URANIUM IN THE PINE CREEK GEOSYNCLINE

PROCEEDINGS OF THE
INTERNATIONAL URANIUM SYMPOSIUM ON THE PINE CREEK GEOSYNCLINE
SYDNEY, 4–8 JUNE 1979
JOINTLY SPONSORED BY BMR AND CSIRO
IN CO-OPERATION WITH IAEA



INTERNATIONAL ATOMIC ENERGY AGENCY, VIENNA, 1980

Cover picture:

The cover shows the Alligator Rivers area, Northern Territory. Cliff-forming sandstone of the Kombolgie Formation (Middle Proterozoic) overlies Lower Proterozoic schists. Mount Brockman, in the foreground, rises 250 m above the plain. Photograph by R.S. Needham.

URANIUM IN THE PINE CREEK GEOSYNCLINE

PROCEEDINGS SERIES

URANIUM IN THE PINE CREEK GEOSYNCLINE

PROCEEDINGS OF THE
INTERNATIONAL URANIUM SYMPOSIUM
ON THE PINE CREEK GEOSYNCLINE
JOINTLY SPONSORED BY THE
BUREAU OF MINERAL RESOURCES, GEOLOGY AND GEOPHYSICS
AND THE
CSIRO INSTITUTE OF EARTH RESOURCES
IN CO-OPERATION WITH THE
INTERNATIONAL ATOMIC ENERGY AGENCY
AND HELD IN SYDNEY, AUSTRALIA
4–8 JUNE 1979

Editors:
John Ferguson and Ann B. Goleby

Organizing Committee:
John C. Rowntree, Chairman
John Ferguson
Geoff H. Taylor
V. Le R. Furlong, Executive Secretary
Ann B. Goleby, Scientific Secretary

INTERNATIONAL ATOMIC ENERGY AGENCY
VIENNA, 1980

Supported by:
Agip Nucleare Australia Pty. Limited
Afmeco Pty. Limited
Chevron Exploration Corporation
Consolidated Gold Fields Australia Limited
C.R.A. Exploration Pty. Limited
Esso Australia Limited
Getty Oil Development Company Limited
Pancontinental Mining Limited
Peko-Wallsend Limited
Uranerz Australia Pty. Limited
Urangesellschaft Australia Pty. Limited

Phototypesetting by:
The Canberra Times, A.C.T., Australia

Typographical Layout and Design by:
W.R. Greentree, A.C.T. Australia

The following persons acted as referees of the papers contributed to this volume:

Robert Balde
R.A. Binns
L.P. Black
C.F. Blain
B. Blangy
Peter Blattner
W.E. Cameron
William Compston
I.H. Crick
Laurence Curtis
D.H. Dahlem
R.H. De Voto
E.C. Druce
P.J. Eadington
G.S. Eupene
G.R. Ewers
James Ferguson
John Ferguson
C.J. Finlay
W.J. Fraser
V.L.R. Furlong
A.J. Gancarz
John Goulevitch
G.J.S. Govett
R.I. Grauch
D.C. Green
L.B. Gustafson
J.A. Hallberg
H.J. Harrington
R.J. Hart
M.R. Hegge
J.H. Hills
Jan Hoeve
Kevin Johnson
B.W. Logan
K.R. Ludwig
John McAndrew
G.J. McArthur
R.H. McMillan
Yanis Miezitis
Alan Morley
J.T. Nash
R.S. Needham
R.W. Page
R.T. Pidgeon
Bernard Poty
C.E. Prichard
J.R. Richards
G.H. Riley
J.C. Rowntree
Rick Ruker
Vladimir Ruzicka
A.K. Scott
T.I.I. Sibbald
P.G. Stuart-Smith
J.S. Stuckless
G.H. Taylor
Kevin Wills
P.J.M. Ypma

© IAEA, 1980

Permission to reproduce or translate the information contained in this publication may be obtained by writing to the International Atomic Energy Agency, P.O. Box 100, A-1400 Vienna, Austria.

Printed by the IAEA in Austria
March 1980

URANIUM IN THE PINE CREEK GEOSYNCLINE
IAEA, VIENNA, 1980
STI/PUB/555
ISBN 92–0–140080–2

FOREWORD

The International Uranium Symposium on the Pine Creek Geosyncline was designed to present original data and interpretations of the Geosyncline derived from a three year co-ordination study by the sponsoring organisations: Bureau of Mineral Resources, Geology and Geophysics (BMR); Commonwealth Scientific and Industrial Research Organisation, Institute of Earth Resources (CSIRO) and participating industry groups. Papers contained in this volume were presented at the Symposium held in Sydney, Australia, June 4–8, 1979. The sponsoring organisations wish to express their gratitude to the International Atomic Energy Agency (IAEA) for its co-operation in the Symposium and the publication.

Uranium exploration in the Pine Creek Geosyncline was stimulated by the discovery in 1949 of secondary uranium mineralization near Rum Jungle by the prospector J.M. White. This was followed by a decade of intense exploration activity resulting in the discoveries of uranium at Rum Jungle and in the South Alligator Valley. The first systematic mapping survey of the region also commenced during this period. The potential similarity of the Alligator Rivers area to the Rum Jungle Uranium Field was shown by a re-interpretation of the geology as shown on the second edition of the 1:500 000 scale map of the Geosyncline (Walpole *et al.*, *Bull. Bur. Miner. Resour. Geol. Geophys., Aust., 82*, 1968). All the major uranium deposits of the Alligator Rivers Uranium Field have been discovered since 1970. The present resources (RAR) of the Geosyncline are approximately 289,000 tonnes U_3O_8, more than 15 percent of the Western World's uranium resources.

The papers contained in this volume deal with regional and detailed aspects of exploration, geophysics, stratigraphy, geochemistry and petrology. In addition to the coverage of many aspects of uranium distribution and mineralization within the Pine Creek Geosyncline, vein-type uranium deposits in Lower Proterozoic rocks in other countries are discussed and compared with the Australian deposits. Particular emphasis is given to the Athabasca margin deposits in Canada.

A pleasing aspect of the Symposium was the diverse range of hypotheses advanced to account for the 'unconformity type' uranium deposits. It became clear that workers on the Canadian Athabasca margin deposits put much more emphasis on the genetic role of the unconformably deposited Middle Proterozoic rocks than do the Australian workers.

Although the Symposium acted as a landmark in the progress towards an understanding of the uranium mineralization in the Pine Creek Geosyncline, it is natural to expect that further studies will confirm or modify some of the concepts put forward here.

CONTENTS

PINE CREEK GEOSYNCLINE

Regional Studies

Regional geology of the Pine Creek Geosyncline 1
R.S. Needham, I.H. Crick & P.G. Stuart-Smith

Evolution of the Pine Creek Geosyncline 23
P.G. Stuart-Smith, Kevin Wills, I.H. Crick & R.S. Needham

Geochronology and evolution of the late-Archaean basement and Proterozoic rocks in the Alligator Rivers Uranium Field, Northern Territory, Australia 39
R.W. Page, William Compston & R.S. Needham

Granite ages in the Pine Creek Geosyncline 69
G.H. Riley

Granitoids in the Pine Creek Geosyncline 73
John Ferguson, B.W. Chappell & A.B. Goleby

Metamorphism in the Pine Creek Geosyncline and its bearing on stratigraphic correlations 91
John Ferguson

The characteristics and interpretation of regional gravity, magnetic and radiometric surveys in the Pine Creek Geosyncline 101
D.H. Tucker, D.C. Stuart, I.G. Hone & Narayanan Sampath

A study of the Pine Creek Geosyncline using integrated Landsat and Aeromagnetic data 141
C.J. Simpson, J.F. Huntington, John Leishman & A.A. Green

An overview of metallic mineralization in the Pine Creek Geosyncline 157
R.S. Needham & M.J. Roarty

Rare earth elements in sedimentary rocks, granites and uranium deposits of the Pine Creek Geosyncline 175
S.M. McLennan & S.R. Taylor

Pine Creek Geosyncline: Statistical treatment of whole rock chemical data 191
John Ferguson & Paul Winer

A Proterozoic tectonic model for northern Australia and its economic implications 209
A.G. Rossiter & John Ferguson

District Studies

Geology of the Alligator Rivers Uranium Field 233
R.S. Needham & P.G. Stuart-Smith

Geologic setting of the East Alligator uranium deposits and prospects 259
M.R. Hegge, D.V. Mosher, G.S. Eupene & P.J. Anthony

The geology and mineralisation of the South Alligator Valley Uranium Field 273
I.H. Crick, M.D. Muir, R.S. Needham & M.J. Roarty

Geology and exploration of the Rum Jungle Uranium Field 287
W.J. Fraser

The geology of the Litchfield province, N.T. 299
D.A. Berkman

Stratigraphy of the Kapalga Formation north of Pine Creek and its relationship to base metal mineralization 307
John Goulevitch

The geology and economic significance of the Golden Dyke Dome, Northern Territory 319
P.M. Nicholson

Geochemical investigations in the Mt. Bundey area, Northern Territory 335
M.B. Hochman

The Mount Fitch copper and uranium deposits, Rum Jungle Uranium Field, N.T. Australia 343
D.A. Berkman & W.J. Fraser

Experience with the track etch method for uranium exploration in Northern Australia 351
C.P. Pedersen, J. Dunbier & J.E. Gingrich

Detailed Studies
(petrology/geochemistry/mineralogy/experimental)

The nature and significance of the occurrence of uranium in the Nanambu Complex of the Pine Creek Geosyncline 357
John McAndrew & C.J. Finlay

Mineralogy of the Jabiluka, Ranger, Koongarra and Nabarlek Uranium deposits 363
G.R. Ewers & John Ferguson

Fluid inclusion and oxygen isotope studies of the Nabarlek and Jabiluka deposits, Northern Territory, Australia 375
P.J.M. Ypma & Kazuo Fuzikawa

A stable isotope study of three deposits in the Alligator Rivers Uranium Field, N.T. 397
T.H. Donnelly & John Ferguson

Natural Reactor Studies 407
G.H. Riley & M.J. Korsch

Petrology and geochemistry of alteration associated with uranium mineralization at Jabiluka, Northern Territory, Australia 417
R.A. Binns, D.E. Ayres, J.R. Wilmshurst & A.R. Ramsden

Lead isotope studies at Jabiluka 439
B.L. Gulson & K.J. Mizon

Rb-Sr chronology of micas at Jabiluka 457
G.H. Riley, R.A. Binns & S.J. Craven

Mercury distribution in the Jabiluka Two orebody and its host rocks 469
W.R. Ryall & R.A. Binns

Ground water geochemistry in the vicinity of the Jabiluka deposits 477
R.L. Deutscher, A.W. Mann, A.M. Giblin

Uraninite and its alteration products, Koongarra uranium deposit 487
A.A. Snelling

Movements of uranium and daughter isotopes in the Koongarra uranium deposit 499
B.L. Dickson & A.A. Snelling

$^{234}U/^{238}U$ activity ratios in clay as a function of distance from primary ore. 509
P.J. Shirvington

The role of clay adsorption in genesis of uranium ores 521
A.M. Giblin

Models for Uranium Mineralization

Evaporites and uranium mineralization in the Pine Creek Geosyncline 531
I.H. Crick & M.D. Muir

Origin of uranium mineralization at Jabiluka 543
R.A. Binns, J. McAndrew & S-S. Sun

Model for the development of economic uranium mineralisation in the Alligator Rivers Uranium Field 563
John Ferguson, G.R. Ewers & T.H. Donnelly

CANADIAN DEPOSITS

Athabasca basin unconformity-type uranium deposits: A special class of sandstone-type deposits? 575
Jan Hoeve, T.I.I. Sibbald, Paul Ramaekers & J.F. Lewry

Uranium geology in the Amer-Dubawnt-Yathkyed-Baker Lakes region, Keewatin District, N.W.T. Canada..... 595
Laurence Curtis & A.R. Miller

The Key Lake U-Ni Deposits: A model for Lower Proterozoic uranium deposition 617
G. Kirchner, K. Lehnert-Thiel, John Rich & J.G. Strnad

Genetic models and their impact on uranium exploration in the Athabasca sandstone basin, Saskatchewan, Canada..... 631
J.G. Strnad

Contribution to some Saskatchewan uranium deposits mainly from fluid inclusion and isotopic data..... 639
Maurice Pagel, Bernard Poty & S.M.F. Sheppard

OTHER DEPOSITS

Present exploration status of the Lianshanguan uranium deposit, Northeast China 655
Qin Fei & Hu Shaokang

Le Gisement d'Oklo et ses reacteurs de fission naturels..... 663
F. Gauthier-Lafaye, F. Weber, R. Naudet, J.P. Pfiffelmann, R. Chauvet, B. Michel & J.C. Reboul

Uraniferous phosphorite and apatite-bearing gneisses in the Proterozoic of Finland..... 675
Olli Äikäs

Geology of uranium vein deposits (including Schwartzwalder Mine) in Proterozoic metamorphic rocks, Front Range, Colorado..... 683
R.H. De Voto & J.A. Paschis

The association of uranium and skarn development in the Mary Kathleen area, Queensland..... 693
B.I. Cruikshank, John Ferguson & G.M. Derrick

GENERAL

The distribution of U, Th and K through a section of the granitic crust of the Vredefort basement..... 707
R.J. Hart, L.O. Nicolaysen & N.H. Gale

Syngenetic model for some early Proterozoic uranium deposits: evidence from Oklo..... 709
D.G. Brookins

Continental weathering and development of palaeosurface-related uranium deposits: some genetic considerations 721
J.E. Tilsley

A comparison of exploration techniques in Saskatchewan and the Northern Territory 733
C.W. Armstrong & N.W. Brewster

Uranium deposits of the future 743
D.M. Taylor & James Cameron

RETROSPECT & PROSPECT

The Symposium - Retrospect and Discussion 751
G.H. Taylor & J.C. Rowntree

AUTHOR INDEX 759

TEXT APPENDICES

Microfiche: Analyses A — John Ferguson & Paul Winer (this volume).
Analyses B — John Ferguson, B.W. Chappell & A.B. Goleby (this volume).
Analyses C — A.G. Rossiter & John Ferguson (this volume).

Maps: 1:500 000 Solid Geology Map of the Pine Creek Geosyncline.
1:500 000 Gravity Map of the Pine Creek Geosyncline.
1:500 000 Magnetic Map of the Pine Creek Geosyncline.
1:500 000 Radiometric Map of the Pine Creek Geosyncline.

REGIONAL GEOLOGY OF THE PINE CREEK GEOSYNCLINE

R.S. Needham, I.H. Crick and P.G. Stuart-Smith

Bureau of Mineral Resources, P.O. Box 378, Canberra City, A.C.T. 2601, Australia

ABSTRACT

The Pine Creek Geosyncline comprises about 14km of chronostratigraphic mainly pelitic and psammitic Lower Proterozoic sediments with interlayered tuff units, resting on granitic late Archaean complexes exposed as three small domes. Sedimentation took place in one basin, and most stratigraphic units are represented throughout the basin. The sediments were regionally deformed and metamorphosed at 1800Ma. Tightly folded greenschist facies strata in the centre grade into isoclinally deformed amphibolite facies metamorphics in the west and northeast. Pre and post-orogenic continental tholeiites, and post-orogenic granite diapirs intrude the Lower Proterozoic metasediments, and the granites are surrounded by hornfels zones up to 10km wide in the greenschist facies terrane. Cover rocks of Carpentarian (Middle Proterozoic) and younger ages rest on all these rocks unconformably and conceal the original basin margins.

The Lower Proterozoic metasediments are mainly pelites (about 75 percent) which are commonly carbonaceous, lesser psammites and carbonates (about 10 percent each), and minor rudites (about 5 percent). Volcanic rocks make up about 10 percent of the total sequence. The environment of deposition ranges from shallow-marine to supratidal and fluviatile for most of the sequence, and to flysch in the topmost part. Poor exposure and deep weathering over much of the area hampers correlation of rock units; the correlation preferred by the authors is presented, and possible alternatives are discussed. Regional geological observations pertinent to uranium ore genesis are described.

INTRODUCTION

The Pine Creek Geosyncline was studied at 1:250 000 and partly at 1:63 000 scale in the 1950's and early 1960's (Walpole *et al.*, 1968). Systematic 1:100 000 scale mapping of about half of the area during the last 8 years has resulted in substantial changes in geological understanding. Up to 14km of Lower Proterozoic metasediments with interbedded volcanics and mafic sills are preserved in a sequence which generally thins westwards near Rum Jungle, where some units lens out. A regional metamorphic event at 1800Ma metamorphosed the sediments to mainly greenschist facies; however, amphibolite facies dominates in the northeastern part of the Geosyncline, in the Alligator Rivers region. The higher grade terrane was considered by Walpole *et al.* (1968) to be Archaean basement, but our work has indicated a metamorphic gradation in the metasediments between the two metamorphic regimes. Proven Archaean rocks are restricted to the mainly granite-gneiss Rum Jungle, Waterhouse and Nanambu Complexes, which form mantled gneiss domes near the presently exposed western and eastern margins of the Geosyncline.

The higher grade metasediments grade northeastwards into the migmatitic Nimbuwah Complex, where in places sedimentary 'resisters' indicate the sedimentary parentage of the gneissic rocks which form the outer parts of the Complex. These rocks mantle tonalitic to granitic igneous rocks which form the inner parts of the Complex. The intensity of folding in the Geosyncline also increases generally towards the Nimbuwah Complex — tight to isoclinal folds with steep limbs in the central parts progress through overturned tight to isoclinal folds in the South Alligator area, to polyphase isoclinal folds in the Alligator Rivers region.

The Lower Proterozoic metamorphics are intruded by early Carpentarian (Middle Proterozoic)* granites and dolerite, and these are unconformably overlain by valley-fill felsic volcanics and pyroclastics. All these rocks are overlain with marked regional

* The age of the Lower-Middle Proterozoic boundary used in this paper and on the 1:500 000 scale solid geology map of the Pine Creek Geosyncline is 1800Ma, placing the granite and dolerite intrusions of the 'transitional igneous activity' in the early Carpentarian (Middle Proterozoic). The 1700± 30Ma age suggested for the boundary by Plumb *et al.* (in press) places these rocks in the late Lower Proterozoic.

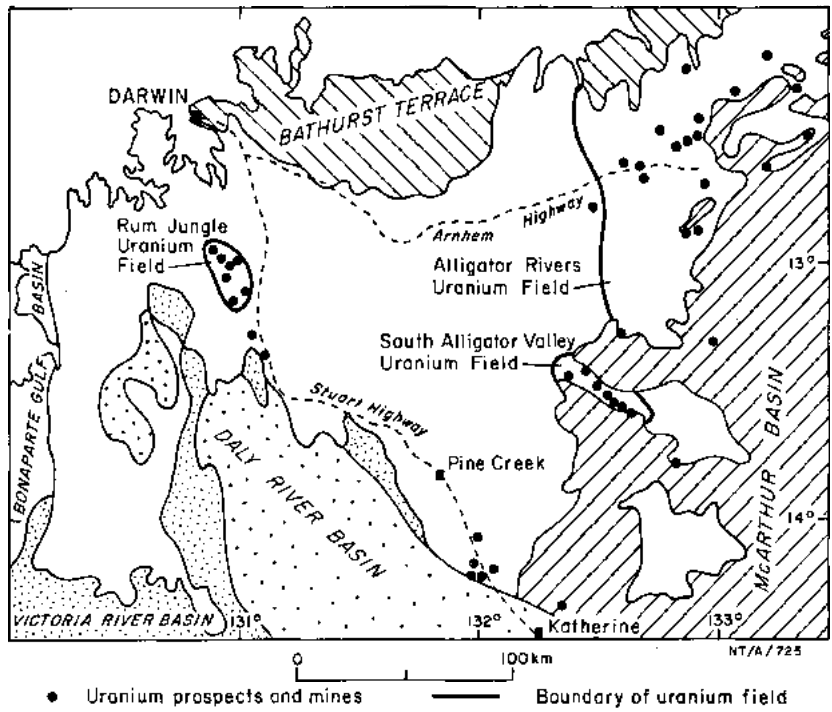


Figure 1. General structural setting of the Pine Creek Geosyncline with location of uranium mines and prospects.

unconformity by Carpentarian (Middle Proterozoic) plateau sandstone with interbedded intermediate to mafic volcanics of the McArthur Basin in the east; by Adelaidean (Upper Proterozoic) mainly siltstone, sandstone and carbonate of the Victoria River Basin in the southwest; by Palaeozoic mainly sandstone, limestone and basalt of the Daly River Basin in the south, and sandstone of the Arafura Basin in the northeast, and by Permian siltstone and sandstone of the Bonaparte Gulf Basin in the west. Mesozoic sandstone and siltstone overlie older rocks in many places, mainly in the north in the Bathurst Terrace (Fig. 1). The Carpentarian (Middle Proterozoic) and younger rocks are largely undeformed, but in places are extensively faulted.

In this paper, the rocks of the Pine Creek Geosyncline are divided into basement, geosynclinal pile, transitional igneous activity*, and cover rocks. The stratigraphy of each group is given separately in tables 1-4. The text concentrates on the stratigraphy of the geosynclinal pile, its structure, metamorphism, problems in correlations, and regional aspects pertinent to uranium ore genesis. Discussion of cover rocks is restricted to those immediately overlying the areas of uranium mineralisation in the Geosyncline, which may have played a part in uranium ore genesis. Generalised stratigraphy is shown in figure 2, and the geology of the Pine Creek Geosyncline is shown on the 1:500 000 solid geology map accompanying this volume.

TOPOGRAPHY AND OUTCROP

Lower Proterozoic rocks crop out over about 66 000km² east and south of Darwin (Fig.

* See footnote previous page.

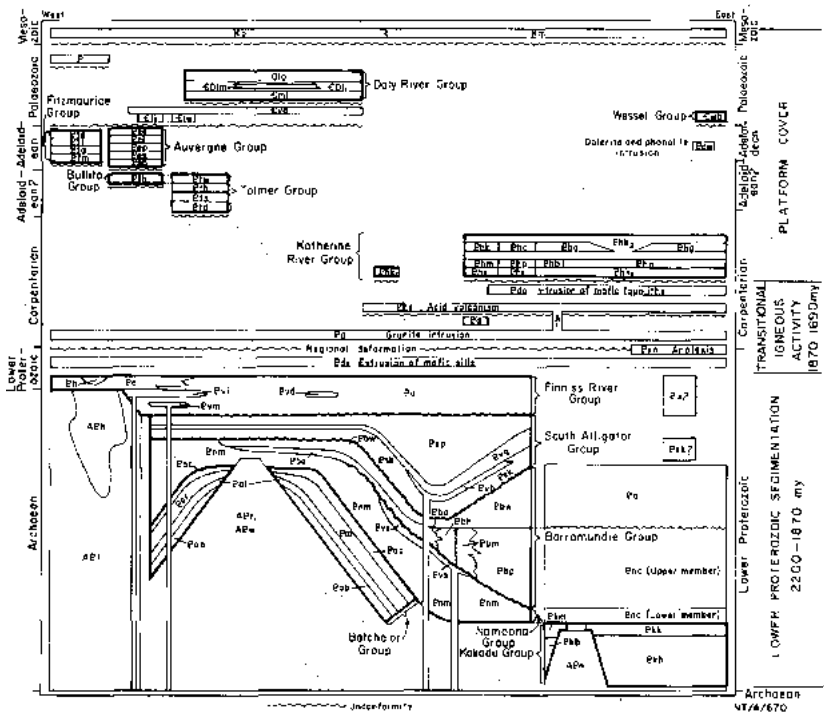


Figure 2. Diagrammatic stratigraphy of the Pine Creek Geosyncline and cover rocks.

1), rising from coastal and estuarine flats in the north, through undulating wooded sand plains with an elevation of up to 50m, to rocky ridges and rubbly rises up to 300m elevation in the south. Fair outcrop is limited to the south where arenaceous, ferruginous or hornfelsic rocks form most of the prominent exposures. The granites generally have a low relief although bouldery outcrop interspersed with lightly wooded sand plains is common. Outcrop on the undulating sand plains and coastal flats is very rare and generally confined to incised creeks or isolated rock pavements at the margins of the larger drainage systems. The metasediments have undergone multiple phases of weathering, which in places extends to a depth of 100m — much of the area is lateritised and/or covered with transported laterite. Carbonaceous pyritic shale and carbonate are two common lithologies, but the shale is almost always altered to brick-red slate at surface and the carbonate is usually totally silicified unless stripped by recent erosion. Extensive Cainozoic sand deposits 5-100m thick cover much of the northern part of the area, where study of the Lower Proterozoic rocks is particularly difficult. Exposure of the cover rocks is poor, except for the Carpentarian (Middle Proterozoic) and Adelaidean (Upper Proterozoic) units. Photogeology is generally only useful in the areas of rocky ridges and rubbly rises, i.e. in the southern part of the Geosyncline.

BASEMENT COMPLEXES

Archaean ages are established for the Rum Jungle and Waterhouse Complexes in the western part of the Geosyncline, and for parts of the Nanambu Complex in the east (Page, 1976; Page *et al.*, this volume; Richards *et al.*, 1977). Walpole *et al.* (1968) interpreted the

	Unit		Lithology
?ARCHAEAN-LOWER PROTEROZOIC	Hermit Creek Metamorphics		quartz mica schist, phyllite, tremolite schist, amphibolite, migmatite
	Litchfield Complex		granodiorite, tonalite, granite, adamellite, migmatite, pegmatite, garnetiferous in places
ARCHAEAN-LOWER PROTEROZOIC	Nanambu Complex		pegmatoid leucocratic gneiss, migmatite, biotite chlorite schist; garnetiferous in places
			porphyroblastic foliated biotite granite and augen gneiss
			muscovite biotite granite, massive to foliated
ARCHAEAN	Rum Jungle Complex	Unit 7	leucocratic granite
		Unit 6	large feldspar granite
		Unit 5	coarse-medium granite
		Unit 4	metadiorite
		Unit 3	granite gneiss, migmatite
		Unit 2	schist, gneiss
		Unit 1	metasediments, banded iron formation
	Waterhouse Complex	Unit 5	aplitic leucocratic granite, garnetiferous granite, pegmatite
		Unit 4	fine-coarse granite, adamellite, pink porphyritic granite
		Unit 3	dolerite, amphibolite
		Unit 2	schist, gneiss, granite gneiss, migmatite
		Unit 1	metasediments, banded iron formation, volcanics

Table 1. Stratigraphy of Archaean and Archaean-Lower Proterozoic basement complexes (Main sources: Crick,

Litchfield Complex and Hermit Creek Metamorphics, in the extreme west, as wholly or partly Archaean; no isotopic work has been done on these rocks, but Berkman (this volume) reports muscovite-biotite schist in the Litchfield Complex as a probable correlative of the Burrell Creek Formation (topmost unit in the geosynclinal pile), and suggests that granites in the Complex have some features in common with the migmatitic granites. The stratigraphy of the basement complexes and the Litchfield Complex is summarised in table 1.

Rum Jungle and Waterhouse Complexes

The Rum Jungle and Waterhouse Complexes are roughly oval granite-gneiss domes up to 400km^2 in the west of the Geosycline. They are the dominant rock units in the Rum Jungle district, with anomalous concentrations of uranium (Ferguson & Winer, this volume), and are a possible source of the uranium deposited in the overlying sediments. Each Complex contains several granite and gneissic granite phases with veins and dykes of pegmatite and

Relationships	Age Ma * Page *et al.*, this volume ● Richards *et al.*, 1977 □ Page, 1976
accreted metamorphosed Kakadu Group	* 1800
metamorphosed Archaean basement	
Archaean basement	* 2400-2500
	□ ● 2400
Archaean basement (the ordering of units represents an ordering from oldest (Unit 1) to youngest (Unit 7) based on field relationships)	
	□ 1755 (reset)
Archaean basement (the ordering of units represents an ordering from oldest (Unit 1) to youngest (Unit 5) based on field relationships)	□ 2400

1978; Johnson *et al.*, 1977; Rhodes, 1965; Needham & Stuart-Smith, this volume; Walpole *et al.*, 1968)

amphibolite and tourmaline veins. Metasediments, banded iron formation, volcanics and metabasics in the Complexes are thought to pre-date the granites (Table 1). Most of the phases of the Rum Jungle Complex were determined by Rhodes (1965). Johnson (1974) recognised the same units in the Waterhouse Complex and also noted the presence of banded iron formation in both Complexes. On field relationships the leucocratic granite of the Rum Jungle Complex is considered to be the youngest phase; this rock type gives an age of about 2400Ma (Richards & Rhodes, 1967; Page *et al.*, this volume). Rhodes (1965) compared the Rum Jungle Complex to a mantled gneiss dome; Stephansson and Johnson (1976) suggested that both Complexes were domed by solid-state diapiric intrusion of granite during the 1800Ma orogeny.

Nanambu Complex

Rocks of this Complex are poorly exposed over an area of about 45km by 80km between the South and East Alligator Rivers in the northeast of the Geosyncline. Needham & Stuart-

Unit	Lithology
FINNISS RIVER GROUP (FLYSCH, 1500-5000m)	
Henschke Breccia	Coarse ferruginous sedimentary breccia and conglomerate with sandstone fragments, minor sandstone
Meeway Volcanics	Porphyritic felsic lavas, tuffs
Chilling Sandstone	White quartz sandstone, ripple-marked and cross-bedded; minor conglomerate, siltstone and tuff
Berinka Volcanics	Felsic and minor intermediate lavas, minor sandstones and tuff interbeds, granophyric felsic intrusive rocks
Dorothy Volcanics	Mafic lavas, pyroclastic rocks, and tuffaceous sediments
Burrell Creek Formation	Siltstone, shale, greywacke siltstone; greywacke increases to west
SOUTH ALLIGATOR GROUP (SHALLOW MARINE CHEMICAL, VOLCANIC, 5000m)	
Kapalga Formation	Ferruginous siltstone; chert bands and nodules in places, commonly carbonaceous at depth; minor tuff
Gerowie Tuff	Black-green cherty tuff, green argillite, pale green tuffaceous greywacke, minor ferruginous chert nodular siltstone and banded iron formation
Shovel Billabong Andesite	Variolitic andesite
Koolpin Formation	Ferruginous siltstone with chert bands and nodules, pyritic carbonaceous shale, silicified dolomite, minor phyllite, jasper and banded iron formation
MOUNT PARTRIDGE GROUP (FLUVIATILE, 5000m)	
Nourlangie Schist	Quartz mica schist, mica quartz schist, minor quartzite
Wildman Siltstone	Siltstone, in places carbonaceous at depth, red and cream laminated siltstone, minor quartzite and quartz greywacke
Acacia Gap Sandstone Member	Quartz sandstone and feldspathic sandstone with pyritic carbonaceous siltstone and quartz siltstone interbeds
Mount Hooper Sandstone	Medium quartz sandstone and quartzite with some chert fragments, siltstone, phyllite; feldspathic quartzite, pebbly in places; chert pebble conglomerate. Cross-bedded
Mundogie Sandstone	Coarse-medium quartz sandstone and orthoquartzite, commonly pebbly quartz pebble conglomerate, siltstone, cross-bedded, scoured and graded beds. Minor schist, amphibolitic in places
NAMOONA GROUP (SHALLOW MARINE, CHEMICAL, DETRITAL, <3500m)	
Stag Creek Volcanics	Mafic volcanic breccia, hawaiite, tuff, tuffaceous shale, tuffaceous greywacke
Cahill Formation	Mica feldspar quartz schist, quartz mica schist, with garnet, amphibole and kyanite in places, carbonaceous schist, crystalline dolomite-magnesite, and calc-silicate gneiss near base
Masson Formation	Ferruginous shale (mostly pyritic and carbonaceous at depth), fine-coarse calcareous and volcanic greywacke, calcarenite, sandstone, limestone
BATCHELOR GROUP (RECURRENT FLUVIATILE, CHEMICAL 1500m)	
Coomalie Dolomite	Dolomite, magnesite, dolomite breccia, trémolite schist, calcilutite, algal structures and evaporite pseudomorphs in places
Crater Formation	Feldspathic sandstone, pebble conglomerate, siltstone, pyritic in part, basal ferruginous conglomerate in places
Celia Dolomite	Dolomite, magnesite, silicified or with algal structures in places, trefnolite schist, minor sandstone, arkose, carbonaceous sediments
Beestons Formation	Arkose, feldspathic sandstone, conglomerate, siltstone
KAKADU GROUP (FLUVIATILE, 1000m)	
Munmarlary Quartzite	Gneissic massive to friable orthoquartzite, minor schist
Mount Howship Gneiss	Very coarse white feldspathic leucogneiss, minor schist; rare garnet and amphibole
Kudjumarndi Quartzite	Orthoquartzite, quartz gneiss, minor schist, rare cross-bedding, rare amphibole
Mount Basedow Gneiss	White-grey-pink coarse muscovite biotite gneiss, granitoid gneiss, minor schist

Table 2. Stratigraphy of Lower Proterozoic metasediments and extrusives. (Main sources: Needham & Stuart-

Thickness	Relationships
<1000	relationship with older units unknown owing to faulting; overlain with marked unconformity by ?Adelaidean (Upper Proterozoic) Moyle River Formation
<1650	overlie and interbedded with Chilling Sandstone confined to southwest
<4800	conformable on Burrell Creek Formation, apparently intertongues with Meeway Volcanics
sills <75	overlies and possibly intertongues with Burrell Creek Formation; confined to southwest
~1000	overlies Burrell Creek Formation; confined to Katherine area
~3000	gradational into Kapalga Formation; onlaps onto Coomalie Dolomite near Waterhouse Complex
<5000	mainly conformable and in places interbedded with Gerowie Tuff, apparently unconformable onto Koolpin Formation north of South Alligator Valley
<750	conformable and in places interbedded with Koolpin Formation
<100	flows near base of Gerowie Tuff
<1000	angular unconformity to disconformity at base
unknown	metamorphic equivalent of Wildman Siltstone and possibly Burrell Creek Formation; locally unconformable on Cahill Formation upper member
1000	conformable on Mount Hooper Sandstone and Mundogie Sandstone, correlates with Nourlangie Schist
0-1200	conformable near base of Wildman Siltstone
<5000	contains pebbles of silicified carbonate probably derived from Cahill Formation lower member, facies variant of Cahill Formation upper member
2400	locally unconformable over Masson Formation and Stag Creek Volcanics; correlates with Mount Hooper Sandstone and facies variant of Cahill Formation upper member
1000	conformable at top of Masson Formation, restricted to South Alligator Valley area
3000	apparently conformable on Kakadu Group, in places onlaps onto Nanambu Complex Archaean granite; lower member facies and metamorphic equivalent of Masson Formation, upper member with Mundogie Sandstone and Mount Hooper Sandstone
3000	lowest exposed unit in centre; apparently conformable on Coomalie Dolomite in west, correlates with Cahill Formation lower member in east
~300	conformable on Crater Formation
300-600	mainly apparently conformable on Celia Dolomite, onlaps onto Rum Jungle Complex in places
<300	conformable on Beestons Formation
<200	rests unconformably on Rum Jungle and Waterhouse Complexes
>200	eastern equivalent of Mummarlary Quartzite
unknown, >2000	eastern equivalent of Mount Basedow Gneiss
150	flanks and in places is within Nanambu Complex accreted leucogneiss
unknown, >1500	transitional into accreted leucogneiss of Nanambu Complex

Smith, 1978; Crick, 1978; Stuart-Smith *et al.*, in prep.; Sweet *et al.*, 1974; Walpole *et al.*, 1968)

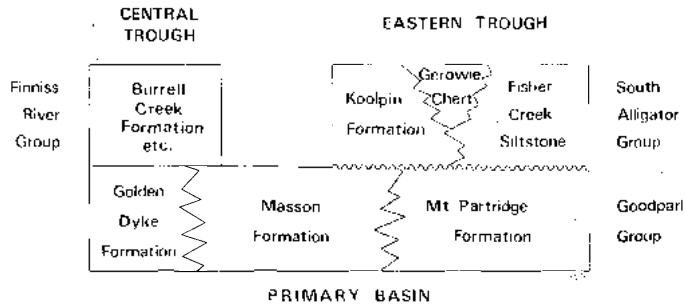


Figure 3. The laterally disposed lithofacies groups proposed by Walpole *et al.* (1968). Modified from Walpole *et al.* (1968) by Crick *et al.* (1978).

Smith (this volume) defined three groups of rocks in the Complex: Archaean two-mica granite; porphyroblastic foliated biotite granite and augen gneiss which is Archaean granite metamorphosed by the 1800Ma event; and pegmatoid leucocratic gneiss, migmatite and schist which is Lower Proterozoic arkosic material accreted to the granitic Complex at 1800Ma. Field distinction of the 3 phases is not always clear. The age relationships of the phases were indicated by isotopic dating techniques (Page *et al.*, this volume). On the southern and western margins of the Complex the leucocratic gneiss may contain resisters of Lower Proterozoic quartzite, and the leucocratic gneiss grades out into meta-arkose of the Lower Proterozoic metasedimentary sequence.

The Nanambu Complex is a likely source of uranium for the Alligator Rivers region uranium deposits, as the two-mica Archaean granite gneiss is known to contain accessory uraninite (McAndrew & Finlay, this volume).

GEOSYNCLINAL SEDIMENTATION

The stratigraphy of the Lower Proterozoic sediments and interbedded volcanic rocks is summarised in table 2, and diagrammatic relationships are shown in figure 2. Details of stratigraphy, particularly the distribution and types of lithologies in each unit, and perhaps some stratigraphic relationships, may be modified as the current study is extended to cover all of the Pine Creek Geosyncline.

At least 14km of sediments and volcanics were deposited in parts of the basin. The margins of the basin are concealed by younger strata, so the size of the basin in unknown. The basin is probably continuous under cover with other Lower Proterozoic sequences in northern Australia such as the Arnhem, Tennant Creek, Granites-Tanami and Arunta Blocks. Sedimentation probably took place between 2400Ma (the age of the youngest basement rocks) and 1870Ma (the age of premetamorphic granodiorites in the northeast; Page *et al.*, this volume). There is no geochronological data on volcanics interbedded with the sediments. The sediments are mainly pelites, which are commonly carbonaceous and/or pyritic and/or calcareous at depth. Other lithologies present are sandstone, crystalline carbonate, calcarenite, tuff and conglomerate.

Basin Configuration

Walpole *et al.* (1968) advanced a concept of deposition in a number of basins. They grouped the rocks into laterally-disposed lithofacies (Fig. 3). Deposition in the 'Primary Basin' was considered to have been succeeded by deposition in the 'Central Trough' and 'Eastern Trough' which were formed by upfaulting of a ridge of Archaean basement volcanics, the Stag Creek Volcanics. Our work has shown that units can be traced through much of the Pine Creek Geosyncline, indicating deposition in one continuous basin — these

units continue through the major lateral facies groupings of Walpole *et al.* (1968). Conformity of the sedimentary units with interbedded tuff units across the basin indicate the chronostratigraphic nature of the geosynclinal pile (Crick *et al.*, 1978). The Stag Creek Volcanics are known from the work of Foy & Miezitis (1977) and ourselves to be interbedded with the sediments and not basement to them. As a consequence of this change in concept much of the rock unit nomenclature has been revised. A table relating the old and the new nomenclature is given by Needham *et al.* (1979, Table 3), who also list the main changes in the stratigraphy. The new stratigraphy is incorporated in the 1:500 000 scale solid geology map of the Pine Creek Geosyncline enclosed in this volume.

Stratigraphy

The geosynclinal succession is made up essentially of an alternating sequence of mainly psammites (Batchelor, Kakadu and Mount Partridge Groups) and pelites (Namoona, South Alligator and Finniss River Groups, Table 2). The Namoona and South Alligator Group pelites are commonly pyritic and carbonaceous and may be calcareous or contain beds of massive carbonate. Carbonate in the psammitic groups is confined to the Batchelor Group. The South Alligator Group is typified by iron-rich chemical sediments and tuffs. Greywacke, once thought to be the dominant lithology in the region, is largely confined to the Finniss River Group.

The psammitic units are mainly fluviatile. The provenance of the Batchelor and Kakadu Groups was probably the adjacent basement complexes, whilst grainsize distribution suggests a northern provenance for the Mount Partridge Group, and a western source for the Finniss River Group (Stuart-Smith *et al.*, this volume). Widespread algal carbonate and evaporite pseudomorphs indicate mainly very shallow to supratidal environments for the carbonates (Crick & Muir, this volume). The pelites and greywackes were probably mainly deposited in neritic conditions.

Sedimentation took place in an intracratonic basin covering at least 100 000km^2. The earliest known Lower Proterozoic sediments, the *Batchelor and Kakadu Groups*, rest unconformably on Archaean basement and exposure is generally confined to areas adjacent to exposed basement. These basal sediments may extend over much of the basin at depth. The Batchelor Group, which surrounds the Rum Jungle and Waterhouse Complexes, contains arkosic rudite, psammite, conglomerate, and minor shale of the Beestons and Crater Formations, and massive crystalline carbonate of the Celia and Coomalie Dolomites. The Kakadu Group, which is best developed adjacent to the Nanambu Complex, comprises mainly meta-arkose and paragneiss, which in places grade into leucogneiss of the Complex.

The two basal groups are overlain by carbonaceous and calcareous pelites and psammites of the *Namoona Group*. The dominant unit in this group is the Masson Formation, which extends from west of the Rum Jungle Complex almost to the South Alligator River; further east it is equivalent to the lower member of the Cahill Formation, a partly calcareous and carbonaceous sequence of micaceous quartzo-feldspathic schist, with lenses of massive carbonate near its base (Needham & Stuart-Smith, 1976). These two correlative units are host to uranium and other mineralisation in the Alligator Rivers and Rum Jungle areas. Volcanic breccia and basalt of the Stag Creek Volcanics are conformable on the Masson Formation in the central part of the Geosyncline. Elsewhere a wedge-shaped assemblage of sandstone and siltstone, the Mount Partridge Group, overlies the Masson Formation. It contains the Mundogie Sandstone, Mount Hooper Sandstone, and Wildman Siltstone between the Wildman and South Alligator Rivers, where the group is thickest; it thins westwards, and correlates with the Acacia Gap Sandstone in the Rum Jungle area. East of the South Alligator River, the Mundogie Sandstone correlates with feldspathic quartz schist of the upper member of the Cahill Formation, and the overlying Wildman Siltstone correlates with the Nourlangie Schist.

A distinctive assemblage of iron-rich sediments, carbonate, and tuff of the *South Alligator Group* rests, in places unconformably, over the older groups. The lowest member of this group, the Koolpin Formation, is mostly pyritic carbonaceous shale which commonly contains chert-bands and nodules, algal carbonate, and banded iron formation. These rocks are generally altered near-surface to chert-banded hematite siltstone and massive siliceous rocks. Chert-banded hematitic siltstone also crops out as interbeds in the overlying Gerowie Tuff; this is the main tuff unit in the Pine Creek Geosyncline, and together with the Koolpin Formation provides the main line of evidence for correlating the strata of the western (Rum Jungle area) and central (Burnside-Mount Bundey-South Alligator Valley) parts of the Geosyncline. Both have distinctive outcrop and photo-tone characteristics (crags of gossan-like iron-rich rocks on ridges and stands of high timber on dark brown soil, with a dark photo-tone for the Koolpin Formation; rubbly to well-bedded cherty rocks with devitrified skins, poor soil development with short gnarled broad-leafed gum trees, and a white photo-tone for the Gerowie Tuff). Rocks similar to the ferruginous siltstone of the Koolpin Formation also crop out in the Alligator Rivers Uranium Field, and are critical to correlation in the northeastern part of the Geosyncline.

Conformity between the ash-fall rocks of the Gerowie Tuff, and other sediments verifies the chronostratigraphic nature of the sedimentary pile. The Gerowie Tuff is overlain by Kapalga Formation rocks, which are a transitional suite between Koolpin-type rocks (less iron-rich and less chert than in the Koolpin Formation) and greywacke of the Finniss River Group, with interbeds of Gerowie Tuff-type tuff and argillite. The Kapalga Formation is up

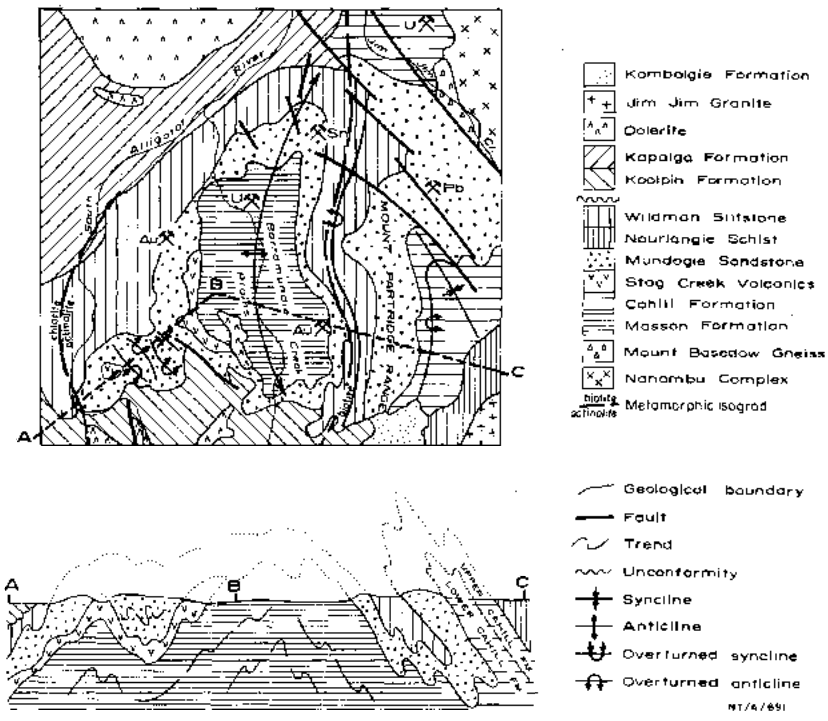


Figure 4. Schematic solid geology and cross-section of the Mount Partridge Area.

to 5km thick in the Kapalga area, where it locally rests unconformably on the two older units of the South Alligator Group.

The upper part of the Lower Proterozoic succession is represented by a monotonous sequence of siltstone, slate, shale, greywacke, and minor arkose, quartzite, conglomerate, and schist, termed the *Finniss River Group*. In the west, greywacke and conglomerate of the Burrell Creek Formation, made up largely of volcanic detritus, grade laterally and upwards to quartz sandstone and minor conglomerate of the Chilling Sandstone (Walpole *et al.*, 1968). In the South Alligator Valley area the group is represented by the Fisher Creek Siltstone, a correlative of the Burrell Creek Formation. The Burrell Creek Formation commonly displays turbiditic sedimentary features, including graded beds, scour marks, flute casts and flame structures.

Alternative correlations

Correlation between amphibolite-grade and greenschist-grade terranes

The correlation given in this paper between metasediments of the two main metamorphic domains in the Pine Creek Geosyncline, is based on four main observations. Firstly, the metamorphic gradation between the two domains is, at least in places, 50km wide, and is best established from rock exposures and drill core in the Mundogie/Mount Partridge Range area (Fig. 4), where the position of the chlorite/actinolite and biotite isograds has been established (a gradation of 10km between these isograds has also been established in the Kapalga area 30km to the north; Stuart-Smith, 1977). Secondly, rocks of the Mundogie Sandstone and Wildman Siltstone can be traced through these isograds, and themselves grade from shale, slate, and quartz sandstone in the chlorite zone, into phyllite and foliated quartzite in the actinolite zone, and into mica schist, quartz gneiss and foliated quartzite in the biotite zone. Thirdly, although the rocks of this area form overturned tight to isoclinal folds, on their regional disposition they are seen to form a major dome under the Barramundie Creek Plains, and an overturned syncline in the Mount Partridge Range. The cross-section of figure 4 thus indicates the reasoning behind correlation across the Mount Partridge Range. The correlative units are similar in lithology, but the difference in thickness and metamorphic grade necessitates a difference in nomenclature. Finally, in the Kapalga area, conglomerate of the Mount Hooper Sandstone, which underlies the Koolpin Formation, contains pebbles of silicified carbonate indicating the presence of an older carbonate unit. The only known possible older carbonate unit is the Cahill Formation, which contains massive carbonate and lies between the Mount Hooper Sandstone and Nanambu Complex in this area. Thus there are two carbonate-bearing units, above and below the Mount Hooper Sandstone, which is a correlative of the Mundogie Sandstone. Elsewhere the higher carbonate-bearing unit is the Koolpin Formation; the lower one is Masson Formation in the lower-grade domain, whereas in the higher-grade domain this carbonate-bearing unit is represented by the lower member of the Cahill Formation.

Wright (1976), after detailed mapping in the Barramundie Creek Plains area, concluded that a sequence of consistently eastwards-dipping strata consisting mainly of sandstone was continuous across the plains. He considered that conglomerate on the west side of the plains indicated an unconformity between Mundogie Sandstone, and overlying 'Mount Partridge Formation' sandstone which he suggested occurred subsurface below the Barramundie Creek Plains. Subsequent work in the area by the Bureau of Mineral Resources, Geology and Geophysics (BMR, 1979) revealed overturned dips in the conglomerate (i.e. the rocks on the western edge of the plains young westwards), and drilling of geophysical anomalies stratigraphically below the conglomerate confirmed this by intersecting Stag Creek Volcanics (Needham *et al.*, 1978). The Barramundie Creek Plains are thus developed over Masson Formation, which lies in the core of a dome, as shown in figure 4.

Unit	Lithology
OENPELLI DOLERITE	differentiated continental tholeiitic basalt: olivine dolerite, commonly porphyritic, quartz dolerite, granophyre
EDITH RIVER VOLCANICS	rhyolite, dacite, tuff, ignimbrite, minor syenite, basalt, volcanic breccia; sandstone and conglomerate lenses
GRANITE EMPLACEMENT	mainly biotite granite, adamellite, syenite and granodiorite; many plutons, commonly each with several phases; Cullen Granite composed of several coalesced plutons
NIMBUWAH COMPLEX	
Granitoid Core	Homogeneous to foliated leucocratic granite, porphyroblastic hornblende biotite granodiorite, grey biotite granite, coarse porphyritic granite; charnockite in south
Migmatite Zone	Granitic to tonalitic migmatite, garnetiferous in places
Lit-par-lit Gneiss Zone	Muscovite biotite feldspar quartz schist and gneiss commonly with amphibole and garnet, and quartz-rich pods and bands
Transitional Zone	quartz schist, pelitic schist, minor quartz-rich differentiated bands
ZAMU DOLERITE	layered continental tholeiitic dolerite; mainly quartz dolerite, olivine dolerite, granophyre and commonly metamorphosed to amphibolite
TI TREE GRANOPHYRE	altered granophyre, minor adamellite

Table 3. Stratigraphy of late Lower Proterozoic to early Carpentarian (early Middle Proterozoic) igneous rocks

1978; Ferguson & Needham, 1978;

Ferguson (this volume) advances an alternative theory which explains the differences in metamorphic grade in the two domains as reflecting two ages of metamorphism. He suggests that the higher-grade rocks reflect a metamorphic event at about 1900Ma, and that these rocks were the source area for later sedimentation. These later sediments, and presumably the older ones too, were subjected to a milder (greenschist grade) metamorphic event at 1800Ma. No stratigraphic or geochronological evidence has been found which supports this theory, and the proven metamorphic gradation mentioned previously, and the continuation of the Mundogie Sandstone from areas of greenschist grade to amphibolite grade, suggest that the concept of stratigraphic equivalence advanced in this paper is preferable to Ferguson's theory, which demands a 'dramatic contrast of metamorphic grade between the two domains'. Ferguson speculates that about 20km of cover rocks are required to produce the higher grades of metamorphism. He questions the feasibility of removing such a thickness of cover rocks by erosion from the higher-grade domain, and having correlative units in each domain still preserved. The higher-grade rocks have, however, been subjected to at least two phases of isoclinal deformation (see later heading), and given that development of a pervasive foliation must indicate substantial shortening of supracrustals, then the complex structure of the higher-grade rocks must indicate a considerable thickening of the observed 14km stratigraphic sequence. Subsequent erosion of 20km of cover therefore need remove only a small portion of the pre-folding 14km sequence, and thus maintain the opportunity to correlate between the two domains.

Ferruginous banded quartz-rich rocks in the Cannon Hill area, 16km north of Jabiluka

Relationships	Age Ma (Page *et al.*, this volume)
<250 thick, and minor dykes	
several lopoliths in Alligator Rivers region, hornfelses Nimbuwah Complex; forms basement ridges to Kombolgie Formation	1688
valley-fill volcanics and pyroclastics, probably comagmatic with granites; markedly unconformable on older rocks, including Carpentarian (Middle Proterozoic) granites.	minimum 1725 (Leggo, 1968 recalculated)
conformable to highly transgressive intrustions commonly hornfelsing country rocks	~1800
contacts with other units not seen; probably emplaced about the time of the end of Lower Proterozoic sedimentation and partly migmatitised by the 1800 m.y. event	1870 1870
transitional into Transitional Zone, contains resisters of some Cahill Formation and Kakadu Group lithologies	1800
transitional into Lit-par-lit Gneiss Zone and Nourlangie Schist	1800
sills and minor dykes folded and metamorphosed with enclosing Lower Proterozoic metasediments	
confined to southwest; sills in Burrell Creek Formation; discordant in Burrell Creek Formation and Chilling Sandstone; equivalent to Zamu Dolerite	

(Transitional igneous Activity) (Main sources: Needham & Stuart-Smith, this volume; Stuart-Smith & Ferguson, Walpole *et al.*, 1968; Sweet *et al.*, 1974).

in the Alligator Rivers region, are similar in appearance to the iron-rich rocks of the Koolpin Formation and are interbedded with garnet actinolite mica schist, carbonaceous schist, and magnetitic and chloritised actinolite biotite schist (Swingler, 1977). Gravity data (Tucker *et al.*, this volume) indicates a thickening of the rock pile in this area, such that the rocks exposed may be the highest seen in the Lower Proterozoic sequence east of the South Alligator River. The correlation of these rocks with the Koolpin Formation is therefore possible, although the poor exposure does not allow determination of all the lithologies in the sequence, or their relationships with other units.

Correlation between the Litchfield Complex and the Geosyncline

The Litchfield Complex has been generally regarded as a basement block west of the Pine Creek Geosyncline. However, as discussed above (under 'Basement Complexes'), schist appears to correlate with the Burrell Creek Formation, and some granites may be Carpentarian (Middle Proterozoic). D. Tucker (pers. comm.) has noted the similarity in magnetic response between schist of the Litchfield Complex and rocks of the Masson Formation.

Only about half the area of the Pine Creek Geosyncline has been systematically re-examined in the current phase of study, which began in 1971. Further work will probably change our view of the stratigraphy in outlying parts of the Geosyncline, particularly in the southeast and southwest, and drilling in the north may define Lower Proterozoic stratigraphy under Mesozoic and Cainozoic cover.

TRANSITIONAL IGNEOUS ACTIVITY

At or near the end of sedimentation, a suite of continental tholeiites with a composite thickness of about 2.5km intruded the sediments, mainly as sills. The sills were folded and metamorphosed with the host rocks by the 1800Ma regional event (Ferguson & Needham, 1978). In the medium to high grade metamorphic domain and in the contact aureoles of Carpentarian (Middle Proterozoic) granite the rocks are amphibolite, but elsewhere the original textures and mineralogy are partly to wholly preserved; in places hornfelsic zones in the adjacent sediments are apparent. This suite of rocks, known as the Zamu Dolerite, ranges vertically in composition from sills of olivine dolerite nearer the base of the Lower Proterozoic sequence, — mainly in the Masson Formation — to quartz dolerite with felsic differentiates, to dacite, — mainly in the South Alligator Group (Stuart-Smith *et al.*, in prep.).

The close of Lower Proterozoic sedimentation is probably indicated by intrusion of granodiorite and tonalite of the Nimbuwah Complex, in the extreme northeast of the Geosyncline, at about 1870Ma (Page *et al.*, this volume). This event may also have triggered off a long period of deformation and metamorphism which culminated at about 1800Ma, the age which is ubiquitously recorded by K-Ar isotopic systems in the metamorphics and many of the basement rocks of the region. The tonalites and granodiorites of the Nimbuwah Complex appear to have undergone migmatisation at 1800Ma to produce the Migmatite Zone and Granitoid Core of the centre of the Complex. The outer gneissic Lit-par-Lit Gneiss Zone and Transitional Zone contain resisters of Lower Proterozoic quartzite, carbonaceous schist, calc-silicate gneiss and marble, and are the product of partly differentiated Lower Proterozoic metasediments. The igneous parentage of the granitoid rocks is supported by their *I*-type affinities (Ferguson *et al.*, this volume); lack of regrowth textures or rounding of zircons, and low Rb/Sr initial ratios, also support a magmatic origin (Page *et al.*, this volume).

The metamorphics were intruded by numerous early Carpentarian (early Middle Proterozoic) granite plutons, which have a minimum age of about 1740Ma (Page *et al.*, this volume). Several plutons coalesced to form the Cullen Granite batholith in the centre of the Geosyncline. This is the largest granitic body (3600km^2), and extends under cover rocks of the Daly River Basin (Tucker *et al.*, this volume). Diapiric intrusion of 'solid state' granite below the Rum Jungle and Waterhouse Complexes has been described as a mechanism for rejuvenation of these Complexes by uplift (Stephansson & Johnson, 1976).

Felsic and minor mafic volcanics and volcaniclastics of the early Carpentarian (early Middle Proterozoic) Edith River Volcanics (~ 1760Ma; Leggo *in* Walpole *et al.*, 1968) are probably comagmatic with the diapiric granites. However, a significant period of erosion between the 1800Ma metamorphic and deformational event, and extrusion of the Edith River Volcanics is indicated by the valley-fill nature of the volcanics.

The final igneous event prior to Carpentarian (Middle Proterozoic) platform sedimentation was intrusion at 1688Ma (Page *et al.*, this volume), of a series of continental tholeiitic lopoliths — the Oenpelli Dolerite — at about 1-2km depth (Stuart-Smith & Ferguson, 1978). These intrusions consist of porphyritic olivine dolerite, quartz dolerite and granophyre sheets, in places over 250m thick, and minor dykes <1m across. The lopoliths form long, arcuate basement ridges to Carpentarian (Middle Proterozoic) platform sedimentation, indicating another substantial period of erosion. Previously the Edith River Volcanics were placed in the Katherine River Group of Carpentarian (Middle Proterozoic) platform sedimentation. However this erosional cycle, and the comagmatic nature of the volcanics and the diapiric granites places the Edith River Volcanics in the period of transitional activity.

The pattern of sedimentation followed by orogenesis and a period of post-orogenic

igneous activity seen in the Pine Creek Geosyncline is consistent with the model of evolution of Proterozoic mobile belts described by Glikson (1976), and which has been applied by Stuart-Smith *et al.*, (this volume)

COVER ROCKS

Plateau-forming sandstone and minor interbedded, mainly intermediate, volcanics of the Kombolgie Formation rest with marked unconformity on older rocks, covering the eastern extent of the Lower Proterozoic metasediments and their gneissic equivalents, which are exposed in a few inliers within the sandstone plateau. Minor dolerite intrusions of Adelaidean (Upper Proterozoic) age cut the sandstone in places; some additional similar intrusions may be represented by long linear magnetic patterns coincident with major fractures in the sandstone. These intrusions, and Adelaidean (Upper Proterozoic) phonolite dykes which intrude the Nanambu and Nimbuwah Complexes, represent the final known igneous events in the region (Page *et al.*, this volume).

Adelaidean (Upper Proterozoic) sediments are exposed at the margins of extensive Cretaceous tablelands in the southwest of the Pine Creek Geosyncline. The age of the sandstone-dominant Tolmer Group which crops out in the same area is obscure, as no relationships are exposed between it and proven Adelaidean (Upper Proterozoic) rocks; it appears basal to the Adelaidean (Upper Proterozoic) sequence, but alternatively may be Carpentarian (Middle Proterozoic), and thus a possible correlative of the Katherine River Group. The northern and southern margins of the Geosyncline are concealed by Mesozoic and Palaeozoic strata.

A palaeo-weathering profile is common below the Kombolgie Formation, and a rare regolith is developed in some places. A regolith is common below the Cretaceous, and lateritisation took place during the Tertiary. Hays (1965) identified three Cainozoic land surfaces, which are commonly superimposed and extensive deep weathering profiles (up to 60m) are developed.

Relationship of cover rocks to uranium mineralisation

The proximity of Kombolgie Formation sandstone to the uranium deposits of the Alligator Rivers Uranium Field and South Alligator Valley Uranium Field, and of the Depot Creek Sandstone Member to the uranium deposits of the Rum Jungle Uranium Field, has focused attention on the sandstone as a possible source of uranium or as a vital part of uranium ore genesis. The Kombolgie Formation is not however rich in uranium (Ferguson & Winer, this volume) and airborne radiometric anomalies in the Formation are restricted to laterites developed downslope from interbedded intermediate to mafic volcanic members (Needham *et al.*, 1973). Heavier elements may be concentrated in purple beds which are common in some areas near the base of the unit. The lithologies are mainly coarse, clean moderately well-sorted subangular to sub-rounded buff to white quartz sandstone, with pebbly horizons and conglomerate beds more common near the base. Clasts are mainly moderately to well-rounded quartzite and vein quartz; clasts of Lower Proterozoic rocks are rare. There are very rare siltstone beds up to 5cm thick. The sandstone is commonly devoid of a matrix except nearer the base where a white clay matrix is often present. The rock ranges from loose and friable, to well indurated, to silicified on stable exposed surfaces and along joints.

The unconformity plane has a morphology similar to that of the undulating sand plains which cover much of the Geosyncline today. The unconformity undulates gently with an amplitude of about 20m although there are scattered basement hills and ridges up to 250m. The Oenpelli Dolerite forms large arcuate basement ridges up to 100m high and the Jim Jim Granite forms a plateau about 100m above the general level of the unconformity. The unconformity plane is displaced by numerous faults which mainly throw the sandstone only

	Unit	Lithology	Thickness	Relationships	Age Ma (Page *et al.*, this volume)
MESOZOIC	BATHURST ISLAND FORMATION	Fine to medium sandstone, siltstone, mainly marine	<1350	unconformable on older units. Thins southwards to continental deposits <100m	
PALAEOZOIC	PORT KEATS GROUP	Siltstone, silty sandstone, minor limestone, basal conglomerate, diamictite	~2000	unconformable on Precambrian	
	DALY RIVER GROUP				
	Oolloo Limestone (Dlo)	Flaggy pink-grey limestone, commonly silicified	60	conformable on Jinduckin Formation	
	Jinduckin Formation (€Dj)	Ferruginous sandstone and siltstone, minor marl, dolomite and chert, halite pseudomorphs common	60	conformable on Tindall Limestone	
	Manbulloo Limestone Member (€Dm)	Limestone, commonly partly silicified	<60	lenses in Jinduckin Formation	
	Tindall Limestone (€mt)	Crystalline limestone with minor calcilutite, chert nodules	160	unconformable on Antrim Plateau Volcanics, Tolmer Group and Cullen Granite	
	ANTRIM PLATEAU VOLCANICS (€va)	Massive and vesicular basalt, minor agglomerate	150	unconformable on Precambrian units	
	JARONG CONGLOMERATE (€j)	Boulder and pebble conglomerate	3-75	unconformable on Precambrian units	
	WITCH WAI CONGLOMERATE (€w)	Ferruginous sandy boulder and pebble conglomerate	10	unconformable on Precambrian units	
	WESSELL GROUP				
	Buckingham Bay Sandstone (€wd)	Coarse white sandstone, clayey sandstone, massive to blocky	~200	unconformable on Nimbuwah Complex and Kombolgie Formation	
	WURUGOIJ DOLERITE (Pdw) AND MINOR DOLERITE DYKES	Quartz dolerite and alkaline dyke rocks		Wurugoij Dolerite forms small stock hornfelsing Kombolgie Formation sandstone in northeast, minor dykes are undeformed and are indicated by magnetic linears over 100km long in places	1700 ± 170
ADELAIDEAN (Upper Proterozoic)	ALVERGNE GROUP (SHALLOW WATER, 600m):				
	Spencer Sandstone (Pec)	Quartz sandstone, minor silty and dolomitic sandstone	<60	conformable sequence	
	Lloyd Creek Formation (Pel)	Algal and oolitic dolomite, minor sands and silty dolomite and greyish-green siltstone	<35	conformable sequence	
	Pinkerton Sandstone (Pep)	White massive quartz sandstone, minor siltstone and shale	<50	conformable sequence	
	Saddle Creek Formation (Pes)	Basal blocky cross-bedded sandstone, upper flaggy quartz sandstone and siltstone	20-90	conformable sequence	
	Argalarri Siltstone (Pea)	Greyish-green siltstone and shale, interbedded minor silty sandstone	>300	conformable sequence	
	FITZMAURICE GROUP (SUBSIDING TROUGH 3000-12000m thickening westwards):				
	Legune Formation (Pfe)	Interbedded sandstone, siltstone and shale	2100	conformable on Lalngang Sandstone	
	Lalngang Sandstone (Pfl)	Sandstone with minor siltstone, grit and conglomerate	1800	unconformable in places on Goobalerri and Moyle River Formations	
	Goobalerri Formation (Pfg)	Grey shale, grey and greenish-grey siltstone and fine sandstone, interbeds of fine white sandstone	600	conformable on Moyle River Formation	
	Moyle River Formation (Pfm)	Fine to medium sandstone, lenses of siltstone and basal conglomerate	<10000	unconformable on Carpentarian and Lower Proterozoic rocks	
	BULLITA GROUP (PARALIC – SHALLOW MARINE):				
	Bynoe Formation (Plb)	Purple and green siltstone, dolomitic siltstone, minor dolomite	<200	base of this group not observed	

	MUDGINBERRI AND MUNMARLARY PHONOLITES (Egs, Epl)				
	Phonolite dykes		<1	undeformed dykes cutting Nanambu and Nimbuwah Complexes	1316
ADELAIDEAN? (Upper Proterozoic?)	TOLMER GROUP (SHALLOW MARINE 1000m)				
	Waterbag Creek Formation (Ptw)	Ferruginous sandstone and siltstone, minor dolomite and marl, baritic pseudomorphs	<300	conformable on Hinde Dolomite; unconformable under Cambrian Antrim Plateau Volcanics	
	Hinde Dolomite (Pth)	Dolomite and minor limestone, dolomite siltstone	120	conformable between Hinde Dolomite and Waterbag Creek Formation	
	Bukalara Sandstone Stray Creek Sandstone Member (Pts)	Flaggy quartz sandstone, green siltstone and shale	180	conformable between Depot Creek Sandstone Member and Hinde Dolomite	
	Depot Creek Sandstone Member (Ptd)	Massive cross-bedded quartz sandstone, pebble bands	300-600	unconformable on early Carpentarian (early Middle Proterozoic) granite; conformable under Stray Creek Sandstone Member	
CARPENTARIAN (Middle Proterozoic)	KATHERINE RIVER GROUP (Fluviatile, and mainly flood volcanics <1600m)				
	Kombolgie Formation (Phk_u, Phk_l)	Medium to coarse quartz sandstone, cross-bedded and rippled marked; minor siltstone, pebbly beds and conglomerate	<1410	overlies all pre-Carpentarian (pre-Middle Proterozoic) rocks with marked conformity	
	Gilruth Volcanic Member (Phg)	Vesicular basalt, tuffaceous siltstone, minor banded quartz-jasperite	5	interbedded with Kombolgie Formation sandstone in Arnhem Land Plateau	correlative upper volcanic units
	Callanan Volcanic Member (Phc)	Andesite, vesicular in places	20	interbedded with Kombolgie Formation sandstone in Callanan Basin	
	Hunwood Creek Volcanic Member (Phh)	Basalt, andesite, minor tuff	170	interbedded with Kombolgie Formation sandstone in Edith River Basin	
	Nungbalgarri Volcanic Member (Phn)	Andesite to rhyodacite flows and minor dykes, vesicular and in places jasper-rich at top, minor intercalated sandstone	170	interbedded with Kombolgie Formation sandstone in Arnhem Land Plateau	1648
	Birdie Creek Volcanic Member (Phb)	Andesite, vesicular	250	interbedded with Kombolgie Formation sandstone in southern part of Arnhem Land Plateau	correlative lower volcanic units
	Plum Tree Creek Volcanic Member (Php)	Ignimbrite, vesicular andesite	370	interbedded with Kombolgie Formation sandstone in Callanan Basin	
	McAdams Creek Volcanic Member (Phm)	Vesicular basalt and andesite, minor tuff and rhyolite	300	interbedded with Kombolgie Formation sandstone in Edith River Basin	
	Kurrumie Member (Phr)	Purple quartz greywacke	220	basal member in Callanan Basin	

TABLE 4. Stratigraphy of Carpentarian (Middle Proterozoic) to Mesozoic cover units (Main sources: Sweet *et al.*, 1974; Walpole *et al.*, 1968; Needham & Stuart-Smith, 1978).

IAEA

a few tens of metres. However, a throw of at least 200m has been substantiated for the Koongarra reverse fault (Foy & Pedersen, 1975). Extensive faulting of blocks of Kombolgie Formation sandstone is recorded in or near the Ranger 1 and Jabiluka One ore bodies (Eupene *et al.*, 1975; Hegge, 1977). There does not appear to be any broad relationship between the elevation of the unconformity and the distribution of mineralisation. The contact at the base of the Depot Creek Sandstone Member is regionally anomalously radioactive, but the uncomformity of the base of the Kombolgie Formation has no radiometric expression. However, metamorphics and granites below the Kombolgie Formation are commonly altered, in places to more than 50m below the unconformity. Granite and gneiss at the top of this palaeo-weathering-profile are commonly altered to a blotchy pale-green and purple quartz-clay rock. In places this profile may be more radioactive than its unweathered parent, but no analyses are available of the amount and distribution of uranium within this profile.

STRUCTURE

Near-vertical foliations trend west to northwest in the Rum Jungle Complex, northwest in the Waterhouse Complex, and mainly north in the Archaean component of the Nanambu Complex. In the low-grade metamorphic terrane the Lower Proterozoic rocks form tight

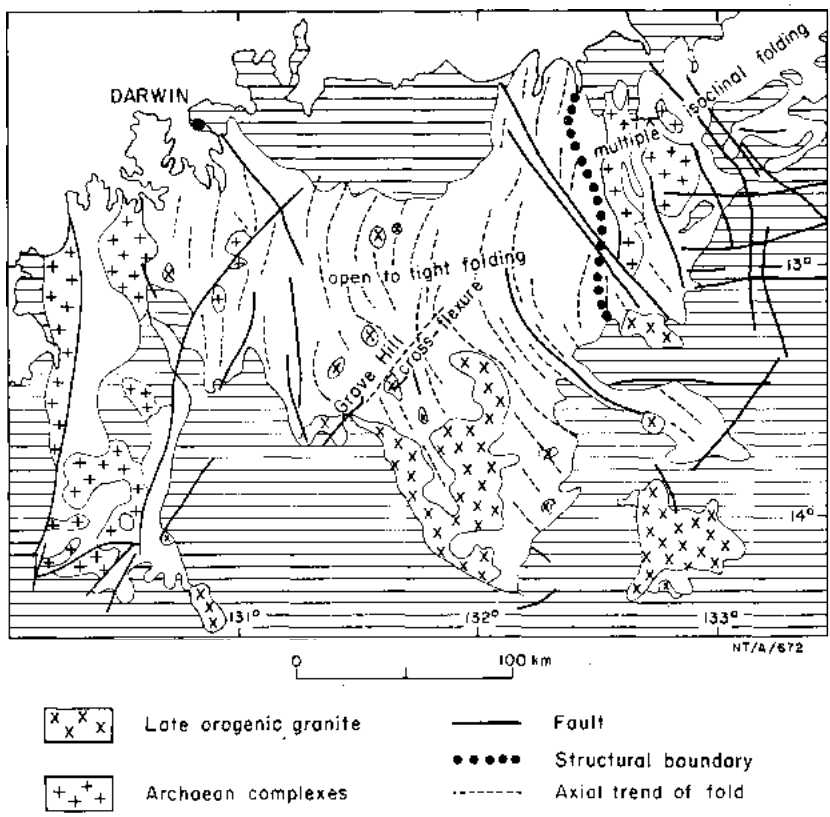


Figure 5. Generalised structural map of the Pine Creek Geosyncline.

folds with steep limbs, which trend about north in the northern part of the area, and northwest in the southern part. This change in the direction in the fold axes occurs about the northeast-trending 'Grove Hill Cross-Flexure' (Fig. 5). Folding increases in intensity eastwards through tight overturned folds in the Mundogie area to isoclinal folds with steep limbs near the boundary of the low and medium-grade metamorphic domains, into polyphase folding involving at least two isoclinal events in the medium-grade domain (Needham & Stuart-Smith, 1976). Fold axes are commonly concentrically disposed around the granitoid complexes, and around some of the concordant diapiric granites.

The unconformity at the base of the Koolpin Formation separates lower, more intensely deformed (tight to isoclinal folds) strata mainly of the Namoona and Mount Partridge Groups from the more broadly and openly-folded rocks of the South Alligator and Finniss River Groups. The main pre- and post-Koolpin Formation deformation fold axes both trend northwest; the difference in fold styles is generally only evident when the regional strike is about northeast — for example northwest of the Cullen Granite between Mount Masson and Mount Douglas. At the northern end of the South Alligator Valley, 30km north of El Sherana, the Koolpin Formation has overstepped the Wildman Siltstone to rest directly on the Mundogie Sandstone (southern edge of figure 4).

Major fault directions are northwest and northeast (mainly strike-slip), and also curvilinear east to northeast (mainly dip-slip). The greatest proven displacement is 5.5km lateral movement on the Giants Reef Fault at Rum Jungle.

Deformation of the Carpentarian (Middle Proterozoic) and younger strata is confined to warping, jointing and faulting. Jointing and faulting are particularly well developed in the Kombolgie Formation in the east, and in the Tolmer Group in the west. Many of the faults which displace the cover rocks are reactivated faults which previously displaced Lower Proterozoic formations. A major set of north-northeasterly faults in the west, including the Giants Reef Fault, is a northern continuation of the Halls Creek Mobile Zone. The major set of northwesterly faults in the east are along or parallel to the Bulman Fault Zone, another major fracture trend of northern Australia.

METAMORPHISM

Two regional metamorphic domains are known in the Pine Creek Geosyncline province (Ferguson & Needham, 1978; Ferguson, this volume); the Litchfield Complex on the western side of the Geosyncline (Berkman, this volume) may represent a third (Fig. 6). The Nanambu-Nimbuwah domain in the east contains metamorphics mainly of the staurolite-almandine subfacies, and in the extreme northeast the sillimanite-almandine-orthoclase subfacies, of the amphibolite facies (Smart *et al.*, 1975). Berkman (this volume) reports garnet-magnetite-muscovite-biotite schist, an assemblage suggesting amphibolite facies in the Litchfield domain. The central domain is mainly greenschist facies, but has extensive zones of upper greenschist facies up to 10km wide surrounding some of the diapiric granites, which are superimposed by andalusite and cordierite hornfels within 1km of the granite contact. Ferguson (this volume) describes the Nanambu-Nimbuwah domain as 'medium to high-grade' and the central domain as 'low-grade'. Ferguson's mineral assemblages containing biotite from the central domain are more typical of the upper greenschist facies zones around the granite diapirs, which possibly reflect regional metamorphism above 'hot spots', which developed in the granitic basement prior to granite intrusion and attendant contact metamorphism.

URANIUM MINERALISATION WITHIN A REGIONAL GEOLOGICAL FRAMEWORK

The distribution and classification of metallic mineral deposits in the Pine Creek Geosyncline is described by Needham & Roarty (this volume). Uranium deposits are

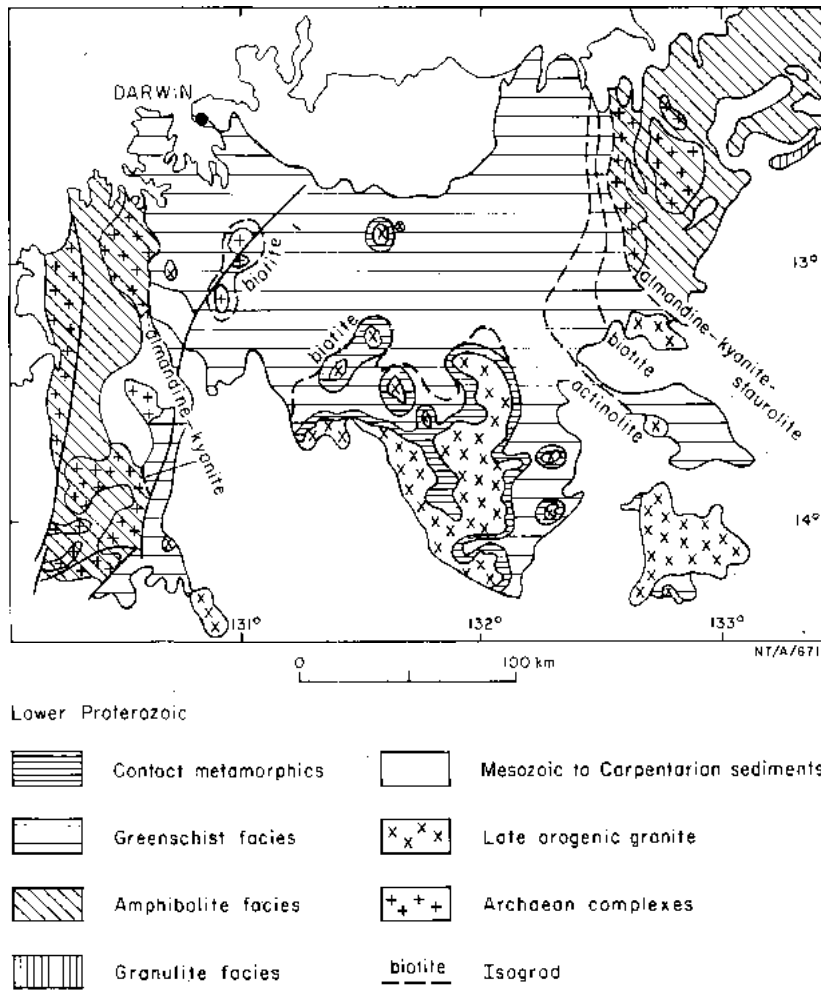


Figure 6. Metamorphic map of the Pine Creek Geosyncline.

undisputably stratabound in the main, and the deposits of the two main uranium fields (Alligator Rivers and Rum Jungle) all probably lie at the same stratigraphic position. The broad lithological associations are the same — mainly in carbonaceous pelites adjacent to massive carbonate rocks — and the deposits are generally within 10km of exposed granitic Archaean basement. The basement is enriched in uranium (Ferguson & Winer, this volume) in a form amenable to removal by leaching (McAndrew & Finlay, this volume). Similar lithologies at the same stratigraphic level are not mineralised in uranium, so the proximity of source rock and a particular environment of deposition seem necessary for accumulation of uranium to take place. Future search would therefore appear most successful near areas of proven or postulated granitic Archaean basement, in sequences containing carbonaceous pelites and/or massive carbonate.

The deposits of the South Alligator Valley Uranium Field are not close to exposed basement, but are commonly situated at the contact of Lower Proterozoic carbonaceous shale and the Edith River Volcanics. The Edith River Volcanics are rich in uranium and are probable source rocks. Although high-grade, the deposits of this area are small and are no longer attractive exploration targets.

Two things the uranium deposits of the Pine Creek Geosyncline have in common are chloritisation of the host rock, and proximity vertically — and in most cases laterally — to plateau sandstone cover rocks. The chloritisation may be associated with periods of epigenetic activity which are commonly thought to have concentrated the ore. The absence of the massive chloritisation of host strata seen in the Alligator Rivers deposits away from the uranium deposits (i.e. more than 200m away) suggests that the chloritisation was formed from a source close to the present ore bodies. Evaporite precursors to the massive carbonate adjacent to the ore bodies, from which much of the ore-zone breccias developed, are a probable source for the magnesium necessary in such a metasomatic process. The role of the plateau sandstone cover rock is enigmatic. There is no evidence to support it as a likely source rock, and more probable source rocks are known in each of the uranium fields. It may have played a role in channelling groundwater to the site of ore deposition, although as mineralisation is found at deeper levels below the sandstone cover rocks, this role seems less tenable. The sandstone has probably acted as a cap rock in protecting the ore bodies. Little Cainozoic cover in areas near the sandstone escarpment facilitates conventional exploration techniques in that area, and has resulted in a very close spatial relationship between ore and the edge of the sandstone. Exploration by drilling into favourable strata close to suitable source rocks in the future may prove this relationship more apparent than real.

ACKNOWLEDGEMENTS

M.J. Roarty and D.A. Wallace have assisted in fiedwork on which this paper is based. K. Wills refereed the paper and made helpful suggestions. This paper is published with the permission of the Director, Bureau of Mineral Resources, Geology and Geophysics, Canberra, Australia.

REFERENCES

Berkman, D.A., this volume: Uranium exploration in the Litchfield Province, N.T., Australia. *Proceedings of the International Uranium Symposium on the Pine Creek Geosyncline.*

Crick, I.H. & Muir, M.D., this volume: Evaporites and uranium mineralisation in the Pine Creek Geosyncline. *Proceedings of the International Uranium Symposium on the Pine Creek Geosyncline.*

Crick, I.H., Stuart-Smith, P.G. & Needham, R.S., 1978: Stratigraphic significance of a discovery of Lower Proterozoic tuff in Pine Creek Geosyncline. *BMR J. Aust. Geol. Geophys., 3,* 163-165.

Eupene, G.S., Fee, P.H. & Colville, R.G., 1975: Ranger Ore uranium deposits. *in* (ed. C.L. Knight) *Economic Geology of Australia and Papua New Guinea Australas. Inst. Min. Metall., Monograph Series No. 5., 1. Metals,* 308-317.

Ferguson, J., this volume. Metamorphism in the Pine Creek Geosyncline and its bearing on stratigraphic correlations. *Proceedings of the International Uranium Symposium on the Pine Creek Geosyncline.*

Ferguson, J., Chappell, B.W. & Goleby A.B., this volume: Granitoids in the Pine Creek Geosyncline. *Proceedings of the International Uranium Symposium on the Pine Creek Geosyncline.*

Ferguson, J. & Needham, R.S., 1978: The Zamu Dolerite: A Lower Proterozoic preorogenic continental tholeiite suite from the Northern Territory, Australia. *J. geol. Soc. Aust., 25,* 309-322.

Ferguson, J. & Winer, P., this volume: Pine Creek Geosyncline: statistical treatment of whole rock geochemical data. *Proceedings of the International Uranium Symposium on the Pine Creek Geosyncline.*

Foy, M.J. & Miezitis, Y., 1977: Uranium mineralisation at Anomaly 2J, South Alligator Valley, Northern Territory, and its significance concerning regional structure and stratigraphy. *Proc. Australas. Inst. Min. Metall., 261,* 1-11.

Foy, M.F. & Pedersen, C.P., 1975: Koongarra uranium deposit. *in* (ed. C.L Knight) *Economic Geology of Australia and Papua New Guinea. Australas. Inst. Min. Metall, Monograph Series, No. 5, 1. Metals,* 317-321.

Glikson, A.Y., 1976: Archaean to Early Proterozoic Shield elements: relevance of plate tectonics. *Geol. Assoc. Can. Spec. Pap. 14.*

Hays, J. 1965: The relations between laterite and land surfaces in the northern part of the Northern Territory of Australia. *22nd Int. geol. Congr., Delhi.*

Hegge, M.R., 1977: Geologic setting and relevant exploration features of the Jabiluka uranium deposits. *Proc. Australas. Inst. Min. Metall., 264,* 19-32.

Johnson, K., 1974: Progress report: geological review and revision of the Rum Jungle area, Northern Territory, 1973. *Rec. Bur. Miner. Resour. Geol. Geophys. Aust., 1974/41* (unpubl.).

McAndrew, J. & Finlay, C.J., this volume: The nature and significance of the occurrence of uranium in the Nanambu Complex of the Pine Creek Geosyncline. *Proceedings of the International Uranium Symposium on the Pine Creek Geosyncline.*

Needham, R.S., Crick, I.H., Stuart-Smith, P.G. & Roarty, M.J., 1978: Mundogie 1:100 000 Sheet area data record. *Rec. Bur. Miner. Resour. Geol. Geophys. Aust. 1978/103* (unpubl.).

Needham, R.S., Ferguson, J. & Prichard, C.E., 1979: Excursion guide for the International Uranium Symposium on the Pine Creek Geosyncline, Australia, Sydney, June 4-8, 1979.

Needham, R.S. & Roarty, M.J., this volume: An overview of metallic mineralisation in the Pine Creek Geosyncline. *Proceedings of the International Uranium Symposium on the Pine Creek Geosyncline.*

Needham, R.S. & Stuart-Smith, P.G., 1976: The Cahill Formation — host to uranium deposits in the Alligator Rivers Uranium Field, Australia. *BMR J. Aust. Geol. Geophys., 1*, 321-333.

Needham, R.S. & Stuart-Smith, P.G., this volume: Geology of the Alligator Rivers Uranium Field. *Proceedings of the International Uranium Symposium on the Pine Creek Geosyncline.*

Needham, R.S., Wilkes, P.G., Smart, P.G. & Watchman, A.L., 1973: Alligator Rivers region fact-finding study, geological and geophysical reports. *Rec. Bur. Miner. Resour. Geol. Geophys. Aust., 1973/208* (unpubl.).

Page, R.W., 1976: Geochronology of Archaean and Lower Proterozoic rocks in the Rum Jungle-Alligator Rivers area, Northern Territory, Australia. *25th Int. geol. Congr., Abstracts Section 1A, Sydney.*

Plumb, K.A., Derrick, G.M., Needham, R.S. & Shaw, R.D., in press: The Proterozoic of Northern Australia. *in* (ed. D.R. Hunter) *Precambrian of the Southern Hemisphere*. Elsevier.

Rhodes, J.M., 1975: The geological relationships of the Rum Jungle Complex, Northern Territory. *Rep. Bur. Miner. Resour. Geol. Geophys. Aust., 89*, 10p.

Richards, J.R. & Rhodes, J.M., 1967: Geochronology of the Rum Jungle Complex. *Aust. J. Sci. (Abstracts) Melb. Congress.*

Richards, J.R., Ruxton, B.P. & Rhodes, J.M., 1977: Isotopic dating of the leucocratic granite, Rum Jungle, Australia. *Proc. Australas. Inst. Min. Metall., 264*, 33-34.

Smart, P.G., Wilkes, P.G., Needham, R.S. & Watchman, A.L., 1976: Geology and Geophysics of the Alligator Rivers Region. *in* (ed. C.L. Knight) *Economic Geology of Australia and Papua New Guinea. Australas. Inst. Min. Metall., Monograph Series No. 5, 1. Metals*, 285-301.

Stephansson, O. & Johnson, K., 1976: Granite diapirism in the Rum Jungle area, Northern Australia. *Precambrian Research, 3*, 159-185.

Stuart-Smith, P.G., 1977: Shallow stratigraphic drilling in the Kapalga 1:100 000 Sheet area, Alligator Rivers region, N.T., 1974-76. *Rec. Bur. Miner. Resour. Geol. Geophys. Aust., 1975/53* (unpubl.).

Stuart-Smith, P.G. & Ferguson, J., 1978: The Oenpelli Dolerite – a Precambrian continental tholeiitic suite from the Northern Territory, Australia. *BMR. J. Aust. Geol. Geophys., 3*, 125-133.

Stuart-Smith, P.G., Roarty, M.J., Needham, R.S. & Crick, I.H. (in prep): Geology of the Mundogie 1:100 000 Sheet area, Northern Territory. *Rec. Bur. Miner. Resour. Geol. Geophys. Aust.* (unpubl.).

Stuart-Smith, P.G., Wills, K., Crick, I.H. & Needham, R.S., this volume: Evolution of the Pine Creek Geosyncline. *Proceedings of the International Uranium Symposium on the Pine Creek Geosyncline.*

Swingler, N., 1977: Exploration in an area adjoining the area under application for a special mineral lease covering the Jabiluka uranium deposits, Northern Territory, Australia. *Aust. Atomic Energy Comm. Expl. Rep., UB9*, 173p (unpubl.).

Tucker, D.H., Stuart, D.C., Hone, I.G. & Sampath, N., this volume: The characteristics and interpretation of regional gravity, magnetic and radiometric surveys in the Pine Creek Geosyncline. *Proceedings of the International Uranium Symposium of the Pine Creek Geosyncline.*

Walpole, B.P., Crohn, P.W., Dunn, P.R. & Randal, M.A., 1968: Geology of the Katherine-Darwin region, Northern Territory. *Bull. Bur. Miner. Resour. Geol. Geophys. Aust., 82*, 304p.

Wright, J.H., 1976: Exploration license no. 120 Northern Territory. Report on 1976 investigations. *Noranda Australia Ltd report No. 260* (unpubl.).

EVOLUTION OF THE PINE CREEK GEOSYNCLINE

P.G. Stuart-Smith[1], K. Wills[2], I.H. Crick[1] and R.S. Needham[1]

1. Bureau of Mineral Resources, P.O. Box 378, Canberra City, A.C.T. 2601, Australia.
2. C.R.A. Exploration Pty Ltd., P.O. Box 3959, Winnellie, N.T., 5789, Australia.

ABSTRACT

Previous accounts of the Early Proterozoic evolution of the Pine Creek Geosyncline have been dominated by geosynclinal concepts in which sedimentation began in a primary basin that later divided into two basins separated by a median ridge. Rock units were thought to interfinger and represent diachronous facies changes from marginal through transitional to trough environments. Recent work has established chronostratigraphic rock units within the Early Proterozoic sequences. The sediments were deposited under alternating, rather than laterally disposed, continental and shallow marine environments. An interpretation of the evolution of the geosyncline is described in four main stages.

Stage 1. The geosyncline began to develop in the Early Proterozoic probably during incipient rifting and subsidence of Archaean basement. Continental and shallow marine sediments were deposited at the margins of the geosyncline while in its centre a thicker sequence of fine clastic and chemical sediments, and volcanics accumulated.

Stage 2. Uplift of Archaean basement resulted in partial erosion of Stage 1 sediments and an influx of clastic material into the geosyncline. Sandstone and conglomerate formed extensive alluvial fans flanking the uplifted areas and graded distally into littoral and subtidal deposits which later transgressed over them.

Stage 3. The third stage started with a tectonic event which caused uplift, folding and subsequent peneplanation of Stage 1 and 2 sediments. A new phase of sedimentation, dominated by chemical and organic sediments and felsic volcanics, accompanied a shallow marine transgression. A major shift in the locus of tectonic activity within the geosyncline from the centre to the west resulted in faulting and volcanism on the western margin and caused an influx of flysch-type sediment into the geosyncline to form an eastwards-thickening wedge. At the close of sedimentation sills of tholeiitic basalt were emplaced into the Early Proterozoic sediments.

Stage 4. Continued subsidence of the geosyncline resulted in deformation, metamorphism and partial anatexis of the Early Proterozoic sediments, and some subsequent igneous activity. The sediments were uplifted, eroded and overlain by flat-lying Middle Proterozoic, younger Proterozoic, Palaeozoic and Mesozoic rocks, indicating continued tectonic stability since early Middle Proterozoic times.

INTRODUCTION

The Pine Creek Geosyncline is an inlier of about 66 000km^2 south and east of Darwin, Northern Territory (BMR, 1979). Here small Archaean domes are surrounded by Early Proterozoic metasediments and minor volcanics; these rocks are intruded by early Middle Proterozoic granite and dolerite. The geosynclinal sequence is overlain in the east by the essentially undeformed Middle Proterozoic sediments of the McArthur Basin, in the south by Palaeozoic sediments of the Daly River Basin, and in the north by Mesozoic sediments of the Bathurst Terrace. The only exposed possible margin of the geosyncline is in the west where the Early Proterozoic sediments abut the supposed Archaean to Early Proterozoic Litchfield Complex. Granites exposed in small inliers within the McArthur Basin give similar ages to those in the Pine Creek Geosyncline (McDougall *et al.*, 1965), indicating that the geosyncline may be the western extremity of a much larger structure.

This paper reconstructs the Early Proterozoic development of the geosyncline. Details of the stratigraphy on which this reconstruction is based are given by Needham *et al.* (this volume).

PREVIOUS CONCEPTS OF EVOLUTION

The geosynclinal character of the Early Proterozoic rocks in the Katherine-Darwin Region was recognised by Noakes (1949). Following systematic 1:250 000 mapping of the Pine Creek Geosyncline, Walpole (1960) and Walpole *et al.* (1968) equated a number of facies assemblages recognised within the Early Proterozoic rocks with various geosynclinal environments as defined by Stille (1941) and Kay (1951). The facies were thought to be partly diachronous lateral equivalents, and two major episodes in the development of the geosyncline

were proposed. The Pine Creek Geosyncline was thought to have been a shallow elongate basin ('Primary Basin') initially, with a long axis trending southeast, in which sediments of the Goodparla Group (the Golden Dyke Formation, Masson Formation and Mount Partridge Formation) were deposited. The formations were thought to interfinger and represent facies changes (Fig. 1) from a trough environment in the west (Golden Dyke Formation) through a transitional environment (Masson Formation) to a marginal environment in the east (Mount Partridge Formation).

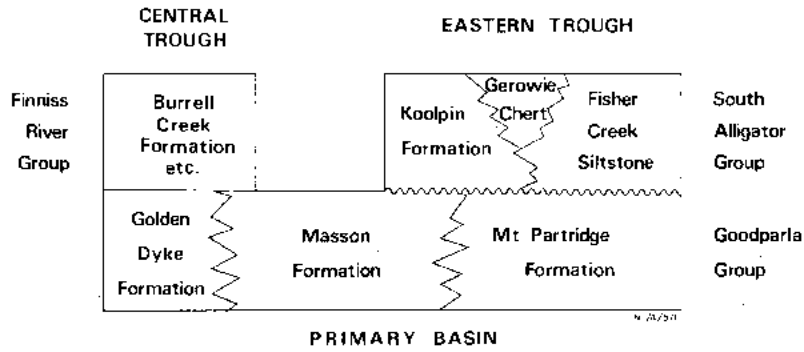


Figure 1. Diagrammatic relationships of the Finniss River, South Alligator and Goodparla Groups. After Crick *et al.* (1978). Modified from Walpole *et al.* (1968).

During or soon after the last stages of deposition of the Goodparla Group, the Primary Basin was considered to have become divided into two basins by the upfaulting of Archaean basement (Stag Creek Volcanics), which formed a barrier trending parallel to the South Alligator Valley. The South Alligator Group sediments (the Koolpin Formation, Gerowie Chert, and Fisher Creek Siltstone) were deposited in a shallow-water environment to the east of this barrier in the 'Eastern Trough'; to the west, the Finniss River Group (the Burrell Creek Formation and others) was deposited in the 'Central Trough'. The Gerowie Chert was considered to be a dolomitic facies variant of the Koolpin Formation and the Fisher Creek Siltstone, lying laterally between and interfingering with them.

Following the major uranium discoveries in the Alligator Rivers region during the last decade, semi-detailed mapping by BMR and exploration companies has revealed that the rock units are chronostratigraphic rather than lateral facies equivalents.

The Stag Creek Volcanics, previously interpreted by Walpole *et al.* (1968) as forming an upfaulted Archaean ridge between the Central and Eastern Troughs, is now known to be interbedded with Early Proterozoic Masson Formation metasediments (Foy & Miezitis, 1977; Stuart-Smith *et al.* in prep), and there is no longer any evidence for basement ridges separating depositional areas in the geosyncline.

Using a 'one-basin' model, Foy & Miezitis (1977) described lithological similarities between many of the formations, some previously noted by Walpole *et al.* (1968), and suggested a new correlation scheme. They retained a facies relationship between the Koolpin Formation, Gerowie Chert (now re-named Gerowie Tuff) and the Fisher Creek Siltstone, and likened the evolution of igneous rocks of the Pine Creek Geosyncline to the broad pattern of igneous activity related to the orogenic cycle, as discussed by Turner & Verhoogen (1960).

More recently Needham *et al.* (1978) have reported the presence of a tuff unit (mapped previously as part of the Golden Dyke Formation or Gerowie Chert) within the Early

Proterozoic metasediments. Crick *et al.* (1978) have identified this tuff unit in the South Alligator Valley and Burnside areas. This is further evidence for the one-basin concept, and provides the first tangible evidence for some of the correlations suggested by Foy & Miczitis (1977). However, now that the volcanic origin of the Gerowie Chert has been demonstrated,

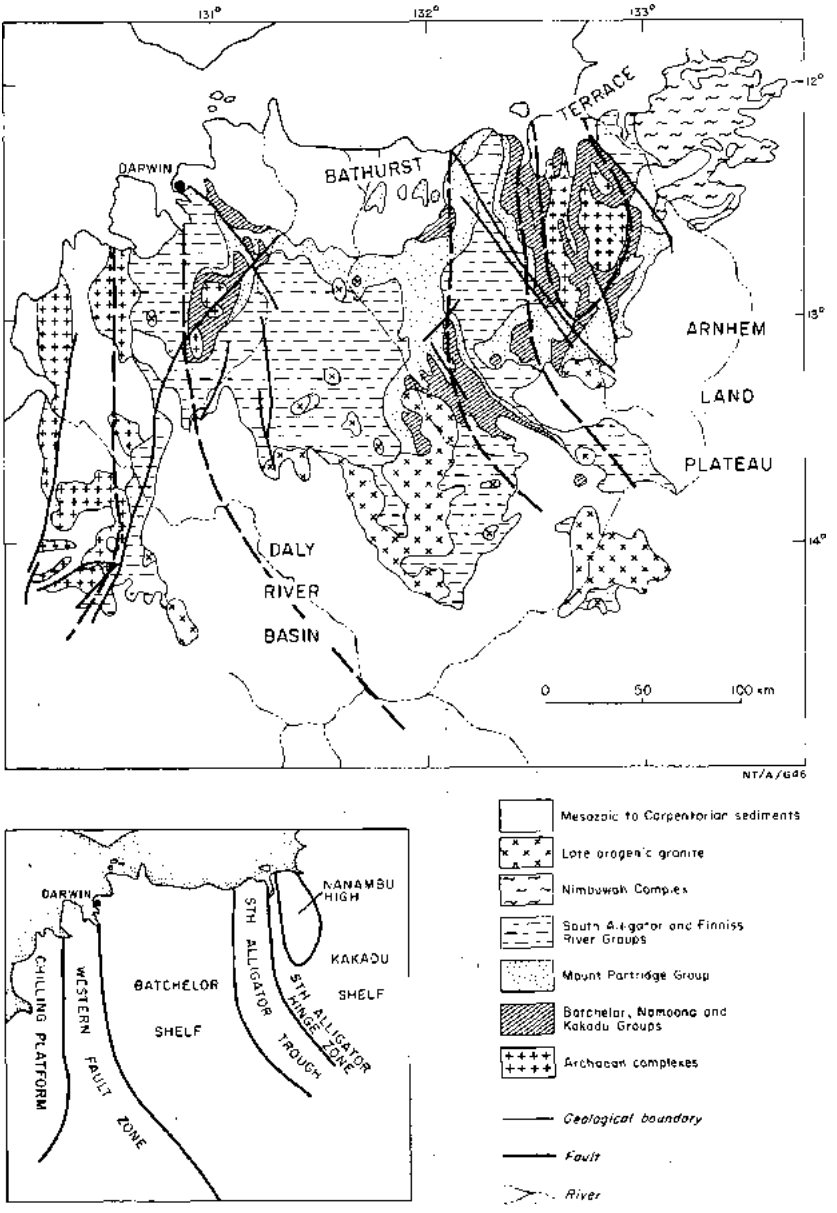


Figure 2. Generalised geology and major structural elements, Pine Creek Geosyncline.

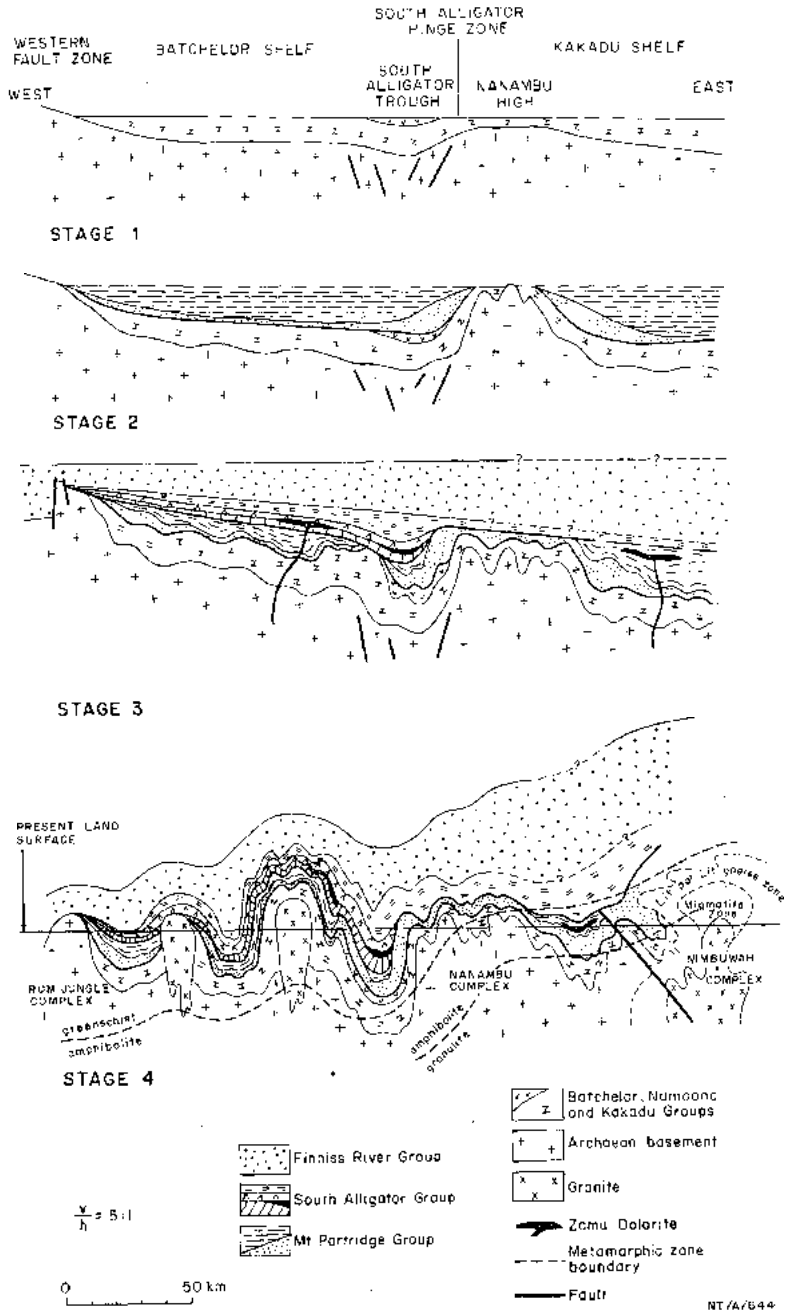


Figure 3. Evolution of the Pine Creek Geosyncline.

the facies relationship between tc Koolpin Formation, Gerowic Chert and Fisher Creek Siltstone can be discarded.

EVOLUTION OF THE GEOSYNCLINE

Seven major structural elements controlled sedimentation, tectonic development, and location of uranium and base metal mineralisation within the geosyncline during the Early Proterozoic.

These are shown in figure 2 and from west to east are: the Chilling Platform, Western Fault Zone, Batchelor Shelf, South Alligator Trough, South Alligator Hinge Zone, Nanambu High and Kakadu Shelf. The South Alligator Trough, which trends north to northwesterly, forms the axis of the geosyncline and separates the adjoining Batchelor and Kakadu Shelves. The Nanambu High formed a relatively unstable block on the Kakadu Shelf, an is separated from the South Alligator Trough by the South Alligator Hinge Zone. The Western Fault Zone separates the Batchelor Shelf from the Chilling Platform, which was a stable block throughout the development of the geosyncline.

The Early Proterozoic sediments were deposited in an intracratonic basin under alternating continental and shallow marine environments between 1870 and 2470 m.y. (Page *et al.*, this volume). The evolution of the basin can conveniently be described in four main stages (Fig. 3), each reflecting fundamental changes in environment and tectonics. They are:

1) deposition of the Batchelor, Kakadu and Namoona Groups;
2) deposition of the Mount Partridge Group;
3) deposition of the South Alligator and Finniss River Groups, and dolerite intrusion; and
4) deformation, metamorphism, granite intrusion, and erosion.

Pre-Stage 1.

Granitoid Archaean rocks are exposed in the Rum Jungle, Waterhouse, Nanambu and possibly Litchfield Complexes, and are considered by some workers to form the basement to the Pine Creek Geosyncline (Tucker *et al.*, this volume).

The Rum Jungle and Waterhouse Complexes in the west, consist of coarse to medium-grained granite and prophyritic granite, lesser aplitic and garnetiferous granite, migmatite, gneiss and schist, and minor quartzite, banded ironstone, metadiorite and felsic volcanics (Rhodes, 1965; BMR, 1976). Several granite types have been dated, and broadly conform to a 2400 m.y. Rb-Sr isochron (Richards *et al.*, 1977).

The Nanambu Complex in the east of the geosyncline contains leucocratic granite and gneiss with minor quartzite and schist, and is intruded by dolerite, mainly altered to amphibolite (Needham & Stuart-Smith, this volume). Medium-grained leucogranite is randomly distributed throughout the complex, and is thought to have crystallised at about 2500 m.y. (Page *et al.*, this volume). Other granites and gneiss in the Nanambu Complex give Rb-Sr ages of 2000 to 1755 m.y., but have high Sr^{87}/Sr^{86} initial ratios indicating that they are probably Archaean rocks which have been partly or wholly re-equilibrated by the 1800 m.y. metamorphism of Stage 4 (Page *et al.*, this volume).

Stage 1.

The Pine Creek Geosyncline developed during the Early Proterozoic, possibly by rifting and subsidence of Archaean basement, when a north to northwest-trending trough (the South Alligator Trough) and two adjoining shelves (the Batchelor and Kakadu Shelves) were formed.

Up to 1500m of quartz sandstone, arkose, conglomerate, siltstone and shale, and interbedded carbonate (algal or evaporitic in places), dolomitic sediments and carbonaceous shale were deposited along the western margin of the Batchelor Shelf (the Batchelor Group), and on the Kakadu Shelf on and around the Nanambu High (the Kakadu Group and part of

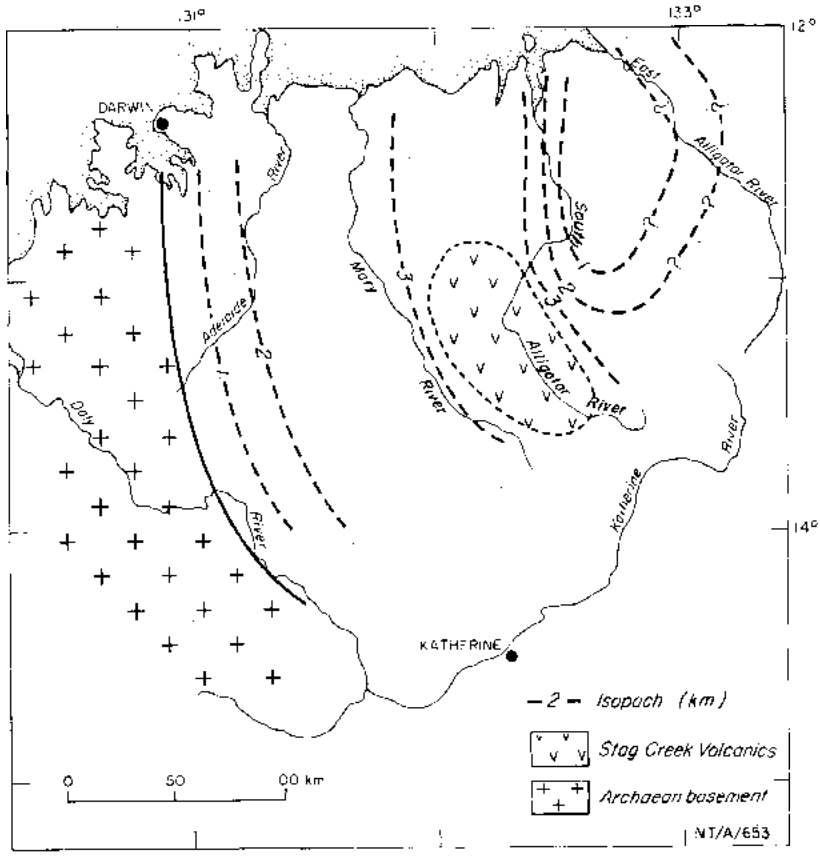


Figure 4. Stage 1, Palinspastic Map of the Batchelor, Namoona and Kakadu Groups.

the Namoona Group). In the centre of the geosyncline, over most of the Batchelor Shelf and the South Alligator Trough, and also on parts of the Kakadu Shelf, a thicker sequence (at least 2500m) of black shale and siltstone, which are calcareous or pyritic in places, and dolomite, lithic fine to coarse greywacke, and calcareous sandstone, was deposited (the Namoona Group, Fig. 4). The calcareous sandstones contain pelloids of dolomite, indicating some reworking of carbonate.

The psammitic and rudaceous sediments interbedded in places with carbonate near the base of the Early Proterozoic succession commonly exhibit cross-bedding and ripple marks, and were probably fluviatile deposits, as suggested by French (1970) for the Crater Formation. The presence of granite pebbles (French, 1970) and the feldspathic nature of the detrital sediments indicates that they were derived from the Archaean basement; pebbles of BIF in a conglomerate within the Crater Formation are identical to Archaean BIF in the Rum Jungle and Waterhouse Complexes (Johnson, 1974). Considerable variation in thickness and grainsize of the basal units (Beestons Formation and Kakadu Group) indicates that the Archaean surface probably had a high relief.

Dolomite in the marginal sequences (i.e., Celia Dolomite, Coomalie Dolomite, and lower

member of the Cahill Formation) commonly contains several types of stratiform stromatolites, including *conophyton* sp., and carbonate pseudomorphs after gypsum and halite. These features indicate deposition in a high intertidal to supratidal environment (Crick & Muir, this volume). In contrast dolomite in the Namoona Group in the South Alligator Trough is well bedded, and contains neither stromatolites nor pseudomorphs after evaporitic minerals; it may have been deposited in a deeper water environment. Carbonaceous sediments interbedded with some of the carbonate rocks were probably deposited in restricted reducing environments in depressions within the generally oxygenated carbonate-terrigenous sediment environment.

Stage 1 concluded with felsic to mafic volcanic activity, possibly resulting from deep fracturing and rifting, or thinning of continental crust associated with formation of the South Alligator Trough, as indicated by the part oceanic and part continental tholeiitic affinities of the Stag Creek Volcanics formed at this time. The volcanics are 1000m thick and consist of interbedded mafic volcanic flows, flow-breccia, tuff, tuffaceous shale, siltstone and greywacke. The Stag Creek Volcanics were deposited over at least 100km^2 of the South Alligator Trough (fig. 4) and may have been originally more extensive, but were either subsequently removed by erosion before the deposition of the Mount Partridge Group or were rendered indistinguishable from metamorphosed mafic intrusive rocks by the 1800 m.y. metamorphic event. The mafic extrusive rocks have been described variously as "greenstones" (Raggat, 1958), "altered basalt and basalt agglomerate" (Walpole, 1962), and "altered basalts or basaltic andesite" (Foy & Miezitis, 1977). Pillow structures have been recognised in the breccia rocks, and interbedded sediments indicate a subaqueous environment. Some subaerial explosive activity may also have occurred.

Stage 2

Following deposition of the Stag Creek Volcanics, the Archaean provenance areas were rejuvenated. As a result, the chemical sedimentation that typified sedimentation of Stage 1 ceased, and an influx of clastic material, represented by the Mount Partridge Group took place. The uplift probably caused slight warping and minor local subaerial exposure of the Stage 1 sediments; warping was probably about north to northwest-tending axes, as a slight angular unconformity beneath the Mount Partridge Group is only obvious where sediments strike east.

The three psammitic formations (the Mundogie Sandstone, Mount Hooper Sandstone, and Acacia Gap Sandstone) at the base of the Mount Partridge Group, typically consist of interbedded coarse quartz sandstone, arkose, minor pelitic rocks and conglomerate. Pebbles in the conglomerate consist of quartz, chert, quartzite, and rare mafic volcanic and banded amphibolitic rocks. These formations range in thickness from over 3000m in the northern part of the Batchelor Shelf (along the present coastline between Darwin and Field Island) and in the South Alligator Trough to less than 500m in the central part of the Batchelor Shelf (Fig. 5). On the western margin of the Batchelor Shelf the Acacia Gap Sandstone pinches out against the Chilling Platform. East of the Nanambu High on the Kakadu Shelf a similar sequence of metapsammitic rocks (upper member of the Cahill Formation) 2500m thick is probably a correlative (Needham *et al.*, this volume). The decrease in thickness towards the centre of the Batchelor Shelf corresponds with a decrease in grainsize and feldspar content. This feature is consistent with current directions indicated by cross-bedding, which suggest nearby sediment sources to the north and east (Walpole *et al.*, 1968; Stuart-Smith *et al.*, in prep.).

Archaean granitic gneiss, schist, and metasediments of the Nanambu High and a granitic complex interpreted by Tucker *et al.* (this volume) to underlie the present Van Diemen Gulf in the north were probably the major source areas for the Mount Partridge Group. An extensive belt of massive dolomite of the lower member of the Cahill Formation on

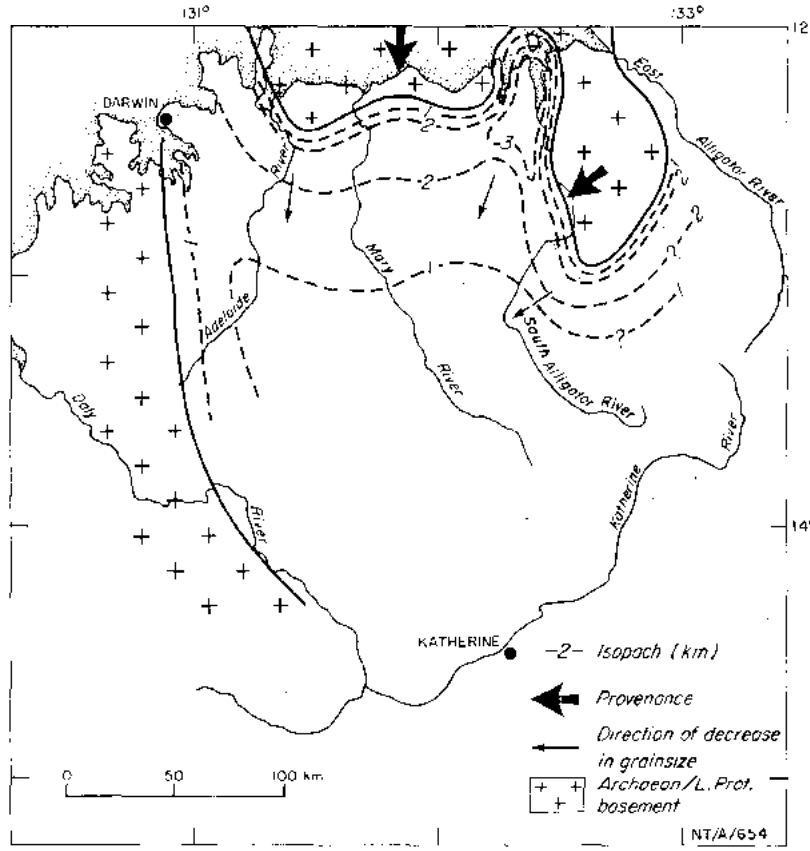


Figure 5. Stage 2, Palinspastic map of basal sandstone formations in the Mount Partridge Group.

the northwestern flank of the Nanambu High was probably the source for the abundant chert pebble conglomerates in the overlying Mount Hooper Sandstone. Many of the chert pebbles contain limonite pseudomorphs after carbonate rhombohedra, indicating that they are probably silicified dolomite (Needham & Stuart-Smith, 1978). Structures present in sandstone and conglomerate such as lenticular cross-bedding, graded-bedding and scours, the presence of oxidised grain boundaries, and the relationship between thickness and composition indicate that the psammitic formations were deposited in a continental environment, probably as coalesced alluvial fans flanking the provenance areas. The fans graded distally to subtidal deposits of laminated siltstone, shale, and minor quartz sandstone of the Wildman Siltstone and its metamorphic equivalent, the Nourlangie Schist. The sandstone commonly displays ripple marks, load casts, and lenticular cross-bedding, and is typically thinly bedded, well sorted and fine to medium-grained. The subtidal deposits transgressed over the alluvial fans and possibly onto parts of the provenance areas. By the time the Wildman Siltstone had been deposited the Chilling Platform was probably the only exposed basement in the region.

Stage 3

A tectonic event which caused uplift, folding, and subsequent erosion of the Stage 1 and

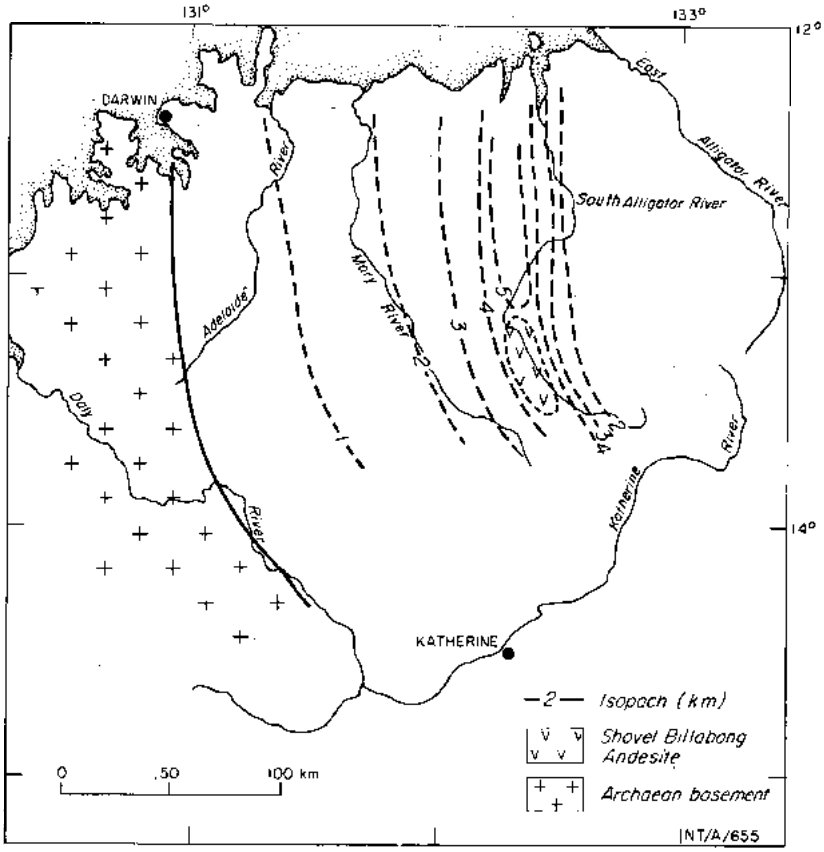


Figure 6. Stage 3, Palinspastic map of the South Alligator Group.

2 sediments, preceded a new phase of sedimentation, dominated by chemical and organic sediments (South Alligator Group), which accompanied a shallow marine transgression - initially over the Batchelor Shelf and the South Alligator Trough, and later the Kakadu Shelf (Fig. 6). The sediments of this phase form an eastward-thickening sequence (Koolpin Formation) of dolomite (algal and evaporitic in places), pyritic carbonaceous shale containing bands, lenses and nodules of chert, and carbonaceous siltstones. They reach a maximum thickness of 1000m in the South Alligator Trough, indicating continuing subsidence in this area.

Peneplanation of the older sediments and of the Archaean basement exposed west of the Batchelor Shelf (the Chilling Platform) and possibly on the Nanambu High is indicated by the lack of terrigenous material in the sediments and the lack of local variations in thickness of the Koolpin Formation. A ferruginous, sandy quartz breccia rarely containing quartz pebbles commonly forms the base of the sequence and may be a regolith. Siliceous breccia is also associated with massive silicified dolomite and is considered by Walpole *et al.* (1968) to be reef breccia associated with biohermal reefs. Although the reefs are commonly silicifed, the preservation of some collenia-type algae and the relationship between massive and brecciated

dolomite indicates that they were bioherms. Muir & Jackson (1978) also report the presence of domal and columnar stromatolitic dolomites and possible gypsum casts.

The association of pyritic carbonaceous rocks, including shungite (Muir & Jackson, 1978), with algal dolomite in the Koolpin Formation indicates a restricted environment, possible in a back reef. Crick *et al.* (this volume) suggest that those rocks may have formed in a fresh to slightly brackish water environment. The reefs probably developed in a high-energy shallow-marine environment within the photic zone, which had restricted access to the sea. A low or distal provenance area is indicated by the lack of terrigenous material.

Chemical sedimentation was temporarily interrupted by widespread felsic subaerial volcanism (Gerowie Tuff and Shovel Billabong Andesite) centred in the South Alligator Trough.

The Shovel Billabong Andesite was deposited as a conformable unit about 40km long, 10km wide and 100 to 300m thick within the South Alligator Trough. The unit consists of numerous flows which interfinger with the overlying Gerowie Tuff in places.

The Gerowie Tuff consists of pelite, fine-grained black cherty tuff, coarse feldspathic tuff, coarse lithic tuff and minor tuffaceous arenite, and possible felsic flow rocks (Crick *et al.* 1978; Stuart-Smith *et al.*, in prep.). The tuffs and sediments are commonly laminated to thinly bedded, and micro-crossbedding and graded bedding are rearly present in coarse feldspathic and lithic tuffs. The sequence reaches a maximum thickness of 750m in the South Alligator Trough and thins westwards across the Batchelor Shelf. It has not been recognised on the Kakadu Shelf.

The Gerowie Tuff probably formed as subaqueous accumulations of fine wind and water-born siliceous ash and, possibly, minor flows, intercalated with pelitic sediments containing chert nodules in places. Pyritic carbonaceous sediments and carbonates typical of the other formations in the South Alligator Group are absent.

The subaerial acid volcanoes from which the Shovel Billabong Andesite and the Gerowie Tuff were derived were probably in, or marginal to, the South Alligator Trough. The thickest and coarsest accumulations of tuff are in the trough, and the andesite occurs only in the trough. During deposition of the Gerowie Tuff the geosyncline probably remained shallow, with continued subsidence in the South Alligator Trough. The Chilling Platform and possibly the Nanambu High land areas, were of low relief, and provided relatively insignificant terrigenous material.

Chemical and minor organic sedimentation followed the volcanism, and resulted in the deposition of an eastward-thickening sequence of interbedded ferrugionous siltstone containing bands, lenses and nodules of chert, carbonaceous shale, greywacke and minor massive dolomite (Kapalga Formation). This sequence was deposited on the Batchelor Shelf and in the subsiding South Alligator Trough, where it attained a maximum thickness of about 5000m. It onlapped the Gerowie Tuff, Koolpin Formation and Mount Partridge Group on the western side of the Nanambu High, and may have possibly covered the Nanambu High and extended onto the Kakadu Shelf.

A major shift in the locus of tectonic activity within the geosyncline from the centre to the west is represented by formation of the Western Fault Zone and felsic to intermediate volcanism west of the Batchelor Shelf. Volcanism and probable basement uplift west of the Western Fault Zone resulted in an influx of flysch-type sediment into the geosyncline as evidenced by the presence of greywackes in the Kapalga Formation and deposition of the overlying Finniss River Group, which thickens eastwards from less than 1500m on the Batchelor Shelf to over 5000m on the Kakadu Shelf, indicating continued subsidence of the South Alligator Trough and the Kakadu Shelf. Up to 4200m of sediment (Sweet, 1977) was also deposited in the Western Fault Zone which probably formed a north-trending trough between the Chilling Platform and the Batchelor Shelf. The Finiss River Group comprises two

minor volcanic units, the Berinka and Dorothy Creek Volcanics together with the Burrell Creek Formation in the Western Fault Zone, the Burrell Creek Formation on the Batchelor Shelf, and the Fisher Creek Siltstone in the South Alligator Trough and on the Kakadu Shelf. The sediments include siltstone, slate, shale, greywacke, arkose, quartzite, schist, and minor conglomerate commonly containing pebbles of felsic volcanic rocks. A westerly source for the sediments is indicated by a decrease eastwards in grainsize and volcanic component and by sedimentary structures (Walpole *et al.*, 1968). Common sedimentary features include graded bedding, flow casts, load casts, incipient pull-aparts, and washouts (Walpole *et al.*, 1968) - all indicative of deposition by turbidity currents (Kuenen, 1953), and characteristic of flysch deposits. In places the complete turbidite sequence as defined by Bouma (1962) is present (Johnson, 1974).

As a distinct late stage development, a 4800m sequence (the Chilling Sandstone) of medium grained quartz sandstone, which is commonly rippled-marked and cross-bedded, and rare quartz pebble conglomerate and siltstone was deposited in the Western Fault Zone. Walpole *et al.* (1968) suggested that these rocks onlapped westwards onto Archaean rocks of the Chilling Platform, and that rapid lateral variations in the sequence were largely controlled by faulting. Sweet (1977) questioned the existence of the Chilling Platform, and suggested it was further west than proposed by Walpole *et al.* (1968). The full extent of the Chilling Sandstone, the youngest unit of the Early Proterozoic sequence preserved, is not known.

At the close of sedimentation tholeiitic basalt (Zamu Dolerite) was emplaced, mainly as sills, into the Early Proterozoic sediments (Ferguson & Needham, 1978). The Zamu Dolerite is thicker in the South Alligator Trough and Kakadu Shelf sediments than elsewhere, possibly reflecting deep fracturing in the underlying basement associated with formation of the trough. The intrusions constitute a tholeiitic suite which is differentiated into olivine dolerite, quartz dolerite and minor granophyre. In the South Alligator Trough they show a broad vertical differentiation; olivine dolerite is restricted to the Namoona Group and granophyre is best developed at the tops of quartz dolerite sills in the South Alligator Group. The Zamu Dolerite intrudes mainly the South Alligator Group in the centre of the Batchelor Shelf and the Finniss River Group in the South Alligator Trough, which possibly reflects the increase in sediment thickness eastwards across this part of the geosyncline, as the intrusions were probably emplaced at similar depths.

Stage 4

The tensional regime which characterised the depositional history of the geosyncline changed to east-west compression resulting in deformation, metamorphism, and partial anatexis of the Early Proterozoic sediments, and in some subsequent igneous activity (Fig. 3). Deformation and metamorphism increased in intensity eastwards, and was mainly controlled by the original basement configuration, such as the psition of basement highs, the South Alligator Hinge Zone, and thickness of the sedimentary pile. Sediments of the Batchelor Shelf and the South Alligator Trough were metamorphosed to lower greenschist facies, and were folded about north to northwest-trending non-cylindrical axes. The folds are typically composite and tight to isoclinal, with shallow-dipping axes, and axial plane cleavages are well developed (Stephansson & Johnson, 1976). East of the South Alligator Hinge Zone the Kakadu Shelf sediments were more complexly deformed and were involved in at least four phases of folding, including two events that produced isoclinal folds (Needham & Stuart-Smith, 1976).

Accompanying the east-west compression of the sediments, diapiric growth of the Nimbuwah Complex in the northeast of the region caused marginal overfolding and intense isoclinal folding of the sedimentary pile. This was accompanied by amphibolite facies and in places granulite facies regional metamorphism. Marginal overfolding and thrusting occurred along the southwest flank of the Nimbuwah Complex, suggesting that it may have formed by

the upward and outward movement of a mobile mass of granitised material over less granitised material, like the migmatite diapirs described by Haller (1956, p. 162) (Smart *et al.* 1975).

During this period of deformation the Nanambu High was reactivated and partly migmatised; leucocratic gneissic material, probably derived from the Kakadu Group, was accreted to it to form the Nanambu Complex (Needham & Stuart-Smith, this volume). The folded sediments were draped around it to form complex refolded synclinal structures. A marked foliation developed parallel to the axial plane of these folds, and gave rise to the dominant regional schistosity.

During the later stages of formation of the Nimbuwah Complex, complex small-scale cross-folding, with an axial plane crenulation cleavage, developed in the less competent rock types. This may have been related to further movements of the migmatite and Archaean granite masses, and to the intrusion of anatectic granites as the grade of metamorphism reached its peak (Needham & Stuart-Smith, 1976). Biotite which grew during the development of the crenulation cleavage has yielded a K-Ar isotopic age of about 1800 m.y. and dates the climax of late Early Proterozoic tectonism (Page *et al.*, this volume).

Changes in metamorphic grade across the geosyncline have hindered correlation of rock units. Needham *et al.* (this volume) and Ferguson (this volume) present two different interpretations of stratigraphic correlations across the South Alligator Hinge Zone. Recent BMR stratigraphic drilling across the zone (Stuart-Smith, 1977) indicates that the change between greenschist and amphibolite facies is gradational, over distances of 10 to 50km wide, and not abrupt as proposed by Ferguson (this volume). The gradational eastwards increase in metamorphic grade across the hinge zone is consistent with the general eastwards increase in metamorphic grade east of the zone, observed in amphibolite of the Zamu Dolerite by Ferguson & Needham (1978) from the high-temperature end of the medium-grade (i.e. upper amphibolite) to the low-temperature end of high-grade (i.e. granulite) (Winkler, 1976).

The maximum preserved thickness of Early Proterozoic sediments in the Pine Creek Geosyncline is about 14km (Needham *et al.*, this volume). This cannot account for the observed metamorphic grades, as these require depths of burial in excess of 20km for amphibolite grade (Ferguson, this volume). The indicated depths of burial could have been attained, at least in part, by the intense overfolding and thrusting of sediments east of the South Alligator Hinge Zone. The eastwards gradient from greenschist to amphibolite facies is steepened across the South Alligator Hinge Zone by a relative uplift of about 5 to 8km east of the zone (Needham *et al.*, this volume; Tucker, pers. comm.). This displacement was possibly associated with diapirism of the Nimbuwah and Nanambu Complexes.

Some igneous activity followed deformation and metamorphism of the geosynclinal sediments. Firstly, at 1730-1780 m.y. (Compston & Arriens, 1968), numerous plutons of biotite granite, adamellite, and minor syenite and granodiorite domed and hornfelsed the surrounding metasediments in the less deformed and metamorphosed areas (Walpole *et al.*, 1968). Small hydrothermal deposits of Pb, Zn, Cu, Au, Sn, W and U were associated with contact aureoles around the intrusions. Apart from minor marginal phases possibly due to contamination, all the granitoids are classified as *I-type* (Ferguson *et al.*, this volume). During this phase of igneous activity the folded Early Proterozoic sediments were peneplaned and unconformably overlain by the Edith River Volcanics. The volcanics, centred in the South Alligator Trough (1760 m.y. Leggo *in* Walpole *et al.*, 1968) are probably the final product of this felsic igneous phase. Subsequent deep crustal fracturing may be reflected by intrusion of the tholeiitic Oenpelli Dolerite (1688 m.y.), phonolite dykes (1312 m.y.), and minor dolerite dykes (1200 m.y.).

The Oenpelli Dolerite and Early Proterozoic metasediments are unconformably overlain by flat-lying Middle Proterozoic sediments in the east, and elsewhere by younger Proterozoic,

Palaeozoic, and Mesozoic cover rocks, indicating tectonic stability since early Middle Proterozoic times.

CONCLUSIONS

Previous concepts of evolution of the Pine Creek Geosyncline considered that the Early Proterozoic sediments formed a thick basin-like accumulation. Sedimentary units were thought to represent diachronous facies changes from shallow to deep water environments. The model of evolution presented in this paper is based on the recently recognised chronostratigraphy outlined by Needham *et al.* (this volume).

The Early Proterozoic sediments were deposited in an intracratonic basin under alternating continental and shallow marine environments. The intracratonic setting of the geosyncline is indicated by:

a) the prevalence of shallow-marine and continental deposits and the absence of undoubted deep-water deposits.
b) the presence of continental tholeiites, such as the Zamu Dolerite (Ferguson & Needham, 1978) and the Oenpelli Dolerite (Stuart-Smith & Ferguson, 1978).
c) gravity patterns suggesting that the basement to the geosyncline has the same density and is continuous with the exposed granitoid Archaean complexes in the region.

The geosyncline was initiated by incipient rifting and marginal subsidence of the Archaean crust, leading to the formation of the South Alligator Trough and the adjoining Batchelor and Kakadu Shelves. Such a mechanism has been suggested for the evolution of other Early Proterozoic geosynclines or mobile belts (Hoffman, 1973; Glikson, 1976); it is indicated in the Pine Creek Geosyncline by:

a) the concentration of igneous activity, including volcanic centres, in the South Alligator Trough (e.g. the Stag Creek Volcanics, Shovel Billabong Andesite, Gerowie Tuff, and the Zamu Dolerite).
b) the inferred presence of a major boundary fault, the Western Fault Zone (other boundaries are not exposed)
c) uplift of the Nanambu High and other margins of the South Alligator Trough, particularly during Stage 2. Marginal uplift is a feature common to rifts produced by upwarping and extension of the crust (Cloos, 1955).

Glikson (1976), in discussing a rift-valley model for Proterozoic mobile belts, suggested that such a model can explain the evolution of ensialic mobile belts by the subsidence of downfaulted troughs and an accompanying rise of subjacent mantle diapirs. Such features have been demonstrated by geophysical surveys in the east African rift system (Baker *et al.*, 1972) and result in metamorphism and felsic igneous activity preceding mafic igneous activity. Thus the formation of the Nimbuwah Complex and the 1800 m.y. regional metamorphism precede granite intrusion (1730-1780 m.y.) and felsic volcanism (Edith River Volcanics) which precede the intrusion of the tholeiitic Oenpelli Dolerite (1688 m.y.).

ACKNOWLEDGEMENTS

The authors are grateful to M.J. Roarty and D.A. Wallace for discussion and many helpful suggestions to the ideas expressed in this paper. We also thank D. Blake, C. Blain and C.E. Prichard for critically reading the manuscript.

This paper is published with the permission of the Director, Bureau of Mineral Resources, and the Manager, CRA Exploration Pty Ltd.

REFERENCES

BMR, 1976: *Geology of Rum Jungle, 1:100 00. Bureau of Mineral Resources, Australia.*
BMR, 1979: *Solid Geology of the Pine Creek Geosyncline, 1:500 000, Bureau of Mineral Resources, Australia.*
Baker, B.H., Mohr, R., & Williams, L.A.J., 1972: Geology of the eastern rift system of Africa: *Spec. Pap. geol. Soc. Am.*, 136.
Bouma, A.H., 1962: *Sedimentology of some flysch deposits.* Elsevier, Amsterdam.
Cloos, E., 1955: Experimental analysis of fracture patterns. *Bull. geol. Soc. Am., 66*, 241-256.
Compston, W., & Arriens, P.A. 1968: The Precambrian geochronology of Australia. *Can. J. Earth Sci., 5*, 561-583.

Crick, I.H., Stuart-Smith, P.G., & Needham, R.S., 1978: Stratigraphic significance of a discovery of Lower Proterozoic tuff in the Pine Creek Geosyncline. *BMR J. Aust. Geol. Geophys., 3,* 163-165.
Crick, I.H., & Muir, M.D., this volume: Evaporites and uranium mineralisation in the Pine Creek Geosyncline. *Proceedings of the International Uranium Symposium on the Pine Creek Geosyncline.*
Crick, I.H., Muir, M.D., Needham, R.S., & Roarty, M.J., this volume: The geology and mineralisation of the South Alligator Uranium Field. *Proceedings of the International Uranium Symposium on the Pine Creek Geosyncline.*
Dunn, P.R., 1962: Alligator River, N.T. — 1:250 000 Geological Series. *Explan. Notes Bur. Miner. Resour. Geol. Geophys. Aust., D/53-1.*
Ferguson, J., this volume: Metamorphism in the Pine Creek Geosyncline and its bearing on stratigraphic correlations. *Proceedings of the International Uranium Symposium on the Pine Creek Geosyncline.*
Ferguson, J., Chappell, B.W., & Goleby, A.B., this volume: Granitoids in the Pine Creek Geosyncline. *Proceedings of the International Uranium Symposium on the Pine Creek Geosyncline.*
Ferguson, J., & Needham, R.S., 1978: The Zamu Dolerite: A Lower Proterozoic preorogenic continental tholeiitic suite from the Northern Territory, Australia. *J. geol. Soc. Aust., 25(6),* 309-322.
Foy, M.F. & Miezitis, Y., 1977: Uranium mineralisation at Anomaly 2 J, South Alligator Valley, Northern Territory, and its significance concerning regional structure and stratigraphy. *Proc. Australas. Inst. Min. Metall., 261,* 1-11.
French, D.J., 1970: Crater Formation investigation, Rum Jungle district, Northern Territory. *Rec. Bur. Miner. Resour. Geol. Geophys. Aust., 1970/65* (unpubl.).
Glikson, A.Y., 1976: Archaean to Early Proterozoic shield elements: relevance of plate tectonics. *Spec. Pap. geol. Ass. Can., 14.*
Haller, J., 1956: Probleme der Tiepentektonik, Bauformen im Migmatite — Stockwerk der ost-gronlandischen Kalendoniden. *Geol. Rdsch. 45,* 159-167.
Hoffman, P., 1973: Evolution of an early Proterozoic continental margin: the Coronation geosyncline and associated aulacogens of the northwestern Canadian shield. *Phil. Trans. R. Soc. (London), A. 273,* 547-581.
Johnson, K., 1974: Progress report: geological review and revision of the Rum Jungle area, Northern Territory, 1973. *Rec. Bur. Miner. Resour. Geol. Geophys. Aust. 1974/41* (unpubl.).
Kay, M., 1951: North American Geosynclines. *Mem. geol. Soc. Am.,* 48.
Kuenen, Ph.H., 1953: Features of graded bedding. *Bull. Am. Ass. Petrol. Geol. 37(5).*
McDougall, I., Dunn, P.R., Compston, W., Webb, A.W., Richards, J.R., & Bofinger, V.M., 1965: Isotopic age determinations on Precambrian rocks of the Carpentarian region, Northern Territory, Australia. *J. geol. Soc Aust., 12(1),* 67-90.
Muir, M.D., & Jackson, M.J., 1978: Report on a visit to the Batchelor and South Alligator River areas 27-28 September 1978. *Prof. Op. Bur. Miner. Resour. Geol. Geophys. Aust., 1978/31* (unpubl.).
Needham, R.S., Crick, I.H., & Stuart-Smith, P.G., 1978: Pine Creek Geosyncline in Geological Branch Summary of Activities. *Rep. Bur. Miner. Resour. Geol. Geophys. Aust., 208.*
Needham, R.S., Crick, I.H., & Stuart-Smith, P.G., this volume: Regional geology of the Pine Creek Geosyncline. *Proceedings of the International Uranium Symposium on the Pine Creek Geosyncline.*
Needham, R.S., & Stuart-Smith, P.G., 1976: The Cahill Formation — host to uranium deposits in the Alligator Rivers Uranium Field, Australia. *BMR J. Aust. Geol. Geophys., 1* 321-333.
Needham, R.S., & Stuart-Smith, P.G., 1978: Alligator River Party: Final progress record. *Rec. Bur. Miner. Resour. Geol. Geophys. Aust., 1978/113* (unpubl.).
Needham, R.S., & Stuart-Smith, P.G., this volume: Geology of the Alligator Rivers Uranium Field. *Proceedings of the International Uranium Symposium on the Pine Creek Geosyncline.*
Noakes, L.C., 1949: A geological reconnaissance of the Katherine-Darwin region, Northern Territory. *Bull. Bur. Miner. Resour. Geol. Geophys. Aust., 16.*
Page, R.W. Compston, W., & Needham, R.S., this volume: Geochronology and evolution of the late Archaean basement and Proterozoic rocks in the Alligator Rivers Uranium Field, Northern Territory, Australia. *Proceedings of the International Uranium Symposium on the Pine Creek Geosyncline.*
Raggatt, H.G., 1958: Finding ore: some Australian case histories and their bearing on future discovery. *Aust. J. Sci., 21(4a),* 60-77.
Richards, J.R., Ruxton, B.P., & Rhodes, J.M., 1977: Isotopic dating of the leucocratic granite, Rum Jungle, Australia. *Proc. Australas. Inst. Min. Metall., 264.* 33-43.
Rhodes, J.M. 1965: The geological relationships of the Rum Jungle Complex, Northern Territory. *Rep. Bur. Miner. Resour. Geol. Geophys. Aust., 89.*
Smart, P.G., Wilkes, P.G., Needham, R.S., & Watchman, A.L., 1975: Geology and Geophysics of the Alligator Rivers Region *in* (ed. C. L. Knight) *Economic Geology of Australia and Papua New Guinea., Australas. Inst. Min. Metall., Monograph Series No. 5, 1. Metals,* 285-301.
Stephansson, O., & Johnson, K., 1976: Granite diapirism in the Rum Jungle area, northern Australia. *Precambrian Research, 3,* 159-85.
Stille, H., 1941: *Ein Fuhrung in den Bau Amerikas.* Berlin, Borntraeger.
Stuart-Smith, P.G., 1977: Shallow stratigraphic drilling in the Kapalga 1:100 000 Sheet area, Alligator Rivers Region, N.T., 1974-6. *Rec. Bur. Miner. Resour. Geol. Geophys. Aust. 1977/53* (unpubl.).
Stuart-Smith, P.G., & Ferguson, J., 1978: The Oenpelli Dolerite — a Precambrian continental tholeiitic suite from the Northern Territory, Australia. *BMR J. Aust. Geol. Geophys., 3.* 125-133.
Stuart-Smith, P.G., Roarty, M.J., Needham, R.S., & Crick, I.H. (in prep.). Geology of the Mundogie 1:100 000 Sheet area, Northern Territory. *Rec. Bur. Miner. Resour. Geol. Geophys. Aust* (unpubl.).

Sweet, I.P., 1977: The Precambrian Geology of the Victoria River Region, Northern Territory. *Bull. Bur. Miner. Resour. Geol. Geophys. 168.*

Tucker, D.H., Hone, I., & Sampath, N., this volume: The characteristics and interpretation of regional gravity, magnetic, and radiometric surveys in the Pine Creek Geosyncline. *Proceedings of the International Uranium Symposium on the Pine Creek Geosyncline.*

Turner, F.J., & Verhoogen, J., 1960: *Igneous and metamorphic Petrology.* 2nd Edition, McGraw-Hill, New York.

Walpole, B.P., 1960: Evolution of the Pine Creek Geosyncline. *Ph.D. thesis, Australian National University, Canberra* (unpubl.).

Walpole, B.P., 1962: Mount Evelyn, N.T. 1:250 000 Geological Series. *Explan. Notes Bur. Miner. Resour. Geol. Geophys. Aust., SD/53-5.*

Walpole, B.P., Crohn, P.W., Dunn, P.R., & Randall, M.A., 1968: Geology of the Katherine-Darwin region, Northern Territory. *Bull. Bur. Miner. Resour. Geol. Geophys. Aust., 82.*

Winkler, H.G.F., 1976: *Petrogenesis of Metamorphic Rocks,* 4th Edition, Springer-Verlag, Berlin, 334 p.

GEOCHRONOLOGY AND EVOLUTION OF THE LATE-ARCHAEAN BASEMENT AND PROTEROZOIC ROCKS IN THE ALLIGATOR RIVERS URANIUM FIELD, NORTHERN TERRITORY, AUSTRALIA

R.W. Page[1], W. Compston[2] and R.S. Needham[1]

1. Bureau of Mineral Resources, P.O. Box 378, Canberra City, A.C.T., 2601, Australia.
2. Research School of Earth Sciences, ANU, P.O. Box 4, Canberra City, A.C.T., 2600, Australia.

ABSTRACT

U-Pb zircon and monazite studies, together with Rb-Sr and K-Ar total-rock and mineral studies, have been undertaken on various suites of amphibolite-grade gneisses and schists, granulites, intrusive granites, volcanic rocks, and dolerites in the Alligator Rivers Uranium Field. These studies cover all the major rock units of the region, and lead to the establishment of an overall chronology which is geologically consistent, and with which any petrogenetic hypothesis or model of mineralization is constrained.

The Nanambu Complex granitic basement, onto which the Lower Proterozoic Pine Creek Geosynclinal sediments were deposited, gives concordant U-Pb zircon and Rb-Sr total-rock ages at about 2470 Ma. The age of the Lower Proterozoic metasediments themselves can only be estimated, and for the Ranger 1 'Footwall Sequence', such an estimate is 2000-2200 Ma. Granitoids and charnockitic granulites in the Nimbuwah Complex gives U-Pb zircon results, interpreted as crystallisation ages, between 1886 and 1866 Ma. These magmas had had no crustal residence prior to this time, and their emplacement into the Pine Creek Geosyncline is envisaged as the initiation, perhaps the triggering mechanism, of the principal regional metamorphism, dated herein at 1800 Ma. This latter event is ubiquitous, and is reflected in most Rb-Sr total-rock and mineral systems, and in all K-Ar mineral systems. The U-Pb age of a monazite from a 2470 Ma old gneiss is also updated by this event, but U-Pb isotopic systems in zircon, and a few Rb-Sr total-rock systems, have withstood such modifications.

Post-tectonic, Middle Proterozoic (Carpentarian) granites (Jim Jim, Tin Camp, and Nabarlek Granites) and dolerites (Oenpelli Dolerite) have Rb-Sr total-rock and mineral ages of 1730 and 1780 Ma and 1688 ± 13 Ma, respectively. The formation of retrograde chlorite-rich haloes in the vicinity of the uranium deposits, post dates not only the above intrusive rocks, but it also transgresses the regional unconformity above which are the flat-lying Kombolgie Formation sandstones. The latter contain two basaltic members, for one of which a Rb-Sr isochron age of 1648 ± 29 Ma has been obtained. The main chloritisation associated with the Nabarlek and Jabiluka One orebodies is reflected in locally disturbed Rb-Sr total-rock systems which give an age of ca. 1600 Ma for this event; at Nabarlek, an even younger alteration episode, less than 920 Ma, is also recognised. This last result coincides with published U-Pb pitchblende ages on the Nabarlek deposit, and evidently represents the last re-deposition of uranium ore and growth of secondary chlorite-sericite aggregates during a further low-temperature metasomatism.

INTRODUCTION

Isotopic methods of dating rocks, and geochemical constraints inferred from initial isotopic ratios, are of prime importance in understanding Precambrian evolution. Without such data, establishment of the igneous and metamorphic geological history, and correlation of Precambrian rock sequences into the geological time-scale can be extremely tenuous arguments, even when attempted in an approximate fashion.

The Precambrian rocks in the Alligator Rivers Uranium Field comprise a suite of Lower Proterozoic metasedimentary units which surround two large centres of gneissic-granitic and migmatitic rocks, and associated more massive granitic bodies; the whole is intruded by both pre- and post-orogenic mafic igneous rocks, and is overlain unconformably by Middle Proterozoic (Carpentarian) plateau sandstone with interbedded mafic volcanic members. This Middle Proterozoic (Carpentarian) sequence is itself intruded by younger doleritic bodies (Fig. 1). The geological setting is described by Walpole *et al.* (1968), Needham *et al.* (this volume), and Needham & Stuart-Smith (this volume).

Detailed isotopic evidence, relevant to each salient rock formation amenable to geochronological study, is presented in this paper. Use of Rb-Sr, U-Pb, and K-Ar isotopic systems, coupled with a geologically-controlled sampling strategy, provides the age framework, as well as several isotopic constraints, within which any model of the geological

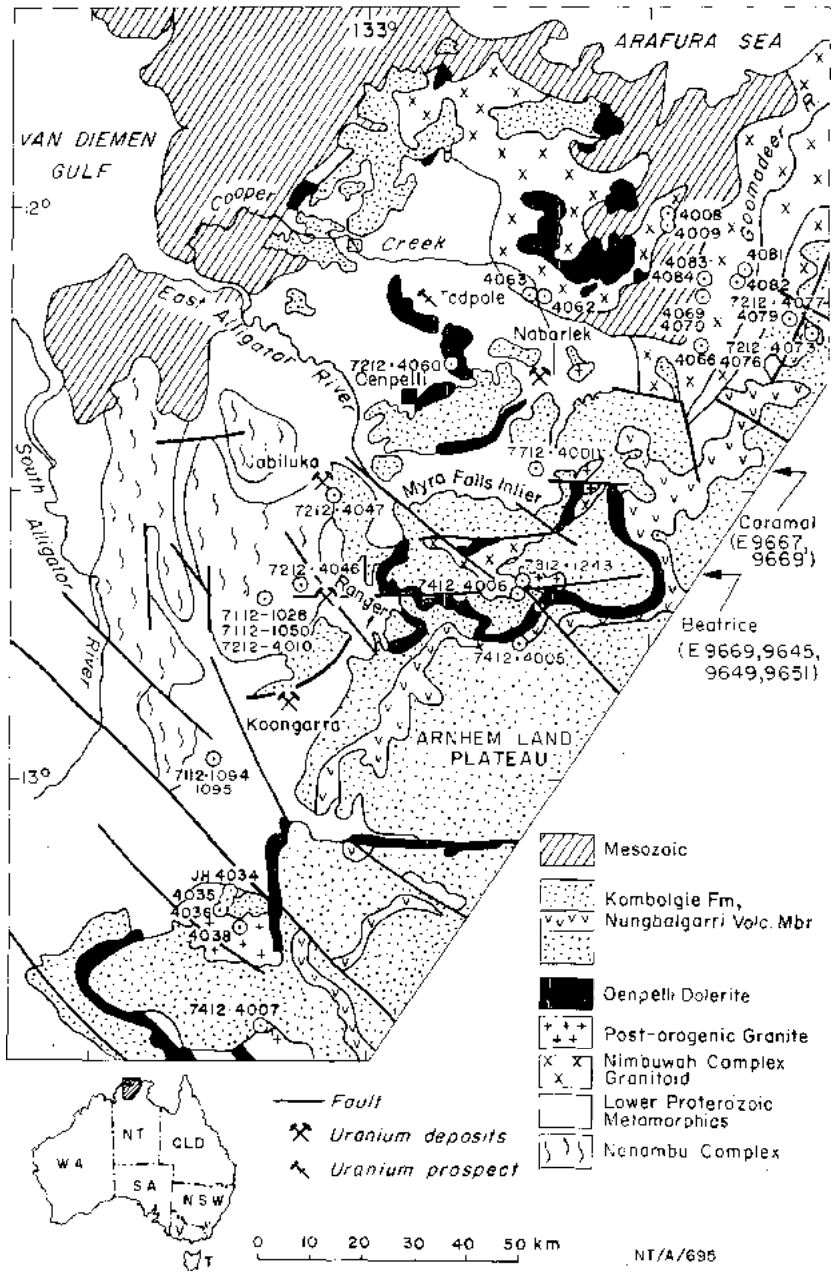


Figure 1. Geological map of the Alligator Rivers region showing location of samples, other than those from the Nanambu Complex and the uranium deposits.

development of the region must comply. For the study, various suites of gneiss, schist, granite, volcanics, and dolerite were sampled and analysed, including several near the uranium deposits. One major problem has been establishing the existence and eastward extent of Archaean rocks comparable to those which are basement to Lower Proterozoic metasediments in the Rum Jungle area, 200km to the west. Another has centred on the unknown stratigraphic relationship between the two terranes of medium to high grade gneisses (Nanambu and Nimbuwah Complexes), and between them and the Pine Creek Geosyncline metasediments. A further objective has been to obtain information on the timing and temperature threshold of the alteration processes evident in mineralized areas.

All the ages measured and referred to throughout this paper are calculated (and previously published ages recalculated) using decay constants recommended by the IUGS Subcommission on Geochronology (Steiger & Jäger, 1977). Analytical techniques and statistical treatment of the data are as described in Krogh (1973) and Page (1978). Errors quoted for Rb-Sr isochron results are at the 95% confidence level; K-Ar ages, and U-Pb zircon intersection ages with concordia have errors quoted at the 1σ and 2σ level, respectively.

AGE OF THE BASEMENT TO THE PINE CREEK GEOSYNCLINE

In the western part of the Pine Creek Geosyncline at Rum Jungle, geological relationships between basement granitoids and unconformably overlying Lower Proterozoic sediments have been documented for many years. The antiquity of this basement in the form of the Rum Jungle and Waterhouse Complexes is supported by previous geochronological studies (Richards *et al.*, 1966 and 1977) and by the present authors' unpublished data. These combined U-Pb zircon and Rb-Sr total rock ages show that the Rum Jungle and Waterhouse basement granitoids are at least 2400 Ma old. In the Alligator Rivers region, no contacts with basement are exposed, and suggestions that the Nanambu Complex is basement comparable to that at Rum Jungle have been the subject of much conjecture (Walpole *et al.*, 1968; Needham *et al.*, 1974; Dodson *et al.*, 1974).

As at Rum Jungle, the Nanambu Complex includes a range of *S*- and *I*-type granitoids (Ferguson *et al.*, this volume), dominantly granitic gneiss and coarse leucogneiss. It extends over about 3500 km² (Figs. 1 & 2) between the South and East Alligator Rivers. It is interpreted and defined by Needham & Stuart-Smith (this volume) to include partly metamorphosed Archaean granitoid rocks, with an accreted mantle of paragneisses and schists belonging to the Lower Proterozoic sequence.

It will be seen that the granitoid and orthogneissic rocks of the bulk of the Nanambu Complex can be distinguished on isotopic grounds from the paragneisses and schists which predominate nearer the margin. Hence, the U-Pb and Rb-Sr isotopic data presented in this section relate to granitoids and orthogneisses, and data on the paragneisses are more aptly discussed in terms of their relevance to the age of metamorphism (discussed below). The mineralogy of the Nanambu orthogneisses is dominated by quartz, K-feldspar, plagioclase, biotite, and amphibole, with minor epidote, muscovite and garnet.

Archaean ages in the Nanambu Complex

a) U-Pb zircon data

Zircons (and monazite) were separated from a 30kg block of biotite granite-gneiss, from the eastern most outcrop of the Nanambu Complex, known as 'Granite Hill', 3km south of Jabiluka (Fig. 2). Here the basement rocks are unconformably overlain by Kombolgie Formation sandstone. Most of the granitic outcrop is biotite gneiss, but there is also local development of muscovite-rich gneiss and muscovite-bearing pegmatoid.

The procedure followed throughout this study involved splitting the 100% pure zircon concentrate into several size and magnetic fractions, to achieve a dispersion in their U concentrations and U/Pb ratios. The resultant analyses provide in-built tests to determine (i)

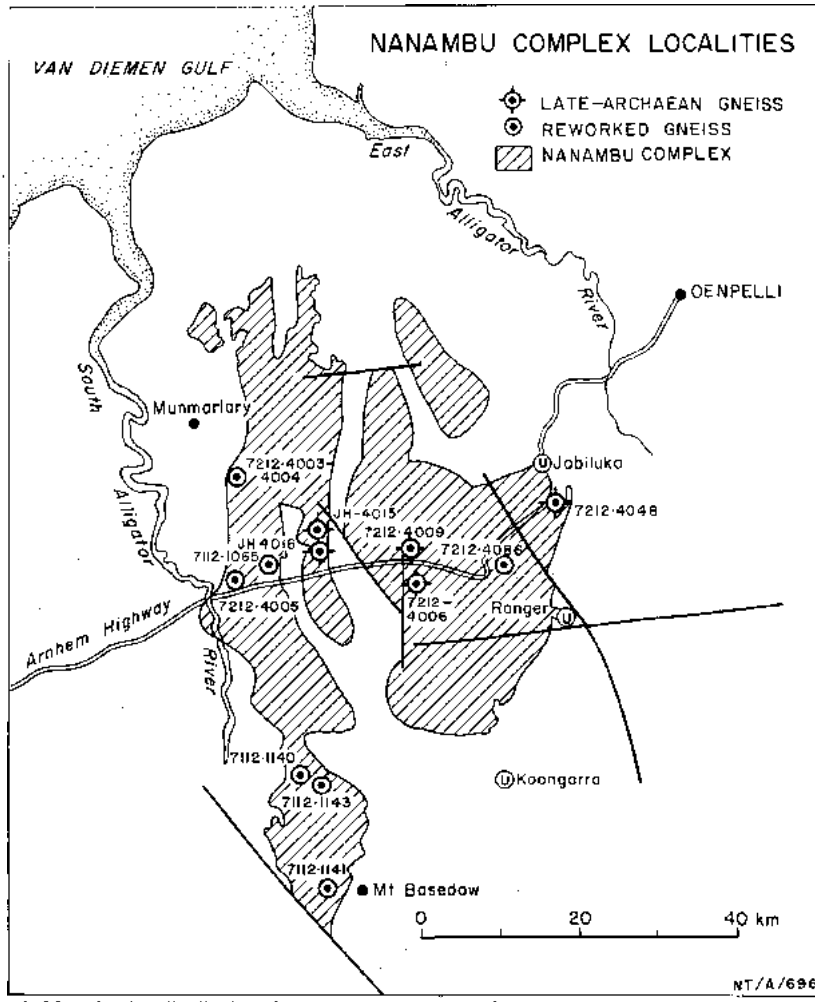


Figure 2. Map showing distribution of the Nanambu Complex. Sample localities which give late-Archaean ages are marked ⊙, and localities in which the isotopic systems of the gneisses are modified are marked ⊙

the igneous crystallisation age if the zircon suite is cogenetic, or (ii) if there is more than one zircon generation present, or (iii) if the U-Pb systems of the zircons have been modified.

All the non-magnetic fractions (Table 1) are clear, colourless to pink, and generally free of inclusions, whereas the two magnetic fractions (9, 10) include zircons with small dark inclusions and have grey, opaque margins, which are partly metamict. Most fractions are euhedral to subhedral and have a fine magmatic zoning parallel to the crystal faces. Several percent of the coarsest (-150μ) zircon fraction contain small, relict (optically discontinuous) zircon cores, suggestive of a non-resorbed, pre-magmatic zircon generation. No such cores were verified amongst the finer (-75μ and -45μ) grainsize fractions. It is conceivable that relict grains act as nucleii which enhance more rapid and larger zircon growth, explaining their dominance in the coarsest zircon population.

	Sample	Size in microns and magnetic susceptibility	Sample fraction (Figs 4,8,14)	Weight (mg)	$^{206}Pb/^{204}Pb$ (meas'd)	Concentration (ppm)* U	Concentration (ppm)* Total Pb	Atom % Pb* ^{206}Pb = 100 204	207	208	Atomic Ratios $^{207}Pb/^{206}Pb$	$^{206}Pb/^{238}U$	$^{207}Pb/^{235}U$
NANAMBU COMPLEX	7212.4048	+150 NM? clear	1	0.15	414.2	2666.3	1215.7	0.2264	17.764	13.664	0.14857	0.37243	7.62909
		+150 NM? pink	2	0.16	531.9	2103.6	954.0	0.1800	17.059	10.706	0.14745	0.37487	7.62118
		-150 NM? pink	2	2.70	374.9	1796.5	833.7	0.2650	17.815	22.576	0.14399	0.36852	7.31640
		-150 NM1	3	1.54	371.5	1826.7	804.6	0.2672	17.233	28.587	0.13761	0.34056	6.46182
		-75 NM1 clear	4	0.07	400.1	1170.0	531.2	0.2167	17.419	19.122	0.14629	0.39037	7.87410
		+75 NM1 pink	5	0.64	360.6	2176.2	1015.7	0.2354	17.788	27.565	0.14228	0.36982	7.25493
		-75 NM2	6	3.00	377.7	1981.8	904.3	0.2555	17.372	22.104	0.14007	0.36569	7.06250
		-75 M2	7	2.05	296.2	2075.2	981.6	0.3366	17.865	33.485	0.13475	0.34455	6.40147
		-45 NM2	8	4.04	344.1	2148.4	975.9	0.2902	17.349	25.702	0.13570	0.34969	6.54262
		-45 M2	9	0.12	224.2	3546.5	1941.0	0.4394	18.618	40.477	0.12851	0.29640	5.26213
		-75 M3	10	4.91	193.0	2180.5	780.8	0.5172	18.575	52.702	0.11639	0.22406	3.59594
		-150, Monazite	M	1.41	2070	4046.1	7718.6	0.0470	12.037	560.87	0.11406	0.32482	5.10821
NIMBUWAH COMPLEX	7212.4081A	-250 NM1	1	1.87	2402	296.5	95.3	0.0342	14.688	16.241	0.11229	0.29042	4.49339
		-250 M1	2	2.53	1055	423.7	130.2	0.0905	12.236	17.351	0.11067	0.26506	4.02280
		-150 NM1	3	3.21	2280	309.3	102.6	0.0420	11.774	16.793	0.11231	0.29782	4.61183
		-150 NC	4	6.52	2214	318.5	104.3	0.0392	11.690	16.938	0.11152	0.29370	4.52062
		-75 NM2	5	3.12	1382	332.7	112.9	0.0682	12.142	19.196	0.11228	0.29682	4.59356
		-75 M2	6	6.10	1843	346.0	113.4	0.0525	11.886	17.687	0.11176	0.29133	4.49065
		-45 NM2	7	3.28	1650	375.1	124.4	0.0345	11.696	17.045	0.11231	0.29762	4.60880
	7212.4081C	-250 NM2	8	2.00	2123	315.2	105.9	0.0384	11.926	15.963	0.11411	0.30453	4.78796
		-150 NM2	9	6.96	3104	338.0	116.2	0.0286	11.683	16.485	0.11298	0.31025	4.83281
		-75 NM3	10	7.28	2813	386.4	131.0	0.0322	11.671	16.639	0.11237	0.30531	4.73039
		-45 NM2	11	1.58	2855	442.6	147.0	0.0288	11.619	15.667	0.11237	0.30176	4.67262
		-45 NM2	12	1.92	4090	413.6	136.4	0.0270	11.582	15.659	0.11219	0.29977	4.63691
		-45 NM3	13	2.05	1754	431.6	143.1	0.0335	11.693	15.885	0.11242	0.30038	4.65583
	7312.1243	-250 NM2	1	2.51	1570	547.2	171.5	0.0597	12.005	11.922	0.11201	0.28096	4.49362
		-150 NM2	2	2.88	1355	529.5	179.9	0.0709	12.097	12.242	0.11141	0.28514	4.38000
		-150 NO.5	3	4.42	872.1	572.0	197.6	0.1112	12.481	13.418	0.10977	0.26635	4.03139
		-75 NM2	4	4.30	1311	513.7	182.8	0.0797	11.983	12.168	0.11028	0.27598	4.21174
		-45 NM2	5	1.00	927.0	715.0	202.1	0.0978	12.215	13.049	0.10892	0.25501	3.97474
MYOA FALLS SCHIST	7712.4001	-250 NM5	1	1.92	1774	348.2	141.4	0.0306	15.067	14.867	0.14676	0.36042	7.29343
		-150 NM2 clear	2	3.07	2410	257.8	116.7	0.0360	15.006	13.492	0.14544	0.34528	7.00428
		-150 NM2	3	6.49	1841	364.2	135.2	0.0519	15.197	13.471	0.14531	0.33256	6.66303
		-75 NM3	4	8.69	1117	435.7	167.0	0.0875	14.930	13.698	0.13795	0.30438	5.78939
		-75 M1	5	2.17	826.0	583.5	202.7	0.1185	14.449	13.968	0.12900	0.26321	4.68166
		-45 NM2	6	1.14	1340	426.0	139.5	0.0876	14.942	12.934	0.13807	0.30392	5.86280

Size fractions of -250 + 150μ, -150 + 75μ, -75 +45μ, and -45μ, are designated -250, -150, -75 and -45, respectively.

Magnetic (M) and non-magnetic (NM) splits are indicated after each size fraction, together with the tilt angle (0.1°,2°, etc.) of Frantz isodynamic separator.

Composition blank lead: 206/204 17.97, 207/204 15.55, 208/204 37.21.

Common lead corrections: according to 2.45 Ga values from Cumming and Richards (1975) for 7212 4048; for other samples, according to Konasawich's (1968) single stage diffusion age of each sample (Tilton, 1960)

*Corrected for blank. Pb blank < 0.5 ng, U blank = 0.05 ng.

Table 1. U-Pb analytical data for zircons and monazite from the Alligator Rivers region.

The U-Pb zircon results were achieved by analysing very small amounts (0.1 to 4.9 mg) of zircon, representing extreme variations in size and magnetic susceptibility present in the bulk sample (Table 1). Data for the eight non-magnetic fractions and two relatively magnetic fractions are plotted on the U-Pb concordia diagram (Fig. 3).

The analysed zircon fractions have a wide variation in U content from 1120 to 3500 ppm. Concentrations in fractions with 0.1 mg (or less) zircon, have large uncertainties due to weighing errors with such small samples, but there is nevertheless a clear average U concentration for the population at around 2100 ppm.

On the concordia diagram, the U-Pb analyses define a wedge-shaped area, so that no single Pb-loss trajectory could validly account for all the data. However, the two magnetic (partly metamict) fractions 9 and 10 can be ignored for present purposes, because they are some 40 to 50 percent discordant, and their disposition with respect to the other 8 analyses cannot be accounted for by a single Pb-loss pattern. Their gross discordancy is probably due to an initial Pb-loss episode onto which further recent lead loss has been superimposed.

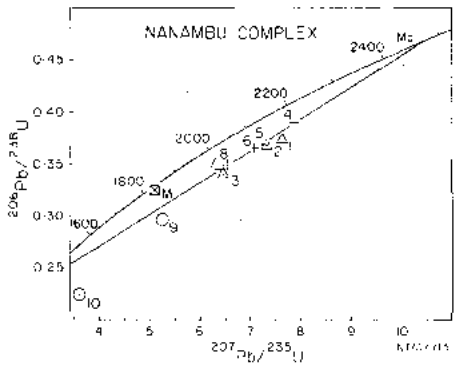


Figure 3. U-Pb concordia diagram for zircons from the Nanambu Complex. Crosses mark the least magnetic finer fractions (4-8), triangles mark the coarsest (-150μ) fractions (1-3), and open circles mark the two magnetic fractions (9, 10). The monazite analysis is marked M. Numbers refer to the analytical data in table 1.

The 8 non-magnetic fractions lie in a better-defined discordant group, in which there is a systematic bias between the 3 coarsest (-150μ) fractions and the remaining 5 finer fractions. The finer fractions are all on a well-defined chord which has upper and lower concordia intercepts corresponding to ages of 2470 $^{+47}_{-46}$ Ma and 1362 ± 80 Ma, respectively. The off-set of the -150μ fractions appears to be a real effect, and one of these analyses (fraction 1) is well duplicated. The isotopic data on the three coarse-grained fractions therefore imply that an inherited older component is present. These three fractions are not perfectly aligned (as might be expected if variable amounts of inheritance are present in such small samples) yet the upper intercept off-set on the chord to which they best fit is some 30 Ma older than that for the finer fractions. The existence of visible cores in the coarse zircons, and the fact that this part of the Nanambu Complex is of *S*-type granitic origin (Ferguson *et al.*, this volume), are consistent with this inheritance interpretation. A more precise age for the coarse fractions or their cores cannot be given, except they are at least 2500 Ma old.

It might be argued that the finer zircon fractions which define the 2470 Ma chord are in fact less reliable age indicators than the coarser fractions, because they would be more influenced by effects of the 1800 Ma (see below) metamorphism. Such effects could include the formation of new zircon grains and overgrowths, or the addition of U or loss of Pb at the time of metamorphism. The presence in the same rock of anhedral (?recrystallised) monazite which has a $^{207}Pb/^{206}Pb$ age (nearly concordant) of 1865 Ma (Table 1, Fig. 3) does suggest that U and Pb were mobile at or near the time of metamorphism. However, the linearity of the 5 fine zircon data points on the concordia plot, and their apparent inertia from the 1800 Ma metamorphism (as the lower intercept age is 1362 ± 80 Ma), suggests that the resultant chord does have real age significance. For these reasons and because these finer fractions are free of visible cores, their interpreted age of 2470 $^{+47}_{-46}$ Ma is considered to be the age of magmatic crystallisation of the zircons, approximating the emplacement age of this part of the Nanambu Complex.

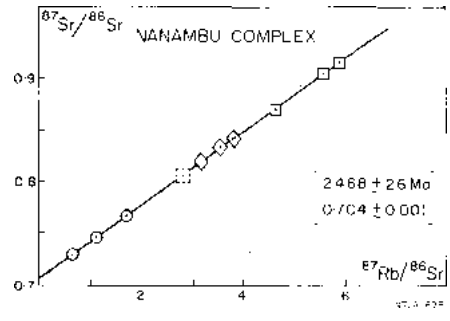


Figure 4. Rb-Sr isochron diagram of total-rock analyses of late-Archaean gneisses of the Nanambu Complex.

b) Rb-Sr total-rock data

The antiquity of the granitoid at 'Granite Hill', as well as other scattered low outcrops of granitic gneiss in the central and western parts of the Nanambu Complex (Fig. 2) has also been established by the use of Rb-Sr total-rock data (Table 2). Ten samples from 5 widespread localities define the oldest Rb-Sr isochron (model 3, mean square of weighted deviates (MSWD) 3.9). The isochron (Fig. 4) has an age of 2468 ± 26 Ma, and an initial $^{87}Sr/^{86}Sr$ of 0.704±0.001.

Because of the agreement of the U-Pb

Sample	Rb ppm	Sr ppm	$^{87}Rb/^{86}Sr$	$^{87}Sr/^{86}Sr$
LEAST-DISTURBED LATE-ARCHAEAN ORTHOGNEISSES				
7212.4006	177.7	182.5	2.8473	0.80515
7212.4009A	145.4	250.5	1.7316	0.76490
4009B	90.6	231.7	1.1337	0.74545
4009D	52.4	221.6	0.6835	0.72857
7212.4043A	159.0	120.8	3.8606	0.84078
	156.7	118.7	3.8615	0.84158
4043B	157.3	128.6	3.5765	0.83308
4043H	146.8	133.2	3.2025	0.81880
7212.4015	242.4	150.6	4.7174	0.87307
4015A	246.8	123.7	5.8705	0.91403
7212.4016	237.9	120.5	5.6881	0.90777
ISOTOPICALLY MODIFIED NANAMBU ORTHOGNEISSES*				
7212.4048B	136.8	94.7	4.2791	0.84562
4048D	141.9	93.7	4.3734	0.85449
4048F	275.2	85.2	9.5814	0.99300
	276.0	85.2	9.6117	0.99401
7212.4086A (163')	18.9	546.6	0.0998	0.71694
4086B (154')	133.6	429.2	0.9013	0.73651
4086C (159')	77.1	248.6	0.2572	0.72066
4086G (162')	40.3	921.3	0.1265	0.71816
4086D (177')	167.6	660.4	0.7345	0.73048
4086E (183')	49.8	577.7	0.2517	0.71700
4086I (182')	137.3	408.3	0.9735	0.73534
7212.4003A	262.2	67.8	8.8941	1.03239
4003D	245.5	71.5	10.318	1.08191
4003H	359.6	78.4	13.672	1.16721
7212.4004A	396.8	48.5	25.449	1.50568
	386	47.5	25.781	1.50427
4004B	217.4	57.7	11.315	1.11120
4004C	379.4	72.6	15.088	1.24509
4004D	409.3	78.3	15.388	1.23103
7212.4035A	260.9	78.6	9.896	1.04212
4035B	344.4	88.4	11.662	1.08569

*4040F and 4004 are micaceous pegmatoidal gneisses
4048B,D and 4003 are muscovite-rich gneisses.
Others are mainly biotite-granitic gneisses (± garnet, ± amphibole).

Table 2. Rb-Sr total-rock data from the Nanambu Complex.

zircon and Rb-Sr total-rock systems, and because of the widespread locations of the Rb-Sr samples, we regard the 2470 Ma result as a regionally significant age for the primary formation of Nanambu Complex granitoids.

Post-Archaean apparent ages in the Nanambu Complex

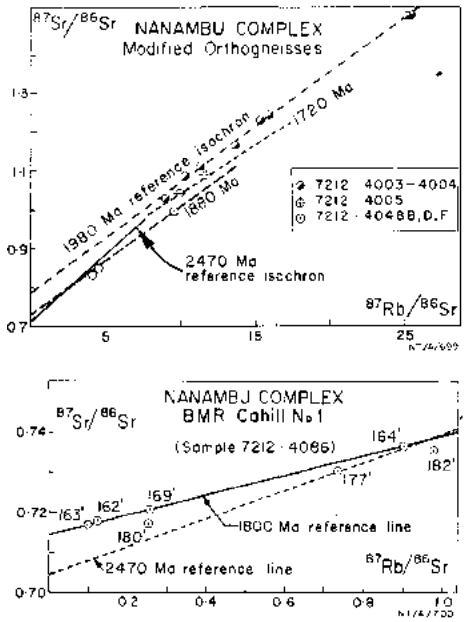
Other parts of the Nanambu Complex that have been studied do not yield this late Archaean age, but nevertheless retain clear isotopic evidence of such a pre-history. Such rocks have undergone metasomatism and partial or complete isotopic mixing during the 1800 Ma metamorphism, and on a local outcrop (or smaller) scale there has been a tendency towards isotopic homogenisation, which masks (but does not obliterate) the primary age.

Rb-Sr analyses are shown in table 2 and Fig. 5A of two muscovite gneisses (4048B, D) and a muscovite-bearing pegmatoidal rock (4048F) sampled from the 2468 Ma 'Granite Hill' locality. These rock types fall significantly below the 2468 Ma isochron, and suggest a younger (rotated) isochron with a slope corresponding to an apparent age of 1880 Ma and a high initial ratio of 0.733. The presence of recrystallised muscovite implies Rb addition as the chief mechanism of updating of these rocks, although some loss of daughter Sr probably also occurred.

Further examples of isotopically

Sample		Rb ppm	Sr ppm	$^{87}Rb/^{86}Sr$	$^{87}Sr/^{86}Sr$	Rb-Sr (K-Ar) Age (Ma) (Ri=0.705)
7112.1141	Musc.	466.2	28.1	54.531	2.12397	1809 (1815)
	Bio.	802.6	12.0	371.83	10.2487	1785 (1797)
7212.4003A	Musc.	741.0	13.3	295.30	9.30892	2023
	Bio.	1371.7	14.4	900.57	23.9948	1798
7212.4004A	Musc.	697.0	10.9	357.13	10.3388	1875
	Bio.	681.5	8.85	494.05	13.1997	1759
7212.4006	Bio.	860.4	11.4	479.70	13.0805	1794
7212.4009A	Bio.	598.9	8.20	451.342	12.3735	1797

Table 3. Rb-Sr data and ages of muscovites and biotites from the Nanambu Complex.



Figures 5A, 5B. Rb-Sr isochron diagrams of total-rock analyses of isotopically modified Nanambu Complex gneisses, with the slope (shown for reference) of the 2470 Ma gneiss isochron.

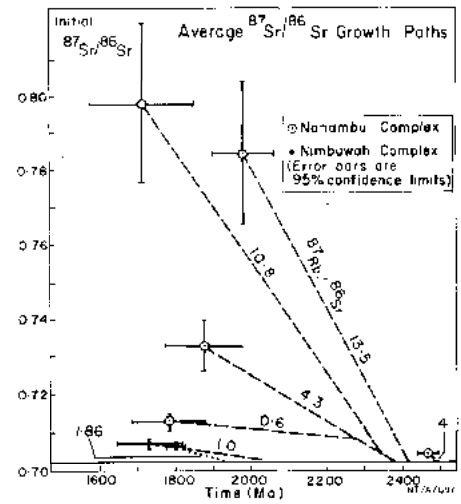


Figure 6. $^{87}Sr/^{86}Sr$ evolutionary paths for various total-rock suites from the Nanambu Complex (open circles) and Nimbuwah Complex (solid dots). Slope of each path is determined by averaged $^{87}Rb/^{86}Sr$ ratio shown for each suite. Error bars are the 95 percent confidence limits.

modified Rb-Sr systems within the Nanambu Complex are now documented. Gneiss samples from a drill hole (BMR Cahill No. 1, 9km WNW of Ranger 1) plot approximately about two sub-parallel 1800 Ma isochrons having high initial $^{87}Sr/^{86}Sr$ ratios of 0.711 and 0.715 (Fig. 5B). In like manner, the young two-point isochron for a granite-gneiss outcrop near the South Alligator River (4005) is demonstrably a metamorphosed late Archaean rock because of the high indicated R_i of 0.80 ± 0.02 (Fig. 5A). A large pavement of leucogneiss, cut by pegmatoidal veins and mica-rich schlieren (4003, 4004; 6km south of Munmarlary) exhibits similar Rb-Sr systematics (Fig. 5A, secondary isochron, apparent age 1980 ± 92 Ma, R_i 0.785 ± 0.020) attributed to incomplete isotopic homogenisation of late-Archaean rocks in the ca. 1800 Ma amphibolite-grade regional metamorphism.

None of these modified Rb-Sr isochrons are considered to define a discrete event, because isotopic equilibration of the total-rock systems cannot be demonstrated. Alkali metasomatism and redistribution of radiogenic Sr are the processes which led towards Rb and Sr homogenisation on the outcrop scale. Despite the effects of this metamorphism, there is sufficient sampling to show that all the modified gneisses retain the imprint of their 2500 Ma pre-history. This is illustrated in a strontium-evolution diagram (Fig. 6) which allows extrapolation (assuming an average $^{87}Rb/^{86}Sr$ for a particular suite) back in time for each Rb-Sr system. All five of the modified Nanambu gneiss systems require an interpretation which involves primary derivation from a late-Archaean protolith, ca. 2500 Ma old.

Mica ages from the Nanambu Complex

Rb-Sr and K-Ar ages for muscovites and biotites verify the importance of the 1800 Ma event (Tables 3 & 4). Six K-Ar ages on both micas form a tight group between 1791 and 1815 Ma, with a mean of 1799 ± 9 Ma. Most of the biotite Rb-Sr ages show good agreement with the K-Ar ages in this range, but the muscovite Rb-Sr ages from the outcrop southeast of Munmarlary (4003A, 4004A)

possess inherited (pre-1800 Ma) and variable radiogenic strontium, indicated by their old ages of 1875 and 2023 Ma.

In summary, it is clear that most of the Nanambu Complex micas have mainly responded to the 1800 Ma regional metamorphism, as has the U-Pb system in monazite. However, total-rock systems either record their 2470 Ma initial formation, or show a disturbed isotopic evolution which can be traced back to the same late-Archaean event.

Sample	Mineral	Avge % K	$\frac{^{40}Ar^*}{^{40}K}$	$\%^{40}Ar^*$	K-Ar Age (Ma)
7112.1065	Biotite	8.76	0.17833	99.9	1791 ± 35
7112.1140	Muscovite	8.43	0.17585	99.8	1803 ± 35
7112.1143	Muscovite	8.96	0.17466	99.9	1793 ± 35
	Biotite	6.36	0.17592	99.8	1800 ± 35
7112.1141	Muscovite	8.75	0.17817	99.9	1815 ± 35
	Biotite	6.97	0.17541	99.9	1797 ± 35

Table 4. K-Ar mica ages on gneisses from the Nanambu Complex.

EMPLACEMENT OF LOWER PROTEROZOIC GRANITOID ROCKS

The Nimbuwah Complex is another terrane of metamorphosed granitoid and metasedimentary rocks, and covers 2500km² in the north east of the Alligator Rivers region. The meta-igneous rocks have amphibolite-to granulite-facies assemblages and are considered to be solely of *I*-type origin (Ferguson *et al.*, this volume). They are coarse porphyroblastic granitic gneisses, banded medium-grained hornblende-biotite-tonalitic gneisses, mafic pyroxene-granulite gneisses, and several migmatitic variants. There is a transition from metamorphosed Lower Proterozoic supracrustal rocks, through migmatite, to true granitoids and deep-seated granulites. Several workers have suggested that the granitoid rocks result from partial melting of the supracrustals; however, they may represent juvenile igneous material extracted from much deeper levels. One of the aims of this isotopic study is to test these hypotheses. Outcrops of all these phases have been studied using Rb-Sr techniques, and the two main granitoid types and a mafic granulite have also been the subject of zircon U-Pb investigation.

A suite of detrital zircons from the metasedimentary units in the Nimbuwah Complex, south of Nabarlek in the Myra Falls area, has also been measured, and those data are given later in dealing with the Lower Proterozoic sequence.

U-Pb zircon data

a) Granitic rocks

A coarse porphyroblastic granitic gneiss (7212.4081A), and a medium-grained biotite-rich tonalitic gneiss (7212.4081C) which it invades, were selected as representing two dominant, but contrasting igneous rock types of the Nimbuwah Complex. Both samples are hornblende-bearing *I*-type granitoids typical of much of the Complex between the Goomadeer River and Cooper Creek. Both suites of zircons consist of colourless, magmatically zoned euhedral grains with no evidence of older cores.

Thirteen relatively non-magnetic size fractions from four size populations have been analysed (Table 1). Uranium concentrations range from 300 to 440 ppm, and are generally 10 to 30 percent higher in the more mafic rock (4081C). Within the non-magnetic fractions of each zircon population, there is a systematic increase in U from the coarsest to finest grain sizes. The disposition of the data points on the concordia plot (Fig. 7A) does not, however, bear any consistent relationship to U content, except that the less magnetic fraction of any particular size has less U and is always more concordant.

The U-Pb data for twelve fractions define an unambiguous discordance pattern, the chord to which gives an upper intercept with concordia at 1866 $^{+8}_{-7}$ Ma, and a lower intercept at 421 ± 75 Ma. This pooled age is not distinguishable from the independently regressed age

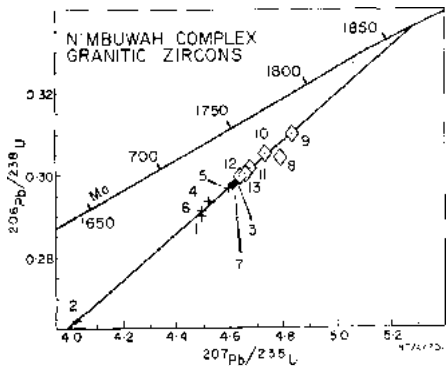


Figure 7A. U-Pb concordia diagram for zircons from the Nimbuwah Complex granitoids. Sample 7212.4081A marked as crosses, 7212.4081C as diamonds. Numbers refer to the analyses in table 1.

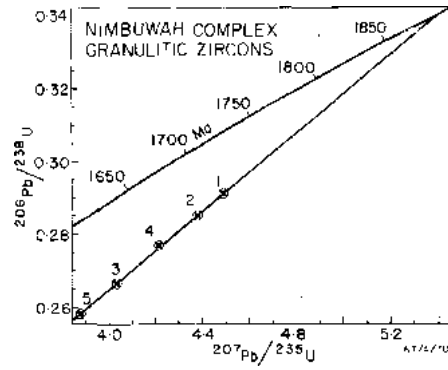


Figure 7B. U-Pb concordia diagram for zircons from the Nimbuwah Complex granulite sample 7312.1243.

result of either the 4081A or 4081C populations. The igneous character of these rocks, the zircon morphology, and the linear distribution of the data, suggest a simple cogenetic suite. The 1866 $\pm\frac{8}{9}$ Ma age cannot therefore be interpreted as anything other than the time of primary magmatic crystallisation.

This pooled age does not include one aberrant point (4081C - 250 NM2, fraction 8), which has a $^{207}Pb/^{206}Pb$ age and an approximate trajectory age on concordia, some 20 Ma older than the remainder of the population. It will be seen that such an age (1885 Ma) is not inconsistent with the granulite zircon age from the Nimbuwah Complex. This agreement may be fortuitous, although it has been suggested by Ferguson *et al.* (this volume) that the granulites may represent the deep precursors or restite material from which the granitic melts were initially derived in the lower crust.

The zircons from the more mafic tonalitic rock, 4081C, are a more concordant population than those from 4081A, the granitic gneiss. This is despite the fact that uranium concentrations in 4081C are 10-30 percent higher. Radioactivity of zircons is therefore not of overriding importance in determining the degree of discordance, but rather the rock chemistry must have affected the alteration processes that led to different amounts of Pb loss from these zircons.

b) Granulite rocks

The granulites of the Nimbuwah Complex are mainly confined to the eastern Beatrice Inlier (Fig. 1). The granulites contain two pyroxenes, garnet, quartz, plagioclase, biotite, and accessory zircon. The various size and magnetic fractions of zircons extracted from one of the granulites (7312.1243) are euhedral, zoned, and clear, and generally similar to the zircon populations of the Nimbuwah granitic rocks. However, the U concentrations of the granulite zircons are much higher (550 to 715 ppm), and there is a direct correspondence between grainsize, U content, and degree of discordance (Table 1 & Fig. 7B).

Four of the five fractions form an excellent linear array having an upper intercept age of 1886 ± 5 Ma, and a lower intercept with concordia at 555 ± 21 Ma. Inclusion of the -75 NMO data (fraction 4) does not significantly affect these intercept ages, but it increases the 2 sigma errors on the ages by a factor of 4. Once again, our interpretation of this result relates it to an age of zircon crystallisation and granulite formation.

The apparent 20 Ma difference between this age and the 1866 Ma granitoid ages is real, but geological conclusions drawn from this observation should be constrained by remembering

Sample	Rb ppm	Sr ppm	$^{87}Rb/^{86}Sr$	$^{87}Sr/^{86}Sr$
GRANITIC ROCKS				
7212.4062	90.3	410.9	0.6355	0.72255
7212.4063B	147.8	319.9	1.3378	0.73971
4063E	163.9	324.0	1.4659	0.74421
4053G	145.5	336.2	1.2530	0.73857
7212.4066B	146.1	296.8	1.4164	0.74339
4066C	147.3	280.3	1.5225	0.74768
4066F	134.9	309.9	1.2605	0.74014
4066G	66.9	449.1	0.4302	0.71815
7212.4069A	214.5	238.3	2.6163	0.77447
4069B	147.8	314.5	1.3612	0.74333
4069C	216.5	300.8	2.0894	0.76209
4069G	183.1	293.7	1.8088	0.75483
4069I	195.4	381.5	0.7992	0.72783
4069J	205.6	161.3	3.7136	0.80110
7212.4082	342.0	138.7	7.2508	0.99494
7412.4008A	131.7	391.1	0.9746	0.73160
4008B	179.2	301.2	1.7252	0.75067
4008C	195.3	271.1	2.0917	0.76030
4008F	233.1	154.8	4.3961	0.82010
7412.4009D	178.4	227.0	2.2815	0.76256
4009E	192.3	399.3	1.3953	0.74141
4009T	101.1	267.9	1.0924	0.73462
4009G	182.2	265.0	1.9954	0.75787
4009H	151.5	329.5	1.3315	0.74024
4009I	278.6	196.1	4.1450	0.81378
4009J	126.4	434.0	0.8426	0.72696
4009L	198.5	244.5	2.3575	0.76547
4009N	148.8	349.7	1.2323	0.73833
4009O	208.4	142.6	4.7646	0.81752
4009P	198.8	279.0	2.0679	0.75832
GRANULITE ROCKS				
7412.4006A	73.9	426.3	0.5011	0.71910
4006C	157.3	763.1	1.7334	0.75024
4006D	120.5	309.0	1.1293	0.73559
4006E	177.1	72.5	7.1626	0.87193
4006F	58.1	366.7	0.4579	0.71811
4006G	11.5	471.7	0.0704	0.70944

Rb and Sr concentrations measured by XRF for samples of prefix 7212.

All other concentrations measured by isotope dilution.

Table 5. Rb-Sr total-rock data for the Nimbuwah Complex.

Outcrop No.	No. of Samples	Isochron Regression		
		MSWD	Age Ma	Initial $^{87}Sr/^{86}Sr$
7212.4066	4	11.3	1834 ± 150	0.7068 ± 0.0017
7212.4069	6	11.5	1795 ± 86	0.7075 ± 0.0018
7412.4008	4	0.72	1793 ± 45	0.7064 ± 0.0011
7412.4009	11	15.6	1794 ± 60	0.7057 ± 0.0014
7412.4006	5	33.0	1730 ± 95	0.7071 ± 0.0013
All samples, except the granulites (7412.4006)	30	25.3	1800 ± 24	0.7064 ± 0.0006

Table 6. Rb-Sr total-rock isochron regression results for the Nimbuwah Complex.

that the Beatrice Inlier granulites are some 70km southwest of the 1866 Ma granite localities. The zircon data indicate the *I*-type granitoid development and crystallisation of granulitic assemblages at depth are stages in the one magmatic episode.

There is a further significant single U-Pb age (published by Hills & Richards, 1976) on a uraninite grain from a pegmatitic veinlet found in drill core at the Tadpole Prospect, in the northwestern part of the Nimbuwah Complex (Fig. 1). The analysis is virtually concordant, giving a $^{207}Pb/^{206}Pb$ age of 1855 Ma. This is coincident with our zircon results, and supports the present interpretation involving the genesis of igneous rocks in the Nimbuwah Complex at about this time.

These events recorded by U-Pb systems are seen as lower crustal precursors of the 1800 Ma metamorphic event, which is manifested in the following Rb-Sr and K-Ar results on both Nimbuwah plutonic rocks and host supracrustal rocks.

Rb-Sr total-rock data

Various granitoid rock types from eight sites within the Nimbuwah Complex have been studied (Fig. 1, Table 5). Most of the sites are in the northeastern part of the Complex, and the granulites are from the Beatrice Inlier in the southern part. The individual sites were selected to contain rock types with a suitable dispersion in Rb/Sr. For a single outcrop site, one can usually assume that each sample became closed to Rb and Sr at the same time, and it is likely that all samples shared the same initial $^{87}Sr/^{86}Sr$.

Rb-Sr isochron results from individual sites and the combined sites are summarised in table 6. The fit of the individual isochrons is comparable to that of the combined isochron involving all 30 samples (Fig. 8), and the ages and initial ratios are the same to within the stated uncertainties.

The regressions fit various of the McIntyre *et al.*, (1966) models, and the pooled 1800 ± 24 Ma age is appropriately a model 4 result, which suggests a combination of geological factors as responsible for the observed disposition of the data. The pooled age denotes a time at, or close to, the peak of high-grade metamorphism at which Rb and

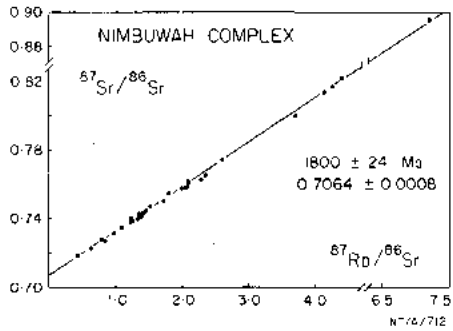


Figure 8. Pooled Rb-Sr isochron diagram of total-rock analyses of Nimbuwah Complex granitoids.

Sr became fixed in the various samples. Given our knolwedge (from the zircon U-Pb results) of the 70-80 Ma pre-metamorphic history of these granitoids, we can conclude that the $^{87}Sr/^{86}Sr$ ratio of 0.7064 is, in part, an artifact of metamorphic redistribution, and hence is only a maximum value for the igneous source. Using the average measured $^{87}Rb/^{86}Sr$ of 1.86 derived from the 30 Nimbuwah Complex granitoids as an estimate, we can subtract the inferred 80 Ma radiogenic component, and find that the source-rock initial $^{87}Sr/^{86}Sr$ would have been about 0.7043. This $^{87}Rb/^{86}Sr$ estimate probably errs on the low side, since high-grade metamorphism probably causes a decrease in Rb/Sr (Moorbath, 1975). However, by arbitrarily increasing the average $^{87}Rb/^{86}Sr$ by 15 percent (to 2.13), the inferred initial $^{87}Sr/^{86}Sr$ of the source would change only slightly, to 0.7040.

The Rb-Sr data on the 5 gneissic granulites from the Beatrice Inlier (7412.4006, Table 5) yield an isochron (4006E, a jointed pegmatite vein, is not included) of 1730 ± 95 Ma. This is somewhat equivocal on its own, but is nevertheless within the limits of the regionally determined 1800 ± 24 Ma age of the principal metamorphic event.

Implications of the isotopic data

The isotopic data have revealed that three contrasting granitoids of the Nimbuwah Complex - exclusively of *I*-type origin (Ferguson *et al.*, this volume) - initially intruded the Lower Proterozoic supracrustals, and some 70 to 80 Ma later were metamorphosed along with the supracrustals, enabling all Rb-Sr total rock systems to be reset at ca. 1800 Ma. The normal intrusive granitic rocks, exemplified by the zircon-dated samples 7212.4081A and C, had their zircon U-Pb systems evolve from 1866 $^{+8}_{-4}$ Ma. The pyroxene-granulite gneisses give a U-Pb zircon age about 20 Ma older than this, but they are considered to be part of the same igneous generation, which, instead of reaching the upper crust and crystallising as normal intrusives, were cooled early and trapped in the lower crust - at 700-800°C and 25-30km, (Ferguson, this volume) - to crystallise with magmatic igneous textures, yet with typical granulite facies mineralogy. These magmatic developments are considered to be forerunners of the main 1800 Ma metamorphism of the Pine Creek Geosyncline.

The isotopic data demonstrate beyond doubt that the Nimbuwah Complex rocks cannot have been derived by the reworking of earlier gneisses such as those exposed in the Nanambu Complex, or by the anatexis of metasediments such as those of the Lower Proterozoic sequences. Neither the zircon morphology, nor the U-Pb or Rb-Sr systematics, give any hint of ancient Archaean components in the Nimbuwah Complex, indicating that these rocks are some 600 Ma younger than those of the nearby Nanambu Complex granitoids, and have had an entirely different evolution. This is illustrated in figure 6 by the relative $^{87}Sr/^{86}Sr$ growth paths, calculated from the mean of the measured $^{87}Rb/^{86}Sr$ values for each individual outcrop site.

These granitoids, as deep-seated precursors to, yet as integral parts within, the Nimbuwah Complex, can be considered as mainly juvenile additions to the crust at, or close to, the measured age. Their inferred intitial $^{87}Sr/^{86}Sr$ of about 0.704 is slightly higher than suggested from the upper mantle growth line at this time, and hence might allow for minor crustal contamination. However, their relatively constant Sr isotopic composition over the entire Complex, would not support any model calling for major sialic involvement.

1800 Ma REGIONAL METAMORPHISM AND ASSOCIATED POST-OROGENIC GRANITOIDS

Metamorphism

Widespread isotopic effects of the metamorphic event have already been discussed in relation to the Nanambu and Nimbuwah Complexes. In some cases in the former, and in all cases in the latter, pre-existing Rb-Sr systems are reset at or about 1800 Ma.

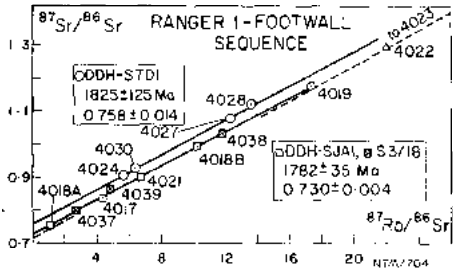


Figure 9. Rb-Sr isochron diagram of total-rock analyses from Lower Proterozoic gneisses and schists of the Ranger 1 'Footwall Sequence'.

Paragneisses and schists of the Lower Proterozoic metasediments have also been metamorphosed to amphibolite-grade assemblages. These units have an inferred stratigraphic age of between 2400 and 1800 Ma, but invariably given measured Rb-Sr (total-rock and mica) and K-Ar (mica) ages of close to 1800 Ma (Tables 7-10). This indicates virtually complete Ar loss and Sr isotopic homogenisation at 1800 Ma, and the sub-parallel Rb-Sr isochrons so generated have high and variable initial $^{87}Sr/^{86}Sr$ ratios. This is illustrated by two Rb-Sr isochrons on the Ranger 1 'Footwall Sequence' (Fig. 9), which have similar ages (1782 ± 35 Ma and 1825 ± 125 Ma) yet entirely different initial $^{87}Sr/^{86}Sr$ (0.730 ± 0.004 and 0.758 ± 0.014). Total rock samples of a pegmatite, which intrudes the 1825 Ma paragneisses in DDH STD-1, have virtually the same Rb-Sr age of 1815 ± 60 Ma, the indicated initial $^{87}Sr/^{86}Sr$ from the two point line being 0.722.

Table 8 summarises the K-Ar mica data on some of the same 'Footwall Sequence' samples, and on other gneisses and schists from Ranger 1 and elsewhere in the Lower Proterozoic metasediments. The 15 biotite and muscovite results are markedly concordant and have a mean (±1 s.d.) age of 1800 ± 11 Ma. The similar Lower Proterozoic sequence, but of somewhat lower metamorphic grade, present at Jabiluka contains muscovite-chlorite schists and muscovite-pegmatites, whose K-Ar ages (Table 9) are virtually identical to the mica ages at Ranger. The mean of the 8 Jabiluka muscovite ages is 1804 ± 7 Ma. Two of these ages are from schists in a mineralized zone of the Mine Sequence (4053, 4054), yet they are consistent with the remainder of the population.

Mica K-Ar ages on biotite and muscovite-chlorite schists near the Nabarlek deposit, are more variable and somewhat younger than in the other Lower Proterozoic metasediments (Table 10). The single biotite age is much younger (1583 Ma), and the muscovite ages range from 1737 to 1791 Ma.The muscovite Rb-Sr age of 1817 Ma and biotite Rb-Sr age of 1733 Ma (Table 7) are also variable, but these and the K-Ar ages are in accord with the usual pattern of radiogenic daughter-product loss, as a result of elevated temperatures in the area after the main 1800 Ma metamorphic event. Increased temperatures were almost certainly due to local contact metamorphic effects of either or both of the Nabarlek Granite and Oenpelli Dolerite, which are younger, major intrusive bodies (see later sections) directly below the Nabarlek orebody. The metamorphic aureole of the Oenpelli Dolerite is though to be at least 50m wide and is known to have reached the pyroxene hornfels facies (Stuart-Smith & Ferguson, 1978).

In summary, there is compelling evidence for advocating an important metamorphic event at or about 1800 Ma. The relevant isotopic systems so affected are: (a) Rb-Sr total-rock and mica, and K-Ar mica, systems in many parts of the Nanambu Complex, (b) all the Rb-Sr total rocks studied in the Nimbuwah Complex, (c) Rb-Sr total rocks and micas, and K-Ar mica systems of most of the studied Lower Proterozoic metasedimentary sequence. The

Sample*	Location	Rb ppm	Sr ppm	$^{87}Rb/^{86}Sr$	$^{87}Sr/^{86}Sr$	Rb-Sr (K-Ar) Age (Ma)
JABIRU TAILINGS DAM, DDH STD1						
7212.4022	16.7m	197.8	18.3	33.958	1.60871	
7212.4023	19.5m	119.1	16.6	21.966	1.29560	
7212.4024	20.5m	295.3	153.0	5.681	0.90730	
7212.4027	22.5m	265.3	69.1	12.353	1.07846	
7212.4028	23.3m	259.4	56.9	13.695	1.12106	
7212.4030	27.7m	237.0	109.5	6.382	0.92471	
JABIRU AIRSTRIP, DDH S3A1						
7212.4017	24.3m	135.1	90.8	4.353	0.83926	
7212.4018A	24.8m	39.6	98.7	1.164	0.75891	
7212.4018B	24.9m	215.1	61.6	10.369	0.99488	
7212.4019	26.4m	259.0	45.7	17.305	1.17376	
7212.4021	33.5m	118.0	51.8	6.707	0.90385	
No. 3 OREBODY, DDH S3/1B						
7212.4037	240.5m	122.0	131.5	2.703	0.79921	
7212.4038	244.8m	201.4	50.4	11.907	1.03480	
7212.4039	248.0m	85.1	50.6	4.929	0.86179	
OTHER LOWER PROTEROZOIC SCHISTS						
7112.1095 Biotite	5 km NE of	654.5	7.8	618.36	16.5255	1778 (1789)
7112.1095 Muscovite	Mt. Basedow	314.3	17.6	59.446	2.2929	1851 (1784)
7023.0050 Biotite	Nabarlek, DDH 47,	411.3	22.1	61.915	2.2520	1733 (1583)
7023.0050 Muscovite	344.1m	229.5	17.3	42.548	1.8220	1817 (1791)
E9670 t.r.	Myra Falls Inlier	93.8	213.8	1.273	0.74600	
Biotite		572.6	27.3	71.58	2.5569	1794
Muscovite		322.5	31.4	32.11	1.5453	1809

*All rock types are micaceous gneisses and schists, except 4022,4023 which are pegmatites.

Table 7. Rb-Sr total-rock data on the Ranger 'Footwall Sequence' (7212-series), and Rb-Sr data on other Lower Proterozoic schists.

majority of these are markedly consistent at ca. 1800 Ma, indicating that the main regional metamorphism of the Pine Creek Geosyncline ended abruptly at this time. Later retrogression and metasomatism, however, locally affected some isotopic systems (see below).

Emplacement of post-orogenic granitoids

High-level granitoids which intrude the metasediments of the Pine Creek Geosyncline are considered on textural grounds to post-date the main regional metamorphism. There are several intrusions, ranging from 3km² to 2800km². Most are felsic, and of *I*-type origin (Ferguson *et al.*, this volume). New Rb-Sr data are presented here for the Jim Jim, Tin Camp, and Nabarlek Granites, the three known late-orogenic granitoids in the Alligator Rivers area. The Nabarlek Granite outcrops 8km east of Nabarlek and has been intersected 400m below the orebody.

Data on the Jim Jim Granite come from both of its northern and southern outcrop regions (Fig. 1), separated by 20km of unconformably overlying Kombolgie Formation sandstone. Rb-Sr data (Table 11) for 8 total-rock samples fit a model 1 isochron (Fig. 10, MSWD 0.89), giving an age of 1732 ± 11 Ma, initial $^{87}Sr/^{86}Sr$ of 0.7072 ± 0.0008. Inclusion of the slightly aberrant sample 4007D increases the age by a few million years, but this is not warranted as the MSWD of the fitted line then increases by a factor of 6.

The Tin Camp Granite is exposed at two centres, near the Caramal prospect 20km southeast of Nabarlek, and near the Beatrice prospect 20km further south (Fig. 1). Most of the six total-rock samples from the Tin Camp Granite are very enriched in radiogenic ^{87}Sr (Table 11). The fitted isochron for the four Beatrice area samples gives an age of 1787 Ma, but as the indicated initial $^{87}Sr/^{86}Sr$ is unrealistically low (0.670 ± 0.016), due to the weighting of the isochron at the low end by sample 9644, we have to assume either that this sample does not belong to the population, or that it has been significantly altered after original emplacement. Therefore, model ages of the remaining samples (1764, 1736 and 1774 Ma)

Sample	Location	Mineral	Avge % K	$\frac{^{40}Ar^*}{^{40}K}$	$\%\ ^{40}Ar^*$	K-Ar Age (Ma)
(a) OUTSIDE MINERALIZED ZONES						
7212.4016	DDH SPS22, 22.9m	Biotite	6.62	0.17696	99.8	1807 ± 30
7212.4022	DDH ST01, 16.7m	Muscovite	8.62	0.18027 0.17754	99.6 99.6	1829 ± 30 1811 ± 30
7212.4023	DDH STB1, 19.5m	Muscovite	8.71	0.17669	99.7	1806 ± 30
7212.4030	DDH STB1, 27.7m	Muscovite	8.84	0.17706	99.8	1808 ± 30
		Biotite	6.50	0.17443	99.5	1792 ± 30
7212.4045	DDH S1/96, 308.0m	Biotite	7.18	0.17467	99.6	1793 ± 30
(b) BELOW NO. 3 OREBODY						
7212.4038	DDH S3/18, 244.8m	Muscovite	8.75	0.17663	99.8	1805 ± 30
7212.4039	DDH S3/18, 245.0m	Muscovite	8.81	0.17749	99.8	1811 ± 30
		Biotite	7.13	0.17647	99.7	1804 ± 30
7212.4039A	DDH S3/18, 245-250m	Muscovite	8.85	0.17437	99.8	1791 ± 30
7212.4041	DDH S3/23, 382.1m	Muscovite	8.78	0.17373	99.8	1787 ± 30
7212.4043	DDH S3/23, 382.4m	Muscovite	8.50	0.17543	99.8	1797 ± 30
(c) OTHER LOWER PROTEROZOIC SCHISTS						
7112.1094		Muscovite	8.99	0.17665	99.9	1805 ± 35
7112.1095		Muscovite	8.68	0.17334	99.9	1784 ± 35
		Biotite	7.82	0.17406	99.9	1789 ± 35

Table 8. K-Ar mica ages from gneisses, schists and pegmatite in the Ranger 1 Footwall Sequence *(a,b)*, and two schists *(c)* 5km NE of Mt. Basedow.

Sample	Location	Mineral	Avge %K	$\frac{^{40}Ar^*}{^{40}K}$	$\%^{40}Ar^*$	K-Ar Age (Ma)
7212.4049	DDH 24, 128.8m	Muscovite	8.58	0.17527 0.17940	99.7 99.7	1796 ± 30 1823 ± 30
7212.4050	DDH 24, 135.3m	Muscovite	8.35	0.17519	99.6	1796 ± 30
7212.4058	DDH 24, 137.6m	Muscovite	8.37	0.17767	99.7	1812 ± 30
7212.4055	DDH 35, 50.2m	Muscovite	8.61	0.17681	99.9	1806 ± 30
7212.4056	DDH P34, 102.4m	Muscovite	8.65	0.17547	99.9	1798 ± 30
7212.4057	DDH 1, 103.6m	Muscovite	8.44	0.17699	99.8	1808 ± 30
7212.4053	DDH 22, 69.3m	Muscovite	8.52	0.17514	99.9	1795 ± 30
7212.4054	DDH 22, 40.1m	Muscovite	8.72	0.17745	99.8	1811 ± 30

Table 9. K-Ar ages from six schists and two pegmatites (4049, 4057) in the Jabiluka One Footwall Schist Series and the Mine Sequence (4053, 4054).

based on an initial $^{87}Sr/^{86}Sr$ of 0.707, may give a more valid average age (±1 s.d.) for the Beatrice area Granites, which is 1758 ± 20 Ma. Analyses of the two Tin Camp Granite samples from near Caramal indicate a common initial ratio of 0.709 ± 0.002, and an age of 1748 ± 18 Ma. Combined with the Beatrice area analyses, the resultant 5-point isochron (Fig. 11) may be interpreted as indicating an average age for the Tin Camp Granite of 1755 ± 15 Ma (initial $^{87}Sr/^{86}Sr$ 0.708 ± 0.003).

The Jim Jim and Tin Camp Granites are therefore only marginally older than other Pine Creek Geosyncline granites, as assessed by Compston & Arriens (1968), but are some 30 to 60 Ma younger than the granite ages reported by Riley (this volume). Although all of these post-orogenic granite ages are consistent with overall geochronological constraints (i.e. they are younger than the 1800 Ma metamorphism which they post-date), we cannot be confident that they are real ages of igneous crystallisation until independent U-Pb zircon ages are measured (see discussion in Page, 1978).

Sample	Location	Mineral	Avge %K	$\frac{^{40}Ar^*}{^{40}K}$	$\%^{40}Ar^*$	K-Ar Age (Ma)
7023.0050	DDH 47, 344.1m	Biotite	7.27	0.14422	99.9	1583 ± 32
		Muscovite	8.34	0.17435	99.8	1791 ± 35
7212.4103	DDH 1, 8m	Muscovite	8.59	0.16980	99.9	1761 ± 30
7212.4104	DDH 1, 18.5m	Muscovite	8.47	0.16617	99.8	1737 ± 30
7212.4105	DDH 207, 14.2m	Muscovite	8.43	0.16759	99.8	1746 ± 30

Table 10. K-Ar ages on schists from Nabarlek.

A cautionary example is illustrated by Rb-Sr data on the Nabarlek Granite: the biotite age (Table 11) indicates emplacement at least 1780 Ma ago, but a secondary, probably metasomatically induced, isochron involving 8 of the 9 total-rock samples (Fig. 12), has an age of 1561 ± 17 Ma, and high initial $^{86}Sr/^{86}Sr$ of 0.726 ± 0.005. This is interpreted as the age of low-temperature alteration of the Nabarlek Granite; it is noted that a still younger chemical alteration is required to account for the isotopic composition of sample 1901.

ESTIMATE OF THE STRATIGRAPHIC AGE OF PINE CREEK GEOSYNCLINE METASEDIMENTS

The ages of the basement granitoids in the Nanambu Complex and the intrusive components of the Nimbuwah Complex indicate that the Lower Proterozoic metasediments are between 2470 and 1870 Ma old.

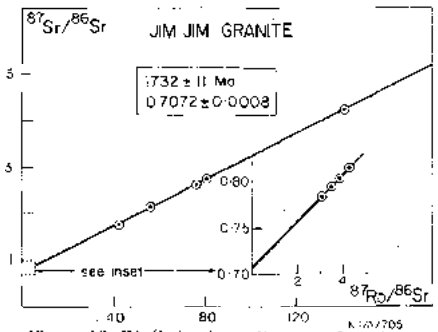


Figure 10. Rb-Sr isochron diagram of total-rock analyses from the Jim Jim Granite.

Sample	Rb ppm	Sr ppm	$^{87}Rb/^{86}Sr$	$^{87}Sr/^{86}Sr$
JIM JIM GRANITE				
JH 4034	238.3	192.9	3.5979	0.79700
JH 4035	207.1	189.4	3.1812	0.78579
JH 4037	227.5	175.5	3.7771	0.80163
JH 4038	233.5	159.3	4.2762	0.81414
7412.4003A	426.9	21.8	141.451	4.22304
7412.4003E	414.0	18.5	76.841	2.61387
7412.4003D	394.5	23.0	55.546	2.15756
7412.4003A	356.8	15.7	80.946	2.72740
7412.4003C	393.3	29.4	47.637	1.76877
TIN CAMP GRANITE (BEATRICE)				
E 5644	106.5	16.2	19.90	1.1823
E 5645	411.5	18.5	76.48	2.6473
E 5649	329.6	16.8	63.87	2.3008
E 5651	592.9	14.2	172.0	5.0951
TIN CAMP GRANITE (CARAVALL)				
E 5667	375.2*	137.7	6.718	0.87767
E 5669	458.8	5.544	579.2	15.766
NABARLEK GRANITE				
F 1901	318.5	18.7	54.65	1.8573
	321.6	19.3	54.44	1.8565
E 1913	337.9*	149.7	6.623	0.87106
E 1928	369.1*	170.7	6.352	0.86020
E 1928 B10	1964.0	27.9	409.3	11.1975
N636	362.3	14.1	98.51	2.7049
N537	306.4	12.5	83.09	2.5493
N639	333.7	64.7	15.42	1.0714C
NAB3/4			17.026**	1.1158
NAB3/5			9.329**	0.9364
NAB3/6			8.454**	0.9126

* Rb,Sr determined by XRF

**Rb/Sr determined by XRF by AMDL for Queensland Mines Ltd.

Table 11. Rb-Sr data on total-rock and biotite samples from post-orogenic granitoids.

The source of the Lower Proterozoic sediments has mostly been assumed to be a basement of Nanambu-type and age. To substantiate this, and to check the maximum age of the sediments, U-Pb isotopic measurements were made on a suite of detrital zircons from a Lower Proterozoic schist in the Myra Falls Inlier (7712.4001, Fig. 1). The rock is a contorted, quartz-muscovite-garnet schist in which there are concordant and discordant synkinematic quartz-rich lenticles. There is no evidence of partial melting of the rock or of the outcrops nearby. In general, the sample is typical of the amphibolite-grade supracrustals, which, although mapped here as paragneiss and schist of the Nimbuwah Complex, are probably equivalents of the Cahill Formation, the lower part of which hosts most of the uranium deposits of the region (Needham & Stuart-Smith, 1976). Ferguson (this volume) estimates that the temperature/pressure of recrystallisation of these rocks is 600 + 50°C and 5-8 kb.

The zircons are a generally sub-rounded, clear, colourless population; a few euhedral grains remain, but overall the population is detrital in origin. Uranium contents (Table 1) are variable but moderately low (300 to 680 ppm), and in general smaller grains are more U-rich. Analytical data are discordant on the U-Pb concordia diagram (Fig. 13), and despite the fact that the zircons are detrital, the data still indicate a fairly uniform apparent age for the population. Taken at face value, the chord trajectory through all data points indicates an age of 2440 ± 40 Ma. This agrees with the established age of the basement Nanambu Complx, and essentially confirms it is provenance for this part of

the Lower Proterozoic sediments. The data especially emphasise the stability of the U-Pb isotopic systems in zircon, since they are not at all perturbed during the major 600°C amphibolite-grade metamorphism which recrystallised most other minerals at 1800 Ma.

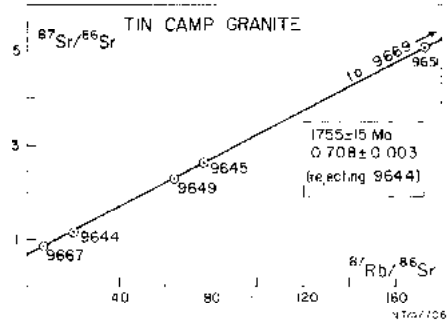


Figure 11. Rb-Sr isochron diagram of total-rock analyses from the Tin Camp Granite.

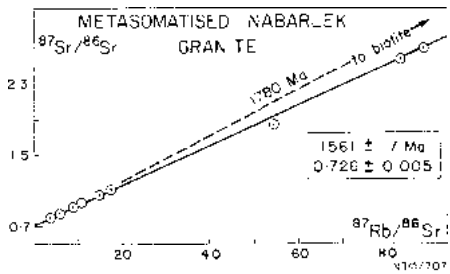


Figure 12. Rb-Sr isochron diagram of total-rock analyses from the metasomatically altered Nabarlek Granite.

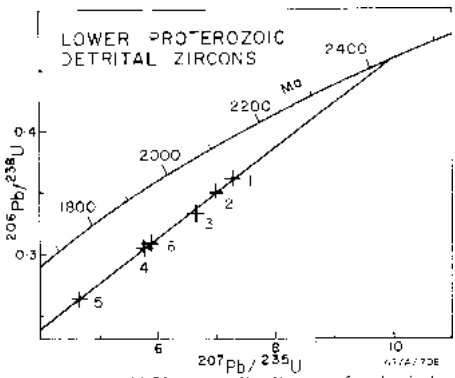


Figure 13. U-Pb concordia diagram for detrital zircons from a Lower Proterozoic (?Cahill Formation) schist (7712.4001) in the Myra Falls Inlier. Numbers refer to the analytical data in table 1.

Certain additional estimates can be made from the Rb-Sr data regarding the age of actual sedimentation of the Lower Proterozoic rocks. These models assume no bulk loss of Rb and Sr at the time of isotopic homogenisation (metamorphism), and employ an average Rb/Sr based on the measurements for each suite. With such modelling, and using an assumed pre-metamorphism initial $^{87}Sr/^{86}Sr$ of 0.71, the maximum depositional age of the 'Footwall Sequence' at Ranger 1 is estimated at between 2000 and 2200 Ma. If either the Rb/Sr or initial $^{87}Sr/^{86}Sr$ of the sediments are higher than estimated, then the resultant model 'depositional ages' will be younger than this.

These findings based on the evolution of Rb-Sr isotopic systems, have relevance to interpretation of the gneisses and schists underneath the uranium deposits. For example, the 'Footwall Sequence' at Ranger 1 is commonly termed Nanambu Complex. Although this terminology concurs with the broad definition of the Complex (Needham & Stuart-Smith, this volume), it is plain that the 2.0 to 2.2 Ga 'Footwall Sequence' is not crystalline basement to the Lower Proterozoic uranium-bearing deposits; it is part of the accreted Lower Proterozoic leucocratic gneisses, a far more juvenile formation, and a *derivative* of the more primitive, late-Archaean (2.47 Ga) Nanambu Complex.

Similar Rb-Sr models are not appropriately applied to the chlorite schists and paragneisses of orebody alteration zones of the Cahill Formation, because of the gross metasomatism evident in these areas.

OENPELLI DOLERITE EMPLACEMENT

This tholeiitic intrusive suite is an important time-marker in the geological framework of the region, not only because of its extremely large areal extent (about 20,000km²), but also because it demonstrably postdates the 1800 Ma metamorphism, as well as the post-orogenic (1730 to 1780 Ma) granitic rocks such as the Jim Jim and Nabarlek Granites.

The Oenpelli Dolerite crops out as a number of discordant, ellipsoidal lopoliths over a distance of 200km between the Jim Jim area (in the south), and north of Oenpelli to the coast (Fig. 1). Geological, petrographic and chemical data for these rocks are given in Smart *et al.* (1975), and Stuart-Smith & Ferguson (1978).

This Rb-Sr isotopic study was undertaken on drill-core samples from Nabarlek and two surface samples. At Nabarlek, the sill-like intrusion is 250m thick, and its primary mineralogy is well-preserved, except near the margins. The main sill intrudes Lower Proterozoic schist and paragneiss, and a minor apophysis (also thought to be Oenpelli Dolerite) intrudes the Nabarlek Granite (Anthony, 1975). In the south of the Alligator Rivers region, an intrusion of Oenpelli Dolerite cuts the Jim Jim Granite, and so the age of the latter (1732 ± 11 Ma) is a further maximum constraint on the age of Dolerite emplacement. Below the Nabarlek orebody, as elsewhere, the Dolerite is highly differentiated (ranging from olivine dolerite to quartz gabbro and granophyre), and total-rock analyses (Table 12) have a very suitable dispersion in Rb/Sr. A well-fitted total rock Rb-Sr isochron (Fig. 14, 13 samples, MSWD = 5.6) has values for age and initial $^{87}Sr/^{86}Sr$ (1682 ± 64 Ma, 0.7044 ± 0.0004) that register the time of differentiation and original cooling.

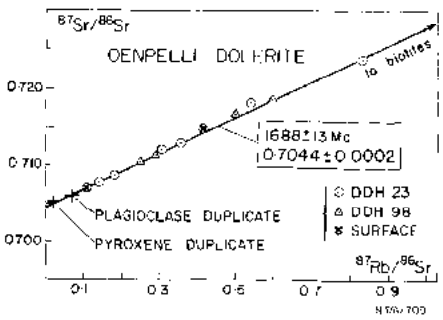


Figure 14. Rb-Sr isochron diagram of total-rock and mineral analyses from the Oenpelli Dolerite.

Plagioclase, clinopyroxene, biotite, and a chloritised biotite fraction were separated from one of the total-rock samples (1894). The resultant internal isochron gives an independent age determination of 1688 ± 19 Ma. In principle, because it is mainly controlled by the biotite, this age should be regarded as a minimum estimate of the emplacement age. However, because it is the same as the total-rock age and has an equally low value for the initial $^{87}Sr/^{86}Sr$, 0.7043 ± 0.0006, it is probable that little or no radiogenic ^{87}Sr has moved from the biotite. The plagioclase and clinopyroxene data lie slightly off the isochron, and the good analytical duplication suggests that these are real effects.

Combination of all the total-rock and mineral data for the Oenpelli Dolerite gives a result of 1688 ± 13 Ma (initial $^{87}Sr/^{86}Sr$ 0.7044 ± 0.0002), which is a reliable estimate of its age of emplacement. Two K-Ar ages on pyroxenes from the Dolerite (Table 13) are some 60 to 90 Ma younger than the Rb-Sr result. It is probable that these younger K-Ar ages are due to post-emplacement loss of a few percent of radiogenic argon. However, K-Ar ages on the Dolerite (4060) 11km northeast of Oenpelli are substantially older than the Rb-Sr isochron age suggesting that this sample contains excess radiogenic argon. The Rb-Sr analysis of this rock lies on the 1688 Ma isochron, but it is not sufficiently radiogenic to allow any model Rb-Sr age comparisons to be made with the argon data. Stuart-Smith & Ferguson (1978) considered that the initial $^{87}Sr/^{86}Sr$ ratio (0.7044) is low enough to be consistent with magma genesis from an uncontaminated tholeiitic source in the upper mantle. However, a value of 0.7044 is actually somewhat higher than the minimum permissible value of 0.703 for the average contemporary mantle at 1700 Ma. Hence the Sr isotopic characteristics, and the fact that the Oenpelli Dolerite is underlain by Archaean and Lower Proterozoic granitoids, are not inconsistent with a minor degree of crustal contamination.

In summary, the 1688 ± 13 Ma age of the Oenpelli Dolerite is compatible with other geological and isotopic evidence, in so far as the Dolerite is known to post date the 1800 Ma metamorphic event, and the 1730 to 1780 Ma post-orogenic granitoids. As the Oenpelli

Sample	Location	Rb ppm	Sr ppm	$^{87}Rb/^{86}Sr$	$^{87}Sr/^{86}Sr$
7212.4100D	DDH 23, 96.6m	44.0	153.7	0.8283	0.72395
7212.4100E	96.7m	52.4	280.4	0.5401	0.71814
6212.4100F	99.1m	28.0	227.6	0.3546	0.71291
7212.4100K	207.9m	13.3	268.6	0.1428	0.70784
E1892	12.2m	30.0	285.0	0.3043	0.71188
E1894	114.0m	18.0	281.6	0.1848	0.70862
E1894 biotite		370.3	11.13	95.97	3.0324
Bio (recalcr.)		315.6	43.9	20.72	1.2074
plagioclase 1		11.6	435.8	0.0770	0.70580
plagioclase 2		14.1	521.1	0.0779	0.70598
pyroxene 1		0.191	22.8	0.0242	0.70520
pyroxene 2		0.183	22.9	0.0231	0.70530
7212.4101B	DDH 98, 45.7m	28.2	136.7	0.5956	0.71869
7212.4101C	46.6m	42.5	246.1	0.4994	0.71676
7212.4101D	56.4m	13.5	271.7	0.1433	0.70793
7212.4101E	60.7m	19.8	194.9	0.2928	0.71144
7212.4101F	66.4m	26.7	307.3	0.2504	0.71067
7212.4060	Surface	11.9	304.9	0.1125	0.70697
E1912	Surface	36.0	250.2	0.4156	0.71473
HIGHLY ALTERED DOLERITE					
E1860	DDH 3, < 12m	64.4	10.3	17.97	1.0572
		65.3	11.9	15.88	1.0151
E1891	DDH 23, < 12m	107.5	10.3	29.99	1.3552
		112.2	10.7	30.23	1.3334

Table 12. Rb-Sr data on the Oenpelli Dolerite. All are total-rock analyses except where specified

Dolerite is overlain by sandstone of the Kombolgie Formation, the 1688 Ma age is a realistic maximum age for deposition of this Formation. Further constraints on the age of the Kombolgie Formation are presented later in the paper.

Highly altered samples of Oenpelli Dolerite

Near the margins of the Oenpelli Dolerite localised metamorphism gives rise to serpentinitic rocks and assemblages dominated by sericite, chlorite, albite and prehnite (Anthony, 1975; Stuart-Smith & Ferguson, 1978); two such samples (Table 12) from near the top of the sill have had their Rb/Sr chemistry grossly changed and are much younger than the 1688 Ma age for the unaltered dolerites. The altered dolerites do not lie on a line through 0.7044, indicating that the ages of the two samples were altered by different amounts. The model ages for the two samples, relative to 0.7044, are 1367 Ma and 1481 Ma. No age can be given for the alteration process (which on this evidence might have been continuous over a long period) other than younger than 1367 Ma.

ISOTOPIC EVIDENCE FOR LOCALISED METASOMATIC ALTERATION EVENTS

1600 Ma evidence

In the vicinity of the U deposits of the Alligator Rivers region, the host metasediments are affected by extensive chloritisation. The close association between U mineralisation and Mg-metasomatism is ubiquitous. The chloritisation has a variety of forms, including retrograde chlorite associated with sericitic alteration, and 'replacive' or massive chlorite, genetically linked with specific mineralisation features (Anthony, 1975; Hegge, 1977).

At Nabarlek, mineralisation zone schists, and the margins of the Oenpelli Dolerite and Nabarlek Granite immediately below mineralisation, are extensively chloritised and sericitised. If these effects are a result of the same metasomatic event, that event must be younger than 1688 ± 13 Ma, the age of the Dolerite.

Sample	Location	Mineral	Avge % K	$\frac{^{40}Ar^*}{^{40}K}$	$\%^{40}Ar^*$	K-Ar age (Ma)
AMPHIBOLITE DYKES						
7212.4031	Ranger 1, DDH 51/84, 49.7m	Amphibole	0.440	0.15193	97.7	1638 ± 25
7212.4058A	Jabiluka, DDH 24, 204m	Amphibole	0.325	0.15348	97.8	1647 ± 25
Nab. 23/3	Nabarlek, DDH 23, 115.8m	Amphibole	0.468	0.15634	98.6	1670 ± 25
OENPELLI DOLERITE						
Nab 23/1	Nabarlek DDH 23, 47.8m	Pyroxene	0.0247	0.15113	88.3	1633 ± 65
Nab 23/2	Nabarlek DDH 23, 63.9m	Pyroxene	0.0219	0.14704	89.5	1604 ± 35
7212.4060	11 km N.E. of Oenpelli	T.R.	0.419	0.21893 0.22335	97.8 98.1	2060 ± 50 2083 ± 50
		Plagioclase	0.598	0.19441	98.1	1918 ± 50

Table 13. K-Ar ages on amphibolitic dykes and Oenpelli Dolerite.

Sample	Rb ppm	Sr ppm	$^{87}Rb/^{86}Sr$	$^{87}Sr/^{86}Sr$	Rb-Sr model age (0.705)
SERICITE-CHLORITE SCHISTS - NABARLEK					
E1864	446.4	25.6	52.22	2.1025	1699
E1880	198.0	26.4	22.81	1.7584	1688
E1856	101.5	29.3	10.22	0.93396	1560
E1863	136.6	42.2	9.55	0.92818	1627
E1893	109.3	5.87	34.34	1.4653	1553
	111.6	12.8	26.61	1.2825	1512
	106.9	6.44	39.75	1.5973	1565
E1852	67.7	65.4	3.010	0.77528	1625
E1867	111.0	10.7	32.23	1.4647	1641
	112.0	12.4	27.73	1.3563	1635
E1877	102.6	38.9	16.29	1.0860	1628
	105.1	21.0	14.96	1.0557	1612
E1857	155.5	76.0	5.99	0.84582	1648
SERICITE-CHLORITE SCHISTS - JABILUKA 1					
7212.4050	133.4	11.0	38.09	1.60518	1647
7212.4051	163.8	17.3	29.12	1.37468	1601
7212.4053	99.6	9.4	32.70	1.41230	1617
7212.4054	80.3	7.0	35.99	1.59290	1736
7212.4055	101.1	3.7	94.47	2.72650	1491
7212.4056	108.6	7.2	48.19	1.79569	1576
7212.4058	119.0	11.7	31.55	1.46023	1666
7212.4049*	415.2	26.2	52.18	2.14354	
7212.4057*	333.2	17.3	63.11	2.22095	
MINERALISED SERICITE-CHLORITE SCHISTS - NABARLEK ORE ZONE					
E1872	21.4	30.6	2.011	0.71792	450
E1873	151.5	46.2	9.807	0.83044	924
E1873 sericite	108.0	31.6	9.981	0.8251	842
E9516	129.0	29.0	13.35	0.89185	998
E9605	92.9	19.8	13.87	0.95550	1260
E1854	161.7	26.1	18.44	1.0048	1136
E1871	0.28	23.1	0.035	0.71476	

*Muscovite-bearing pegmatites

Table 14. Rb-Sr data for alteration zone total-rock samples at Nabarlek and Jabiluka One.

Rb-Sr measurements (Table 14) were made on a number of chlorite-sericite schists from the Nabarlek alteration zone. Under hydrothermal metasomatic conditions, where there are local temperature gradients, it is probable that samples from different locations will have their isotopic systems disturbed and set at different times, or they may have non-uniform initial $^{87}Sr/^{86}Sr$ ratios. The isotopic data for the alteration zone schists are plotted in figure 15 and do not conform to a single isochron. They plot on or below the Oenpelli Dolerite reference isochron, and are best interpreted as outlined above. However, as most of the alteration zone schists are quite enriched in radiogenic ^{87}Sr, it is possible to look at their model ages (Table 14) for some meaningful pattern.

The two samples (1864, 1880) that plot on the Oenpelli Dolerite reference line are from within 50m of that intrusion, and may have had their isotopic systems reset in the contact aureole at that time. Both samples appear to have remained closed systems since then.

The other seven alteration zone schists all have model ages less than the Oenpelli Dolerite age of 1688 Ma. Their model ages range from 1542 to 1648 Ma, and have a

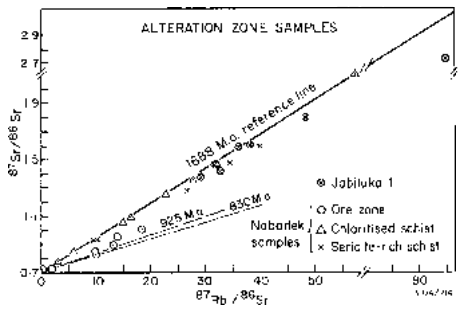


Figure 15. Rb-Sr isochron diagram of total-rock and mineral analyses from alteration and ore zone schists at Nabarlek, and alteration zone schists at Jabiluka One.

mean (±1 s.d.) of 1610 ± 40 Ma. This is interpreted as an average estimate for the age of metasomatic alteration of these schists. The age of alteration earlier obtained for the nearby Nabarlek Granite (1561 ± 17 Ma) is statistically the same as the schist alteration age, and provides strong support for the present assessment.

Similar chloritic-sericitic schists (of the retrograde-chlorite type) from the Cahill Formation at Jabiluka One have had their Rb-Sr systematics (Fig. 15) as equally disturbed as the altered Nabarlek schists. Model ages are again the most useful way to assess the data, as the 7 samples exhibit no clear isochron relationships. The average Rb-Sr alteration age of 1600 ± 80 Ma is essentially identical to the Nabarlek result.

The alteration event that disturbed the Rb-Sr systems had no effect on K-Ar muscovite ages of several of the same schists and two pegmatites (Table 9). The K-Ar ages are very consistent at 1804 ± 7 Ma, and this indicates that the 1600 Ma metasomatic event took place well below the K-Ar muscovite threshold retention temperature of about 350°C.

There is other isotopic evidence from the region for mild, but perhaps significant post-1800 Ma events. This includes: (a) three K-Ar ages (Table 13) of average 1648 ± 17 Ma on amphibolite dykes from Nabarlek, Jabiluka and the Ranger areas, (b) two clinopyroxene K-Ar ages of 1630 and 1600 Ma from the Oenpelli Dolerite, and (c) 1630 Ma average K-Ar ages (Hurley *et al.*, 1961) on several of the granites (known to be at least 1730 Ma) which intrude the Pine Creek Geosyncline. The U-Pb age of 1600-1700 Ma measured on the Ranger deposit pitchblendes (Hills & Richards, 1976, Fig. 5) may also be related to the 1600 Ma metasomatic event recorded by the Nabarlek and Jabiluka chloritic schists.

900-1260 Ma evidence

Rb-Sr analyses on four schists and a sericite from the ore zone at Nabarlek provide evidence of a second alteration episode at between 900 and 1260 Ma ago (Table 14). Evidence of an alteration younger than 1367 Ma was previously suggested by two grossly altered samples of the Oenpelli Dolerite (Table 12). Not all the ore zone schists have responded fully to this event, and hence its age cannot be precisely determined. However, if we assume that the sample (1873 total-rock) with the lowest model age did respond fully, then its age of about 920 Ma is the age of this process. If the response was not complete, then the alteration event would have occurred later than 920 Ma. One of the altered Nabarlek schists (1872) has a substantially younger age (450 Ma) than any of the others. This could be due to continued formation or recrystallisation of chlorite by hydrothermal activity, or to the effects of groundwater movement. Another analysis (1871) is a rich ore sample which is so low in Rb and so poorly enriched in $^{87}Sr/^{86}Sr$ that no significance can be attached to its age.

The bulk of the Rb-Sr data on the Nabarlek ore zone leads us to conclude that it was last altered at or after 920 Ma ago. In general, this result coincides with the Hills & Richards (1976) interpretation of pitchblende and uraninite U-Pb data on the deposit, and evidently represents the last re-deposition of uranium ore and growth (or isotopic resetting) of secondary sericite and chlorite during a further low-temperature metasomatism. The earlier 1600 Ma alteration is considered as a more regional metasomatic event, which not only affected the Lower Proterozoic rocks, but also parts of the overlying Middle Proterozoic (Carpentarian) sandstone sequence.

AGE OF THE MIDDLE PROTEROZOIC (CARPENTARIAN) KOMBOLGIE FORMATION

The Kombolgie Formation forms an extensive, flat-lying sandstone plateau up to 500m thick, and unconformably overlies the 1688 Ma Oenpelli Dolerite and all older rock units of the Pine Creek Geosyncline. It is not metamorphosed, except in the contact aureole of intrusive dolerites, and near some of the U deposits, where metasomatically derived chloritic, dolomitic, and uraniferous veins intrude across the unconformity (Eupene *et al.*, 1975; Rowntree & Mosher, 1975).

The Nungbalgarri Volcanic Member (up to 170m thick) contains basaltic to rhyodacitic flows, tuffs, and cherty sediments, and lies about in the middle of the Kombolgie Formation. The volcanic rocks are commonly very altered, making it difficult to obtain a precise stratigraphic age determination for the unit. The least altered samples known to us are from one of the northern-most outcrops, about 55km east of Nabarlek (Fig. 1). Three of the basalts analysed (Table 15) consist dominantly of fresh plagioclase laths (0.1 to 0.5mm long) and sub-ophitic clinopyroxene grains in a groundmass of devitrified glass, with minor chlorite and carbonate. The fourth (4074) is a more altered basalt in which the pyroxene is almost completely chloritised, and plagioclase pseudomorphed by carbonate and sericite. Hence the analysis of this last sample is rejected for any realistic stratigraphic age determination.

Five Rb-Sr total-rock analyses of the three fresh basalts define a model 1 isochron (Fig. 16, MSWD = 0.63) with an age of 1641 ± 219 Ma, and initial $^{87}Sr/^{86}Sr$ of 0.7059 ± 0.0027. The large errors at this 95% level are due to the fact that there are only three samples in the regression, the t-multiplier being 12.7.

Five mineral phases and two mixed phases (Table 15) were separated from one of the basalts with a view to establishing a Rb-Sr mineral isochron. Plagioclase is the only phase which is aligned with the total-rock points (Fig. 16), and the resultant regression is an improved model 1 isochron (MSWD = 0.42). The age, unchanged from the total-rock isochron, is 1648 ± 29 Ma with an initial $^{87}Sr/^{86}Sr$ of 0.7058 ± 0.0002. The other mineral data lie off the isochron by significant amounts, and the good analytical duplication of the pyroxene and mesostasis fraction suggest that these are real effects. It is doubtful if the implied chemical alteration of these phases is due to any single event; most phases have lost radiogenic ^{87}Sr (or gained Rb), whereas the mesostasis has gained ^{87}Sr (or lost Rb).

The excellent fit of the plagioclase data to the model 1 total-rock isochron, leads us to conclude that the indicated 1648 ± 29 Ma result is a reliable age for the Nungbalgarri Volcanic Member, and hence it is the first direct age determination on the Kombolgie Formation itself.

It is apparent that the 1648 Ma Kombolgie Formation result is a reasonable age for this lower-Middle Proterozoic (lower Carpentarian) sequence. It fits all other geochronoloical constraints: (a) the Kombolgie Formation overlies the 1688 Ma Oenpelli Dolerite, and, most importantly (b) it is itself post-dated by chlorite alteration haloes, which elsewhere we have dated at 1600 Ma and $\leq$ 920 Ma.

LATE MIDDLE PROTEROZOIC (LATE CARPENTARIAN) AND EARLY PALAEOZOIC INTRUSIVES

Mudginberri and Maningkorrirr Phonolites

Phonolite dykes up to 1m wide and 1km long intrude the Nanambu and Nimbuwah Complexes (Fig. 1). They postdate the 1800 Ma metamorphism but their relationship with the Kombolgie Formation sandstones is not apparent. They possess primary igneous minerals (sanidine, anorthoclase, nepheline, aegirine-augite and biotite) and textures, and generally have only minor groundmass alteration.

The total-rock, biotite, and pyroxene K-Ar ages (Table 16) show quite a large range. Geological constraints demand that the apparent 2190 Ma age of sample 4010 pyroxene is due to the presence of excess argon. The biotite results provide the best minimum age of 1200 to

Sample	Rb ppm	Sr ppm	$^{87}Rb/^{86}Sr$	$^{87}Sr/^{86}Sr$
NUNGBALGARRI VOLCANIC MEMBER				
7212.4073 t.r.	35.4	161.0	0.6354	0.72099
7212.4074 t.r.	63.6	75.9	2.4233	0.75360
	105.9	249.0	1.2499	0.73585
7212.4075 t.r.	107.5	251.7	1.2439	0.73502
	43.6	166.3	0.7574	0.72171
7212.4076 t.r.	44.6	169.4	0.7616	0.72357
	12.15	350.2	0.1002	0.70582
7212.4076 plagioclase	12.37	348.8	0.1024	0.70882
	1.48	17.16	0.2491	0.70585
pyroxene	1.51	17.23	0.2531	0.71013
sericite	104.8	151.8	2.0010	0.76873
sericite residue	85.2	144.0	1.7141	0.74232
chlorite	10.4	75.9	0.3957	0.71176
chlorite residue	14.6	91.8	0.4449	0.71417
	98.4	154.6	1.6759	0.74755
mesostasis	85.5	154.8	1.6759	0.74504
MUDGINBERRI PHONOLITE				
7212.4046 t.r.	61.1	553.3	0.3185	0.71250
pyroxene	14.5	412.2	0.1013	0.70841
biotite	522.9	27.8	60.754	1.82015
7212.4047 t.r.	67.4	595.4	0.3013	0.71221
pyroxene	6.19	261.4	0.06837	0.70716
biotite	257.1	75.7	9.8536	0.84395
7212.1138*t.r.			0.4523	0.7155
7212.1088*t.r.			0.2715	0.7111
7212.1056*t.r.			0.4016	0.7136
WURUGOIJ DOLERITE				
7212.4077 t.r.	33.6	713.7	0.4590	0.71334
7212.4078 t.r.	30.7	750.3	0.3479	0.71205
7212.4079 t.r.	23.0	206.8	0.3207	0.71055

*ANOL analyses, Rb/Sr ratios determined by XRF.

Table 15. Rb-Sr data for the Nungbalgarri Volcanic Member, Mudginberri Phonolite and Wurugoij Dolerite.

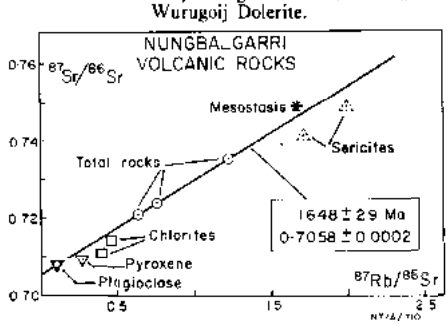


Figure 16. Rb-Sr isochron diagram of total-rock and mineral analyses of basalts from the Nungbalgarri Volcanic Member.

1300 Ma. One of the pyroxene ages is unrealistically low, and the total-rock ages are marginally younger than the biotites, probably due to the groundmass alteration.

The Rb-Sr data on the Mudginberri Phonolite samples (Table 15) are plotted in figure 17. The two biotite ages (assuming initial ratio of 0.706) are 1290 and 1303 Ma, which are in excellent agreement with the K-Ar ages for the same samples. The Rb-Sr isochron age is dominated by the biotite results. Scatter on the isochron exceeds experimental uncertainties having MSWD of 19.4. The resultant model 4 age is 1316 ± 40 Ma (initial $^{87}Sr/^{86}Sr$ 0.7063 ± 0.0004), which we regard as the best determined age for the emplacement of the phonolites.

Wurugoij Dolerite and equivalents

Dolerites which intrude the Kombolgie Formation provide a minimum age for that unit. The Wurugoij Dolerite (7212.4077-4079, Fig. 1) is one such body, about 100m in diameter, which has baked the surrounding sandstones which it intrudes. The two K-Ar ages of the pyroxenes (Table 16) are in good agreement at about 1200 Ma. This is a minimum value for the age of intrusion of the Dolerite.

Rb-Sr data (Table 15) on three samples from the same body are inconclusive in terms of assessing an independent age, because they are not sufficiently enriched in radiogenic ^{87}Sr and do not align on any single isochron. Assuming the 1200 Ma K-Ar age is a real age of intrusion, we can find the average initial $^{87}Sr/^{86}Sr$ ratio of the suite, which is about 0.7055.

An equivalent dolerite (7712.5001) is known near Ranger 1, and is traceable as a prominent aeromagnetic feature and photolineament which cross-cuts the Kombolgie Formation. Its K-Ar age from pyroxene measurements (Table 16) is 1370 ± 30 Ma. The duplicate analyses agree within experimental error and confirm that this is a late-Middle Proterozoic (late-Carpentarian) intrusion. This result infers a minimum age for the Kombolgie Formation, and is entirely consistent with our earlier geochronological interpretations regarding that unit.

Early Palaeozoic dyke intruding the Nungbalgarri Volcanic Member

K-Ar measurements were made on total rocks, plagioclases, and pyroxenes from two samples of a 20cm wide basaltic dyke (7412.4005A, B) which cuts the Nungbalgarri Volcanic Member (Fig. 1). It was considered likely that the dyke was part of the Nungbalgarri suite. The dyke rock is, however, unusually fresh compared to the normal Nungbalgarri basalts. The

K-Ar ages (Table 16) have a very large scatter from 522 to 152 Ma, but they almost certainly demonstrate that the dyke is not part of the ca. 1650 Ma Nungbalgarri Volcanic Member association. For both samples, the total-rock ages are lower than the mineral ages, due to the presence of chlorite and other secondary minerals in the groundmass. There is no obvious reason why the pyroxene ages should be less than those for the plagioclase, and if there is no inherited argon present, the minimum age of the dyke is about 522 Ma.

Sample	Mineral	Avge % K	$\frac{^{40}Ar^*}{^{40}K}$	$\pm^{40}Ar^*$	K-Ar age (Ma)
MUDGINBERRI PHONOLITE					
7212.4010	pyroxene	0.209	0.24471	97.7	2199 ± 40
			0.24240	97.5	2182 ± 40
7212.4046	t.r.	2.67	0.09621	99.5	1193 ± 30
	biotite	7.4	0.10947	99.9	1309 ± 30
	pyroxene	0.275	0.09017	98.1	1137 ± 30
7212.4047	biotite	6.61	0.10913	99.9	1306 ± 30
	pyroxene	0.231	0.04734	93.1	684 ± 15
			0.04614	95.2	670 ± 15
7112.1118	biotite	7.33	0.09759	99.9	1205 ± 22
MANINGKORRIRR PHONOLITE					
7212.4070	t.r.	3.05	0.07950	99.9	1035 ± 25
7212.4083	t.r.	3.25	0.09960	99.5	1223 ± 25
7212.4084	t.r.	3.85	0.07428	99.9	982 ± 20
MURGOIJ DOLERITE (4078, 4079) AND EQUIVALENT (5001)					
7212.4078	pyroxene	0.089	0.09731	92.3	1203 ± 40
7212.4079	pyroxene	0.037	0.09649	86.9	1195 ± 35
7712 5001	pyroxene	0.0610	0.11601	92.2	1363 ± 35
			0.11760	89.8	1377 ± 35
DYKE INTRUDING NUNGBALGARRI VOLCANIC MEMBER					
7412 4005A	t.r.	0.498	0.00906B5	70.9	153 ± 3
			0.0089849	71.5	152 ± 3
	plagioclase	0.319	0.034477	93.6	522 ± 10
	pyroxene	0.0387	0.011667	56.4	194 ± 10
7412 4005B	t.r.	0.510	0.017197	88.1	280 ± 5
			0.017288	89.5	281 ± 5
	plagioclase	0.354	0.029428	95.9	454 ± 15
	pyroxene	0.0669	0.015637	74.8	315 ± 20

Table 16. K-Ar data for various phonolitic and doleritic intrusives.

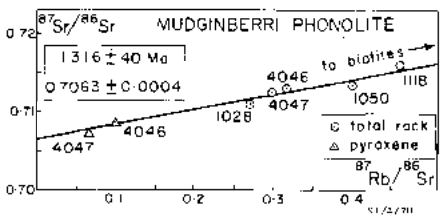


Figure 17. Rb-Sr isochron diagram of total-rock and clinopyroxene analyses from the Mudginberri Phonolite.

Three groups of post-Kombolgie Formation intrusives have been dated: (i) the phonolites yield Rb-Sr and K-Ar ages of close to 1300 Ma, (ii) dolerites which cross-out the Kombolgie Formation yield K-Ar ages of 1200 Ma and 1370 Ma, and (iii) a narrow basalt dyke has a probable early Palaeozoic minimum age of 522 Ma. The late-Middle Proterozoic (late-Carpentarian) 1200-1400 Ma intrusives are similar in age to more widespread dolerites intruding the Roper Group in eastern Arnhem Land (McDougall *et al.*, 1965).

CONCLUDING REMARKS AND SUMMARY

Significance of lower discordia intercepts on U-Pb concordia diagrams

The discordance patterns of U-Pb systems in zircons give rise to linear or sub-linear arrays of data on the concordia diagrams (Figs. 3, 7 & 13). Models of lead-loss which account for such discordance are usually attributed to episodic loss (Wetherill, 1956) or loss by continuous diffusion (Tilton, 1960). The interpretation of zircon data espoused in this paper relates primarily to the upper intercept ages, and they are quite independent of which lead-loss model is operative. Comparison of the various lower intercept ages (Table 17) might be expected to provide some information in this regard. However, the fact that no single lower intercept age is apparent suggests that discordance is not related to any single geologically and isotopically recognisable event.

Lower intercept ages for the three zircon suites (4081A, 4081C, and 1243) from the Nimbuwah Complex are 440 Ma, 500 Ma, and 555 Ma, respectively. This can be considered a distinct grouping compatible with either the continuous diffusion lead-loss model, or perhaps with an uplift-dilatancy (episodic) model (Goldich & Mudrey, 1972). The latter

Unit	Mineral Age		Pooled Rb-Sr isochron age	U-Pb zircon age	U-Pb lower intercept age
	K-Ar	Rb-Sr			
Nanambu Complex		1800	2468 ± 26	2470^{+47}_{-40}	1362±80
Nanambu Complex reworked gneisses	1800	1800 (bio.) 1875-2020 (musc.)	1750,1800,1880,1980 (apparent ages only)		
Nimbuwah Complex-granites			1800 ± 24	1866^{+8}_{-7}	421±75
Nimbuwah Complex - granulites			1730 ± 95	1886±5	555±21
Lower Proterozoic metamorphics	1800	1800	1782 ± 35 1825 ± 125 1815 ± 60		
Lower Proterozoic sedimentation:					
(a) model age estimate			2000 - 2200		
(b) zircon provenance				2440±40	840±85
Jim Jim Granite			1732 ± 11		
Tin Camp Granite			1755 ± 15		
Nabarlek Granite		1780			
Oenpelli Dolerite			1688 ± 13		
Alteration ages:					
(a) Nabarlek			1610 - 40		
(b) Nabarlek ore zone			~ 920		
(c) Jabiluka 1			1600 ± 80		
(d) Nabarlek Granite			1560 ± 16		
Amphibolite dykes	1648				
Nungbalgarri Volcanic Member (Kombolgie Formation)			1648 - 79		
Phonolite dykes	1200-1300	1300	1316 ± 40		
Wurugoij Dolerite	1200				
Other Dolerite	1370				
Palaeozoic Dyke	522				

Table 17. Summary of the principal ages (Ma) and age constraints for various units in the Alligator Rivers region.

implies alteration of the zircons (involving lead-loss) during an episode of uplift of the terrane at 450-550 Ma in early Palaeozoic. However, the hypothesis can be no further advanced until fission-track age measurements, on minerals such as apatite which tend to be reset at temperatures as low as 100°-120°C, are undertaken (cf. Table 7, Page, 1978).

Summary and implications of the isotopic data

The data presented in this paper provide an internally consistent framework within which there are substantial constraints relevant to any modelling of geological processes which affected the Alligator Rivers region. All the isotopic results are summarised in table 17, and for every case, are in excellent accord with known geological relationships.

At least six generations of clearly defined magmatic activity punctuate the late Archaean to Proterozoic record: at 2470 Ma, 1866-1886 Ma, 1730-1760 Ma, 1688 Ma, 1648 Ma and

1200-1370 Ma. Additional igneous rock-forming events include the formation of migmatites and pegmatitic mobilizates during the 1800 Ma regional metamorphism, pre-1800 Ma dolerites (Zamu Dolerite, probably 1800-2000 Ma, and perhaps even akin to the Nimbuwah Complex granitoids), and a small Palaeozoic dyke about 520 Ma old (perhaps akin to Antrim Plateau magmatism).

U-Pb zircon and Rb-Sr total-rock measurements agree closely at 2470 Ma, and therefore provide good documentation for the age of the oldest known granitoid rocks of the region, which belong to the Nanambu Complex. This age, as well as the age of the Rum Jungle Complex, and isotopic evidence inferred from reworked gneiss components in the Nanambu Complex, are unequivocal geological data which indicate the existence of this late Archaean basement, upon which part of the Lower Proterozoic (2200-2000 Ma) Pine Creek Geosyncline sequences were later deposited.

U-Pb data on zircons and Sr isotopic evidence from Nimbuwah Complex granitoids, indicate that these rocks were derived from outside their present environment, and were juvenile additions to the crust at the time of their 1866 to 1886 Ma crystallisation and intrusion into the Pine Creek Geosyncline. The isotopic data rule out the possibility that the granitoids were derived *in situ* by anatexis of Pine Creek Geosyncline sediments, or by reworking of Nanambu Complex-type gneisses. The Rb-Sr total-rock ages of the granitoids and migmatites of the Nimbuwah Complex are not distinguishable from each other at ca. 1800 Ma, and are a reflection of the regional metamorphic event.

Lower Proterozoic schists, host rocks to the uranium deposits in the area, contain detrital zircons whose provenance age (2440 ± 40 Ma) corresponds with the age of the late Archaean (ca. 2470 Ma) Nanambu basement. However their superimposed fabric and amphibolite-facies mineralogy were produced during the 1800 Ma event. K-Ar and Rb-Sr mica ages from the Complexes and from the metasediments indicate the same 1800 Ma event. This age is so widespread and the isotopic evidence so compelling, there can be little doubt that it is recording anything other than the main amphibolite-facies regional metamorphism. The presence of externally-derived granitic magma, crystallised 70 to 80 Ma before the end of the 1800 Ma metamorphism, lends support to the idea that such magmatic intrusion within the Nimbuwah Complex, may be the cause of, or perhaps the triggering mechanism for, increased geothermal gradients and the ensuing regional metamorphic event.

Post-orogenic felsic intrusives (Jim Jim Granite, Tin Camp Granite, and Nabarlek Granite) and mafic intrusives (Oenpelli Dolerite) dated in this study have Rb-Sr ages of 1730-1780 Ma and 1688 ± 13 Ma, respectively. An episode of low-grade retrogressive metamorphism and metasomatism post-dates emplacement of the Oenpelli Dolerite, and its products envelope uranium mineralisation in all known deposits. At Nabarlek and Jabiluka One, this metasomatic event is reflected in disturbed Rb-Sr total-rock systems, and has an age of 1600 Ma. A localised, younger low-grade event is also recognised at Nabarlek, and has an age no older than 920 Ma.

Kombolgie Formation sandstones blanket the 1800 Ma metamorphic rocks and the post-tectonic felsic and mafic intrusive rocks, but are affected by, and are hence older than, the pervasive chloritic metasomatism in the vicinity of the uranium deposits. These relationships give inferred constraints on the age of the Kombolgie Formation of 1688 to 1600 Ma. Our direct Rb-Sr measurement of the age of a mafic volcanic unit (Nungbalgarri Volcanic Member) within the Kombolgie Formation is 1648 ± 29 Ma. This result agrees with all known geological and geochronological parameters, and is the most reliable age yet documented for the Kombolgie Formation of the Katherine River Group, or its correlative in the McArthur Basin, the Tawallah Group. Also, the 1648 Ma result is consistent with previous age measurements in the Tawallah Group (McDougall *et al.*, 1965; Plumb & Derrick, 1975), which, until now, could only be said to have an age of 1570 Ma or older.

ACKNOWLEDGEMENTS

Mr P.G. Smart assisted in collecting some of the samples. The authors also acknowledge with thanks the staff of Geopeko Ltd. (Ranger), Pancontinental Mining Ltd. (Jabiluka), and Queensland Mines Ltd. (Nabarlek), who allowed ready access to drill-core material at their respective deposits. Mr D. Pohl and Dr J.M. Worden of Esso Australia Ltd. arranged for us to isotopically analyse their samples collected from the Nabarlek Granite, Tin Camp Granite, and Nabarlek alteration zone. Esso Australia Ltd. were also responsible for expediting our Rb-Sr analytical program on some samples from the Nimbuwah Complex and Oenpelli Dolerite, and arranged for Dr B.W. Chappell to carry out Rb and Sr XRF determinations on some of these samples. The K-Ar analyses reported in this paper were carried out at the Australian Mineral Development Laboratories, South Australia, under the supervison of Dr A.W. Webb. The Rb-Sr and U-Pb analytical work was performed with capable assistance in sample preparation, mineral separation, and isotope-dilution chemistry, from Messrs M.J. Bower, N.C. Hyett, M.W. Mahon, D.J. Millar, and T.K. Zapasnik. R.W. Page and R.S. Needham publish with the permission of the Director, Bureau of Mineral Resources, Geology and Geophysics, Canberra.

REFERENCES

Anthony, P.J., 1975: Nabarlek uranium deposit. *in* (ed. C.L. Knight) *Economic Geology of Australia and Papua New Guinea, Australas. Inst. Min. Metall., Monograph Series No. 5, 1. Metals*, 304-308.

Compston, W. & Arriens, P.A., 1968: The Precambrian geochronology of Australia. *Can. J. Earth Sci., 5*, 561-583.

Cumming, G.L. & Richards, J.R., 1975: Ore lead isotope ratios in a continuously changing Earth. *Earth Planet. Sci. Lett., 28*, 155-171.

Dodson, R.G., Needham, R.S., Wilkes, P.G., Page, R.W., Smart, P.G. & Watchman, A.L., 1974: Uranium mineralisation in the Rum Jungle-Alligator Rivers province, N.T., Australia. *in, Formation of Uranium Ore Deposits. Proceedings of a Symposium, Athens.* International Atomic Energy Agency, Vienna, 551-568.

Eupene, G.S., Fee, P.H. & Colville, R.G., 1975: The Ranger One uranium deposits. *in* (ed. C.L. Knight) *Economic geology of Australia and Papua New Guinea, Australas. Inst. Min. Metall., Monograph Series No. 5, 1, Metals*, 308-317.

Ferguson, John,: this volume, Metamorphism in the Pine Creek Geosyncline and its bearing on stratigraphic correlations. *Proceedings of the International Uranium Symposium on the Pine Creek Geosyncline.*

Ferguson, John, Chappell, B.W. & Golcby, A.B., this volume: Granitoids in the Pine Creek Geosyncline. *Proceedings of the International Uranium Symposium on the Pine Creek Geosyncline*

Goldich, S.S. & Mudrey, M.G., Jr., 1972: Dilatancy model for discordant U-Pb zircon ages; *in* (ed. A.I. Tugarinov) *Contributions to Recent Geochemistry and Analytical Chemistry (Vinogradov Volume).* Nauka Press, Moscow, 415-418.

Hegge, M.R., 1977: Geologic setting and relevant exploration features of the Jabiluka Uranium Deposits. *Proc. Australas. Inst. Min. Metall., 264*, 19-32.

Hills, J.H. & Richards, J.R., 1976: Pitchblende and galena ages in the Alligator Rivers Region, Northern Territory, Australia. *Miner. Deposita, 11*, 133-154.

Hurley, P.M., Fisher, N.H., Pinson, W.H. & Fairbairn, H.W., 1961: Geochronology of Proterozoic Granites in Northern Territory, Australia, Part I. K-Ar and Rb-Sr age determinations. *Bull. geol. Soc. Am., 72*, 653-662.

Kanasewich, E.R., 1968: The interpretation of lead isotopes and their geological significance; *in* (eds E.I. Hamilton & R.M. Farquar), *Radiometric Dating for Geologists.* Interscience Publ., New York, 147-223.

Krogh, T.E., 1973: A low contamination method for hydrothermal decomposition of zircon and extraction of U and Pb for isotopic age determinations. *Geochim. cosmochim. Acta, 37*, 485-494.

McDougall, I., Dunn, P.R., Compston, W., Webb, A.W., Richards, J.R. & Bofinger, V.M., 1965: Isotopic age determinations on Precambrian rocks of the Carpentaria region, Northern Territory, Australia. *J. geol. Soc. Aust., 12*, 67-90.

McIntyre, G.A., Brooks, C., Compston, W. & Turek, A., 1966: The statistical assessment of Rb-Sr isochrons. *J. geophys. Res., 71*, 5459-5468.

Moorbath, S., 1975: Evolution of Precambrian Crust from strontium isotopic evidence. *Nature, Lond., 254*, 395-398.

Needham, R.S., Smart, P.G. & Watchman, A.L., 1974: A reinterpretation of the geology of the Alligator Rivers Uranium Field. *Search, 5*, 397-399.

Needham, R.S. & Stuart-Smith, P.G., 1976: The Cahill Formation-host uranium deposits in the Alligator Rivers Uranium Field, Australia. *BMR J. Aust. Geol. Geophys, 1*, 321-334.

Needham, R.S. & Stuart-Smith, P.G., this volume: Geology of the Alligator Rivers Uranium Field. *Proceedings of the International Uranium Symposium on the Pine Creek Geosyncline.*

Needham, R.S., Crick, I.H. & Stuart-Smith, P.G., this volume: Regional Geology of the Pine Creek Geosyncline. *Proceedings of the International Uranium Symposium on the Pine Creek Geosyncline.*

Page, R.W., 1978: Response of U-Pb zircon and Rb-Sr total-rock and mineral systems to low-grade regional metamorphism in Proterozoic igneous rocks, Mount Isa, Australia. *J. geol. Soc. Aust., 25*, 141-164.

Plumb, K.A. & Derrick, G.M., 1975: Geology of the Proterozoic rocks of the Kimberley to Mount Isa region. *in* (ed. C.L. Knight) *Economic geology of Australia and Papua New Guinea, Australas. Inst. Min. Metall., Monograph Series No. 5, 1, Metals*, 217-252.

Richards, J.R., Berry, H. & Rhodes, J.M., 1966: Isotopic and lead-alpha ages of some Australian zircons. *J. geol. Aust., 13*, 69-96.

Richards, J.R., Ruxton, B.P. & Rhodes, J.M., 1977: Isotopic dating of the Leucocratic granite, Rum Jungle, Australia. *Proc. Australas. Inst. Min. Metall., 264*, 33-43.

Riley, G.H., this volume: Granite ages in the Pine Creek Geosyncline. *Proceedings of the International Uranium Symposium on the Pine Creek Geosyncline.*

Rowntree, J.C. & Mosher, D.V., 1975: Jabiluka Uranium Deposits. *in* (ed. C.L. Knight) *Economic geology of Australia and Papua New Guinea. Australas. Inst. Min. Metall., Monograph Series No. 5, 1. Metals,* 321-326.

Smart, P.G., Wilkes, P.G., Needham, R.S. & Watchman, A.L., 1975: Geology and geophysics of the Alligator Rivers Region. *in* (ed. C.L. Knight). *Economic geology of Australia and Papua New Guinea, Australas. Inst. Min. Metall., Monograph Series No. 5, 1. Metals,* 285-301.

Steiger, R.H. & Jäger, E., 1977: Subcommission on geochrology: convention on the use of decay constants in geo- and cosmochronology. *Earth Planet. Sci. Lett., 36,* 359-362.

Stuart-Smith, P.G. & Ferguson, John, 1978: The Oenpelli Dolerite-a Precambrian continental tholeiitic suite from the Northern Territory, Australia. *BMR J. Aust. Geol. Geophys., 3,* 125-133.

Tilton, G.R., 1960: Volume diffusion as a mechanism for discordant lead ages. *J. geophys. Res., 65,* 2933-2945.

Walpole, B.P., Crohn, P.W., Dunn, P.R. & Randal, M.A., 1968: Geology of the Katherine-Darwin Region, Northern Territory, *Bull. Bur. Miner. Resour. Geol. Geophys. Aust., 82,* 304p.

Wetherill, G.W., 1956: Discordant U-Pb ages, I. *Trans. Am. geophys. Un., 37,* 320-326.

APPENDIX — SAMPLE LOCATION LIST

Unit	Sample No.	1:100,000	Sheet Name, grid reference
Nanambu Complex (late-Archaean)	7212.4006	Cahill	513025
	7212.4009	Cahill	521038
	JH 4015	Cahill	352052
	JH 4016	Cahill	353050
	7212.4048	Cahill	722131
Nanambu Complex (reworked gneisses)	7212.4003	Kapalga	265151
	7212.4004	Kapalga	265151
	7212.4005	Cahill	298989
	7212.4086	Cahill	642001
	7112.1065	Cahill	337008
	7112.1140	Cahill	358840
	7112.1141	Cahill	410616
	7112.1143	Cahill	389830
Nimbuwah Complex	7212.4062	Oenpelli	200493
	7212.4063	Oenpelli	197493
	7212.4066	Goomadeer	475422
	7212.4069	Goomadeer	458546
	7212.4081	Goomadeer	554610
	7212.4082	Goomadeer	530582
	7312.1243	Howship	119067
	7412.4006	Howship	068995
	7412.4008	Goomadeer	415669
	7412.4009	Goomadeer	416676
Ranger 1 'Footwall Sequence'	7212.4016	Cahill	275958 DDH SPS 22
	7212.4017	Cahill	712997 DDH SJA 1
	7212.4018	Cahill	712997 DDH SJA 1
	7212.4019	Cahill	712997 DDH SJA 1
	7212.4021	Cahill	712997 DDH SJA 1
	7212.4022	Cahill	720966 DDH STD 1
	7212.4023	Cahill	720966 DDH STD 1
	7212.4024	Cahill	720966 DDH STD 1
	7212.4027	Cahill	720966 DDH STD 1
	7212.4028	Cahill	720966 DDH STD 1
	7212.4030	Cahill	720966 DDH STD 1
	7212.4031	Cahill	736960 DDH S1/84
	7212.4037	Cahill	736972 DDH S3/18
	7212.4038	Cahill	736972 DDH S3/18
	7212.4039	Cahill	736972 DDH S3/18
	7212.4041	Cahill	739979 DDH S3/23
	7212.4043	Cahill	739979 DDH S3/23
	7212.4045	Cahill	736970 DDH S1/96
Other Lower Proterozoic chists	7112.1094	Cahill	487641
	7112.1095	Cahill	520649
	7712.4001	Oenpelli	117227
	E 9670		
Jabiluka Ore	7212.4049	Cahill	708172 DDH 24
	7212.4050	Cahill	708172 DDH 24
	7212.4051	Cahill	708172 DDH 24
	7212.4053	Cahill	708172 DDH 22
	7212.4054	Cahill	708172 DDH 22
	7212.4055	Cahill	708172 DDH 35
	7212.4056	Cahill	708172 DDH P34
	7212.4057	Cahill	708172 DDH 1
	7212.4058	Cahill	708172 DDH 24
Nabarlek	7023.0050	Oenpelli	175384 DDH 47
	7212.4103	Oenpelli	175384 DDH 1
	7212.4104	Oenpelli	175384 DDH 1
	7212.4105	Oenpelli	175384 DDH 207
Nabarlek, alteration zone schists	E 1864	Oenpelli	175384
	E 1880	Oenpelli	175384
	E 1856	Oenpelli	175384
	E 1863	Oenpelli	175384
	E 1893	Oenpelli	175384
	E 1852	Oenpelli	175384
	E 1867	Oenpelli	175384
	E 1877	Oenpelli	175384
	E 1857	Oenpelli	175384
	E 1872	Oenpelli	175384
	E 1873	Oenpelli	175384
	E 9616	Oenpelli	175384
	E 9605	Oenpelli	175384
	E 1854	Oenpelli	175384
	E 1871	Oenpelli	175384
Jim Jim Granite	JH 4034	Jim Jim	560410
	JH 4035	Jim Jim	549393
	JH 4037	Jim Jim	537379
	JH 4038	Jim Jim	572344
	7412.4007	Jim Jim	616103
Tin Camp Granite (Beatrice)	E 9664	Howship	160000
	E 9645	Howship	160000
	E 9649	Howship	160000
	E 9651	Howship	160000
Tin Camp Granite (Caramal)	E 9667	Oenpelli	265185
	E 9669	Oenpelli	265185
Nabarlek Granite	E 1901	Oenpelli	175384
	E 1913	Oenpelli	175384
	E 1928	Oenpelli	175384
	N 636	Oenpelli	175384
	N 637	Oenpelli	175384
	N 639	Oenpelli	175384
	NA 23/4	Oenpelli	175384 DDH 23
	NA 83/5	Oenpelli	175384 DDH 83
	NA 83/6	Oenpelli	175384 DDH 83
Oenpelli Dolerite	7212.4100	Oenpelli	175384 DDH 23
	E 1892	Oenpelli	175384 DDH 23
	E 1894	Oenpelli	175384 DDH 23
	7212.4101	Oenpelli	175384 DDH 98
	7212.4060	Oenpelli	970440
	E 1912	Oenpelli	
	E 1860	Oenpelli	175384 DDH 3
	E 1891	Oenpelli	175384 DDH 23
	Nab. 23/1	Oenpelli	175384 DDH 23
	Nab. 23/2	Oenpelli	175384 DDH 23
Amphibolite	Nab. 23/3	Oenpelli	175384 DDH 23
Nungbalgarri Volcanic Member	7212.4073	Goomadeer	691483
	7212.4074	Goomdeer	691483
	7212.4075	Goomadeer	691483
	7212.4076	Goomadeer	690489

Unit	Sample No.	1:100,000	Sheet Name, grid reference
Mudginberri Phonolite	7212.4010	Cahill	587000
	7112.1028	Cahill	587000
	7112.1050	Cahill	587000
	7212.4046	Cahill	657017
	7212.4047	Cahill	722131
	7112.1118	Cahill	722131
Maningkorrier Phonolite	7212 4070	Goomadeer	458546
	7212 4083	Goomadeer	462554
	7212 4084	Goomadeer	462554
Wurugoj Dolerite	7212.4077	Goomadeer	680498
	7212.4078	Goomadeer	680498
	7212.4079	Goomadeer	680498
	7712.5001	Cahill	720950 NMF 1
Palaeozoic dyke	7412.4005	Howship	130895

GRANITE AGES IN THE PINE CREEK GEOSYNCLINE

G.H. Riley

C.S.I.R.O. Division of Mineral Physics, P.O. Box 136, North Ryde, N.S.W., 2113, Australia.

ABSTRACT

Rb-Sr data on high-level, late orogenic granitoid intrusions in the Pine Creek Geosyncline indicate that their emplacement was essentially synchronous. Low initial $^{87}Sr/^{86}Sr$ ratios strongly suggest that they did not originate by anatexis of crustal material of high Rb/Sr ratio but from a source of primitive strontium with low enrichments of ^{87}Sr. The Allia Creek granite may be an exception. The geographic distribution of sampling sites demonstrates that this intrusive event was widespread throughout the Geosyncline in the early Proterozoic. The age of 1780 $\pm$ 20 m.y. is therefore interpreted as representing a minimum age for the regional metamorphism of the Pine Creek Geosyncline and a maximum age for the development of high grade, vein type, uranium mineralization.

INTRODUCTION

The Pine Creek Geosyncline is a Precambrian mobile belt containing metasediments of Lower Proterozoic age. Crystalline rocks of granitic composition occur throughout the Geosyncline but age relationships are not always evident from field mapping.

The western margin of the Geosyncline is bounded by the Litchfield Complex, comprised of granite and metamorphic rocks considered to be Archaean to Lower Proterozoic. Elsewhere in the western area the sediments are characterized by low metamorphic grade and clearly overlie an Archaean crystalline basement complex exemplified by the Rum Jungle Complex and the Waterhouse Complex. In the eastern area of the Geosyncline, the metamorphic grade is higher, increasing from lower greenschist in southern areas to upper amphibolite and granulite facies in the north-east (Smart *et al.*, 1975; Ferguson, this volume). The degree of metamorphism in the north-east was sufficiently intense to migmatise the sedimentary

Granite	Sample	Sample No	Rb (ppm)	Common Sr (ppm)	$^{87}Rb/^{86}Sr$	$^{87}Sr/^{86}Sr$
Cullen	Whole rock	D53/9/10	323	90.3	10.3615	0.9728
Cullen	Whole rock	D52/8/5	253	128	5.7100	0.8542
Cullen	Whole rock	D53/9/1	144	328	1.2707	0.7382
Cullen	Biotite	D53/9/1	579	16.3	102.64	3.3357
Cullen	K-Feldspar	D53/9/1	241	490	1.4257	0.7427
Burnside	Whole rock	D52/8/25	439	65.1	19.539	1.1991
Burnside	Whole rock	D52/8/26	359	72.9	14.271	1.0637
Mt Bundey	Whole rock	D52/4/5	257	397	1.8849	0.7535
Mt Bundey	K-Feldspar	D52/4/5	468	459	2.9538	0.7811
Mt Bundey	Hornblende	D52/4/5	38	336	0.3317	0.7136
Allia Creek	Whole rock	D52/8/7	346	36.3	27.609	1.4148
Allia Creek	Duplicate	Duplicate	344	36.1	27.638	1.4178
Allia Creek	Muscovite	D52/8/7	956	9.5	290.27	8.1275
Allia Creek	K-Feldspar	D52/8/7	602	62.4	27.955	1.4221
Prices Springs	Whole rock	D52/8/20	264	378	2.0243	0.7569
Prices Springs	Whole rock	D52/8/21	236	214	3.1983	0.7888

Table 1. Rb-Sr data for Pine Creek granites, whole rocks and minerals.

sequence and so generate the Nimbuwah Complex, gneissic members of the Kakadu Group (Anthony, 1975), and the Nanambu Complex (Needham & Smart, 1972).

A series of granitic plutons and stocks intrude the basement complexes, the migmatites and the regionally metamorphosed Proterozoic sediments. These granites have been variously described as "late intrusive leucogranite" (Richards *et al.*, 1977), as typical of "post-tectonic or late-syntectonic magmas" (Smart *et al.*, 1975), as "solid state diapiric intrusions" (Stephansson & Johnson, 1976) and as "anatectic" in the case of the (undated) granite at Nabarlek (Anthony, 1975). It is clear that the granitic rocks of the Geosyncline do not comprise a single set and that major variations in composition (Ferguson *et al.*, this volume) result from distinct genetic types.

Ferguson *et al.* (this volume) have subdivided the granitoids into two classes: those related to complexes and those which are clearly intrusive, high-level, late orogenic types. These authors give extensive data on the uranium content of each class. Both are enriched compared with average crustal values, the late orogenic types containing higher average concentrations of uranium.

Clearly the ages of these various granite intrusions are important features in the development of the Geosyncline. The relevance of the granitic and volcanic rocks as possible ultimate sources of uranium mineralization has been previously discussed (Ayres & Eadington, 1975; Dodson & Prichard, 1975; Smart *et al.*, 1975).

Descriptive models proposed to reconstruct the genesis of the high grade uraninite deposits are critically dependent on the timing of events in the Geosyncline. Previous and contemporary U-Pb and Pb-Pb isotopic data (Hills & Richards, 1976; Gulson & Mizon, this volume) indicate an apparent complex history for each deposit; no single model based on discrete 'events' is appropriate for all four deposits in the Alligator Rivers Uranium Field. Rather, each orebody appears to have undergone substantial (repeated?) remobilization after initial uranium concentration and deposition, so that isotopic data specifically on the mineralized samples are unlikely to be definitive.

It is clear that high grade mineralization occurred after the regional metamorphism, and, if the intrusive granitoids are classic late orogenic/post-kinematic magmas, their geochronology defines the upper age limit for ore zone development. One simple test to relate the intrusive episode to the final stage of regional metamorphism is to examine granite age data on a very broad geographic scale. If, indeed, all high-level granites were emplaced in a single episode, then energy considerations strongly suggest a temporal association with the regional metamorphism. A further appropriate test is to consider the genetic model of their origin. Derivation by partial or complete anatexis would suggest an intimate association of protogranitic material during metamorphism but not necessarily the terminal phase of the event.

The objective of the regional study described here is to determine whether the widespread occurrence of high level granites in the Pine Creek Geosyncline can be documented as a single episode of emplacement and whether there is isotopic evidence relating to their origin.

RESULTS

Acquisition of granitic samples from the eastern area of the Geosyncline is hampered by lack of outcrop and availability of fresh material. Consequently, this survey is restricted to the northern, southern and western zones. Samples were obtained from the Cullen granite, Allia Creek granite, Burnside granite, Prices Springs granite, and Mt Bundey granite. Their locations are shown on the map of figure 1.

Rb-Sr data for minerals from the Allia Creek granite, Cullen granite and Mt. Bundey granite as well as whole rock data for samples from all localities are listed in table 1. The ages,

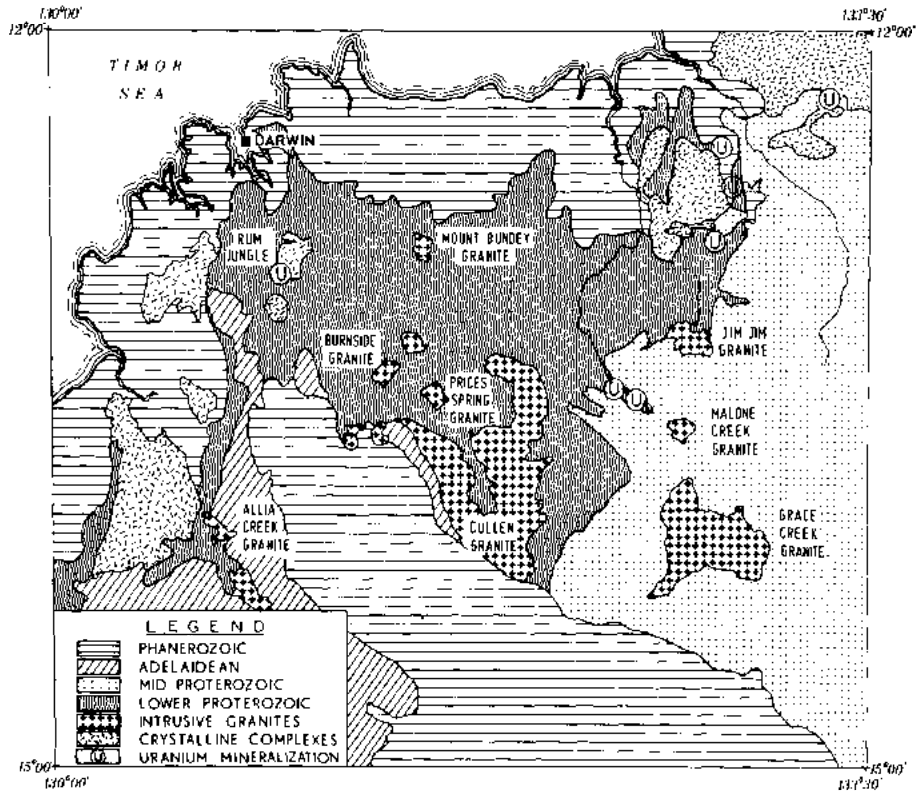


Figure 1. Schematic geologic map of the Pine Creek Geosyncline showing intrusive granite distribution, uranium mineralization localities and sampling sites for Rb-Sr analyses.

based on a ^{87}Rb decay constant of 1.42×10^{-11} disintegrations/atom/year (Steiger & Jager, 1977), and initial $^{87}Sr/^{86}Sr$ are summarized as follows:

Allia Creek (muscovite, whole rock, feldspar)	1780± 80m.y.	0.709 ± .040
Mt. Bundey (whole rock, feldspar, hornblende)	1790±110m.y.	0.7051±.0017
Cullen (3 whole rocks, biotite, feldspar)	1790± 40m.y.	0.7058±.0017
All locations (9 whole rocks)	1780± 20m.y.	0.7057±.0010

Grouping the whole rock samples to a common isochron analysis is of questionable validity. However, the empirical fit of data points results in a grouped age error of 20 m.y. (Model I, M.S.W.D. = 1.32) implying both a common age and a very similar initial $^{87}Sr/^{86}Sr$ for these granites (Fig. 2). The sampled area which includes about 50% of the Geosyncline, has thus suffered a very widespread synchronous event which, by implication, was closely related in time to the regional metamorphism.

The initial $^{87}Sr/^{86}Sr$ ratios are similarly in agreement, with the exception of the Allia Creek data. The initial ratio of this granite is not easily determined and the isochron intercept has a large associated error because of the lack of samples with low Rb/Sr ratio. However, the data from the Mt. Bundey granite, the Cullen granite and the grouped whole rock isochron yield low initial ratios supporting the conclusion of Ferguson *et al.* (this volume), that, with the exception of Allia Creek, the late orogenic granites studied here are *I*-type.

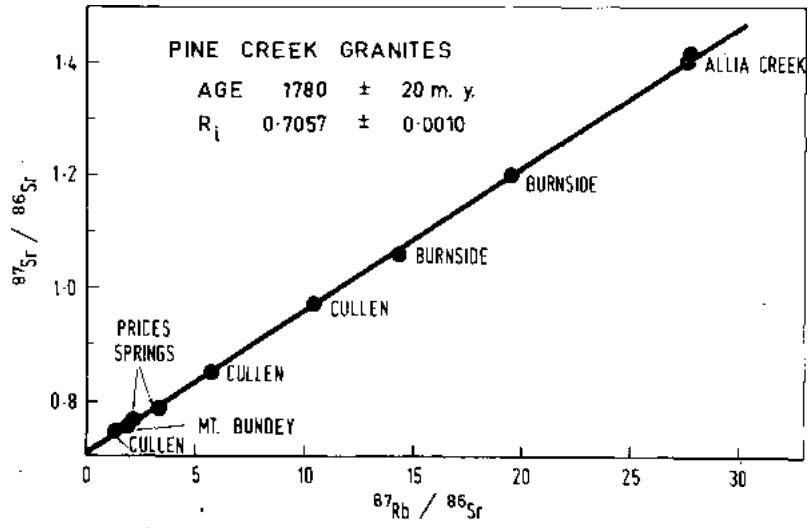


Figure 2. Isochron diagram for Pine Creek granites, 10 whole rock samples. Model I age, MSWD = 1.32.

CONCLUSION

Regional Rb-Sr data on high-level, intrusive granites from the northern, western and eastern areas of the Pine Creek Geosyncline indicate a single age in the region of 1780-1790 m.y. Their low initial $^{87}Sr/^{86}Sr$ ratio suggests an *I*-type origin. These results are strongly indicative that the granite emplacement episode was a terminal-phase event in the regional metamorphism of the Pine Creek Geosyncline sediments. As the high grade uranium mineralization was developed subsequent to this metamorphism, the upper limit to its age is 1780±20m.y.

REFERENCES

Anthony, P.J. 1975: Nabarlek Uranium Deposit. *in* (ed. C.L. Knight) *Economic Geology of Australia and Papua New Guinea. Australas. Inst. Min. Metall., Monograph Series No. 5, 1. Metals*, 304-308.

Ayres, D.E. & Eadington, P.J., 1975: Uranium mineralization in the South Alligator River Valley. *Miner. Deposita, 10*, 27-41.

Dodson, R.G. & Prichard, C.E., 1975: Uranium in the Pine Creek Geosyncline. *in* (ed. C.L. Knight) *Economic Geology of Australia and Papua New Guinea. Australas. Inst. Min. Metall., Monograph Series No. 5, 1. Metals*, 281-284.

Ferguson, J., this volume: Metamorphism in the Pine Creek Geosyncline and its bearing on stratigraphic correlations. *Proceedings of the International Uranium Symposium on the Pine Creek Geosyncline.*

Ferguson, J., Chappell, B.W. & Goleby, A.B., this volume: Granitoids in the Pine Creek Geosyncline. *Proceedings of the International Uranium Symposium on the Pine Creek Geosyncline.*

Gulson, B.L. & Mizon, K.J., 1979: Lead isotope studies at Jabiluka. *Proceedings of the International Uranium Symposium on the Pine Creek Geosyncline.*

Hills, J.H. & Richards, J.R., 1976: Pitchblende and galena ages in the Alligator Rivers Region, Northern Territory, Australia. *Miner. Deposita, 11*, 133-154.

Needham, R.S. & Smart, P.G., 1972: Progress report Alligator River Party, N.T., 1971. *Rec. Bur. Miner. Resour. Geol. Geophys. Aust., 1972/1* (unpubl.).

Richards, J.R., Ruxton, B.P. & Rhodes, J.M., 1977: Isotopic dating of the leucocratic Granite, Rum Jungle, Australia. *Proc. Australas. Inst. Min. Metall., 264*, 33-43.

Smart, P.G., Wilkes, P.G., Needham, R.S. & Watchman, A.L., 1975: Geology and geophysics of the Alligator Rivers Region. *in* (ed. C.L. Knight) *Economic Geology of Australia and Papua New Guinea. Australas. Inst. Min. Metall., Monograph Series No. 5, 1. Metals*, 285-301.

Steiger, R.H. & Jager, E., 1977: Subcommission on Geochronology: Convention on the use of decay constants in geo- and cosmochronology. *Earth Planet. Sci. Lett., 36*, 359-362.

Stephansson, O. & Johnson, K., 1976: Granite diapirism in the Rum Jungle area, Northern Australia. *Precambrian Research, 3*, 159-185.

GRANITOIDS IN THE PINE CREEK GEOSYNCLINE

John Ferguson,[1] B. W. Chappell [2] and A. B. Goleby[3]

1. Bureau of Mineral Resources, P.O. Box 378, Canberra City, A.C.T. 2601, Australia
2. Dept. of Geology, A.N.U., P.O. Box 4, Canberra, A.C.T. 2600, Australia
3. 112 McInnes St., Weston, A.C.T. 2611, Australia

ABSTRACT

Granitoid rocks are extensively developed in the Pine Creek Geosyncline. These granitoids are of two distinct ages — Archaean and late Lower Proterozoic to early Middle Proterozoic. Whole-rock Rb-Sr isochrons and zircons record Archaean ages for the Rum Jungle and Waterhouse Complexes; K-Ar dates on minerals from Rum Jungle record an ~1800 m.y. regional metamorphic event. Isotopic dating of the Nanambu Complex indicates an Archaean age, but also reactivated ~1800 m.y. granitoid components. These complexes have features in common with mantled gneiss domes. The little known Litchfield Complex appears to have a history similar to that of the Nanambu Complex. The Nimbuwah Complex is atypical in that the zircons record an 1870 m.y. orogenic event and the Archaean component is apparently absent. Post ~1800 m.y. regional metamorphism, granitoids formed late-orogenic semi-conformable to highly transgressive plutons with ages ranging from late lower Proterozoic to early Middle Proterozoic.

The complexes contain a mixture of *S*- and *I*-type granitoids except the Nimbuwah which is exclusively of *I*-type. The Nimbuwah Complex differs from the other complexes: it is the most mafic, impoverished in lithophile elements including U and Th, has a low initial $^{87}Sr/^{86}Sr$ ratio, and is associated with granulites. The late-orogenic granitoids are generally more felsic than the complex granitoids, are almost exclusively *I*-type, and are richer in the lithophile elements including U and Th. Granitoids of the Pine Creek Geosyncline are enriched in uranium by a factor of 2 to 6 times the world average abundance for these rock types, except for the Nimbuwah Complex which has an average uranium content of 3 ppm.

The data suggest alternative interpretations: the late-orogenic granitoids may represent products of a small degree of partial melting ('minimum temperature'), end products of fractionation or derivation from a source moderately high in potassium and silica. However, the complex granitoids, particularly the *I*-types, could be interpreted as products of a large degree of partial melting ('non-minimum temperature') from a source rich in silica and calcium or of mildly fractionated rocks. The mafic Nimbuwah Complex, with marked low lithophile content, may represent residuum after extraction of a more felsic component.

INTRODUCTION

Granitoids comprise a large area of the rocks exposed in the Pine Creek Geosyncline. The five complexes in which multi-deformational events have occurred are Rum Jungle, Waterhouse, Litchfield, Nanambu and Nimbuwah complexes. Most of these complexes record two orogenic events, with dates ranging from Archaean to Lower Proterozoic. Numerous high level late-orogenic granitoids intrude the Lower Proterozoic sediments to form semi-conformable to highly transgressive plutons. These granitoids are considered to postdate the ~1800 m.y. regional metamorphic event — an age relationship confirmed by isotopic dates on the granitoids, which give late Lower Proterozoic to early Middle Proterozoic ages.

Prior to 1946 geological investigations were confined to broad traverses of a reconnaissance nature. With the discovery of economic gold mineralisation in 1872 in the Pine Creek area and at Grove Hill in 1873, active prospecting was generated and geological reports were largely confined to details of the deposits and prospects. For a review of this earlier geological work, see Walpole *et al.* (1968, p.3-5).

As a result of the Bureau of Mineral Resources, Geology and Geophysics (BMR), activity in the region in 1946, the first geological map of the area was compiled by Noakes (1949). Further regional work was undertaken by the BMR, and as a result of this activity a 1:500 000 geological map was published as well as a comprehensive geological account (Walpole *et al.*, 1968). These authors dealt with aspects of the granitoid rocks in considerable detail, including field and tectonic settings, isotopic age measurements, and petrology. Limited analyses were also carried out.

With the discoveries of airborne radiometric anomalies in the Alligator Rivers Region in 1969 the BMR undertook semi-detailed mapping of the new uranium field. Thereafter a better understanding of the age relationships and distribution of the granitoids was reached, particularly for the Nanambu and Nimbuwah Complexes (Needham *et al.*, 1974; this volume).

Since the 1968 publication (Walpole *et al.*) further isotopic dating of the granitoids has been carried out by Compston & Arriens (1968), Page (1976), Richards *et al.* (this volume) and Riley (this volume). Stephansson & Johnson (1976) investigated the tectonic setting of the granitoids in the western half of the Pine Creek Geosyncline. Petrochemical studies on granitoids have been confined to certain individual plutons: Rum Jungle (Johnson, 1974); Cullen Granite (Ewers & Scott, 1977) and Mount Bundey Granite (Hochman, 1979).

For this study we have compiled all existing chemical analyses on the Pine Creek Geosyncline granitoids, including 79 new whole-rock analyses; they are presented in microfiche in the pocket at back of the Proceedings. The new whole-rock chemical data includes analysis of 41 elements and oxides; statistical treatment of these data includes: correlations, means, variances, and clustering (Ferguson & Winer, this volume). The broad petrochemistry of the granitoids in the Pine Creek Geosyncline is investigated here and models are postulated to account for the generation of these rocks.

REGIONAL GEOLOGY (Fig. 1)

Within the Pine Creek Geosyncline, there are five complexes in which multi-deformational events have taken place involving granitoid rocks, migmatites and, in places,

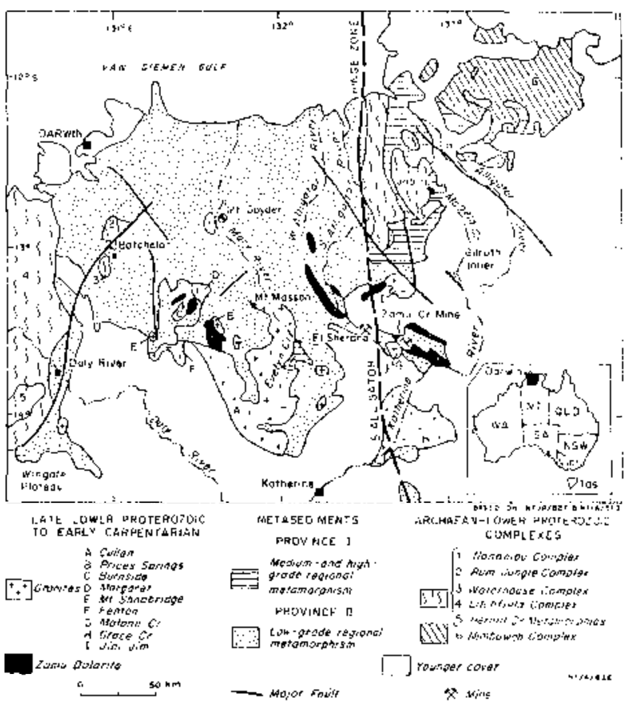


Figure 1. Generalised geology of the Pine Creek Geosyncline.

supracrustal rocks (see Page *et al.*, this volume for a summary of chronology). Two orogenic events have been recorded in most of the complexes, with dates ranging from Archaean to late Lower Proterozoic. Archaean ages (2500 m.y. ± 100 m.y.) have been determined in three of the complexes from whole rock Rb-Sr isochrons and the U-Pb method, namely the Rum Jungle, Waterhouse, and Nanambu Complexes (Richards *et al.*, 1966 and 1977; Richards & Rhodes, 1967; Page, 1976). The Nanambu Complex has the unique distinction of recording an ~2000 m.y. orogenic event (Page, 1976). Recent interpretation of this age suggests that it could have resulted from isotopic inhomogenisation (Page *et al.*, this volume). An ~1800 m.y. late Lower Proterozoic orogenic event is documented by whole rock Rb-Sr dates in the Litchfield, Nanambu and Nimbuwah Complexes (Compston & Arriens, 1968; Page, 1976), by K-Ar mineral ages at Rum Jungle (Richards *et al.*, 1977), and is also confirmed by K-Ar on micas from the Nanambu and Litchfield Complexes (Hurley *et al.*, 1961; Page, 1976).

U-Pb zircon studies from the crystalline rocks of the Nimbuwah Complex record an orogenic event between 1866 and 1886 m.y. (Page *et al.*, this volume). The Rb-Sr total-rock isochrons for these rocks give an age of 1803 ± 20 m.y., denoting a time shortly before the peak of metamorphism. Using an assumed mantle $^{87}Sr/^{86}Sr$ ratio of 0.7023, the regression analysis gives an age of 1950 ± 28 m.y. for these same rocks; this date is the maximum estimate of the mean age of the unmetamorphosed granitoids (Page *et al.*, this volume).

The Rum Jungle and Waterhouse Complexes do not intrude overlying Lower Proterozoic sediments. The doming of the Archaean basement and cover rocks in these two areas was caused by polyphase folding (Ruxton, B.P. & Shields, J., Unpubl. report 1962; Rhodes, 1965; Walpole *et al.*, 1968). Ruxton & Shields (op. cit.) and Stephensson & Johnson (1976) compared the Rum Jungle Complex to a mantled gneiss dome (Eskola, 1948); doming has resulted in the formation of a rim syncline around the Waterhouse Complex, and shearing has developed at the basement-sediment contact of both complexes. This essentially solid-state diapirism is thought to have been driven by intrusion of younger underlying granitoids by a mechanism of gravitational instability (Stephansson & Johnson, 1976). The origin of the Nanambu Complex may be similar, but during the 1800 m.y. metamorphism, Lower Proterozoic basal arkosic rocks were accreted to the Archaean granitoids (Needham *et al.*, this volume). Contacts between the Archaean and younger rocks, and between the Archaean-Lower Proterozoic granitoids and the surrounding rocks, are not exposed. The Nimbuwah Complex comprises outer partly migmatitised schist and gneiss which grade into Lower Proterozoic metasediments, and inner migmatitic and massive granitoid rocks. Very little information is available on the Litchfield Complex, but parts of it appear to have had a style of development similar to that of the Nanambu and Nimbuwah Complexes. In all these Complexes it is possible to trace the transition from granitoid rocks through migmatites into metamorphosed supracrustal rocks. Using an unconformity which separates Lower Proterozoic metasediments from granitoids of the Litchfield Complex south of the Daly River, Berkman (this volume) assigns an Archaean age to this granitoid terrain.

High-level diapiric granitoids intrude the Lower Proterozoic metasediments; these granitoids are considered to slightly postdate the ~1800 m.y. regional metamorphic event (Needham *et al.*, this volume; Ferguson, this volume). This age relationship is confirmed by isotopic dates which range from 1780 to 1710 m.y. (Compston & Arriens, 1968; Hurley *et al.*, 1961; Page, 1976; Page *et al.*, this volume; Riley, this volume) indicating late Lower Proterozoic to early Middle Proterozoic ages. The area of these granitoid plutons ranges from the 3km² Mount Shoobridge Granite to the >2800km² Cullen Granite. Intrusive relations vary from semi-conformable, as exemplified by the Burnside Granite, to highly transgressive intrusive varieties, as typified by the Cullen Granite. Contact metamorphism is associated with all these late-orogenic granitoids, and has produced hornfelsic aureoles up

to 5km wide (Walpole *et al.*, 1968). Low-pressure medium-grade mineral assemblages occur in these contact metamorphic aureoles (Ferguson, this volume).

The Malone Creek and Grace Creek Granites are hypersolvus and, as pointed out by Walpole *et al.* (1968), are spatially associated with the extrusive felsic rocks of the Edith River Volcanics which are dated at 1760 m.y. The other granitoids are subsolvus. Walpole *et al.* (1968) suggested that the Malone Creek Granite "may have been intruded not long before the deposition of the Edith River Volcanics". Further, the earlier isotopic dating of the Grace Creek Granite suggested that this granitoid was much younger than the Edith River Volcanics. Later reinterpretation of the isotope dating by Compston (see Walpole *et al.*, 1968; Appendix 2) indicates similar ages for these two rock units. The similar ages and spatial association of these two granitic plutons with the Edith River Volcanics, taken in conjunction with the hypersolvus nature of the granitoids, suggests that they may be coeval - an opinion shared by Needham *et al.* (this volume).

In all cases, the major rock units of the complexes are an admixture comprising granitic banded gneisses, foliated granitoids, migmatites, agmatites, pegmatites, aplites, and mylonites. Rocks of obvious supracrustal affinity include quartzose rocks, meta-pelitic schists, amphibolites, meta-volcanics, and metamorphosed calcareous and siliceous chemical sediments. Where outcrop is good, and detailed mapping has been carried out, as in the Rum Jungle Complex (Rhodes, 1965; Johnson, 1974), relative age relationships of major rock units can be ascertained, which in decreasing age are, schists and gneisses, granite gneiss, meta-diorite, coarse granite, large feldspar granite and leucocratic granite. In the case of the Nimbuwah Complex, Needham *et al.* (1974) distinguished granitoid core, migmatite zone, lit-par-lit gneiss zone, and transitional zone (mostly supracrustals). At times, clear-cut intrusive relations can be seen within the granitoid varieties of the Nimbuwah Complex, where porphyritic granitoids intrude gneisses producing agmatitic textures.

CHEMISTRY AND PETROLOGY

Using chemical, mineralogical, and field criteria Chappell & White (1974) have distinguished two types of granitoids in the Palaeozoic Lachlan Fold Belt of southeastern Australia. The differences between these two are interpreted as a reflection of different source rocks: partial melting of peraluminous sedimentary rocks is thought to produce *S*-type granitoids whereas *I*-types have an igneous source. The rationale for this concept is that the production of pelitic sedimentary rocks involves loss of sodium to sea-water and evaporites and calcium to carbonates, so that the main sedimentary pile is relatively enriched in aluminium. Granitoids from such a source will reflect this prior chemical fractionation. In contrast, this style of fractionation does not occur in igneous rocks; hence there is no enrichment of aluminium relative to alkalis and calcium in *I*-type granitoids. These chemical differences are reflected in the mineralogy, of the two granitoid varieties. The distinctive chemical, mineralogical and field criteria of *S*- and *I*-type granitoids are summarised in table 1. In that the atmosphere was generally oxygenous as far back as 2500 m.y. ago (Cloud, 1976), and so probably similar to later climatic conditions, the rationale of *S*- and *I*-type granitoid production through anatexis of sedimentary and igneous rocks respectively, should be applicable back to at least Lower Proterozoic times. The parameters outlined here have been applied to the granitoids of the Pine Creek Geosyncline.

The granitoid complexes have mixed *S*- and *I*-type parentage (Fig. 2). The Nanambu, Waterhouse and Rum Jungle Complexes have an approximately equal distribution of *S*- and *I*-types. The little information available on the Litchfield Complex suggests that it is dominated by *S*-types, whereas granitoids of the Nimbuwah Complex are exclusively *I*-type. Within the complexes the granitoids consist mostly of adamellite, other compositions include granite, granodiorite, quartz monzonite, quartz monzodiorite, and rare tonalite and

I-types	*S*-types
CHEMICAL CRITERIA	
Sodium normally high, $Na_2O \gtrsim 3.2\%$ in felsic varieties, decreasing to 2.2% in more mafic types.	Sodium may be low, Na_2O normally $<3.2\%$ in rocks with approximately 5% K_2O, decreasing to $>2.2\%$ in rocks with approximately 2% K_2O.
Mol. $Al_2O_3/(Na_2O + K_2O + CaO) < 1.1$	Mol. $Al_2O_3/(Na_2O + K_2O + CaO) > 1.1$
Broad spectrum of compositions from felsic to mafic.	Relatively restricted in composition to high SiO_2 types
Regular inter-element variations within plutons; linear or near-linear variation diagrams	Variation diagrams more irregular
C.I.P.W. normative diopside or $<1\%$ normative corrundum	Always have C.I.P.W. Normative corrundum
$Fe^{3+}/(Fe^{2+} + Fe^{3+})$ high (usually >0.2)	$Fe^{3+}/(Fe^{2+} + Fe^{3+})$ low (usually <0.2)
Initial $^{87}Sr/^{86}Sr$ ratios generally low (usually <0.708)	Initial $^{87}Sr/^{86}Sr$ ratios generally high (usually >0.708)
$<65\%$ SiO_2 most common	$>65\%$ SiO_2 most common
$\delta^{18}O$ values from 7.9 to 9.4	$\delta^{18}O$ values from 9.9 to 12.0
MINERALOGICAL CRITERIA	
Hornblende present (hornblende-bearing xenoliths common)'	Hornblende absent
Minor muscovite in very felsic rocks	Muscovite common, sometimes abundant (2-3%)
Cordierite, garnet, andalusite and sillimanite absent	Cordierite, garnet, andalusite and sillimanite may be present
Accessories: Magnetite, allanite and primary sphene; sulphides uncommon; zircon, monazite and apatite can be present	Accessories: Ilmenite, cassiterite and tourmaline; sulphides common; zircon, monazite and apatite can be present

From: Chappell & White, 1974; White *et al.*, 1977; O'Neil & Chappell, 1977; Hine *et al.*, 1978.

Table 1. Distinctive chemical and mineralogical properties of *I*- and *S*-type granitoids

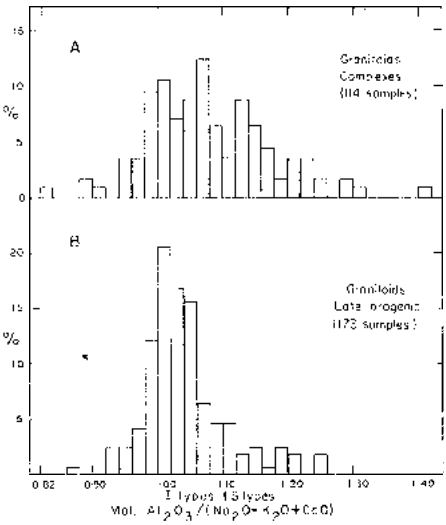


Figure 2. Histograms showing frequency mol. $Al_2O_3/(Na_2O + K_2O + CaO)$ for complex and late-orogenic granitoids (A & B respectively). Those analyses for which this ratio was >1.50 are not plotted. Analyses of obviously altered rocks are not plotted.

monzonite (Fig. 3A). These varieties of granitoids can occur exposed as separate units or make up composite exposures with all textural varieties present. The pegmatites and aplites are generally the only non-foliated granitoids encountered in the complexes. The foliation in the granitoids is defined by any, or a combination of, the following: elongate feldspar phenocrysts, platey and small elongate clots of biotite or hornblende or a combination of these two mafic minerals, xenoliths and, rarely, lensoid aggregates of quartz. In some cases, the feldspar phenocrysts define a marked lineation in the plane of lamination. The banded gneisses owe their lamination to alternating concentrations of mafic and felsic units, grain size variation and to textural contrasts. The bands vary considerably in thickness and extent, producing irregular lensoid units and broad uniform tabular units which are invariably contorted into wild-folds. Contorted and irregular mafic schlieren also define the banding in places. The non-banded gneisses have a marked foliation produced by planar alignment of elongate minerals and small aggregates of minerals which also produce a lineation in some places. Where banded and non-banded varieties of gneiss are juxtaposed, the foliation in both units is parallel, furthermore the rafts of early gneisses in these rocks are flattened with their long axes parallelling the foliation. Where narrow late-porphyritic granitic veins and pegmatites and aplites crosscut the foliation at high angles, they are ptygmatically folded. Generally the granitoids are medium-grained but coarse-grained and fine-grained varieties are present locally which help to produce a banded texture. In some places narrow coarse grained units are transgressive to the general foliation. All varieties of granitoids can by porphyritic, the K-feldspar phenocrysts reach 3cm long in the coarse grained varieties and 0.8cm in the medium-grained varieties. Although the mineral proportions vary considerably the same suite generally occurs within the mafic and felsic units of the granitoids. In the *I*-type granitoids, the pristine assemblage includes quartz, two-feldspars, biotite, ± hornblende, ± sphene, ± apatite, ± allanite, ± zircon. With the exception of the absence of hornblende and allanite, the *S*-type granitoids can include any or all of the following: garnet, muscovite, cordierite, and sillimanite. The quartz usually exhibits two size populations. The larger grains occur as anhedra in areas interstitial to the other major rock-forming minerals, varying in size, from 1 to 4mm, whereas the smaller grains included in the K-feldspars are subhedral and range in size from 0.1 to 0.4mm. The larger interstitial grains commonly cluster into aggregates up to 1cm long with a poorly defined lensoid character which is, in part, responsible for the foliation. The quartz generally shows undulose extinction. In the granites and felsic granodiorites, K-feldspar is in excess of plagioclase; the reverse is true in the more mafic granodiorites and monzodiorites. Two feldspars are always present; generally these are a micro-perthitic microcline and a polysynthetically twinned Na-rich plagioclase. In the coarser grained rocks, stringlet perthite tends to develop in the microcline. A micro-vermicular texture between quartz and feldspar is only sparsely developed at and

near the margins of the K-feldspar over areas not exceeding 1mm. The phenocrysts take on lath habit, otherwise the K-feldspar form irregular anhedra. Plagioclase has a fairly strong lath development throughout ranging from elongate to stumpy. The plagioclase can show a weak zoning; in many instances it has been extensively altered to muscovite along cleavage and fracture directions.

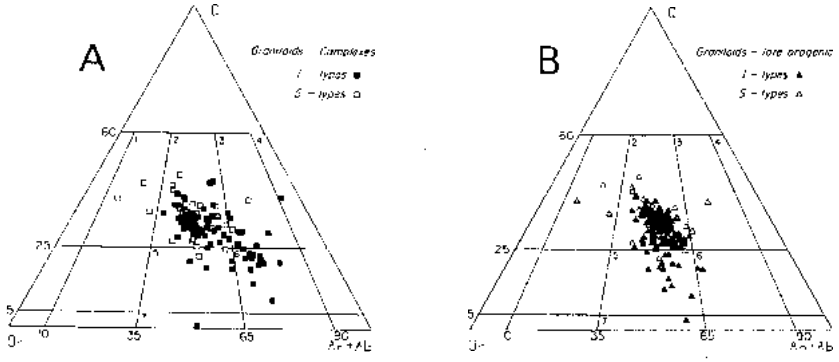


Figure 3. Normative compositions of complexes and late-orogenic granitoids (A and B respectively) plotted in terms of Q, Or and An + Ab. The classification scheme is modified from the modal classification of Streckeisen (1976): 1 = granite; 2 = adamellite; 3 = granodiorite; 4 = tonalite; 5 = quartz monzonite; 6 = quartz monzodiorite; 7 = monzonite. All available analyses plotted.

Biotite and hornblende are the main mafic minerals in the *I*-types, the two minerals generally coexist, but hornblende may be absent. Where hornblende and biotite occur in the same rock, they most commonly form small aggregates of interlocking grains and sphene is usually intergrown with these aggregates. The hornblende is usually markedly poikilitic and the biotite less so, the inclusions can comprise quartz and euhedral apatites, zircons, fluorite and opaques. Biotite is readily altered to chlorite, hornblende less so, and epidote group minerals are also an alteration product of both minerals. Individual grains of hornblende and biotite rarely exceed 3mm but clotted aggregates of these minerals can produce elongate lensoid masses several centimetres long which are generally less than 8mm diameter. The minor zircon inclusions produce metamict haloes in the two mafic minerals. Garnet and biotite are the main mafic minerals in the *S*-type granitoids, occurring either as 2mm diameter grains in the general matrix of the rock or more commonly as poikilitic anhedra up to 2cm diameter with inclusions of feldspar and quartz. Muscovite and cordierite commonly occur with the garnet; sillimanite has been reported as a common phase in the granitoids of the Litchfield Complex (Walpole *et al.*, 1968). Biotite can occur with muscovite-the two minerals commonly intergrown. Zircon and apatite are common accessories minerals in these rocks and opaque(s) less so.

The pegmatities are commonly interlayered with fine-grained aplite, both phases are typically granitic and contain abundant muscovite, and in places, tourmaline.

The gradation between *S*-type granitoid and obvious meta-sedimentary units can be difficult to monitor when meta-pelitic rocks are involved. The granitoids commonly take on a *S*-type character near these meta-pelitic units. Garnet, cordierite, muscovite, and sillimanite appear in granular hypidomorphic rocks and can also be found juxtaposed in obvious metapelitic rocks but the boundary may be indistinct.

The late-orogenic granitoids are mainly *I*-type (Fig. 2), but *S*-type phases are commonly developed near the margins which suggests contamination of *I*-types. These granitoids are dominantly adamellite; granite compositions are found exclusively as *S*-type. Other compositions include granodiorite, quartz monzonite, and some less common quartz

monzodiorite and monzonite (Fig. 3B). The late-orogenic granitoids have polyphased granitoid development with as many as five major rock phases, as is the case for the Cullen Granite (Ewers & Scott, 1977). Even the small Mount Shoobridge Granite is made up of three granitoid types (Rhodes, 1969). The major rock units are generally coarse to medium-grained with granitic to porphyritic texture. Minor phases include pegmatites, aplites, microgranites, felsic porphyry dykes, granophyric chill phases, quartz ± tourmaline veins, quartz breccias, mafic xenoliths, and mafic mineral segregations.

In the major granitoid phases of the late-orogenic plutons, textural contrasts range from coarse to fine-grained, and granular hypidomorphic to porphyritic. Phenocrysts usually comprise alkali-feldspar up to 6cm long, but plagioclase and quartz can be rare additional phenocrystic phases. Only minor foliation is present in these rocks produced by the platey alignment of feldspars and elongate mafic xenoliths. Some flaser texture is developed at the margins of some plutons. The alkali feldspar is generally perthitic to microperthitic in the medium to coarse-grained varieties and cryptoperthitic in the fine-grained varieties. Plagioclase may form phenocrysts in the more mafic varieties; the composition varies from albite/oligoclase in the more felsic varieties, to andesine in the more mafic. Quartz occurs as discrete anhedral grains up to 6mm in diameter and as clusters of several grains reaching 15mm in diameter. The quartz generally displays undulose extinction as well as fracturing. Myrmekitic and micrographitic textures are particularly prevalent in the medium and fine-grained granitoid phases. As most of the late-orogenic granitoids are *I*-type, the main mafic minerals are hornblende and biotite. These two minerals tend to aggregate, the hornblende is commonly poikilitic, the inclusions are the felsic minerals. Apatite, zircon, allanite, and fluorite are the main accessory minerals. Near the margins of some of these plutons muscovite ± garnet ± cordierite are developed. These may be *S*-type phases implying a sedimentary source rock component, or else are the result of contamination. Figure 2B shows that a small percentage of late-orogenic granitoids plot in the *S*-type field. In some cases, the *S*-type character is due to a pristine condition, but where petrographic control is unavailable

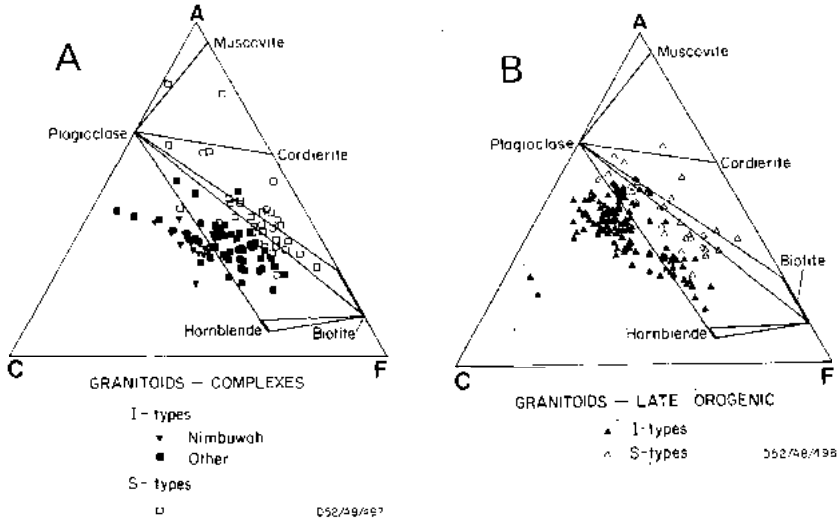


Figure 4. Granitoid compositions plotted in terms of $A(Al_2O_3 + Fe_2O_3) - (Na_2O + K_2O)$, $C(CaO - 3.3xP_2O_5)$, and F(FeO + MgO + MnO) for complex and late-orogenic granitoids (A & B respectively). All available analyses plotted.

the peraluminous character may be caused by extensive alteration of the feldspar to clay and micaceous minerals.

In the *I*-type granitoids, the xenoliths are amphibolite and hornblende-rich granitoids. These xenoliths rarely exceed 30cm in length. In the *S*-type granitoids, the xenoliths are meta-pelites which commonly contain garnet, cordierite, and andalusite. Xenoliths of country rock are common in the marginal parts of the plutons, particularly in the transgressive varieties.

The main elements determining mineralogical assemblages of granitoid types are Al, Na, K and Ca, and hence the ACF and A'KF plots (Figs. 4 & 5) are well suited to demonstrate these differences. These two figures show that there is a broad separation of *S*- and *I*-types in all the granitoid rocks of the Pine Creek Geosyncline. In the ACF plots (Fig. 4A & B), the *I*-types populate on the C-rich side of the plagioclase-biotite join whereas the *S*-types are displaced towards the A-apex of this tie-line. The mafic-rich character of the granitoids in the complexes relative to the late-orogenic granitoids is reflected by their relative displacement towards the F-apex (Figs. 4 & 5). The calcic-rich nature of the Nimbuwah Complex granitoids is shown by their displacement towards the C-apex as compared to most other complex granitoids (Fig. 4A). In some cases the A' component in the A'KF plot gave a negative value. This anomaly stems from the fact that in some cases petrographic control was absent, and as all CaO is subtracted from Al_2O_3 in the A' component, the calculation does not accommodate calcium that may be present in places other than in CaAl and $CaFe^{3+}$ silicates. The peraluminous character of the *S*-type granitoids is shown by their displacement towards the A' component, as compared to the *I*-type granitoids which lie close to the K-F side of the ternary plot.

The PCG set of analyses (microfiche, this volume) were used for the correlation testing of elements, as these samples contained sufficient trace element data to make the exercise meaningful. Another requirement for this test was a minimum of five samples per rock unit. On this basis, the correlation of elements was computed at the 99 percent confidence limit

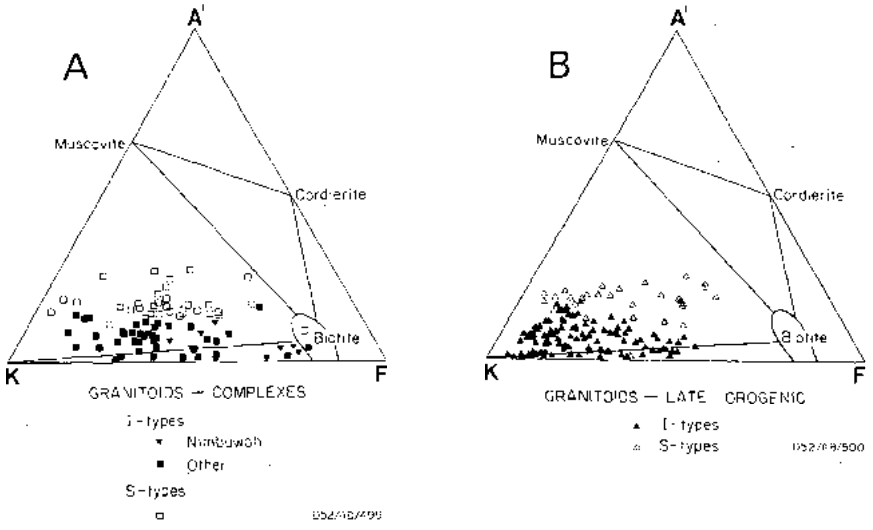


Figure 5. Granitoid compositions plotted in terms of A'(Al_2O_3 + Fe_2O_3) – (Na_2O + K_2O + CaO), K(K_2O) and F(FeO + MgO + MnO) for complex and late-orogenic granitoids (A & B respectively). All available analyses plotted.

for the granitoid groups: Waterhouse Complex, Nanambu Complex, Nimbuwah Complex and late-orogenic granitoids (Ferguson & Winer, this volume, Table 5).

The granitoid rocks usually show a high degree of correlation between major elements. This is particularly true where standard deviations (S.D.) are high (Ferguson & Winer, this volume, Table 7); in such instances there is a strong negative correlation of Si with the other major elements.

The Waterhouse Complex granitoids display a moderate degree of correlation of most major and some trace elements and, as can be seen from the S.D.'s, they also have a moderately restricted compositional range (Ferguson & Winer, this volume, Table 7). The only moderate correlation of the major elements is related to the mixed *S*- and *I*-type parentage. The high degree of correlation of the trace elements, Y, Zr, La, Ce, V and Hf is probably related to accessory and minor mineral phases.

The Nanambu Complex displays a high degree of correlation despite the more varied composition as shown by high S.D.'s. Due to the large variance of Si in these *S*- and *I*-type granitoids there is a strong negative correlation of this element with most of the major elements excepting Ca and alkalis. The negative correlation of Si with Mg and Fe reflects the inverse correlation of mafic and felsic minerals, a factor exaggerated by the common replacement of feldspars by chlorite. The lack of a correlation between Si and Ca and alkalis can also be attributed to replacement of feldspars by chlorite. The relatively enriched sulphur content of the Nanambu Complex, found particularly in the *S*-type granitoids, results in a good correlation with the chalcophile elements, Ni, Cu, Zn, As and Mo. The high degrees of correlation of other trace elements are attributed to accessory and minor mineral phases.

The mafic-rich granitoids of the Nimbuwah Complex, all of which are *I*-types, have a high degree of correlation of major elements. The inverse relationship between felsic and mafic minerals in these rocks accounts for the negative correlation of Si and Ti, Σ Fe, Mn, Mg and Ca. High degrees of correlation are shown for the trace elements, S, Ni, Zn, Rb, Sr, Th, La, Ga, Ce, Pb, V, F and Sc. With the probable exception of Rb and Sr the remaining trace elements distribution showing strong correlation is probably governed by accessory mineral phases.

The high-level late-orogenic granitoids (Ferguson & Winer, this volume, Table 7) comprise a mixed suite of rocks from six different plutons; these rocks were grouped into one unit because insufficient analyses were available for statistical treatment of individual bodies. This composite suite of analyses, not surprisingly, has a moderately high S.D. for most elements and does not have a particularly high degree of correlation. Not unexpectedly, Si shows a negative correlation with all the major elements except alkalis. The lack of correlation with alkalis probably reflects the degree of alteration of feldspar to sheet silicates. The high degree of correlation of Rb, Sr and Ba is probably controlled by substitution in the major minerals, whereas, P, Y, Ni, Zr, U, Ga, V, F and Sc is probably fixed in minor and trace minerals in these rocks.

Figures 6 and 7 display clearly the negative correlation between SiO_2 and MgO, TiO_2 and Al_2O_3 for the granitoids from the complexes and late-orogenic granitoids. The more felsic nature of the *S*-type granitoids is demonstrated by general higher SiO_2 relative to the *I*-type granitoids. The average K_2O content of the granitoids is about 5 percent, except for the Nimbuwah Complex which averages less than 4 percent. Higher Rb in the more evolved felsic granitoids results in a negative correlation between K/Rb and SiO_2 (Figs. 6G & 7G). The negative correlation between Ba/Rb versus SiO_2 results from higher Ba relative to Rb in the more mafic granitoids — a condition reversed in the more felsic, SiO_2- rich, varieties (Figs. 6H & 7H). The higher Sr contents of the more mafic granitoids and the presence of

more Rb in the felsic varieties results in a positive curve for a plot of Rb/Sr versus SiO_2 (Figs. 6E & 7E).

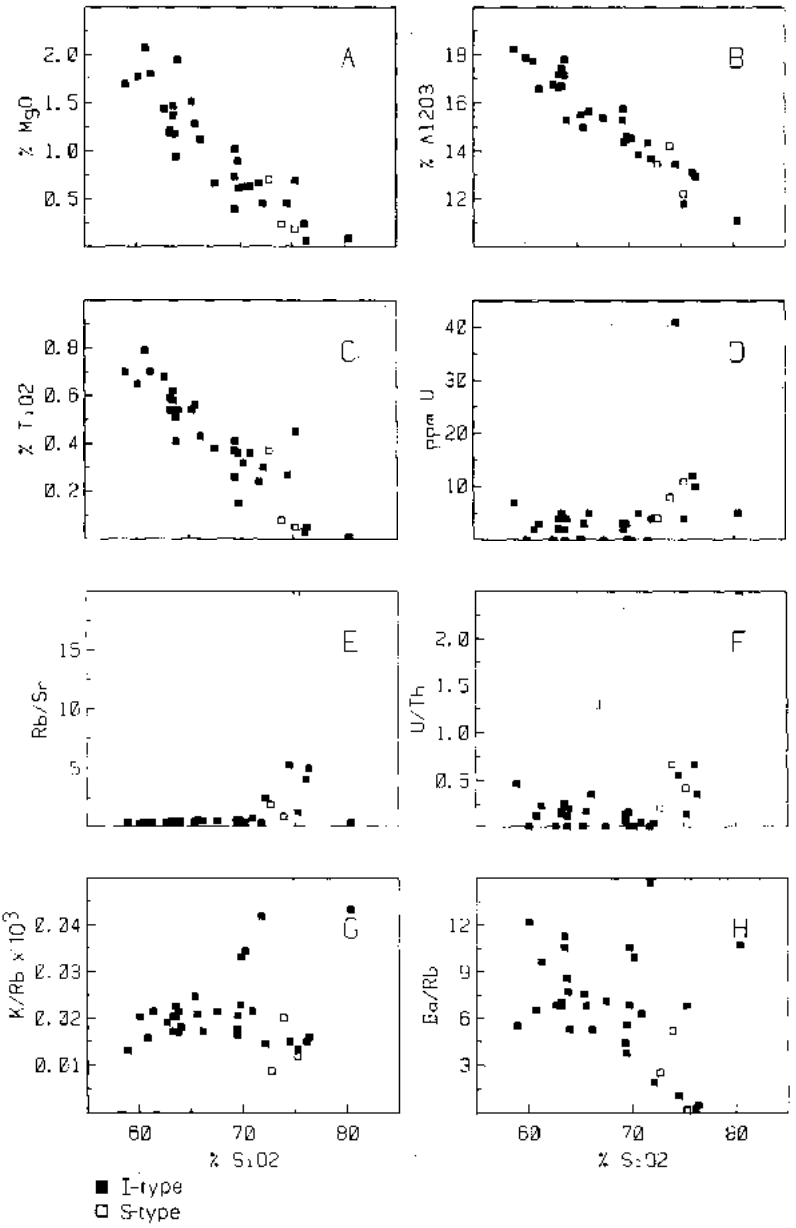


Figure 6. Plots of silica versus some oxides and ratios for complex granitoids. Only those analyses for which petrographic control is available are plotted.

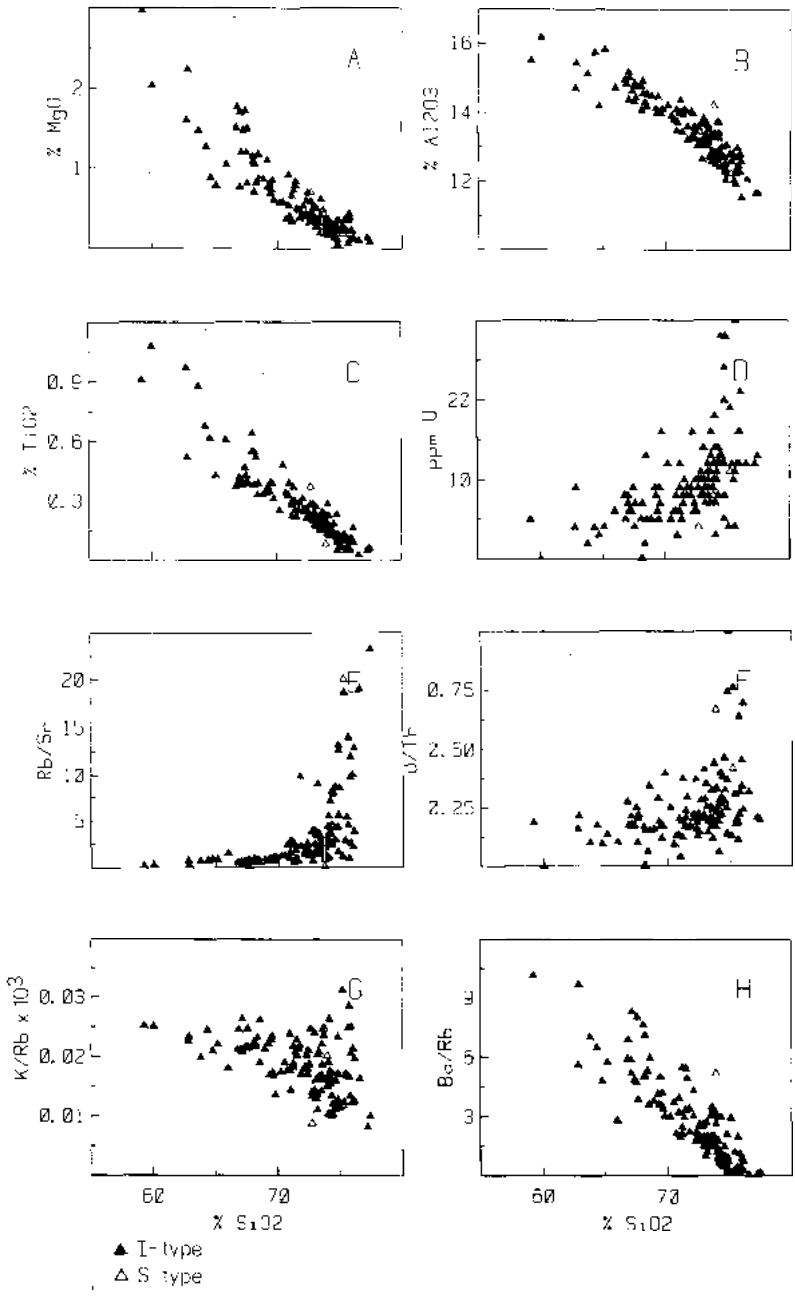


Figure 7. Plots of silica versus some oxides and ratios for late-orogenic granitoids. Only those analyses for which petrographic control is available are plotted.

The ternary relationship between Rb-Ba-Sr has been used to trace the differentiation patterns in granitoid rocks (El Bouseily & El Sokkary, 1975). Figure 8A & B shows the patterns encountered for granitoids of the Pine Creek Geosyncline; a large percentage of values fall into the 'anomalous granite' field; those which have 'suffered from metasomatism' (El Bouseily & El Sokkary, 1975). Although the granitoids which occur in the Pine Creek Geosyncline do not always fall into their nominated fields the samples plot along the

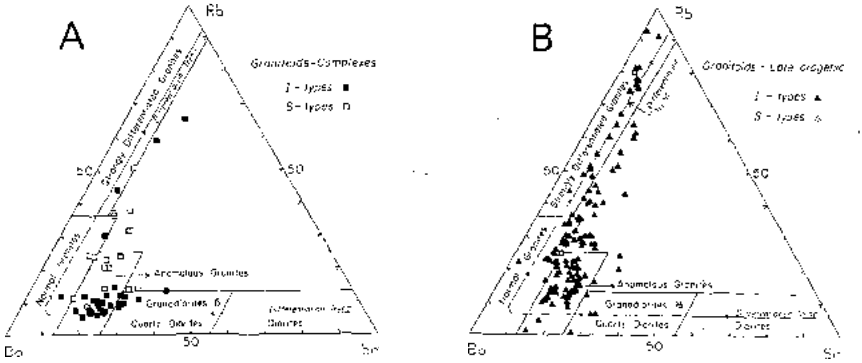


Figure 8. Rb-Ba-Sr variation diagram for complex and late-orogenic granitoids (A & B respectively) (after El Bouseily & El Sokkary, 1975). Only those analyses for which petrographic control is available are plotted.

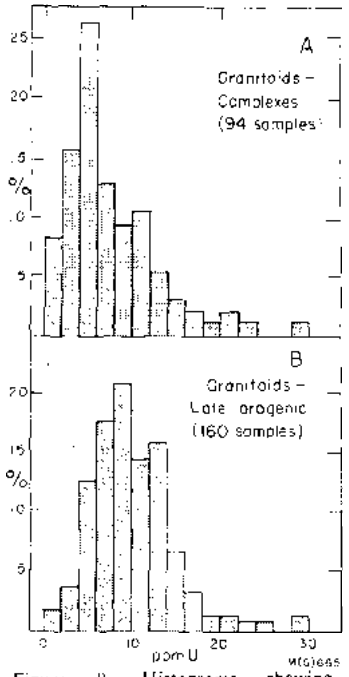


Figure 9. Histograms showing frequency of U(ppm) for complex and late-orogenic granitoids (A & B respectively). Some analyses plotted in figure 2 where uranium analysed.

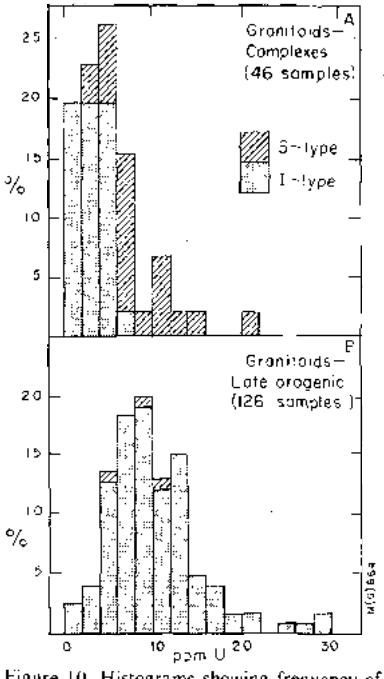


Figure 10. Histograms showing frequency of U(ppm) in the complexes and late-orogenic granitoids for *S*- and *I*-types (A & B respectively). Only those analyses for which petrographic control is available are plotted.

	COMPLEXES					LATE OROGENIC					
	Rum Jungle	Waterhouse	Nanambu	Nimbuwah	Litchfield	Allia Creek	Burnside	Cullen	Fenton	Jim Jim	Malone Creek
No. of analyses*	30	12	48	28	6	2	10	106	14	12	2
SiO_2	71.37	75.93	71.45	65.69	72.65	67.40	73.75	71.62	71.57	73.16	75.18
TiO_2	0.38	0.18	0.25	0.45	0.19	0.49	0.17	0.28	0.32	0.24	0.06
Al_2O_3	13.64	13.38	14.16	15.99	14.74	16.39	13.43	15.58	14.05	13.14	12.16
Fe_2O_3	0.95	0.84	2.04	1.05	0.85	0.52	1.93	2.98	2.72	0.97	0.89
FeO	1.49	0.94		2.77	1.37	3.35				1.35	1.21
MnO	0.04	0.03	0.04	0.06	0.04	0.05	0.04	0.04	0.04	0.05	0.02
MgO	0.85	0.61	1.27	1.15	0.81	0.93	0.28	0.60	0.65	0.62	0.27
CaO	1.23	0.77	1.21	4.14	1.42	2.23	0.91	1.53	1.46	0.96	0.46
Na_2O	3.24	4.00	3.76	2.89	3.15	2.74	3.47	3.17	3.23	2.30	1.54
K_2O	5.19	4.98	4.72	3.83	3.85	4.27	5.05	5.01	4.81	5.78	6.65
P_2O_5	0.16	0.07	0.16	0.14	0.05	0.22	0.03	0.09	0.09	0.07	0.03
Ba	202	830	426	1025			360	550	1435	475	66
Rb	278	256	179	152			372	294	193	275	320
Sr	60	147	143	337			56	149	278	103	8
Pb	25	28	16	26			51	29	169	19	15
Th	44	44	32	25	10	27	48	40	36	43	84
U	11	13	10	3	7	5	17	9	11	8	23
Zr	130	170	175	234			284	169	318	162	136
Nb	59	11	6	9				11		25	54
Y	32	32	31	23			57	25	28	41	82
La	71	51	38	76			66	66	113	65	52
Ce	109	96	72	134			156	126	181	125	177
Li	4	16	24	26			66	26	52	26	70
Cs	3	5	5	3						4	4
Sc	9	4	6	15						6	3
V	6	13	40	45				57		40	<2
Cr			133								
Co	3	5	36	18				7		7	3
Ni	1	2	15	6				5		2	1
Cu	5	7	14	9			6	6	6	9	3
Zn	8	25	32	51			50	29	67	22	23
Ga	25	18	19	20				17		19	25
Be	4										
As	<2										
Mo	<2										
Sn	3										
Wf	9										
Ag	<2										

* 'Number of analyses' refers to major-element analyses, and does not necessarily correspond to the number of trace element analyses.

All analyses used for these averages are on microfiche in the pocket at the back of this volume.

PCGr Nos.	1-30	31-42	43-90	91-118	119-124	125-136	136-137	138-243	244-257	258-269	270-271

Table 2. Averaged Chemical Analyses of Granitoids in the Pine Creek Geosyncline

differentiation trend showing Rb enrichment with increasing fractionation. Good contrasts are provided by the more evolved felsic nature of the late-orogenic granitoids.

Th content is rather uniform with the exception of the Nimbuwah Complex granitoids which have a relatively low average content of 25 ppm (Table 2). U contents are higher in the felsic granitoids giving a positive slope for plots of U versus SiO_2 and U/Th versus SiO_2 (Figs. 6D, F & 7D, F). Uranium concentration in granitoids of the complexes is generally high compared to the world abundances of 4.8 ppm in granitoids and 2.7 in the crust (Taylor, 1964; (Fig. 9A)). Most of the U values fall in the 4 to 16 ppm range with the exception of the Nimbuwah Complex where all but one of the values are below 4 ppm (Table 2). The *S*-types have a slightly higher U content than the *I*-types (Fig. 10A). A larger percentage of the late-orogenic granitoids plot in the 4 to 16 ppm U range (Fig. 10B). Not enough of these granitoids are *S*-type to draw statistically valid conclusions concerning U distribution in the two granitoid types. The granitoids of the Nimbuwah Complex are anomalous compared to those elsewhere in the Pine Creek Geosyncline: mafic granitoids and granulites dominate, uranium content is less than 4 ppm and they have a low initial $^{87}Sr/^{86}Sr$ ratio. These features suggest multi-orogenesis, and the formation of a uranium-depleted residuum.

In the quartz-saturated ternary feldspar system at 1000 bars (Fig. 11 A & B) most late-orogenic granitoids fall close to the univariant boundary curve which separates the quartz-

LATE OROGENIC (Cont'd)

Mt. Sandev	Mt. Boyce	Mt. Snowbridge	McKinley	Naharlek	Prices Springs	Roberts Ck.	Tin Cap	Wolfcamp Hill	
2	2	16	2	10	7	2	2	1	
71.92	80.08	66.49	62.38	74.97	70.62	73.20	76.12	68.41	SiO_2
0.26	0.29	0.41	0.49	0.20	0.35	0.08	0.13	0.43	TiO_2
15.79	16.80	15.12	15.97	12.89	14.33	15.02	11.85	17.26	Al_2O_3
1.25	1.69	1.70	0.65	0.75	0.75	0.94	0.36	1.32	Fe_2O_3
1.25	0.18		2.60	1.15	2.14	0.93	0.73	2.15	FeO
0.04	0.03	0.05	0.10	0.04	0.05	0.04	0.02	0.05	MnO
0.86	0.02	1.72	2.03	1.13	0.70	0.63	0.16	0.96	MgO
1.56	3.08	2.24	3.71	0.39	1.68	1.13	0.51	0.56	CaO
3.56	4.11	3.51	7.08	0.96	2.99	4.40	3.03	3.31	Na_2O
4.52	5.12	4.59	5.34	4.34	5.14	2.98	5.00	4.37	K_2O
0.13	0.09	0.21	0.21	0.06	0.12	0.06	0.03	0.09	P_2O_5
696		1445		232	853		203		Ba
280		182		304	254		382		Rb
420		639		86	289		42		Sr
36		62		10	34		43		Pb
49		50		50	45		63		Th
10		12		25	10		11		U
206		241		261	231		242		Zr
22		16		16	17		15		Nb
19		13		70	25		41		Y
106		60		88	59		158		La
109		145		109	139		209		Ce
33		24		18	30		21		Li
<1		2		2					Ga
1		2		9			3		Sc
19		26		25	20		9		V
									Cr
6		13		3	7				Co
4		17		2	6		3		Ni
4		11		3	5		4		Cu
79		36		4	37		15		Zn
20		19		20	18		19		Ga
6									Be
<2									As
3									Mo
2									Sn
30									Hf
2									W
272-275	276-277	278-293	294-295	296-305	306-312	313-314	315-316	317	

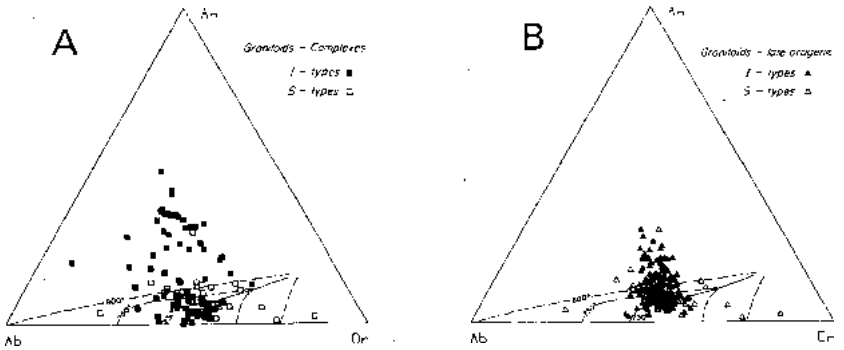


Figure 11. Normative Ab-Or-An diagrams for the complex and late-orogenic granitoids (A & B respectively) showing parts of the liquidus surface at the quartz-saturated ternary feldspar system at 1000 bars water pressure projected onto the Ab-Or-An face of the tetrahedron (after James & Hamilton, 1969). All available analyses plotted.

plagioclase and quartz-alkali feldspar fields. By contrast, the complex granitoids show a greater variation and are displaced towards the An corner which reflects their more mafic character and higher temperature of formation.

Normative compositions were used to construct phase diagrams for the simple granite systems Q-Ab-Or-H_2O and Q-Ab-Or-An-H_2O (Fig. 12 A & B). The centre of gravity for the plots of the late-orogenic granitoids falls evenly between the quartz-feldspar field boundaries at 500-3000 bars water pressure whereas the complex granitoids show a wide variation displaced towards the An_5 'piercing point'.

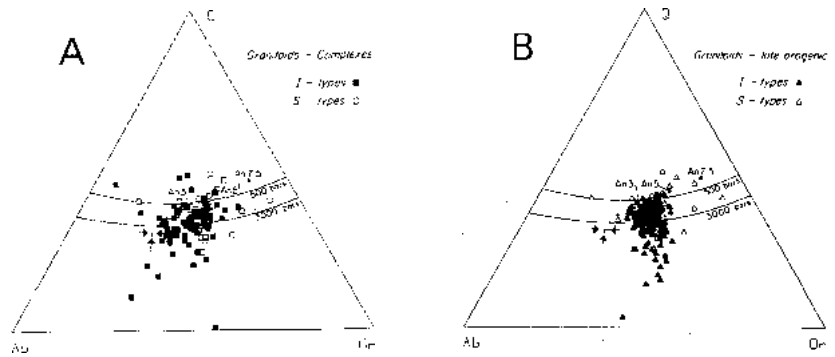


Figure 12. Normative Q-Ab-Or-H_2O diagrams for the complex and late orogenic granitoids (A & B respectively) showing quartz-feldspar field boundaries at 500 and 5000 bars water pressure and positions of quaternary isobaric minima (after Tuttle & Bowen, 1958). 'Piercing points' are also shown for the system Q-Ab-Or-An-H_2O at 1000 bars water pressure for An contents 3.5 and 7.5 percent projected onto the base of the tetrahedron (after James & Hamilton, 1969). All available analyses plotted.

CONCLUSIONS

The presence of granitised and granitoid engulfed metasediments and abundant *S*-type granitoids in some of the Archaean Complexes in the Pine Creek Geosyncline indicates that sediments predate 2500 ± 100 m.y. The little information available on the Litchfield Complex suggests that this Complex had a development similar to that of the Rum Jungle, Waterhouse, and Nanambu Complexes. The Nimbuwah Complex offers marked contrasts with the other complexes: there is no Archaean component; the granitoids are more mafic; there is depletion in compatible elements including U and Th; the granitoids have low initial $^{87}Sr/^{86}Sr$ ratios; *I*-type granitoids develop exclusively and granulites are present. These features and the estimated P-T conditions (Ferguson, this volume) suggest that this Complex is the lowermost exposed portion of the Pine Creek Geosyncline and represents a terrain that has undergone multi-orogenesis and formation of a residuum depleted in large-ion lithophile elements. The exposed inliers of granulites may represent unfaulted blocks. Hart *et al.*, (this volume) indicate a similar geochemical crustal profile for the upper and middle crust at Vredefort, South Africa.

The granitoids occurring in the complexes, particularly the *I*-types, could be interpreted either as products of a large degree of partial melting ('non-minimum temperature') from a source enriched in silica and calcium, or as products of mildly fractionated rocks. On the other hand the late-orogenic granitoids may represent products of a small degree of partial melting ('minimum temperature') or end products of fractionation derived from a source moderately enriched in potassium and silica.

That the basement was originally enriched in U is indicated by the high values present in the Archaean granitoids, in particular, the *S*-types. The Archaean rocks are thought to be

representative of the provenance areas to the Lower Proterozoic sediments of the Pine Creek Geosyncline. Uranium was selectively enriched in some sediments, resulting in development of syngenetic protore. The late-orogenic granitoids were probably derived from a uranium-enriched igneous component of the basement, as represented by some of the Archaean granitoids in the area. They have a slightly higher U-content than the Archaean granitoids.

Rossiter & Ferguson (this volume) suggest that uranium enrichment of this province resulted from mantle-plume development with attendant incompatible element enrichment of the derived magmas.

ACKNOWLEDGEMENTS

The authors are grateful to G. R. Ewers, J. McAndrew and J. F. Truswell for their comments on the manuscript.

This paper is published with the permission of the Director of the Bureau of Mineral Resources, Geology and Geophysics, Canberra, Australia.

REFERENCES

Berkman, D.A., this volume: Uranium exploration in the Litchfield province, N.T., Australia. *Proceedings of the International Uranium Symposium on the Pine Creek Geosyncline.*

Chappell, B.W., & White, A.J.R., 1974: Two contrasting granite types. *Pacific Geology, 8,* 173-174.

Cloud, P., 1976: Major features of crustal evolution. *Du Toit Memorial Lecture, 14, Geol. Soc. Sth. Africa, Annexure to Volume 79.*

Compston, W., & Arriens, P.A., 1968: The Precambrian geochronology of Australia. *Can. J. Earth Sci., 5,* 561-583.

El Bouseily, A.M. & El Sokkary, A.A., 1975: The relationship between Rb, Ba and Sr in granitic rocks. *Chem. Geol., 16,* 207-219.

Eskola, P.E., 1948: The problem of mantled gneiss domes. *Q. Jl. geol. Soc. Lond., 104,* 461-476.

Ewers, G.R., & Scott, P.A., 1977: Geochemistry of the Cullen Granite, Northern Territory, *BMR J. Aust. Geol. Geophys., 2,* 165-176.

Ferguson, John, this volume: Metamorphism in the Pine Creek Geosyncline and its bearing on stratigraphic correlations. *Proceeding of the International Uranium Symposium on the Pine Creek Geosyncline.*

Ferguson, John, & Winer, Paul, this volume: Pine Creek Geosyncline: Statistical treatment of whole rock chemical data. *Proceedings of the International Uranium Symposium on the Pine Creek Geosyncline.*

Hart, R.J., Nicolaysen, L.O., & Gale, N.H., this volume: The distribution of U, Th and K through a section of the granitic crust of the Vredefort basement. *Proceedings of the International Uranium Symposium on the Pine Creek Geosyncline.*

Hine, R., Williams, I.S., Chappell, B.W., & White, A.J.R., 1978: Contrasts between *I*- and *S*-type granitoids of the Kosciusko Batholith. *J. geol. Soc. Aust., 25,* 219-234.

Hochman, M., 1979: Geochemical investigations in the Mount Bundey area. *Extended Abstracts of the International Uranium Symposium on the Pine Creek Geosyncline,* 108-111.

Hurley, P.M., Fisher, N.H., Pinson, W.H., & Fairbairn, H.W., 1961: Geochronology of Proterozoic granites in Northern Territory, Australia. Part I: K-Ar and Rb-Sr age determinations. *Bull. geol. Soc. Am., 72,* 653-662.

James, R., & Hamilton, D., 1969: Phase relations in the system $NaAlSi_3O_8$-$KAlSi_3O_8$-$CaAl_2Si_2O_8$-SiO_2 at 1 kb water vapor pressure. *Contrib. Mineral. Petrol., 21,* 111-141.

Johnson, K., 1974: Progress report: geological review and revision of the Rum Jungle area, Northern Territory, 1973. *Rec. Bur. Miner. Resour. Geol. Geophys. Aust., 1974/41.*

Needham, R.S., Crick, I.H., & Stuart-Smith, P.G., this volume: Regional Geology of the Pine Creek Geosyncline. *Proceedings of the International Uranium Symposium on the Pine Creek Geosyncline.*

Needham, R.S., Smart, P.G., & Watchman, A.L., 1974: A reinterpretation of the geology of the Alligator Rivers Uranium Field. *Search, 5,* 397-399.

Noakes, L.C., 1949: A geological reconnaissance of the Katherine-Darwin region, N.T., with notes on the mineral deposits. *Bull. Bur. Miner. Resour. Geol. Geophys. Aust., 16.*

O'Neil, J.R., & Chappell, B.W., 1977: Oxygen and hydrogen isotope relations in the Berridale Batholith. *Jl. geol. Soc. Lond., 133,* 559-572.

Page, R.W., 1976: Geochronology of Archaean and Lower Proterozoic rocks in the Rum Jungle - Alligator River Area, Northern Territory, Australia. *25th Int. geol. Congr., Section 1A, Abstracts, Sydney.*

Page, R.W., Compston, W., & Needham, R.S., this volume: Geochronology and evolution of the late Archaean basement and Proterozoic rocks in the Alligator Rivers Uranium Field, Northern Territory, Australia. *Proceedings of the International Uranium Symposium on the Pine Creek Geosyncline.*

Rhodes, J.M., 1965: The Geological Relationships of the Rum Jungle Complex, Northern Territory. *Rep. Bur. Miner. Resour. Geol. Geophys. Aust., 89,* 10p.

Rhodes, J.M., 1969: The application of cluster and discriminatory analysis in mapping granite intrustions. *Lithos, 2,* 223-238.

Richards, J.R., Berry, H., & Rhodes, J.M., 1966: Isotopic and lead-alpha ages of some Australian zircons. *J. geol. Soc. Aust., 13,* 69-96.

Richards, J.R., & Rhodes, J.M., 1967: Geochronology of the Rum Jungle Complex. *Aust. J. Sci. (Abstracts) Melb. Congress.*

Richards, J.R., Ruxton, B.P., & Rhodes, J.M., 1977: Isotopic dating of the leucocratic granite, Rum Jungle, Australia. *Proc. Australas. Inst. Min. Metall., 264,* 33-43.

Riley, G.H., this volume: Granite ages in the Pine Creek Geosyncline. *Proceedings of the International Uranium Symposium on the Pine Creek Geosyncline.*

Rossiter, A.G., & Ferguson, John, this volume: A Proterozoic tectonic model for northern Australia and its economic implications. *Proceedings of the International Uranium Symposium on the Pine Creek Geosyncline.*

Stephansson, O., & Johnson, K., 1976: Granite diapirism in the Rum Jungle Area, Northern Australia. *Precambrian Research, 3,* 159-185.

Streckeisen, A., 1976: To each plutonic rock its proper name. *Earth Sci. Rev., 12,* 1-33.

Taylor, S.R., 1964: Abundance of chemical elements in the continental crust: a new table. *Geochim. cosmochim. Acta, 28,* 1273-1285.

Tuttle, O.F., & Bowen, N.L., 1958: Origin of granite in the light of experimental studies in the system $NaAlSi_3O_8$-$KAlSi_3O_8$-SiO_2-H_2O. *Mem. geol. Soc. Am., 74,* 153.

Walpole, B.P., Crohn, P.W., Dunn, P.R., & Randal, M.A., 1968: Geology of the Katherine-Darwin Region, Northern Territory. *Bull. Bur. Miner. Resour. Geol. Geophys. Aust., 82,* 304p.

White, A.J.R., Williams, I.S., & Chappell, B.W., 1977: Geology of the Berridale 1:100 000 Sheet 8625. *Geol. Surv. NSW Dept. Mines, 138.*

METAMORPHISM IN THE PINE CREEK GEOSYNCLINE AND ITS BEARING ON STRATIGRAPHIC CORRELATIONS

John Ferguson

Bureau of Mineral Resources, P.O. Box 378, Canberra City, A.C.T., 2601, Australia.

ABSTRACT

Within the Pine Creek Geosyncline two broad zones of regional metamorphic grade are present. The boundary which separates these two provinces coincides, in part, with the northerly trending South Alligator Hinge Zone at approximately 132°30'E. Rocks to the northeast of this divide (Province I) are regionally metamorphosed to medium and high-grade, whereas elsewhere in the Pine Creek Geosyncline low-grade regional metamorphism is encountered (Province II).

P-T estimates for the medium-grade metamorphism are in the range 5-8 kb and 550°-630°C; these rocks grade into anatectic granitoids. Also present in Province I are granulites falling within an estimated P-T field of 7-10 kb and 700°-800°C. Mineral parageneses encountered in the regionally metamorphosed rocks of Province II point to a P-T regime of P < 4 kb (possibly < 2 kb) and a temperature range of about 400°-500°C.

The dramatic contrast of metamorphic grade across the South Alligator Hinge Zone and the 15-30km of cover rocks needed to produce the medium to high-grade metamorphism in Province I raises problems if these rock units have correlatives in Province II. Consideration is given to the possibility that the rocks east of the South Alligator Hinge Zone in Province I may have been basement as well as provenance area during the sedimentation in the Pine Creek Geosyncline.

INTRODUCTION

Within the area of the Pine Creek Geosyncline there have been at least two major periods of regional metamorphism and anatexis. Minor meta-strata and extensive development of *S*-type granitoids in some of the Archaean complexes (Ferguson *et al.*, this volume) record the earlier event of 2500 ± 100 m.y. (Page *et al.*, this volume). Anatexis and extensive development of high-level late-orogenic granitoids are associated with a major regional metamorphic event dated at about 1800 m.y. (Page *et al.*, this volume). U-Pb dating on zircons from the crystalline rocks of the Nimbuwah Complex record an orogenic event dated between 1866 and 1886 m.y. (Page *et al.*, this volume). Two broad zones of regional metamorphism are present in the Pine Creek Geosyncline; they are separated, in part, by a northerly trending tectonic hinge zone. Most of the rocks to the east of this zone belong to medium- and high-grade regional metamorphism (Province I, Fig. 1). The low-grade regional metamorphic rocks of Province II have been locally contact metamorphosed by the late-orogenic granitoids.

Early metamorphic studies on the Pine Creek Geosyncline were piecemeal descriptions dealing mostly with individual map areas. Notable exceptions were excellent regional studies on metamorphosed mafic igneous rocks (Stewart, 1959; Bryan, 1962). Walpole *et al.*, (1968) synthesised the earlier circumscribed investigations on metamorphism, as well as advancing additional information in their regional investigations of the Pine Creek Geosyncline. Needham & Stuart-Smith (1976) briefly discussed the metamorphic pelitic assemblages of the Cahill Formation. Ferguson & Needham (1978) studied the metamorphosed pre-orogenic Zamu Dolerite suite, which has extensive distribution in the Geosyncline. On the basis of this study, the Pine Creek Geosyncline was divided into two major zones of regional metamorphic grade.

This paper deals with the broad regional study of metamorphism in the Geosyncline, and attempts to establish pressure - temperature (P-T) regimes for the observed mineral parageneses. The estimated P-T regimes of the metamorphic Provinces pose problems for the accepted stratigraphic correlations in the Pine Creek Geosyncline (Needham *et al.*, this volume; Stuart-Smith *et al.*, this volume).

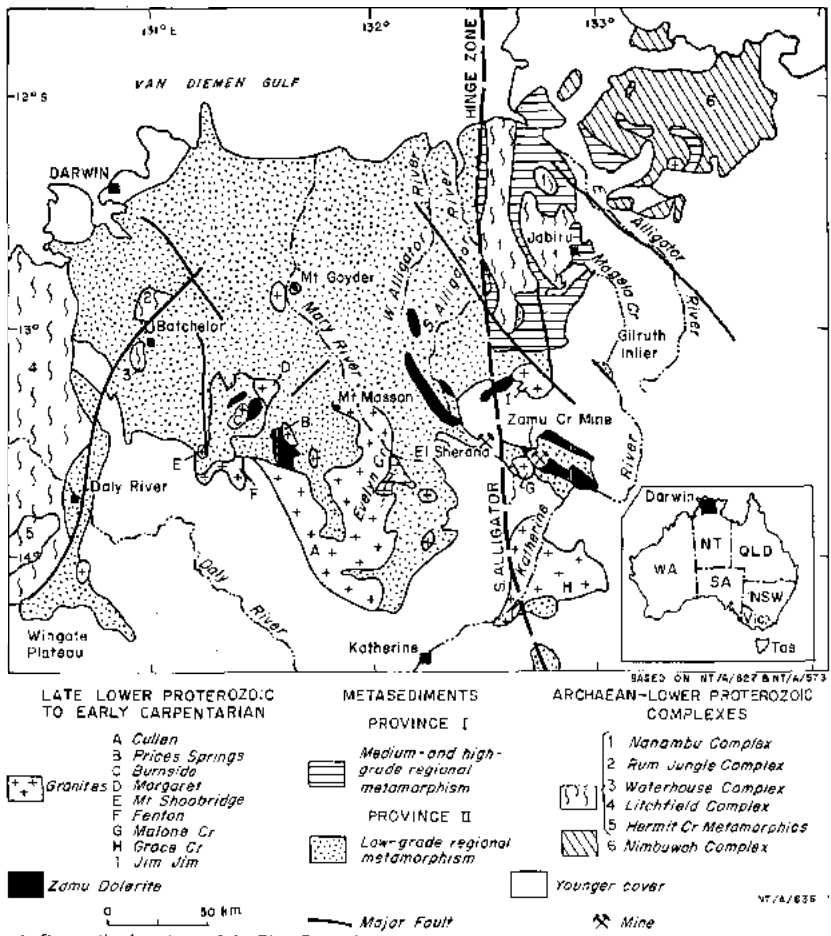


Figure 1. Generalised geology of the Pine Creek Geosyncline showing broad metamorphic divisions (modified from Ferguson & Needham, 1978).

REGIONAL SETTING

The two broad zones of regional metamorphism in the Pine Creek Geosyncline are partly separated by the northerly trending South Alligator Hinge Zone (S.A.H.Z.) at approximately 132°30′E (Fig. 1). Rocks east of this divide in Province I (Fig. 1) are regionally metamorphosed to medium or high-grade, whereas elsewhere in the Geosyncline, the regional metamorphism is low-grade (Province II, Fig. 1). Late-orogenic high-level granitoid plutons have locally superimposed a contact metamorphism on the ~1800 m.y. regional metamorphic event in Province II (Fig. 1).

In Province II, the Lower Proterozoic rocks form northerly trending tight folds with steep limbs. Folding increases in intensity eastwards, producing isoclinal folds in the region of the S.A.H.Z. Polyphase isoclinal folding is present in Province I and at least four deformation phases recognised (Needham & Stuart-Smith, 1976; Needham *et al.*, this volume). A number of the late-orogenic plutons in Province II are semi-conformable,

resulting in concentric disposition of fold axes around these plutons. In the case of the ~1800 m.y. reactivated Archaean Nanambu Complex, as well as the Litchfield and Nimbuwah Complexes, it is possible to trace the transition from granitoid rocks through migmatites into metamorphosed supractrustals.

PETROLOGY

Province I

Medium-grained banded gneissic granulites are found in the southern part of the Nimbuwah Complex. The rocks are generally mesocratic. The compositional banding ranges from a few millimetres to tens of centimetres. Textural changes usually coincide with compositional banding, the darker units are usually finer grained. Additional textural contrasts result from granular and porphyroblastic development; alkali feldspar and garnets constitute the porphyroblasts. Orthopyroxene is extensively developed throughout the granulites; it is dominantly hypersthene and rarely ferrohypersthene ($En_{45.5\text{-}52.1}$; Al_2O_3 <1.6%). Orthopryroxene was not found to coexist with garnet or clinopyroxene; clinopyroxene coexists with garnet in some cases. Irrespective of the associated minerals, the clinopyroxene compositions display a restricted chemical range, namely $Ca_{45.1\text{-}46.2}Mg_{30.4\text{-}29.7}Fe_{24.5\text{-}24.1}$, and the Ca-Tschermak's molecule is less than 2.2 percent. Equally restricted in compositional range are the almandine-rich garnets ($alm_{61.6\text{-}65.2}$, $spes_{4.1\text{-}4.0}$, $pyp_{11.9\text{-}13.8}$, $grs_{22.4\text{-}17.0}$). As in other granulite terrains the crypto- to microperthitic alkali feldspars may contain a high Ab component (up to 45.1%); the compositional range is $Or_{48.8\text{-}74.2}$ with a maximum of $An_{6.2}$. Plagioclase ranges from $An_{27\text{-}80}$ with most compositions falling in the andesine/labradorite field. Olive-green magnesio-hornblende with a moderate titanium content (up to 2.17% TiO_2) is present. The red-brown biotite is high in magnesium (up to 12.6% MgO) and has a moderate titanium content (up to 4.8% TiO_2).

The medium-grade metamorphic rocks of Province I, most of which are from the Cahill Formation, are characterised by well-developed segregation banding and crenulation cleavage. Segregation banding in the meta-pelitic assemblages is produced by alternating concentrations of mafic and felsic minerals. Generally, the segregation banding is on a scale of less than 1cm, but boudinaged quartz-rich bands can have widths up to 25cms. These banded schists are tightly folded with the occasional presence of ptygmatic veins. Porphyroblasts in the meta-pelitic assemblages comprise garnet, staurolite, kyanite and magnetite. All of these minerals tend to be poikiloblastic and show pre- and para-deformation features. Muscovite and biotite commonly show two ages of development namely pre- and post-deformation. Original compositional variations between arenaceous and pelitic-rich units produce a continuum of metamorphosed rocks corresponding to quartzite-feldspathic (±mica) quartzite-micaceous quartzite-meta-pelitic schists. Some sedimentary features can still be observed within the arenite-rich units, and the rocks are generally thinly cleaved along micaceous-rich zones. In the pelitic assemblages, the garnets range from almandine to spessartine-rich ($alm_{34.1\text{-}72.5}$, $spes_{54.8\text{-}11.8}$, $pyp_{8.4\text{-}8.6}$, $grs_{2.8\text{-}7.1}$). The alkali feldspars are well ordered microclines with low albite (up to $Ab_{1.6}$) and anorthite (up to $An_{0.7}$) contents. Plagioclase ranges from albite to oligoclase with a maximum anorthite content of $An_{18.5}$.

Meta-calcareous arenites are also present, occurring as thinly banded calc-silicate rocks. These calc-silicate rocks can grade into para-amphibolites characterised by a pale green felted texture produced by acicular actinolite. The calc-silicate rocks contain amphiboles ranging from hornblende to actinolite. Diopside ($Ca_{49.8}Mg_{46.4}Fe_{2.8}$) is commonly developed in assemblages which contain microcline ($Or_{95.3}Ab_{4.6}An_{0.6}$), epidote/zoisite, calcite and scapolite (mizzonite range). Where the carbonate content reaches major proportions, flow-banded marble assemblages are developed. Calcite,

dolomite and magnesite-rich marbles are common; grossularite-rich garnet is present in some cases.

Dark green, fissile orthoamphibolite of the Zamu Dolerite (Ferguson & Needham, 1978) is common throughout the Geosyncline. They occur as pre-orogenic sills up to 300m thick. Hornblende (magnesio, ferro, and hastingsitic varieties) make up between 50 and 85 percent of these rocks. Besides plagioclase ($An_{85.5-54.2}$), quartz, biotite and accessory minerals and alteration products, clinopyrozene and garnet, may also be present. The clinopyroxene ($Ca_{49.5-48.5}Mg_{42.3-28.1}Fe_{8.3-23.4}$) and almandine-rich garnet ($alm_{52.0-59.9}$, $spes_{13.5-4.7}$, $pyp_{4.8-8.9}$, $grs_{29.7-26.5}$) are antipathetic.

Province II

The low-grade regional metamorphic rocks generally have a well developed cleavage, and where mica, chlorite, or graphite occurs there is a phyllitic texture. Sedimentary features are commonly preserved; these include turbidity structures, stromatolitic lamination, ripple marks, current and graded bedding. Where well developed folding or shearing has taken place, mica, chlorite, graphite, and quartz-rich segregation bands are present. Terrigenous sediments range from rudites to argillites. The meta-conglomerates, sandstones, greywackes and shales may contain low albite, well ordered microcline, chlorite, biotite, muscovite, and epidote group minerals. Ortho- and allochemical rocks include abundant carbonate and minor banded iron formation. The carbonate-rich units can contain dolomite, calcite, magnesite, and tremolite. In the orthoamphibolites of the Zamu Dolerite ophitic textures are generally preserved; where shearing has taken place the rock is fissile. Magnesio-hornblende coexists with albite/oligoclase and quartz. Additional major minerals that can be present include prehnite, chlorite, biotite, and epidote-group minerals.

Hornsfels facies rocks are developed where late-orogenic high-level granitoid plutons have locally superimposed a contact metamorphism on the ~1800 m.y. regional metamorphic event. These contact metamorphic aureoles may be up to 5km wide but are generally less than 1km wide. The pelitic/greywacke assemblages are characterised by the development of andalusite and cordierite porphyroblasts. In calcareous and calc-silicate rocks, the minerals found are diopside, wollastonite, dolomite, calcite, magnesite, talc, tremolite, and some scapolite. The orthoamphibolites are recrystallised and plagioclase has the composition andesine to labradorite.

MINERAL PARAGENESES

Province I : High-grade metamorphism

In the granulite terrain of the southern Nimbuwah Complex, the most common parageneses encountered are Ho + Bio + Opx + Qz + Plag ± Ksp, and Ho + Bio ± Cpx ± Ga + Qz + Plag ± Ksp. The high grossularite content of the almandine-rich garnets places these compositions close to the plagioclase-hypersthene tie-line in the ACF diagram (Fig. 2). The granulites have mafic compositions which also plot close to this line (Fig. 2). The antipathy of hypersthene with garnet or clinopyroxene indicates that metamorphic conditions are those of the hypersthene-plagioclase-granulite subzone of the regional hypersthene zone of high-grade metamorphism (Fig. 2). However, the one assemblage which contains coexisting garnet and clinopyroxene suggests the reaction:

orthopyroxene + plagioclase = clinopyroxene + garnet + quartz.

The right hand side of this reaction takes place at a slightly higher pressure at constant temperature, or at lower temperatures at constant pressure (Winkler, 1976), and belongs to the clinopyroxene-almandine-quartz-granulite subzone of the regional hypersthene zone. The absence of an assemblage with coexisting clino- and orthopyroxene is probably related to the limited chemical range of the granulites falling as they do close to the plagioclase-hypersthene tie-line.

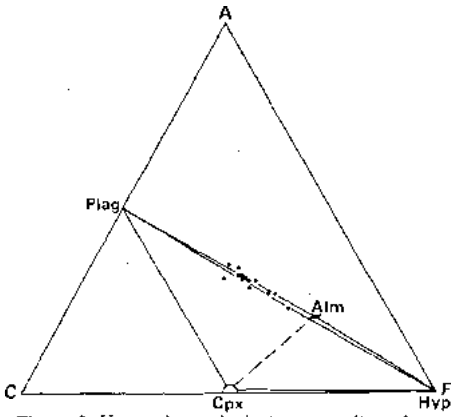


Figure 2. Hypersthene-plagioclase-granulite subzone of the regional hypersthene zone of high grade metamorphism (Winkler, 1976). The tie-line Cpx-Alm takes place at slightly higher pressures at constant temperatures or at lower temperatures at constant pressure. Hornblende, biotite, quartz ± K-feldspar are also present. See figure 5 for abbreviations.

: Medium-grade metamorphism

Within the area of medium-grade metamorphism of Province I, the meta-pelites of the Cahill Formation contain the mineral parageneses Alm + Kya/Sil + Bio + Musc ± Stt ± Plag ± Ksp (Figs. 3 & 4), which signify (almandine)-medium grade metamorphism (Winkler, 1976). Coexistence of Kya/Sil and Alm + Stt, with biotite, is a normally observed natural assemblage (Winkler, 1976). Chlorite is found as a marginal replacement to biotite and garnet, but rarely as separate flakes.

The orthoamphibolite suite of the Zamu Dolerite contains the mineral suite Ho + Plag + Qz ± Cpx ± Ga ± Bio, and accessory minerals that can include sphene, apatite, opaque(s) and carbonate. Figure 4 shows that all compositions plot near the Plag/Zo - Ho tie-line; those that are displaced from this tie-line contain either garnet or clinopyroxene as additional phases. These rocks belong to the labradorite/bytownite-amphibolite (medium) grade of metamorphism.

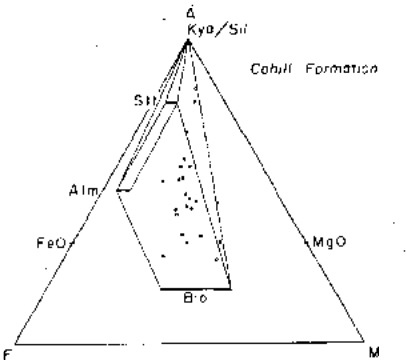


Figure 3. AFM plot of (almandine) medium-grade metamorphism for Cahill Formation. Quartz, plagioclase and muscovite are additional phases (after Winkler, 1976). See figure 5 for abbreviations.

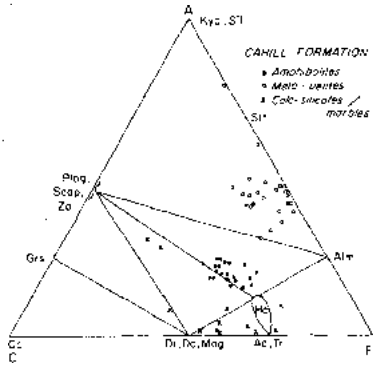


Figure 4. ACF plot of medium-grade metamorphism for amphibolites, metapelites and calc-silicates/marbles of the Cahill Formation (after Winkler, 1976). See figure 5 for abbreviations.

The calc-silicate rocks and marbles of the Cahill Formation have a wide chemical range and corresponding mineralogy. Compositional variations are shown in the ACF diagram (Fig. 4). The calc-silicates are dominated by the assemblage Ho + Di + Do + Plag + Zo + Scap (Fig. 4), whereas the marbles are dominated by Do + Mag + Ac/Tr + Di; Cc + Grs + Di; Cc + Ksp + Scap + Epi/Zo + Ho; Cc + Qz + Zo + Ho + Scap + Ksp. These assemblages, and the presence of scapolite, clearly confirm that these rocks have been subjected to a medium-grade of metamorphism.

Province II : Low-grade regional metamorphism

The rocks have been regionally metamorphosed to low-grade. The meta-pelitic assemblages here contain Na-plag + Ksp + Bio + Musc + Chl + Epi/Zo. The calcareous units contain Do + Cc + Mag ± Tr. Mafic intrusives of the Zamu Dolerite belong to the albite/oligoclase amphibolite grade (Ferguson & Needham, 1978).

: Contact metamorphism

Of the contact metamorphosed areas investigated the highest grades were observed in rock units dominated by the South Alligator and Finniss River Groups adjacent to the Burnside, Prices Springs and Cullen Granites. In the pelitic/greywacke assemblages, contact metamorphism produces andalusite and cordierite, which at times coexist with Ksp + Qz + Musc + Bio.

Contact metamorphism of the calcareous units produces Cc + Di + Wo; Cc + Do + Ta + Tr; and Tr + Cc + Di. Additionally, Stephenson & Johnson (1976), report scapolite in the eastern Waterhouse Complex. The mafic intrusives of the Zamu Dolerite are contact metamorphosed to amphibolite and are commonly sheared; they contain Ho + Andesine/Labradorite + Qz.

P - T ESTIMATES

Estimated P-T regimes for the respective metamorphic Provinces are plotted in figure 5. The 'Stt-in' curve places a minimum temperature of about 500°C on Province I. The minimum pressure constraint can be derived from the presence of kyanite and sillimanite and the absence of andalusite in the pelitic assemblages. The use of Winkler's (1976) preferred triple point for the alumino-silicates would give a minimum plot of ~6 kb (Fig. 5). However, curves calculated for the triple point (Wall & Essene, 1972), fitting experimental determinations (Richardson *et al.*, 1969), suggest that a figure of ~4.5 kb is a more likely pressure for this system (Fig. 5). The upper temperature for the medium-grade metamorphic assemblage of Province I is fixed by the water-saturated granite melting curve at about 630°C. Garnet-bearing amphibolites of the Zamu Dolerite have a composition similar to the quartz tholeiitic compositions used experimentally by Green & Ringwood (1972). The 'Ga-in' curve for quartz tholeiite (Fig. 5) is that of Green & Ringwood (1972), extrapolated to lower P-T regimes. The coexistence of plagioclase and garnet in the tholeiitic compositions confines the P-T conditions to the area bounded by the 'Ga-in' and 'Plag-out' curves.

These reactions place an approximate P-T grid on the medium-grade metamorphic assemblage of Province I at around 5-8 kb and 550°-630°C.

In the granulite terrain of the Nimbuwah Complex, two mineral exchange equilibria were employed to determine P-T equilibration curves. These include Mg-Fe exchange between garnet and clinopyroxene (curve 11, Fig. 5), recently calibrated by D.J. Ellis (pers. comm.), and Mg-Fe exchange between biotite and garnet (Ferry & Spear, 1978; curve 12, Fig. 5). Curves 11 and 12 represent the extreme P-T space derived from these co-existing mineral pairs. Cpx-Ga pairs give consistently lower temperatures than the Bio-Ga pairs. Most of the granulite compositions correspond closely to quartz tholeiite compositions of Green & Ringwood (1972), and therefore a maximum T is fixed by the intersection of the mineral pair curve 12 with the extrapolated 'Ga-in' curve at about 820°C (Fig. 5). Minimum T is determined by the intersection of the 'Plag-out' curve for quartz tholeiite and the partition curve for the observed mineral pair curve 11 (Fig. 5). These intersections in P-T space define an approximate field of 7-10 kb and 700°-800°C for the granulite terrain (Fig. 5). The presence of semi-autochthonous anatectic granitoids in the Nimbuwah Complex suggests that the granulites may represent the residuum after extraction of a granitic component.

In the regionally metamorphosed rocks of Province II, the absence of

cordierite/staurolite and presence of chlorite, biotite, muscovite, and epidote-group minerals places these rocks in the field of low-grade metamorphism, with a temperature range of about 400°-500°C. There are no diagnostic mineral assemblages to define pressures involved; however, absence of almandine indicates a pressure less than 4 kb at 500°C (Winkler, 1976), whereas the absence of andalusite probably indicates a P_f less than 2 kb (Winkler, 1976), as shown by field IIR on figure 5.

The presence of cordierite in the contact metamorphosed rocks of Province II places them above low-grade metamorphism. Absence of sillimanite and presence of andalusite defines an upper temperature of about 680°C. Coexistence of K-feldspar with andalusite, to the exclusion of muscovite, indicates that temperatures were at times sufficient to allow the breakdown of Musc + Qz $\rightleftarrows$ Ksp + And (curve 9, Fig. 5). Given the presence of andalusite and absence of sillimanite, the upper pressure is confined to approximately 2.5 kb (Althaus *et al.*, 1970). The presence of wollastonite in calcareous units points to a temperature above 500°C (Winkler, 1976). The reaction curve Cc + Qz $\rightleftarrows$ Wo + CO_2 is plotted in figure 5 for

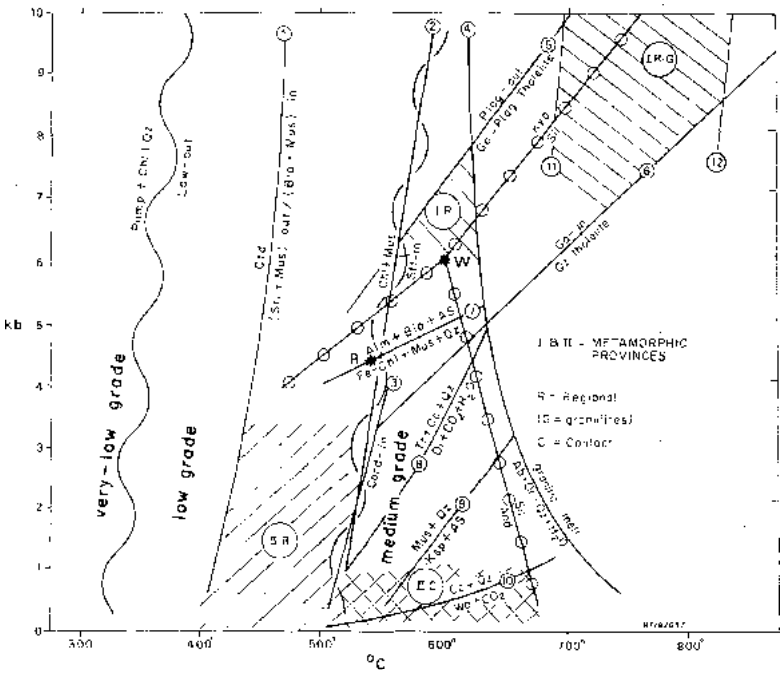


Figure 5. P-T diagram showing approximate fields of regional metamorphism (Provinces IR, IR-G & IIR) and contact metamorphism (Province IIC) in the Pine Creek Geosyncline. Reaction curves: 1 — Nitsch (1970) and Brown (1971); 2 — Hoscheck (1967) and Ganguly & Newton (1968); 3 & 7 — Hirschberg & Winkler (1968); 4 — Tuttle & Bowen (1958), and Merrit *et al.* (1970); 5 & 6 — Green & Ringwood (1972); 8 — Metz & Puhan (1970, 1971); 9 Althaus *et al.* (1970); 10 — Greenwood (1967); 11 & 12 — P-T curves based on coexisting mineral pairs in granulite facies (see text). W is the triple point for the alumino-silicates after Winkler (1976) and R is the preferred triple point of Richardson *et al.* (1969). Abbreviations used in figures 2 to 5 and text: Ab = albite; Ac = actinolite; And = andalusite; Alm = almandine; As = Al_2SiO_5; Bio = biotite; Cc = calcite; Chl = chlorite; Cord = cordierite; Cpx = clinopyroxene; Ctd = chloritoid; Di = diopside; Do = dolomite; En = enstatite; Ga = garnet; Grs = grossularite; Ho = hornblende; Hyp = hypersthene; Kya = kyanite; Ksp = K-feldspar; Law = lawsonite; Mag = magnesite; Musc = muscovite; Or = orthoclase; Plag = plagioclase; Pump = pumpellyite; Pyp = pyrope; Qz = quartz; Scap = scapolite; Sil = sillimanite; Spes = spessartine; Sti = stilpnomelane; Stt = staurolite; Ta = talc; Tr = tremolite; Wo = wollastonite; Zo = zoisite.

the condition $X_{CO_2} = 1.0$ (Greenwood, 1967). This curve intersects the And/Sil curve at a pressure of slightly less than 1 kb. The above P-T constraints indicate $P < 1$ kb and T 500°-680°C for contact metamorphism in Province II.

DISCUSSION

The dramatic contrast in metamorphic grade and style of deformation across some parts of the South Alligator Hinge Zone, and the necessary 15 to 30km of cover rocks needed to produce the medium to high-grade metamorphism of Province I, are factors which raise some interesting speculations. If the Kakadu and Namoona Groups of Province I have correlatives in low grade regionally metamorphosed Lower Proterozoic rocks in Province II (Fig. 1) as suggested by Smart *et al.* (1975), Needham *et al.* (this volume) and Stuart-Smith *et al.* (this volume), then an exceptionally high heat flow, and the removal of at least 15km of cover rocks, has to be invoked to explain the conditions that pertained for Province I during orogenesis. As acknowledged by Stuart-Smith *et al.* (this volume) some of the area to the east of the S.A.H.Z. must have been provenance to the dominantly rudite assemblage of the Mount Partridge Group to the west. For such uplift to have taken place in Province I during the main sedimentary cycle of Lower Proterozoic deposition would produce even greater difficulties in securing the necessary thickness of cover rocks to account for the mineral parageneses found in Province I. Consideration must be given to the possibility, first suggested for the Myra Falls Metamorphics by Walpole *et al.* (1968), that some or all of the rocks in Province I are older than the low-grade metamorphic sediments found in Province II (Fig. 1). If this interpretation is correct, rocks of the Kakadu and Namoona Groups in Province I, as well as the Nimbuwah Complex, would have been part basement and provenance area to the main sedimentation occurring in the Pine Creek Geosyncline.

Recently completed U-Pb dating on zircons from granitoid rocks in the Nimbuwah Complex give an age of 1866 ± 8 m.y. and zircons from a granulite in this Complex give 1886 ± 5 m.y. These dates reflect the crystallisation age (Page *et al.*, this volume). Rb-Sr whole rock isochrons on these rocks record the omnipresent ~1800 m.y. metamorphic event of the geosyncline. This Rb-Sr isochron is a Model 3 fit; with an assumed contemporary mantle initial ratio of 0.7023 an age of 1905 ± 28 m.y. is the maximum estimate of the igneous protoliths of the gneiss (Page *et al.*, this volume). The 1870 to 1905 m.y. time span falls into the transitional tectonism period of 1950 to 1850 m.y. belonging to the Older Domain of the early Proterozoic North Australian Orogenic Province (Plumb, in press). This event occurs extensively throughout northern Australia including the Arnhem Block, a suggested eastward continuation of the Pine Creek Geosyncline (Plumb & Derrick, 1975), where the anatectic Bradshaw Granite has an age of ~1900 m.y. The outlined foregoing events provide a contrast to the main sedimentation of the Pine Creek Geosyncline which could be regarded as typical Younger Domain followed by ~1800 m.y. metamorphism and transitional tectonism with emplacement of discordant granitoids and extrusions of felsic volcanics in the period 1780-1760 m.y. (Page *et al.*, this volume). The age(s) of the metasediments within the Geosyncline could be decisive in establishing the orogenic history of the area. Paragneiss and schists of the Lower Proterozoic metasediments invariably give Rb-Sr total rock and mica, and K-Ar mica, ages close to 1800 m.y. (Page *et al.*, this volume). Similarly, the mineral ages in the Archaean Rum Jungle Complex also record the 1800 m.y. metamorphic event. The only U-Pb dates on zircons from the metasedimentary units come from a quartz-mica schist of the Cahill Formation in the Myra Falls Inlier, which indicated an age of about 2400 m.y. (Page *et al.*, this volume). These authors consider that the zircons are detrital, and attribute the age to the provenance area.

To evaluate the tectonic history of the area further an extensive study should be undertaken on dating zircons from the metasediments of the geosyncline. East of the

S.A.H.Z. rocks of the Namoona and Kakadu Groups have been metamorphosed to medium-grade at temperatures around 600°C and pressures > 5 kb; in places they grade into anatectic granitoids. The zircons within these Groups may be recrystallised thereby recording orogenic events. Stratigraphic correlations are at present sufficiently equivocal to suggest that the rocks within Province I may belong to an older Orogenic Province that acted as the provenance area, as well as basement to the main Lower Proterozoic sedimentation within the Pine Creek Geosyncline. Further work should test the possibility that the rocks of the Kakadu and Namoona Groups being of Archaean age or belonging to the period 2500-1870 m.y. The high percentage of *S*-type granitoids and minor metasediments in the Archaean Complexes of the Pine Creek Geosyncline (Ferguson *et al.*, this volume) as well as possibly abundant Archaean metasediments in the Hermit Creek Metamorphics indicates that sedimentary development was extensive prior to 2500 ± 100 m.y.

The presence of low-grade metamorphic strata of Province II lying to the east of the S.A.H.Z. in the area north of Jim Jim Granite and the South Alligator Valley (Fig. 1) could be interpreted as younger strata onlapping basement comprising Province I metamorphites and/or granitoids.

ACKNOWLEDGEMENTS

Rock specimen donations by I. H. Crick, R. S. Needham and R. W. Page are gratefully acknowledged. W. Cameron, C. F. Prichard, J. F. Truswell and K. Wills made helpful suggestions for improving the manuscript. N. Davis and A. B. Goleby assisted greatly in preparing the figures.

Published with the permission of the Director, Bureau of Mineral Resources, Geology and Geophysics, Canberra, A.C.T., Australia.

REFERENCES

Althaus, E., Nitsch, K.H., Karotke, E., & Winkler, H.G.F., 1970: An experimental re-examination of the upper stability limit of muscovite plus quartz. *Neues Jb. Miner. Mh., 1970,* 325-336.

Brown, E.H., 1971: Phase Relations of biotite and stilpnomelane in the Greenschist Facies. *Contrib. Mineral. Petrol., 31,* 275-299.

Bryan, R., 1962: Lower Proterozoic basic intrusive rock of the Katherine-Darwin area, Northern Territory. *Rec. Bur. Miner. Resour. geol. Geophys. Aust., 1962/7,* 46p.

Ferguson, J., Chappell, B.W., & Goleby, A.B., this volume: Granitoids in the Pine Creek Geosyncline. *Proceedings of the International Uranium Symposium on the Pine Creek Geosyncline.*

Ferguson, J., & Needham, R.S., 1978: The Zamu Dolerite: A Lower Proterozoic preorogenic continental tholeiitic suite from the Northern Territory, Australia. *J. geol. Soc. Aust., 25,* 309-322.

Ferry, J.M., & Spear, F.S., 1978: Experimental calibration of the positioning of Fe and Mg between biotite and garnet. *Contrib. Mineral. Petrol., 66,* 113-117.

Ganguly, J., & Newton, R.C., 1968: Thermal stability of chloritoid at high pressure and relatively high oxygen fugacity. *J. Petrology, 9,* 444-466.

Green, D.H., & Ringwood, A.E., 1972: A comparison of recent experimental data on the gabbro-garnet granulite-eclogite transition. *J. Geol., 80,* 277-288.

Greenwood, H.J., 1967: Wollastonite: Stability in H_2O-CO_2 mixtures and occurrence in a contact - metamorphic aureole near Salmo, British Columbia, Canada. *Am. Miner., 52,* 1169-1680.

Hirschberg, A., & Winkler, H.G.F., 1968: Stabilitatsbeziehungen zwischen Chlorit, Cordierit und Alamdin bei der Metamorphose (Stability Relations between Chlorite, Cordierite and Almandine during metamorphosis). *Contrib. Mineral. Petrol., 18,* 17-42.

Hoschek, G., 1967: Untersuchungen zum Stabilitatsbereich von Chloritoid und Staurolith. *Contrib. Mineral. Petrol., 14,* 123-162.

Merrill, R.B., Robertson, J.K. & Wylie, P.J., 1970: Melting reactions in the system $NaAlSi_3O_8$-$KAlSi_3O_8$-SiO_2-H_2O to 20 kilobars compared with results for other Feldspar-Quartz-H_2O and rock-H_2O systems. *J. Geol., 78,* 558-569.

Metz, P., & Puhan, D., 1970: Experimentelle Untersuchung der Metamorphose von kieselig dolomitisch en Sedimenten. *Contrib. Mineral. Petrol., 26,* 302-314.

Metz, P., & Puhan, D., 1971: Korrektur zur Arbeit. Experimentelle Untersuchung der Metamorphose von Kieselig dolomitisch en Sedimenten. *Contrib. Mineral Petrol., 31,* 169-170.

Needham, R.S., Crick, I.H., & Stuart-Smith, P.G., this volume: Regional Geology of the Pine Creek Geosyncline. *Proceeding of the International Uranium Symposium on the Pine Creek Geosyncline.*

Needham, R.S., & Stuart-Smith, P.G., 1976: The Cahill Formation - host to uranium deposits in the Alligator Rivers Uranium Field, Australia. *BMR J. Aust. Geol. Geophys., 1,* 321-334.

Nitsch, K.H., 1970: Experimentelle Bestimmung der eberen Stabilitatsgrenze von Stilpnomelan. *Fortschr. Miner., 47,* 48-49.

Page, R.W., 1976: Geochronology of Archaean and Lower Proterozoic rocks in the Rum Jungle - Alligator Rivers Area, Northern Territory, Australia. *25th Int. geol. Congr., Section 1A, Abstracts, Sydney.*

Page, R.W., Compston, W., & Needham, R.S., this volume: Geochronology and evolution of the late Archaean basement and Proterozoic rocks in the Alligator Rivers Uranium Field, Northern Territory, Australia. *Proceeding of the International Uranium Symposium on the Pine Creek Geosyncline.*

Plumb, K.A., 1979: The tectonic evolution of Australia. *Earth Sci. Rev., 14*, 205-250.

Plumb, K.A., in press: Structure and tectonic style of the Precambrian shields and platforms of northern Australia. *Tectonophysics.*

Plumb, K.A., & Derrick, G.M., 1975: Geology of the Proterozoic rocks of the Kimberley to Mount Isa region. *in* (ed. C.L. Knight), *Economic Geology of Australia and Papua New Guinea, Australas. Inst. Min. Metall., Monograph Series No. 5, 1. Metals*, 217-252.

Richardson, S.W., Gilbert, M.C., & Bell, P.M., 1969: Experimental determination of Kyanite - Adalusite and Andalusite - Sillimanite equilibria: The aluminum silicate triple point. *Am. J. Sci., 267*, 259-272.

Smart, P.G., Wilkes, P.G., Needham, R.S., & Watchman, A.L., 1975: Geology and geophysics of the Alligator Rivers Region. *in* (ed. C.L. Knight) *Economic Geology of Australia and Papua New Guinea, Australas. Inst. Min. Metall., Monograph Series No. 5, 1. Metals*, 285-301.

Stephansson, O., & Johnson, K., 1976: Granite diaprism in the Rum Jungle Area, Northern Territory. *Precambrian Research, 3*, 159-185.

Stewart, J.R., 1959: Proterozioc igneous rocks in the Katherine-Darwin region, Northern Territory. *M.Sc. thesis, University of New England* (unpubl.).

Stuart-Smith, P.G., Wills, K., Crick, I.H., & Needham, R.S., this volume: Evolution of the Pine Creek Geosyncline. *Proceedings of the International Uranium Symposium on the Pine Creek Geosyncline.*

Tuttle, O.F., & Bowen, N.L., 1958: Origin of granite in the light of experimental studies in the system $NaAlSi_3O_8$-$KAlSi_3O_8$-SiO_2-H_2O. *Mem. geol. Soc. Am., 74*, 153 p.

Wall, V.J., & Essene, E.J., 1972: Subsolidus Equilibria in CaO-Al_2O_3-SiO_2-H_2O. *Abstract with Programs geol. Soc. Am., 4*, 700.

Walpole, B.P., Crohn, P.W., Dunn, P.R., & Randal, M.A., 1968: Geology of the Katherine-Darwin Region, Northern Territory. *Bull. Bur. Miner. Resour. geol. Geophys. Aust., 82*, 304p.

Winkler, H.G.F., 1976. *Petrogenesis of metamorphic rocks*. Springer-Verlag, New York (4th Edition), 334p.

THE CHARACTERISTICS AND INTERPRETATION OF REGIONAL GRAVITY, MAGNETIC AND RADIOMETRIC SURVEYS IN THE PINE CREEK GEOSYNCLINE

D.H. Tucker, D.C. Stuart, I.G. Hone and N. Sampath

Bureau of Mineral Resources, P.O. Box 378, Canberra City, A.C.T. 2601, Australia.

ABSTRACT

Most of the Bouguer anomaly features in the Pine Creek Geosyncline can be explained by the presence of low-density granitic complexes within a more dense, Lower Proterozoic metasedimentary column.

There is no apparent density or magnetic contrast between the granitic complexes and the basement of the Pine Creek Geosyncline. Modelling constrained by surface geology indicates that the granitic complexes commonly slope outwards and merge with the basement at a depth of generally less than 5000m.

A regional model based on this hypothesis indicates that relatively shallow basement at a depth of approximately 1000m links some of the more extensive granitic complexes, for example the Litchfield Complex with the Cullen and Grace Creek Granites, and the Nanambu Complex with postulated near-surface granites fringing Van Dieman Gulf. Similarly a basement high links the Jim Jim and Malone Creek Granites.

Thick sediments of the Pine Creek Geosyncline appear to lie in an essentially east-west-trending belt, mainly confined by these basement highs in the western area but also extending eastwards from the Nanambu Complex/Grace Creek chain of basement highs, to as yet unrecognised limits beneath Middle Proterozoic (Carpentarian) cover rocks.

Much of the regional magnetic data recorded over Lower Proterozoic metasediments and the Archaean and Middle Proterozoic (Carpentarian) rocks of the region has little or no magnetic relief.

Broad curvilinear magnetic zones of high relief occur as isolated features throughout the region and are composed of narrow anomalies with amplitudes of from 500 to 1500 nT. Most of the known uranium deposits lie within these zones. The curvilinear anomalies appear to have at least three different sources, the most widespread of which are associated with steeply dipping Lower Proterozoic sediments commonly adjacent to granitic and metamorphic complexes. Other sources of curvilinear anomalies appear to be mafic intrusive sills, and volcanic members of the Middle Proterozoic (Carpentarian) rocks.

Other prominent magnetic features are suites of long, linear anomalies and a few discrete bulls-eye anomalies of small area. The linear anomalies are caused by Middle Proterozoic (Carpentarian) dolerite dykes. The bulls-eye anomalies occur near or within granitic complexes and are probably the result of mafic intrusions.

The sources of individual anomalies within curvilinear magnetic zones over Lower Proterozoic rocks are conformable with the metasediments, are mostly less than 100m thick and are locally continuous for 10-50km. Similar sources often reappear at approximately the same stratigraphic level throughout the Geosyncline. Magnetic units with the highest amplitude anomalies appear to occur in the shalier or siltier parts of the section - notably in the Koolpin Formation and stratigraphically equivalent rocks.

In the central part of the Geosyncline including Rum Jungle, curvilinear magnetic anomalies result from strongly remanently magnetised iron sulphides in the sedimentary section. However, in the east, in the Alligator Rivers Uranium Field, and in the west, in the Litchfield Block, the anomalies result from inductively magnetised iron oxides.

The magnetic results suggest that the Litchfield Block is an integral part of the Pine Creek Geosyncline, and that the primary sedimentation and/or subsequent metamorphic history of the central part of the Geosyncline was distinctly different from the eastern and western margins of the Geosyncline.

In the radiometric data there are three distinct levels of total count-rate which broadly correspond with different types of rocks. A low count-rate is recorded over approximately 40 percent of the area and is in general restricted to regions where rocks of the Pine Creek Geosyncline are covered by younger sediments. Approximately 50 percent of the region has a medium count-rate observed over outcropping and subcropping Early Proterozoic metasediments of the Pine Creek Geosyncline. Count-rates observed over reasonably exposed Early Proterozoic rocks are similar to those observed over regions where Early Proterozoic rocks are covered by various weathering products.

Other medium count zones are observed over Middle Proterozoic (Carpentarian) felsic volcanics, the Edith River Volcanics, and some of the Archaean to Proterozoic aged granites and metamorphics.

Discrete, well defined zones with a high count-rate are observed throughout the region and with few exceptions are located over Middle Proterozoic (Carpentarian) granites.

The stripped count-rates observed over the region have different characteristics depending primarily on the age and lithology of the rocks. The results suggest that the granitic rocks of the Geosyncline are enriched in all radioelements relative to generally accepted levels for granites. Similarly the Early Proterozoic metasediments appear to be enriched in uranium and thorium relative to generally accepted concentration levels for arenaceous and argillaceous sediments. The Middle Proterozoic (Carpentarian) granites are probably distinguishable from the Archaean granitic complexes on the basis of their apparently higher potassium, uranium and thorium concentrations. The Early Proterozoic metasediments appear to be enriched in uranium relative to thorium

compared to the Archaean or Middle Proterozoic (Carpentarian) granitic rocks. The high total-count readings observed over the Middle Proterozoic (Carpentarian) granites appear to be predominantly due to the substantial concentration of potassium rather than locally abnormal concentrations of uranium or thorium.

INTRODUCTION

The Bureau of Mineral Resources, Geology and Geophysics (BMR) has covered the Pine Creek Geosyncline with helicopter gravity stations on an 11,000m grid, and airborne magnetic and gamma spectrometer surveys along east-west lines 150m above ground level and 1500m apart. These data are available as maps at various scales, and most recently at 1:500 000 scale to overlay a geological map of the region at the same scale (BMR 1979a, 1979b, 1979c & 1979d).

Inspection of the new regional maps shows that most of the known uranium deposits lie in areas of magnetically disturbed metasediments near residual Bouguer anomaly lows associated with radioactive granites. Some of these regional associations have been reported elsewhere (Stephansson & Johnson, 1976; Horsfall & Wilkes, 1975; Tucker, Hone, Sampath & Ewers, 1979).

To better understand the links between the regional geophysics and regional geology, BMR undertook a multidisciplinary investigation of the geophysical characteristics of the Pine Creek Geosyncline during 1977 and 1978. The investigation included detailed ground surveys over anomalies, field and laboratory studies of rock physical properties, mineralogy studies, geological mapping, and computer modelling of anomaly sources.

GEOLOGY

The geology of the Pine Creek Geosyncline has most recently been described by Needham *et al.* (this volume).

As indicated in figure 1, the Pine Creek Geosyncline consists of Early Proterozoic, predominantly clastic sediments surrounded and overlain by younger sediments of the McArthur Basin, Daly River Basin, and Bathurst Terrace to the north. The Litchfield Block forms the western margin of the Geosyncline and contains granites and metamorphic rocks of (probably) Archaean to Middle Proterozoic (Carpentarian) age. A summary of the distribution of Early Proterozoic metasediments and their stratigraphic relations is provided in Needham *et al.* (op. cit.).

Metasediments of the Pine Creek Geosyncline are domed by Archaean to Early Proterozoic granitic rocks, for example at Rum Jungle, and in the east, surround or grade into domes of migmatite and granitic rocks (Nanambu Complex, Nimbuwah Complex). The metasediments are extensively intruded by Middle Proterozoic (Carpentarian) granites (Stephansson & Johnson, 1976) and at least two phases of mafic sills, including the Early Proterozoic Zamu Dolerite (Bryan, 1962; Ferguson & Needham, 1978) and the Middle Proterozoic (Carpentarian) Oenpelli Dolerite (Stuart-Smith & Ferguson, 1978).

The Early Proterozoic metasediments are moderately to tightly folded along north-south axes, and dips are mostly steep. Faulting of the metasediments is generally parallel to the fold axes. Regional metamorphism, is generally of low grade (greenschist facies) but reaches medium and/or high grade (amphibolite facies) east of a line drawn at about 132°30'E (Ferguson, this volume).

DENSITY OF ROCKS IN THE PINE CREEK GEOSYNCLINE

A program of rock sampling and physical property measurements was undertaken to assist in understanding the source of gravity anomalies in the Pine Creek Geosyncline. Although the rock densities measurement program was hindered by sparse outcrop, severe weathering of surface rocks, and the scarcity of representative drillcore, sufficient

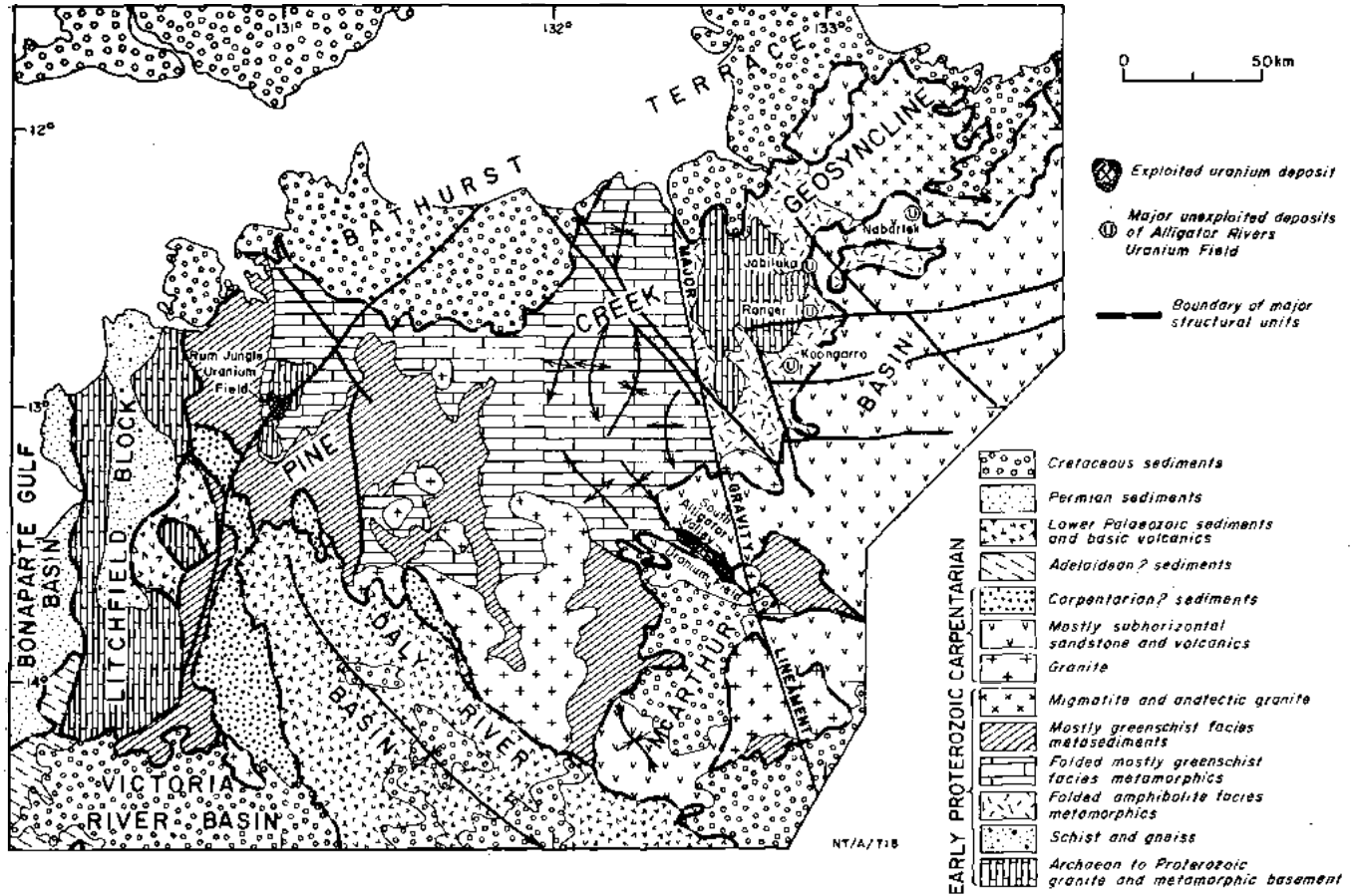


Figure 1. Simplified geology and major structural units (after BMR 1979a).

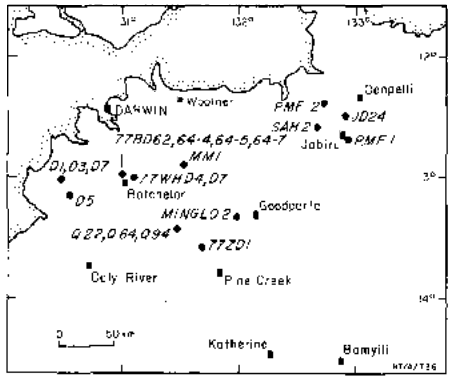


Figure 2. Drillhole locality map.

information was obtained to identify the characteristic density of individual lithologies, and some specific formations and stratigraphic units.

Density measurements were made on samples selected from 20 deep diamond drillholes some of which are described in Price (1974), Prichard (1964), Muggeridge (1977) and Fraser (1977); and from the bottom cores of 95 of BMR's shallow stratigraphic holes described, in Crick (1976) and Stuart-Smith (1977) and from approximately 250 surface samples of Early Proterozoic rocks and various granites. The location of the deep drillholes is indicated in figure 2.

The specific gravity measurements made in the Pine Creek Geosyncline are summarised in table 1. A more comprehensive listing of the specific gravity measurements is given in a BMR Microfiche Report (Tucker, in prep.).

Measurements were made on samples ranging in mass from 100 to 2000 grams. Measurement techniques included wet and dry specific gravity determination using Archimedes principle, and porosity determination using a mercury porosimeter.

Effect of weathering

Measurements of porosity and dry specific gravity on selected samples show that weathered rocks have a porosity of between 3 and 17 percent compared with a porosity of about 1 percent for samples from deep drillholes. An analysis of the specific gravity and porosity results indicates that the density of fresh rocks can be estimated from weathered samples if sufficient measurements are available to permit an interpolation of the specific gravity at the 1-percent porosity value. However, as surface sampling in the Pine Creek area commonly favours the collection of siliceous rocks which are resistant to weathering, care must be taken to ensure that weathered samples are representative of the lithology or formation sampled.

Density of Early Proterozoic Rocks

The results of specific measurements shown in table 1 indicate that there are three main groupings of density characteristics for the Early Proterozoic rocks. High density rocks have a specific gravity of from 2.9 to 3.0 and include mafic igneous units such as the Stag Creek Volcanics and Zamu Dolerite, and calcareous rocks such as the Coomalie Dolomite and Celia Dolomite. Rocks with an intermediate density have a specific gravity of from 2.75 to 2.85 and are mainly the shaley and schistose rocks such as the Koolpin Formation, Masson Formation and the Cahill Formation. Rocks with a low density have a specific gravity of from 2.67 to 2.75 and tend to be the sandy or silty units such as the Burrell Creek Formation, Fisher Creek Siltstone, Acacia Gap Sandstone, Mundogie Sandstone and possibly rocks of the Kakadu Group.

Density of Granites and Granitic Complexes

Basement complexes and migmatite zones are essentially granitic in composition although digestion of metasediments may affect the overall density of the complexes of some extent. Specific gravity measurements on the granitic rocks of the Geosyncline ranged from 2.63 to 2.68.

Density of Middle Proterozoic (Carpentarian) Doleritic Intrusives

Some of the Early Proterozoic metasedimentary units are extensively intruded by doleritic sills, such as the Oenpelli Dolerite, which have a specific gravity of around 3.00.

Formation	Dominant lithologies Intersected and Sampled	Hole/Area	Depth range sampled (m)	Dry specific gravity			
				Mean	SD	Ranged	N
Koombolgie Fmn	Pink, grey or green fine to coarse silicified sandstone	Geopeko S9/1	140-260	2.63	0.03	2.58-2.66	7
Burrell Creek Fmn	Interbedded siltstones and grits	Crae 77WHD7	20-124	2.73	.0.05	2.68-2.79	23
Gerowie Tuff	Crystal tuff-chert	Mundogie 1:100,000	Surface	2.69*	—	2.57-2.74	16
Koolpin Formation	Quartzite, chert, silicified dolomite	Mundogie 1:100,000	Surface	(2.66)*		2.61-2.74	25
Koolpin Formation	Black carbonaceous sulphide rich shale	Geopeko Quest 22	60-94	2.87	0.10	2.77-2.99	4
Koolpin Formation	Chloritic shale & siltstone, sulphide rich shale	Geopeko Quest 94	31-98	2.94*	0.14	2.69-3.09	10
Coirwong Greywacke	Quartz sandstone, feldspathic sandstone	Mundogie 1:100,000	Surface	(2.66)*	—	2.60-2.72	19
Mundogie Sandstone	Quartzite	Mundogie 1:100,000	Surface	(2.66)*		2.62-2.70	10
Masson Formation	Grey graphic pyritic shale with chert nodules	Crae 77WHD7	270-352	2.78	0.02	2.74-2.83	17
Masson Formation	Interbedded dolomitic shales & siltstones	Crae 77WHD7	124-270	2.79	0.04	2.71-2.89	30
Zamu Dolerite in Koolpin Formation	Amphibolite	Geopeko Quest 94, 62, 22	95-120	2.98	0.02	2.96-3.02	6
Stag Creek Volcanics	Basalt	Mundogie 1:100,000	Surface	3.00*	—	2.99-3.30	7
Coolamie Dolomite	Dolomite	Crae 77WHD7	454-500	2.93	0.05	2.84-3.00	9
Cahill Formation	Quartz chlorite schist PMF1 S/1	Geopeko	40-238	2.75	0.12	2.65-3.05	11
Cahill Formation	Muscovite biotite quartz schist	Geopeko PMF2 S/1	62-194	2.81	0.11	2.69-3.03	8
	Amphibolite (after ?sediments)	SAH2	284-404	3.00	0.05	2.92-3.02	31
Metasediment in Litchfield Block	Quartz mica feldspar schist	BHP EL71 D1	20-68	2.75	0.04	2.68-2.80	8
" "	Chlorite quart feldspar mica schist	BHP EL71 D5	40-176	2.86	0.10	2.60-3.13	39
" "	Quartz mica garnet amphibole schist	BHP EL71 D3	52-110	2.94	0.14	2.71-3.31	23
" "	Quartz mica garnet magnetite schist	BHP EL71 D7	41-133	2.98	0.12	2.76-3.25	25
Various	Phyllite	Mundogie 1:100,000	15-45	2.87*		2.76-2.87	5
Cullen Granite	Various granite phases (Ewers & Scott, 1977)	Cullen granite	Surface	2.65	0.06	2.61-2.71	50
Nimbuwah Complex	Granite	Alligator River	Surface	2.68	0.06	2.57-2.77	10
Rum Jungle Complex	Granite (Major, 1978)	Rum Jungle	Various	2.63	0.04	?	?
Nanambu Complex	Granite	Alligator River	Surface	2.63	0.05	2.58-2.80	14

*SG from interpolation of porosity & SG measurements ()Mean values in brackets are considered less reliable than the others

Table 1. Dry specific gravities of selected rock units, Pine Creek Geosyncline.

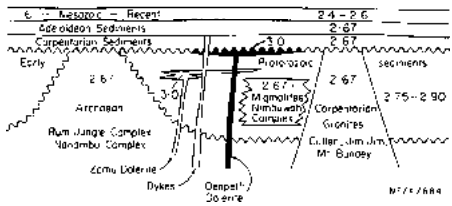


Figure 3. A specific gravity model for rocks of the Pine Creek Geosyncline.

Density of Middle Proterozoic (Carpentarian) and Younger Sediments

Few density measurements were made on Middle Proterozoic (Carpentarian) sedimentary rocks or post Proterozoic sediments. However, the lack of metamorphism and the geological descriptions of these rocks suggest they are all of relatively low density compared to the density of the Early Proterozoic rocks.

Density Profile through the Upper Crust

The specific gravity measurements on rocks of the Pine Creek Geosyncline and interpretation of geological, gravity and magnetic data suggest a simple model of the upper crust in the region of the Pine Creek Geosyncline as shown in figure 3. In this model we have a low density basement which consists variously of Archaean to Middle Proterozoic (Carpentarian) crystalline rocks overlain by high density metasediments of Early Proterozoic age which are in turn overlain by thin, flat lying, low density sediments. The section is cut by high density doleritic sills and dykes of various ages and parts of the Early Proterozoic section consist of low-medium density migmatised zones.

The assumption of a granitic basement is inferred from the presence of exposed granitic Archaean complexes with outward sloping contacts in the Rum Jungle, Litchfield and Nanambu Complexes, and the virtual absence of magnetic features in the basement.

REGIONAL GRAVITY CHARACTERISTICS

A regional view of the gravity characteristics of the Pine Creek Geosyncline is provided by BMR gravity surveys of the region as indicated in figure 4 and the map accompanying this volume (BMR, 1979b). The Bouguer anomaly data shown in these figures is based on the results of BMR helicopter surveys on an 11,000m grid and numerous BMR ground traverses with station spacings of from 200m to 300m over areas of special interest such as Rum Jungle. All of these results are available from the Australian national gravity repository in BMR, Canberra (Murray, 1974; Anfiloff *et al.*, 1976). The Bouguer anomalies have been calculated using a reduction density of 2.67 t/m^3 and the map is contoured on a four-minute grid surface at 10 μm/s^2 intervals.

The Bouguer anomaly values recorded in the Pine Creek Geosyncline are essentially positive and achieve a maximum value of 400 μm/s^2. The positive Bouguer anomaly values in the Geosyncline contrast strongly with the negative Bouguer anomaly values observed over the younger sedimentary basins which surround the Geosyncline to the south, east and west.

Trend surface analyses indicate a gentle north-south trending regional gradient of approximately 2 μm/s^2/km to the north, and an average Bouguer anomaly over the Geosyncline of approximately 200 μm/s^2. Superimposed on this fairly uniform regional surface are numerous and predominantly north-south closure patterns and gradients which frequently correspond with geological boundaries and units. The majority of closure patterns are relative lows, and these correspond with the granitic complexes of the region. Other features observed in the regional data are a reduction in Bouguer anomaly along the coast of Van Diemen Gulf, and various lineaments and gradients. Some of the important characteristics of the regional Bouguer anomaly data are shown in figure 4.

The positive Bouguer anomaly observed within the Pine Creek Geosyncline is interpreted as the result of the high density of the upper crust in this region as proposed in

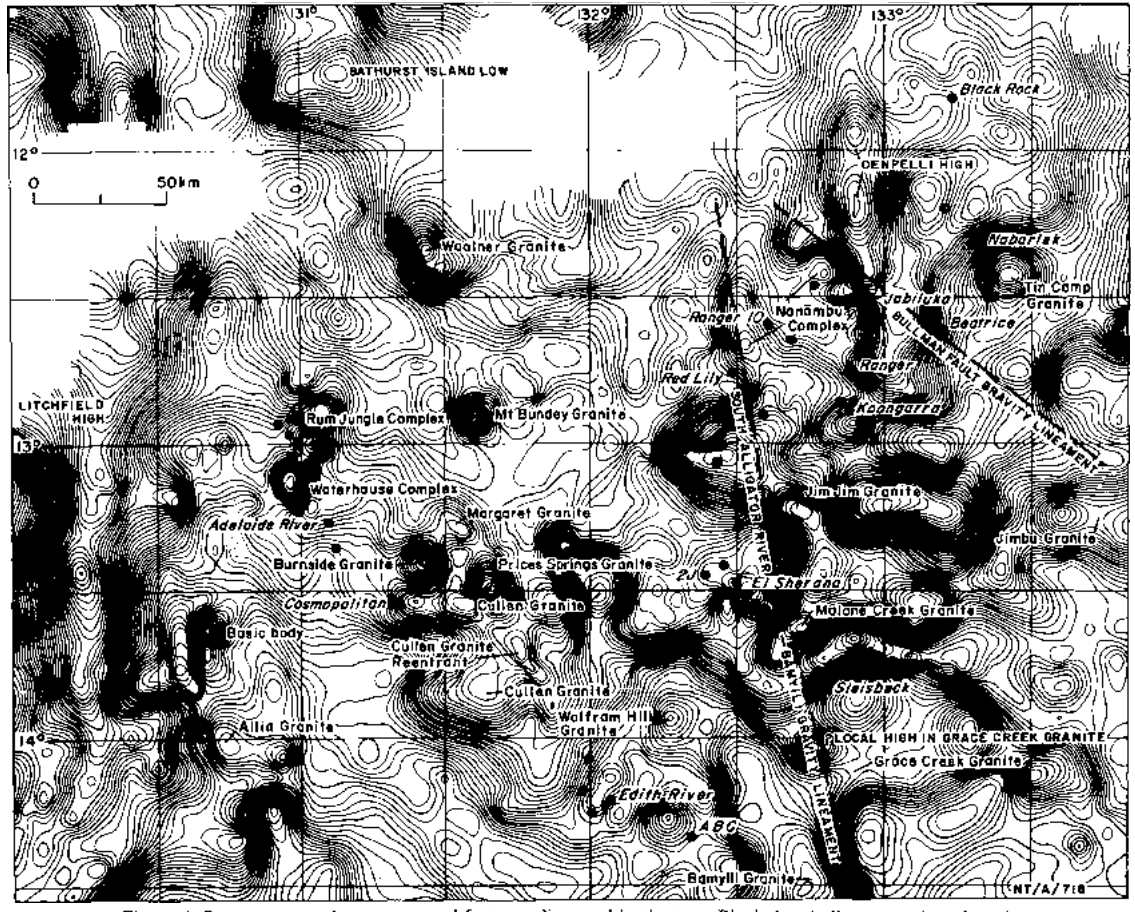


Figure 4. Bouguer anomaly contours and features discussed in the text. Black dots indicate uranium deposits.

IAEA

the model shown in figure 3. The local closures and gradients appear to reflect differences in rock density and structural elements of the Geosyncline.

SOURCE OF LOCALIZED GRAVITY LOWS

The source of the localized, relative low anomalies was investigated by detailed gravity traverses, geological mapping, rock property measurements, and modelling. Anomalies of this type frequently occur over, or are associated with, outcropping granitic rocks surrounded by Lower Proterozoic metasediments. The most prominent localized low anomalies lie in a belt which includes the Rum Jungle and Waterhouse Complexes, Burnside Granite, Prices Springs Granite, Cullen Granite, and the Jim Jim Granite and Tin Camp Granite in the Alligator River area. Some localized anomalies, such as those over the Jim Jim and Malone Creek Granites, appear to be linked over a large area and have a common source.

With the available rock property information and geological constraints provided by field mapping, the sources of localized low anomalies are shown to be granitic complexes lying within the metasedimentary section. Localized low anomalies have either a flat bottom or a smooth symmetrical low depending on the width of the anomaly. A guide to the relationship between possible models of the granitic-metasedimentary boundary and the shape of the localized low anomalies is indicated in figure 5. Sensitivity analyses of two dimensional inversion constraints suggest the most probable model for the granitic sources is that in which the density contrast between the granitic and metasedimentary rocks has a depth extent of less than 5000m, and the contacts between the two rock types commonly slope outwards.

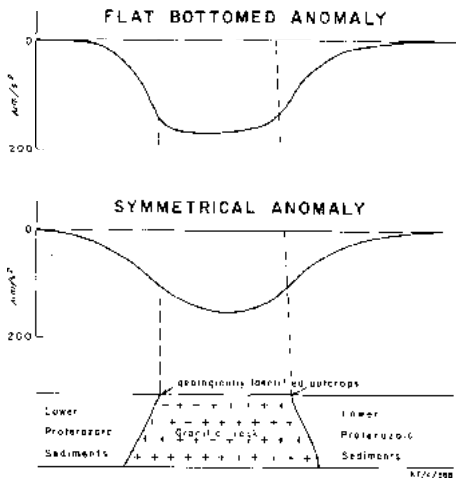


Figure 5. Sketch of typical Bouguer anomaly lows developed across granites in the Pine Creek Geosyncline. (a) A flat bottomed residual low and (b) a smooth symmetrical low, both of which on modelling with the available geological constraints indicate outward sloping contacts and limited depth extent, the case (b) applying to narrower bodies than does (a).

Possible geological interpretations of this model are shown in figure 6. The idealised Bouguer anomaly (a) can be interpreted using constraints on the surface extent to give the theoretical model (b) of low density contrast material in a zero-density background. Contacts slope outwards and the model has limited depth extent. However, this basic model is indistinguishable from models (c), (d), or (e). Of those possible models only (e) satisfies all the available geological and geophysical constraints and is therefore preferred. In this model, localized Bouguer anomaly lows indicate the presence of the low-density granitic bodies, either Archaean or Middle Proterozic (Carpentarian), which are surrounded by high-density Early Proterozoic sediments and merges at depth with a low density basement.

Modelling of Rum Jungle and Waterhouse Complexes

Detailed gravity traverses by Major (1977) using station spacings of as little as 200m show that the Waterhouse Complex and Rum Jungle Complex are mostly overlain by relative Bouguer anomaly lows which exhibit a flat bottom. As shown in figure 7 modelling of the Complex with the assumptions of a

simple density contrast and contacts which slope steeply outwards beneath the Lower Proterozoic sediments limits the probable depth extent of the granitic complex to less than 5,000m. A limited depth extent of the complexes is also indicated by an analysis using excess mass calculations (Major, op. cit). Northeast of the Rum Jungle Complex there is no gravity low developed across a granitic to metasediment contact and this may indicate that part of the Rum Jungle Complex comprises rocks which have a similar density to the enclosing Lower Proterozoic sediments.

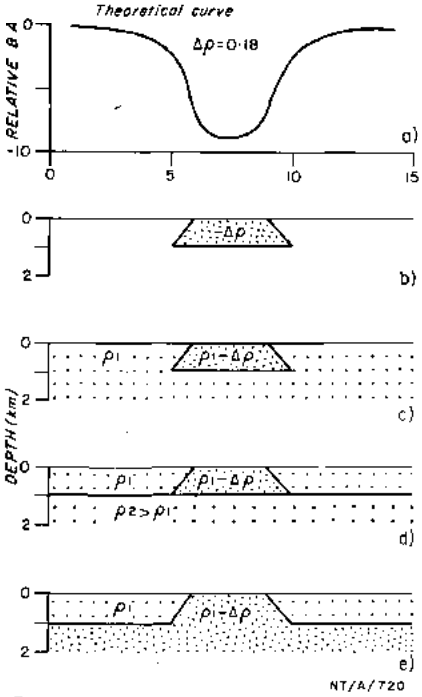


Figure 6. Inversion of typical Bouguer anomaly low. For explanation see text.

Modelling of the Mount Bundey Granite

A detailed gravity traverse across this small body shows a smooth symmetrical relative low anomaly. As indicated in figure 8 the anomaly can be modelled as a low density granitic body with outward sloping contacts and a depth extent of less than 5,000m.

Modelling of the Jim Jim Granite

The negative Bouguer anomaly profile over the Jim Jim granite shows a well developed flat bottomed low (Fig. 9). This anomaly can be modelled as a low density granitic body with an outward sloping contact on the southwestern side and vertical to inward dipping contact on the northeastern side.

Modelling of Other Localized Low Anomalies

The results of modelling of the source of other localized lows throughout the Geosyncline are summarised in table 2. The results show that modelled depth extents are generally less than 5,000m and most granitic bodies have a batholith-type geometry. The proposition that there is no density contrast between the granitic complexes and the basement of the Geosyncline implies that the depth extent of the modelled granitic bodies is a guide to the thickness of the surrounding metasediments.

SOURCE OF LOCALIZED GRAVITY HIGHS

Anomalies of this type can rarely be associated with specific geological units or features. Detailed gravity traverses by Wronski (1978) across various steeply dipping Lower Proterozoic metasediments west of 132°30'E show that only small anomalies of from 10 to 30 $\mu m/s^2$ can be attributed to density differences in the steeply dipping metasediments. These small anomalies are very minor when compared with the 200 to 300 $\mu m/s^2$ anomalies observed over the Litchfield Block and north of the Alligator Rivers area. Low density contrasts within the Lower Proterozoic metasediments are also indicated by the results of specific gravity measurements.

As the large localized high anomalies in the east and west cannot be attributed to density contrasts between exposed Lower Proterozoic metasedimentary rock bodies, it seems probable that the anomalies result from either thickening of the metasedimentary section or the presence of very dense rock units at depth. Unfortunately the lack of geological constraints means that the source of these high anomalies cannot be modelled with much confidence.

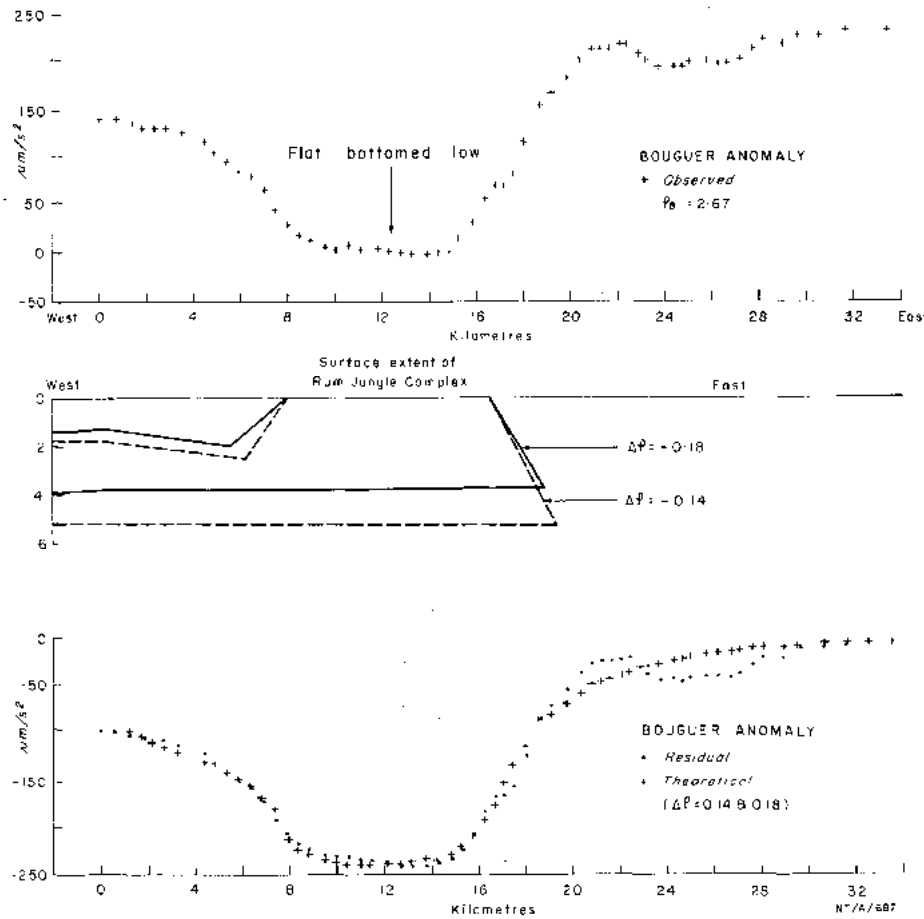


Figure 7. Gravity profile and model across Rum Jungle Complex.

Modelling of the High Anomaly over the Litchfield Block

This feature is an elongate high of 300 m/s^2 which extends north-south over the Litchfield Block, and may extend northwards onto Bathurst Island. Owing to the lack of geological constraints, modelling of the feature was not definitive and presented several plausible possibilities. The most favoured model indicates an elongate high density body of density approximately 3.0 t/m^3 within a depth of 10-15km, beneath or within the Litchfield Block. This might be attributed to metasediments or mafic rocks at depth.

Modelling of the Oenpelli Bouguer Anomaly High

This anomaly is a prominent north-side trending feature some 200 $\mu m/s^2$ above the local background. The gradients are not sufficiently well defined to permit definitive modelling in the region of the highest amplitude peaks. However, modelling based on a detailed gravity traverse by Wronski (1978) along the road southeast of Oenpelli indicates that the feature could be caused by a shallow high density unit up to 12,000m wide with near vertical contacts, extending to approximately 6,000m. This model approximately coincides

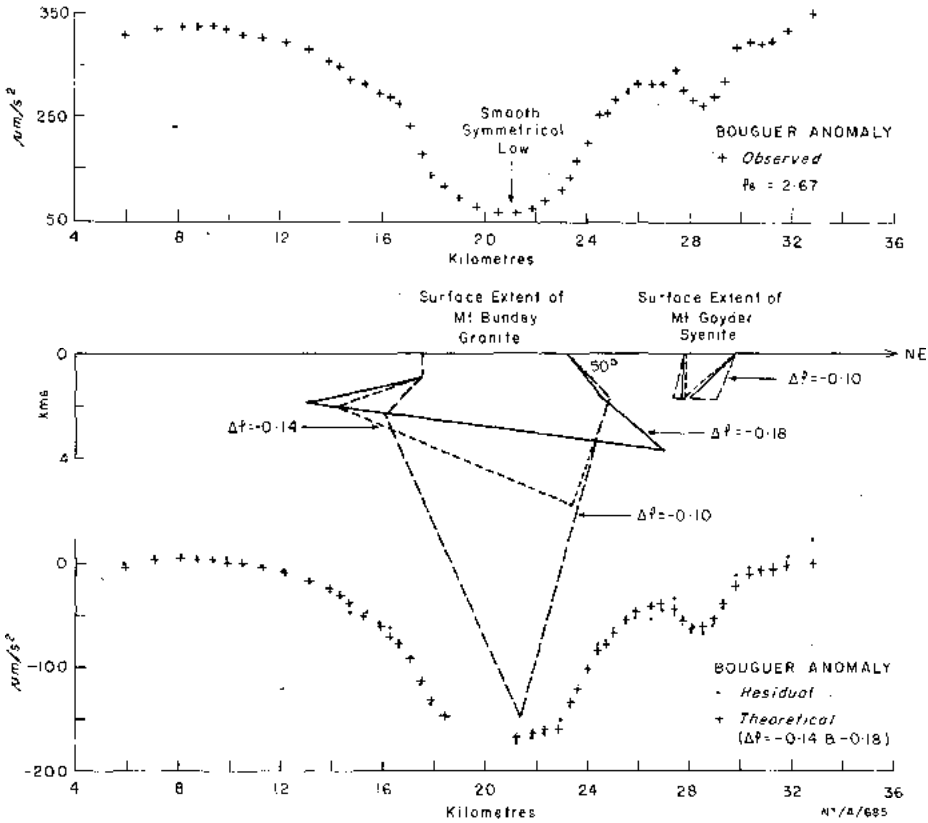


Figure 8. Gravity profile and model across Mount Bundey Granite.

in position and trend with the mapped Finniss River Group, and Nourlangie Schist in the area. Perhaps these are particularly high-density units.

Modelling of the High Anomaly North of Daly River

This anomaly of 250 μm/s² above local background lies over a mapped igneous mafic body and can be modelled as a high-density block with outward sloping contacts with a depth extent of 4,000m.

Modelling of the High Anomaly within the Grace Creek Granite

This high anomaly which appears to be fringed by shallow curvilinear magnetic anomalies is underlain by granite and is an unusual feature for the area. Fieldwork indicates that the granite contains more mafic minerals in the region of the gravity high (J. Ferguson, pers. comm.). The anomaly is not well defined but can be modelled as a high-density plug 8,000m across, with near-vertical contacts.

GRAVITY LINEAMENTS

A second derivative map of Bouguer anomalies in the Geosyncline is shown in figure 10 and highlights the distribution of gradients associated with the contact between blocks with different density occurring in the top 10km of crust. In the second derivative presentation the zero contours lie over the steepest parts of the Bouguer anomaly gradients and approximate

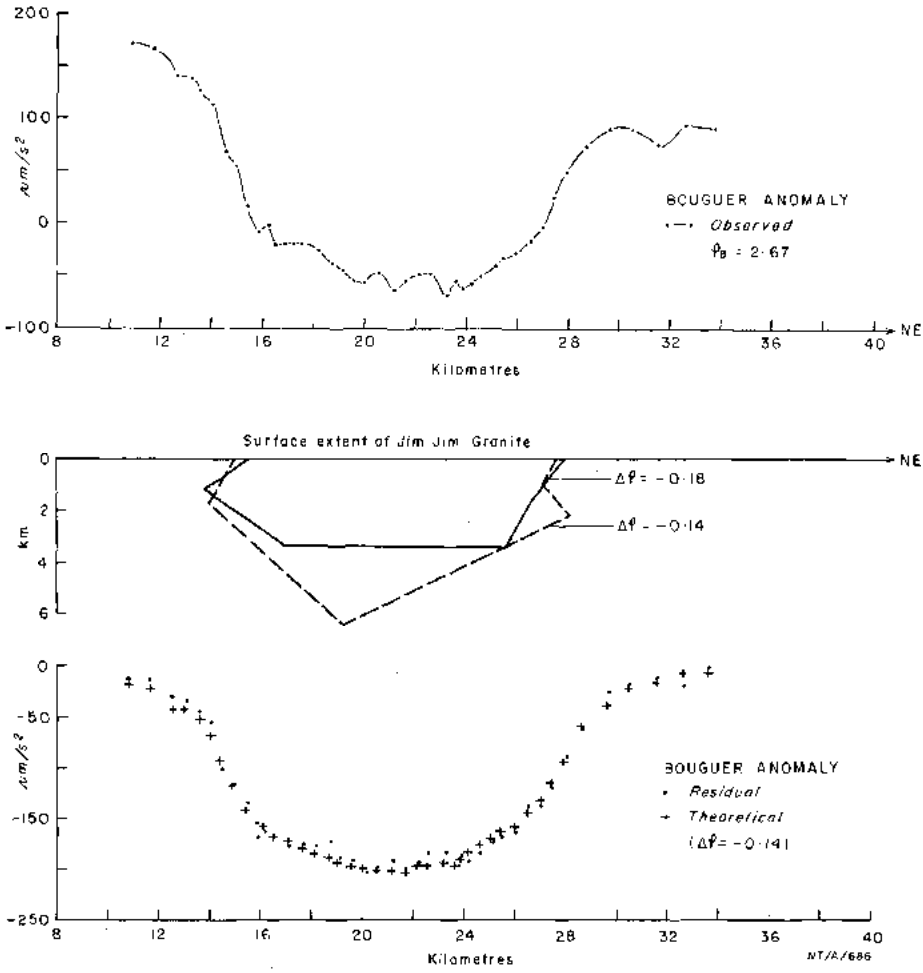


Figure 9. Gravity profile and model across Jim Jim Granite.

the position of contacts between high and low density rock units. The study of Bouguer anomaly maps, augmented by second derivative and other presentations indicate that the major geological blocks in the Geosyncline are predominantly oriented in northwest, north-south and east-west directions. Dislocations and alignments of some of these features generate lineaments in the gravity data which might be interpreted as faults or structural boundaries. Some of the lineaments identified in this manner appear to correlate with geologically identified structural or geomorphological features. As examples two major features are indicated in figure 4 and are discussed below. Others are evident in figures 4 and 10, but these will not be discussed here.

Bullman Fault Lineament

There appears to be a dislocation and some 10 to 15km sinistral offset of north-south gravity trends (Fig. 4) along a line which extends northwest through the East Alligator River

	Localised Residual Anomaly Characteristics		2D Model Geometry (for Δ = -0.18)				
	Residual amplitude $\mu m/s^2$	Shape*	Surface width	Bottom width	Depth extent	Contact dips	Remarks
Litchfield Complex	-60	F	11,000+	8,100+	900	Inwards	Contacts inferred
Roberts Creek Granite	-70	S	2,000	9,500	1,000	Outwards	Contacts mapped
Rum Jungle Complex (Major, 1977)	-180	F	17,000	21,000	2,500	Outwards	Contacts mapped, dips 45°-90°
Waterhouse Complex (Major, 1977)	-240	F	8,600	13,000	3,700	Outwards	Contacts mapped, dips 20°-75°
Woolner	-180	F	7,500	20,000+	4,000	Outwards	Contacts inferred by magnetics
Mt. Bundey Granite	-180	S	5,800	14,000	3,000	Outwards	Contacts mapped
Cullen Granite Re-entrant	80	N	6,000	nil	2,500	Inwards	Contacts mapped
Jim Jim Granite	-200	F	12,400	5,600	3,300	Complex	Contacts mapped
Namamba Complex	-150	?S	7,000	19,000	2,000	Outwards	Poor fit; Contacts mapped
			7,800	23,000	2,100	Outwards	Good fit; Contacts inferred
Malone Creek Granite	-200	?S			6,000	Outwards	Contacts mapped

* F = Flat bottom; S = Smooth symmetrical; N = Narrow high over EE sediments.

Table 2. Characteristics of 2-Dimensional models for selected granites.

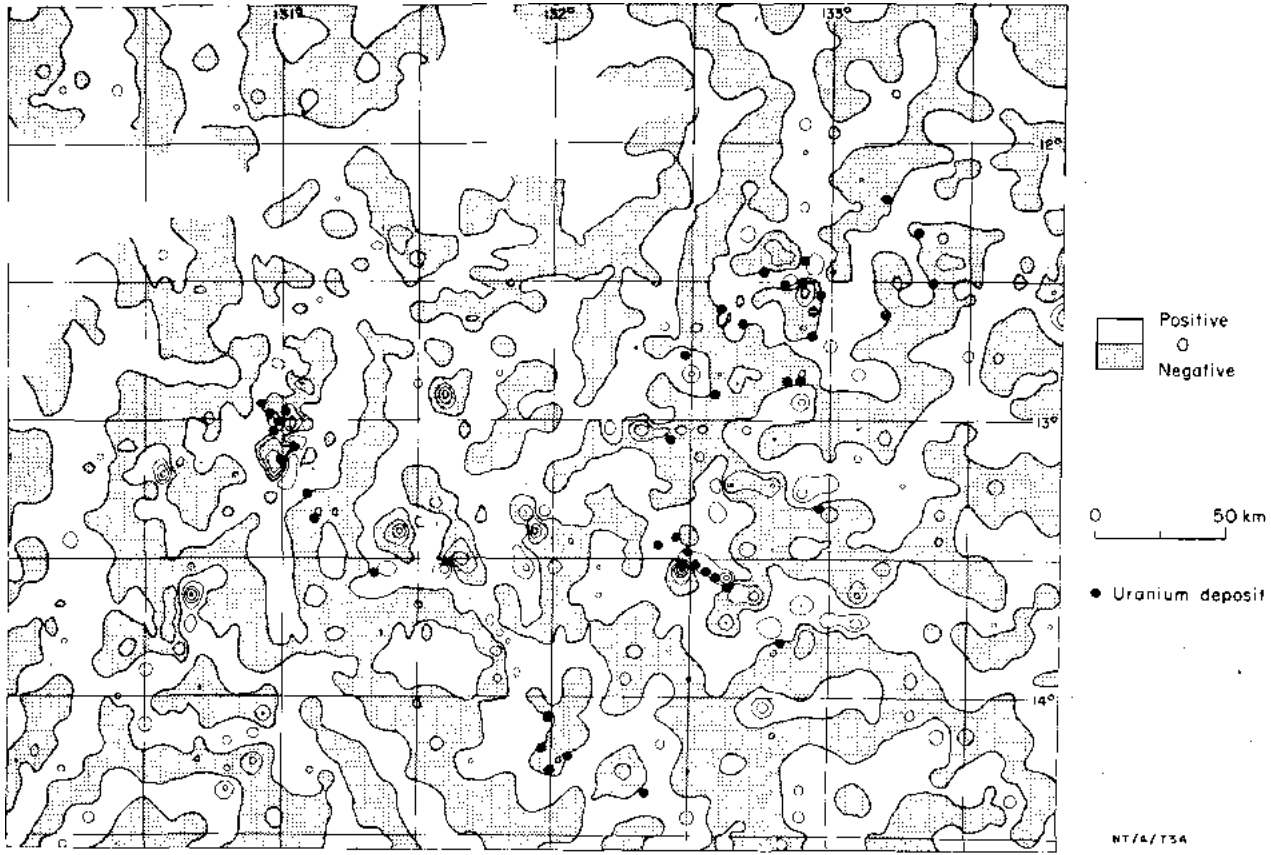


Figure 10. Second derivative of Bouguer anomalies computed for a sample interval of two minutes shows closures due predominantly to relatively near surface features. The zero contour may indicate the contact between adjacent blocks of differing density.

and is roughly coincident with the Bullman Fault as identified by geological mapping. This gravity feature is mirrored in the magnetic contour maps by linear anomalies attributed to dolerite dykes, and extends southeastwards out of the study area. It is in addition parallel to other structural features such as the South Alligator Syncline (see 1:500 000 Geological Map BMR 1979a).

South Alligator River - Bamyili Lineament

A roughly north-south lineament defined mainly by the gradient of gravity features associated with granitic bodies passes through and is parallel to the South Alligator River over much of its course. Few gravity trends of any prominence cross this lineament; Bouguer anomaly closure patterns are predominantly north-south and east-west to the east of the line, and predominantly northwest and northeast to the west of it. The nature of these features suggests that the lineament is a reflection of a major lateral change in structure and composition.

SOURCE OF GRAVITY LOW ALONG THE COAST OF VAN DIEMEN GULF

There is a reduction in the average Bouguer anomaly of some 50 $\mu m/s^2$ along the south coast of Van Diemen Gulf. Proterozoic rocks in this area are covered by a thin veneer of Mesozoic and Quaternary cover of approximately 100m which thickens to over 500m to the north on Bathurst and Melville Islands. The reduction in Bouguer anomaly in this area can in part be explained by this cover if a large density contrast between it and Early Proterozoic rocks is assumed. Thus, if adequate control is used it is probable that variations in Bouguer anomaly values along the Van Diemen Gulf coast can be used to indicate the thickness of Mesozoic and Quaternary cover.

The 50 $\mu m/s^2$ reduction in average Bouguer anomaly discussed above is largely overshadowed by a 250 $\mu m/s^2$ localized low near Woolner, and another on the eastern end of Melville Island. The Woolner low can be modelled as a low density body with outward sloping contacts similar to the cases of the Rum Jungle Complex and Jim Jim Granite (Table 2).

A BASEMENT MODEL OF THE PINE CREEK GEOSYNCLINE

Density measurements and modelling indicate that the specific gravity of the Lower Proterozoic metasediments is approximately 2.85, and the specific gravity of the granite complexes is approximately 2.67. Furthermore in most areas there is no apparent density or magnetic contrast between the granitic complexes and the basement of the Pine Creek Geosyncline. Modelling constrained by surface geology indicates that the granitic complexes commonly slope outwards and merge with the basement at a depth of generally less than 5,000m. Accordingly the depth extent of the granitic complexes determined by modelling can be used as a control on the thickness of Lower Proterozoic sediments and hence on the extent and structure of the Geosyncline.

A regional model based on this hypothesis and using a contrast of 0.18 was estimated from a residual gravity map calculated to give anomaly zeros over granitic outcrop. The prominent Bouguer Anomaly high over the Litchfield Block was removed in the residual calculation on the basis that this area is largely underlain by granite and the anomaly could thus be set to zero. The regional model is shown in figure 11. It indicates that a relatively shallow basement at a depth of approximately 1000m links some of the more extensive granitic complexes, for example the Litchfield Complex with the Cullen and Grace Creek Granites, and the Nanambu Complex with predicted very near-surface granites fringing Van Diemen Gulf (Fig. 11). Similarly a basement high links the Jim Jim and Malone Creek Granites.

Sediments up to 6000m thick are developed in the Pine Creek Geosyncline in an

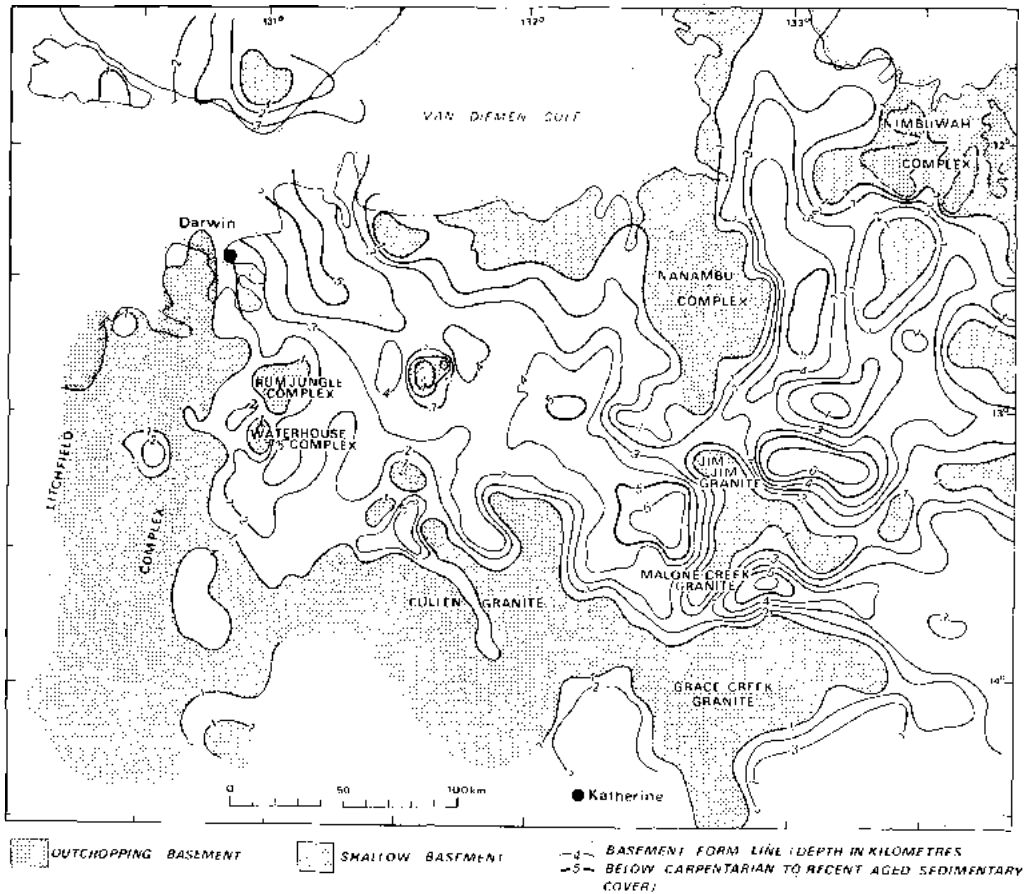


Figure 11. Basement form lines for the Pine Creek Geosyncline.

essentially east-west trending belt confined by these basement highs. This belt appears to extend eastwards beneath Middle Proterozoic (Carpentarian) cover rocks.

ASSOCIATIONS BETWEEN THE DISTRIBUTION OF URANIUM DEPOSITS AND GRAVITY ANOMALIES

Regional gravity anomalies have been shown to be caused by extensive rock units and the distribution of known uranium deposits is shown in relation to the gravity pattern in figures 4 and 10. The deposits appear to lie in zones exhibiting a disturbed gravity pattern; the zones reflect lateral changes in the density across granite, metasediment boundaries.

The major deposits in the Alligator Rivers area lie on the fringe of a regional gravity high zone which may indicate a higher density or greater-thickness of the metasediment column. The small deposits in the vicinity of Rum Jungle and Adelaide River may have a similar relationship with the regional gravity high zone which extends southeastwards from Darwin to near Mount Bundey. Basement depth analysis supports the thicker metasediments hypothesis, but it should not be overlooked that a regional increase in dense minerals, for example mica or iron sulphides or oxides, could contribute to the gravity high.

Even though it may be empirically attractive to draw northwest and northeast straight lines to connect some of the uranium deposits and then construct conjugate sets of parallel lines to take in others, there does not appear to be a direct relationship between the major gravity lineaments, such as the South Alligator River-Bamyili Lineament or the Bullman Fault Lineament, and the deposits. However, the major known deposits all lie to the east of the former of these two features, and hence appear to be located in a region of essentially north-south and east-west basement trends, while the smaller deposits including the South Alligator Valley Uranium Field lie to the west of it and appear to be located in a region of essentially northwest basement trends. It is possible that the deposits are somehow related to a very deep seated fault system, which extends down to 6000m or more.

REGIONAL MAGNETIC CHARACTERISTICS

A regional view of the magnetic characteristics of the Pine Creek Geosyncline is provided by the residual total magnetic intensity (TMI) contour map shown in figure 12 and the map accompanying this volume (BMR, 1979c). These maps have been compiled mainly from the results of BMR reconnaissance airborne magnetic surveys along east-west traverses flown 1500m apart and at a mean terrain clearance of 150m, and to a lesser extent from various company surveys. In the area bounded by longitude 132°E and 133°30'E and latitudes 12°S and 13°30'S and magnetic results were recorded by analogue methods; elsewhere results were recorded and processed by digital methods. The results of BMR reconnaissance airborne magnetic surveys (Gerula, 1979) in the Pine Creek Geosyncline are available at 1:250 000 scale from the Australian Government Printer, Canberra, as TMI contour maps, stacked TMI profiles and flight path maps, and for part of the area as digital records on magnetic tape. Preparation of the contour maps has involved some smoothing of data and removal of the International Geomagnetic Reference Field. In the Pine Creek Geosyncline, the total magnetic field intensity is approximately 47,000 nT, inclination is -40°, and the declination is 4°E (Finlayson, 1973).

Many of of the features seen in the magnetic field in the area, are indicated in figure 12.

Long-Wavelength Features

Owing to the masking effect of high-amplitude short-wavelength features in the residual TMI data, it is difficult to identify low-amplitude long-wavelength features. However, smooth elongate gradients can be observed in the southwest of the Geosyncline and probably indicate deep-seated contacts which may reflect structural or lithological changes at considerable depth. Additional long wavelength features are indicated in figure

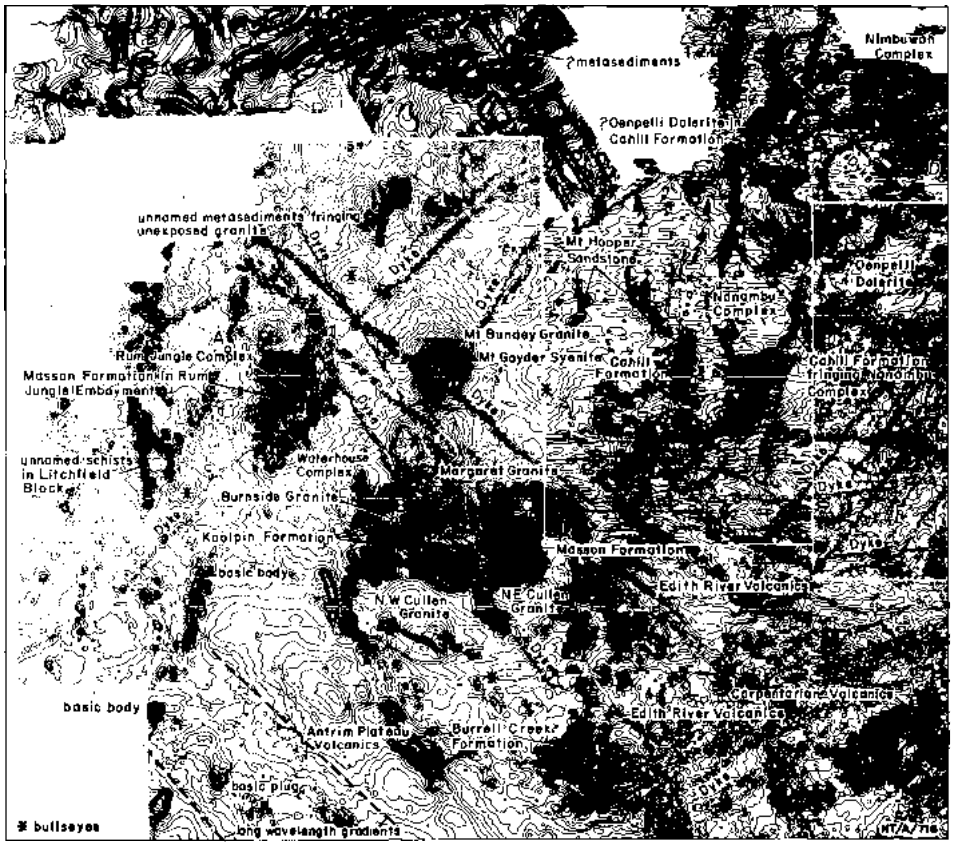


Figure 12. Total Magnetic Intensity Contours, showing sources of selected curvilinear zones, linear anomalies, bullseyes, and long wavelength gradients.

12 and include bullseye or dipole anomalies, as for instance, 15km north of the Rum Jungle Complex.

Short-Wavelength Elongate Features

The most prominent features in the residual TMI data are elongate anomalies which, have a short wavelength and are bounded by steep gradients. Analysis indicates that the sources of the features are very shallow and mainly occur within rocks which outcrop or sub-outcrop. Correlations between short wave-length features and surface geological units are indicated in figure 12.

Curvilinear Zones:

The most widespread and prominent short wave-length features observed in the regional magnetic data are broad curvilinear zones which are located over steeply dipping Lower Proterozoic sedimentary formations, sills of Oenpelli Dolerite, and Middle Proterozoic (Carpentarian) Volcanic members. The curvilinear zones consist of complex, narrow elongate (often subparallel) magnetic anomaly patterns which extend over several hundred square kilometres. The amplitude of individual anomalies range from 10 nT to over 1000 nT. The boundary between curvilinear and low-relief zones is sharp, and frequently corresponds with boundaries between rock units.

Linear Anomalies:

Other prominent short-wavelength features are suites of long, linear anomalies of both positive and negative sign which cut across the regional geological strike of the Lower Proterozoic metasediments. As indicated in figure 12 most of the linear anomalies trend approximately northwest or northeast and a few in the eastern part of the area trend approximately east-west. These directions parallel the orientation of faulting in the region and the linear features are commonly coincident with faults or photo lineaments. For example one of the largest of the linear anomalies extends southwest from near Woolner and for 50km is co-incident with the Giants Reef Fault where it cuts the Rum Jungle Complex. In the east of the area the linear features frequently lie over joints in the flat-lying Kombolgie Formation. There appear to be few linear anomalies in the region 132° to 132°30'E. A fuller discussion of associations of the linears and geological features is given by Simpson *et al.* (this volume).

Dipole or Bullseye Anomalies

Near-circular positive anomalies usually with adjacent magnetic lows are observed in areas of low magnetic relief and are typical of sources of limited areal but considerable depth extent. As indicated in figure 12 the size of these anomalies is quite variable. The most prominent which lies over the northern part of the Mount Bundey Granite/Mount Goyder Syenite where magnetite deposits were mined and has an amplitude of 500 nT; it appears to have components from both shallow and deep sources.

The more common amplitude of the features lies in the range 50-150 nT. For example a bullseye anomaly of 50 nT amplitude which may have a source as deep as 2500m below the surface, lies 15km north of the Rum Jungle Complex.

Owing to the wide flight line spacing and the prominence of the curvilinear magnetic zones it is difficult to detect small or low intensity anomalies of this kind.

MAGNETIC PROPERTIES OF ROCKS IN THE PINE CREEK GEOSYNCLINE

Studies of the magnetic properties of rocks, and sources of magnetic anomalies in the Pine Creek Geosyncline, were made on core samples selected from 20 deep and 50 shallow holes which passed through or near sources of magnetic anomalies. The distribution of the deep holes is shown in figure 2. Suitable holes for magnetic property studies occur in only a few localities and mainly test economically important units of the Lower Proterozoic Nonetheless the holes are widely distributed across the Geosyncline.

Formation	Area	Main lithology intersected and sampled	Background magnetic properties				
			Susceptibility SIx10⁻⁶			Koenisberger Q (Field 50 000nT)	
			Mean	Common range	N	Mean	Common range
Cahill	Fringe of Nanambu Complex	Quartz chlorite/mica schist	190	60-200	37	-	0.02-3 5
Cahill		Biotite/muscovite quartz schist					
Cahill		Quartz chlorite feldspar pegmatoid	12				
Cahill		Amphibolite (sedimentary?)	560	400-750	78	0.03	0.004-0.32
Cahill		Sandstone	110	60-400	9	0.3	0.06-0.8
Cahill		Mica-schist	500	120-1200	24	0.4	0.16-0.88
Masson	Fringe of	Marble	250	60-250	6		
Zamu	Cullen	Amphibolite (igneous)	1000	400-1900	27	16	0.04-42
Koolpin, Masson	Granite	Black carbonaceous shale	750	60-1100	25	-	0.002-0.14
Koolpin	"	Chloritic garnetiferous phyllitic shale	500	120-750	9		
Koolpin	"	Chlorite & chlorite chert siltstone	1100	400-3000	30	0.06	0.004-0.16
Koolpin	"	Dolomite shale	1000	750-1500	11		
	Rum Jungle Embayment	Dolerite (near Dolerite Ridge)	950	400-1600	27	2.0	0 2-2.6
Masson	"	Black slate	880	500-1300	11		
Masson	"	Graphitic argillite	380	200-450	9		
Masson	"	Calcareous amphibolite (sedimentary)	250	60-1400	11		
unamed schists	Litchfield Block	Chloritic quartz feldspar mica schist	500	250-5000	77	0.006	-
"	"	Quartz mica garnet amphibole schist	1000	400-1600	21		
"	"	Quartz biotite garnet magnetite schist					
" amphibolite	"	Amphibolite (igneous texture	90	—	4		
" "	"	Amphibolite	1200	750-1900	6	0.02	-
Oenpelli Dolerite	vicinity of Oenpelli	Dolerite					
Northwest negative linear	NW of Mount Bundey Granite	Dolerite					
Dolerite sill	Jabiluka	Dolerite	720	560-860	3	0.1	0.004-0.028
Stag Creek Volcanics	South Alligator River Valley	Basalt	500	100-800	3		
Edith River Volcanics	East of Katherine	Felsic volcanics	500	200-1300	13		

Magnetic susceptibility measured on drill core with BISON AC susceptibility meter in the field. Koenigsberger ratio Q determined on 2.5 x 2.5cm plugs in BMR physical property laboratory are expressed in terms of a field of 50 000 nT. N = number of samples.

Table 3. Summary of magnetic susceptibility and remanence measurements made on drill core and surface samples.

Properties of magnetic intersections								Magnetic minerals present
Susceptibility SIx10⁻⁶			Koenigsberger Q (Field 50 000nT)				Thickness	
N	Mean	Common range	N	Mean	Range	N	(m)	
2	50000	13000-160000	15	-	0.08-1.00	2	25	Magnetite
9 3 6	7500	5000-13000	6	-	0.06-1.4	2	2-10	Magnetite
3	9000	6000-13000	20	35	16-44	5	15+	Pyrrhotite
2	19000	2500-60000	29	71	12-185	3	30	Pyrrhotite
3	30000	7500-50000	6	98	48-175	3	30	Pyrrhotite
3	10000	4000-50000	15	3.4		1	20	Pyrrhotite
	19000	9500-28000	18				10-50	Pyrrhotite
	9000	5000-18000	30		1.3-7.8	2	50+	Pyrrhotite
1	7500	4000-11000	3				6	Magnetite
	25000	10000-290000	14	50	0.06-100	3	3-15	Magnetite Pyrrhotite
	160000	50000-375000	30	0.1	0.002-0.22	4	40+	Magnetite
1	210000	140000-325000	4	0.44	-	1	2	Magnetite
	14000		1	2.0	-	1	sfce	Magnetite
	32000	3700-44300	5	4.1	3.3-5.3	5	30	Pyrrhotite
3							170+	Magnetite
	48000		1				sfce	?
	22500	22000-23000	2				sfce	?

Table 3 continued.

Laboratory investigations of the magnetic properties of core samples included opaque mineralogy, magnetic susceptibility, remanence and magnetic mineralogy measurements (Tucker *et al.*, 1979).

Susceptibility

The results of magnetic susceptibility measurements are summarised in table 3 which shows the susceptibility, remanence and magnetic mineralogy of various rock units and magnetic sources in the Pine Creek Geosyncline. The mean background susceptibility of all rock units investigated is less than 1200 x 10^{-6} SI units and for more than half of the samples is less than 500 x 10^{-6} SI units. The magnetic susceptibility of magnetic sources falls into two groups depending on their magnetic mineralogy. Pyrrhotite-bearing rocks have a mean susceptibility of about 15 000 x 10^{-6} SI units and magnetite bearing rocks have a mean susceptibility of about 60 000 x 10^{-6} SI units. Magnetic metasediments, penetrated in drillholes, are usually strongly weathered near the surface for 10-50m, in which zone they are found to be essentially non-magnetic.

Remanence

The strength of remanent magnetisation is here indicated by the Koenigsberger ratio (Q) and was determined for a field of 50 000 nT to permit comparison between induced and remanent magnetisation. The results of remanence measurements shown in table 3 indicate that remanence is the major factor determining the magnetisation of pyrrhotite-bearing sources but is relatively minor for magnetite bearing sources. The direction of remanence in pyrrhotite-bearing sources was investigated by crudely orientated samples and the results of these measurements show the remanence to be parallel to the present direction of the earth's magnetic field. Modelling supports this observation as dips calculated for magnetic profiles over pyrrhotite sources approximate geological dips.

SOURCE OF LONG-WAVELENGTH MAGNETIC FEATURES

Interpretation of the long-wavelength features shown in the profile drawn between ABCD in the total-magnetic-intensity-map (BMR, 1979c and figure 13), indicates that their source could be small lateral compositional changes across wide blocks of basement at depths of 2000-5000m. However, owing to the lack of supporting geological information and on physical properties, this interpretation is at best speculative.



Figure 13. Magnetic profile across the Pine Creek Geosyncline showing long wavelength features (dashed).

SOURCES IN CURVILINEAR MAGNETIC ZONES

The source of curvilinear anomalies has been investigated by the analyses of airborne and ground magnetic surveys, geological observations and rock-property measurements.

Magnetic Sources in Early Proterozoic Rocks

The results from field studies of curvilinear zones observed over steeply dipping Early Proterozoic rocks indicate that the zones consist of narrow, sub-parallel anomalies separated by as little as 200m (see figure 14 after Tucker *et al.*, 1979). On the ground, single anomalies identified in airborne data can commonly be resolved into two or more anomalies. The sources of individual anomalies appear to be conformable with the metasediments, they are mostly less than 50m thick in computer derived models and drillhole intersections, and are

locally continuous for 10-50km. Depth estimates for the top surface of the sources range from 20m to 50m and are consistent with the weathering profiles observed in the region. Laboratory studies of core from holes intersecting magnetic sources in Early Proterozoic metasediments (Table 3) confirm the view that the sources of these curvilinear zones are thin units within the Lower Proterozoic formations. The source of the magnetisation in these units is one to five percent of inductively magnetised magnetic or remanently magnetised pyrrhotite.

Proximity of granites:

Many of the prominent curvilinear zones over Lower Proterozoic rocks form haloes up to 10km wide around areas of outcropping granitic rocks, and thus appear to be related to them in some way, perhaps through metamorphism of appropriate sediments during emplacement of the granites. Good examples of such zones occur around the Rum Jungle

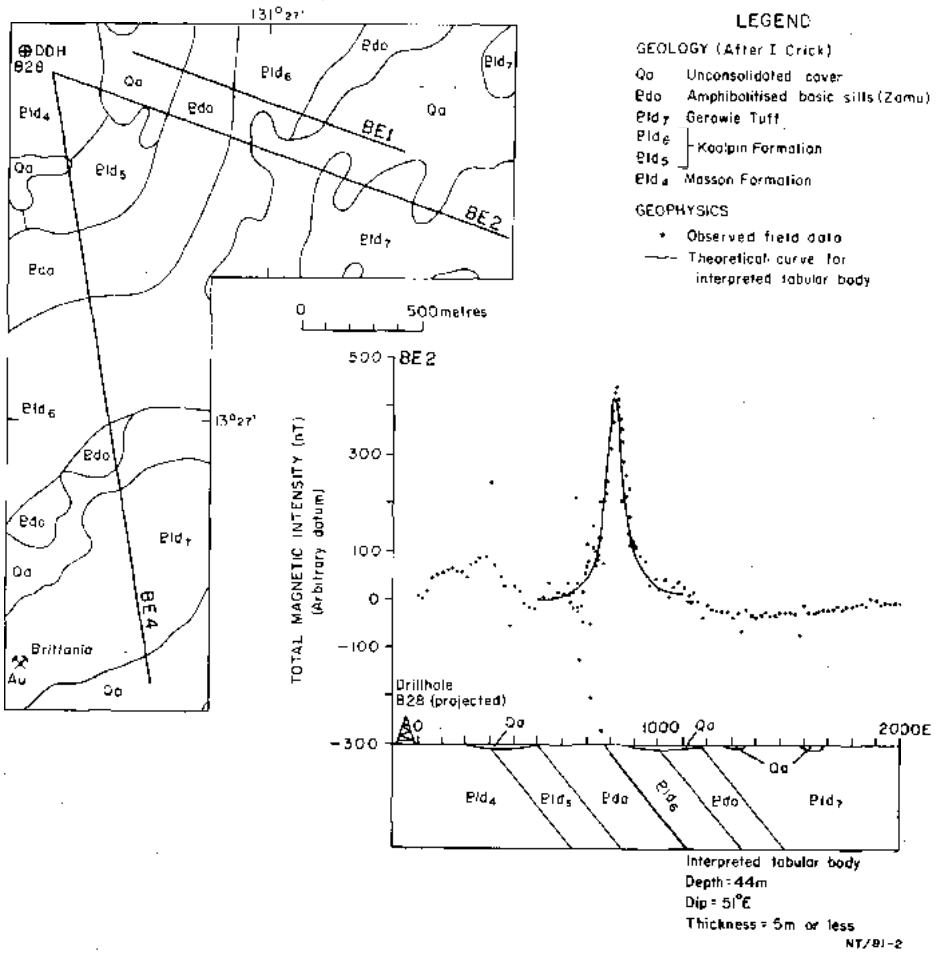


Figure 14. Ground magnetometer profiles and theoretical models across metasediments southeast of the Burnside Granite (after Tucker *et al.*, 1979).

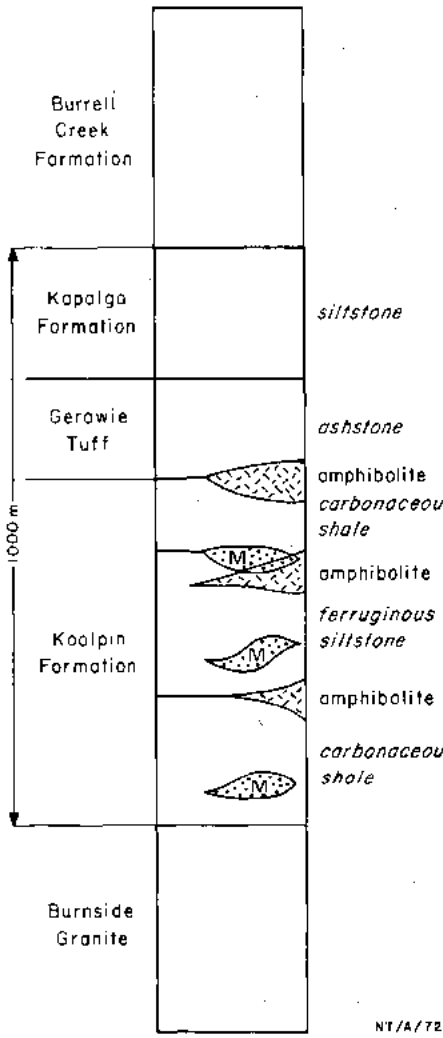


Figure 15. Positions of magnetic sources (m) in Koolpin Formation intruded by Zamu Dolerite (now amphibolitised) in the vicinity of the Burnside Granite.

and Waterhouse Complexes, the Burnside, Prices Springs and Cullen Granites and the Nanambu Complex. However, such an association is not universal as there are granites which are not surrounded by curvilinear magnetic zones, (e.g. the Margaret and Mount Bundey Granites), and west of the Nanambu Complex there are curvilinear zones over sediments which are 30 km away from known granitic rocks.

It seems probable that a combination of favourable lithology and granitic intrusion has produced the largest curvilinear zones in the Geosyncline. However, in the absence of favourable lithology, the effects of granitic intrusions do not markedly increase the magnetic susceptibility of the surrounding metasediments.

Association with metamorphic grade:

Around most of the granitic bodies the metamorphic grade reaches low grade (greenschist facies) or medium grade (amphibolite facies) for widths of up to 10 km, and it is here that high amplitude anomalies are found.

East of the South Alligator River the metamorphic grade is consistently medium grade to high grade, and curvilinear magnetic zones are well developed over Early Proterozoic rocks in this area, even in the absence of granitic bodies.

West of the South Alligator River (about 132°30'E), where the regional metamorphic grade of the Lower Proterozoic sediments is relatively low, magnetic anomalies are not observed away from granitic intrusions.

Association with Zamu Dolerite:

Field mapping and photogeological interpretation indicate that metasediments containing sources of strong magnetic anomalies are frequently intruded by sills of amphibolitised Zamu Dolerite. A preliminary correlation of the airborne magnetic data and geology suggested that the Zamu Dolerite might be the source of the magnetic anomalies. However, interpretation of detailed magnetic data and susceptibility logging of core from drillholes around the Burnside Granite shows that the dolerite usually is relatively non-magnetic in comparison to the enclosing metasediments. These same studies indicate that the source of the magnetic anomalies around the Burnside Granite are thin units within the metasediments which are commonly close to the contact with the sills (Figs. 14 & 15). In some cases magnetic minerals are also found in the sills adjacent to magnetic units in the metasediments.

Other Anomalies

Field investigations of curvilinear zones observed over relatively flat-lying Oenpelli Dolerite and Middle Proterozoic (Carpentarian) volcanic members of the Kombolgie Formation show these zones consist of an irregular pattern of close spaced anomalies. The shape of these anomalies is attributed to the influence of weathering giving lateral variability of the intrinsic bulk magnetic properties of these rocks as indicated by the high susceptibility of Oenpelli Dolerite and other extrusive igneous units recorded in table 3.

SOURCE OF LINEAR MAGNETIC ANOMALIES

Modelling of anomalies recorded by airborne and ground magnetic surveys indicates that the linear anomalies are typical of those produced by thin vertical dykes. Some linear anomalies are negative and can be modelled as vertical dykes only if a strong component of remanent magnetisation is assumed. Modelling indicates the source of the linear anomalies to be near vertical and from 5 to 30m thick.

Holes drilled by the Northern Territory Geological Survey northwest of the Mount Bundey Granite (location 1 in figure 16) to test the source of a northwest-trending negative linear anomaly, and by Geopeko Pty. Ltd. south of Jabiru (location 3) to test the source of an east-west negative anomaly, penetrated dolerite containing magnetite and pyrrhotite respectively. Model depth estimates from ground surveys to the top surface of the sources at locations 1 to 4 were 10-30m, which was consistent with observations that the dolerite dykes do not crop out. The depth of these sources is probably the result of weathering, plus surficial cover.

As indicated in figure 16 both positive and negative anomalies are observed. The positive anomalies appear to result from normally magnetised bodies. However the negative anomalies appear to be the result of remanent magnetisation which is opposite to the present earth's field. While the negative linears are attributed to pyrrhotite or magnetite bearing dolerite the sources of the positive linears are not known but are assumed to be similar.

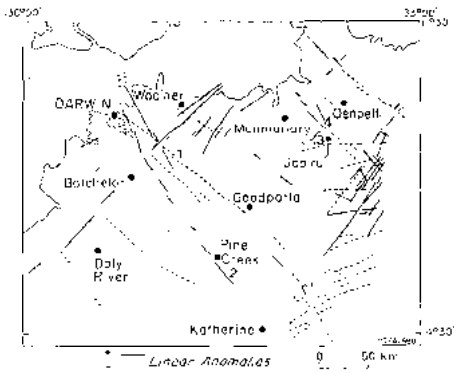
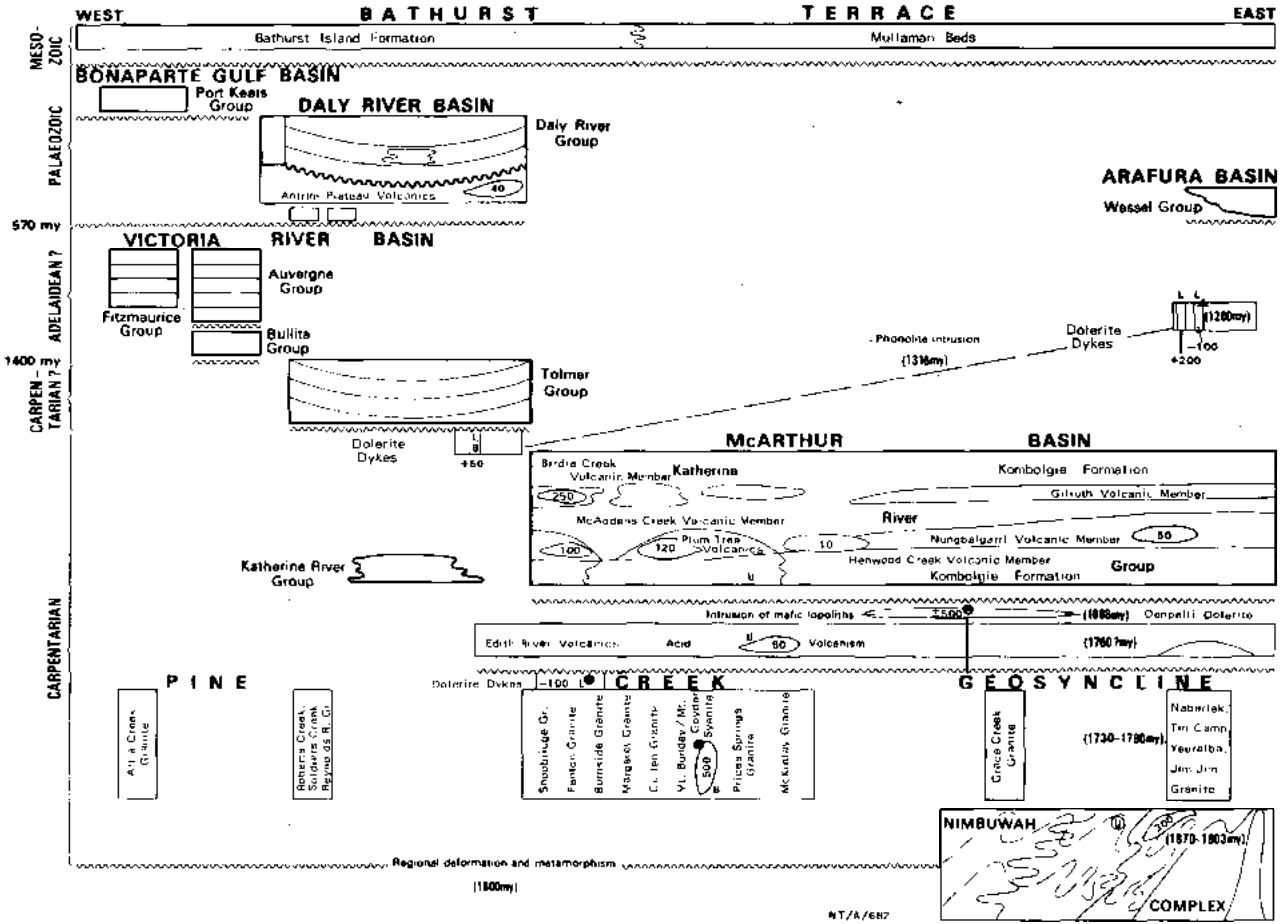


Figure 16. Linear features attributed to dolerite dykes.

At present there is insufficient evidence to indicate the timing and mechanism of remanence acquisition. Field evidence on the age of the dykes is provided in table 4 which suggests that at least some of the dykes may have been emplaced after deposition of the Kombolgie Formation and before deposition of the Tolmer Group. However, this proposition may be in conflict with a radiometric dating of 1370 m.y. (Page, pers. comm.) on a sample of dolerite from an east-west, negative anomaly near Jabiru. According to the stratigraphic table in Needham *et al.* (this volume), an age of 1370 m.y. would postdate the Tolmer Group sediments.

SOURCE OF DIPOLE AND BULLSEYE MAGNETIC ANOMALIES

The adjacent positive-and-negative (dipole) anomalies which these features exhibit in the regional magnetic data suggest the presence of large, relatively uniform and deeply extending plug-like bodies intruded into the near-surface rocks. This proposition is supported by the presence of the magnetic syenite intrusive coincident with the circular-


WEST
BATHURST TERRACE
EAST
MESO-ZOIC
Bathurst Island Formation
Mullaman Beds
BONAPARTE GULF BASIN
Port Keats Group
DALY RIVER BASIN
Daly River Group
Antrim Plateau Volcanics
40
ARAFURA BASIN
Wessel Group
PALAEOZOIC
570 my
VICTORIA RIVER BASIN
Auvergne Group
Fitzmaurice Group
Bullita Group
ADELAIDEAN ?
1400 my
CARPEN-TARIAN ?
Tolmer Group
Dolerite Dykes
+50
Phonolite intrusion
(1316my)
Dolerite Dykes
(1280my)
-100
+200
McARTHUR BASIN
Birdie Creek Volcanic Member
Katherine River Group
Katherine
Kombolgie Formation
250
Gilruth Volcanic Member
McAddens Creek Volcanic Member
River
Plum Tree Volcanics
100
120
10
Nungbalgarri Volcanic Member
50
Henwood Creek Volcanic Member
Kombolgie Formation
Group
Intrusion of mafic lopoliths
+500
(1688my)
Donpalli Dolerite
Edith River Volcanics
Acid Volcanism
60
(1760 ?my)
CARPENTARIAN
PINE CREEK GEOSYNCLINE
Dolerite Dykes
-100
Ami a Creek Granite
Roberts Creek, Soldiers Creek, Reynolds R. Gr.
Snowbirdge Gr.
Fenton Granite
Burnside Granite
Margaret Granite
Cullen Granite
Mt. Burdidy / Mt. Copyton Syenite
500
Prices Springs Granite
McKinlays Granite
Grace Creek Granite
(1730-1790my)
Nabarlek
Ten Camp
Yeuralba
Jim Jim Granite
NIMBUWAH COMPLEX
300
(1870-1803my)
Regional deformation and metamorphism
(1500my)
NT/A/687

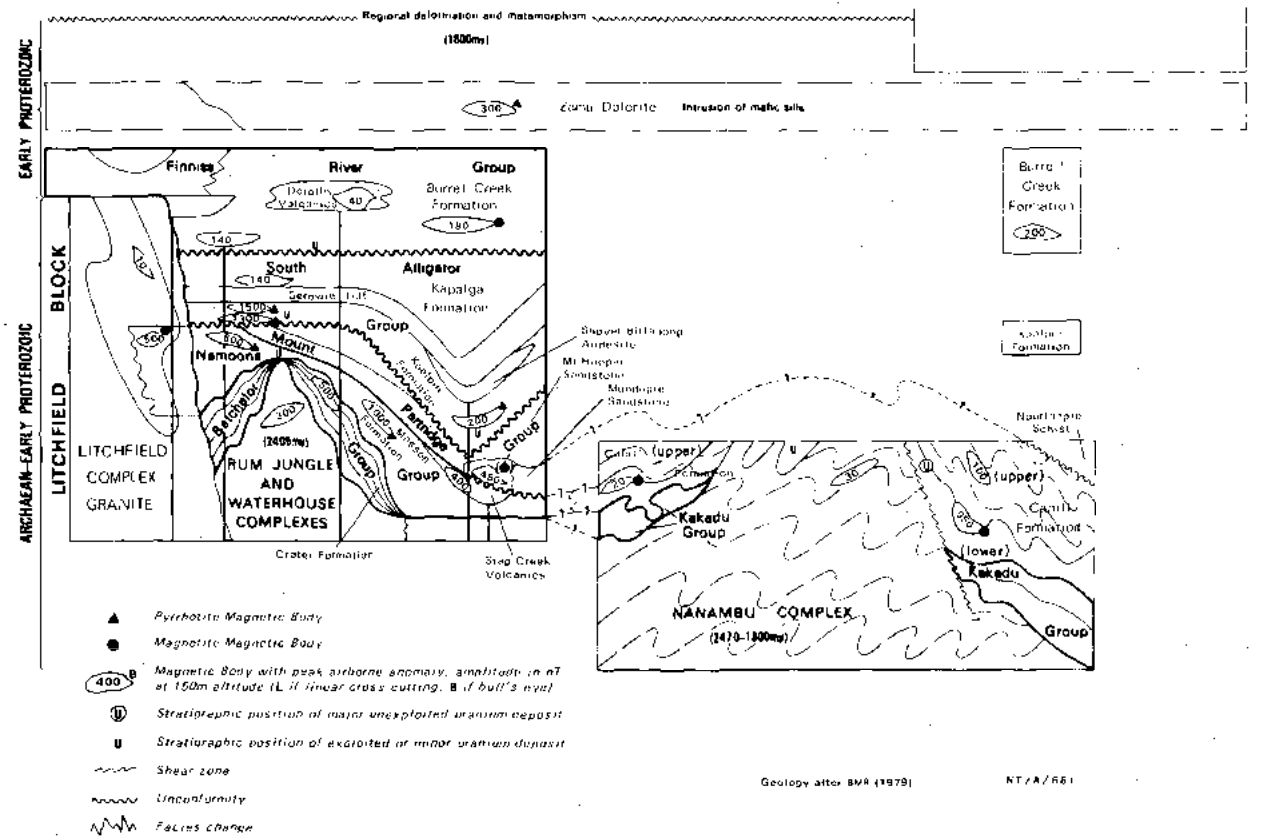


Figure 17. Position of magnetic sources in the stratigraphic column of the Pine Creek Geosyncline.

dipole anomaly near Mount Bundey, and by the presence of a large magnetic mafic plug 15km north of Daly River discussed by Shelley (1969). Some dipole or bullseye anomalies could be caused by unexposed domes of metasediments with magnetic properties similar to those in table 3.

Linear anomaly character	Youngest formations cut by sources	Oldest formations overlying sources
positive sign	Kombolgie Formation in ALLIGATOR RIVER and MT EVELYN	Mullaman Beds (Cretaceous)
	Cullen Granite in PINE CREEK	Tolmer Group in PINE CREEK
negative sign	Kombolgie Formation in ALLIGATOR RIVER and MT EVELYN	(Source near Jabiru dated at 1370 m.y. by K-Ar method, R. Page, pers. comm.)
	Mount Bundey Granite in DARWIN	Mullaman Beds

Table 4. Stratigraphic relationships for sources of linear anomalies.

STRATIGRAPHIC LOCATION OF SHORT WAVELENGTH MAGNETIC SOURCES

A summary of the approximate location of magnetic anomalies in the stratigraphic column of the Pine Creek Geosyncline is shown in figure 17. This figure is based on the stratigraphy of Needham *et al.* (this volume), and indicates the type of magnetic source, the typical maximum anomaly amplitude recorded in the regional data, and if known, the magnetic mineral responsible for the observed response.

Sources in Archaean Rocks

Most Archaean rocks in this area are granitic complexes and have associated low relief zones indicating a low concentration of magnetic minerals. Exceptions are the Rum Jungle Complex, which is overlain by curvilinear zones of up to 300 nT amplitude and the Hermit Creek Metamorphics of the Litchfield Complex which are locally overlain by weak curvilinear zones of 10-20 nT amplitude.

Sources in Early Proterozoic Rocks

The Crater Formation in the Batchelor Group is locally magnetic around the Rum Jungle and Waterhouse Complexes and a peak amplitude of 400 nT is observed over the Formation. In the Namoona Group the Masson Formation is extensively overlain by high amplitude curvilinear zones of amplitude up to 1000 nT. These anomalies are attributed to horizons of 1-5 percent pyrrhotite over thickness of 5-50m in shales and black carbonaceous shales, particularly in the Rum Jungle Embayment and around the northern part of the Cullen Granite. The Stag Creek Volcanics in the South Alligator Valley are in part overlain by a curvilinear zone of amplitude 400 nT. This unit is not magnetic at every place where it is mapped in outcrop. The lower part of the Cahill Formation is overlain by weak curvilinear zones of amplitude 20 nT. A strong curvilinear zone of amplitude 950 nT, occurs over the boundary between the upper and lower parts of the Cahill Formation as geologically mapped, and is attributed to 1-5 percent magnetite over a thickness of 5-50m in pelitic schists. A curvilinear zone of amplitude 100 nT lies over part of the upper Cahill Formation.

A curvilinear zone of amplitude 450 nT lies over the Mt. Hooper Sandstone and is attributed to magnetite in quartzites.

Curvilinear zones of amplitude 500 nT in the general area of the Litchfield Complex, west of Rum Jungle, are attributed to 1-5 percent magnetite which has been intersected over 5-50m in pelitic schists.

The Koolpin Formation of the South Alligator Group is associated with curvilinear zones with multiple sources and amplitude up to 1500 nT. In the Burnside Granitic area these anomalies are attributed to horizons or lenses of 1-5 percent pyrrhotite in 5-50m thick units of shale and black shale, and are often close to intruded sills of Zamu Dolerite containing pyrrhotite. However, the sills are much less magnetic than the enclosing Koolpin Formation. The Kapalga Formation is associated with a curvilinear zone for which the mineralogy of the source is unknown.

Few magnetic anomalies occur over the extensive Burrell Creek Formation of the Finniss River Group. However, to the southwest of the Cullen Granite the formation is associated with curvilinear zones of amplitude up to 180 nT which are attributed to magnetite-bearing mudstones. Also the Dorothy Volcanics within the Burrell Creek Formation are associated with a 40 nT amplitude curvilinear zone.

Sources in Middle Proterozoic (Carpentarian) Rocks

Most of the granites in the Pine Creek Geosyncline are of this age and in the main have a low magnetic relief. However, most are fringed by curvilinear zones associated with the Early Proterozoic sediments surrounding the granites. An exception is a prominent and very broad circular dipole anomaly of 500 nT amplitude which is located over the Mount Bundey Granite/Mount Goyder Syenite bodies. The anomaly is mainly attributed to the magnetic properties of the Syenite, and to a lesser extent to magnetite-bearing blocks of sediments within the Syenite.

The Edith River Volcanics are consistently overlain by curvilinear zones of 50 nT amplitude which are attributed to the magnetite content of these rocks.

The Oenpelli Dolerite extensively intrudes rocks east and northeast of Jabiru, and curvilinear zones of up to 500 nT amplitude are usually observed over these rocks. These zones sometimes exhibit a sign reversal which suggests remanent magnetisation (Horsfall & Wilkes, 1975). The work of Stuart-Smith & Ferguson(1978) indicates that the magnetic response of the dolerite sill is due to a small content of magnetite.

In the Katherine River Group nine thin volcanic members lie in the Kombolgie Formation, and five of these, namely the Birdie Creek, McAddens Creek, Plum Tree, Henwood Creek and Numbulgarri Volcanic members, are associated with curvilinear zones of amplitude as high as 250 nT. The source of these anomalies is believed to be the magnetite content of the volcanic rocks.

Sources in Upper Proterozoic (Adelaidean) Rocks

Sedimentary rocks of this age appear to contain no magnetic sources. However, it is possible that some of the suites of long linear anomalies attributable to dolerite dykes may be of Middle Proterozoic (Carpentarian) to lower Upper Proterozoic (Adelaidean) age, or even younger.

Sources in Palaeozoic and Mesozoic Rocks

With the exception of curvilinear zones of 40 nT amplitude over the Antrim Plateau Volcanics on the western side of the Daly River Basin rocks of these ages exhibit no magnetic response. The anomalies over the Antrim Plateau Volcanics are attributed to the magnetite content of the volcanic rocks.

DISTRIBUTION OF MAGNETIC MINERALS IN EARLY PROTEROZOIC ROCKS

Large prominent curvilinear zones account for the bulk of the features observed in the

regional magnetic data, and these zones mostly occur over the shalier, siltier and more carbonaceous parts of the Early Proterozoic section. In particular large curvilinear zones with peak amplitudes in excess of 500 nT are mainly restricted to associations with the Koolpin and Masson Formations and their equivalents in the eastern and central parts of the Geosyncline. Smaller-amplitude and less prominent magnetic anomalies are fairly widespread over the Lower Proterozoic rocks and appear to be associated with local lithological units which are not easily linked across the Geosyncline.

Field and laboratory studies of the source of most of the strong magnetic anomalies over Lower Proterozoic metasediments below the Finniss River Group suggest a regional zoning of magnetic minerals as shown in figure 18. In the central part of the Geosyncline most of the magnetic anomalies are due to pyrrhotite in shales and carbonaceous shales and slates; others are due to magnetite in siltstones. In the eastern part of the Geosyncline, and in the Litchfield Block to the west the magnetic anomalies are due to magnetite in pelitic schists. Further sampling and analysis of the source of magnetic anomalies is required to confirm this regional zoning.

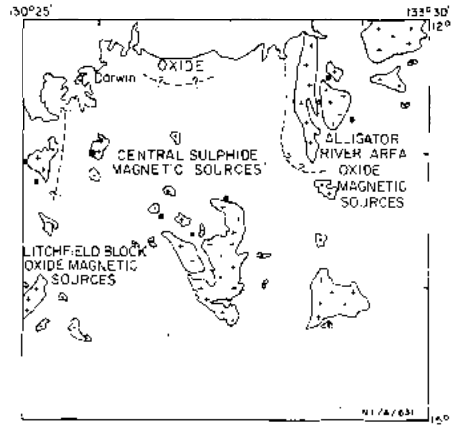


Figure 18. Predominant magnetic iron facies in Early Proterozoic sidements beneath Finnis River Group. Black dots include drill holes.

This apparent distribution of magnetic iron minerals in the Geosyncline suggests several hypotheses regarding the original distribution of iron minerals in, and the subsequent metamorphic history of, the Geosyncline.

The distribution of magnetite and pyrrhotite may be the result of different metamorphic processes throughout the Geosyncline. Magnetite, hematite, pyrrhotite and pyrite are common accessory iron minerals in slates, phyllites, mica schists and gneisses formed by regional metamorphism of elastic sediments; these processes are discussed by Thompson (1972) and French (1973). Magnetite and pyrrhotite are common accessory minerals when the metamorphism is of greenschist or higher grade. Hence, hematite and pyrite contained in shales in the Alligator Rivers area and in the Litchfield Block may have altered to magnetite under the effects of medium to high grade regional metamorphsim as indicated by the presence of mica schists. In the central area pyrite present in shales, phyllites, and carbonaceous shales has altered to pyrrhotite under the effects of the rather lower grades of metamorphism around the granites, whereas hematite present in some sedimentary units appears to have been unaffected.

A second model is equally likely and is based on the proposition that the extensive, strong magnetic anomalies in the Pine Creek Geosyncline may occur at a broadly equivalent stratigraphic level. In this model the present magnetic mineral distribution is a reflection of primary sedimentation and subsequent regional metamorphism. The stratigraphic unit which is now the source of most of the strong magnetic anomalies is equivalent to the Masson Formation and is likely to have been deposited as an iron-sulphide-rich zone in the centre of the Geosyncline and an iron oxide rich zone at the Geosyncline margins. This model suggests that the magnetic schists of the Litchfield Block have had a similar geological history to the Cahill Formation rocks in the Alligator Rivers area. Recent geological studies add some support to this proposition.

The observed magnetic iron distribution can also be explained by a third model in which the different magnetic iron facies may represent different levels in the section and different metamorphic histories. The different levels may have been brought into apparent lateral equivalence by regional deformation and faulting.

The validity of any of the models suggested will have to be tested by further fieldwork, including geological mapping and geophysical studies. However, current geological and geophysical knowledge of the area tends to support the proposition that the present distribution of most of the magnetic mineral concentrations in Lower Proterozoic sediments is a reflection of primary sedimentation of iron-rich minerals in stratigraphic units equivalent to the Koolpin and Masson Formations.

ASSOCIATIONS BETWEEN THE DISTRIBUTION OF URANIUM DEPOSITS AND MAGNETIC ANOMALIES

Ground magnetic mapping, and magnetic susceptibility logging of drillcore at Jabiluka indicates that the deposits are not magnetic targets, even though trace quantities of sulphides are present in the drillcore. However, most of the large deposits including Nabarlek, Ranger, Jabiluka and Koongarra lie within or close to high amplitude curvilinear magnetic zones. These are in the main associated with the Cahill Formation (Needham & Stuart-Smith, 1976), Masson Formation and Koolpin Formation. Hence the extent of high amplitude curvilinear magnetic zones appears to define stratigraphic horizons which are favourable for the concentration of uranium mineralization. Deposits which do not occur in magnetic rocks include the Edith River Deposits within the Cullen Granite, the Adelaide River deposits within the Burrell Creek Formation and deposits within the Nimbuwah Complex northeast of Oenpelli.

Linear anomalies attributable to dolerite dykes in general do not appear to have a direct association with the known uranium deposits. However, they are more common in the eastern part of the Geosyncline where the larger uranium deposits occur. Similarly dykes are also common in the Rum Jungle area.

REGIONAL RADIOMETRIC SURVEYS

A regional view of the radiometric characteristics of the Pine Creek Geosyncline is provided by the BMR reconnaissance airborne spectrometer surveys of the region. The surveys were made with a four-channel spectrometer employing a 3700cm³ (225 cubic inch) NaI detector which was flown at 220km/hr along east-west lines 1500m apart and 150m above ground level. The Alligator Rivers and the northern half of the Mount Evelyn, 1:250 000 sheet areas were flown with an analogue recording system. All other data were recorded digitally and corrections have been made for background, altitude and Compton scattering. The results of these surveys are available from the Australian Government Printer Copy Service, Canberra, in various forms including stacked profiles and contour maps at 1:250 000 scale. An investigation of the results of the analogue spectrometer surveys in the Alligator Rivers and northern Mount Evelyn 1:250 000 sheets areas has been described by Horsfall & Wilkes (1975).

(a) Stripping Ratios	(b) Sensitivity	
$\alpha = 0.6$	7.5 cps (ch 1) ≈ 1μR/h	(on the ground)
$\beta = 0.75$	5.0 cps (ch 2) ≈ 1%k	"
$\gamma = 1.1$	0.55 cps (ch 3) ≈ 1 ppm eU	"
	0.45 cps (ch 4) ≈ 1 ppm eTh	"

Table 5. System characteristics: BMR spectrometer surveys, Pine Creek Geosyncline.

Radiation Intensity	Mean stripped Countrate (Sec)				Stripped Countrate						
					1 Sec Sample				10 Sec Sample		
	T	K	U	Th	T	K	U	Th	T	K	U
High (Rum Jungle Complex)	160	18	6	15	10	55	90	29	3	17	28
Medium (Koolpin Formation)	100	16	6	8	13	56	80	35	4	18	25
Low (Kombolgie Formation)	15	5	2	2	64	134	185	120	21	42	60

Table 6. Typical Counting Statistics for BMR spectrometer surveys, Pine Creek Geosyncline.

Detailed or quantitative interpretation of the BMR spectrometer data is not possible owing to the small detector used and the lack of quantitative calibration data. An estimate of the calibration constants for the BMR spectrometer system was obtained by theoretical calculations and a comparison of airborne results with chemical analyses of rock samples. The calibration constants of the system obtained by these comparisons and as applied in standard stripping formulae (Wilkes, 1979), are shown in table 5. Note, however, that these estimates are subject to uncertainties which will preclude quantitative interpretation of radio-elements concentrations, and may introduce substantial errors into the qualitative interpretation if the relative concentration of radio-elements changes significantly. The small detector results in low count-rates. Hence, the statistical accuracy of data collected over small areas is poor. The spectrometer data are most useful in a regional reconnaissance role when large blocks of data can be summed together to produce a large number of counts. The statistical accuracy of the spectrometer data over typical rocks in the Pine Creek Geosyncline as a function of counting time is indicated in table 6. Note that meaningful results in the uranium channel are obtained only for counting times in excess of 100 seconds or approximately 6km of traverse.

REGIONAL RADIOMETRIC CHARACTERISTICS

A regional view of the radiometric characteristics is provided by the BMR total count survey of the area which is shown in figure 19 as a photo reduction of the 1:500 000 scale contour map which accompanies this volume (BMR, 1979d).

A comparison of the average count-rates observed over different lithologies and stratigraphic units is shown in table 7 and suggests that characteristics of the radio-element geology of the Geosyncline and surrounding regions are reflected in the total-count data. There appears to be three distinct levels of count-rate which broadly correspond with different types or rocks. It is interesting to note that the average count-rate of approximately 100 cps corresponds to an exposure rate of some 13 R/hr which is a relatively high figure for a region composed mainly of poorly exposed metasediments.

Low Count Zones

Approximately 40 percent of the survey area has a low count-rate of less than 50 counts per second. In general these low count areas are restricted to regions where rocks of the Pine Creek Geosyncline are covered by younger sediments as in indicated in figure 20.

Standard Deviation %									Chemical Assays		
	100 Sec Sample				1000 Sec Sample				K	U	Th
Th	T	K	U	Th	T	K	U	Th	%	ppm	ppm
9	0,9	3	9	2.9	0.3	1.7	2,8	0.9	5,2	11	47
14	1.3	6	8	3.5	0.4	1.8	2.5	1.4	1.8	7	9
38	6	13	18	12	2.1	4	6	3.8	0.03	7	10

Table 6 continued.

In the east, low-count zones are observed over the exposed sandstones of the McArthur Basin, especially the Kombolgie Formation. In the south, low-count zones are observed over the partly exposed arenaceous and calcareous sediments of the Daly River Basin and the Victoria River Basin. Low-count zones are observed over the Mesozoic sediments which in places cap the area, and over large areas of semi-tidal mud flats in the west and north. The most consistent and low count-rates are observed over the Kombolgie Formation.

Medium Count Zones

Approximately 50 percent of the area has a count-rate of between 50 and 150 counts per second and of this, perhaps two-thirds of the area has a count-rate between 50 and 100.

An extensive medium count zone is observed over most of the area underlain by outcropping and subcropping Early Proterozoic metasediments of the Pine Creek Geosyncline. Closure patterns are frequently elongate and appear to parallel geological strike, or in some places major water courses. The elongate zones are best developed over the more quartz-rich metasediments such as the Burrell Creek Formation. Over shalier metasediments such as the Koolpin Formation, the elongate zones are less well developed:- probably a result of the relatively deep weathering of these rocks. Count-rates observed over reasonably exposed Early Proterozoic rocks are similar to those observed over regions where Early Proterozoic rocks are covered by various weathering products. Hence, the medium-count zones appear to be due to the intrinsic radio-element concentration of Early Proterozoic metasediments and the weathering products derived from them. No detailed analyses of the spectral signatures of bedrock and residual soil is possible with the BMR regional data. However, it seems probable that within the medium count zones the spectral signature of the underlying bedrock may have been preserved in overlying residual soils. Ground surveys using surface and downhole spectrometry support this suggestion (A. Mutton, pers. comm.).

Other medium-count zones are observed over Middle Proterozoic (Carpentarian) felsic volcanics, the Edith River Volcanics, and some of the Archaean to Proterozoic aged granites and metamorphics.

High Count Zones

Discrete, well defined zones with a count-rate of greater than 150 cps are observed throughout the region and with few exceptions are located over Middle Proterozoic (Carpentarian) granites. Some of these granites are abnormally radioactive and count-rates

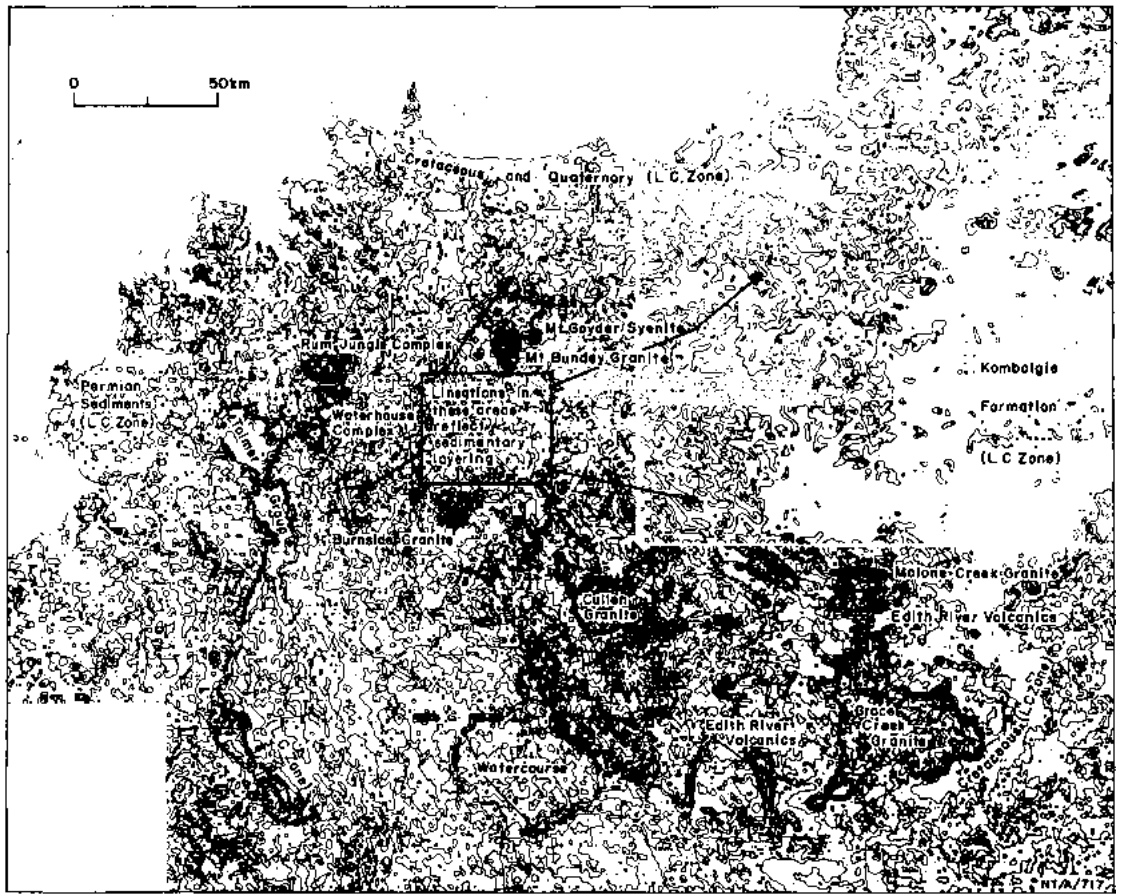


Figure 19. Total count radiometric contours and selected features referred to in the text.

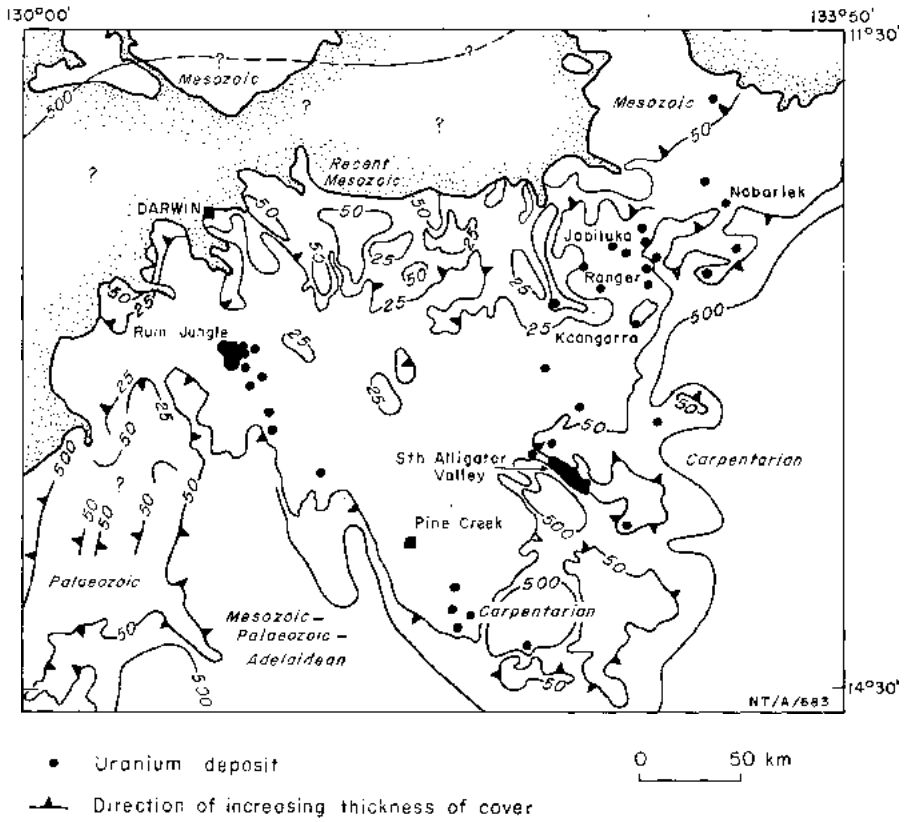


Figure 20. Thickness of cover to Pine Creek Geosyncline rocks. Contours in metres.

as high as 400 are locally recorded over the Mount Goyder Syenite, and Malone Creek Granite.

RADIO-ELEMENT CONCENTRATION OF ROCKS IN THE GEOSYNCLINE

An indication of the relative concentration of radio-elements in the rocks of the Pine Creek Geosyncline is provided by a comparison of mean stripped count-rates accumulated over rock units which are reasonably well exposed over large areas. The mean stripped count-rates with chemical analyses of rock units of the Geosyncline are compared with chemical analyses of rock samples in table 8. The spectrometer results shown in this table are for data accumulated for over 1000 seconds or approximately 60km of traverse. The geochemical data have been extracted from Heier & Rhodes (1966); Ferguson & Winer (this volume); Ferguson, Chappell & Goleby (this volume); and Rossiter & Ferguson (this volume).

The spectrometer and chemical data are in reasonable agreement with regard to the relative concentration of radioelements in the rocks listed in table 8. Furthermore, estimates of radioelement concentration based on the spectrometer sensitivity characteristics listed in table 5 also show a reasonable agreement with the chemical data.

As noted for the total count data, the stripped count-rates observed over the region

Age	Generalised rock systems	Total Count Rates (per sec) - Typical Means		
		Low	Medium	High
Adelaidean - Recent (Upper Proterozoic)	Black soil plains	50		
	Cretaceous sediments	35		
	Permian sediments	35		
	Lower Palaeozoic-sediments		90	
	-mafic volcanics		65	
	Adelaidean to Carpentarian sediments in the west of the area	40		
Carpentarian (Middle Proterozoic)	Sediments - mainly sandstones	25		
	Volcanics - mainly felsic		140	
	Granites (hot)			300
	Granites			175
Early Proterozoic and older	Migmatite and anatectic granite		75	
	Low grade metasediments		85	
	Folded medium grade metamorphics		85	
	Archaean to Proterozoic granites and metamorphics		145	

Table 7. Mean Total Count response over generalised rock systems classified by age.

appear to have different characteristics depending primarily on the age and lithology of the rocks. The results suggest that the granitic rocks of the Geosyncline are enriched in all radio-elements relative to generally accepted levels for granites (Clark *et al.*, 1966). Similarly the Early Proterozoic metasediments appear to be enriched in uranium and thorium relative to generally accepted concentration levels for arenaceous and argillaceous sediments. The Middle Proterozoic (Carpentarian) granites are possibly distinguishable from the Archaean granitic complexes on the basis of their apparently higher potassium, uranium and thorium concentrations and perhaps lower uranium to thorium ratio. The Early Proterozoic metasediments appear to be enriched in uranium relative to thorium compared to the Archaean or Middle Proterozoic (Carpentarian) granitic rocks. The high uranium to thorium ratios observed over the black soil areas may indicate a scavenging of uranium by humic material. The high total count readings observed over the Middle Proterozoic (Carpentarian) granites appears to be due to the substantial concentration of potassium rather than locally abnormal concentrations of uranium or thorium. The very low counts

Age	Rock Unit	Lithology	Mean Stripped Countrate (CPS)					Chemical Assay		
			T	K	U	Th	U:Th	K%	U ppm	Th ppm
Q		black soil	75	12	4	6	0,7	-	-	-
Mesozoic		sandstone and shale	35	3	3	6	0,5	-	-	-
Upper Proterozoic	Depot Creek Sandstone	sandstone	50	9	3	3	1.0	-	-	-
	Kombolgie	quartzite	15	5	2	2	1.0	0.03	7	10
?Middle Proterozoic	Grace Creek Granite	granite	160	26	8	12	0.8	-	-	-
	Malone Creek Granite	granite	275	29	14	26	0.5	8.0	23	84
	Burnside Granite	granite	175	39	8	14	0.6	5	18	48
	Cullen Granite (NE)	granite	270	39	6.5	21	0.3	5.0	10	40
	Cullen Granite (S)	granite	175	25	6	13	0.5	5.0	10	40
Early Proterozoic	Burrell Creek	siltstone	125	24	5	7	0.7	3.6	5	23
	Koolpin	shales and black shales	100	16	6	8	0.8	1.8	7	9
	Masson	shales and black shales	100	16	5	7	0.7	3.5	15	13
?Archaean	Litchfield Complex	granitic	65	8	3	5	0.6	4.0	8.6	6.6
	Hermit Creek Metamorphics	meta-sediments	80	12	4	6	0.7	-	-	-
	Waterhouse Complex	granitic	120	14	4	10	0.4	4.9	13	44
	Rum Jungle Complex	granitic	160	18	6	15	0.4	5.2	11	47

Table 8. Some examples of mean stripped count-rates and chemical analyses for selected rock units, Pine Creek Geosyncline.

over the Kombolgie Formation appear to be due to an overall low radioelement concentration but particularly a very low potassium concentration.

ASSOCIATIONS BETWEEN THE DISTRIBUTION OF URANIUM DEPOSITS AND RADIOMETRIC ANOMALIES

Airborne gamma ray spectrometry has been the principal prospecting tool used to explore for uranium in the Pine Creek Geosyncline and large anomalies detected over Nabarlek (Tipper & Lawrence, 1972), Ranger (Ryan, 1972) and Koongarra (Foy & Pedersen, 1975) were a direct indication of the presence of these deposits. Smaller ground and airborne radiometric anomalies have been attributed to some of the smaller or less well exposed deposits in the region. BMR surveys were flown with a line spacing, system

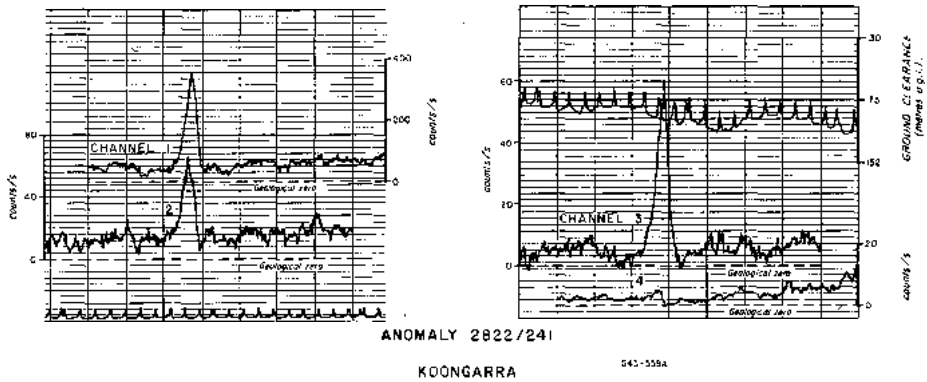


Figure 21. Analogue radiometric records across Koongarra uranium deposit (after Wilkes, 1979).

sensitivity and altitude appropriate to regional geological investigation and not detailed exploration. However, several known uranium deposits were directly overflown by BMR surveys and high uranium to thorium ratios were recorded (Fig. 21). In general the anomalies attributed to uranium mineralization were recorded on single flight lines and extensive radioactive haloes could not be recognised in the regional data. However, the area containing the Ranger deposit produces radiometric anomalies on three flight lines, and the area around Rum Jungle open cut mines which is now heavily contaminated produces radiometric anomalies of large extent.

The Koolpin and Cahill Formation, which host most of the known uranium deposits in the Geosyncline cannot be distinguished from other Early Proterozoic rock units on the basis of the BMR regional spectrometric data. However, a more sensitive and detailed spectrometer survey may reveal more subtle characteristics which might be used as aids to exploration.

ACKNOWLEDGEMENTS

This study was aided by discussions with colleagues including Messrs I.A. Crick, P.G. Stuart-Smith, and R.S. Needham of the BMR's Pine Creek Geosyncline Geological Party, and with exploration company personnel especially Messrs G.S. Eupene and J. Goulevitch of Geopeko Limited, and G. Steemson and D.R. Kennedy of C.R.A. Exploration Pty. Limited. The rock physical property study was aided by the willing provision of drillcores by various exploration companies including Geopeko, C.R.A.E., and Pancontinental.

Considerable help in the study was provided by Mr. A.S. Murray of B.M.R. who produced the various gravity maps by computer from the Australian Gravity Data Bank, and in addition spent considerable time experimenting with methodology of data manipulation including derivatives of several orders and polynominal surfaces, and residuals.

The work of the B.M.R. cartographic group in preparing the figures and plates for this paper is gratefully acknowledged.

This paper is published by permission of the Director, Bureau of Mineral Resources, Geology and Geophysics, Canberra, Australia.

REFERENCES

Anfiloff, W., Barlow, B.C., Murray, A.S , Denham, D. & Sandford, R., 1976: Compilation and production of the 1976 Gravity Map of Australia. *BMR J. Aust. Geol. Geophys. 1*, 273-276.

BMR, 1979a: Pine Creek Geosyncline Solid Geology Map, 1:500,000 scale. *Bureau of Mineral Resources, Geology and Geophysics, Australia.*

BMR, 1979b: Pine Creek Geosyncline Bouguer Anomaly contours, 1:500,000 scale. *Bureau of Mineral Resources, Geology and Geophysics, Australia.*

BMR, 1979c: Pine Creek Geosyncline Total Magnetic Intensity contours, 1:500,000 scale. *Bureau of Mineral Resources, Geology and Geophysics, Australia.*

BMR, 1979d: Pine Creek Geosyncline Total Count Radiometric contours, 1:500,000 scale. *Bureau of Mineral Resources, Geology and Geophysics, Australia.*

Bryan, R., 1962: Lower Proterozoic basic intrusive rocks of the Katherine-Darwin ara, Northern Territory. *Rec. Bur. Miner. Resour. Geol. Geophys. Aust., 1962/7* (unpubl.).
Clark, S.P., Peterman, Z.E. & Heier, K.S., 1966: Abundances of uranium, thorium and potassium. *in, Handbook of Physical Constants. Mem. geol. Soc. Am., 47.*
Crick, I.H., 1976: Shallow stratigraphic drilling in the Burnside Granite area, Batchelor 1:100,000 Sheet, Northern Territory, 1975. *Rec. Bur. Miner. Resour. Geol. Geophys. Aust , 1976/101* (unpubl.).
Ewers, G.R., & Scott, P.A., 1977: Geochemistry of the Cullen Granite, Northern Territory. *BMR J. Aust. Geol. Geophys., 2,* 165-176.
Ferguson, John, this volume: Metamorphism in the Pine Creek Geosyncline and its bearing on stratigraphic correlations. *Proceedings of the International Uranium Symposium on the Pine Creek Geosyncline.*
Ferguson, John, Chappell, B.W. & Goleby, A.B., this volume: Granitoids in the Pine Creek Geosyncline. *Proceedings of the International Uranium Symposium on the Pine Creek Geosyncline.*
Ferguson, J. & Needham, R.S., 1978: The Zamu Dolerite: a Lower Proterozoic continental tholeiitic-suite from the Northern Territory, Australia. *J. geol. Soc. Aust., 25,* 309-322.
Ferguson, John & Winer, Paul, this volume: Pine Creek Geosyncline: Statistical treatment of whole-rock chemical data. *Proceedings of the International Uranium Symposium on the Pine Creek Geosyncline.*
Finlayson, D.M., 1973: Isomagnetic maps of the Australian region for epoch 1970.0. *Rep. Bur. Miner. Resour. Geol. Geophys. Aust., 159.*
Foy, M.F. & Pedersen, C.P., 1975: Koongarra uranium deposit. *in* (ed. C.L. Knight) *Economic Geology of Australia and Papua New Guinea, Australas. Inst. Min. Metall., Monograph Series No. 5, 1. Metals,* 317-321.
Fraser, W.J., 1978: EL610 Waterhouse, Rum Jungle, N.T. Final Report. *C.R.A. Exploration Pty. Ltd. Report No. 9408* (unpubl.).
French, B.M., 1973: Mineral assemblages in diagenetic and low grade metamorphic iron formation. *Econ. Geol., 68,* 1063-1074.
Gerula, W.J., 1979: Airborne magnetic and radiometric surveys up to December 1977. *Rep. Bur. Miner. Resour. Geol. Geophys. Aust., 204*
Heier, K.S. & Rhodes, J.M., 1966: Thorium, uranium and potassium concentrations in granites and gneisses of the Rum Jungle Complex, Northern Territory, Australia. *Econ. Geol., 61,* 563-571.
Horsfall, K.R. & Wilkes, P.G., 1975: Aeromagnetic and radiometric survey of Cobourg Peninsula, Alligator River and Mount Evelyn (part) 1:250 000 Sheet areas Northern Territory 1971-1972. *Rec. Bur. Miner. Resour. Geol. Geophys. Aust., 1975/89* (unpubl.).
Major, J.A., 1977: Rum Jungle Area Gravity Survey Northern Territory 1974. *Rec. Bur. Miner. Resour. Geol. Geophys. Aust., 1977/9* (unpubl.).
Muggeridge, G.D., 1977: EL610 Waterhouse, Rum Jungle N.T. Exploration of the Waterhouse No. 2 and Mt Minza Prospects April 1976-December 1976. *C.R.A. Exploration Pty. Ltd. Report 8778* (unpubl.).
Murray, A.S., 1974: The Australian national gravity repository computer system. *Rec. Bur. Miner. Resour Geol. Geophys. Aust., 1974/68* (unpubl.).
Needham, R.S., Crick, I.H. & Stuart-Smith, P.G., this volume: Regional Geology of the Pine Creek Geosyncline. *Proceedings of the International Uranium Symposium on the Pine Creek Geosyncline.*
Needham, R.S. & Sturart-Smith, P.G., 1976: The Cahill Formation — host to uranium deposits in the Alligator Rivers Uranium Field, Australia. *BMR J. Aust. Geol. Geophys., 1,* 321-333.
Price, D.G., 1974: 1973 Exploration for base metals and uranuim, CR1541, EL 71 Finnis River, NT, EL 897 Mt. Tolmer NT. *The Broken Hill Proprietary Company Limited Australia* (unpubl.).
Prichard, C.E., 1964: Progress report on diamond drilling, Rum Jungle area 1964. *Rec. Bur. Miner. Resour. Geol. Geophys. Aust., 1964/7* (unpubl.).
Rossiter, A.G. & Ferguson, John, this volume: A Proterozoic tectonic model for northern Australia and its economic implications. *Proceedings of the International Uranium Symposium on the Pine Creek Geosyncline.*
Ryan, G.R., 1972: Ranger 1: a case history. *in* (eds. S.H.U. Bowie, M. Davis & D. Ostle), *Preceedings of a NATO-sponsored Advanced Study Institute on Methods of Prospecting for Uranium Minerals, London. Inst. Min. Metall.,* 296-300.
Shelley, E.P., 1969: Daly River detailed aeromagnetic survey, Northern Territory 1966. *Rep. Bur. Miner. Resour. Geol. Geophys. Aust., 139.*
Simpson, C.J., Huntington, J.F., Leishman, J. & Green, A.A., this volume: A study of the Pine Creek Geosyncline using integrated Landsat and aeromagnetic data. *Proceedings of the International Uranium Symposium on the Pine Creek Geosyncline.*
Smart, P.G., Wilkes, P.G., Needham, R.S. & Watchman, A.L., 1975: Geology and geophysics of the Alligator Rivers Region. *in* (ed. C.L. Knight) *Economic Geology of Australia and Papua New Guinea, Australas. Inst. Min Metall., Monograph Series No. 5, 1. Metals,* 285-301.
Stephensson, O. & Johnson, K., 1976: Granite diapirisms in the Rum Jungle area, Northern Australia. *Precambrian Research, 3,* 159-185.
Stuart-Smith, P.G., 1977: Shallow stratigraphic drilling in the Kapalga 1:100,000 sheet area, Alligator Rivers Region N.T., 1974-6. *Rec. Bur. Miner. Resour. Geol. Geophys. Aust., 1977/53* (unpubl.).
Stuart-Smith, P.G. & Ferguson, John, 1978: The Oenpelli Dolerite - a Precambrian continental tholeiitic suite from the Northern Territory, Australia. *BMR J. Aust. Geol. Geophys., 3,* 125-133.
Thompson, J.B., 1972: Oxides and sulphides in regional metamorphism of pelitic schists. *24th Int. geol. Congr., Abstracts, Section 10,* 27-35.

Tipper, D.P. & Lawrence, G., 1972: The Nabarlek area, Arnhemland Australia, a case history. *in* (eds. S.H.U. Bowie, M. Davis & D. Ostle) *Proceedings of a NATO-sponsored Advanced Study Institute on Methods of Prospecting for Uranium Minerals, London. Inst. Min. Metall.*, 301-304.

Tucker, D.H., Hone, I.G., Sampath, N. & Ewers, G.R., 1979: Geological and Physical Characteristics of Some Magnetic Sources in Lower Proterozoic Metasediments Pine Creek Geosyncline N.T. *Bull. of the Australian Society of Exploration Geophysicists, 10*, 54-66.

Tucker, D.H., in prep: Rock physical property data for the Pine Creek Geosyncline N.T. *Rep. Bur. Miner. Resour. Geol. Geophys. Aust.*

Wilkes, P.G., 1979: Acquisition, processing, and interpretation of airborne gamma-ray spectrometry data. *Rep. Bur. Miner. Resour. Geol. Geophys. Aust.*, 186.

Wronski, E.B., 1978: Gravity Survey, Alligator River 1:250 000 Sheet Area, Northern Territory, 1972-73. *Rec. Bur. Miner. Resour. Geol. Geophys. Aust., 1978/9* (unpubl.).

A STUDY OF THE PINE CREEK GEOSYNCLINE USING INTEGRATED LANDSAT AND AEROMAGNETIC DATA

C.J. Simpson,[1] J.F. Huntington,[2] J. Leishman[2] and A.A. Green[2]

1. Bureau of Mineral Resources, P.O. Box 378, Canberra City, A.C.T. 2601., Australia.
2. CSIRO Division of Mineral Physics, P.O. Box 136, North Ryde, N.S.W. 2113., Australia.

ABSTRACT

Computer-enhanced Landsat imagery with newly developed Landsat/Stereo-Magnetics imagery has been used to map lineaments in the Pine Creek Geosyncline. Comparison of lineaments with the distinct aeromagnetic lineaments caused by dolerite dykes suggests that the dykes are of different ages and are associated with different fracture sets. Landsat lineaments were combined with mapped faults, veins, and magnetic lineaments to provide a total fracture distribution for the geosyncline. Six major fracture directions were identified and some new structural zones defined, the most intensive being a northwesterly zone from Katherine to Noonamah. Statistical analysis of uranium, and gold mineralization suggests that there is a non-random relationship between both types of occurrences and the total fracture distribution. Though further refinements to the study methods are indicated the techniques have application to exploration strategy in the Geosyncline.

INTRODUCTION

Landsat satellite imagery of the Pine Creek Geosyncline (PCG) was studied in an attempt to extract additional structural information. Enhanced Landsat scenes used in the study were specially processed by the Commonwealth Scientific and Industrial Research Organisation (CSIRO) Division of Mineral Physics. In addition, CSIRO developed aeromagnetic data products in photographic form were evaluated to assess their usefulness as photo-interpretation aids.

During the study, conventional airphoto mosaics and geophysical data were examined in an endeavour to substantiate features detected on Landsat. The geophysical data included, for the whole PCG, total magnetic intensity contour maps, Bouguer anomaly contour maps, and total count radiometric contour maps. The geophysical data were used specifically to examine their responses to known structures, and thus to assist the interpretation of structural data from Landsat. Detailed interpretations of the geophysical data were not attempted.

DATA PRODUCTS USED

Two types of Landsat imagery were generated for the study. For the scenes identified on figure 1 digitally enhanced imagery was produced directly from NASA Landsat computer-compatible tapes. Techniques of Landsat digital enhancement to increase image detail have been discussed by Simpson (1978), and the various methods employed by CSIRO Division of Mineral Physics have been reported by Green *et al.* (1978). After processing, panchromatic prints were produced at various scales between 1:1 140 000 and 1:78 000.

In addition to the individual Landsat scenes a digital Landsat mosaic of the two central images over the PCG was prepared from two consecutive scenes acquired on the same day. The scenes were enhanced and joined by computer to form a continuous mosaic with consistent tonal ranges.

Two types of aeromagnetic products were prepared:

1) Grey tone images of the total magnetic field were derived from the Bureau of Mineral Resources, Geology and Geophysics (BMR) digital data. This was done by resampling, geometric correction, and suitable enhancement by the contrast modification techniques typically used for digital Landsat data. Light tones in these images reflect higher

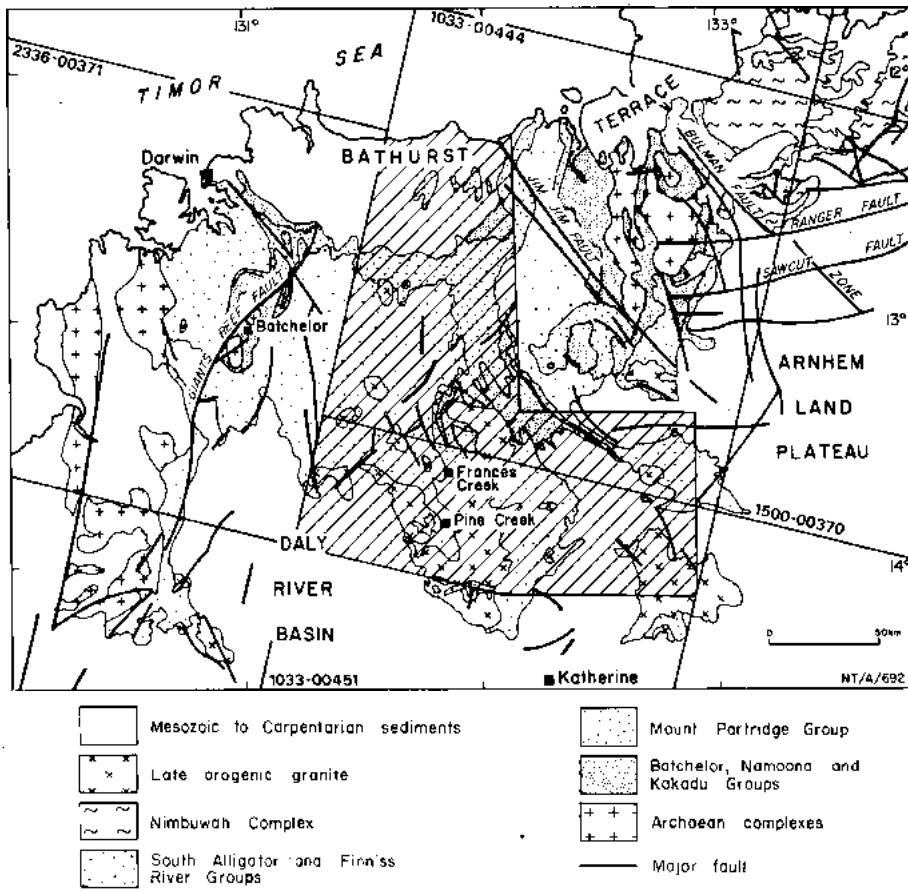


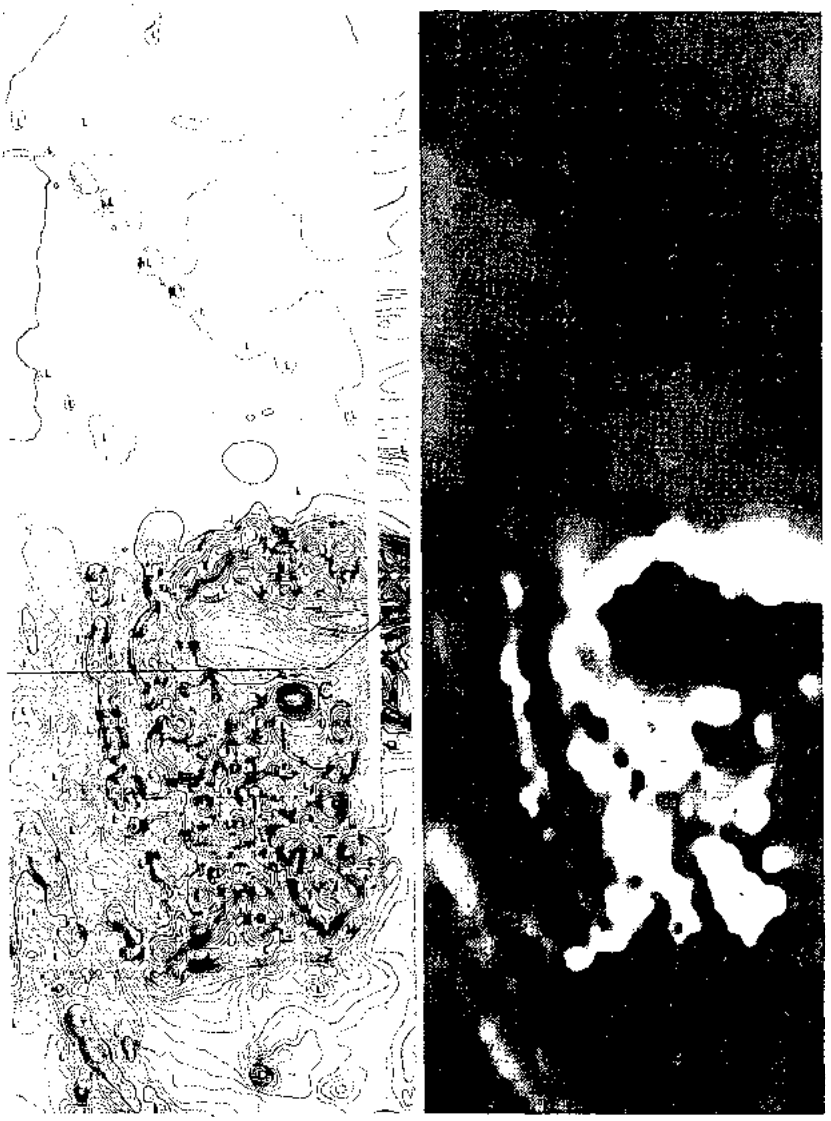
Figure 1. Generalized geology of the Pine Creek Geosyncline (after Stuart-Smith *et al.*, this volume). Landsat scenes used are identified. Area covered by Landsat/Stereo-Magnetics imagery is hachured.

magnetic intensities. Figure 2(a) illustrates conventional total magnetic intensity contours (BMR, 1979b) for that part of the PCG within latitudes 12°53′S and 13°44′S, and longitudes 131°42′E and 132°01′E. Figure 2(b) is a 'magnetics image' of the same data, enhanced to reveal low amplitude features such as the subtle north-trending grey tones in the top-left corner. These represent magnetic responses from specific rock units, including carbonaceous and ferruginous shale with algal carbonate, banded iron formation, jaspilite and tuff. Such features are not apparent on the more commonly used contoured aeromagnetic data, but are identifiable in the stacked profiles. Different contrast enhancement methods can be applied to such 'magnetics images' to assist in interpretation of data, in stacked profile form, of various amplitudes.

2) Merged Landsat/Stereo-Magnetics (LSM) images. Figure 3 shows part of a LSM image covering the same area as figure 2.

In the preparation of LSM images each picture element of a single Landsat band is individually shifted, parallel to the scan direction, by an amount proportional to the total magnetic intensity value at that point. When viewed stereoscopically with an ordinary

unshifted image, the introduced parallax results in a three-dimensional model in which magnetic highs appear as hills and lows as valleys (Fig. 3). The merging of Landsat and aeromagnetic data has been further discussed by Huntington & Green (in press).



(a) (b)

Figure 2. Example of areomagnetic contours (a) from BMR 1979b, and aeromagnetics image (b) for the area contained by 12°53'S-13°44'S and 131°42'E-132°01'E. (Approximate scale 1:600 000).

'Magnetics images' and LSM images were available only for that part of the PCG covered by digital aeromagnetic data (Fig. 1). Conventional contour maps based on digital and analog magnetic data were consulted throughout the study.

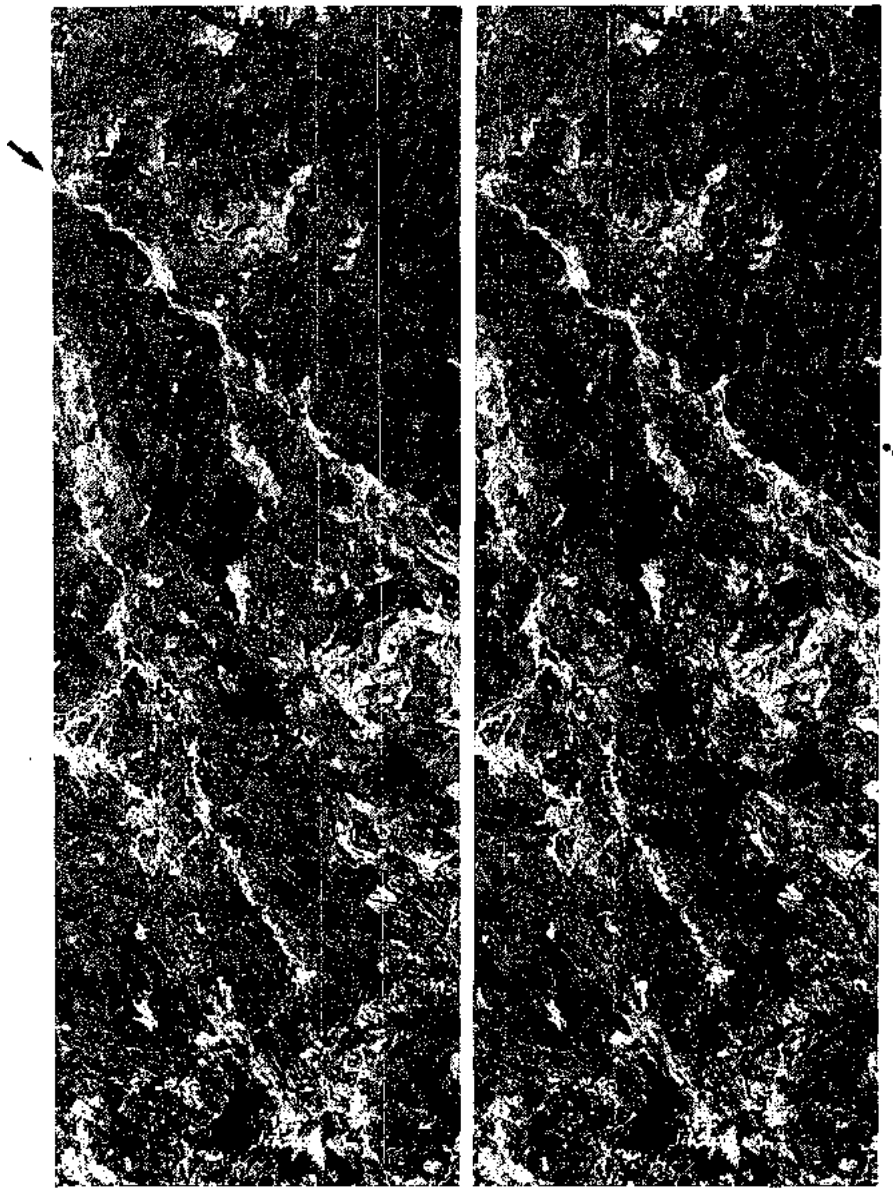


Figure 3. Stereoscopic pair for the area shown in figure 2 illustrating part of a Landsat/Stereo-Magnetics (LSM) image. (Total magnetic intensity shown in three dimensions). Arrow indicates Mary River, dots show trend of linear magnetic low (refer Fig. 2).

Sets	Azimuth		Significant zones and features
1	135-155	p-q	(Noonamah-Katherine Zone);
		r-s	(extends into South Alligator Valley);
		t-u	(Jim Jim Fault);
		v-w	(Bulman Fault Zone).
2	160-175	x-y	(Mount Goyder - Pine Creek)
3	090-105	n-o	(Mount Shoobridge-Sleisbeck lineament);
		k-m.	
4	035-060	e-f	(Giants Reef Fault Zone-north);
		g-h	(incorporates Grove Hill cross flexure).
5	010-025	a-b	(Giants Reef Fault Zone-south);
		c-d.	
6	065-085	i-j	

Table 1. Major fracture sets of the PCG.

Other orthogonal pairs may also be present within the PCG. Thus in table 1, set 1 might be paired with 4; 2 with 6; and 3 with 5.

Lineament-aeromagnetic relationships

Comparison of independently determined Landsat lineaments and the magnetic lineaments* displayed on the 1:500 000 solid geology map of the PCG (BMR, 1979a) showed that 40% of the magnetic lineaments had some coincident Landsat expression (Class 1). Furthermore, the coincident lineaments occur in well defined groupings. Linear positive magnetic anomalies (Tucker *et al.*, this volume) trending approximately 150° were almost all detected in the Landsat analysis (Fig. 8), as were those magnetic lineaments with trends between 30-40° throughout the eastern part of the Geosyncline. However, linear negative magnetic anomalies with trends of about 130°, or linear positive anomalies with trends of about 40°, in the west of the Geosyncline, were not detected (Class 2). In the southeast corner of figure 8, a group of magnetic lineaments with trends between 60°-70°, showed poor Landsat expression. Combination of Classes 1 and 3 delineates a major 20-25 km wide zone, extending across the centre of the Geosyncline at about 150°, through Noonamah and Katherine (Fig. 8; Fig. 7. p-q). Gravity data (BMR, 1979d), shear zones, dykes and the alignment of minor folds (BMR, 1979a), distributed along this zone all support the belief that it is a major structural feature, here designated the 'Noonamah-Katherine Lineament Zone'.

A zone of Class 2 Lineaments (without Class 3 extensions) trending at about 130° through Noonamah and Mount David (Fig. 8) is named here the 'Noonamah-Mount David Lineament Zone'. Further evidence for its existence is provided by alignments of folds and dykes, and gravity alignments. It is similar in width to the Noonamah-Katherine Zone. The overall lack of Class 3 lineaments in this zone was unexpected. Some Landsat lineaments - e.g. the broad linear zone of the Mary River (Fig. 3) - which at first appeared to coincide with magnetic lineaments were shown by the LSM images to have sufficient directional disparity to eliminate them from Class 1.

Lineament-gravity relationships

The existence of a number of the interpreted lineaments is supported by Bouguer anomaly contours (BMR, 1979d).

* These features are generally considered to be caused by mafic igneous rocks in the basement, or intrusive into the Lower Proterozoic sequence.

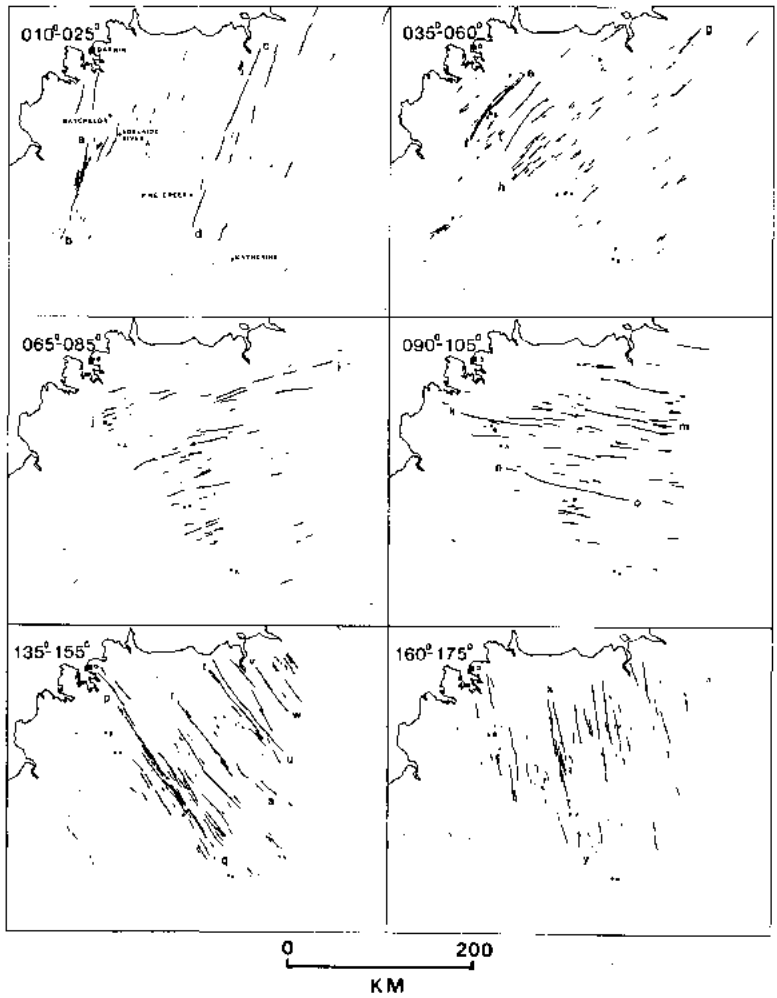


Figure 7. Plots of specific trends and zones from figure 5.

Along the western fringe of the Pine Creek Geosyncline the gravity features conform to known northerly and northeasterly trending structures, which include the Giants Reef Fault.

The northern margin of the Daly River Basin is paralleled by a northwest-trending lineament zone. The margins of the Edith River Basin, and of its associated gravity low, are broadly coincident with northwest-trending (part of the Noonamah-Katherine Lineament Zone) and northeast-trending lineaments. For much of their length, both the Noonamah-Katherine and Noonamah-Mount David Lineament Zones coincide with aligned gravity features (mainly Bouguer highs).

In the east and south of the region, the general grain of the gravity contours conforms well to the trends of the orthogonal northeast-northwest lineament sets. Within the Arnhem Land Plateau close coincidence between margins of gravity features and zones of

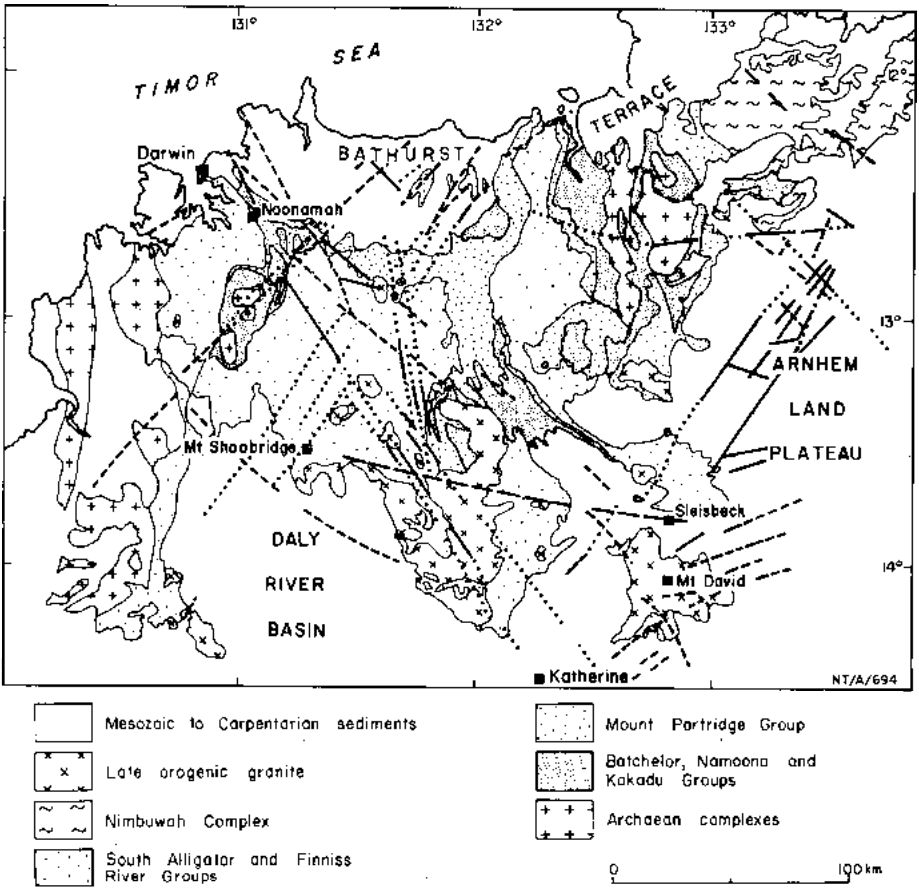


Figure 8. Lineaments derived from Landsat and/or magnetics interpretations.
——— aeromagnetic coincident with Landsat (class 1).
– – – – aeromagnetic without coincident Landsat (class 2).
· · · · · Landsat without coincident aeromagnetic but with Landsat extentions of aeromagnetic (class 3).
— — Mount Shoobridge-Sleisbeck lineament.

concentrated northwest-trending (including the Jim Jim and Bulman Fault Zones) and northeast-trending lineaments is evident. In the northern part of the Plateau the Bouguer anomaly contours trend northerly; a major Bouguer high extending northwards through Jabiru and Oenpelli has broad coincidence with a meridional lineament cluster.

Tucker *et al.* (this volume) suggest that most of the regional Bouguer features in the Geosyncline can be explained by the distribution of intrusive and basement granitic complexes. The sympathetic gravity-lineament relationships suggest that basement fracturing has been important in controlling this distribution.

Lineaments-radiometrics relationships

The regional distribution of zones of high surface radiometric intensity (BMR,1979c) appears to be largely a function of outcrop conditions, of the locations of granitic complexes and felsic-intermediate volcanics, and of drainage patterns. The last control can have three

effects — the concentration of radiometrically anomalous material, the exposure of radiometrically anomalous rock types, or the masking of alluvial cover.

These factors generally preclude the confident drawing of any relationships between lineaments and regional radiometric intensity, except in areas where linear structures have obviously controlled the distribution of radiometrically anomalous rocks. Such areas include those along the Giants Reef Fault to the east of Daly River (BMR, 1979c), to the west of the Waterhouse Complex, and in the Rum Jungle Embayment; along the meridional structures associated with the Mount Shoobridge Fault; and in the Adelaide River area. The large circular feature associated with the Cullen Granite between Frances Creek and Pine Creek (cf. Figs. 1 & 4) defines quite precisely the margins of a zone of high radiometric intensity.

Lineaments which may in themselves have been the cause of radiometric highs are not identifiable, although in the Ranger 10 area there is some correlation of elongate radiometric highs with northwest-trending lineaments. Regional radiometric highs associated with the major uranium deposits do not appear to be controlled by lineaments.

Lineament-mineralization relationships

The observed and expected frequency distribution of distances from uranium and gold occurrences to the nearest lineament are shown on figure 9. The expected frequency is based on the probability model of locating a lineament within any given radius of a randomly

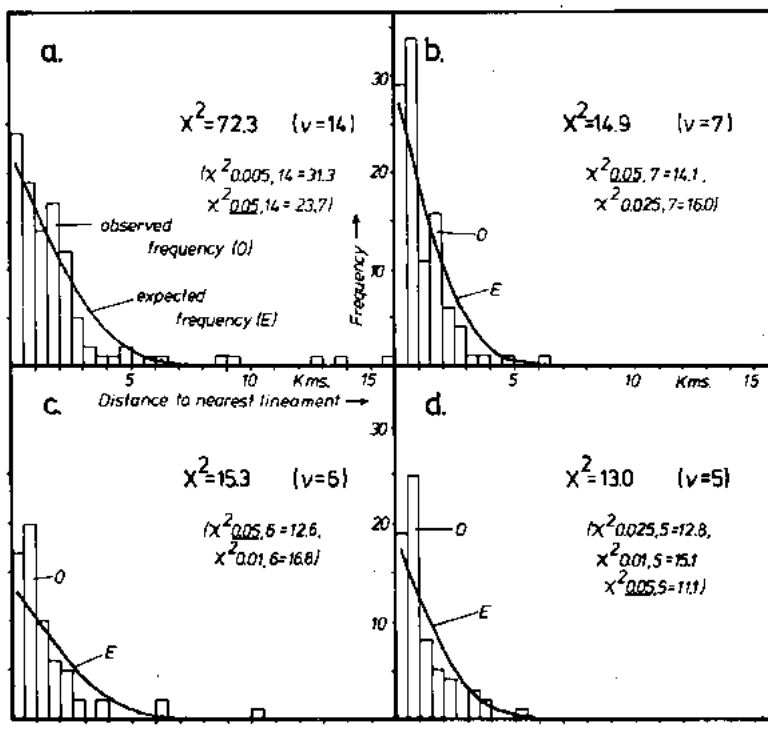


Figure 9. Observed (O) and expected (E) frequency distributions of distances from mineral occurrences to the nearest lineament. (a) uranium to lineaments, (b) uranium to lineaments, mapped faults etc. (c) gold to lineaments, (d) gold to lineaments, mapped faults etc. V = number of degrees of freedom; X^2 is the critical value derived from chi-squares tables for the indicated percentiles and degrees of freedom, $X^2 = \sum \frac{(O-E)^2}{E}$

INTERPRETATION TECHNIQUES

Landsat lineaments

Conventional photo-interpretation principles were employed to detect linear, curvilinear and circular features and various techniques were applied in an attempt to arrive at an objective lineament map. At this stage published maps were examined only to ensure that bedding trends and man-made features were not incorporated into the lineament map.

Two interpreters using 1:1 140 000 and 1:500 000 scale Landsat imagery produced a total of four independent lineament maps by both vertical and low-angle viewing techniques. Four confidence levels of detection were used and only observable segments of lineaments were annotated, extrapolation between segments not being attempted at this stage. Line gratings known as Ronchi rulings (Offield, 1975) were used during one interpretation, particularly as an aid to defining and extending subtle lineaments.

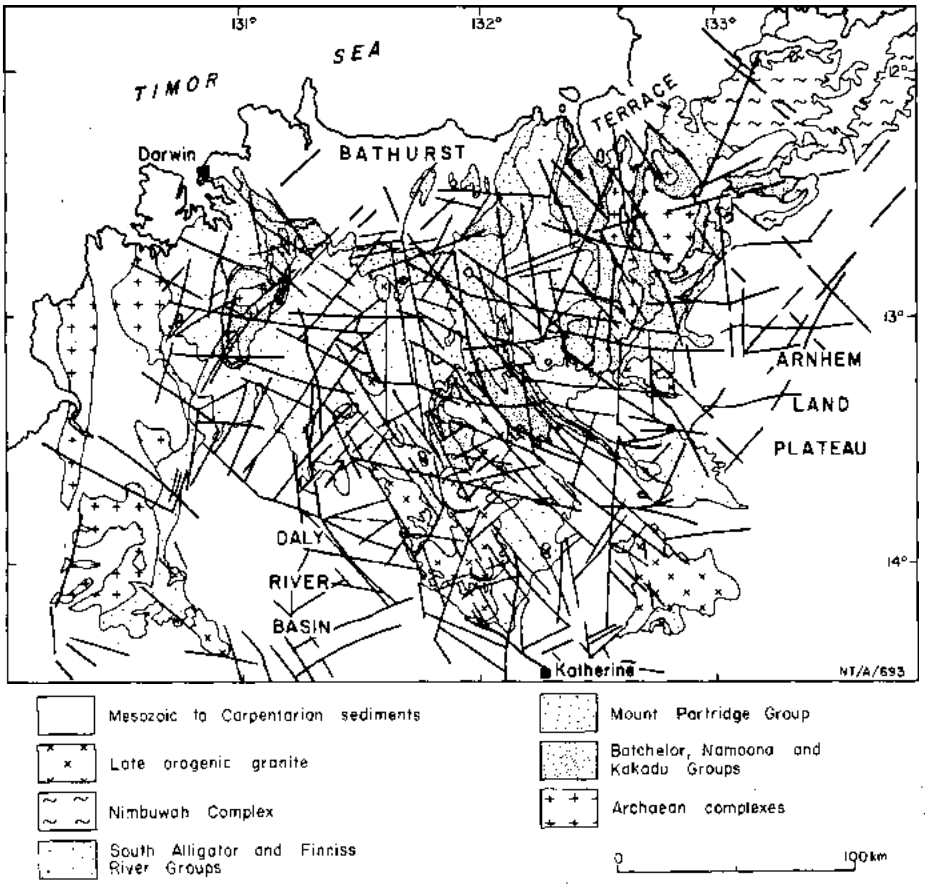


Figure 4. Map of the edited Landsat lineaments.

The many lineaments from the four interpretations were compiled onto a 1:500 000 scale controlled base and rigorously edited to produce a final interpretation (Fig. 4). In an attempt to achieve a measure of objectivity in the final edited map only those segments of

lineaments coincident on two or more independent interpretations were plotted. Extensions and/or joins to the edited lineaments were added from all four lineament interpretations after comparison with known geology, faults, and major joint sets had established their validity.

A separate integration of the final lineament map with all faults, veins, linear dykes and magnetic lineaments within pre-Middle Proterozoic (pre-Carpentarian) rocks from BMR, 1979a, was then prepared (Fig. 5) to allow all fracturing in the Geosyncline to be synthesised.

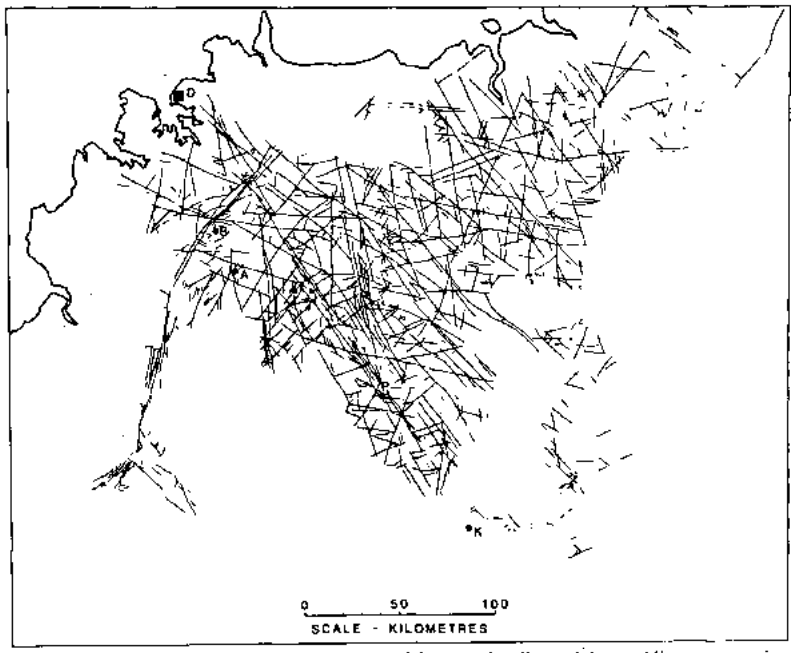


Figure 5. Composite of all interpreted lineaments, mapped faults, veins, linear dykes and linear magnetic anomalies within pre-Middle Proterozoic (pre-Carpentarian) rocks.

The two final maps (Figs. 4 & 5) were digitised on a table digitiser, and a package of computer programs for the analysis of geometric and spatial distribution of linear features applied. These plotted the digitised lineaments, rose diagrams (including those of lineament frequency, total length and average length for the various azimuth classes) and histograms of lineament lengths. A capacity to edit the lineament maps by omitting or enhancing lineaments with various azimuths was used to derive figure 7.

Landsat-aeromagnetic lineaments

The relationships between the lineaments and aeromagnetic information were considered both locally and regionally. Three classes of lineaments were recognised:

Class 1 — Aeromagnetic coincident with Landsat
Class 2 — Aeromagnetic without coincident Landsat
Class 3 — Landsat without coincident aeromagnetic but with Landsat extensions of aeromagnetic.

'Magnetics images', aeromagnetic contour maps (BMR, 1979b) and the geology map (BMR, 1979a) provided an overview of magnetic lineaments and trends. Detailed study of

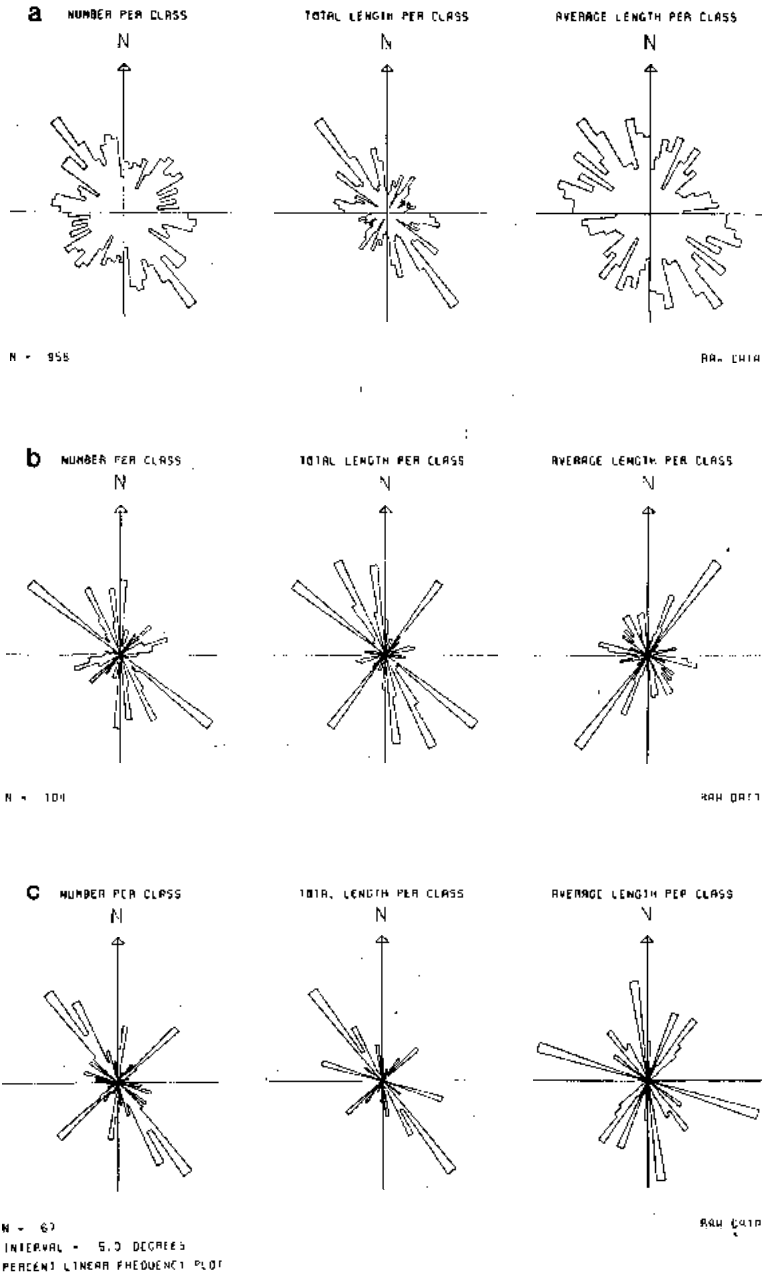


Figure 6. Rose diagrams of (a) all data in figure 5.
(b) data in figure 5 closest to uranium occurrences
(c) data in figure 5 closest to gold occurrences

some of these in the available LSM images showed that all three classes listed above were identifiable by stereoscopic examination. The value of this form of LSM integration was borne out by subtle aeromagnetic features (alignments, offsets or parallel gradient zones) providing local support for the existence of many Landsat lineaments. In an attempt to further enhance subtle aeromagnetic features selected areas of both magnetic and merged LSM data were examined at considerably larger scale, using an interactive computer display unit.

Mineralization relationships

In addition to using the interpreted lineament pattern as part of a regional structural synthesis of the PCG a study was conducted of the often sought for relationship between lineaments and certain mineralization. Uranium was considered because of its topical interest and gold because of its common structural association. Given the contentious nature of such studies a more quantitative approach than is commonly adopted was taken to:

1) identify individual lineaments or faults closest to mineralization and to record these distances.
2) indicate the directional and length characteristics of those lineaments closest to mineral occurrences.
3) test the observed spatial association of mineralization to lineaments against a random model.

If mineralization and genuine structural lineaments are assumed to be non-random events then we might expect them to be capable of statistical vertification. This may be done by graphical or chi-square comparison of the observed distribution of distances between mineral occurrences and the nearest lineament, with a theoretical distribution of distances of points (chosen independently of the location of the lineaments), to the nearest lineament. This method, derived by Berman (1977) and applied by Huntington & Green (1978) tests the worst case (random) association, the implication being that if a spatial association does exist then it must be better than random to be worthy of any further study.

Using this approach 104 uranium and 67 gold occurrences were studied, each being compared against the lineament interpretation alone, and the total data set of lineaments, mapped faults, veins, linear dykes and linear magnetic anomalies. No subdivision as to size of deposit or type of mineralization was made since over-subdivision of such a sample could easily yield individual samples too small to be meaningful.

RESULTS

Landsat lineaments

In general there was good agreement between Landsat lineaments and the known faults (BMR, 1979a). Many faults are expressed as subtle linear zones (up to 2km wide) and as such were more often detected by low angle than by vertical viewing.

Fracture trends shown in figure 5 are classified in figure 6a. Six major peaks were considered significant (Table 1) and all have a regional distribution throughout the Geosyncline (Fig. 7). Features of the 065°-085° and 090°-105° sets are relatively evenly spaced, whereas some clustering into lineament zones is evident within the other four sets. In addition there is a suggestion of regular spacing of zones, most evident in the 135°-155° and 160°-175° sets, where the separation is in the order of 50-70km. Spacings of a higher frequency have also been recognised.

The very obvious faults and fracture traces in the well exposed, relatively undeformed subhorizontal Kombolgie Formation capping the Arnhem Land Plateau (Fig. 1), reflect the various sets detected in the PCG but are more systematically and densely developed. There is also a suggestion of an anticlockwise rotation of trends (in the orthogonal east-west and north-south sets) passing eastwards into the plateau.

chosen point. Using a chi-square comparison between the two distributions the random model is rejected in all cases at the 5% significance level, though cases b, c, and d (Fig. 9) appear random at lower significance levels.

Though the observed relationship appears to be non-random at the 5% level this does not necessarily imply a controlling influence by lineaments, but rather that mines cluster at varying distances from lineaments in a manner which departs from the model. Such may or may not be geographically significant.

In all cases in figure 9 there are more mines in close proximity to lineaments than the model predicts. In addition there is a corresponding paucity at greater distances away from lineaments. As expected, gold shows a closer affinity to lineaments than uranium. However a pre-requisite of the model is that the lineaments are uniformly distributed on a plane (a situation sometimes difficult to attain in practice as illustrated in figure 5). The departure from randomness may partly be due to such spatial inhomogeneities in the lineament data. Despite this some other spatial affinity between the mines and their closest lineaments appears likely. The random model predicts that 99.9% of mineral occurrences should occur within 6-7km of a lineament, however some uranium and gold occurs further away indicating larger than predicted 'holes' in the lineament pattern.

The trends of those lineaments, mapped faults, veins, linear dykes and linear magnetic anomalies closest to uranium and gold occurrences are indicated in figures 6b and 6c respectively. Though a number of preferred orientations are evident the trends should be compared against figure 6a to compensate for high frequency trends in the total data set. Such a normalization merely changes the relative importance of the peaks.

Five main uranium trends (from Fig. 6b), the percentage of lineaments within them, and their known counterparts are listed below.

125°-130°	(16%)	— South Alligator Valley Uranium Field deposits
150°-155°	(9%)	— Jim Jim and Bulman Fault Zone trends (east Alligator only)
170°-185°	(16%)	— Ranger 28 fault trend and N-S faults near Jabiluka (eastern area only)
35°-45°	(7%)	— Giants Reef Fault Zone (western area only)
70°-75°	(9%)	— basement trends east of, and faulting just south of, Jabiluka

Without more specific genetic information this number of trends, coupled with the small number of occurrences closest to each trend (maximum = 16%), definitive directional associations for the entire PCG do not appear warranted. However over smaller areas, specific fracture orientation may assume greater significance.

Uranium mineralization in both the Rum Jungle Embayment and the South Alligator Valley Uranium Field has some spatial association with, respectively, major northeast (Giants Reef Fault), and northwest-trending fault zones. Such trends are reflected in the actual structures controlling mineralization. Two lineaments detected on Landsat and with azimuths of 100° and 110° intersect the Giants Reef Fault in the vicinity of Whites mine immediately north of Batchelor. Shears with a similar trend have been reported in the Whites orebody.

A lineament expressed as discontinuous segments for over 100km length on a strike of about 75° passes immediately south of Jabiluka. It crudely defines one direction of elongation of the Alligator Rivers Uranium Field. Between Jabiluka and Barote Spring (some 9km to the west) the lineament approximates to the Nanambu Complex-Cahill Formation contact. To the east of Jabiluka it is reflected by fracture traces in the Kombolgie Formation.

The lineaments, mapped faults, veins, dykes, and linear magnetic anomalies, closest to gold occurrences (Fig. 6c) define three major trends which are listed below (the percentage of lineaments within each trend is show in brackets).

140°-150°	(34%)	Pine Creek Shear Zone and associated trends. Largely contained within the longer Noonamah-Katherine lineament zone (Fig. 7, p-q).
45°-50°	(11%)	Clustered near and parallel with the axis of the Burnside Granite. Trend of the Grove Hill Cross Flexure and faults south of Burnside Granite.
105°-110°	(4%)	Mount Shoobridge-Sleisbeck lineament.

DISCUSSION

This study has confirmed that the several specific approaches adopted for the joint analysis of Landsat and geophysical data can assist in a re-appraisal of the regional geology of the PCG and can bring out new information of relevance to regional tectonics and possible mineralization relationships. An appropriate strategy in such a study is vitally important and the four main techniques which have contributed to this study are:

1) The integration and editing of *several* Landsat interpretations to arrive at a single reliable data set.
2) The digital integration of Landsat and aeromagnetic data.
3) The graphical processing of lineament/fault data to enhance specific spatial patterns and zones.
4) The quantitative analysis of spatial associations between mineral occurrences and lineaments.

The stereoscopic merging of Landsat and magnetics was found to be extremely useful in regional structural analysis. The intimate association of such a merging increases both the confidence and reliability of image interpretation by the convergence of evidence from the two independent data sources. The integrated imagery provided a valuable medium for analysing dyke relationships and predicting the occurrence of both dykes and faults in poorly exposed parts of the Geosyncline such as soil-covered, vegetated, or fireburn areas where Landsat information was only faintly expressed. LSM images should prove useful for assisting collaboration between geologists and geophysicists in projects requiring integration of data from both disciplines. Further refinements to data presentation and interpretation techniques are desirable. Higher resolution aeromagnetic data with closer line spacings, and use of gravity and radiometric data in the integrating process, are planned.

The coincidence of lineaments with many known faults and several of the structures indicated by geophysics supports the belief that the edited Landsat lineaments represent a reliable data set. Of the numerous Landsat lineaments detected during the study only some of those which appear to have structural and/or economic significance have been discussed. A more comprehensive analysis of the lineaments would require additional field work.

The newly defined Noonamah-Katherine and Noonamah-Mount David lineament zones are considered representative of two well defined lineament directions in the PCG. Though the two lineament zones are similar in width they differ with respect to: fracture intensity (as displayed on Landsat imagery), orientation (between 15°-20° difference), responses of magnetic lineaments, and some mineralization associations (notably gold), all of which suggest the separate zones and associated magnetic lineaments are of different ages. Tucker *et al.* (this volume) propose that the magnetic lineaments are responses of post-Middle Proterozoic (post-Carpentarian) dolerite dykes. The coincidence of dolerite dykes and some gravity trends with many of the northeast and northwest-trending Landsat lineament sets suggests they are expressions of deep basement fractures.

Relationships, if any, between these dolerite dykes, lineaments and mineralization are uncertain but are worthy of further investigation. The Alligator Rivers Uranium Field exhibits a very similar geological setting to the uranium deposits in the Athabasca Basin of

northern Saskatchewan. Although origins of those deposits are debatable, both faults and dolerite dykes have been involved in some genetic models as being significant for uranium localisation (Munday, 1979).

Another well defined lineament, identified on Landsat and at least 170km long, extends south-southeast from Mount Shoobridge through the Golden Dyke (Au), Coronet Hill (Cu, Pb) and Sleisbeck (U) prospects. The feature named the Mount Shoobridge-Sleisbeck lineament (Fig. 7, n-o; Fig. 8) warrants further examination because of its size and apparent relation to different mineralization.

The preliminary statistical evaluations indicate that gold and uranium occurrences are more closely associated with fractures that a random distribution model would predict. Since it was anticipated that gold would have this relationship it served as a check on the statistical approach. Thus we believe that we have demonstrated that the uranium in the PCG has better than non-random association with fractures. Some 32% of the uranium occurrences studied in the PCG are indicated as having some relationship to two sets of fractures (125° -130°, and 170°-185°).

To those explorationists who choose to incorporate structural lineaments into their strategy within the PCG such features become more favourable search areas if there is association with the several other criteria (e.g. lithologic, stratigraphic) that are believed to influence or control mineralization.

The non-random distance association suggests the need for more detailed analysis along the following lines.

1) Further subdivision of the mineralization into size and type categories.
2) Study of smaller areas within the PCG where lineaments may be more uniformly distributed and where the style of mineralization may be more homogeneous.
3) The incorporation of more genetic factors (e.g. stratigraphy) into the analysis.

ACKNOWLEDGEMENTS

The authors wish to acknowledge the helpful criticism and comments of V.L.R. Furlong. C.J. Simpson publishers with the permission of the Director, Bureau of Mineral Resources, Geology and Geophysics, Canberra.

REFERENCES

Berman, M., 1977: Distance distributions associated with poisson processes. *Appl. Probability, 14*, 702-712.

BMR, 1979a: *Solid geology of the Pine Creek Geosyncline Northern Territory, 1:500 000 map.* Bureau of Mineral Resources, Australia.

BMR, 1979b: *Total magnetic intensity contours of the Pine Creek Geosyncline Northern Territory, 1:500 000 map.* Bureau of Mineral Resources, Australia.

BMR, 1979c: *Radiometric contours — Total count. Pine Creek Geosyncline Northern Territory, 1:500 000 map.* Bureau of Mineral Resources, Australia.

BMR, 1979d: *Bouguer anomaly contours of the Pine Creek Geosyncline Northern Territory, 1:500 000 map.* Bureau of Mineral Resources, Australia.

Green, A.A., Huntington, J.F. & Roberts, G.P., 1978: Landsat digital enhancement techniques for mineral exploration in Australia. *Proceedings of twelfth International Symposium on Remote Sensing of Environment, (Manila, 20-26 April, 1978), volume 2*, 1755-1762.

Huntington, J.F. & Green, A.A., (in press): The application of Landsat imagery and related remote sensing techniques to mineral resources exploration in Australia. *International Journal of Remote Sensing, 1(1).*

Huntington, J.F. & Green, A.A., 1978: A method of testing if significant spatial correlations exist between lineaments and mineral occurrences. *Abstracts of the fifth International Symposium on the genesis of ore deposits, Snowbird, Utah, August 1978.*

Munday, R.J., 1979: Uranium mineralization in northern Saskatchewan. *Bull. Can. Inst. Min. Metall., 72(804)*, 102-111.

Offield, T.W., 1975: Line-grating diffraction in image analysis: Enhanced detection of linear structures in ERTS images, Colorado Front Range. *Modern Geology, 5*, 101-107.

Simpson, C.J., 1978: Landsat: developing techniques and applications in mineral and petroleum exploration. *BMR J. Aust. Geol. Geophys., 3*, 181-191.

Tucker, D.H., Stuart, D.C., Hone, I.G. & Sampath, N., (this volume): The characteristics and interpretation of regional gravity magnetic and radiometric surveys in the Pine Creek Geosyncline. *Proceedings of the International Uranium Symposium on the Pine Creek Geosyncline.*

AN OVERVIEW OF METALLIC MINERALISATION IN THE PINE CREEK GEOSYNCLINE

R.S. Needham[1] and M.J. Roarty[2]

1. Bureau of Mineral Resources, P.O. Box 378, Canberra City, A.C.T. 2601, Australia
2. Northern Territory Geological Survey, P.O. Box 2901, Darwin, N.T. 5794, Australia

ABSTRACT

Although renowned for its relatively recently discovered large uranium deposits, the Pine Creek Geosyncline has a history of exploitation dating back to 1865, during which time 16 metals have been extracted. Uranium makes up 96.8 percent of the value of recorded production and reserves at present metal prices, lead 1.9 percent, gold and zinc 0.32 percent each, iron 0.2 percent, silver 0.2 percent and all other metals 0.3 percent. The Alligator Rivers Uranium Field accounts for 95 percent of the total value of recorded production and reserves, the Rum Jungle Uranium Field 4 percent, and all other areas 1 percent.

Deposits range from stratiform through stratabound to vein-type. Most have undergone some degree of alteration or remobilisation, and extreme metasomatism in some masks clues to the earlier evolution of the deposits.

Small vein-type hydrothermal deposits, clustered around intrusive granites, predominate. Other deposits can be sub-divided into those associated with the basement, those associated with the Masson and Cahill Formations, and those associated with the Gerowie Tuff, Koolpin, and Kapalga Formations. Many deposits have undergone supergene concentration near the surface, and some have been formed predominantly by this process.

Uranium appears to have been mainly derived from Archaean source rocks, and base metals and some precious metals from volcanic exhalative sources. Main areas of potential are the Alligator Rivers region for uranium and possibly gold, and the central part of the geosyncline for base metals.

INTRODUCTION

Sixteen metals have been exploited in the Pine Creek Geosyncline since 1865 (Ag, As, Au, Bi, Cd, Co, Cu, Fe, Mn, Mo, Pb, Sn, Ta, U, W, Zn). Uranium (most of which has been discovered since 1970) makes up 96.8 percent of the value of recorded production and reserves, lead 1.9 percent, gold and zinc 0.32 percent each, iron 0.2 percent, silver 0.2 percent and all other metals 0.3 percent (Table 1; Needham, 1978). Individual mineral fields are shown in figure 1. The Alligator Rivers Uranium Field accounts for 95 percent of the total value of recorded production and reserves in the Pine Creek mineral province, the Rum Jungle Uranium Field 4 percent, and all other areas 1 percent (Table 2; Needham, 1978).

HISTORY OF EXPLORATION

The first discovery in the Pine Creek Geosyncline was gold at Blackmore River in 1865; the Pine Creek and Grove Hill strikes of the early 1870's resulted in a rush of prospectors to the region. Hundreds of prospects were located, but none was worked to any great depth. By 1881 mining activity was widespread and most of the major mineral deposits now known, other than uranium and iron ore, were being worked by the turn of the century; these included gold at Pine Creek, Union Reefs, Brocks Creek and Northern Hercules; tin at West Arm, Mount Finniss, Mount Wells and Mount Shoobridge; silver-lead at the Evelyn mine; copper at Daly River and copper-gold at Iron Blow (Fig. 2). Discoveries of tin at Maranboy, Hayes Creek and Horseshoe Creek, and wolfram at Wolfram Hill, between 1900 and 1915 did little to boost a steadily declining production record; by 1946 production had declined in value to 3 percent of the annual production of the 1880 to 1900 boom years (Noakes, 1949).

Government action and incentives in the 1940's aimed at extending and intensifying search for uranium in Australia led to the discovery of uranium at Rum Jungle in 1949. A decade of intense activity ensued during which the uranium-copper-lead deposits of Rum Jungle and the uranium-gold deposits of the South Alligator Valley (Fig. 1) were discovered. The first systematic survey of the region was conducted during this period by the Bureau of Mineral Resources, Geology and Geophysics (BMR), and several tin, lead and iron

Metal	Total recorded production and reserves		No. of mines and deposits	Value $A (as at May 1978)	% of total value
U_3O_8	338,607.75	T	22	29,785,294,000	96.76
Pb	1,178,315	T	22	589,157,500	1.91
Au	647,943	oz	48	97,418,230	0.32
Zn	198,861	T	5	97,243,030	0.32
Fe	3,900,000	T	2	62,400,000	0.20
Ag	12,601,310	oz	23	54,437,660	0.19
Sn	6,275	T concentrate	52	42,361,897	0.14
Cu	29,692	T	23	33,848,880	0.10
Co	861	T	1	10,564,470	0.03
WO_3	600.24	T	3	7,503,000	0.02
Bi	40	T	1	720,000	0.0023
MnO_2	294	T	2	310,464	0.0010
Cd	104,773	lb	1	209,564	0.00068
As	36	T	1	158,400	0.00051
Ta	12.2	T concentrate	2	152,500	0.0050
Mo	0.125	T	1	2,140	0.000006
				30,781,680,000	

T = tonnes oz = ounces lb = pounds

Table 1. Metals of the Pine Creek Geosyncline in order of value. (Data in Tables 1-6 from a compilation by Needham (1978 unpubl.) of information in Crohn (1968) and Northern Territory Department of Mines and Energy records).

prospects were located during this survey and others conducted by private prospectors. Apart from uranium, the most significant discovery came in 1964, when the Woodcutters silver-lead-zinc deposit was first indicated by a routine systematic geochemical survey designed to explore for uranium and base metals along a favourable stratigraphic contact (Dodson & Shatwell, 1965). Base metal exploration subsequently increased, but was soon overshadowed by the exceptional success of airborne radiometric prospecting undertaken by several companies in 1969-70. This was prompted by improvement in uranium market forecasts and by a reinterpretation of the geology of the Alligator Rivers region published by the BMR as the second edition of a 1:500 000 scale geological map of the geosyncline, which enhanced

Mineral field	Metals in order of value (minor amounts in parentheses)	Value $A (as at May 1978)	% total value
Alligator Rivers	U, Au (Sn)	29,371,400,161	95.42
Rum Jungle	U, Pb, Ag, Cu, Zn, (Co, Au)	1,118,118,373	3.63
Cullen	Au, Ag, Sn, Pb, Zn, Cu	125,322,870	0.41
	W, (As, Bi, Cd, Mn, Mo, U)		
South Alligator Valley	U, Au (Ag, Pb)	78,391,498	0.25
Frances Creek	Fe, Au (Ag)	62,425,500	0.20
Maranboy	Sn	9,451,260	0.03
Finniss River	Sn, Ta, Au	3,973,868	0.01
Daly River	Cu	1,556,100	0.005
Baldiva	Au, Sn	943,537	0.003
Yeuralba	W, Sn (Cu)	601,422	0.002
Isolated mines	U, Au, Sn (Mn, Ag, Cu, Pb, Fe)	10,400,772	0.04

Table 2. Recorded production and reserves for the mineral fields in the Pine Creek Geosyncline

its similarity to the Rum Jungle area (Walpole *et al.*, 1968). Since 1970, the Nabarlek, Ranger 1, Koongarra, and Jabiluka One and Two deposits have been discovered and several other prospects hold great promise, particularly Jabiluka Three, Hades Flat and Caramal (Fig. 2). The Jabiluka Two deposit contains gold: it is the only one of these known to contain economic quantities of any metal other than uranium.

Exploration in the Alligator Rivers Uranium Field has almost reached a standstill following progressive governmental annexation of lands and by deliberations on future land use in the area, particularly the Kakadu National Park and extensions, and pending Aboriginal land claims. Presently, mining of known deposits appears likely to proceed; exploration, if allowed to recommence, is likely to be restricted. Exploration mainly for base metals and uranium has continued in the remainder of the Pine Creek Geosyncline.

Geological research, like exploration, tailed off from the late 1950's to the late 1960's, but has grown dramatically following discovery of major uranium deposits in the Alligator Rivers area. Detailed geological mapping by the BMR and Northern Territory Geological Survey has provided a radically altered framework for current research and exploration. The earlier concept of a greywacke-dominated sequence with lateral interfingering of facies representing units deposited in a number of basins, has been replaced by one of chronostratigraphic units, dominantly shallow sediments which in places are evaporitic, which may be traced with little facies variation through almost the entire geosyncline (Needham *et al.*, this volume). The new stratigraphy is most relevant to studies of mineralisation in the Pine Creek Geosyncline, as many of the mineral occurrences are related to particular strata. The recognition of this relationship has facilitated the classification of the deposits according to type, and has enabled us to make some speculations on their genesis.

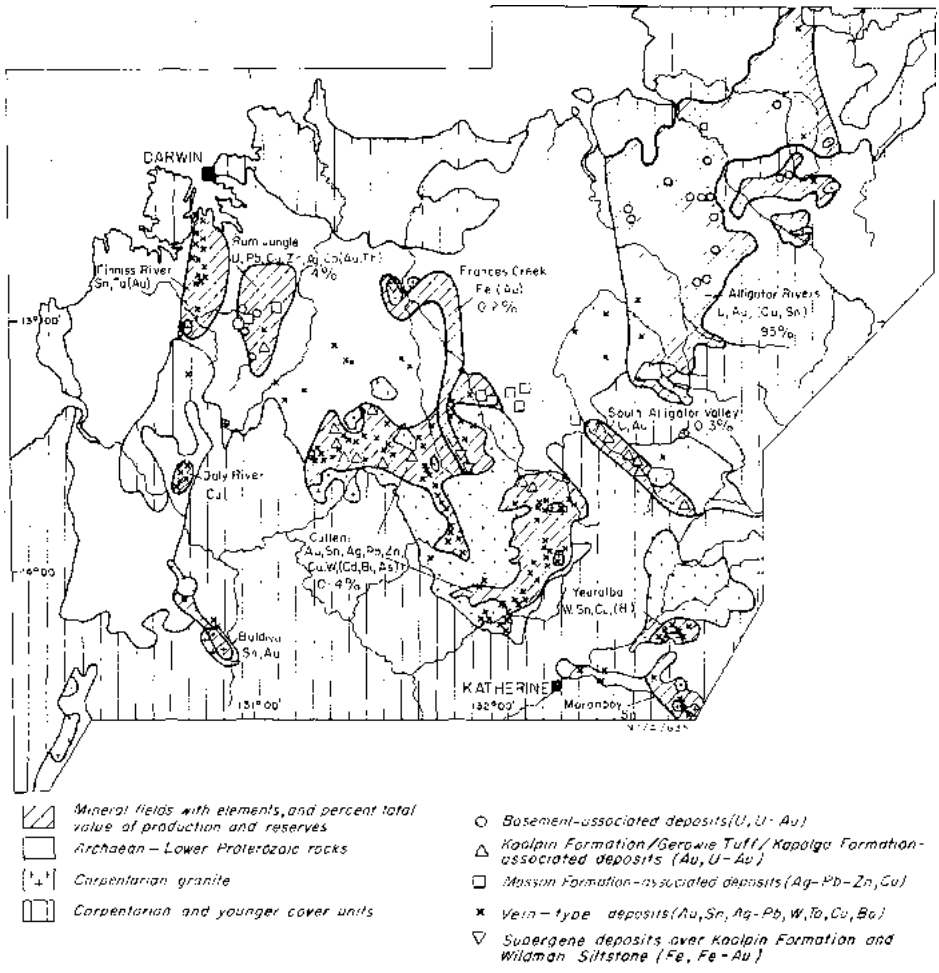


Figure 1. Mineral fields, showing deposit types and percentage of total value of production and reserves for each field.

CLASSIFICATION OF MINERAL DEPOSITS

Crohn (1968) prepared the first systematic treatise of mines and mineral deposits of the Katherine-Darwin region, which includes most of the Pine Creek Geosyncline, and gave the first geographical grouping of mines and prospects. The most notable addition to the mineral fields described by Crohn is the Alligator Rivers Uranium Field, which overshadows all others in size and value; the Woodcutters Ag-Pb-Zn deposit at Rum Jungle was also discovered after Crohn's work was completed.

Crohn (1975) later defined two main types of mineral deposits (excepting the iron deposits) in the geosyncline: firstly, the uranium and associated base metal deposits of the Rum Jungle and Alligator Rivers regions, which occur in a restricted and distinctive section of the Lower Proterozoic succession and are regarded as broadly syngenetic; and secondly the smaller 'hydrothermal' deposits scattered throughout the geosyncline around many of

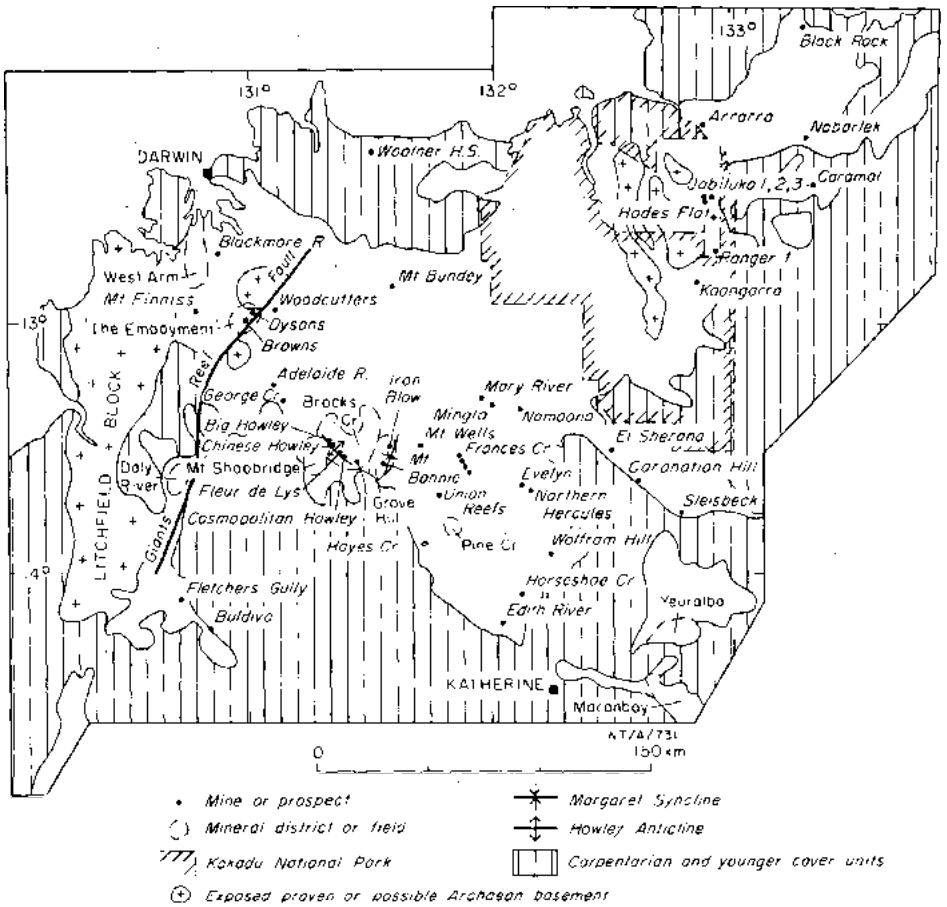


Figure 2. Locality map of some mines and prospects in the Pine Creek Geosyncline.

the granitoid bodies; these are mainly gold, tin, copper, lead and zinc. He also noted that some deposits of this group appeared to be conformable in pyritic black slate and do not conform to the general pattern of the other 'hydrothermal' deposits.

Most of the mineral deposits in the Pine Creek mineral province have undergone some degree of alteration or remobilisation, and extreme metasomatism in some deposits masks clues to any earlier evolution. Deposit types grade from stratiform to stratabound and into vein-type, and epigenetic and/or supergene processes are superimposed on these to some degree. Accordingly, classifications based purely on detailed characterisation of each deposit, for example, as either stratiform, stratabound or vein-type, are difficult to make owing to the gradations between these types, and a classification based on style of epigenetic processes tells little of the underlying reason for the deposit being where it is. A classification is chosen here based partly on broad deposit type and partly on the regional geological associations of the deposits. This approach has yielded a number of groups of deposits which have clear relationships with stratigraphy and particular geological processes, from which conclusions on the metallogenesis of each group can be made.

In this paper, mineral occurrences are broadly grouped into stratabound and vein-type deposits. The stratabound deposits are futher sub-divided according to their stratigraphic associations. Main mineralised horizons are the Masson and Cahill Formations which are lateral equivalents, and the superposed Koolpin Formation, Gerowie Tuff and Kapalga Formation (Fig. 3). In the lower horizons (Masson and Cahill Formations), U and U-Au deposits are found only where the host rocks are close to exposed granitic basement complexes, whereas Ag-Pb-Zn, Cu deposits occur throughout the basin of deposition. Other deposits have been formed by supergene processes acting on certain strata, particularly rocks of the Wildman Siltstone. Accordingly, the mineral occurrences of the Pine Creek Geosyncline metalliferous province can be placed in the following categories:

1) stratabound deposits in the Masson and Cahill Formations close to areas of basement rocks — U, U-Au
2) stratiform or stratabound deposits in the Masson and Cahill Formations throughout the basin — Ag-Pb-Zn, Cu
3) stratiform deposits in the Koolpin Formation, Gerowie Tuff, and Kapalga Formation — Au, U-Au, Pb-Zn, Cu
4) vein-type deposits associated mainly with early Carpentarian (early Middle Proterozoic) granites — Au, Sn, Ag-Pb, W, Ta, Cu, Bi
5) supergene deposits, mainly in the Wildman Siltstone — Fe, Fe-Au

MINERAL FIELDS

Crohn (1968) classified his mineral fields mainly on geographical criteria. We have reclassified them in accordance with the categories of mineral deposit outlined above (Fig. 1). The largest is the *Cullen mineral field*, surrounding the early Carpentarian (early

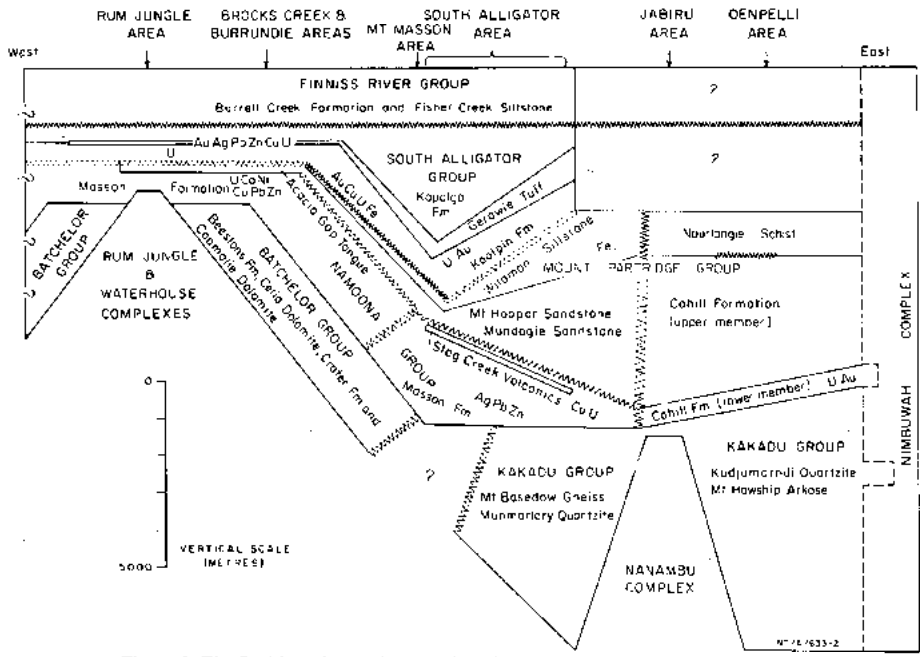


Figure 3. The Position of stratabound mineralisation in the Pine Creek Geosyncline.

Middle Proterozoic) Cullen Granite batholith in the centre of the province. Deposits within it are mainly vein-type, containing a wide variety of metals (Au, Sn, Ag, Cu, W, Cd, Bi, As), and the value of recorded production and reserves is only 0.4 percent of the total for the province. The *Finniss River, Daly River, Buldiva, Yeuralba* and *Maranboy mineral fields* along the western and southeastern margins of the province contain most of the remaining vein-type deposits (Sn, Au, W, Bi, Cu, Ta). Mineralisation in these is mostly associated with early Carpentarian (early Middle Proterozoic) granite, exposed in the Finniss River, Buldiva, Yeuralba and Maranboy fields. The copper mineralisation in the Daly River field is probably related to an adjacent body of dolerite. Some of the Au deposits of the Cullen mineral field range from stratiform deposits in the Koolpin Formation/Gerowie Tuff/Kapalga Formation, through intermediate types, into deposits of vein-type appearance. This gradation suggests that syngenetic metals have been remobilised, probably during regional metamorphism, and concentrated in or near siliceous veins. The two Ag-Pb-Zn deposits of the Cullen mineral field, which make up 25 percent of recorded production and reserves for that field, also belong to the group of stratiform deposits in the Koolpin Formation, Gerowie Tuff and Kapalga Formation.

Partly within and extending north of the Cullen mineral field is the *Frances Creek Iron Field*. The iron deposits, some with minor gold, are supergene bodies over iron-rich rocks of the Wildman Siltstone and Koolpin Formation. Production accounts for about 0.2 percent of the total of value of production and reserves for the province. The *South Alligator Valley Uranium Field* contains U and U-Au deposits mainly in rocks of the Koolpin Formation although mineralisation commonly extends into overlying Carpentarian (Middle Proterozoic) sandstone and volcanics. In one deposit mineralisation is in a Carpentarian (Middle Proterozoic) volcanic diatreme which contains blocks of carbonaceous shale probably derived from the underlying Koolpin Formation. Minor copper mineralisation is associated with this deposit, and some deposits in the field carried minor silver (Threadgold, 1960).

The two most significant mineral-producing areas in the province are both dominated by deposits associated with the Masson and Cahill Formations. The *Rum Jungle Uranium Field* (U, Pb, Cu, Zn, Ag, Co) provides 3.6 percent of the total of production and reserves of the Pine Creek Geosyncline, and the *Alligator Rivers Uranium Field* (U, U-Au) 95 percent. Most of the deposits are within 5 km of exposed granitic Archaean basement; the most significant exception is the Nabarlek deposit in the Alligator Rivers Uranium Field, which differs markedly from the other mainly disseminated stratabound deposits in its essentially vein-type character. Some minor uranium mineralisation occurs in the Koolpin Formation at Rum Jungle.

DEPOSIT TYPES

1) U, U-Au stratabound deposits in the Masson and Cahill Formations close to areas of basement rocks.

These are in the Rum Jungle and Alligator River Uranium Fields and account for 96.6 percent of total value of production and reserves of all metals, and 96.8 percent of uranium production and reserves (Tables 1 & 3). The majority of deposits are located in breccia zones in partly or wholly carbonaceous pelitic rocks, adjacent to crystalline carbonate rocks which commonly contain pseudomorphs of supratidal evaporite minerals (Crick & Muir, this volume). The absence of U and U-Au deposits in similar rocks at the same stratigraphic level in the geosyncline away from basement suggests that the association with basement is an important factor in uranium ore genesis. The ore bodies are generally tabular to basin-shaped and conformable to some degree. The ore zone breccias do not extend appreciably beyond the perimeter of the orebody (e.g. Ranger 1).

	tonnes	grade	contained U_3O_8 tonnes
Jabiluka One	1,367,000	0.256% U_3O_8	3 484
Jabiluka Two	529,000	10 dwt Au (15.3 gm/T)	
	51,900,000	0.39% U_3O_8	203 800
Koongarra	3,555,272	0.346% U_3O_8	12 301
Nabarlek*	494,470	1.84% U_3O_8	9 550
Ranger 1	41,000,000	0.2007% U_3O_8	100 700
Whites	682,000	0.16% U_3O_8, 0.6% Pb, 2.2% Cu, 0.92 oz Ag	1 069
Dysons	154,000	0.34% U_3O_8	534
Mount Burton	6,000	0.17% U_3O_8, 1.3% Cu	10
Rum Jungle Creek South	653,000	0.4% U_3O_8	2 612
			334 060

Table 3. Tonnage/grade figures for some U ± Au stratabound deposits in the Masson and Cahill Formations.
* Nabarlek is in Nimbuwah Complex rocks probably derived by metamorphism of Cahill formation.

At Rum Jungle, the deposits lie on or close to the contact between massive crystalline dolomite/magnesite of the Coomalie Dolomite, and the overlying calcareous carbonaceous shales of the Masson Formation. They occur on the northern limb of a syncline between two granite complexes (the Archaean Waterhouse and Rum Jungle Complexes), along shear zones on or near the crest of a subsidiary anticline on this structure (Fraser, 1975). The syncline has been displaced about 4.8km by the Giants Reef Fault to form the Embayment, a re-entrant of Lower Proterozoic metasediment into the Rum Jungle Complex in which the metasediments form a broad, west-plunging syncline. Most of the mineral deposits at Rum Jungle occur in the Embayment.

In the Alligator Rivers region, most of the U and U-Au deposits are near the base of the Cahill Formation and adjacent to lenses of massive dolomite and/or magnesite. This common proximity between uranium deposits and carbonate rocks may be relevant to ore genesis. Eupene *et al.* (1975) suggest the ore zone at Ranger 1 developed by volume reduction following replacement of carbonate by chert. Ferguson *et al.* (this volume) infer that the collapse structures are related to near-surface karsting, and suggest that they were infilled with alluvium after the main period of introduction of uranium. However, Crick & Muir (this volume) suggest that the ore-zone breccias developed as diapiric breccias, resulting from the density instability of evaporite beds which were later replaced by carbonate.

All the deposits are located in zones of chloritisation, ranging from minor in the Rum Jungle deposits, to massive and pervasive in the Alligator Rivers deposits. In each the chloritisation is localised around the deposit; for example, at Jabiluka the alteration halo exceeds 200m from the uranium deposits (Binns *et al.*, this volume). Massive chloritisation is rare in rocks removed from the uranium deposits. In the Alligator Rivers region minor chloritisation away from the ore bodies has been noted along structural and stratigraphic

breaks and along quartz-filled micro-fractures (Needham & Stuart-Smith, 1976), and near the contact of the Oenpelli Dolerite (Needham *et al.*, 1975). The chloritisation of the ore zones appears to have taken place mainly at about 1610 Ma (Page *et al.*, this volume). Low-temperature events took place in some deposits at about 900 Ma (Hills & Richards, 1976; Gulson, B.L., Hills, J.H., Page, R.W. & Riley, G.H., pers. comm.). These ages approximate pitchblende and uraninite ages measured in some of the deposits, and may indicate significant mineralisation episodes (Page *et al.*, this volume).

The primary ore mineral of this deposit type is uraninite, mostly as disseminated and massive (colloidal and vein-type) pitchblende, and as 'paint' on fractures. The Alligator Rivers deposits contain gold, but only Jabiluka Two contains economically recoverable quantities. Minor chalcopyrite, galena and pyrite also are present. Secondary uranium minerals include sklodowskite, saleeite, gummite, and metatorbenite.

The Rum Jungle deposits are 'best developments' of mineralisation within a series of overlapping mineral zones (Fraser, 1975), and grade from uranium alone in the north at Dysons, through U-Co-Cu-Pb-Ag at Whites and Cu at Intermediate, to Ag-Pb-Zn at Browns. The primary ore minerals in the base metal deposits were sulphides, but significant amounts of production came from secondary minerals in some of the deposits, mainly malachite and cerussite. Secondary uranium minerals included torbenite, autunite, phosphuranylite, 'gummite' and saleeite.

These deposits are described in more detail in this volume by Fraser (Rum Jungle deposits) and Hegge *et al.* (Alligator Rivers deposits).

Some uranium deposits occur as massive mineralisation in planar dislocation or crush structures which extend beyond the outer limits of the ore body. They are shown as vein-type deposits on figure 1, and include the Adelaide River and George Creek mines in the west of the Pine Creek Geosyncline, and the Nabarlek deposit in the northeast of the Alligator Rivers Uranium Field (Fig. 2). The Adelaide River and George Creek mines, together with minor vein and disseminated patchy uranium in the south of the Cullen Granite near Edith River, are probably magmatic in origin. The massive vein-type uranium mineralisation at Nabarlek is, however, probably genetically related to the other mainly stratabound deposits of the Alligator Rivers region in the Cahill Formation. The Nabarlek orebody is located in a chloritised shear zone in quartz-mica schist and paragneiss of the Nimbuwah Complex, which in places contains recognisable resisters of carbonaceous and calc-silicate rocks correlated with the Cahill Formation (Needham & Stuart-Smith, this volume). The schist and paragneiss are probably also equivalent to the Cahill Formation, but metamorphism has obliterated the sedimentary character of the parent rocks (carbonaceous schist was discovered adjacent to the orebody during mining — Ferguson *et al.*, this volume — supporting the Cahill Formation parentage of these rocks). The migration of uranium away from its stratigraphic locus adjacent to carbonate bodies (which is the common association for the other Alligator Rivers region uranium deposits), into low-pressure sites may indicate a different temperature and pressure regime at Nabarlek during the 1800 Ma orogenesis, or a different transport and/or concentrating mechanism. Transporting fluids may have been provided by the partial melting of the host rocks.

2) Ag-Pb-Zn, Cu stratiform or stratabound deposits in the Masson and Cahill Formations.

These occur in the Rum Jungle Uranium Field, and as scattered deposits spread between the Frances Creek and South Alligator Valley mineral fields. They account for about 2.5 percent of total value of production and reserves (not counting contained U_3O_8) and about 85 percent of Ag-Pb-Zn production and reserves (Table 4). They are at the same stratigraphic level as the U, U-Au deposits discussed above, but are not restricted to areas near the basement complexes. The Rum Jungle Ag-Pb-Zn deposits overlap zones of uranium mineralisation, suggesting a similar genesis for the base metal and uranium deposits. These

	tonnes	grade	tonnes contained metal
Woodcutters	720,000	7.5% Pb, 12.9% Zn, 154 gm/T Ag	92 880 Zn, 54 000 Pb (3.6 million oz Ag)
Whites	682,000	0.16% U_3O_8, 0.6% Pb, 2.2% Cu, 0.92 oz Ag	15 000 Cu, 4 100 Pb, 1 069 U_3O_8, 861 Co (64 000 oz Ag)
Intermediate	373,000	2.45% Cu	9 140 Cu
Browns	20,500,000	5.4% Pb, 0.3% Zn, 12 gm/T Ag	1 107 000 Pb, 61 500 Zn (7.9 million oz Ag)
Mary River	750,000	10% Zn	75 000 Zn
Minglo	18	58% Pb, 4.5 oz Ag	10 Pb

Table 4. Tonnage/grade figures for some Ag-Pb-Zn, Cu stratiform to stratabound deposits in the Masson and Cahill Formations.

deposits include the Browns, Intermediate and Woodcutters deposits at Rum Jungle, and the Namoona, Minglo and Mary River deposits northeast of the Cullen mineral field (Fig. 2).

All the deposits are contained within pyritic carbonaceous and dolomitic shales of the Masson Formation, although the Woodcutters deposit transgresses the underlying unconformity with the Coomalie Dolomite. This deposit (Pb-Zn-Ag-Cd) comprises five discrete transgressive en echelon lodes, along the axis of a north-pitching anticline (Roberts, 1975). The ore minerals are mainly sphalerite, galena, pyrite, lead and antimony/arsenic sulphosalts, contained in veins which are generally transgressive. The gangue is dolomite, silica and accessory anatase, tourmaline and muscovite. Roberts (1973; 1975) considered that sedimentary and diagenetic processes concentrated metals in the sediments and formed the ore solutions, and that the conditions which resulted in the dolomitisation also played an essential part in the genesis of the deposit. He considered that the metals were co-precipitated within a restricted basin with the precursors to the dolomite, and were concentrated in the pore solutions during diagenesis. He suggested the metals were possibly transported as organo-metallic complexes in sulphide and carbonate-bearing solutions to sites in the axial zone of an anticline during tectonism, where lower pressure, and temperatures below 160°C, prevailed.

The Minglo mine and Mary River and Namoona prospects crop out as a group of hematitic gossans discordant to the Masson Formation country rocks, within 10km north of the Cullen Granite (Fig. 2). The Minglo gossan is rich in Pb; the Mary River gossan is rich in Pb and Au, but is depleted in Zn, Ag, Cd and Co relative to the lode, and the Namoona gossan in places contains visible galena. The Namoona gossan strikes slightly discordant to the country rocks and discontinuous gossans to the northwest indicate that this deposit may lie on the same linear structure as the Mary River prospect.

The Namoona prospect consists of two lodes, one Pb-Zn and the other Pb, in calcarenite and pyritic carbonaceous shale of the Masson Formation which dips 60° to the southwest. In places the lodes appear bedded and elsewhere are located in minor shears. The Mary River mineralisation consists of sphalerite with inclusions of pyrite and stannite and subordinate pyrite and galena in a brecciated shear zone. The Minglo mine is located in a quartz-breccia zone 1-2m wide, and at surface the breccia contains secondary lead ochres and films. The host is pyritic carbonaceous shale of the Masson Formation, which is hornfelsed by the Cullen Granite, exposed 1.25km away. The vertical ore zone breccia cuts the host rocks

which dip 30° SSW. The ore consisted of galena and anglesite masses in the breccia and has been worked to a maximum depth of 15m.

Many of the Ag-Pb-Zn stratiform deposits in the Masson Formation appear to be confined to a 300m-thick sequence of siltstone and shale with calcarenite and sandstone in places. The pelitic rocks are carbonaceous and pyritic at depth, but commonly altered to brick-red hematitic siltstone at surface. This sequence underlies mafic volcanics, tuffaceous shale and greywacke of the Stag Creek Volcanics, about 1000m thick, which host minor copper and uranium deposits. The 300m-thick sequence in which the stratiform deposits occur is therefore at the top of the Masson Formation in the central part of the geosyncline. The Woodcutters and other base metal deposits at Rum Jungle are however located at the bottom of the Masson Formation, at or close to the contact with the underlying Coomalie Dolomite (Fig. 3).

3) Au, U-Au and Ag-Pb-Zn, Cu stratiform or stratabound deposits in the Koolpin Formation, Gerowie Tuff and Kapalga Formation.

The deposits of this category can be further divided into mainly Au deposits in tuff and ashstone of the Gerowie Tuff, U-Au deposits in carbonaceous shale of the Koolpin Formation, and Ag-Pb-Zn and Cu deposits in interlaminated ashstone, greywacke and siltstone of the Gerowie Tuff and Kapalga Formation. They make up about 0.3 percent of uranium production and reserves in the Pine Creek Geosyncline, and about 6 percent of total production and reserves of metals other than uranium (Table 5). Iron deposits are also formed from Koolpin Formation rocks by supergene processes, and are discussed under a subsequent heading. The three host formations constitute a distinctive suite of iron-rich carbonate rocks, banded iron formation, pelitic rocks and volcanics extending from the Rum Jungle area to the South Alligator Valley.

The mineralisation may be stratified and stratiform, or transgressive. The Ag-Pb-Zn deposits are stratiform; Goulevitch (this volume) describes conformable lenses of massive pyrrhotitic sulphide, with internal banding and foliation parallel to bedding, in the Iron Blow and Mount Bonnie mines, which exploit the same stratigraphic level in the Margaret Syncline in the western part of the Cullen mineral field (Fig. 2). Both deposits are represented at the surface by well developed stratabound gossans. The lodes consist of pyrrhotite, pyrite, sphalerite, galena, arsenopyrite, chalcopyrite and minor silver and antimony sulphides, in a gangue of dolomite, chlorite, talc, actinolite and quartz. At the Mount Bonnie mine several periods of faulting are represented which have affected the lode to varying degrees. Thrust-faulting parallel to the lode has caused pinching and swelling, and high-angle cross-faults and shears have displaced portions of the lode (Ivanac, 1974). Goulevitch proposed that dewatering of the underlying ashstones of the Gerowie Tuff provided a saline solution capable of transporting the metals. Devitrification of the ashstones could have provided a heat source and a means of liberating metals to the saline solution. Sea water in restricted sea floor depressions would have provided the source of reduced sulphur to precipitate the sulphides.

The Howley Anticline (Fig. 2) is another fold structure in the west of the Cullen mineral field that is well-endowed with stratabound mineralisation. The Cosmopolitan Howley (Au), Fleur de Lys (U, Cu), Chinese Howley (Au) and Big Howley (Cu) mines or prospects all lie at similar stratigraphic levels on this structure, in an interbedded sequence of slate, arenite, tuff, quartzite and chert. Gold occurrences are common in the cores of folds and may be concentrated in areas where the pitch of the fold changes, or in drag folds or areas of crumpling. Favourable horizons include chloritised carbonaceous schist with quartz and carbonate, some tuff beds, and nodular and lenticular chert-banded siltstone. The Cosmopolitan Howley deposit follows a contact between graphitic shale and underlying chlorite schist.

The base-metal deposits of the Margaret Syncline and Howley Anticline are most probably syngenetic, and metals were probably derived from the carbonaceous pelites and/or pyroclastics in the sequence. The gold deposits are associated with tourmalinites in the Koolpin Formation and Wildman Siltstone, suggesting concentration of metal in hot sea-floor brines (Nicholson, this volume). The concentration of deposits adjacent to granite

	tonnes	grade	contained metal (tonnes unless otherwise stated)
Cosmopolitan Howley	50,000	12.55 dwt Au	33,780 oz Au
Zapopan	40,000	13.4 dwt Au	26,650 oz Au
Brittania	220	3.8 oz Au	
Mount Ellison	3,250	20% Cu	650 Cu, 3 As
Iron Blow	13,700	5 dwt Au, 0.1-1.0% Cu (4-5% Pb, 6-14% Zn, 10-20 oz Ag in places	60 Cu
Mount Bonnie	500,000	1.5% Pb, 7.7% Zn, 6 gm/T Ag	96 460 oz Ag, 7 500 Pb, 38 500 Zn
Phillip Greets	360	25-30% Zn	90 Cu
Evelyn	80,000	5.5% Pb, 7.5% Zn, 275 gm/T Ag	784 300 oz Ag, 243 oz Au, 104 770 lb Cd, 4 990 Cu, 5 980 Zn
McCarthys	570	70% Pb, 10 oz Ag	5 700 oz Ag, 400 Pb
Coronation Hill	25,700	0.3% U_3O_8	75 U_3O_8
Saddle Ridge	29,800	0.2% U_3O_8	78 U_3O_8
El Sherana	38,400	0.5% U_3O_8	226 U_3O_8
El Sherana West	21,300	0.8% U_3O_8	185 U_3O_8
Rockhole-Teagues	13,200	1.1% U_3O_8	152 U_3O_8
Palette	4,700	2.5% U_3O_8	124 U_3O_8
Scinto 5	5,700	0.4% U_3O_8	22 U_3O_8
Scinto 6	1,700	0.15% U_3O_8	3 U_3O_8
Koolpin Creek	2,300	0.12% U_3O_8	3 U_3O_8
Skull	530	0.5% U_3O_8	3 U_3O_8
Sleisbeck	600	0.4% U_3O_8	3 U_3O_8

Table 5. Tonnage/grade figures for some Au, U-Au and Ag-Pb-Zn, Cu stratiform deposits in the Koolpin and Kapalga Formations and Gerowie Tuff.

suggests that heat associated with the intrusive event may have assisted in any post-lithification mobilisation of metal. Ore-carrying fluids may have been derived from dewatering of the sequence, or from the granite. Low-pressure structures are apparently the main control of ore deposition sites.

The mine with the highest value of production in this category in the Cullen mineral field is the Evelyn mine (Ag-Pb-Zn-Cd-Au, Fig. 2), which worked a small group of lodes in limestone and calcareous slate of the Koolpin Formation. Although the deposit is stratabound, some parts of it appear to be skarn, suggesting that the ore solutions in this ore body may have been magmatic; metals may then have accompanied magmatic solutions, as an alternative to being mobilised from Koolpin Formation sediments.

The primary ore zone mainly contained galena and sphalerite; hydrozincite, smithsonite, cerussite, anglesite and secondary copper minerals occurred in the secondary zone (Rowston, 1957). The lodes transgressing the bedding are up to 2m wide, situated 'en echelon', and can be traced on the surface for up to 80m. The area is dominated by a large east-striking fault at which all lodes terminate. Small fractures related to this main fault are thought to have provided favourable channels for the ore solutions during the Cullen Granite intrusion. The Cullen Granite has an extensive contact metamorphic aureole. Near the granite limestone has been altered to marble and calcium-magnesium-silicate rocks rich in tremolite and diopside, garnet?, chrysotile, anthophyllite and antigorite. carbonaceous shale has been altered to cordierite-andalusite and/or chiastolite hornfels, and psammitic rocks to a variety of hornfels.

Most of the U and U-Au deposits of the South Alligator Valley are stratabound in the Koolpin Formation (Crick *et al.*, this volume). The mineralisation is mainly pitchblende, which is usually associated with gold, minor iron and copper, and in places silver, niccolite, cobalt-nickel arsenides and galena (Threadgold, 1960). Most of the deposits are in faults, shears or fractures in carbonaceous shale of the Koolpin Formation. About 35 percent of past production comprised secondary U minerals with minor primary uranium ore in overlying Carpentarian (Middle Proterozoic) felsic volcanics and sandstone (Edith River Volcanics). The metals may be derived from the uranium-enriched Edith River Volcanics or black shales of the Koolpin Formation. Another possible source is volcanism associated with the Gerowie Tuff, although this unit is not known to be enriched in U in the South Alligator Valley area.

4) Au, Sn, Ag-Pb, W, Ta, Cu, Bi vein-type deposits mainly related to early Carpentarian (early-Middle Proterozoic) granites.

Most of these deposits are either close to exposed granite or overlie concealed granite; they are commonly concentrated on major shear zones. They account for about 10 percent of production and reserves for all metals except uranium, and about 3 percent of uranium production and reserves are in vein-type deposits (Table 6). Cusp areas are characterised by a greater number of pegmatites and a range of metals, and in places copper may indicate the presence of concealed granite (e.g. the Daly River mineral field, Fig. 2). Mineralisation associated with deeper parts of granite bodies, as in the Cullen mineral field, is mainly in quartz veins or quartz-filled shears. Many deposits in this field are in cross-cutting quartz veins within Koolpin Formation rocks, suggesting hydrothermal remobilisation of syngenetic metals. However the bulk of the deposits are hosted in the Burrell Creek Formation and undoubtedly have a magmatic origin.

The Union Reefs group of mines (Fig. 2) is typical of vein-type gold deposits in the Burrell Creek Formation. The mines are in a major NNE-trending shear zone within an embayment in the Cullen Granite. The host rocks are tuffaceous greywacke, slate and siltstone, with minor amphibolite dykes, metamorphosed in places to andalusite-mica schist and mica schist (Shields *et al.*, 1967). Most workings are on two near-vertical zones of

intense shearing. The ore is native gold, pyrite, arsenopyrite, chalcopyrite, galena and marcasite in quartz reefs up to 5m wide, with minor carbonate veinlets. Some deposits have undergone supergene enrichment. Production records are incomplete, but probably more than half of the recorded gold production came from nearby alluvial deposits.

The Yeuralba mines (Fig. 2) exemplify the other metal groups occurring in vein-type deposits. The Yeuralba Granite is surrounded by a narrow metamorphic aureole in the Burrell Creek Formation. Metals are contained in quartz reefs, pegmatites and greisens. The Yeuralba deposit comprises Cu, Sn, W and minor Bi mineralisation in a tourmaline-topaz

	tonnes	grade	contained metal (tonnes unless stated otherwise)
Maranboy (several mines)	55,000	1.6% Sn	1 400 Sn
Mount Wells	100,000	1% Sn	1 530 Sn, 3 Cu
Jessops + Billy Can	10,000	1% Sn	354 Sn
Mount Masson	5,700	1.10% Sn	94 Sn
Mt Harris + Margaret + Buffalo	3,900	1.10% Sn	43 Sn
Coronet Hill	250	22% Cu	55 Cu
Waldens	1,220	8-10% Cu	100 Cu
Daly River	6,000	20% Cu	1 200 Cu
Empire	133	8% Cu	15 Cu
Wallaby	30	35% Cu	10 Cu
Pine Creek	68,000	1.4 oz Au	95,500 oz Au, 255 oz Ag, 1 Pb, 1.6 Sn
Copperfield	2,140	12% Cu	260 Cu
Kellys	32	4.4% Sn	? Sn
Wolfram Hill	230	30% Cu	440 WO_3, 70 Cu
Wests	25	70% Pb, 34 oz Ag	850 oz Ag, 17.5 Pb
Driffield	10,700	10 dwt Au	5 300 oz Au
Jones Bros Reef	1,140	16 dwt Au	915 oz Au
Yeuralba	50	24% Cu	40 WO_3, 13 Sn, 12 Cu
Nabarlek	494,470	1.84% U_3O_8	9 550 U_3O_8
Adelaide River	5,300	0.5% U_3O_8	45 U_3O_8
George Creek	371	0.26% U_3O_8	1 U_3O_8
King River	111	2.8% Sn	4.7 Sn

Table 6. Tonnage/grade figures for some vein-type deposits in the Pine Creek Geosyncline.

greisen and associated quartz-tourmaline lodes on the western margin of the granite; some lodes also carry fluorite and apatite (Walpole,1958).

Minor vein-type Au and Sn occurrences in Mount Partridge Group sediments north of the South Alligator Valley mineral field appear to be related to a marked gravity low which may represent a concealed granite body. Minor Pb-Zn occurs in quartz breccia zones in the Nanambu Complex in the southwest part of the Alligator Rivers mineral field.

5) Supergene iron deposits in the Wildman Siltstone and Koolpin Formation.

Outcrops of the Koolpin Formation, and in places the Wildman Siltstone, are commonly rich in iron, and in many places ridges of these rocks are capped with false gossans overlying pyritic black shales. Banded iron formation is developed in both formations in some areas. Surface iron enrichment is most pronounced in the Frances Creek Iron Field, where the Frances Creek and Mount Bundey deposits represent particularly strong concentrations of supergene iron ore along a line of more or less continuous near-surface iron enrichment over favourable strata.

The Frances Creek mine (Fig. 2) consisted of 5 deposits cropping out intermittently over a strike length of 15km, along the bedding of the host arenite, siltstone and pyritic black shale of the Wildman Siltstone. Individual deposits are generally tabular to lenticular, up to 600m long and 20m wide; several of the deposits were prominent outcrops before mining, with sheer walls in places up to 20m high (Crohn, 1968). The Mount Bundey deposit (Fig. 2) consisted of two tabular ironstone bodies (consisting of a martite cap over a magnetite-martite-pyrite lode) interbedded with banded carbonaceous and pyritic siltstone, within a raft of Koolpin Formation in the Mount Bundey Granite (Ryan, 1975). Both orebodies appear to have resulted from supergene enrichment of ferruginous beds in pre-Cretaceous times, as the Cretaceous Petrel Formation unconformably overlies part of the Frances Creek deposit. In the Mount Bundey deposit, syngenetic disseminated and bedded pyrite within the siltstone was probably converted to magnetite during granite intrusion, and futher continuous supergene enrichment by the formation of martite, hematite and goethite, resulted in the development of the iron ore lodes (Ryan, 1975).

METALLOGENESIS

The character of the deposits and their stratigraphic, structural and petrological associations suggest that metals were derived from three major sources. The first is the early Carpentarian (early Middle Proterozoic) granites, which are undoubtedly the major source for most of the vein-type deposits. The second is the Archaean inliers, which are widely held to be the source of the uranium in the Masson and Cahill Formations; this is supported by the close spatial relationship between uranium deposits and exposed basement, and the recognition of the presence of uranium in the Archaean rocks in forms amenable to leaching and weathering, mainly as accessory uraninite (McAndrew & Finlay, this volume). Attention should be paid to other possible areas of Archaean basement in the hope of discovering additional basement associated deposits, particularly in the Litchfield Block — if further geochronological work supports an Archaean age for some of the rocks in this area — and a possible occurrence of concealed basement near Woolner homestead (80km east of Darwin, Fig. 2). The third source, for stratabound base-metal and related deposits in the Lower Proterozoic rocks of the Pine Creek Geosyncline, is probably volcanic. These deposits occur at stratigraphic levels close to volcanic rocks, and the presence of banded iron formation at one of these levels suggests that metals were introduced into the system in brines formed by submarine volcanic exhalative activity. The recent recognition of more volcanic rocks in the Lower Proterozoic sequence in Wildman Siltstone (P.G. Stuart-Smith, pers. comm., 1979), improves the base-metal potential of this generally poorly exposed unit.

The origin of uranium in the South Alligator Valley deposits remains equivocal. The

uranium enrichment of the Edith River Volcanics and broad spatial relationship between mineralisation and the volcanics suggest that uranium was leached from those rocks and was transported to nearby low-pressure sites in fault breccias at or near the Edith River Volcanics/Koolpin Formation contact, where precipitation took place under reducing conditions in pyritic carbonaceous shale of the Koolpin Formation. Subsequent erosion and exhumation changed the chemical environment of the deposits, and resulted in oxidation of much of the ore on the volcanic side of the stratigraphic contact. Alternatively, syngenetic uranium in the Koolpin Formation may have been mobilised and concentrated by epigenetic processes into the fault breccias.

CONCLUDING REMARKS

The history of the Pine Creek Geosyncline is mainly concerned with the development of numerous small shallow workings of a range of metals. Only in relatively recent times have large deposits been discovered requiring more than a decade to mine. These have all been uranium deposits, but the presence of more gold in the Jabiluka Two deposit than all previously recorded production for that metal in the province is encouraging for the future prospects for gold. However, gold is likely to be a by-product of uranium mining as it has not been found alone in this type of deposit and as direct exploration for gold in this terrane is difficult.

The recognition of extensive favourable strata for base metals has encouraged exploration in the central part of the geosyncline. Here exposure is relatively good and exploration is not hampered by the deep weathering and surficial deposits so common elsewhere. No significant announcements of exploration successes have been made to date, although several prospects have been located.

The main potential for the province remains uranium. The large deposits are confined to the Alligator Rivers region, and the only major feature of those deposits not shared by others in the province is the regional amphibolite-grade metamorphism of the host rocks. It is likely therefore that the 1800 Ma orogenesis played an important but as yet poorly understood role in ore genesis, and that future discoveries of large uranium deposits are likely to be confined to the northeast part of the geosyncline. The amphibolite-grade metasediments of the Litchfield Block may also be prospective, particularly if Archaean rocks are discovered in the area. So far exploration has been based mainly on follow-up of airborne and ground radiometric surveys, but owing to the generally extensive overburden this must be regarded as largely ineffective in much of the region. Future methods for exploration, if permitted in the national park which covers the most prospective areas, must be designed primarily to define concealed stratigraphy. This concept has already been applied on a local scale, and has paid enormous dividends in adding 52 million tonnes of 0.4 percent U_3O_8 to the 1.4 million tonnes of 0.26 percent U_3O_8 initially discovered at Jabiluka.

ACKNOWLEDGEMENTS

We wish to thank Ian Crick and Peter Stuart-Smith for helpful discussions in the draft stage, and John Goulevitch and David Trail for their extensive constructive criticism of the paper. This paper is published with the permission of the Director, Bureau of Mineral Resources, Geology and Geophysics, Canberra.

REFERENCES

Binns, R.A., McAndrew, J. & Sun, S-S, this volume: Origin of uranium mineralisation at Jabiluka. *Proceedings of the International Uranium Symposium on the Pine Creek Geosyncline.*

Crick, I.H. & Muir, M.D., this volume: Evaporites and uranium mineralisation in the Pine Creek Geosyncline. *Proceedings of the International Uranium Symposium on the Pine Creek Geosyncline.*

Crick, I.H., Muir, M.D., Needham, R.S. & Roarty, M.J., this volume: The geology and mineralisation of the South Alligator Valley Uranium Field. *Proceedings of the International Uranium Symposium on the Pine Creek Geosyncline.*

Crohn, P.W., 1968: The mines and mineral deposits of the Katherine-Darwin region. *in* Walpole, B.P., Crohn, P.W., Dunn, P.R., & Randal, M.A., Geology of the Katherine-Darwin Region, Northern Territory. *Bull. Bur. Miner. Resour. Geol. Geophys. Aust., 82,* 171-282.

Crohn, P.W., 1975: Mineralisation in the Pine Creek Geosyncline. *in* (ed. C.L. Knight) *Economic Geology of Australia and Papua New Guinea. Australas. Inst. Min. Metall., Monograph Series No. 5, 1, Metals,* 269-271.

Dodson, R.G. & Shatwell, D.O., 1965: Geochemical and radiometric survey, Rum Jungle, N.T. 1964. *Rec. Bur. Miner. Resour. Geol. Geophys. Aust., 1965/254* (unpubl.).

Eupene, G.S., Fee, P.H. & Colville, R.G., 1975: Ranger 1 uranium deposits. *in* (ed. C.L. Knight), *Economic Geology of Australia and Papua New Guinea. Australas. Inst. Min. Metall. Monograph Series No. 5, 1. Metals,* 308-317.

Ferguson, J., this volume: Metamorphism in the Pine Creek Geosyncline and its bearing on stratigraphic correlation. *Proceedings of the International Uranium Symposium on the Pine Creek Geosyncline.*

Ferguson, J., Ewers, G.R. & Donnelly, T.H., this volume: Model for the development of economic uranium mineralisation in the Alligator Rivers Uranium Field. *Proceedings of the International Uranium Symposium on the Pine Creek Geosyncline.*

Fraser, W.J., 1975: The Embayment line of mineralization, Rum Jungle. *in* (ed. C.L. Knight) *Economic Geology of Australia and Papua New Guinea. Australas. Inst Min. Metall Monograph Series No. 5, 1, Metals,* 271-277.

Fraser, W.J., this volume: Geology and exploration in the Rum Jungle Uranium Field. *Proceedings of the International Uranium Symposium on the Pine Creek Geosyncline.*

Goulevitch, J., this volume: Stratigraphy of the Kapalga Formation in the Pine Creek area and its relationship to base metal mineralisation. *Proceedings of the International Uranium Symposium on the Pine Creek Geosyncline.*

Hegge, M.R., Mosher, D.V., Eupene, G.S. & Anthony, P.J., this volume: Geologic setting and comparative review of the East Alligator uranium deposits and prospects. *Proceedings of the International Uranium Symposium on the Pine Creek Geosyncline.*

Hills, J.H. & Richards, J.R., 1976: Pitchblende and galena ages in the Alligator Rivers region, N.T., Australia. *Miner. Deposita, 11,* 133-154.

Ivanac, J.F., 1974: Exploration licence 615 Northern Territory. Results of exploration to 1st May 1974. *Central Pacific Minerals N.L.* (unpubl.).

McAndrew, J. & Finlay, C.J., this volume: The nature and significance of the occurrence of uranium in the Nanambu Complex of the Pine Creek Geosyncline. *Proceedings of the International Uranium Symposium on the Pine Creek Geosyncline.*

Needham, R.S., 1978: A regional analysis of the Pine Creek Geosyncline N.T. progress report. *James Cook Univ. Nth Qld Seminar Paper GL503* (unpubl.).

Needham, R.S., Crick, I.H. & Stuart-Smith, P.G., this volume: Regional geology of the Pine Creek Geosyncline. *Proceedings of the International Uranium Symposium on the Pine Creek Geosyncline.*

Needham, R.S., Smart, P.G. & Watchman, A.L., 1975: Progress report, Alligator River Party N.T., 1972 (Oenpelli Region). *Rec. Bur. Miner. Resour. Geol. Aust., Geophys., 1975/39* (unpubl.).

Needham, R.S. & Stuart-Smith, P.G., 1976: The Cahill Formation - host to uranium deposits in the Alligator Rivers Uranium Field, Australia. *BMR J. Aust. Geol. Geophys., 1,* 321-333.

Needham, R.S. & Stuart-Smith, P.G., this volume: Geology of the Alligator Rivers Uranium Field. *Proceedings of the International Uranium Symposium on the Pine Creek Geosyncline.*

Nicholson, P.M., this volume: The geology and economic significance of the Golden Dyke Dome. *Proceedings of the International Uranium Symposium on the Pine Creek Geosyncline.*

Noakes, L.C., 1949: A geological reconnaissance of the Katherine-Darwin region, N.T., with notes on the mineral deposits. *Bull. Bur. Miner. Resour. Geol. Geophys. Aust., 16,* 54p.

Page, R.W., Compston, B.W. & Needham, R.S., this volume: Geochronology and evolution of the late Archaean basement and Proterozoic rocks in the Alligator Rivers Uranium Field, Northern Territory, Australia. *Proceedings of the International Uranium Symposium on the Pine Creek Geosyncline.*

Roberts, W.M.B., 1973: Dolomitization and the genesis of the Woodcutters lead-zinc prospect, Northern Territory, Australia. *Miner. Deposita, 8,* 35-56.

Roberts, W.M.B., 1975: Woodcutters L5 lead-zinc prospect. *in* (ed. C.L. Knight), *Economic Geology of Australia and Papua New Guinea. Australas. Inst. Min. Metall. Monograph Series No. 5., 1. Metals,* 277-281.

Rowston, D.L., 1957: Geophysical survey at the Evelyn mine, Pine Creek district, Northern Territory. *Rec. Bur. Miner. Resour. Geol. Aust., Geophys., 1957/101* (unpubl.).

Ryan, G.R., 1975: Mount Bundey iron ore deposit, N.T. *in* (ed. C.L. Knight) *Economic Geology of Australia and Papua New Guinea. Australas. Inst. Min. Metall. Monograph Series No. 5, 1, Metals,* 952-958.

Threadgold, I.M., 1960: The mineral composition of some uranium ores from the South Alligator River area, Northern Territory. *Sci. ind. Res. Org., Melb., minerogr. Inv. tech. Pap. 2.*

Walpole, B.P., 1958: The Maranboy tinfield, Northern Territory. *Bull. Bur. Miner. Resour. Geol. Geophys. Aust., 27*

Walpole, B.P., Crohn, P.W., Dunn, P.R. & Randal, M.A., 1968: Geology of the Katherine-Darwin region, Northern Territory. *Bull. Bur. Miner. Resour. Geol. Geophys. Aust., 82,* 304p.

RARE EARTH ELEMENTS IN SEDIMENTARY ROCKS, GRANITES AND URANIUM DEPOSITS OF THE PINE CREEK GEOSYNCLINE

Scott M. McLennan and S.R. Taylor

Research School of Earth Sciences, Australian National University, Canberra A.C.T. Australia

ABSTRACT

Rare earth elements (REE) and other trace elements have been analysed in fine-grained sedimentary rocks from several important Lower Proterozoic units in the Pine Creek Geosyncline. Samples from the lower part of the sequence (Group I) appear slightly evolved from typical Archaean sedimentary rocks (AAS) towards typical Post-Archaean sedimentary rocks (PAAS). They have slightly lower Eu/Eu* and higher LREE/HREE than AAS. Samples from the upper part of the sequence (Group II) resemble typical post-Archaean sedimentary rocks. These observations are consistent with REE patterns in the Lower Proterozoic Huronian succession of Canada and support the suggestion of a major, episodic change in the composition of the exposed upper crust at the Archaean-Proterozoic boundary. This change was probably related to large scale emplacement of K-rich granitic rocks into the upper crust at the end of the Archaean.

Analyses of U-rich sedimentary rocks from the Cahill Formation indicate significant REE mobility. Samples are highly fractionated and show decreasing La/Yb and increasing ΣREE (for samples with U $\geq$1900 ppm) with increasing U content. These patterns also display a chondrite-normalized negative Eu-anomaly. U-rich samples (U $\geq$1900 ppm) have a chondrite-normalized maximum at Tb. High HREE, U and low Th can be explained by carbonate complexing of U and REE in a low temperature hydrothermal ore solution. The solution was probably oxidizing with a pH >7.5.

No evidence for a natural fossil nuclear reaction was observed in any of the samples. The high abundances of the HREE seem typical of U-ores from the Pine Creek Geosyncline and Rabbit Lake uranium deposit, Canada. Many of these elements are extremely efficient neutron absorbers and would thus significantly inhibit spontaneous chain reactions.

INTRODUCTION

The average concentration of rare earth elements (REE) in fine-grained sedimentary rocks appears to reflect the composition of the exposed crust (see reviews by Nance & Taylor, 1976, 1977; Taylor, 1977, 1979; McLennan *et al.*, 1979). Any temporal variations of REE in sedimentary rocks bears significant information on important questions concerning the evolution of the continental crust. A major difference appears between typical REE patterns in Archaean and younger sedimentary rocks (Wildeman & Haskin, 1973; Jakeš & Taylor, 1974; Nance & Taylor, 1976, 1977; Taylor, 1977, 1979; Taylor & McLennan, 1980, for example). Typical Archaean sedimentary rock (AAS) patterns are less fractionated (LREE/HREE ~5.3), have lower total abundances (ΣREE ~71ppm) and less relative depletion of Eu (Eu/Eu* ~1.0, where Eu* is a theoretical value for no chondrite-normalized Eu anomaly) compared to typical post-Archaean sedimentary rock (PAAS) patterns (LREE/HREE ~9.4; ΣREE ~183 ppm; Eu/Eu* ~0.67; see Table 1). In a study of the Lower Proterozoic Huronian succession of Canada, McLennan *et al.* (1979) observed the changeover in REE patterns and noted the short time interval over which it occurred. From these observations, they concluded that a major episodic change in the composition of the exposed crust took place at the end of the Archaean. The change was probably related to pervasive emplacement of K-rich granitic rocks into an Archaean upper crust previously dominated by a 'tonalite' - greenstone suite. This would be compatible with an overall compositional change for the *upper* crust from andesite to granodiorite (Taylor, 1979). The Lower Proterozoic Pine Creek Geosyncline (PCG) was probably deposited sometime between 2400-1870 m.y. (Page *et al.*, this volume) and thus provides a good Australian example for studying these trends.

There is very little information available on REE distribution in sedimentary uranium deposits. These elements are not normally affected by metamorphism (Green *et al.*, 1969, 1972; Cullers *et al.*, 1974). Since the chemical behaviour of REE is fairly predictable (see

Gschneidner & Eyring, 1979 for most recent summary), REE may prove useful for looking at conditions of uranium ore formation. For these reasons, REE distributions in the U-rich Cahill Formation (Needham & Stuart-Smith, 1976) have also been examined.

Discovery of the natural nuclear reactor at Oklo, Gabon, has led to intensification of the search for other occurrences in rocks of similar age. Examining the possibility of finding a fossil nuclear reactor in the Pine Creek Geosyncline is, in fact, a major purpose of the present proceedings. Understanding the REE distributions in a potential reactor area is crucial in analysing the feasibility and characteristics of a natural nuclear reactor (Loubet & Allegre, 1977). This aspect is considered in the present work.

SAMPLES

Sedimentary rocks of the Pine Creek Geosyncline lie unconformably on an Archaean basement and were deposited sometime during the interval of about 2400-1870 m.y. (Page *et al.*, this volume). The most recent stratigraphic analysis has been summarized by Needham *et al.* (this volume).

For the present study, sedimentary rock samples from the Pine Creek Geosyncline (PCG) have been subdivided into three groups. Group I includes primarily fine-grained sedimentary rocks from the lower part of the PCG succession, including samples from the Batchelor and Namoona Groups and the lower Mount Partridge Group (excluding the Nourlangie Schist and Wildman Siltstone). Two samples from this part of the succession (PCG213, PCG41) are considered anomalous and are discussed separately. Group II represents samples from the upper part of the Pine Creek Geosyncline succession encompassing the upper Mount Partridge Group (Nourlangie Schist and Wildman Siltstone) and the South Alligator and Finniss River Groups. Sample PCG26, from this part of the succession is considered separately. This stratigraphic subdivision is essentially arbitrary and is based solely on REE characteristics. The U-rich Cahill Formation is considered as a separate group.

Three granitic rock samples from the late Archaean (ca.2500 m.y.), Nanambu Complex (Page *et al.*, this volume) were also analysed in order to assess possible effects on the sedimentary REE patterns.

Details of location and petrography, for all PCG-numbered samples, are given in Ferguson & Winer (this volume), who also give complete major and trace element analyses (including La, Ce and Y).

ANALYTICAL METHODS

Most samples were analysed for trace elements by spark source mass spectrometry using the method described by Taylor & Gorton (1977). This technique provides data for Th, U, Hf, Nb, Ba, Pb, Cs, Zr, Tl, W, Mo, Sn, Bi, Y and 12 REE (excluding Tm and Lu). Analytical precision and accuracy is typically about $\pm$ 5%. Four U-rich samples (PCG52, PCG57, PCG148, 75080260) from the Cahill Formation were analysed for REE only, by a modified version (Fryer, 1977a) of an ion exchange — X-ray fluorescence procedure of Eby (1972). Analytical error for this technique is estimated at about $\pm$10%. U and Th values for samples PCG52, PCG57, and PCG148 were taken from Ferguson & Winer (this volume). The U value for sample 75080180 was made available by J. Ferguson.

In the tables, a dash indicates that no determination was made in this study, while an asterisk indicates that the element was below detection limits. LREE represents the sum of La, Ce, Pr, Nd and Sm while HREE represents the sum of Gd, Tb, Dy, Ho, Er, Tm (estimated), Yb and Lu (estimated). Chondrite values used for normalizing are given in table 1.

Sample	AAS[a]	PAAS[b]	CHONDRITES[c]
La	12.6	38	0.315
Ce	26.8	80	0.813
Pr	3.13	8.9	0.116
Nd	13.0	32	0.597
Sm	2.78	5.6	0.192
Eu	0.92	1.1	0.0722
Gd	2.85	4.7	0.259
Tb	0.48	0.77	0.047
Dy	2.93	4.4	0.325
Ho	0.63	1.0	0.0718
Er	1.81	2.9	0.213
Tm	-	-	0.0300
Yb	1.79	2.8	0.208
Lu	-	-	0.0323

a) Data from Taylor and McLennan (1980).

b) Data from Nance and Taylor (1976).

c) Data from Taylor and Gorton (1977).

Table 1. Rare Earth Elements (REE) in AAS, PAAS and Chondrites (in ppm).

RESULTS AND DISCUSSION

Group I

Analytical results for Group I samples are presented in table 2. Chondrite-normalized REE plots are given in figure 1. These samples have slightly more relative depletion in Eu (average $Eu/Eu^* = 0.85$) and are significantly more fractionated (average LREE/HREE = 12.5) than Archean sedimentary rocks (see below; Fig. 8).

Sample PCG213 (Beestons Formation, sandstone) is similar to other Group I samples (Fig. 2) but has very much lower total abundances (ΣREE = 19.1 ppm) and a concave upwards heavy REE pattern (chondrite-normalized Gd/Yb = 0.90) suggestive of some HREE enrichment. The low ΣREE is easily explained by a dilution effect of quartz (SiO_2 = 89.67%; Ferguson & Winer, this volume), which contains very low REE content. The cause of the HREE enrichment is less certain. Some heavy minerals (e.g. zircon) do contain highly enriched HREE patterns and could cause

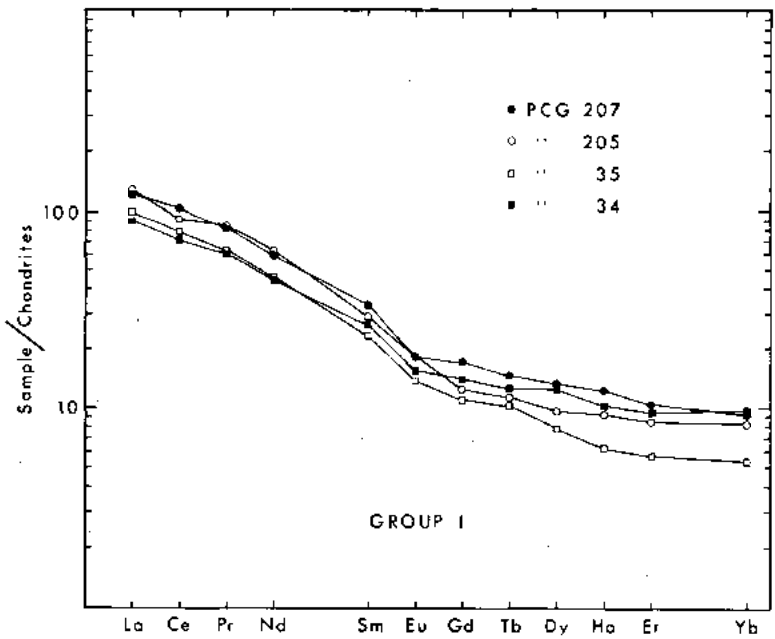


Figure 1. Chondrite - normalized REE patterns for samples from the lower part of the Pine Creek Geosyncline succession (Group I).

HREE enrichment (McLennan *et al.*, 1979). On the other hand, the low concentrations of other heavy mineral-related trace elements (e.g. Th, U, Hf, Zr) in this sample, do not clearly support such a mechanism.

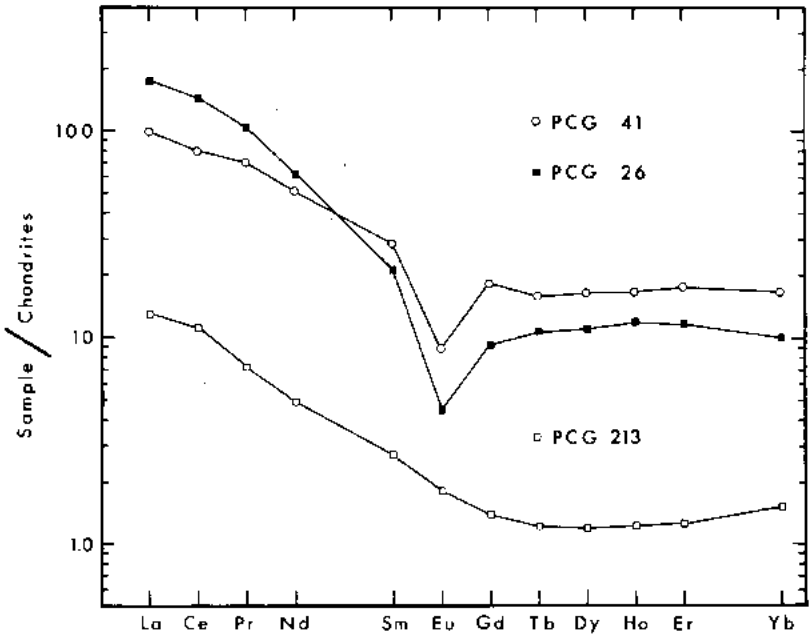


Figure 2. Chondrite - normalized REE patterns for selected samples from the Pine Creek Geosyncline. See text for discussion.

Sample PCG41 (Masson Formation, grey slate; Fig. 2) is unlike any other Group I sample, and is very similar to typical Group II samples (see below). This rock is from the Rum Jungle area (131°07'E, 12°56'S) and was originally included in the Golden Dyke Formation (Walpole *et al.*, 1968). Stratigraphic relations are obscure in this region and not yet fully resolved (Needham *et al.*, this volume). We remain unconvinced that this sample originates from the lower part of the Pine Creek Geosyncline sequence.

Group II

Results from Group II samples are given in table 2 and chondrite-normalized REE plots in figure 3. The Group II samples appear very similar to typical post-Archaean sedimentary rocks though some are even more depleted in Eu (average $Eu/Eu^* = 0.56$ compared to 0.67 for PAAS).

Sample PCG26 (Koolpin Formation, black shale) has a REE pattern similar to most Group II samples (Fig. 2) but has significantly less Eu than expected ($Eu/Eu^* = 0.32$) and less fractionated HREE (chondrite-normalized Gd/Yb = 0.92). PCG26 also has significantly higher U than other Group II samples (U = 26 ppm) and this possibly could have affected the REE pattern (see below).

Clear differences between Groups I and II can also be seen in the concentrations of several other trace elements. Group II has more abundant Zr and Hf, less aboundant Nb(?), Ba, Tl, Mo and Bi and higher Th/U.

Nanambu Complex granitic rocks

Trace element results for the 3 samples from the Nanambu Complex are presented in

	GROUP I						GROUP II					
Sample	PCG273	PCG34	PCG35	PCG47	PCG205	PCG207	PCG26	PCG200	PCG201	PCG23	PCG20	PCG21
Formation	Beestons	Masson	Masson	Masson(?)	Mundogie biot.-musc. -qtz. phyllite	Mundogie	Koolpin	Kapalga	Kapalga	Burrell Creek	Nourlangie	Nourlangie
Lithology	sandstone	siltstone	siltstone	slate		argillite	shale	mica schist	slate	siltstone	siltstone	siltstone
Th	4.1	17	14	16	11	14	17	12	43	12	8.4	11
U	0.60	5.9	2.8	5.9	3.2	4.4	26	2.9	11	3.5	2.1	1.8
Hf	0.80	6.9	2.0	3.3	2.8	2.8	6.3	5.7	6.1	5.3	4.3	6.5
Nb	2.9	18	14	11	12	17	22	13	23	14	6.0	6.5
Ba	223	1114	1244	258	742	868	165	407	733	420	590	468
Pb	7.2	126	5.9	18	7.4	28	9.0	30	9.8	10	5.1	8.9
Cs	0.59	4.5	6.0	2.5	8.9	10	7.0	11	8.9	9.9	0.78	0.44
Zr	19	137	58	116	82	101	176	194	191	119	134	191
Tl	0.56	1.4	1.1	0.36	1.1	1.4	1.5	0.72	1.1	0.79	0.44	*
W	*	0.82	0.34	0.54	0.56	0.2	2.0	*	1.3	0.85	0.17	*
Mo	*	0.98	0.33	0.25	0.26	*	1.3	*	*	*	*	*
Sn	0.46	4.7	2.9	3.3	2.8	6.1	4.9	5.1	12	7.2	2.0	2.0
Bi	0.09	0.60	*	0.48	0.25	0.11	0.10	0.15	*	0.27	0.07	*
La	4.0	28	31	31	40	38	55	27	73	46	31	32
Ce	9.1	57	63	63	74	84	117	55	150	97	70	60
Pr	0.83	6.8	7.2	8.1	9.7	9.4	12	5.5	16	11	7.4	6.3
Nd	2.9	26	27	30	37	35	37	21	59	41	26	22
Sm	0.63	5.0	4.4	5.4	5.5	6.3	4.1	4.8	11	6.9	5.6	4.0
Eu	0.13	1.1	0.98	0.63	1.3	1.3	0.32	0.91	2.4	1.1	0.88	0.65
Gd	0.36	3.6	2.8	4.7	3.2	4.4	2.4	4.7	9.1	5.2	3.3	3.0
Tb	0.06	0.61	0.50	0.76	0.55	0.71	0.53	0.73	1.5	0.78	0.57	0.48
Dy	0.39	4.0	2.5	5.3	3.1	4.3	3.6	4.1	7.8	4.7	3.3	2.6
Ho	0.09	0.74	0.45	1.2	0.67	0.89	0.88	0.91	1.7	0.91	0.62	0.56
Er	0.27	2.0	1.2	3.7	1.8	2.2	2.5	2.3	5.1	2.5	1.7	1.6
Yb	0.32	2.0	1.1	3.4	1.7	1.9	2.1	2.1	4.7	2.1	1.6	1.6
ΣREE	19.1	137.5	142.5	158.2	179.0	189.0	238.1	129.7	341.7	220.0	152.5	135.1
Y	2.8	31	12	36	19	16	29	18	47	28	14	15
ΣREE+Y	21.9	168.5	154.5	194.2	198.0	205.0	267.1	147.7	388.7	248.0	166.5	150.1
Eu/Eu*	0.88	0.80	0.87	0.39	0.95	0.77	0.32	0.59	0.43	0.57	0.53	0.58
La/Yb	12.5	14.0	28.2	9.1	23.5	20.0	26.2	12.9	15.5	20.9	19.4	21.3
LREE/HREE	11.9	9.1	14.9	6.8	34.4	11.5	17.8	7.3	9.9	11.9	12.1	12.2
Th/U	6.8	2.9	5.0	2.7	3.4	3.2	0.65	4.1	3.9	3.4	4.0	6.1

Table 2. Trace element analyses of Group I and Group II samples from the Pine Creek Geosyncline (in ppm).

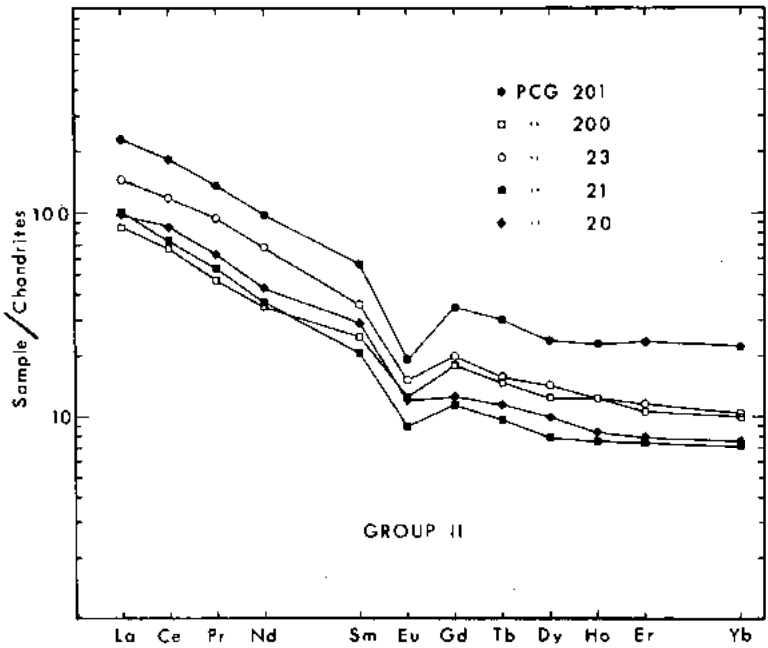


Figure 3. Chondrite - normalized REE patterns for samples from the upper part of the Pine Creek Geosyncline succession (Group II). Note the negative Eu - anomaly in all of the samples.

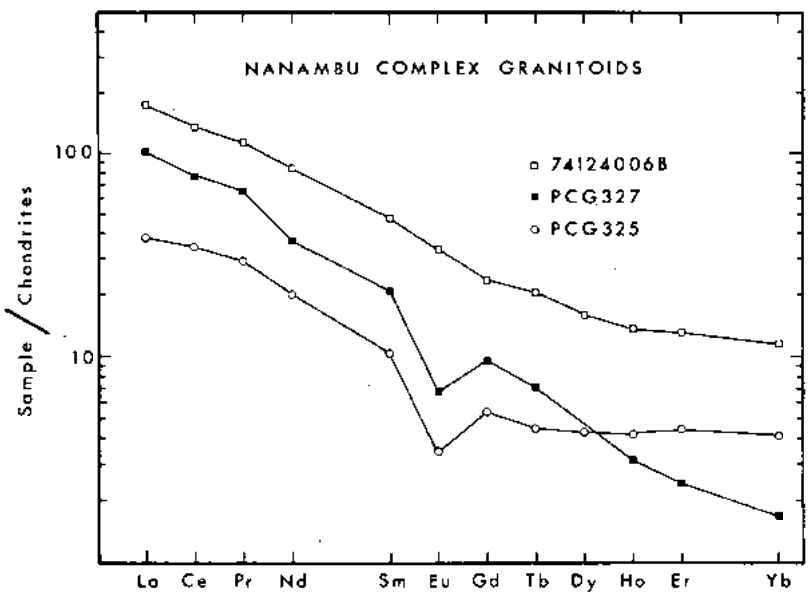


Figure 4. Chondrite - normalized REE patterns for granitic rocks from the Late Archaean Nanambu Complex. Note the negative Eu-anomalies in samples PCG325 and PCG327.

Sample	PCG325	PCG327	741240068
Th	17	21	6.2
U	5.3	3.5	0.61
Hf	2.2	3.2	7.8
Nb	16	5.4	13
Ba	308	352	1396
Pb	35	53	12
Cs	3.7	1.4	1.3
Zr	68	77	219
Tl	1.3	0.91	*
W	*	*	*
Mo	1.5	*	0.59
Sn	7.5	0.83	1.4
Bi	*	*	*
La	12	32	54
Ce	28	62	109
Pr	3.4	7.6	13
Nd	12	22	50
Sm	2.0	4.0	9.1
Eu	0.25	0.49	2.4
Gd	1.4	2.5	6.1
Tb	0.22	0.35	1.0
Dy	1.4	-	5.2
Ho	0.31	0.23	1.0
Er	0.95	0.62	2.8
Yb	0.86	0.35	2.4
ΣREE	63.1	134.0	256.7
Y	13	5.7	26
REE+Y	76.1	139.7	282.7
Eu/Eu*	0.46	0.48	1.00
La/Yb	14.0	91.4	22.5
LREE/HREE	10.6	23.8	12.2
Th/U	3.2	6.0	10.1

Table 3. Trace element analyses of granitic rock samples from the Nanambu Complex, Pine Creek Geosyncline (in ppm).

table 3. Chondrite-normalized REE plots are displayed in figure 4. Cursory examination shows that there is a wide variation in trace element concentrations among these three samples (for example, Ba: 308-1396 ppm, Zr: 68-219 ppm, La/Yb: 14.0-91.4 and Th/U: 3.2-10.1). Such variations are typical for rocks of granitic composition (Hanson, 1978).

Of particular interest to this study is the observation that two of three samples (PCG325, PCG327) exhibit strong negative Eu-anomalies (Eu/Eu* = 0.46, 0.48). The K_2O contents are 4.53 and 5.17 percent, respectively (Ferguson & Winer, this volume). The most probable mechanism of producing such Eu depletion is partial melting where feldspar (most likely plagioclase) is a residual phase. Plagioclase is not stable below about 40km (10 kb) suggesting that such melting would be a relatively shallow, intracrustal process.

Cahill Formation

Trace element analyses for samples from the Cahill Formation are given in table 4. Chondrite-normalised REE plots are presented in figure 5.

Sample PCG132 does not have anomalous U content (U = 1.4 ppm; Th/U = 4.7) and thus represents a normal, unmineralized sample. REE distributions for this rock are essentially intermediate between Group I and Group II samples (cf. Table 5) but the chondrite-normalised plot suggests it is most similar to Group II (Fig. 3). No clear distinction can be made on the basis of other trace element concentrations. Consideration of metamorphic grades led Ferguson (this volume) to suggests that the Cahill Formation was part of the basement during Pine Creek Geosyncline sedimentation and may, in fact, belong to the Older Domain of the early Proterozoic North Australian Orogenic Province. This differs substantially from the interpretation of Needham *et al.* (this volume), who correlate the Cahill Formation with rocks of the Namoona Group to the west. Distinction on the basis trace element concentration is equivocal. In any event, we would never date or correlate any suite of rocks solely on the basis of chemical composition.

As U content increases in the Cahill Formation, REE patterns change drastically (Fig. 5). There is a strong inverse correlation between U content and La/Yb (Fig. 6). For rocks with U $\gtrsim$1900 ppm, there is also a correlation of U and ΣREE (see Fig. 5). Samples with U $\gtrsim$1900 ppm also show a chondrite-normalized maximum at Tb. No systematic variations in Eu behaviour are apparent. Sample 75080260 is an impure uraninite (uraninite + fourmarierite + secondary U and Pb minerals) and has a REE pattern which parallels other U-rich samples. Simple mixing calculations involving PCG132 and 75080260 indicate that uraninite alone cannot control the REE patterns of the U-rich samples. For example, a theoretical mixture corresponding to about 10% uraninite would yield ΣREE<300 ppm.

Sample	PCG52	PCG57	PCG66	75080180	PCG106	PCG132	PCG148	75080260
Lithology	graph.-chl.-qtz.schist	chl.-qtz. schist	chl.-musc.-qtz.schist	qtz.-mica-chl.-hem. schist	chl.-musc.-qtz.schist	musc.-biot.-qtz.schist	musc.-chl.-qtz.schist	impure uraninite
Th	10	13	20	15	16	6.6	9	-
U	12,580	1,900	455	48,230	229	1.4	3,720	-
Hf	-	-	5.6	4.3	4.6	3.8	-	-
Rb	-	-	15	19	13	7.6	-	-
Ba	-	-	551	301	149	408	-	-
Pb	-	-	80	-	39	26	-	-
Cs	-	-	3.1	1.6	2.4	4.1	-	-
Zr	-	-	187	220	116	64	-	-
Tl	-	-	0.40	*	0.32	0.55	-	-
W	-	-	1.5	*	1.6	0.44	-	-
Mo	-	-	3.9	61	1.4	1.1	-	-
Sn	-	-	6.4	4.5	6.4	2.0	-	-
Bi	-	-	2.3	50	0.15	0.19	-	-
La	4.2	1.7	31	5.6	7.9	27	1.5	30
Ce	23	4.8	79	43	15	58	6.5	92
Pr	-	-	12	11	1.7	6.2	-	-
Nd	32	6.2	52	77	6.5	21	7.9	200
Sm	28	4.2	10	79	1.7	3.9	5.8	214
Eu	11	1.4	1.6	24	0.20	0.80	2.1	61
Gd	47	6.6	8.4	183	2.0	3.1	13	277
Tb	13	1.8	1.5	55	0.47	0.53	3.6	83
Dy	73	10	8.8	329	3.6	3.2	23	490
Ho	-	-	1.8	55	0.84	0.58	-	-
Er	23	3.6	4.8	128	2.7	1.7	10	144
Yb	19	2.9	3.7	89	2.6	1.5	7.9	127
ΣREE	294.8	47.2	215.8	1075.5	46.0	128.0	89.3	1853
Y	137	30	40	-	15	13	85	735
ΣREE+Y	431.8	77.2	255.8	-	61.0	141.0	174.3	2588
Eu/Eu*	0.94	0.82	0.54	0.63	0.34	0.71	0.75	0.78
La/Yb	0.22	0.59	8.4	0.062	3.0	18.0	0.19	0.24
LREE/HREE	0.46	0.65	5.1	0.26	2.9	10.5	0.36	0.45
Th/U	0.0013	0.0068	0.044	0.0003	0.079	4.7	0.0024	-

Table 4. Trace element analyses of samples from the Cahill Formation, Pine Creek Geosyncline (in ppm).

Sample 75080180, which has only about 5% U, contains ΣREE = 1075.5 ppm. Also, the low values of La, Ce, Pr and Nd seen in several U-rich samples cannot be achieved by such mixing.

There also appears to be a correlation among U, ΣREE and Pb and Bi (Table 3). The Pb content is obviously due to a radiogenic species formed from uranium. The Bi correlation is also predictable since there is commonly a strong coherence between Bi and HREE (Ahrens & Erlank, 1969). Another important observation is the total absence of systematic behaviour between U and Th as shown by the strong inverse correlation between U and Th/U (Fig. 7).

IMPLICATIONS FOR CRUSTAL EVOLUTION

Table 5 summarises the important REE statistics for Group I and II rocks as well as AAS and PAAS (Nance & Taylor, 1976; Taylor, 1979; Taylor & McLennan, 1980). Group I samples are essentially intermediate between AAS and PAAS particularly with respect to the critical value of Eu/Eu* and, to a lesser extent, ΣREE, and can be considered evolved from AAS towards PAAS. Group II is essentially identical to PAAS except for slightly lower Eu/Eu*.

These findings are similar to those of McLennan *et al.* (1979) for the Lower Proterozoic Huronian succession of Canada (deposited unconformably on an Archaean basement sometime between about 2.6 and 2.2 b.y.). There, fine-grained sedimentary rocks at the base (McKim and Pecors Formations) have REE distributions which are similar to typical

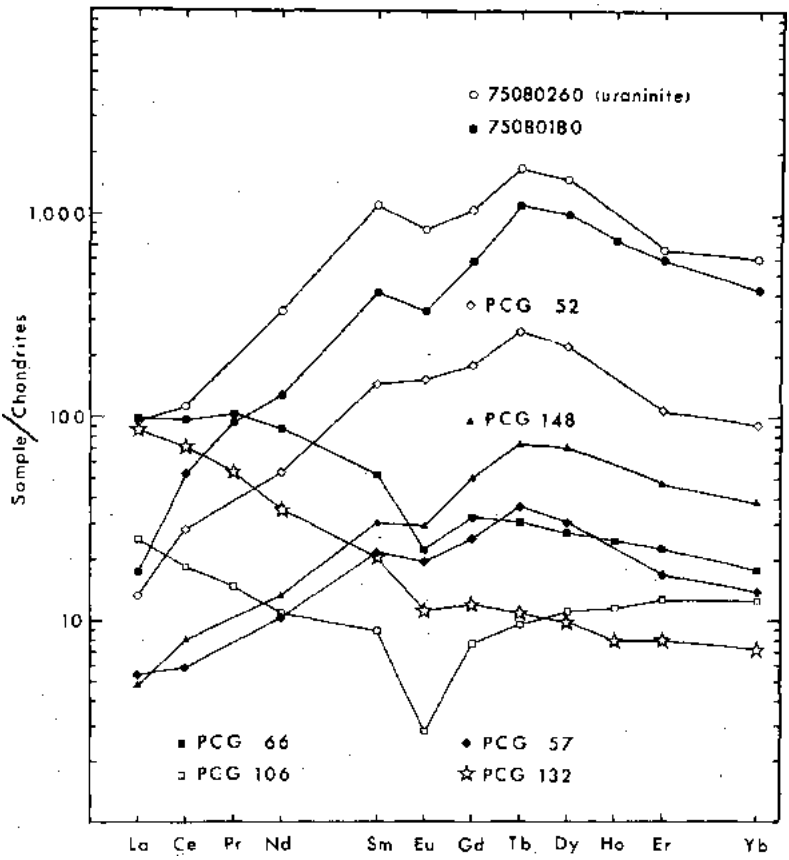


Figure 5. Chondrite - normalized REE patterns for samples from the Cahill Formation. See text for discussion.

Archaean patterns. Towards the top of the section, REE patterns change, resembling typical post-Archaean patterns in the Gordon Lake Formation.

McLennan *et al.* (1979) related these changes in REE patterns in the Huronian sequence to the emplacement of granitic rocks at the end of the Archaean (Kenoran orogeny in Canada). In the Pine Creek Geosyncline, comparable activity is preserved in the Rum Jungle, Waterhouse and Nanambu Complexes (Page *et al.*, this volume). As post-Archaean erosion proceeded, continually greater amounts of Late Archaean granitic rocks were incorporated into Proterozoic sedimentary rocks. Late Archaean granitic rocks of the Superior Province seem commonly to have significant negative Eu-anomalies (McLennan *et al.*, 1979). This, essentially episodic event, caused a fundamental change in the composition of the upper continental crust. If this intrusive event was part of an episode of crustal growth, it may have also caused a change in the bulk composition of the crust. In any regard, it must have resulted in significant vertical redistribution of many elements (Taylor & McLennan, 1979).

Isotopic evidence supports such an episodic event in the upper crust at the Archaean-Proterozoic boundary. Veizer (1976) and Veizer & Compston (1976) made estimates, from carbonate rocks, of the Sr isotopic composition of seawater through geologic time. Archaean

values were similar to those of the upper mantle $(^{87}Sr/^{86}Sr)_i$ values. An extremely sharp increase of the radiogenic component (approximate increase in $(^{87}Sr/^{86}Sr)_i \approx 0.0025$) occurred between 2500-2100 m.y. followed by a gradual increase through the Proterozoic and Phanerozoic (to about $(^{87}Sr/^{86}Sr)i \approx 0.710$). This sharp increase was interpreted as being a result of significant fractionation of the crust associated with the Archaean-Proterozoic boundary. Sm-Nd systematics also suggest a major event at this time. Studies in the Canadian Shield (McCulloch & Wasserburg, 1978) indicate that much of the exposed Superior, Slave and Churchill structural provinces were formed in the period 2700-2500 m.y.

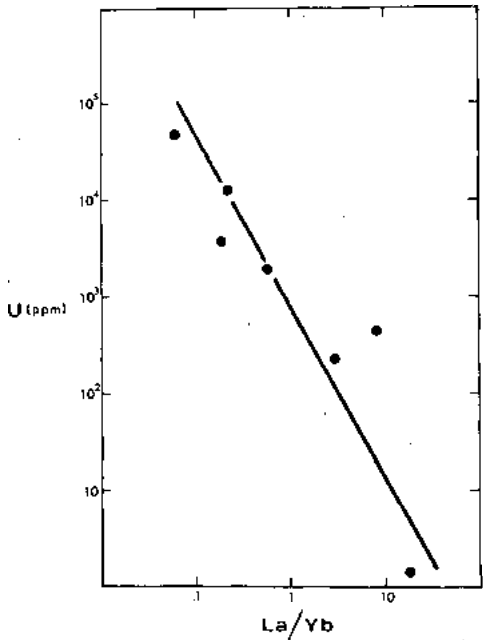


Figure 6. Plot of U versus La/Yb for whole rock samples (75080260 excluded) from the Cahill Formation. Note the inverse correlation.

The Pine Creek Geosyncline samples fit such a model. If negative Eu-anomalies such as those found in the Nanambu Complex (Fig. 4), are common in all late Archaean granitic complexes of the Pine Creek Geosyncline, a greater contribution to Group II sedimentary rocks as compared to Group I can explain the REE patterns.

Pine Creek Geosyncline samples differ from the normally expected pattern in at least one respect. Group I samples are significantly depleted in HREE compared to AAS, Group II and even PAAS (Fig. 8). In a recent review of early Archaean rocks, O'Nions & Pankhurst (1978) noted that early Archaean granitic rocks from Greenland commonly have extremely depleted HREE patterns. Similar HREE-depleted patterns are very common in early Archaean rocks from the high-grade gneiss complexes (and related granitoids) of Barberton Mountain Land (Condie & Hunter, 1976; Glikson, 1976; Hunter *et al.*, 1978) and Scotland (Drury, 1978). Unusually large proportions of these rocks in the provenance of Group I could easily explain the REE patterns. Also, if late Archaean K-rich granitic rocks are responsible for the change seen in the sedimentary REE patterns than the lower LREE/HREE seen in Group II is also predictable. Late Archaean K-rich granitic rocks are much less depleted in HREE than the early Archaean Na-rich varieties. Thus incorporation of the K-rich granitic rocks into the Lower Proterozoic sedimentary rocks would have the effect of lowering LREE/HREE.

URANIUM MINERALIZATION OF THE CAHILL FORMATION

The remarkable correlation of REE patterns and U in the Cahill Formation is most unusual and has not been previously observed. The REE patterns of the U-rich samples (Fig. 5) are unlike any terrestrial or extraterrestrial rock. Several REE minerals, such as samarskite, fergusonite, xenotime, gadolinite, tholenite and kainosite, do display heavy rare earth enrichment (Herrmann, 1970). However, the occurrence of some of these should be associated with either Th, Zr coherence (samarskite), Nb coherence (samarskite, fergusonite), P coherence (xenotime) or selective enrichment of individual REE (gadolinite) (Herrman, 1970). None of these correlations are apparent (see Table 4). None of these

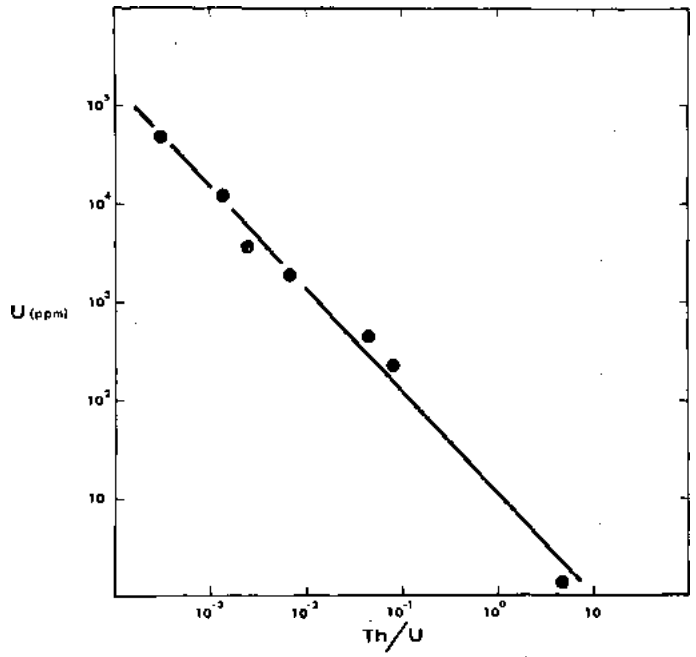


Figure 7. Plot of U versus Th/U for whole rock samples from the Cahill Formation. The strong negative correlation indicates lack of coherence between U and Th distributions.

minerals have been previously reported for these deposits or discovered in the present study.

Although common rock forming minerals such as zircon and garnet commonly show HREE enrichment (Herrmann, 1970), concentrations of such minerals (from major and trace element data) could not have been high enough (if present at all!) to cause such patterns. The impure uraninite sample (75080180) does show a REE pattern parallel to other samples. Heavy REE enrichment in uraninite has also been reported by Zhirov *et al.* (1961). High REE content for uraninite, and particularly igneous uraninites, is very common (Berman, 1957). As pointed out above, however, uraninite alone cannot account for the REE patterns seen in many Cahill samples. It seems possible therefore that most of the rare earth elements are tied up in clay minerals and alteration products. Significant adsorption of REE on clays is a well documented phenomenon (Roaldset, 1973).

The observed REE patterns are suggestive of massive REE mobilization associated with U movement. The HREE are either selectively incorporated into the ore solution or selectively deposited with U. The depletion of LREE in some Cahill samples implies that REE are being leached from sedimentary rocks and would support a sedimentary source for REE. A HREE-depleted parent material has not been identified. If a very large volume of parent material were involved, a HREE depletion may not be apparent.

Transport of REE and particularly HREE during any metamorphic process is very uncommon. Collerson & Fryer (1978) suggested HREE mobility by soluble complexes during early Archean granulite metamorphism of granitic rocks. The abundances of CO_2 in granulite fluid inclusions (Hollister & Burruss, 1976; Touret, 1977) led them to suggest carbonate complexing (in the form $[REE(CO_3)_3]^{-3}$) as the important mechanism. This followed the early work of Kosterin (1959) who pointed out the importance of hydrothermal REE mobility by complexing with such anionic species as CO_3^{2-}, SO_4^{2-} and halogens. The

	REE (ppm)	LREE/HREE	Eu/Eu*
PAAS	183	9.4	0.67
GROUP II[a]	196±89	10.7±2.1	0.56±.08
GROUP I[b]	162±28	12.5±2.7	0.65±.08
AAS	71	5.3	1.03

a) Excludes PC626
b) Excludes PC0213, PC04[illegible]

Table 5. Summary of important REE statistics for AAS, PAAS, Group I and Group II.

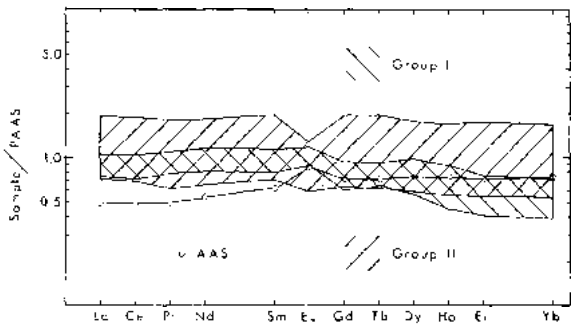


Figure 8. PAAS - normalized REE diagram plotting the fields of Group I and Group II samples. Also included is the average Archaean sedimentary rock (AAS). Note the depletion of HREE in Group I compared to AAS, Group II and even PAAS.

general importance of complexing of REE in hydrothermal solutions has also been discussed by Beus (1958), Mineyiv (1963), Tugarinov & Naumov (1973) and Parekh & Moller (1977). Fryer (1977b) appealed to REE mobility by carbonate complexing to explain HREE-enriched patterns in Precambrian iron-formations. Kerrich & Fryer (1979) concluded that REE concentrations in hydrothermal carbonate and quartz veins had been affected by carbonate complexing.

The lack of Hf/U, Zr/U and Th/U coherence (see Fig. 7) strongly suggests that U was primarily transported in solution at U^{+6} since U^{+4} would be expected to behave in a similar fashion to Th^{+4} (i.e. $-U^{+4}$ complexes, such as phosphate complexes (Adams *et al.*, 1959) can be discounted). The most likely form of transport would be complexing (Langmuir, 1978; also see Rich *et al.*, 1977 for summary). Naumov (1959) discussed carbonate complexing for the transport of U (in the form $[UO_2(CO_3)_3]^{4-}$).

From the above discussion, it seems likely that U and the REE were transported together in a hydrothermal solution. Such a solution was probably at low temperature (Ferguson *et al.*, this volume). Halogen complexing is unlikely as Th is also commonly transported in such a way (Kosterin, 1959). Sulphate complexing though possible, appears to be relatively uncommon and inefficient (Kosterin, 1959). Carbonate complexing is thus the most likely mechanism of transportation. This model is particularly attractive since solubility increases for the HREE, causing HREE enrichment in ore solutions and in late stage deposition (Kosterin, 1959).

Present understanding of REE and U chemistry allows us to place certain constraints on the properties of such a solution. REE and uranyl carbonate complexes are stable under relatively alkaline and oxidized conditions (Kosterin, 1959; Langmuir, 1978). From the uranium data it seems likely that the solutions had Eh greater than about 0.2V and pH greater than about 7.5 (Langmuir, 1978).

Conditions of deposition are less certain but lowering of pH, Eh and/or carbonate concentration would be efficient mechanisms. CO_2 could be effectively decreased by a lowering of total pressure upon entrance of solution into vugs or cavities (Kosterin, 1959). This would be in accordance with the geological setting of the ores (Ferguson *et al.*, this volume; Ewers & Ferguson, this volume). Adsorption of REE and U on clay minerals seems to be a viable mechanism for deposition (Ferguson *et al.*, 1979; see above). If this is the case

a pH greater than 5.5 is most conducive for U adsorption (Giblin, this volume) and an intermediate pH is best for REE, as suggested by the Eu data (Nowak, 1978).

Mobilization of REE by carbonate complexing should result in anomalous Eu behaviour since Eu^{+2} would not complex in the same way as Eu^{+3}. This does not appear to occur (Fig. 5, Table 4). It seems unlikely that either Eu^{+2} was transported by another complexing mechanism (see above discussion) or Eu^{+2} was oxidized to Eu^{+3} since the ore-forming solutions only appear to have varied from moderately reducing to moderately oxidizing (Ferguson *et al.*, this volume). An interesting possibility is the Eu^{+2} was not present in the source material. If the source was sedimentary rocks, this suggests that Eu^{+2} is oxidized to Eu^{+3} during sedimentary processes, so that the Eu anomalies preserve a memory of igneous precursors.

COMPARISON WITH OTHER URANIUM DEPOSITS

Meaningful comparison of results from this study and other areas is hampered by a lack of high quality REE data for U-deposits in general. Brookins *et al.*, (1978) found enriched Eu and Tb and ΣREE in U deposits of the San Juan Basin, New Mexico. They suggested deposition under low Eh conditions. The findings of Rimsaite (1977) for U-ores of the Rabbit Lake deposit, Saskatchewan, are interesting since this deposit has many characteristics which are comparable to the Pine Creek Geosyncline ores (Knipping, 1974). Rimsaite (1977) noted high ΣREE and low LREE/HREE in U-ores from Rabbit Lake (one sample has ~1900 ppm Dy). In this deposit, however, there is an inverse correlation of ΣREE and U content. The significance of these data is uncertain since only three samples were analysed with U_3O_8 ranging from 59-74%. Also, in this example, REE are related to the presence of the REE phase, yttrilite ($Y_2(Th,U,Pb)Si_2O_7$). The association of REE with Th (up to 800 ppm ThO_2 in one REE-rich Rabbit Lake sample) is in marked contrast to the Pine Creek Geosycline.

PINE CREEK GEOSYNCLINE AS A NATURAL NUCLEAR REACTOR

The discovery of the natural reactor at Oklo, Gabon (Neuilly *et al.*, 1972; Bodu *et al.*, 1972) raises the possibility that similar phenomena occurred elsewhere. The Pine Creek Geosyncline and Rabbit Lake deposits are obvious potential candidates for such an occurrence. Both deposits are found in rocks >1800 m.y. (Knipping, 1974; Page *et al.*, this volume) and both deposits contain extensive concentrations of uraninite. In both cases, however, much of the uranium may have been deposited at a later stage (Knipping, 1974; Hills & Richards, 1976).

The REE are extremely important in understanding natural nuclear reactors (Bassiere *et al.*, 1975; Dozal & Neuilly, 1975; Neuilly & Naudet, 1975; Loubet & Allegre, 1977). Sample 75080180 (U > 5%) was analysed by spark source mass spectrometry. Within the precision of the method, no abnormal isotopic ratios were found for $^{143}Nd/^{146}Nd$ or $^{147}Sm/^{149}Sm$. It seems safe to conclude that no fission reactions associated with a natural reactor have affected this sample. The sub-parallel nature of REE patterns in all U-rich samples suggests distributions that the observed REE distributions are a primary feature of the Cahill Formation. Although isotopic analyses are unavailable for the Rabbit Lake deposit, it is unlikely that the samples reported by Rimsaite (1977; see above) were affected by fission from a natural reactor.

The HREE enrichment noted in the Pine Creek and Rabbit Lake deposits is in marked contrast with the Oklo deposit. Original (i.e. pre-reactor) REE concentrations at Oklo were similar to typical post-Archaean sedimentary rocks. Even the addition of reactor fission products does not significantly change the general shape of the REE pattern with the exception of Nd and Eu enrichments (Loubet & Allegre, 1977). Table 6 compares Gd and Gd/Nd for U-rich samples from Oklo (Bassiere *et al.*, 1975), Rabbit Lake (Rimsaite, 1977)

and the Pine Creek Geosyncline (this study). The Oklo values are estimates of natural (i.e. pre-reactor) concentrations (Brassiere *et al.*, 1975). The Pine Creek and Rabbit Lake deposits have much higher Gd concentrations and Gd/Nd ratios.

	CAHILL FORMATION			RABBIT LAKE DEPOSIT				OKLO DEPOSIT			
Sample	75080180	75080260	Average	Orange ore	Green ore	Yellow ore	Average	642	1294	882/1	Average
Gd	153	277	215	855*	67*	28*	317	7	2.5	8.5	6.0
Gd/Nd	1.99	1.39	1.69	1.26	2.75	3.50	2.52	0.07	0.09	0.09	0.08

*values estimated from chondrite-normalized plots.

Table 6. Comparison of Gd and Gd/Nd for ores from the Cahill Formation, Rabbit Lake Deposit and Oklo Deposit.

Sustaining a nuclear reaction is strongly dependent on the availability of free neutrons. Many elements effectively absorb neutrons, thus lowering the possibility of a sustained reaction. A convenient measure of an element's ability to absorb neutrons is given by the thermal neutron absorption cross-section. Many of the heavy REE elements are extremely efficient absorbers. For example Gd, Sm, Eu and Dy have thermal neutron absorption cross sections of 40,000, 5,600, 4,300 and 1,100 barns (Anderson, 1971) respectively. For comparison, Cd and B, common commercial reactor moderators, have cross-sections of 2,500 and 755 barns, respectively.

At this point, it is convenient to note that the Rabbit Lake deposit contains appreciable boron (up to 1,000 ppm), mainly in tournaline (Rimsaite, 1977). Boron analyses have not been reported for the Cahill Formation U-ores but tourmaline is a common accessory in the host rocks (Ewers & Ferguson, this volume). Also, B is found in appreciable quantities in the uraninite (Ferguson *et al.*, this volume).

Based on the few samples analysed and lack of detailed knowledge of grade, volume and dimensions of ore zones for Rabbit Lake and Pine Creek deposits, we feel that detailed calculations of fission reaction probalities are unwarranted. However, the present knowledge of the geochemistry of the Rabbit Lake and Pine Creek Geosyncline U-deposits suggests that conditions were not favourable for initiation of a natural nuclear reactor.

ACKNOWLEDGEMENTS

We are grateful to B.J. Fryer for performing several REE analyses, to P.E. Oswald-Sealy and J.M.G. Shelley for technical assistance, to W. Sinclair and H.N.C. Cutten for XRD determinations and John Ferguson for samples, analytical assistance and many stimulating conversations. J. Ferguson and R.J. Hart provided helpful reviews. We also thank Ms. C. Neagle for assistance in preparation of the manuscript.

REFERENCES

Adams, J.S., Osmond, J.K. & Rogers, J.J.W., 1959: The geochemistry of thorium and uranium. *Physics Chem. Earth, 3,* 298-348.

Ahrens, L.H. & Erlank, A.J., 1969: Bismuth. *in.* (ed. K.H. Wedepohl) *Handbook of Geochemistry* Springer-Verlag.

Anderson, W.K., 1971. Nuclear applications of yttrium and the lanthonons. *in,* (eds. F.H. Spedding and A.A. Daane) *The Rare Earths* Robert E. Krieger Publ. Co., 522-569.

Brassiere, H., Cesario, J., Pouperd, D. & Naudet, R., 1975: Analyse isotopique et ponderale de terres rares dans divers enchantillons d'Oklo. *in, The Oklo Phenomenon,* IAEA, 385-399.

Berman, R.M., 1957: The role of lead and excess oxygen in uraninite. *Am. Miner., 42,* 705-731.

Beus, A.A., 1958: The role of complexes in the transfers and accumulations of rare elements in endogenic solutions. *Geochemistry. 1958,* 388-396.

Bodu, R., Borizigues, H., Murin, N., & Pfiffelmann, J.P., 1972: Sur l'existence d'anomalies isotopiques rencontrees dan l'uranium du Gabon. *C.R. Acad. Sci. Paris, 275, Ser. D.,* 1731.

Brookins, D.G., Della Valle, R.S. & Lee, M.J., 1978: Rare earth element study of whole rocks and clay minerals from the southern San Juan Basin, New Mexico (abstract). *EOS, 59,* 388.

Collerson, K.D. & Fryer, B.J., 1978: The role of fluids in the formation and subsequent development of early continental crust. *Contrib. Mineral. Petrol., 67,* 151-167.

Condie, K.C. & Hunter, D.R., 1976: Trace element geochemistry of Archean granitic rocks from the Barberton region, South Africa. *Earth Planet. Sci. Lett., 29,* 389-400.

Cullers, R.L., Yeh, L.-T., Chaudhuri, S. & Guidotti, C.V., 1974: Rare earth elements in Silurian pelitic schists from N.W. Maine. *Geochim. cosmochim. Acta, 38,* 389-400.

Dozol, J.F. & Neuilly, M., 1975: Analyse isotopique des terres rares contenues dans minerai d'Oklo. *in, The Oklo Phenomenon*, IAEA, 357-369.
Drury, S.A., 1978: REE distributions in a high-grade Archaean Gneiss Complex in Scotland: implications for the genesis of ancient sialic crust. *Precambrian Research, 7*, 237-257.
Eby, G.N., 1972: Determination of rare earth, yttrium and scandium abundances in rocks and minerals by an ion exchange - X-ray fluorescence procedure. *Analyt. Chem., 44*, 2137-2143.
Ewers, G.R. & Ferguson, J., this volume: Mineralogy of the Jabiluka, Ranger, Koongarra and Nabalek uranium deposits. *Proceedings of the International Uranium Symposium on the Pine Creek Geosyncline.*
Ferguson, J., this volume: Metamorphism in the Pine Creek Geosyncline and its bearing on stratigraphic correlations. *Proceedings of the International Uranium Symposium on the Pine Creek Geosyncline.*
Ferguson, J. & Winer P., this volume: Pine Creek Geosycline: statistical treatment of whole-rock chemical data. *Proceedings of the International Uranium Symposium on the Pine Creek Geosyncline.*
Fryer, B.J., 1977a: Rare earth evidence in iron-formations for changing Precambrian oxidation states. *Geochim. cosmochim. Acta, 41*, 361-367.
Fryer, B.J., 1977b: Trace element geochemistry of the Sokoman iron formation. *Can. J. Earth Sci., 14*, 1598-1610.
Glikson, A.Y., 1976: Trace element geochemistry and origin of early Precambrian acid igneous series, Barberton Mountain Land, Transvaal. *Geochim. cosmochim. Acta, 40*, 1261-1280.
Green, T.H., Brunfelt, A.O. & Heier, K.S., 1969: Rare-earth element distribution in anorthosites and associated high grade metamorphic rocks, Lofotenvesteraalen, North Norway. *Earth Planet. Sci. Lett., 7*, 93-98.
Green, T.H., Brunfelt, A.O. & Heier, K.S., 1972: Rare-earth element distribution and K/Rb ratios in granulites, mangerites and anorthosites, Lofotenvesteraalen, Norway. *Geochim. cosmochim. Acta, 36*, 241-257.
Gschneidner, K.A. & Eyring, L. (eds.), 1979: *Handbook on the Physics and Chemistry of Rare Earths* (4 volumes). North-Holland Co.
Hanson, G.N., 1978: The application of trace elements to the petrogenesis of igneous rocks of granitic composition. *Earth Planet. Sci. Lett., 38*, 26-43.
Herrmann, A.G., 1970: Yttrium and the lanthanides. *in*, (ed. K.H. Wedepohl), *Handbook of Geochemistry* , Springer-Verlag.
Hills, J.H. & Richards, J.H., 1976: Pitchblende and galena ages in the Alligator Rivers Region, Northern Territory, Australia. *Miner. Deposita, 11*, 133-145.
Hollister, L.S. & Burruss, R.C., 1976: Phase equilibria in fluid inclusions from the Khtada Lake metamorphic complex. *Geochim. cosmochim. Acta, 40*, 163-175.
Giblin, A., this volume: Experiments on the role of clay adsorption in genesis of uranium ores. *Proceedings of the International Uranium Symposium on the Pine Creek Geosyncline.*
Hunter, D.R., Barker, F. & Mellard, H.T., 1978: The geochemical nature of the Archean Ancient Gneiss Complex and granodiorite suite, Swaziland: a preliminary study. *Precambrian Research, 7*, 105-127.
Jakeš, P. & Taylor, S.R., 1974: Excess Eu content in Precambrian rocks and continental evolution. *Geochim. cosmochim. Acta., 38*, 739-745.
Kerrich, R. & Fryer, B.J., 1979: Archean precious-metal hydrothermal systems, Dome mine, Abitibi greenstone belt II. REE and oxygen isotope relations. *Can. J. Earth. Sci., 16*, 440-458.
Knipping, H.D., 1974: The concepts of supergene versus hypogene emplacement of uranium at Rabbit Lake, Saskatchewan, Canada. *in, Formation of Uranium Ore Deposits, IAEA, 531-549.*
Kosterin, A.V., 1959: The possible modes of transport of the rare earths by hydrothermal solutions. *Geochemistry, 1959*, 381-387.
Loubet, M. & Allegre, C.J., 1977: Behaviour of the rare earth elements in the Oklo natural reactor. *Geochim. cosmochim Acta, 41*, 1539-1548.
McCulloch, M.T. & Wasserburg, G.J., 1978: Sm-Nd and Rb-Sr chronology of continental crust formation. *Science, 200*, 1003-1011.
Langmuir, D., 1978: Uranium solution-mineral equilibria at low temperatures with applications to sedimentary ore deposits. *Geochim. cosmochim. Acta, 42*, 547-569.
McLennan, S.M., Fryer, B.J. & Young, G.M., 1979: Rare earth elements in Huronian (Lower Proterozoic) sedimentary rocks: composition and evolution of the post-Kenoran upper crust. *Geochim. cosmochim. Acta, 43*, 375-388.
Mineyev, D.A., 1963: Geochemical differentiation of the rare earths. *Geochemistry, 1963*, 1129-1149.
Nance, W.B., & Taylor, S.R., 1976: Rare earth patterns and crustal evolution I: Australian post-Archean sedimentary rocks. *Geochim. cosmochim. Acta, 40*, 1539-1551.
Nance, W.B. & Taylor, S.R., 1977: Rare earth element patterns and crustal evolution II: Archean sedimentary rocks from Kalgoorlie, Australia. *Geochim. cosmochim. Acta, 41*, 225-231.
Naumov, G.B., 1959: Transporation of uranium in hydrothermal solution as a carbonate. *Geochemistry, 1959*, 5-20.
Needham, R.S., Crick, I.H. & Stuart-Smith, P.G., this volume: Regional geology of the Pine Creek Geosycline. *Proceedings of the International Symposium on the Pine Creek Geosyncline.*
Needham, R.S. & Stuart-Smith, P.G., 1976: The Cahill Formation — host to uranium deposits in the Alligator Rivers uranium field, Australia. *BMR J. Aust. Geol. Geophys., 1*, 321-333.
Neuilly, M., Bussac, J., Frejacques, C., Nieff, G., Vendryres, G. & Yvon, J., 1972: Sur l'existence dans un passe recule d'une reaction en chaine naturalle de fissions dans le gisement d'uranium d'Oklo (Gabon). *C.R. Acad. Sci. Paris, 275, Ser. D.*, 1847.
Nowak, E.J., 1978: The migration of Eu through geologic media (abstract). *EOS, 59*, 1224.
O'Nions, R.K. & Pankhurst, R.J., 1978: Early Archean rocks and geochemical evolution of the Earth's crust. *Earth Planet. Sci. Lett., 38*, 211-236.

Page, R.W., Compston, W. & Needham, R.S., this volume: Geochronology and evolution of the Late Archaean basement and Proterozoic rocks in the Alligator Rivers uranium field, Northern Territory, Australia. *Proceedings of the International Uranium Symposium on the Pine Creek Geosyncline.*

Parekh, P.P. & Moller, P., 1977: Revelation of the genesis of minerals in paragenesis with fluorites, calcites and phosphates via rare earths fractionation. *IAEA International Symposium on Nuclear Techniques in Exploration Extraction and Processing of Mineral Resources.*

Rich, R.A., Holland, H.D. & Peterson, U., 1977: *Hydrothermal Uranium Deposits.* Elsevier.

Rimsaite, J., 1977: Mineral assembalges at the Rabbit Lake uranium deposit, Saskatchewan: a preliminary report. *Geol. Surv. Pap. Can., 77-1B,* 235-246.

Roaldset, E., 1973: Rare earth elements in Quaternary clays of the Numedal area, southern Norway. *Lithos, 6,* 349-372.

Taylor, S.R., 1977: Island arc models and the composition of the continental crust. *Am. Geophys. Union Maurice Ewing Series I,* 325-335.

Taylor, S.R., 1979: Chemical composition and evolution of the continental crust: the rare earth element evidence. *in,* (ed. M.W. McElhinny), *The Earth: It's Origin, Structure and Evolution.* Academic Press, 353-376.

Taylor, S.R. & Gorton, M.P., 1977: Geochemical application of spark source mass spectrography — III. Element sensitivity, precision and accuracy. *Geochim. cosmochim. Acta, 41,* 1375-1380.

Taylor, S.R. & McLennan, S.M., 1979: Discussion on "Chemistry, thermal gradients and evolution of the lower continental crust". *Jl. geol. Soc. London, 136.*

Taylor, S.R. & McLennan, S.M., 1980: The rare earth element evidence in Precambrian sedimentary rocks: implications for crustal evolution. *in,* (ed. A. Kroner), *Precambrian Plate Tectonics,* Elsevier, in press.

Touret, J., 1977: The significance of fluid inclusions in metamorphic rocks. *in,* (ed. D.G. Fraser), *Thermodynamics in Geology,* Dordrecht-Holland: D. Reidel.

Tugarinov, A.I. & Naumov, V.B., 1972: Physicochemical parameters of hydrothermal mineral formation. *Geochem. Int., 9,* 161-167.

Veizer, J., 1976: $^{87}Sr/^{86}Sr$ evolution of seawater during geologic history and its significance as an index of crustal evolution. *in.* (ed. B.F. Windley), *The Early History of the Earth,* Wiley, 569-578.

Veizer, J. & Compston, W., 1976: $^{87}Sr/^{86}Sr$ in Precambrian carbonates as an index of crustal evolution. *Geochim. cosmochim. Acta, 40,* 905-914.

Walpole, B.P., Crohn, P.W., Dunn, P.R. & Randal, M.A., 1968: Geology of the Katherine-Darwin Region, Northern Territory. *Bull. Bur. Min. Resour. Geol. Geophys. Aust., 82,* 304p.

Wildeman, T.R. & Haskin, L.A., 1973: Rare earths in Precambrian sediments. *Geochim. cosmochim. Acta, 37,* 419-438.

Zhirov, K.K., Bandurkin, G.A., & Laurent'yev, Yu.G., 1961: Geochemistry of rare earth elements in pegmatites of northern Karelia. *Geochemistry, 1961,* 1107-1118.

PINE CREEK GEOSYNCLINE: STATISTICAL TREATMENT OF WHOLE ROCK CHEMICAL DATA

John Ferguson[1] and Paul Winer[2]

1. Bureau of Mineral Resources, P.O. Box 378, Canberra City, A.C.T. 2601, Australia.
2. Department of Statistics, Australian National University, P.O. Box 4, Canberra, A.C.T. 2600, Australia.

ABSTRACT

Statistical treatment of whole rock analyses was undertaken on 350 specimens collected within the Pine Creek Geosyncline which were analysed for 41 elements. Particular emphasis is given to main host rocks associated with uranium deposits, and to granitoids. Statistical methods employed include cluster analysis, correlation coefficients, means and variances. Correlations on the rock units that are host to the uranium deposits give the following results for uranium at the 99 percent confidence limit:

Cahill Formation:	U correlates with W, As, Nb, Mo, Pb, Li, Sc & Co
Masson Formation:	U correlates with Li
Koolpin Formation:	U correlates with Ti, P, Y, Ni, Cu, Zn, W, Nb, Pb & Li.

The large number of rocks analysed in the Cahill Formation (143) made it possible to exercise correlation 'filters' at the 99 percent confidence limit, namely:

a) U in excess of 500 ppm — U correlates with As, Nb, La, Ce, Mo, Pb & Co
b) U in excess of 40 ppm — U correlates with As, Nb, Mo, Pb, Sc & Co
c) U less than 40 ppm — U correlates with P
d) U less than 30 ppm — U shows no correlation

The correlation of uranium with the above elements suggests that they were transported in the uranium mineralising solutions.

Of the granitoids studied the mafic-rich Nimbuwah Complex has the highest degree of correlation and clustering, which is attributed to its exclusively *I*-type nature and limited compositional range. The other granitoids investigated are of mixed *S*-and *I*-type parentage and range from mafic to felsic varieties; these factors account for the low to moderate degree of correlation of the elements.

INTRODUCTION

Statistical treatment of whole rock analyses was undertaken on 350 specimens collected within the Pine Creek Geosyncline, each of which was analysed for a combined total of 41 elements and oxides. The analyses are the PCG set of analyses on microfiche in the pocket at the back of this volume.

Previous statistical treatment of chemical data from the Pine Creek Geosyncline has been limited to individual granitoid plutons. Rhodes (1969) applied cluster analysis techniques to the Mount Shoobridge Granite and Ewers & Scott (1977) determined means, variances, coefficient matrices and cluster analyses on 108 granitic samples from the Cullen Granite.

In this study, correlation coefficients, means, variances and cluster analyses were carried out. Emphasis has been placed on the rock units that are the main hosts to the uranium deposits, namely, the Cahill, Masson and Koolpin Formations; and to the granitoids, which are thought to have played a significant role in uranium genesis. The statistical results are used as a guide to enable geological relationships to be better interpreted, and to test element mobility during the uranium mineralising event(s).

METHODS

The correlation coefficients, means and variances were all calculated by means of standard FORTRAN algorithms.

The cluster analyses were calculated by a modified version of the CLUSTAN computer package. In cluster analysis the choice of a suitable distance measure is always a problem. It often happens that a cluster analysis provides a set of clear clusters, but that these clusters

reflect a structure imposed on the data by the choice of a distance metric rather than a structure in the data themselves. For example, in most applications the Minkowski metrics are the popular choice.

Let $\underset{\sim}{X}_i' = \{X_{1i}, X_{2i}, \ldots, X_{Ni}\}$

and $\underset{\sim}{X}_i' = \{X_{1j}, X_{2j}, \ldots, S_{Nj}\}$

be two vectors (both with N elements) representing the measured concentrations of N elements in the ith and j^{th} rocks. Then the metric distance function (the Minkowski metric) is given by

$$d_r(i,j) = \left[\sum_{k=1}^{N} |X_{ki} - X_{kj}|^r \right]^{1/r}$$

In this system $d_2(i,j)$ is the Euclidean distance between the two vectors. However, it is obvious that for our purposes these metrics have disadvantages. They are sensitive to absolute rather than proportional differences. This means that the elements occurring in high concentrations are given much more weight than the elements occurring in low concentrations. The subsequent cluster analysis may well yield a set of clear clusters, but these clusters may be relatively insensitive to differences between important elements that happen to occur in low concentrations.

In order to minimise these difficulties it was decided to use the 'Canberra Metric', developed by Lance & Williams (1967). This metric is defined as

$$d_{CAN.}(i,j) = \sum_{k=1}^{N} \left\{ \frac{|X_{ki} - X_{kj}|}{(X_{ki} + X_{kj})} \right\} \qquad (1)$$

For positive character states, i.e. for $X_{ki} > 0$ (all k, i) it has attractive properties. Firstly, this metric is a property of only the 2 vectors being compared. In other words it does not impose its own structure on the data as a whole. Secondly, the denominator in (1) ensures that the metric is self-scaling in the sense that it is sensitive to proportional rather than absolute differences between the elements in the vectors being compared.

Although the Canberra Metric is listed as one of the options available in the CLUSTAN package, it was found that the metric actually available was

$$d(i,j) = \frac{\sum_{k=1}^{N} |X_{ki} - X_{kj}|}{\sum_{k=1}^{N} |X_{ki} + X_{kj}|} \qquad (2)$$

This metric also appears in Lance & Williams (1967), where the authors suggest (1) as an improvement on (2).

It was therefore necessary to write our own program for calculating (1). The resulting values of $d_{CAN}(i,j)$ were then inserted at the appropriate step in the CLUSTAN package to complete the cluster analysis. Details of these modifications are available from P. Winer.

In the past it has been fairly common practice, in geological investigations, to use the correlation coefficient

$$d(i,j) = r_{ij} = \frac{\sum_{k=1}^{N} \{(X_{ki} - \bar{X}_i)(X_{kj} - \bar{X}_j)\}}{\left[\sum_{k=1}^{N} (X_{ki} - \bar{X}_i)^2 \sum_{k=1}^{N} (X_{kj} - \bar{X}_{kj} - \bar{X}_j)^2\right]^{\frac{1}{2}}}$$

as a measure of the distance between $\underset{\sim}{X}'_i$ and $\underset{\sim}{X}'_j$ in cluster analysis. This is a very unreliable method which simply does not make statistical sense. For example, the elements of the vectors are not independent and neither are they necessarily measured on the same scale. It is difficult to see what such a statistic means. Furthermore, it is easy to show that the correlation coefficient is not a metric. In particular it does not satisfy the triangle inequality

$$d(i,k) \leq d(i,j) + d(j,k).$$

Another serious objection is that if the vector $\underset{\sim}{X}'_i$ is a scalar multiple of $\underset{\sim}{X}'_j$ the correlation coefficient will be 1. That is, the correlation coefficient will classify the vectors as identical when they may, in fact, be very different. Eades (1965) and Minkoff (1965) have pointed out some of the undesirable properties of the correlation coefficient when applied to clustering techniques. It is suggested that the clustering methods used above are more reliable than methods using correlation coefficients as distance measures.

Three methods were used to define clusters. These are

a) Simple linkage, where the distance between two clusters is defined to be the distance between the nearest neighbours in the two clusters;
b) Average linkage, where the distance between two clusters is defined as the average distance between members of the two clusters;
c) Complete linkage, where the distance between two clusters is defined as the distance between the furthest neighbours in the two clusters.

It was found in every case that (a) gave very poor results, but that (b) and (c) gave satisfactory dendrograms, exhibiting clearly delineated clusters. Furthermore, the dendrograms resulting from (b) and (c) were similar. It seems that with simple linkage the distances between the nearest neighbours in two clusters are of the same order of magnitude as the distances between vectors within clusters. This ensures that, in the presence of internal rounding off errors in the calculations, it is difficult to identify separate clusters. Since, in (b) and (c), the distances between clusters tend to be greater than within clusters, better definition of separate clusters is obtained. Since the algorithm for (b) requires much more computing than the algorithm for (c), it was decided to use (c) in this study.

RESULTS

Correlations were calculated for rock units for which there were five or more analysed samples (Tables 1, 2, 3 and 5). In table 1 the correlations are presented for the rock units that are the main hosts to the uranium deposits, namely, Cahill, Masson, and Koolpin Formations.

Rock types analysed include terrigenous, allochemical and orthochemical as well as impure varieties of these end series. These highly varied compositions produce a moderate degree of correlation between the major elements (Table 1). The generally higher degree of correlation of minor and trace elements is mainly a function of accessory mineral contents and metasomatism produced by the uranium mineralising solutions. The large number of rocks analysed in the Cahill Formation (143), made it possible to exercise correlation 'filters' at the 99 percent confidence limit (Table 2), namely:

a) U in excess of 500 ppm — U correlates with As, Nb, La, Ce, Mo, Pb and Co
b) U in excess of 40 ppm — U correlates with As, Nb, Mo, Pb, Sc and Co
c) U less than 40 ppm — U correlates with P
d) U less than 30 ppm — U shows no correlation.

A large percentage of the Cahill Formation analyses are from Jabiluka One and Two so that correlation matrices (Table 3) for uranium were tested at the 99 percent confidence limit for the following conditions:

a) U in excess of 40 ppm — U correlates with Cu, W, As, Nb, Mo, Pb, Sc and Co
b) U less than 40 ppm — U correlates with As and Mo.

It is not possible to interpret the cluster matrices directly, so a two-dimensional hierarchical clustering diagram or dendrogram was used (Fig. 1). By selecting an arbitrary distance coefficient of 20.0, the rocks of the Cahill Formation are divided into 16 clusters (Fig. 1, Table 4). There are only four major clusters, namely 1, 4, 5 and 6. Cluster 1 is dominated by brecciated micaceous meta-pelites which have a moderate average uranium content (87 ppm). Clusters 4 and 5 are very similar uranium rich brecciated chloritic meta-pelites from the ore zones; they can be separated by their higher magnesium and uranium contents from Cluster 1 (Table 4). Cluster 6 is dominated by brecciated chlorite rich meta-pelites which contain only moderate amounts of uranium (average 160 ppm). The remaining cluster groups include calc-silicate rocks (Cluster 14); weathered limonitic rocks (Cluster 2); chlorite rich rocks with low and high uranium contents (Clusters 3 and 9 respectively); quartzitic rocks with low and moderate uranium contents (Clusters 8, 16; and 11 respectively); dolomitic limestones (Clusters 13 and 15); brecciated chert-rich rocks (Cluster 12); brecciated mica schists with high and low uranium contents (Clusters 10 and 7 respectively).

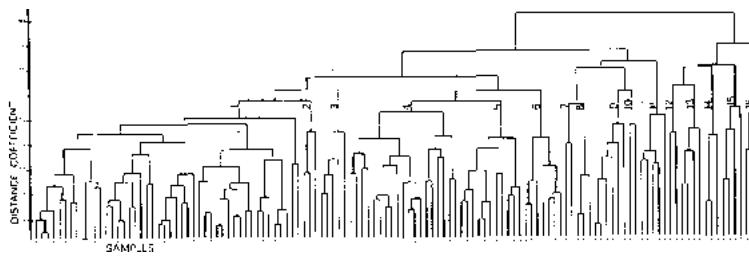


Figure 1. Dendrogram of rocks belonging to the Cahill Formation.

In addition to the elements and oxides shown in Table 1, 40 rocks of the Cahill Formation were analysed for gold. A plot of Au versus U shows that high gold contents (greater than 40 ppm) are restricted to rocks high in uranium (greater than 1000 ppm), but there is no statistical correlation between the two elements (Fig. 2).

At an arbitrary distance coefficient of 16.0 the granitoids cluster into 10 groups (Fig. 3, Table 6). Clusters 1 and 2 are dominated by adamellites; granites are concentrated in Clusters 4 and 5; the remaining minor cluster groups comprise quartz monzonite (6), 'minimum' melt

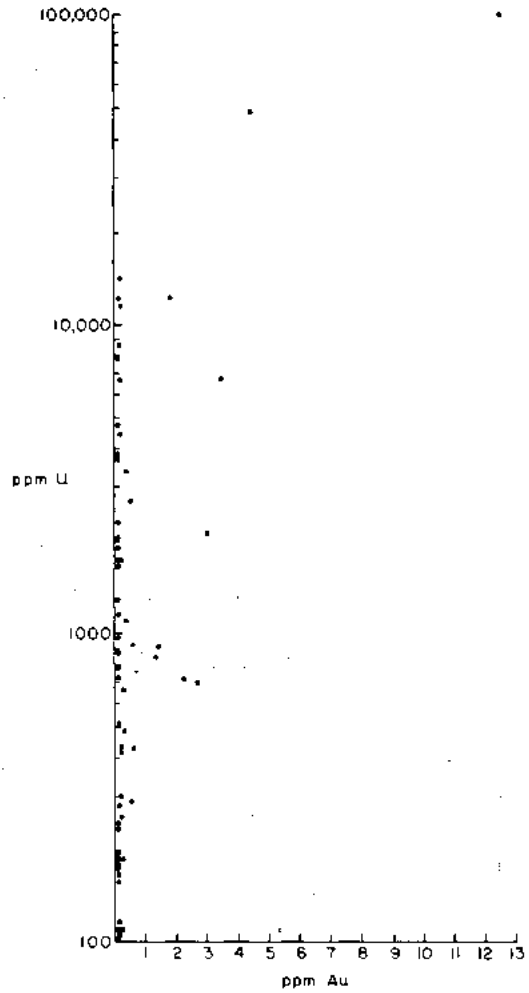


Figure 2. Uranium versus gold; Cahill Formation.

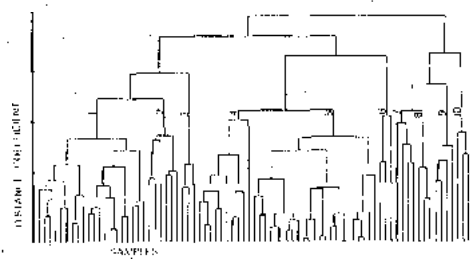


Figure 3. Dendrogram of granitoid rocks.

granites (7 & 8), low Na_2O altered granitoids (9) and altered granitic pegmatites (10). The Nimbuwah Complex granitoids have a restricted compositional range, and, with two exceptions, they all fall into cluster group 5. Despite this restricted compositional range, the elements and oxides have a high degree of correlation (Table 5), suggesting that they are genetically related. Granitoids of the Waterhouse Complex also have a restricted compositional range, but, by contrast, show a small degree of correlation (Table 5). This is reflected in the lack of close clustering of these rocks and their distribution among four cluster groups (1, 2, 4 and 7; Fig. 3). The poor correlation is related to the mixed *S*-and *I*-type parentage of these rocks (Ferguson, Chappell & Goleby, this volume). Equally, the late-orogenic granitoids show a poor correlation (Table 5), and are scattered through cluster groups 1, 4, 7, 8 and 9 (Fig. 3). This is not unexpected, as five different granitoid bodies are represented collectively in this group. Hence, differing source rocks and degrees of fractionation and partial melting could explain the poor correlation. Granitoids from the Nanambu Complex show a moderate degree of correlation owing essentially to the large standard deviation of the major elements. The high degree of correlation for some of the trace elements probably reflects the accessory mineral content. The mixed *S*- and *I*-type parentage of the Nanambu Complex, together with the imposition of multi-orogenesis and anatexis, probably accounts for the dispersion of these rocks through cluster groups 1, 2, 3, 4, 6, and 10 (Fig. 3).

Within each of the rock groups that are genetically related, namely, Zamu Dolerite, Stag Creek Volcanics and the Nungbalgarri Volcanic Member (Table 6), the poor degree of correlation is caused by alteration. The moderately homogeneous rudaceous and arenaceous units of the Kombolgie Formation produce a limited degree of correlation between the elements. Averages and standard deviation of all rock types analysed in the Pine Creek Geosyncline are presented in table 7.

DISCUSSION

The application of statistical analysis to whole rock chemical data from the main hosts to uranium mineralisation in the Pine Creek Geosyncline indicates markedly different sets of correlations for most elements; this is particulary true for uranium. These differences can probably be attributed to original environments of deposition, as well as to metasomatism associated with uranium mineralisation. Cluster analysis on rocks of the Cahill Formation effectively separates the major rock types of this varied suite and additionally groups the metasomatically altered rocks found in the uranium ore-zones. The correlation, at the 99 percent confidence limit, of U with W, As, Nb, Mo, Pb, Li, Sc & Co for the Cahill Formation indicates that these elements were probably also transported in the uranium mineralising solutions. These data have been interpreted in some detail in relation to modelling of uranium mineralisation in the Alligator Rivers Uranium Field (Ferguson, Ewers & Donnelly, this volume).

The high degree of correlation of elements in the Nimbuwah Complex and resulting close clustering emphasises the uniqueness of these granitoids compared to the other granitoids found in the Pine Creek Geosyncline which are more varied and display moderate to low degrees of correlation. The significance of the statistical results pertaining to the granitoids of the Pine Creek Geosyncline is reported in Ferguson, Chappell & Goleby (this volume).

ACKNOWLEDGEMENTS

The authors gratefully acknowledge the work of their assistants A. B. Goleby and Jack Pemn in processing the data for presentation in this study, and the help of B. W. Chappell in producing the microfiche of analyses.

Published with permission of the Director of the Bureau of Mineral Resources, Geology and Geophysics, Canberra, Australia.

	CAHILL FORMATION 140 analyses except for: Co - 111 analyses; Fe^2 and Fe^3 — 125 analyses		MASSON FORMATION 13 analyses except for Co - 11 analyses		KOOLPIN FORMATION 8 analyses except for Co - 7 analyses		
	99%	95%	99%	95%	99%	95%	
Si	Fe^2 Mn Mg Ca	Be	Mn Mg Ca F Sr Zr Mo		Al Mg Ca Th	K Rb Zr Ba La Ga Ge V Sc	Si
Ti	Al K Zr Ga V Sc	Rb Th	Σ Fe Nb V Sc Co	Ga F	P Y Ni Cu Zn Zr U W Nb Pb Li	Al	Ti
A	T Ca K Rb Zr Th Sn Ga Li V F Sc Hf	Mn Mg Nb Ce	K Rb Th La Ga Co	Mn Mg Ca Sr Zr Ba Ce Sc	Si Na Zr Ga F	Ti Ca K Rb Ba Th W Sn Nb Ce Pb V	A
Σ Fe			Ti Nb	Sc Co	S	Mn Na F	Σ Fe
Fe^3	W	Hf					Fe^3
Fe^2	Si Mn Mg K S Ni Zn	Rb Ba					Fe^2
Mn	Si Fe^2 Mg Ca K Ni Rb Zr Ba Th Ce	Al K Nb Zn Zr Li F	Si Mg Ca P Sr Zr Mo	Al K Th Ga	S	Σ Fe Na As	Mn
Mg	Si Fe^2 Mn Ca K Ni Rb Zr Ba Th Ce	Al Na La Li	Si Mn Ca P Zr Mo	Al K Rb Sr Th Ga	Si Ca	K Th Sc	Mg
Ca	Si Al Mn Mg Zr Th Ce Li	K Si Nb V	Si Mn Mg Sr Zr Ga	A P Th Nb Mo	Si Mg Sc	Al Mo	Ca
Na	Sr	Mg Li		V	Al Zr Ga F	Σ Fe Mn K Rb Ba Th Ce V	Na
K	Ti A Fe^2 Mg Rb Zr Ba Th La Ce Sc Hf	Mn Ca F Ni Zn Sr Sr	Al Rb Th La Ga Sr Ce	Mn Mg Ba W Ce	Rb Ba Th V	Si Al Mg Na Ga	K
P	Ti Ga F	K Rb Zr	Si Mn Mg Mo	Ca Th	Ti Y Ni Cu Zn U Ce	W Nb Pb Li	P
S	Fe^3 Cl	As	Ni Cu Sn Co	Zr Th La Ce	Σ Fe Mn As		S
Y	Th Sc	Zr U Nb Ca Mo	Zr	Na Ni	Ti P Ni Cu Zn U W Nb Pb Li	Zr Co	Y
Ni	Fe^2 Mg	Mn K Rb Zr Th Hf	S La Ce V Co	Y Zr Sc	Ti P Y Cu Zn U W Nb Pb Li	Zr Co	Ni
Cu	S Mo	Ti Ni Pb	S Sn		Ti P Y Ni Zn U W Nb Pb Li	Zr Co	Cu
Zn	Fe^2 Sr F	Mn K V	Pb	Ba	Ti P Y Ni Cu U W Nb Pb	Zr Co	Zn
Rb	Al Mg K Sr Zr Ba Th Sn La Ce Li Hf	Ti Fe^2 P Ni U Pb	Al K Ba Th Ga Co	Mg Pb	K Th	S Al Na Ba La Ga Ce V	Rb
Sr	Na Rb Ba La Ce	Ca K Li	S Mn Co Zr	Al Mg Nb Ca			Sr
Zr	T Al Mg Ca K Rb Th Sn Ga V Sc Hf	Mn F Y Ni Nb	S Mn Mg Ca Y Sr	Al S Ni Ti La Ga Ce Cc	T Al Na W Sn Ni Ga Pb Li F	Si Y Ni Cu Zn Ba U Ce V	Zr
Ba	Mg K Rb Sr La Ce	Si Fe^3 Th F Hf	Rb	Al K Zn Ga	K Th Sr Ga V	Si Al Na Rb Zr F	Ba
Th	Al Mg Ca K P Y Rb Zr Sr Ga Hf	T Ni Ba Ce Sc	Al K Rb La Ce Co	Mn Mg Ca F S Zr Sn	S K Rb Ba La	Al Mg Na Ga Ce V F	Th
U	W As Nb Mo Pb Li Sc Co	Y Cu Rb V	L		Ti P Y Ni Cu Zn W Nb Pb Li	Zr Co	U
W	Fe^3 U Nb Sc	As Mo V		K As	Ti Y Ni Cu Zn Zr U Nb Pb Li	Al P Sn Ga F	W
Sn	Al Zr Rb Zr Th Ga F	X	S Cu	Th	Zr Ba Ga Pb V F	A W	Sn
As	U Nb Mo Pb Sc	S W V		W Ga	S	Mn	As
Nb	U W As Mo Pb Li V Sr Co	Al Ce Y Cu Zr Ga	Ti Σ Fe V Sc Co	Ca Sr Ga	Ti Y Ni Cu Zn Zr U W Pb Li	Al P Ga F	Nb
La	K Rb Sr Ba Ce	Mg Hf	A K N Th Ce	S Zr V Sc	Th Co	Si Rb	La
Ga	Ti Al Mn Ca P Zr Th Sn Li V F Sc	Nb	A Ca K Rb Th Sc Co	Ti Mn Mg Sr Zr Ba As Nb	A Na Zr Ba Sr V F	Si K Rb Th W Nb Ce Pb	Ga
Ce	Mg K Rb Sr Ba La	Al Y Th Hf	Ni Th La	Al K S Zr V	La	Si Al Na Rb Zr Th Ga	Ce
Mo	Cu U As Nb Pb Li Sc Co	Y W	Si Mn Mg P	Ca		Ca Sc	Mo
Pb	U As Nb Mo V Sc	Cu Rb Li Co	Zn	Rb	Ti Y Ni Cu Zn Zr U W Sn Nb Li	Al P Ga F	Pb
Li	A Ca Rb Ba U Nb Ga Mg F	Mn Mg Na Sr Pb V Sc	U	Co	Ti Y Ni Cu Zn Zr U W Nb Pb	P	Li
V	Ti A Zr Nb Ga Pb Sc	Ca Zn U W As Li F	Ti Ni Nb Sc	La Ce F	K Ba Sn Ga	Si Al Na Rb Zr Th F	V
F	Al P Zn Sn Ga Li	Mn Ba V		Ti V Sc	Al Na Zr Sr Ga	Σ Fe Ba Th W Nb Pb V	F
Sc	Ti A K Y Zr U W As Nb Ga Mo Pb V Co	Th Li	Ti K Nb Ga V	Al Σ Fe Ni La F Cc	Ca	Si Mg Mn	Sc
Hf	Al K Rb Zr Th	Fe^2 Ni Ba La Ce Co					Hf
Co	U Nb Mo Sc	Pb Hf	Ti A K S Ni Rb Th Nb Ga	Σ Fe Zr Li Sc	P	V Ni Cu Zn L	Co

Table 1. Correlations at the 99 and 95 percent confidence limits for the Cahill, Masson and Koolpin Formations.

	U> 500ppm 33 Analyses (Co only 25 analyses)		U ≥ 40ppm 59 analyses (Co only 50 analyses)		U< 40ppm 58 analyses (Co only 43 analyses)
	99%	95%	99%	95%	99%
Si	Al Na K Cu Zr Ba Ga Li F Sc	Mg V	Mg Ca	Al Fe Y Sr	Fe Mn Mg Ca Zr
Ti	Ca K P Zr W Ga V F Sc	Al	Al K Zr Ca V Sc	Rb Y	Al K Y Rb Zr Sr Nb Ga V Sc Co
Al	Si Na K Si Zr Be Ga Li F Sc	Ti Cu Rb	Ti Na K Rb Zr Ba Th Ga Li Sc Hf	Si Ca Cu V	Ti Mn Mg Ca K Y Rb Zr Th Sr Nb La Ga Ce Li V F Sc Hf Co
Fe	Cu	Mn La	W Ga		Ce Si Ni Zn Mo Y Co
Mg	Mg Ni Zn	K	Mg Zr	Si Na K Si Ba Th	Si Fe Mn Mg K Ni Zn Li V
Mn	Zn Sr	Fe	Zn Sr	Ba	Si Al Fe Mg Ca K Zr Nb Ga Hf
Mg	Fe K Ni	Si Rb	Si Fe Ce K P Ni Rb Ba F	Na Zn Ga Li	Si Al Fe Mn Ca K Ti Zr Ba Th Nb Ce
Ca	Ti Ba Ga V		Si Mg Li F	Al Sr Zr	Si Al Mn Mg K Zr Nb Ga Hf
Na	Si Al K Si Ba F Sc Ce	Zr	Al K Rb Zr Ba Sc	Fe Mg Sr Th Co	Si
K	Si Ti Al Mg Na Ni Rb Si Zr Ba F Sc	Fe Ni Ca	Ti Al Mg Na Ni Rb Zr Ba Th Sc	Fe	Ti Al Fe Mn Mg Ca Y Rb Zr Ba Th Sr Nb La Ga Ce Hf
P	Ti Ca Ga V	Ba Li Sc	Mg Ni Ti Ga F	Rb Ba	U F
Si		Ni	Cu Pb		Fe Mo
Y				Si	Ti Al K Pb Zr Th Sr Nb La Ce Sc
Ni	Fe Mg Rb Ba	K Si Li	Mg K P Rb Ba Ga Li F	Zr Ti	Fe Fe
Cu	Si Mg	Al Ba Ti F Hf	Si Mg Hf	Al U Nb Pb Co	Li Hf
Zn	Fe Mn Sn		Fe Mn Sn	Mg	Fe Fe Ga V F Co
Rb	K Ni Ba	Al Mg Zr Pb	K Mg Na K Ni Zr Ba Th Sr Hf	Ti F Li	Y Al Mg K Y Zr Ba Th Sr Nb La Ga Ce Hf
Sr	Al Na K	Nb Sr	La Ce	Si Fe Zr Ca Na Th	Na
Zr	Si Ti Al K Th Ga V Sc	Na Rb W F	Ti Al Na K Rb Th Ca V Sc Hf	Li Ni	Si Ti Al Mn Mg Ca K Y Rb Th Sr Nb La Ce Hf
Ba	Si Al Cu Na K Ni Rb	P Cu	Al Mg Na K Ni Rb Hf	Fe Mn Sr Th	Mg K Rb As
Th	Zr Hf	Cu V Ga Rb F	Al Ca K P Rb Zr Hf	Fe Na Ni Si Ba	Al Mg K Y Th Zr Sn Nb La Ga Ce Hf
U	As Nb La Ce Mo Pb Co	Sr	As Nb Mo Pb Sr Co	Cu W	P
W	Ti V	Zr Nb Ga Li F Sc	Fe V	Ti U Nb	
Sn	Mn Zr		Mn Zr Rb		Ti Al K Y Rb Zr Th Nb La Ga Ce Sc Hf
As	U Nb Mo	Ce	U Nb Mo Pb	Co	Ba
Nb	U As La Ce Mo Pb Sr Co	Sr W Li	U As Mo Pb Sr Co	Cu W Li	Ti Al Mn Mg Ca K Y Rb Zr Th Sn La Ga Ce V Sc Hf
La	Li Nb Ce	Fe	Sr Ce		Al K Y Rb Zr Th Sn Nb Ce
Ga	Si Ti Al Ca P Zr V F Sc	K Cu	Si Al Fe Ti Na Zr Li V F Sc	Mg	Ti Al Mn Ca K Zn Rb Zr Th Sn Nd Li V F Sc Hf Co
Ce	Fe Li Nb La	As	Si La		Al Mg K Y Ba Zr Th Sn Na La Sc
Mo	Ti U As Nb Co	Th F	Cu U As Nb Pb Co		Fe Si Pb
Pb	Li Nb	Rb Th	Si U As Nb Mo	Cu V Sc	Mo
Li	Si Al	P N W Nb	Al Ni Ga F	Mg Rb Na Sc	Al Fe Cu Ga V F
V	Ti Ga P Zr W Ga Sc	Si F	Ti Zr W Ga Sc	Al Pb	Ti Al Fe Fe Zn Na Ga Li Sc Co
F	Si Ti Al Na K Ga Sc	Cu Zr Th W Mo V	Mg P Ni Ga Cl		Al P Zn Ga Li Co
Sc	Si Ti Al Na K Zr Li Nb Ga V F	P Si U W	Ti Al Na K Zr Li Nb Ga V	Pb Li Co	Ti Al Y Sn Nb Ga Ce V Co
Hf	Th	Cu	Al Cu Rb Zr Ba Th		Al Mn Ca K Cu Rb Zr Th Sn Nb Ba
Co	Na U Nb Mo		U Nb Mo	Na Cu As Sc	Ti Al Fe Zn Ga V F Sc

CAHILL CORRELATIONS

Table 2. Correlations at the 99 and 95 percent confidence limits for the Cahill Formation for different uranium contents.

U< 40ppm 58 analyses (Co only 43 analyses)	U≥ 30ppm 71 analyses (Co only 52 analyses)		U< 30ppm 54 analyses (Co only 41 analyses)		
95%	90%	85%	80%	85%	
K Ba	Al Fe² Mg Ca	Y Sr Sc	Fe² Mn Mg Ca K Zr Ba	Rb As	Si
Fe² Fe³ Ca Ce Hf	Al K Zr Ga V Sc	Na Rb W	Al Y Zr Nb Ga V Sc Co	Ca K Rb Ce	Ti
	Si Ti Na K Rb Zr Ba Th Ga Li Sc Hf	Ca Nb V	Ti Mn Mg Ca K Y Rb Zr Th Sn Nb La Ga Ce Li V F Sc Hf Ca		Al
Ti Mn	W	Ca	Fe² S Ni Zn Mo V Co	Mn	Fe³
Ti S Rb Ba Sc	Si Mg Zn	Na K Si Ba Th	Si Fe³ Mn Mg K Ni Zn Rb Li V	Ba La Sc	Fe²
Fe³ Ni Rb Th	Zn Sn	Ba Th	Si Al Fe² Mg Ce K Rb Zr Nb Ga Hf	Fe³ Ni Th	Mn
Ni	Si Fe² Ca K P Ni Rb Ba F	Na Zn Ga Li	Si Al Fe² Mn Ca K Rb Zr Ba Th Nb Ce	Ni	Mg
Ti Th Li V	Si Mg Si Th	Al Zr	Si Al Mn Mg K Zr Nb Ga Hf	Ti Rb Th Li V	Ca
	Al K Pb Zr Ba Sc	Ti Fe² Mg Ni Sr Th Co	Sr		Na
Sr Ni Sc	Ti Al Mg Na Ni Rb Zr Ba Th Sc	Fe² P Ga Hf	Si Al Fe² Mn Mg Ca Y Rb Zr Ba Th Sn Nb La Ga Ce Hf	Ti Ni Sc	K
	Mg Na Th F	K Rb Zr Ba Ga		U F	P
Fe²	Cu Pb	Hf	Fe³ Mo		S
		Sr	Ti Al K Rb Zr Th Sn Nb La Ce Sc		Y
Mn Mg K Zr Ce Hf	Mg K P Rb Ba Ga Ti F	Na Zr Th	Fe² Fe³	Mn Mg K Zn Th Ce Hf	Ni
	S J Mo Hf	Nb Pb Co	Li Hf		Co
Ni	Fe² Mn Sn	Mg	Fe³ Fe² Ga F Co	Ni V	Zr
Fe² Mn Sc	Al Mg Na K Ni Zr Ba Th Sn Hf	Ti P	Al Fe² Mn Mg K Y Zr Ba Th Sn Nb La Ga Ce Hf	Si Ti Ca Sc	Rb
	Ca La Ce	Si Fe² Na Th	Na		Sr
Sc	Ti Al Na K Rb Th Ga V Sc Hf	Ca P Ni	Si Ti Al Mn Mg Ca K Y Rb Th Sn Nb La Ga Ce Hf	Sc	Zr
Si Fe² La Ce Li	Al Mg Na K Ni Rb Hf	Fe² Mo P Th	Si Mg K Rb As	Fe³ Ce L	Ba
Mn Ca	Al Ca K P Rb Zr Hf	Fe³ Mn Na Ni Sr Ba	Al Mg K Y Rb Zr Sn Nb La Ga Ce Hf	Mn Ca Ni F	Th
	Cu As Nb Mo Pb Sc Co	W		P	U
	Fe³ V	Zr U As Nb Sc			W
	Mn Zn Rb		Ti Al K Y Rb Zr Th Nb La Ga Ce Sc Hf	F	Sn
F Co	Li Nb Mg Pb	W	Ba F	Si Ca	As
F Co	U As Mo Pb Sc Co	Al Cu W Li	Ti Al Mn Mg Ca K Y Rb Zr Th Sn La Ga Ce V F Sc Hf	Nb	Nb
Ba	Si Ce		Al K Y Rb Zr Th Sn Nb Ce	Fe³	La
Ce	Ti Al Ni Zr Li V F Sc	Fe³ Mg K P	Ti Al Mn Ca K Zr Rb Zr Th Sn Nb La V F Sc Hf Co	Ce	Ga
Ti Ni Ba Ga Hf	Sr La		Al Mg K Y Rb Zr Th Sn Nb La	Ti Ni Ba Ga Sc	Ce
	Cu U As Nb Pb Co	Sc	Fe³ S Pb		Mo
	S U As Nb Mo	Cu V Sc	Mg		Pb
Ca Ba Hf	Al Ni Ga F	Mg Nb Sc	Al Fe² Cu Ga V F	Ca Ba Hf	Li
Ca F	Ti Zr W Ga Sc	Al Pb	Ti Al Fe³ Fe² Nb Ga Li Sc Co	Ca Zn P	V
As Nb V	Mg P Ni Ga L		Al Zn As Nb Ga L Co	P Th Sn V Hf	F
Fe² K Pb Zr	Ti Al Na K Zr U Nb Ga V	Si W Mo Pb Li Co	Ti Al Y Sn Nb Ga V Co	Fe³ K Rb Zr Ce	Sc
Ti Ni Ce Li	Al Cu Rb Zr Ba Th	K S Co	Al Mn Ca K Cu Rb Zr Th Sn Nb Ga	Ni Li P	Hf
As Nb	U Nb Mo	Na Cu As Sc Hf	Ti Al Fe³ Zr Ga V F Sc	As Nb	Co

CAHILL CORRELATIONS continued

	U>500ppm (15 analyses)		U>40ppm (31 analyses) (Co only 28 analyses)		U<40ppm (28 analyses)
	99%	95%	99%	95%	99%
Si	Ti Al Cu Zr Ga F	Li Sc	Ti Al Zr Ga Li V Sc	Σ Fe Mg K Y Ni	Σ Fe Mn Mg Cs
Ti	Si Al Cu Zr Ga F	K Sc	Si K P Zr Th Sc	Ca Na Rb Ba V Hf	Al Mg K P Y Rb Zr Th W Sn Nb La Ce Sc Hf
Al	Si Ti Na K Zr Ga F Sc	Cu	Si Ti Na K Rb Zr Ba Ga Sc	V Cu Th	Ti Mn Ca K Rb Sr Zr Ba W Sn Nb La Ga Ce F Sc Hf
Σ Fe	V Hf	S As Co	S As V Hf	Si	Si Mg K Ni
Mn		Zn		Rb Ba	Si Al Mg Ca K Zr Ga
Mg	Ni Li	Na K Zn Rb La	Ca K P Ni Zn Rb Ga Li F	Si Na Sn	Si Ti Σ Fe Mn Ca K V Rb Zr Ba Nb La Ce
Ca	P	Rb	Mg P Ni Sn Ga F	Ti Zn Zr Th Nb Pb	Si Al Mn Mg Ga
Na	Al K La Sc Co	Mg Ni Zn Sr Ba Ce	Al K Ni Zn Rb Ba	Ti Mg Th Sc	
K	Al Na Ba Sc	Ti Mg Ni Rb La	Ti Al Mg Na Ni Rb Zr Ba Th Sc	Si	Ti Al Σ Fe Mn Mg Y Rb Zr Ba Th W Sn Nb La Ce Sc Hf
P	Ca	Zr V	Ti Mg Ca Ni Zn Zr Th Sn Ga F		Ti Sc
S		Σ Fe As Ga V Hf	Σ Fe As V	Hf	Cu As Mo
V	Mn	U Nb Pb		Si Ti Al Sn	Ti Mg K Rb Zr Ba Sn Nb Ce Sc
Ni	Mg Rb Ba Li	Na K La	Mg Ca Na K P Zn Pb Ba Th Sn Ga Li F	Si	Σ Fe Zn Ga Ce F
Cu	Si Ti F	Al Zr Ga V	U Mo Pb	Al Rb Nb	S As Mo
Zn		Mn Mg Na La	Mg Na P N	Ca Li F	Ni Ga Li F
Rb	Ni Ba	Mg Ca K La Cl	Al Mg Na K Ni Ba Th Cl	Ti Mn Cu Zr Hf	Ti Al Mg K Y Zr Ba Th W Sn Nb La Ce Sc Hf
Sr		Na	Sr La Ce		Al
Zr	Si Ti Al Sc	P Cu Nb Ga	Si Ti Al K P Th Hf	Ca Pb F Sc	Ti Al Mn Mg K Y Rb Th Sn Nb La Ga Ce Hf
Ba	K Ni Rb La	Na Ce	Al Na K Ni Rb Th	Ti Mn Cl Hf	Al Mg K Y Rb W Sn Nb La Ce
Th		Pb	Ti K P Ni Rb Zr Ba Hf	Al Ca Na F	Ti K Rb Zr W Sn Nb La Ga Ce F Hf
U	Nb Mo Pb Sc Co	Y Sn As Ce	Cu W As Nb Mo Pb Sc Co	Sn	As Mo
W	Pb	As Nb Hf	U As Nb Mo Pb	V Hf	Ti Al K Rb Ba Th Sn Nb Ce Sn Hf
Sn		Ti Nb	Ca P Ni Sr La Ga	Mg V U Nb Mo F	Ti Al K Y Rb Zr Ba Th W Nb La Ga Ce Sc Hf
As	Nb V Hf	Σ Fe S U W Mo	Σ Fe S U W Nb Mo Pb V Hf	Sc	S Cu U Mo
Mo	U As Mo Pb Sc	Y Zr W Sn Ce Co	U W As Mo Pb Sc Co	Ca Cu Sn	Ti Al Mg K Y Rb Zr Ba Th W Sn La Ga Ce Sc Hf
La	Na Ba Ce	Mg K Ni Zn Rb Sc	Si Sn Cl P		Ti Al Mg K Rb Zr Ba Th Sn Nb Ce Sc
Ce	La Sc	Na Ba U Nb Pb	Sn La		Ti Al Mg K Y Ni Rb Zr Ba Th W Sn Nb La Sc
Mo	Y U Nb Pb F	As Co	Cu U W As Nb Pb Co	Sn F Sc	S Cu U As
Pb	U W Mn Mo	Y Th Ce	Cu U W As Nb Mo Sc	Ca	
Cl	Mg Ni	Si Rb Ga	Si Mg Ni Rb	Zn Ba Ga	Zn
V	Σ Fe As Hf	P S Cu	Si Σ Fe S As Hf	Ti W Sc	Sc
F	Si Ti Al Cu Ga Mo		Mg Ca P Ni Ga	Zn Zr Th Sn Mo	Al Ni Zn F Ga Cu
Sc	Ti Al Na K Zr U Nb Ce	Si Cl	Si Ti Al K U Nb Pb Co	Na Zr As Mo V	Ti Al K P Y Rb W Sn Nb La Ce V
Hf	Σ Fe As V	S W	Σ Fe Ti As V	Ti S Rb Ba W	Ti Al K Pb Zr Th W Sn Nb
Co	Na U	Σ Fe Nb Mo	U Nb Mo Sc		F

JABILUKA CORRELATIONS

Table 3. Correlations at the 99 and 95 percent confidence limits for Jabiluka One and Two for different uranium contents.

U≤40ppm (28 analyses)	U>30ppm (33 analyses) (Co only 28 analyses)		U≤ 30ppm (28 analyses)		
95%	80%	90%	90%	95%	
	Ti Al Zr Ga Li V Sc	Σ Fe Mg K Y Ni	Σ Fe Mn Mg Ca	Zr	Si
Ba V	Si Al K P Zr Th Sc	Ca Na V Rb Ba V Hf	Al Mg K P Y Rb Zr Th W Sn Nb La Ce Sc	Ba V Hf	Ti
Mg Y V	Si Ti Na K Rb Zr Ba Ga Sc	Cu Th	Ti Mn Ca K Rb Zr Ba Th W Sn Nb La Ga Ce F Sc	Mg Y V Hf	Al
Mn Zn Rb Ba W Nb Hf	S As V Hf	Si	Si Mg P Ni Hf	Mn S Zn Rb Ba W Nb	Σ Fe
Σ Fe Th W Nb La V		Rb Ba	Si Al Mg Ca K Zr Th Ga	Σ Fe Rb W Nb La V Hf	Mn
A W V Sc	Ca K P Ni Zn Rb Ga Li F	Si Na Sn	Si Ti Σ Fe Mn Ca K Y Rb Zr Ba Nb La Ce	Al V Sc	Mg
K Zr Th La V	Mg P Ni Sn Ga F	Ti Zn Zr Th	Si Al Mn Mg Zr Ga	K Th Nb La V	Ca
Si	Al K Ni Zn Rb Ba	Ti Mg Zr Th Sc			Na
Ce Ga Li V	Ti Al Mg Na Ni Rb Zr Ba Th Sc	Si	Ti Al Σ Fe Mn Mg Y Rb Ba Th W Sn Nb La Ce Sc Hf	Ca Zr Ga V	K
Y	Ti Mg Ca Ni Zn Zr Th Sr Ga F		Ti Sc	S Y	P
Zr U	Σ Fe As	V Hf	Cu As Mo	Σ Fe P Zr	S
Al P Ni Th La		Si Ti Sn	Ti Mg K Rb Zr Ba Sn Nb Ce Sc	Al P Ni Th La	Y
V Co	Mg Co Na K P Zn Rb Ba Th Sn Ga Li F	Si	Σ Fe Zn Ga Li F	V	Ni
U	U Mo Pb	A Rb Nb	S As Mo	U	Cu
Σ Fe	Mg Na P Ni	Ca Li F	Ni As Ga Li F	Σ Fe	Zn
Σ Fe Ga V	Al Mg Na K Ni Ba Th Li	Ti Mn Cu Zr Hf	Ti Al Mg K V Zr Ba Th W Sn Nb La Ce Sc Hf	Σ Fe Mn Ga V	Rb
Na Ce Sc	Sn La Ce			Sc	Sr
Ca S Sc	Si Ti Al K P Th Hf	Ce Na Rb Ba P Sc	Ti Al Mn Mg Ca Y Ag Th Sn Nb La Ga Ce Hf	Si K S W Sc	Zr
T Σ Fe Th Sc	Al Na K N Rb Th	Ti Mn Zr Li Hf	Al Mg K Y Rb W Sn Nb La Ce	Ti Σ Fe Th Sc	Ba
Mn Ca Y Ba Sc	Ti K P Ni Rb Zr Mg Hf	Al Ca Na F	Ti Al Mn K Rb Zr W Sn Nb La Ga Ce F Hf	Ca Y Ba Sc	Th
S Cu	Cu W As Nb Mo Pb Sc Co	Sn		Cu As Mo V	U
Σ Fe Mn Mg La Ga V	U As Nb Mo Pb	V Hf	Ti Al K Rb Th Sn Nb Ce Sc Hf	Σ Fe Mn Zr La Ga V	W
	Ca P Ni Sr La Ga	Mg Y U Nb Mo F	Ti Al K Y Rb Zr Ba Th W Nb La Ga Ce Sc Hf		Sn
	Σ Fe S U W Nb Mo Pb V Hf	Sc	S Cu Zn Mo	U	As
Σ Fe Mn V	U W As Mo Pb Sc Co	Cu Sr	Ti Al Mg K Y Rb Zr Ba Th W Sn La Ga Ce Sc Hf	Σ Fe Mn Co	Nb
Mn Ca Y W Ga	Sr Sr Ce		Ti Al Mg K Rb Zr Ba Sn Nb Ce Sc	Mn Ca Y W Ga	La
K Rb W La V Sc Hf Co	Si Al Mg Ca P Ni Sn F	Li Sc	A Mn Ca Ni Zn Zr Th Sn Nb F Sc	K Rb W La V Co	Ga
Sr V	Sr La		Ti Al Mg K Y Rb Zr Ba Th W Sn Nb La Sc	V	Ce
	Cu U W As Nb Pb Co	Sn F Sc	S Cu As	U	Mo
	Cu U W As Nb Mo Sc				Pb
K	Si Mg Ni Rb	Zn Ba Ga	Ni Zn	F	Li
Ti Al Mn Mg Ca K Rb W Nb Ga Ce	Si Σ Fe As Hf	Ti S W Sc	Sc	Ti Al Mn Mg Ca K Rb U W Ga Ce	V
	Mg Ca P Ni Ga	Zn Zr Th Sn Mo	Al N Zn Th Ga Co	Li	F
Mg Sr Zr Ba Th Ga	Si Ti Al K U Nb Pb Co	Na Zr As Ge Mo V	Ti Al K P Y Rb W Sn Nb La Ga Ce V	Mg Sr Zr Ba Th	Sc
Σ Fe Ga	Fe Zr Th As V	Ti S Rb Ba W	Σ F K Rb Zr Th W Sn Nb	Ti Al Mn Co	Hf
Nb Ga	U Nb Mo Sc		F	Ga Hf	Co

JABILUKA CORRELATIONS continued

Cluster No	1		2		3		4		5		6		7		8	
No of analyses	46	SD	8	SD	5	SD	19	SD	11	SD	7	SD	2	SD	3	SD
SiO_2	64.24	6.62	62.38	5.12	38.21	7.92	61.61	8.27	62.82	6.98	59.40	5.57	58.90	9.40	81.68	1.48
TiO_2	0.56	0.29	0.56	0.22	0.48	0.15	0.51	0.21	0.41	0.13	0.27	0.15	1.02	0.50	0.32	0.05
Al_2O_3	15.06	2.47	9.87	1.93	16.66	3.43	13.65	4.44	14.08	1.84	11.91	2.40	24.92	5.34	9.52	0.68
Fe_2O_3	1.47	0.80	12.07	5.55	1.58	0.80	2.65	1.23	2.10	0.76	1.52	0.78	1.28	0.64	1.91	0.64
FeO	3.46	2.06	2.69	3.61	8.63	3.17	3.00	1.47	3.61	1.42	2.52	1.13	0.29	0.10	0.40	0.10
ΣFe_2O_3	5.35	2.79	15.05	3.43	13.16	3.17	5.97	2.05	6.11	2.17	4.32	1.83	1.80	0.75	2.35	0.50
MnO	0.05	0.04	0.15	0.28	0.06	0.06	0.03	0.01	0.05	0.05	0.02	0.01	0.01	0.01	0.01	0
MgO	5.91	3.22	2.66	0.85	20.00	1.74	9.18	3.41	9.04	3.25	13.44	1.71	1.62	0.23	1.22	0.16
CaO	0.65	1.38	0.26	0.31	1.72	2.65	0.78	0.16	0.14	0.05	2.05	0.67	0.20	0.18	0.08	0.01
Na_2O	0.43	0.86	0.02	0.01	0.02	0.02	0.05	0.04	0.05	0.02	0.04	0.03	0.20	0.06	0.20	0.12
K_2O	2.68	1.31	0.42	0.39	0.04	0.02	1.47	1.58	1.61	1.06	0.22	0.14	6.91	1.86	2.22	0.14
P_2O_5	0.10	0.05	0.13	0.04	0.24	0.26	0.18	0.13	0.10	0.04	1.29	0.46	0.14	0.11	0.06	0.03
LOI	4.82	2.15	8.72	0.92	11.82	3.61	6.70	1.54	5.96	1.49	7.13	0.89	4.00	0.64	2.11	0.07
S	0.14	0.22	2.58	3.58	0.17	0.23	0.38	0.51	0.09	0.16	0.07	0.05	0.03	0.01	0.04	0.01
Y	22	8.43	27	5.10	5	3.26	19	15.85	21	5.97	24	11.43	35	21.00	15	1.20
Ni	39	18.04	37	6.38	102	49.95	91	26.13	72	24.56	168	59.07	14	6.50	76	14.97
Cu	63	173.18	148	81.39	309	601.21	337	539.59	189	274.55	57	47.41	3	0	3	0.82
Zn	43	22.84	68	9.29	114	46.75	56	34.10	74	98.00	71	29.43	13	3.50	18	10.66
Rb	91	43.99	23	24.75	<2	0	30	32.75	67	53.07	6	3.11	297	169.00	67	2.94
Sr	33	57.56	1	1.70	7	3.31	8	9.78	2	2.02	17	20.11	33	33.50	14	2.62
Zr	183	49.74	103	36.71	155	65.89	144	49.39	184	34.74	76	34.64	318	159.00	196	56.36
Ba	301	235.51	177	126.07	40	5.89	73	53.51	113	65.16	18	10.40	771	170.50	409	147.56
Th	17	5.47	11	0.82	16	6.53	16	6.90	21	4.33	6	2.10	29	29.00	12	2.87
U	87	208.15	243	205.89	34	62.43	1617	1248.38	790	644.33	160	97.64	15	9.00	<2	0.94
W	2	2.12	2	1.76	3	3.10	5	4.40	5	2.97	5	4.07	7	3.50	<2	1.41
Sn	3	2.21	2	1.63	3	0.75	4	1.87	11	13.80	7	3.82	19	15.00	2	0
As	<2	2.33	<2	0.94	<2	0	<2	0.89	<2	0.58	<2	0.70	<2	0	4	2.62
Mo	11	3.17	9	3.68	8	0.75	26	14.61	16	7.06	8	2.32	26	14.50	6	2.05
La	28	14.28	42	15.11	7	12.89	<2	1.46	4	2.46	26	47.63	94	12.00	31	4.19
Ga	23	7.08	13	1.41	38	13.33	41	13.22	34	6.17	47	16.40	40	12.00	12	1.41
Ce	56	23.31	67	23.75	17	13.73	12	5.47	12	8.13	37	58.32	173	40.00	53	5.31
Mo	5	5.40	8	4.08	3	1.55	9	14.79	2	1.54	<2	1.16	5	0.50	3	2.05
Pb	27	21.33	21	11.43	4	5.00	822	1093.24	85	47.53	20	6.57	12	0.50	3	0.82
Li	62	33.35	39	14.61	116	32.65	92	41.01	79	26.32	115	30.03	22	6.50	25	6.65
V	148	96.02	223	58.36	159	45.23	249	109.40	169	48.67	181	28.38	197	42.50	35	13.74
F	669	175.56	423	80.19	1344	591.02	742	222.24	753	121.59	1814	483.08	740	260.00	213	16.99
Sc	17	7.24	22	9.90	13	4.52	20	6.75	14	7.45	20	4.30	31	10.00	8	1.70
Ef	7	2.52	2	1.25	9	6.43	4	3.25	5	1.27	3	1.60	13	4.50	7	2.45

PCG numbers

Cluster 1: 48, 112, 113, 131, 114, 150, 77, 83, 132, 133, 134, 186, 50, 69, 68, 70, 67, 154, 155, 59, 115, 58, 142, 65, 66, 129, 169, 60, 55, 75, 84, 80, 89, 88, 161, 163, 91, 162, 76, 181, 180, 183, 184, 185, 105, 182.

Cluster 2: 74, 82, 159.

Cluster 3: 100, 123, 11, 141, 171.

Cluster 4: 73, 101, 120, 148, 81, 126, 166, 189, 151, 87, 118, 119, 129, 78, 79, 86, 102, 168, 187.

Table 4. Averages and standard deviations of Cahill Formation 16 cluster groups selected at a distance coefficient of 20.0.

9		10		11		12		13		14		15		16		Cluster No
6	SD	2	SD	5	SD	2	SD	4	SD	3	SD	4	SD	3	SD	No of analyses
64.56	7.81	52.38	6.70	76.47	18.87	90.48	3.43	20.84	6.55	48.76	3.35	7.43	2.13	81.91	14.51	SiO_2
0.28	0.21	3.01	2.66	0.09	0.03	0.03	0.02	0.20	0.05	0.61	0.25	0.05	0.04	0.06	0.03	TiO_2
22.16	2.57	25.48	6.82	4.00	1.73	2.05	0.51	6.39	1.94	6.76	2.41	1.30	0.84	3.57	1.15	Al_2O_3
3.07	1.12	0.69	0.45	9.76	18.29	0.30	0.11	1.54	1.00	3.35	0.99	0.66	0.56	0.23	0.06	Fe_2O_3
2.02	0.69	0.35	0.06	1.11	0.38	1.06	0.23	2.78	1.37	8.43	2.65	2.84	2.34	0.59	0.50	FeO
5.31	1.56	5.08	0.38	11.00	18.63	1.47	0.14	4.62	2.48	12.71	1.76	3.82	3.14	0.88	0.57	ΣFe_2O_3
0.06	0.06	0.01	0	0.01	0.01	0.01	0.01	0.11	0.12	0.19	0.03	0.19	0.15	0.05	0.06	MnO
8.11	2.61	2.26	1.09	4.61	2.62	2.35	0.77	19.24	4.21	20.27	1.44	27.82	6.34	4.31	6.03	MgO
0.16	0.05	0.71	0.51	0.49	0.26	1.08	0.82	38.77	3.65	5.43	1.06	16.32	9.75	6.02	8.49	CaO
0.04	0.02	0.16	0.08	0.03	0.02	0.04	0.01	0.03	0.02	0.49	0.32	0.03	0.01	0.31	0.25	Na_2O
0.97	0.58	6.32	1.60	0.01	0.01	0.17	0.13	0.63	1.02	0.08	0.06	0.03	0.02	2.11	1.33	K_2O
0.14	0.08	0.49	0.38	0.28	0.18	0.69	0.52	0.17	0.08	0.06	0.02	0.07	0.02	0.05	0.04	P_2O_5
6.69	1.76	6.34	1.14	2.70	1.25	1.42	0.50	29.20	5.65	1.14	0.35	42.59	2.07	0.42	0.27	LOI
0.11	0.15	0.06	0.04	0.23	0.32	0.03	0.02	0.35	0.49	0.05	0.01	0.07	0.03	0.02	0.01	S
26	13.38	37	5.00	43	33.63	4	2.50	9	4.49	11	3.56	13	14.84	15	13.02	Y
78	32.39	48	5.50	60	31.11	27	5.00	31	22.72	1051	313.02	6	3.77	5	1.70	Nb
288	539.81	223	22.00	398	449.32	9	0	101	150.44	115	14.97	16	18.80	6	3.09	Cu
57	35.13	14	10.50	26	8.13	20	5.00	23	8.12	76	21.35	7	4.15	31	43.72	Zn
24	25.03	68	21.50	<2	0	1	1.00	31	52.55	<2	1.89	<2	0	58	33.18	Rb
8	8.39	19	9.00	7	7.91	8	4.50	32	10.83	35	15.11	21	13.08	37	13.60	Sr
160	51.85	332	86.50	29	12.25	26	22.00	38	7.43	41	18.55	9	6.06	82	4.64	Zr
98	59.87	117	110.00	12	4.76	31	20.50	46	69.24	38	22.07	2	3.00	1743	1471.66	Ba
19	6.66	15	3.50	8	6.89	1	1.00	6	2.17	<2	0.94	<2	0.87	20	10.37	Th
7691	4227.43	6315	5613.00	365	187.84	27	9.00	140	134.19	3	5.77	4	1.73	5	3.30	U
10	4.23	9	3.00	10	11.21	1	1.00	<2	0	21	29.70	<2	1.30	<2	0	W
6	5.03	5	3.00	3	2.68	<2	0	<2	0.67	2	1.25	<2	0	<2	0	Sn
11	4.43	<2	0	<2	0	<2	0	<2	0	<2	0.94	<2	0	3	3.77	Ag
82	40.89	75	47.00	6	1.74	4	3.50	4	0.43	<2	1.25	<2	0	<2	0	Sb
23	26.00	10	10.00	26	46.29	<2	0	6	6.50	5	4.99	20	30.73	38	33.36	La
30	6.70	75	28.50	16	10.68	7	1.00	12	6.38	9	1.25	<2	1.30	4	0.67	Ga
53	31.08	30	20.50	36	94.13	6	7.00	26	12.03	12	8.81	23	10.01	59	44.97	Ce
64	71.19	48	42.00	6	7.11	3	0	3	0.43	4	1.63	3	1.92	3	0.82	Mo
1605	1105.76	723	529.50	44	16.63	11	4.00	14	10.47	3	1.41	<2	1.30	17	11.31	Pb
108	27.41	94	47.00	50	22.46	32	10.50	32	15.14	6	1.25	9	4.56	3	3.09	Li
247	186.37	666	564.50	81	65.89	37	6.00	56	29.93	163	19.82	8	8.38	29	18.03	V
573	220.13	1100	100.00	880	661.30	710	490.00	683	275.15	447	287.67	161	63.09	40	37.42	F
27	7.47	62	3.00	8	2.06	5	0.50	8	6.02	19	4.78	8	5.45	7	7.41	Sc
5	3.20	<2	0	<2	0.80	3	0.50	4	1.50	<2	0	3	0.83	4	2.25	Be

Cluster 5: 95, 96, 105, 106, 107, 108, 158, 164, 180, 172, 167. Cluster 6: 103, 109, 122, 176, 177, 178, 179

Cluster 7: 62, 136. Cluster 8: 118, 119, 140. Cluster 9: 92, 93, 98, 94, 97, 152. Cluster 10: 124, 157.

Cluster 11: 83, 84, 174, 175, 184. Cluster 12: 99, 121. Cluster 13 110, 128, 153, 170. Cluster 14: 135, 137, 188.

Cluster 15: 116, 127, 149, 117. Cluster 16: 130, 123, 136.

Table 4 continued

Cluster No	1		2		3		4		5	
No of analyses	20	SD	6	SD	3	SD	10	SD	23	SD
SiO_2	72.36	1.75	73.96	1.48	75.78	3.28	69.41	3.96	64.27	3.33
TiO_2	0.23	0.60	0.06	0.04	0.01	0	0.47	0.17	0.55	0.15
Al_2O_3	13.91	0.85	13.86	0.61	13.47	1.68	14.21	1.33	16.30	1.28
FFe_2O_3	2.08	0.56	0.94	0.12	0.42	0.17	3.51	0.81	4.80	1.09
MnO	0.02	0.01	0.02	0.02	0.01	0	0.04	0.02	0.06	0.02
MgO	0.55	0.12	0.63	0.68	0.12	0.03	0.95	0.51	1.32	0.44
CaO	1.32	1.08	0.61	0.07	0.83	0.50	1.70	0.65	4.60	1.36
Na_2O	3.22	0.60	3.55	0.28	3.29	0.95	2.76	0.52	2.88	0.60
K_2O	5.05	0.82	5.46	0.27	5.50	2.13	5.42	1.06	3.36	0.67
P_2O_5	0.11	0.09	0.08	0.04	0.06	0.01	0.20	0.14	0.15	0.04
LOI	0.84	0.30	0.79	0.27	0.31	0.13	1.06	0.68	1.56	0.50
S	0.02	0.01	0.03	0.04	0.01	0	0.02	0.01	0.02	0.01
Y	18	8.84	15	12.23	4	1.41	32	15.23	24	5.82
Ni	2	1.55	3	1.34	1	0.94	6	5.38	7	2.55
Cu	6	3.28	13	12.06	4	0.47	10	8.74	11	7.30
Zn	27	9.91	15	3.89	3	1.25	48	20.62	55	14.08
Rb	213	74.50	168	62.32	120	49.03	271	61.56	144	33.84
Sr	160	104.93	88	28.25	209	8.73	296	218.18	351	71.44
Zr	185	51.51	61	30.59	80	65.57	446	304.68	241	39.54
Ba	690	434.57	342	184.70	819	353.71	1049	527.20	1009	222.13
Th	44	19.21	19	13.01	7	8.52	69	27.92	18	5.83
U	9	9.33	17	11.91	5	2.05	8	3.79	3	2.20
W	2	1.72	3	2.52	<2	0	1	1.20	1	1.06
Sn	1	1.47	1	0.94	1	0.94	2	1.37	1	1.73
As	<2	0	<2	0	<2	0	<2	0.60	1	1.06
Nb	12	7.25	5	4.51	<2	0	20	8.98	10	2.90
La	73	28.55	14	12.64	10	6.94	130	64.41	63	19.13
Ga	18	1.98	16	2.50	13	1.25	21	6.71	21	2.50
Ce	126	45.01	31	20.79	26	16.78	250	71.12	115	32.23
Mo	4	2.27	4	3.68	1	2.45	7	7.90	4	2.18
Pb	37	9.58	53	11.95	44	18.35	44	11.04	23	6.66
Li	16	7.23	13	4.41	3	0.94	22	5.26	27	9.92
V	26	16.55	7	4.63	11	4.11	53	41.96	53	17.70
F	516	481.45	121	59.33	<20	0	1013	444.39	800	206.56
Sc	6	4.79	4	2.21	3	1.41	9	4.07	15	3.98
Hf	7	2.01	3	1.70	6	2.05	14	5.52	8	2.69
$\frac{Al_2O_3}{Na_2O+K_2O+CaO}$	0.53		1.08		1.05		1.05		0.97	

POG Numbers:
Cluster 1: 336, 332, 334, 275, 265, 269, 330, 297, 331, 314, 318, 315, 321, 322, 327, 324, 325, 278, 288, 291.
Cluster 2: 329, 326, 335, 310, 312, 308. Cluster 3: 319, 320, 323.
Cluster 4: 33, 262, 271, 280, 281, 317, 313, 316, 272, 16.
Cluster 5: 263, 279, 284, 295, 298, 299, 300, 305, 303, 282, 304, 283, 285, 292, 289, 293, 301, 302, 286, 287, 290, 296, 294.
Cluster 6: 311, 14, 15. Cluster 7: 337, 328, 267, 276. Cluster 8: 270, 266, 268.
Cluster 9: 264, 277, 273, 274. Cluster 10: 306, 307, 309

Table 6. Averages and standard deviations of granitoids 10 cluster groups selected at a distance coefficient of 16.0.

6		7		8		9		10		Cluster No
3	SD	4	SD	3	SD	4	SD	3	SD	No of analyses
50.77	3.32	72.64	2.75	76.54	1.02	77.25	3.77	68.98	2.74	SiO_2
0.86	0.07	0.05	0.01	0.05	0	0.36	0.08	0.01	0	TiO_2
16.17	2.14	12.08	0.70	11.72	0.37	12.73	1.62	15.14	0.61	Al_2O_3
10.82	1.13	1.04	0.30	1.43	0.22	2.50	0.68	2.38	1.39	ΣFe_2O_3
0.15	0.01	0.01	0.004	0.01	0.01	0.01	0	0.02	0.01	MnO
6.96	1.89	0.51	0.42	0.25	0.08	0.61	0.47	4.94	0.93	MgO
3.08	2.61	0.17	0.12	0.31	0.08	0.02	0.01	0.75	0.46	CaO
1.32	0.92	2.03	1.84	1.70	0.73	1.10	0.01	0.08	0	Na_2O
3.42	1.58	4.81	1.19	6.70	1.01	2.66	1.45	2.51	0.80	K_2O
0.22	0.20	0.02	0.01	0.01	0.01	0.06	0.02	0.55	0.36	P_2O_5
3.00	0.65	1.32	0.78	1.12	0.28	2.81	1.22	4.61	1.18	LOI
0.11	0.05	0.01	0.004	0.02	0.01	0.01	0.004	0.06	0.03	S
18	6.85	45	15.04	93	8.38	22	9.21	9	6.60	Y
127	65.56	1	0.80	1	0.47	7	8.50	26	19.69	Ni
44	26.45	6	5.67	7	4.78	7	7.68	10	4.55	Cu
172	87.64	7	1.34	35	14.06	3	2.49	35	6.68	Zn
79	97.57	283	90.24	432	89.36	105	48.93	147	63.59	Rb
120	64.39	76	21.24	7	0.94	41	35.65	28	17.52	Sr
138	97.17	87	7.48	147	38.26	255	43.55	25	7.65	Zr
1086	926.12	44	71.58	62	17.02	288	186.99	12	2.49	Ba
9	6.65	44	17.32	68	11.76	54	37.89	<2	0	Th
3	2.50	10	2.86	17	4.64	3	0	25	14.17	U
<2	0	3	3.00	2	0	7	8.53	2	1.70	W
<2	0	3	1.92	10	5.91	2	1.30	29	26.04	Sn
3	4.24	<2	0	4	2.06	<2	0	<2	0	As
8	6.13	36	29.38	39	10.40	16	8.95	11	4.78	Nb
33	23.70	19	10.86	42	7.12	93	46.57	38	53.27	La
18	5.66	21	4.39	26	0.82	36	4.15	34	13.89	Ce
68	36.13	45	17.47	96	22.22	141	53.99	61	71.00	Ce
6	1.70	2	1.48	3	0.67	3	0.71	4	3.27	Mo
28	29.96	20	17.50	12	4.78	5	1.87	4	2.94	Pb
35	5.32	13	12.46	32	9.81	39	11.15	85	9.46	Li
226	18.06	3	0.50	3	1.63	58	33.51	69	90.39	V
580	249.13	998	600.22	3067	602.77	450	318.04	523	382.98	F
30	7.07	5	3.70	2	2.25	9	1.79	20	3.86	Sc
6	4.50	5	3.11	9	4.24	10	1.30	6	2.36	Hf
1.41		1.36		1.11		4.13		3.60		$\frac{Al_2O_3}{Na_2O+K_2O+CaO}$

Table 6 continued

	Rimbunwah Complex (99 analyses)	Nanambu Complex (118 analyses)	Waterhouse Granite (8 analyses)	Granitoids – Less Organic (15 analyses)	Zamu Dolerite (38 analyses)	Stag Creek Volcanics (8 analyses)	KOMBOLGIE FORMATION Nungalgarri Volcanic Member (5 analyses)	Arenites and Rudites (5 analyses)	
S	Ti Al Σ Fe Mn Mg Ca K Zn Sr W Ga F Sc	Ti Al Σ Fe Mn Mg S Ni Cu Zn As Ga Mo Li V F Sc	As Na Pb	Al Σ Fe Mn Mg Ca F Ni Sr Ba	Al Mg S	S	As Ca Ga Li	Al Σ Fe Mg Zn Ga Mo Li	Si
Ti	Si Al Σ Fe Mg Ca S Zn Sr Zr Ga V F Sc	Si Al Σ Fe Mn Mg P Y Σ Pb Zr Th Nb La Ga Ce Mo Li V F Sc Hf	Σ Fe Mn Ga Zr La Ce V Sc Hf	Σ Fe Mn P Rb Zr Ba V Sc	Σ Fe Mn P Y Zn Zr Nb La Ca Mo V F	P Y Zr Th Nb La Ce Pb Hf	V Fe Mg Ni Ga Pb	Ca P Y Zn Sr Li W As Nb La Ce Sc	T
A	Si Ti Σ Fe Mn Mg Li Na K Zn Sr W Ga F Sc	Si Ti Σ Fe Mn Mg S Ni Cu Zn Rb Ga Mo V Sc	S Na K Y Rb Pb	Si La	Si U S Na S Sr	Sc	Sr Ca Ga Li	Si Σ Fe Mg S Ni Th Ga Mo Li V	A
Σ Fe	Si Ti Al Mn Ca K S Ni Zn Sr Zr Ga V F Sc	Si Ti Al Mn Mg S Ni Cu Zn As Ga Mo Li V F Sc	Ti Mn Ca Zr Zn La Ce V Sc Hf	Si Ti Mn Ca P Zr Ba V Sc	Ti Mn Ca P Y Zn Zr Nb V Sc	Ca Na Sr Zr Zn Ga V F	Ti	Si Al S Ni Th Ge Mo Li V	Σ Fe
Mn	Si Al Σ Fe Mg Ca Na Zr Sr Ni Zn Ga Ge F Sc	Si Ti Al Σ Fe Mg S Ni Cu Zn Rb V Sc	Ti Σ Fe Ce Zn Zr La V Hf	Si Ti Σ Fe Mg Ca P Ni Sr Ba Sc	Ti Σ Fe P Zn Mn Sc		Zn Hf	Ca W As	Mn
Mg	Si Ti Al Σ Fe Mn Ca F S Ni Zn Sr Ga V F Sc	Si Ti Al Σ Fe Mn S Al Cu Zn Rb Ga Li V Sc	V	Si Mn Ca P Ni Sr Ba	Si Al Na Ni Sr Zr Mn Li	K Rb Li	Ti Ni La Sc	Si Al Zr	Mg
Ca	Si Ti Al Σ Fe Mn Mg K S Zn Sr Ga F Sc	Sc	Ti Σ Fe Mn Zr Ce Hf	Si Σ Fe Mn Mg P Ni Sr Ba Sc	Fe S Cl Sc	Si Al Cu Ge Pb Li	Si Al Cu Ge Pb Li	Ti Na P Y Sr U W As Nb La Ce Sc	Ca
Na	Al Mn Y Sr Ga	Sc	S Al K Y Sn Pb	Pb	Al Mg Sr	Fe Ca Si Zr Th Ga V F			Na
F	Si Ti Al Σ Fe Mg Ca S Ni Cu Rb Y Tl La Ga Ce Pb V Sc	Ba	Al Na Y Pb	U F	Rb	Mg Rb Th	Rb Sr Ba		K
P		F Y Zr Nb La Ce Li F Hf	S	Si Ti Σ Fe Mn Mg Ca Ni Sr Ba V Sc	Ti Σ Fe Mn Y Zn Zr Th W Nb La Ce F Hf	Ti Y Zr Th Nb La Ce Hf		Ti Ca Y Sr U W As Nb La Ce Sc	P
S	Si Ti Σ Fe Mg Ca K Cl V F	Si Al Σ Fe Mn Mg Ni Cu Zn As Pb V Sc	P		Si Al Ca Mo	S Cu	H1	Al Σ Fe Ni Cu Th Ga Mo Li V	S
V	Na	F P Zr Nb La Ce F Hf	Al Na K Rb Sn Nb Pb	Rb U Sn As Ga F	Ti Σ Fe F Zn Zr Th W Nb La Ce Mo V F Hf	Th Zr Th Nb La Ge Ce Pb Hf	Cu Sc	Ti Ca P Sr U W As Nb La Ce Sc	V
Ni	Σ Fe Mg F Pb V	Si Al Σ Fe Ni Mg S Ca Zn As Ga V Sc	Cu	Si Mn Mg Ca P Si Ba Sc	Mg		Ti Mg La	Al Σ Fe S Cu Th Ga Mo Li V	Ni
Cu	K S	Si Al Σ Fe Mn Mg S Ni Zn As Pb V Sc	Ni Zr	Mo		S	Ca V Ga	S Ni Ga V	Cu
Zn	Si Ti Al Σ Fe Mn Mg Ca Sr Ga Li F Sc	Si Ti Al Σ Fe Mn Mg S Ni Cu As Ga Li V F	Σ Fe Mn W Li		Ti Σ Fe Mn P Y Zr Nb Ca Mo V F		Mn Ba Th W	Ti Nb La Ce Sc	Zn
Rb	K Th U La Ce Pb	T Zr Th Nb La Ga Ce Li F Hf	V	Si Y Zr Li Sn La Ga F Sc	K Ga	Mg K Th	K Sr Si		Rb
Sr	Si Ti Al Σ Fe Mn Mg Ca Na Zn Ga F	Ba W	Ba	Si Mn Mg Ca P Ni Ba	Al Mg Na Ba La Ce F	Σ Fe Ca Na Zr Th Ga V F	K Rb	Ti Ca P Y U W As Nb La Ce Pb Sc	Sr
Zr	T Σ Fe Hf	F P Y Nb Th Nb La Ce Li F Hf	T Σ Fe Mn Ca Ga La V Sc Hf	Ti Σ Fe Rb V Sc Hf	Ti Σ Fe Mg P Y Zn Ba Th W Nb La Ce F Hf	T Σ Fe Ca Na P Y Sr Th Nb La Ga Ce V F	Nb	Mg Hf	Zr
Be		K Sr	Si La V Hf	Si Ti Zr Fe Mn Mg Ca P Ni Sr V Sc	Sr Zr Th As La Ce Hf	Ca	K Zn W		Ba
U	Rb Nb Mo	Sn	Mo	K Y Rb As Nb F	W Li			Ti Ca P Y Sr W As Nb La Ce Pb Sc	U
W	Si Al Ga	Sr	Zn		P Y Zr U Nb La Ce F Hf		Zn Ba Th V	Ti Mn Ca P Y Sr U As Nb La Ce Sc	W
Sn		U	Na Y Nb	V Rb Ga F			Rb Mo		Sn
As		Si Al Σ Fe Mn Mg S Ni Cu Zn V Sc		Y U Nb Ga	Ba Li			Ti Mn Ca P Y Si L W Nb La Ce Sc	As
Nb	V U Ga F	Ti P Y Rb Zr Th La Ga Ce Li F Hf	Al Y Sn	U As Ga	Ti Σ Fe P Y Zn Zr Th W La Ce F Hf	Ti P Y Zr Th La Ga Ce V Hf	Zr	Ti Ca P Y Zr Si U W As La Ce Pb Sc	Nb
La	V Th K Ga Th Ce Pb	Ti P Y Rb Zr Ti Th Nb Ce Li F Hf	F Σ Fe Mn Zn Zr Ba Ce V Hf	Al Sn Ce	Ti P Y Sr Zr Ba Th W Nb Ca F Hf	Ti P Y Zr Th Nb Ce	Mg Ni Hf	Ti Ca P Y Zn Sr U W As Nb Ce Pb Sc	La
Ga	Si Ti Al Σ Fe Mn Mg Ca Na K Zn Sr W Ni F Sc	Si Ti Al Σ Fe Mn Mg Rb Zn Rb Y Nb La V F		Y Rb Sn As Nb F	Rb	Σ Fe Ca Na Y Sr Zr Th Nb F	S Ti Al Ca Cu Pb Li	Si Al Σ Fe S Ni Cu Th Mo Li V	Ga
Ce	Mn K Rb Th La Pb Hf	Ti P Y Rb Zr Th Nb La Li F Hf	Ti Σ Fe Ca La V Hf	La	Ti P Y Zn Ba Zr Ba Th W Nb La F Hf	Ti P Y Zr Th Nb La		Ti Ca P Y Zr Sr U W As Nb La Pb Sc	Ce
Mo	U	Si Ti Al Σ Fe Sc	U	Cu	Ti Mn Mg S Y Zn V		Sn F	Si Al Σ Fe S Ni Th Ga Li V	Mo
Pb	K Rb Rb Th La Ce V	S Cu	Si Al Na K Y	Na		Ti Y	Ti Ca Ga Li	Sr U Nb La Ce Sc	Pb
Li	Zn	Si Ti Σ Fe Mg P Zn Rb Zr Th Nb La Ga Ce V F	Zn		Mg Ca U	Mg Cu	Si Al Ca Ga Pb	Si Al Σ Fe S Ni Th Ga Mg V	Li
V	Ti Al Fe Mg K S Ni Pb	Si Ti Al Σ Fe Mn Mg S Ni Cu Zn As Ga Li F	Ti Σ Fe Mn Mg Zr Ba La Ce Hf	Ti Σ Fe P Zr Ba Sc	Ti Σ Fe P Y Zn Mo Sc	Σ Fe Ca Na Sr Zr Nb F Sc	W	Al Σ Fe S Ni Cu Th Ga Mo Li	V
F	Si Ti Al Σ Fe Mn Mg Ca S Zn Sr Nb Ga	Si Ti Σ Fe P Y Zn Hf Zr Th Nb La Ga Ce Li V Ni		K Y Rb U Sr Ga	Ti P Y Zn Sr Zr W Nb La Ce Hf	Σ Fe Ca Na Y Sr Zr Th Ga V	Mo		F
Sc	Si Ti Al Σ Fe Mn Mg Ca K Zn Ga	Si Ti Al Σ Fe Mn Mg Ca Na S Ni Cu As Mo	Ti Σ Fe Zr Hf	Ti Σ Fe Mn Ca P Ni Rb Zr Ba V F	Σ Fe Mn Ca V	Al V	Mo Y	Ti Ca P Y Zn Sr U W As Nb La Ce Pb	Sc
Hf	Zr Ce	Ti P Y Rb Zr Th Nb La Ce F	Ti Σ Fe Mn Ga Zr Ba La Ce V Sc	Zr	P Y Zr Ba Th W Nb La Ce	Ti P Y Nb	Mn Sn	Zr	Hf

Table 5. Correlations at the 99 percent confidence limit for a number of rock units in the Pine Creek Geosyncline.

No. of Analyses	Nimbuwah Complex 29 analyses		Namarlun Complex 18 analyses		Waterhouse Complex 8 analyses		Granitoids – Late Orogenic 15 analyses		Zamu Dolerite 38 analyses		Stag Creek Volcanics 8 analyses	
	Mean	SD	Mean	SD	Mean	SD	Mean	SD	Mean	SD	Mean	SD
SiO_2	68.69	4.633	71.67	4.912	74.86	3.049	73.78	4.428	48.79	6.365	49.55	3.826
TiO_2	0.48	0.170	0.27	0.256	0.18	0.122	0.26	0.204	1.26	0.958	1.76	0.830
Al_2O_3	15.79	1.717	14.48	1.565	12.97	0.896	12.91	1.984	14.02	3.414	14.12	1.581
ΣFe_2O_3	4.14	1.250	2.19	2.060	1.76	0.838	2.67	1.551	12.38	4.714	15.62	3.574
MnO	0.05	0.023	0.03	0.035	0.03	0.013	0.02	0.019	0.17	0.047	0.21	0.043
MgO	1.17	0.500	0.75	0.920	0.47	0.176	0.63	0.551	6.39	3.251	6.52	2.528
CaO	4.10	1.672	1.07	0.709	0.74	0.454	0.81	0.907	9.67	4.392	9.43	1.678
Na_2O	2.48	0.838	3.76	0.612	2.89	1.053	1.92	1.279	1.34	0.793	1.04	1.422
K_2O	3.61	1.041	5.28	1.010	4.91	0.814	4.98	1.686	1.04	0.581	2.38	2.296
P_2O_5	0.14	0.078	0.14	0.110	0.09	0.022	0.06	0.060	0.15	0.133	0.24	0.184
LOI	1.47	0.581	0.74	0.518	0.79	0.317	1.65	1.003	2.91	3.246	5.49	2.231
S	0.02	0.014	0.03	0.028	0.02	0.010	0.01	0.006	0.12	0.335	0.03	0.019
Y	23	5.950	13	10.904	32	20.131	41	27.970	23	15.222	40	21.201
Ni	6	4.023	6	13.326	2	2.315	3	4.057	84	91.226	86	42.836
Cu	10	7.056	10	14.872	7	6.685	6	4.484	56	41.685	25	25.956
Zn	50	16.932	37	54.812	25	11.900	21	14.704	97	31.147	84	33.895
Rb	147	54.060	191	76.711	236	41.866	270	135.92	46	23.815	46	48.541
Sr	329	90.983	134	67.770	147	115.42	142	223.23	150	117.89	80	119.94
Zr	237	43.830	205	166.39	173	126.21	187	69.771	93	75.645	138	57.691
Ba	1099	275.02	499	249.79	830	549.72	479	492.34	256	300.51	252	166.30
Th	24	25.262	18	28.91	44	13.777	55	21.685	5	4.273	4	2.727
U	2	2.175	9	5.822	13	9.955	9	5.365	2	5.487	3	3.345
W	<2	1.372	<2	1.83	4	2.736	3	5.039	<2	0	<2	0.375
Sn	<2	1.605	<2	1.5	<2	1.392	3	4.356	<2	0	<2	0.250
As	<2	0.921	<2	2.062	<2	0	<2	1.966	2	10.537	2	2.727
Mo	3	3.216	10	9.789	11	3.773	23	10.853	3	4.031	7	4.689
La	76	33.766	45	36.393	41	40.463	72	75.619	18	14.703	25	19.875
Ga	20	3.199	16	5.533	19	1.642	20	3.861	18	16.054	21	4.357
Ce	133	57.796	97	71.106	96	72.665	137	85.879	39	26.905	48	37.476
Nb	6	2.141	4	2.348	4	3.74	3	1.409	6	2.388	6	2.845
Pb	25	8.593	47	14.140	38	12.893	27	15.331	5	5.136	4	1.933
Cl	26	16.217	34	7.182	16	6.698	23	11.963	17	15.697	20	13.573
V	47	26.074	49	60.204	13	6.351	12	14.938	365	304.43	405	130.43
F	712	269.62	416	461.85	411	217.10	1536	924.93	488	308.66	536	382.13
Sc	14	5.163	7	5.324	5	2.833	6	4.955	42	10.708	40	6.047
HF	6	2.593	8	4.275	7	1.308	8	3.359	2	3.007	4	1.479
RGC nos.	277-305		310-327		328-335		267-276		224-261		192-199	

Table 7. Averages and standard deviations of sundry rock units in the Pine Creek Geosyncline.

Konbolgie Formation: Nungbalgarri Volcanic Member, 5 analyses		Arenites and Rudites, 5 analyses		Kapalga Formation, 3 analyses		Mundogle Sandstone, 4 analyses		Koolpin Formation, 8 analyses		Masson Formation, 13 analyses		Cahill Formation, 143 analyses		
Mean	SD	Mean	SD	Mean	SD	Mean	SD	Mean	SD	Mean	SD	Mean	SD	
51.21	4.193	88.93	6.618	69.05	4.416	72.19	13.793	48.64	28.821	56.83	20.429	60.10	15.814	SiO_2
1.14	0.028	0.25	0.281	0.38	0.093	0.61	0.349	0.64	0.961	0.61	0.503	0.48	0.475	TiO_2
14.62	1.088	2.94	2.271	15.25	2.731	13.64	7.307	7.50	5.472	12.15	6.923	12.87	5.785	Al_2O_3
9.91	0.920	2.28	1.390	5.04	1.090	6.57	5.912	11.92	17.604	6.84	6.357	5.84	5.025	Fe_2O_3
0.20	0.081	0.02	0.028	0.05	0.009	0.03	0.044	0.09	0.140	0.01	0.065	0.05	0.061	MnO
5.80	2.027	1.11	0.950	1.81	0.519	1.32	1.127	6.69	9.600	5.33	6.188	8.68	6.387	MgO
7.46	6.997	0.36	0.620	0.37	0.429	0.06	0.029	7.95	12.659	4.82	6.630	1.79	4.724	CaO
1.55	0.716	0.04	0.027	0.46	1.156	0.29	0.273	0.05	0.023	0.21	0.286	0.14	0.524	Na_2O
3.24	1.428	0.03	0.012	4.46	1.589	3.72	1.997	1.76	1.636	3.34	2.235	1.27	1.716	K_2O
0.15	0.017	0.03	0.095	0.09	0.050	0.25	0.008	0.11	0.086	0.25	0.339	0.20	0.307	P_2O_5
4.13	1.490	2.07	1.268	2.44	1.159	1.21	2.287	12.06	13.617	11.42	11.652	7.82	7.786	LOI
0.05	0.017	0.06	0.050	0.09	0.001	0.02	0.008	0.19	0.366	0.53	0.774	0.50	0.822	S
24	2.191	158	388.43	33	13.225	11	5.527	110	253.36	25	15.120	21	14.269	Y
26	3.514	29	53.820	27	21.929	36	29.534	540	860.76	39	75.289	86	155.31	Ni
135	46.512	120	253.62	24	30.980	4	1.795	158	328.08	36	128.76	187	489.24	Cu
148	91.263	25	56.810	66	37.851	49	58.985	30	29.328	82	115.11	49	44.755	Zn
88	38.217	<2	0	299	67.267	82	66.996	72	90.650	66	63.135	56	61.356	Rb
160	73.675	16	14.885	51	25.650	61	36.082	38	31.042	46	49.944	19	35.957	Sr
152	4.915	128	78.059	169	20.606	86	36.233	97	85.029	147	31.163	142	78.449	Zr
569	469.75	5	2.994	573	325.03	600	278.96	128	136.84	392	413.43	202	369.22	Ba
11	1.186	10	5.280	31	11.776	5	4.265	8	7.953	13	8.334	15	8.377	Th
2	1.557	3	8.424	6	2.494	3	3.961	454	1160.6	15	22.134	1048	2475.2	U
<2	2	10	15.781	3	0.943	2	1.090	6	5.124	2	2.260	5	6.728	W
2	1.633	5	4.332	6	1.885	3	1.765	2	1.937	<2	1.009	4	5.675	Sn
<2	0.8	<2	2.000	271	358.06	2	3.098	2	2.121	8	13.197	2	5.064	As
6	0.748	3	3.919	11	2.494	5	4.717	12	19.449	9	7.307	19	26.812	Sb
29	7.326	42	106.8	17	4.384	25	6.157	24	41.707	28	25.856	19	24.725	La
24	13.876	7	16.134	19	5.437	25	8.437	58	135.257	16	8.678	27	15.700	Ce
63	6.556	158	190.34	84	17.815	53	15.343	48	91.087	55	43.563	41	39.430	Ce
6	1.897	6	6.419	4	4.327	5	1.118	8	5.650	14	17.045	12	27.361	Mo
28	24.961	2	7.032	29	18.185	17	9.055	17	20.115	16	22.917	306	787.75	Pb
59	8.593	16	12.553	18	7.118	34	21.020	29	49.659	29	20.220	76	82.728	Cl
200	17.225	43	55.507	90	25.152	84	25.455	156	340.52	162	122.28	177	141.84	V
368	89.084	416	160.32	1372	409.99	783	376.03	846	674.67	871	431.41	756	422.89	F
26	2.561	6	4.126	12	3.494	13	11.092	15	8.879	16	7.045	17	9.755	Sc
47	9.723	5	2.623	7	2.055	5	0.833	9	15.341	5	3.077	5	3.753	Ni
8-12		3-7		200-202		202-207		76-93		34-46		47-189		

Table 7 continued

REFERENCES

Eades, D. C., 1965: The inappropriateness of the correlation coefficient as a measure of taxonomic resemblance. *Syst. Zool., 14*, 98-100.

Ewers, G. R. & Scott, P. A., 1977: Geochemistry of the Cullen granite, Northern Territory. *BMR J. Aust. Geol. Geophys., 2*, 165-176.

Ferguson, John, Chappell, B. W. & Goleby, A. B. this volume: Granitoids in the Pine Creek Geosyncline. *Proceedings of the International Uranium Symposium on the Pine Creek Geosyncline.*

Ferguson, John, Ewers, G. R. & Donnelly, T. H., this volume: Model for the development of economic uranium mineralisation in the Alligator Rivers Uranium Field. *Proceedings of the International Uranium Symposium on the Pine Creek Geosyncline.*

Lance, G. N. & Williams, W. T., 1967: Mixed-data classificatory programs. *Australian Computer Journal, 1*, 15-20.

Minkoff, E. C., 1965: The effects on classification of slight alterations in numerical technique. *Syst. Zool., 14*, 196-213.

Rhodes, J. M., 1969: The application of cluster and discriminatory analysis in mapping granite intrusions. *Lithos, 2*, 223-237.

A PROTEROZOIC TECTONIC MODEL FOR NORTHERN AUSTRALIA AND ITS ECONOMIC IMPLICATIONS

Allan G. Rossiter[1]* and John Ferguson[1]

1. Bureau of Mineral Resources, P.O. Box 378, Canberra City, A.C.T., 2601, Australia.
* Present Address: Consultant Geologist, 17 Churchill Ave., Bright, Vic., 3741, Australia.

ABSTRACT

It is argued that at the end of Archaean time the Australian continent was confined to the area now occupied by the Yilgarn, Pilbara, Gawler, and Musgrave Blocks, and the southern part of the Arunta Block. During the Early Proterozoic, sedimentary and volcanic rocks were laid down in an extensive depositional zone trending roughly east-west along the northern margin of the Archaean continent. Copper and gold mineralization, commonly showing stratigraphic control, is widespread in this belt. Following deformation and metamorphism of the Early Proterozoic rocks, felsic and mafic igneous activity, and accumulation of platform sediments on the newly stabilized crust, a predominantly north-south depositional zone developed along the eastern margin of the continent during the Middle Proterozoic. Lead and zinc assume much more importance in the mineral deposits of this belt. It is postulated that the present positions of rocks of the Pine Creek and Georgetown regions are due to horizontal displacements of several hundred kilometres along major fault zones. Apparent rifting of these blocks away from palaeo-continental margins may be related to the occurrence of uraniferous granitic rocks and uranium mineralization within them via a mantle plume mechanism. Although current data are limited, tectonic environments suggested for Proterozoic mafic igneous rocks of northern Australia by their geochemistry are compatible with the geological settings of these rocks and with the tectonic model put forward.

INTRODUCTION

Several parts of northern Australia have been the subject of intensive geological study in recent years but relationships between them have received little attention. Although tectonics of individual regions have been described in some detail (e.g. Geological Society of Australia, 1971; Plumb, 1979; Plumb, in press) there have only been a few attempts (e.g. Rutland, 1976) to develop a comprehensive picture of the tectonic evolution of northern Australia, as a whole. Here we endeavour to develop a simple general model consistent with geological observations to date in each region.

The first half of this paper mainly comprises brief accounts of the geological features of the various parts of northern Australia. These are based on conclusions of earlier workers and are provided so that the reader has sufficient background information to follow subsequent development of the tectonic model. References are given under the relevant heading for those requiring a more detailed treatment of a particular region. The review of Plumb & Derrick (1975) provides an excellent starting point for anyone wishing to become better acquainted with the Proterozoic geology of northern Australia.

In the second half of the paper the model is tested by considering the geochemistry of the mafic igneous rocks of northern Australia. The distribution of uraniferous granitic rocks and uranium deposits in northern and eastern Australia is then evaluated (with particular reference to the Pine Creek region) as a possible corollary of the model, and finally some other economic implications are mentioned.

The broad tectonic classification used here is based on the Tectonic Map of Australia and New Guinea (Geological Society of Australia, 1971) in that Orogenic, Transitional, and Platform Cover Domains are distinguished. These terms are defined in relevant sections of the text. Some units were referred to as Blocks on the Tectonic Map, generally because effects of deformation and metamorphism precluded their classification within the above scheme; this practice is continued here.

Subdivision of Precambrian time is still in a state of flux in Australia. Herein the upper limit of the Archaean is taken at 2400 m.y. in accordance with recent work by Richards *et al.* (1977) in the Rum Jungle area. An age of 1800 m.y. is assigned to the Early-Middle

Proterozoic boundary in keeping with the widely-accepted 1770 m.y. date for the Cliffdale Volcanics (Dunn *et al.*, 1966). Demarcation of the lower limit of the Late Proterozoic is still under review - for convenience 1400 m.y. is adopted here but this age is not important to following discussion. In this paper isotopic dates are rounded off to the nearest 50 m.y. because experimental errors, uncertainty in decay constants, and ambiguity as to what the dates actually mean geologically, make it rather meaningless to quote the majority of such figures to greater exactness.

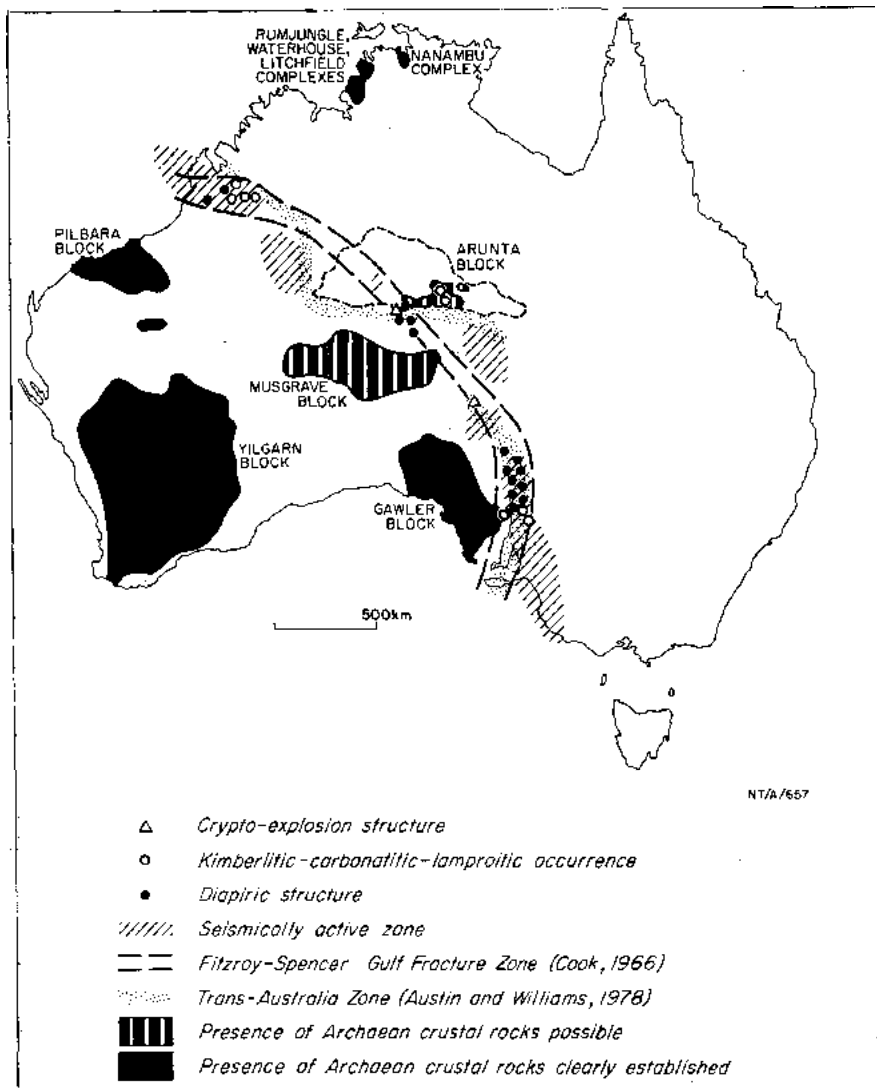


Figure 1. Evidence for the position of the Australian continental margin at the end of the Archaean (~2400 m.y. ago).

THE ARCHAEAN CONTINENT (≳2400 M.Y.)

The tectonic model presented here is based on the premise that at the end of the Archaean the Australian continent extended over the region now occupied by the Yilgarn, Pilbara, Gawler, southern Arunta, and Musgrave Blocks (Fig. 1). It has been clearly established that the first three Blocks contain Archaean rocks but isotopic dates of this age have yet to be obtained from the Arunta and Musgrave Blocks.

Yilgarn/Pilbara Blocks

The oldest rocks in the Yilgarn and Pilbara Blocks (the so-called greenstones) consist of mafic to intermediate extrusives, broadly contemporaneous ultramafic to felsic intrusives, and lesser felsic volcanic and sedimentary material (Williams & De la Hunty, 1975; Blockley, 1975). Such rocks in both Blocks have yielded isotopic ages exceeding 3000 m.y. (Arriens, 1971; Pidgeon, 1978). The ensuing episodes of metamorphism and granitic intrusion peaked ~2600 m.y. ago in the Yilgarn (Cooper *et al.*, 1978) and somewhat earlier in the Pilbara (Oversby, 1976). Mafic dykes considerably younger than the granitoids represent the last significant igneous activity in both regions.

Gawler Block

In the Gawler Block metamorphic rocks dated at ~2650 m.y. are intruded by granitoids ~2400 m.y. old (Cooper *et al.*, 1976; Webb & Thompson, 1977).

Arunta Block

Hypersthene granulites* in the southern Arunta have yielded rubidium/strontium ages of ~1800 m.y. (Black, 1975). The formation of such rocks requires very dry conditions and is only possible in an originally sedimentary terrain when metamorphism continues for an exceptionally long time or when two or more periods of metamorphism occur (Winkler, 1976). It may be, then, that the 1800 m.y. date represents the second episode (or even the last of several episodes) in the metamorphic evolution of these rocks and that deposition occurred much earlier.

Musgrave Block

The oldest isotopic dates so far obtained from the hypersthene granulites of the Musgrave Block cluster around 1650 m.y. (Webb, 1973a) but it can be argued, as with the Arunta rocks, that deposition possibly occurred during the Archaean. From rubidium/strontium investigations, Arriens & Lambert (1969) concluded that the Musgrave granulites probably did not have a pre-metamorphic crustal history of more than 500 ± 300 m.y. However, Arriens (1971) later pointed out that, had the Rb/Sr ratio in these rocks increased during metamorphism then a longer pre-history could not be ruled out. Given the mobility of strontium during metamorphic processes (e.g. Smith & Smith, 1976) this is a distinct possibility. Gray & Oversby (1972) carried out lead isotope measurements on Musgrave granulites and deduced that the U/Pb ratio could not have changed greatly during the pre-metamorphic evolution of these rocks. They acknowledged, however, that as long as this condition was satisfied, an indeterminate length of time could have elapsed between deposition of the rocks and their final metamorphism.

Lambert (1970) noted that hypersthene granulites, charnockitic granitoids, and anorthosites of the Musgrave Block represent the deepest crustal level that can be sampled over any considerable area on the earth's surface; Moore & Goode (1978) have shown that these rocks probably formed at depths of 30-35km. If these rocks were laid down during the Proterozoic, then they must have experienced more rapid burial, metamorphism, and subsequent uplift and erosion than all the Archaean terrains of the world. Pyroxenes of mafic rocks associated with anorthosites of the Musgrave Block are abnormally high in chromium

* In this paper the term 'granulite' is confined to rocks of Winkler's (1976) regional hypersthene zone. Rocks with granoblastic texture but lacking hypersthene, or rocks containing hydrous minerals such as hornblende, have been termed granulites by previous workers in northern Australia but are excluded here.

(Moore, 1971; Goode & Moore, 1975), a characteristic of anorthosites exceeding 3000 m.y. in age (Windley, 1970). More detailed study of the Musgrave anorthosites may shed further light on the question of the Block's age.

The postulated Archaean continental margin coincides (Fig. 1) with the Fitzroy-Spencer Gulf Fracture Zone, a major structural feature dating back at least to the Proterozoic (Cook, 1966, 1971). Mantle-derived diatremes of the kimberlitic-carbonatitic lamprophyric association occur along its length and diapiric structures are coincident in South Australia. Cleary & Simpson (1971) noted that seismic activity still occurs along this line and considered that it marked the boundary between major crustal plates. Their conclusions were subsequently reinforced by Stewart & Mount (1972). Recently, Austin & Williams (1978) have emphasised the importance of the Fitzroy-Spencer Gulf structure as the junction between subcontinental plates of differing crustal mobility. Absence of underlying Archaean crust could explain the greater instability of the block to the north and east.

The only known rocks of Archaean age that do not lie within the postulated continent occur in the Pine Creek region. The Rum Jungle, Waterhouse, and Nanambu Complexes (Fig. 1) have yielded Late Archaean isotopic dates (Page *et al.*, this volume), and Berkman (this volume) assigns an Archaean age to granitic rocks in the Litchfield Complex unconformably underlying Early Proterozoic metasediments. In terms of our model, the present-day position of these rocks can only be explained by a huge northward displacement from the edge of the Archaean continent. The evidence for such movement is discussed later. The existence of Archaean basement has been postulated in several other parts of Australia (e.g. beneath the Kimberley Basin - Gellatly, 1971) but there are no real grounds for such assertions.

EARLY PROTEROZOIC OROGENIC DOMAINS (~2400-1800 M.Y.)

Orogenic Domains were defined on the Tectonic Map of Australia and New Guinea (Geological Society of Australia, 1971) as belts of 'intense tectonism involving development and deformation of ortho-geosynclines or metamorphic and igneous complexes prior to cratonization' typified by 'thick flysch-like sequences in extensive linear troughs; abundant and varied volcanics and plutonics; intense deformation and widespread metamorphism of fill'. In northern Australia (Plumb, in press) has distinguished 'Older Domains' metamorphosed 2000-1950 m.y. ago from 'Younger Domains' metamorphosed 1850-1800 m.y. ago. Orogenic Domains of definite and probable Early Proterozoic age are represented in the Halls Creek, The Granites-Tanami/northern Arunta, Pine Creek, and Tennant Creek regions (Fig. 2).

Halls Creek Orogenic Domain

(Principal references: Dow & Gemuts, 1969; Gemuts, 1971; Gellatly *et al.*, 1974; Plumb & Gemuts, 1976).

The available isotopic data suggest that the Halls Creek Group has a maximum age of 2200 m.y. and may be as young as 2050 m.y. (Page, 1976). The Group is thicker than 10km. The lowermost unit comprises mafic volcanics (Ding Dong Downs Volcanics) and passes up into a sandstone-conglomerate unit (Saunders Creek Formation) deposited in shallow water during a pause in volcanism. The remainder of the Group (Biscay and Olympio Formations) consists of a thick sequence of turbidites with conspicuous intercalated mafic and felsic volcanics. Some of the mafic lavas show pillow structures and Plumb & Gemuts (1976) have suggested that they were possibly extruded in an ancient island arc environment. The Halls Creek Group is intruded by mafic rocks of the 'older' Lamboo Complex; these were emplaced after folding of the sedimentary pile but before the main (Tickalara) metamorphic

episode at ~1950 m.y.. The concordant, gneissic Mabel Downs Granodiorite is considered cogenetic with the Tickalara Metamorphics.

The Granites-Tanami/northern Arunta Orogenic Domain

(Principal references: Blake *et al.*, 1975; Stewart *et al.*, 1976; Blake 1978; Blake *et al.*, in press).

The oldest exposed rocks in The Granites-Tanami region comprise a sequence of sediments and volcanics, probably several thousands of metres in thickness, metamorphosed to low grade (Tanami Complex). The volcanics range from mafic to felsic with both types abundant. Similarities in lithology, regional metamorphism, and deformation between the Tanami Complex and the Halls Creek Group suggest that these units are stratigraphically equivalent (Blake *et al.*, 1975), although Plumb (in press) considers the former to be younger. In either case, it seems likely that the Tanami Complex and the Halls Creek Group were deposited in similar environments. Metasediments of probable Early Proterozoic age (Lander Rock Beds and Mount Stafford Beds) also occur in the northern part of the Arunta Block. Intermediate and mafic flows or sills are commonly associated with these rocks.

Pine Creek Orogenic Domain

(Principal references: Walpole *et al.*, 1968; Smart *et al.*, 1975; Needham *et al.*, this volume; Stuart-Smith *et al.*, this volume).

Sedimentation probably took place in the Pine Creek region sometime between 2400 and 1800 m.y. ago (Richards *et al.*, 1977). More specifically Plumb (in press) has proposed that deposition post-dated reactivation of the Nanambu Complex~2000 m.y. ago (Page, 1974). Page *et al.*, (this volume) now consider, however, that the 2000 m.y. date for the Nanambu rocks is due to isotopic inhomogenization and does not reflect a significant geological event. The Archaean Rum Jungle, Waterhouse, and Nanambu Complexes are overlain unconformably by coarse, clastic sediments which contain interbedded carbonates (Batchelor and Kakadu Groups). These rocks may be continuous across the basin of deposition or they may interfinger distally with the Namoona Group (Needham *et al.*, this volume) which consists of fine clastic and chemical sediments with minor mafic extrusive rocks (Stag Creek Volcanics). The presence of turbidites may indicate rapid subsidence or instability due to volcanic activity and the Namoona Group probably represents the deepest sedimentation in the basin. The Group contains the lower member of the Cahill Formation, host to the main uranium orebodies of the Pine Creek region. The next unit in the sequence comprises sandstone and conglomerate laid down in a shallow-water high-energy regime (Mount Partridge Group). In the overlying South Alligator Group the presence of carbonates and subaerial felsic volcanics suggests that deposition occurred in fairly shallow water under quieter conditions. The uppermost Early Proterozoic unit, the Finniss River Group, contains turbidites. Total original thickness of the Early Proterozoic sequence may have been as much as 20km (Needham *et al.*, this volume). The tholeiitic Zamu Dolerite (Ferguson & Needham, 1978) was intruded into the sedimentary pile shortly before deformation and regional metamorphism occurred ~1800 m.y. ago (Page *et al.*, this volume). It is generally considered (e.g. Stuart-Smith *et al.*, this volume) that the intensity of metamorphism increased towards the northeast where the largely anatectic Nimbuwah Complex formed, although Ferguson (this volume) suggests that consideration be given to the hypothesis that the higher grade rocks represent older basement. The presence of hypersthene granulites among the Nimbuwah rocks tends to support the latter view. Gravity trends and discontinuous outcrops imply that Pine Creek rocks continue into eastern Arnhem Land (Plumb, in press) where pelitic rocks, metamorphosed 1950 m.y. ago, crop out (Plumb & Derrick, 1975).

Tennant Creek Orogenic Domain

(Principal references: Crohn & Oldershaw, 1965; Dunnet & Harding, 1967).

In the Tennant Creek region an Early Proterozoic sequence similar to the Pine Creek one, but which contains more volcanics, is present. The oldest known rocks are pelites metamorphosed to amphibolite facies ~1900 m.y. ago (Black, 1977); the Warramunga Group is only weakly metamorphosed and may be younger (Plumb, in press). It consists of predominantly fine-grained sediments (including turbidites) with abundant intercalated felsic volcanics (belonging mainly to the Bernborough Formation). The main deformation experienced by the Group occurred ~1800 m.y. ago (Black, 1977). The Hatches Creek Group, which lies unconformably on the Warramunga rocks, may also be Early Proterozoic as it is intruded by a granitoid dated at ~1700 m.y. (G.H. Riley, pers. comm. to Compston & Arriens, 1968). It contains both mafic and felsic volcanics. The Tomkinson Creek Group also lies unconformably on the Warramunga Group. In contrast to the Hatches Creek Group it contains no volcanics and is not intruded by granitic rocks; it may therefore be younger.

In the Nicholson River area northwest of Mount Isa a metamorphosed sequence which contains minor volcanics (Murphy Metamorphics) crops out (Roberts *et al.*, 1963). These rocks are intruded by an early phase of the Nicholson Granite Complex dated at ~1850 m.y. (Webb, 1975). The Yaringa Metamorphics are probably Early Proterozoic and appear to be the oldest exposed rocks in the Mount Isa region. Carter *et al.* (1961) suggested that the presence of a strong east-west cleavage contrasting with north-south trends in all other rocks of the region might indicate that the Yaringa metamorphics are older. Metasediments comprise most of this unit but there are some felsic igneous rocks which may be extrusive in origin.

EARLY PROTEROZOIC TECTONIC MODEL

Present-day setting of the Halls Creek Group, the Tanami Complex and related rocks in the northern Arunta Block, the Warramunga Group, and possibly the Hatches Creek Group, is consistent with their accumulation during the Early Proterozoic in a roughly east-west depositional zone along the northern margin of the proposed Archaean continent (Fig. 2). The Murphy Metamorphics and Yaringa Metamorphics may also have been laid down in an easterly extension of the same structure. East-west fold axes, cleavages, and thrust faulting in most of the Early Proterozoic sequences indicate that their stabilization was in response to predominantly north-south compression; this is consistent with the latitudinal orientation of the postulated depositional zone. The zone was probably made up of a number of parallel troughs and, during the 600 m.y. of the Early Proterozoic, older troughs appear to have been filled and deformed and new ones subsequently initiated ('Older Domains' and 'Younger Domains' of Plumb, in press). The character of the sedimentary and volcanic rocks, and abundance of the latter in Early Proterozoic successions of northern Australia, suggest deposition in an environment somewhat similar to the trough complexes associated with modern oceanic-continental plate junctions. In particular the apparent tendencies in some instances for volcanic units to become more felsic with time (especially within the Halls Creek Group) emphasize this similarity.

We propose that Early Proterozoic rocks of the Pine Creek region were laid down close to the Archaean continent (in proximity to The Granites-Tanami rocks) and were then displaced north along major fault zones (Fig. 2); total movement of the order of 500km is implied. Rifting of this type can explain the areas of Archaean rocks in the Pine Creek region; these may simply be a piece (or pieces) broken off the continent and shifted northwards. Therefore, these Archaean remnants do not, in our opinion, constitute compelling evidence that Early Proterozoic sequences of northern Australia are all underlain by pre-existing crustal material. In fact presence of thick turbidite successions indicates considerable instability in the floor of the depositional zone and it is possible that much of it

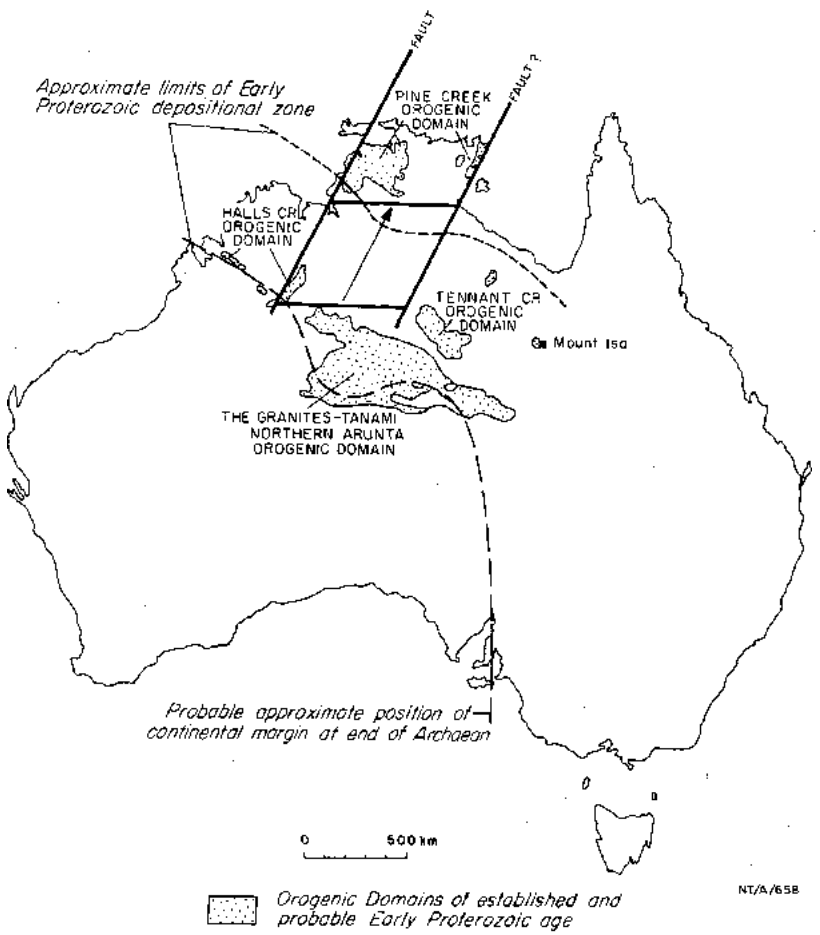


Figure 2. Early Proterozoic (~ 2400-1800 m.y.) geology and tectonic model for northern Australia. The map is very generalised and it should not be inferred that similar events in different regions occurred at precisely the same time.

rested on oceanic crust; greenstone has been reported from the bases of drill holes through the Murphy Metamorphics in the Nicholson River area (Nasca, 1972). Thus the Early Proterozoic depositional pattern may have been largely one of continental accretion. Limited evidence for this proposal, as seen in the geochemistry of the mafic igneous rocks and the nature of the mineral deposits of the belt, will be discussed later.

We suggest that the Halls Creek Mobile Zone (Fig. 3), and its probable extension beneath the Joseph Bonaparte Gulf (Plumb, in press), constitutes the western fault zone along which the Pine Creek rocks were displaced. Dow & Gemuts (1969) have established that movement along faults of the Halls Creek Mobile Zone was east block north, but it has not been possible to accurately gauge the overall displacement. Plumb & Gemuts (1976) set a *minimum* limit of 110km for the total movement and Rod (1966) argued that a post-Cambrian displacement amounting to 230km was a possibility. The Halls Creek Fault (one of many elements of the Mobile Zone) displays many of the characteristics of fundamental

strike-slip faults (Plumb & Gemuts, 1976), namely, long sinuous trace, near vertical dip, large vertical displacements which are periodically reversed, wide shear zone, horizontal slickensides, long history of intermittent movement, and distinct major geological provinces on either side. The strike-slips of such faults can be enormous and a figure of 500km for the Halls Creek Mobile Zone is quite possible. Plumb & Derrick (1975) considered that the north-south trends in the western part of the Pine Creek region are due to deflection against the Halls Creek Mobile Zone but a local flexure in the predominantly east-west depositional zone could also explain them. Meridional trends in The Granites-Tanami region can be similarly accounted for.

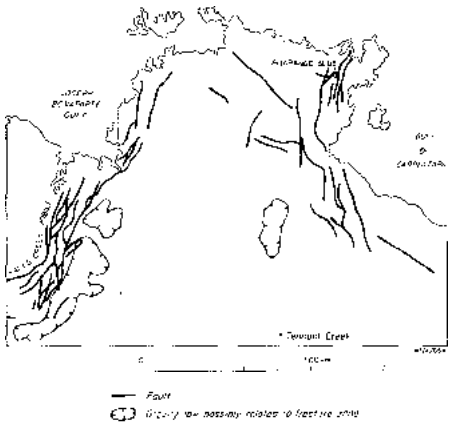


Figure 3. Evidence for major fracture zones which might have controlled northward movement of the rocks of the Pine Creek region.

The eastern margin of the proposed fault block is obscured by Middle Proterozoic sedimentary rocks, by the waters of the Gulf of Carpentaria, and by the imprint of younger structures. It is plausible, however, that the western coast of the Gulf is the modern expression of a major fracture zone dating back to the beginning of the Middle Proterozoic, in much the same way as the present eastern coast of the Joseph Bonaparte Gulf is related to the Halls Creek Mobile Zone. Several faults cutting Middle Proterozoic rocks run roughly parallel to the western margin of the Gulf (Fig. 3) and it can be argued that these are also related to an ancient deep-seated fracture zone of the type proposed. The Ritarango Beds were intensely sheared by close-spaced strike-slip faults parallel with the Gulf Coast prior to deposition of the Middle Proterozoic McArthur Basin sequence (Plumb & Derrick, 1975). Further south the Middle Proterozoic faults bend away to the southeast and perhaps influence of older structures was not as pronounced here. It may be relevant that a large negative gravity anomaly similar to those associated with the Halls Creek Mobile Zone, and coinciding with our postulated eastern fault zone, occurs north of Tennant Creek (Fig. 3).

It seems unlikely that the 500km northwards displacement which we propose for rocks of the Pine Creek region could have occurred by ensialic stretching alone; lateral accretion of upwelling mantle-derived mafic material would almost certainly have accompanied any such movement. Preliminary gravity modelling studies have shown that the lack of any positive gravity feature associated with the postulated accretion zone can be explained by the thick sequence (at least 5km) of low density sedimentary rocks in the Birrindudu and Victoria River Basins overlying the zone, and the presence of high density oceanic crust within about 15km of the surface in the regions surrounding it.

The presumed rifting of the Pine Creek rocks from the rest of the continent would probably have taken place ~1800-1700 m.y. ago. Plumb & Gemuts (1976) noted that field relations are consistent with major movements on the Halls Creek Mobile Zone ~1700 m.y. ago. Emplacement of the Oenpelli Dolerite ~1700 m.y. ago (Page *et al.*, this volume) may be linked to the rifting episode in much the same way that several major mafic suites throughout the world are considered consanguineous with the break-up of Gondwanaland. Metamorphism and deformation of the Arunta Block ~1800 and 1700 m.y. ago (Black, 1975) may also be related. Obviously the present-day position of the Pine Creek rocks

represents the sum total of displacement discussed above and more recent fault movements probably of smaller magnitude.

Other apparent examples of movement of continental crustal blocks oceanwards from palaeo-Australian margins occur in various parts of Australasia (Fig. 10). These include possible separation of the Willyama, Mount Painter, and Denison Blocks from the Gawler Block in Middle Proterozoic time (Katz, 1976) and postulated easterly migration of Tasmania and New Zealand during the Palaeozoic (Harrington *et al.*, 1973), and of the Lord Howe Rise late in Mesozoic time (Hayes & Ringis, 1973).

EARLY-MIDDLE PROTEROZOIC TRANSITIONAL AND PLATFORM COVER DOMAINS (~1900-1700 M.Y.)

Transitional Domains

Transitional Domains (Geological Society of Australia, 1971) consist of 'late to post-orogenic developments associated with cratonization; transitional in time between orogenic and cratonic tectonism'. Manifestations of transitional tectonism include 'downwarps, cauldron subsidences and rifts; molasse-like sediments, abundant volcanic and plutonic rocks; moderate deformation and rare metamorphism of fill'. Transitional Domains were superimposed on all the Early Proterozoic Orogenic Domains discussed above between 1900 and 1700 m.y. ago. Transitional tectonic elements of this age are particularly well-developed

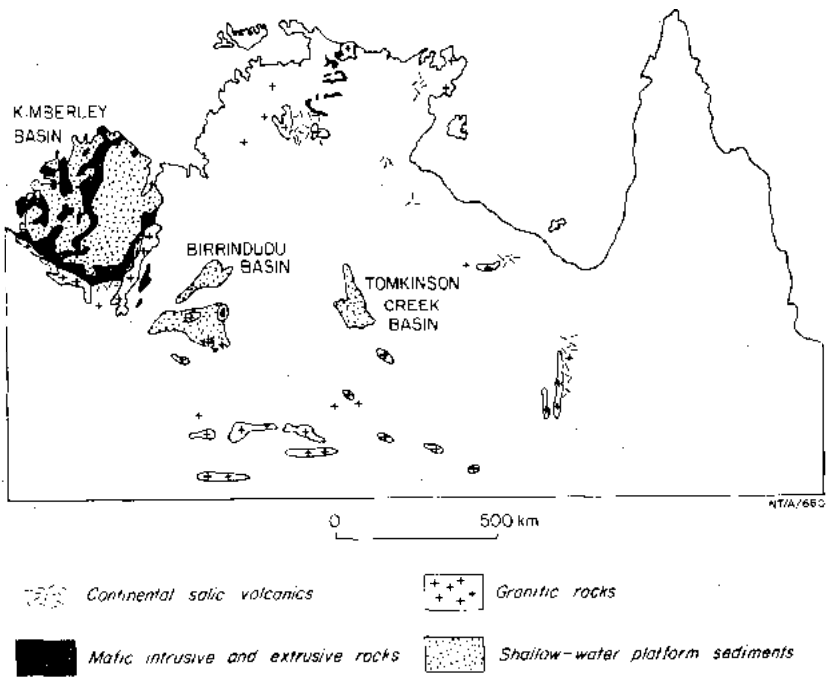


Figure 4. Early-Middle Proterozoic (~1900-1700 m.y.) Transitional and Platform Cover Domains of northern Australia. For convenience the Birrundudu and Tomkinson Creek basins are shown but they may be younger than 1700 m.y.

in the Halls Creek, The Granites-Tanami/northern Arunta, Pine Creek, and Mount Isa regions (Fig. 4).

Halls Creek region

Transitional tectonism affected the Halls Creek region before its influence was felt in any other part of northern Australia; rocks of the 'younger' Lamboo Complex are the result. The Whitewater Volcanics consist largely of ignimbritic rhyolites (Gemuts, 1971) whose isotopic age has yet to be unequivocally established. They postdate regional metamorphism of the Halls Creek Group at ~1950 m.y. and are intruded by post-tectonic granitic rocks (e.g. Bow River, Sophie Downs, and Lennard Granites) whose ages cluster around 1850 m.y. (Bofinger, 1967; Bennet & Gellatly, 1970).

The Granites-Tanami/northern Arunta region

In The Granites-Tanami region the 1800 m.y. old Mount Winnecke Formation comprises felsic lavas and interbedded sediments (Page *et al.*, 1976). Most of the volcanism was probably subaqueous (Page *et al.*, 1976) and in this respect Mount Winnecke Formation rocks differ from all other felsic volcanics in the Transitional Domains of northern Australia. Shallow-water sandstone units (Pargee and Supplejack Downs Sandstones) may be lateral equivalents of the Mount Winnecke Formation (Blake,1978). Post-tectonic granitic intrusions in the region (The Granites, Slatey Creek, and Lewis Granites and the Mount Winnecke Granophyre) yield ages in the 1800-1700 m.y. range (Page *et al.*, 1976). In the northern Arunta the Reynolds Range Group may be the same age as the Mount Winnecke Formation (Blake, 1978). All the granoitoids of this region that have been dated are ~1700 m.y. old (Stewart *et al.*, 1976).

Pine Creek region

Granitic rocks (e.g. Cullen, Burnside, and Jim Jim Granites) and ignimbritic felsic volcanics (Edith River Volcanics) postdating deformation and regional metamorphism of the Early Proterozoic sequence, are widely developed in the Pine Creek region. Many of the granitic rocks are ~1750 m.y. old (P.J. Leggo, pers. comm. to Walpole *et al.*, 1968; Page *et al.*, this volume); the Edith River Volcanics give an identical age and are consequently considered comagmatic with the granitoids. Intrusion of extensive sheets of tholeiitic Oenpelli Dolerite (Stuart-Smith & Ferguson, 1978) marks the end of transitional tectonism. Post-tectonic granitic rocks in eastern Arnhem Land have been dated at ~1800 m.y. (McDougall *et al.*, 1965); felsic volcanics in the region may be related.

Mount Isa region

In the Mount Isa region felsic ignimbritic volcanics now metamorphosed to greenschist and amphibolite facies (Leichhardt Metamorphics) and related granitic rocks (Kalkadoon Granite) have been dated at ~1850 m.y. (Page, 1978). These rocks are similar to the products of transitional tectonism in the Halls Creek region and their existence supports the assertion made earlier that the Yaringa Metamorphics are part of a largely unexposed, Early Proterozoic Orogenic Domain. The Leichhardt Metamorphics are overlain by mafic (Magna Lynn Metabasalt) and felsic (Argylla Formation) volcanic formations. These three units make up the Tewinga Group. The Ewen Granite postdates the Argylla Formation.

In the Tennant Creek region transitional tectonism is represented mainly by post-tectonic granitic intrusions. The Tennant Creek Granite, the North Seismic Adamellite, and the Warrego Granite yield ages in the range 1800-1700 m.y. (Black, 1977). Plumb (in press) considers the Hatches Creek Group to be a manifestation of transitional tectonism but as noted above its age is uncertain. The Cliffdale Volcanics of the Nicholson River area are felsic ignimbritic rocks dated at ~1750 m.y. (Webb, 1973b); they are intruded by comagmatic later phases of the Nicholson Granite Complex.

Platform Cover Domains

The main characteristics of Platform Covers (Geological Society of Australia, 1971)

are 'widespread, generally thin sequences of shallow-water and continental sediments; rare small plutons, basaltic sheets and mild deformation - broad warping and block faulting'

Kimberley Basin

The Kimberley Basin sequence (Plumb & Derrick, 1975) is the only Platform Cover Domain which was laid down in northern Australia during the time interval under consideration (Fig. 4). The rock types include psammitic sediments and carbonates interbedded with mafic, and minor felsic, volcanics; the total thickness is of the order of 5km. The bulk of the succession (Speewah and Kimberley Groups) was deposited after intrusion of the 1850 m.y. granitoids of the Halls Creek region but before emplacement of the 1800 m.y. Hart Dolerite. The younger Bastion and Crowhurst Groups are confined to the eastern

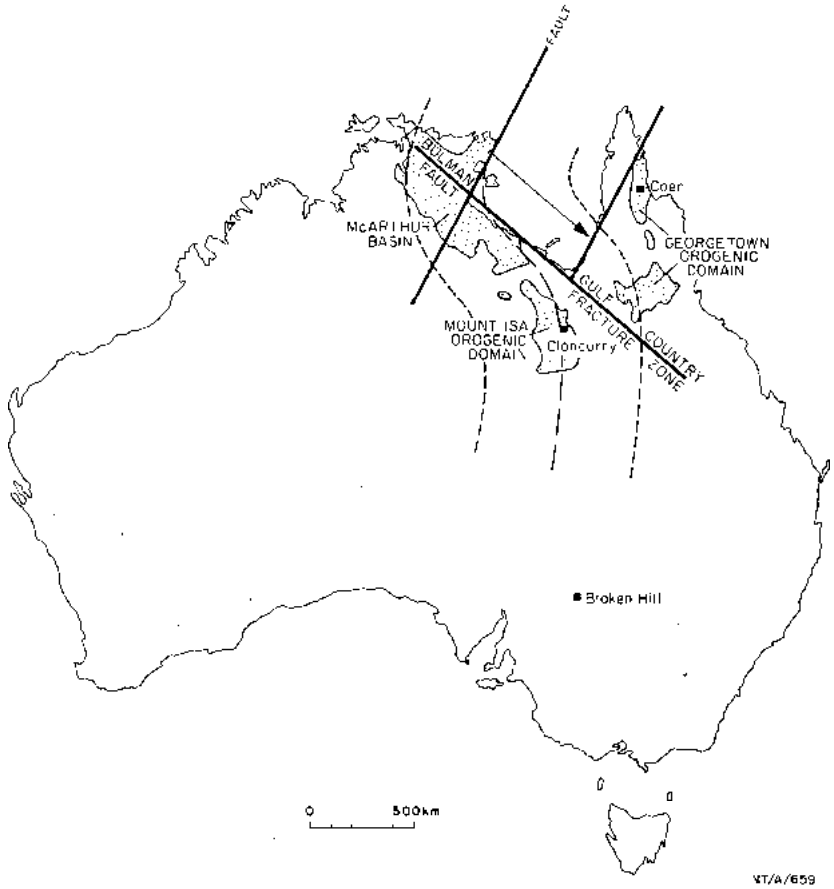


Figure 5. Middle Proterozoic (~1800-1400 m.y.) geology and tectonic model for northern Australia.

part of the basin. Deformation and metamorphism of the basin sequence has generally been slight; felsic plutonic rocks are absent.

MIDDLE PROTEROZOIC OROGENIC AND PLATFORM COVER DOMAINS (1800-1400 M.Y.)

Orogenic and Platform Cover Domains of definite and probable Middle Proterozoic age are best-developed in the Mount Isa, Georgetown, and McArthur regions (Fig. 5).

1. OROGENIC DOMAINS

Mount Isa Orogenic Domain

(Principal references: Carter *et al.*, 1961; Plumb & Derrick, 1975; Wilson & Derrick, 1976; Wilson, 1978; Plumb *et al.*, in press)

A median basement ridge consisting of rocks of the previously discussed Tewinga Group separates the Middle Proterozoic of the Mount Isa region into western and eastern successions. The western succession has been subdivided into the Haslingden and overlying Mount Isa Groups. The rocks of both Groups have been regionally metamorphosed to low grade. The basal unit of the Haslingden Group consists of conglomerate and sandstone deposited in shallow water. The overlying Eastern Creek Volcanics consist of tholeiitic basalts (Glikson *et al.*, 1976) interbedded with sediments laid down during hiatuses in volcanic activity. The uppermost unit of the group, the Myally Sub-group, consists of psammitic sediments which accumulated in a shelf or platform environment (Glikson *et al.*, 1976). The Haslingden Group was deformed ~1650 m.y. ago (Page, 1978) and intruded by the Sybella and Weberra Granites before deposition of the Mount Isa Group began (Glikson *et al.*, 1976). The Mount Isa Group comprises a psammitic basal formation overlain by several pelitic units (including the Urquart Shale which contains the Mount Isa and Hilton orebodies). Presence of carbonates and tuffs in the sequence indicates accumulation in relatively shallow water.

The lowermost units of the eastern succession are the Soldiers Cap and Malbon Groups; these both consist of interbedded sediments and mafic volcanic rocks (Toole Creek Metavolcanics and Marraba Volcanics). The Soldiers Cap rocks include turbidites (Llewellyn Creek Formation) which may imply more open marine conditions in the east in contrast to an epicontinental environment in the west (Glikson *et al.*, 1976). The next unit of the eastern succession is the Mary Kathleen Group which contains shallow-water, commonly calcareous, sediments and minor mafic volcanics; it is overlain unconformably by the psammitic Mount Albert Group. The eastern succession is intruded by mafic rocks (e.g. Lunch Creek Gabbro) and numerous granitoids (e.g. Burstall, Williams, Wimbera, and Wonga Granites). Dolerite dykes of various ages intrude the western and eastern successions as well as basement rocks (D.H. Ellis, pers. comm.).

Georgetown Orogenic Domain

(Principal references: White, 1965; Willmott *et al.*, 1973; Oversby *et al.*, 1975; Bain *et al.*, 1978)

The oldest exposed rocks in the Georgetown region belong to the Etheridge Group whose upper age limit is set by a date of ~1600 m.y. for its regional metamorphism (Black *et al.*, in prep.). The group comprises psammitic, pelitic, and calcareous sediments seemingly deposited in fairly shallow water. Mafic flows and sills (e.g. Cobbold 'metadolerite'), emplaced before folding and metamorphism of the sedimentary pile, are widespread. Metamorphism of the group increases in grade in an easterly direction but whether this phenomenon is real or merely reflects westwards tilting of the sequence, and consequent exposure of older rocks in the east, is not clear. Deformation was accompanied, and followed, by intrusion of numerous granitoids (e.g. Forsayth, Digger Creek, and Esmeralda Granites)

and the extrusion of ~1450 m.y. old (Webb, 1971) ignimbritic felsic volcanics (Croydon Volcanics). Sequences of probable Middle Proterozoic age in the Coen and Yambo regions are similar to the Georgetown rocks but all the granitoids which intrude them appear to be Palaeozoic (Oversby *et al.*, 1975).

2. PLATFORM COVER DOMAINS

McArthur Basin

(Principal reference: Plumb & Derrick, 1975)

The rocks of the McArthur Basin sequence are similar to those of the Mount Isa Orogenic Domain although they are only slightly metamorphosed and mildly deformed (mainly in response to block faulting). Volcanic units are relatively thin and felsic plutonic rocks are virtually absent. The Tawallah Group (and equivalents) and the McArthur Group (and equivalents) have been correlated with the Haslingden Group and the Mount Isa Group respectively (Plumb & Sweet, 1974), although recent mapping suggests that much (if not all) of the Tawallah Group may post-date the Haslingden Group (I.P. Sweet, pers. comm.). The Tawallah Group and its equivalents consist of basal sandstone and conglomerate (e.g. Kombolgie Formation and Westmoreland Conglomerate) overlain by extensive flood basalts and lesser felsic volcanics (e.g. Seigal and Peters Creek Volcanics). These in turn pass up into psammitic sediments, carbonates and minor, mainly mafic, volcanics (e.g. Settlement Creek Volcanics and Gold Creek Volcanic Member of the Masterton Formation). Intrusion of the Packsaddle Microgranite ~1600 m.y. ago (Webb, 1974) places an upper age limit on the Group.

The unconformably overlying McArthur Group and its equivalents include carbonates, psammitic sediments, and evaporites. Some pelitic and tuffaceous rocks were deposited in the deeper water of the Batten Trough (such rocks include the Barney Creek Formation which contains the HYC orebody). The Tawallah and McArthur Groups were laid down, in the main, under shallow-water shelf conditions and total about 5km in thickness except in the fault-bounded Batten Trough where 12km of sediments occur. The Roper and Malay Road Groups were deposited in the McArthur Basin subsequent to deformation in the Mount Isa region ~1500 m.y. ago (Plumb, in press); they are intruded by dolerite sills. The McArthur Basin Platform Cover Domain and the Mount Isa Orogenic Domain merge on the Lawn Hill Platform where the rocks of the McNamara Group (equivalent to the Mount Isa Group) combine the characteristic features of both Domains.

Shallow-water platform sediments of probable Middle Proterozoic age occur in the intracontinental Birrindudu and Tomkinson Creek Basins, but these are mentioned here only for sake of completeness.

MIDDLE PROTEROZOIC TECTONIC MODEL

We propose that at the beginning of the Middle Proterozoic the edge of the Australian continent was in about the position shown in figure 5. The best evidence for this assertion comes from the Mount Isa region (Glikson *et al.*, 1976; Wilson, 1978). These authors make the following observations:

1) As previously mentioned sediments of the Soldiers Cap Group seem to have been deposited in more open marine conditions than rocks of apparently the same age which occur to the west where the environment was epicontinental.

2) The Soldiers Cap rocks have experienced more intense regional metamorphism (up to amphibolite facies) than rocks of apparently similar age to the west and, if it is assumed that there is an inverse relationship between crustal thickness and geothermal gradient, eastward crustal thinning is implied.

3) Faulting is the main tectonic influence in the western part of the Mount Isa region

whereas folding predominates in the east. Crustal thinning and associated increasing ductility in an easterly direction may be responsible.

4) Mafic metavolcanics of the Soldiers Cap Group are more closely related in trace element composition to oceanic basalts than are the Marraba and Eastern Creek Volcanics.

These facts are consistent with the edge of the continent being in the Cloncurry area at the beginning of the Middle Proterozoic.

Extrapolation of the proposed continental margin southwards to the Broken Hill region* seems logical given the similarity between rocks and mineralization there and those of the Mount Isa region, and the predominance of north-south structural trends in the Middle Proterozoic depositional zone. It is possible, however, that deposition in the vicinity of the continental limit began somewhat earlier to the south as the Broken Hill rocks underwent regional metamorphism 1700 m.y. ago (Shaw, 1968).

Continuation of the edge of the continent north of the Mount Isa region is more problematical. According to Plumb (in press) gravity trends indicate that the Mount Isa Orogenic Province continues up the east coast of the Gulf of Carpentaria; these trends could be related to much younger rocks though. The epicontinental nature of the McArthur Basin sequence is reflected in the character of the sediments it contains, in the mildness of deformation it has undergone, and in the virtual absence of metamorphism and felsic plutonism. In the Georgetown Orogenic Province, however, the older rocks are intensely deformed, metamorphosed to high grade, and extensively intruded by granitic rocks. These features suggest that the Georgetown rocks were laid down in an environment where continental crust was thinner (and in places perhaps even absent). To the east of the McArthur Basin no remnants of Early Proterozoic Orogenic Domains or Early-Middle Proterozoic Transitional Domains crop out. Thus the proposed continental margin shown in figure 5 is based on the distribution of actual outcrops representing such Domains. Although it can be argued that there are unexposed rocks of this type beneath the Carpentaria Basin, it seems more logical to base an hypothesis on known outcrops than to postulate existence of unexposed rocks. That a continental boundary can occur quite close to a pre-existing Transitional Domain is suggested by the proximity of the Mount Isa basement rocks to the probable edge of the continent in the Cloncurry area.

The Middle Proterozoic rocks of the Georgetown region appear at first glance to have been deposited a long way from the proposed continental margin. If, however, one accepts the suggestion of Harrington *et al.*, (1973) that the major Australian sedimentary basins formed by the separation of lithospheric plates, this may not necessarily have been the case. It is possible that the Georgetown rocks were deposited fairly close to the continental edge (not far removed from the McArthur Basin) and that they were subsequently displaced some 600km eastwards. The anomalous east-west trends in the Georgetown rocks could indicate a local flexure in the predominantly north-south Middle Proterozoic depositional zone. The proposed rifting (Fig. 5) may have been controlled by the previously assumed fault zone along the western coast of the Gulf of Carpentaria and the Gulf Country Fracture Zone postulated by Harrington (1974). The suggested rifting probably began in the Late Proterozoic (Harrington *et al.*, 1973).

LATE PROTEROZOIC PLATFORM COVER DOMAINS (< 1400 M.Y.)

The Late Proterozoic in northern Australia was very quiet tectonically. Shallow-water platform sediments accumulated over large areas (Fig. 6) and these sequences are still flat-lying or only gently folded. No significant igneous activity of this age has been recorded.

* It should be borne in mind that the Broken Hill rocks may have lain some 250km to the south-west prior to Middle Proterozoic rifting (Katz, 1976)

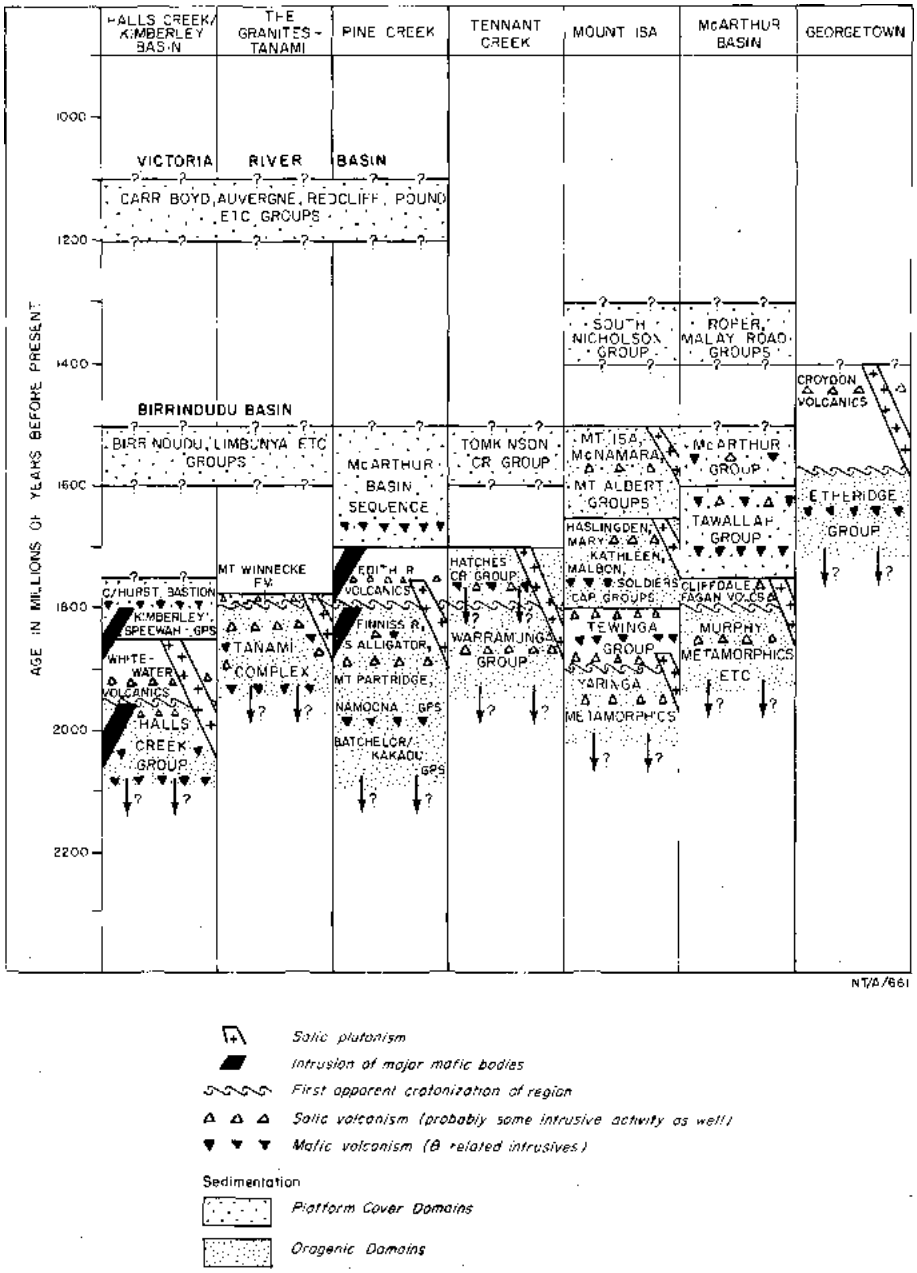


Figure 6. Tectono-magmatic and stratigraphic scheme for the Proterozoic of northern Australia. Many uncertainities still exist and the diagram is designed to show only the similarity of events in different regions at roughly equivalent times.

A TEST OF THE TECTONIC MODEL - GEOCHEMISTRY OF THE EARLY-MIDDLE PROTEROZOIC MAFIC IGNEOUS ROCKS OF NORTHERN AUSTRALIA

Since they were pioneered by Pearce & Cann (1971, 1973) geochemical methods have been used by many workers as a means of identifying original tectonic setting of supracrustal mafic igneous rocks. The validity of this approach for very old rocks is still subject to debate but some authors (e.g. Glikson *et al.*, 1976; Ferguson & Needham, 1978; D.H. Ellis, pers. comm.) have reported meaningful results in studies of Australian Proterozoic rocks. Accordingly, an extensive literature survey was undertaken to collate all available chemical analyses of supracrustal mafic igneous rocks from the Early and Middle Proterozoic sequences of northern Australia to see how these agreed with the tectonic environments suggested by our model (the data collated are reproduced on microfiche in the back pocket of this volume). Although this approach is unfortunately hampered at the moment by lack of analyses for the Early Proterozoic mafic units of the Halls Creek, The Granites-Tanami/northern Arunta, and Tennant Creek regions, some interesting trends have emerged.

Most of the chemical plots that have been used to discriminate between mafic igneous rocks of different tectonic situations were tested but the majority proved unsatisfactory. When plotted on Ti-Zr-Sr (Pearce & Cann, 1973) and TiO_2-K_2O-P_2O_5 (Pearce *et al.*, 1975) diagrams, for example, data for most of the mafic units showed excessive scatter suggesting considerable post-depositional redistribution of strontium and potassium. The FeO-MgO-Al_2O_3 plot of Pearce *et al.*, (1977) was ineffectual because analyses from the one unit usually fell within several fields. We found the Ti-Zr-Y diagram (developed by Pearce & Cann, 1973) to be the most consistently useful, no doubt because of the relative immobility of these elements during metamorphic processes (e.g. Smith & Smith, 1976).

Mafic rocks of the Pine Creek region for which relevant chemical data are available, are the Stag Creek Volcanics, Zamu Dolerite, Oenpelli Dolerite, and the Nungbalgarri Volcanic Member of the Kombolgie Formation. The Stag Creek Volcanics show an affinity with ocean-floor basalts when plotted on a Ti-Zr-Y diagram (Fig. 7); this is consistent with their extrusion early in the depositional history of the Early Proterozoic sequence. The Zamu Dolerite plots in both the calc-alkali and ocean-floor basalt fields of the Ti-Zr-Y diagram (Ferguson & Needham, 1978), and this unit may include both continental and oceanic

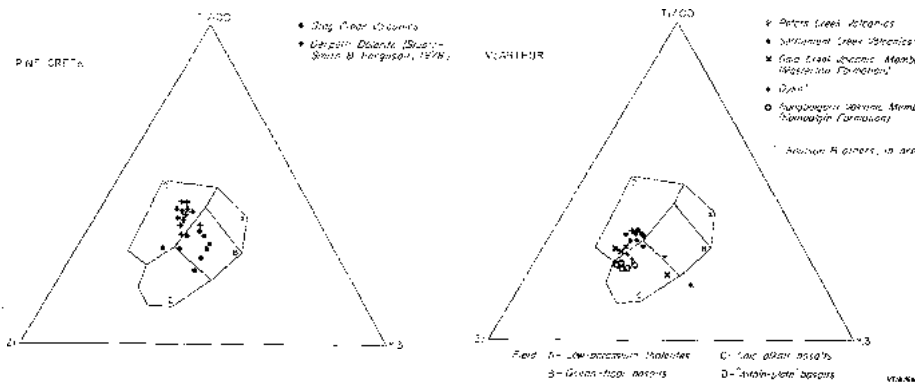


Figure 7. Mafic igneous rocks of northern Australia plotted on the Ti-Zr-Y discrimination diagram of Pearce & Cann (1973). Only rock units for which this diagram has not been previously published are shown. Of the northern Australia mafic rocks for which data are available, only the Stag Creek Volcanics, flows within the Soldiers Cap Group (Glikson *et al.*, 1976) and related dykes (D.H. Ellis, pers. comm.), and the Cobbold 'metadolerites' (I.W. Withnall, pers. comm.) plot consistently in the ocean-floor basalt field.

types. The Nungbalgarri Volcanic Member falls within the calc-alkali basalt field of the plot (Fig. 7) and the Oenpelli Dolerite (Stuart-Smith & Ferguson, 1978) shows continental tendencies; this is in accord with emplacement of these rocks after cratonization of the Early Proterozoic Pine Creek rocks.

Some data are available for the Peters Creek Volcanics, Settlement Creek Volcanics, and the Gold Creek Volcanic Member of the Masterton Formation in the McArthur Basin sequence. Rocks of the last two units range from mafic to intermediate in composition and have been altered to low temperature mineral assemblages enriched in iron, magnesium, potassium, and possibly aluminium (Knutson *et al.*, in press). When plotted on a Ti-Zr-Y diagram (Fig. 7) these rocks all fall within the calc-alkali and 'within-plate' basalt fields. As noted earlier there is good evidence that the McArthur Basin was floored by pre-existing continental crust and so trace element compositions of mafic volcanic rocks from this region are consistent with our tectonic model.

The geochemistry of the mafic igneous rocks of the Mount Isa region has recently been studied in some detail. Glikson *et al.*, (1976) noted that apparently continental tholeiites (Eastern Creek Volcanics and Marraba Volcanics) dominate the western part of the region but give way to tholeiites with some oceanic affinities (metavolcanics of the Soldiers Cap Group) in the east. D.H. Ellis (pers. comm.) investigated the mafic dykes of the province and found that these also tend to become more oceanic in trace element composition in an easterly direction. In addition he noted that younger dykes are more continental than ones emplaced earlier in the same general vicinity. He suggests that these spatial and temporal variations could imply the existence of an island arc environmental association with a westerly-dipping subduction zone in the region during the Middle Proterozoic.

When plotted on a Ti-Zr-Y diagram the intrusive and extrusive rocks of the Cobbold 'metadolerite' of the Georgetown region plot in the ocean-floor basalt field (I.W. Withnall, per. comm.). The proposal presented earlier, that these rocks formed in an environment with oceanic tendencies adjacent to the McArthur Basin, thus agrees with the current geochemical evidence.

A POSSIBLE EXPLANATION OF THE DISTRIBUTION OF URANIFEROUS GRANITIC ROCKS (AND URANIUM DEPOSITS) IN NORTHERN AUSTRALIA IN TERMS OF THE TECTONIC MODEL

A chemical characteristic of the granitic rocks of the Pine Creek region is their enrichment in uranium (Ferguson *et al.*, this volume). The Halls Creek and Tennant Creek granitoids, however, appear to have relatively low uranium contents, although the data for the former are very limited (Fig. 8). No uranium determinations are available for the granitic rocks of The Granites-Tanami region but uranium-rich granitoids are reported from the northern Arunta (Stewart & Warren, 1977). In this section the tectonic model is used to see if the distribution of uraniferous granitic rocks in the abovementioned parts of northern Australia can be explained. Later the ideas developed are applied to the rest of the continent.

It is difficult to see how a massive regional enrichment of uranium such as that in the Pine Creek region could occur without some mantle process being instrumental. Even if the uranium was carried to higher levels following its expulsion from lower crustal rocks it must be conceded that an external (i.e. mantle or, less likely, upper crustal) influence caused elimination of uranium from the lower crust at Pine Creek but not in the surrounding regions. Anderson (1975) introduced the concept of chemical plumes rich in uranium and other incompatible elements rising from the lower mantle as a corollary of the hypothesis of inhomogeneous planetary accretion. He proposed that such plumes are triggered by gravitational instabilities set up when refractory calcium-aluminium silicates and oxides (plus uranium, etc.) condensed closer to the centre of the accreting Earth than heavier ferromagnesian compounds. Sillitoe (1974) cited evidence that mantle plumes enriched in

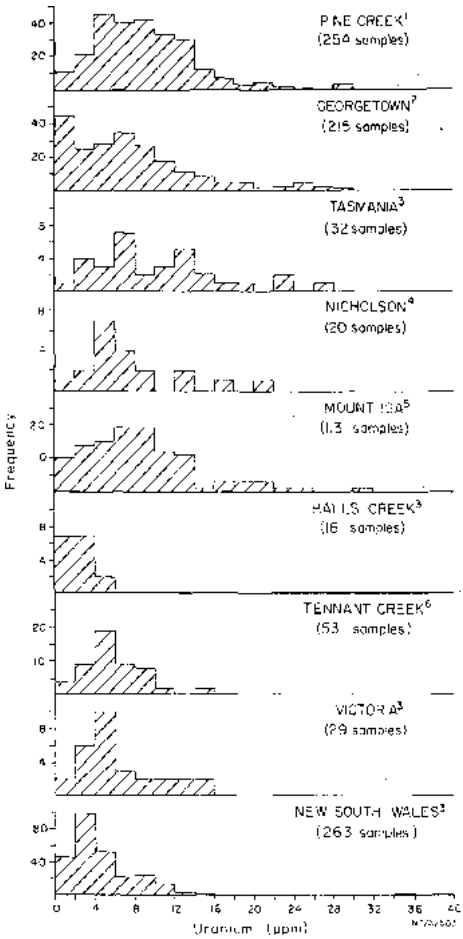


Figure 8. Uranium distribution in the granitic rocks of various parts of Australia. Data from: 1. Ferguson *et al.* (this volume); 2. Sheraton & Labonne (1978); 3. Heier & Lambert (1978); 4. Gardner (1978); 5. Derrick (pers. comm.); 6. Haldane (pers. comm.).

tin and other lithopile elements (presumably including uranium) have periodically penetrated the Earth's crust.

We speculate below on a course of events in which a uranium-rich plume, originating as Anderson (1975) suggested, rose to crustal levels in about the position shown in figure 9 late in the Archaean when the Rum Jungle, Waterhouse, Nanambu, and Litchfield Complexes were juxtaposed with the rest of the postulated Archaean continent. The influx of heat could have caused anatexis of felsic crustal rocks and the melts so formed may have mixed with the uraniferous low-melting fraction of the plume (probably largely anorthite (Anderson, 1975)) to produce the parent magmas of the uranium-rich Late Archaean granitic rocks of the Pine Creek region. Plume activity could have waned following the heat loss accompanying expulsion of the low-melting material and a long hiatus may have followed.

An extensive reactivation of the plume as its internal heat was replenished by radioactive decay, could have occurred towards the end of the Early Proterozoic and the younger Pine Creek and northern Arunta uraniferous granitic rocks formed in analogous fashion to the Archaean ones. Lateral spreading of the plume within the asthenosphere could have produced rifting similar to the type proposed by Burke & Dewey (1973), although development of a triple point may have been prevented here by major pre-existing crustal fractures. Temperatures could then have risen to the point where mafic plume and surrounding upper mantle material began to melt and the magmas produced may have filled the rift zone and produced the Oenpelli Dolerite. The uranium deposits of the Pine Creek region could be related to such plume activity in either of two ways:

1) The Archaean complexes enriched in uranium in the above manner may have constituted the provenance area of the Early Proterozoic sediments from which the uranium was subsequently remobilized.
2) Sea-floor, plume-related volcanic activity might have been responsible for syngenetic uranium enrichment in the Early Proterozoic sequence.

It could be argued that the Halls Creek and Tennant Creek granitic rocks are not uraniferous because they formed beyond the region of influence of the mantle plume.

A similar plume in the present Gulf of Carpentaria region could have provided the

driving force for the possible easterly migration of the Georgetown rocks mentioned above. It may be significant that the Proterozoic Georgetown granitic rocks are markedly uraniferous. Renewed igneous activity in the Carboniferous, when presumably the older granitoids were remelted, produced uranium deposits in this region. It is of further interest that the majority of uranium-rich granitic rocks and uranium deposits in eastern Australia lie within crustal blocks that may have broken away from a continental margin and moved oceanwards (Fig. 9). Thus uranium mineralization occurs in the Willyama and Mount Painter Blocks and highly uraniferous granitoids are common in Tasmania. The uranium mineralization and uranium-rich granitic rocks of the Mount Isa region and the Nicholson River area appear to be an exception to the rule, although they could have formed within the area of influence of the alleged Gulf of Carpentaria plume.

ECONOMIC IMPLICATIONS

The possibility of a genetic link between formation of uranium deposits, mantle-plume activity, and rifting of blocks from continental margins raises interesting exploration

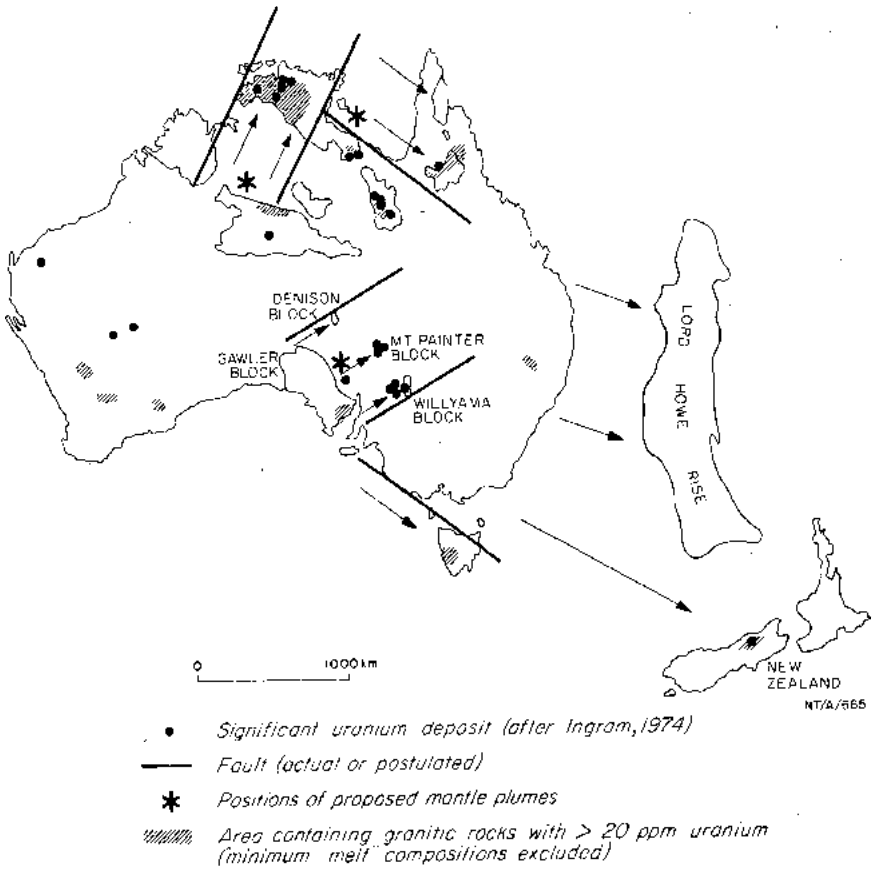


Figure 9. Apparent relationship between uranium mineralization, uraniferous granitic rocks, and rifting in northern and eastern Australia. All areas of uraniferous granitic rocks in Australia known to the authors are shown – data from the same sources as figure 8.

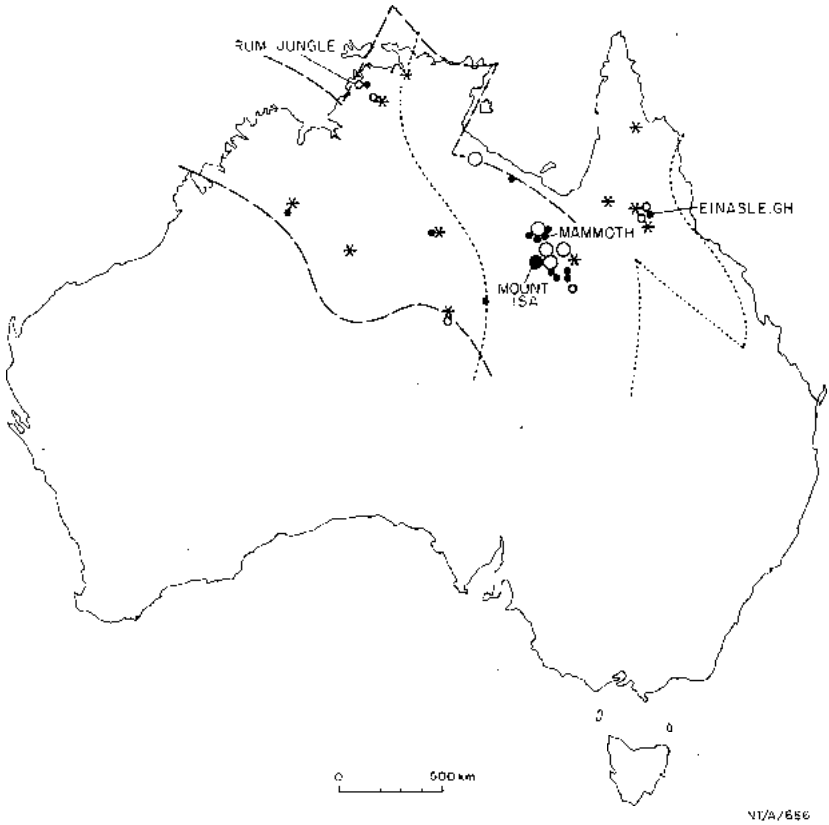


Figure 10. Mineral deposits of northern Australia in relation to the postulated Early and Middle Proterozoic depositional zones. The only significant lead-zinc mineralization occurring within the rocks of the Early Proterozoic zone is that at Rum Jungle. The only significant copper (Einasleigh) and gold deposits lying outside the Early Proterozoic zone are situated in the more oceanic parts of the Middle Proterozoic zone.

possibilities. If the mantle plume model is valid, The Granites-Tanami/northern Arunta region would seem to have potential for discovery of uranium deposits similar to those of the Pine Creek region. The model provides no reason to expect the presence of significant uranium mineralization in the Kimberley and Tennant Creek regions. Exploration for uranium has been relatively active in most of the apparently rifted blocks of eastern Australia, but Tasmania may warranty more attention than it has received to date. Presence of tin mineralization in the Pine Creek and Georgetown regions and in Tasmania suggests that a mantle-plume model may have application in the search for this metal as well.

Copper and gold (Fig. 10) appear to dominate the non-uraniferous mineral deposits of our proposed Early Proterozoic depositional zone and undoubtedly further discoveries of these metals will be made here. Copper deposits found in the zone so far are fairly small although the copper in the Mount Isa and Mammoth orebodies appears to have been remobilized and may have come from underlying Early Proterozoic rocks. Lead-zinc deposits in the Early Proterozoic rocks of northern Australia are both rare and fairly small and do not seem to be a very attractive exploration target. An absence of continental crust beneath most of the Early Proterozoic sequences could explain the scarcity of syngenetic lead-zinc deposits within them as the volcanic concentration of lead (and perhaps to a lesser degree zinc), appears to require partial melting of sialic material (Hutchinson 1973; Jacobsen, 1975). It is probably significant that the only notable lead-zinc deposits in the depositional zone occur in the only part in which older continental crust can be identified, although it is possible that plate tectonics as we know them today did not operate during the Early Proterozoic, and that although there was Archaean sialic material present elsewhere, there was no mechanism by which it could be subducted and melted.

The proposed Middle Proterozoic depositional zone differs markedly from the Early Proterozoic one in that lead and zinc become far more important in its metallogenesis. The fact that pre-existing continental crust underlies much of the belt is clearly significant in this respect. Nearly all copper deposits in Middle Proterozoic rocks show evidence of remobilization and the only one in an area seemingly not underlain by Early Proterozoic rocks is the Einasleigh deposit. Gold mineralization is important only in the more oceanic parts of the Middle Proterozoic belt. If the rocks of the Georgetown and McArthur regions were once juxtaposed, recent revival of base metal exploration in the former would appear to be justified. Stratabound lead-zinc deposits probably offer the best prospects, although the depositional environment was probably more oceanic than in the McArthur region and copper could assume more importance, as in fact gold does.

FUTURE INVESTIGATIONS SUGGESTED BY THE TECTONIC MODEL

We concede that some of the preceding discussion is rather speculative, but feel that the tectonic model put forward goes a long way towards explaining the facts as they are now known. Obviously as more geological and geochemical data become available the model will need to be refined and modified. Eventually it may have to be abandoned altogether but if it has provided a useful basis for more detailed research and exploration programs it will have served its purpose. Additional isotopic dating in the Arunta and Musgrave Blocks (preferably by uranium/lead measurements on zircon separates), geochemical characterization of mafic volcanic rocks of the various remnants of our proposed Early Proterozoic depositional zone, and more uranium determinations for the Halls Creek, The Granites-Tanami/northern Arunta, and Mount Isa granitic rocks, appear to deserve priority. A detailed Landsat interpretation might shed more light on the possible existence of a concealed fault zone in line with the western margin of the Gulf of Carpentaria.

ACKNOWLEDGEMENTS

We wish to pay tribute to officers of the Bureau of Mineral Resources, the Geological Survey of Western Australia, and the Geological Survey of Queensland who have worked in northern Australia during the last 25

years. If it were not for their efforts the synthesis presented here would clearly not have been possible. We would also like to thank A.B. Goleby for her most considerable assistance (especially in collating the chemical analyses for the mafic igneous rocks). A.D. Haldane, G.M. Derrick, and J. Knutson kindly permitted use of unpublished chemical data. Our appreciation also goes to D.H. Blake, W.B. Dallwitz, A.Y. Glikson, J.A. Hallberg, H.J. Harrington, B.S. Oversby, K.A. Plumb, C.E. Prichard, A.J. Stewart, I.P. Sweet, and J.F. Truswell who made helpful criticisms of earlier drafts, although this in no way implies their agreement with all aspects of the final paper.

REFERENCES

Anderson, D.L., 1975: Chemical plumes in the mantle. *Bull. geol. Soc. Am., 86,* 1593-1600.

Arriens, P.A., 1971: The Archaean geochronology of Australia. *Spec. Publs geol. Soc. Aust., 3,* 11-24.

Arriens, P.A., & Lambert, I.B., 1969: On the age and strontium isotope geochemistry of granulite-facies rocks from the Fraser Range, Western Australia, and the Musgrave Ranges, Central Australia. *Spec. Publs geol. Soc. Aust., 2,* 377-388.

Austin, P.M., & Williams, G.E., 1978: Tectonic development of Late Precambrian to Mesozoic Australia through plate motions possibly influenced by the earth's rotation. *J. geol. Soc. Aust., 25,* 1-21.

Bain, J.H.C., Oversby, B.S., Withnall, I.W., & Mackenzie, D.E., 1978: Precambrian and Palaeozoic geology of the Georgetown region, *in* (ed. M.J. Rubenach), *Excursions Handbook.* Third Australian Geological Convention, Geological Society of Australia.

Bennett, R., & Gellatly, D.C., 1970: Rb-Sr age determinations of some rocks from the West Kimberley region. *Rec. Bur. Miner. Resour. Geol. Geophys. Aust., 1970/20,* (unpubl.).

Berkman, D.A., this volume: Uranium Exploration in the Litchfield province, N.T., Australia. *Proceedings of the International Uranium Symposium on the Pine Creek Geosyncline.*

Black, L.P., 1975: Present status of geochronological research in the Arunta Block, Northern Territory in Proterozoic Geology. *Abstract of First Australian Geological Convention, geol. Soc. Aust.*

Black, L.P., 1977: A Rb-Sr geochronological study in the Proterozoic Tennant Creek Block, central Australia. *BMR J. Aust. Geol. Geophys., 2,* 111-122.

Black, L.P., Bell, I.H., Rubenach, M.J. & Withnall, I.W., in prep., Geochronology of discrete structural-metamorphic events in a multiply deformed terrain.

Blake, D.H., 1978: The Proterozoic and Palaeozoic rocks of The Granites - Tanami region, Western Australia and Northern Territory, and interregional correlations. *BMR J. Aust. Geol. Geophys., 3,* 35-42.

Blake, D.H., Hodgson, I.M., & Smith, P.A., 1975: Geology of the Birrindudu and Tanami 1:250 000 Sheet areas, Northern Territory. *Rep. Bur. Miner. Resour. Geol. Geophys. Aust., 174.*

Blake, D.H., Hodgson, I.M., & Muhling, P.C., in press: Geology of The Granites-Tanami region, Northern Territory and Western Australia. *Bull. Bur. Miner. Resour. Geol. Geophys. Aust., 197.*

Blockley, J.G., 1975: Pilbara Block *in* Geology of Western Australia. *Mem. geol. Surv. W. Aust., 2,* 81-91.

Bofinger, V.M., 1967: Geochronology in the East Kimberley area of Western Australia. *Ph.D. Thesis, Australian National University.* (unpubl.).

Burke, K., & Dewey, J.F., 1973: Plume generated triple junctions : key indicators in applying plate tectonics to old rocks. *J. Geol., 81,* 406-433.

Carter, E.K., Brooks, J.H., & Walker, K.R., 1961: The Precambrian mineral belt of North-Western Queensland. *Bull. Bur. Miner. Resour. Geol. Geophys. Aust., 51.*

Cleary, J.R., & Simpson, D.W., 1971: Seismotectonics of the Australian continent. *Nature, Lond., 230,* 239-241.

Compston, W., & Arriens, P.A., 1968: The Precambrian geochronology of Australia. *Can. J. Earth Sci., 5,* 561-583.

Cook, P.J., 1966: The Illamurta Structure of central Australia, Its development and relationship to a major fracture zone. *Rec. Bur. Miner. Resour. Geol. Geophys. Aust., 1966/46,* (unpubl.).

Cook, P.J., 1971: Illamurta diapiric complex and its position on an important central Australian structural zone. *Bull. Am. Ass. Petrol. Geol., 55,* 64-79.

Cooper, J.A., Fanning, C.M., Flock, M.M., & Oliver, R.L., 1976: Archaean and Proterozoic metamorphic rocks on southern Eyre Peninsula, South Australia. *J. geol. Soc. Aust., 23,* 287-292.

Cooper, J.A., Neshitt, R.W., Platt, J.P., & Mortimer, G.E., 1978: Crustal development in the Agnew region, Western Australia, as shown by Rb-Sr isotopic and geochemical studies. *Precambrian Research, 7,* 31-59.

Crohn, P.W., & Oldershaw, W., 1965: The geology of the Tennant Creek one mile sheet area. *Rep. Bur. Miner. Resour. Geol. Geophys. Aust., 83.*

Dow, D.B., & Gemuts, I., 1969: Geology of the Kimberley region Western Australia : the East Kimberley. *Bull. Bur. Miner. Resour. Geol. Geophys. Aust., 106.*

Dunn, P.R., Plumb, K.A., & Roberts, H.G., 1966: A proposal for time-stratigraphic subdivision of the Australian Precambrian. *J. geol. Soc. Aust., 13,* 593-608.

Dunnet, D., & Harding, R.R., 1967: Geology of the Mount Woodcock 1-mile sheet area, Tennant Creek, Northern Territory. *Rep. Bur. Miner. Resour. Geol. Geophys. Aust., 114.*

Ferguson, J., this volume: Metamorphism in the Pine Creek Geosyncline and its bearing on stratigraphic correlations. *Proceedings of the International Uranium Symposium on the Pine Creek Geosyncline.*

Feguson, J., Chappell, B.W. & Goleby, A.B., this volume: Granitoids in the Pine Creek Geosyncline. *Proceedings of the International Uranium Symposium on the Pine Creek Geosyncline.*

Ferguson, J., & Needham, R.S., 1978: The Zamu Dolerite : a Lower Proterozoic preorogenic continental tholeiitic suite from the Northern Territory, Australia. *J. geol. Soc. Aust., 25,* 309-322.

Gardner, C.M., 1978: Precambrian geology of the Westmoreland region, northern Australia Part III : Nicholson Granite Complex and Murphy Metamorphics. *Rec. Bur. Miner. Resour. Geol. Geophys. Aust., 1978/32,* (unpubl.).
Gellatly, D.C., 1971: Possible Archaean rocks of the Kimberley region, Western Australia. *Spec. Publs geol. Soc. Aust., 3,* 93-101.
Gellatly, D.C., Sofoulis, J., Derrick, G.M., & Morgan, C.M., 1974: The older Precambrian geology of the Lennard River 1:250 000 Sheet area, Western Australia. *Rep. Bur. Miner. Resour. Geol. Geophys. Aust., 153.*
Gemuts, I., 1971: Metamorphic and igneous rocks of the Lambco Complex, East Kimberley region, Western Australia. *Bull. Bur. Miner. Resour. Geol. Geophys. Aust., 107.*
Geological Society Australia, 1971: Tectonic Map of Australia and New Guinea.
Glikson, A.Y., Derrick, G.M., Wilson, I.H., & Hill, R.M., 1976: Tectonic evolution and crustal setting of the middle Proterozoic Leichhardt River fault trough, Mount Isa region, northwestern Queensland. *BMR. J. Aust. Geol. Geophys., 1,* 115-129.
Goode, A.D.T., & Moore, A.C., 1975: High pressure crystallization of the Ewarara, Kalka and Gosse Pile Instrusions, Giles Complex, Central Australia. *Contrib. Mineral. Petrol., 51,* 77-97.
Gray, C.M., & Oversby, V.M., 1972: The behaviour of lead isotopes during granulite facies metamorphism. *Geochim. cosmochim. Acta, 36,* 939-952.
Harrington, H.J., 1974: The Tasman Geosyncline in Australia *in* (eds. A.K. Denmead, G.W. Tweedale, & A.F. Wilson), *The Tasman Geosyncline - a Symposium, Geological Society of Australia, Queensland Division, Brisbane.*
Harrington, H.J., Burns, K.L., & Thompson, B.R., 1973: Gambier - Beaconsfield and Gambier-Sorrell fracture zones and the movement of plates in the Australia-New Zealand region. *Nature Phys. Sci., 245,* 109-112.
Hayes, D.E., & Ringis, J., 1973: Sea-floor spreading in the Tasman Sea. *Nature, Lond., 243,* 454-458.
Heier, K.S., & Lambert, I.B., 1978: A compilation of potassium, uranium and thorium abundances and heat productivites of Australian rocks. *Technical Report, R.S.E.S., Australian National University.*
Hutchinson, R.W., 1973: Volcanogenic sulfide deposits and their metallogenic significance. *Econ. Geol., 68,* 1223-1246.
Ingram, J.A., 1974: Uranium deposits. *Miner. Resour. Rep. Bur. Miner. Resour. Geol. Geophys. Aust., 6.*
Jacobsen, J.B.E., 1975: Copper deposits in time and space. *Minerals, Science and Engineering, 7,* 337-371.
Katz, M.B., 1976: Lineament tectonics of the Willyama Block and its relationship to the Adelaide autocogene. *J. geol. Soc. Aust., 23,* 275-286.
Knutson, J., Ferguson, J., Roberts, W.M.B., Donnelly, T.H., & Lambert, I.B., in press: Petrogenesis of the copper-bearing breccia pipes, Redbank, N.T., Australia. *Econ. Geol.*
Lambert, I.B., 1971: The composition of the deep continental crust. *Spec. Publs geol. Soc. Aust., 3,* 419-428.
McDougall, I., Dunn, P.R., Compston, W., Webb, A.W., Richards, J.R., & Bofinger, V.M., 1965: Isotopic age determination on Precambrian rocks of the Carpentaria region, Northern Territory, Australia. *J. geol. Soc. Aust., 12,* 67-90.
Moore, A.C., 1971: Mineralogy of the Gosse Pile ultramafic intrusion, central Australia. II. Pyroxenes. *J. geol. Soc. Aust., 18,* 243-258.
Moore, A.C., & Goode, A.D.T., 1978: Petrography and origin of granulite facies rocks in the western Musgrave Block, central Australia. *J. geol. Soc. Aust., 25,* 341-358.
Nasca, S.U., 1972: Project No. 923 : Benmara, Northern Territory, Final Report. *Unpublished Report, Esso Australia Ltd.*
Oversby, B.S., Palfreyman, W.D., Black, L.P., Cooper, J.A., & Bain, J.H.C., 1975: Georgetown, Yambo and Coen Inliers - regional geology *in* (ed. C.L. Knight), *Economic Geology of Australia and Papua New Guinea, Australas. Inst. Min. Metall., Monograph Series No. 5, 1. Metals,* 511-516.
Oversby, V.M., 1976: Isotopic ages and geochemistry, of Archaean acid igneous rocks from the Pilbara, Western Australia. *Geochim. cosmochim. Acta, 40,* 817-829.
Page, R.W., 1974: Implications of new geochronological data in the Alligators River area, Northern Territory, *in* BMR Symposium abstracts, Canberra, 1974. *Rec. Bur. Miner. Resour. Geol. Geophys. Aust., 1974/35,* (unpubl.).
Page, R.W., 1976: Reinterpretation of isotopic ages from the Halls Creek Mobile Zone, northwestern Australia. *BMR J. Aust. Geol. Geophys., 1,* 79-81.
Page, R.W., 1978: Response of U-Pb zircon and Rb-Sr total-rock and mineral systems to low-grade regional metamorphism in Proterozoic igneous rocks, Mount Isa, Australia. *J. geol. Soc. Aust., 25,* 141-164.
Page, R.W., Blake, D.H., & Mahon, M.W., 1976: Geochronology and related aspects of acid volcanics, associated granites, and other Proterozoic rocks in The Granites-Tanami region, northwestern Australia. *BMR J. Aust. Geol. Geophys., 1,* 1-13.
Page, R.W., Compston, W. & Needham, R.S., this volume: Geochronology and evolution of the large Archaean basement and Proterozoic rocks in the Alligator Rivers Uranium field, Northern Territory, Australia. *Proceedings of the International Uranium Symposium on the Pine Creek Geosyncline.*
Pearce, J.A., & Cann, J.R., 1971: Ophiolite origin investigated by discriminant analysis using Ti, Zr and Y. *Earth Planet. Sci. Lett., 12,* 339-349.
Pearce, J.A., & Cann, J.R., 1973: Tectonic setting of basic volcanic rocks determined using trace element analyses. *Earth Planet. Sci. Lett., 19,* 290-300.
Pearce, T.H., Gorman, D.E., & Birkett, T.C., 1975: The TiO_2-K_2O-P_2O_5 diagram : a method of discriminating between oceanic and non-oceanic basalts. *Earth Planet. Sci. Lett., 24,* 419-426.
Pearce, T.H., Gorman, D.E., & Birkett, T.C., 1977: The relationship between major element chemistry and tectonic environment of basic and intermediate volcanic rocks. *Earth Planet. Sci. Lett., 36,* 121-132.

Pidgeon, R.T., 1978: 3450 m.y. old volcanics in the Archaean layered greenstone succession of the Pilbara Block, Western Australia. *Earth Planet. Sci. Lett., 37*, 421-428.
Plumb, K.A., 1979: The tectonic evolution of Australia. *Earth Sci. Rev., 14*, 205-249.
Plumb, K.A., in press: Structure and tectonic style of the Precambrian shields and platforms of northern Australia. *Tectonophysics*.
Plumb, K.A., & Derrick, G.M., 1975: Geology of the Proterozoic rocks of the Kimberley to Mount Isa region *in* (ed. C.L. Knight), *Economic Geology of Australia and Papua New Guinea, Australas. Inst. Min. Metall., Monograph Series No. 5, 1. Metals*, 217-252.
Plumb, K.A., Derrick, G.M., & Wilson, I.H., in press: Precambrian geology of the McArthur River - Mount Isa Region, northern Australia *in* (eds. P.J. Stephenson & R.A. Henderson), *Geology and geophysics of northeastern Australia, Geological Society of Australia, Queensland Division, Brisbane*.
Plumb, K.A., & Gemuts, I., 1976: Precambrian geology of the Kimberley region, Western Australia. *25th Int. geol. Congr., Sydney, Excursion Guide, 44C*.
Plumb, K.A., & Sweet, I.P., 1974: Regional significance of recent correlations across the Murphy Tectonic Ridge, Westmoreland area *in* Papers presented at the regional meeting on recent technical and social advance in the north Australian mineral industry *Melbourne Australas. Inst. Min. Metall.*, 199-206.
Richards, J.R., Ruxton, B.P., & Rhodes, J.M., 1977: Isotopic dating of the leucocratic granite, Rum Jungle, Australia. *Proc. Australas. Inst. Min. Metall., 264*, 33-43.
Roberts, H.G., Rhodes, J.M., & Yates, K.R., 1963: Calvert Hills, Northern Territory 1:250 000 Geological Series. *Explan. Notes Bur. Miner. Resour. Geol. Geophys. Aust., SE/53-8*.
Rod, E., 1966: Clues to ancient Australian geosutures. *Eclog. geol. Helv., 59*, 849-883.
Rutland, R.W.R., 1976: Orogenic evolution of Australia. *Earth Sci. Rev., 12*, 161-196.
Shaw, S.E., 1968: Rb-Sr studies of the mine sequence rocks at Broken Hill, *in* (eds. M. Radmanovitch & J.T. Woodcock), *Broken Hill Mines, 1968, Australas. Inst. Min. Metall., Monograph Series 3*, 185-198.
Sheraton, J.W., & Labonne, B., 1978: Petrology and geochemistry of acid igneous rocks of northeast Queensland. *Bull. Bur. Miner. Resour. Geol. Geophys. Aust., 169*.
Sillitoe, R.H., 1974: Tin mineralisation above mantle hot spots. *Nature, Lond., 248*, 497-499.
Smart, P.G., Wilkes, P.G., Needham, R.S., & Watchman, A.L., 1975: Geology and geophysics of the Alligator Rivers region, *in* (ed. C.L. Knight), *Economic Geology of Australia and Papua New Guinea, Australas. Inst. Min. Metall., Monograph Series No. 5, 1. Metals*, 285-301.
Smith, R.E., & Smith, S.E., 1976: Comments on the use of Ti, Zr, Y, Sr, K, P and Nb in classification of basaltic magmas. *Earth Planet. Sci. Lett., 32*, 114-120.
Stuart-Smith, P.G., & Ferguson, J., 1978: The Oenpelli Dolerite - a Precambrian continental tholeiitic suite from the Northern Territory, Australia. *BMR J. Aust. Geol. Geophys., 3*, 125-133.
Stuart-Smith, P.G., Wills, K., Crick, I.H. & Needham, R.S., this volume: Evolution of the Pine Creek Geosyncline. *Proceedings of the International Uranium Symposium on the Pine Creek Geosyncline*.
Stewart, A.J., Langworthy, A.P., Warren, R.G., Offe, L.A., Glikson, A.Y., Wells, A.T., Le Messurier, P., & Gardener, J.E.F., 1976. Precambrian structures and metamorphic rocks of central Australia and Tennant Creek, N.T. *25th Int. geol. Congr., Sydney, Excursion Guide 47C*.
Stewart, I.C.F., & Mount T.J., 1972: Earthquake mechanisms in South Australia in relation to plate tectonics. *J. geol. Soc. Aust., 19*, 41-52.
Stewart, A.J., & Warren, R.G., 1977: The mineral potential of the Arunta Block. *BMR J. Aust. Geol. Geophys., 2*, 21-34.
Walpole, B.P., Crohn, P.W., Dunn, P.R., & Randal, M.A., 1968: Geology of the Katherine-Darwin Region, Northern Territory. *Bull. Bur. Miner. Resour. Geol. Geophys. Aust., 82*.
Webb, A.W., 1971: Australian Mineral Development Laboratories Report, AN 5188/71 (unpubl.).
Webb, A.W., 1973a: The geochronology of the younger granites of the Musgrave Block. Progress Report II Australian Mineral Development Laboratories AN1/1/123 (unpubl.).
Webb, A.W., 1973b: Carpentaria age determination project. Australian Mineral Development Laboratories Report AN2/1/O - 1814/73 Part Report 4 (unpubl.).
Webb, A.W., 1974: Australian Mineral Development Laboratories Report AN 2250/74 (unpubl.).
Webb, A.W., 1975: Geochronology of 22 rock samples from Nicholson Granite Complex. Australian Mineral Development Laboratories Report AN2/1/O - 2850/75 (unpubl.).
Webb, A.W., & Thompson, B.P., 1977: Archaean basement rocks in the Gawler Craton, South Australia. *Search, 8*, 34-36.
White, D.A., 1965: The geology of the Georgetown/Clarke River area, Queensland. *Bull. Bur. Miner. Resour. Geol. Geophys. Aust., 71*.
Williams, I.R., & De la Hunty, L.E., 1975: Yilgarn Block, *in* Geology of Western Australia. *Mem. Geol. Surv. W. Aust., 2*, 33-81.
Willmott, W.F., Whitaker, W.G., Palfreyman, W.D., & Trail, D.S., 1973: Igneous and metamorphic rocks of Cape York Peninsula and Torres Strait. *Bull. Bur. Miner. Resour. Geol. Geophys. Aust., 135*.
Windley, B.F., 1970: Anorthosites in the early crust of the Earth and on the Moon. *Nature, Lond., 226*, 333-335.
Winkler, H.G.F., 1976: *Petrogenesis of Metamorphic Rocks* (4th edition) Springer-Verlag, Berlin, 334 p.
Wilson, I.H. 1978: Volcanism on a Proterozoic continental margin in northwestern Queensland. *Precambrian Research, 7*, 205-235.
Wilson, I.H., & Derrick, G.M., 1976: Precambrian geology of the Mount Isa region, northwest Queensland, *25th Int. geol. Congr., Sydney, Excursion Guide, 5A, 5C*.

GEOLOGY OF THE ALLIGATOR RIVERS URANIUM FIELD

R. S. Needham and P. G. Stuart-Smith

Bureau of Mineral Resources, P.O. Box 378, Canberra City, A.C.T. 2601, Australia.

ABSTRACT

The uranium deposits of Ranger 1, Koongarra, Jabiluka One and Two, and Nabarlek are in the Alligator Rivers Uranium Field, the northeastern part of the Pine Creek Geosyncline. Lower Proterozoic metasediments, which were metamorphosed mainly to amphibolite-grade and multiply isoclinally folded at about 1800 Ma, host much of the uranium and overlie or grade into the Archaean to Lower Proterozoic granitoid Nanambu Complex. In the northeast of the Field the metasediments grade into schist and gneiss forming the outer parts of the Lower Proterozoic Nimbuwah Complex; the inner parts of this Complex contain granodioritic and tonalitic migmatite and granitoid rocks which were emplaced before the 1800 Ma event. The metasediments are intruded by pre-orogenic and post-orogenic tholeiitic dolerite, by synorogenic granite, and by later minor phonolite and dolerite dykes. All but the minor dykes are overlain with marked unconformity by Carpentarian (Middle Proterozoic) sandstone with basalt flows, which conceals older rocks over most of the southeastern half of the area. The pre-Carpentarian (pre-Middle Proterozoic) rocks are deeply weathered and lateritised and are covered extensively by Mesozoic and Cainozoic sediment.

The uranium is mainly contained in the lower member of the Cahill Formation, comprising mica quartz schist, magnesite and carbonaceous schist, which is chloritised around the uranium occurrences and along faults, shears and some stratigraphic breaks. The ore zones are located in breccia. The stratabound nature of the ore suggests that it has formed partly syngenetically; however, epigenetic processes appear essential for the development of such high-grade deposits.

INTRODUCTION

The Alligator Rivers Uranium Field covers about 22 500km^2 in the northeast of the Pine Creek Geosyncline (Fig. 1), east of the South Alligator River and Mount Partridge Range, and north of latitude 13°20'S. The field contains the major uranium discoveries of Ranger 1, Koongarra, Jabiluka One and Two and Nabarlek (Fig. 2). Before these were discovered, the geology of the area was poorly understood. Exploration interest in the area grew as a result of broad similarities between the Lower Proterozoic rocks of this area and the Rum Jungle Uranium Field (Fig. 1) revealed by mapping undertaken by the Bureau of Mineral Resources, Geology and Geophysics (BMR), and portrayed on a regional geological map of the area published in 1967 (BMR, 1967), and between the Carpentarian (Middle Proterozoic) rocks of this area and uranium-bearing equivalents in the Westmoreland area in northwest Queensland. Since the discovery of the Alligator Rivers uranium deposits, the area has been re-mapped at 1:100 000 scale (Needham & Smart, 1972; Needham *et al.*, 1975a & b; Smart *et al.*, 1975; Needham & Stuart-Smith, 1976 & 1978). Exposure is sparse and contacts are rarely exposed; radiometric age determination has been used to verify relationships postulated between many units. As a result of the recent studies, similarities between this area and the Rum Jungle area have been confirmed. Archaean granitoid rocks are basement to arkosic, psammitic, pelitic and carbonate-bearing Lower Proterozoic metasediments which are partly carbonaceous; these rocks in turn are overlain by younger, essentially undeformed plateau-forming sandstone. The uranium is stratabound in the carbonate-bearing and carbonaceous part of the Lower Proterozoic sequence (Needham & Stuart-Smith, 1976). However, the metamorphic grade and intensity

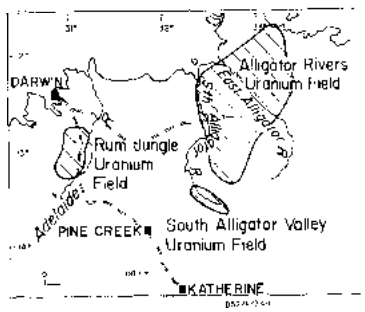


Figure 1. Location of the Alligator Rivers Uranium Field in the Pine Creek Geosyncline.

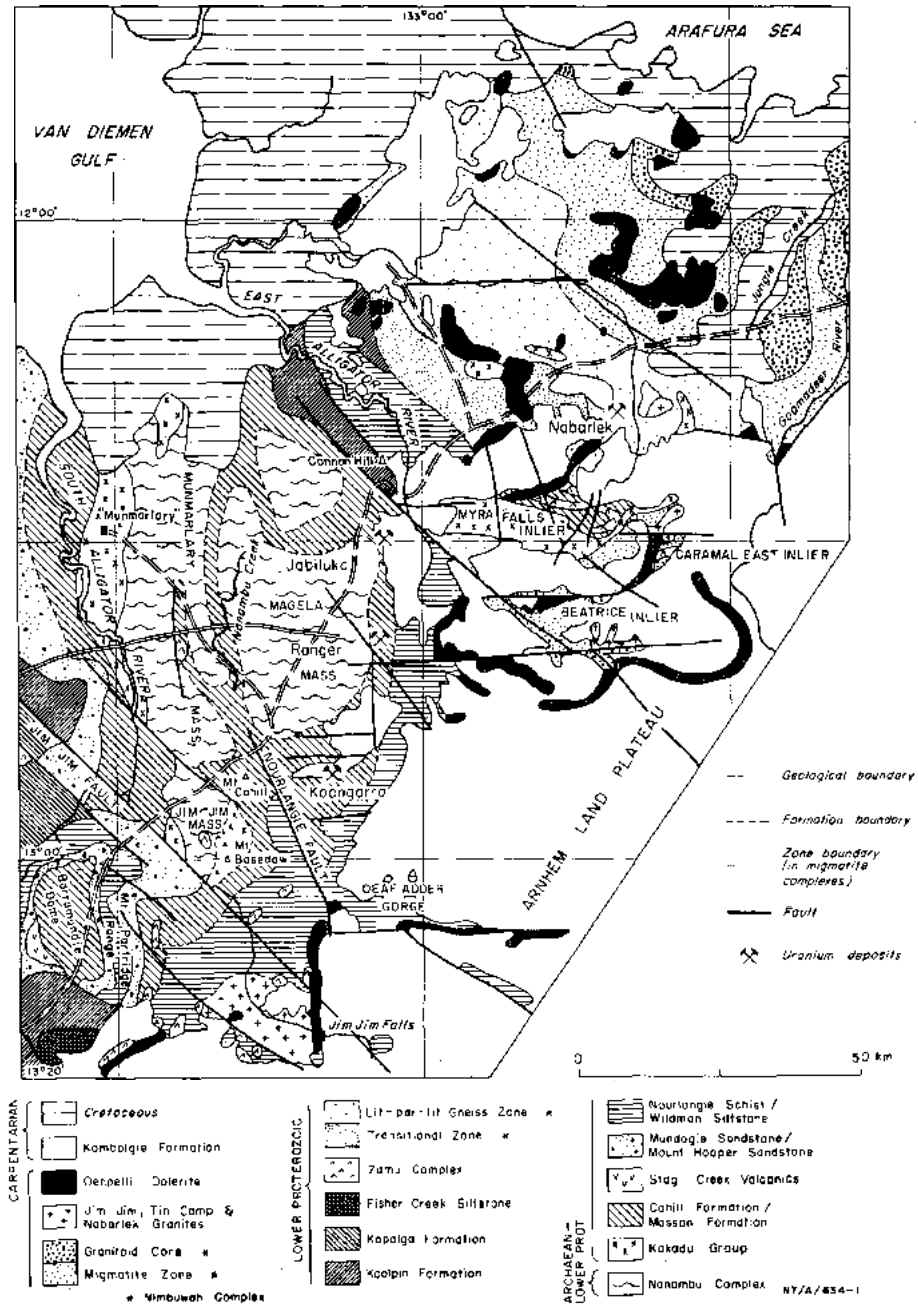


Figure 2. Generalised geology of the Alligator Rivers Uranium Field (after Needham & Stuart-Smith, 1976).

Table 1. Summary of Stratigraphy (Cainozoic units omitted) Ages after Page *et al.* (this volume) unless otherwise stated.

		Age Ma	Unit	Thickness m	Main Lithologies	Stratigraphic Relationships	Definition or Best Descriptions
PLATFORM COVER	MESOZOIC	L. Neocomian -Aptian (Hughes, 1978)	Bathurst Island Formation Marligur Member Darwin Member	60 20	fine to coarse sandstone fine sandstone, siltstone; mudstone	facies equivalents; disconformably overlies Petrel Fm	Hughes (1978)
		E. Jurassic-Neocomian (Hughes, 1978)	Petrel Formation	100	claystone, coarse sandstone	unconformable on older units	
	ADELAIDEAN (Upper Proterozoic)	1200	Wurugoij Dolerite		quartz dolerite	intrudes Kombolgie Fm	Needham *et al.* (1975a)
		1316	Mudginberri Phonolite, Maningkorrirr Phonolite	1	phonolite	as dykes intrude Nanambu Complex and Nimbuwah Complex	Smart *et al* (1975)
		1370		2	quartz dolerite	as dykes intrudes Cahill Fm and Nourlangie Schist	
	KATHERINE RIVER GROUP	1648	Kombolgie Formation upper sandstone unit	150	sandstone, minor pebbly sandstone, conglomerate, siltstone	conformable over Nungbalgarri Volcanic Mbr; locally unconformable over lower sandstone unit	Needham & Stuart-Smith (1978) Walpole *et al.* (1968)
			Gilruth Volcanic Mbr	5	tuffaceous siltstone, banded quartz-jasper rock, vesicular basalt	conformable within Kombolgie Fm upper sandstone unit	
			Nungbalgarri Volcanic Mbr	0-170	basalt, trachy-basalt; cherty rhyolite and ignimbrite at top in places	conformable over lower sandstone unit	

IAEA

	CARPENTARIAN (Middle Proterozoic)		lower sandstone unit	300	sandstone, pebbly sandstone, conglomerate, minor siltstone. Local unconformable ferruginous sandstone	markedly unconformable over most older rocks; apparently conformable over Edith River Volcs	
TRANSITIONAL IGNEOUS ACTIVITY		1688	Oenpelli Dolerite	250	olivine dolerite, quartz dolerite, granophyric dolerite and granophyre	intrudes older rocks as lopoliths. Forms basement ridges under Kombolgie Fm	Smart *et al* (1975) Stuart-Smith & Ferguson (1978)
		1760 (Walpole *et al.*, 1968)	Edith River Volcanics	10	tuff, tuffaceous siltstone, altered rhyolite	valley-fill deposits over Lower Prot. rocks	Needham & Smart (1972). Needham & Stuart-Smith (1978)
		1760-1780	Nabarlek, Tin Camp and Jim Jim Granites		altered biotite granite	intrude Lower Prot. metaseds., overlain by Kombolgie Fm	Needham & Stuart-Smith (1978), Needham *et al.* (1975 & b)
	PROTEROZOIC	1870-1803	Nimbuwah Complex		granodiorite, granite, migmatite, gneiss, schist	contacts of inner granitoid rocks with other units not seen; outer gneiss and schist grade into and contain resisters of Lower Prot. metasediments	Needham *et al.* (1975a) Needham & Stuart-Smith (1978)
			Zamu Dolerite	170	ortho-amphibolite	sills folded and metamorphosed with enclosing metasedments	Ferguson & Needham (1978)
SEDIMENTATION		SOUTH ALLIGATOR GROUP	Fisher Creek Siltstone?	unknown	mica quartz schist	possibly overlies Koolpin Fm?	Needham (in prep., b)
			Koolpin Formation?	unknown	mica quartz schist, quartzite, magnetitic and graphitic in places, commonly with iron-rich bands, minor amphibolite	possibly overlies Cahill Fm and/or Nourlangie Schist	
			Nourlangie Schist	unknown	quartz and mica schist	in places unconformable over Cahill Fm; metamorphic equivalent of Wildman Siltstone	Needham (in prep., a)

PROTEROZOIC	LOWER		Cahill Formation	3000	mica and quartz feldspar schist and gneiss; lower member is calcareous and carbonaceous in places and contains para-amphibolite and lenses (250 m) crystalline dolomite-magnesite near base	not clear. Probably conformable on Mount Basedow Gneiss and onlapping Nanambu Complex. Lower member is equivalent to Masson Fm and upper member to Mt. Hooper Sst. and Mundogie Sst., though of different sedimentary and metamorphic facies	Needham & Stuart-Smith (1976)
LOWER	LOWER	KAKADU GROUP	Kudjumarndi Quartzite	150	quartzite, minor feldspar quartz gneiss	lowest known meta-sedimentary units in east. Equivalent to Munmarlary Qt and Mt Basedow Gneiss	Needham & Stuart-Smith (1978)
			Mt Howship Gneiss	unknown	meta-arkose, coarse pegmatoid gneiss		
			Munmarlary Quartzite	200	quartzite	lowest known meta-sedimentary units in west. Transitional into Lower Prot. part of Nanambu Complex. Equivalent to Kudjumarndi Qt and Mt Howship Gneiss	
			Mt Basedow Gneiss	unknown	meta-arkose, pebbly in places; gneiss, minor schist		
BASEMENT	ARCHAEAN LOWER PROTEROZOIC	1800	Nanambu Complex		leucogneiss, pegmatoid gneiss, schist	transitional into Mount Basedow Gneiss	Needham (in prep., a)
		1800-2000			foliated granite, augen gneiss	metamorphosed Archaean granite	
	ARCHAEAN	2400-2500			granite, foliated granite	oldest known rocks in Alligator Rivers region	

Table 1 continued.

Proterozoic rocks in the Alligator Rivers region is, in the main, markedly greater than in the Rum Jungle area. Although the Carpentarian (Middle Proterozoic) rocks of the Alligator Rivers region are similar in age and rock type to those of the Westmoreland area, they are not known to host any significant uranium mineralisation.

STRATIGRAPHY

Generalised geology and schematic stratigraphy of the Alligator Rivers region are shown in figures 2 and 3; the stratigraphy is summarised in table 1.

ARCHAEAN-LOWER PROTEROZOIC GRANITOIDS

Nanambu Complex

Gneiss, granite and schist of the Nanambu Complex occupy much of the western part of the Alligator Rivers Uranium Field. The name 'Nanambu Granite' was used by Condon & Walpole (1955) and Dunn (1962) to describe gneissic and garnetiferous granite in the Nanambu Creek area; Needham & Smart (1972) modified the name to Nanambu Complex to reflect the presence of a range of granitic and metamorphic lithologies. The Complex is poorly exposed (mostly as weathered rock in the banks of incised creeks, or small pavements of fresh rock near the margins of flood plains) in three areas enclosed by Lower Proterozoic metasediments, named the Magela, Jim Jim and Munmarlary Masses by Needham & Smart (1972). Geochronological studies have obtained three groups of ages between 2500 and 1800 Ma, indicating formation between the late Archaean and the late Lower Proterozoic (Page *et al.*, this volume). Three groups of rocks can be distinguished on the basis of these different ages. The oldest group (2500-2400 Ma) is massive to foliated granite, which grades into strongly foliated gneiss (1980-1800 Ma) indicating partial response to the 1800 Ma regional amphibolite-grade metamorphism. These rocks are surrounded by a concordant sheath of Lower Proterozoic (1800 Ma) gneiss, schist, migmatite and metasediment. Where possible the Lower Proterozoic rocks are incorporated in the Lower Proterozoic stratigraphy; elsewhere (mainly interlayered leucocratic gneiss and schist, and migmatite) they are included in the Nanambu Complex. The Nanambu Complex occupies domes within the metasediments, which suggests that Archaean granite was reactivated, i.e. uplifted and metamorphosed with the enclosing rocks during the 1800 Ma event, to form a mantled gneiss dome.

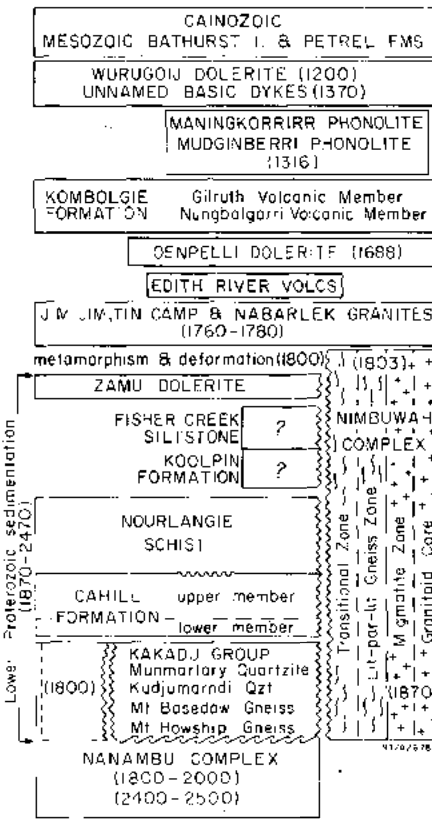


Figure 3. Schematic stratigraphy of the Alligator Rivers Uranium Field. Numbers in parentheses are age determinations (Ma) from Page *et al.* (this volume).

In the *massive to foliated granite* (2504-2400 Ma), the foliation is generally northerly and vertical, and augen can be seen in vertical sections parallel to the foliation where the foliation is strongly developed. The rocks are white to light grey, and medium to coarse grained, and contain quartz, microcline, plagioclase and biotite with accessory muscovite and opaque minerals. Muscovite may be as abundant as biotite in the more massive varieties. The granites form mainly small scattered domes and pavements along the eastern side of the South Alligator River floodplain, and in the headwaters of Nanambu Creek, and also form basement hills in the Kombolgie Formation 4km south of Jabiluka and 12km north of Koongarra.

Well foliated gneiss yields ages between 1980 and 1800 Ma with generally high initial $^{87}Sr/^{86}Sr$ ratios, indicating that the gneiss has an Archa ean origin and has only partly responded to the 1800 Ma regional metamorphism (Page *et al.*, this volume). Common minerals are quartz, K-feldspar and/or plagioclase and biotite. Muscovite may be present, but is generally subordinate to biotite, and almandine is a rare accessory. Granuloblastic textures are common, characteristic of the almandine-amphibolite facies of metamorphism. In places augen textures are well developed.

Leucogneiss, schist and migmatite yield ages of 1800 Ma, consistent with time of late Lower Proterozoic regional metamorphism, and normal initial isotopic ratios indicate a metasedimentary origin (Page *et al.*, this volume). The term leucogneiss has been applied to a diverse group of coarse, mostly massive pegmatitic rocks, consisting essentially of quartz, alkali feldspar, and plagioclase. Accessory muscovite, and lesser biotite may also be present as subparallel plates, giving the rock a weak foliation. In particularly coarse specimens, however, feldspar may form layers up to 12cm thick. In places, muscovite and quartz commonly form differentiated layers up to 2cm across which mark the foliation. Almandine is a common accessory.

In some areas, particularly in the south, leucogneiss is interlayered with biotite schist. Because of gradation of leucogneiss into meta-arkose of the Kakadu Group in this area (described below) the layering probably represents preserved sedimentary compositional banding. Northeast of Munmarlary homestead in the north of the Complex, migmatites are present showing the vein, layered, dilatation, folded, ptygmatic, augen and schlieren structures described by Mehnert (1968). These rocks probably represent a progression of partial anatexis from the layered leucogneiss and schist, and suggest that metamorphic grade increases northwards.

The distribution of Archaean granite in the Nanambu Complex is shown on the Cahill 1:100 000 geological map (BMR, 1977). In places the granite crops out near the margin of the Complex, less than 1km from rocks of the Cahill Formation, which lie stratigraphically above the Kakadu Group. This proximity suggests that in some areas the Kakadu Group may thin or be overlapped by the Cahill Formation. The patchy distribution of Archaean rocks both in the centre and near the margin of the Complex indicates that the structural relationship between the granite and its sheath of metasedimentary rocks is not simple, most probably as a result of polyphase isoclinal folding during the 1800 Ma regional metamorphic and deformational episode, and faulting.

LOWER PROTEROZOIC METASEDIMENTS

Kakadu Group

Meta-arkose, leucocratic gneiss and quartzite flank the Nanambu Complex on the west and south, and are in places (e.g. Mount Basedow) transitional into leucogneiss of the Complex; similar leucocratic gneiss and quartzite occupying the core of an anticline and a dome in the Myra Falls Inlier 20km south of Nabarlek are in the same stratigraphic position (i.e. below the Cahill Formation, Needham & Stuart-Smith, 1978). These rocks, which form

the Kakadu Group, are the oldest recognisable Lower Proterozic metasediments in the region, and were probably deposited on Archaean basement. They are distinguished from leucogneiss of the Nanambu Complex by commonly preserved bedding and compositional banding, rare cross-bedding, relatively good, continuous, ridge-forming exposures, finer grain size and less massive and pegmatoid, better foliated appearance.

The gradation between granitoids of the Nanambu Complex and meta-arkose of the Kakadu Group is apparent at Mount Basedow, in the southernmost exposures of the Nanambu Complex. Here the *Mount Basedow Gneiss* contains both leucogneiss and meta-arkose which are well foliated parallel to compositional layering, and which appear to be cross-bedded in places, although no younging directions could be determined. Feldspars impart a pink, grey or yellow colour to these rocks; they are usually poorly-sorted, and consist of angular and irregular grains of microcline (in places perthitic), subrounded to angular quartz, and flakes of muscovite with albite, rare chlorite and magnetite, in a groundmass of cryptocrystalline quartz. These rocks grade into well foliated leucogneiss of the Nanambu Complex, which is exposed in the banks of creeks incised in the lowlands west of Mount Basedow.

Quartzite and meta-arkose form strike ridges of *Munmarlary Quartzite* on the western flank of the Nanambu Complex north of the Arnhem Highway. These rocks are similar to quartzite of the Mount Basedow Gneiss, consisting entirely of a granuloblastic quartz mosaic, which in places is sheared and contains muscovite or feldspar. Feldspar may constitute up to 20 per cent of the rocks, but is usually interstitial between quartz grains. Most of the quartz is strained and fractured; it forms elongate grains or lensoid lamellae, which give the rocks a bedded appearance. The quartzite is in places surrounded by gneiss of the Nanambu Complex, suggesting that the quartzite was originally sandstone in a sequence predominantly consisting of arkose which has been metamorphosed to form the granitoid leucogneiss of the Nanambu Complex. The quartzite remains a mappable unit as its essential monomineralic nature is preserved and it forms prominent and continuous outcrops.

Feldspathic quartzite correlated with the Munmarlary Quartzite was intersected by drilling 1000m west of the South Alligator bridge (Stuart-Smith, 1977), and appears to rest directly on Archaean rocks of the Nanambu Complex.

The Munmarlary Quartzite and Mount Basedow Gneiss largely occupy a zone of upper greenschist facies metamorphism in the west and south of the Alligator Rivers Uranium Field, defined by mineral assemblages in nearby pelitic and calcareous rocks (Needham & Smart, 1972; Needham & Stuart-Smith, 1976; Wallace, in prep. — see under 'Structure and Metamorphism').

Coarse pegmatoid meta-arkose and leucogneiss *(Mount Howship Gneiss)* form the lowest part of the sequence in the Myra Falls Inlier 20km south of Nabarlek, and are overlain by quartzite (*Kudjumarndi Quartzite*), which is commonly sheared, although cross-bedding is preserved in places. These rocks are mineralogically the same as representatives of the Mount Basedow Gneiss and Munmarlary Quartzite. Outcrop of the Mount Howship Gneiss is confined to the Myra Falls Inlier, but isolated exposures of Kudjumarndi Quartzite north and northwest of Nabarlek, surrounded by lit-par-lit gneiss of the Nimbuwah Complex, indicate that the latter is probably the differentiated equivalent of the Mount Howship Gneiss.

Cahill Formation

The Cahill Formation consists of a *lower member* composed partly of carbonate and carbonaceous rocks passing transitionally upwards into a more psammitic *upper member*. The formation is very poorly exposed (less than 1 percent); its stratigraphy is known mainly from fences of shallow drill holes (Fig. 4; Needham & Stuart-Smith, 1976). Needham

Crick & Stuart-Smith (this volume) suggest that the lower member may be correlated with the Masson Formation of the Namoona Group, and the upper member with the Mount Hooper Sandstone and Mundogie Sandstone of the Mount Partridge Group west of the Alligator Rivers Uranium Field.

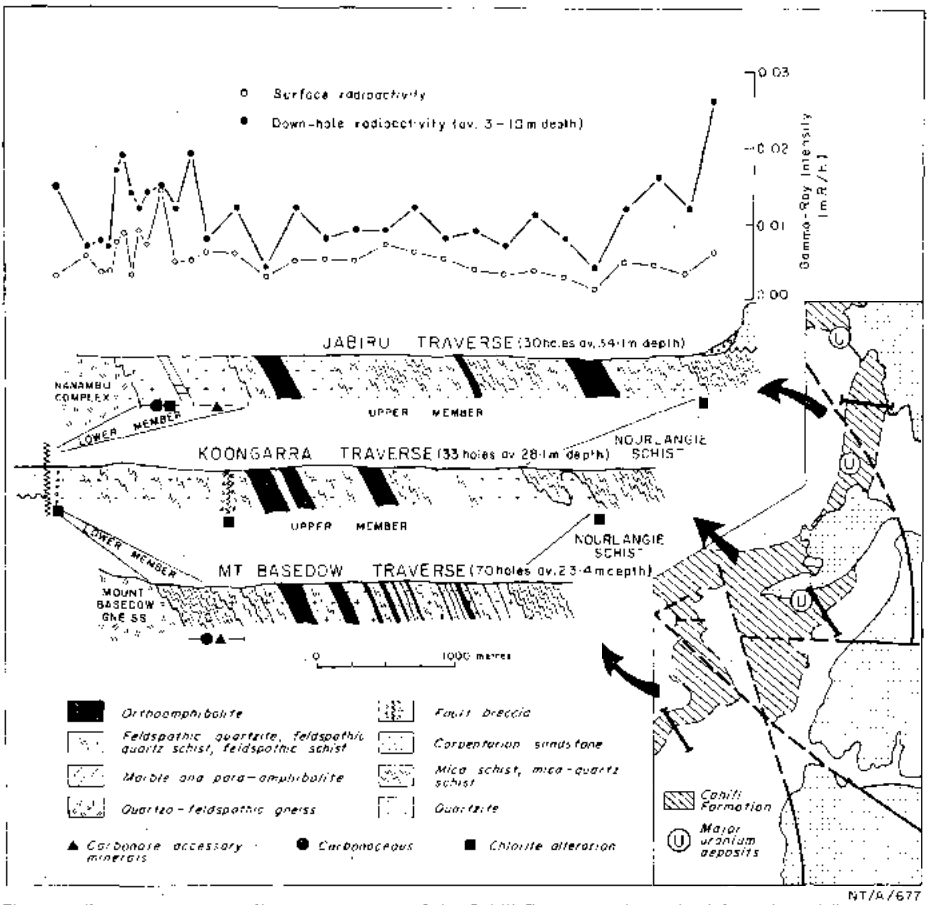


Figure 4. Stratigraphy and radiometric response of the Cahill Formation, determined from three drill traverses (after Needham & Stuart-Smith, 1976).

Wright (1976) advanced an alternative correlation based on detailed mapping in the 'Barramundie Dome', in the extreme southwest of the Alligator Rivers Uranium Field (Fig. 2). He considered that rocks of the Mount Partridge Range area extended across the centre of the dome (an area of subdued relief and very poor exposure) and were unconformable over similar sandstone and conglomerate on the west side of the dome. The presence of two psammitic units at different stratigraphic levels was thus implied, which possibly correlated with the Kakadu Group and Mount Partridge Group. Subsequent mapping (BMR, 1979) located overturned conglomerate beds on the west side of the dome, and drilling intersected underlying Stag Creek Volcanics (Needham *et al.*, 1978), indicating the presence of Masson Formation in the centre of the dome and a major dip reversal across the dome. Traceable

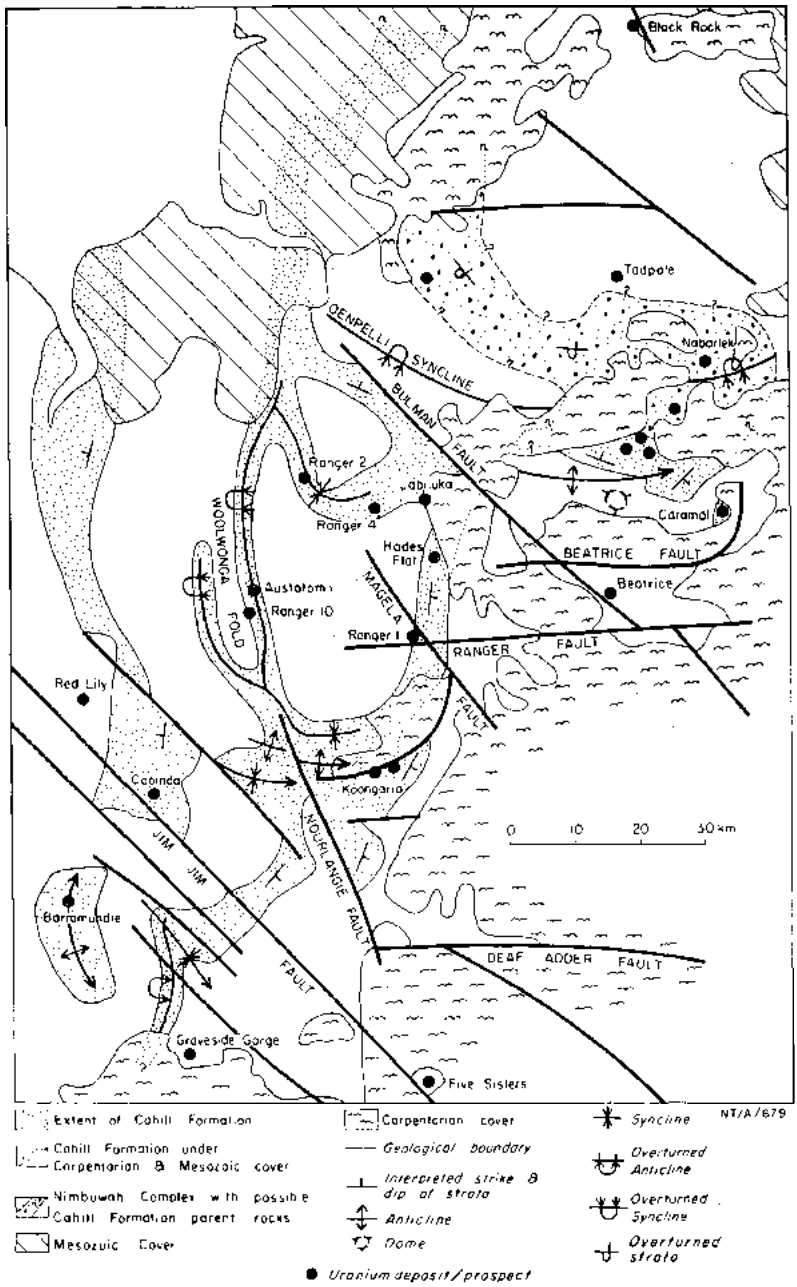


Figure 5. Known and postulated extent of the Cahill Formation showing major structural elements and distribution of uranium occurrences.

marker units around the dome confirmed the correlation of psammitic units across it and support the stratigraphic correlation between the Cahill and Masson Formations favoured by the authors.

Cahill Formation rocks form a belt generally about 5km wide surrounding and folded into the Nanambu Complex in the western part of the region, and in the eastern part are restricted to the central and eastern parts of the Myra Falls Inlier. The lower member contains the major uranium deposits of the area, and the majority of uranium prospects (Fig. 5).

Lower Member

The lower member is a sequence of interbanded pyritic carbonaceous mica schist, chloritised feldspathic quartzite and quartz schist, para-amphibolite and calc-silicate rock, with lenses of massive dolomite up to 500m thick. It ranges in thickness from 300 to 600m and probably up to 1000m (G.S. Eupene, pers. comm. 1979) and is characterised by numerous sharp changes in rock type. In areas well away from known mineralisation, rocks of the lower member generally contain higher values of Mg, F and Th than in the upper member and have a lower Fe/Mg ratio (Table 2). Within the Cahill Formation, carbonaceous rocks have the highest U content (Table 2). The rocks of the lower member are generally slightly more radioactive than adjacent metasediments (Fig. 4) which is consistent with the slightly higher uranium contents in some rock types in the member (Table 2). The higher radioactivity is apparently too subtle to be detected by airborne techniques, and surficial cover generally causes the radioactivity to be attenuated at surface (Fig. 4). Furthermore, the radioactivity of Nanambu Complex and Nourlangie Schist rocks is commonly erratic and in places is markedly higher than that of the Cahill Formation. Consequently surface and airborne radiometric techniques generally do not reflect geological patterns.

Carbonaceous schist makes up less than 10 percent of the lower member, and consists of fine-grained foliated carbon, quartz, and minor disseminated pyrite and pyrrhotite; the schist is interlayered with quartz-rich bands. Fine-grained graphite is present along sheared foliation and crenulation cleavage surfaces. The carbonaceous schist contains phlogopite in places, and also tremolitic amphibole, accessory scapolite, epidote, and carbonate minerals. This assemblage suggests that the rock was derived from a magnesium carbonate-bearing sediment similar to the pyritic carbonaceous dolomitic shale and siltstone found throughout the central and western parts of the Pine Creek Geosyncline.

Marble, calc-silicate rock and para-amphibolite are mainly confined to the lower member of the Cahill Formation. The most common variety is massive crystalline carbonate rock, which ranges in composition from calcitic dolomite to magnesite (Needham, 1976). It crops out, mostly in the Woolwonga Fold (Fig. 5), as discontinous ridges, up to 10m high, of iron-stained vuggy, cherty rock with rare possible algal structures, which are usually columnar. Near-surface and surface silification and ferruginisation are common; fresh crystalline magnesian dolomite has been intersected less than 10m below an outcropping ridge of ferruginous silicified dolomite near Nanambu Creek (Needham, 1976). Exposures of fresh carbonate rock are near the prominent escarpment which marks the edge of the Carpentarian (Middle Proterozoic) plateau sandstone (e.g. 9km SSE of Ranger 1, 17km south of Nabarlek); these rocks have probably been exhumed by scarp retreat since the early Tertiary period of ferruginisation and silicification (silicification of carbonate in the Ranger 1 orebody (Eupene *et al.*, 1975) may represent an earlier period of near-surface weathering).

Pseudomorphs of magnesite and chert after gypsum are evident in some exposures of carbonate, and are also present in massive and brecciated carbonates at Jabiluka, Ranger 1 and Koongarra (Crick & Muir, this volume), but have not been seen in drill cores from carbonates on the western side of the Nanambu Complex (Wallace, in prep.). Evaporites

	LOWER MEMBER				UPPER MEMBER	
	quartzite(8)	schist(5)	carbonaceous schist(6)	carbonate(2)	quartzite(4)	schist(8)
Oxides, wt%						
SiO_2	77.54	60.90	57.28	26.15	76.04	66.08
TiO_2	0.40	.50	.61	.02	.43	.59
Al_2O_3	13.7	17.52	18.17	.41	11.15	15.97
Fe_2O_3	0.90	1.46	1.76	.55	.56	1.24
FeO	1.58	5.57	4.02	-	2.49	4.04
MnO	.05	.06	.05	.04	.04	0.07
MgO	2.71	5.56	4.31	27.60	1.26	2.29
CaO	1.04	.39	3.13	15.97	1.24	.70
Na_2O	1.49	1.45	.86	.04	1.25	1.29
K_2O	2.69	2.95	4.24	.09	2.68	4.17
P_2O_5	.15	.11	.08	.06	.11	.11
loss	2.87	5.18	4.59	28.97	1.49	3.03
Total	99.51	99.65	99.10	99.88	99.74	99.58
Traces, ppm						
F	760[1]	1290[2]	920[2]	n.a.	450	650
Co	10	19	18	n.d.	6	18
Ni	15	44	54	3	25	43
Cu	42	78	48	n.d.	8	82
Zn	51	82	109	6	39	109
Pb	14	7	14	2	12	17
Th	21	15	17	n.d.	12	12
U	5	3	7	n.d.	4	4
Fe/Mg	1.14	1.13	1.68	.03	3.06	2.90

Table 2. Average geochemical analyses of some rocks from the Cahill Formation in 'unmineralised' areas (G. R. Ewers, unpublished data). Apart from the two carbonate samples all samples are drill core obtained from the three drilling traverses shown in figure 4. The number of analyses of each rock type is shown in parentheses. 1-one sample only; 2-two samples only.

may have been deposited in a sabkha environment east of the Nanambu Complex, and carbonates in a deeper marine environment on the western side.

Cahill Formation exposures in the Myra Falls Inlier are predominantly calc-silicate gneiss, and include soft, green massive fibrous actinolitic hornblende gneiss, granular orange quartz-carbonate-actinolitic hornblende gneiss, banded quartz-actinolitic hornblende-diopside gneiss (in places with plagioclase), quartz-microcline-carbonate-actinolitic hornblende gneiss; plagioclase-quartz-actinolitic hornblende-diopside gneiss (in places with garnet), and fibrous to coarsely crystalline white marble (Needham & Stuart-Smith, 1978). These rock types are metamorphosed calcareous feldspathic quartz sandstone, feldspathic quartzose limestone and pure limestone. They are coarsely interlayed with muscovite-feldspar-quartz schist (in places with garnet and amphibole) containing quartz-feldspar pods elongated parallel to the main foliation, which represents interbeds of pelitic sandstone within the calcareous sediments.

The actinolitic hornblende gneiss is almost monomineralic; it represents a metamorphosed impure dolomite.

The granular quartz-carbonate-actinolitic hornblende gneiss is thinly layered with alternating bands enriched in quartz, carbonate, microcline or actinolitic hornblende; a few medium to coarse lenses of quartz occur generally in association with the microcline. The rock is probably a metamorphosed calcareous quartz sandstone.

In the banded quartz-plagioclase-actinolitic hornblende-diopside gneiss, the diopside forms anhedra about 2mm across, and a few poikiloblastic anhedra up to 10mm long with inclusions of quartz and subhedral actinolitic hornblende. In quartz-rich layers other minerals are interstitial. Sphene is an accessory mineral in the banded gneiss, and sericite after plagioclase is common in interstitial areas. Plagioclase is more prominent in actinolitic hornblende-rich areas, where it forms small laths or rare poikilitic anhedra up to 2mm across. Red garnet is present in some bands, which are about 10mm wide. The garnet forms poikiloblastic anhedra up to 5mm across, and contains inclusions of all the other minerals present in the banded gneiss.

Where quartz and K-feldspar occur in higher than usual proportions in the banded gneiss, and plagioclase and diopside are absent, carbonate minerals are commonly prominent constituents of the rock. This quartz-K-feldspar-carbonate-actinolitic hornblende gneiss is typified by fine layering, each layer enriched in one mineral. The actinolitic hornblende layers are accompanied preferentially by clinozoisite. The more mafic bands contain minor biotite and chlorite, and accessory sphene and opaques.

The marble is composed entirely of calcite and tremolite. Tremolite makes up about 20 percent of the rock and is scattered among the polygonal calcite crystals as layers and pods up to 6mm thick, or as individual anhedra and laths in the finer parts. The rock is a metamorphosed sandy dolomite.

Steeply dipping layers of thinly banded magnetite-calcite-biotite-hornblende-diopside-quartz schist have been intersected in drill holes in a layered sequence of mica schist and feldspathic schist near Mount Basedow, and represent an intermediate stage in the transformation of a sediment to a para-amphibolite. Mineralogical banding in this rock is distinct, and probably reflects compositional banding typical of thinly bedded dolomite marls. In contrast, ortho-amphibolite of the Zamu Dolerite, which inter-fingers with rocks of the Cahill Formation, is homogeneous in composition, widespread in occurrence, thicker (up to 600m), and generally lacks distinct mineralogical banding.

Other rock types. The non-carbonaceous and non-carbonate rocks of the lower member are similar to the mica schist, feldspathic quartzite, and quartz schist of the upper member, but amphibole and sphene are accessory minerals in feldspathic quartzite of the lower member only, and reflect the calcareous nature of t he original sediments. The rocks of the lower member are also less quartz-rich than their counterparts in the upper member, which is commonly apparent in outcrop (e.g. at Mount Brockman 3km south of Ranger 1). and which is reflected in generally lower silica values for rocks of the lower member (Table 2).

Upper member

The upper member grades into the lower member, and is composed of interlayered feldspathic quartz schist, feldspathic schist, feldspathic quartzite, and minor mica schist and quartzo-feldspathic gneiss. Minor carbonate lenses occur in places (G. S. Eupene, pers. comm. 1979). Its boundary with the overlying Nourlangie Schist (referred to previously as a metamorphic equivalent of Fisher Creek Siltstone) is marked by an increase in the proportion of mica schist, and in places by a change in magnetic response (Horsfall & Wilkes, 1975). The thickness of the upper member ranges up to 2500m or more near Jabiluka (Needham & Stuart-Smith, 1976).

Exposure of the upper member is confined to low, discontinuous ridges or rubbly rises

of quartzite (some of which also contain schist) best developed south of Mount Cahill where the member is characterised by a smooth white photo-pattern on aerial photographs. The quartzites are similar to those in the Mount Basedow Gneiss and Munmarlary Quartzite, but it can be definitely demonstrated that they occur much higher in the sequence. Other rock types which crop out in this area are clayey quartzite, banded and cross-bedded fine-grained quartzite, quartz-pebble meta-conglomerate, banded hematite rock, and hematite-quartz breccia (Needham & Smart, 1972).

Quartz-feldspar-gneiss

The quartzo-feldspathic rocks of the upper member are composed of quartz + feldspar and muscovite with or without biotite and chlorite; the rocks contain accessory apatite, tourmaline, magnetite and garnet, and rare calcite and clinozoisite. They are medium-grained, foliated, banded, or, rarely, massive rocks. The absence of mineral elongation and shearing generally distinguishes them from Mount Basedow Gneiss and Munmarlary Quartzite rocks. Macroscopic and microscopic banding is common, and probably relates to original compositional layers in the parent sedimentary rock. Phyllosilicates form thin planar folia, along which the rock readily parts, defining its schistosity. The rocks are cut by minor veins of quartz and tourmaline-quartz-alkali feldspar.

Mica and mica-quartz schist

These rocks are typically composed of quartz, biotite and chlorite, muscovite and feldspar, with or without garnet and iron oxides, and are distinguished from the quartzo-feldspathic rocks only by a greater proportion of mica and a lower feldspar content (less than 10 percent). However, the mica schist is intimately associated with quartz-feldspar schist, and commonly forms thin bands in it. Markedly kinked, very micaceous bands in the mica schist contain boudins and fold noses of quartz and feldspar.

Porphyroblasts of almandine and magnetite are common, and magnetite is generally altered to hematite. Lesser staurolite and kyanite commonly occur with almandine and titano-magnetite, and all these four minerals generally form porphyroblasts up to 1cm across. Hematite forms small hexagonal plates parallel to the foliation, and replaces magnetite octahedra. Banding within the staurolite and kyanite schist is intensely kinked and folded.

The upper member is probably a metamorphosed sequence of well-bedded feldspathic arenite and siltstone, minor conglomerate, and thin bands of pelite. The high proportion of Fe and Al-bearing silicates in the schists suggests that they represent metamorphosed iron-rich pelites.

Nourlangie Schist

The Nourlangie Schist crops out mostly in the footslope of the Arnhem Land escarpment, and occurs as deeply weathered, micaceous rubbly rises on the lowlands. It is a monotonous sequence of quartz-mica and mica-quartz schist, commonly containing one or more of the following minerals: garnet, feldspar, amphibole, magnetite, kyanite, and staurolite. Minor quartzite and feldspathic quartz schist are present in the formation. Minerals other than quartz and mica are rarely apparent in outcrop. The convergence of, and discontinuity between, two sets of trends seen on air-photos coincide with the Cahill Formation/Nourlangie Schist boundary established by drilling east of Koongarra, and indicate an unconformable relationship in this area between the two formations (Needham & Stuart-Smith, 1976). Needham *et al.* (this volume) suggest that the Nourlangie Schist is equivalent to the Wildman Siltstone of the Mount Partridge Group west of the Alligator Rivers Uranium Field. The Nourlangie Schist includes the entire sequence of pelitic schist east of Mount Partridge Range and the Nanambu Complex stratigraphically above the Cahill Formation, except for pelitic schist in the Cannon Hill area (Fig. 2) within the Koolpin? Formation. With further drilling, the Nourlangie Schist north of Cannon Hill may

prove to be stratigraphically above the Koolpin? Formation and equivalent to the Finniss River Group west of the Alligator Rivers Uranium Field.

Koolpin Formation?

Siliceous and ferruginous banded rocks form discontinous strike ridges 20km north of Jabiluka (Swingler, 1977). They lie in a large syncline east of the Nanambu Complex and may be 2-5km stratigraphically higher than the base of the Cahill Formation. In their resemblance to banded ironstone and their carbon content, they are similar to Koolpin Formation of South Alligator Valley area 100km to the southeast. The Koolpin Formation in that area is about 2km higher in the stratigraphic sequence than the Masson Formation, (Stuart-Smith *et al.*, in prep.), which correlates with the Cahill Formation.

Swingler (1977) described the exposures north of Jabiluka as thinly banded mica quartz schist and quartzite, with some thicker (0.1-0.2m) quartzite, magnetite quartzite, and amphibolite bands. Near the base there are bands of graphitic and porphyroblastic schist, and amphibolite. The schist contains bands and lenses 4-10mm wide of medium to coarse mosaic quartz interlayered with biotite-amphibolite-feldspar schist ± quartz ± magnetite. The quartzite includes a black type containing thin layers of magnetite, amphibole (?actinolite) and chloritised ?biotite. The graphitic rocks contain thin parallel bands of microcrystalline quartz with included and intergranular graphite, alternating with thin laminae and lenses of limonite, probably after feldspar. The porphyroblast rock is a banded and lensoid quartz-biotite schist with rare, altered porphyroblasts about 4mm across; their polygonal outlines suggest they were garnet. They are more abundant in graphite-rich layers.

Fisher Creek Siltstone?

Mica-quartz schist which crops out along the East Alligator River floodplain north of Jabiluka occupies the axis of the Oenpelli Syncline (Fig. 5) between the Nanambu and Nimbuwah Complexes. On figure 2 it is shown as Nourlangie Schist as it is lithologically similar, but because of its possible stratigraphic position above the nearby Koolpin Formation? rocks, it may be a correlative of the Finniss River Group siltstone, which overlies the Koolpin Formation in the South Alligator Valley area.

TRANSITIONAL IGNEOUS ACTIVITY AND METAMORPHISM

Near the close of Lower Proterozoic sedimentation a period of igneous activity began which was related to the regional metamorphism and deformation, and which affected the whole of the Pine Creek Geosyncline at about 1800 Ma. The event was strongest in the Alligator Rivers Uranium Field; its climax was marked by widespread migmatitisation of Lower Proterozoic rocks in the northeast of the Alligator Rivers region to form the Nimbuwah Complex. During the period of igneous activity and metamorphism (1870-1690 Ma), pre- and post-orogenic dolerite and synorogenic granite were intruded, and post-orogenic felsic volcanics extruded. Deposition of Carpentarian (Middle Proterozoic) platform cover marked the end of this transitional period and the beginning of an age of stability which has persisted with little disturbance to the present day.

Zamu Dolerite

The Zamu Dolerite is a widespread pre-orogenic continental tholeiitic suite in the Pine Creek Geosyncline (Ferguson & Needham, 1978). The dolerite is metamorphosed to foliated, dark green to black, fine to medium-grained amphibolite in the Alligator Rivers region, and intrudes the Nanambu Complex, Cahill Formation, Nourlangie Schist and Nimbuwah Complex as sill-like bodies commonly 1-10m thick, but up to 70m thick in the Myra Falls Inlier; two sills of amphibolite 290m and 15m thick underlie the Jabiluka One orebody and are interlayered with chloritic sericitic schist. Where more than 10m thick the sills are medium-grained towards their centres, and in places relict igneous textures are

preserved. Hornblende makes up between 50 and 85 percent, and plagioclase and quartz together form up to 45 percent of the amphibolite; minor interstitial K-feldspar may be present. Chlorite alteration is common, and biotite, usually an accessory, may be a major phase in areas of intense chloritisation, for example near the uranium orebodies. Biotite is always partly altered to chlorite, and is usually intermixed with amphibole and parallel to foliation; in places it is at a considerable angle to the foliation. Some of the chlorite forms veins less than 4m wide, with opaques and muscovite ± epidote ± prehnite. Sphene, apatite, carbonate, ilmenite, chalcopyrite and pyrite are common accessories in the amphibolite.

Nimbuwah Complex

East of the East Alligator River, the Lower Proterozoic metasediments grade into differentiated schist and gneiss in the outer parts of the Nimbuwah Complex, which was formed by metamorphism and progressive migmatitisation of Lower Proterozoic rocks at about 1800 Ma. The Complex contains four 'zones', the *Transitional Zone, Lit-par-lit Gneiss Zone, Migmatite Zone* and *Granitoid Core* (see Fig. 2; Needham *et al.*, 1975a). The outer Transitional and Lit-par-lit Gneiss Zones contai n resisters representing the Kakadu Group, Cahill Formation and Zamu Dolerite which confirm that the zones formed by metamorphic differentiation of Lower Proterozoic sediments. Cahill Formation rocks around the Nanambu Complex have in places undergone partial differentiation as well; fine leucosome bands and knots are developed, but overall the parent stratigraphy is preserved.

The inner Migmatite Zone and Granitoid Core consist of granitoid, mainly granodioritic, rocks and lack resisters of Lower Proterozoic metasediments common in the outer zones of the Complex. Geochronological studies (Page *et al.*, this volume) indicate that these granitoids crystallised from a melt at about 1870 Ma, and were later subjected to the 1800 Ma metamorphism when they underwent partial anatexis to form metatexite and diatexite. As Lower Proterozoic sedimentation is assumed to have ceased at the time of the earlier event, 1870 Ma is a minimum age for sediment deposition in the Pine Creek Geosyncline.

The boundary between the Nimbuwah Complex and the Lower Proterozoic metasediments is defined by the appearance of metamorphic feldspar as bands of leucosome. In the *Transitional Zone* pegmatoid leucosome is only sporadically developed in the quartz-feldspar-biotite schist, garnet-quartz-feldspar schist, quartz-mica schist, quartz-chlorite schist, leucogneiss, banded biotite gneiss, feldspathic quartzite and micaceous quartzite. The rocks become more gneissic to the east.

The *Lit-par-lit Gneiss Zone* is characterised by the development of subparallel leucocratic layers in gneisses which represent an early stage in the formation of migmatite by metamorphic differentiation of the parent rock into leucosome and palaeosome. The leucosome consists almost entirely of quartz and feldspar, and the palaeosome consists of biotite with some feldspar and quartz and minor garnet and opaque minerals. Finely banded biotite gneiss represents metamorphic differentiation on a microscopic scale, whereas lit-par-lit gneiss is formed by differentiation on a macroscopic scale. The incipient development of quartz-feldspar augen in feldspathic schist and banded biotite gneiss reflects a more advanced stage of metamorphic differentiation.

Essential minerals in the Lit-par-lit Gneiss Zone are quartz, potash feldspar (generally microcline), plagioclase, and biotite. Plagioclase and potash feldspar are generally equally abundant. Plagioclase ranges between albite and andesine, and is relatively resistant to alteration. The potash feldspar is mostly sericitised, and may be completely replaced. Mafic minerals are mainly biotite; hornblende is present in places. Muscovite, where present, is intimately associated with biotite as interlocking flakes, and rarely exceeds biotite in abundance. Pink garnet porphyroblasts are a common minor accessory. Other accessory minerals are apatite, sphene, iron oxides, and zircon.

The schists of the Lit-par-lit Gneiss Zone are mineralogically similar to the gneisses, apart from the predominance of biotite (and, in places, muscovite) over quartz and feldspar. Porphyroblastic garnet is the most common accessory mineral.

The *Migmatite Zone* contains granitoid rocks, which are mainly granodiorite and consist of quartz, plagioclase, microcline, biotite and hornblende, and minor clinopyroxene (Needham *et al.*, 1975a). Accessory minerals are magnetite, muscovite, apatite, tourmaline, sphene and zircon. Biotite is commonly altered to chlorite, plagioclase to chlorite and sericite, and potash feldspar to sericite. The rocks are mostly well foliated and are segregated into lighter and darker bands, which contain the same mineral assemblages but with different mineral proportions. In places, clots of biotite and hornblende form very dark lenses and schlieren, up to 50cm by 5cm. Needham *et al.*, (1975a) applied the terms 'leucosome', 'palaeosome' and 'melanosome' to these bands, and described a wide variety of interpenetration fabrics which are typical of migmatic terranes (Mehnert, 1968). These rocks are 'metatexites' — rocks which have undergone partial anatexis. Veins of coarse leucocratic pegmatite cut across the foliation of these migmatitic rocks and again have the same mineral assemblage. Augen gneiss is confined to outer parts of the zone, particularly in an area 30km east of Nabarlek. Thirty-five kilometres south of Nabarlek, in the 'Beatrice Inlier', and 25km southeast of Nabarlek in the 'Caramal East Inlier' (Fig. 20, the migmatitic rocks are tonalitic and commonly contain garnet; in places they contain coexisting orthopyroxene and clinopyroxene (Ferguson, this volume) and are charnockites.

Near the inner margin of the zone in areas of schlieren and nebulitic migmatite, patches of non-foliated, coarsely porphyritic granodiorite indicate transition of the metatexites into 'diatexite' — that is, rocks which have undergone high-grade anatexis, and which constitute the Granitoid Core of the Nimbuwah Complex.

Porphyritic granodiorite crops out mainly at the margin of the *Granitoid Core*, and is distinguished by the large phenocrysts — up to 5cm by 3cm. The mineral assemblages of the rocks of the Granitoid Core are similar to that of the Migmatite Zone rocks, but in the equigranular granitoids nearer the centre of the Granitoid Core hornblende is rare and biotite is less prominent. These rocks are generally white to pink, massive, homogeneous and poorly foliated. In places discrete types are distinguished by higher biotite content, marked foliation, grain size, or contained graphite. One discrete type follows a major photolineament, suggesting it is a younger body whose emplacement was tectonically controlled.

Regional metamorphism and deformation

The Lower Proterozoic rocks of the Alligator Rivers region were metamorphosed in the staurolite-almandine subfacies of the amphibolite facies and underwent polyphase deformation during the 1800 Ma orogenic event (Smart *et al.*, 1975; Needham & Stuart-Smith, 1976). Almandine is found in most rock types, but is more abundant in mica schist. Kyanite is found only with staurolite, indicating that the metamorphic grade does not reach the kyanite-almandine subfacies (Winkler, 1967).

The western edge of the Alligator Rivers region coincides roughly with the greenschist/amphibolite facies boundary; the biotite isograd lies along the South Alligator River and on the western side of the Mount Partridge Range (Needham *et al.*, this volume). The metamorphic grade increases subtly towards the northeast (Smart *et al.*, 1975); rocks between the South and East Alligator Rivers belong to the 'high-temperature end of medium-grade metamorphism' and rocks east of the East Alligator River to the 'low-temperature end of high-grade metamorphism' (Ferguson & Needham, 1978).

Later retrograde metamorphism at about 1610 Ma (Page *et al.*, this volume) has resulted in chloritisation of ferro-magnesian minerals and sericitisation of feldspars. Garnet, biotite, and amphibole commonly show complete or partial alteration to chlorite; chloritised

haloes surrounding small quartz veins are common in the Lower Proterozoic metasediments. This alteration is most pervasive in the lower member of the Cahill Formation, where rocks are relatively enriched in Mg to those of the upper member (Table 2), and chlorite had replaced feldspar in feldspathic quartzite, to give rise to quartz-chlorite schist. Chloritisation is particularly intense in some sheared and brecciated schists of the lower member near the contact with the Nanambu Complex, suggesting that chloritisation followed cataclastic deformation. However, the association of chlorite with the sheared contact between the Nanambu Complex and the Cahill Formation and with the unconformity between the Cahill Formation and the Nourlangie Schist suggests that stratigraphic and structural breaks are the main loci of chloritisation, providing channelways for Fe and Mg-rich fluids.

Hematitisation is widespread, and is associated with chlorite alteration, particularly in areas of uranium mineralisation. Hematite is a common vein-filling mineral, also replaces ferromagnesian minerals, and forms pseudomorphs after magnetite.

Owing to poor exposure, structural interpretation is based almost entirely on small-scale structures in drill core, aerial photo trends, and on regional distribution of units. The style and orientation of folds and faults in the Precambrian rocks have been mainly governed by basement configuration (the Archaean rocks of the Nanambu Complex) and development of a large migmatite complex (the Nimbuwah Complex) in the northeast of the Alligator Rivers Uranium Field. The major structural features of the region are shown in figure 5.

Local unconformity between the Cahill Formation and Nourlangie Schist suggests that minor folding took place at times during Lower Proterozoic sedimentation. The main deformation took place after the close of sedimentation, when diapiric growth of the Nimbuwah Complex in the northeast of the region caused marginal overfolding and intense isoclinal folding of the sedimentary pile, which was accompanied by the 1800 Ma regional metamorphism.

During this period of deformation, a block of Archaean granitic material was reactivated and partly migmatitised; leucocratic gneissic material, probably derived from the Kakadu Group, was accreted to it to form the Nanambu Complex (Page *et al.*, this volume). The Cahill Formation was draped around it to form a complex refolded synclinal structure known as the Woolwonga Fold. The isoclinal fold axes were similarly controlled, being concentrically arranged around the Archaean block.

A well developed foliation produced by recrystallisation and transposition of original bedding formed parallel to the axial plane of these folds, and gave rise to the dominant regional schistosity. Relict isoclinal fold noses are preserved in the more competent quartz-rich bands in mica schist. Almandine and magnetite porphyroblasts show deformed, rotational, and crosscutting textures, indicating their development before, during, and after the formation of the schistosity. Complex small-scale crossfolding of the foliation with axial-plane crenulation cleavage developed in the less competent rock types, and may have been related to further movements of the migmatite and Archaean granite masses, and to the intrusion of anatectic granites. The grade of metamorphism probably reached its peak after the formation of the crenulation cleavage as unstrained mica and idiomorphic kyanite and staurolite porphyroblasts cut across the cleavage. Biotite porphyroblasts which grew at this stage yield K-Ar isotopic ages of about 1800 Ma which dates the climax of late Lower Proterozoic tectonism in the Alligator Rivers region.

Faults in the Lower Proterozoic rocks are usually long and straight, and have vertical or dip-slip displacements, which in many places developed parallel to the regional northwest-trending schistosity. They are in the main quartz or quartz-breccia filled, and the adjacent country rocks are sheared. The Jim Jim Fault Zone is a 10km-wide zone of intense shearing

and step-faulting, bounded on the northwest by the Jim Jim Fault. Other major faults in the area may be similarly complex.

Most of the faults were initiated during the 1800 Ma deformation, but displacement of Carpentarian (Middle Proterozoic), Mesozoic and younger rocks on some indicate reactivation at later dates. Several of the major faults show displacements up to 70m of Carpentarian (Middle Proterozoic) strata, and the Koongarra Fault, the only major fault in the area which does not trend northwest or west, has a displacement of at least 200m and probably as much as 600m (Foy & Pedersen, 1975). The rectilinear joint pattern in the Kombolgie Formation probably developed during slight tilting or downwarping of the McArthur Basin succession to the southeast.

The Kombolgie Formation and Nanambu Complex are both closely fault-bounded, although the contacts are rarely exposed and the faulted relationship is generally only evident in drillcore. The Arnhem Land Escarpment is a fault scarp modified by different amounts of scarp retreat.

Synorogenic granites

The *Nabarlek, Tin Camp and Jim Jim Granites* post-date the 1800 Ma orogenic event; they yield Rb-Sr ages of 1760-1780 Ma (Page *et al.*, this volume) and are not foliated. They are even-grained, mainly coarse biotite granites which are generally very altered and in many places are cut by north-trending quartz-breccia reefs. Typical composition is 45-50 percent orthoclase, 30-35 percent quartz, 10-15 percent plagioclase, and 5 percent biotite with rare opaques. The orthoclase is commonly sericitised, most of the plagioclase is saussuritised, and biotite is altered to chlorite. The Tin Camp and Nabarlek Granites are in places composed only of quartz and clayey alteration products. The granite margins appear to be fault-controlled and there is no evidence of contact metamorphism in the country rock. Gravity data suggest that the 'Caramal East Inlier' and 'Beatrice Inlier' exposures of the Tin Camp Granite are connected at depth, and that the Jim Jim Granite extends up to 100km eastwards under the Carpentarian (Middle Proterozoic) cover rocks (Tucker *et al.*, this volume).

Oenpelli Dolerite

Lopoliths of post-orogenic continental tholeiitic Oenpelli Dolerite underlie much of the Alligator Rivers region. The bodies are at least 250m thick in places, and were emplaced after the orogenic event about 1688 Ma ago (Page *et al.*, this volume). The intrusions consist of symmetrically differentiated layers of olivine dolerite, minor felsic differentiates, and rare cross-cutting gabbroic pegmatites (Stuart-Smith & Ferguson, 1978). Within the thicker sheets minor rhythmic layering is found in olivine dolerite. Cross-cutting contacts are evident with the country rocks, which in places are contact metamorphosed to cordierite hornfels, or have undergone Fe-Mg metasomatism. The dolerite was emplaced at depths between 1 and 2 km (Stuart-Smith & Ferguson, 1978), indicating substantial erosion before deposition of Carpentarian (Middle Proterozoic) cover rocks.

Edith River Volcanics

Tuffaceous sediments and felsic flow rocks, occurring as rubble in valleys at Mount Basedow and below the Kombolgie Formation 12 km east of Ranger 1 and 16 km ESE of Jabiluka, are probably flow remnants and correlatives of the Edith River Volcanics. The volcanics unconformly overlie Lower Proterozoic strata mainly in the South Alligator Valley Uranium Field (Fig. 1), where they have been described by Stewart (1965).

The volcanics in the Alligator Rivers Uranium Field are generally pink or grey; they contain phenocrysts of resorbed quartz and highly sericitised and chloritised sanidine crystals up to 5mm in diameter in a groundmass of quartz and feldspar and minor epidote. Chlorite commonly contains magnetite, and the rock displays blotchy hematite staining.

Of the descriptions given by Stewart (1965) of the Edith River Volcanics, the Pul Pul

Rhyolite bears closest resemblance to the volcanics in the Alligator Rivers region, which are tentatively regarded as porphyritic alkali rhyolites. The possibility of a pyroclastic origin cannot be excluded.

CARPENTARIAN (MIDDLE PROTEROZOIC) AND YOUNGER COVER ROCKS

Essentially flat-lying Carpentarian (Middle Proterozoic) to Mesozoic sediments cover most of the older rocks in the Alligator Rivers region, and unconsolidated Cainozoic sand and soil are widespread over the lowlands.

Katherine River Group

Sandstone and volcanics of this formation are the lowest unit in the Katherine River Group, which is the lowest part of the Carpentarian (Middle Proterozoic) sequence in northern Australia. The *Edith River Volcanics*, which Walpole *et al.*, (1968) considered were extruded through vents in the South Alligator Valley Uranium Field (Fig. 1) were included in the Katherine River Group by these workers. The volcanics however predate (1760 Ma, Leggo *in* Walpole *et al.*, 1968) the Oenpelli Dolerite on which the *Kombolgie Formation* rests with unconformity; the Edith River Volcanics and Kombolgie Formation are thus separated by a period during which the Oenpelli Dolerite was emplaced and subsequently exposed by erosion, and cannot be considered as members of the same group.

The *Kombolgie Formation* forms the Arnhem Land Plateau, mainly in the southeast of the region, and a number of outliers in the lowlands. The edges of the plateau and outliers are generally marked by sheer cliffs up to 200m high. Lower Proterozoic rocks are commonly exposed in the footslope to the sandstone cliffs.

The formation comprises upper and lower sandstone units separated by basalt of the Nungbalgarri Volcanic Member. In places the upper sandstone unit contains a thin basaltic member, the Gilruth Volcanic Member (Needham & Stuart-Smith, 1978).

The sandstone contains mainly medium to coarse-grained, moderately well sorted, sub-rounded to sub-angular quartz grains in a matrix or amorphous fibrous clay or iron oxide minerals. Friable varieties are devoid of a matrix and quartzitic varieties may have either interlocking grains or a fine quartz cement.

Other rock types are fine ferruginous siltstone, and conglomerate containing well rounded quartz cobbles up to 20cm. Conglomerate beds range from 20cm to over 30m thick and are more common below the Nungbalgarri Volcanic Member. Basal conglomerates at the base of the formation generally comprise up to 80 percent pebbles of subangular quartz and feldspathic quartzite, up to 20 percent blade-shaped clasts of Lower Proterozoic schist, rodded quartzite, and psammitic shale, and up to 2 percent highly angular chunks of vein quartz. Distribution of the conglomerates is sporadic, and may have been controlled by relief of the pre-Kombolgie surface; thus, basal conglomerate is missing at Nourlangie Rock, a feature 6km west of Koongarra which probably formed a small hill prior to Kombolgie sedimentation.

Accessory minerals in the sandstone appear to be locally related to the basement rock. For example, biotite, pyroxene, and chlorite are present as accessory minerals in sandstone overlying a hill of granite 12km north of Koongarra.

Sandstone above the volcanic member is generally more homogenous, and conglomerate beds are less common. The sandstone throughout the formation is commonly cross-bedded and ripple marked. The cross-bedding ranges from medium (5cm-2m) to large-scale (2m-8m) and is of the 'alpha' type suggesting a shallow freshwater origin (Allen, 1963). Measurements of directional sedimentary structures generally fall within the southern quadrant, suggesting a prevailing current of deposition from the north.

The Lowlands are in part an exhumed pre-Kombolgie Formation land surface, and display a morphology similar to the unconformity at the base of the Kombolgie Formation,

with local relief up to 20m and isolated hills up to 120m. Local drape structures over partly exhumed mafic intrusive bodies and small hills of foliated granites (e.g. 12km north of Koongarra) are depositional in origin, although the low dips in the main scarp probably resulted from an overall tilt to the southeast. Basinal dips in the outliers have been modified by tectonism and faulting, and range up to 70° in places. Minor irregularities are represented by pebble-filled valleys at the base of the Kombolgie Formation.

The *Nungbalgarri Volcanic Member* consists mainly of a series of flows, which range in composition from basalt through trachybasalt and dacite to rhyodacite (Needham & Stuart-Smith, 1978). Cherty rhyolite and ignimbrite overlie the flows in places. The more felsic rock types occur nearer the top of the member. Columnar jointing is common and pillow lavas are evident in places at the bottom of the unit. Giant load casts developed at the base also indicate subaqueous extrusion (Needham, 1978). The member is thickest 30km east of Ranger 1 and thins towards Deaf Adder Gorge (Fig. 2). It pinches out in places south of Deaf Adder Gorge, where its stratigraphic position is marked by a local unconformity between the upper and lower sandstone units, and an intraformational conglomerate. Basalt from the member has been dated at about 1648 Ma (Page *et al.*, this volume).

The *Gilruth Volcanic Member* contains tuffaceous siltstone, banded quartz-jasper rock, and amygdaloidal basalt. These rock types are apparent only as rubble amongst nodular laterite scree on a prominent bench commonly marking the base of the member. Sandstone blocks from higher in the formation have collapsed over the volcanic member and concealed the volcanics.

Minor Intrusive Rocks

Phonolite dykes are concentrated in two areas in the Alligator Rivers region — the Maningkorrirr Phonolite which intrudes the Nimbuwah Complex east of Jungle Creek 35km NE of Nabarlek, and the Mudginberri Phonolite which intrudes the Nanambu Complex between Ranger 1 and Jabiluka. Rb-Sr data on these rocks yield an age of 1316 Ma (Page *et al.*, this volume). They form scattered steeply dipping dykes less than 10m thick and more usually less than 1m thick, and can be traced for distances up to 1km. They are typically dark grey-green, fine to medium-grained and porphyritic. The phenocrysts are alkali feldspar, nepheline, Na-pyroxene and brown mica set in a groundmass of the same minerals ± natrolite ± Na-amphibole (Needham *et al.*, 1979).

Minor dykes and small bodies of quartz dolerite are scattered throughout the region. One body near the Goomadeer River, the Wurugoij Dolerite, displays intrusive contacts with the Kombolgie Formation and has a K-Ar age of 1200 Ma (Page *et al.*, this volume). Long, narrow mainly northeast or east-trending magnetic anomalies over joints in the Kombolgie Formation may indicate concealed mafic igneous bodies. A quartz dolerite intruded along a lineament which trends east through the Ranger 1 deposit has a K-Ar age of 1370 Ma (Page *et al.*, this volume). Similar dyke rocks are aligned parallel to the axial plane of a major fold in Cahill Formation rocks east of Mount Partridge Range.

Mesozoic Sediments

Poorly sorted quartzose sandstone, mudstone, siltstone and conglomerate, fossiliferous in places, form low tablelands and mesas, and underlie Cainozoic sand plains, in the north. The Cretaceous rocks consist of two interfingering members of the *Bathurst Island Formation* (Hughes, 1978). The *Marligur Member* contains poorly consolidated, well sorted fine to very coarse quartzose sandstone with rounded grains, and forms lenses within the Darwin Member up to 20m thick, thinning to the west (Needham, 1976; Hughes, 1978). The *Darwin Member* consists of fine argillaceous sandstone, white leached siltstone and micaceous mudstone, which thickens westwards to about 35m. It is the upper part of the sequence previously referred to (e.g. by Walpole *et al.*, 1968) as the Mullaman Beds. The Marligur Member was deposited in a paralic environment, and contains numerous

gastropods, crinoid ossicles, worm borings, and a heteromorphic ammonite ?Baculites sp. (Hughes, 1978). Spores in cuttings are of ?late Neocomian to Aptian age (Burger *in* Hughes, 1978). The Darwin Member was deposited in epicontinental conditions and contains molluscan fauna, described by Skwarko (1966), and belemnites, brachiopods, echinoids, bryozoans, corals and arenaceous foraminifers.

Petrel Formation

Low mesas of white and purple claystone, and medium to coarse-grained friable sandstone are scattered over the Arnhem Land Plateau. These rocks are the lower part of the sequence previously referred to as the Mullaman Beds, but which is now known to disconformably underlie the Darwin and Marligur Members of the Bathurst Island Formation (Hughes, 1978). The Petrel Formation rocks are continental, and are known from data outside the Alligator Rivers Region to be Early Jurassic to Neocomian in age.

Cainozoic sediments

Cainozoic sediments form a veneer over the plains between the Arnhem Land escarpment and the coast; talus slopes and colluvial sand lie on, and adjacent to, the Arnhem Land Plateau. Cainozoic deposits have been divided into laterite, late Tertiary sand, talus, and Quaternary continental and marine sediments.

Laterite is commonly developed on low-lying exposures of pre-Cainozoic rocks, apart from the Kombolgie Formation. The laterites are generally either truncated remnants of the standard laterite profile described by Whitehouse (1940) or are detrital.

Coarse unconsolidated clayey quartz sand of late Tertiary age forms the Koolpinyah Surface of Story *et al.*, 1969. It was probably deposited as a fan and derived mainly from Mesozoic and Carpentarian (Middle Proterozoic) units. Cainozoic sand on the Arnhem Land Plateau has been deposited continuously since the Early Tertiary. Talus slopes are developed against the Arnhem Land escarpment, where the base of the Kombolgie Formation is exposed. Scree mostly conceals the unconformity below the Kombolgie Formation, but quite commonly small cliff-like exposures are found at the top of the talus slope, below an overhang formed by preferential erosion of the Lower Proterozoic rocks. The talus is composed mostly of large blocks of Kombolgie Formation sandstone up to 20m across but rounded to blade shaped pebbles of the underlying rocks are commonly present.

Quaternary continental sediments include alluvial silt, sand, and clay deposited along rivers and creeks, and in abandoned river channels; silty levee deposits along the banks of major rivers; and black humic soils deposited in poorly drained depressions within drainage systems.

Quaternary marine sediments include coastal deposits of silt and clay, clay pans, and beach ridges. Beach ridges have developed parallel to the present coast, and less commonly at the edge of the inner margin of the coastal plain adjacent to the higher-level Upper Tertiary sand deposits.

ECONOMIC GEOLOGY

Uranium

In the Alligator Rivers Uranium Field all major and most minor uranium mineralisation is stratabound in the Cahill Formation, particularly in the lower member, where carbonaceous and carbonate rocks are common. In fact throughout the Pine Creek Geosyncline uranium is almost invariably found in sequences containing carbonaceous and carbonate rocks. This association indicates that carbon and/or carbonate rocks probably played an important role in the formation of the uranium deposits. Carbon may have fixed uranium in reducing conditions from surface and groundwaters, before or after lithification. Uranium may have been concentrated peripherally to, or within open fractures in the carbonate rocks by adsorption onto clays (Ferguson *et al.*, this volume) or during

dewatering. Alternatively, Crick & Muir (this volume) suggest that much of the carbonate has replaced evaporites, and that brines released during dewatering, or Mg- and carbonate-rich ground-waters which replaced the evaporites after the 1800 Ma metamorphism, were important metasomatising and ore-forming fluids.

The size and grade of the uranium deposits suggest that ore-forming processes may have taken place over a long time; this suggestion is supported by uranium dates ranging from 1700 to 900 Ma (Hills & Richards, 1976).

Each of the major deposits in the Cahill Formation occurs in zones of brecciation, faulting, and ferromagnesian alteration. Page *et al.* (this volume) suggest the alteration took place about 1610 Ma ago; chloritisation of Kombolgie Formation sandstone in the Ranger 1 (Eupene *et al.*, 1975) and Jabiluka (Binns *et al.*, this volume) deposits indicates deposition of the sandstone before this date. Mechanisms suggested to produce the brecciation include carbonate solution and collapse (Eupene *et al.*, 1975), and evaporite diapirism (Crick & Muir, this volume).

Details of ore genesis are still far from resolved. The essentially stratabound nature of the uranium deposits, and their close relationship with carbonaceous and carbonate rocks suggest that the orebodies have formed partly syngenetically. Epigenetic processes, probably associated with chloritisation, appear essential in the development of such high-grade deposits, and stratigraphic and structural breaks, which are commonly chloritised (Needham & Stuart-Smith, 1976), could have provided pathways for mineralising and metasomatising fluids. However, there has been no significant movement of uranium away from the lower part of the Cahill Formation, underlining the essentially stratabound nature of the mineralisation. Any ore genesis model must explain the apparently autochthonous association of the chlorite alteration with the ore zone breccias and adjacent rocks.

Gold

Gold is the only metal besides uranium known to occur in economically viable quantity, and then it occurs only in association with uranium in the Jabiluka Two deposit (minor gold occurs in association with arsenopyrite but no uranium in magnetite schist at the Ranger 43 prospect 20.5km NNE of Munmarlary homestead, G.S. Eupene, pers. comm. 1979). All known gold deposits in the South Alligator Valley Uranium Field are associated with uranium, and there appears to be little potential for direct exploration for gold in the Alligator Rivers Uranium Field. Minor hydrothermal gold at the Yemelba and Mundogie mines in the Mount Partridge Range, in the southwest of the area, is associated with a gravity low, which may indicate a concealed granite body.

Other metals

Minor lead and zinc mineralisation occurs in quartz breccia-filled faults in the Nanambu Complex west of Mount Cahill, and copper accompanies uranium in some as yet insufficiently tested areas of mineralisation. Minor hydrothermal and alluvial tin in the Mount Partridge Range and Myra Falls Inlier is associated with concealed or exposed Carpentarian (Middle Proterozoic) granite. In the past, attention has been given to a minor supergene concentration of iron in a quartz-hematite rock developed over Nourlangie schist, 6km NNE of Jim Jim Falls.

ACKNOWLEDGEMENT

This paper is published with the permission of the Director, Bureau of Mineral Resources, Geology and Geophysics, Canberra, Australia. G. S. Eupene and D. S. Trail assisted extensively in the final preparation of the manuscript. R. Balde and G. J. McArthur also reviewed the manuscript.

REFERENCES

Allen, J.R.L., 1963: The classification of cross-stratified units with notes on their origin. *Sedimentology, 2*, 93-114.

Binns, R.A., McAndrew, J. & Sun, S-S., this volume: Origin of uranium mineralisation at Jabiluka. *Proceedings of the International Uranium Symposium on the Pine Creek Geosyncline.*

BMR, 1967: Geological map of the Katherine-Darwin region, scale 1:500 000.

BMR, 1977: Cahill 1:100 000 scale geological map, preliminary edition, 5472.

BMR, 1979. Mundogie 1:100 000 scale geological map, preliminary edition, 5371.

Condon, M.A. & Walpole, B.P., 1955: Sedimentary environment as a control of uranium mineralisation in the Katherine-Darwin region, N.T. *Rep. Bur. Miner. Resour. Geol. Geophys. Aust., 24.*

Crick, I.H. & Muir, M.D., this volume: Evaporites and uranium mineralisation in the Pine Creek Geosyncline. *Proceedings of the International Uranium Symposium on the Pine Creek Geosyncline.*

Dunn, P.R., 1962: Alligator River, N.T. — 1:250 000 Geological Series. *Explan. Notes Bur. Miner. Resour. Geol. Geophys. Aust. D/53-1.*

Eupene, G.S., Fee, P.H. & Colville. R.G., 1975: Ranger 1 uranium deposits. *in* (ed. C.L. Knight) *Economic Geology of Australia and Papua New Guinea. Australias. Inst. Min. Metall. Monograph Series No. 5, 1. Metals,* 308-317.

Ferguson, John, this volume: Metamorphism in the Pine Creek Geosyncline and its bearing on stratigraphic correlations. *Proceedings of the International Uranium Symposium on the Pine Creek Geosyncline.*

Ferguson, John & Needham, R.S., 1978: The Zamu Dolerite: A Lower Proterozoic pre-orogenic continental tholeiitic suite from the Northern Territory, Australia. *J. geol. Soc. Aust., 25(6), 309-322.*

Foy, M.F. & Pedersen, C.P., 1975: Koongarra uranium deposit. *in* (ed. C.L. Knight) *Economic Geology of Australia and Papua New Guinea. Australas. Inst. Min. Metall. Monograph Series No. 5, 1. Metals,* 317-321.

Hills, J H. & Richards, J.R., 1976: Pitchblende and galena ages in the Alligator Rivers region, N.T., Australia. *Miner. Deposita, 11,* 133-154.

Horsfall, K.R. & Wilkes, P.G., 1975: Aeromagnetic and radiometric survey of Cobourg Peninsula, Alligator River and Mount Evelyn (part) 1:250 000 sheet areas, Northern Territory 1971-1972. *Rec. Bur. Miner. Resour. Geol. Geophys. Aust., 1975/89* (unpubl.)

Hughes, R.J., 1978: The geology and mineral occurrences of Bathurst Island, Melville Island, and Cobourg Peninsula, Northern Territory. *Bull. Bur. Miner. Resour. Geol. Geophys. Aust., 177.*

Mehnert, K.R., 1968: *Migmatites and the origin of granitic rocks.* Amsterdam, Elsevier.

Needham, R.S., 1976: BMR Rotary-percussion and auger drilling in the Cahill and East Alligator 1:100 000 Sheet areas, Alligator Rivers region, 1972-3. *Rec. Bur. Miner. Resour. Geol. Geophys. Aust., 1976/43* (unpubl.)

Needham, R.S., 1978: Giant-scale hydroplastic deformation structures formed by the loading of basalt onto water-saturated sand, Middle Proterozoic, Northern Territory, Australia. *Sedimentology, 25,* 285-295.

Needham, R.S., (in prep, a): Cahill 1:100 000 Sheet area. *Bur. Miner. Resour. Geol. Geophys. Aust. Map Commentary 5472.*

Needham, R.S., (in prep, b): East Alligator 1:100 000 Sheet area. *Bur. Miner. Resour. Geol. Geophys. Aust. Map Commentary 5473.*

Needham, R.S., Crick, I.H. & Stuart-Smith, P.G., this volume: Regional geology of the Pine Creek Geosyncline. *Proceedings of the International Uranium Symposium on the Pine Creek Geosyncline.*

Needham, R.S., Crick, I.H., Stuart-Smith, P.G. & Roarty, M.J., 1978: Mundogie 1:100 000 Sheet area data record. *Rec. Bur. Miner. Resour. Geol. Geophys. Aust., 1978/103* (unpubl.).

Needham, R.S., Ferguson, John & Prichard, C.E., 1979: *Excursion guide for the International Uranium Symposium on the Pine Creek Geosyncline, Australia.*

Needham, R.S. & Smart, P.G., 1972: Progress report, Alligator River Party N.T., 1971. *Rec. Bur. Miner. Resour. Geol. Geophys. Aust, 1972/1* (unpubl.).

Needham, R.S., Smart, P.G. & Watchman, A.L., 1975a: Progress report, Alligator River Party N.T., 1972 (Oenpelli Region). *Rec. Bur. Miner. Resour. Geol. Geophys. Aust., 1975/39* (unpubl.).

Needham, R.S., Smart, P.G. & Watchman, A.L., 1975b: Progress report, Alligator River Party N.T., 1972 (Jim Jim region). *Rec. Bur. Miner. Resour. Geol. Geophys. Aust., 1975/35* (unpubl).

Needham, R.S. & Stuart-Smith, P.G., 1976: The Cahill Formation — host to uranium deposits in the Alligator Rivers Uranium Field, Australia. *BMR J. Aust. Geol. Geophys., 1,* 321-333.

Needham, R.S. & Stuart-Smith, P.G., 1978: Progress report of the Alligator River Party, 1973-6 Fieldwork. *Rec. Bur. Miner. Resour. Geol. Geophys. Aust., 1978/113* (unpubl.).

Page, R.W., Compston, W. & Needham, R.S., this volume: Geochronology and evolution of the late Archaean basement and Proterozoic rocks in the Alligator Rivers Uranium Field, Northern Territory, Australia. *Proceedings of the International Uranium Symposium on the Pine Creek Geosyncline.*

Skwarko, S.K., 1966: Cretaceous stratigraphy and palaeontology of the Northern Territory. *Bull. Bur. Miner. Resour. Geol. Geophys. Aust., 73.*

Smart, P.G., Wilkes, P.G., Needham, R.S. & Watchman, A.L., 1975: Geology and geophysics of the Alligator Rivers Region. *in* (ed. C.L. Knight) *Economic geology of Australia and Papua New Guinea. Australas. Inst. Min. Metall., Monograph Series No. 5, 1. Metals,* 285-300.

Stewart, J.R., 1965: Middle Proterozoic volcanic rocks in the Katherine-Darwin area, Northern Territory. *Rep. Bur. Miner. Resour. Geol. Geophys. Aust., 90.*

Story, R., Williams, M.A.J., Hooper, A.D.L., O'Ferrall, R.E. & McAlpine, J.R., 1969: Lands of the Adelaide-Alligator area, Northern Territory. *CSIRO Land Research Series 25,* 153p.

Stuart-Smith, P.G., 1977: Shallow stratigraphic drilling in the Kapalga 1:100 000 Sheet area, Alligator Rivers Region N.T., 1974-6. *Rec. Bur. Miner. Resour. Geol. Geophys. Aust., 1977/53* (unpubl.)

Stuart-Smith, P.G. & Ferguson, John, 1978: The Oenpelli Dolerite — a Precambrian continental tholeiitic suite from the Northern Territory, Australia. *BMR J. Aust. Geol. Geophys., 3,* 125-133.

Stuart-Smith, P.G., Roarty, M.J., Needham, R.S. & Crick, I.H., in prep: Geology of the Mundogie 1:100 000 Sheet area, N.T. *Rec. Bur. Miner. Resour. Geol. Geophys. Aust.,* (unpubl.)

Swingler, N., 1977: Exploration in an area adjoining the area under application for a special mineral lease covering the Jabiluka uranium deposits, Northern Territory, Australia. *Aust. Atomic Energy Comm. Expl. Rep. UB9.*

Tucker, D.H., Stuart, D.C., Hone, I.G. & Sampath, N., this volume: The characteristics and interpretation of regional gravity, magnetic and radiometric surveys in the Pine Creek Geosyncline. *Proceedings of the International Uranium Symposium on the Pine Creek Geosyncline.*

Wallace, D.A., in prep: Drilling in the Munmarlary area, Alligator Rivers Uranium Field, 1978. *Rec. Bur. Miner. Resour. Geol. Geophys. Aust.* (unpubl.)

Walpole, B.P., Crohn, P.W., Dunn, P.R. & Randal, M.A., 1968: Geology of the Katherine-Darwin region, Northern Territory. *Bull. Bur. Miner. Resour. Geol. Geophys. Aust.*, 82.

Whitehouse, F.W., 1940: Studies in the late geological history of Queensland. *Pap. Dept. Geol. Univ. Qld.*, 2(1).

Wright, J.H., 1976: Exploration licence no. 120 Northern Territory. Report on 1976 investigations. *Noranda Australia Ltd. Report no. 260* (unpubl.)

GEOLOGIC SETTING OF THE EAST ALLIGATOR URANIUM DEPOSITS AND PROSPECTS

M.R. Hegge[1], D.V. Mosher[1], G.S. Eupene[2] and P.J. Anthony[3].

1. Pancontinential Mining Limited, 50 Bridge Street, Sydney, N.S.W., 2000, Australia.
2. Geopeko Limited, 10 km Stuart Highway, Darwin, N.T., 5789, Australia.
3. Queensland Mines Limited, 50 Margaret Street, Sydney, N.S.W., 2000, Australia.

ABSTRACT

Since 1969, four major uranium deposits and a number of important prospects have been discovered in the East Alligator region of the Northern Territory. The region is now considered one of the most prospective areas for uranium exploration in the World. Exploration activity in the region has been hampered as a result of government delays in processing new applications for exploration tenements. It is expected that this situation will continue until such time as the government has resolved the political problems associated with establishment of the Kakadu National Park, Aboriginal Lands Rights and current mine development.

The uranium deposits are located in Lower Proterozoic metasediments of the Cahill Formation. These occupy a north-trending synclinorium infolded between granitic migmatite complexes that have apparently been derived from older Lower Proterozoic metasediments and Archaean inliers. Two lower submembers of the Cahill Formation are the most favourable stratigraphic horizons for uranium mineralization and are comprised of metamorphosed pelites and impure carbonates totalling approximately 1000 metres in thickness. Host rocks are typically quartz chlorite schists with variable amounts of graphite and phyllosilicate minerals. These directly overlie up to 300 metres of dolomite or magnesite containing minor interbedded schist units which also contain local mineralization. Approximately 2000 metres of more micaceous schists comprise the upper part of the Cahill Formation. Regional metamorphism has occurred to at least amphibolite facies and has been followed by retrograde metamorphism to a greenschist facies equivalent. The metasediments are intruded by masses of granitic pegmatites and dolerite. Unconformably overlying these rocks are sandstones and conglomerate of the Middle Proterozoic Kombolgie Formation.

A comparative review of these deposits and prospects reveals some striking geological similarities in addition to their occurrence within the same stratigraphic succession. These include:

1) Structural controls, specifically open spaces, appear to be the main localizing feature although most deposits are grossly conformable to enclosing lithologies.
2) The intense and pervasive chloritization, magnesium metasomatism, and lesser sericite alteration of the mineralized and surrounding lithologies including the Kombolgie Formation.
3) Pitchblende is the main ore mineral and, although disseminated sulphides occur in varying amounts, gold is the only associated metal which is concentrated in economic quantities.
4) The spatial relationship of the deposits to the Middle Proterozoic unconformity or the erosional margin of the Kombolgie Formation.
5) The proximity to the older granitic migmatite complexes and their pegmatitic apophyses.
6) A regional association with carbonate bearing strata but a common antipathetic relationship with carbonate within the ore zones.
7) A common, major mineralizing phase (900 m.y.) which postdates deposition of the Kombolgie Formation.

The Nabarlek deposit is the most notable exception to some of the aforementioned characteristic features.

INTRODUCTION

Since 1969, four major uranium deposits and a number of important prospects have been discovered in the East Alligator region of the Northern Territory (Fig. 1). The region is now considered to be one of the most prospective in the world for locating further uranium reserves. Exploration activity in recent years, however, has been hampered as a result of government delays in processing new applications for exploration tenements. It is expected that this situation will continue until such time as the government has resolved the political problems associated with establishment of the Kakadu National Park, Aboriginal Land Rights and current mine development in the area.

This paper briefly describes the geology of some deposits and prospects. It should be noted that certain prospects have not been included in this discussion because of the lack of sufficient data. The common geologic features are summarized to determine the most important similarities and possible ore controls. A brief comparison with the Athabasca Basin in Canada is presented.

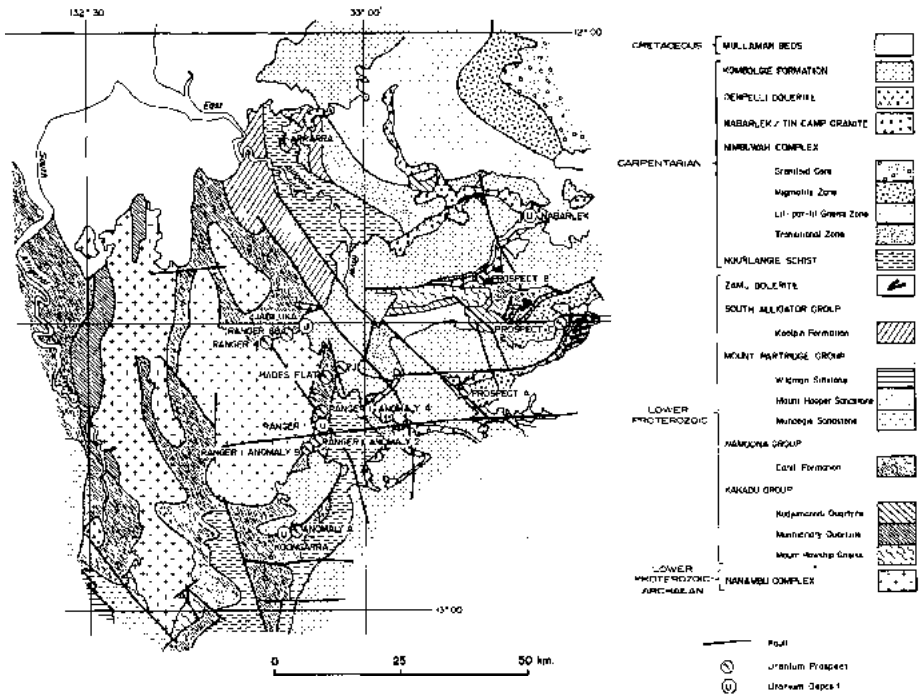


Figure 1. Regional Geology of the East Alligator River area (Modified from BMR Pine Creek Geosyncline 1:500,000 geological map, 1979).

The regional geology has been presented by other authors (Needham & Stuart-Smith, this volume) and will not be repeated in this discussion (Fig. 1). In summary, the authors hope to provide a greater insight into the different geologic environments of uranium mineralization in the East Alligator region and in this way aid in elucidating the metallogenesis.

DESCRIPTION OF DEPOSITS AND PROSPECTS

Koongarra

The uranium mineralization at Koongarra (Fig. 1) occurs in metamorphic rocks of the Cahill Formation just above a reverse faulted contact with the Kombolgie Formation (Foy & Pedersen, 1975). The most prominent structural feature is the north-east trending Koongarra Reverse Fault which dips at about 55° to the south-east and marks the geological footwall of the mineralized zones (Fig. 2). Vertical displacement is probably about 600 metres. Strong brecciation and shearing persist well into the overlying quartz chlorite schists and intensely sheared zones are present in adjacent graphitic units.

Uranium ore occurs in two distinct but clearly related mineralized bodies separated by a barren gap about 100 metres in length. Both strike and dip more or less parallel to the Koongarra Reverse Fault. The primary mineralization is largely confined to the quartz chlorite schists and the graphitic rocks immediately above but in places it continues into the overlying garnetiferous quartz muscovite chlorite schists.

The south-west mineralized zone, termed the No.1 orebody, has a strike length of 450 metres and persists to a depth of approximately 100 metres. Secondary uranium minerals are

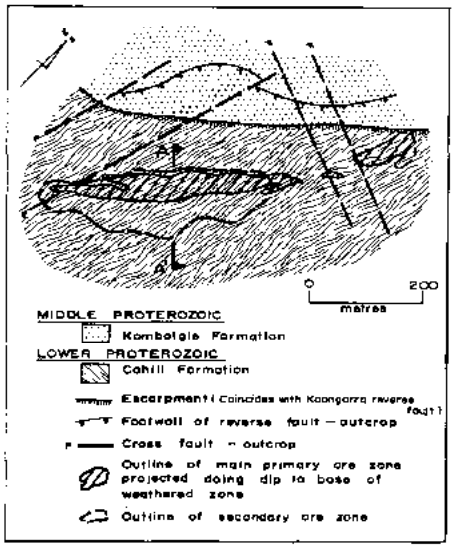


Figure 2. Generalized geologic plan of the Koongarra deposit (After Foy & Pedersen, 1975).

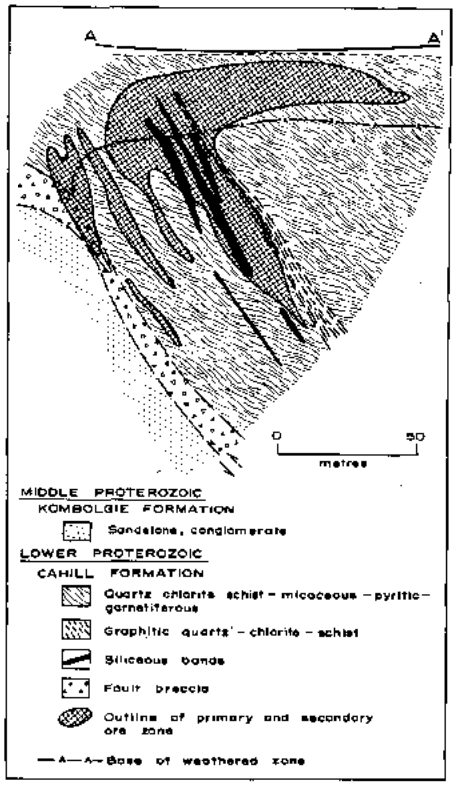


Figure 3. Geologic cross section of the Koongarra deposit (Modified from Foy & Pedersen, 1975). Location of cross section shown on figure 2.

present from just below surface down to the base of weathering at about 25 metres (Snelling, this volume). The primary mineralization occurs in a series of coalescing lenses which together form an elongated wedge dipping at 55° to the south-east. True widths, averaging 30 metres at the top of the unweathered zone, taper out at about 100 metres below surface and along strike (Fig. 3). The strongest mineralization is over a thickness of several metres just below the graphitic unit which tends to form a well defined hanging wall.

To the north-east mineralization occurs over a strike length of about 100 metres. There is little indication of secondary mineralization. The primary zone, first intersected in unweathered rocks at a depth of 50 metres, persists to at least 250 metres below surface. In cross section the ore zone tends to be oval, narrow at the top, thickening, and then thinning again at depth. This again is made up of a series of partially coalescing lenses. Ore grade is lower than at the No. 1 orebody. Mineralization has been dated at 870 m.y. (Hills & Richards, 1976).

Ranger 1, No. 1 Orebody

The No.1 Orebody at Ranger 1 contains about 50,000 tonnes of recoverable U_3O_8 at a grade of 0.3% U_3O_8 (Fig. 4). The deposit has been described in some detail previously (Eupene *et al.*, 1975) and only a brief up-dated summary is presented here. The deposits are located in altered microgneiss, schist and silicified carbonate near the base of the lower Cahill Formation (Needham & Stuart-Smith, this volume). Minor mineralization extends into the underlying Nanambu Complex.

The Orebody can be divided into two major host rock types — the Upper Mine Sequence (UMS) and the Lower Mine Sequence (LMS) (Fig. 5). The UMS is chloritised schist and

microgneiss whereas the LMS is silicified carbonate. These major rock types grade downdip into their unaltered parent material. Both sequences are intensely brecciated in the ore zones and extensively intruded by chlorite veins. It is this chlorite which carries the majority of the mineralization. Syn-metamorphic, chloritized pegmatite dykes intrude the sequence, along with post-metamophic mafic dykes but neither are mineralized.

No Kombolgie Formation sandstone has been noted in the immediate area of the orebody, though the unconformity could only have been a few tens of metres at most above the present land surface.

The deposit appears to be structurally, rather than chemically controlled at all scales of observation. Although a little carbonaceous matter is present in parts of the UMS, this appears to have played a minimal chemical role in precipitation of pitchblende (Eupene, 1979).

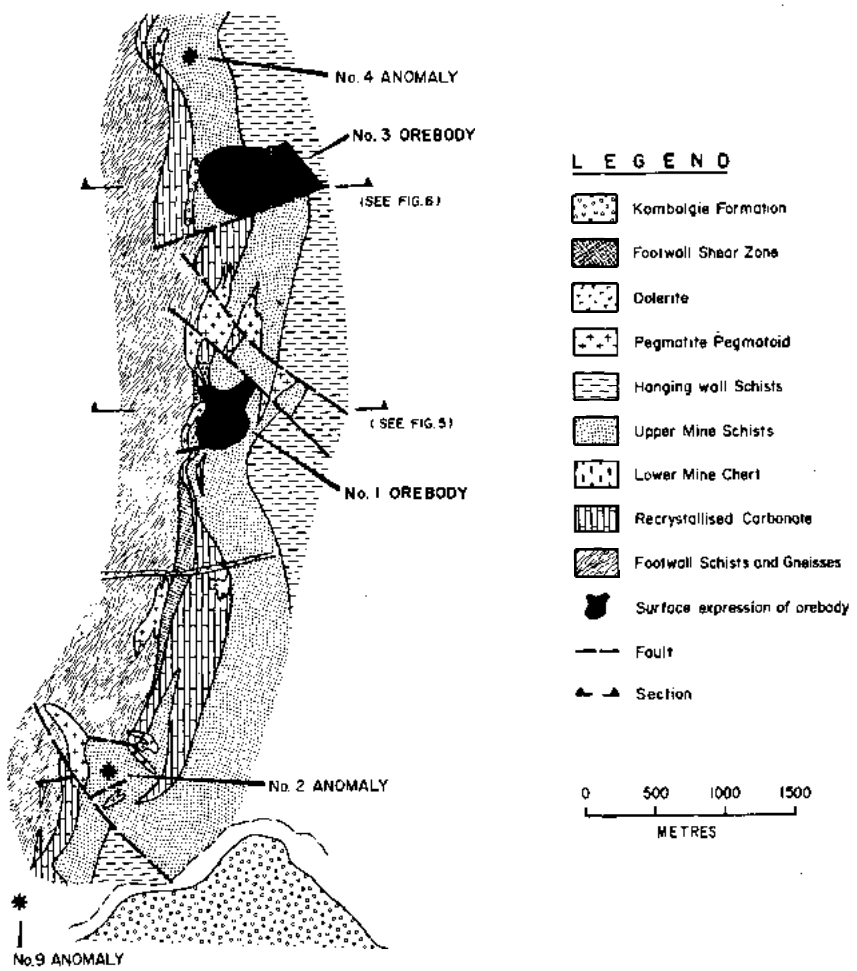


Figure 4. Generalized geologic plan of the Ranger One orebodies and prospects (Modified from Eupene *et al.*, 1975).

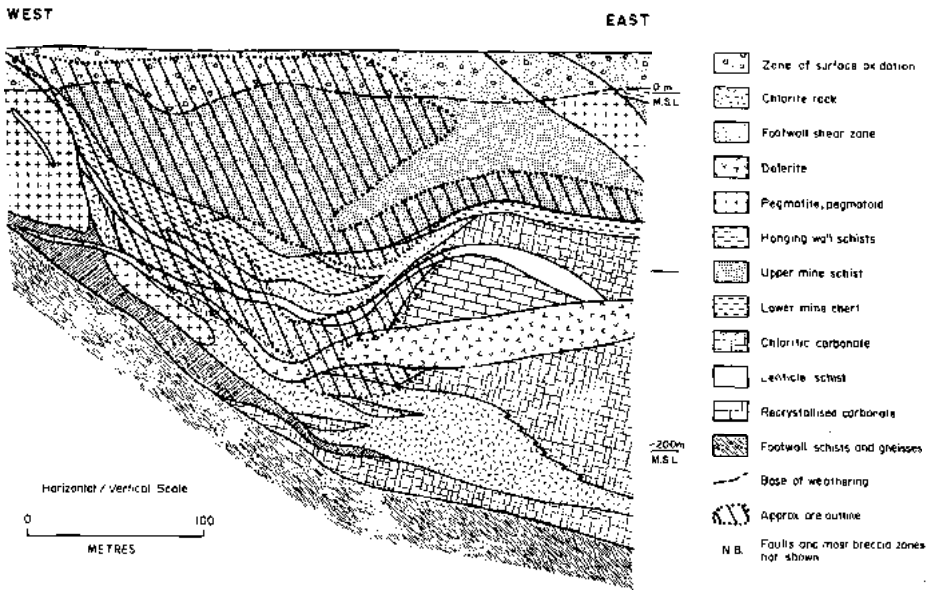


Figure 5. Geological cross section of the Ranger One Number 1 orebody (Modified from Eupene *et al.*, 1975). Location of section shown on figure 4.

There is strong evidence that the deposit is located in a collapse structure developed in silicified carbonate of the LMS and extending into the overlying chloritic schist and microgneiss of the UMS. The source of the chlorite in the ore zones is believed to be those sections of the LMS which demonstrate post-metamorphic recrystallization.

Ranger 1, No. 3 Orebody

The No. 3 Orebody at Ranger contains about 50,000 tonnes of U_3O_8 at an average grade lower than that in the No. 1 Orebody. It is located approximately 1500 metres north of the No. 1 Orebody in an identical stratigraphic position within the lowermost members of the Cahill Formation (Fig 4). The deposit has only been drilled on 100 metre centres and is still open. The geology, therefore, is not known in as much detail as that of the No. 1 Orebody.

Whilst the rock types and stratigraphy are similar at this deposit, there are some differences in ore distribution patterns and structural setting (Fig. 6). The majority of indicated mineralization is in the UMS. There is no strongly developed mineralized zone in the LMS and silicification of the LMS carbonate, though well-developed, is not as extensive as at the No. 1 Orebody.

A blind deposit has been discovered in chloritic lenses within the LMS carbonate rocks on the eastern extremity of the drilling grid. This is approximately 700 metres down-dip from the unconformity surface, and over 250 metres vertical from the present surface. It does not appear to be connected by mineralization to the near-surface deposit. Uranium mineralization within carbonate host rocks is epigenetic in form and is associated with chlorite.

A large block of chloritized Kombolgie Formation sandstone has been 'dropped in' on the western margin of the deposit and lends weight to the collapse structure hypothesis for the localization of the major Ranger 1 deposits.

Ranger 1, Anomaly 2

Anomaly 2 at Ranger 1 has been excluded from the Ranger Project area as a result of

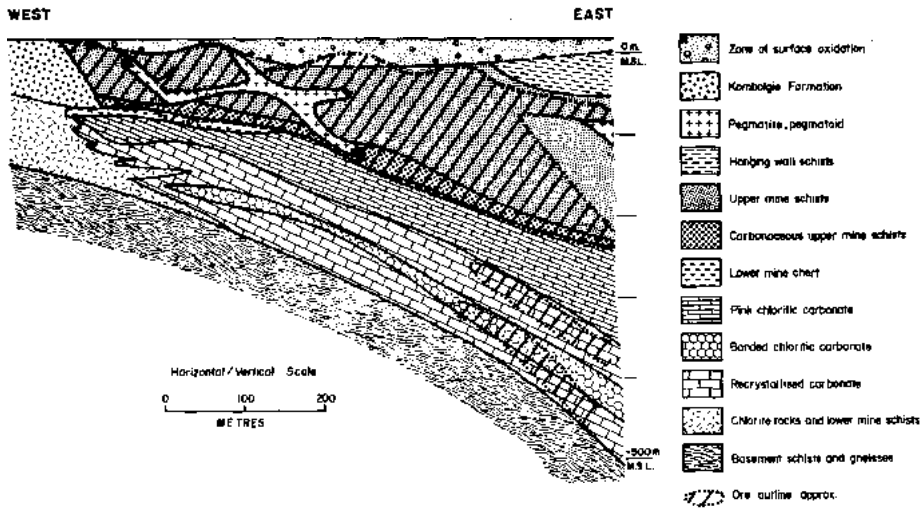


Figure 6. Geologic cross section of the Ranger One Number 3 orebody. Location of section shown on figure 4.

the government adopting the recommendations of the Ranger Uranium Environmental Inquiry (Fig. 4). No diamond drilling has been undertaken on the deposit, though it has been extensively auger drilled and 53 percussion holes have been completed. Significant uranium mineralization, both primary and secondary has been intersected, and there is every chance of establishing a mineable resource.

The anomaly, which is characterized by three separate radiometric highs, commences about two kilometres south of the No. 1 Orebody and follows the arcuate strike of the Nanambu Complex/Cahill Formation contact. Radiometric anomalies and uranium intersections seem to be restricted to carbonaceous and chloritic schists near the base of the UMS. The LMS in the area appears to be largely carbonate, with little of the widespread silicification present in the larger Ranger 1 deposits. Mineralization occurs preferentially in brecciated zones.

Ranger 1, Anomaly 4

Anomaly 4 at Ranger 1 is the northernmost anomaly of the Ranger 1 group and occurs 800 metres north-west of the No. 3 Orebody (Fig. 4). Four percussion drill holes and one diamond drill hole have been completed to date on the prospect. Only thin, low grade uranium mineralization has been intersected to date but further work is warranted. Mineralization has been intersected in brecciated schists, chert and chloritized pegmatites at the contact between the UMS and LMS. In addition, mineralization is present in a chloritic breccia on the contact between the LMS and the Nanambu Complex.

Ranger 1, Anomaly 9

Anomaly 9 at Ranger 1 lies beneath out-wash sand, derived from Kombolgie Formation about 1,000 metres south-west of Anomaly 2 (Fig. 4). There is no radiometric expression at surface. Two shallow core holes have intersected medium grade secondary uranium mineralization in decomposed UMS schists. No deeper drilling has been undertaken. A gossanous outcrop in the area contains malachite, and may represent basal Kombolgie Formation.

This area has been excluded from the Ranger Project Area for the same reason as Anomaly 2.

Ranger 4

Ranger 4 is about 10 kilometres west-southwest of Jabiluka and about 20 kilometres north-northwest of Ranger 1 No. 1 Orebody and was detected in 1970 as the result of an airborne survey (Fig. 1). The prospect has been trenched, and several percussion and diamond holes have been drilled. Results to date indicate a small body of medium to low grade uranium mineralization. The radiometric anomaly occurs over a window of laterised bedrock within an area largely covered by Recent alluvium, and Cretaceous sand. A down thrown block of sandstone of the Kombolgie Formation (?) is present to the north of the anomaly. The general stratigraphy is similar to that seen elsewhere in the lower part of the Cahill Formation. The mineralization occurs in chloritised and brecciated pegmatoid rocks within a dolomite bearing sequence at or near the Cahill Formation/Nanambu Complex contact. There appears to be an embayment in the contact in the vicinity of the deposit.

Ranger 68

Ranger 68 occurs along the Nanambu Complex/Cahill Formation contact between Ranger 4 and Jabiluka (Fig. 1). The deposit is totally covered by about 30 metres of Recent alluvium and Cretaceous sand. No radiometric anomaly is present. A low-order radon anomaly in the area could possibly be related to the mineralization. The deposit was located by scout drilling along the favourable Cahill Formation/Nanambu Complex contact. Only 12 holes have been drilled into the prospect so far. These indicate a significant and unclosed mineralized body of medium grade.

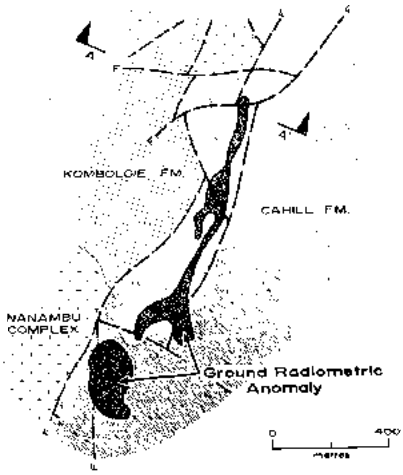


Figure 7. Generalized geologic plan of the Hades Flats deposit.

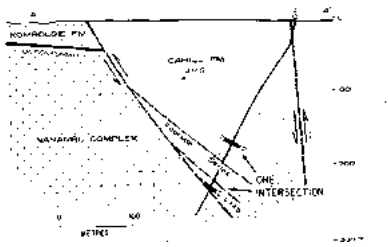


Figure 8. Geologic cross section of the Hades Flats deposit. Location of section shown on figure 7.

The mineralization is present in chloritised breccia, pegmatoids and to a lesser extent in quartz sericite chlorite schists which occur in a sequence similar to that at Ranger 4. Primary mineralization consisting of sooty and colloform pitchblende, occurs immediately below the Cretaceous unconformity. Limited secondary mineralization was observed in one hole. There is some chalcocite mineralization associated with higher uranium grades. The absence of a readily-identifiable regolith below the Cretaceous sand is of notable interest.

The deposit appears to be localized in and near a massive breccia zone at the contact between lower carbonate of the Cahill Formation and the Nanambu Complex. Although structural relations are at this stage uncertain there is a possibility that the Cahill Formation in the area is overturned.

Hades Flats

The Hades Flats deposit is located 10 kilometres north and along strike from the Ranger deposits (Fig. 1). The uranium mineralization occurs in rocks of the lower Cahill Formation which are similar to the Ranger mine series (Fig. 7). The host rocks in the upper part of the metasedimentary succession are mainly chlorite feldspar schist with adjacent unmineralized graphite schist and dolomite. A footwall series of

hematitic chlorite muscovite schist is also unmineralized. The lower mine series is 50 metres thick and is composed of chlorite schist and breccia with local intercalated dolomite horizons. These units are in faulted contact with quartzite, gneiss, schist and pegmatite of the Nanambu Complex (Fig. 8).

The uranium mineralization consists of pitchblende in fractures or breccia zones in the chlorite schists. Chlorite-healed breccia zones at the faulted contact with the Nanambu Complex provide another host for pitchblende mineralization. Thucolite occurs randomly in small fractures but is not economically significant. Some secondary uranium minerals have been noted in the weathered zone. Remnants of the Middle Proterozoic Kombolgie Formation indicate the present land surface represents a close proximity to the unconformity between the Lower and Middle Proterozoic rocks.

7J

The 7J prospect is located approximately three kilometres northeast of Hades Flats at the edge of the Arnhem Land Plateau (Fig. 1). It is within Stage One of the Kakadu National Park and no work has been carried out on the prospect since 1973. The surface showing exhibits secondary uranium minerals in Lower Proterozoic metasediments, probably of the Cahill Formation, and also in the basal conglomeratic sandstone of the Kombolgie Formation (Fig. 9). The mineralization in the sandstone appears to have been introduced by groundwater movement along the unconformity.

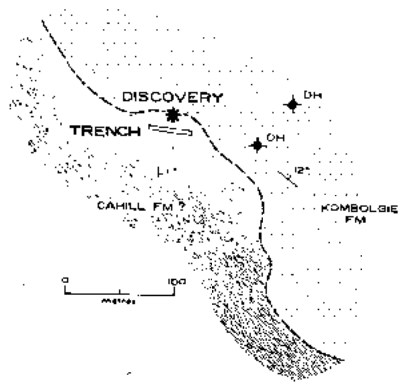


Figure 9. Generalized geologic plan of the 7J

Secondary mineralization exposed in a trench occurs as stringers in hematite-stained chlorite schist overlying graphite schist. Anomalous gold values are present in some of the discovery boulders.

Pitchblende has been intersected in chlorite schists downdip from the showing but the ore controls and exact stratigraphic position remain unsolved due to the lack of data. The nearest identified Nanambu Complex rocks were intersected in drill holes approximately 2000 metres to the west.

Jabiluka One and Two

The Jabiluka One and Two deposits are hosted by the lower member of the Cahill Formation and occur within 300 metres of each other (Fig. 10) near the eastern edge of the Nanambu Complex. Jabiluka One coincides with an erosional window through unconformably overlying sandstone of the Kombolgie Formation. To the east, Jabiluka Two is covered by between 20 and 220 metres of sandstone which locally exhibits faulting along the unconformity. A third deposit, Jabiluka Three, has been indicated by one drill hole south of Jabiluka One.

The observed part of the Cahill formation at Jabiluka contains four separate ore-bearing horizons, each comprised of a number of distinct lithologies. These have been folded into an open, asymmetric flexure, striking east-southeast and dipping to the south (Fig. 11).

Host rocks are mainly chlorite and/or graphite schists and their brecciated equivalents. Mineralization consists of pitchblende which occurs as vein-fillings, disseminated grains in chloritic gangue material, and as selvages to chloritic veins or local replacement zones. Minor coffinite and brannerite have also been reported (Binns *et al.*, this volume). Accompanying sulphides include pyrite with lesser amounts of chalcopyrite and galena. Major gangue minerals are chlorite, quartz and sericite. Magnesium metasomatism is an intimate alteration

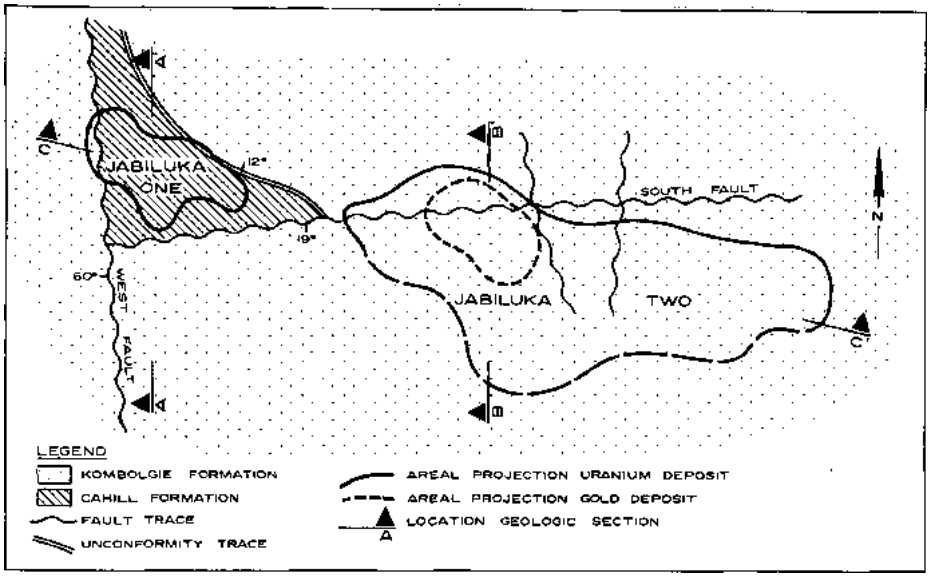


Figure 10. Generalized geologic plan of the Jabiluka One and Two ore deposits (Modified from Hegge, 1977).

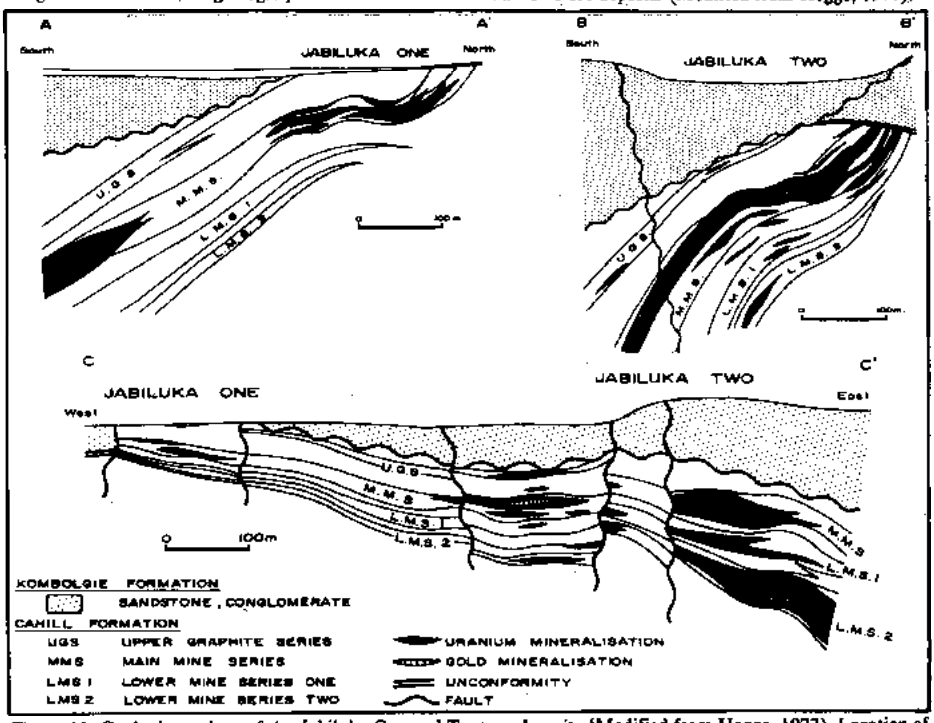


Figure 11. Geologic sections of the Jabiluka One and Two ore deposits (Modified from Hegge, 1977). Location of sections shown on figure 10.

feature of the mineralized zones. A portion of Jabiluka Two contains economic amounts of native gold accompanied by traces of lead, bismuth, and nickel tellurides. There is no apparent positive correlation on a local scale between uranium and gold mineralization. An age date of 920 m.y. has been obtained for uranium mineralization at Jabiluka One (Hills & Richards, 1976).

Nabarlek

The Nabarlek deposit occurs in altered metapelites which flank the western edge of the Nimbuwah Complex (Anthony, 1975). Uranium mineralization is localized along a chlorite-filled structure which is clearly transgressive to the enclosing rocks (Fig. 12). The host rocks, which include quartz mica, chlorite mica and quartz chlorite schist and minor amphibolite are more intensely deformed than those at other deposits and graphitic or dolomitic units are conspicuously absent. The mineralized structure, which exhibits breccias and flow banding, continues both north and south of the orebody and is truncated at a maximum depth of 85 metres by a sheet of Oenpelli Dolerite.

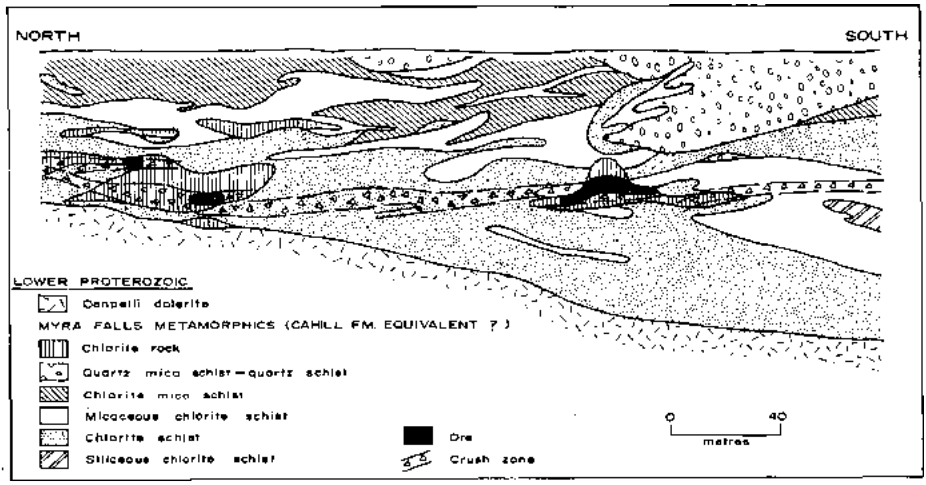


Figure 12. Geologic long section of the Nabarlek ore deposit (Modified from Anthony, 1975).

Uranium mineralization consists of massive and disseminated pitchblende with a halo of secondary minerals (Fig. 13). There is an intimate association of uranium mineralization and intrusive chlorite which is best developed where adjacent country rocks are chloritic. Hematite is also a major constituent towards the centre of the orebody.

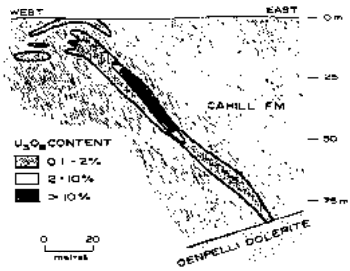


Figure 13. Generalized cross section of the Nabarlek ore deposit (Modified from Anthony, 1975).

As at Ranger and Koongarra, the present-day land surface is believed to approximate the Lower Proterozoic/Middle Proterozoic unconformity.

Arrarra

The Arrarra prospect is located approximately 35 kilometres north of Jabiluka and is within the Arnhem Land Aboriginal Reserve (Fig. 1). Uranium mineralization occurs in chloritized quartz sericite schists which have been intruded by a thick sheet of Oenpelli Dolerite, then unconformably overlain by the Kombolgie Formation (Fig. 14). The lithologies located to date indicate that the metasediments may be

part of the upper Cahill Formation. The Nimbuwah Complex crops out approximately 30 kilometres to the east although geophysical data indicates similar rocks may exist to the immediate southwest of the property along the East Alligator River. Mineralization consists of secondary uranium minerals which appear to be concentrated at the base of the Middle Proterozoic weathered zone (Fig. 15). The mineralized zones are adjacent to major fault structures which also exhibit local radiometric anomalies.

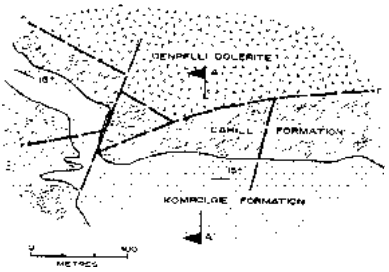


Figure 14. Generalized geologic plan of the Arrarra prospect.

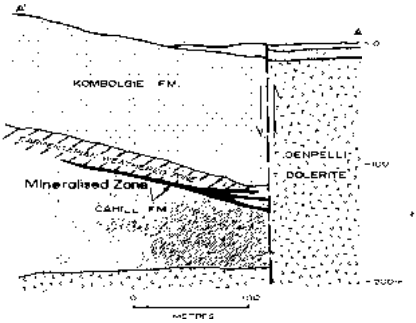


Figure 15. Geologic cross section of the Arrarra prospect. Location of section shown on figure 14.

No primary mineralization has been located to date.

Other Prospects

Several other prospects occur in the Arnhem Land Aboriginal Reserve. Only three, however, can be described due to the lack of available information (Fig. 1).

Prospect 'A'

Prospect 'A' is reported to occur in the marginal Migmatite Zone of the Nimbuwah Complex. This zone is characterized by the development of augen gneisses which have been cut by quartz stockwork breccias consisting of silicified rock fragments healed by quartz and lesser hematite. The breccias appear to be within shear zones.

Mineralized lithologies, particularly those proximal to quartz breccias, exhibit chloritic, sericitic and minor hematitic alteration. Mineralization consists of sooty pitchblende occurring as tiny disseminations or along hairline veins within altered gneiss. Pyrite and minor chalcopyrite are common. Some secondary uranium minerals occur in the weathered zone.

Prospect 'B'

Prospect 'B' is similar to 'A' and consists of secondary uranium mineralization which is exposed in trenches cutting across schists adjacent to a quartz stockwork breccia. Host rocks include quartz schists with variable amounts of chlorite, mica, hematite and graphite. The quartz breccia occupies a structure which cuts sandstone of the Kombolgie Formation in one part of the prospect but no mineralisation is reported to occur in that area.

Prospect 'C'

Prospect 'C' is located at the base of a scarp of sandstone of the Kombolgie Formation. This unconformably overlies hematitic chlorite quartz schist which has been locally brecciated and healed by quartz and chlorite veins. A sheet of Oenpelli Dolerite, which exists from near surface to almost 100 metres below the unconformity, has also chloritized the enclosing rocks. Mineralization occurs in an arcuate band extending from surface showings near the scarp to depths of up to 50 metres below the unconformity.

Sooty pitchblende is concentrated in veins containing chlorite and brecciated fragments of quartz which cut the chlorite quartz schist at a low angle. Some pyrite is also present.

DEPOSIT OR PROSPECT	PUBLISHED RESERVES (TONNES U_3O_8)	HOST ROCKS RELATION TO UNCONFORMITIES		HOST ROCKS PROXIMAL TO		ALTERATION				STRUCTURAL CONTROL		ASSOCIATED METALS	
		ARCHAEAN / L. PROT	LOWER / MIDDLE PROT	GRAPHITE	DOLOMITE	CHLORITE	SILICA	CLAY	HEMATITE	FAULTING	BRECCIATION	ECONOMIC	NON-ECONOMIC
RANGER 1, No 1 OREBODY	50,000	FAULT CONTACT	PRESENT LAND SURFACE	WEAK	x	x	x	x	WEAK	x	x		Pb,Cu,As
RANGER 1, No 3 OREBODY	50,000	"	" " "	"	x	x	x	x		x	x	-	Pb,Cu
RANGER 1, ANOMALY 2	N A	"	" " "	x	x	x	WEAK	x	-	x	x	"	NOT KNOWN
RANGER 1, ANOMALY 4	N A	"	" " "	x	x	x	x	x	"	x	x	"	"
RANGER 1, ANOMALY 9	N A	"	" " "	NOT KNOWN	NOT KNOWN	x	NOT KNOWN	x	NOT KNOWN	x	x	-	Cu
HADES FLATS	N A	IN FAULT CONTACT	" "	x	x	x	x	x	x	x	WEAK	-	-
RANGER 4	N A	FAULT CONTACT	ADJACENT FAULT BLOCK	-	x	x	NOT KNOWN	x	x	x	x		
RANGER 68	N A	" "	PROX MAL	-	x	x	NOT KNOWN	x	x	x	x		Cu
JABILUKA ONE & TWO	207,000	PROXIMAL	UNCONFORMABLY OVERLAIN (FAULTED IN PART)	x	x	x	x	x	WEAK	x	x	As	Pb,Cu,Ni,Bi,Te,Pd,Hg
KOONGARRA	53,000	"	REVERSE FAULT	x	x	x	x	x	WEAK	x	x	-	Pb,Cu,As
7J	N A	NOT KNOWN	UNCONFORMABLY OVERLAIN	x	NOT KNOWN	x	x	x	x	x	NOT KNOWN	As(?)	
ARRARRA	N A	" "	" "	-		x	x	x	x	x	WEAK	-	-
NABARLEK	9,300	" "	PRESENT LAND SURFACE	-	-	x	x	WEAK	x	x	x	-	Pb,Cu
PROSPECT "A"	N A	MIGMATITE ZONE	NOT KNOWN	-	-	x	x	WEAK	x	x	x	-	NOT KNOWN
PROSPECT "B"	N A	" "	UNCONFORMABLY OVERLAIN IN PART	WEAK	-	x	x	WEAK	x	x	x	-	NOT KNOWN
PROSPECT "C"	N A	" "	" "	-	-	x	x	x	x	x	x	-	NOT KNOWN

x = PRESENT
- = NOT PRESENT

Table 1. Comparative features — East Alligator Deposits and Prospects.

The footwall rocks may be either quartz chlorite feldspar schist or dolerite. In some zones of extensive faulting, mineralization may occur in schists below masses of up-thrown dolerite.

CONCLUSIONS

A comparative review of the deposits and prospects reveals some striking geological similarities in addition to their occurrence within the same general stratigraphic succession (Table 1). These include:

1) The structural controls, such as faulting and brecciation, which appear to be the main ore localizing feature although most deposits are generally conformable to enclosing lithologies.
2) The intense chloritization of the host rocks and surrounding lithologies — including the Kombolgie Formation. This suggests that the ore fluids either contained chlorite or precipitated chlorite during the mineralizing events.
3) The proximity of the deposits to rejuvenated Archaean migmatite complexes and their pegmatitic apophyses, the latter of which may locally intrude the Lower Proterozoic metasediments.
4) The spatial relationship of the deposits to the Middle Proterozoic unconformity or erosional margin of the Kombolgie Formation, the significance of which is not clearly evident.
5) A regional association for the majority of the deposits with carbonate-bearing strata but a common antipathetic relationship with carbonate within the ore zones. Evidence suggests solution of the carbonate could have allowed the formation of overlying collapse breccias and also provided suitable channelways for mineralizing fluids.
6) The late-state mineralizing or reconcentrating events which post-date deposition of the Kombolgie Formation.

As previously mentioned, Nabarlek is the major exception to some of these characteristic features, most important of which is the lack of graphitic and carbonate-bearing strata within the host stratigraphy. Similarly, some of the smaller prospects exhibit obvious differences but this may be due, in part, to the lack of sufficient data.

COMPARISON WITH ATHABASCA BASIN DEPOSITS IN CANADA

In comparing the East Alligator deposits with those of the Athabasca Basin in northern Saskatchewan, Canada, it is generally agreed that the regional geological setting is essentially the same. In formulating respective exploration models based on genesis, therefore, it might be more useful to examine some of the most outstanding dissimilarities. These appear to be:

1) The lack of ore in the Kombolgie Formation. There are no known East Alligator equivalents of deposits such as Collins Bay 'B' or Fond-du-lac which are hosted entirely by Middle Proterozoic sandstone.
2) The lack of high grade mineralization concentrated at the Lower/Middle Proterozoic unconformity with lower grade zones extending into both the metasediments and overlying sandstones. Environments for uranium deposition such as those at Key Lake, Midwest Lake and West Bear exist at Jabiluka and 7J, for example, but no enrichment of primary mineralization occurs at the uncomformity. The overlying sandstones, although altered to some extent in a similar manner to the mineralized Cahill Formation, are completely barren of primary uranium minerals. No imprints of oxidation-reduction conditions are apparent such as those in mineralized sandstone at, say Midwest Lake. The

contrasting physico-chemical environment, which is reported to have existed near the Athabasca unconformity and is typified by the generation of carbon-dioxide and methane (Hoeve & Sibbald, 1978a), does not appear to have been active in the Kombolgie Formation. This unique environment could possibly be viewed as an additional upgrading event for mineralization formed initially near the unconformity and under similar conditions in both regions. This might also account for the higher average ore grades encountered in the Saskatchewan deposits.

3) The lack of other economic metal concentrations in the East Alligator area other than gold at Jabiluka. There are no complex metallic mineral assemblages such as those at Cluff Lake or the nickel sulphide and arsenide associations at Key Lake.

It is suggested that further studies on the mineralization involving these metals in the Athabasca deposits might aid in a better understanding of the uranium genesis in both regions.

ACKNOWLEDGEMENTS

The writers wish to thank the managements of Geopeko Limited, Queensland Mines Limited, Noranda Australia Limited and Pancontinental Mining Limited for permission to publish the presented information. A critical review of the manuscript by J. C. Rowntree is gratefully acknowledged. We are also indebted to Terry Rust for his preparation of the illustrations and to Valerie Froome for typing the manuscript.

REFERENCES

Anthony, P.J., 1975: Nabarlek uranium deposit. *in* (ed. C.L. Knight) *Economic Geology of Australia and Papua New Guinea, Australas. Inst. Min. Metall., Monograph Series No. 5, 1. Metals*, 304-308.

Binns, R.A., McAndrew, J. & Sun, S-S., this volume: Origin of uranium mineralization at Jabiluka. *Proceedings of the International Uranium Symposium on the Pine Creek Geosyncline.*

Eupene, G.S., 1979: Stratigraphic and Temporal Control of Mineralization in the Alligator Rivers Uranium Province, Northern Territory, Australia. *in* (ed. J.D. Ridge) *Proceedings of the fifth International Symposium on the genesis of ore deposits, Snowbird, Utah, August 1978.* (in press).

Eupene, G.S., Fee, P.H. & Colville, R.G., 1975: Ranger One uranium deposits, *in* (ed. C.L. Knight) *Economic Geology of Australia and Papua New Guinea, Australas. Inst. Min. Metall., Monograph Series No. 5, 1. Metals*, 308-317.

Foy, M.F. & Pedersen, C.P., 1975: Koongarra Uranium. *in* (ed. C.L. Knight) *Economic Geology of Australia and Papua New Guinea, Australas. Inst. Min. Metall., Monograph Series No. 5, 1. Metals*, 317-321.

Hegge, M.R., 1977: Geologic setting and relevant exploration features of the Jabiluka uranium deposits. *Proc. Australas. Inst. Min. Metall., 264*, 19-32.

Hills, J.H. & Richards, J.R., 1976: Pitchblende and galena ages in the Alligator Rivers region, Northern Territory, Australia. *Miner. Deposita., 11*, 133-154.

Hoeve, J. & Sibbald, T.I.T., 1978a: Mineralogy and geological setting of unconformity-type uranium deposits, northern Saskatchewan, Canada *in* (ed. M. M. Kimberley) *Short course in Uranium Deposits: their Mineralogy and Origin. Mineralogical Association of Canada*, 457-474.

Hoeve, J. & Sibbald, T.I.T., 1978b: Uranium concentration related to the sub-Athabasca unconformity, northern Saskatchewan, Canada *in* (ed. M. M. Kimberley) *Short course in Uranium Deposits: their Mineralogy and Origin. Mineralogical Association of Canada*, 475-484.

Needham, R.S. & Stuart-Smith, P.G., this volume: Geology of the Alligator River Uranium Field. *Proceedings of the International Uranium Symposium on the Pine Creek Geosyncline.*

Snelling, A.A., this volume: Pitchblende and its alteration products, Koongarra uranium deposit. *Proceedings of the International Uranium Symposium on the Pine Creek Geosyncline.*

THE GEOLOGY AND MINERALISATION OF THE SOUTH ALLIGATOR VALLEY URANIUM FIELD

I.H. Crick,[1] M.D. Muir,[1] R.S. Needham[1] and M.J. Roarty[2]

1. Bureau of Mineral Resources, P.O. Box 378 Canberra City, A.C.T., 2601, Australia.
2. Mines Division, Department of Mines and Energy, Darwin, N.T., Australia.

ABSTRACT

The South Alligator Valley Uranium Field contains thirteen small worked out mines and over fifteen prospects most of which are within a north-west trending belt 24km long by 3km wide.

Uranium mineralisation is commonly associated with gold and is (1) epigenetic, (2) occurs in a variety of rock types but commonly within the Lower Proterozoic Koolpin Formation, (3) occurs close to a major unconformity between Lower Proterozoic and Middle Proterozoic (Carpentarian) rocks and (4) has ages of about 800 m.y. and 500 m.y.

New evidence concerning the environment of deposition and possible age of the Koolpin Formation is discussed.

Models of uranium mineralisation in this field range from syngenetic, with minor remobilisation, to hydrothermal. Models which best explain most features of the mineralisation propose that uranium was leached from the Edith River Volcanics by low-temperature groundwaters and redeposited in a reducing environment along faults and fractures in the unconformably underlying Koolpin Formation.

INTRODUCTION

The South Alligator Valley Uranium Field (SAVUF) is by far the smallest uranium field in the Pine Creek Geosyncline. It contains thirteen worked-out mines (total production 874 tonnes U_3O_8) and over fifteen prospects mostly within a northwest trending belt 24km long and 3km wide located about 220km southeast of Darwin (Fig. 1). The field has been reviewed by Prichard (1965), Crohn (1968), Taylor (1969), Dodson *et al.* (1974), Ayres & Eadington (1975), and Foy (1975). In this paper we revise the Lower Proterozoic stratigraphy, present new data on the Koolpin Formation, the host for most of the uranium mineralisation, and consider models for uranium mineralisation as well as review the literature on this area. Subdivisions of the Proterozoic used in this paper are as defined by Dunn *et al.* (1966).

GEOLOGY

The geology of the SAVUF was described by Walpole *et al.* (1968); that of the northern third has been revised by Needham *et al.* (1978), (Fig. 2). Changes in the interpretation of the Lower Proterozoic stratigraphy are summarised in Needham *et al.* (this volume).

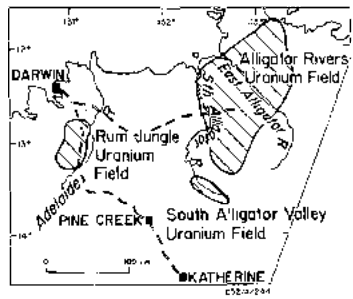


Figure 1. Location of the Uranium Fields in the Pine Creek Geosyncline.

The Lower Proterozoic sediments in the SAVUF are exposed unconformably beneath a thick sequence of mainly flat-laying Middle Proterozoic (Carpentarian) arenite, rudite, and volcanics. Most of the uranium mineralisation in the SAVUF is close to the unconformity.

The Lower Proterozoic sequence in the SAVUF has an exposed thickness of about 2.5km, and is considered to occupy a basement low, the South Alligator River Trough, formed by incipient rifting (Stuart-Smith *et al.*, this volume). Basement to the succession was considered by Walpole *et al.* (1968) to be the Archaean 'greenstones' of the Stag Creek Volcanics. Recently, Foy & Miezitis (1977) and Needham *et al.* (1978) have reported that mafic flows and breccias of this unit are interlayered with Lower Proterozoic tuffaceous sediments, and are underlain by Masson Formation quartzite,

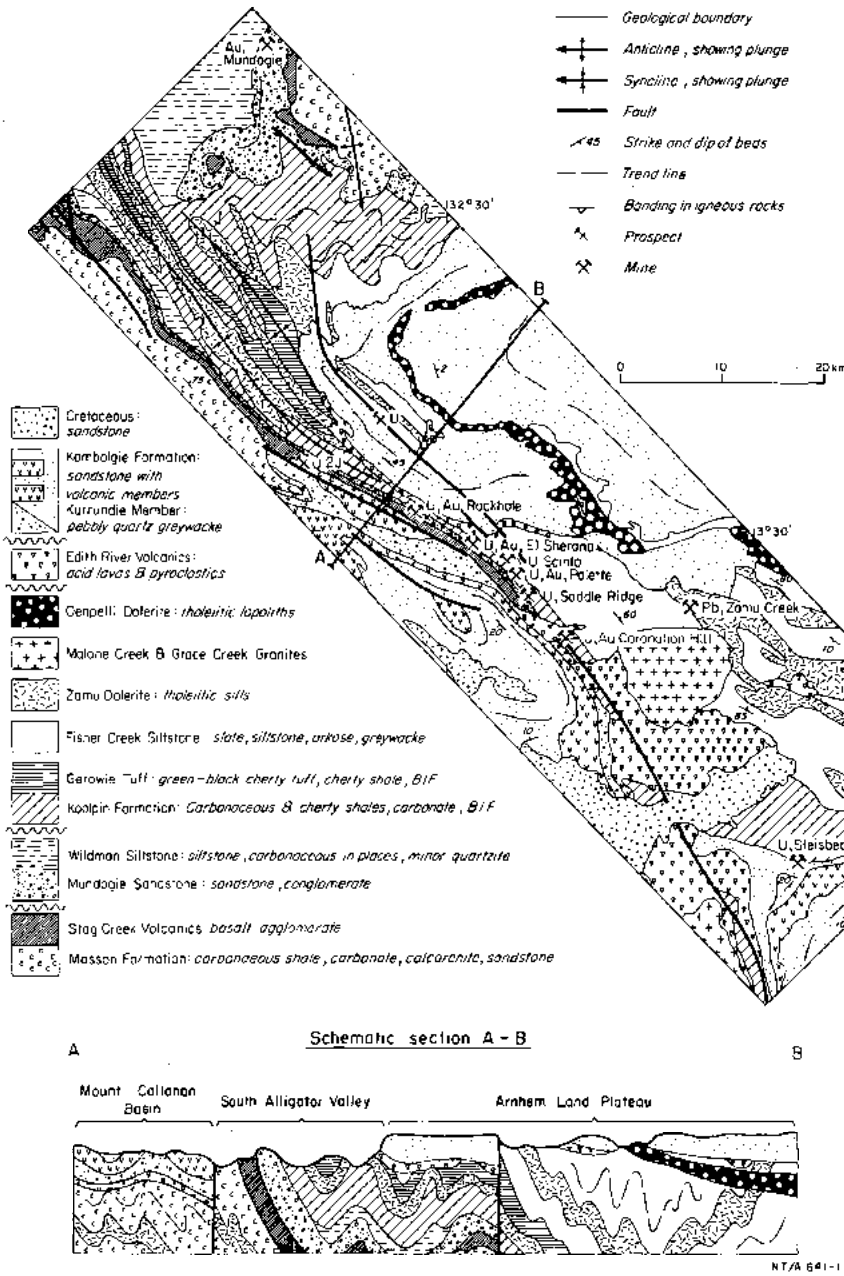


Figure 2. Geology of the South Alligator Valley Uranium Field.

siltstone, and calcareous sandstone. No Archaean basement is exposed, and Tucker *et al.* (this volume), using gravity modelling, consider depth to such basement to be 4-6km.

The Stag Creek Volcanics are unconformably overlain by the Mundogie Sandstone, which consists of quartz rudite and arenite. This unit, in turn, is unconformably overlain by the Koolpin Formation, the host to most of the uranium mineralisation in the SAVUF. The mineralisation was previously considered to occur at the same stratigraphic level as the uranium mineralisation in the Rum Jungle and Alligator Rivers Uranium Fields (Dodson *et al.*, 1974), but the Koolpin Formation is now considered to be at a higher stratigraphic level (Crick *et al.*, 1978a).

The Koolpin Formation in the SAVUF consists mainly of pyritic and carbonaceous pelitic sediments commonly containing bands, lenses and nodules of chert, and rare large lenses of stromatolitic carbonate. Pyritic argillites containing cherty interbeds (banded iron formation), carbonaceous slate, phyllitic shale and slate which in places are carbonaceous and rare fine grain calcareous sediments or marls are present in this formation (Shepherd, 1967). Overall, the Koolpin Formation is an iron formation belonging to the sulphide facies in the SAVUF.

A massive stromatolitic carbonate lens, near the base of the formation, crops out intermittently between Saddle Ridge and Coronation Hill. One large outcrop, 3km southeast of Saddle Ridge, has a thickness of 200-400m, and contains beds 2-3m thick of ripple-marked, slumped, and flaser-bedded dololutite and dolarenite, and stromatolitic dolomite (Muir & Jackson, 1978). The stromatolites present include distinctive branching columnar forms which are identified as *Katernia perlina* (Bertrand-Sarfati & Eriksson, 1977), and cf. *Pilbaria perplexa* (Walter, 1972). Both forms are found exclusively in Lower Proterozoic rocks. *Katernia perlina* (or very closely related forms) is known from the Labrador Geosyncline (Donaldson, 1963), dated at between 1800-2440 m.y. (Stockwell, 1964), from the Frere Formation of the Nabberu Basin (Hall & Goode, 1978) dated as greater than 1700 m.y. (identification confirmed by M.R. Walter, pers. comm.) and from the Transvaal Dolomite (Truswell & Eriksson, 1973) dated at 2224 ± 21 m.y. (D. Crompton, pers. comm. to Truswell & Eriksson, op. cit.).

The chert in the Koolpin Formation is considered by Walpole *et al.* (1968) to be silicified dolomite whereas Shepherd (1967) considers most of it to be primary. Stevens & Roberts (p.290 *in* Walpole *et al.*, 1968) observed that nodules and bands of chert were confined to bands containing a dolomite matrix in a drill-core sample of a thinly bedded pyritic carbonaceous marl from Rockhole mine. In places the dolomite matrix was partly replaced by cryptocrystalline silica to produce incipient chert nodules containing numerous dolomite lenticles. Rare dolomolds occur in chert bands and in places the bedding planes of pelitic sediments appear draped around chert nodules (Shepherd, 1967). It is therefore, probable that both primary and secondary chert occurs in the Koolpin Formation.

Conformably overlying the Koolpin Formation in the northern part of the SAVUF is the felsic Gerowie Tuff, formerly regarded as a silicified carbonate rock interfingering with the Koolpin Formation, but now known to be a mainly tuffaceous unit (Crick *et al.*, 1978b) which contains some variolitic basic flows (Needham *et al.*, 1978), minor ferruginous chert-nodular siltstones and banded iron formation. In the southern part of the SAVUF, the Koolpin Formation is faulted against the Fisher Creek Siltstone, the uppermost Lower Proterozoic unit.

Sills of Zamu Dolerite (Ferguson & Needham, 1978) were intruded into the Lower Proterozoic sequence at about the end of geosynclinal sedimentation. Non-radiogenic lead and zinc mineralisation occurs as veins associated with fluorite in one such sill at the Zamu Creek Mine (Hills & Richards, 1976).

The Lower Proterozoic sediments in the southern part of the field are intruded by the

Malone Creek Granite. This unit is a fine to medium-grained, massive aplitic granite containing accessory fluorite, allanite and monazite (Walpole *et al.*, 1968). Its age is about 1750 m.y. (Compston & Arriens, 1968), similar to that of the Edith River Volcanics, dated at 1760 m.y. (Leggo, p. 286, *in* Walpole *et al.*, 1968).

The Edith River Volcanics which unconformably overlie the Lower Proterozoic sediments in the SAVUF, have been subdivided into three inter-fingering members; the Coronation Member, which contains valley-fill deposits of arenite, rudite, and volcanics; the Scinto Breccia Member, composed of quartz breccia which is hematitic in places; and the Pul Pul Rhyolite Member, consisting mainly of green and pink rhyolite and ignimbrite (Walpole *et al.*, 1968). Three volcanic necks near Coronation Hill containing volcanic and Lower Proterozoic sedimentary rock fragments are probably local feeder centres for the Edith River Volcanics (Walpole *et al.*, 1968). Uranium and minor gold and copper mineralisation occurs in one of the breccias (Coronation Hill Deposit). A disconformable to unconformable contact between the Edith River Volcanics and the overlying Kombolgie Formation probably represents a considerable time-break (Needham *et al.*, this volume).

The Kombolgie Formation is represented by a 1500m thick sequence of sandstone and volcanics on the southwestern side of the South Alligator River valley, but consists of only 600m of sandstone on the northeastern side.

Correlations and Environment of Deposition of the Koolpin Formation

The Koolpin Formation carbonate sequence has many parallels with the Transvaal Dolomite, in addition to the overall stromatolite sequences. The rock-types of the Koolpin Formation for example, are strikingly similar to those of the Chuniespoort and Campbell-Griquatown Groups (which include the Transvaal Dolomite) in South Africa and the Hamersley Group of Western Australia. Button (1976) considers the Chuniespoort, Campbell-Griquatown and Hamersley Groups to have formed contemporaneously. We suggest the Koolpin Formation is probably similar in age to these rocks (between 2000 and 2300 m.y.).

Bertrand-Sarfati & Eriksson (1977) have used the model developed by Truswell & Eriksson (1973) to determine the depositional environments of the Transvaal Dolomite stromatolites. Both the stromatolites identified from the Koolpin Formation are intertidal forms, and this interpretation is supported by evidence for high-energy, shallow water environments provided by interbedded clastic carbonates. Small prismatic gypsum pseudomorphs are common in some beds in the Koolpin Formation, indicating a certain degree of hypersalinity. They differ markedly in type and quantity from the gypsum pseudomorphs of the Rum Jungle and Alligator Rivers Uranium Fields (Crick & Muir, this volume), and may represent primary gypsum deposited directly from sea water. There does not appear to have been sufficient gypsum present here to initiate diapirism as may have occurred in the other two uranium fields in the geosyncline, and we do not believe that this Koolpin Formation gypsum played any significant role in mineralisation.

The upper part of the Koolpin Formation, the 'carbonaceous siltstones' of Walpole *et al.* (1968), consists of interbeds of cherty iron formations and pyritic carbonaceous shale. The carbonaceous shale contains abundant highly carbonised kerogen and graphite and in places resembles anthracite. Similar coaly rocks ('shungite', 'anthracite', 'thucholite') have been found in Greenland, Karelia, Labrador, U.S.A., Brazil, South Africa (Penge Iron Formation - Transvaal Dolomite and Witwatersrand Group) (Muir, 1979), and in the Glengarry Sub-Basin of the Nabberu Basin (Horwitz & Smith, 1978). With the exception of the Witwatersrand thucholite occurrences, these coaly rocks fall within the age range 1700-2400 m.y. (Muir, 1979). One sample from El Sherana suspected to be thucolite was thoroughly tested but contained no hydrocarbons (Shepherd, 1967). Traces of uranium, thorium and gold occur in the South Alligator shungite (Karkhanis, 1976).

From collections at the tips of Rockhole, O'Dwyers, Teagues, and El Sherana Mines, it is evident that the shungite and pyritic carbonaceous shale are abundant. Organic matter can only accumulate under reducing (Hemingway, 1968) and acid conditions (Nicholls, 1968). Such conditions are not normally encountered in marine environments, as oxidising and neutral to alkaline conditions prevail at the sediment-water interface. Thus for substantial accumulations of coal to be preserved, fresh to only very slightly brackish water conditions are essential (Hemingway, 1968). Fresh-water depositional conditions in the Koolpin Formation carbonaceous beds are not inconsistent with their association with ironstone. Modern bog iron ores are precipitated under fresh-water conditions in lakes formed in depressions on peat surfaces; at the fresh water-peat surface, iron is oxidised and precipitated as hydroxide, but between peat layers it is deposited as siderite or vivianite (Carlson *et al.*, 1978). If the Koolpin ironstones were formed in a similar manner, it is possible that the carbonaceous beds of the Koolpin Formation were precipitated under fresh-water, stagnant conditions.

URANIUM DEPOSITS

General

Uranium mineralisation occurs in a variety of rock types, mainly within the Koolpin Formation but also within the Edith River Volcanics, Stag Creek Volcanics (Foy & Miezitis, 1977) and possibly in the Masson Formation. Mineralisation is located mainly in faults, shears, breccias and joints close to and on the contact between the Lower Proterozoic and Middle Proterozoic (Carpentarian) rocks.

Rockhole Area

Deposits in this area, the most northwesterly in the field, are closely spaced and consist of three main concentrations (Rockhole, Teagues & O'Dwyers) having a total recorded production of 152 tonnes of U_3O_8 (Ingram, 1974). Secondary uranium mineralisation and pitchblende with a gummite sheath was originally found on the surface along a shear zone about 750m long developed in prominently banded marls containing lenses and elongate nodules of chert in the Koolpin Formation and, at the southeast end, in the Edith River Volcanics (Ostle, 1956).

Uranium ore was extracted by underground mining mainly from stringers, pods and lenses of pitchblende and from sooty fracture coatings in shoots 2cm to 2m wide (Taylor, 1969). Prichard (1957) reports anastomozing veins of pitchblende in carbonaceous dolomitic shales adjacent to a band of sheared graphitic slate in the Koolpin Formation, and pitchblende veins up to 7cm wide in fractures within the Coronation member of the Edith River Volcanics.

At the Rockhole mine (Fig. 3) the ore occurs in the Koolpin Formation mainly at the contact of carbonaceous shales and cherty ferruginous siltstones in the hanging wall of at least two moderate to high-angle reverse faults, and also in joints and shears in the footwall in the Coronation Member of the Edith River Volcanics (Taylor, 1969). Threadgold (1960) reports that some of the ore occurred as pitchblende veinlets less than 2mm wide in chert. The ore was associated with up to 2% pyrite, a little marcasite and chalcopyrite, trace lead, iron and copper selenides and gold; the only sample analysed was thorium free (Threadgold, 1960). A major reverse fault with a throw in excess of 100m, which separates the Edith River Volcanics from the Koolpin Formation, lies adjacent to the mineralisation and in places contains ore (Hare, 1961). The fault-plane has been affected by later faulting and folding and both Hare (op. cit.) and Shepherd (1967) consider that the ore was introduced at this stage, and was concentrated in 'kinks' or tension cracks.

El Sherana area

This area is 7km southeast of the Rockhole area and is probably near the same major fault that passes through the Rockhole area. Two deposits here were mined for uranium and gold, El Sherana (226 tonnes, U_3O_8; Needham, 1978) and El Sherana West (185 tonnes, U_3O_8; Needham, 1978) (Fig. 4), both mainly in Koolpin Formation.

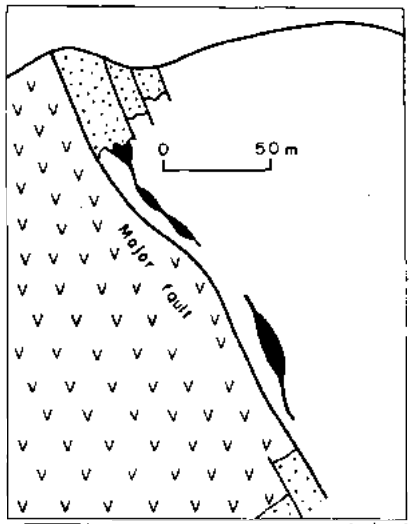


Figure 3. Composite cross-section of the Rockhole Mine. After Hare (1961) and Ayres & Eadington (1975).

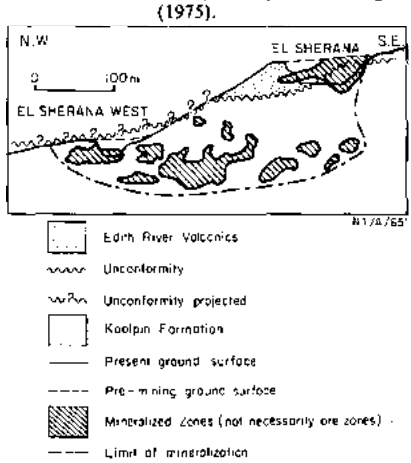


Figure 4. Longitudinal projection of El Sherana and El Sherana West. After Foy (1975).

Mineralisation consists of massive segregations, veins, and disseminations of pitchblende, mainly in fractures in cherty ferruginous siltstone and only rarely in carbonaceous beds (Taylor, 1969). The massive pitchblende occurred in places as nodules, up to 25cm in diameter, commonly displaying radial and concentric cracks. Gold was found in one specimen in a concentric crack, suggesting it had formed after the pitchblende (Shepherd, 1967). Galena and anglesite stringers are common, and the lead content of pitchblende ore from El Sherana was in places as high as 5% (Shepherd, op. cit.). The ore-body at El Sherana is carrot shaped, resulting from a secondary uranium mineral dispersion halo, some of the secondary minerals having dispersed into overlying sandstone of the Coronation Member of the Edith River Volcanics (Shepherd, op. cit.). In places, massive pitchblende encloses fragments or residuals of chert containing minor arsenides (Threadgold, 1960).

Mineralisation occurs patchily along strike to El Sherana West (Foy, 1975).

Scinto/Koolpin Creek Area

Between El Sherana and the next major deposit, Palette, about 6km to the southeast, lie three small deposits; Koolpin Creek, Scinto 5 and Scinto 6, and a number of prospects.

Mineralisation at Koolpin Creek lies within a sheared zone of the Koolpin Formation (Ostle, 1956) and consists of sooty pitchblende and some thin stringers of pitchblende occupying fractures in black shales and phyllite. Middle Proterozoic (Carpentarian) rocks originally overlying the deposit have been removed by erosion but the projected unconformity surface must have been in excess of 30m above the present land surface indicating that most of the ore has probably been eroded away (Shepherd, 1967).

Scinto 5 (recorded production 22 tonnes U_3O_8) is located in bleached white and red ferruginous shales of the Koolpin Formation near a steep sheared contact with the Edith River Volcanics (Dunn, 1960). Scinto 6 (3 tonnes, U_3O_8) occurs in sheared and jointed volcanics possibly belonging to the Edith Creek Volcanics (Matheson, 1960; Ostle, 1956) but may be Lower Proterozoic Zamu Dolerite (Shepherd,

1975). Some pitchblende was found at Scinto 5, but only secondary uranium mineralisation was found at Scinto 6.

A number of prospects, some merely radioactive anomalies, are found in this area in either the Koolpin Formation or Edith River Volcanics, close to their contact. Of particular interest is the Stockpile Prospect, which occurs in an outlier of Edith River Volcanics overlying the Mundogie Sandstone (Matheson, 1960). A yellow powdery unidentified uranium mineral was found distributed in aphanitic rhyolite which in thin section showed 'nests' of fine-grained pitchblende and secondary alteration products, unrelated to microfractures, indicating that at least some of the uranium is syngenetic (Shepherd, 1967).

Palette Deposit

This deposit (124 tonnes U_3O_8; Ingram, 1974) is located in sandstone of the Coronation Member of the Edith River Volcanics and Koolpin Formation just beneath the unconformity (Fig. 5). Most mineralisation occurs within small shears and fractures of the sandstone (Dunn, 1960), but some occurs in greenish siltstone and weathered banded ironstone of the Koolpin Formation (Matheson, 1960).

The deposit contained rich ore shoots composed of vein and nodular pitchblende similar to that of El Sherana; some of the nodular pitchblende shows imperfectly developed radial and concentric cracks (Shepherd, 1967). Significant quantities of native gold occur as veins in the pitchblende, along with minor amounts of pyrite, chalcopyrite, galena and marcasite. Fine hematite is associated with the pitchblende in the sandstone, which is a coarsely mottled greyish pink rock studded with creamy-white ellipsoidal patches. The greyish pink sandstone contains apatite which is more or less completely replaced by a fine-grained aggregate of phosphouranylite within about 8cm of pitchblende veins. It also contains fine hematite, sericite and minor tourmaline. These minerals are not found in the creamy-white ellipsoidal patches, indicating that they were introduced into the sandstone during the pitchblende mineralisation (Threadgold, 1960).

Saddle Ridge Area

Between the Palette Deposit and the Coronation Hill deposit, 7km to the southeast, lie two small deposits and a number of prospects, some only radioactive anomalies, all clustered within a 1.5km radius of the Saddle Ridge deposit, 2km south-southeast of Palette.

The Saddle Ridge deposit (78 tonnes, U_3O_8; Needham, 1978) is elongated along a steeply dipping cross-fault separating rhyolites and tuffs of the Edith River Volcanics from bleached shales of the Koolpin Formation (Sherpherd, 1967). It is composed almost entirely of secondary uranium minerals (Ostle, 1956), mainly meta-torbernite, which occur within the Koolpin Formation and to a lesser extent within the Edith River Volcanics (Ostle, 1956). Shepherd & Grenning (1961) report that sooty pitchblende occurred in a 2m length of drill core, obtained 85m below surface beneath the present open cut from an inclined drill hole. The other small deposit, Skull, 300m southeast of Palette, consisted of small nodules of pitchblende in shears in carbonaceous shale of the Koolpin Formation adjacent to the Middle Proterozoic (Carpentarian) unconformity (Shepherd, 1967).

One of the small prospects in this area, the BMR No. 1 anomaly, or Saddle Ridge South Prospect, lies 800m southeast of Saddle Ridge in phosphatic, hematitic cherty breccia (Ostle, 1956) belonging to the Scinto Breccia Member of the Edith River Volcanics. A shaft sunk into the breccia at this prospect passed down into massive carbonate containing fissures of anomalously radioactive red clay (Dunn, 1960). This indicates that the breccia, rather than being a discrete unit formed at the same time as the Edith River Volcanics, probably formed as a carbonate hardground or regolith. Similar phosphatic cherty breccias are found at Sleisbeck, and also in the Rum Jungle area (Walpole *et al.*, 1968).

Another interesting prospect, Saddle Ridge East, 800m east of Saddle Ridge, contains minor amounts of torbernite, some of which fill amygdales in lavas of the Edith River

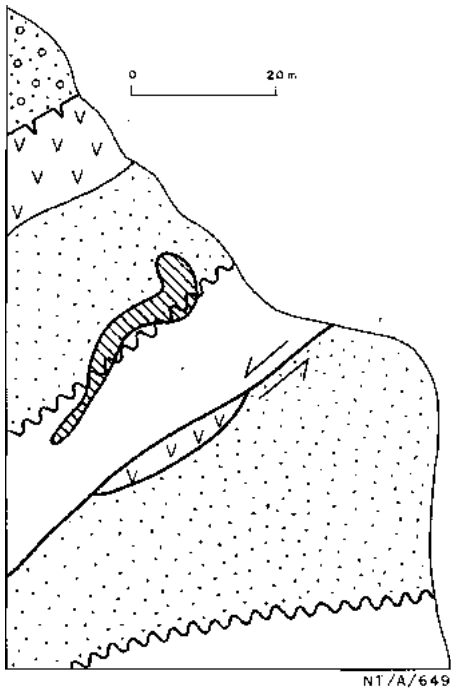


Figure 5. Generalised cross section of Palette. After Shepherd (1967).

Volcanics close to unconformably underlying Lower Proterozoic sediments (Shepherd, 1967).

Coronation Hill Area

The Coronation Hill deposit (75 tonnes, U_3O_8; Ingram, 1974) is located 6km southeast of Saddle Ridge. Mineralisation occurs within a 20m diameter volcanic pipe filled with fragments of altered Edith River Volcanics and Lower Proterozoic rocks (Walpole *et al.*, 1968). This pipe is one of several known in this area, but is the only one mineralised. Pitchblende, much of it the sooty variety, is the primary ore. It is associated with gold which is places forms separate ore-shoots in the ore-body (Shepherd, 1967). Minor secondary uranium mineralisation, associated with wavellite, occurs in highly faulted quartzites of the Edith River Volcanics, well above the unconformity, about 120m southwest of the Coronation Hill deposit.

Sleisbeck Deposit

Sleisbeck is an isolated deposit (3 tonnes, U_3O_8; Ingram, 1974) some 30km southeast of Coronation Hill. It is included in the SAVUF as it lies along the same general trend as the other deposits. The ore consists of pitchblende and secondary uranium minerals associated with phosphate and minor, Cu, Ni, Co and As, and occurs in chloritic and carbonaceous schists, quartzites and mudstones (Newton, 1955). The quartzite is generally homogeneous at depth but is fractured and hematite-veined on the surface, and may have been originally a calcareous sandstone (Newton, op. cit.) similar to that of the Masson Formation, exposed 60km to the northwest (Needham *et al.*, 1978). The exposed fractured hematitic quartzite is associated with phosphatic rock, and is considered by Walpole *et al.* (1968) to have been originally a carbonate belonging to the Koolpin Formation.

Ores at Rockhole, El Sherana and Palette

Threadgold (1960) reports that there is a minor development of a second generation of pitchblende commonly occurring as veinlets cross-cutting older pitchblende. At the surface at El Sherana and Palette and to a lesser extent at Rockhole, the pitchblende ores have been extensively oxidised, giving rise to a wide variety of secondary minerals - oxides, carbonates, sulphates, phosphates, vanadates, and silicates. Rutherfordine was the most abundant secondary uranium mineral at El Sherana but was not found at Palette. Phosphouranylite and uranophane are the most abundant secondaries at Palette.

Threadgold (1960) comments that the paragenesis of the ores is not wholly clear but the apparent sequence is:

1) Niccolite, cobalt-nickel arsenides, gersdorffite, (?) pyrite
2) Pitchblende (main)
3) (?) Pyrite, marcasite, chalcopyrite, galena-clausthalite, (?) nickel selenide, gold, quartz, siderite, hematite
4) Pitchblende (very minor).

Age of the Deposits

Hills & Richards (1972), re-interpreting the data of Greenhalgh & Jeffrey (1959), found that five pitchblende samples from the El Sherana, Palette and Sleisbeck deposits give a concordant age of about 800 m.y., and two from Palette lie close to concordia at 500 m.y. Cooper (1973), using the same data, came to much the same conclusions, and suggested that the five samples from El Sherana, Palette and Sleisbeck show either an episodic lead loss age of 710 m.y. or a continuous diffusion age of 815 m.y., whereas the two samples from Palette suggest another mineralization or a secondary solution and redeposition of uranium at 500 m.y. The 500 m.y. age may be related to the minor development of second generation pitchblende in the Rockhole, El Sherana and Palette ores observed by Threadgold (1960).

URANIUM ORE GENESIS MODELS

Models proposed for uranium ore genesis in the SAVUF range from syngenetic, with minor remobilization, to hydrothermal.

Condon & Walpole (1955) note that the uranium was commonly associated with quartz-hematite or quartzite breccia which they considered to be silicified carbonate breccia formed originally by wave-action on algal bioherms. They suggest that chemical changes over short distances near bioherms were responsible for concentrating uranium during deposition of the Koolpin Formation and elsewhere, and that diagenetic or orogenic processes mobilized and concentrated uranium in nearby structural traps. Prichard (1965) considers the source of uranium was the Koolpin Formation, and that the ore-bodies were formed by supergene processes, the carbonaceous beds forming a suitable reducing environment for precipitation of uranium. Dodson *et al.* (1974) also consider the Koolpin Formation to be the source, and suggest that concentration of uranium occurred during the major 1800 m.y. igneous and tectonic event, and was later relocated and redeposited nearby by circulating leaching fluids. They suggest the Saddle Ridge deposit was formed by supergene enrichment, as it is close to the present-day land-surface, and that other deposits, such as Palette, were formed through hypogene enrichment.

Threadgold (1960) considers the association of colbalt nickel arsenides, selenium-bearing sulphides, and native gold at El Sherana and Palette as indicating that ascending hydrothermal fluids were responsible for the pitchblende ores, a view supported by Stewart (1965), Taylor (1969) and Shepherd (1967).

Stewart (1965) considers the uranium mineralization originated from the same magmatic source as the Edith River Volcanics because the volcanics, especially the Pul Pul Rhyolite Member, commonly show high radioactivity. Taylor (1969) points to the paragenetic association of the ores given by Threadgold (1960) and the kaolinisation and bleaching of carbonaceous shales, even in unoxidised zones of some deposits, plus introduction of sericite, tourmaline and apatite into the wall-rocks of the Palette mine (Threadgold, op. cit.), as indicating a hydrothermal origin. He considers magmatic activity at depth, associated with the Edith River Volcanics, and the ore-forming fluids are interrelated, the fluids being introduced through the major fault structures common to many deposits.

Shepherd (1967) describes the ore-bodies as "epigenetic fissure vein deposits occurring

in faults", and states that the presence of mercury, tellurium, selenium, lead, copper and phosphorous, indicates a magmatic source.

Foy (1975) favours an epigenetic model in which acidic oxidised groundwaters leached uranium from the Edith River Volcanics and passed through porous sandstone until a fracture zone allowed them to descend and be deposited in the reducing environment of the underlying Koolpin Formation. A similar model is also proposed by Ayres & Eadington (1975), who cite the preliminary sulphur isotope results from Rockhole and El Sherana as being typical of a low-temperature sedimentary source, and the geochemical association of uranium with vanadium and gallium as indicating transportation of uranium in groundwaters.

Donnelly & Ferguson (this volume) find, from sulphur isotope studies, that the bedded sulphides in the Pine Creek Geosyncline have a magmatic origin, whereas sulphides in the ore-zones in the Alligator Rivers Uranium Field have a wide range of values indicative of low-temperature biological sulphate reduction processes. They suggest that Ayres & Eadington's (1975) results also fit this model.

DISCUSSION

Syngenetic concentration of uranium in carbonaceous shales is commonly advocated by workers in the Pine Creek Geosyncline. In support of this, analyses of shales in the Koolpin Formation by Ayres & Eadington (1975) in the SAVUF show above average uranium contents. Also, Crick *et al.* (1978b) report that the Gerowie Tuff overlying the Koolpin Formation in the SAVUF is anomalously radioactive. Both formations are exposed extensively in the Pine Creek Geosycline but only one small deposit of uranium, the Fleur de Lys (0.15 tonnes, U_3O_8) is found at this stratigraphic level outside the SAVUF. Therefore the Koolpin Formation or Gerowie Tuff probably did not contribute significant quantities of syngenetic uranium to form the ore bodies of the SAVUF.

The suggestion by Ayres & Eadington (1975) and Foy (1975) that the Edith River Volcanics is the source appears to be the most plausible as the volcanic members are commonly radioactive and contain syngenetic pitchblende (Shepherd, 1967). As most of the deposits lie close to the contact between the Edith River Volcanics and the underlying Koolpin Formation it seems likely that descending waters, not ascending waters as suggested by some authors, leached uranium from the Edith River Volcanics before depositing it in suitable chemical-structural traps found mainly in the Koolpin Formation.

Although the sulphur isotope and geochemical results of Ayres & Eadington (1975) suggest low-temperature emplacement of the ores at El Sherana and Rockhole by groundwaters, mineralogy of the gangue at Palette and presence of ore in a volcanic neck at Coronation Hill is highly suggestive of hydrothermal emplacement. Heated uranium-enriched groundwaters which had passed through the volcanic members of the Edith River Volcanics during or soon after their deposition at about 1760 m.y. could have played a role. The ca. 800 m.y. pitchblende from Palette may only be remobilized uranium from an earlier concentration. However, more research is required, especially on the Coronation Hill deposit where very few details are known, before any firm answer can be given on this aspect.

No obvious local geological evidence points to an event that explains the pitchblende ages, which appear to be reliable ages, of ca. 800 m.y. and 500 m.y. There is a gap in the geological record of about 1500 m.y. between deposition of the Kombolgie Formation at ca 1650 m.y. (Page *et al.*, this volume) and the Cretaceous Petrel Formation which unconformably overlies the Kombolgie Formation in the southwestern part of the SAVUF.

Post-Kombolgie Formation faulting and jointing may have allowed leaching and transporting groundwaters access to the Edith River Volcanics and Koolpin Formation or remobilised pre-existing concentrations. Most of the deposits are on, or close to, major faults.

Hegge & Rowntree (1978) consider rejuvenation of the South Alligator River lineament and parallel block faulting of the Kombolgie Formation in the Late Proterozoic may have remobilised uranium in the Alligator Rivers Uranium Field. The 500 m.y. pitchblende age from Palette in the SAVUF coincides with the age of formation of the Daly River Basin but it is uncertain as to what affect this had on the SAVUF, about 100km to the northeast.

One possibility, not previously considered, is that major climatic changes, such as the onset of a pluvial period (i.e. a period of abundant rainfall) commonly associated with a glacial period (Flint, 1957), may have rejuvenated or expanded the groundwater regime in the SAVUF, thus substantially increasing the amounts of uranium being leached from the Edith River Volcanics, primarily, and being deposited or remobilisd to form the present concentrations. There is widespread evidence that glaciation, dated at 723 ± 30 m.y. and 651 ± 43 m.y. in the Kimberleys (Bofinger, 1967) affected large areas of Australia during the Late Proterozoic (Dunn *et al.*, 1971). Glaciogenic sediments of the same age in the Victoria Rivers Region adjacent to the Pine Creek Geosyncline and in the Kimberleys, unconformably overlie sediments containing carbonates, red-beds and evaporites indicating that arid conditions commonly prevailed before the onset of glaciation. Although there are no preserved sediments of that age in the Pine Creek Geosyncline, indicating it may have been above sea-level at that time, these glacial periods probably had an impact on the climatic and groundwater regimes. The oldest pitchblende dated in the SAVUF (710-815 m.y., Cooper, 1973) from El Sherana, Palette and Sleisbeck may therefore have been transported to form these deposits during a pluvial period associated with the Late Proterozoic glacial periods. The 500 m.y. age obtained for two samples from Palette indicates a minor degree of remobilisation possibly in response to tectonic activity related to the formation of the Daly River Basin.

However, the ca. 800 m.y. pitchblende age may only indicate that a major period of remobilisation of pre-existing concentrations of uranium took place at that time. The presence of an unconformity between the Edith River Volcanics and Kombolgie Formation (Needham *et al.*, this volume) suggests that there was ample time (about 150 m.y.) for leaching of the volcanics to take place prior to deposition of the Kombolgie Formation, unless climatic conditions were particularly arid.

SUMMARY

Uranium mineralization in the SAVUF is mainly associated with carbonaceous pyritic argillites, which are commonly chert banded, of the Lower Proterozoic Koolpin Formation. In one deposit (Palette) the mineralization is found in both the Koolpin Formation and in sandstones of the unconformably overlying Edith River Volcanics. Most deposits occur close to this unconformity, on or near major faults. Primary mineralization is commonly nodular to vein-type pitchblende which has been dated at about 800 m.y. and 500 m.y. Substantial secondary uranium mineralization and gold is commonly associated with the pitchblende.

Models proposed for the genesis of the deposits range from syngenetic with minor remobilisation within the Koolpin Formation, to hydrothermal related to magmatic activity. We consider that syngenetic uranium in the Koolpin Formation did not significantly contribute towards formation of these deposits and that the Edith River Volcanics were the most likely source. The ores at El Sherana and Rockhole were probably formed through the action of ground-waters depositing uranium, leached from the Edith River Volcanics, in the reducing environment of the Koolpin Formation.

The mineralogy associated with the Palette deposit and the location of ore in a volcanic neck at Coronation Hill is suggestive of hydrothermal emplacement although further research into this aspect is necessary. It is possible that some uranium concentrations were initially formed by hydrothermal activity during deposition of the Edith River Volcanics at

1760 m.y. and during the period before deposition of the Kombolgie Formation by ground-water activity.

Pitchblende ages of about 800 m.y. and 500 m.y. appear to be reliable and cannot be directly correlated to local geological events in the SAVUF. Emplacement of ore at 800 m.y. may be related to tectonic activity or, as we suggest, possibly due to a relatively rapid expansion of the ground-water system in response to a pluvial period associated with a major glacial period. The 500 m.y. pitchblende, found only at Palette, indicates a minor episode of emplacement possibly related to tectonic acitivity associated with the formation of the Daly River Basin.

ACKNOWLEDGEMENTS

We gratefully thank J.H. Shepherd for permission to quote from his Ph.D. thesis and Y. Miezitis, J. Jackson, C.P. Pedersen, D.H. Blake and W.B. Dallwitz for their comments.

This paper is published with the permission of the Director of the Bureau of Mineral Resources, Geology and Geophysics, Canberra, Australia.

REFERENCES

Ayres, D.E., & Eadington, P.J., 1975: Uranium mineralization in the South Alligator Valley. *Miner. Deposita, 10,* 27-41.

Bertrand-Sarfati, J., & Eriksson, K.A., 1977: Columnar stromatolites from the early Proterozoic Schmidtsdrift Formation, Northern Cape Province, South Africa - Part 1: Systematic and diagnostic features. *Palaeont. Afr., 1977,* 1-26.

Bofinger, V.M., 1967: Geochronology in the East Kimberley area of Western Australia. *Ph.D. thesis, Australian National University,* (unpubl.).

Button, A. 1976: Transvaal and Hamersley Basins - Review of Basin Development and Mineral Deposits. *Minerals, Science and Engineering, 8,* 262-293.

Carlson, L., Koljonen, T., & Vuorinen, A., 1978: The precipitation of iron and manganese in Fennoscandia: geology and geochemistry. *in* (W.E. Krumbein) *Environmental Biogeochemistry and Geomicrobiology Volume 2: The Terrestrial Environment.* Ann Arbor Science, Ann Arbor, Michigan, 503-513.

Compston, W., & Arriens, P.A., 1968: The Precambrian geochronology of Australia. *Can. J. Earth Sci., 5,* 561-583.

Condon, M.A., & Walpole, B.P., 1955: Sedimentary Environment as a control of uranium mineralization in the Katherine-Darwin Region, Northern Territory. *Rep. Bur. Miner. Resour. Geol. Geophys. Aust., 24,* 17p.

Cooper, J.A., 1973: On the age of uranium mineralization at Nabarlek, N.T., Australia. *J. geol. Soc. Aust., 19,* 483-486.

Crick, I.H. & Muir, M.D., this volume: Evaporites and uranium mineralization in the Pine Creek Geosyncline. *Proceedings of the International Uranium Symposium on the Pine Creek Geosyncline.*

Crick, I.H., Stuart-Smith, P.G., & Needham, R.S., 1978a: Recent advances in the understanding of the Lower Proterozoic stratigraphy, Pine Creek Geosyncline. *Rec. Bur. Miner. Resour. Geol. Geophys. Aust., 1978/21.*

Crick, I.H., Stuart-Smith, P.G., & Needham, R.S., 1978b: Stratigraphic significance of a discovery of Lower Proterozoic tuff in the Pine Creek Geosyncline. *BMR J. Aust. Geol. Geophys., 3,* 163-165.

Crohn, P.W., 1968: The mines and mineral deposits of the Katherine-Darwin region *in* Walpole, B.P., Crohn, P.W., Dunn, P.R., & Randal, M.A., 1968, Geology of the Katherine-Darwin Region, Northern Territory. *Bull. Bur. Miner. Resour. Geol. Geophys. Aust., 82,* 304p.

Dodson, R.G., Needham, R.S., Wilkes, P.G., Page, R.W., Smart, P.G. & Watchman, A.L., 1974: Uranium mineralisation in the Rum Jungle - Alligator Rivers Province, Northern Territory, Australia *in* Formation of Uranium Ore Deposits, International Atomic Energy Agency, Vienna, 551-568.

Donaldson, J.A., 1963: Stromatolites in the Denault Formation, Marion Lake, coast of Labrador, Newfoundland. *Bull. geol. Surv. Can., 102,* 33p.

Donnelly, T.H., & Ferguson, John, this volume: A stable isotope study of three deposits in the Alligator Rivers Uranium Field, N.T. *Proceedings of the International Uranium Symposium on the Pine Creek Geosyncline.*

Dunn, P.R., 1960: Report on a quarterly inspection of the South Alligator River Uranium area, Northern Territory. *Bur. Miner. Resour. Geol. Geophys. Aust., unnumbered Record,* (unpubl.)

Dunn, P.R., Plumb, K.A., & Roberts, H.G., 1966: A proposal for time-stratigraphic subdivision of the Australian Precambrian. *J. geol. Soc. Aust., 13(2),* 593-608.

Ferguson, John, & Needham, R.S., 1978: The Zamu Dolerite: A Lower Proterozoic pre-orogenic continental tholeiitic suite from the Northern Territory, Australia. *J. geol. Soc. Aust., 25,* 309-322.

Flint, R.F., 1957: *Glacial and Pleistocene Geology.* John Wiley and Sons, N.Y.

Foy, M.F., 1975: South Alligator Valley Uranium Deposits *in* (ed. C.L. Knight) *Economic Geology of Australia and Papua New Guinea, Australas. Inst. Min. Metall., Monograph Series No. 5, 1. Metals,* 301-304.

Foy, M.F., & Miezitis, Y., 1977: Uranium mineralization at Anomaly 2J, South Alligator Valley, Northern Territory, and its significance concerning regional structure and stratigraphy. *Proc. Australas. Inst. Min. Metall., 261,* 1-11.

Greenhalgh, D., & Jeffery, P.M., 1959: A contribution to the geochronology of Australia. *Geochim. cosmochim. Acta, 16,* 39-57.

Hall, W.D.M., & Goode, A.D.T., 1978: The early Proterozoic Nabberu Basin and associated iron formations of Western Australia. *Precambrian Research, 7,* 129-184.

Hare, R., 1961: *Structural control of pitchblende mineralization at the Rockhole Mine, N.T., Australia.* (unpubl.).
Hegge, M.R., & Rowntree, J.C., 1978: Geologic setting and concepts on the origin of uranium deposits in the East Alligator River region, N.T., Australia. *Econ. Geol., 73(8),* 1420-1429.
Hemingway, J.E., 1968: Sedimentology of Coal-Bearing Strata. *in* (eds. D.G. Murchison & T.S. Westoll) *Coal and Coal-Bearing Strata.* Oliver & Boyd, Edinburgh, 43-70.
Hills, J.H., & Richards, J.R., 1972: The age of uranium mineralization in northern Australia. *Search, 3,* 382-385.
Hills, J.H., & Richards, J.R., 1976: Pitchblende and galena ages in the Alligator Rivers Region, Northern Territory, Australia. *Miner. Deposita, 11,* 133-154.
Horwitz, R.C., & Smith, R.E., 1978: Bridging the Yilgarn and Pilbara Blocks, Western Australia. *Precambrian Research, 6,* 293-322.
Ingram, J.A., 1974: Uranium Deposits. *Min. Resour. Rep. Bur. Miner. Resour. Geol. Geophys. Aust., 6.*
Karkhanis, S.N., 1976: Chemical studies on Organic Matter from Precambrian Rocks. *Ph.D. Thesis, Imperial College, University of London,* (unpubl.).
Matheson, R.S., 1960: *Report on holdings of United Uranium N.L., South Alligator River Area, Northern Territory.* (unpubl.).
Muir, M.D., 1979: A sabkha model for deposition of part of the Proterozoic McArthur Group of the Northern Territory, and implications for mineralization. *BMR J. Aust. Geol. Geophys., 4,* 149-162.
Muir, M.D., & Jackson, M.J., 1978: Report on a visit to the Batchelor and South Alligator River areas, 27-28 Sept. 1978. *Prof. Opinion, Bur. Miner. Resour. Geol. Geophys. Aust., 31,* 4. (unpubl.).
Needham, R.S., 1978: A regional analysis of the Pine Creek Geosyncline N.T., progress report. *James Cook University of Northern Queensland, Seminar Paper EL503,* (unpubl.).
Needham, R.S., Stuart-Smith, P.G., Crick, I.H. & Roarty, M.J., 1978: Mundogie 1:100,000 Sheet area, data record. *Rec. Bur. Miner. Resour. Geol. Geophys., 1978/103.*
Needham, R.S., Crick, I.H., & Stuart-Smith P.G., this volume: Regional Geology of the Pine Creek Geosyncline. *Proceedings of the International Uranium Symposium on the Pine Creek Geosyncline.*
Newton, H.J., 1955: The occurrence of uranium ore at Sleisbeck, N.T. *Proc. Australas. Inst. Min. Metall., 76,* 1-15.
Nicholls, G.D., 1968: The geochemistry of coal-bearing strata *in* (eds. D.G. Murchison & T.S. Westoll), *Coal and coal-bearing strata.* Oliver & Boyd, Edinburgh & London, 269-307.
Ostle, D., 1956: *Preliminary field report on the South Alligator-Sleisbeck Uranium Field. BMR Technical Files,* (unpubl.).
Page, R.W., Compston, W. & Needham, R.S., this volume: Geochronology and evolution of the late Archaean basement and Proterozoic rocks in the Alligators Rivers Uranium Fields, Northern Territory, Australia. *Proceedings of the International Uranium Symposium on the Pine Creek Geosyncline.*
Prichard, C.E., 1957: Report on a quarterly inspection of the South Alligator River Uranium area, Northern Territory. *Bur. Miner. Resour. Geol. Geophys. Aust., unnumbered Record* (unpubl.).
Prichard, C.E., 1965: Uranium ore deposits of the South Alligator River, *in* (ed. C.L. Knight) *Geology of Australian Ore Deposits. 8th Commonwealth Mining and Metallurgical Congress, 1,* 207-209.
Shepherd, J.S., 1967: Uranium in Northern Australia. *Ph.D. Thesis, University of Queensland* (unpubl.).
Shepherd, J.S. & Grenning, P.J., 1961: *Ore bodies of United Uranium N.L. holdings, South Alligator River, N.T.* (unpubl.).
Stewart, J.R., 1965: Middle Proterozoic rocks in the Katherine-Darwin area, Northern Territory. *Rep. Bur. Miner. Resour. Geol. Geophys. Aust., 90,* 23p.
Stockwell, C.H., 1964: Fourth report on structural provinces, orogenies, and time-classifications of the Canadian Precambrian Shield. *Geol. Surv. Pap. Can., 64-17 (11),* 1-21.
Stuart-Smith, P.G., Wills, K., Crick, I.H. & Needham, R.S., this volume: Evolution of the Pine Creek Geosyncline. *Proceedings of the International Uranium Symposium on the Pine Creek Geosyncline.*
Taylor, J., 1969: Origin and controls of uranium mineralization in the South Alligator Valley. *Atom. Energy, Sydney, 12,* 18-24.
Threadgold, I.M., 1960: The mineral composition of some uranium ores from the South Alligator River area, N.T. *CSIRO, Melbourne, Mineragraphic Investigations Technical Paper No. 2,* 53.
Truswell, J.F., & Eriksson, K.A., 1973: Stromatolitic associations and their palaeoenvironmental significance; re-appraisal of a Lower Proterozoic locality from the Northern Cape Province, South Africa. *Sediment Geol., 10,* 1-23.
Walter, M.R., 1972: Stromatolites and the biostratigraphy of the Australian Precambrian & Cambrian. *Spec. Pap. Palaeontol., 11,* 1-190.
Walpole, B.P. Crohn, P.W. Dunn, P.R. & Randal, M.A., 1968: Geology of the Katherine-Darwin Region, Northern Territory. *Bull. Bur. Miner. Resour. Geol. Geophys. Aust., 82,* 304p.

GEOLOGY AND EXPLORATION OF THE RUM JUNGLE URANIUM FIELD

W. J. Fraser

C.R.A. Exploration Pty Ltd., P.O. Box 39598, Winnellie, N.T., 5789, Australia.

ABSTRACT

The Rum Jungle Uranium Field was discovered by a private prospector in 1949. A total of 3530 tonnes of uranium oxide was mined and treated from four ore-bodies by Territory Enterprises Pty. Limited who managed the Rum Jungle Project on behalf of the Australian Atomic Energy Commission until the closure of operations in 1971. One small low grade uranium orebody remains to be developed. Lead, zinc, copper, cobalt and nickel were found zoned sub vertically with uranium at one deposit. One medium sized lead, zinc, copper, cobalt and nickel deposit remains to be developed and one small copper deposit with minor uranium was mined. The basemetal deposits show a regional zoning relationship with the known uranium mineralization. Uranium and basemetal mineralization is hosted by graphitic or chloritic, pyritic shales at the contact with a magnesite. These rocks are in the lower part of a sequence of Lower Proterozoic sediments which uncomforably overlie Archaean basement complexes. The sediments and complexes are displaced by Giants Reef Fault and sub-parallel shears and linears may further control mineralization. Nearly 50km of the prospective shale/magnesite contact was tested by total count radiometric surveys, various electrical methods, auger, rotary percussion and diamond drilling. The soure for the uranium mineralization was probably the Archaean basement complexes from which uranium was initially deposited as protore by either chemical precipitation or clay adsorption in the shale units or as detrital placers in quartz pebble conglomerates immediately overlying the basement complexes.

INTRODUCTION

The Rum Jungle Uranium Field is about 70km south east of Darwin. The township of Batchelor, population 250, is central to the field.

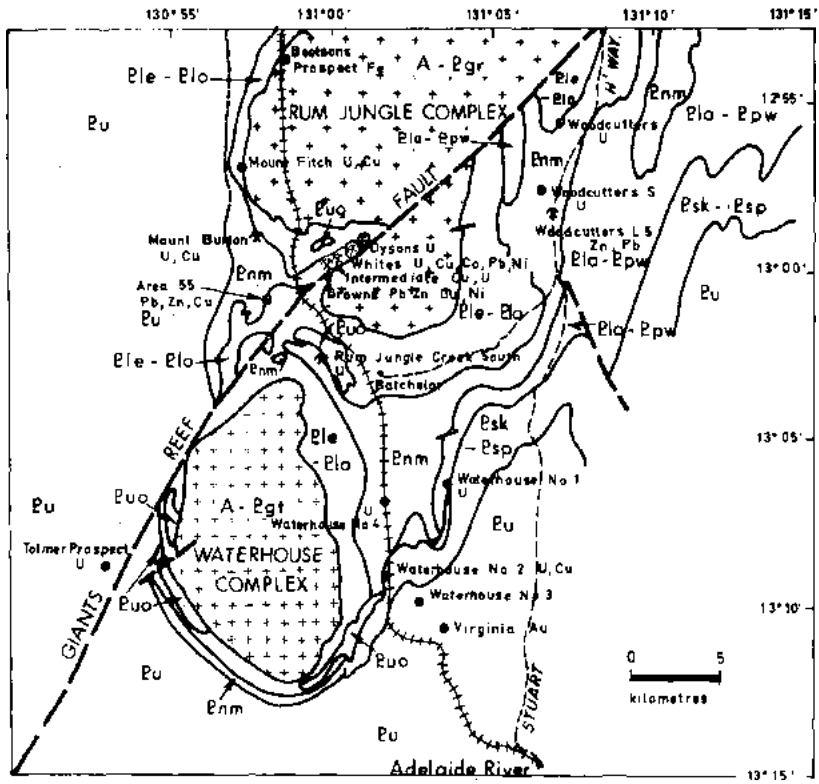
The first records of mineralization were made by Goyder, Surveyor General of South Australia in 1869. A green platey mineral and copper cabonates were noted near the Overland Telegraph Line about 90km south along the route from Darwin. This site was later deduced to be that from which Mr. J.M. (Jack) White, a local prospector and pastoralist, collected specimens of torbernite in November, 1949. White's discovery led to the mobilization of a large Bureau of Mineral Resources (BMR) geotechnical team in 1950. By 1953 reconnaissance geological mapping, ground and airborne radiometric surveys were completed and several important radioactive anomalies discovered and investigated. BMR trenching, drilling and underground exploration outlined Jack White's find as a significant uranium deposit and White received a (maximum) $50,000 reward from the Commonwealth.

During 1953 Territory Enterprises Pty. Limited (TEP) was formed as a subsidiary of Consolidated Zinc Proprietary Limited (CZP), now Conzinc Riotinto of Australia Limited (CRA), to mine White's Deposit for the Australian Atomic Energy Commission (AAEC). TEP remained manager of the Rum Jungle Project and was responsible for the mining and treatment of uranium ores from three other deposits until the closure of operations in 1971. The total quantity of uranium oxide produced was estimated at 3530 tonnes U_3O_8 (Warner, 1976).

Australian Mining and Smelting (AM & S) then a subsidiary of CZP (and later CRA), explored for base-metals in the Field from 1955 to 1971. AM & S discovered Brown's Deposit, a medium sized lead body and mined and treated by flotation, copper ores at the Intermediate Mine.

GEOLOGY

The geological setting is dominated by two domed Archaean granitic complexes, the Rum Jungle and Waterhouse Complexes (Fig. 1).



REFERENCE

UPPER PROTEROZOIC

TOLMER GROUP

Puo — Buldiva Sandstone
Depot Creek Sandstone Member

LOWER PROTEROZOIC

FINNISS RIVER GROUP

Pu — Burrell Ck. Formation

SOUTH ALLIGATOR GROUP

Psk, Psp — Kapalga Formation
Gerowie Tuff
Koolpin Formation

MOUNT PARTRIDGE GROUP

Plo - Ppw — Wildman Siltstone
Acacia Gap Sandstone

NAMOONA GROUP

Pnm — Masson Formation

BATCHELOR GROUP

Ple, Plo — Coomalie Dolomite
Crater Formation
Celia Dolomite
Beestons Formation

ARCHAEAN – ? MIDDLE PROTEROZOIC

A - Pgt — Waterhouse Complex
A - Pgr — Rum Jungle Complex

Geological boundary
Fault
Prospects
Mines

Figure 1. Solid Geology Map of the Rum Jungle Area (modified after Stephansson & Johnson, 1976).

The *Rum Jungle Complex* consists of coarse grained, large feldspar granite and leucogranite with minor belts of gneiss, schist, banded iron formation (BIF) and migmatite and metadiorite. Detailed mapping by Rhodes (1965) and geochronological studies by Richards *et al.*, (1966) showed that all units were Archaean.

The *Waterhouse Complex* is poorly exposed but was mapped (Johnson, 1974) as gneiss, schist and migmatite in the north and a coarse grained large feldspar granite in the south. Page (1976), determined a 2400 m.y. Rb-Sr isochron on zircons from the complex.

The Rum Jungle and Waterhouse Complexes are overlain unconformably by sediments of the Pine Creek Geosyncline. The stratigraphic nomenclature used here (Needham *et al.*, this volume) conforms to the code adopted for this symposium but differs considerably from earlier maps. This present code was established in the central part of the Pine Creek Geosyncline and was traced to the eastern margins of the Rum Jungle and Waterhouse Complexes

The Batchelor Group is an assemblage of arenite, dolomite-magnesite, rudite, arenite and dolomite-magnesite. The lowest unit, the *Beestons Formation*, rests unconformably on the east and south of the basement complexes and ranges up to 300m. It consists of grit, arkose and greywacke often containing grains of pale blue opaline quartz which are a common component of the coarse granite types of the Rum Jungle Complex. The unconformity is commonly sheared with quartz injection at the contact. The Beestons Formation is overlain by the *Celia Dolomite* ranging up to 300m thick which is essentially a magnesite but with algal dolomite lenses in the middle and chert and chert breccia lenses at the upper contact with the *Crater Formation*. The Crater Formation transgresses both the Beestons Formation and Celia Dolomite and overlies unconformably Archaean granitic basement in the west and north. It ranges in thickness up to 600m with a discontinuous boulder and cobble conglomerate at the base. The clasts are well rounded and are commonly of BIF. D.J. French (pers. comm.) considered this conglomerate to be part of a fluvial channel system and the clasts derived from BIF mapped within the complexes. The upper units of the Crater Formation are grits and arkose with several discontinuous beds of radioactive oligomictic quartz pebble conglomerate (French, 1970). The Crater Formation is transgressed by quartz tourmaline veins which originate in the complexes and can be traced into the Coomalie Dolomite. The *Coomalie Dolomite* is conformable on the Crater Formation and ranges up to 300m in thickness. Like the Celia Dolomite it is essentially a magnesite, but chert, shale, micaceous, hematitic, tremolitic and talcose lenses have been mapped within the unit.

A sachariodal quartzite crops out on the Coomalie Dolomite southwest of Brown's Deposit near Mt. Fitch Deposit but K.J. Wills (pers. comm.), considered this to be of Cretaceous age.

The *Namoona Group* contains the *Masson Formation* (former Golden Dyke Formation) and is the host for all major uranium and base-metal mineralization. It is a sequence of pyritic, graphitic, sericitic, chloritic and calcareous shales and amphibolite with minor quartzite, which range up to 1000m in thickness. Outcrop is generally poor with extensive soil or laterite cover. The best exposures are on the flanks of the Acacia Gap Sandstone.

The Mount Partridge Group comprises the *Acacia Gap Sandstone* and *Wildman Siltstone*. The Acacia Gap Sandstone (formerly Acacia Gap Tongue) was thought to be a transgressive member within the Golden Dyke Formation. It is an indurated pyritic quartzite ranging up to 1000m in thickness. The Acacia Gap Sandstone and overlying Wildman Siltstone pinch out near Waterhouse No. 2 Prospect south east of the Waterhouse Complex. However, a similar quartzite unit occurs near the base of the Masson Formation in the south

west of the Rum Jungle Complex at Mt. Burton. K.J. Wills (pers. comm.) considers this to be unconformable on the Namoona Group.

The *South Alligator Group* consists of the *Koolpin Formation, Gerowie Tuff* and the *Kapalga Formation*. These units range up to 700m in thickness and pinch out south east of the Waterhouse Complex. The lowest unit, the Koolpin Formation, is essentially a hematitic quartzite, hematitic quartzite breccia and BIF. Drilling Waterhouse No. 2 Prospect has shown a transition to chloritic and pyritic quartzites with carbonate lenses at depth. The hematitic quartzites are overlain by graphitic shales with chert nodule beds, blocky graphitic shales containing a thin bed of crenulated hematitic quartzite, with a transition to hematitic siltstone and greywacke grits of the Burrell Creek Formation.

Finniss River Group. The *Burrell Creek Formation* is conformable on the South Alligator Group on the east side of the Waterhouse Complex but onlaps the Masson Formation and Coomalie Dolomite on the south and west sides of the Waterhouse Complex. On the west side of the Rum Jungle Complex it is mapped as conformable on the Namoona Group. In areas where detailed mapping and drilling were carried out e.g. Mount Fitch, a broad transition zone was noted. However, detailed relogging of drill core from this area may lead to the recognition of marker units from the central part of the Pine Creek Geosyncline.

The *Tolmer Group* of possible Middle Proterozoic (Carpentarian) age overlies unconformably the Lower Proterozoic assemblage. The main exposures are the Tolmer Plateau (Tabletop Range) south west of Rum Jungle and south of Adelaide River township. The lowest unit, the *Depot Creek Sandstone Member* of the Buldiva Sandstone, is a fine indurated quartzite and quartz sandstone with occasional pebble, cobble conglomerate and breccia lenses. The mauve to purple tuffaceous sandstones of the Kombolgie Formation in the Alligator River area were not noted in the Depot Creek Sandstone Member. At Rum Jungle, outcrop is rare but noteably close to known uranium mineralization. The unit is a sequence of hematitic and chloritic mudstones, hematitic quartzite breccia (HQB) and hematitic sandstones. It is commonly phosphatic and crops out on the Coomalie Dolomite Crater Formation and calcareous units of the Masson Formation. It is remarkably similar to a basal member of the Athabasca Sandstone at Wollaston Lake, Saskatchewan. One feature requiring clarification is the apparent inter-fingering (open cut mapping) of the HQB with shales of the Masson Formation particularly at Dyson's Deposit. Fraser (1975) suggested that the HQB was folded into an isoclinical trough during movements on Giants Reef Fault although Spratt (1965) and Berkman (1968) noted considerable shearing along the contact. However, the situation could be more complex and it is suggested that the 'HQB' that interfingers with the shales may be sheared Koolpin Formation overlain by HQB of the Depot Creek Sandstone. This relationship has been noted near Stapleton Siding south of the Waterhouse No. 2 Prospect.

STRUCTURE AND METAMORPHISM

Rhodes (1965) suggested that the Rum Jungle Complex was a mantled gneiss dome and Stephansson & Johnson (1976) considered that both Archaean Complexes correspond to Eskola's type of mantled gneiss domes, but that a diapiric intrusion of early Middle Proterozoic (Carpentarian) granitoids caused the doming of the complex. The metasediments were regionally metamorphosed to low grade greenschist facies and folded along north and north east trending axes.

The Rum Jungle and Waterhouse Complexes and Proterozoic sediments are displaced laterally approximately 4-5km, by Giants Reef Fault. This is a dextral wrench fault with probable movement similar to that of plough share. At Rum Jungle it has displaced a wedge shaped mass of sediments called the Embayment, against the south western margin of the Rum Jungle Complex. Within the Embayment the sediments show evidence of tension

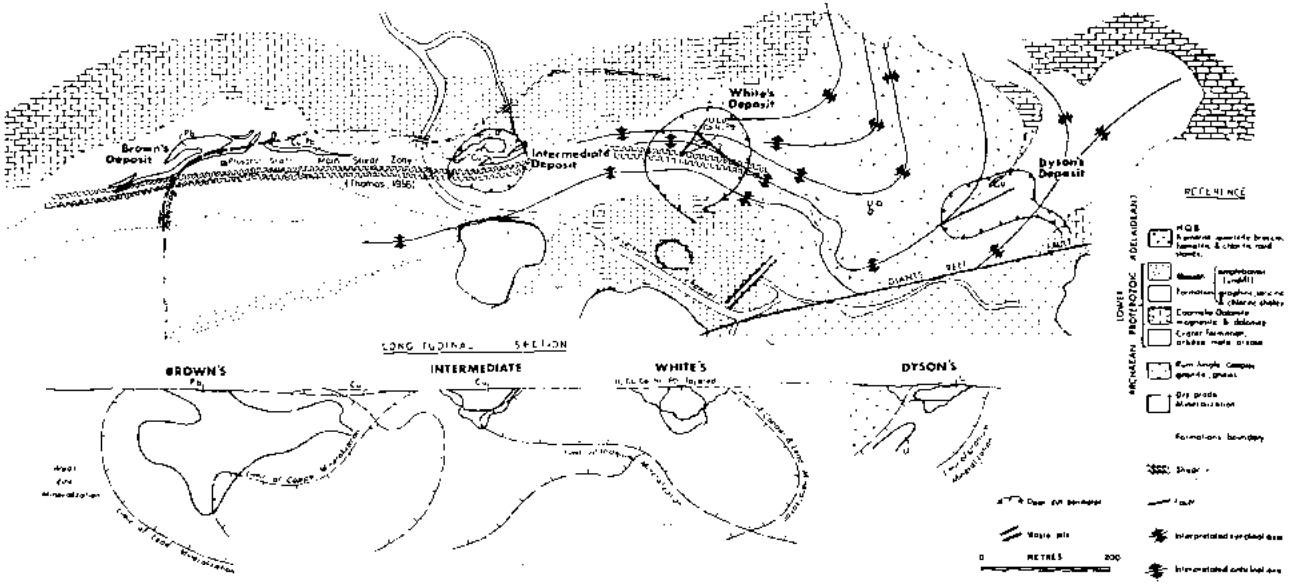


Figure 2. Rum Jungle Uranium Field - Geological Plan of the Embayment area (modified after Fraser, 1975).

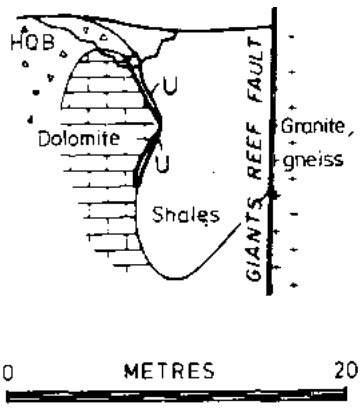


Figure 3. Diagrammatic section of Dyson's Deposit.

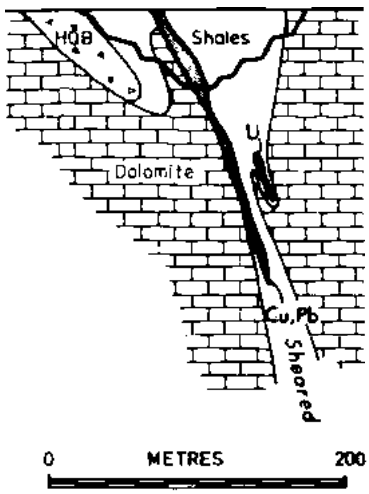


Figure 4. Diagrammatic section of White's Deposit.

flexure folding caused by movement on the fault. The Main Shear Zone (Thomas, 1956) parallels Giants Reef Fault and transgress known mineralization in the Embayment. This feature and several other parallel linears are visible on Landsat imagery and are noted to transgress mineralization in the Masson Formation at Mount Burton and Rum Jungle Creek South. Other linears remain to be tested.

MINERALIZATION

Four significant mineral deposits were found along a 1.5km strike length of the Embayment: Dyson's (uranium), White's (uranium, copper, lead, cobalt and nickel), Intermediate (copper, uranium) and Brown's (lead, zinc, copper, cobalt and nickel).

Drilling along the Embayment showed that from Dyson's to Brown's, mineralization was a near continuous line of onlapping mineral zones and each deposit the best development within a zone (Fig. 2). It was also noted that the deposits within the Embayment showed a periodicity of about 400m between centres. Scout drilling was carried out to the south west of Brown's Deposit to test for further periodicity but found only strongly pyritic shales with minor sphalerite.

Dyson's Deposit (Fig. 3).

This deposit was found by BMR geophysicist, D.F. Dyson, by ground radiometric traversing in 1950. It was initially mined on a small scale by both underground and open cut methods by TEP in 1953-1954. TEP carried out further open cut mining in 1957-1958. A total of 157,000 tonnes of ore with an average grade of 0.34% U_3O_8 were mined to 65m depth from a deposit with dimensions approximately 60m long, 8m wide and 100m depth. The deposit was contained in strongly sheared graphitic shales of the Masson Formation at the Coomalie Dolomite contact. Saleeite with minor autunite and sklodowskite persisted to 40m but pitchblende as veins and dissemination was found from 25m depth. Drilling by TEP in 1968-1969 showed that mineralization continued in a narrow zone beneath the open pit to a depth of +100m. The highest grades were in sheared and strongly hematitized dolomite at the contact with Masson Formation shales.

White's Deposit (Fig. 4).

This deposit was discovered by a local prospector Jack White in 1949. It was initially mined underground by TEP in 1953 but after further evaluation the deposit was mined by open cut methods by Geo Wimpey Ltd. from 1954-1958. The deposit was described by Spratt (1965), as consisting of four conformable zoned layers in sheared graphitic, sericitic, chloritic and pyritic shales of the Masson Formation at the Coomalie Dolomite contact. These were as follows from the contact:

1) pitchblende and chalcopyrite with minor galena, aikinite, native bismuth and

gersdorffite ranging up to 18m;
2) pyrite, bornite, chalcocite, linnaeite and carrollite ranging up to 3m;
3) a very fine grained linnaeite, carrollite, bravoite and gersdorffite zone ranging up to 3m;
4) very fine grained galena with minor sphalerite and carrollite ranging up to 5m.

These zones did overlap however, in particular the copper-cobalt and cobalt-nickel zones. Only the uranium copper zone outcropped. It was recorded as a narrow gossanous zone containing torbernite and autunite, with lesser phosphuranylite, gummite, saleeite and johannite. Pitchblende occurred from 8m depth as veins and disseminations and is known to persist to 180m depth. The copper-cobalt and lead-cobalt zones continue to +300m depth but become very narrow. Ore mined and treated totalled 396,000 tonnes a an average grade of 9.27% U_3O_8, 2.7% Cu and an additional 295,000 tonnes at an average grade of 2.8% Cu and 9.3% Co.

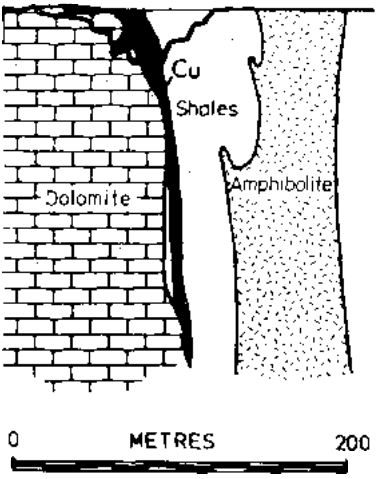


Figure 5. Diagrammatic section of Intermediate Deposit.

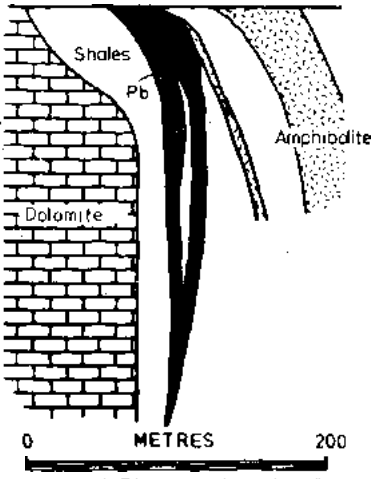


Figure 6. Diagrammatic section of Brown's Deposit.

Intermediate Deposit (Fig. 5).

Malachite was gauged from small surface exposures from the 1880's at a site nearby known as Rum Jungle Copper Mines. Evaluation drilling by AM & S in 1963 indicated a supergene and primary copper deposit with dimensions 150m long, 40m wide, and 350m depth. Mining was carried out to 70m depth by open cut methods by Davis Contractors in 1964-1965. Ore mined and treated by flotation totalled 395,000 tonnes at an average grade of 2.7% Cu and a further 367,000 tonnes at an average grade of 1.79% Cu was treated by acid leaching.

Malachite and native copper were found to 10m depth and chalcocite to 20m. Chalcopyrite with very minor pitchblende occurred from 20m depth. Berkman (1966) described the deposit as contained in a breccia of large blocks of graphitic and talcose shales enveloped by strongly sheared and contorted graphitic shales. These were in the Masson Formation at the Coomalie Dolomite contact.

Brown's Deposit (Fig. 6).

In 1954, very fine grained galena was recognised in the cores from TEP drill holes on a radiometric anomaly at Brown's Camp south west of the site of the Rum Jungle Copper Mines. In 1956-1957 by an agreement with the AAEC, AM & S carried out further drilling and by 1958 had indicated a substantial low grade lead deposit.

Further evaluation was carried out by AM & S from 1967-1970 by shaft sinking to 120m depth with drives and crosscuts at 122m, 73m and 30m. Horizontal diamond drill holes were placed at 30m centres. This work and earlier drilling indicated an orebody ranging up to 700m long, 50m wide and persisting to 450m depth. Cerussite, malachite and pyromorphite with very minor galena were found from the suface to 30m and finely divided galena with very minor chalcopyrite, sphalerite, linnaeite, covellite and gersdorffite from 30m. The host rocks were sheared graphitic sericitic and pyritic shales of the Masson Formation close to the Coomalie Dolomite contact. The deposit was found to be divided by an irregular bed of near barren blocky chloritic mafic tuffaceous shales and amphibolite. Amphibolite lenses were found on the hanging wall. Metallurgical tests are continuing to determine economic methods for treating the very finely divided galena.

Further mineralization was found in the Masson Formation at the Coomalie Dolomite contact, outward from the Embayment and peripheral to the basement complexes, at Mount Fitch (uranium and copper), Mount Burton (uranium and copper), Area 55 (lead, zinc and copper) and at Rum Jungle Creek South (uranium). Reconstruction of the geology prior to Giants Reef Faulting and a plot of these deposits (Fig. 7) has suggested an extension of the Embayment mineral zoning with base-metals predominating in the west and uranium in the east along an arc peripheral to the Waterhouse Complex.

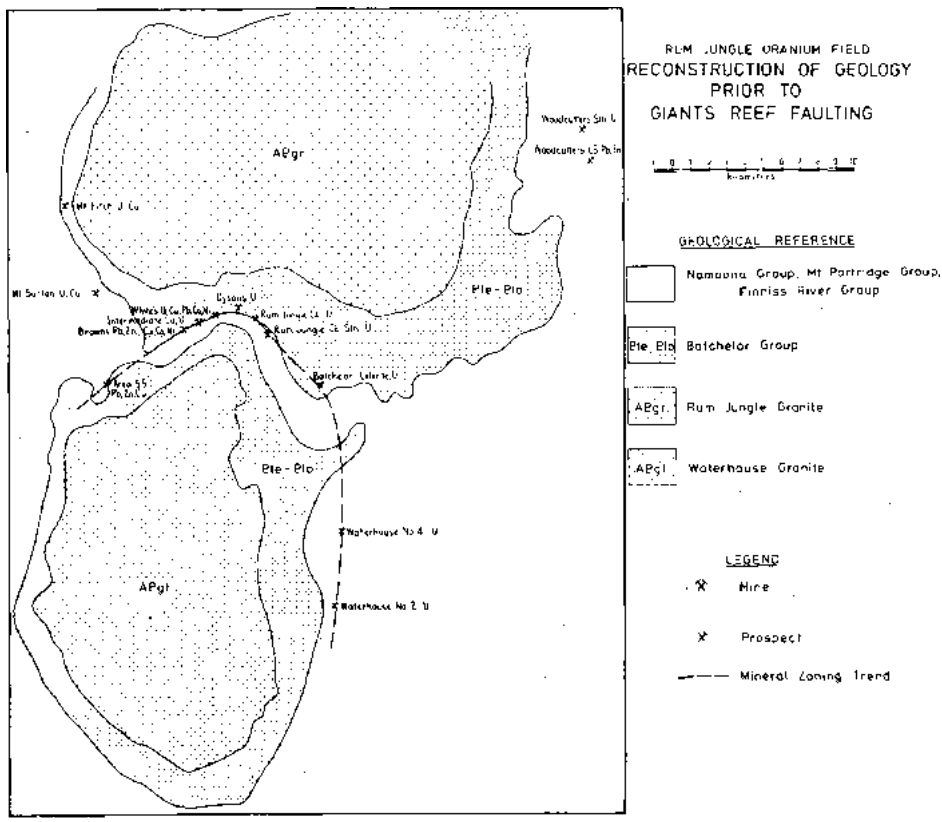


Figure 7. Rum Jungle Uranium Field - Reconstruction of Geology prior to Giant's Reef faulting.

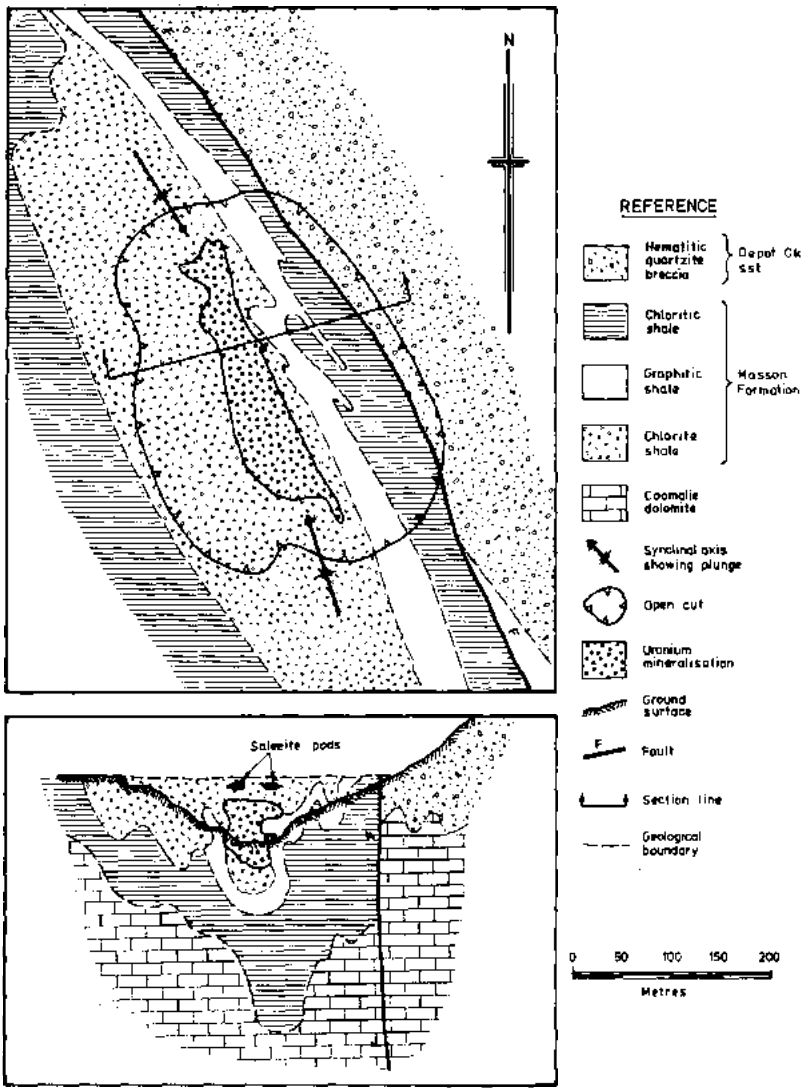


Figure 8. Rum Jungle South Deposit (modified after Berkman, 1968).

Rum Jungle Creek South (Fig. 8).

Grid drilling by TEP in 1959, of a weak surface radioactive anomaly led to the discovery of the largest uranium orebody at Rum Jungle. Initial drilling programmes however, indicated only a broad zone of apparently random uranium mineralization. Berkman (1968) described that a detailed diamond drilling programme and a prospecting shaft ultimately indicated continuity of high grade uranium mineralization within a zone 245m long, 60m wide and 80m depth. This deposit was mined by Davis Contractors during 1961-1963. A total of 663,500 tonnes of ore with an average grade of 9.43% U_3O_8 and a further 115,800 tonnes at an average

grade of 0.6% U_3O_8 were extracted. The host rocks were Masson Formation pyritic and chloritic shales overlying graphitic shale in a synclinical structure close to the Coomalie Dolomite contact. HQB is downfaulted on the eastern limb of the syncline and amphibolite overlies Coomalie Dolomite on the western limb. Moderate to severe weathering of the shales was noted to 30m depth and this zone was nearly brren of mineralization except for three small near surface pods of saleeite. Berkman (op.cit.) recorded that pitchblende was the sole uranium ore in the ore zone and the base-metal sulphides were virtually absent. The pitchblende occurred as a fine sooty coating on cleavage planes and joints but some veins and stockworks were developed on a minor scale at the contact with the underlying graphitic shale.

Mount Fitch

Mount Fitch is a small low grade uranium deposit in Masson Formation shales and brecciated Coomalie Dolomite. The principal features of this deposit are summarized by Berkman & Fraser (this volume). This deposit has not been mined.

EXPLORATION METHODS

All significant uranium and base-metal mineralization is found at or very close to the contact between the Coomalie Dolomite and the lower graphitic shale unit of the Masson Formation. This control was apparent from the very earliest days of AAEC financed exploration and it dominated the exploration strategy. For more than fifteen years, exploration programmes of the following type were carried out concurrently over the Hundred of Goyder land subdivision and Mining Reserve: Reconnaissance soil sampling (BMR); auger drilling to bed rock or watertable (BMR); scout, follow up auger and percussion drilling (TEP); costeaning (TEP); various electrical geophysical methods (BMR); total count radiometric surveys (BMR and TEP); scout, follow up and evaluation diamond drilling (TEP). These programmes tested nearly 50km of prospective strike length of the Masson Formation/Coomalie Dolomite contact and led to the discovery of two further uranium ore bodies, Rum Jungle Creek South (1959) and Mount Fitch (1965).

Other controls were noted e.g. in the presence of HQB adjacent to uranium mineralization in the Embayment and at Rum Jungle Creek South. Johnston (1974) regarded the HQB as a regolith and a basal member of the Depot Creek Sandstone i.e. represented an unconformity. The impact of the realization consolidated by models of the Alligator Rivers and Athabasca Basin areas is now being applied to exploration programmes in the south and west of the Waterhouse Complex.

BMR airborne radiometric surveys in 1952, identified a number of prominent total count radioactive anomalies in the Crater Formation, particularly in the north and south of the Rum Jungle Complex. Those in the north were investigated by BMR and Riotinto Finance and Exploration Limited (RIOFINEX) (Clark, 1954) and BMR carried out investigations of the southern anomalies until 1971. Analyses of surface rock chip samples and drill core of oligomictic quartz pebble conglomerate showed that thorium minerals were the principal radioactive minerals present. However, the discouraging surface uranium: thorium ratios, initially encountered at Blind River, Ontario, are noted and it is suggested that similar situations may be found in the Crater Formation. The application of portable differential spectrometer surveys may now assist in the identification of favourable drill targets which were impossible to determine in the past.

Very few gaps of blind drill targets remain in the lower Masson Formation. However future explorers should consider differential spectrometer surveys on the prospective contact assisted by 'Track Etch' or alphameter surveys, improved analytical drilling and bore hole logging techniques.

Past exploration programmes investigated very little of the units overlying the Masson

Formation. In essence, the possible target size based on on known mineralization e.g. the Tolmer Prospect and Adelaide River Deposit, discouraged most explorers.

GENESIS

Fraser (1975) considered that the Masson Formation contained syngenetic protore which was mildly remobilized during doming of the granites. The area was then weathered, the HQB being a regolith of this surface, and supergene enrichment, particularly of uranium, occurred.

During the initial movement on Giants Reef Fault, the HQB was drapped into flexures, accompanied by further mobilization of the protore.

Berkman (1968) discussed previous opinions and thought that the uranium deposits had the same origin. He considered a period of remobilization and low temperature hydrothermal mineralization during the orogenesis of the Pine Creek Geosyncline.

The initial source of the uranium was probably the Archaean basement complexes. The processes following are complicated by final supergene processes which Berkman (op.cit.) considered to have occurred at Rum Jungle Creek South Deposit. The main alternatives are chemical precipitation at the shale/magnesite contact during deposition of the sediments or detrital protore in the Crater Formation which was later remobilized by low temperature metasomatic processes.

The size differences between known uranium deposits in the Alligator Rivers Field and those of the Rum Jungle Field is an enigma. However, it is speculated that it may be related to metamorphic grade and possibly that the Rum Jungle uranium deposits are in younger sediments.

ACKNOWLEDGEMENTS

Permission by CRA Exploration Pty. Limited and the Australian Atomic Energy Commission to publish this paper is gratefully acknowledged. A F.McQueen, K. Johnson and K.J. Wills critically reviewed the paper and offered many helpful suggestions.

REFERENCES

Berkman, D.A., 1966: The Geology of the Intermediate Copper Mine, Rum Jungle, N.T. *Unpublished Report, CRA Exploration Pty. Ltd., Report No. 656.*

Berkman, D.A. 1968: The Geology of the Rum Jungle Uranium Deposits. *in, Uranium in Australia Symposium. Australas Inst. Min. Metall.*, 12-31

Berkman, D.A. & Fraser, W.J., this volume: The Mount Fitch Copper and Uranium deposits, Rum Jungle Uranium Field N.T. Australia. *Proceedings of the International Uranium Symposium on the Pine Creek Geosyncline.*

Clark, A.B., 1954: Report on Manton Reserve Authority to Prospect No. 130. *Unpublished Report, Riotinto Finance and Exploration.*

Fraser, W.J., 1975: The Embayment line of mineralization, Rum Jungle. *in* (ed. C.L. Knight), *Economic Geology of Australia and New Guinea. Australas. Inst. Min. Metall. Monograph Series No. 5. 1. Metals*, 271-277.

French, D.J., 1970: Crater Formation investigation, Rum Jungle district, N.T. 1969. *Rec. Bur. Miner. Resour. Geol. Geophys. Aust., 1970/65* (unpubl.).

Johnson, K. 1974: Progress report: geological review and revision of the Rum Jungle area, N.T. 1973. *Rec. Bur. Miner. Resour. Geol. Geophys. Aust., 1974/41* (unpubl.).

Needham, R.S., Crick, I.H. & Stuart-Smith, P.G., this volume: Regional Geology of the Pine Creek Geosyncline. *Proceedings of the International Uranium Symposium on the Pine Creek Geosyncline.*

Page, R.W., 1976: Geochronology of Archaean and Lower Proterozoic rocks in the Rum Jungle-Alligator Rivers Area, N.T. Australia. *25th Int. geol. Congr. Section 1A. Abstracts, Sydney.*

Richards, J.R., Berry, H. & Rhodes, J.M., 1966: Isotopic and lead-alpha ages of some Australian zircons. *J. geol. Soc. Aust., 13*, 69-96.

Rhodes, J.M., 1965: The geological relationships of the Rum Jungle Complex, N.T. *Rep. Bur. Miner. Resour. Geol. Geophys. Aust., 89*, 10p.

Spratt, R.N., 1965: Uranium Ore deposits of Rum Jungle, *in* (ed. J. McAndrew). *Geology of Australian Ore Deposits, 8th Commonwealth Mining and Metallurgical Congress, Melbourne*, 201-206.

Stephansson, O. & Johnson, K., 1976: Granite diapirism in the Rum Jungle Area, Northern Australia. *Precambrian Research, 3*, 159-185.

Thomas, W.N., 1956: The geological investigation of the Rum Jungle Uranium field, N.T. *TEP Report* (unpubl.).

Warner, R.K., 1976: The Australian Uranium industry. *Atom. Energy, Sydney, 19(2)*, 19-31.

THE GEOLOGY OF THE LITCHFIELD PROVINCE, N.T.

D.A. Berkman

Australian Oil and Gas Co. Ltd., 261 George Street, Sydney, N.S.W., 2000, Australia

ABSTRACT

The Litchfield province is herein defined as the westernmost outcropping unit of the Pine Creek Geosyncline extending from the Giant's Reef Fault at about longitude 130°50'E westerly to the edge of the Bonaparte Gulf basin. The northern half of the province has been remapped using company drillhole data and a Bureau of Mineral Resources air magnetic-radiometric survey.

Five areas have been found to be entirely granitoid, garnetiferous and gneissic in part, with composition in the range adamellite to granodiorite. A single Rb/Sr age of about 1800 m.y. has been published. The granitoid margins are migmatised and transitional into large areas of metasediments, varying in metamorphic grade from greenschist (fine grained chloritic graphitic schist) to upper amphibolite/granulite grade (course grained quartz - feldspar gneiss). The regional strike is northerly to northwesterly, and these metasediments are thought to merge into the Burrell Creek Formation beyond the border of the province. Two periods of metamorphism affected the Litchfield province metasediments, but only one phase can be detected in the granitoids, thus these are assumed to be younger, probably formed during the 1800 m.y. orogenesis known elsewhere in the Geosyncline.

Minor areas of unmetamorphosed gabbro, dolerite and quartz-diorite occur, probably of Middle Proterozoic age. Cover rocks include quartz sandstones of the (?) Middle Proterozoic Moyle River Formation and Depot Creek Sandstone, and Cambro-Ordovician sandstones of the Daly River Basin.

The formation boundaries in the Litchfield province are not particularly confused or complicated, nor are the igneous lithologies particularly diverse. There is no evidence for an Archaean age for the part of the Litchfield province north of the Daly River, and it is thus proposed that the term 'Litchfield Complex' should be abandoned.

INTRODUCTION

The Pine Creek Geosyncline is basement - the oldest exposed rock - for the northwest part of the Northern Territory, and rocks of Pine Creek Geosyncline age continue beyond the area of outcrop under younger basins on all sides. The Litchfield province is the westernmost outcropping unit of the Geosyncline, of area about 8500km^2, and defined as the area between the eastern margin of the Permo-Triassic Bonaparte Gulf Basin and the Giant's Reef Fault, as far east as 130°50'E.

The outcrop geology is shown on the Cape Scott, Darwin, Fog Bay, and Pine Creek 1:250 000 geological maps. The lack of outcrop in this area has led to minimal interest of stratigraphers and prospectors, and the present areas of interest in exploration are restricted because access to the better known and more obviously prospective parts of the Geosyncline is considerably limited.

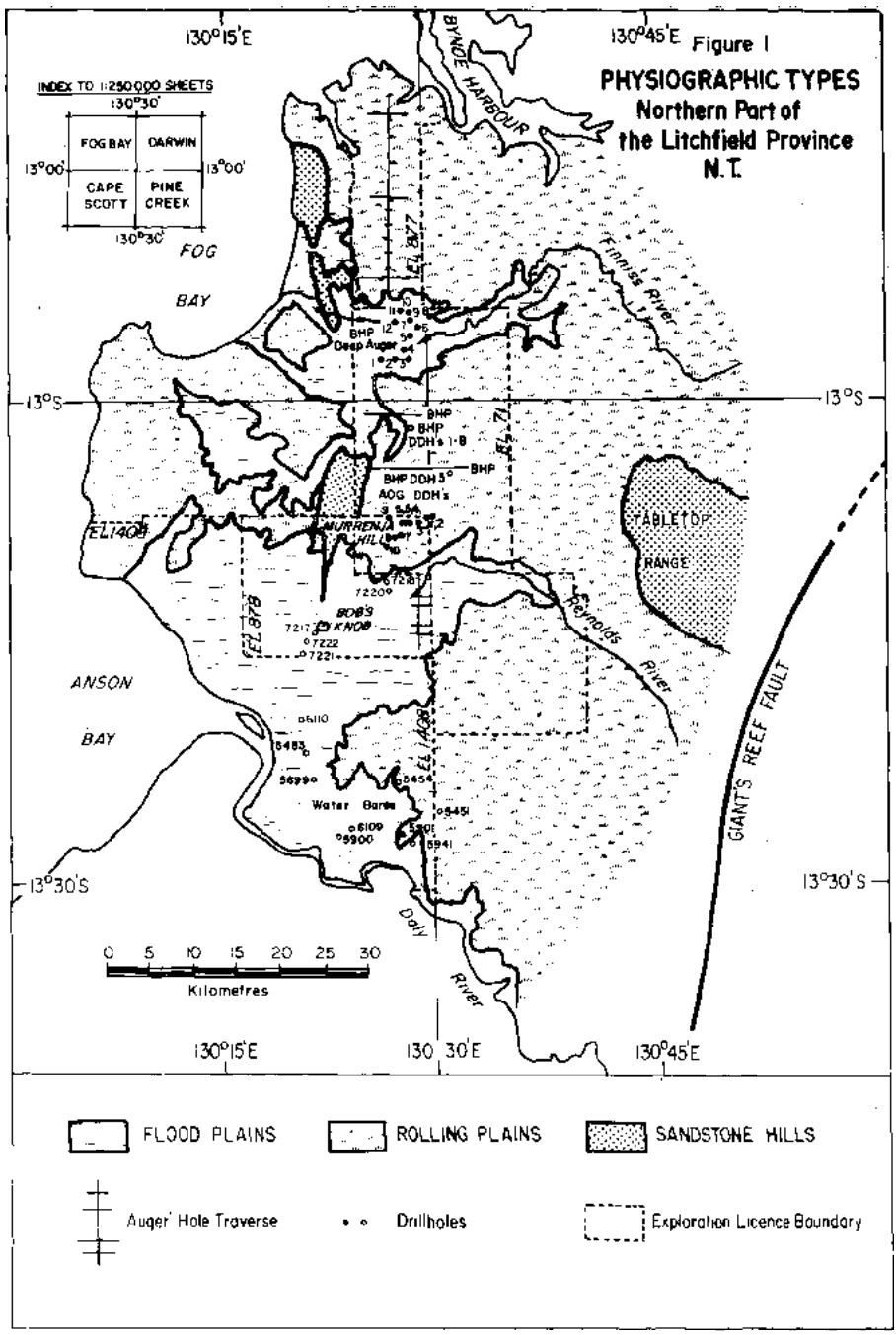
The first geological report arose from Hossfeld's (1937) work on the Daly River copper mines. He briefly noted an amphibolite at Marion hill and a body of granite further west, which he named (after its highest point) the Mt. Litchfield Granite. A geologist was included in the regional pastoral and agricultural survey of the Darwin - Katherine area in 1946, and his reconnaissance was published as the first regional geological map.

Hossfeld's Mt. Litchfield Granite was renamed the Litchfield Granite, and its boundaries were extended to a much larger area, about 160km long northsouth by at least 50km wide (Noakes, 1949).

Regional geological mapping on 1:250 000 scale was largely completed by 1953, and this work was combined in a major regional report by Walpole, *et al.* (1968). New lithological information was obtained in recent company mineral exploration programmes (Fig. 1), particularly in Exploration Licences 71 (The Broken Hill Proprietary Company Limited), 877 and 878 (Esso Australia Limited) and 1408 (AOG Minerals Pty. Limited). Permission to publish this information is gratefully acknowledged.

PHYSIOGRAPHY

The flood plains extend inland up to 50km from the coast, and are rarely higher than


Figure 1
PHYSIOGRAPHIC TYPES
Northern Part of
the Litchfield Province
N.T.
130°15'E
130°45'E
INDEX TO 1:250 000 SHEETS
130°30'
FOG BAY
DARWIN
CAPE SCOTT
PINE CREEK
13°00'
130°30'
FOG
BAY
BYNOE HARBOUR
Finniss River
EL 877
EL 878
EL 1408
BHP
Deep Auger
BHP DDH's 1-8
BHP DDH 3°
AOG DDH's
HURRENJI HILL
BOB'S KNOB
TABLETOP RANGE
Reynolds River
GIANT'S REEF FAULT
ANSON
BAY
Water Bore
Daly River
13°S
13°30'S
0 5 10 15 20 25 30
Kilometres
FLOOD PLAINS
ROLLING PLAINS
SANDSTONE HILLS
Auger Hole Traverse
Drillholes
Exploration Licence Boundary

15m above sea level (Fig. 1). This physiographic type was tested by 12 auger drillholes, to an average depth of 25m, on the Finniss River flood plains. (BHP, 1974). This drilling shows the typical sequence to be a metre or so of black clayey soil, then an average of 20m (maximum 30m) of grey clay containing shell fragments (including nautilus and forams), overlying weathered rock.

This succession is interpreted as a littoral and deltaic deposit of marls and river sediments, of Cainozoic age.

Thus the area of swamp between the end of the permanent course of the Finniss and Reynolds Rivers and the sea is thought to have a deep cover of transported sediment. This alluvial cover extends southerly from the Reynolds River delta to join the Daly River flood plains.

The rolling plains are all less than 60m above sea level, with only minor undulations, and a cover of open stunted forest and native grasses. The dendritic drainage pattern is quite distinctive. Plains developed on granitoids have some knoll and tor outcrops, separated by dark grey clayey soils, whereas those on metasediments have a brown clayey loam, which can contain small tabular rock fragments, but more commonly no surface lithological information is presented.

The sandstone hills provide the highest ridges in the area, reaching about 150m above sea level on Murrenja Hill and the Tabletop Range. The hills are only lightly forested, and provide ample outcrop, although no formation contacts are known.

STRATIGRAPHY

The northern part of the province may be separated into seven major stratigraphic/lithological units, based on outcrop and drillhole data, or inferred from physiographic and airmagnetic patterns where definite information is not available. The units are the granitoids, with five bodies postulated in this northern area, and five areas of mafic igneous rocks, all separated by metasediments tentatively assigned to the Lower Proterozoic. On the north and east sides of the province the granitoids are flanked by greywackes and siltstones of the Burrell Creek Formation. These older rocks are partly covered by unmetamorphosed Moyle River Formation sandstones, in a band northerly from Murrenja Hill, by flaggy sandstones in the Litchfield station area, and by Permian sediments in a band along the west coast (Fig. 2).

1. Granitoids

a) *Fog Bay granite*

The boundaries of this mass are defined by mapping on the Fog Bay 1:250 000 sheet (Senior & Hughes, 1975), by mapping on the Darwin sheet (Malone, 1962a), and by auger drillholes in EL 877 (Lindemann, 1974). Lithologies are listed as a garnetiferous granite and a two-mica grandiorite. Malone (1962 a) states that a faulted contact separates this granite from the Lower Proterozoic Burrell Creek Formation, and that quartz-tourmaline veins transgress the contact.

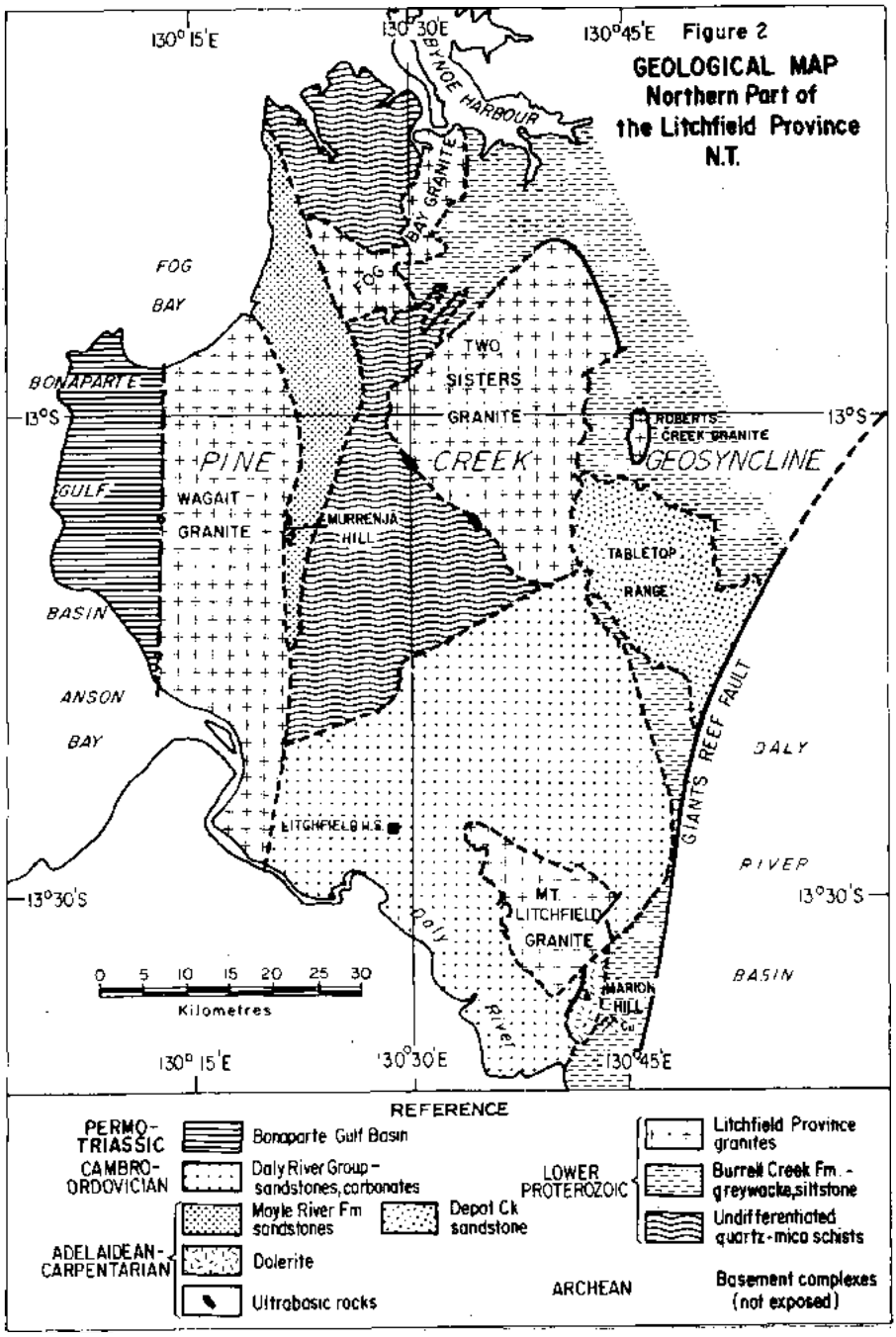
b) *Roberts Creek Granite*

This body occurs in the southwest corner of the Darwin sheet, and continues southerly on to the Pine Creek sheet. It is completely encircled by the Lower Proterozoic Burrell Creek formation. Malone (1962 a) describes the mass as "a garnetiferous granodiorite containing blebs of quartz-feldspar-tourmaline-muscovite pegmatite . . . probably an apophysis of the Litchfield Complex".

c) *Two Sisters Granite*

Information on this body is provided by Malone (1962 a, b), BHP (1974) and unpublished AOG mapping.

Thin sections have been described from four localities:


Figure 2
GEOLOGICAL MAP
Northern Part of
the Litchfield Province
N.T.
130°15'E
130°30'E
130°45'E
13°S
13°30'S
BYNOE HARBOUR
BAY GRANITE
FOG
BAY
BONAPARTE
GULF
BASIN
ANSON
BAY
TWO
SISTERS
GRANITE
ROBERTS
CREEK GRANITE
PINE
CREEK
GEOSYNCLINE
WAGAIT
GRANITE
MURRENJA
HILL
TABLETOP
RANGE
GIANTS REEF FAULT
DALY
RIVER
BASIN
LITCHFIELD M.S.
MT.
LITCHFIELD
GRANITE
MARION
HILL
Cu
Daly
River
0 5 10 15 20 25 30
Kilometres
REFERENCE
PERMO-
TRIASSIC
Bonaparte Gulf Basin
CAMBRO-
ORDOVICIAN
Daly River Group –
sandstones, carbonates
Moyle River Fm
sandstones
Depot Ck
sandstone
ADELAIDEAN-
CARPENTARIAN
Dolerite
Ultrabasic rocks
LOWER
PROTEROZOIC
Litchfield Province
granites
Burrell Creek Fm. –
greywacke, siltstone
Undifferentiated
quartz-mica schists
ARCHEAN
Basement complexes
(not exposed)

i) At about 130°35'E, 13°05'S: Outcrops of a fine grained hornblende-biotite-quartz-oligoclase/andesine gneiss, of trondhjemite composition; a biotite-microcline-oligoclase-quartz gneiss, of biotite adamellite composition; and a biotite-microcline-oligoclase-quartz augen gneiss. All of these contain rounded accessory zircon grains, and are thought to be formed by tectogenesis.
ii) At about 130°34'E, 13°03'S: An outcropping equigranular biotite microgranite (quartz-microcline-oligoclase-biotite and muscovite).
iii) At about 130°29'E, 13°02'S: from BHP drillhole 1, garnetiferous microgranite and pegmatite and quartz-biotite-garnet microgneiss; both are interbanded with schists, and thought to be regionally metamorphosed pelitic sediments, of upper greenschist - lower amphibolite grade.
iv) At about 130°33'E, 13°06'S: Outcrops of a coarse muscovite granite. A single outcrop of biotite granodiorite at about 130°28E, 13°05'S, may be an isolated pinnacle of this granite.

d) *Wagait Granite*

This granite is described by Mendum (1972) and AOG mapping. It is a northerly trending body, bounded by the Murrenja Hill sandstone to the east and the faulted contact with Permian sediments to the west. In thin sections from two outcrops the rock is described as a coarse grained hornblende-biotite adamellite, and a third outcrop is a coarse grained biotite granite; all have common accessory zircon, and metamict allanite.

The coarse grained garnetiferous quartzo-feldspathic gneiss intersected in AOG hole 9 is possibly the eastern rim of granitisation of this body.

e) *Mt. Litchfield Granite*

Walpole *et al.* (1968, p.133) describes this granitoid body in some detail, as a massive and gneissic adamellite and granodiorite, well exposed over an area of about 250km^2. A recent thin section is described as a coarse grained muscovite-biotite granodiorite, containing partly sericitised quartz, muscovite, lesser fine grained biotite, and accessory zircon. There is a platey flow structure, trending at about 340°, on the eastern margin, parallel to the bedding in the adjacent Lower Proterozoic metasediments, and the gneissic foliation trends at 075° and 285° (Walpole *et al.*, 1968).

2. Mafic igneous rocks

Mafic to ultramafic igneous rocks are known from five areas north of the Daly River:

a) At about 130°30'E, 13°02'S: outcrops of serpentinised peridotite and weathered carbonate rock.
b) At about 130°33'E, 13°07'S: a tremolite-talc-chlorite rock, formed from a serpentinised peridotite and a uralitised microgabbro or dolerite. These two outcrops of mafic rock mark the eastern margin of three major airmagnetic anomalies, and are interpreted as a major geological boundary.
c) B.H.P. drillhole 2 intersected two bands of orthoamphibolite, a contact metamorphosed dolerite or microgabbro.
d) A fault-bounded valley in the centre of the Murrenja Hill sandstone contains fresh and undeformed coarse grained quartz-andesine-augite gabbro, and produces a circular magnetic anomaly.
e) The Marion Hill dolerite, on the southeast flank of the Mt. Litchfield Granite, is briefly noted by Bryan (1962).

3. Undifferentiated Quartz-Mica Schists

a) *Graphitic-Chloritic Schists*

BHP drillholes 1 and 2, and AOG holes 2 and 3, contain fine grained crenulated pyritic schists, with up to 10% graphite and up to 35% normal chlorite (i.e. formed from biotite). These have hydromuscovite, quartz, and potassium feldspar layers, providing a prominent

schistosity, and fine graphite flakes occur in all layers. The shapes of lenticular patches of quartz and chlorite in core from the AOG holes suggest that these schists may be metamorphosed tuffs. There appears to be an older phase of regional metamorphism, to greenschist facies, producing the mineral layering, then a period of quartz-carbonate-sulphide veining, then a further episode of metamorphism which produced the crenulations.

b) *Magnetite Schists*

AOG hole 2 intersected a fine grained grey quartz-feldspar-biotite-muscovite-garnet schist, with a fine network of streaks and bands of reddish hematite replacing magnetite. BHP hole 2 found a banded quartz-feldspar-biotite-garnet-grunerite schist, with very fine magnetite grains in the garnets. Both give rise to a linear air magnetic anomaly, and both are thought to be regionally metamorphosed iron rich sediments. The trend of the anomaly is northerly at AOG 2, and northwesterly at BHP 2, suggesting that this may be the trend of the original sedimentary layering in each area.

c) *Muscovite-Biotite Schists*

Medium to coarse grained schists, in which pale grey 'silky' sericite is the most striking mineral, were found in BHP drillholes 1 and 2 at air magnetic anomaly 1, and in AOG holes 4, 5, 6, 7, 8 and 10.

The usual constituents are quartz, microcline, oligoclase, muscovite/sericite, biotite and garnet. The location of outcrops on the eastern rim of anomaly 1 suggests a north-northwest regional trend, and the foliation in one outcrop is northwest. All these schists are thought to be formed from fine grained quartzose pelitic sediments, by a primary regional metamorphism followed by a thermal metamorphic episode. There is a striking increase in metamorphic grade westerly in the AOG drillholes, from greenschist in hole 3 to upper amphibolite/granulite in hole 9.

4. Burrell Creek Formation

This is largely greywackes and siltstones and includes the Noltenius Formation of Walpole *et al.* (1968). It forms the north, east and south boundaries of the Province, and Sweet (1977) is the most recent reference.

5. Moyle River Formation

White, pink or brown sandstone, with some pebble bands, extends from Bob's Knob on the Cape Scott sheet, through Murrenja Hill, terminating at the coast on the Fog Bay sheet. The formation has been described by Mendum (1972) and AOG mapping as quartz sandstones with well rounded grains of high sphericity, and commonly with authigenic quartz cement. In some cases the quartz cement is partly replaced by late diagenetic hematite; tourmaline and zircon are common accessories.

The formation is only metamorphosed along regional faults, and is here much quartz veined and altered to a sericitic quartzite. It is lithologically identical to the (?) Middle Proterozoic Depot Creek sandstone, as exposed on the northern Tabletop Range road crossing.

6. Daly River Group

Low-lying black soil plains in the Litchfield station area have occasional large floaters in erosion gutters, described as feldspathic sandstones and arkoses. The well rounded quartz grains may have been derived from the Moyle River Formation sandstones, and the feldspars from the older grantoids and metasediments. They lie unconformably on the Mt. Litchfield Granite, and are correlated with the sandy units of the Cambrian/Ordovician Daly River Group further to the east.

7. Permian Sediments (Bonaparte Gulf Basin)

Up to 1980m of sandstones and shales, with thin coal seams, are known in coal exploration drillholes and in offshore wildcat wells (Mendum, 1972). The sequence onshore has a lateritic capping, and no outcrops are known north of the Daly River.

RELATIONSHIP

South of the Daly River the metasediments (Hermit Creek Metamorphics) have been assigned an Archaean age on the basis of "the structural and metamorphic unconformity between them and the Lower Proterozoic rocks of the Pine Creek Geosyncline" (Randal, 1962). In the same district, Sweet (1977) reports that Lower Proterozoic Burrell Creek Formation unconformably overlies a granitoid, thus this particular granitoid is allocated an Archaean age. Parts of this granitoid have migmatised contacts with the Hermit Creek Metamorphics, and these parts are thought to be intrusive of age 1800 million years, which is the usual age of the plutons which intrude the Pine Creek Geosyncline sequence further east.

Different evidence is available north of the Daly River. The banding in the metasediments and the long dimension of the air magnetic anomalies all strike north to northwest, parallel to the regional trends in the Pine Creek Geosyncline. The Burrell Creek Formation is known from the north and east of the Province, and broadly similar 'quartz-mica schists' can be traced, as an extension of this formation, southerly to the area of Cambrian-Ordovician sandstone cover. A sequence of finer grained graphitic-chloritic schists, lithologically very similar to the uranium host rock elsewhere in the Geosyncline, has been found within this zone. Two periods of metamorphism are noted in the metasediments, an older regional phase and a younger thermal phase.

Five pluton-like granitic masses are known from this northern zone, and the margins are known to be migmatised, with extensive granitisation of the surrounding metasediments. A flow structure was noted in the Mt. Litchfield Granite, parallel to the bedding in the adjacent Lower Proterozoic rocks of the Pine Creek Geosyncline. In the AOG drillholes there is an obvious increase in metamorphic grade from fine grained chloritic schist of greenschist facies in the east, through upper greenschist and amphibolite facies to a coarse grained gneiss of upper amphibolite/granulite facies in the west.

Age determinations are available for two areas:

a) Mt. Litchfield Granite, at about 130°42'E,13°30'S, whole rock Rb/Sr of about 1800 m.y. (Compston & Arriens, 1968), and
b) Quartz diorite, from about 530m depth in AAP Moyle No. 1, at about 129°46'E, 14°17'S, K/Ar of 1393-1537 m.y. (Page, 1968).

The event at about 1800 m.y. is now considered to be the time of emplacement of the 'younger' granitoids of the Pine Creek Geosyncline and remobilisation of the older basement complexes. The quartz diorite and other mafic igneous rocks are obviously younger than this on field evidence.

More detailed work has shown that the Litchfield Complex, as defined (Walpole *et al.*, 1968) is not an assemblage of widely different igneous rocks, nor are the formation boundaries particularly intricate or interwoven. There is no evidence of an Archaean age for the granitoids or metasediments north of the Daly River, and the regional geology there is generally similar to the adjacent parts of the Pine Creek Geosyncline. Thus the term 'Complex' has been discarded, and the district identified as a geographical unit only, i.e. as the Litchfield province.

REFERENCES

Bryan, R., 1962: Lower Proterozoic basic intrusive rocks of the Katerine-Darwin area, Northern Territory. *Rec. Bur. Miner. Resour. Geol. Geophys. Aust., 1962/7.*

B.H.P., 1974: Exploration Licence 71, Finniss River, Northern Territory. Report for the year ended 6th September, 1974. *Unpublished Report, N.T. Mines Department No. CR 75/35.*

Compston, W., & Arriens, P.A., 1968: The Precambraian Geochronology of Australia. *Can. J. Earth Sci., 5,* 561-583.

Hossfeld, P.S., 1937: The Daly River copper and silver-lead area, Daly River district. *Aerial geological and geophysical surveys North. Aust., N.T. Report No. 19.*

Lindemann, W.L., 1974: Final report of exploration conducted on Exploration Licence 877, Northern Territory. *Unpublished Report, Esso Australia Limited, N.T. Mines Department No. CR 74/65.*

Lindemann, W.L., 1974: Final report of exploration conducted on Exploration Licence 878, Northern Territory. *Unpublished Report, Esso Australia Limited, N.T. Mines Department No. CR 74/65.*

Malone, E.J., 1962(a): Darwin 1:250 000 geological sheet. *Explan. Notes Bur. Miner. Resour. Geol. Geophys. Aust., D/52-4.*

Malone, E.J., 1962(b): Pine Creek 1:250 000 geological sheet. *Explan. Notes Bur. Miner. Resour. Geol. Geophys. Aust., D/52-8.*

Mendum, M.R., 1972: Cape Scott 1:250 000 geological sheet. *Explan. Notes Bur. Miner. Resour. Geol. Geophys. Aust., SD/52-7.*

Morgan, C.M., Sweet, I.P., Mendum, J.R. & Pontifex, I.R., 1970: The geology of the Cape Scott, Port Keats, Fergusson River and Delamere 1:250 000 sheet areas, Northern Territory. *Rec. Bur. Miner. Resour. Geol. Geophys. Aust., 1970/3.*

Noakes, L.C., 1949: A Geological Reconnaissance of the Katherine-Darwin Region Northern Territory; with Notes on the Mineral Deposits. *Bull. Bur. Miner. Resour. Geol. Geophys. Aust., 16.*

Page, R.W., 1968: Catalogue of age determinations carried out on Australian rocks in 1966. *Rec. Bur. Miner. Resour. Geol. Geophys. Aust., 1968/30.*

Randal, M.A., 1962: Fergusson River 1:250 000 geological sheet. *Explan. Notes Bur. Miner. Resour. Geol. Geophys. Aust., SD/52-12.*

Senior, D. & Hughes, R.J., 1975: Fog Bay 1:250 000 geological sheet. *Explan. Notes Bur. Miner. Resour. Geol. Geophys. Aust., SD/52-3.*

Sweet, I.P., 1977: The Precambrian Geology of the Victoria River Region, Northern Territory. *Bull. Bur. Miner. Resour. Geol. Geophys. Aust., 168.*

Walpole B.P., Crohn, P.W., Dunn P.R., & Randal, M.A., 1968: Geology of the Katherine-Darwin Region, Northern Territory. *Bull. Bur. Miner. Resour. Geol. Geophys. Aust., 82.*

STRATIGRAPHY OF THE KAPALGA FORMATION NORTH OF PINE CREEK AND ITS RELATIONSHIP TO BASE METAL MINERALIZATION

John Goulevitch

Geopeko, P.O. Box 39443, Winnellie, N.T., 5789, Australia

ABSTRACT

The lithology, stratigraphy and mineralization of the Kapalga Formation (South Alligator Group) is described from the Margaret Syncline in the Pine Creek area of the Northern Territory of Australia. An interdigitation of carbonaceous siltstones and mudstones, chert, ashstones and tuffaceous chert, greywacke, siltstone, mudstone and minor banded iron formation (b.i.f.) characterises the Formation. These rocks define a vertical facies transition between low energy sediments of the underlying Koolpin Formation, and high energy sediments of the overlying Burrell Creek Formation. This transition is interlayered with numerous ashstone-tuffaceous chert horizons which were deposited during the waning stage of Gerowie Tuff sedimentation.

The boundary between the Kapalga Formation of the South Alligator Group and the Burrell Creek Formation of the Finniss River Group is strictly conformable in this part of the Pine Creek 'Geosyncline'.

Relict devitrified shards have been recognised in the Gerowie Tuff in the Margaret Syncline and these observations along with whole-rock chemical analyses conclusively support claims by previous investigators that these rocks are volcanic derivatives.

Base metal mineralization at Iron Blow and Mt. Bonnie occurs as massive, stratiform, sulphide-silicate-carbonate lodes. The deposits are at the same stratigraphic level towards the base of the Kapalga Formation and minor stratification parallel with bedding has been observed. These features, and the association of the lodes with mud-flow breccias, lead to the conclusion that the lodes are syngenetic in origin.

Thermochemical consideration of the sulphide assemblages together with the temporal relationship between the mineralization and Gerowie Tuff point to diagenetic devitrification of the underlying tuffaceous rocks as the source of the mineralization. Recent publications of experimental data from reaction of seawater and volcanic glass provide information which supports this thesis, and suggests a seawater origin for the sulphur present.

INTRODUCTION

In the Grove Hill area, 180km SSE of Darwin (Fig. 1) some of the best exposures of Lower Proterozoic sediments, volcanics and metadolerites of the Pine Creek Geosyncline sequence are present. Between Burrundie and Hayes Creek the bulk of the South Alligator Group as defined by Needham *et al.* (this volume) and the lower portion of the Burrell Creek Formation of the Finniss River Group are well represented together with sills of Zamu Dolerite.

Mineralization is abundant throughout the area with, among many other deposits, tin at Jimmy's Knob, Mundic and Hayes Creek, gold at Yam Creek, Golden Dyke and Spring Hill, and base metal sulphide deposits at Iron Blow, Mt. Bonnie and the McKinlay Silver Mine (Walpole *et al.*, 1968). With the exception of gold mineralization of the Golden Dyke type, (Nicholson, this volume) which occurs in the Koolpin Formation, the basal unit of the South Alligator Group, these mineral occurrences mostly occur within the upper portion of the South Alligator Group i.e. within the Kapalga Formation.

Recent exploration of the base metal mineralization at Iron Blow and Mt. Bonnie mines has enabled detailed study of the Kapalga Formation within a major syncline, here called the Margaret Syncline (Fig. 1).

In this paper the stratigraphy and lithology of the Kapalga Formation as it appears in the Margaret Syncline is presented. In addition the major geological characteristics of the base metal mineralization at Iron Blow and Mt. Bonnie are described and the inter-relationship between the stratigraphy and the mineralization is discussed. Mineralogical and chemical aspects of the mineralization are considered in an attempt to arrive at an understanding of the physical and chemical properties of both the mineralising solution and the depositional environment which existed during mineralization. Based on this, one particular theory of the

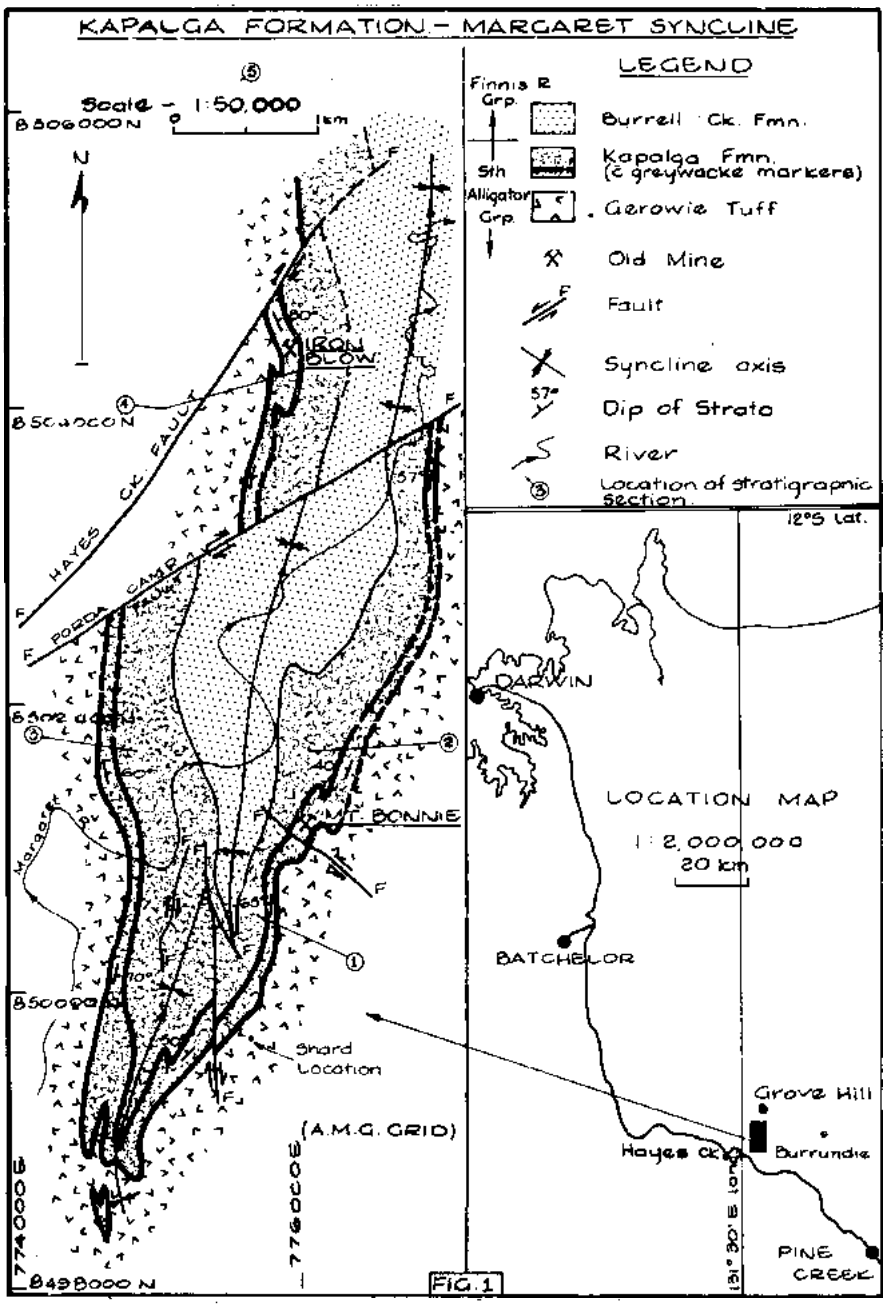


Figure 1. Kapalga Formation in the Margaret Syncline.

genesis of the mineralization is explained. Finally, the changes in the chemical characteristics of the depositional environment during sedimentation of the entire Kapalga Formation, as indicated by iron sulphide/oxide assemblages, are described.

GENERAL GEOLOGY

Prior to this Symposium the bulk of the sediments between Burrundie and Hayes Creek had been grouped in the 'Golden Dyke Formation' and a minor amount allocated to the Burrell Creek Formation (Walpole *et al.*, 1968). The revised stratigraphy of this area is illustrated on the 1:500 000 map accompanying this volume and described by Needham *et al.* (this volume).

Briefly, the Koolpin Formation, Gerowie Tuff, and Kapalga Formation of the South Alligator Group, and Burrell Creek Formation of the Finniss River Group are all present. The Mt. Partridge Group may occur in the Hayes Creek area (Nicholson, this volume) though it is not exposed further to the east towards Burrundie where the overlying Koolpin Formation appears to be much thicker (Goulevitch, 1979, unpubl.). Despite such thickness variations the layered stratigraphy of the South Alligator Group as initially proposed by Crick *et al.*, (1978) has been firmly established in this belt.

At least three major (150-200m) layers of Zamu Dolerite (Ferguson & Needham, 1978) are interleaved with the sediments of the Koolpin Formation and Gerowie Tuff. Contacts between dolerites and sediments in drill core are strictly conformable (Goulevitch, 1979,

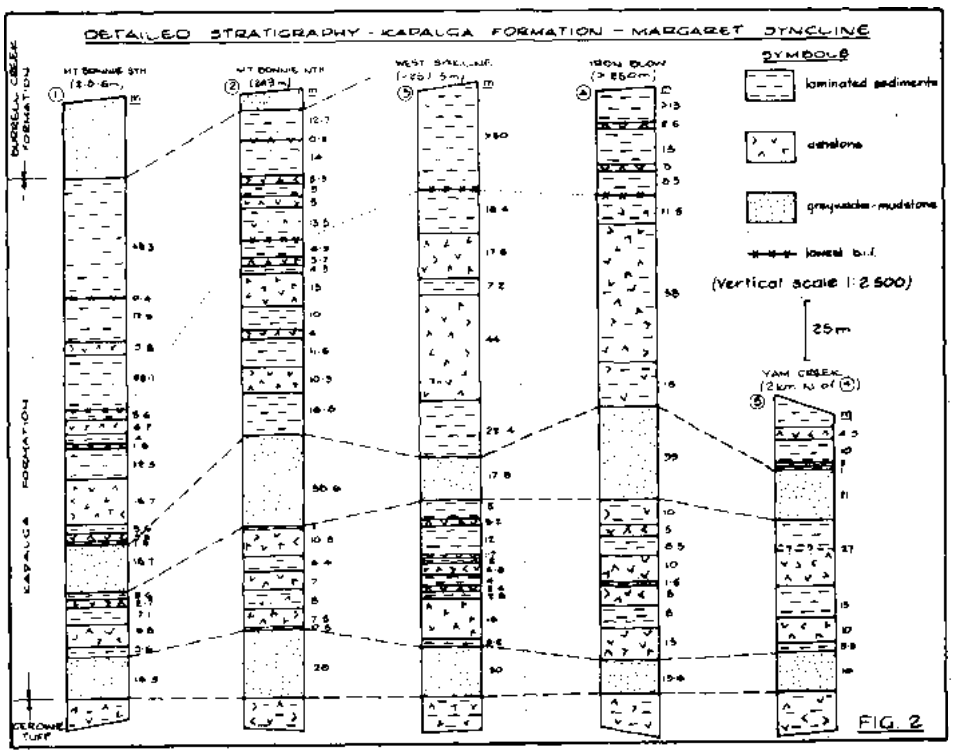


Figure 2. Detailed stratigraphy of the Kapalga Formation in the Margaret Syncline.

unpubl.) but because of later metamorphic events it is not possible to categorically state whether the metadolerites represent intrusion sills or thick lava flows in this area.

STRATIGRAPHY and LITHOLOGY

Essentially, the Kapalga Formation (200-300m) is a transitional sequence between underlying low-energy sediments of the Koolpin Formation (i.e. 'Koolpin facies') and overlying high-energy sediments of the Burrell Creek Formation (i.e. 'Burrell Creek facies'). Superimposed on this transition are layers of ashstone-tuffaceous chert which belong to the phase of volcanism which produced the Gerowie Tuff (i.e. 'Gerowie Tuff facies' rocks) (Fig. 2.).

From detailed mapping and core logging, the details of the stratigraphy of the Kapalga Formation have been elucidated in the Margaret Syncline. Stratigraphic columns from five locations are shown in figure 2.

The base of the Kapalga Formation is defined as the base of the lower of two major greywacke-mudstone units because this unit is the first recognisable input of 'Burrell Creek facies' sediment to the sequence, it is extensively developed, and it is distinctive.

The upper boundary of the Kapalga Formation is ideally defined by the cessation of 'Koolpin facies' sediments in this area. However, isolated thin (0.1m) laminated chert and laminated ferruginous mudstone layers are present 50-100m above the base of otherwise continuous greywacke-siltsone-mudstone sedimentation of the 'Burrell Creek facies'. Because of this, the Kapalga Formation-Burrell Creek Formation boundary in the Margaret Syncline has been selected to correspond with the top of the uppermost significant (0.2-0.3m) layer of banded iron formation (b.i.f.)-laminated chert (see below), which in many places is coincident with the start of uninterrupted greywacke-siltstone-mudstone sedimentation. This boundary has been accurately positioned at several locations. Nevertheless, as minor greywacke has been mapped within the b.i.f. sequence in one area, this definition of the Kapalga Formation-Burrell Creek Formation boundary may be revised or redefined as further information becomes available.

The three lithofacies constituting the Kapalga Formation (i.e. 'Koolpin facies', 'Gerowie Tuff facies' and 'Burrell Creek facies') are reflected by three distinct lithological groups.

Chert, b.i.f, finely bedded pyritic carbonaceous mudstones and siltstones, and argillaceous mudstones and siltstones constitute 40-50% of the sequence and represent the contribution of the low-energy 'Koolpin facies' to the Formation. The 'chert' is recrystallised to sugary quartzite and occurs, both as finely laminated thin bands (0.5m-30cm thick) and, as ellipsoidal nodules (0.5-1.5cm in diameter) which are concentrated in layers parallel to bedding. It is generally accompanied by calcitic, pyritic, chloritic and carbonaceous bands (0.5-15cm) and laminae (1-5mm) though such bands can also occur without chert. Towards the top of the sequence hematite, magnetite and pyrite laminae (1-5mm) commonly accompany the chert resulting in b.i.f. layers up to 30cm thick. In the Margaret Syncline, hematite is the dominant iron oxide phase in these layers; however, elsewhere in the Pine Creek area magnetite is the dominant phase.

Unlike in the Koolpin Formation in this area, where the carbonaceous sediments normally contain in excess of 10% carbonaceous matter, the carbonaceous mudstones and siltstones of the Kapalga Formation generally contain only a percent or two of this material. The carbonaceous laminae associated with chert bands may however, contain 20-30% carbonaceous material. This drastic variation in the carbon content is reflected by the colour of the rocks. In the Kapalga Formation the bulk of the carbonaceous sediments are grey-black in colour as opposed to the jet-black colour of the equivalent sediments in the Koolpin Formation in the Burrundie-Hayes Creek area.

The contribution of the 'Burrell Creek facies' to the Kapalga Formation is characterised by two greywacke-siltstone-mudstone units which can be traced continuously around a significant portion of the syncline (Fig. 1). These two major units, which constitute about 25% of the Formation, have been intersected in several diamond drill holes where hey each consist of 10-20 discrete greywacke-siltstone-mudstone beds 0.5-2m thick. Graded bedding is very common; in most cases individual layers display a sandy or silty greywacke basal section and a massive mudstone upper section separated by an intermixed transition zone. In some layers the upper few centimetres of the mudstone portion are distinctly laminated, and in one case cross-bedding has been observed.

These textural observations are consistent with a turbidity current origin for these rocks, and this possibility is further strengthened by the common occurrence of small (3-10mm) isolated mudstone pellets in the basal greywacke section. Minor carbonaceous matter is also present in these rocks and this indicates some reworking of 'Koolpin facies' sediments.

Ashstones and tuffaceous cherts of the 'Gerowie Tuff facies' account for the remaining 25-35% of the Formation, and are for the most part texturally and mineralogically very similar to the rocks described by Crick *et al.* (1978). Splinters (0.05-0.1mm) of microcline, albitic plagioclase, and quartz in extremely fine (0.005-0.03mm) quartz-feldspar (-sericite) matrix strongly suggest, but do not prove, a volcanic origin for these rocks (H.W. Fander, pers. comm.). In addition the major element chemistry (Table 1) strongly suggests the rocks are rhyodacitic volcanic derivatives.

Confirmation of the volcanic origin of these rocks is given by the discovery of well defined devitrified shards in a specimen of Gerowie Tuff from the south-east margin of the Margaret Syncline (Fig. 1). To date, the shards have only been found in one rock specimen (GS

%	GS3638 3642 Ø	GS3641	GS3640	GS3643	GS1-31 *	GS36	GS37	GS38	GS39	GS40	GS41
SiO_2	73·6	76·6	79·7	60·6	80·6	77·1	80·4	76·2	74·9	79·2	81·7
Al_2O_3	14·4	13·0	11·0	19·5	10·5	12·4	10·2	11·9	12·9	10·7	9·95
TiO_2	0·23	0·16	0·10	0·15	0·13	0·15	0·12	0·12	0·14	0·12	0·09
Fe_2O_3	0·78	0·70	0·57	2·12	0·26	0·19	0·10	0·68	0·19	0·27	0·18
FeO	0·90	0·90	0·79	0·79	0·60	1·18	0·45	0·87	0·95	1·02	0·60
MnO	0·06	0·04	0·03	0·06	0·04	0·04	0·03	0·15	0·10	0·05	0·03
CaO	0·22	0·24	0·09	0·06	0·52	0·19	0·38	0·23	0·50	0·32	0·46
MgO	0·80	0·76	0·57	2·16	0·35	0·15	0·08	0·86	0·12	0·19	0·33
Na_2O	3·78	4·05	1·62	2·84	4·86	4·72	4·04	3·88	4·34	3·40	4·99
K_2O	3·93	2·80	4·40	9·85	1·29	3·10	2·80	4·20	4·65	3·15	0·15
LOI	1·25	1·1	1·2	3·0	0·8	0·4	0·4	0·9	0·4	0·7	0·7
	99·95	100·44	100·27	101·12	99·78	99·62	99·00	99·99	99·09	99·12	99·18
U	8	5	6	10	5	4	X	5	X	5	6
Th	47	40	25	55	26	35	20	25	25	25	20
Rb	190	110	190	450	39	75	65	100	150	120	10
Sr	75	60	70	60	75	30	40	60	90	70	70
Cu	57	25	40	40	20	20	10	40	20	10	60
Pb	32	30	35	25	95	9	55	20	15	15	20
Zn	28	25	25	25	28	15	50	30	50	15	20
Cl	50	50	395	X	3095	1920	2880	3300	430	230	260
F	527	287	568	1411	510	570	410	400	480	510	330
S	80	70	95	65	175	80	170	170	300	110	90

X Not detected.
Ø Avg of 2 samples from same hand specimen.
* Avg. of 30 samples from same horizon. (excl. GS 6)

Table 1. Chemistry of Ashstones (Analysed by Analabs Pty, Ltd).

3639/3642 Table 1) taken from near the base of a 1.5m thick ashstone bed. The bed is characterised by massive basal (GS 3639/42) and central (GS 3641) portions and a finely laminated cherty upper section (GS 3640). The data in table 1 highlight the chemical variation across the bed. It also indicates that hornstone cobbles which characterise sub-outcrop areas of 'Gerowie Tuff facies' rocks in the Margaret Syncline only represent the upper cherty laminated section of the individual ashstone layers (cf.GS 3640 with GS 1-31, Table 1). Specimen GS 3643 is from a thin (0.3m) more pelitic bed in the sequence of ashstone beds from which GS 3629-42 were obtained. The high K_20 content reflects the more pelitic nature of the rock whereas the Na_20 content still indicates a high volcanic component

A feature of some ashstone horizons in the Kapalga Formation is the presence of lenses and/or beds of pebble-breccia. These rocks consist of rounded and sub-angular fragments (0.2-10cm) of metamudstone, siltstone and tuffaceous chert, set in a microcrystalline quartz-albite matrix which closely resembles the recrystallised matrix of the ashstones. Minor calcite is a common constituent of the matrix in the pebble-breccias, particulary in those closely associated with massive sulphide mineralization (see below).

Delicate fragment shapes, the well bedded nature of the breccias and the presence of symmetrically graded bedding (coarse midsection, finer margins) in some beds, are all features consistent with a mud-flow origin for these rocks (J.N. Elliston, pers. comm.). Only three restricted occurrences of these rocks are known in the Kapalga Formation in the Margaret Syncline despite good exposure of the ashstone units in which they lie.

BASE METAL MINERALIZATION

Base metal mineralization was discovered in the Margaret Syncline in the later part of the nineteenth century. The Iron Blow mine was extensively worked between 1886-1914 (Rayner *et al.*, 1937) and the Mt. Bonnie mine was well developed by 1915 (Jenson, *et al.*, 1915) but never went into production.

Renewed exploration of these deposits over the past twenty years has revealed that at each mine the main mineralization occurs in stratiform massive sulphide-silicate-carbonate lodes which are roughly lens shaped, up to thirty metres thick, and in excess of 150m across.

The main sulphide minerals present are pyrrhotite and sphalerite with minor amounts of pyrite, galena, chalcopyrite and arsenopyrite. Significant silver and traces of gold occur with these sulphides. The silicate gangue minerals are chlorite, talc, quartz, actinolite, phlogopite and minor garnet. Calcite is the dominant carbonate gangue mineral though minor dolomite is present. Within the lodes the bulk of the sulphides are concentrated in discrete tabular zones containing 40-50% sulphide minerals with sulphide-deficient gangue zones below and to the sides.

RELATIONSHIP BETWEEN STRATIGRAPHY AND MINERALIZATION

The lodes are stratabound within the sediment-ashstone sequence between the two greywacke-mudstone units of the Kapalga Formation described above. At both mines the lodes occur in the position of an ashstone-rich horizon about a third of the way up from the lower greywacke-mudstone unit (Fig. 2).

Layers of pebble-breccia (described previously) occur above, below and within the lodes. In drill holes which have not intersected mineralization, the pebble-breccia (1.5m) occurs in the same stratigraphic position as the lodes, though laterally removed from them. The thickest intersections of pebble-breccia located to date (more than 20m) come from directly below the thickest accumulation of massive sulphide at Iron Blow.

A weak, though distinct, mineral foliation is present in the sulphide rich zones and measurements on oriented core from both mines show this is parallel with bedding in the

adjacent host rocks. Distinct laminations of sphalerite and carbonaceous mudstone have also been observed in a narrow core intersection from Iron Blow.

Because of the stratiform, stratabound and stratified character of the lodes and consequent implied syngenetic origin, the importance of defining the detailed stratigraphy in the area is very obvious.

The flat lensoid shape of the lodes and the association with restricted developments of pebble-breccias suggest together that a sea-floor depression or trough was the localising control of the mineralization. It is pertinent that at this stratigraphic level, the sequence is well exposed around the entire syncline, particularly near the Iron Blow mine, but pebble-breccia has only been discovered either within the lodes or in their near vicinity.

PROPERTIES OF THE SYSTEM DURING MINERALIZATION

The method employed in the analysis of the possible conditions prevailing in the system was introduced by Barnes & Kullerud (1961). Their theoretical treatment of the subject was later upgraded with more refined thermochemical data by Helgeson (1969).

Barnes & Kullerud (1961) explained how the state of hydrothermal solutions, from which observed sulphide mineral assemblages were deposited, could be described in terms of four variables, viz. temperature (T), acidity (pH), oxygen fugacity (f_{O_2}), and total activity of all sulphur species in solution (S_t).

Although it is possible to consider the behaviour of all mineral phases in this way, only the sulphide minerals will be considered here. These enable a relatively simple, first order approach to the problem to be undertaken. Consideration of the gangue minerals would allow further refinement of parameters outlined below but they are unlikely to drastically alter the ore-genesis theory to follow.

Because of the abundance of iron sulphides in the lodes at Iron Blow and Mt. Bonnie, the Fe-S-O system is the most useful to consider in this case. Thermochemical data used to construct the graphs for this system (Figs. 3-6) are listed in table 2. Sulphur fugacity data were obtained from Barnes & Kullerud (1961, p.662).

Initial assumptions of this analysis are that at the sea floor during deposition of the carbonaceous and pyritic sediments of the lower Kapalga Formation ('Koolpin facies') the following conditions normally existed:— T, 25°C; pH, 8 (present ocean value); S_t, 10^{-3}m; NaCl, 0.5m (Turner & Gustafson, 1978).

The value for S_t may appear to be very high but is is pertinent to note that water in the lower levels of the Black Sea (where similar sedimentation is occurring) contain about

Reaction	Log $K_{(T)}$ 25°C	100°C	Reference
$3\,Fe_2O_3 = 2Fe_3O_4 + \frac{1}{2}O_{2(g)}$	-34.43	-26.02	Helgeson (1969)
$FeS_2 \rightleftharpoons FeS + \frac{1}{2}S_{2(g)}$	-17.26	-12.50	"
$2\,FeS_2 + \frac{3}{2}O_{2(g)} \rightleftharpoons Fe_2O_3 + 2S_{2(g)}$	46.33	38.39	"
$3\,FeS_2 + 2O_{2(g)} \rightleftharpoons Fe_3O_4 + 3S_{2(g)}$	52.27	44.57	"
$3\,Fe + 2O_{2(g)} \rightleftharpoons Fe_3O_4$	177.9	137.7	Barnes & Kullerud (1961)
$Fe + \frac{1}{2}S_{2(g)} \rightleftharpoons FeS$	24.8	18.7	" "
$3\,FeS + 2O_{2(g)} \rightleftharpoons Fe_3O_4 + \frac{3}{2}S_{2(g)}$	103.8	81.5	" "

Table 2. Equilibrium constants (used in derivation of figures 3-6).

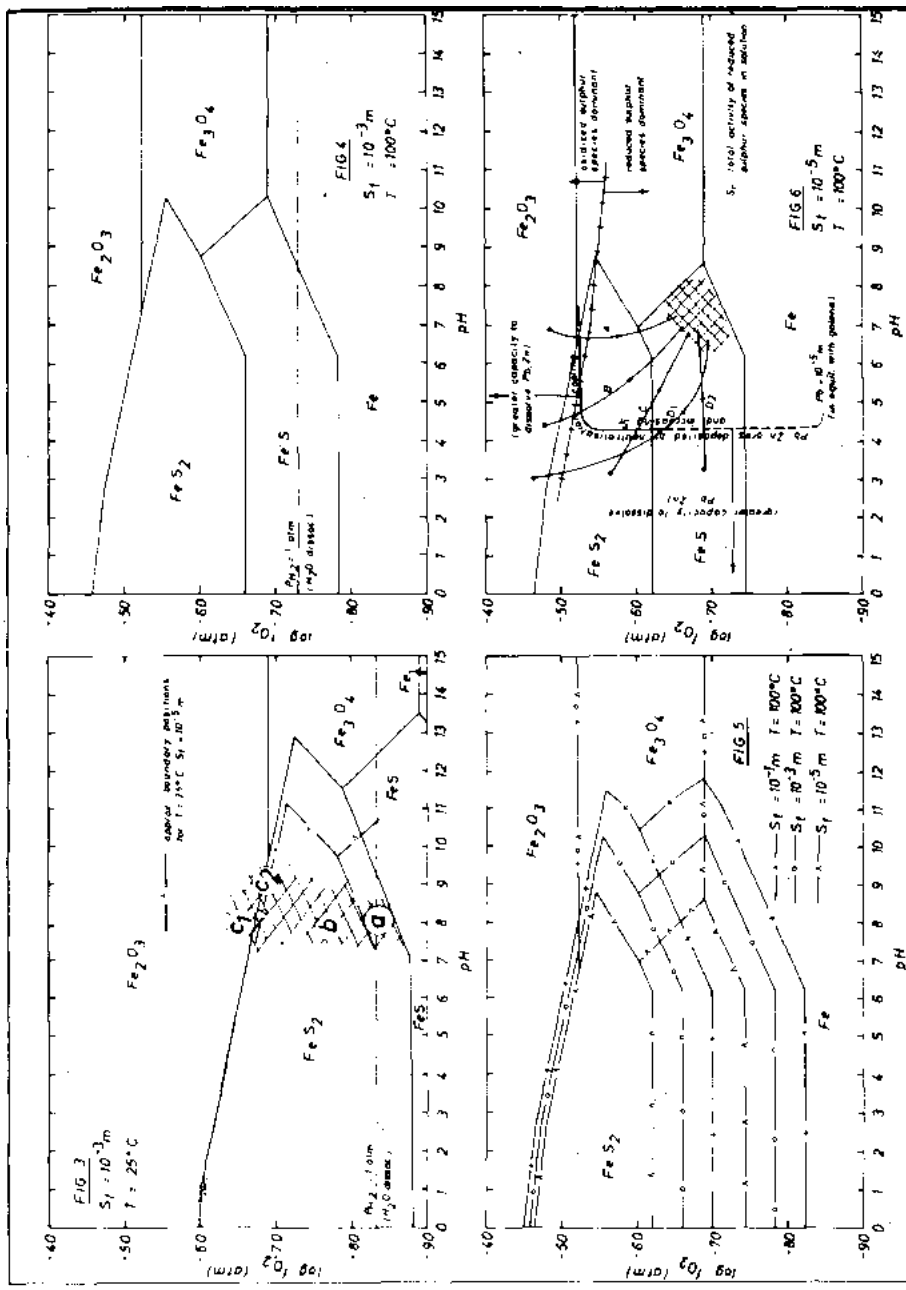


Figure 3-5. Stability of Fe-S-O minerals as functions of f_{O_2} and pH for various values of T and S.
Figure 6. Stability fields of Fe-S-O minerals as functions of f_{O_2} and pH at T = 100°C and S_t = 10^{-5}m with metal solubility data for NaCl = 3m from Anderson, 1975.

$10^{-3.5}$m dissolved H_2S (Ryabinin & Bogaschuk, 1977). (Under the conditions assumed above HS^- or $SO_4^=$ rather than H_2S would be the dominant sulphur species in solution, Barnes & Kullerud, 1961).

The presence of pyrite as the dominant syngenetic Fe-S phase in the Kapalga Formation (excluding the mineralized horizons) determines the f_{O_2} range is $10^{-67.5}$ to 10^{-86}atm (Fig. 3). At lower f_{O_2}, pyrrhotite becomes the dominant Fe-S phase although at these levels H_2O dissociation is an interfering factor (Barnes & Kullerud, 1961). While this situation is not impossible to overcome in some circumstances, there are two simpler ways by which pyrrhotite can become the dominant syngenetic Fe-S phase.

Comparison of figures 3 and 4 reveals that by increasing the temperature to 100°C pyrrhotite becomes the dominant Fe-S phase between f_{O_2} levels of 10^{-62} to 10^{-74} atm at pH8. Alternatively, by decreasing the total activity of the sulphur species in solution (S_t), the stability field of pyrrhotite can again be lifted to higher f_{O_2} levels (Fig. 5).

In contrast to these effects, variation of pH has very little effect on the stability field of pyrrhotite (in terms of f_{O_2}) below pH8 at fixed T and S_t (Figs. 3-5).

From the foregoing considerations, it is evident that a temperature rise to a value as low at 100°C, or a reduction in S_t, or some combination of these two changes will allow pyrrhotite to become the dominant Fe-S species at f_{O_2} levels which correspond to pyrite dominance under the normal sea-floor conditions assumed to exist during deposition of Kapalga Formation.

At temperatures above 100°C (e.g. 150°-250°C) pyrrhotite is stable at even higher f_{O_2} though it is not necessary to expand the discussion to include higher temperature systems here.

At this stage, it is convenient to direct attention to the other sulphide phases in the massive sulphide lodes at Iron Blow and Mt. Bonnie. Consideration of conditions necessary for the transport of Pb, Zn and Cu and deposition of sphalerite, galena and chalcopyrite further assists in defining the properties of the metalliferous solutions responsible for the mineralization.

Anderson (1975) has provided a basis for understanding the phenomena of base metal transport in, and deposition from hydrothermal solutions. He indicates that, at 100°C, sufficient lead and zinc to form an ore deposit can be transported in mildly acid, sodium chloride-rich, brine solutions. He further states that, with decreasing reduced sulphur in solution, decreasing pH, and increasing temperature, the metal-bearing capacity of such solutions is markedly improved.

In figure 6, a portion of Anderson's information is presented for some of the conditions that were applied in figure 5 (viz. 100°C, $S_t = 10^{-5}$m) and several possible paths of ore-deposition are suggested. Paths A,B and to a lesser extent C, pass through the pyrite stability field (inside the sphalerite, galena deposition line) before reaching the pyrrhotite stability field. Had any of these paths been followed (especially A and B), a major earlier pyritic zone would be expected to underlie the pyrrhotitic accumulations at Iron Blow and Mount Bonnie. As zoning of this type has not been recognised to date, Paths A, B and C will not be further considered here.

In contrast to those possibilities, Paths D_1 and D_2 both highlight methods of forming pyrrhotitic base metal deposits. A solution following either of these paths precipitates the base metal sulphides by cooling, neutralisation, and increase in the amount of reduced sulphur in solution (up from 10^{-5}m for the ore solution to 10^{-3}m for the seawater). In both cases as the solution cools and S_t rises (Figs. 3,5), the pyrrhotite stability field is displaced downwards and replaced by the pyrite stability field. Consequently an upper or lateral rim of pyritic ore would be expected to reflect this later change. Limited drilling around the lode margins at Iron Blow indicates such a zone may exist in places.

It is also possible to illustrate from figure 6 and Anderson (1975) that under the assumed

normal sea-floor conditions (low temperature, high S_t with reduced species dominant, slightly alkaline water) almost any trace of base metal in solution would be immediately deposited. This means that the solution from which the ore deposits formed, could not have been generated by accumulation of dissolved base metal at this location over a long period of time with a subsequent change in environmental conditions to trigger precipitation. Conditions conducive to precipitation of base metal sulphides were in existence well before ore deposition, as evidenced by the presence of pyrite in the sediments below the ores. Hence it is concluded that ore deposition resulted from a single inflow of metalliferous brine into an existing favourable environment.

From the information gained from the Fe-S-O system and solubilities of base metal in hydrothermal solutions, suitable likely properties of the solution responsible for deposition of the Iron Blow and Mt. Bonnie lodes appear to be:— T: 75-125°C; S_t: less than 10^{-5}m; pH: below 4.5; Pb and Zn in solution: above 1-2ppm; f_{O_2}: 10^{-50} to 10^{-70}atm; NaCl: 1-3m (this final parameter not only improves the capacity of the solution to transport base metals - Anderson, 1975 - but also ensures that the specific gravity of the ore solution exceeds the specific gravity of the seawater at moderate temperatures - Ellis & Mahon, 1977).

These figures are the minumum requirements of a feasible system to explain these lodes. Higher T, lower S_t and lower pH all enhance the solubility of Pb and Zn in brine solutions (Anderson, 1975) and consequently the figures stated represent only one end of a spectrum of possibilities. However, as this is the low temperature end it is extremely important and it is hoped to exhibit in the following section that ore-forming processes are feasible in this range.

SOURCE OF THE MINERALIZING FLUID

A feasible theory to explain the source of any mineralization must satisfy two major criteria. Firstly it must account for the chemical and physical characteristics of the mineralizing fluid as indicated by mineral assemblages, textures, fluid inclusions, and isotope ratios. Secondly, and equally important (as it is this criterion which decides the probability, as opposed to feasibility, of the preferred theory), it must be compatible with all other aspects of the local and, to a lesser extent, regional geology.

The chemical and physical characteristics of the mineralising fluid which formed the lodes at Iron Blow and Mt. Bonnie have several possible explanations. Space does not permit examination of all of these in this paper. Instead, a theory which closely complies with all the geological data has been selected for detailed consideration.

The probable temporal relationship between the mineralization and the enveloping (though mostly underlying) sequence of volcanogenic sediments, viz, the Gerowie Tuff, is a key element in determining the source of the mineralization. This point was pre-empted in the predeeding section where it was shown that the mineralization probably resulted from a single influx of a suitable fluid into an environment which favoured deposition of the metals being carried in that solution. Furthermore, the widespread presence of well bedded, very fine-grained pyrrhotite in Koolpin Formation sediments between Burrundie and Hayes Creek (Goulevitch, 1979, unpubl.) indicates that similar conditions existed in this area throughout the time that the earlier 'Koolpin facies' sediments were deposited. In spite of this, significant accumulations of base metal sulphides have only been discovered in this area much higher in the sequence towards the top of the 'Gerowie Tuff facies' in the Kapalga Formation.

In view of this implied temporal relationship, it is suggested that the ore fluid was generated during diagenetic devitrification of the Gerowie Tuff. The process envisaged produced a mildly acid, base metal-bearing brine solution of moderate temperature and low sulphide activity. Such developments can be explained in the following ways.

Temperature

According to Ellis (1967), the devitrification of ignimbrites to quartz and feldspar is an

exothermic process. Ellis states that the process is capable of providing sufficient heat to account for high temperature waters in some geothermal areas. Because the process is exothermic, it is irrelevant which reaction path is followed e.g. via solid diffusion, colloidal state, or complete dissolution and redeposition (ionic or colloidal). The important feature is that heat is released in the process.

Acidity

Because of the formation of clay minerals (and ultimately mica) during diagenesis a pH drop is to be expected as OH^- ions are incorporated in the clay lattice and H^+ ions remain in the interstitial water. Experimental reaction of artificial brines and natural seawater with glasses of acid (Holland, 1972) and basic (Mottl & Holland, 1978: Bischoff & Dickson, 1975) composition at moderate (200°C) to high (above 500°C) temperatures has confirmed that a significant pH drops occurs in all cases.

Sulphur

The experiments of Mottl & Holland (1978) and Bischoff & Dickson (1975) also show that, in seawater-basalt reactions, sulphate is removed from the seawater to extremely low concentrations.

Therefore, it appears that a solution characterised by moderate temperature, midly acid pH (4-5) and very low content of sulphur species can be generated during devitrification of glassy volcanic rocks. These changes are the three main requirements which improve the base metal carrying capability of a sodium chloride brine solution (Anderson, 1975).

Bischoff & Dickson (1975) further revealed that the resultant solution (after seawater-basalt reaction of 200°C) was enriched in Fe and Cu, but because of detection limitations were unable to confirm that the same occurred with Pb and Zn. Nevertheless, a release of these metals into solution would be expected provided a sufficient concentration of complexing agent were present (in this case Cl^- to prevent the metal from immediately reprecipitating (cf. Walton, 1978).

A further observation made by Mottl & Holland (1978) and Bischoff & Dickson (1975) is that in the basalt-seawater reaction at elevated temperatures, Mg was very rapidly removed from the seawater by reaction with SiO_2 which had been leached from the basalt. This at first seems to be a disadvantage of the theory being reviewed as both chlorite and talc are very common gangue minerals in the Iron Blow and Mt Bonnie deposits. However, the experimental work also revealed that the SiO_2 (dissolved) content in the reacted seawater rose from less than 1 ppm before reaction to over 500 ppm after reaction (200°C). Thus, although resultant solution is devoid of Mg it is enriched in potentially reactive SiO_2. When such a solution is subsequently re-mixed with an excess of normal seawater abundant Mg is then available to react with the dissolved SiO_2 to ultimately form the chlorite and talc common around the lodes.

An analogous scheme provides a method for deposition of the metals as sulphides. Recalling that the experimental work also highlighted the very efficient removal of sulphate from the seawater, one is led to conclude that the sulphur in the lodes was obtained at the site of deposition either from the seawater or from a sulphur-bearing hydrothermal solution from another source.

Recent investigations in the Black Sea provide pertinent information in this regard. Not only has it been found (Berner, 1974) that sediments being deposited on the floor of the Black Sea are rich in iron sulphides and carbonaceous matter (i.e. similar to 'Koolpin facies' sediments) but it has also been discovered that seawater in the lower levels of the Black Sea are characterised by high concentrations of H_2S (around $10^{-3.5}$m) near the sea floor particularly in the deeper areas (Ryabinin & Bogachuk, 1977).

In the light of this, it is suggested that a smiliar situation existed during deposition of the lower Kapalga Formation and that the sulphur in the Iron Blow and Mt Bonnie sulphide

minerals was obtained from the seawater at the site of deposition. Sulphur isotope data from Mt Bonnie (T. H. Donnelly, pers. comm.) is consistent with such a source though other interpretations of the data are possible.

The final aspect of the ore solution to be considered is the NaCl concentration of the solution. The experimental data referred to previously (Mottl & Holland, 1978; Bischoff & Dickson 1975) resulted in very little change in the Na and Cl concentrations in the reacted seawater - if anything, the Na content decreased slightly in some experimental runs.

The necessity to increase the NaCl concentration above the normal content of 0.5m (Turner & Gustafson, 1978) arises not because of base metal solubility and complexing, but because of the density requirements of the mineralizing fluid when it is exhaled onto the sea floor. In view of the likelihood of a temperature increase during devitrification it is advantageous for the mineralizing fluid to have a salinity high enough to compensate for the density reduction which results from the increased temperature. Normally, such a solution would flow along the sea floor into depressions or troughs, though the variations and limitations to such a scheme, as indicated by Turner & Gustafson (1978), are appreciated. As stated previously, the pebble breccias in the ore environment at Iron Blow and Mt Bonnie suggest that sea floor depressions capable of localising high density ore solutions were present during sedimentation.

Apart from Holland's (1972) high temperature experiments, the literature appears devoid of other experimental work involving seawater and acid (rather than basaltic) glass. However, the investigations of Surdam & Eugster (1976) into the formation of zeolites from trachytic glass at Lake Magadi in Kenya make up for this deficiency to some extent. Sea-floor brines at Lake Magadi are vastly more saline than any of the inflowing solutions and overlying waters. From this it appears that the salinity of a solution may be significantly increased by the removal of H_2O to form hydrous zeolite minerals during early diagenesis of alkali-rich volcanic glass. Base metals released during this initial break-down would be concentrated in the uncombined more saline interstitial water because of the abundance of chloride ions to form soluble complexes (after Walton, 1978).

During sedimentary compaction and initial dewatering, this metalliferous saline interstitial water would be the first to be expelled from the tuffaceous sequence. During later diagenesis and early metamorphism the loosely combined less saline water and water of crystallisation would be expelled as albite, quartz and K-feldspar formed as the final products we see today.

Finally, it must be again emphasised that other theories of ore genesis can be proffered. The theory presented here is aimed primarily at explaining the apparent temporal relationship between the mineralization and the underlying (for the most part) sequence of alkali-rich tuffaceous rocks. The relative simplicity of the process, and fact that it incorporates a 'closed-system' approach (i.e. no spurious external source of metals, heat, or acid water) are factors which make the theory extremely attractive.

CHEMICAL CONDITIONS DURING KAPALGA FORMATION DEPOSITION

In a preceeding section the stability fields of mineral species in the Fe-S-O system were used to investigate the chemical environment during mineralization (Figs. 3-6). Since all mineral species of this system (excluding elemental Fe) are represented in the Kapalga Formation, the data can also be used to trace the chemical evolution of the sea floor environment (excluding the mineralizing event) during sedimentation of this unit.

The lithological composition of the Kapalga Formation was shown above to be essentially a transition between earlier 'Koolpin facies' sediment and later 'Burrell Creek facies' sediment. Below the Gerowie Tuff, the 'Koolpin facies' rocks in this area (i.e. Koolpin

Formation) are characterised by large accumulations of bedded pyrrhotite with minor pyrite (Goulevitch, 1979, unpubl.).

The difficulty of forming syngenetic pyrrhotite at low temperatures is apparent in figure 3 as the degree of H_2O dissociation becomes excessive at low f_{O_2}. Unless the temperature at the sea floor was higher than 25°C or S_t less than 10^{-3}m pyrrhotite would be unlikely to deposit around pH8. An S_t reduction to 10^{-4}m is sufficient to shift an acceptable portion of the FeS stability field above the H_2O dissociation line at pH8. Consequently, during deposition of the Koolpin Formation the sea floor would be expected to have exhibited the properties of 'a' in figure 3 with S_t of 10^{-4}m or less.

In the lower Kapalga Formation, however, the 'Koolpin facies' sediments - carbonaceous mudstones and siltstones, laminated cherts and minor carbonate - contain pyrite as the dominant, and for the most part sole, representative of the Fe-S-O system. From figure 3 it can be seen that this change in iron sulphide species can result from a change in f_{O_2} from 'a' to 'b' in the hatched area which covers the likely pH range during deposition. In addition, an increase in S_t from 10^{-4} to 10^{-3}m would assist this phase change from pyrrhotite to pyrite.

Towards the top of the Kapalga Formation the 'Koolpin facies' is represented by slightly carbonaceous mudstones and siltstones, and hematite-pyrite (± magnetite) b.i.f. In figure 3 the hematite-pyrite case is shown at 'c_1'. For magnetite to be present, either S_t must drop significantly (e.g. $S_t = 10^{-5}$m line in figure 3) to draw the magnetite field to lower pH, or the pH must increase slightly from 'c_1' towards 'c_2'. Because of the thickness and abundance of the chert bands at this point a pH rise is not unexpected as this also assists silica deposition.

To summarise, the transition from pyrrhotite to pyrite to hematite (+ pyrite ± magnetite) across the Kapalga Formation essentially represents a gradual increase in the f_{O_2} of the seawater at the sea floor with minor variations due to S_t and pH changes. The influx of Burrell Creek Formation greywacke-mudstone turbidites either was the cause of this change, or along with the f_{O_2} change, was the result of a more encompassing geological event e.g. regional uplift, or sea regression.

CONCLUSIONS

From the information presented in the preceding sections the following conclusions seem justified.

1) In the Margaret Syncline, the Kapalga Formation is a transition between underlying low energy, probably hemipelagic, sediments of the Koolpin Formation and overlying high energy, probably terrigenous, sediments of the Burrell Creek Formation. This sequence is interlayered with ashstone beds which were deposited during the waning stage of Gerowie Tuff sedimentation.
2) This transition was accompanied by a change from more reducing to more oxidising conditions at the sea floor during sedimentation as is reflected by the syngenetic iron sulphide-iron oxide mineral assemblages.
3) The identification of devitrified shards in Gerowie Tuff ashstone confirms claims by earlier workers that these rocks are volcanic derivatives.
4) Massive sulphide-silicate-carbonate mineralization at Iron Blow and Mt Bonnie is stratabound, stratiform and (in places) stratified. This, together with the presence of associated pebble-breccias, strongly suggests a syngenetic origin for the mineralization.
5) Divitrification of the Gerowie Tuff ashstones provides a simple model which adequately explains the presence of the Iron Blow and Mt. Bonnie mineralization, and which is compatible with the local and regional geology.

ACKNOWLEDGEMENTS

The author is indebted to Dr. M.J. Wilson, Mr. K.G. Burlinson, Dr. R.R. Large, Mr. P. Nicholson and other Geopeko personnel for their constructive criticism of earlier drafts of this paper. In addition he is appreciative of the

efforts of Judy Burke and Margo Bellis for typing and drafting respectively. The paper is presented with permission from the directors of Peko-Wallsend Ltd. and for this the author is extremely grateful.

REFERENCES

Anderson, G.M., 1975: Precipitation of Mississippi Valley-type ores. *Econ. Geol., 70,* 937-942.

Barnes, H.L. & Kullerud, G., 1961: Equilibria in sulphur-containing aqueous solutions in the system Fe-S-O and their correlation during ore deposition. *Econ. Geol., 56,* 648-688.

Berner, R.A., 1974: Iron sulphides in Pleistocene deep Black Sea sediments and their palaeo-oceanographic significance. *in* (eds. E.T. Degens & D.A. Ross) *The Black Sea - Geology, Chemistry and Biology, Am. Ass. Petrol. Geol., Tulsa,* 524-531.

Bischoff, J.L. & Dickson, F.W., 1975: Seawater-basalt interaction at 200°C and 500 bars: implications for the origin of sea-floor heavy-metal deposits and regulation of seawater chemistry. *Earth Planet. Sci. Lett., 25,* 385-397.

Crick, I.H., Stuart-Smith, P.G. & Needham, R.S., 1978: Stratigraphic significance of a discovery of Lower Proterozoic tuff in the Pine Creek Geosyncline. *B.M.R. J. Aust. Geol. Geophys., 3,* 163-165.

Ellis, A.J., 1967: The chemistry of some explored geothermal systems. *in* (ed. H.L. Barnes) *Geochemistry of Hydrothermal Ore Deposits.* Holt Rinehart and Winston, New York, 465-514.

Ellis, A.J. & Mahon, W.A.J., 1977: *Chemistry and Geothermal Systems,* Academic Press, N.Y., 392p.

Ferguson, J. & Needham, R.S., 1978: The Zamu Dolerite: a Lower Proterozoic preorogenic contiental tholeiitic suite from the Northern Territory, Australia. *J. geol. Soc. Aust., 25,* 309-322.

Goulevitch, J., 1979: Exploration results:- Quest 10, Quest 23/37, Quest 62, Quest 67, Burrundie/Grove Hill area. *Geopeko Report, D79/9,* 22p. (unpubl.).

Helgeson, H.C., 1969: Thermodynamics of Hydrothermal systems at elevated temperatures and pressures. *Am. J. Sci., 267,* 729-804.

Holland, H.D., 1972. Granite, solutions, and base metal deposits. *Econ. Geol., 67,* 281-301.

Jenson, H.I., Gray, G.J. & Winters, R.J., 1915: The geology of the Woggaman Province, Northern Territory of Australia. *Bull. Nth Terr. Aust., 16,* 72p.

Mottl, M.J. & Holland, H.D., 1978: Chemical exchange during hydrothermal alteration of basalt by seawater - 1. Experimental results for major and minor components of seawater. *Geochim. cosmochim. Acta, 42,* 1103-1115.

Rayner, J.M. & Nye, P.B., 1937: Geophysical report on the Iron Blow area, Pine Creek district, Northern Territory. *Aer. Surv. Nth Aust., N.T. Report 13.*

Ryabinin, A.I., & Bogachuk, V.M. 1977: On the geochemistry of hydrogen sulphide in the waters of the Black Sea. *Geochem. Int., 14,* 117-184.

Surdam, R.C., & Eugster, H.P., 1976: Mineral reactions in the sedimentary deposits of the Lake Magadi region, Kenya. *Bull. geol. Soc. Am., 87,* 1739-1752.

Turner, J.S., & Gustafson, L.B., 1978: The flow of hot saline solutions from vents in the sea floor - some implications for exhalative massive sulphide and other ore depositis. *Econ. Geol., 73,* 1082-1100.

Walpole, B.P., Crohn, P.W., Dunn, P.R. & Randal, M.A., 1968: Geology of the Katherine Darwin region, Northern Territory. *Bull. Bur. Miner. Resour. Geol. Geophys., Aust., 82,* 304p.

Walton, A.W. 1978: Fate of uranium during open system diagenesis of glass-rich volcanic sediment of the Tascotal Formation (oligocene), Trans-Pecos, Texas. *Econ. Geol., 73,* 1399.

THE GEOLOGY AND ECONOMIC SIGNIFICANCE OF THE GOLDEN DYKE DOME, NORTHERN TERRITORY

P.M. Nicholson

Peko Mines, P. O. Box 156, Tennant Creek, N.T., 5760, Australia.

ABSTRACT

Rocks of the Lower Proterozoic South Alligator Group were deposited in a restricted basin. Mudstones were typically deposited, although during periods of restricted, clastic sedimentation, banded, ferruginous, chemical sediments, carbonates and cherts accumulated.

An exhalative model is proposed for some stratiform mineralization hosted by these sediments. High geothermal gradients caused the circulation of oceanic and meteoric waters through the sediment pile and the underlying basement rocks. Resultant brines, which were both metal- and boron-rich, were periodically discharged onto the seafloor. These migrated towards, and collected in, local troughs where metal- and boron-rich sediments formed. Iron and base-metal sulphides were deposited from these brines when they encountered reducing conditions. Gold occurs in the iron-rich sediments. The base metal content of the brines and subsequent deposits increased markedly after tuffaceous sediments were added to the pile as these contained potentially accessible metals, and their leaching agent, chlorine.

INTRODUCTION

The Golden Dyke Dome is located 5km north-east of the Hayes Creek in the Pine Creek area (Fig. 1).

Within the Hayes Creek-Burrundie area sediments and intrusives of the Lower Proterozoic Pine Creek Geosyncline crop out. These include chemical and argillaceous sediments of the South Alligator Group, flysch-type sediments of the Finniss River Group, sills of the Zamu Dolerite, and granite of the Cullen batholith. Mineralization occurs throughout this area with different types of gold, silver, base metals and tin deposits represented.

A continuous sequence of sediments which belongs to the South Alligator Group is exposed around the Golden Dyke Dome. These sediments contain examples of Mt Isa-McArthur River-type, base metal mineralization, Homestake-type, gold mineralization and bedded, tourmaline rocks. All of these deposit types have been considered to have a syngenetic, sedimentary-exhalative origin (eg. Croxford *et al.*, 1975; Sawkins & Ryc, 1974; Ethier & Campbell, 1977).

The aim of this study is to examine the relationships between the various types of mineralization in the Golden Dyke Dome area, their associated sediments and the local stratigraphy and thus gain insights into the controls on ore deposition and the genesis of the mineralizing fluids.

GENERAL GEOLOGY

The Golden Dyke Dome area contains the type locality of the Golden Dyke Formation as defined by Walpole *et al.* (1968). According to the revised stratigraphy (Needham *et al.*, this volume) the sediments of the Dome now belong to the Koolpin Formation, Gerowie Tuff and Kapalga Formation of the South Alligator Group (Table 1). Several sheets of the Zamu Dolerite are interlayered with this sediment pile.

The sediments and dolerites experienced mid-greenschist facies, regional metamorphism at about 1800 m.y. (Page *et al.*, this volume). This coincided with, or preceded two episodes of ductile deformation which produced a dome-shaped structure consisting of two closely spaced, double plunging anticlines (Fig 1). A number of later faults complicate this structure.

Intrusion of the Cullen Granite occurred at 1765 ± 90 m.y (Leggo *in* Walpole *et al.*,

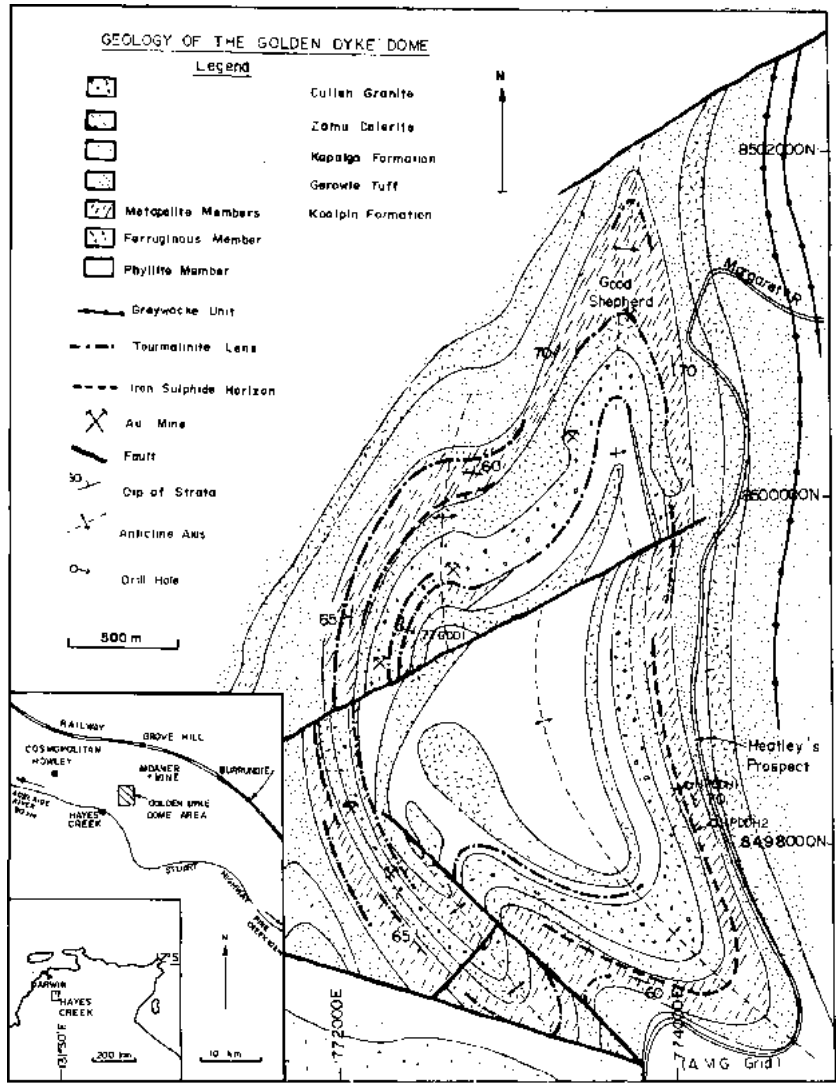


Figure 1: Geology of the Golden Dyke Dome

1968). This granite and its 500m wide metamorphic aureole lie to the south of the Dome (Fig. 1).

STRATIGRAPHY AND SEDIMENTARY GEOLOGY OF THE KOOLPIN FORMATION

The Koolpin Formation is divided here into 4 informal members; the Phyllite Member, the Banded Ferruginous Member and the Upper and Lower Carbonaceous Metapelite Members. Interlayered with these are a number of tourmalinite lenses and metadolerite sills (Table 1, Fig. 1).

Formation	Member	Lithology	Thickness (metres)
Kapalga Formation		Phyllite, greywacke, iron formation, chert, tuffaceous chert	500
Gerowie Tuff		Tuffaceous chert, chert, tuffaceous pelite, phyllite.	300
Koolpin Formation	Upper Carbonaceous Metapelite Member	Carbonaceous and sulphidic metapelite, tourmalinite.	80 - 150
	Banded Ferruginous Member	Ferruginous sediment, Carbonaceous metapelite, tourmalinite.	50 - 100
	Lower Carbonaceous Metapelite Member	Carbonaceous metapelite, tourmalinite, greywacke	0 - 50
	Phyllite Member	Phyllite, tourmalinite	at least 220

Table 1: Stratigraphy of the Rocks of the Golden Dyke Dome

Phyllite Member

A thickness of about 220m of the Phyllite Member is exposed in the centre of the Dome. It is comprised of pink, quartz-muscovite phyllites, laminated, green, muscovite-chlorite-quartz metapelites and tourmalinites. The tourmalinites will be described later. Carbonaceous metapelites are only minor constituents of this Member. Poor outcrop and complex folding prevent determination of the relationships between lithologies.

Lower Carbonaceous Metapelite Member

The carbonaceous metapelite sequence can be divided into Upper and Lower Members separated by the Banded Ferruginous Member.

The Lower Member only appears on the western side of the Dome where it is up to 50m thick and is comprised of dark-coloured, carbonaceous, quartz-biotite metapelites which contain minor interbeds of greywacke and light coloured K-feldspar-chlorite-muscovite-quartz metapelite. Core from drill hole 77GDD1 (Fig. 1) indicates minor, conformable sulphide bands present near the bottom of the unit. These are composed of pyrite with trace chalcopyrite. Relatively coarse-grained garnet, biotite and chlorite, which are in equilibrium with the regional metamorphic, fine grained quartz and biotite, are commonly associated with the sulphide bands.

A 50cm thick bed of greywacke was also found in drill-hole 77GDD1. It contains 30% subangular, detrital, quartz grains and rounded lithoclasts of metapelite. These grains and lithoclasts lie in a matrix of quartz-biotite metapelite. The large grain sizes contained in the greywacke compared with the surrounding pelites, and the presence of pelite inclusions suggests these sediments may have been deposited by turbidity currents.

Banded Ferruginous Member

The Banded Ferruginous Member ranges from 50 to 100m thick and lies in the carbonaceous metapelite sequence (Table 1, Fig. 1). It is characterized by the presence of banded, iron-rich, sedimentary rocks. These rocks can be classified as belonging to the different facies of banded iron formations (James, 1954). The Member consists of seven or

eight beds of banded, ferruginous sediment alternating with beds of carbonaceous, quartz-biotite metapelite. Three different types of ferruginous sediment, texturally and mineralogically distinguishable, occur at the Dome. These are the silicate, silicate-oxide and oxide types.

The Silicate-rich rocks

The silicate-rich rocks are composed of alternating green and darker, green-brown bands. The green bands are 2mm to 7mm thick and composed entirely of ferroactinolite whereas the green-brown bands are usually thinner and composed of approximately equal proportions of ferroactinolite and stilpnomelane. Sugar-textured, re-crystallized chert pods vary from 1cm to 2cm in diameter. They are slightly ellipsoidal in shape and flattened parallel to bedding. Stilpnomelane-rich bands invariably border the pods and are distorted around them.

The Silicate-oxide rocks

The Silicate-oxide rocks contain different scales of banding. Iron-rich bands 2mm to 4mm thick alternate with quartz-rich bands of approximately the same thickness. The iron-rich bands are themselves composed of finer alternations of quartz- and iron-rich bands. The quartz-rich bands contain minor white mica and the iron-rich bands contain an equilibrium, metamorphic assemblage of hematite, biotite and quartz. These bands range from 0.1mm to 1mm in thickness, and can be slightly contorted and disrupted. Sugar-textured, chert pods and lenticles are ubiquitous. They commonly exceed 10cm in length with elongation ratios ranging between 1:1 and 6:1. Necking of chert lenses is common and in places chert pods can be traced along strike into continuous chert beds. When observed perpendicular to bedding planes, the chert is seen to form irregular, anastomosing networks. These features indicate that the chert podding is mainly a result of boudinaging of originally continuous, gelatinous, chert beds during compaction.

The Oxide-rich rocks

The oxide-rich rocks are almost entirely composed of quartz and hematite. A weak banding is defined by the differing proportions of these minerals. It is uncertain whether all the hematite is of hypogene origin.

The lack of detrital textures, iron-rich composition and fine banding in these rocks indicates they represent metamorphosed, chemically precipitated sediments. High iron activities (Eugster & Chou, 1973) and very low detrital influx (Klein & Bricker, 1977) must have prevailed during their deposition.

Upper Carbonaceous Metapelite Member

The Upper Carbonaceous Metapelite Member contains grey and black metapelites which are generally carbonaceous. Quartz-biotite metapelites are found throughout the Member, whereas quartz-muscovite metapelites are only found near the top of the Member. Thin, conformable chert bands are numerous. A gossanous, ferruginous bed of metapelite can be traced discontinously around the Dome. This horizon ranges in thickness from 10 to 20m and lies within 10 or 20 metres of the unit's boundary with the underlying Banded Ferruginous Member. Magnetic anomalies coincide with this horizon in the northern and eastern parts of the Dome. Drilling shows it to be very pyrrhotite-rich below the zone of oxidation.

Metadolerite Sills

Three major and several minor sheets of the Zamu Dolerite are interlayered with the South Alligator Group sediments. The local, slightly transgressive nature and discontinuity of these units infers an intrusive origin. However, regional conformability of the three major sills has allowed previous workers to use them in correlating stratigraphy within the Hayes Creek-Burrundie area (eg. Hossfeld, 1936; Voisey, 1938; Goulevitch, 1977).

The positions of the three major sills are shown in figure 1. These range between 40 and 100m in thickness. Three thinner and less continuous sills occur between the major middle and upper sills. These are up to 50m in thickness.

The metadolerite sills are composed of sphene, biotite, plagioclase and actinolite. Relic, ophitic textures and chilled margins are present. No contact metamorphic effects are evident in adjacent sediments, and there is no apparent spatial relationship between the metadolerite sills and the mineralization described in the subsequent sections.

A DESCRIPTION AND DISCUSSION OF MINERALIZATION IN THE KOOLPIN FORMATION

Mineralization in the Banded Ferruginous Member

The Banded Ferruginous Member contains anomalous, and at times economic, gold concentrations. Sampling by Hossfeld (1936) and Blanchard (1937) indicated one bed of ferruginous sediment, called the Main Reef, contained almost 1 gram per tonne gold over a strike length of at least 3km. Within this bed grades averaged 10 grams per tonne over a 110m strike length and 3m thickness at the Golden Dyke mine (Hossfeld, 1936). Economic concentrations of gold are also present in other ferruginous beds within the Member, and within correlatable ferruginous sediments at several locations, including the Moaner Mine, 3km to the east, and the Cosmopolitan Howley Mine to the west (Fig. 1).

The gold within these deposits is associated with disseminated pyrite, arsenopyrite and minor chalcopyrite (Hossfeld, 1936). Tourmaline has been reported as an accessory mineral at the Cosmopolitan Howley (Twist, 1975). Although quartz veining is commonly present, it does not consistently contain gold, and never contains all the gold ore at any one locality.

Because the gold and sulphide concentrations are conformable and mainly disseminated through the sediment, it is suggested that the mineralization is syngenetic in origin. Moreover, a chemical, sedimentary origin is proposed for similar gold deposits found in Precambrian iron-rich rocks of the Homestake area, South Dakota (Sawkins & Rye, 1974) and in the Archaean banded iron formations of Rhodesia (Fripp, 1976). These authors envisaged that gold was deposited on the seafloor from hot brines. At the Golden Dyke Dome, one tourmalinite lens is contained within the Banded Ferruginous Member (Fig. 1). As will be shown later, these tourmalinites are also thought to be of sedimentary-exhalative origin.

Auriferous quartz veins associated with these deposits probably represent later remobilization of syngenetic gold and silica.

Mineralization in the Upper Carbonaceous Metapelite Member

In the eastern part of the Dome, at Heatley's Prospect (Fig. 1), soil geochemical lead, zinc and copper anomalies coincide with the Upper Carbonaceous Metapelite Member over a 1000 metre strike length (Shields & Pietsch, 1971). The anomalies are elongated parallel to strike and coincide with a major magnetic anomaly of the same shape. Diamond drill holes HPDDH1 and HPDDH2 tested these anomalies and intersected anomalous, although sub-economic, metal concentrations (Baarda, 1972). Apart from several zones of discordant, vein mineralization, the base-metal concentrations can be explained by the presence of base-metal sulphides visible in polished section, which originally crystallized during sedimentation or diagenesis. This is indicated by the occurence of these sulphides in conformable lenses and lines of aggregates, and their association with iron sulphides which exhibit soft sediment deformation structures such as irregular lens contortion and sedimentary dykes. With the exception of areas containing discordant mineralisation and two anomalous zones, metal concentrations in the metapelites range between the following values; copper, 100 to 300 ppm; lead, 50 to 150 ppm; and zinc, 500 to 1000 ppm.

The Upper Carbonaceous Metapelite Member can be divided into two units in the

Heatley's Prospect area, depending on the iron sulphide species present and their abundance. The lower unit comprises the bottom 50 to 60m of the Member whereas the upper unit comprises the top 20 to 30m.

The lower unit is characterized by pyrrhotite which occurs as fine grains 0.01mm in diameter or thin lenses 0.5mm thick. Concentrations of fine grains define laminae of 0.3mm. Fine-grained galena, sphalerite and chalcopyrite appear to have formed with the pyrrhotite as they are intergrown with pyrrhotite or have similar grain sizes and distributions. Coarser pyrite lenses averaging 1mm thick and blebs 0.5mm in diameter are usually present with the previously mentioned sulphides. The pyrite postdates the finer sulphides though is still conformable and shows soft-sediment deformation structures. This pyrite is often associated with chert beds and lenses and co-exists with minor amounts of chalcopyrite, arsenopyrite and galena.

The pyrrhotite-rich bed mentioned previously is intersected in HPDDH1 10 metres above the Banded Ferruginous Member. Pyrrhotite reaches a local maxima concentration of 20 percent over a 10m thickness. Elsewhere in the lower unit sulphides comprise two to five percent of the metapelite.

The pyrrhotite is probably of syngenetic or diagenetic origin. Formation by conversion of pyrite to pyrrhotite during metamorphism is considered very unlikely. Plimer & Finlow-Bates (1978) state that this conversion probably only occurs by reaction between pyrite and ferromagnesian silicates. No such reactions are evident in this area, and there appears to be no spatial relationship between the relative distribution of pyrite and pyrrhotite and any metamorphic heat source (such as the dolerite sills). Furthermore, as mentioned above, pyrite of probable diagenetic origin postdates the pyrrhotite.

A conformable layer of massive fine grained sulphide 5cm thick occurring near the top of the lower unit was intersected in HPDDH1. This layer reportedly contained over one percent zinc, one percent lead and 30 grams per tonne silver (Baarda, 1972). As no samples were available for this study, it is not certain how this layer was formed. However, sulphides of syngenetic origin occur immediately above and below the layer.

The boundary between the upper and lower units is gradational. Pyrrhotite gradually becomes less common. Pyrite commonly occurs as lenses and globular aggregates 1mm to 2mm in diameter which may define conformable bands up to 5cm thick. Fine-grained

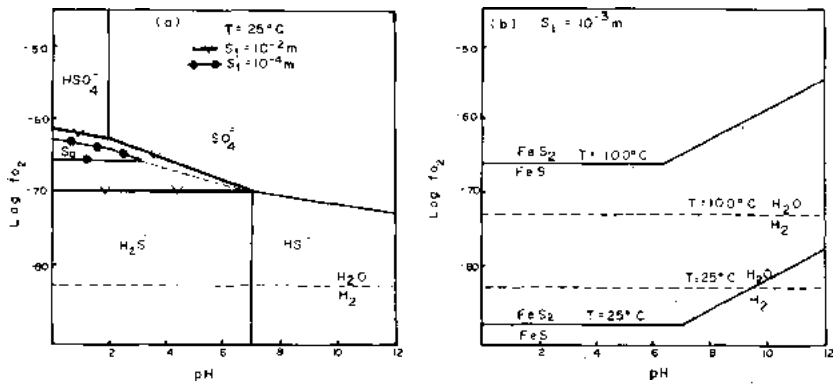


Figure 2. (a) Stability fields of sulphur species in fo_2-pH space at 25°C and total dissolved sulphur : $S_t = 10^{-2}$ and 10^{-4} molal
(b) Relative stability fields of FeS and FeS_2 in log fo_2-pH space at 25°C and 100°C, and total dissolved sulphur = $S_t = 10^{-3}$ molal
(Thermodynamic data from Helgeson, 1969)

sphalerite, galena, chalcopyrite and rare pyrite are disseminated through the rest of the upper unit. The average total volume of sulphides is about three percent. Fifteen metres below the top of the upper unit a 2m thick bed containing ten percent pyrite, 1000 ppm copper, 1000 ppm lead and 2000 ppm zinc was interesected in HPDDH2 (Baarda, 1972).

According to the data of Helgeson (1969), iron monosulphides are generally metastable with respect to pyrite at 25°C and one atmosphere pressure. However, the study of pyrite formation in the sedimentary environment shows that an iron monosulphide phase is the first to precipitate (Berner, 1967; Sweeney & Kaplan, 1973). This reacts with elemental sulphur to form pyrite, or its precursor, greigite (Fe_3S_4). Considering the stability of elemental sulphur, figure 2a shows the conditions in which iron monosulphide is most likely to be preserved. These are high pH, low oxygen fugacity, and low total sulphur activity. Figure 2b shows that iron monosulphide is also increasingly stable at higher temperatures.

The formation of iron monosulphides in the Golden Dyke Dome area due to low sulphur activity is hard to reconcile with the exceedingly high sulphur contents of these horizons (up to 15% by weight). Moreover, iron silicates become increasingly stable relative to iron sulphides at low sulphur activities and high silica activities (Fig. 3), which are evidenced by the deposition of chert. Formation due to low oxygen fugacity is unlikely as minimum values of oxygen fugacity are limited by the stability field of water (Fig. 2b). Lastly, the effect of pH is limited to alkaline conditions (Fig. 2a, 2b), which are unlikely to prevail in normal sedimentary environments.

It is therefore considered that the pyrrhotite-rich horizon at the Golden Dyke Dome, and a number of similar horizons further to the east (Goulevitch, 1977), were formed during periods of relatively high temperature. Pyrite may have formed during diagenesis as temperatures dropped, or as the monosulphide was partially sulphidized.

Although the base-metal concentrations at Heatley's Prospect are generally within the limits sometimes found in normal carbonaceous shales, these concentrations are anomalous for Koolpin Formation sediments. Moreover, the metals are present in syngenetically or diagenetically formed sulphides which are in places closely associated with high concentrations of pyrrhotite. It is therefore considered the base-metals were derived from brine activity. This is substantiated by the spatial relationships between sulphide concentrations and tourmalinites (see below). A similar origin is proposed for the McArthur River and Mt. Isa deposits (Croxford *et al.*, 1975; Mathias & Clark, 1975).

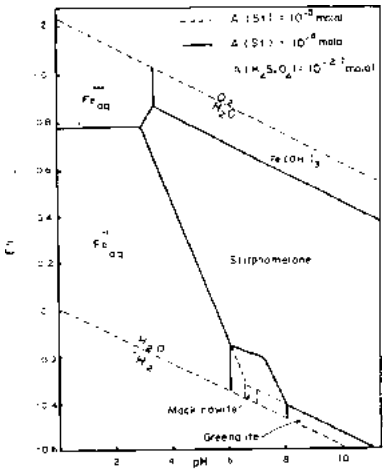


Figure 3. Stability fields in Eh-pH space of some minerals in the system Fe - H_2O-O_2-S at 25°C, one atmosphere total pressure, saturated with amorphous silica, and at two activities of total dissolved sulphur. Boundaries between acqueous species and solids at A (aq) = 10^{-6} (after Klein & Bricker, 1977)

The upper pyrite-rich unit may have formed in more oxidising conditions close to the ferruginous shale facies boundary to the east (see below). This would explain the dominance of pyrite instead of pyrrhotite, and the presence of a relatively chalcopyrite-rich bed. Brines which were cooling, and migrating into anoxic conditions, would tend to deposit the relatively insoluble copper first.

TOURMALINITE LENSES

In the Golden Dyke Dome tourmalinite lenses are found throughout the Koolpin Formation (Fig. 1). Four distinct horizons have been recognized as

well as uncorrelated occurrences in the Phyllite Member. The lenses are discontinuous and grade laterally and vertically into the sediments surrounding them. They rarely exceed 10m in thickness although they extend up to 3km along strike.

Composition

Tourmalinites are defined here as laminated rocks containing over 15% (by volume) tourmaline and over 90% (by volume) combined quartz and tourmaline. At the Dome the proportion of tourmaline varies from 15% to 60%. Minor rutile and carbon are also present. Rocks transitional to metapelites contain biotite or muscovite. X-ray and optical methods (Epprecht, 1953; Winchell, 1932) indicate the tourmalines are composed mainly of dravite (magnesium) and uvite (calcium) components, with a minor schorl (iron) component. Ratios of Mg/(Mg + Fe) were 0.85 and 0.91, and of Ca/(Ca + Na), 0.34 and 0.68.

Using the tourmaline contents mentioned above, and the average boron content of tourmaline (Deer *et al.*, 1972), it can be calculated that the tourmalinites contain 0.7 to 2.2% boron (by weight). Comparing these with the concentrations of boron found in other rocks and minerals (Harder, 1970) it is obvious that tourmalinites contain anomalous boron concentrations.

Texture

The tourmaline in these rocks is generally preferentially orientated parallel to the steeply dipping, slatey cleavage produced during the first episode of regional, ductile deformation. This indicates that tourmaline crystallized during this event or was reorientated to this position during cleavage development.

The tourmalinites usually have a banded texture, which consists of alternate tourmaline-rich and tourmaline-poor bands. The former vary from 2 to 20mm in thickness, and the latter from 6 to 30mm. In places a banding is defined by the presence of spherical clots 1mm in diameter which are composed of a quartz nucleus surrounded by randomly orientated tourmaline laths. Similar tourmaline-rich clots are also found flattened parallel to the slatey cleavage.

The compositional banding is invariably parallel to bedding in adjacent rocks.

Metapelites associated with the lenses have tourmaline disseminated throughout the rock or concentrated into thin conformable bands less than 1mm thick.

Cross-cutting bodies of massive textured, coarser quartz and tourmaline are common. These probably represent remobilization of finer, banded material.

Origin

The pronounced stratigraphical control; the bedded nature; and the pre- or syndeformational crystallization of the tourmalinites points strongly to a syngenetic origin for the boron concentrations.

The lack of detrital textures, the presence of fine, regular banding and their simultaneous depositions with sediments deposited in low energy environments (carbonaceous, sulphidic mudstones and iron formation) indicate that these rocks were formed chemically.

Boron contents of the tourmalinites are probably too high to have been inherited from boron-rich, clayey material that converted to tourmaline during diagenesis or metamorphism. To concentrate sufficient boron in the sediments and produce a banded texture a boron-rich phase must have formed at the sediment-water interface or close to it. The lack of metamorphic equivalents of clay material within most tourmalinites suggests tourmaline or the initial boron-rich precursor formed by reaction between clays and boron-rich solutions. Frondel & Collette (1957) synthesized tourmaline by such a process and Ontoev (1956) attributes other tourmalines with high aluminium content (which accompanies a high calcium content) to the assimilation of clay and shale material during crystallization.

Boron-rich sediments can be formed in extremely saline, evaporitic lakes (Read, 1973; Rankama & Sahama, 1950). However, the position of the tourmalinite lenses within rocks which display no evidence of evaporitic deposits and appear to be deposited in a trough (see below) suggests some other mechanism is responsible for tourmalinite formation.

The boron content of 6 samples of Koolpin Formation metapelite found some distance away from tourmalinites, ranged between 5 and 78ppm. Wedepohl (1974) states that boron is not lost from pelitic rocks until upper greenschist facies metamorphism. Furthermore, one sample of metapelite which contained no tourmaline although it was found adjacent to a tourmalinite lens, contained 2,000 ppm boron. Therefore, the low boron contents of the Koolpin Formation metapelites suggests boron was added to the environment in discrete impulses.

Tourmaline has been widely reported as an accessory in gold and base metal deposits, some of which are of probable exhalative origin. For example: The Big Stubby copper-zinc deposit in Western Australia (Both *in* Ethier & Campbell, 1977), the gold-arsenopyrite deposits of Passagem de Mariana, Brazil (Fleischer & Routhier, 1973), and the lead-zinc deposits at Sullivan, British Columbia (Ethier & Campbell, 1977).

At the Golden Dyke Dome, and possibly in neighbouring areas, tourmalinite lenses occur along strike from various types of mineralization. For example:

1) A tourmalinite lens occurs within the gold-bearing Banded Ferruginous Member (Fig. 1), although it may occur within a non-ferruginous, pelitic bed.
2) The pyrrhotite-rich horizon and a tourmalinite lens both lie 10 to 20m above the upper boundary of the Banded Ferruginous Member (Fig. 1). Furthermore, the pyrite-rich bed at Heatley's Prospect containing anomalous concentrations of base-metals roughly correlates with the uppermost tourmalinite in the Koolpin Formation. Both occur about 10 or 15m below the lower boundary of the Gerowie Tuff (Fig. 1).
3) A tourmalinite lens found by Stephens (1978) 3km west of the Dome lies between two prominent greywacke-mudstone units in the Kapalga Formation. The base

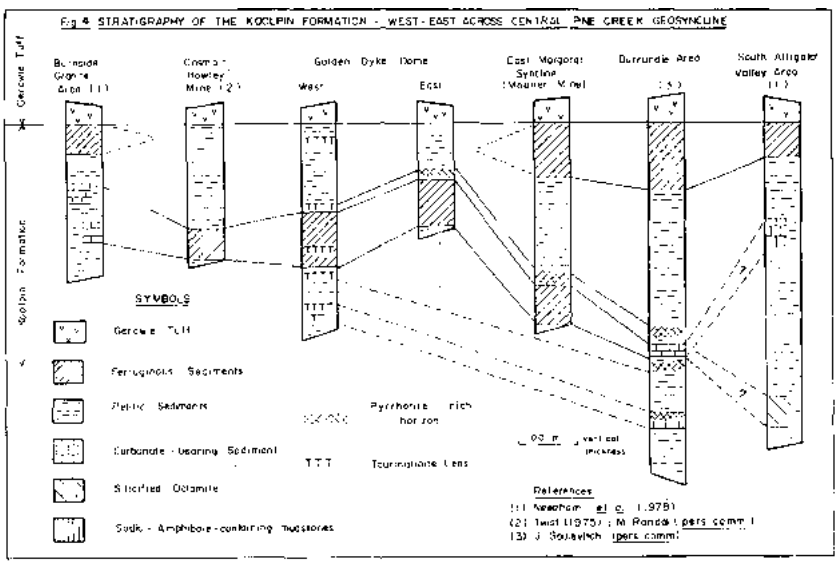


Figure 4. Stratigraphy of the Koolpin Formation — west to east across central Pine Creek Geosyncline.

metal lodes of Iron Blow and Mt Bonnie also lie between these two units (Goulevitch, this volume).

4) All of the pyrrhotite-rich units within the Koolpin Formation in the Burrundie-Grove Hill area found by Goulevitch *(pers. comm.)* can be correlated (by the present author) with tourmalinite lenses in the Golden Dyke Dome (Fig. 4).
5) At the Good Shepherd mine in the northern part of the Dome (Fig. 1), gold and silver has been won from a tourmalinite lens. Jenson (1915) visited the mine and described an apparently conformable lode zone. Although quartz veins are present, Jenson infers that the country rock (the tourmalinite) itself comprises most of the lode material. Fleischer and Routhier (1973) describe similar gold mineralization in tourmalinites where they suggest the gold and tourmaline were deposited together.

The unusual composition of these rocks, and their association with apparent sedimentary-exhalative mineralization, suggest the tourmalinites of the Golden Dyke Dome are products of periodic, seafloor, brine activity.

GEROWIE TUFF

This formation is characterised by a predominance of rocks displaying evidence of volcanic activity. On the eastern side of the Dome, it is approximately 300m thick.

Rock types present included tuffaceous pelites, phyllites, chert, tuffaceous non-albitic chert and tuffaceous albitic chert. Considering the lower boundary of this unit as a time line, the areal distribution of the various rock types above this boundary indicates the position of the different depositional environments at that time.

The west side of the Dome is typified by tuffaceous pelites and cherts. Phyllites are also present.

The tuffaceous pelites contain 25 percent silt-sized, angular grains of quartz, plagioclase and K-feldspar. The shape and composition of these grains suggests they have a tuffaceous origin. The grains define laminae, some of which are graded. The rest of the rock is composed of fine grained (0.02mm diameter) muscovite and minor quartz.

The cherts are usually well laminated and contain approximately 80 percent quartz and 20 percent white mica. Angular silt grains are present in some places.

Beds of tuffaceous albitic chert dominate the Gerowie Tuff on the eastern side of the Dome. Chert, tuffaceous non-albitic chert and phyllite are also present.

The tuffaceous albitic cherts are composed of 5 to 10 percent angular grains of quartz, plagioclase and microcline. These lie in a very fine-grained (less than 0.02mm diameter) matrix of 50 to 60 percent quartz, 40 to 50 percent albite and 5 to 10 percent biotite. In some specimens carbonate clots comprise 5 percent of the rock. Goulevitch (1978) describes thin carbonate laminae in a tuffaceous albitic chert near the Iron Blow mine.

Goulevitch (this volume) notes a gradation in texture and composition upwards through the tuffaceous albitic chert beds. The beds are characterized by massive basal and central portions with finely laminated tops. Silica concentrations increase towards the top of the beds.

Goulevitch (1978) lists the average whole rock chemical analyses of 30 samples of the hard, laminated, upper sections of tuffaceous albitic chert beds. Table 2 shows the average of these analyses compared with the chemistry of selected rocks.

Because of interaction between seawater and volcanic particles, the chemistry of water-laid tuffs cannot be directecly correlated with the chemistry of extrusive igneous rocks. Low rubidium and zinc and high silica (up to 87 percent), and selenium (up to 0.50ppm) contents in the tuffaceous albitic cherts compared with the ranges possible in pure volcanics (Wedephol, 1974), suggests that considerable interaction has occurred with the sedimentary

environment. The influence of the sedimentary environment is also illustrated by the different lithologies (tuffaceous cherts and tuffaceous pelites) produced simultaneously within a small area. The variation in silica concentrations upwards through individual beds suggests alteration may have started soon after deposition.

The fine-grained matrix of the tuffaceous albitic cherts is considered to represent the metamorphic or authigenic produce of an original, chemical, sedimentary component. There is no textural evidence to suggest original, crystalline, clastic material has broken down during metamorphism. The similar proportion of clastic grains and the absence of fine grained albite in the neighbouring lithologies (tuffaceous pellites, non-albitic tuffaceous cherts) also shows that the matrix could not have been wholly formed by the metamorphic breakdown of glass.

The mineralogy and textural features of the tuffaceous albitic cherts are very similar to

%	1	2	3	4
SiO_2	80.6	69.1	74.22	51.50
TiO_2	0.15	0.04	0.28	1.26
Al_2O_3	10.3	9.3	13.27	10.65
Fe_2O_3	0.26	0.17	0.88	9.76
FeO	0.87	0.28	0.92	
MgO	0.33	0.1	0.28	2.66
CaO	0.52	0.5	1.59	4.20
Na_2O	4.85	5.2	4.24	13.98
K_2O	1.29	8.4	3.18	5.99
P_2O_5	0.033		0.05	
H_2O^-	0.04	2.8	0.23	
H_2O^+	0.20		0.80	
C	0.18			
L.O.I.	0.8			

Trace Element Chemistry of Tuffaceous Albitic Cherts (p.p.m.) (Goulevitch, 1978)

Cr	80	Rb	39	Se	0.21
S	175	Zn	28	Hg	0.02
SO_4	124	P	155		
Zr	111.	Cl	3095		
Ba	325	F	510		
Th	26	Cu	20		
Sr	73	Ni	16		

1. Average for upper sections of tuffaceous albitic cherts (Goulevitch, 1979).
2. Zeolite - containing tuffaceous deposits, Green River Formation (Bradley and Eugster, 1969).
3. Average rhyolite (Carmichael et. al., 1974)
4. Anhydrous gels, Lake Magadi, Kenya (Eugster and Jones, 1968).

TABLE 2: Chemistry of Tuffaceous Albitic Cherts Compared with Other Rock Types

expected metamorphic equivalents of tuffaceous illite-quartz-analcite deposits formed in Lake Magadi, Kenya and similar deposits in the Green River Formation, Wyoming. Variations in chemistry (Table 2) may be due to differences in volcanic chemistry, rate of silica deposition and/or rate of clay deposition. Surdam & Eugster (1976) studied the Lake Magadi deposits and postulated the events leading to their formation. Alkali-rich solutions appear to be formed by the leaching of tuffaceous glass and feldspar in the basin and surrounding catchment areas. During evaporation calcium and magnesium are precipitated as carbonates and silica is precipitated as magadiite, which later inverts to chert. Zeolites and sodium-silica-gels are formed when sodium- and silica-rich solutions react with tuffaceous material. Potassium reacts with clay material to form authigenic illite. Connate solutions may evolve higher salinities, until authigenic trona, flourite and halite are deposited.

It is suggested that similar processes may have operated during the deposition of Gerowie Tuff. However, as zeolites can also be formed by reactions between normal dilute surface or ground water and glass fragments (Surdam and Eugster, 1976), it is uncertain how high sodium activities were during the deposition of the Gerowie Tuff. High silica activities must have prevailed for chert, or a chert-precursor, to have precipitated.

As suggested by Goulevitch (this volume), the removal of HO during the formation of hydrous zeolite minerals may have increased the salinity of the pore fluids. Base metals released during the breakdown of tuffaceous material may have been concentrated in the pore fluids as soluble chloride complexes.

The tuffaceous pelites in the western side of the Dome may have been deposited in deeper, less restricted environments with lower silica and sodium activities, and higher clastic inputs.

KAPALGA FORMATION

A thickness of about 500m of the Kapalga Formation is exposed in the north eastern part of the area. Strongly hornfelsed sediments of this formation are also exposed in the fault block adjacent to the Cullen Granite (Fig. 1).

The formation is generally composed of tuffaceous cherts, phyllites, banded iron formation and greywackes. Goulevitch (this volume) describes the stratigraphy of the formation in detail, in the adjacent Margaret Syncline. He considers that the sequence represents a vertical facies transition between the hemipelagic sediments of the underlying Koolpin Formation and the terrigenous sediments of the overlying Burrell Creek Formation. Tuffaceous sediments of the Gerowie Tuff interrupt this sequence.

Of interest to this study is the presence of two horizons containing tourmalinites immediately to the west of the Dome (Stephens, 1978). Also of interest are the syngenetic base metal lodes at Iron Blow and Mt. Bonnie in the adjacent Margaret Syncline, to the east (Goulevitch, this volume). One of the horizons containing tourmalinites and both base metal lodes lies between the two major greywacke-mudstone units found in the Hayes Creek-Burrundie area.

Within the Dome tourmaline is found disseminated in sediments in the fault block adjacent to the granite. Pervasive contact metamorphism prevents the exact determination of the stratigraphic position of these occurrences.

Apart from the interruptions marked by tuff and greywacke sedimentation, the environmental conditions that prevailed during the deposition of Kapalga Formation rocks appear to be similar to those that prevailed during Koolpin-times. Banded, ferruginous sediments, carbonaceous, sulphidic pelites and boron-rich sediments were deposited.

STRATIGRAPHIC CORRELATIONS AND FACIES DISTRIBUTIONS

There are a number of significant differences in the sequences found on either side of the Golden Dyke Dome. These include the following features:

1) The tourmalinite lenses are concentrated in the western part of the Dome. Drilling indicates that they are completely absent in the Upper Carbonaceous Metapelite Member, in the south eastern quarter (Fig. 1).
2) Known gold mineralization associated with ferruginous sediments (Homestake-type?) is restricted to the west side of the Dome.
3) A thickening of Koolpin Formation carbonaceous metapelites occurs in the western half of the Dome. The lower Member is not present in the eastern half of the Dome and the upper Member thickens from 80m in the east to 150m in the west.
4) Tuffaceous pelites are found mainly in the west, whereas tuffaceous albitic cherts are mainly found in the east.

These factors indicate deeper water in the west during the accumulation of the Koolpin Formation and lower Gerowie Tuff. Brines tended to collect and to deposit their gold and boron contents in the deepest parts of the basin.

Figure 4 shows the lithostratigraphic sequences of the Koolpin Formation in different parts of the central Pine Creek Geosyncline. The following important correlations can be made:

1) The banded ferruginous sediments of the Golden Dyke Dome and Cosmopolitan Howley area are correlated with carbonate-bearing horizons in the Burnside Granite and Burrundie areas using the major metadolerite sills as stratigraphic markers. Both represent intervals of chemical sedimentation in a sequence of the fine grained clastic sediments. This correlation is supported by the work of Eugster & Chou (1973) who predicted the formation of calcium and magnesium carbonates in restricted, iron-depleted areas marginal to areas depositing ferruginous sediments.
2) Tourmalinite lenses in the Golden Dyke Dome can be correlated with pyrrhotite-rich units in the Burrundie-Grove Hill area. Both rock types are thought to have formed from exhalative brines.
3) Using the first occurrence of tuffaceous sediments as a time marker, the spatial distribution of lithofacies can be determined at the top of the Koolpin Formation. A black shale facies in the Golden Dyke Dome and Cosmopolitan Howley areas is chronostratigraphically equivalent to ferruginous shale/chert facies bordering it to the north, west and east. The transition zone between the black shale and ferruginous shale/chert must have occurred close to the eastern boundary of the Dome as ferruginous metapelites underlie the Gerowie Tuff near the Moaner gold mine, 2km to the east (Goulevitch, 1977).

From these correlations it is concluded that a trough existed in the Golden Dyke-Cosmopolitan Howley area during the deposition of rocks of the Koolpin Formation and of the lower Gerowie Tuff. The sequence on the eastern side of the Dome was deposited near the edge of this trough. During upper Koolpin-times a deeper, more rapidly subsiding trough existed in the Burrundie-Grove Hill area to the east in which a thick sequence of carbonaceous metapelites accumulated.

CONCLUSIONS

Brines were exhaled periodically during the deposition of the Koolpin and Kapalga Formations. Exhalative deposits accumulated in troughs, one of which occurred in the Golden Dyke-Cosmopolitan Howley area during Koolpin-times.

The composition and location of the exhalative deposits formed depended upon environmental conditions prevailing in the trough. For example iron and base-metal sulphides were deposited with carbonaceous pelites. Environments in which carbonaceous pelites accumulate are recognized as being suitable for base-metal sulphide accumulation

(eg. Croxford *et al.*, 1975). The base metals, which are probably soluble as chloride complexes (Anderson, 1975), are ideally precipitated and accumulated in quiescent, reducing, hydrogen sulphide-rich and neutralising conditions.

Gold with minor sulphides is found in banded ferruginous sediments. The transport of gold in solution can occur in a number of ways. Gold-thio complex species, gold-chloride complex species and gold in a colloidal state appear to be the most important of these. Gold deposition may have occurred in the ferruginous sediments, rather than the interbedded carbonaceous pelites, due to differences in environmental conditions. For example, if the gold was transported in thio complexes, higher oxygen fugacities may have caused gold deposition (Seward, 1973). Alternatively, colloidal gold may have been precipitated from solution by absorption reactions with amorphous ferric hydroxides (Goni *et al.*, 1967). Amorphous ferric hydroxides have been suggested as precursors for iron oxide minerals in iron formations (Eugster & Chou, 1973).

The tourmalinites appear restricted to pelitic horizons. This may be due to the formation of a boron-rich phase by the reaction of boron-rich solutions and clay particles.

The separation of different exhalative deposit types within certain stratigraphic horizons may be due to the evolution of brine chemistry over time and/or space. Alternatively this separation may be explained by brine differentiation, as described by Turner & Gustafson (1978).

There are marked similarities between all of the exhalative deposits in the Cosmopolitan Howley-Burrundie area. Some of these are:

1) Pyrrhotite, with sphalerite as the major, base-metal sulphide, occurs at Heatley's Prospect and in the Iron Blow and Mt Bonnie lodes.
2) Arsenopyrite occurs at Heatley's Prospect, Iron Blow, Mt. Bonnie and in the Ferruginous Member gold deposits.
3) Silver is found at Heatley's Prospect, Iron Blow, Mt. Bonnie and the Good Shepherd mine.
4) Gold is found at the Iron Blow, Mt. Bonnie and Good Shepherd localities as well as in the Ferruginous Member deposits.
5) Tourmalinite lenses occur on the same stratigraphic plane as most of the mineralised horizons.

These factors indicate that throughout the deposition of the South Alligator Group rocks in the Cosmopolitan Howley-Burrundie area the brines had similar compositions, and therefore probably a similar genesis occurred.

There are present-day occurrences of metal- and boron-rich brines emanating from basin floors. Numerous hot, metal-rich brine pools have been found along the axis of the Red Sea (Degens & Ross, 1976) and hot springs on the floor of Lake Kivu, in the East African Rift Valley, emit zinc-, iron-, boron-and silica-rich brines (Degens & Kulbicki, 1973). The sources of both these brines is considered to be hot, circulating ocean and meteoric waters which leach the country rocks of chlorine, boron and metals. Circulation is driven by the higher geothermal gradients which exist in the sediment and volcanic piles of these active rift areas (Craig, 1969; Degens & Ross, 1976).

A similar mechanism is proposed for brine formation during deposition of South Alligator Group rocks. It would be expected that the composition of the brines will therefore be dependent on the nature of the underlying strata. This may explain why the iron sulphide beds of the Kapalga Formation contain far higher concentrations of base-metals than those of the Koolpin Formation, in Cosmopolitan Howley-Burrundie area. The Gerowie Tuff underlying the Kapalga Formation contains potentially accessible metal contents in pore fluids and unstable tuff particles as well as high chlorine contents ideal for the leaching of these metals. No such tuffaceous material exists close to and below the exhalites in the

Koolpin Formation. The formation of exhalative deposits well before the deposition of the Gerowie Tuff indicates that igneous processes are not necessarily directly responsible for brine genesis.

ACKNOWLEDGEMENTS

This work is part of an honours thesis submitted to the University of Queensland. The author particularly thanks Dr. M.M. Wilson who supervised the thesis. Constructive criticism of the manuscript by J. Goulevitch, J.V. Main and G.S. Eupene is gratefully acknowledged.

Thanks are due to K. Wills of C.R.A.E. and the Northern Territory Mines Branch for access to drill core, M. Randall for information about the Cosmopolitan Howley Mine, M. Schmahl for draughting of the diagrams and G. Vaccaro for typing of the manuscript. The author is indebted to Geopeko for their financial and logistic support during the field work for this study.

REFERENCES

Anderson, G.M., 1975: Precipitation of Mississippi Valley-type ores. *Econ. Geol., 70,* 937-942.

Baarda, F.D., 1972: Diamond drilling at Heatley's Prospect, 1971-71. *Unpublished Report, Central Pacific Minerals N.L.*

Berner, R.A., 1967: Thermodynamic Stability of sedimentary iron sulphides. *Am. J. Sci., 265,* 773-785.

Blanchard, R., 1937: Interim Report on Golden Dyke (Shackle) Property. *Unpublished Report, Anglo-Queensland Mining P.L.*

Bradley, W.H. & Eugster, H.P., 1969: Geochemistry and paleolimnology of the trona deposits and associated authigenic minerals of the Green River Formation of Wyoming. *Prof. Pap. U.S. geol. Surv., 496-13.*

Carmichael, I.S.E., Turner, F.J. & Verhoogen, J., 1974: *Igneous Petrology.* McGraw-Hill, New York.

Craig, H., 1969: Geochemistry and Origin of the Red Sea Brines. in (eds. E.T. Degens & D.A. Ross), *Hot Brines and Recent Heavy Metal Deposits in the Red Sea,* Springer-Verlag, New York, 208-242.

Croxford, N.J.W., Gulson, B.L. & Smith, J.W., 1975: The McArthur Deposit: A review of the Current Situation. *Miner. Deposita, 10,* 302-304.

Deer, W.A., Howie, R.A. & Zussman, J., 1972: *An Introduction to the Rock-Forming Minerals.* Longman Group Ltd., London.

Degens, E.T. & Kulbicki, G., 1973: Hydrothermal origin of metals in some East African Rift Lakes. *Miner. Deposita, 8,* 388-404.

Degens, E.T. & Ross, D.A., 1976: Strata-bound metalliferous deposits in or near active rifts, in (ed. K. H. Wolf), *Handbook of stratabound and stratiform ore deposits.* Elsevier, Amsterdam.

Epprecht, W., 1953: Die Gutterkonstated der Turmaline. *Schwiez miner. petrogr. Mitt., 39,* 481-505.

Ethier, V.G. & Campbell, F.A., 1977: Tourmaline concentrations in Proterozoic sediments of the Southern Cordillera of Canada and their economic significance. *Can. J. Earth Sci., 14,* 2348-2363.

Eugster, H.P. & Chou, J-Ming, 1973: The depositional environments of Precambrian banded iron-formations. *Econ. Geol., 68,* 1144-1188.

Eugster, H.P. & Jones, B.F., 1968: Gels composed of sodium-aluminium silicate, Lake Magadi, Kenya. *Science, 161,* 160-163.

Fleischer, R. & Routhier, P., 1973: The 'consanguineous' origin a tourmaline-bearing gold deposit: Passagem de Mariana (Brazil). *Econ. Geol., 68,* 11-22.

Fleet, M.E., 1967: Spectrophotometric method for determining trace amounts of boron in rocks and minerals. *Analyt. Chem., 39(2),* 253.

Fripp, R.E.P., 1976: Stratabound Gold Deposits in Archaean Banded Iron-Formation, Rhodesia. *Econ. Geol., 71,* 58-75.

Frondel, C. & Collette, R.L., 1957: Synthesis of tourmaline by reaction of mineral grains with $NaCl$-H_3BO_3 solution, and its implication in rock metamorphism. *Am. Miner, 42,* 754-758.

Goni, J., Guillemin, G. & Sarcia, C., 1967: Geochemie der l'or exogene — Etude experimentale de la formation des despersions colloidales d'or et de leur stabilite. *Miner. Deposita, 1,* 259-286.

Goulevitch, J., 1977: Photo-interpretation of geology in the Burrundie-Grove Hill area and consequent exploration philosophy. *Unpublished Report D77/6, Geopeko Ltd.*

Goulevitch, J., 1978: Regional Geology in the Burrundie-Grove Hill Area and its Economic Significance. *Unpublished Report D78/2, Geopeko Ltd.*

Goulevitch, J., this volume: Stratigraphy of the Kapalga Formation in the Pine Creek Area and its Relationship to Base Metal Mineralization, *Proceedings of the International Uranium Symposium on the Pine Creek Geosyncline.*

Harder, H., 1970: Boron Content of Sediments as a Tool in Facies Analysis. *Sediment. Geol., 4,* 153-175.

Helgeson, H.C., 1969: Thermodynamics of hydrothermal systems at elevated temperatures and pressures. *Am. J. Sci., 267,* 729-804.

Hossfeld, P.S., 1936: The Golden Dyke Dome and Adjacent Areas. *Unpublished Report, Aerial geological and geophysical Surveys North. Aust., N.T. Report No. 19.*

James, H.L., 1954: Sedimentary Facies of Iron-formation. *Econ. Geol., 49,* 235-291.

Jenson, H.I., 1915: The Geology of the Woggaman Province. *Bull. Nth. Terr. Aust., 16.*

Klein, C. & Bricker, O.P., 1977: Some Aspects of the Sedimentary and Diagenetic Environment of Proterozoic Banded Iron-Formation. *Econ. Geol., 72,* 1457-1470.

Mathias, B.V. & Clark, G.J., 1975: Mt. Isa Cu and Ag-Pb-Zn orebodies — Isa and Hilton Mines. *in:* (ed. C.L. Knight), *Economic Geology of Australia and Papua New Guinea, Australas. Inst. Min. Metall., Monograph Series, No. 5., 1. Metals,* 351-372.
Needham, R.S., Crick, I.H. & Sturt-Smith, P.G., 1978: Pine Creek Geosyncline, *Rep. Bur. Miner. Resour. Geol. Geophys Aust., 208.*
Needham, R.S., Crick, I.H. & Stuart-Smith, P.G., this volume: Regional Geology of the Pine Creek Geosyncline. *Proceedings of the International Uranium Symposium on the Pine Creek Geosyncline.*
Ontoev, D.O., 1956: About the compositon of some ore forming tourmalines. *Trans. Inst. Geology, Ore Deposits, Petrography, Mineralogy and Geochemistry, 3,* 340-346.
Page, R.W. Compston, W. & Needham, R.S., this volume: Geochronology and Evolution of the Late Archaean Basement and Proterozoic Rocks in the Alligator Rivers Uranium Field, Northern Territory, Australia. *Proceedings of the International Uranium Symposium on the Pine Creek Geosyncline.*
Plimer, I.R. & Finlow-Bates, T., 1978: Relationship between Primary Iron Sulphide Species, Sulphur Source, Depth of Formation and Age of Submarine Exhalative Sulphide Deposits. *Miner. Deposita, 13,* 399-410.
Rankama, K. & Sahama, T.G., 1950: *Geochemistry.* University of Chicago Press, Chicago.
Read, M.H., 1973: *Rutley's Elements of Mineralogy.* Thomas Murby & Co., London.
Sawkins, F.J. & Rye, D.M., 1974: Relationships of Homestake-type gold deposits to iron-rich Precambrian sedimentary rocks. *Trans. Inst. Min. Metall., 83,* B56-B59.
Seward, T.M., 1973: Thio complexes of gold and the transport of gold in hydrothermal ore solutions. *Geochim. cosmochim. Acta, 37,* 379-400.
Shields, J.W., & Pietsch, B.A., 1971: Progress Report, Authority to Prospect 1959 Pine Creek — Northern Territory. *Unpublished Report N.T.-11, Central Pacific Minerals N.L.*
Stephens, C.S., 1978: Initial Report: Regional geology of the Western E.L.'s, Hayes Creek, N.T. *Unpublished Report D78/17, Geopeko Ltd.*
Surdam, R.C. & Eugster, H.P., 1976: Mineral Reactions in the sedimentary deposits of the Lake Magadi region, Kenya. *Bull. geol. Soc. Am., 87,* 1739-1752.
Sweeney, R.E. & Kaplan, I.R., 1973: Pyrite framboid formation: Laboratory synthesis and marine sediments. *Econ. Geol., 68,* 618-634.
Turner, J.S. & Gustafson, L.B., 1978: The flow of hot saline solutions from vents in the sea floor — some implications for exhalative massive sulphide and other ore deposits. *Econ. Geol., 73,* 1982-1100.
Twist, R., 1975: Cosmo-Howley Area. *Unpublished Report, Geopeko Ltd.*
Voisey, A.H., 1938: Notes on the Stratigraphy of the Northern Territory of Australia with special reference to the Jurassic. *Proc. R. Soc. N.S.W., 72.*
Walpole, B.P., Crohn, P.W., Dunn, P.R. & Randall, M.A., 1968: Geology of the Katherine-Darwin region, Northern Territory. *Bull. Bur. Miner. Resour. Geol. Geophys. Aust, 82.*
Wedepohl, K.H. (ed.), 1974: *Handbook of Geochemistry.* Springer-Verlag, Berlin.
Winchell, A.N., 1932: Ferrotremolite, oxyhornblende and tourmaline. *Am. Miner, 17,* 472-477.

GEOCHEMICAL INVESTIGATIONS IN THE MT. BUNDEY AREA, NORTHERN TERRITORY

M.B. Hochman

Department of Economic Geology, University of Adelaide, P.O. Box 498, Adelaide S.A., 5000, Australia.

ABSTRACT

A geochemical study of the Mt. Bundey Granite/Mt. Goyder Syenite involving major elements and the trace elements Ba, Sr, Rb, Y, Zr, Nb, Ce, Nd, Sc and U has been carried out.

The results indicate that the granitoids were formed by fractionation from an intermediate liquid which may have been produced by partial melting of a siliceous granulite in the lower crust.

Samples of dolerites, lamprophyres, volcanics of the Gerowie Tuff and sediments of the Koolpin Formation were also analyzed, but the limited number of samples prevents any interpretation of these results.

INTRODUCTION

In view of the similarity in age between Lower Proterozoic (Carpentarian) granitoids of the Pine Creek Geosyncline and the oldest known mineralization of this area (1700-1800 m.y.) an understanding of source and mechanism of formation of the granites may prove useful in determining the origin of mineralization. The Mt. Bundey Granite is one of the Lower Proterozoic (Carpentarian) granitoids and as such forms the basis of this paper.

Samples of granite were collected from evenly spaced intervals along the Arnhem Highway and the remaining rock types from the area between the eastern edge of the granite and Mary River. The location of the study area is shown in figure 1.

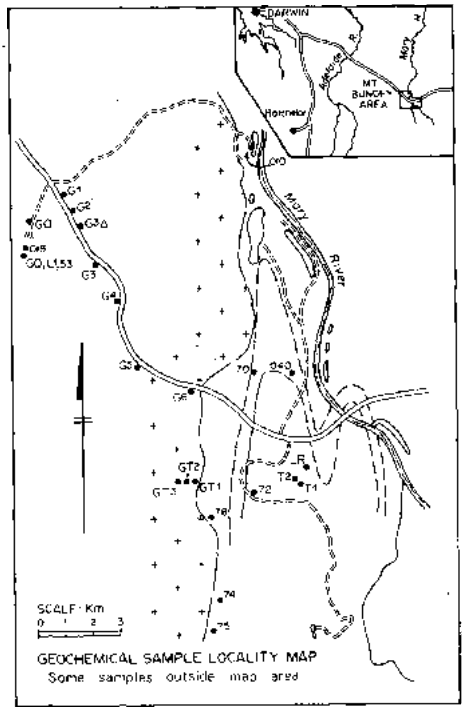


Figure 1. Geochemical Sample Locality Map.

GRANITOIDS

The granitoid rocks found in the Mt. Bundey area are granites, syenites and also minor aplite which intrudes the granite. The major element geochemistry is shown in table 1 which also includes analyses for an average granite (Taylor, 1968) and an average syenite (Daly, 1933). The Mt. Bundey Granite differs from the average in having less total iron, CaO, and Y, but more alkalis, Ba, Rb, Sr, Ce and U, with higher K_2O/Na_2O and Rb/Sr ratios.

The Mt. Goyder Syenite also averages less total iron and CaO but has more total alkalis and P_2O_5, and it also appears enriched in Ba, Sr, and to a lesser extent in Ce, Zr, Sc, and Ni. The aplite is extremely siliceous and also has a high proportion of total alkalis, but is depleted in most trace elements apart from Rb. The dominance of K_2O over Na_2O in all of the granitoids reflects the dominance of potash feldspar over plagioclase, with the low total iron contents being due to low modal percentages of iron-bearing minerals such as biotite.

	SYENITES				GRANITES						
	G1	G2	GS	GS1	G3	G3A	G4	G5	G6	GT1	GT2
SiO_2	61.05	59.95	62.24	61.49	71.97	72.02	72.03	72.03	67.25	72.36	70.99
Al_2O_3	14.74	14.16	14.21	14.19	13.77	13.54	13.66	13.16	13.12	13.50	13.62
Fe_2O_3	4.99	5.59	5.09	5.12	2.35	2.24	2.37	2.62	4.50	2.52	2.84
MnO	0.10	0.10	0.07	0.07	0.02	0.02	0.02	0.04	0.10	0.04	0.04
MgO	2.40	3.26	3.12	3.13	0.57	0.55	0.55	0.55	1.93	0.53	0.65
CaO	2.53	3.26	3.53	3.74	1.47	1.23	1.42	1.52	2.50	1.42	1.29
Na_2O	4.62	3.91	3.54	3.67	3.91	3.80	3.79	3.54	3.47	3.67	3.71
K_2O	6.96	6.89	5.85	5.90	5.01	5.08	5.06	4.87	5.16	4.80	5.09
TiO_2	0.72	0.76	0.63	0.59	0.27	0.26	0.28	0.30	0.46	0.29	0.31
P_2O_5	0.49	0.74	0.44	0.43	0.11	0.10	0.10	0.11	0.38	0.11	0.12
LoI	0.35	0.39	0.43	0.74	0.47	0.59	0.43	0.48	0.38	0.43	0.68
Total	98.94	99.01	99.15	99.07	99.91	99.42	99.71	99.20	99.24	99.67	99.33
Ba	2300	2850	2840	3130	920	1000	890	820	855	760	845
Sr	1670	1790	1470	1535	430	400	430	375	365	400	400
Rb	225	220	220	195	255	275	265	285	345	275	275
Y	18	16	23	-	10	-	12	17	29	14	17
Zr	805	740	390	400	210	180	200	245	250	225	205
Nb	90	50	35	33	23	25	24	28	30	26	22
Ce	310	250	285	265	115	97	120	155	195	150	145
Nd	110	95	105	85	32	31	35	42	81	41	44
Sc	9	12	16	-	4	-	3	4	9	5	4
U	12	12.3	15.7	-	14	-	-	-	11.1	-	-

	GRANITES			APLITE				Mpageni type	
	GT3	GQ	GQ2	O18	Average granite	Average syenite	MBPL	Ngwempisi Pluton	Kwetta Pluton
SiO_2	71.00	70.15	71.78	76.13	71.2	60.19	67.90	68.6	69.0
Al_2O	13.74	13.95	13.63	12.67	14.7	16.28	14.60	13.8	14.3
Fe_2O_3	2.59	2.72	2.33	0.91	3.6	6.02	4.06	3.78	2.28
MnO	0.04	0.03	0.01	0.02	0.05	0.14	0.04	-	-
MgO	0.63	0.87	0.56	0.16	0.55	2.49	1.28	0.67	0.80
CaO	1.36	1.65	1.31	0.46	2.00	4.30	2.25	2.17	2.33
Na_2O	3.75	3.85	3.73	4.00	3.54	3.98	3.35	4.25	3.21
K_2O	5.10	5.32	5.05	5.12	4.18	4.49	6.06	5.13	4.85
TiO_2	0.31	0.34	0.24	0.08	0.40	0.67	0.76	0.58	0.66
P_2O_5	0.11	0.16	0.10	0.01	0.16	0.28	0.10	-	-
LoI	0.54	0.31	0.51	0.30	-	1.16	-	-	-
Total	99.17	99.35	99.25	99.86	100.38	100.00	100.4	98.98	99.44
Ba	905	1170	850	215	600	-	1530	1430	1150
Sr	430	665	405	190	285	-	829	343	328
Rb	270	250	295	305	145	-	253	184	216
Y	18	13	-	13	40	-	16	-	-
Zr	220	260	120	89	180	-	334	-	-
Nb	25	30	55	30	-	-	34	-	-
Ce	140	120	110	35	57	-	178	250	206
Nd	46	33	29	15	-	-	58	-	-
Sc	3	5	-	1	-	-	-	-	-
U	-	12.3	-	11.5	-	-	-	-	-

Table 1. Geochemistry of granitoids.

Classification of the Granitoids

Alkaline vs Calc-alkaline:

A plot of SiO_2 vs alkalinity (Fig. 2) indicates that the granitoids plot mainly in the alkaline field of the diagram with some divergence into the calc-alkaline field. Petrologically, neither syenite nor granite can be classified as alkaline, as both contain hornblende rather than sodic amphiboles. They have no pyroxene and the syenite contains quartz rather than feldspathoids. Therefore, both syenite and granite belong in the calc-alkaline field.

S- or I-type granite:

An attempt has been made to classify the Mt. Bundey Granite according to the scheme proposed by Chappell & White (1974) using geochemical, mineralogical and field data. Mineralogically the dominant ferromagnesium minerals in *S*-type granites are biotite, muscovite, cordierite, garnet and ilmenite, and in *I*-types are biotite, hornblende, sphene and magnetite. The Mt. Bundey Granite contains biotite, hornblende, sphene and magnetite but no muscovite, cordierite or garnet. The $Al_2O_3/(Na_2O+K_2O+CaO)$ ratio can be used as a classification tool being less than 1.1 in *I*-type granites and greater than 1.1 in *S*-types. The value obtained for the Mt. Bundey Granite is 1.27. CIPW calculated mineralogy shows normative diopside present with normative corundum being absent or present in minor amounts. Field evidence suggests that *I*-type granites should contain mafic xenoliths whereas *S*-types should contain metasedimentary xenoliths. The Mt. Bundey Granite contains mafic biotite hornblende-bearing xenoliths. Initial $^{87}Sr/^{86}Sr$ ratios (Riley, this volume) yield a value of 0.7051 for the Mt. Bundey Granite. This value is low enough to discount the possibility of a magma forming by the melting of sediments. The above results therefore indicate that the Mt. Bundey Granite is best referred to as an *I*-type granite.

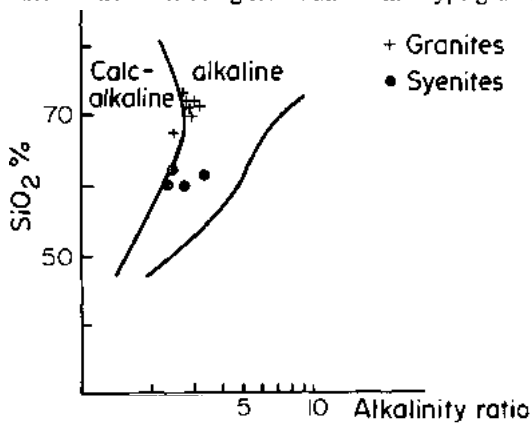


Figure 2. Alkalinity variation diagram for the Mt. Bundey Granite/Mt. Goyder Syenite (after Wright, 1969).

The establishment of this granite as *I*-type neither proves nor disproves any relationship with mineralization. As reported by Ewers & Scott (1977), it has also proved difficult to determine a relationship between the Cullen Granite and the mineralization in its surrounding sediments.

Source of the Granitoids

Three possible mechanisms for the formation of the granitoids are considered.

1) Metasomatism

Metasomatism or granitization is immediately rejected as field evidence shows a contact aureole around the granite, and a sharp contact with the sediments.

2) Partial melting

The position of the granites on figure 3 (Ab-An-Or) indicates that they could have been produced by partial melting. Although they plot on a cotectic, they do not fall on a eutectic minimum, and formation by partial melting would therefore necessitate temperatures above those required for incipient melting.

The syenites however could not be produced by direct partial melting of a source rock,

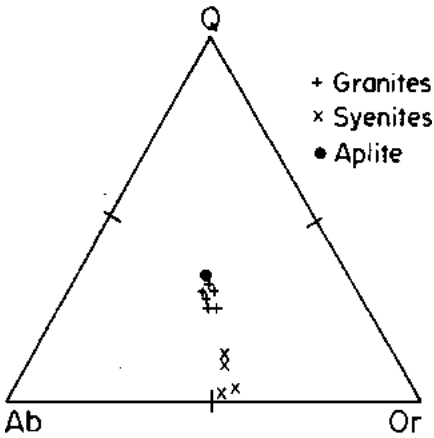


Figure 3. Q-Ab-Or ternary diagram.

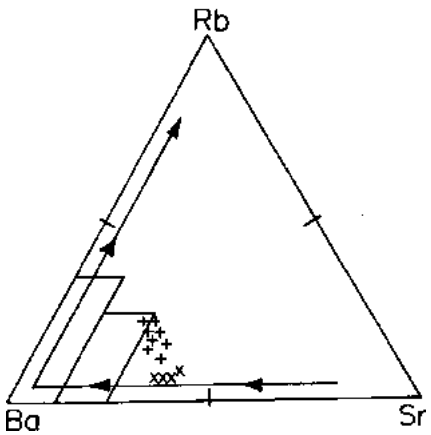


Figure 4. Rb-Sr-Ba variation diagram (after El Bouseily & El Sokkary, 1975).

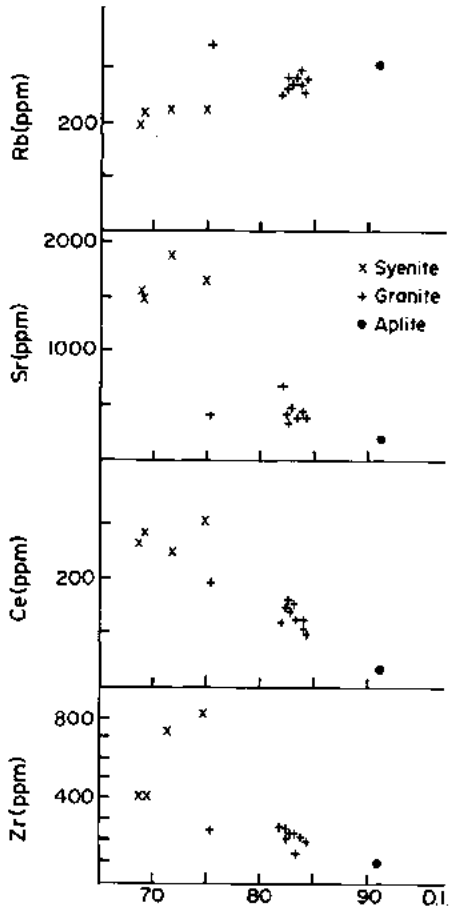


Figure 5. Variation of Rb, Sr, Ce, Zr with differentiation index (after Thornton & Tuttle, 1960).

as their position on figure 3 indicates that this would require pressures far in excess of realistic estimates.

3) Fractional crystallization

This appears a viable mechanism for the formation of the suite of granitoids from syenite through to aplite. Differentiation plots show linear trends, such as the trend toward Rb with increasing SiO_2 (Fig. 4), and the plots in figure 5 of differentiation index vs Rb, Sr, Ce, Zr.

If fractionation is the mechanism of formation for the granitoids then intermediate members between the granite and the syenite would be expected. Sample 549/G6 appears to be such a rock, being intermediate between the two end members in most major and minor elements.

Elemental abundances and ratios (Hochman, 1978) indicate that the syenite represents the first cumulate from a parent liquid and the granite represents a further fractionation

with the aplite being the last phase. Hence, a model involving crystal fractionation seems the most likely mechanism for producing the granitoids.

Composition and source

An attempt has been made to calculate the composition of a liquid from which the granitoids fractionated. This initial composition of liquid (the Mt. Bundey Primary Liquid or MBPL) was derived by taking a weighted average of the syenite plus the granite, assuming that the syenite represented one-third of the pluton and the granite the remaining two-thirds. (This estimation was made from field exposures of both granite and syenite). The initial composition was then refined by varying percentages of all major elements until a liquid with a composition of the Mt. Bundey Granite was left after crystallization of a syenite with the modal proportions of the Mt. Goyder Syenite given in Hasan (1958). A full description of the calculations is given in Appendix 1 of Hochman (1978).

The author would like to stress at this point that the remainder of this section depends on the composition of the MBPL being accurate and that the MBPL is only a calculated entity rather than a measured one. Bearing this in mind, possible sources for the MBPL include the upper and lower crust, and the upper mantle. Many of the upper crustal rocks appear to be unsuitable sources in view of their low K_2O/Na_2O ratios. It has been suggested that the Archaean granite gneisses of the Pine Creek Geosyncline are parents of the Lower Proterozoic (Carpentarian) granitoids, but this is unlikely, as they are too enriched in Rb, (i.e. the Rb/Sr ratio of the Rum Jungle and Waterhouse Complexes is 4.6 and 1.6 respectively, while the MBPL is only 0.3).

The author favours a model such as that proposed in Condie (1978) for the formation of the MBPL. This involves mantle plume activity into the lower crust which triggers partial melting of a siliceous granulite. The liquids produced by this are represented by the Mpageni batholiths from the Barberton region of South Africa (Condie & Hunter, 1976), (Table 1). A comparison of these batholiths with the MBPL shows that the two are similar and hence this mechanism is considered plausible.

Comparison of the Mt. Bundey Granite with other granitoids in the Pine Creek Geosyncline

The Mt. Bundey Granite appears geochemically quite similar to other Lower Proterozoic (Carpentarian) granitoids in the Pine Creek Geosyncline. All of these rocks show the same major element trends such as the dominance of K_2O over Na_2O, the high total alkali content, and the depleted CaO content. A minor element comparison of the Mt. Bundey Granite with the Cullen Granite also shows similarities. All minor elements of the Mt. Bundey Granite which have been considered fall within the corresponding limits found for those of the Cullen Granite (Ewers & Scott, 1977). The Mt. Bundey Granite does appear to be higher in Ce, Zr and U but the major difference is the Rb/Sr ratio which is 0.65 compared to 1.5 in the Cullen Granite.

OTHER ROCK TYPES

A number of other rock types were analyzed and have been included in table 2. A further description of some is as follows:

The Volcanics

The samples consist of Gerowie Tuff and are listed under 549/T1, 549/T2 and 549/LR in table 2. The former two mentioned are vitric tuffs with flow banding in thin section. The latter is a spherulitic obsidian.

The two tuffaceous samples are very dark and chert-like in hand specimen with a white weathered shell and thus appear similar to those described by Crick *et al.* (1978) in the Burnside area. Thin section shows that the tuffs consist of curved and some elongate fragments of quartz and K-feldspar in a cryptocrystalline matrix of quartz, K-feldspar and

	LAMPROPHYRES		VOLCANICS			DOLERITES		SEDIMENTS					
	549/53	549/L1	549/T2	549/T1	549/LR	549/78	549/54	549/75	549/74	549/010	549/40	549/70	549/77
SiO_2	49.89	49.18	71.76	75.27	84.57	60.01	44.59	60.56	0.49	62.95	15.78	87.95	86.76
Al_2O_3	11.48	11.10	14.37	13.40	7.93	12.41	13.72	17.56	0.14	18.39	0.96	0.13	0.45
Fe_2O_3	7.99	8.02	2.21	1.33	0.56	9.89	13.59	7.26	0.52	2.49	72.20	8.69	11.58
MnO	0.19	0.19	0.14	0.02	0.02	0.15	0.28	0.21	0.05	0.02	0.16	0.00	0.03
MgO	8.21	9.16	0.40	0.31	0.11	3.73	6.92	3.36	20.80	1.23	0.05	0.05	0.20
CaO	7.12	6.62	0.45	0.56	0.80	4.35	8.55	1.43	30.57	0.03	0.03	0.02	0.09
Na_2O	0.80	1.01	1.04	5.63	3.19	1.10	2.74	1.16	0.11	0.10	0.08	0.01	0.01
K_2O	7.66	7.44	8.11	3.10	0.50	4.47	1.27	4.16	0.04	4.93	0.05	0.04	0.11
TiO_2	1.55	1.49	0.12	0.16	0.09	0.46	3.19	0.63	0.01	0.63	0.05	0.38	0.01
P_2O_5	2.04	1.99	0.02	0.03	0.02	0.47	0.55	0.06	0.08	0.05	0.86	0.06	0.15
LoI	0.62	0.75	1.05	0.39	2.36	2.31	3.82	2.75	45.88	8.92	9.53	2.22	0.61
Total	97.54	96.94	99.67	100.19	100.14	99.35	99.22	99.14	98.69	99.74	99.73	99.58	99.99
Ba	6690	5670	1650	660	76	340	730	225	< 1	185	22	31	675
Sr	2580	2380	-	170	58	86	225	120	240	59	10	5	89
Rb	359	285	-	120	34	180	30	185	1	240	10	2	9
Y	21	-	-	17	26	-	33	-	-	-	13	-	-
Zr	660	705	180	125	104	55	135	72	ND	155	3	81	ND
Nb	42	43	15	11	7	11	21	18	2	15	4	11	< 1
Ce	495	455	-	99	59	66	56	77	16	84	24	3	18
Nd	195	200	-	44	21	46	29	31	4	37	11	1	21
Sc	23	-	4	3	3	-	25	-	-	13	8	-	-
U	4.9	-	-	6	4	4	0.4	3.7	-	7.7	14.1	6.7	-

Geochemistry of rocks other than granitoids

- not determined

ND not detected

549/75 Shale
549/74 Dolomite
549/010 Andalusite schist

549/40 Gossan
549/70
549/77 Iron cherts

Table 2. Geochemistry of rocks other than granitoids.

plagioclase. Some of these curved fragments are thought to be shards. Thin section examination also shows that 549/T2 has been extensively altered.

The spherulitic obsidian consists of large (1mm long) ellipsoidal spherulites in a cryptocrystalline matrix similar to the tuffs, and also has the same devitrification textures and small crystal growths. Both the tuffs and obsidian are very siliceous and have high Al_2O_3 contents. Minor element analyses indicate that both rock types are enriched in Zr and to a lesser extent in Ce also.

It is unlikely that these volcanics were derived from the same source as the granitoids since the former have sodium dominating over potassium, whereas the reverse is true for the granitoids. It is possible, though, that the tuffs and obsidian form part of the same extrusive event as both have similar mineralogy, devitrification textures, and share a common cryptocrystalline matrix.

Lamprophyres

These femic rocks had been noted by previous workers and are found transgressing both the granite and the sediments. The presence of biotite, dominance of orthoclase over plagioclase, and REE pattern indicate that the lamprophyres are minettes. They are geochemically similar to other known minettes apart from a higher K_2O content. Due to the extremely limited number of analyses of the above-mentioned, and other rock types, no definite conclusions can be drawn regarding these rocks and hence they are included merely as a guide to future workers in the area.

CONCLUSIONS

The granitoids in the Mt. Bundey area are quite similar to those in other parts of the geosyncline. They are best described as calc-alkaline *I*-type granites which are thought to have formed by fractionation from an intermediate liquid. It is suggested that this liquid (the MBPL) is derived by melting of a siliceous granulite in the lower crust.

ACKNOWLEDGEMENTS

This work partially fulfilled the requirements of an honours degree at the University of Adelaide in 1978. The project was sponsored by Geopeko Ltd., and as such I am extremely grateful to Mr. G. Eupene and Mr. A. L. Browne for assistance rendered throughout the year. For assistance in the theoretical considerations of this work at the University, I would particularly like to thank Professor P.J. Ypma and Dr. R.W. Nesbitt, and finally I would like to thank Dr. G.R. Ewers from the Bureau of Mineral Resources for his critical appraisal of this manuscript.

REFERENCES

Chappell, B.W. & White, A.J.R., 1974: Two contrasting granite types. *Pacific Geology, 2,* 173-174.

Condie, K.C., 1978: Geochemistry of Proterozoic granitic plutons from New Mexico, U.S.A. *Chem. Geol., 21,* 131-151.

Condie, K.C. & Hunter, D.R., 1976: Trace Element Geochemistry of Archaean Granitic Rocks from the Barberton Region, South Africa. *Earth Planet. Sci. Lett., 29,* 389-400.

Crick, I.H., Stuart-Smith, P.G. & Needham, R.S., 1978: Stratigraphic significance of a discovery of Lower Proterozoic tuff in the Pine Creek Geosyncline. *BMR J. Aust. Geol. Geophys., 3(2),* 163-165.

Daly, R.A., 1933: *Igneous Rocks and the Depths of the Earth.* (McGraw Hill, 598p.

El Bouseilly, A.M. & El Sokkary, A.A., 1975: The relation between Rb, Ba, and Sr in granitic rocks. *Chem. Geol. 16,* 207-219.

Ewers, G.R. & Scott, P.A., 1977: Geochemistry of the Cullen Granite, Northern Territory. *BMR J. Aust. Geol. Geophys., 2,* 165-176.

Hasan, S.M., 1958: Petrography and Petrology of the Mt. Bundey Granite and the Mt. Goyder Syenite, Northern Territory. *Rec. Bur. Miner. Resour. Geol. Geophys. Aust., 1958/36* (unpubl.).

Hochman, M.B., 1978: Geochemical Investigations in the Mt. Bundey Area. *B.Sc. Hons. thesis, University of Adelaide* (unpubl.).

Riley, G.H., this volume: Granite ages in the Pine Creek Geosyncline. *Proceedings of the International Uranium Symposium on the Pine Creek Geosyncline.*

Taylor, S.R., 1968: Geochemistry of andesites. *in* (ed. L.H. Ahrens) *Origins and Distribution of the Elements* Pergamon, London, 559-583.

Thornton, C.P. & Tuttle, O.F., 1960: Chemistry of igneous rocks. I. Differentiation Index. *Am. J. Sci. 258,* 664-684.

Wright, J.B., 1969: A simple alkalinity ratio and its application to questions of non-orogenic granite genesis. *Geol. Mag., 106,* 370-384.

THE MOUNT FITCH COPPER AND URANIUM DEPOSITS, RUM JUNGLE URANIUM FIELD, N.T., AUSTRALIA

D. A. Berkman[1] and W. J. Fraser[2]

1. Australian Oil & Gas Corporation Limited, 261 George Street, Sydney, N.S.W., 2000, Australia.
2. C.R.A. Exploration Pty. Ltd., P.O. Box 39598, Winnellie, N.T., 5789, Australia.

ABSTRACT

The Mount Fitch copper and uranium deposits are contained in chloritic, sericitic and graphitic schists of the Namoona Group and magnesite of the Batchelor Group. The main uranium deposit is confined to a major breccia zone in the magnesite. Total ore reserves are approximately 1500 tonnes U_3O_8. Secondary copper mineralization is contained in residual clays overlying the magnesite and reserves are estimated at 290,000 tonnes of ore with an average grade of 0.65 Cu. An interpretation of the structure suggests that the metasediments were initially folded during the orogenesis of the Pine Creek Geosyncline. Later faulting and cross folding, complimentary to Giants Reef Fault intensively brecciated the metasediments. It is suggested that the mineralization is syngenetic or introduced during the orogenesis of the Pine Creek Geosyncline and upgraded by later weathering which was most effective in the breccia zone, facilitated by the high permeability. The copper mineralization represents a major enrichment by removal of magnesite during weathering.

INTRODUCTION

The Mount Fitch deposits are about 60km south of Darwin and 7km northwest of the former uranium treatment plant at Rum Jungle. The deposits were extensively tested between 1950 and 1970 by the Bureau of Mineral Resources, Geology and Geophysics (BMR) and Territory Enterprises Pty. Limited (TEP). Each of the authors worked for TEP between 1960 and 1970, and most of the data herein are from our unpublished company reports, and from BMR records. Permission to publish this information is gratefully acknowledged.

GEOLOGY

Correlation of the regional stratigraphy with the Rum Jungle information is incomplete, thus reference is made to the detailed local mapping of Pritchard & French (1965) and Johnson (1974). However, the metasediments which they allocate to the 'Golden Dyke Formation' are now assigned to the 'Masson Formation' of the Namoona Group (Figs. 1 & 2) (Needham *et al.*, this volume).

The northwestern edge of the Rum Jungle Complex is about 500m east of the Mt. Fitch deposits, and is mapped in this area as leucocratic granite (Rhodes, 1965). It is a pink or grey, fine to medium even-grained adamellite. Near the deposits the leucocratic granite is grey, and coarser grained than usual, and it contains tourmaline rosettes and quartz-tourmaline veins along joints. Some quartz-tourmaline veins transect the granite-metasediment contact, and displace small pegmatite veins.

The Complex is unconformably overlain by the Batchelor Group metasediments (Fig. 2), with the basal members dipping away from the granite. The individual members in the Mt. Fitch area are, in order from the base:

Crater Formation, the basal sedimentary unit near Mt. Fitch, here comprising coarse grained quartz-feldspar schists and fine grained grey quartzites, with minor bands of angular white quartz pebbles. This formation contains several outcrops of quartz-tourmaline rock striking at 310°-350°, parallel to the regional foliation.

Coomalie Dolomite is a carbonate sequence containing minor schists, and apparently conformable on the Crater Formation (the contact in drillholes is invariably sheared and altered). The Dolomite has a distinctive weathering profile, of dark reddish brown to orange brown clays of very variable thickness, usually about 10m to 40m, but occasionally much

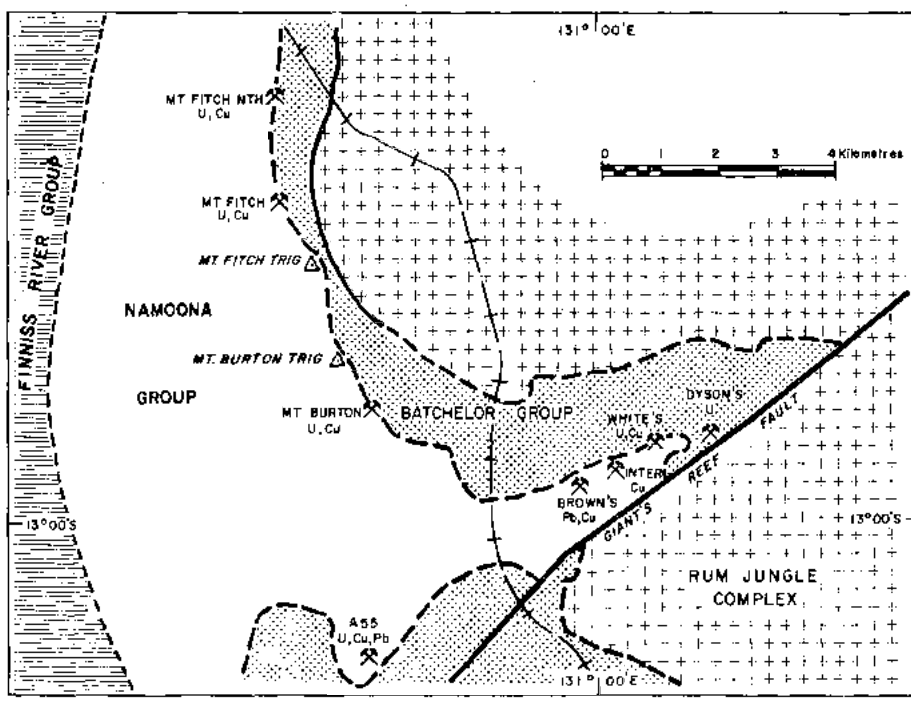


Figure 1. Regional Geology of the Mount Fitch Area.

thicker. Within this clay zone are rafts of fresh, coarsely crystalline magnesite marble, boulders of tremolite schist and tremolitic jasper, nodules of brilliant white secondary magnesite, and boulders of white quartzite. The surface is occasionally marked by large sinkholes, and major cavities, to 15m depth, have been found at all depths drilled.

The Formation varies considerably in composition along strike. Outcrop and drillhole data indicate a minimum thickness of 60m at the outcrop near Tamblyn's shaft, which increases to a maximum of about 700m in a strike distance of about 2km to the north, and also increases rapidly down dip to the west. The large rhombohedra invariably contain more than the stoichiometric 45 percent $MgCO_3$ required for dolomite, and many assays show more than 90 percent $MgCO_3$. (Note that only the fine grained calcilutites, unknown at Mt. Fitch, are of dolomite composition (Crohn *et al.*, 1968)).

The typical Coomalie succession at the Mt. Fitch deposits is a white coarse grained magnesite marble, a green chloritic magnesite, and a grey silty medium grained magnesite (Fig. 3).

The Batchelor Group is overlain by the *Namoona Group* with the *Masson Formation* as the basal member. They are trough sediments, and form a northerly trending band about 3½km wide. Individual members are, from the base:

1) The Masson Formation comprises a black pyritic chloritic and carbonaceous schists, often finely banded with chlorite-rich and chlorite-poor layers, and a maximum drill-hole length of 27m.
2) A fine grained grey carbonate, maximum drillhole length of 34m.
3) Grey to black quartz-sericite schist, invariably pyritic, and of considerable thickness

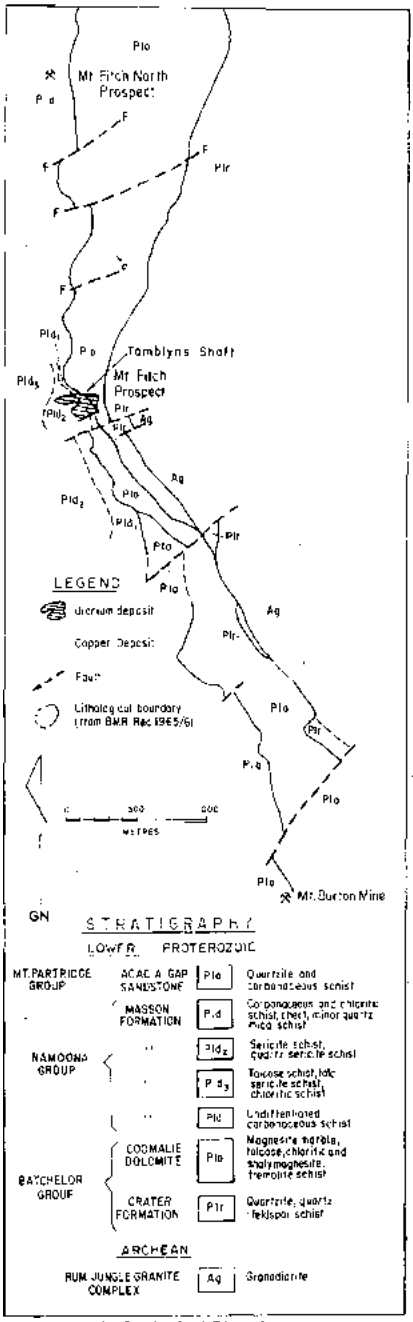


Figure 2. Geological Plan, Mount Burton to Mount Fitch North.

- certainly greater than 100m. There are several bands of green chloritic schist and pale yellow meta-argillites in the upper part.

4) A very fissile medium grey quartz-sericite schist. Drilling has shown that this unit is conformable with the remainder of the sequence, and the shear zone at the base (previously the 'Mt Fitch Fault') is not particularly remarkable.

STRUCTURE

The close pattern of drillholes shows that the upper surface of the Coomalie Dolomite forms an eastern trough, a central ridge, then a steep westerly slope. Foliation patterns from surface mapping in the schists also indicate north to northwesterly folding, and the boundaries between the various rock units parallel this foliation, all confirming that this is the primary fold direction. These folds and the associated cleavage are assumed to have originated during orogenesis at about 1800 m.y.

The mineralization is terminated at its southern end by a near vertical, northeasterly fault which has displaced the southern block down. Regional mapping identified an extension to this fault, and a nearby parallel fault, which have displacement in the sense north block east (Fig. 2). These folds and faults are broadly parallel to the Giant's Reef Fault, and are thought to be the same age.

In the eastern trough the Dolomite and overlying schists have been intensely brecciated; the magnesite has been recrystallised in part, to form rhombohedra with side lengths up to 20mm, and the schists have flowed so as to surround angular schist and magnesite fragments. In the chloritic magnesite horizon the large angular magnesite fragments are enclosed in a matrix of fine chlorite and magnesite grains. This breccia zone is thought to be of Giant's Reef age, produced at the intersection of a major zone of shearing (which is parallel and complementary to the main displacement along the Giant's Reef Fault) with the regional cleavage due to the 1800 m.y. folding.

COPPER MINERALIZATION

Isolated high copper values, to 200 ppm, are known from soils from the northern tip of the Mt. Burton quartzite to the Mt. Fitch North Prospect, over a strike length of about 4km. The primary mineral is chalcopyrite, occasionally with a thin bornite rim, and is found as fine disseminated grains and occasional veins in most of the schist and magnesite sections drilled. This primary mineralization is usually quite low grade, less than 400 ppm, with occasional magnesite breccia sections containing veins of chalcopyrite, so that assays of a few percent copper are known over a few metres drill hole length.

Three higher grade bodies are known; each is about 70m wide, with northerly lengths of 300, 120 and 130m (Fig 3). The deposits are flat-lying, extending from the surface to a maximum of 40m depth, and entirely restricted to the residual clays overlying the Coomalie Dolomite. The copper minerals are malachite, native copper and chalcocite, as fine grains and thin smears, associated with iron and manganese oxides. Reserves from non-core drilling are estimated as 290,000 tonnes of grade 0.6 percent copper, but the recovered grade is sure to be much lower than this. These surficial deposits represent at least a tenfold enrichment, by removal of the carbonate host rock during weathering.

URANIUM MINERALIZATION

Striking patches of brilliant green platey meta-torbernite have been found in several costeans, as joint coatings in grey sericite schists and yellow meta-argillites of the Pld 2 unit. Minor mineralization of this type is also found in drill core at the Mount Fitch North Prospect. The magnesite breccia fragments on surface dumps and walls at the trial pit are commonly coated with a yellow secondary uranium mineral, apparently a weathering bloom.

The primary ore mineral is extremely fine grained, and somewhat enigmatic. It was originally described as thucholite, but electron probe work at AMDEL in 1968 (Emberton & Fraser, 1969) and C.S.I.R.O. research (S. J. Craven, 1979 pers. comm.) did not detect

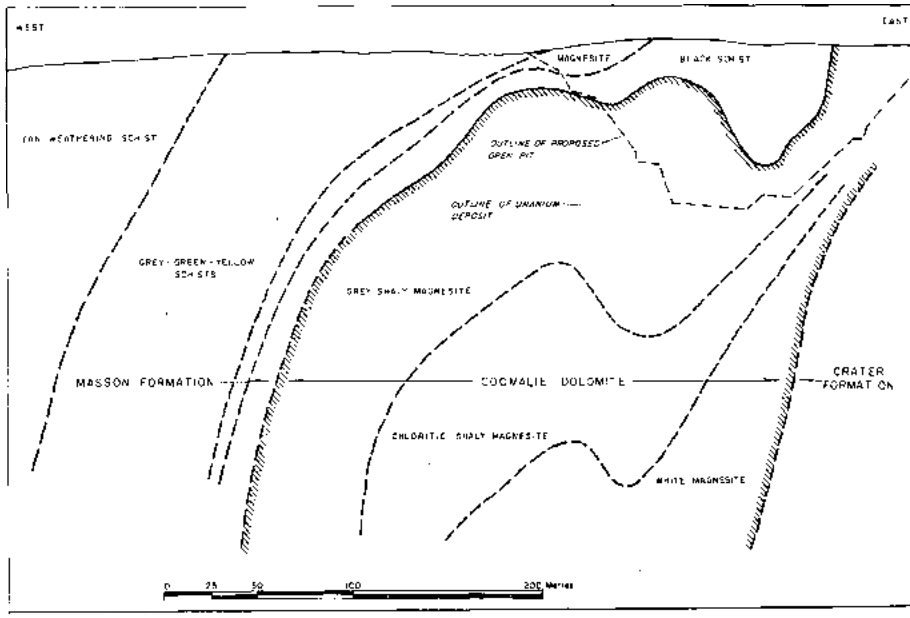


Figure 3. Cross-section 43930N, Mount Fitch.

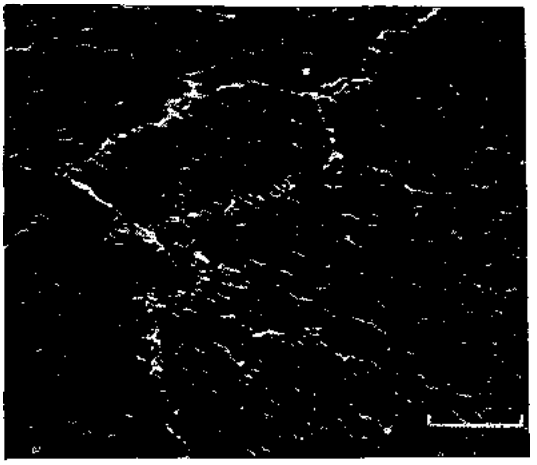


Figure 4. Mount Fitch magnesite breccia. Scanning electron microscope photograph using secondary electrons and back scattered electrons. Note the cleavage directions which identify individual magnesite fragments; the white vein material also defines fragment boundaries (CSIRO photograph. Scale bar is 0.04mm long).

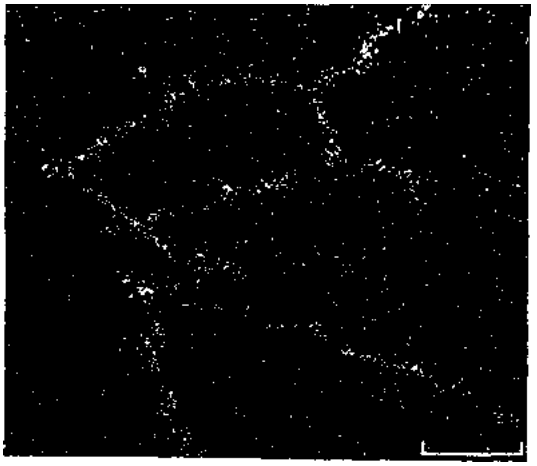


Figure 5. M α uranium radiation map of same area as figure 4. Note that the uranium mineralization is confined to the vein areas (CSIRO photograph. Scale bar is 0.04mm long).

thorium or rare earths. Both conclude that the primary uranium mineral probably occurs as amorphous oxides. The C.S.I.R.O. work found pyrite associated with this mineral. Uranium is distributed:

1) In the carbonaceous schists of the Masson Formation, concentrated in narrow friable clayey carbonaceous bands, with a lesser quantity disseminated through the rock,

and

2) In the Coomalie Dolomite, concentrated in anastomosing veinlets (usually around five microns wide) in the matrix part of the magnesite breccias and noticeably absent from the massive 'pure magnesite' fragments (Figs. 3 & 4).

This mineralization occurs in two masses, joined by a low grade corridor. The northernmost is a near vertical slab, about 110m long eastwest and 30m wide, and of average depth about 20m. The larger body is a flattened ellipsoid, about 160m long north-south by 110m wide, with maximum depth about 100m. Reserves in both deposits, total approximately 1500 tonnes U_3O_8 contained in ore with an average grade of 0.042% U_3O_8.

Each of the uranium deposits is directly related to the eastern trough and the zone of brecciation therein; the major body lies directly in the northerly trending portion of the trough, while the smaller slab is directly over the westerly extension of this trough. Grades diminish rapidly outside the breccia zone. The few deeper exploration holes show that low grade mineralization extends beyond the outlines of the main deposit, and has been found to 219m depth. The accepted base of the deposit is an economic limit, related to the optimum open pit design, while the geological limit is the transition from chloritic magnesite to 'pure' magnesite.

The upper surface of the deposit is generally the base of the weathered zone, which is

occasionally only 5m below the ground surface, deepening to a maximum of 70m. The depth of weathering contours are reasonably similar to the shape of the eastern trough, and the authors assume that the deeper weathering here is due to higher permeability in the breccia zone. There is an indication of some supergene enrichment, with the highest assays in each drillhole less than 50m below the base of the weathered zone.

METALLOGENESIS

Each of the Pine Creek Geosyncline Formations is unusually thin in the Mt. Fitch area, suggesting that this was an isolated sub-basin during the deposition of these rocks. The strikingly wide transition zone between the magnesite and schist units, which merge into each other over a present thickness of about 200m, is further evidence of a near shore and isolated depositional environment.

Copper and uranium mineralization are common at the Coomalie Dolomite-schist interface for a strike length of more than 4km, although the Mt. Fitch deposits are the only major concentrations known in this belt. Finely disseminated copper and uranium minerals are thought to be either primary sedimentary constituents, at quite low concentrations (only a few hundred ppm of uranium and copper) or widespread low temperature hydrothermal mineralization, emplaced perhaps at the 1800 m.y. orogenesis.

In the absence of geochronological data on the deposits it is presently postulated that concentration of this primary mineralization to a higher grade deposit occurred after Giant's Reef faulting, in an area of intense brecciation with increased permeability. In this area weathering of sulphides provided dilute acid to dissolve uranium and copper, and the uranium ions were precipitated preferentially on the shaley fragments, at some distance below the zone of weathering. Copper minerals were formed near the ground surface, in a terra rossa horizon.

GUIDES TO EXPLORATION

The Mt. Fitch information suggests that the search for uranium deposits has the best chance of success in areas with the following characteristics:

1) Areas of depositional thinning, particularly areas in which the Dolomite-shale boundary is transgressive or poorly defined.
2) Zones of brecciation in carbonates and schists within 4km of the edge of Archaean granite complexes, which are favourable for supergene enrichment of low grade primary deposits.
3) Significant uranium (and copper) mineralization may occur in carbonate horizons, as well as the better known graphitic schists — the carbonate units in the Pine Creek Geosyncline have not usually been thoroughly prospected.

REFERENCES

Berkman, D.A. 1966: Authority to Prospect 1281, Final Report. *Unpublished Report, Australian Mining and Smelting Company Limited.*

Berkman, D.A., 1968: The geology of the Rum Jungle uranium deposits. *in, Uranium in Australia Symposium, Australas. Inst. Min. Metall., 12-31.*

Crohn, P. W., Prichard, C. E. & Gardener, J., 1968: Summary of BMR exploration — Rum Jungle Area, 1968. *Rec. Bur. Miner. Resour. Geol. Geophys. Aust., 1968/102,* (unpubl.).

Emberton, J. & Fraser, W. J., 1969: Mount Fitch uranium prospect geological report, October, 1969. *Unpublished Report, Territory Enterprises Pty. Limited.*

Emberton, J. & Fraser, W. J., 1970: Mount Fitch uranium prospect: geological report for the year ending 31st December, 1969. Rum Jungle, January, 1970. *Unpublished Report, Territory Enterprises Pty. Limited.*

Haldane, A. D. & Debnam, A. H., 1959: Geochemical prospecting survey, Rum Jungle, Northern Territory. *Rec. Bur. Miner. Resour. Geol. Geophys. Aust., 1959/3,* (unpubl.).

Johnson, K., 1974: Progress report: geological review and revision of the Rum Jungle area, Northern Territory, 1973. *Rec. Bur. Miner. Resour. Geol. Geophys. Aust., 1974/41,* (unpubl.).

Pritchard, P. W. & French, D. J., 1965: Rum Jungle geochemical survey, 1963: The Mount Burton mine — North Mount Fitch prospect area. *Rec. Bur. Miner. Resour. Geol. Geophys. Aust., 1965/6,* (unpubl.).
Rhodes, J. M., 1964: The geological relationships of the Rum Jungle Complex, Northern Territory. *Rep. Bur. Min. Resour. Geol. Geophys Aust., 89,* 10p.
Walpole, B. P., Crohn, P. W., Dunn, P. R. & Randal, M. A., 1968: Geology of the Katherine - Darwin Region, N.T. *Bull. Bur. Miner. Resour. Geol. Geophys. Aust., 82.*
Ward, H. J., 1953: Mount Fitch prospect Rum Jungle, Northern Territory. *Rec. Bur. Miner. Resour. Geol. Geophys. Aust., 1953/140,* (unpubl.).
Warin, O. N., 1959: Report of investigation of radiometric anomalies discovered by Auster aircraft in the Rum Jungle district, Northern Territory. *Rec. Bur. Miner. Resour. Geol. Geophys. Aust., 1959/18,* (unpubl.).
Wood, R. W. & McCarthy, E., 1952: Preliminary report on scintillometer airborne surveys over the Rum Jungle area and other portions of the Northern Territory. *Rec. Bur. Min. Resour. Geol. Geophys. Aust., 1952/79,* (unpubl.).

EXPERIENCE WITH THE TRACK ETCH METHOD FOR URANIUM EXPLORATION IN NORTHERN AUSTRALIA

C.P. Pedersen[1], J. Dunbier[1] and J. E. Gingrich[2].

1. Noranda Australia Limited, 440 Collins Street, Melbourne, Vic., 3000, Australia.
2. Terradex Corporation, 460 N. Wiget Lane, Walnut Creek, California, 94598, U.S.A.

ABSTRACT

The Track Etch* technique for uranium exploration is a radon detection system which has been found to be helpful in exploring for 'hidden' uranium ore bodies. These 'hidden' bodies have little or no surface expression that can be detected with the usually employed airborne or ground radiometric detection methods. Radon from these 'hidden' bodies can migrate to the surface where it can be detected with Track Etch detectors and it can thus provide a clue which helps in discovering ore bodies which may be located at significant depths. A test of the Track Etch method was conducted in the Alligator Rivers Uranium Field in 1972 by Noranda in a uranium prospect area located 7km east-northeast of the Koongarra deposit near the base of the southeast escarpment of the Mt. Brockman outlier. The Track Etch readings measured a background radon level in the area of 7.3 T/mm² with a peak value of 702 T/mm² or almost 100 times background. The Track Etch technique, in this instance, successfully delineated the primary uranium mineralization buried by transported overburden. The radon anomaly covered a much larger surface area than the surface projection of the known primary mineralization. The strongest portion of the Track Etch anomaly appeared to be some 70m east of primary mineralization at a point where the shallowest primary mineralization was approximately 35m deep. The displacement of the anomaly peak from the centre of the primary mineralization is thought to be due to secondary uranium mineralization dispersal from the primary source caused by ground water movement or gaseous radon transport. In areas where dispersion of uranium daughter products occurred, spurious anomalies were detected remote from the primary uraniferous source. In most instances these surface anomalies (swampy black soils) could be identified by simultaneous measurements with both scintillometer and Track Etch methods. The results of these tests indicate that the Track Etch radon detection method can provide valuable information in exploring for the 'hidden' deposits found in this area and in areas of similar geology.

* The Track Etch system is covered by U.S., Australia, and other patents.

INTRODUCTION

Radon has been used as a uranium exploration tool for several years (Miller & Ostle, 1976). It has the advantage over methods which are either indirect (resisitivity, magnetic, etc.) or which are limited by the penetration of gamma rays to the detectors (geiger counters or scintillometers). Radon originating from deeply buried uranium deposits can be transported by gaseous or aqueous movement to the surface where it can be detected by several gaseous alpha radiation detection methods and it can thus provide a useful clue in finding these 'hidden' deposits.

Several factors influence the measurement of radon and its application to uranium exploration. It has been found that radon concentrations in the near-surface soil will vary by large amounts because of changing meteorological conditions and soil gas radon concentrations can vary by more than a factor of 100 in a 24 hour period due to variations in temperature, barometric pressure, wind speed and direction, moisture and other conditions (Gableman, 1974). Weekly integrated readings can also vary by more than a factor of 10 and it is for this reason that longer term integrated measurements are needed to provide reliable radon data. It should be noted that these changing meteorological conditions may contribute significantly to the transport of radon to the surface from the buried uranium deposits.

There is a significant contribution of radon in the soil gas from the background uranium mineralization in the soil at the point of measurement. A recent technical paper describes the relationship of the soil gas radon content to the uranium concentration measured in the same areas (Alter, 1978). Areas with heavy surface leaching conditions (such as the one tested on this program) commonly have low levels of near-surface uranium and hence have low

background radon levels in the soil gas. For this reason, these highly leached areas may show much stronger radon anomalies (X background) than other areas where there is more uranium in the soils, and hence it may be possible to detect deeper sources of significant uranium mineralization in these environments.

Another major factor influencing radon concentrations at the surface is the permeability of the rocks over the buried uranium mineralization. Rocks with high permeability obviously can allow more radon to be transported to the surface by either gaseous or aqueous transport and thus make it possible to detect deeper mineralized targets. Faults and fractures in the overlying rocks provide areas with high permeability. Since economic uranium deposits are often found in conjunction with faults, this phenonemon can sometimes be used to advantage in applying radon detection methods.

The grade, amount and emanating rate of the uranium mineralization directly affect the amount of radon released from the ore body. Higher grades, larger amounts and greater emanating power of certain uranium minerals all contribute to higher amounts of radon released. As radon moves upward from a buried source, its concentration decreases as it decays. For this reason, a deep high-grade deposit can produce the same quantity of radon at the surface as a shallow low-grade deposit. At the present time it is not known what the depth limitations for radon detection are since its movement and measurement is influenced by many different factors in different areas but it is believed that ore bodies at depths of 100 to 200m can be detected in many circumstances and that depths of up to 300m are possible in very favorable circumstances.

One advantage in using radon as an exploration tool is the fact that it is a pure alpha emitting gas. By making the detection system for radon sensitive only to gaseous alpha emitters, the sensitivity can be made to be very high and very precise for radon gas. This can be particularly important in eliminating background noise problems like those often encountered with other radiometric detection systems.

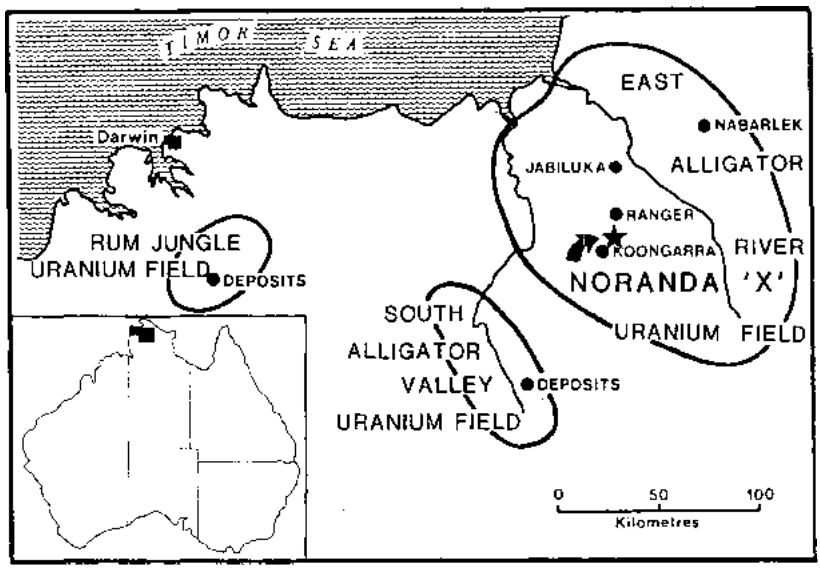


Figure 1. General Location of the Survey Area.

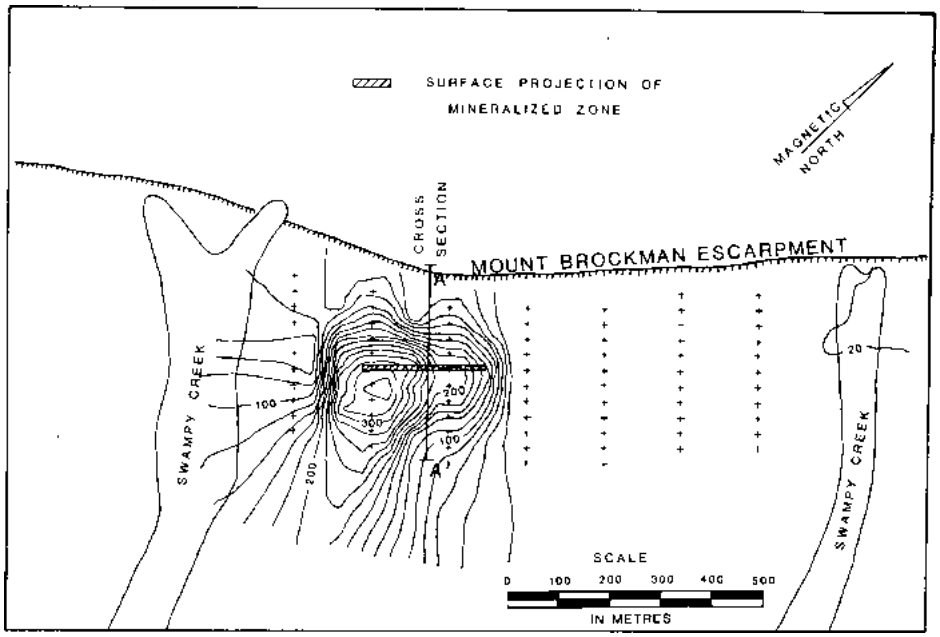


Figure 2. Location of Test Area and Track Etch Radon Map of Results.

THE TRACK ETCH DETECTION METHOD

The Track Etch system for uranium exploration has been previously described in detail in several technical papers (Gingrich & Fisher, 1976; Fisher, 1976). Essentially, it uses special alpha radiation sensitive detectors enclosed in small sampling cups to detect the radon content of the soil gas. These Track Etch cups are placed in shallow holes in the earth and left undisturbed for several weeks. By leaving the detectors for a period of time they continuously accumulate the readings produced by the varying radon soil concentrations, and thus they produce readings indicative of the long term average radon concentrations in the areas being sampled. It has been found that the short-term variations in soil-gas radon content measured by other methods caused significant problems in interpreting radon data. These problems are eliminated with the Track Etch method.

One of the other significant advantages of the Track Etch method is its extreme simplicity and the fact that the sampling cups can be easily deployed by unskilled personnel. The detectors and cups are simply pieces of rugged plastic material and they have no complicated mechanical or electrical parts to cause problems.

In the field the Track Etch cups are normally used in a grid pattern with spacings ranging between 30 and 1000m depending on the size of the area being explored, the dimensions of the expected mineralized area, the local structural trends, and other factors.

Recent research with the Track Etch system has resulted in the development of Thoron Filters to remove unwanted thoron gas (Rn-220) from thorium mineralization and in the improvement in the sensitivity of the detectors by a factor of 10 over the detectors used in this program.

TRACK ETCH SURVEY AREA

A test of the Track Etch method was conducted in the Alligator Rivers Uranium Field in

1972 by Noranda in a uranium prospect area located 7km east-northeast of the Koongarra deposit near the base of the southeast escarpment of the Mt. Brockman outlier (Figs. 1 and 2). This prospect (identified as Anomaly X) was recognized as being geologically similar to the area around Koongarra.

A cross section of the geology in the immediate test area is shown in figure 3. The uranium occurs as steeply dipping veinlets and disseminations of uraninite in a zone of sheared chloritic schists adjacent to a branch of the Koongarra Reverse Fault zone. The schists are a portion of the Lower Proterozoic Cahill Formation which has been upthrown against the Middle Proterozoic Kombolgie Formation. In this area the Koongarra Reverse Fault has up to 600m of post-Kombolgie vertical displacement. The Kombolgie Formation, which is the footwall of the fault, is a sheared, silicified, hematitic sandstone, commonly metamorphosed to quartzite. The primary mineralization is overalin by a diffuse zone of lower grade secondary uranium mineralization. The bedrock is covered by a 1 to 3m thick layer of sandy alluvium and lateritic soil. This cover is not enriched in uranium mineralization and it masks the major mineralized zones.

PREVIOUS PROSPECTING IN THE TEST AREA

The initial exploration in the test area commenced in 1969. During that year and in 1970 two systematic airborne spectrometric surveys, including several special escarpment flightlines failed to detect any anomalies in the prospected area. Subsequently, in 1971 ground prospecting delineated a composite radiometric anomaly consisting of: a localized zone of highly radioactive termite mounds in an area of sandy alluvium; a weak, diffuse radioactive anomaly associated with scattered laterite outcrops downslope from the termite mounds; some small laterite outcrops downslope from the termite mounds; and some small moderate intensity radioactive anomalies in swamply black soils around springs along strike from the termite mound anomalies. The termite mounds had readings up to 10 times the normal background. The weaker diffuse anomaly (associated with laterite outcrops) had readings of 1.5 to 3.5 times background and the highest readings were extremely localized. Further evaluation of these anomalies showed that the laterite zone was an expression of a weak, near surface secondary mineralized dispersion tongue, while the swamp concentrations reflected aqueous radon dispersion from an unknown source. The swampy black soil anomalies are a common occurrence along the entire Mt. Brockman Escarpment.

Following initial exploration effort, auger and percussion drilling indicated that beneath a 1 to 3m sand veneer the termite mound anomaly was underlain by clayey, weathered schists containing scattered uranium mineralization increasing in concentration downwards. Inclined diamond drilling indicated the presence of steeply dipping pods of uranium mineralization at depth. The mineralization consisted of veinlets and disseminations of uraninite hosted in sheared chloritic schists of the Lower Proterozoic Cahill Formation.

In October 1972 additional drilling was undertaken with the goal of penetrating through the reverse fault well into the underlying Kombolgie. Primary mineralization was intersected in Cahill Formation schists at depths between 25 and 50m and the drill hole passed through the fault into the Kombolgie at 52m and continued into the Kombolgie to a total depth of 164m (Fig. 3).

THE TRACK ETCH SURVEY

In late 1972 the Track Etch radon detection system became available in Australia and a test of the method was conducted by Noranda in the area of interest around this prospect. The Track Etch cups were placed in 60cm holes on a 160 by 30m grid for some 4600m along the strike of the Koongarra fault zone at the base of the Mt. Brockman escarpment. (A portion

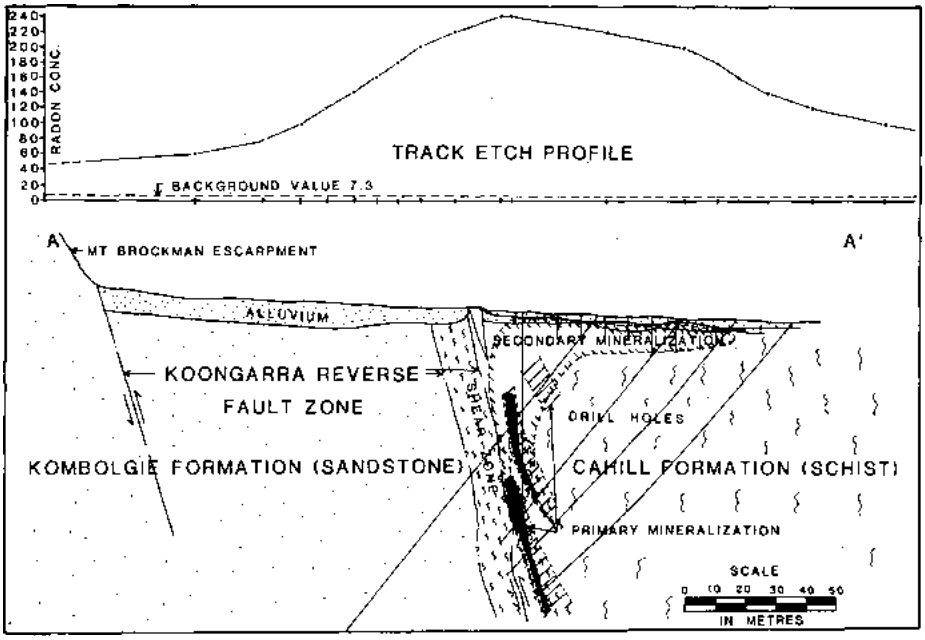


Figure 3. Cross section of Geology and Track Etch Profile.

of this area is shown in figure 2.) The Track Etch sample spacing was selected as a compromise between detecting the target zone and providing the most cost-effective coverage. For logistical reasons the cups had to be placed during the early wet season which was not considered ideal at the time. (The wet conditions which were encountered have subsequently been shown to cause no significant problems in making adequate Track Etch radon measurements in either this area or many others with similar conditions.) The Track Etch cups were left in place for approximately three weeks (to provide adequate integrating time) after which they were returned to Terradex for processing, reading and evaluating.

The Track Etch readings measured a background radon level in the area of 7.3 T/mm^2 with a peak value of 702 T/mm^2 or almost 100 times background. Approximately 26% of the readings were anomalous and the majority of the high points were concentrated in the one anomalous zone shown in figure 2. Surface scintillometer readings made in this area were only weakly anomalous. The strongest portion of the Track Etch anomaly appeared to be some 70m east of primary mineralization. At this point the shallowest primary mineralization is approximately 35m deep. The displacement of the anomaly peak from the primary mineralization is though to be due to secondary uranium mineralization dispersal from the primary source caused by ground water movement or other factors. The Track Etch anomaly continues from the peak value in a south easterly direction as shown in figure 2.

The Track Etch background level measured in the test area (7.3 T/sq.mm) is significantly lower than the world wide average value of 20 T/sq.mm but is typical of background measurements made on other Track Etch surveys in the Alligator Rivers area. The low background value is indicative of low surface uranium mineralization due to strong surface leaching that occurs because of the heavy rainfall in the area. The low background value to some degree made it easier to see the more subtle radon anomalies associated with minor amounts of mineralization.

The Track Etch survey also found some lower magnitude radon anomalies associated with mineralized laterites and black soil swampy areas. Exploration of these associated anomalies showed that the laterite zone was an expression of a weak, near surface secondary dispersion tongue, whereas swamp concentrations reflect radon dispersion from an unknown source. The swampy areas also had moderate radioactive anomalies that could be detected with hand-held scintillometers. Some of these anomalies had been tested by shallow drilling early in the project, but once it was realised that they probably presented aqueous dispersion no further direct work was undertaken.

Following the Track Etch survey additional systematic geological mapping and other exploration work was performed in the area but no additional exploration drilling was undertaken and since January 1974 all exploration work in the area was stopped because of government regulations. Because of this, it is not possible to relate the full extent of the primary Track Etch anomaly to the full extent of the primary uranium miniralization. It is known, however, that the Track Etch anomaly covered a much larger surface area than the surface projection of the known primary mineralization. This may have been partially due to the dispersed halo of secondary uranium mineralization and partially due to gaseous radon movement from the primary uranium source. In evaluating the Track Etch data from the survey, it is believed that future surveys in this type of area could be conducted by a wider Track Etch cup spacings, i.e. in the order of 60 by 150m or possibly greater. If such a wide spaced survey were performed it then might be desirable to follow it with closer samples in the areas of interest.

SUMMARY AND CONCLUSIONS

It was concluded from these results that the surface and airborne radiometric expression of the more significant uranium mineralization in the test area was suppressed by a thin layer of transported overburden. Dispersion of uranium or its daughter product elements had generated weak surface radiometric anomalies, but these were often subtle and only tenuously related to primary mineralization. The Track Etch technique in this instance, because of its much greater sensitivity and ability to measure radon transported from the buried source, successfully delineated the primary uranium mineralization. The Track Etch radon anomaly provided a strong contrast to background and covered a much larger surface area than the surface projection of the primary mineralization.

In areas where aqueous dispersion of uranium daughter products occurred, spurious anomalies were detected remote from the primary uraniferous source. In most instances these surface anomalies (swampy black soils) could be identified by simultaneous measurements with both scintillometer and Track Etch methods.

The result of this test program has indicated that the Track Etch radon detection method can provide valuable information in exploring for these 'hidden' types of uranium deposits in this area and in areas with similar geology. Further improvements in radon detection sensitivity may provide a useful tool in exploring for even deeper types of targets.

REFERENCES

Alter, H. Ward, 1978: Track Etch Ratios in Soil Uranium and a New Uranium Abundance Estimate. *Symposium on the Natural Radiation Environment, III, Houston, Texas.*

Fisher, J.C., 1976: Application of Track Etch Radon Prospecting to Uranium Deposits, Front Range, Colorado. *Proceedings of the joint meeting of Am. Inst. Min. Metall. Engrs and Min. Metall. Inst. Japan. Denver, Colorado.*

Gableman, John W., 1974: Economic Geology and Uranium Prospecting in Frontier Areas. *Am. Inst. Min. Metall. Pet. Engrs. 103rd. Annual Meeting, Dallas, Texas.*

Gingrich, J.E. & Fisher, J.C., 1976: Uranium Exploration Using the Track Etch Method. *Exploration for Uranium Ore Deposits, IAEA, Vienna,* 213-227.

Miller, J.M. & Ostle, D., 1976: Radon Measurements in Uranium Prospecting. *Exploration for Uranium Ore Deposits. IAEA, Vienna,* 107-125.

THE NATURE AND SIGNIFICANCE OF THE OCCURRENCE OF URANIUM IN THE NANAMBU COMPLEX OF THE PINE CREEK GEOSYNCLINE

J. McAndrew and C. J. Finlay

CSIRO Division of Mineralogy, P.O. Box 136, North Ryde, N.S.W., 2113, Australia.

ABSTRACT

The mineralogy of the occurrence of the uranium in granitic rock types from the Nanambu Complex has been studied for seven localities in the Complex. Uranium is present in accessory zircon, monazite, xenotime, uranothorite, uraninite and apatite; in pseudomorphs of altered uraninite and uranothorite; in ferruginized and chloritized biotite; and as very minor amounts disseminated through altered feldspar. There is no concentration along grain boundaries, or fractures. Uraninite or pseudomorphs of altered, oxidized uraninite have been recognized at five of the localities. The accessory uraninite provides a source of mobile uranium for hydrothermal as well as supergene processes. Zircon in uraninite-bearing granitic rocks of the Nanambu Complex has a relatively high uranium content of 0.18-0.36%. This may represent the saturation level for uranium in zircon at the conditions under which the granitic rocks formed, and be a guide to the potential occurrence of uraninite, and thus of labile uranium, in such rocks.

INTRODUCTION

In igneous and metamorphic terranes, any initial concentration of uranium, at the trace element level, is normally observed in silicic and alkaline igneous rocks. Granitic associations are thus prospective sources for uranium to form mineral deposits and, as in the Canadian Shield (Darnley *et al.*, 1977), uranium mineralization may be associated with a regional concentration of uranium in granites above the average abundance of 4 ppm (Rogers & Adams, 1969). The Pine Creek Geosyncline is one such district, containing granitoids which are enriched in uranium relative to this value (Ferguson *et al.*, this volume). However some uranium districts are associated with granites which, except very locally, lack notable enrichment in uranium, as in the western USA (Larsen & Gotterfried, 1961; Stuckless *et al.*, 1977), and the probable source rocks may not contain uranium appreciably in excess of the Clarke value.

An important factor influencing the lack of simple correlation between mineralization and regional enrichment of uranium is the wide variation in the availability of uranium in crystalline rocks for further concentration. This is determined by the mineralogical manner in which the uranium is present, and for this purpose four main types of occurrence may be recognized. Commonly the major portion occurs in the accessory resistate minerals. This fraction is relatively immobile, and is not readily available for reconcentration by either hydrothermal or supergene processes. Three types of labile uranium can be distinguished and these are of restricted occurrence, in contrast to the ubiquity of uraniferous resistate minerals. They consist of the following. (1) Uranium along grain boundaries and microfractures can either be primary, or of secondary supergene origin derived from primary labile uranium rather than being a source of it (Barbier & Ranchin, 1969). (2) Uraniferous chlorite, formed as a replacement of biotite during deuteric alteration, from which uranium may be subsequently released (Renard, 1974). (3) Accessory uraninite provides a ready source of labile uranium. Normally it is absent. Exceptionally, disseminated uraninite forms ore grade concentrations, as at Rössing for which some studies suggest a primary plutonic origin (Berning *et al.*, 1976). However, hydrothermal processes may also deposit disseminated uraninite within a silicic pluton (Cuney, 1978). As a minor accessory its relic from alteration in the zone of supergene oxidation is insignificant and difficult to recognize, although uraninite may carry a substantial fraction of the total rock uranium (Barbier *et al.*, 1967).

The mode of occurrence of uranium in silicic intrusions and complexes in the Alligator

Rivers Uranium Field may thus have an important bearing on their potential as source rocks for mineralization, and consequently on genetic hypotheses for ore formation. We have therefore investigated the mineralogy of the occurrence of uranium in granitic-type rocks from the Nanambu Complex, which represent a possible source for uranium in the major deposits fringing the Complex.

METHODS

The friable nature of secondary minerals formed by supergene oxidation of uraninite and the extremely fine grain size of the uraniferous accessory minerals preclude satisfactory general use of heavy mineral concentrates.

The study is therefore based on microscopic investigation of polished thin sections, coordinated with measurement of their uranium distributions. The latter were determined by fission tracks recorded on polycarbonate and mica detectors in contact with the polished surfaces, the fission being induced by irradiation with dosages in the vicinity of 10^{15}neutrons/cm^2 slow neutrons in the HIFAR reactor of the Australian Atomic Energy Commission. Conventional etching techniques were used to reveal the tracks (Fleischer *et al.*, 1975).

The detectors sample a surface layer of the section equivalent to a thickness of about 6 μm, within which the distribution of uranium across the section can be recognized to within a few micrometres. However the extremely fine grain size of the uraniferous phases makes determination of the concentration of uranium in individual grains difficult, except for those with similar cross-sectional area over the upper 8 μm of the section. The values given are for grains more favourable for measurement; those by fission tracks may have an accuracy not better than $\pm$ 20%, and within this error agree with microprobe analysis made on a Cambridge Geoscan V and corrected by the Magic IV programme.

ROCK TYPES

The rocks studied contain quartz, microcline, alkali-plagioclase, and two micas, and vary in texture from gneissic granite to granitic gneiss. They are from seven localities in the Nanambu Complex (Fig 1). All contain phenocrysts of perthitic microcline, some also of alkali feldspar. The amount of muscovite ranges from more to much less than that of biotite. In addition to occurring with or in a similar texture to biotite, muscovite forms patches within microcline and abundant inclusions within alkali plagioclase. Much finer grained ?kaolinization is also present in some sericitized plagioclase, which normally has a clear unaltered rim. There is some myrmekitic to graphic quartz in plagioclase. Fine-grained quartz-feldspar lenticles may become abundant. At only one locality is biotite together with muscovite segregated into thin parallel sheets of pronouncedly tabular crystals. Biotite is occasionally chloritized.

These rocks were selected to cover a range of uranium and thorium content; uranium analyses range from 2 to 50 ppm and the Th/U ratio from 0.4 to 33. However, it is evident from fission track studies of thin sections that uranium can vary at a hand specimen scale. The alkaline nature of the specimens is shown by their $(K_2O + Na_2O)/CaO$ ratio of 5.4 to 14.0, while K_2O/Na_2O ranges from 1.2 to 2.1. The extent of variation of composition of granitoids in the Nanambu Complex is given by the comprehensive study of Ferguson *et al.* (this volume).

URANIUM LOCALIZATION

The uranium is present in four distinct modes. These are (1) in accessory zircon, monazite, xenotime, uranothorite, uraninite and apatite; (2) in small pseudomorphs consisting of very fine-grained to cryptocrystalline aggregates; (3) in ferruginized and chloritized biotite,

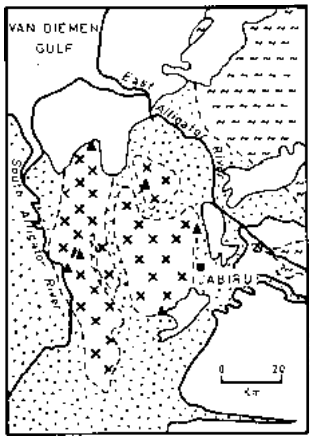


Figure 1. Map showing localities of specimens studied. Geology after Needham & Stuart-Smith (1976).

and (4) as very minor quantities disseminated through altered feldspar. There is no appreciable uranium along either grain boundaries of the major minerals or microfractures. We have not observed sphene or allanite, which accords with the alkali-rich nature of the rocks. These accessory minerals are very fine grained, seldom exceeding 100 μm, and commonly 5 to 30 μm in maximum dimension. While occurring within all major rock minerals, they do not show any preferential concentration within biotite or muscovite.

Monazite and zircon are ubiquitous, each varying in the amount present as well as in its uranium content. Zircon can be more abundant either in feldspar or in quartz and, in the latter, cracks occasionally radiate out from the zircon, indicative of expansion accompanying partial metamictization. The uranium content of the *monazite* was observed to vary from 0.1% to 0.8%, with a general tendency for higher values in specimens containing uraninite or pseudomorphs after uraninite. The finer, more equidimensional grain size of monazite relative to zircon makes fission track determination of the uranium concentration less accurate, and this variation needs further examination. *Zircons* in uraninite-bearing specimens from five localities have a uranium content of 0.18% to 0.36% by fission track analysis. Microprobe analysis of five grains gave a uranium variation from 0.24% to 0.35%, with Th/U from 0.7 to less than 0.01. Growth zoning is visible in some grains, and in polished section higher refractive index zones predominate. Bands of lower reflectivity and hardness may be partly metamict, and slightly higher in uranium. In contrast, zircon from two localities where uraninite or its pseudomorph were not recognized is less uraniferous, containing 0.05% to 0.13% uranium.

Two types of *uraniferous pseudomorphs* are distinguished in particular by their uranium content. One type is highly uraniferous; it tends to have a subcubic shape and is considered to represent pseudomorphs after uraninite. The other contains smaller amounts of uranium and may be pseudomorphous after uranothorite. In a deep drill core at 350m vertical depth accessory *uraninite* shows minor to appreciable alteration. Microprobe analysis gave a thorium content varying from 1.4% to 2.3%. This is much higher than that of the vein uraninites, and accords with the thorium content of accessory uraninite in some leucogranites of the Massif Central (Carrat, 1976). The 14.0% to 20.4% of lead within this uraninite may represent retained radiogenic lead. The highest concentration represents lead forming in 1650 m.y. from the uraninite, which is well within the 2,500 m.y. to 1800 m.y. ages determined for the Nanambu Complex (Page *et al.*, this volume). The small quantity of associated galena reveals only very minor sulphurization of this lead, distinctly less than commonly observed in uraninite in the Jabiluka orebody (Binns *et al.*, this volume). Zonal alternation of some grains to secondary minerals is distinct from the alteration observed by near surface weathering, unlikely at this depth, and may indicate a hydrothermal effect, with some leaching of uranium. Grains in alkali plagioclase (Fig. 2), have characteristic extinction haloes arising from radiation damage (McAndrew, 1957). Uraninite appears to be a normal accessory mineral, occurring as cubes and subhedral grains in feldspar and quartz. Uraninite in granites has also been considered to be of deuteric origin. However some textural evidence is indicative of this, as well as an association with strong corrosion of other uraniferous accessory minerals



Figure 2. Uraninite at the centre of an extinction halo in feldspar. Crossed polars.

(Cuney, 1978). These features have not been observed in the Nanambu Complex.

Uraninite or pseudomorphs after uraninite have been found at five of the seven localities studied. Two localities lacking this are in the western and north-western part of the Complex. The mineralogical distribution of uranium is, in general, concordant with the chemical variation in uranium and thorium. The low Th/U ratios are found in rocks where uranium occurred particularly in accessory uraninite and uraniferous zircon. Uraniferous ferruginized and chloritized biotite also contributes to lower ratios; however, this is of secondary origin and thus does not provide a primary source of labile uranium.

DISCUSSION

The uranium in accessory uraninite in the granitic rocks of the Nanambu Complex is readily mobilized by oxidation to provide a viable source of uranium for supergene concentration. However the presence of uraninite may also result in enrichment in uranium of hydrothermal fluids which penetrate such granites. An example of this is provided by recent studies of the uranium vein deposit in the uraninite-bearing Bois Noirs granite in France (Cuney, 1978). Utilizing fluid inclusion studies, Cuney deduced that the vein uranium was mobilized from this uraninite by hydrothermal activity.

Heat generated by abnormally high trace concentrations of radioactive elements in granite plutons can create continued convective fluid circulation in and around such plutons (Fehn *et al.*, 1978). The nature of such convection cells depends closely on the permeability of the pluton and adjacent country rock, but does provide a mechanism for movement of potentially mobile uranium over an extended period of time. The alteration of feldspars, noted above, reveals that hydrothermal activity has occurred within the Nanambu Complex. Evidence of possible hydrothermal movement of uranium may be provided by the unexpected observation of alteration of uraninite in granitic gneiss at a depth of 350m below surface.

Unambiguous criteria are lacking for simple recognition of silicic source rocks capable of providing a source of mobile uranium. Favourable alkaline leucocratic two-mica granites which contain accessory uraninite (e.g. Renard, 1974) are not necessarily distinguished by either a high uranium or a low Th/U content, and these in fact may vary widely. Moreover the presence of accessory uraninite may not be readily recognised in near surface specimens, particularly in deeply weathered terranes, unless its insignificant oxidized relics are especially sought.

In the Nanambu Complex, however, uraninite occurs in association with particularly uraniferous zircon. The range in uranium content of these zircons is about 0.18% to 0.35%. This lies in the uppermost part of the range 0.015% to 0.4% in uranium reported for zircon in granitic rocks, and exceeds that commonly found (Ahrens *et al.*, 1967; Berzina *et al.*, 1974). However similar uranium contents have been found in zircon in uraninite-bearing alkaline leucogranites of the Massif Central (Renard, 1974).

Both accessory zircon and uraninite appear to be normal accessory minerals of the Nanambu granitoids. Neither show evidence of being deposited from later deuteric-

hydrothermal activity; criteria for such formation can however be lost e.g. cracks along which deuteric deposition occurred may be destroyed by subsequent healing. We suggest that the unusually high uranium content of the zircon represents the saturation level under high temperature igneous-metamorphic conditions of formation appropriate to such rocks. An immediate corollary is that the presence of zircons containing this amount of uranium is an indication that uraninite could have formed in a granitic body. The presence of zircons with less uranium would then indicate that there was insufficient uranium for the crystallization of primary uraninite.

Thus a uranium content of 0.2% to 0.3% in zircon may provide a useful assessment of a granitic body being a potential source of primary labile uranium.

While distinguishing granitoids which may contain primary uraninite, this criterion would not necessarily apply to those containing uraninite hydrothermally introduced subsequent to crystallization, as has been deduced for disseminated uraninite found in parts of French plutons (Cuney, 1978). Association of this type of occurrence with zircon lower in uranium may provide supporting evidence for an epigenetic origin.

Our proposal parallels and extends a suggestion of Adler (1977) which was preceded by the recognition (Silver, 1976) that a belt of igneous rocks in the Precambrian basement of the Colorado Plateau contained zircons with two to twenty times the normal uranium content. It requires data readily obtained with modern facilities. If borne out by further studies, such an appraisal has the advantage of utilizing a resistate mineral, and hence can be applied to the evaluation of source rocks irrespective of surface weathering. Moreover it would be applicable to zircons in sediments, for ascertaining the likely presence of source rocks for labile uranium in their provenance.

ACKNOWLEDGEMENTS

We gratefully acknowledge the provision of specimens for this study by Dr J. Ferguson and the Bureau of Mineral Resources, Geology and Geophysics, and the cooperation received from Pancontinental Mining Ltd., Ranger Uranium Mines Pty. Ltd. and Noranda Australia Ltd.

REFERENCES

Adler, H.H., 1977: Geochemical factors contributing to uranium concentration in alkalic igneous rocks. *in, Recognition and Evaluation of Uraniferous Areas.* International Atomic Energy Agency, Vienna, 35-43.

Ahrens, L.H., Cherry R.D. & Erlank, A.J., 1967: Observations on the Th-U relationship in zircons from granitic rocks and from kimberlites. *Geochim. cosmochim. Acta, 31,* 2379-2387.

Barbier, J. & Ranchin, G., 1969: Influence de l'alteration meteorique sur l'uranium à l'état de traces dans le granite à deux micas de St-Sylvestre. *Geochim. cosmochim. Acta, 33,* 39-47.

Barbier, J., Carrat, H.G. & Ranchin, G., 1967: Presence d'uraninite en tant que minéral accessoire usuel dans les granites à deux micas uranifères du Limousin et de la Vendée. *C.R. Acad. Sci. Paris, 264,* 2436-2439.

Berning, J., Cooke, R., Hiemstra, S.A. & Hoffman, U., 1976: The Rössing uranium deposit, South West Africa. *Econ. Geol., 71,* 351-368.

Berzina, I.G., Yeliseyeva, O.P. & Popenko, D.P. 1974: Distribution relationships of uranium in intrusive rocks of Northern Kazadhstan. *Int. Geol. Rev., 16,* 1191-1204.

Binns, R.A., McAndrew, J. & Sun, S-S., this volume: Origin of uranium mineralization at Jabiluka. *Proceedings of the International Uranium Symposium on the Pine Creek Geosyncline.*

Carrat, H.G., 1976: Le role de la géochimie de l'uranium et du thorium dans la recherche des gisements uraniferes intragranitiques. *Sciences Terre, 20,* 131-164.

Cuney, M., 1978: Geologic environment, mineralogy, and fluid inclusions of the Bois Noirs-Limouzat uranium vein, Forez, France. *Econ. Geol., 73,* 1567-1610.

Darnley, A.G., Charbonneau, B.W. & Richardson, K.A., 1977: Distribution of uranium in rocks as a guide to the recognition of uraniferous regions. *in, Recognition and Evaluation of Uraniferous Areas.* International Atomic Energy Agency, Vienna, 55-86.

Fehn, U., Cathles, L.M. & Holland, H.D., 1978: Hydrothermal convection and uranium deposits in abnormally radioactive plutons. *Econ. Geol., 73,* 1556-1566.

Ferguson, J., Chappell, B.W. & Goleby, A.B., this volume: Granitoids in the Pine Creek Geosyncline. *Proceedings of the International Uranium Symposium on the Pine Creek Geosyncline.*

Fleischer, R.L., Price, P.B. & Walker, R.M., 1975: *Nuclear Tracks in Solids.* Univ. Calif. Press, Berkeley.

Larsen, E.S., Jr. & Gotterfried, D., 1961: Distribution of uranium in rocks and minerals of Mesozoic batholiths in western United States. *Bull. U.S. Geol. Surv., 1070C.*

McAndrew, J., 1957: Natural radiation damage in albite. *Am. J. Sci., 255,* 715-723.

Needham, R.S. & Stuart-Smith, P.G., 1976: The Cahill Formation — host to uranium deposits in the Alligator Rivers Uranium Field, Australia. *BMR J. Aust. Geol, Geophys.,* 1, 321-333.

Page, R.W., Compston, W. & Needham, R.S., this volume: Geochronology and evolution of the late Archaean basement and Proterozoic rocks in the Alligators Rivers Uranium Fields, Northern Territory, Australia. *Proceedings of the International Uranium Symposium on the Pine Creek Geosyncline.*

Renard, J., 1974: Etude petrographique et géochimique des granites du district uranifère de Vendée. *Sciences Terre, Memoir 30,* 216p.

Rogers, J.J.W. & Adams, J.A.S., 1969: Uranium. *in* (ed. K.H. Wedepohl) *Handbook of Geochemistry.* Springer-Verlag, Berlin.

Silver, L.T., 1976: A regional uranium anomaly in the Precambrian basement of the Colorado Plateau. *Geol. Soc. Am. Abst. Prog., 1976 Annual Meeting.*

Stuckless, J.S., Bunker C.M., Bush, C.A., Doering, W.P. & Scott, J.H., 1977: Geochemical and petrological studies of a uraniferous granite from the Granite Mountains, Wyoming. *J. Res. U.S. Geol. Surv.,* 5, 61-81.

MINERALOGY OF THE JABILUKA, RANGER, KOONGARRA, AND NABARLEK URANIUM DEPOSITS

G.R. Ewers and John Ferguson

Bureau of Mineral Resources, P.O. Box 378, Canberra City, A.C.T., 2601, Australia.

ABSTRACT

The Alligator Rivers uranium deposits are stratabound within the Lower Proterozoic Cahill Formation. Quartz-muscovite-chlorite schists predominate in all deposits. Within areas of uranium mineralization, chloritization is intense with the partial or complete replacement of biotite, muscovite, garnet, amphibole, and feldspar. The two most striking features common to the ore zones of all deposits are the tendency for mineralization to occur within zones of brecciation, and for it to be intimately associated with the chlorite cementing these breccias. The breccia fragments are typically chloritic and/or sericitic quartzite, chert (which in places is silicified carbonate) and strongly chloritized material. They are usually angular, laminated, and rotated. The textures and lithology indicate that brecciation occurred after the ~1800 m.y. regional metamorphic event, and that there was a high percentage of voids between the fragments. Breccia fragments have been cemented by chlorite ± quartz ± hematite ± chert ± graphite ± sulphides ± uraninite. The primary uranium mineralization is uraninite, though brannerite and coffinite have been reported. The uraninite occurs as disseminated cubes, which may coalesce to form clusters and strings; veins coating foliation planes; narrow lenses; rare spherules; and massive uraninite. Textures establish that uranium has been remobilized and redeposited within the ore zones. The limited extent of carbonaceous and sulphide-rich zones and their poor correlation with mineralization suggests that any deposition of uranium as a result of reducing conditions, has been localized rather than widespread.

The textural relations and composition of the chlorite cementing the breccia fragments vary considerably, and their significance in terms of ore genesis is open to interpretation. It is suggested that the presence of gibbsitic material, clay minerals, and clay-sized chlorite in this fracture filling chlorite may indicate an environment in which uranium was concentrated through adsorption. The tendency for the Fe^{2+}/Fe^{3+} ratio of the chlorite cementing breccia fragments to decrease with increasing whole-rock uranium values, suggests that redox reactions involving Fe may have led to uranium deposition.

INTRODUCTION

The major uranium deposits of the Alligator Rivers Uranium Field have been described by Hegge, 1977 (Jabiluka); Eupene *et al.*, 1975 (Ranger 1); Foy & Pederson, 1975 (Koongarra); and Anthony, 1975 (Nabarlek). This study enlarges on the petrographic work contained in these papers, and compares and contrasts the main petrologic features of each deposit. Particular attention has been given to primary mineral relations in the ore zones to assist in the formulation of a model for the genesis of the deposits. Secondary mineralization in the weathered zone has not been considered.

The dominant feature of the mineralogy is the ubiquitous occurrence of chlorite. Although chlorite is present in unmineralized zones within all the deposits of the Alligator Rivers Uranium Field, it is invariably and intimately associated with the primary uranium mineralization in each deposit. Clearly, chlorite or the minerals from which it formed, provides a key to understanding the genesis of these deposits.

GEOLOGIC SETTING

A description of the regional geological setting, and a comparative review of the uranium deposits has been given by Needham *et al.* (this volume), Needham & Stuart-Smith (this volume), and Hegge *et al.* (this volume).

Host Rocks To Mineralization

The Alligator Rivers uranium deposits are stratabound within the Lower Proterozoic Cahill Formation. According to Needham & Stuart-Smith (this volume), the Cahill Formation overlies the Kakadu Group with apparent conformity, and in many places is adjacent to the Nanambu Complex. In turn, it is overlain, in places unconformably by the Nourlangie Schist. Needham & Stuart-Smith (1976) have divided the Cahill Formation into two members:

1) a lower member, which ranges in thickness from 300 to 600m and which contains the major uranium deposits of the area, is characterized by the presence of carbonaceous units and carbonate rocks, and includes an interlayered sequence of mica schist, chloritized feldspathic quartzite, quartz schists, para-amphibolite, and calc silicate rock;
2) an upper member, which is more psammitic and contains quartz schist, feldspathic schist, feldspathic quartzite, and conglomerate.

Both members contain ortho-amphibolite and have been regionally metamorphosed to medium or amphibolite grade in an anatectic environment (Ferguson & Needham, 1978). Recent estimates suggest that temperatures of 600°C ± 50°C, and pressures of 5 to 8 kilobars prevailed at the time (Ferguson, this volume).

Quartz-muscovite-chlorite schists predominate in all deposits and are commonly characterized by segregation banding (in places accompanied by crenulation) where any one of the three minerals may be dominant in individual bands. The quartz tends to be tabular and to show horse-tail fractures passing continuously across adjacent grains and containing minute inclusions. Typically, the muscovite, and less commonly the chlorite, show two periods of growth. Early distorted flakes define the schistosity, and later undeformed flakes are superposed on the foliation. Fine white mica (sericite) is also generally present, and may occur as an alteration product of K-feldspar. Thin quartz veins, and to a lesser extent carbonate veins (± quartz, ± sulphides), are frequently either discordant or concordant to the schistosity.

Within the areas of uranium mineralization, chloritization is often intense. The chlorite ranges from cryptocrystalline to flaky, and generally occurs as a partial or complete replacement of biotite and muscovite. At Jabiluka, it completely pseudomorphs garnet and amphibole, and in the tourmaline-bearing granitoid pegmatite dykes, the alkali feldspar has also been extensively chloritized. At Ranger 1, the chloritization is more restricted and less intense. The Hangingwall Sequence contains fresh garnet and K-feldspar in pelitic schist; unaltered hornblende and plagioclase occur in interbedded amphibolite. Minor K-feldspar, plagioclase, and hornblende persist in the Upper Mine Sequence. Chloritization is most intense in the ore zones, especially the Lower Mine Sequence, where feldspars in granitic pegmatites have altered to chlorite and dolerites have been completely chloritized. At Koongarra, garnet is either completely chloritized or surrounded by an outer layer of chlorite elongated parallel to the schistosity. The garnet may contain helical trails of opaque inclusions producing a snowball effect indicating rotation. Foy & Pedersen (1975) have reported feldspar in several drillholes, and have also noted the presence of partially or completely chloritized hornblende.

With the exception of Nabarlek, the uranium deposits all lie close to massive bedded dolomite and/or magnesite (Eupene, 1979). Quartz and chlorite are common in the carbonate rocks and impart a poikiloblastic texture in which chlorite parallels the foliation. With the possible exception of the Ranger 1 No. 3 orebody, carbonate does not persist into the mineralized zones. It has been suggested that at Jabiluka and Ranger 1 No. 1, the carbonate has been replaced by chert in the ore zones (Eupene *et al.*, 1975; Hegge, 1977). At Koongarra, dolomite has been intersected southwest and northeast of the mineralized zones (Foy & Pedersen, 1975); however, well banded siliceous units which are lenticular, brecciated, and up to 5 metres thick, overlap the ore zones, and may represent silicified carbonate.

Carbonaceous material, thought to be mainly graphite, occurs throughout the sequence at Jabiluka. However, it is confined to the base of the Upper Mine Sequence at Ranger 1, and is restricted to a schist overlying the primary mineralization at Koongarra. It has also been recognized recently at Nabarlek (R. Tammekand & S. Lees, pers. comm.). Typically, the carbonaceous material is both fine-grained and platey, and occurs in thin bands parallel to the

schistosity, or as a coating on shear planes. Although mineralized zones may contain carbonaceous material, there appears to be no broad relationship between the uranium mineralization aand the presence of carbon.

Accessory minerals found in the wall rocks of some or all of the deposits include sulphides (mainly pyrite), hematite, tourmaline, apatite, sphene, zircon, epidote-group minerals, and gypsum. The sulphides occur in veins and as small conformable lenses, commonly in chlorite-rich zones. Euhedral prisms of pleochroic, green tourmaline (usually less than 0.1mm long) are also common, and tend to be concentrated in muscovite and chlorite-rich zones. Larger grains of tourmaline are rare, and appear to have been derived from the tourmaline-bearing pegmatites which intrude the Cahill Formation. Apatite, hematite, epidote-group minerals, and sphene are common accessory minerals; the last two tending to concentrate within mica-rich zones. At Koongarra and Jabiluka, flaky biotite, either partially or completely altered to chlorite, commonly contains minute inclusions surrounded by metamict alteration haloes. These inclusions appear to be zircon. Rutile and gypsum are rare accessory minerals.

Ore Zone Textures

The two most striking features of the ore deposits are the tendency for mineralization to occur within zones of brecciation, and for it to be intimately associated with chlorite (Figs. 1 and 2). Though the brecciation is particularly well developed at Jabiluka, Ranger 1, and Koongarra, it also occurs at Nabarlek. The breccia fragments are typically chloritic and/or sericitic quartzite, chert (which in places is silicified carbonate), and strongly chloritized material. Occasionally, fragments are graphitic or contain hematite. The fragments are usually angular, commonly laminated as a result of segregation banding, and typically rotated. The textures and lithology indicate that the brecciation developed after the regional metamorphism, and that there was a high percentage of voids (at times reaching 50 percent by volume) between the fragments. The breccias are cemented by chlorite ± quartz ± hematite ± chert ± graphite ± sulphides ± uraninite. At Ranger 1, in particular, there is evidence that late



Figure 1. Chloritized breccia fragments (grey) cemented by chlorite and uraninite. Scale bar = 3mm.



Figure 2. Angular, rotated, and laminated fragments of quartz-muscovite-chlorite schist cemented by chlorite, uraninite, and graphite. Scale bar = 3mm. Transmitted light.

deformation has caused some breccias to be rebrecciated before being cemented a second time with chlorite. Where chlorite is the fracture-filling material it occurs as one or more textural varieties. It is often pleochroic, from colourless through varying shades of green and brown. The interference colours are commonly grey-green and blue-mauve, and the habit ranges from cryptocrystalline to flaky. Cryptocrystalline varieties sometimes appear to be more highly birefringent, suggesting that minerals other than chlorite may be present. In these instances, microprobe analyses have indicated a high K_2O content, and X-ray diffraction has confirmed the presence of fine K-mica and/or illite.

At Ranger 1, vugs and fractures which remained open at the time the breccias were initially cemented, have subsequently been infilled with euhedral quartz and chlorite, and may also contain hematite, sulphides and carbonate. In some of these cavities, a paragenetic sequence is evident: chlorite often lines the cavities, and is followed by quartz, which may be interrupted by repeated chlorite deposition. In one instance, a spherulitic intergrowth of hematite in quartz was observed to complete the sequence, indicating that the Eh-pH conditions of the depositing solutions had undergone a change with time.

The primary uranium mineralization in each deposit is uraninite. However, coffinite, brannerite and rare thucolite are known from Jabiluka (Binns *et al.*, this volume), and Eupene *et al.*, (1975) have reported minor quantities of brannerite and amorphous mixtures of uranium with titania and phosphates at Ranger 1. Thucolite has also been reported from the Ranger 1 No. 3 orebody (G.H. Taylor, *in* Eupene, 1979). Many forms of uraninite, invariably associated with the chlorite, fill interstices between the breccia fragments (Fig. 3). A disseminated form occurs as cubes 10 to 100 μm across, but these may coalesce, and form clusters, strings and massive uraninite (anhedral and subhedral grains are also common). A common feature of the disseminated form is for only the rims of the cubes to take a polish, producing an 'atoll-type' texture, suggesting replacement of the cores. At Ranger 1, in

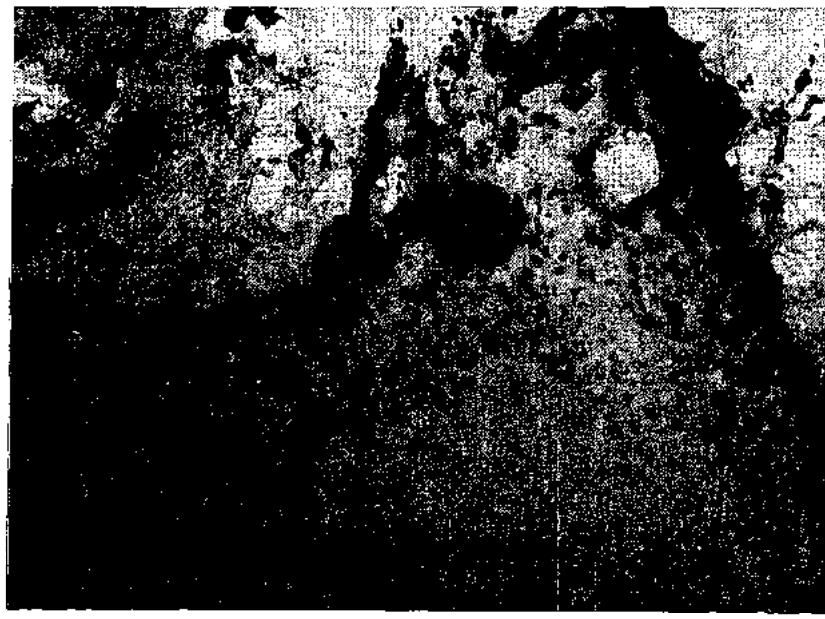


Figure 3. Breccia fragments (light grey) cemented by chlorite (medium grey) containing disseminated uraninite. Scale bar = 0.3mm. Transmitted light.

particular, uraninite cubes are found in progressive stages of replacement by chlorite from the core outwards, and in some areas are completely pseudomorphed by chlorite (Fig. 4). It is not clear why the cores of the uraninite cubes should be preferentially replaced, though this may be a function of growth zoning and/or variable oxygen content. However, it establishes direct evidence that, at different times, uranium has been remobilized.

Uraninite also forms thin veins coating foliation planes, and may occupy hairline fractures which are discordant to the foliation. In some cases, these fractures appear to postdate the earliest mineralization. Hairline fractures containing uraninite may pass from chlorite cement into adjacent grains of quartz within breccia fragments. The veins coating foliation planes frequently become braided where the uraninite becomes interstitial to flaky varieties of chlorite. Narrow lenses of uraninite are also found within and parallel to the cleavage of flaky chlorite.

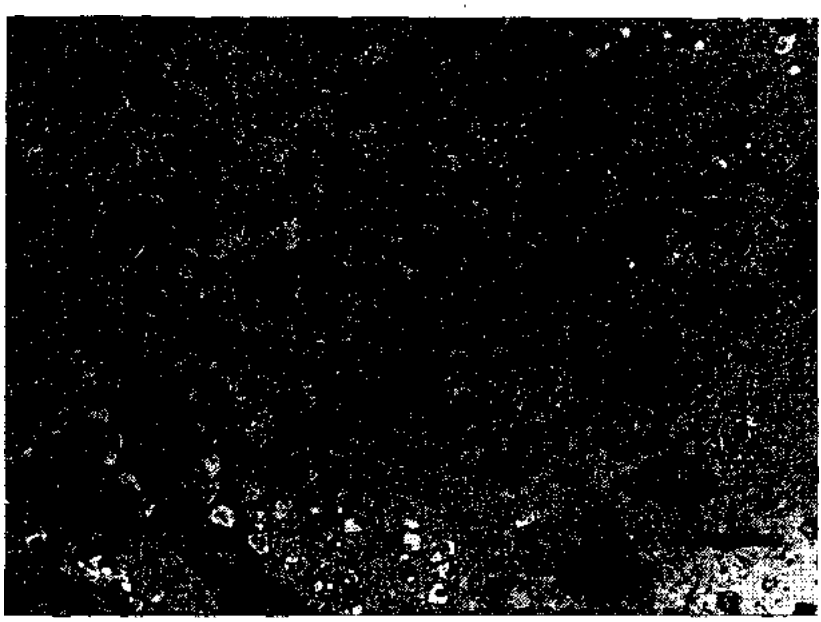


Figure 4. Progressive replacement of disseminated uraninite cubes (light grey) by chlorite at Ranger 1. Scale bar = 0.1mm. Reflected light.

Massive colloform uraninite with characteristic concentric banding and radial fractures is common at Jabiluka, Koongarra, and Nabarlek, but appears to be rare at the Ranger 1 deposit. At Jabiluka, reticulated and lacework patterns are produced in colloform uraninite where silicate inclusions are abundant. Rare massive spherules of uraninite up to 0.7mm in diameter are also found at Jabiluka.

Evidence that carbonaceous and sulphide-rich zones have produced a widespread reducing environment in which uraninite has deposited is not strong. There is no correlation between the presence of sulphur and the concentration of uranium (Ferguson & Winer, this volume; Binns *et al.*, this volume). However, at Ranger 1, there are some instances in which uraninite may have precipitated around sulphides as a result of localized reducing conditions. At Jabiluka, veins of uraninite invade brecciated pyrite enclosing isolated remnants of pyrite.

Galena is commonly disseminated as minute inclusions (usually less than 5 μm)

throughout the various forms of uraninite, and may fill fractures within the uraninite. It also occupies hairline fractures within the chlorite that cements the breccia fragments, and may occur as isolated grains up to 200 μm across. At Ranger 1, galena replaces pyrite, and at Jabiluka, it appears that cubes of galena are being replaced by chlorite. Hills & Richards (1976) have concluded that the lead in the galena is highly radiogenic.

Other common sulphides are pyrite and chalcopyrite, with pyrite usually dominant. These minerals may occur within breccia fragments and/or the cement, and are found in various forms: as isolated grains (up to 200 μm); as aggregates; as narrow lenses within and parallel to the basal cleavage of muscovite and chlorite; and as stringers which form both concordant and transgressive to the foliation. Rarely, the pyrite may be massive. As isolated grains, pyrite in particular retains its subhedral to euhedral habit where it is protected within quartz grains from the effects of fracturing. However, when exposed, the pyrite and chalcopyrite are often fractured, sometimes extensively, and the pyrite may show signs of solution. At Ranger 1, pyrite is often partially replaced by chalcopyrite and galena.

Hematite occurs throughout the ore zone at Nabarlek, and is a major constituent towards the centre of the orebody. Although the distribution of hematite and uraninite appears to be related at Nabarlek, hematite is found only in accessory (though locally high) amounts in each of the other deposits, and its distribution cannot be correlated with the concentration of uranium. Gold has been noted in all the deposits except Nabarlek. There does not, however, appear to be a positive correlation between gold and uranium (Ferguson & Winer, this volume). Traces of chalcocite and covellite have been found in all deposits, and Anthony (1975) has also reported the presence of bornite and marcasite in the Nabarlek deposit. Altaite (PbTe), melonite ($NiTe_2$), and tellurbismuth (Bi_2Te_3) have been identified from microprobe studies as rare accessory minerals at Jabiluka, confirming earlier observations reported by Hegge (1977).

FRACTURE FILLING CHLORITE AND ITS POSSIBLE GENETIC SIGNIFICANCE

The significance of the association between the chlorite cementing breccia fragments and the uranium mineralization, and its relevance to ore genesis, has been investigated by examining the varieties of chlorite within and outside the mineralized zones. Chlorite is the only mineral which is common, in quantity, to all deposits.

Methods

Quantitative electron microprobe analyses of chlorite were made using an energy dispersive X-ray spectrometer. The technique that was followed has been published by Reed & Ware (1975).

X-ray diffractometer traces were recorded at Amdel and BMR for a selection of breccias from each of the four deposits. Traces were made for whole-rock samples using either copper or cobalt radiation on finely powdered material mounted in specimen spinners. A portion of this powder was also dispersed in water and allowed to settle before pipetting off the -2 μm material held in suspension. It was anticipated that the -2 μm fraction would largely contain the chlorite filling the interstices between breccia fragments. The mineralogy of this -2 μm or 'clay' size fraction was investigated by diffractometry using oriented preparations, which had been either glycolated or saturated with Mg^{2+} ions, and subsequently heated.

A microanalytical spectrophotometric technique was used to determine the Fe^{2+} and total Fe content of chlorite cementing breccia fragments in mineralized and unmineralized breccias. The technique for Fe^{2+} has been reported by Kiss (1974), and involves the addition of a suitable Fe chromogen to a dissolving acid mixture, such that, as the Fe^{2+} is released from the silicate mineral, it is complexed in situ to form a stable, coloured Fe^{2+} complex. Total Fe was determined after the conversion of all Fe in the sample to Fe^{2+}. The Fe^{3+} content was obtained by difference.

Where reported, uranium has been analysed by X-ray fluorescence spectrometry.

Results

The chlorite filling intestices between breccia fragments consists of one or more textural varieties. These varieties may range from cryptocrystalline to flaky. They are often pleochroic, from colourless through varying shades of green and brown, and exhibit a range of interference colours, including the anomalous blue so characteristic of chlorite. The paragenesis for this fracture filling chlorite is complex and open to interpretation. However, there are instances where a later generation of chlorite occasionally crosscuts earlier formed fracture filling chlorite. At Ranger 1, in particular, vugs and fractures, which remained open at the time the breccias were initially cemented, have subsequently been filled with chlorite which has deposited from solution and developed a growth zoning.

The results for more than 350 electron microprobe analyses indicate a wide range in composition for the varieties of chlorite cementing breccia fragments. Those analyses in which the $Na_2O + K_2O + CaO$ content exceeds one percent have been rejected, since there is no

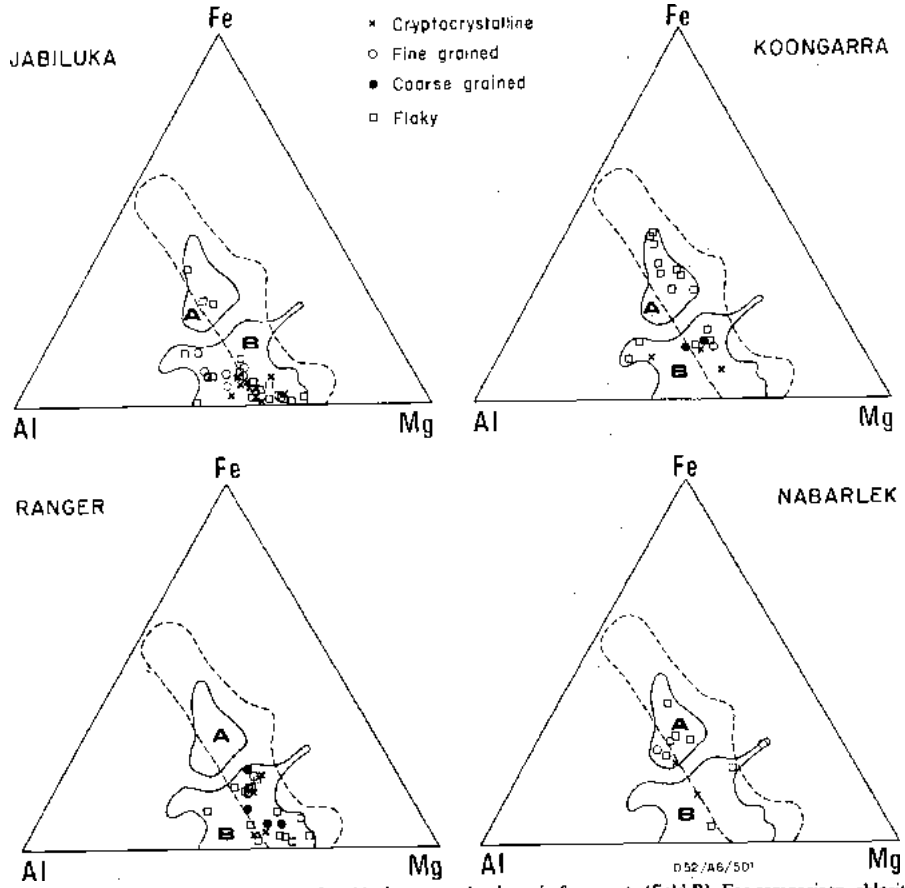


Figure 5. Fe-Al-Mg variation diagram for chlorite cementing breccia fragments (field B). For comparison, chlorite formed by the replacement of biotite plots within field A, and chlorites tabulated by Deer *et al.* (1962) plot within the dashed field.

	1	2	3	4	5
SiO_2	33.22	33.03	31.33	30.33	25.11
Al_2O_3	21.46	21.52	21.27	20.04	21.16
TiO_2	0.00	0.00	0.00	0.00	0.12
FeO*	4.84	7.81	3.95	12.46	28.07
MnO	0.00	0.00	0.00	0.00	0.11
MgO	24.62	21.57	27.53	22.67	12.09
CaO	0.09	0.00	0.00	0.00	0.00
K_2O	0.00	0.17	0.00	0.17	0.00
Na_2O	0.20	0.00	0.00	0.21	0.37
TOTAL	84.43	84.10	84.08	85.88	87.03
$Mg/_{Mg+Fe}$	0.90	0.83	0.93	0.76	0.43

* total Fe expressed as FeO

1. colourless flaky chlorite - Jabiluka

$$(Al_{1.64}\ Fe^{2+}_{0.39}\ Mg_{3.53})\ (Si_{3.20}\ Al_{0.80})\ O_{10}\ (OH)_8$$

2. green coarse-grained chlorite - Ranger I

$$(Al_{1.73}\ Fe^{2+}_{0.54}\ Mg_{3.15})\ (Si_{3.24}\ Al_{0.76})\ O_{10}\ (OH)_8$$

3. colourless fine-grained chlorite - Jabiluka

$$(Al_{1.46}\ Fe^{2+}_{0.32}\ Mg_{3.97})\ (Si_{3.03}\ Al_{0.97})\ O_{10}\ (OH)_8$$

4. green cryptocrystalline chlorite - Nabarlek

$$(Al_{1.37}\ Fe^{2+}_{1.04}\ Mg_{3.36})\ (Si_{3.02}\ Al_{0.98})\ O_{10}\ (OH)_8$$

5. green-brown pleochroic flaky chlorite alteration of biotite - Koongarra

$$(Al_{1.40}\ Ti_{0.01}\ Fe^{2+}_{2.53}\ Mg_{1.94}\ Mn^{2+}_{0.01})(Si_{2.71}\ Al_{1.29})\ O_{10}\ (OH)_8$$

Table 1. Microprobe analyses (wt. percent) of typical chlorites with corresponding structural formulas.

place in the chlorite structure for cations as large as Na^+, K^+, and Ca^{2+}, and their presence, in quantity, suggests interlayering and/or admixture with micas, clays, or other silicates. The late stage vug and open fracture filling chlorite exhibits no systematic change in composition from the edge of a vug or fracture to its centre, despite the well developed growth zoning. The Si content shows little variation, while changes in the Mg, Fe, and Al content of the chlorite are unpredictable.

Table 1 presents some typical analyses for the varieties of chlorite found cementing breccias in the four deposits. For comparison, an analysis for chlorite replacing biotite (analysis 5) has been included. Structural formulas have also been given and were calculated on the basis of the theoretical O(OH) content of the unit cell for chlorite. Typically, the fracture filling chlorites are aluminous and magnesium rich. They generally have Mg/Mg + Fe ratios between 0.70 and 0.90, give consistently low totals (compare analyses 1-4 with analysis 5), and do not conform to the ideal structural formula. Some of these features are illustrated in figure 5, where analyses for the varieties of fracture filling chlorite plot within a restricted field (B). For comparison, field A encloses predominantly flaky chlorites which appear to replace biotite and possibly muscovite, and the dashed field encloses a variety of chlorites tabulated by Deer *et al.*, (1962). The field B or fracture filling chlorite is predominantly penninite and clinochlore, according to the nomenclature of Hey (1954).

In figure 6, structural formulas have been used to illustrate the relationship between the formula positions occupied by Al in octahedral coordination and those occupied by Al in tetrahedral coordination. The 1:1 relation between tetrahedral and octahedral Al is represented by the diagonal line. The dashed field encloses points for about 150 chlorite analyses drawn from the literature and plotted by Foster (1962). Although these analyses plot near the 1:1 relation, Foster (1962) found that in most of the chlorites represented, octahedral Al was less than tetrahedral Al. In comparison, the fracture filling chlorites from the Alligator Rivers deposits contain a clear excess of Al in octahedral sites. The inclusion of Fe^{3+} in an analysis, and subsequent recalculation of the structural formula, has the effect of slightly displacing points toward the tetrahedral field. However, the conversion of Fe^{2+} entirely to Fe^{3+} in microprobe analyses of even the most Fe rich chlorites from the Alligator Rivers deposits, is insufficient to cause significant changes to the distribution of points in figure 6. It cannot be determined whether this excess of octahedral Al occupies sites in the brucite layer or the talc layer of the chlorite structure. However, X-ray diffraction traces suggest that gibbsitic material is present occupying interlayer positions in chlorite and minor vermiculite. The fact that many chlorites contain more octahedral Al than is required to balance the negative tetrahedral charge indicates that the chlorite structure can accommodate an excess of trivalent octahedral cations.

Attempts to characterize those chlorites which are genetically related to the mineralization and distinguish them from unrelated generations of chlorite met with limited success. The colour, grainsize, and major and minor element chemistry are not distinctive. However, there is a tendency for the Fe^{2+}/Fe^{3+} ratio of chlorites to decrease with increasing uranium content in whole-rock samples (Fig. 7).

Interpretation

While the textural relations and composition of the fracture filling chlorites do not give a clear indication of their origin, it is possible to put forward an interpretation of the origin and significance of the chlorite in terms of ore genesis. Clearly, it is not the only interpretation, but it is the one favoured by the authors.

Although of limited extent, the X-ray diffraction traces have indicated the presence, in some samples, of poorly crystalline, true clay chlorite and illite-like mica. They have also suggested that gibbsitic material is present and may have accumulated in interlayer positions in chlorite and minor vermiculite. It should be noted that gibbsite commonly forms under

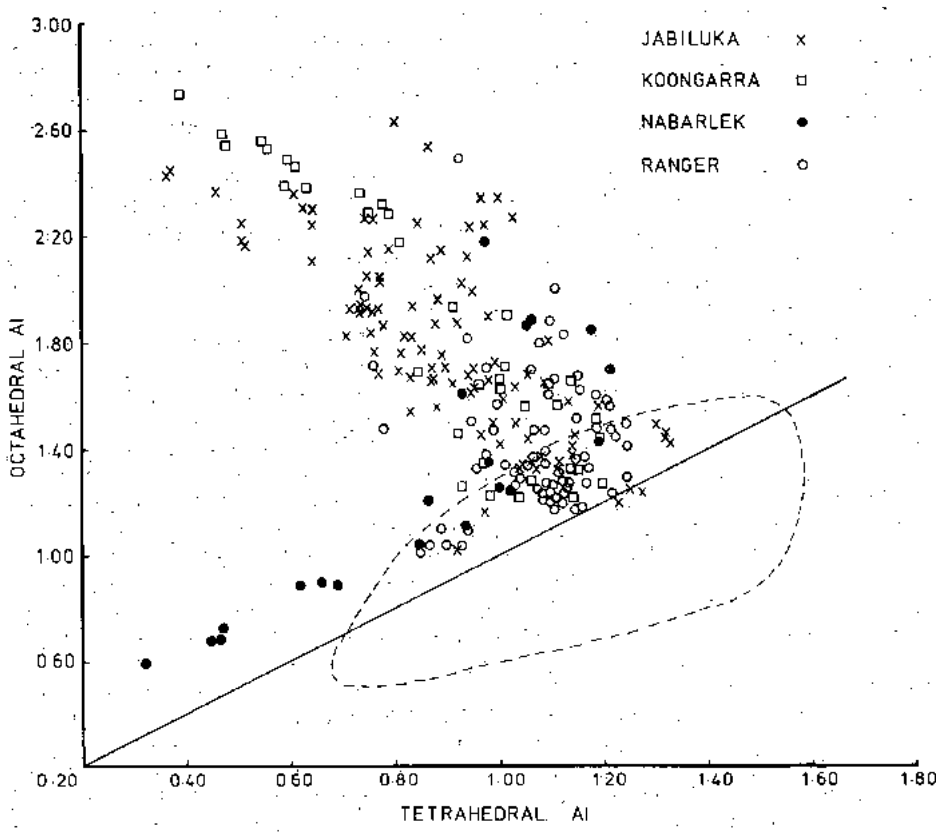


Figure 6. Relation between tetrahedral Al and octahedral Al in chlorite cementing breccia fragments.

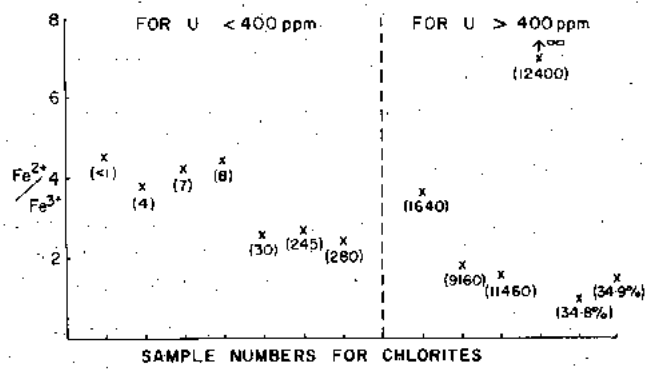


Figure 7. Relationship between the Fe^{2+}/Fe^{3+} ratio of chlorite cementing breccia fragments and the corresponding whole-rock uranium content (U given in ppm in parentheses unless otherwise indicated).

conditions of prolonged leaching and weathering. Hegge (1977) has reported kaolinite and montmorillonite associated with the uranium mineralization at Jabiluka, and has observed sepiolite (a white, fibrous, magnesian clay mineral) in Main Mine Series equivalent dolomite units between Jabiluka One and Two.

It is difficult to assess whether these other minerals associated with the chlorite are of recent origin or whether they existed within the ore zones at the time of the main mineralizing event. It is equally difficult to evaluate whether the chlorite was deposited from solution, introduced to the ore zones as chlorite, or formed from clay minerals during diagenesis. The concentration of uranium by clays has been widely canvassed in the literature (e.g. Keys & Dodd, 1958; Katayama, 1958; Doi *et al.*, 1975) and its importance in terms of ore genesis has been demonstrated experimentally (Muto *et al.*, 1965; Giblin, this volume). If clay minerals were originally present, and concentrated uranium through adsorption, as the model of Ferguson *et al.*, (this volume) would suggest, it is not surprising to find little evidence now of their prior existence. The formation of chlorite from clay minerals during diagenesis is well documented (e.g. Rowsell & De Swardt, 1976; Dunoyer de Segonzac, 1970) and would virtually remove all trace of the original clay mineralogy. The heat dissipated by an intrusion, such as the Oenpelli Dolerite or Nungbalgarri Volcanic Member, would also facilitate the formation of chlorite from clays.

Whether adsorption or some other mechanism is invoked for the concentration of uranium to ore grade levels, it is clear that the fracture filling chlorite, or the minerals from which it formed, provide a key to understanding the genesis of these deposits. Chlorite is the only mineral which is common, in quantity, to all deposits, and wherever primary uraninite is found, it is intimately associated with chlorite. The tendency for the Fe^{2+}/Fe^{3+} ratio of chlorites to decrease with increasing uranium content in whole-rock samples (Fig. 7), suggests that redox reactions involving Fe in the chlorite may lead to uranium deposition. If uranium in the form of uranyl complexes were absorbed onto clays and/or chlorite, the reduction of these complexes to give uraninite may have been facilitated by the oxidation of Fe^{2+} to Fe^{3+}.

ACKNOWLEDGEMENTS

We are indebted to Geopeko Ltd., Noranda Australia Ltd., Pancontinental Mining Ltd. and Queensland Mines Ltd. for allowing us to sample drillcore from each deposit.

We also wish to thank N.G. Ware and E. Kiss from the Research School of Earth Sciences, Australian National University for their assistance with the analytical work, and J.T. Nash, J.F. Truswell, and W.B. Dallwitz for their constructive comments in reviewing the manuscript.

Published with the permission of the Director, Bureau of Mineral Resources, Geology & Geophysics, Canberra, A.C.T.

REFERENCES

Anthony, P.J., 1975: Nabarlek Uranium Deposit *in* (ed. C.L. Knight) *Economic Geology of Australia and Papua New Guinea, Australas. Inst. Min. Metall., Monograph Series No. 5, 1. Metals*, 304-308.

Binns, R.A., McAndrew, J., & Sun, S-S., this volume: Origin of uranium mineralization at Jabiluka. *Proceedings of the International Uranium Symposium on the Pine Creek Geosyncline.*

Deer, W.A., Howie, R.A., & Zussman, J., 1962: *Rock-Forming Minerals. Vol. 3: Sheet Silicates.* John Wiley & Sons Inc., New York.

Doi, K., Hirono, S., & Sakamaki, Y., 1975: Uranium mineralization by ground water in sedimentary rocks, Japan. *Econ. Geol. 70,* 628-646.

Dunoyer de Segonzac, G., 1970: The transformation of clay minerals during diagenesis and low grade metamorphism: a review *Sedimentology, 15,* 281-347.

Eupene, G.S., 1979: Stratigraphic, structural and temporal control of mineralization in the Alligator Rivers uranium province, Northern Territory, Australia *in* (ed. J.D. Ridge) *Proceedings of the Fifth International Symposium on the Genesis of Ore Deposits, Snowbird, Utah, August 1978* (in press).

Eupene, G.S., Fee, P.H., & Colville, R.G., 1975: Ranger One Uranium Deposits *in* (ed. C.L. Knight) *Economic Geology of Australia and Papua New Guinea, Australas. Inst. Min. Metall., Monograph Series No. 5, 1. Metals*, 308-317.

Ferguson, John, this volume: Metamorphism in the Pine Creek Geosyncline and its bearing on stratigraphic correlations. *Proceedings of the International Uranium Symposium on the Pine Creek Geosyncline.*

Ferguson, John, Ewers, G.R., & Donnelly, T.H., this volume: Model for the development of economic uranium mineralization in the Alligator Rivers Uranium Field. *Proceedings of the International Uranium Symposium on the Pine Creek Geosyncline.*

Ferguson, John & Needham, R.S., 1978: The Zamu Dolerite: a Lower Proterozoic pre-orogenic continental tholeiitic suite from the Northern Territory, Australia. *J. geol. Soc. Aust., 25,* 309-322.

Ferguson, John & Winer, P., this volume: Pine Creek Geosyncline: Statistical treatment of whole-rock chemical data. *Proceedings of the International Uranium Symposium on the Pine Creek Geosyncline.*

Foster, M.D., 1962: Interpretation of the composition and a classification of the chlorites. *Prof. Pap. U.S. geol. Surv., 414A.*

Foy, M.F., & Pedersen, C.P., 1975: Koongarra Uranium Deposit *in* (ed. C.L. Knight) *Economic Geology of Australia and Papua New Guinea, Australas. Inst. Min. Metall., Monograph Series No. 5, 1. Metals,* 317-321.

Giblin, Angela, this volume: Experiments on the role of clay adsorption in genesis of uranium ores. *Proceedings of the International Uranium Symposium on the Pine Creek Geosyncline.*

Hegge, M.R., 1977: Geologic setting and relevant exploration features of the Jabiluka uranium deposits. *Proc. Australas. Inst. Min. Metall., 264,* 19-32.

Hegge, M.R., Mosher, D.V., Eupene, G.S. & Anthony, P.J., this volume: Geologic setting and comparative review of the East Alligator uranium deposits and prospects. *Proceedings of the International Uranium Symposium on the Pine Creek Geosyncline.*

Hey, M.H., 1954: A new review of the chlorites. *Mineralog. Mag., 30,* 277-292.

Hills, J.H., & Richards, J.R., 1976: Pitchblende and galena ages in the Alligator Rivers region, Northern Territory, Australia. *Miner. Deposita, 11,* 133-154.

Katayama, N., 1960: Genesis of uranium deposits in sedimentary rocks. Part 15 -- Genetic Problems of Uranium and Thorium Deposits. *21st Int. geol. Congr. Copenhagen,* 7-14.

Keys, W.S., & Dodd, P.H., 1958: Lithofacies of continental sedimentary rocks related to significant uranium deposits in the Western United States. *Proceedings of the Second United Nations International Conference on Peaceful Uses of Atomic Energy, Geneva, 2,* 367-378.

Kiss, E., 1974: Synthesis of a sulphonated ferroin reagent for chelating iron (II) in strong acid — spectrophotometric determination of the oxidation state of iron in silicates. *Analytica chim. Acta, 72,* 127-144.

Muto, T., Hirono, S., & Kurata, H., 1965: Some aspects of fixation of uranium from natural waters. *Mining Geol. (Tokyo), 15(74),* 287-298.

Needham, R.S., Crick, I.H., & Stuart-Smith, P.G., this volume: Regional geology of the Pine Creek Geosyncline. *Proceedings of the International Uranium Symposium on the Pine Creek Geosyncline.*

Needham, R.S., & Stuart-Smith, P.G., 1976: The Cahill Formation — host to uranium deposits in the Alligator Rivers Uranium Field, Australia. *BMR J. Aust. Geol. Geophys., 1,* 321-333.

Needham, R.S., & Stuart-Smith, P.G., this volume: Geology of the Alligator Rivers Uranium Field. *Proceedings of the International Uranium Symposium on the Pine Creek Geosyncline.*

Reed, S.J.B., & Ware, N.G., 1975: Quantitative electron microprobe analysis of silicates using energy dispersive X-ray spectrometry. *J. Petrology, 16,* 499-519.

Rowsell, D.M., & De Swardt, A.M.J., 1976: Diagenesis in Cape and Karroo sediments, South Africa, and its bearing on their hydrocarbon potential. *Trans. geol. Soc. S. Africa, 79,* 81-145.

FLUID INCLUSION AND OXYGEN ISOTOPE STUDIES OF THE NABARLEK AND JABILUKA URANIUM DEPOSITS, NORTHERN TERRITORY, AUSTRALIA

Peter J.M. Ypma and Kazuo Fuzikawa

Department of Economic Geology, University of Adelaide, P.O. Box 498, Adelaide S.A., 5000, Australia.

ABSTRACT

Fluid inclusion and oxygen isotope studies of silicates and carbonates spatially associated with pitchblende and uraninite deposits of Nabarlek and Jabiluka indicate the following limitations on genetic models for these deposits:

1) Late metamorphic fluids with NaCl and high density CO_2 occur as remnants in pockets of quartz in the ore zone, but are more common in the non-retrograde amphibolite facies metamorphic sequence of the Lower Cahill Formation. Their homogenization temperatures are well above 350°C; decrepitation is very common; entrapment pressures exceed 1200kg/cm².
2) Highly specialized fluid inclusions in quartz and carbonates seem to be restricted to the immediate host rock of the deposits.
3) Heterogeneous entrapment of chlorite, sericite and pitchblende in fluid inclusions in quartz point to contemporaneity between alteration products of host rock, uranous-oxide mineralization, and fluid inclusions.
4) The fluids were heterogenous as they feature the mixing of a very saline brine with a more dilute carbon dioxide-rich fluid, both of which occur in the same growth zones of quartz crystals coeval with the mineralization.
5) As a result of mixing, exsolution of CO_2 occurred. The brines vary in salinity with compositions of up to 20-30 wt% $CaCl_2$ plus 5-10 wt% $MgCl_2$ plus 10-20 wt% NaCl, and minor amounts of KCl, and $FeCl_2$. The brines are rarely over-saturated at 25°C. Homogenization temperatures vary between 160° and 110°C, featuring a decrease in temperature of a quartz I-pitchblende-quartz II paragenesis. The decrease in temperature is accompanied by an increase in salinity. The small vapour-phase of the brine inclusions may contain CH_4.
6) Vapour-rich inclusions contain medium density CO_2 and CH_4 with up to 45 vol.% CH_4 in the CO_2-rich phase. Salinities of these fluids are generally less than those of the brines. Entrapment pressures were probably in the 250-350kg/cm² range.
7) Oxygen isotope data of material of known homogenization temperature points to water of meteoric origin with $\delta^{18}O$ values between -5 and +1 per mil.

The data are compatible with a genetic model in which uranium deposition occurred at the confluence of a dilute carbon dioxide-rich phase of meteoric origin with a hypersaline brine causing the exsolution of CO_2 and CH_4. This event could have effected uranium precipitation as: a) uranyl carbonates carried by the CO_2-rich solutions were decomposed; b) uranyl compounds adsorbed to clay minerals were desorbed, and c) the pH decreased at the contact with the more acid hypersaline brine. Fluid inclusions point to numerous salinity reversals and hence a multiple process of uranyl adsorption, desorption, reduction and precipitation, presumably lasting for many millions of years where the uranium concentration itself formed the thermal drive for circulating fluids.

INTRODUCTION

We lack a basic understanding of the solutions producing the uranium deposits of the Alligator Rivers Uranium Field (ARUF). Several theories have been proposed ranging from syngenetic (Crick & Muir, this volume), epigenetic hydrothermal (Gulson & Mizon, this volume), epigenetic metamorphogenic (Binns, McAndrew & Sun, this volume), surficial origin (Ferguson *et al.*, this volume), and mobilization by evaporite deposits (Crick & Muir, this volume). As for a precipitation mechanism, we do not seem to find much beyond the presence of graphite in some ore-bearing and intra-formational strata, and pre-uranium sulphides, none of which reducing factors are common throughout all ore bodies.

This study was initiated with the aim of obtaining direct fluid inclusion evidence of the solution transport and precipitation of uranium. The following geological parameters are important in considering the significance of fluid inclusion data.

The host rock of the mineralization is the Lower Cahill Formation which can be

bracketed between the 2470 m.y. Archaean basement age and an 1800 m.y. regional metamorphic age (Page *et al.*, this volume). This formation consists largely of iron-rich and pelitic sediment with intercalations of magnesites and dolomites featuring pseudomorphs of halite and gypsum (Crick & Muir, this volume), carbonaceous shales, now transformed to graphite schists and more siliceous layers. Pre-metamorphic dolerite sills (Zamu Dolerite) also occur in the Cahill Formation.

Metamorphism (Ferguson, this volume) reached amphibolite facies in the Jabiluka-Ranger area, and granulite facies in the Nimbuwah Complex, east of Jabiluka, which possibly does not extend into the Nabarlek area. Pelitic, arkosic and quartzose rocks of the Kakadu Group underlie the Cahill Formation at Jabiluka and form an integral part of the Nimbuwah migmatites. As the outcrop of the Cahill Formation at Nabarlek is very restricted it is not known whether the host rock of the Nabarlek deposit belongs to the Cahill Formation. Characteristic markers such as the Mg-rich carbonates have not been observed, but could easily be present.

Metamorphism produced garnet, biotite and staurolite schists in the ferriferous members of the Cahill Formation and muscovite gneisses in the pelitic members at Jabiluka and muscovite schists, amphibolites, and mica gneisses at Nabarlek. The proximity to the migmatitic Nimbuwah Complex appears from crosscutting pegmatites and pegmatoids or para-conformable bodies of felsic composition. Elsewhere anatectic and diapiric granites appear, possibly contemporaneous with the Edith River Volcanics (1760 m.y.; Needham *et al.*, this volume).

Deformation of the Cahill Formation is multiphase, the last stage being coeval with the major metamorphic event. The results are tight isoclinal folds, with attenuated limbs and a

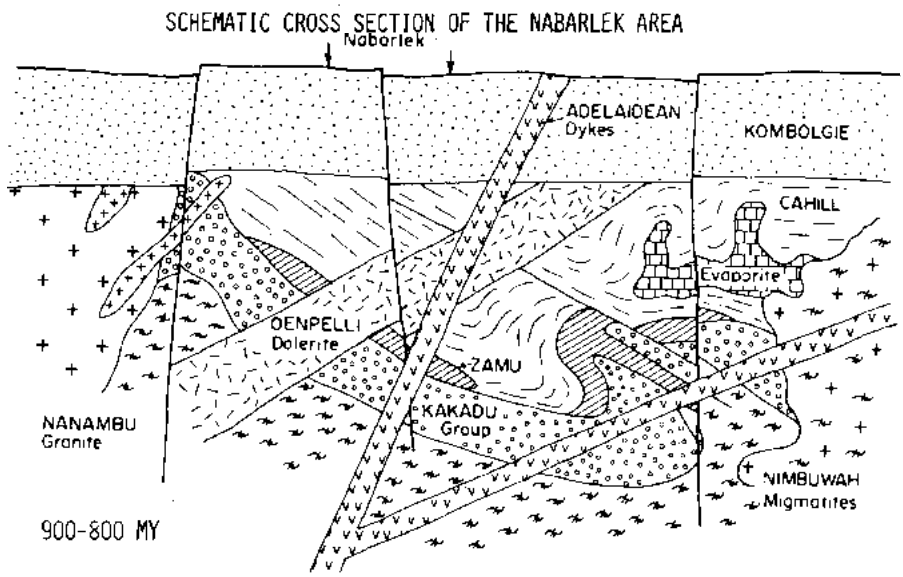


Figure 1. Schematic cross section (W-E) of the Nabarlek area at the termination of U-mineralization and start of Upper Proterozoic (Adelaidean) sedimentation.

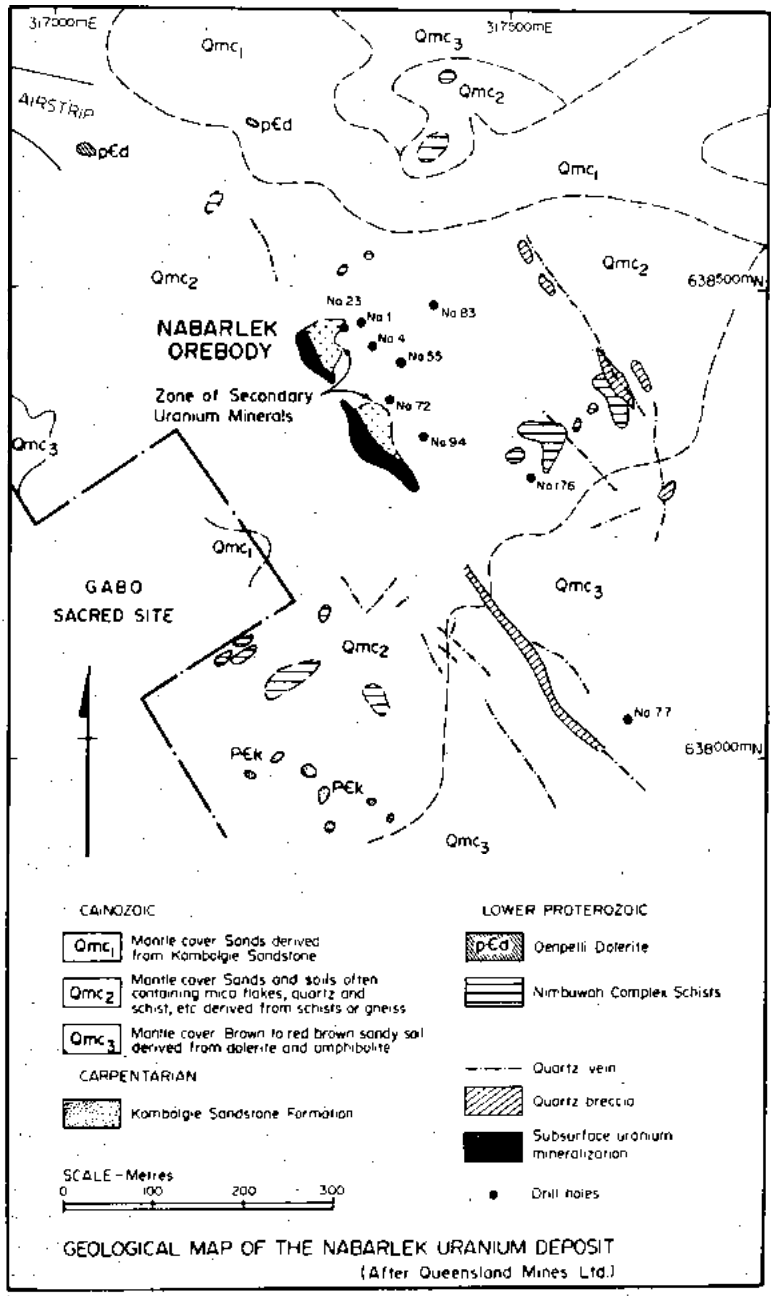


Figure 2. Geological outcrop map of the Nabarlek area. Drill cores which have been sampled are indicated.

scarcity of fold hinges, which renders the reconstruction of local stratigraphy very difficult. Emplacement of the Oenpelli Dolerite sills at 1688 m.y. is post-metamorphic and before an erosional interval of Middle Proterozoic age. The whole Nabarlek orebody is situated above the Oenpelli Dolerite. Middle Proterozoic Kombolgie Sandstone has been deposited on this erosional surface. The regolith of the palaeosurface is restricted to a few metres. Intraformational volcanics have established an age of about 1650 m.y. (Page *et al.*, this volume) for the Kombolgie Sandstone which is the basal formation of Middle Proterozoic (Carpentarian) sedimentation. Phonolite dykes of 1316 m.y. (Needham *et al.*, this volume) mark the last known Proterozoic intrusive event in the region. Upper Proterozoic (Adelaidean) sand and siltstones covered the Middle Proterozoic (Carpentarian) formations. Possible mineralization ages as indicated by isotope data on micas are about 1600 m.y. (Page *et al.*, this volume); ~1340 m.y. on chalcopyrite (Gulson & Mizon, this volume) and U-Pb ages of ~900 m.y. (Hills & Richards, 1976).

LOCAL GEOLOGY AT NABARLEK

The local geology for the Jabiluka deposit is extensively dealt within this volume (Hegge *et al.*, this volume), and need not be discussed here. A more complete account of the geology at Nabarlek is contained in Anthony (1975).

A schematic cross-section of the Nabarlek area is in figure 1, which gives the geological development up to the stage of faulting of the Kombolgie Formation. Several generalizations have been made in this diagram which are not necessarily true for the immediate Nabarlek area. The following qualifying statements have to be made:

1) a distinct Kakadu Group has not been unambiguously identified; it is more likely that the Kakadu Group is highly migmatized and has become an indistinguishable part of the Nimbuwah Complex;
2) there are no known occurrences of Nanambu granite near Nabarlek;
3) carbonates and evaporites are common for the Jabiluka area but are not known from the Nabarlek area;
4) post-Kombolgie dykes are known in a 60km radius of Nabarlek but not near the deposit.

Figure 2 gives drillhole locations at Nabarlek which have been sampled in this study. It can be seen that outcrop is very sparse and does not allow correlation with rock units of the Cahill Formation at Jabiluka. However, there are some indications that the host rock at Nabarlek is the Cahill Formation because of its pelitic and ferriginous nature and the recent identification of graphite schists at both ends of the north lens (pers. comm., P. Anthony, Queensland Mines).

A WSW-ENE cross-section of the northern part of the orebody is in figure 3. A conformable attitude of orebody with regard to host rock layering is only indicated by parallel amphibolite bands which have been correlated with the Zamu Dolerite of the ARUF. In detail, mica and chlorite schists are closely interwoven and cannot easily be correlated between drillholes. The brecciated hematitic ore zone stands out as a dominant ore controlling structure, which grades into hematitic quartz veins and breccias along strike. Several features which run parallel to the ore-bearing structure are seen in figure 3.

The Nabarlek orebody is underlain by the Oenpelli Dolerite sill, which is locally about 200m thick. Zamu Dolerite amphibolites are more intensively altered than the Oenpelli Dolerite, whose alteration is restricted to its margins and numerous cross-cutting features. Deep vertical holes reaching below the Oenpelli Dolerite sill did not reveal any mineralization. Samples for fluid inclusion and oxygen isotope studies have been obtained from retrograde schists below the Oenpelli Dolerite.

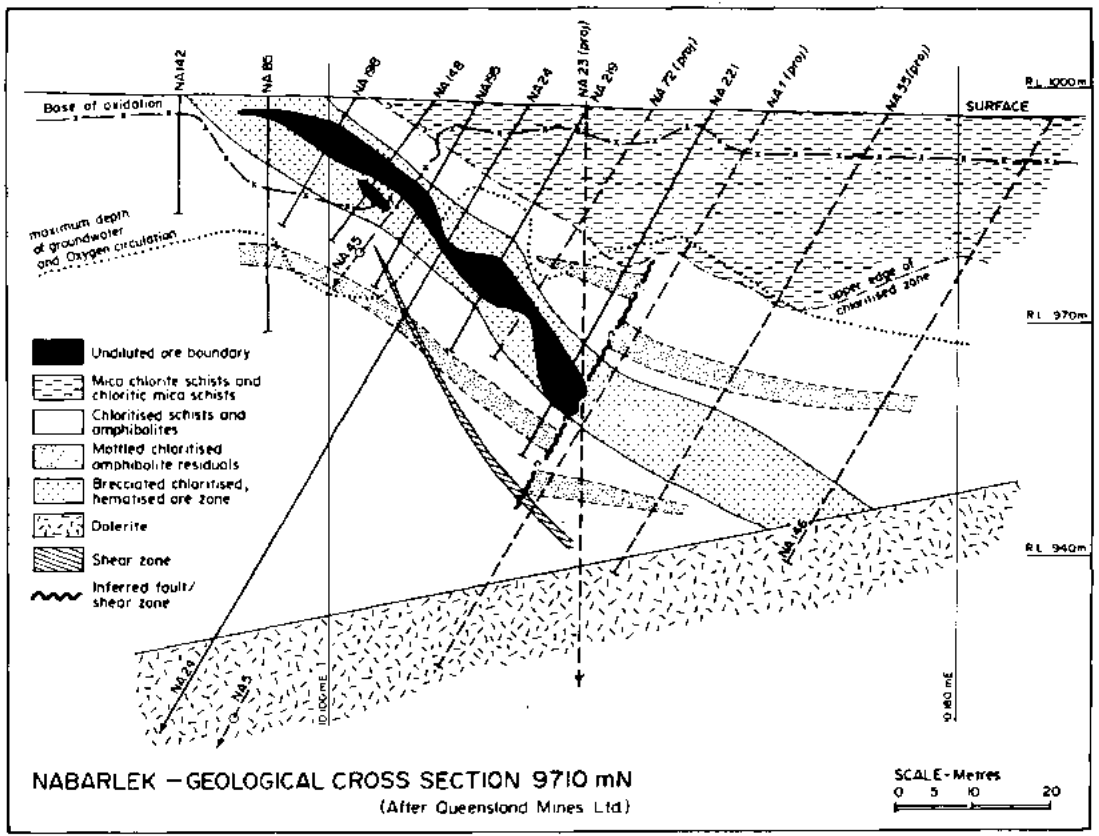


Figure 3. Cross section (WSW-ENE) through Nabarlek orebody with projection of drill holes.

FLUID INCLUSION STUDIES

This study represents the results of some 1500 heating tests and 1000 cooling tests on fluid inclusions from Nabarlek, and 600 heating tests and 600 cooling tests on material from Jabiluka Two. About 30 samples from Nabarlek were tested with the scanning electron microscope (SEM) and some 15 from Jabiluka, with the purpose of identifying daughter minerals and evaporation residues from fluid inclusions according to a technique described by Metzger *et al.*, (1977).

One of the main problems and limitations associated with a study of this kind is the selection of material. Obtaining suitable fluid inclusion material from drusy veins and euhedral crystals, is not difficult. However, the significance of such late-stage material within the contexts of the mineralization is generally very limited.

In this study we were mainly interested in transparent minerals closely associated with the uranium mineralization. The latter, as such, is not easily defined, as repeated mobilizations have taken place and most of the disseminated uranium mineralization is devoid of any coeval and transparent gangue material. Moreover, recognition of paragenetical sequences is very difficult for both Jabiluka and Nabarlek. A generalized paragenetic scheme for Nabarlek appears to be as follows, in order of decreasing age:

1) Quartz I, dolomite
2) Pitchblende I, hematite, chlorite
3) Quartz II, chlorite-sericite
4) Pitchblende II, goethite, calcite.

Figure 4 shows the paragenetic relationship between pitchblende and Quartz II.

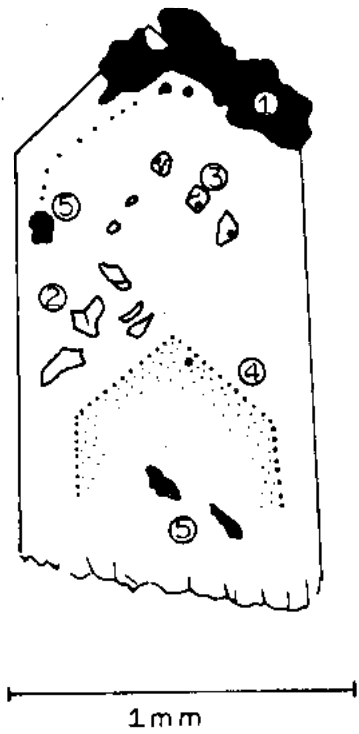


Figure 4. Quartz II from Nabarlek Na 77, -58.05m. Primary solid inclusion of pitchblende (5) formed during growth of crystal. Zone of primary two phases (brine + vapour) inclusions (4). Zone of coeval two phase (2) and three phase (brine + vapour + heterogeneous daughter mineral) inclusions (3). Late stage pitchblende (1). Decreasing temperature of the sequence 4→3+2 indicated by fluid inclusion homogenization temperature (120°→100°C)

The association between fluid inclusions and the deposition of uranous-oxides has been studied by autoradiography. About 30 thin sections of quartz containing fluid inclusions were investigated by this method. An unambiguous relationship between fluids and pitchblende or uraninite has been established in six cases. In four of them fluids were trapped on solid inclusions of uranous-oxides in quartz, others showed uraninite as solid cubes in a trail of fluid inclusions in quartz. The lack of success in other samples is due to the fact that 12 microns of quartz effectively absorbs all α-radiation.

Numerous cases of primary trapment of fluids on solid inclusions such as chlorite and dolomite did establish the significance of the fluids in terms of mineralization and alteration. Both at Nabarlek and Jabiluka two distinct generations of fluid inclusions can be recognised in quartz.

1) One is associated with regional metamorphic fluids and occurs in quartz pods, quartzose strata in gneisses and schists and quartz veinlets in the Nanambu and Nimbuwah basement rocks, and their metamorphic mantle.

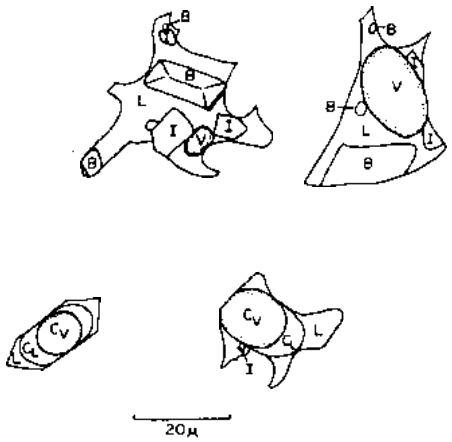


Figure 5. Fluid inclusions in quartz of Nabarlek Na 77, -111.4m. Separation of fluids into a saline brine with NaCl (I), and birefringent daughter minerals (B) and CO_2 rich fluids with liquid CO_2 (C_L) and CO_2 rich vapour (C_V) and brine (L). Temperature of observation is 25°C.

2) Another is associated with vein quartz, breccias and open space fillings.

In samples where both generations occur, the first one always predates the second.

Metamorphogenic quartz

The first one is characterized by the co-occurrence of CO_2-rich inclusions, and complex brines with numerous daughter minerals (Fig. 5). The CO_2-rich inclusions feature a liquid CO_2-rich phase and a CO_2 vapour-phase which disappears between 25° and 31°C; this applies to both Nabarlek and Jabiluka Two. The CO_2-rich phase melts at between -65° and -56°C which points to essentially pure CO_2 (which prevails) to 40 mol.% CH_4. The brines of the CO_2-rich inclusions also have significant salinities as indicated by melting temperatures of ice between -22° to -15°C.

The inclusions with numerous daughter minerals occur in the same field as the CO_2-rich ones. Most show signs of necking down and fracturing which probably did separate brine and daughter minerals from CO_2-rich fluids. Those brines which have apparently become separated have small vapour bubbles which disappear between 140° and 160°C. Decrepitation may take place before complete disappearance of the vapour-phase. None of the inclusions with daughter minerals could be made to homogenize, decrepitation between 300° and 350°C destroyed the content well before the dissolution of daughter minerals. The following products have been identified with the SEM and its Energy Dispersive Analysis of X-rays (EDAX):

NaCl
KCl
$CaCl_2$ + hydrates
Fe-chloride
Mg,Ca,Fe carbonates (ankerite, dolomite, calcite)
Zn,Na,Fe sulphates
Ca-silicates.

Fluid inclusions of metamorphogenic quartz outside the chlorite alteration envelope such as quartz pods in Nanambu granites and Nimbuwah migmaties, show a more regular pattern of inclusions with NaCl daughters in the same inclusion containing high density CO_2. Complete homogenization could not be achieved in most of these because of decrepitation but has been estimated to occur between 450° and 600°C. The fluids have most likely been associated with the waning stages of amphibolite facies metamorphism.

Metamorphogenic quartz from the chlorite-rich orebody envelope - as described above - is commonly disrupted and shows a more complicated pattern. These quartz masses may also contain pseudo-secondary and secondary inclusions belonging to the vein quartz. Disappearance of a vapour-phase between 140° and 160°C also points to disruption of these earlier inclusions at the quartz vein-stage. There are no differences between the metamorphogenic inclusions from Nabarlek or Jabiluka.

Homogeneity of the saline brine and dense CO_2-rich phase could not have occurred

below 1200kg/cm² for the homogenization temperatures envisaged (>400°C) according to data from Takenouchi & Kennedy (1965). The pressure domains of entrapment of these fluid inclusions are definitely of a regional metamorphic category.

Finally, as quartz of this pre-uranium stage commonly contains sulphates of Zn and Fe in the inclusions, it would seem that the sulphide mineralization found in and around Jabiluka could have been tied to this event. Narrow sulphur isotope ratios close to zero (Donnelly & Ferguson, this volume) support this point of view.

Vein quartz

Two stages of vein quartz have been recognized, an early xenomorphous or massive quartz (Quartz I of the paragenesis) and a later, largely idiomorphic quartz.

The main fluid inclusion difference between the two stages is one of temperature disappearance of the vapour-phase in dominantly saline inclusions. The ranges of homogenization temperature overlap, but their modal values differ by about 40°C. The older quartz-stage has a modal value of homogenization temperatures of 150°C, whereas the younger averages around 110°C. This observation applied to both Nabarlek and Jabiluka Two.

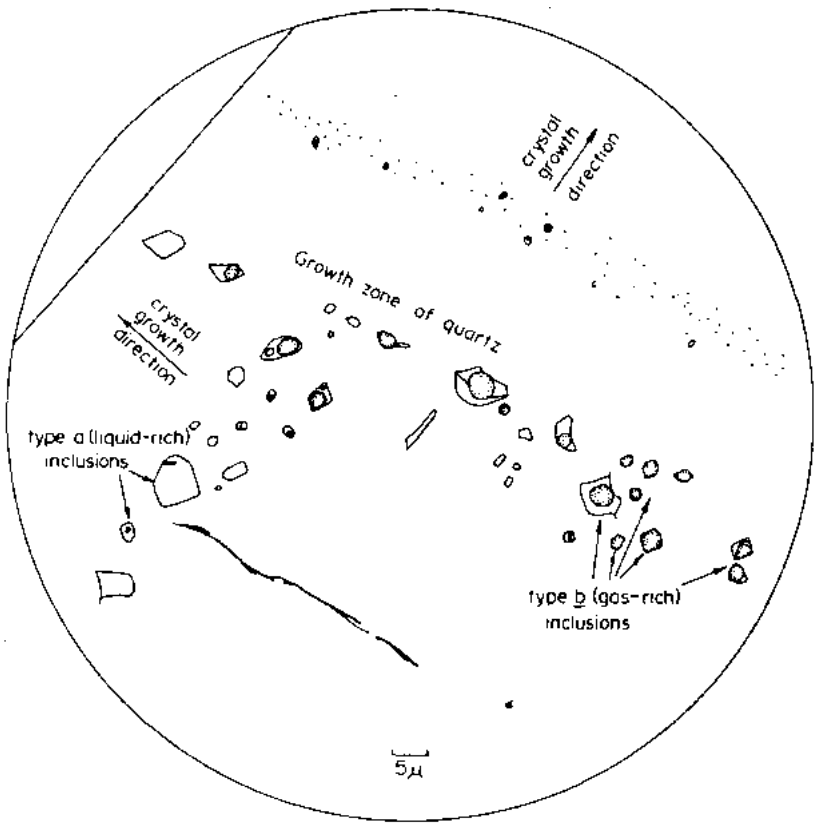


Figure 6. Vein quartz featuring separation of CO_2 rich and brine inclusion in the same zone of growth of the crystal. Sample from Nabarlek, quartz II, Na 77, -46.8m.

Another common characteristic of the inclusions of both deposits is the co-occurrence of saline inclusions with a very small vapour-phase and less saline inclusions with a very large vapour-phase with highly variable liquid:vapour ratios (Fig. 6). Other generalizations which apply to both deposits is that the vapour-rich inclusions contain gas under pressure, which is a mixture of CO_2 and CH_4; and finally, the dominant solute in both deposits is $CaCl_2$, followed by NaCl, and $MgCl_2$ of equal importance. Daughter minerals in the genetic sense are rare and limited to NaCl. Other daughter minerals from heterogeneous entrapment and solid inclusions are:

chlorite
sericite (white mica)
dawsonite ($NaAlCO_3(OH)_2$)
hematite
geothite
carbonates
pitchblende.

All these products of heterogeneous entrapment have been identified with the SEM. Investigation by SEM also proved to be very useful for the identification of evaporative residues in or near the fluid inclusion cavities. Complex compounds of Ca, Mg and K chlorides have been identified with Energy Dispersive X-ray Analysis.

There is very little difference in fluid chemistry between the early-and late-stage quartz. In fact, both quartz stages show inclusions that span the whole gamut of low salinity to 30 wt% $CaCl_2$ equivalent. These widely varying salinity values are perhaps the most distinguishing characteristic of fluid inclusions associated with the uranium mineralization, both at Nabarlek and Jabiluka. Even in the euhedral quartz where brine-rich inclusions clearly can be assigned a primary origin (Figs. 4 & 6), gross salinity differences still occur within growth zones. As daughter minerals resulting from homogeneous entrapment are very rare (and limited to NaCl and its hydrate in the -20° to +30°C temperature bracket) we may exclude the possibility of supersaturation to explain these rapid changes. Mixing of brines appears to be the only alternative. The latter is also suggested by contemporaneity between brine-rich and vapour-rich inclusions in the same zone of growth (Fig. 6). As the salinity would effectively prevent boiling in the temperature range (of 110°-150°C) under consideration, we have to assume exsolution of gases upon mixing of CO_2-rich fluid with a concentrated saline brine.

The presence of gas under moderate pressure, rather than a void of shrinkage is indicated by the crushing test of the vapour-rich inclusions. The gases included in the vapour-phase of inclusions with highly variable liquid:vapour ratios (Fig. 6) are CO_2 and CH_4, as determined by $BaCl_2$ reactions and solubility in kerosene. We preferred these methods over bulk analysis by gaschromatography because of the heterogeneity of all samples which commonly enclosed solids like carbonates and thucholite. All vapour-rich inclusions of the vein quartz failed to feature liquifaction of the CO_2-rich phase on cooling, which is probably due to a combination of low density and methane content of the vapour-phase. CO_2 and CH_4 were identified within the inclusions by the formation of gas-clathrates, melting between -1.0° and +11°C. As it is very unlikely that the pressure between individual stages of trapping varied by a large amount, and the internal pressure was not high enough to liquify CO_2, the variable clathrate melting temperatures are likely to indicate changes of CO_2:CH_4 ratios at a constant pressure between 10 and 30km/cm^2 for 5°C (Miller, 1974). CO_2 and CH_4 have equal clathrate structures and form a solid solution series. Freezing of the CO_2-rich phase below -56°C also points to the presence of CH_4. Melting of a CO_2-rich solid as low as -65° has been observed. Testing with a microbarometric stage (Ypma, 1965) indicated gas pressures of 60kg/cm^2 at 21°C. The gas mixture could not be liquified at this

pressure and -10°C. The latter, again, supports the conclusion of substantial amounts of CH_4 in the vapour-phase (Hollister & Burruss, 1976). CO_2:CH_4 volumetric ratios very between 3:1 to 1:4. As will be shown, we may expect that the concentrated brines carried CH_4. On mixing, CH_4 probably would fractionate into the exsolved CO_2-rich phase, although the solubility of CH_4 in the mixed brine will also have increased because of lower salinity.

With the uncertainty of the CO_2:CH_4 ratio it is difficult to estimate the pressure at a homogenization temperature of 160°C. Assuming an upper density limit of 0.6 of the CO_2-rich phase - which seems certain to be borne out by the lack of liquifaction - we may safely set an upper pressure limit of 500kg/cm², and more probably a range of 250-350kg/cm² for the entrapment pressure. A pressure of 300kg/cm² corresponds to hydrostatic pressure of 3000m overburden (the Kombolgie now measures 1000m) or a lithostatic load of 1200m of Middle Proterozoic (Carpentarian) sediments.

CO_2-rich inclusions are much less common than brine-rich inclusions, and where they do occur they do so in clusters or on a particular side of the quartz crystal (Fig. 6). As the CO_2-rich inclusions are most likely to be the result of heterogeneous trapping, one would expect such to take place where CO_2 bubbles were trapped under a growing crystal face. The CO_2-rich phases were never found in inclusion material of deep-seated origin such as within, or below the Oenpelli Dolerite sill at Nabarlek. Sampling at Jabiluka has not been extensive enough to make a similar statement. The CO_2-rich inclusions are most common within the high-grade ore zone. As brecciation facilitated premeability and mixing of fluids, one would indeed expect most CO_2 to have been exsolved here.

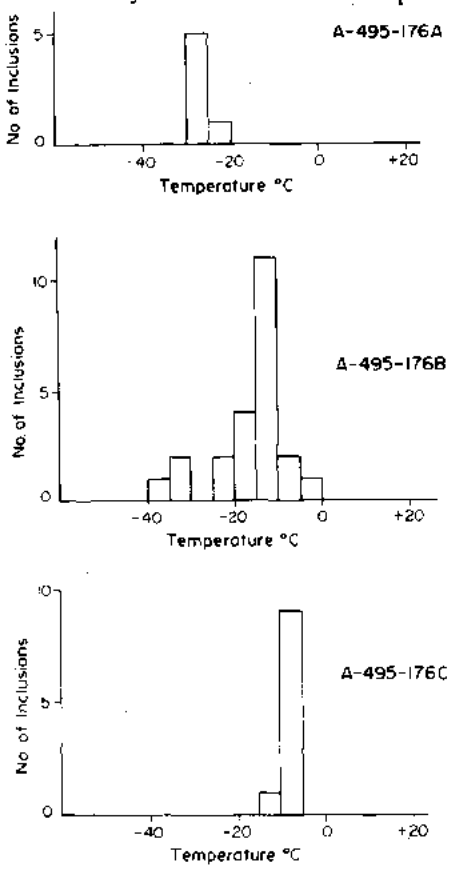


Figure 7a. Freezing temperatures histogrammes of quartz 1 of Nabarlek, Na 77, -67.4m.

Correlations between CO_2 content of fluids and high-grade uranium mineralization has been established for many deposits (Cuney, 1978; Naumov & Mironova, 1969). It equally applies to Nabarlek, except the mechanism proposed here is exsolution because of mixing with a saline brine, rather than boiling (Poty *et al.*, 1974) or decompression (Leroy, 1978).

Homogenization temperatures of CO_2-rich inclusions are meaningless as they result from heterogenous trapment.

Histogrammes of homogenization temperatures and phase changes below 0°C for the early quartz of Nabarlek are in figures 7a and b. Inclusion data of late-stage quartz of Jabiluka are in figure 9. Figure 8 shows the inverse relationship between homogenization and freezing temperatures for a quartz which contains both early-type and late-stage inclusions.

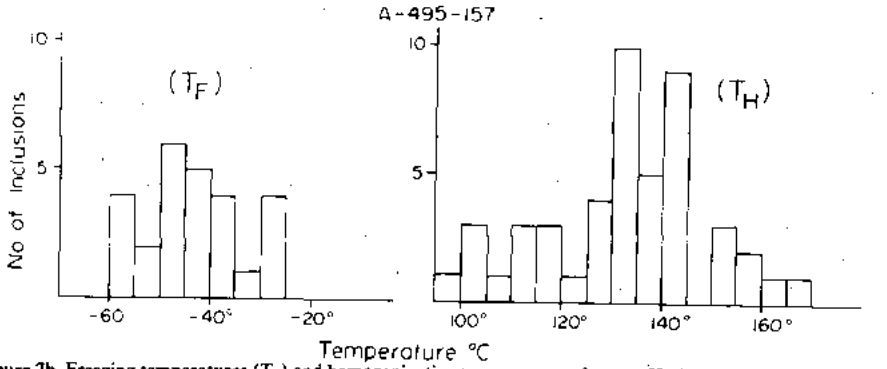


Figure 7b. Freezing temperatures (T_F) and homogenization temperatures of quartz II of Nabarlek, below ore zone, Na 55, -89.0m.

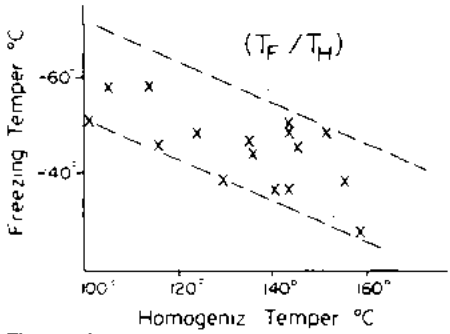


Figure 8. Histogrammes of freezing and homogenization temperatures of late stage (quartz II) from Jabiluka, DDH 143, -104m.

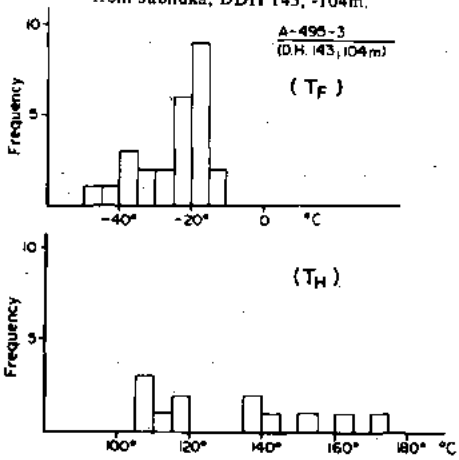


Figure 9. Histogramme of freezing and homogenization temperature of quartz II from Nabarlek, below ore zone. Decrease of temperature and increase of salinity. Na 55, -89.0m.

The picture that emerges from all these data is that of highly varying constitution of fluid inclusions and homogenization temperatures. Although steep salinity gradients have been observed in mineralizing environments, due to density separation of fluids, the concept of steep thermal gradients is much less acceptable, even when mixing of separate fluids is involved. Phase metastability could be invoked to explain the temperature range but is not entirely satisfactory as the range also includes very large inclusions, in which phase kinetics are normally less of a problem. The answer is possibly in the discernable CH_4 content dissolved in the brine. This follows from the observation that many brine inclusions show a very small vapour-phase persisting well above the temperature at which one would have expected homogenization, judging from the rate of retreat of the 'vapour'-phase on heating. As CH_4 is reasonably soluble in concentrated brines at +30°C (much more than CO_2, for instance, 0.04 mol.% CH_4 is soluble in a brine of 2.5 mol.% $CaCl_2$) and solubility rapidly decreases with temperature (Duffy *et al.*, 1961), one would expect CH_4 to be exsolved during the heating test until the volume expansion of the brine is sufficient to increase the internal pressure to dissolve CH_4 again. This mechanism explains why many brine-rich inclusions start to leak or decrepitate before full homogenization, which could not have occurred if the vapour-phase had been a pure 'void of shrinkage'. An early

decrepitation of brine-rich inclusions and tests for CH_4 with kerosene support the presence of CH_4 in the brines.

As the solubility of CH_4 in a brine is so sensitive to salinity, we should expect that salinity gradients and mixing with more dilute solutions would change the homogenization temperatures of the system brine + CH_4. Undiluted concentrated brines which have a very small CH_4 content will feature a homogenization temperature largely due to the disappearance of the 'void of shrinkage', whereas diluted brines could accommodate more CH_4 which leads to a homogenization temperature due to a process where the internal pressure increase of the fluid causes dissolution of the gas-phase, with all the inherent kinetic uncertainties of such a process.

Nothwithstanding this cautious interpretation of homogenization temperatures, real temperature differences did exist as will be shown in the oxygen isotope section.

A most useful indication as to the Eh of the inclusions is given by the presence of $FeCl_2$ and $FeSO_4$ in the brines. The presence of iron chlorides and sulphates in inclusions has been demonstrated with the SEM but their oxidation state was not known until several inclusions in sample Nabarlek Na77, 58.05m, and Jabiluka DDH169, 200.4m, showed leakage and subsequent irreversable formation of hydrous ferric oxide, probably goethite. This occurred after several thermal cycles up to 200°C of a very concentrated brine which presumably was not diluted by a CO_2-rich fluid. Hydrogen leakage was probably small in the natural environment as the formation temperatures were low, which shifts the $CO_2+4H_2= 2H_2O+CH_4$ equilibrium towards CH_4. Hematite is a common daughter mineral in fluid inclusions of the ore zone where mixing was common. This would suggest that the CO_2-rich fluids were more oxidizing than the concentrated brines.

Many inclusions feature unusual phase changes below 0°C, which have not been mentioned before in the fluid inclusion literature. The inclusions generally belong to the late-stage quartz, or a late-stage calcite (sample Na23, 305m; Table 1). Salt hydrates were formed below -50°C. By retaining the inclusions at this temperature for 1 hour or more, course-grained salt hydrates develop. Between -45° and 35° these change into an hexagonal shaped hydrate that has been identified as $CaCl_2 \cdot 6H_2O$. Given thefrequency with which Mg chloride has been fund with the SEM it seems that we are dealing with solutions close to the eutectic of $CaCl_2$ and $MgCl_2$ (Yanatieva, 1946) with possibly the addition of NaCl and KCl. Yanatieva's (op.cit.) data indicate that a solution of 23±2 wt% $CaCl_2$ and 10±2 wt% $MgCl_2$ will crystallize first $MgCl_2 \cdot 12H_2O$ between -55° and -43°C, which will revert to $CaCl_2 \cdot 6H_2O$ between -50° and -35°C.

Similar pheomena have been observed in the system $CaCl_2$-NaCl. Yanatieva's (op.cit.) phase diagram indicates the formation of $NaCl \cdot 2H_2O$ at temperatures below -21.2°C for brines containing $CaCl_2$, down to -52°C for 29 wt% $CaCl_2$ and only 3 wt% NaCl. It is important to notice that for a $CaCl_2$ content of slightly less than 29%, $NaCl \cdot 2H_2O$ will form at ~-40°C and melt incongruently to NaCl + liquid at ~-20°C. $CaCl_2$ will form no hydrates under these conditions, thus the formation of NaCl could be very misleading. Many inclusions from Nabarlek and Jabiluka displayed the above-mentioned behaviour of the formation of NaCl by incongruently melting of $NaCl \cdot 2H_2O$ below +0.2°C, which dissolves again below +20°C. This has been taken as evidence for $CaCl_2$ or $MgCl_2$ in the solution. The low initial melting temperature of ice (Roedder, 1963) should also be taken as an indication for $CaCl_2$ in solution. As $CaCl_2$ is the dominant species, all salinities have been quoted in $CaCl_2$ equivalent.

The inverse correlation between salinity and homogenization temperatures (Fig. 8) is a general feature for all young vein quartz at Jabiluka and Nabarlek. The significance is not well understood. In general, the later solutions tend to be more saline and are of lower temperature. The same trend can be approximately observed with regard to the position of

Sample No.	Description	Phase change	Tm range Tm(mode)	Th range Th(mode) Tm (dm)	Salinity wt% eq.$CaCl_2$	Gas release	SEM analysis
			Uraniferous samples				
Na77	L+V,NaCl	ice	-31 to -43	70 to	26		Sericite, chlorite, NaCl
-58.05mA	dawsonite	$CaCl_2$-$6H_2O$	+13.9	130V	29		KCa chloride, Fe-salt
	hematite	clathrates	+11,+14			***	
	carbon "button"						
-58.05mB	L(only)KCl	vapovr,-10	-46	89dm	29		KCl, $CaCl_2$ hydrates
	NaCl,L+V	new goethite		94V		*	$MgCl_2$
	hematite						
-58.05mD	L(only)	ice	- 5		9		NaCl + $CaCl_2$ hydrates
	L+V	ice	- 9 to -37	85V	11-27		
-58.05 F	L+V	ice + cubic XL	-44 to	93 to	28		NaCl + $CaCl_2$ hydrates
	NaCl	$CaCl_2$-$6H_2O$	-61	142V	30	*	
Na77	L(only)	ice	-11 to	95-	16 to		NaCl + $CaCl_2$ hydrates
-46.8m	L+V		-33.5	108V	26	***	
Na77	L only(QII)			120-200			
-56.7	L+V(QI)			(140)V			
Na72	L only	ice	-0.3,-0.9	95-190	0.5	**	$CaCl_2$ hydrates
-29.6m	L+V	clathrate	-31.5	(130)V			sericite, kaolinite
			Uraninites				
Na 1						CH_4	calcite, dolomite
						CO_2	gypsum
						He	galena, chlorite
			Non-mineralized samples				
Na77	L+V	ice	-24,-28	150-200	26 to		sericite
-67.3mA	(QI)			(150)V	29		$CaCl_2$
-67.3mB	L+V	ice	- 5,-40	140-170	17.5	**	KCl
	NaCl(QI)		(-16)	(160)V			$FeSO_4$-hydrate
-67.3mC	L+V(QI)	ice	- 5 to -15	140-170	13.5		basalts
-67.3mD	L+V(QI)			(165)V			dolomite
-67.3mE	L+V(QII)	inhom.entrap.	-20,-35	>500	22-30	CO_2	ankerite
	L(QII)	ice		133		CH_4	
-67.3mF	L+V(QI	ice		120-160			
	(QII)			(130)V			
Na77	L(QII)			(85)V			
-61.7m	L+V(QI)			(140)V			
Na55	L+V(QI)	ice	-26 to -58	100-170	24-	*	$CaCl_2$,NaCl
-89m		$CaCl_2$-$6H_2O$	(-46)	(135)V	31	CO_2	KCl (near ore)
Na55	L+V(QII)	ice	-22,-36	110-150	21 to		Ca+Na chloride
-83.9m			(-30)	(120)V	27		(near ore)
Na1	L+V(QI)	ice	-41,-46	(150)V	20-29	***	$CaCl_2$,NaCl
-59.8m	L+V(QII)	$CaCl_2$-$6H_2O$	- 8,+ 4	(120)V	32-33	CH_4	$MgCl_2$?
Na23	L	ice	- 1,-22		15-16		
-305m	dawsonite		(-12)				
Na83	L+V	ice		100			
-93.3m	(in dolerite)						
			Calcite				
Na23	L+V	ice, several	-45,-35	96-104	+34		$CaCl_2$,NaCl
-305m	post-dates QII	hydrates	- 3 to - 2				probably $MgCl_2$
Na176	L+V	ice	- 7,-23	125-170	9-23	*	$CaCl_2$, NaCl
-44m			(-18)	(135)V		CO_2	

Table 1. Fluid inclusions from Nabarlek.

the orebody at Nabarlek. Fluid inclusions below the orebody are more saline and often fail to develop a vapour-phase (Table 1).

Naumov & Dorofeyeva (1975) produced data on the theoretical effect on pH by Na and K salt solutions at different temperatures. The general tendency is that solutions of the kind envisaged in this study reach a low pH of 5 to 5.5 near 120°C. This low pH will have facilitated the precipitation of uraninite once the uranyl carbonate complexes were broken down by exsolution of CO_2, and uranyl ions were reduced by CH_4.

The process would gain efficiency assuming an intermediate absorption stage to clay minerals (chlorite) as proposed by Giblin (this volume) and Giblin *et al.* (1969), particularly as the saline brines would have been instrumental in desorbing uranium ions from the clay mineral surfaces.

It is remarkable that those brine inclusions below the orebody and below the Oenpelli Dolerite at Nabarlek feature a lower homogenization temperature (~100°C) than the mixed brines of the ore zone. This implies that we have to postulate that the diluting waters were warmer, or that the heat source was located on the site of the present orebody. Fehn *et al.* (1978) have developed a model for heat and fluid convection around anomalously radioactive bodies, which could be applied here.

It is considered that the heat generated by dilution of a $CaCl_2$-rich brine is insufficient to explain the surge in temperature.

Fluid inclusions in uraninite and pitchblende escape observation, however, some general observations can be made from crushing tests and SEM investigations. The same volatiles as found in the associated quartz viz: CO_2 and CH_4, have been found in pitchblende of Nabarlek, in addition to another gas that has been tentatively identified as He. Inclusion cavities contained heterogeneously trapped daughter minerals of calcite, dolomite, gypsum, chlorite and galena. It is significant that calcite seems to be a common solid inclusion in pitchblende while it is very rare in quartz I and not much more common in quartz II. Apparently the postulated reaction between saline $CaCl_2$-rich brines and CO_2-rich fluids which are thought to have reduced and precipitated uranous oxides from carbonate fluids, produced also precipitation of calcite.

OXYGEN ISOTOPE STUDIES

A combination of oxygen isotope studies and fluid inclusion thermometry enables the determination of the nature of the fluids which affected the country rock and produced the mineralization.

Oxygen extraction and mass spectrometry were carried out by the Institute of Nuclear Sciences, Department of Scientific and Industrial Research, Lower Hutt, New Zealand. Experimental parameters of this laboratory are given by Blattner (1975). All values are recorded in per mil (‰) relative to Standard Mean Ocean Water (SMOW).

Most of the oxygen isotope studies were on samples from Nabarlek. The results are comparable and are shown to be comparable to those of the Jabiluka Two orebody (Binns, McAndrew & Sun, this volume). The samples from Nabarlek can be categorized as follows:

1) The Oenpelli Dolerite and its alteration products.

The Oenpelli Dolerite at Nabarlek occurs close to the Kombolgie unconformity but predates this event. Crystallization or weathering under near-surface conditions could cause a wholesale change of O-isotope ratios of the material affected, as has been demonstrated for Sky (Taylor, 1968), and many other igneous rocks (Taylor, 1974).

Altered dolerite, which consist largely of chlorite, white mica, opaques and remnants of mafic minerals has a $\delta^{18}O$ value of 6.9±0.1‰ as an average whole rock value of 12 samples. The average $\delta^{18}O$ value of three fresh dolerites with plagioclase, pyroxene and olivine is 6.6 ±0.2‰. Both are normal values for tholeiitic magma of this type. These results clearly

indicate that the alteration must have been achieved in an essentially closed system in which the cause of hydration (meteoric water or metamorphogenic solutions) had a limited volume compared to the O-reservoir of the igneous rock mass. The restricted volume relationship during the alteration process between solution and dolerite are also indicated by the $\delta^{18}O$ values of individual minerals of the altered dolerite, iron-oxide-rich portions of the altered dolerite have retained their low $\delta^{18}O$ values. Furthermore, a plagioclase ($\delta^{18}O = 7.8 \pm 0.5‰$) and pyroxene ($\delta^{18}O = 5.7 \pm 0.5‰$) pair of a fresh dolerite represents an equilibrium temperature of 500±180°C (Friedman & O'Niel, 1977).

However, not all alterations occurred under restricted conditions. Some alteration products, in particular those near veins and fractures, show equilibration with water which cannot be considered to be magmatic or metamorphic. A sample from the Oenpelli Dolerite in core Na22-110.6m contains a chlorite ($\delta^{18}O = 4.8 \pm 0.1‰$) and sericite ($\delta^{18}O = 10.2 \pm 0.1‰$) pair which represents an equilibrium temperature of 150±10°C. Yet most results are more compatible with an alteration process of the dolerite under deep-seated conditions, presumably an auto-hydration following the dolerite's emplacement under >2000m meta-sedimentary cover (Needham *et al.*, this volume).

2) Granites and granite gneisses of the Nimbuwah Complex.

Few, if any of the granites near Nabarlek can be considered to be unaltered. Even cores (from Na23) at depths of -482 and -487 metres showed alteration. Nevertheless, $\delta^{18}O$ values of these granites showed little difference from normal values for granites. An average of four samples (Na23 and Na83, -470 and -488m) gave a $\delta^{18}O$ value of 10.6±0.4‰, against 9.0±0.5‰ for average granites (Taylor, 1968). This slight increase could be the result of anatexis, but could also be due to white mica, which is the sole mineral which shows a lower temperature equilibration ($\delta^{18}O = 9.8 \pm 0.3‰$), compared to quartz which retained its magmatic value of 10.7±0.2‰). The general inference is that alteration of the granites also took place under conditions of restricted supply of volatile material. Assuming a temperature of 235°C for the formation of sericite, its $\delta^{18}O$ value could be an equilibrium value with water of juvenile origin (+7.0‰).

3) Metasediments and igneous rocks

The metasediments and igneous rocks show a predominance of igneous components resulting in whole rock $\delta^{18}O$ values of +10.0 to 11.0‰. Actinolite schists and amphibolites (probably the Nabarlek equivalent of the Zamu Dolerite) reveal their magmatic derivation by $\delta^{18}O$ values of +9 to 10‰. Retrograde features do not change the $\delta^{18}O$ values of the amphibolites.

4) Quartz and calcite veins

Material was obtained from quartz-chlorite breccias, quartz veinlets in barren chlorite-sericite schists, quartz veinlets in mineralized chlorite rock, a hematitic chlorite matrix, and mineralized veinlets in quartz-sericite-chlorite schists. Previously - see fluid inclusion section - a distinction has been made between early-stage and late-stage quartz, based on crystal habits and paragenesis. A further justification for this distinction is clearly provided by the O-isotope data. The late-stage quartz clusters closely around a $\delta^{18}O$ value of 15.6±0.3‰ (for 12 samples). The early-stage quartz is less homogeneous and averages 10.7±0.3‰ (for 11 samples). This difference in oxygen isotope composition could be a result of:

a) shift in $\delta^{18}O$ composition of the mineralizing solutions;
b) drop in temperature between early and late-stage quartz at constant values of $\delta^{18}O$ for water;
c) change in salinity at constant temperature and source of water.

Although we are dealing with extremely complicated and concentrated solutions and the effect of salinity on oxygen isotope fractionation becomes maximal for 120°C (Truesdell, 1974) the maximal shift is still insufficient to explain the discrepancy between early- and

late-stage quartz. For instance, a complex brine of 2M $CaCl_2$, 0.5M NaCl and 0.2M KCl causes at 120°C a decrease in quartz-water fractionation by about 2‰ when compared with pure water. Moreover, fluid inclusion data indicate that there is no difference in salinity of such magnitude between early- and late-stage quartz, although minor differences do exist.

Hole No.	Sample No.	Depth (m)	Dist.to sill(m)	$\delta^{18}O$ qu. (‰SMOW)	T_H(°C)	$\delta^{18}O$ sol. (‰SMOW)	Mode	
Na-23	A-495-144	305.5	10	16.8±.1	~100	-5.5	-5.5	3M NaCl
Na-55	-156	83.9	3.0	15.1±.5	120	-4.5- -3.5	-4.0	2.7 M $CaCl_2$
" "	-157	89.0	-0.5	17.0±.5	100-145	-5.0- +2.2	-0.6	3.1 M $CaCl_2$
Na-83	-191	93.3	-40.0	15.5±.5	90-110	-10.8- -9.4 uncorrected		younger quartz
" "	-191	93.3	-40.0	15	-	-	-	older quartz
" "	-186	416.4	116.0 (below sill)	10.8±.5	~150-200	-7.5- -2.4 uncorrected		
Na-74	-164	39.5	132	13.8±.5	120-140	-9.2- -6.8 uncorrected		younger quartz
" "	-164	39.5	132	12.8±.5	-	-	-	older quartz
Na-72	-162	22.5	75.5	12.3±.5	130-160	-4.6- -1.5	-4.5	0.4 M NaCl

Table 2. Oxygen isotope values of quartz and corresponding brines, calculated* and corrected for temperature and salinity.

*$10^3 \ln\alpha$ (Qu-H_2O) = $3.65(10^6/T^2)$-2.59 (Blattner, 1975)

The observed difference in the temperature of disappearance of the vapour-phase of fluid inclusions associated with each stage of quartz formation, is not quite large enough to explain the O-isotope shift between the successive stages of quartz. Using Blattner's (1975) equation of: $10^3 \ln\alpha$(quartz-water) + $3.65(10^6/T^2)$-2.59‰ a temperature drop from 150° to 110°C or 165° to 120°C is required to account for an ^{18}O shift of 4.5‰. Using Matthews and Beckingsale's (1979) equation of: $10^3 \ln\alpha$(quartz-water = $3.05\,(10^6/T^2)$-2.09 a temperature difference of 50°C (from 170°C for the early quartz to 120°C for the later one) is needed to account for an ^{18}O shift of 4.5‰. Differences in this temperature range are difinitely not borne out by the fluid inclusion data. A temperature decrease from 150° to 100°C is closer to those indicated by the fluid inclusion data, but is still too large. In order to explain the 5.0‰ shift other than by a 50°C temperature differential, we have to postulate that solutions producing the early quartz were less depleted in ^{18}O than later ones, which could have been the result from isotope exchange with the host rock affecting the earlier solutions more than the later ones. Taking the average homogenization temperatures of early quartz (150°C) and later quartz (110°C) a difference in $\delta^{18}O$ values of 4.5‰ can be expected. An additional 0.5‰ could easily have been the result of higher $\delta^{18}O$ values in the earlier brine. In view of the spread in homogenization temperatures, 0.5‰ is always well within the calculated range of solution values. The latter averages out at -4.3‰ SMOW from those ten samples for which both salinity and homogenization temperatures were known (Tables 2 & 3). As expected, CO_2 in solution will shift the oxygen isotope composition of the solution more towards higher $\delta^{18}O$ values as is the case for calcites for which salinities and homogenization temperatures are known (Table 4). The negative values of $\delta^{18}O$ of the mineralizing solutions are incompatible with magmatic or metamorphic origin and points to meteoric water as their main component. The possibility of late metamorphic emplacement of the vein quartz and calcite seems to have been ruled out by oxygen isotopes.

The high salinity of the brines and the very limited oxygen isotope exchange by surface

Sample No.	Depth (m)	Dist.to sill(m)	Early-stage Quartz $\delta^{18}O$ qu. (‰SMOW)	T_H(°C)	$\delta^{18}O$ sol. (‰SMOW)	Mode	Later-stage Quartz $\delta^{18}O$ qu. (‰ SMOW)	T_H(°C)	$\delta^{18}O$ sol. (‰SMOW)	Mode
A-495-167	44.6	117	9.5±.1	-	-		-	-	-	-
168	46.8	115	15.5±.1	-	-		15.9±.1	100	-5.7	-5.7
171	56.7	106	9.5±.5	-	-		14	140	-5.5	-5.5
172	58.0	105	7.1±.5	-	-		16	85-140	- 7.8- -0.8	-3.0
174	61.7	101	10.1±.5	120-165	-12.0- -6.5 uncorrected		16.5±.1	80-100	-12.2- -9.1 uncorrected	
174A	61.8	101	9.3±.1	-	-	-	15.2±.1	-	-	-
176	67.4	96	11.0±.1	160-210	- 5.8- -1.0	-5.5	16.0±.5	125-150	- 4.5- -0.2	-3.7
178	104.4	62	-	-	-	-	16	105-145	- 9.0- -3.6 uncorrected	
179	111.4	56	10.3±.5	135-160	- 8.0- -4.8	-5.0	-	-	-	-

Table 3. Oxygen isotope values of quartz from drill NA77 and corresponding solution calculated* and corrected for temperature and salinity.

*$10^3 \ln \alpha_{(Qu-H_2O)} = 3.65(10^5/T^2)-2.59$ (Blattner, 1975)

waters are in full agreement with the concept of limited solution volume, and the confinement of oxygen isotope exchange to hydrated minerals and hydrothermal vein material. A chlorite-sericite pair from an altered dolerite (Na22;-110m) near a later vein gave an equilibrium temperature of 150±10°C. These sheet silicates are in equilibrium with a solution with a $\delta^{18}O$ value of +0.8‰ SMOW. This temperature confirms fluid inclusion data and points to the contemporaneity of chlorite and sericite as solid inclusions in vein quartz of this temperature range.

Fluid inclusion thermometry of dolomites and quartz associated with dolomite at Jabiluka Two as applied to $\delta^{18}O$ values of dolomite (Binns, McAndrew & Sun, this

Drill-hole No.	Sample No.	Depth (m)	$\delta^{18}O$ calc. (‰SMOW)	T_H(°C)	$\delta^{18}O$ solution (‰SMOW) Calcul.*	Corr.for NH_4Cl	Corr.for Sal.effect	Sal. (mol $CaCl_2$)
Na- 1	A-495-110	39	22.5±.1	50 (estimated)	-0.7	-0.7	<-0.7	
Na- 23	A-495-144	305	13.1±.1	95-105	-4.0- -3.0	-3.0- -2.0	-0.5- +0.5	3
Na-176	A-495-220	38	13.2±.1	125-165	-1.0- +2.1	+0.5- +3.6	+2.5- +4.0	2

Table 4. Oxygen isotope values of calcite and corresponding brines calculated and corrected for temperature and salinity.

*$10^3 \ln \alpha_{(CaCO_3-H_2O)} = 2.78 \times 10^6/T^2-3.39$ (O'Neil et al., 1969).

volume) points to waters with $\delta^{18}O$ values of -4.2‰ for drusy dolomite with an homogenization temperature of 120°C and 1+0‰ for dolomite with an homogenization temperature of 160°C. These data support the concept of a $\delta^{18}O$ shift during the paragenesis, towards more depleted solution values with an increase in the dominance of meteoric waters.

It is of interest to notice that quartz from the greisen and retrogressed schists zone at Jabiluka Binns, McAndrew & Sun, this volume) has a $\delta^{18}O$ value of ~+15.0‰ which is the same as the late vein quartz at Nabarlek. Jabiluka's vein quartz has $\delta^{18}O$ values of ~+17.0 which corresponds to a value of the coexisting fluid of -1.0‰ at 110°C.

DISCUSSION OF RESULTS

Fluid inclusion and oxygen isotope studies clearly place some restraints on the modes of origin of the Jabiluka and Nabarlek deposits.

Although transparent gangue material is rare among the host minerals of the mineralization, and it could be argued that the bulk of chlorite has a different genesis than that of the quartz, the weight of fluid inclusion evidence is such that no fluids have been found other than the three categories described in this study. As replacement by chlorite and formation of quartz-hematite breccias are contemporaneous with the bulk of uranium mineralization (Binns, McAndrew & Sun, this volume), it would seem very unlikely that the fluids involved would not have left a trace in early quartz other than the inclusions observed.

In terms of the regional distribution, the fluid inclusions can be classified as:

1) widespread distribution of high temperature and high pressure $NaCl$-CO_2 brines, presumably of metamorphic derivation;
2) concentrated saline brines of $CaCl_2$, $MgCl_2$ and $NaCl$ occurring demonstrably within, around and below the ore bodies in a domain with an estimated radius of 500 metres, but which could be more expensive;
3) medium pressure CO_2-rich brines which are confined to the ore zone, and above it, the exact lateral extent of which is unknown. One serious short-coming of this study is our lack of investigation of the Kombolgie Sandstone.

Drastic changes in salinity and liquid:vapour ratios of primary fluid inclusions have been explained as the result of mixing of the brines mentioned under 2 and 3. The results of this process are:

1) exsolution of dissolved CO_2 from the dilute fluid, and
2) salinity changes of the concentrated brines.

What is not well understood is:

a) the lack of precipitation of carbonates which could have been expected for such Ca^{2+} and Mg^{2+}-rich solution, and
b) the source of ions in the concentrated brines.

ad a A possible explanation for the lack of precipitation of calcite is the drop in temperature which accompanied mixing of the cool brine and warmer CO_2 fluid, and the increase in salinity which also improves calcite solubility (Holland, 1967).

ad b Crick & Muir (this volume) have drawn attention to the occurrence of carbonate pseudomorphs after evaporate minerals (halite and gypsum) in the Lower Cahill Formation of the ARUF. The high temperature $NaCl$-CO_2 brines of late metamorphic origin have also been shown to contain Ca^{2+} and Mg^{2+} in appreciable quantities. At temperatures of 450°C magnesite will be the carbonate equilibrium species even for a solution with a Ca^{2+} :Mg^{2+} ratio of 9:1 at a total salinity of 2M (Rosenberg *et al.*, 1967). This ratio was easily attained in these fluids. It may be of interest to notice the prevalance of magnesite over dolomite in carbonates of the Pine Creek Geosyncline near basement highs: presumably in areas of high-grade metamorphism and corresponding dominance of CO_2 (Touret, 1972).

Upon cooling, the magnesite stability field yields to dolomite and much lower Ca:Mg ratios are needed to maintain magnesite (Ca:Mg of 6:4 at 225°C; Rosenberg *et al.*, op. cit.). This implies that at the temperatures of uranium precipitation, as derived from fluid inclusions (100°-160°C), one would expect dolomite to be formed - which is indeed quite abundant at Jabiluka - and the release of Mg^{2+} to the solution, explaining the prominent Mg-metasomatism. Under these conditions, calcite should form only at very low temperatures: ~100°C (Rosenberg *et al.*, op.cit.), which conforms with observation.

The increase of salinity towards the end of the mineralization could indicate an end of access of more dilute brines (presumably CO_2-rich fluids) to the area.

CONCLUSIONS

Our conclusions are contained diagrammatically in the following model of the genesis of the Nabarlek deposit, which is considered to be equally applicable to Jabiluka (Fig. 10).

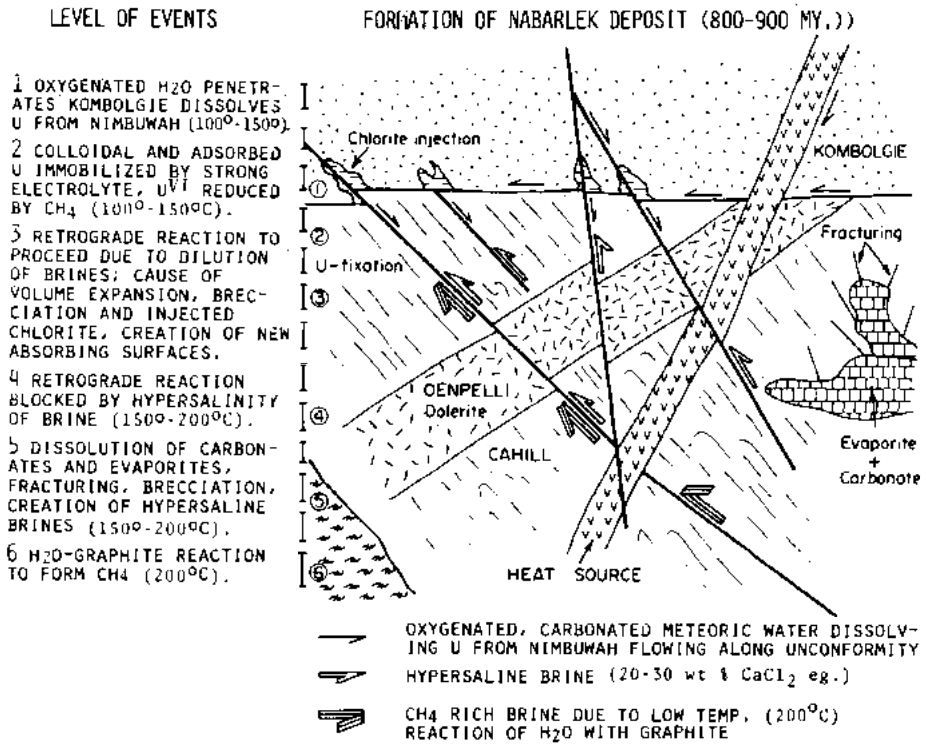


Figure 10. Schematic diagram of the formation of the Nabarlek deposit, as discussed in text.

After a period of metamorphism and deformation, evaporites of the Lower Cahill Formation were transformed by late metamorphic brines into magnesite and/or dolomite. These brines were of metamorphic derivation and featured high(NaCl) salinity and dense CO_2 phases. Temperatures ranged between 450° and 600°C, at a minimum pressure of 1200kg/cm^2. Fluid inclusions of these brines are common throughout the Nabarlek and Jabiluka areas, and not related spatially to the U-mineralization. No mineralization took place until after the deposition of the Kombolgie Formation. This sandstone presumably acted as a thermal insulating blanket enabling a radiogenic heat flow to be built up by the highly uraniferous Nanambu and Nimbuwah complexes (Fehn *et al.*, 1978). Access of water to the metamorphic Cahill was probably very restricted, and extremely saline brines with high calcium activity were the result, possibly derived from evaporites, which effectively blocked retrograde metamorphic reactions of mafic minerals because of the common ion effect, but allowed K and Na metamorphic reactions: e.g. the "greissen" of Binns, McAndrew & Sun (this volume).

Fracturing and (questionable) removal of excess formations above the Kombolgie Sandstone provided access of groundwater to the area. This event could have been coeval with the emplacement of phonolites along faults in the metamorphic basement (1316±50 m.y., Needham *et al.*, this volume). This event also increased the heat flow. Access by groundwater produced convective water movement. Because of the high density of the brines, the fluids' movement was stratified resulting in a saline basal brine with more dilute surface water on top. Areas of dilute water penetration became available for retrograde

metamorphism because of the removal of the common ion effect. Chlorite was injected into the Kombolgie Sandstone.

CO_2-rich surface water whose meteoric origin seems to be indicated by oxygen isotope data were the most likely carriers of uranyl carbonate compounds, whose uranium content was leached from the granitic basement rocks. The creation of newly formed sheet silicates in the retrograde alteration zone were most effective in adsorption of uranyl ions, according to the Giblin model (this volume). Hydrostatic changes moved the interface of brine and surface water in time, causing exsolution of CO_2 from the carbonate-rich meteoric waters. The CO_2-rich meteoric waters were more oxidizing (hematite inclusions) than the saline brine ($FeCl_2$ in solution). The low pH of the brine facilitated decomposition of the uranyl complexes, its salinity caused desorption from clay surfaces, its CH_4 content, the reduction of uranous oxides. The temperature of this process occurred between 110° and 160°C at a pressure of about 300kg/cm², which corresponds to the lithostatic pressure under 1200m of Kombolgie Sandstone or 3000m of overburden at hydrostatic pressures.

The uranium content of the granitic basement, and at a later stage, the uranium concentrations themselves, were sufficient to keep a convective water system going, possibly with very limited new input. Uranous-oxides must have undergone many dissolution and reprecipitation phases, depending on the position and the brine:CO_2-rich fluid interface.

The convective fluid cell probably stopped with the loading of Upper Proterozoic (Adelaidean) sediments on top of the Kombolgie Sandstone (900-800 m.y.), at which age the last regeneration of uranium oxides took place. The ore zone reverted to one of saline brine dominance at this stage, and no major disturbances occurred until the removal of the Kombolgie Sandstone.

ACKNOWLEDGEMENTS

We acknowledge the help from the staff of Queensland Mines and Pancontinental Mining in providing us access to Nabarlek and Jabiluka, respectively. Several samples from the Jabiluka Two deposit were provided by the Mineralogy Division of the Institute of Earth Sciences of the C.S.I.R.O., North Ryde.

We acknowledge the financial support from Nuclebras which enabled Kazuo Fuzikawa to carry out the laboratory and field studies in the Northern Territory.

The oxygen isotope studies would not have been possible without the generous way in which Dr. P. Blattner made available to us his laboratory at the New Zealand Geological Survey Department of Scientific and Industrial Research, Lower Hutt, New Zealand.

REFERENCES

Anthony, P.J., 1975: The Nabarlek Uranium Deposit. *in* (ed. C.L. Knight) *Economic Geology of Australia and Papua New Guinea. Australas. Inst. Min. Metall., Monograph Series No. 5, 1. Metals*, 304-308.

Binns, R.A., McAndrew, J. & Sun, S.S., this volume: Origin of uranium mineralization at Jabiluka. *Proceedings of the International Uranium Symposium on the Pine Creek Geosyncline.*

Binns, R.A., Ayres, D.E., Wilmshurst, J.R. & Ramsden, A.R., this volume: Geochemistry of Jabiluka Ores and Host Rocks. *Proceedings of the International Uranium Symposium on the Pine Creek Geosyncline.*

Blattner, P., 1975: Oxygen isotopic composition of fissure grown quartz-adularia and calcite from Broadlands Geothermal Field, N.Z. *Am. J. Sci., 275*, 785-800.

Crick, I.H. & Muir, M.D., this volume: Evaporites and uranium mineralization in the Pine Creek Geosyncline. *Proceedings of the International Uranium Symposium on the Pine Creek Geosyncline.*

Cuney, M., 1978: Geologic Environment, Mineralogy, and Fluid Inclusions of the Bois Noirs-Limouzat Uranium Vein, Forez, France. *Econ. Geol., 73*, 1567-1610.

Duffy, J.R., Smith, N.O. & Bartholomew, N., 1961: Solubility of natural gases in aqueous salt solutions — I. *Geochim. cosmochim. Acta, 24*, 23-31.

Fehn, V., Cathless, L.M. & Holland, H.D., 1978: Hydrothermal convection and uranium deposits in abnormally radioactive plutons. *Econ. Geol., 73*, 1556-1566.

Ferguson, J., this volume: Metamorphism in the Pine Creek Geosyncline and its bearing on startigraphic correlations. *Proceedings of the International Uranium Symposium on the Pine Creek Geosyncline.*

Ferguson, J., Ewers, G.R. & Donnelly, T.H., this volume: Model for the development of economic uranium mineralization in the Alligator Rivers Uranium Field. *Proceedings of the International Uranium Symposium on the Pine Creek Geosyncline.*

Friedman, I. & O'Neil, J.R., 1977: Compilation of stable isotope fractionation factors of geochemical interest. *In* (ed. M. Fleischer) *Data of Geochmistry, Prof. Pap. U.S. geol. Surv., 440-KK.*

Giblin, A.M., this volume: Experiments on the role of clay adsorption in genesis of uranium ores. *Proceedings of the International Uranium Symposium on the Pine Creek Geosyncline.*

Giblin, A.M., Batts, B.D. & Swaine, D.J., 1979: Laboratory simulation studies of uranium mobility in natural waters. (Manuscript submitted to *Geochim. cosmochim. Acta.).*

Gulson, B.L. & Mizon, K.J., this volume: Preliminary investigation of the use of Pb isotopes in uranium exploration with additional U-Pb 'ages' for Jabiluka uraninite. *Proceedings of the International Uranium Symposium of the Pine Creek Geosyncline.*

Hegge, M.R., Mosher, D.V., Eupene, G.S. & Anthony, P.J., this volume: Geologic Setting and Comparative review of the East Alligator Uranium Deposits and Prospects. *Proceedings of the International Uranium Symposium on the Pine Creek Geosyncline.*

Hills, J.H. & Richards, J.R., 1972: The age of the uranium mineralization in northern Australia. *Search, 3(10),* 382-385.

Holland, H.D., 1964: Gangue minerals in hydrothermal systems. *in* (ed. H.L. Barnes) *Hydrothermal Ore Deposits.* Hold Rinehart, Winston, N.Y., 382-436.

Hollister, L.S. & Burruss, R.C., 1976: Phase Equilibria in fluid inclusions from the Khtada Lake Metamorphic Complex. *Geochim. cosmochim. Acta, 40,* 163-175.

Leroy, J., 1978: The Margnac and Fanay Uranium Deposits of the La Crouzille District (Western Massif Central, France): Geological and Fluid Inclusion Studies. *Econ. Geol., 73,* 1611-1634.

Matthews, A. & Beckingsale, R.D., 1979: Oxygen Isotope equilibration systematics between quartz and water. *Am. Miner., 64,* 232-246.

Metzger, F.W., Kelly, W.C., Nesbitt, B.E. & Essene, E.J., 1977: Scanning Electron Microscopy of daughter minerals in fluid inclusions. *Econ. Geol., 72,* 141-151.

Miller, S.L., 1974: The nature and occurrence of clathrate hydrates. *in* (ed. I.R. Kaplan) *Natural Gases in Marine Sediments.* New York, Plenum Press, 151-177.

Naumov, G.B. & Mironova, O.F., 1969: Das Verhalten der Kohlensäure in hydrothermalen Lösungen bei der Bildung der Quartz-Nasturan-Kalzit-Gänge des Erzegebirges: *Z. angew. Geol., 15,* 240-241.

Naumov, G.B. & Dorofeyeva, V.A., 1975: Chemical nature of the acidity evolution in endogenous solutions. *Geokhomiya, 2,* 248-258, (in Russian). Abstract in *Geochem. Int., 12(1),* 201 (1975).

Needham, R.S. & Roarty, M.J., this volume: Regional survey of metallic mineralization in the Pine Creek Geosyncline. *Proceedings of the International Uranium Symposium on the Pine Creek Geosyncline.*

Needham, R.S., Crick, I.H. & Stuart-Smith, P.G., this volume: Regional Geology of the Pine Creek Geosyncline. *Proceedings of the International Uranium Symposium on the Pine Creek Geosyncline.*

Page, R.W., Compston, W. & Needham, R.S., this volume: Geochronology and evolution of the late Archaean basement and Proterozoic rocks in the Alligator Rivers Uranium Fields, Northern Territory Australia. *Proceedings of the International Uranium Symposium on the Pine Creek Geosyncline.*

Poty, B.P., Leroy, J. & Cuney, M., 1974: Les incusions fluides dans les minerais des gisements d'uranium intragranitiques du Limousin et du Forez (Massif Central, France). *in. Formation of Uranium Ore Deposits. Proceedings of a Symposium, Athens.* International Atomic Energy Agency, Vienna, 569-582.

Riley, G.H., Binns, R.A. & Craven, D., this volume: Rb-Sr chronology of micas at Jabiluka. *Proceedings of the International Uranium Symposium on the Pine Creek Geosyncline.*

Roedder, E., 1973: Studies of fluid inclusions II: Freezing data and their interpretation. *Econ. Geol., 58,* 167-211.

Rosenberg, P.E., Burt, D.M. & Holland, H.D., 1967: Calcite-dolomite-magnesite stability relations in solutions: the effect of ionic strength. *Geochim. cosmochim. Acta, 31,* 391-396.

Sofer, Z. & Gat, J.R., 1972: Activities and concentrations of oxygen-18 in concentrated aqueous salt solution: analytical and geophysical implications. *Earth Planet. Sci. Lett. 15,* 232-238.

Takenouchi, S. & Kennedy, G.C., 1965: The solubility of carbon dioxide in NaCl solutions at high temperatures and pressures. *Am. J. Sci., 263,* 445-454.

Taylor, H.P., Jr., 1968: The oxygen isotope geochemistry of igneous rocks. *Contrib. Mineral. Petrol., 19,* 1-71.

Taylor, H.P., Jr., 1974: The application of oxygen and hydrogen isotope studies to problems of hydrothermal alteration and ore deposition. *Econ. Geol., 69,* 843-883.

Touret, J., 1972: Le facies granulite en Norvige meridionale et let inclusions fluides: paragneiss et quartzites. *Sciences Terre, 17,* 179-193.

Truesdell, A.H., 1974: Oxygen isotope activities and concentrations in aqueous salt solutions at elevated temperatures — Consequences for isotope geochemistry. *Earth Planet. Sci. Lett., 23,* 387-396.

Yanatieva, 1946: *in* Seidell & Linke, 1965: *Solubilities of Inorganic and Metal Organic Compounds,* 4th edition, Volume 2.

Ypma, P.J.M., 1965: An instrument for geobarometry of fluid inclusions. (abstract). *Spec. Pap. geol. Soc. Am., 87.*

A STABLE ISOTOPE STUDY OF THREE DEPOSITS IN THE ALLIGATOR RIVERS URANIUM FIELD, N.T.

T. H. Donnelly[1] and John Ferguson[2]

1. CSIRO Baas Becking Laboratory, P.O. Box 378, Canberra City, ACT, 2601, Australia
2. Bureau of Mineral Resources, P.O. Box 378, Canberra City, ACT, 2601, Australia

ABSTRACT

Major Lower Proterozoic stratabound uranium deposits in the Alligator Rivers Uranium Field occur in the lower member of the Cahill Formation. These Lower Proterozoic sediments have undergone regional metamorphism, at about 1800 m.y., to medium-grade. Peneplanation occurred with collapse dolines being developed in the carbonate-rich units of the Cahill Formation, which became the sites of uranium concentration. At around 1700 m.y. these structures were largely sealed by infill and alluvium. Intrusion of the post-orogenic Oenpelli Dolerite, at around 1688 m.y. predates the deposition of the basal Carpentarian strata of the Kombolgie Formation. The deposits examined in this stable isotope study, Jabiluka One and Two, Koongarra and Ranger 1, have features in common, for example; the absence of massive bedded carbonate within ore-zones and their reappearance outside of these zones, association with retrograde metamorphism found in the breccia zones.

Bedded sulphides adjacent to ore-zones have $\delta^{34}S$ values (av. = +2.2‰, σ = 0.9‰) indicative of a magmatic sulphur source. Preliminary isotope data on sulphides from correlated units across the Pine Creek Geosyncline suggest similar $\delta^{34}S$ values. These values suggest that bacterial sulphate reduction was absent in this area at this period and the seawater sulphate in which the Cahill Formation sediments were laid down had $\delta^{34}S$ values ~0‰.

In contrast, the ore-zone sulphides ($\delta^{34}S$ = -6 to +7‰) formed by either a low temperature process involving bacterial sulphate reduction, or by a hydrothermal process. Coexisting bedded and ore-zone sulphides at Jabiluka record similar temperatures of about 270°C. The thermal event is explained as the effect of a hydrothermal solution entering the area after emplacement of ore-sulphides. It is suggested that this event correlates with an igneous episode such as the emplacement of Oenpelli Dolerite or volcanic units in the Katherine River Group.

Massive and bedded carbonates have $\delta^{13}C$ values indicative of a sedimentary marine origin. Their $\delta^{18}O$ values are similar in range to ore-zone carbonate, and are not primary values. Ore-zone carbonate have $\delta^{13}C$ values which indicate their formation from a mixture of bedded carbonate and organically-derived CO_2. The proportion of the latter carbon source is greater at Koongarra. Graphite from the Jabiluka ore-zone has mainly normal sedimentary marine $\delta^{13}C$ values, whilst from Koongarra all $\delta^{13}C$ values are altered which indicates greater reactions involving organic matter at this deposit; in agreement with carbonate results. Ore-zone carbonate also shows a $\delta^{13}C/\delta^{18}O$ correlation which suggests this trend is primary and the reaction which formed the correlation was *in situ*. The correlation is explained in terms of an oxidising groundwater entering an organic-rich zone, and the $\delta^{18}O$ values are in agreement with the recrystallisation of carbonates throughout the area by groundwaters.

Whilst the isotope data are not unequivocal, the low temperature model (≤85°C) is favoured because, (1) it most simply explains $\delta^{34}S$, $\delta^{13}C$ and $\delta^{18}O$ patterns of ore-zone sulphides and carbonates, and (2) the $\delta^{13}C/\delta^{18}O$ correlation of ore-zone carbonate suggests retention of original isotopic compositions and *in situ* reactions, and is best explained in terms of groundwater reactions in the collapse dolines.

INTRODUCTION

Three major uranium deposits of the Alligator Rivers Uranium Field (Jabiluka One and Two, Koongarra, and Ranger 1), which occur in the Lower Proterozoic Cahill Formation (Fig. 1) have been isotopically examined. This study is so far the most extensive stable isotope investigation of minerals associated with uranium mineralisation in the Pine Creek Geosyncline. The data obtained relate to (1) the evolution of the Geosyncline, from ~2500 m.y. to younger geological periods, (2) the onset of bacterial sulphate reduction as a major process, and (3) the evolution of seawater sulphate sulphur isotope compositions to ^{34}S enriched values, shown from at least the Cambrian onwards. The isotope data have been obtained from sulphides, carbonates and organic matter (identified as graphite in the areas studied), from both ore-zones and adjacent sediments.

REGIONAL GEOLOGY

The uranium deposits examined in this study have been described by Hegge, 1977 (Jabiluka), Foy & Pedersen, 1975 (Koongarra), and Eupene *et al.*, 1975 (Ranger). The

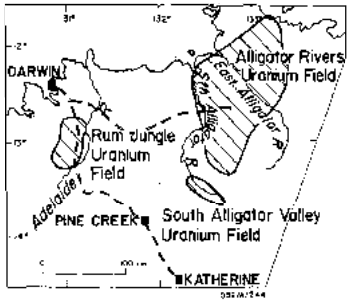


Figure 1. The Alligator Rivers Uranium Field, N.T., in which major stratabound uranium deposits occur.

regional geological setting, and a comparative review of these deposits is described by Needham *et al.* (this volume), Needham & Stuart-Smith, (this volume), Hegge *et al.* (this volume) and Ewers & Ferguson (this volume). For this study only those aspects relevant to the interpretation of the stable isotope data are included.

The basement to the Lower Proterozoic rocks in the area is the mantled gneiss dome of the Nanambu Complex. This complex comprises Archaean granitoids with a primary age of ~2500 m.y. (Page *et al.*, this volume) and accreted Lower Proterozoic feldspathic and quartzitic gneisses and schists developed during an ~1800 m.y. regional metamorphic event. The base of the Lower Proterozoic succession is represented by the Kadadu Group which is overlain, apparently conformably, by the Cahill Formation. The Cahill Formation is overlain, in places unconformably, by an assemblage of dominantly arenite-argillite rocks which belong to the Nourlangie Schist. Extensive intrusion of continental tholeiite sills followed. Orogenesis occurred at about 1800 m.y. and was accompanied by late-orogenic granitic development continuing into the early Middle Proterozoic. This was followed by post-orogenic intrusion of continental tholeiites. Peneplanation and deposition of the basal Middle Proterozoic Kombolgie Formation followed. Rocks in the Alligator Rivers Uranium Field were regionally metamorphosed by the ~1800 m.y. orogenic event to medium or high-grade; within areas of uranium mineralization, very low-temperature retrograde metamorphism is found.

ORE-ZONES

The Alligator Rivers uranium deposits are stratabound within the lower member of the Cahill Formation; a unit dominated by carbonaceous schist and massive carbonates (Needham & Stuart-Smith, 1976). Some features common to the deposits being studied are, the absence of massive bedded carbonates within the ore-zones and their reappearance outside of these zones (Eupene *et al.*, 1975; Foy & Pedersen, 1975), their relationship to the regional unconformity surface separating Lower and Middle Proterozoic, and the intimate association of the uranium mineralisation to zones of post-tectonic brecciation and chloritisation (Ewers & Ferguson, this volume). The zones of brecciation, called collapse dolines (Ferguson *et al.*, this volume) would have been permeable to solutions. Uraninite and galena ages from the Alligator Rivers Uranium Field indicate two different periods of possible mineralisation or mobilisation, namely 1700± m.y. and 800-900 m.y. (Hills & Richards, 1976).

Black shale and organic-rich carbonates have concentrated uranium (Ferguson & Winer, this volume) but no syngenetic deposits have been found, and no appreciable mobilisation appears to have occurred during the ~1800 m.y. regional metamorphism in areas of medium grade (Ferguson, this volume). Peneplanation of the terrain followed with the postulated development of collapse dolines which became the sites of uranium mineralisation. At ~1700 m.y. these structures are thought to to have been largely sealed to permeable solutions by infill and alluvium. Ferguson *et al.* (this volume) postulate that at the time of intrusion of the Oenpelli Dolerite at around 1688 m.y. or during emplacement of volcanic units in the Katherine River Group at about 1650 m.y. (Page *et al.*, this volume) that the heat generated was sufficiently high to metamorphose the diagenetic assemblages present in the collapsed dolines.

EXPERIMENTAL PROCEDURES

Standard techniques were used to separate sulphides and carbonates which included microdrilling and hand picking under a binocular microscope. Organic-rich samples were treated with acid to remove carbonates and silicates. All separated minerals were examined by XRD to check their purity. Some of the carbonate and all the carbonaceous residues were isotopically analysed by Geochron Laboratories, Massachusetts, U.S.A. Sulphides were prepared and purified for mass spectrometry by the methods of Kaplan *et al.* (1970). Carbonates were reacted with phosphoric acid as described by McCrea (1950). The $\delta^{18}O$ values are corrected for acid liberation fractionation according to the modified values of Sharma & Clayton (1965). Reaction times were normally a few days for calcite and several weeks for dolomite.

Purified SO_2 and CO_2 samples were isotopically examined on a Micromass 602D mass spectrometer and the $\delta^{34}S$, $\delta^{13}C$ and $\delta^{18}O$ values have a reproducibility of $\sim\pm 0.2‰$. The $\delta^{34}S$ values are reported relative to Canon Diablo Troilite (CDT), the $\delta^{18}C$ relative to Pee Dee Belemnite (PDB) and $\delta^{18}O$ relative to Standard Mean Ocean Water (SMOW).

STABLE ISOTOPE RESULTS AND DISCUSSION

1. Bedded Sulphides

The $\delta^{34}S$ values for all bedded sulphides, from sediments adjacent to the uranium ore deposits, are shown in figure 2. The bedded sulphides are predominantly pyrite (some chalcopyrite and sphalerite) and their $\delta^{34}S$ values occur in the restricted range +0.5‰ to +3.5‰ (av. $\delta^{34}S = +2.2‰$, $\sigma = 0.9‰$). Similar $\delta^{34}S$ values for bedded sulphides have been obtained in other parts of the Pine Creek Geosyncline. A pyrite sample from carbonaceous shale of the Koolpin Formation (El Sherana uranium deposit, South Alligator River Valley) has a $\delta^{34}S$ value of -1.2‰ (Ayres & Eadington, 1975), whilst the syngenetic base metal sulphide Mount Bonnie deposit, which occurs in the lowest part of the Kapalga Formation (Goulevitch, this volume), also has a restricted $\delta^{34}S$ range with an average value of +2.2‰ (Donnelly *et al.*, in prep). Preliminary isotope studies of bedded sulphides (mainly pyrite and pyrrhotite) from various areas of the Pine Creek Geosyncline, at stratigraphic levels thought to be equivalent to the Cahill Formation, have so far yielded a restricted $\delta^{34}S$ range near zero permil (Donnelly, unpublished data).

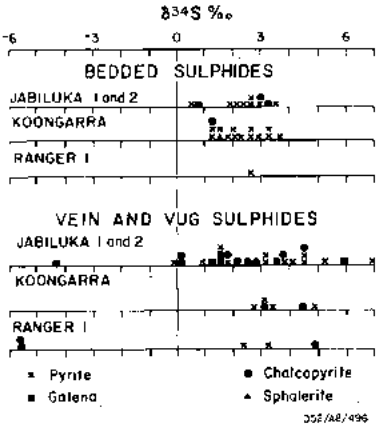


Figure 2. $\delta^{34}S$ values for bedded sulphide sediments adjacent to ore-zones and vein vug sulphides. Note the somewhat wider spread of $\delta^{34}S$ values, with much greater variety of sulphides, in the ore-zones compared to bedded sulphides.

The bedded sulphides of the Alligator Rivers Uranium Field have undergone regional metamorphism to medium-grade. Whilst the thermal event may be recorded by coexisting sulphides (Rye & Ohmoto, 1974), the overall $\delta^{34}S$ range of the dispersed bedded sulphides should not be affected. The bedded sulphides examined in this study formed at some time after 2500 m.y. and before the ~1800 m.y. metamorphic event. They have $\delta^{34}S$ values similar to that found for bedded sulphides of earlier geological periods in Australia (Donnelly *et al.*, 1978; Lambert *et al.*, 1978). These isotopic compositions suggest that the sulphides precipitated from hydrothermal solutions containing magmatic sulphur, probably derived by volcanogenic processes. In contrast, post Middle Proterozoic volcanogenic sulphides are characterised by $\delta^{34}S$ values that are heavier

on the average than normal magmatic values, reflecting reduction of isotopically heavy seawater sulphate (Sangster, 1968; Rye & Ohmoto, 1974) or isotopic exchange between magmatic sulphide and marine sulphate (Sasaki & Kajiwara, 1971).

Whilst the sulphur isotope data for Archaean bedded sulphides could be interpretated as indicating very low levels of sulphate in the contemporaneous hydrosphere, and absence of widespread oxygenated conditions, it appears most probable that photosynthesis was taking place during the Archaean (Eichmann & Schidlowski, 1975; Cloud, 1976). Cloud proposed that photosynthetic micro-organisms were initially dependent upon Fe^{2+} as the oxygen 'sink' until the development of internal oxygen metabolising enzymes, with resultant proliferation around 2300 m.y. Certainly reduced sulphur would have been another important 'sink', and the resultant seawater sulphate, whilst not indicative of an oxygen atmosphere, may have been present at relatively early geological periods, as evidenced by Archaean barite deposits (Lambert *et al.*, 1978). The evidence of Crick & Muir (this volume) indicates the presence of some sulphate during formation of the earliest sediments in the Pine Creek Geosyncline.

Sulphur isotope data for bedded sulphides, so far examined, from the Pine Creek Geosyncline are in agreement with a magmatic sulphur source (probably by volcanogenic processes). It appears most likely that sulphate was present at this stage, but with a $\delta^{34}S$ value also near zero permil. The isotope data also indicate that bacterial sulphate reduction, if present, was a very minor process. The proliferation of bacterial sulphate reduction is the suggested mechanism whereby ocean sulphate $\delta^{34}S$ values evolved from magmatic values to the ^{34}S enriched values noted from Cambrian to younger geological periods (Holser & Kaplan, 1968).

The oldest rocks in which isotope evidence has indicated some bacterial sulphate reduction are in the ~2700 m.y. Michipicoten B.I.F., Canada (Goodwin *et al.*, 1976). In Australia the oldest rocks in which bacterial sulphate reduction is indicated from isotopic evidence is the ~1600 m.y. H.Y.C. deposit in the McArthur Basin, N.T. (Smith & Croxford, 1973). The sulphur isotopic compositions of bedded sulphide, from sediments close to the basement to younger units of the Pine Creek Geosyncline, should change markedly recording the advent of bacterial sulphate reduction. Therefore, it is possible the distinct $\delta^{34}S$ values for bedded sulphides in these uranium bearing lower sequences may be useful for broad-scale stratigraphic correlations across the Pine Creek Geosyncline. This study is at present under investigation (Donnelly *et al.*, unpublished data).

2. Vein or Vug Sulphides

$\delta^{34}S$ values for all vein or vug sulphides from the uranium ore-zones are shown in figure 2. In contrast to the bedded sulphides these are:

1) usually a mixture of two or more of the minerals, pyrite, chalcopyrite, galena and sphalerite,
2) not dominated by pyrite, and
3) characterised by a much wider spread of $\delta^{34}S$ values (-6‰ to +7‰).

This range of $\delta^{34}S$ values is similar to that found for uranium ore sulphides at Rockhole and El Sherana, South Alligator Uranium Field (-6‰ to +12‰) reported by Ayres & Eadington (1975); which they tentatively suggested meant bacterial sulphate reduction and consequently low-temperature processes of uranium ore formation.

Two models can explain the range of $\delta^{34}S$ values found for vein or vug sulphides:

1) Low temperature model.

Anaerobic environment with bacterial sulphate reduction; temperatures may have been ambient, or no higher than ~85°C (Rozanova & Khudiakova, 1974), for survival of bacteria, and under conditions of a restricted sulphate supply.

2) High temperature model.

A multi-step process is necessary to produce the $\delta^{34}S$ range. This involves, (a) the presence of sulphate and sulphide in a hydrothermal solution (changing redox conditions can then produce ^{32}S enriched sulphides; Ohmoto, 1972), (b) organic and/or inorganic sulphate reduction ($\delta^{34}S(SO_4^{2-}) \gtrsim +7‰$) producing ^{34}S enriched sulphides (Ohmoto & Rye, 1979).

Both models would infer that isotopically heavy seawater sulphate was present while the ore-zone metals were accumulating.

3. Temperature Studies

Fluid inclusion studies at Jabiluka by Ypma & Fuzikawa (this volume) have indicated a hydrothermal event. Ferguson *et al.*, (this volume) have detected disseminated euhedral uraninite in each of the deposits examined in this study, with marked development of this form of uranium at Ranger 1, They noted that a Russian study of hydrothermal uranium deposits (Tugarinov & Nanmov, 1969) indicated the euhedral form of uraninite occurs only at temperatures above 250°C.

The application of sulphur isotope geothermometry to the uranium deposits was carried out to try to gain more information on the thermal history of these deposits. This technique is based on the equilibrium sulphur isotope fractionation between coexisting sulphur-bearing minerals. The important sulphur species in hydrothermal systems have been examined and their isotopic fractionations are now known (Rye & Ohmoto, 1974).

Four coexisting sulphide pairs, representing both bedded and ore-zone sulphides were analysed from the Jabiluka deposits (Table 1). Whilst all calculated temperatures (using data from Kajiwarra & Krouse, 1971) are similar this does not necessarily mean there was a reasonable approach to equilibrium. However, the average calculated temperature of around 270°C (± 30°C) is in good agreement with the noted minimum temperature from the presence of euhedral uraninite. Rye & Ohmoto (1974) noted that although pyrite coexisting with various other sulphides (such as galena) have $\Delta\ \delta^{34}S$ values large enough to produce accurate temperature calculations, they rarely give good temperatures because pyrite tends to precipitate over a much larger part of the paragenesis than other sulphides. This is not the case at Jabiluka where both bedded and vein or vug sulphides seem to be recording the one temperature event. As the ~1800 m.y. regional metamorphic event predates uranium

Table 1. $\delta^{34}S$ values of coexisting sulphides from ore zones and adjacent sediments and calculated temperatures from $\Delta\ \delta^{34}S$ values.

Sulphide	Description	$\delta^{34}S$ ‰	$\Delta\ \delta^{34}S$ ‰	Temperature* °C
1. py cpy	Bedded py/cpy in graphitic schist, Mine Sequence, Jabiluka Two	+2.3 +0.7	= +1.6	257°
2. py cpy	Vug filling, Mine Sequence Jabiluka Two	+4.4 +2.6	= +1.8	227°
3. py cpy	Vein, Mine sequence Jabiluka Two	+2.9 +1.6	= +1.3	315°
4. py gn	Vug filling, Mine Sequence Jabiluka Two	+5.2 +1.4	= +3.8	265°

*Temperatures calcuated using isotope fractionation factors of Kajiwarra & Krouse (1971).

mineralisation it is suggested that these calculated temperatures are best explained in terms of a later thermal event, possibly related to the emplacement of the Oenpelli Dolerite at ~1688 m.y. (Page *et al.*, this volume), which caused isotopic exchange in earlier forms of coexisting sulphides.

Coexisting sulphides from Ranger 1 were isotopically examined. Pyrite, chalocpyrite and galena, from bedded sulphides and/or vein or vug sulphides, had the distinct $\delta^{34}S$ values noted previously (Fig. 2), however, either the individual sulphides of each pair examined had the same $\delta^{34}S$ value, or their $\Delta\ \delta^{34}S$ value indicated a disequilibrium situation. Ewers & Ferguson (this volume) noted that at Ranger 1, pyrite is commonly partially replaced by chalcopyrite and in some cases by galena. The isotope data agree with this observation and indicate the replacement took place after the ~1688 m.y. thermal event. The galena was probably derived from radioactive decay of uranium, as all lead examined at this deposit has been found to be radiogenic (Hills & Richards, 1973).

4. Bedded Carbonate

The isotope results for carbonate (predominantly dolomite), in sedimentary strata adjacent to the ore-zones and massive carbonate formations further removed from the deposits, are shown in figures 3 and 4. The carbon isotopic compositions of all these carbonates are compatible with normal sedimentary marine origin (Keith & Weber, 1964). The oxygen isotopic compositions, with an average value around +17‰, are slightly lower than the average value of +20‰ reported by Veizer & Hoefs (1976) for sedimentary dolomite formed during the period ~1600-2500 m.y. The $\delta^{18}O$ ranges for bedded and massive carbonates and ore-zone carbonates are similar, with ore-zone carbonates extended to lower $\delta^{18}O$ values (down to +7‰, as against +13‰ for bedded carbonates). $\delta^{18}O$ changes of this magnitude in carbonates are usually indicative of recrystallisation involving groundwater (c.f. Hudson, 1977).

When recrystallation of extensive areas of carbonates occur, in general, their original $\delta^{13}C$ values are retained but their new $\delta^{18}O$ values will reflect the isotopic composition of the water, and the relative proportions of water and carbonate involved, and the temperature of recrystallation. It has been suggested (Binns *et al.*, this volume) that the temperature and fluid associated with regional metamorphism changed the original massive and bedded

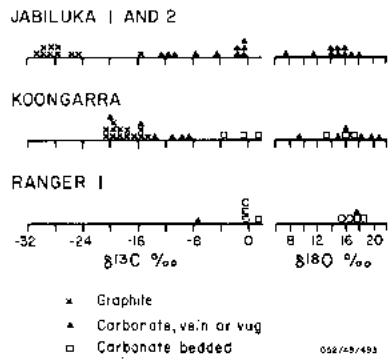


Figure 3. $\delta^{13}C$ and $\delta^{18}O$ values for bedded carbonate in sediments adjacent to ore-zones and vein or vug carbonate. $\delta^{13}C$ values for ore-zone graphite are also shown. Note the narrow range of $\delta^{13}C$ values for bedded carbonate compared to ore-zone carbonate, which shows formation to varying degrees from organically-derived CO_2.

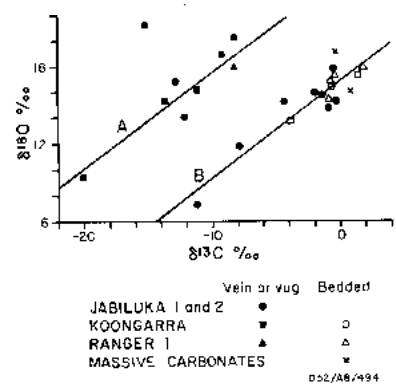


Figure 4. $\delta^{13}C/\delta^{18}O$ correlation diagram for ore-zone carbonates from (A) Koongarra and (B) Jabiluka One and Two. Note similar slopes from the two deposits although there is greater organically-derived CO_2 involved in the formation of carbonates at Koongarra.

carbonate $\delta^{18}O$ values to the values now found for ore-zone carbonate. The metamorphism, which occurred at depths in excess of 15km (Ferguson, this volume), would have mainly involved reactions with a hydrous phase comprising liberated crystalline waters. Even allowing for minor interstitial water the fluid:rock ratio would be low. Therefore, the $\delta^{18}O$ content of the massive carbonates would dominate the system and the dolomitic marbles would tend to retain original $\delta^{18}O$ values. Shieh & Taylor (1969) in their isotopic examination of marbles formed under high and low metamorphic grade and at contact metamorphic zones found only slight lowering of $\delta^{18}O$ (& $\delta^{13}C$) values unless skarn reactions were involved (CO_2 enriched in ^{13}C & ^{18}O is lost from the system). No such reactions have been noted in the areas studied and the low $\delta^{18}O$ values found are best explained in terms of recrystallisation by groundwater. High fluid:rock ratios would be expected during the formation of the unconformity surface and later while the collapse dolines were relatively open structures. The occurrence of the lowest $\delta^{18}O$ values in ore-zone carbonates is in agreement with transport by, and recrystallisation from, groundwater.

5. Vein or Vug Carbonates

The isotope results for all vein or vug carbonates from the uranium ore-zones are shown in figure 3. In contrast to the narrow spread of $\delta^{13}C$ values for bedded and massive carbonates, vein or vug carbonates have a range of $\delta^{13}C$ from normal sedimentary marine carbonate to ^{13}C depleted values (up to -20‰) showing the influence of organically-derived isotopically light CO_2 in their formation. The $\delta^{18}O$ range is basically similar to that found for bedded and massive carbonates, extending to values as low as +7‰.

Vein or vug carbonates show a reasonable correlation between $\delta^{13}C$ and $\delta^{18}O$ for the two most extensively sampled deposits, Jabiluka One and Two and Koongarra (Fig. 4). It is suggested that the two curves shown represent, at least, an approach to equilibrium precipitation of the carbonates from isotopically similar waters; the difference between the two curves implies greater involvement of organically-derived CO_2 at Koongarra, relative to Jabiluka One and Two. The $\delta^{13}C/\ \delta^{18}O$ correlation implies original trends have been retained, and *in situ* reaction. However, the correlation excludes anaerobic oxidation of organic matter, which can be concurrent with biological sulphate reduction, as the process producing the organically-derived CO_2.

The correlation is most satisfactorily explained as the result of oxidising groundwater entering an organic-rich zone. The lack of alteration in $\delta^{13}C$ content of adjacent bedded carbonate suggests these solutions did not contain biologically-derived CO_2. On entering the collapse dolines the groundwaters oxidised organic matter producing CO_2 which combined with marine carbonate in solution, and precipitated vein or vug carbonate. The degree of oxidation of the organic matter was related to the oxygen content of the groundwater.

An alternative to the above model is one involving hydrothermal solutions entering the collapse dolines. French (1966) has shown that at temperatures ~200°C interaction of diagenetic solutions with graphite generates methane and CO_2. If increasing temperature causes greater amounts of CO_2 to be produced the higher temperatures will in turn produce lower $\delta^{18}O$ values (Matthews & Katz, 1978). However, as the carbonate, which has formed to varying degrees from organically-derived CO_2, is apparently confined to the ore-zones this suggests reaction in these areas involved organic carbon distinct to these areas (i.e. fresh organic matter) and the correlation is best explained in terms of the former model.

6. Graphite from Ore-Zones

The samples of graphite were obtained from Jabiluka One and Two and Koongarra, and their $\delta^{13}C$ values are shown in figure 3. Eichmann & Schidlowski (1975) have shown that the isotopic composition of biogenic kerogen in unaltered sedimentary rocks throughout the Precambrian is fairly constant and similar to the values in the Phanerozoic

($\delta^{13}C$ = -25‰±6‰). From figure 3 it can be seen that, except for one ^{13}C enriched value, all Jabiluka graphite samples lie in this range. However, the bulk of the Koongarra graphite samples have $\delta^{13}C$ values outside of this range indicating it has undergone reactions to a greater degree than at Jabiluka.

Carbonate within the ore-zone breccia at these two deposits indicate incorporation of organically-derived CO_2, the degree of incorporation being greater at Koongarra. These data are in agreement with the carbon isotopic compositions of the graphite analysed from these deposits. The ore-zone carbonate was suggested to have formed *in situ*, from CO_2 produced during aerobic oxidation of organic matter by groundwaters and marine carbonate in these waters. The presence of thucholite, which would not have survived the regional metamorphism, has been reported from Ranger 1, No. 3 orebody (G. H. Taylor *in* Eupene, 1979) and Jabiluka (Binns *et al.*, this volume) suggesting also a later generation of relatively fresh organic matter.

The interpretation of the carbon isotopic compositions of ore-zone graphite (and carbonate) suggests the zones were at some stage in their development active areas for the accumulation of organic matter.

CONCLUSIONS

The isotope data obtained from minerals within and adjacent to three uranium ore deposits in the Alligator Rivers Uranium Field have provided some constraints on defining the evolution of these deposits. Whilst the interpretation of ore-zone sulphide $\delta^{34}S$ values does not allow one single model, the low temperature model ($\lesssim$85°C) involving bacterial sulphate reduction under conditions of restricted sulphate supply provides the simplest explanation of the data. Relatively low temperatures are also suggested from the interpretation of the stable isotope results on ore-zone carbonate and graphite. These data are in agreement with relatively low temperature groundwater reactions in zones of relatively fresh organic matter. The fact that coexisting sulphides from ore-zones and adjacent metasediments have recorded the same temperature event is best explained as a thermal event after emplacement of the sulphides.

In contrast to the relatively wide spread $\delta^{34}S$ values for ore-zone sulphides all bedded sulphides from the adjacent Lower Proterozoic sediments have a narrow spread of $\delta^{34}S$ values near zero permil. This suggests a magmatic origin for this sulphur (possibly by volcanogenic processes), and that sulphate reducing bacteria were not present, at least, up to the time of deposition of the Cahill Formation. Because of the distinctive $\delta^{34}S$ value of bedded sulphide in these lower units this isotopic signature may be an aid for broad stratigraphic correlations.

Bedded and massive carbonate have $\delta^{13}C$ values indicative of a sedimentary origin. This is in contrast to ore-zone carbonate $\delta^{13}C$ values which indicate formation involving organically-derived CO_2.

The constraints imposed on the evolution of the uranium deposits by the stable isotope study have resulted in the following suggested model. With the development of brecciated ore-zones produced by a process of collapse dolines these systems acted as structural traps for organic matter, clays, metals and carbonate from groundwaters (Ferguson *et al.*, this volume). Around 1700 m.y. the deposits were effectively sealed by infill and alluvium. Bacterial sulphate reduction under conditions of restricted sulphate supply produced H_2S for formation of vein and vug sulphides. Groundwaters circulated through the area and recrystallisation of carbonates recorded a similar $\delta^{18}O$ range (Fig. 3). This solution did not carry organically-derived CO_2 as the $\delta^{13}C$ values for carbonates away from ore-zones were unchanged. The oxidising groundwaters entered the organic-rich brecciated zones, and oxidation of organic matter formed some CO_2 which, with marine carbonate in solution,

later formed the ^{12}C-enriched vein or vug carbonates. The amount of organic CO_2 produced was proportional to the oxygen content of the water, and therefore resulted in the rough correlations shown in figure 4. Later, epithermal solutions generated at the time of the emplacement of the Oenpelli Dolerite (1688±m.y.) or volcanic units in the Katherine River Group (at about 1650 m.y.) caused isotopic exchange in coexisting sulphides in both sediments and ore-zones. Some lowering of carbonate $\delta^{18}O$ values could occur (depending if the carbonate were recrystallised), however this would not affect the $\delta^{13}C/\ \delta^{18}O$ correlation.

ACKNOWLEDGEMENTS

We are indebted to Geopeko Ltd., Noranda Australia Ltd., Pancontinental Mining Ltd. and Queensland Mines Ltd. for supply of, and access to, rock samples. The following people are thanked for discussion of the isotope data and critically assessing an early draft of this manuscript: G. R. Ewers, I.B. Lambert and J.F. Truswell. P. Ryan and N. Davis are thanked for help in preparing samples for isotope analyses. The Bass Becking Laboratory is supported by the Australian Minerals Industries Research Association Ltd., B.M.R and C.S.I.R.O.

One of the authors (J.F.) acknowledges permission to publish from the Director, Bureau of Mineral Resources, Geology and Geophysics, Canberra, A.C.T.

REFERENCES

Ayres, D.E., & Eadlington, P.J., 1975: Uranium mineralisation in the South Alligator Valley. *Miner. Deposita, 11,* 27-41.

Binns, R.A., McAndrew, J., & Sun, S-S., this volume: Origin of uranium mineralisation at Jabiluka. *Proceedings of the International Uranium Symposium on the Pine Creek Geosyncline.*

Cloud, P., 1976: Major features of crustal evolution. *Du Toit Memorial Lecture, 14, Geol. Soc. Sth. Africa, Annexure to Volume 79.*

Crick, I.H., & Muir, M.D., this volume: Evaporites and uranium mineralization in the Pine Creek Geosyncline. *Proceedings of the International Uranium Symposium on the Pine Creek Geosyncline.*

Donnelly, T.H., Goulevitch, J., & Roberts, W.M.B., in prep.: Preliminary genetic implications of limited stable isotope data from the Mt. Bonnie (Ag, Pb, Au) deposit, Pine Creek Area.

Donnelly, T.H., Lambert, I.B., Oehler, D.Z., Hallberg, J.A., Hudson, D.R., Smith, J.W., Bavington, O.A., & Golding, L., 1978: A reconnaissance study of stable isotope ratios in Archaean rocks from the Yilgarn Block, Western Australia. *J. geol. Soc. Aust., 24,* 409-420.

Eichmann, R., & Schidlowski, M., 1975: Isotopic fractionation between coexisting C(org)- C(carb) pairs in Precambrian sediments. *Geochim. cosmochim. Acta, 39,* 585-595.

Eupene, G.S., 1979: Stratigraphic, structural and temporal control of mineralisation in the Alligator River Uranium Province, N.T., Australia *in* (ed. J.D. Ridge) Proceedings of the fifth International Symposium on the genesis of ore deposit, Snowbird, Utah, August 1978 (in press).

Eupene, G.S., Fee, P.H., & Colville, R.G., 1975: The Ranger One uranium deposits. *in* (ed. C.L. Knight) *Economic Geology of Australia and Papua New Guinea, Australas. Inst. Min. Metall., Monograph Series No. 5, 1. Metals,* 308-317.

Ewers, G.R. & Ferguson, John, this volume: Mineralogy of the Jabiluka, Ranger, Koongarra and Nabarlek uranium deposits. *Proceedings of the International Uranium Symposium on the Pine Creek Geosyncline.*

Ferguson, John, this volume: Metamorphism in the Pine Creek Geosyncline and its bearing on stratigraphic correlations. *Proceedings of the International Uranium Symposium on the Pine Creek Geosyncline.*

Ferguson, John, Ewers, G.R., & Donnelly, T.H., this volume: Model for the development of economic uranium mineralisation in the Alligator Rivers Uranium Field. *Proceedings of the International Uranium Symposium on the Pine Creek Geosyncline.*

Ferguson, John, & Winer, Paul, this volume: Pine Creek Geosyncline: Statistical treatment of whole rock chemical data. *Proceedings of the International Uranium Symposium on the Pine Creek Geosyncline.*

Foy, M.F., & Pedersen, C.P., 1975: The Koongarra uranium deposit. *in* (ed. C.L. Knight) *Economic Geology of Australia and Papua New Guinea, Australas. Inst. Min. Metall., Monograph Series No. 5, 1. Metals,* 317-321.

French, B.M., 1966: Some geological implications of equilibrium between graphite and a C-H-O gas phase at high temperatures and pressures. *Review of geophysics, 4,* 223-253.

Goodwin, A.M., Monster, J., & Thode, H.C., 1976: Carbon and sulphur isotope abundance in Archaean iron-formations and early Precambrian life. *Econ. Geol., 71,* 870-892.

Goulevitch, J., this volume: Stratigraphy of the Kapalga Formation in the Pine Creek Area and its relationship to base metal mineralisation. *Proceedings of the International Uranium Symposium on the Pine Creek Geosyncline.*

Hegge, M.P., 1977: Geologic setting and relevant exploration features of the Jabiluka Uranium Deposits. *Proc. Australas. Inst. Min. Metall., 264,* 19-32.

Hegge, M.R., Mosher, D.V., Eupene, G.S. & Anthony, P.J., this volume: Geologic setting and comparative review of the East Alligator uranium deposits and prospects. *Proceedings of the International Uranium Symposium on the Pine Creek Geosyncline.*

Hills, J.H., & Richards, J.R., 1973: Radiogenic Lead in north Australian Galenas. *Nature Phys. Sci., 241,* 18-19.
Hills, J.H., & Richards, J.R., 1976: Pitchblende and galena ages in the Alligator Rivers Region, Northern Territory, Australia. *Miner. Deposits, 11,* 133-154.
Holser, W.T., & Kaplan, I.R., 1966: Isotope geochemistry of sedimentary sulphates. *Chem. Geol., 1,* 93-135.
Hudson, J.D., 1977: Stable isotopes and limestone lithification. *J. geol. Soc. Lond., 133,* 637-660.
Kajiwara, Y., & Krouse, H.R., 1971: Sulphur isotope partitioning in metallic sulphide systems. *Can. J. Earth Sci., 8,* 1397-1408.
Keith, M.L., & Weber, J.N., 1964: Carbon and oxygen isotopic composition of selected limestones and fossils. *Geochim. cosmochim. Acta, 28,* 1787-1816.
Lambert, I.B., Donnelly, T.H., Dunlop, J.S.R., & Groves, D.I., 1978: Stable isotope compositions of early Archaean sulphate deposits of probable evaporitic and volcanogenic origins. *Nature, 276,* 808-811.
Matthews, A., & Katz, A., 1977: Oxygen isotope fractionation during the dolomitization of calcium carbonate. *Geochim. cosmochim. Acta, 41,* 1431-1438.
Needham, R.S., Crick, I.H., & Stuart-Smith, P.G., this volume: Regional Geology of the Pine Creek Geosyncline. *Proceedings of the International Uranium Symposium on the Pine Creek Geosyncline.*
Needham, R.S., & Stuart-Smith, P.G., 1976: The Cahill Formation — host to uranium deposits in the Alligator Rivers Uranium Field, Australia. *BMR J. Aust. Geol. Geophys., 1,* 321-334.
Needham, R.S., & Stuart-Smith, P.G., this volume: Geology of the Alligator Rivers Uranium Field. *Proceedings of the International Uranium Symposium on the Pine Creek Geosyncline.*
Ohmoto, H., 1972: Systematics of sulphur and carbon isotopes in hydrothermal ore deposits. *Econ. Geol., 67,* 551-578.
Ohmoto, H., & Rye, R.O., 1979: Isotopes of sulphur and carbon, *in* (ed. H.L. Barnes) Geochmeistry of hydrothermal ore deposits, 2nd edition (in press).
Page, R.W., Compston, W., & Needham, R.S., this volume: Geochronology and evolution of the late Archaean basement and Proterozoic rocks in the Alligator Rivers Uranium Field, Northern Territory, Australia. *Proceedings of the International Uranium Symposium on the Pine Creek Geosyncline.*
Rozanova, E.P., & A.J. Khudiakova, 1974: A new con-sporulating thermophilic organism, *Desulfovibrio thermophilus* sp. n., reducing sulphates. *J. Mikro. Biologiya., 43,* 1069-1075.
Rye, R.O., & Ohmoto, H., 1974: Sulphur and carbon isotopes and ore genesis : A review. *Econ. Geol., 69,* 826-842.
Sangster, D.F., 1968: Relative sulphur isotope abundances of ancient seas and stratabound sulphide deposits. *Proc. geol. Ass. Canada, 19,* 79-91.
Sasaki, A., & Kajiwara, 1971: Evidence of isotopic exchange between seawater sulphate and some syngenic sulphide ores. *Spec. Issue Soc. Min, geol. Japan, 3,* 289-294.
Smith, J.W., & Croxford, N.J.W., 1973: Sulphur-isotope ratios in the McArthur lead-zinc-silver deposit. *Nature Phys. Sci., 245,* 10-12.
Tugarinov, A.L., & Naumov, V.B., 1969: Thermobaric conditions of formation of hydrothermal uranium deposits. *Geochem. Int., 6,* 89-102.
Veizer, J., & Hoefs, J., 1976: The nature of O^{18}/O^{16} and C^{13}/C^{12} secular trends in sedimentary carbonate rocks. *Geochim. cosomochim. Acta, 40,* 1387-1395.
Ypma, P.J.M., & Fuzikawa, K., this volume: Fluid inclusion studies as a guide to the composition of uranium ore forming solutions of the Nabarlek and Jabiluka deposits, N.T., Australia. *Proceedings of the International Uranium Symposium on the Pine Creek Geosyncline.*

NATURAL REACTOR STUDIES

G.H. Riley and M.J. Korsch

CSIRO Division of Mineral Physics, P.O. Box 136, North Ryde, N.S.W., 2113, Australia.

ABSTRACT

The Proterozoic uraninite deposits in the East Alligator River area of the Pine Creek Geosyncline contain high grade zones which could have supported natural sustained fission reactions.

Uranium isotopic abundance measurements on 39 samples from Koongarra, Jabiluka and Nabarlek do not provide evidence for significant ^{235}U depletion. Neodymium isotope measurements on a single sample from Nabarlek have no anomalous values that can be related to a fission product origin. A relatively high abundance of ^{143}Nd is interpreted as radiogenic from ^{147}Sm α-decay.

While no evidence for natural sustained fission results from this preliminary study, remobilization of uraninite may have had the effect of diluting isotopic anomalies to below detection levels.

INTRODUCTION

Uranium has three naturally occurring isotopes, all of which are unstable and experience α-decay. The major isotope, ^{238}U, has a half-life of 4.468 x 10^9y., ^{235}U has a half-life of 7.038 x 10^8y., and ^{234}U has a half-life of 2.446 x 10^5y. The natural abundances of ^{238}U and ^{235}U are well established as 99.275 atom % and 0.72 atom % respectively; natural abundance variations are unknown other than those relating to the natural sustained fission events at Oklo (International Atomic Energy Agency, 1975). The minor isotope, ^{234}U, has a secular equilibrium abundance of 55ppm. Large isotopic abundance variations of this isotope are well established in nature; the mechanism(s) causing disequilibrium values are generally well understood (Cherdynstev, 1971).

In addition to natural α-decay, ^{238}U and ^{235}U both suffer natural fission with accompanying neutron emission. The spontaneous fission half-life of ^{238}U is approximately 10^{16}y. and this isotope is dominant in natural neutron production as shown by both half life and isotopic abundance considerations. The current fission rate in 1 gram of uranium is about 1 fission event every 3 minutes, corresponding to almost 1 neutron per minute.

A sustained fission reaction in natural situations is only possible if fission of ^{235}U is induced and sufficient neutrons are contained to sustain the reaction. At the present isotopic abundance of ^{235}U this situation cannot arise; however, due to the relative α-decay half-lives of ^{238}U and ^{235}U, the higher abundance of ^{235}U in the Precambrian was sufficient for a sustained reaction if other conditions were suitable. The ^{235}U abundance in the Lower Proterozoic was >3%, a value comparable with that used in contemporary light water power reactors.

At the Oklo occurrence, nine extinct natural reactor zones have been identified. The uranium occurs as high grade pitchblende located as infillings in fracture zones in the Francevillian Series in the Lower Proterozoic of the Gabon. The age of mineralization is estimated to be approximately 2 x 10^9y. Evidence for natural sustained fission, which continued for approximately 2 to $5x10^5$ years in this deposit, is the isotopic depletion of ^{235}U and the occurence of stable, fission product isotopes: neodymium, samarium, cadmium, tellurium, ruthenium, rubidium, strontium, barium and certain noble gases.

The discovery of the Oklo reactors in 1972 has, not surprisingly, led to an intense search for similar phenomena in other uranium deposits with suitable age and grade thickness characteristics. None, apparently, have been found; it is regrettable, however, that the results of null experiments remain unrecorded. The lack of evidence for duplication of the Oklo event(s) elsewhere may result from implausibly unique circumstances at the Oklo deposit. More likely, however, the absence of data confirming other fission localities is

related to lack of adequate measurements of ore bodies now mined out, to remobilization of reactor zones during metamorphic events causing dilution of diagnostic isotopic anomalies or to dispersal of extinct natural reactors by normal geochemical means.

In the search for evidence for natural fission events in Australian deposits, we should recognize that spectacularly depleted ^{235}U abundances similar to those observed at Oklo may no longer be extant. Remobilization of the ore after initial deposition and enrichment could well have homogenized isotopic anomalies to below the limits of precision of measurement. In this event, extinct reactor zones may only be detectable by seeking isotopic anomalies in elements of very low natural abundance.

ALLIGATOR RIVERS URANIUM FIELD

Some uraninite deposits in the Pine Creek Geosyncline are possible locations where a sustained induced fission event may have occurred. By analysis of the circumstances documented at the Oklo mine, we may infer that for fission events to be sustained, the following requirements should be satisfied:

1) the deposit should be old enough for the fissioning nuclide, ^{235}U, to have an abundance exceeding 2% (i.e. an age $\geq 10^9$ y.);
2) the mineralization should exceed 5-10% over distances of 50cm or more, so that neutron losses do not prevent continuous induced fission;
3) a light element moderator should be present in the ore zone to thermalize fission neutrons to enable further ^{235}U fission;
4) elements with isotopes having high thermal neutron capture cross-sections should be present only at low concentration;
5) to detect and verify the past existence of sustained fission, the reacting zone should not have suffered post-reaction geologic events which could mask identification of diagnostic nuclide abundances.

Isotopic data relevant to the time of mineralization in the deposits of the Alligator River Uranium Field are complex and do not, at present, yield well defined ages. Limits on the age of the Lower Proterozoic metasediments are set by the ages of the Nanambu basement complex and the intrusive Nimbuwah complex (Page *et al.*, 1979). The possible age range under this constraint is between 1870 m.y. and 2470 m.y. Page *et al.* estimate the age of the 'Footwall Sequence' at Ranger 1 as between 2000 m.y. and 2200 m.y.; younger Rb-Sr ages in the region of 1800 m.y. are considered to reflect recrystallization of the metasediments during amphibolite-facies metamorphism.

At Jabiluka, pegmatites which clearly post-date the regional deformation have concordant Rb-Sr muscovite ages of 1830 ± 5 m.y.; biotites from non-retrogressed amphibolite facies schists have apparent ages of 1805 ± 5 m.y. (Riley *et al.*, this volume). A minimum regional age for the last time the host rocks experienced temperatures of ~300°C is, therefore, 1800 m.y., although localized low temperature metasomatism may have occurred subsequently. Uranium-lead systematics on chalcopyrite and pyrite from 'drusy' veins cutting uranium mineralization indicate ages of 1380 m.y. and 1770 ± 80 m.y. (Gulson & Mizon, this volume). The authors interpret the former date as a minimum age for uranium mineralization and the latter as a fortuitous effect due to inherited radiogenic lead derived from uraninite. The age information at Nabarlek, based on K-Ar and Rb-Sr ages of muscovites taken from just outside the metasomatized zone, indicates a minimum age of 1800 m.y. for the host sediments (Page *et al.*, 1979). The metasomatism is dated in the vicinity of 1600 m.y.

Uranium-lead measurements on the ore at Jabiluka indicate a complex post-depositional history. The oldest apparent uraninite ages interpreted by Gulson & Mizon (this volume) are 1100-1300 m.y. with a series of younger events perturbing the isotopic

data. Pitchblende and galena ages (Hills & Richards, 1976) for Nabarlek, Jabiluka, Ranger and Koongarra indicate that only Ranger and Koongarra have isotopic relicts of a 1700-1800 m.y. formational event. Both of these ore bodies suffered an episode of lead mobility at 800-900 m.y.. The data on Nabarlek all indicate no age older than 900 m.y.; all ore bodies may have been remobilized subsequently. There is no published observation of uraninite mineralization in the Kombolgie sandstone, whose deposition occurred between 1680 m.y. and 1370 m.y. (Page *et al.*, 1979). If, in fact, Kombolgie deposition post-dates mineralization, the minimum age for the uraninite is 1370 m.y. and younger ages indicated presumably are due to remobilization affecting U-Pb systematics.

Because the primary mineralization at Ranger, Koongarra, Jabiluka and Nabarlek is exposed only with drill holes, detailed knowledge of grade-thickness is incomplete. However, it is clear that, with the possible exception of Ranger, the deposits have zones with sufficient grade-thickness for local sustained fission to have occurred. The necessary requirement for a light element moderator is easily fulfilled by the presence of water and carbon in the host sediments. However, it is currently unknown whether these constituents were present in oversupply, thus preventing a sustained fission event.

Documentation of rare earth element geochemistry of these four ore deposits is incomplete, so that estimates of the significance of the abundance of elements with high neutron capture cross-sections is not possible. However, most pitchblende deposits are characterized by relatively high rare earth concentrations (2000-4000 ppm); it is perhaps noteworthy that the Oklo ore had only about 400 ppm total rare earths prior to the fission events. Other elements that could cause neutron flux decrease and hence present sustained fission are thorium, vanadium, cadmium, boron and lithium.

Preservation of evidence of postulated sustained fission events in the Alligator Rivers Uranium Field is undoubtedly dependent on the significance of the apparent remobilization of the ore. Detection of anomalies in ^{235}U abundance is crucially dependent on the scale of remobilization and dilution of anomalous uranium isotopic ratios with the normal elemental abundance from adjacent non-reacting zones. Current precision in the measurement of the $^{235}U/^{238}U$ ratio indicates that the detectable dilution ratio limit will be about 100:1 (for a fission event of the scale of Oklo).

ANALYTICAL TECHNIQUES

The strategy for this investigation was to establish a technique for measuring the isotopic composition of uranium in natural ores with a precision goal of <0.1%. Although the well preserved Oklo ores had ^{235}U abundances as low as 0.44% (i.e. depletion of ^{235}U by almost 40%), the situation with Australian pitchblende deposits, which have probably suffered metasomatism and remobilization, demands a high precision. For a fission zone burn-up of 40% and subsequent normal abundance dilution by a factor of 100-200, the analytical precision needed is ~0.1% to ensure that the event is detected. The laboratory is equipped with a thermal ionization mass spectrometer; very high precision UF_6 gas analysis is not available.

In view of the possibility of remobilization of uranium in the deposits masking burn-up depletions of ^{235}U, a follow-up investigation of the occurrence of fission product nuclide abundance anomalies was planned. In this strategy there are two clear choices. One is to determine isotopic compositions in elements of very low geochemical abundance such as tellurium, ruthenium and cadmium, with the expectation that remobilization will dilute these anomalous fission abundances minimally. The alternative is to seek anomalous isotopic compositions in elements which can be measured with high analytical precision using thermal ionization sources. In this study we have chosen to investigate neodymium isotope abundances because available techniques allow very high precision isotopic analysis of this element and because it has several isotopes, thus enabling corrections to compensate for thermionic fractionation arising in the analysis. In Oklo analyses, neodymium isotope ratios deviate from normal compositions by more than a factor of two. If neodymium of a similar isotopic composition occurred as the result of sustained fission in any Australian deposit, then subsequent remobilization would mask the event at a dilution ratio level of ~600.

1. Extraction chemistry

a) Uranium Extraction

Crushed samples are leached with 10M hydrochloric acid at 95°C for 16 h. The acid is evaporated and the residue dissolved in 2M hydrochloric acid, centrifuged and then extracted with 20% w/w bis (2-ethylhexyl)-orthophosphoric acid (HDEHP) in toluene. The toluene layer is washed first with acidified hydrogen peroxide and

then with water. Uranium is back-extracted into 1 M hydrochloric acid, washed with carbon tetrachloride and evaporated to dryness. The sample is then dissolved in dilute nitric acid and loaded onto a rhenium filament.

b) Neodymium Separation

After a 10M hydrochloric acid leach, the dried sample is dissolved in 0.5M sulphuric acid, centrifuged and loaded onto a small, cation-exchange resin column. The uranium is washed through with several column volumes of 0.5M sulphuric acid and the neodymium is recovered with 5.3M hydrochloric acid. This fraction is dried and loaded onto a column of POROSIL B previously silanized and coated with 10% w/w HDEHP. The column is washed with 0.2M hydrocholric acid and the neodymium cut is taken with acid of the same concentration. The cut is evaporated to dryness, dissolved in water and loaded onto a rhenium filament.

2. Mass spectrometry

The instrument used in this project was an AVCO Series 900A, 35-cm radius, single sector mass spectrometer with a thermal ionization source. The instrument has been interfaced with an Interdata 7/16 mini computer (Ridley, 1978), which provides isotope search and identification, magnetic peak switching with Hall probe field stabilization, electrometer range switching and digital data acquisition.

a) Uranium

Uranium samples are loaded as the nitrate in a triple filament source in which all filaments are rhenium. For a sample load of about 40-50 μg, centre filament current of 5.0 A and sample filament currents of 2.6 A, a steady ^{238}U beam of 4×10^{-11} A can be generated. The ion beam is collected by a Faraday cup and amplified by a vibrating reed electrometer. Data are taken by computer switching of the ^{238}U beam on the 10 V electrometer range to the ^{235}U beam on the 100 mV electrometer range. Each peak is digitally sampled by a digital voltmeter for a preset number of sampling periods each of 20 ms duration (i.e. one mains cycle).

A single set of data consists of twelve observations of ^{238}U successively interspersed with thirteen observations of ^{235}U. Each ^{238}U observation has sixty sampling periods (of 20 ms) and each ^{235}U observation has three hundred sampling periods (of 20 ms). Zeroes (i.e. no beam conditions) are measured on the 10 V and 100 mV ranges for 400 sampling periods both before and after each set. Each set of data contains 6220 observations and takes about 8 min to accumulate. The observations of each peak height are statistically filtered and the mean derived. After zero substractions, successive ^{238}U peak heights are averaged to enable the calculation of twelve isotope ratios of $^{235}U/^{238}U$. These ratios have a typical relative standard deviation of 0.02-0.04%.

The dwell time between readings, after beam switching, is important because of the transient response of the magnet and the rise time of the electrometer. In this project, our procedure is to maintain accurate and reproducible, clock-determined dwell times, so that residual errors are systematic. The dwell time for ^{238}U, after the magnet is switched and before data are gated on, is 1500 ms; for ^{235}U, the dwell time is set at 8000 ms. The effect of a small delay time for for ^{235}U is to overestimate its intensity; the final delay time chosen introduces a small error comparable in magnitude with the effect of isotopic fractionation between successive sets of data.

Assessment of the systematic error incurred in these analyses is demonstrated by the data for certified

Sample No	Mean $^{235}U/^{238}U$	σ (%)	Mean $^{234}U/^{238}U \times 10^6$
SRM U-500	1.00044	0.05	
*SRM U-500	0.99970		
DIFFERENCE	0.07%		
SRM-010	0.010171	0.12	54.95
*SRM-010	0.010140		54.66
DIFFERENCE	0.306%		0.54%
SRM-005	0.004936	0.17	22.12
*SRM-005	0.004913		21.91
DIFFERENCE	0.346%		0.96%
SRM-950b	0.0072765		56.72
†SRM-950b	0.0072525		
DIFFERENCE	0.330%		

*U.S. National Bureau of Standards certified values

†Value compatible with Belgian Congo ore standard (Cowan and Adler, 1976)

Table 1. Uranium isotope ratios in standards.

standards (Table 1) produced by the rigid analytical procedure described above. In the case of the 1:1 standard N.B.S. SRM #U-500, the deviation of the mean value for the ratio $^{235}U/^{238}U$ from the certified value is 0.07%.

For the 1:100 standard N.B.S. SRM #U-010, the deviation of the mean value for observed $^{235}U/^{238}U$ from the certified value is +0.31%. For the 1:200 standard N.B.S. SRM #U-005, the deviation of the observed mean from the certified value is +0.36%. It is clear that for 1:1 isotopic abundance of ^{235}U and ^{238}U, the systematic instrument error is small. However, in the vicinity of natural abundance of ^{235}U (i.e. 0.5% and 1% abundance), a systematic error in excess of 0.3% is present.

Results for the N.B.S. (non-isotopic) standard SRM #950b are also shown in table 1. This standard does not have isotopic abundance certification, but is commonly used as a (certified) chemical standard for uranium. For comparative purposes, we assume the ^{235}U abundance for uranium to be identical to the N.B.S. Belgian Congo standard and this value of 0.7110 wt% (Cowan & Adler, 1976) leads to a $^{235}U/^{238}U$ ratio which is 0.330% less than that shown for our analysis of SRM #950b in table 1. As this discrepancy is precisely compatible with the isotopic standardization by SRM #005 and SRM #010, it is accepted as a systematic error for our mass spectrometric technique applied to uranium at natural isotopic abundance levels. Hence all $^{235}U/^{238}U$ ratios determined on ores for this study are normalized to SRM #950b by a correction factor of 0.9967.

The determination of the ^{235}U abundance in ore specimens for this work comprises three successive sets of data (i.e. $^{235}U/^{238}U$ ratios) acquired by the procedure described aboved. Each set of data has a measurement duration of about 8 min; a time delay of 5-6 min is incurred between sets, during which refocussing, initiation and peak search procedures are carried out. The mean of the three sets invariably has a higher standard deviation than any individual set due to unavoidable mass fractionation during the analysis. The mean $^{235}U/^{238}U$ ratio value (and its standard deviation) are converted to the equivalent weight % abundance of ^{235}U.

Measurement of the ^{234}U abundance is by a similar two peak switching procedure, the comparator isotope being ^{235}U. The major variant on the previously described procedure is that an electron multiplier (with a gain of $\sim 10^3$) is used in the current mode for amplification of both ion beams. The ^{234}U determination is carried out after the third set of $^{235}U/^{238}U$ measurements; dwell times of 1500 ms for ^{235}U and 8000 ms for ^{234}U are used. In the reduction of the data, a $(mass)^6$ correction is applied on the assumption that the multiplier gain is velocity dependent.

The measured ^{234}U isotopic (atom) abundances for the N.B.S. standards, SRM # 010 and SRM # 005, are listed in table 1 and compared with the certified abundance value for each standard. The agreement is satisfactory although, in both cases, a small systematic positive error is evident. The measured abundance of ^{234}U in the SRM #950b chemical standard is slightly above the equilibrium value. There is no certified N.B.S. value for SRM #950b.

b) Neodymium

Neodymium isotopic analysis is performed in a different manner. The sample is loaded as a chloride on rhenium filaments and pumped to a vacuum of approximately 5×10^{-6} Torr. With a (rhenium) ionizing filament current of ~4.2 A and radiant heat as the only energy source for the sample filaments, neodymium (metal) beams of $\geq 3 \times 10^{-11}$ A can be sustained for several hours. With this element in natural isotopic abundance, the dynamic range of ion beam intensities is sufficiently small that dwell time considerations in peak switching are unimportant. In this type of analysis, three beams are switched and interleaved in a sequence so that the central mass isotope, regarded as the reference peak, is measured at every second switch event. Thus, in a sequence of ^{146}Nd, ^{144}Nd and ^{143}Nd, the ^{144}Nd beam is regarded as the reference peak for that run.

Dwell times for neodymium are set at 1500 ms and the number of (20 ms) observations on each switched peak is set at ≥30. In any single set, 67 beam switches occur, resulting in 17 ratios of medium mass/high mass (e.g. $^{144}Nd/^{146}Nd$) and 16 ratios of low mass/ medium mass (e.g. $^{143}Nd/^{144}Nd$). The typical standard deviation for such ratios determined in this manner is ≤0.02%; the standard error of the mean for 42 sets of the $^{143}Nd/^{144}Nd$ ratio (normalized to a constant $^{146}Nd/^{142}Nd$ ratio) on a chemical standard is 12.5 ppm. Precision of this order is only attainable where isotopic fractionation can be corrected for by normalization procedures.

RESULTS AND DISCUSSION

In this investigation, we have concentrated on analysing samples from Koongarra, Jabiluka and Nabarlek. Samples were selected from high grade zones (most exceed 5%), with intersection widths exceeding 50cm. The total number of ore samples analysed is 39, made up of Jabiluka 14, Nabarlek 17 and Koongarra 8. In table 2 we list, by ore body, the sample location, uranium grade, thickness of the zone and the isotopic abundances of ^{235}U and ^{234}U.

In assessing these data, it is relevant to consider the relative magnitude of the precision of the determination compared to fractionation during analysis. Averaged over all sets of data, the mean standard error is 0.023%, while the average standard error for the sample means is 0.053%. The discrepancy is considered to reflect isotopic fractionation. This conclusion is supported by the observation that the three sets of ratios comprising each analysis are invariably ordered such that the mean of each set decreases as a function of analysis time, i.e. the light isotope (^{235}U) is less enriched in the ion beam as sample is consumed.

Sample No	Drill hole	U_3O_8 (wt%)	Mean ^{235}U (wt%)	Std. dev. x 10^4	^{234}U Abundance (ppm)
NABARLEK					
9094	243	6.6	0.7105	2	53.7
9095	"	7.1	0.7106	3	55.3
9096	"	11.8	0.7114	9	54.8
9097	"	66.0	0.7111	10	54.7
9098	"	49.9	0.7111	4	55.0
9099	"	10.7	0.7105	3	54.9
7267	193	9.2	0.7107	10	54.6
7268	"	25.9	0.7108	3	54.8
7269	"	39.3	0.7107	5	54.8
7270	"	54.4	0.7111	4	55.1
7271	"	25.8	0.7119	10	55.1
7272	"	25.7	0.7109	6	54.9
7273	"	15.4	0.7100	4	54.7
*75080530	-	-	0.7111	4	55.7
*75080532	-	-	0.7114	1	60.9
*75080533	-	-	0.7094	2	43.1
*75080260	-	-	0.7109	3	55.2
JABILUKA					
54957	219	7.8	0.7110	10	55.0
54961	"	6.9	0.7114	6	55.1
54962	"	6.9	0.7111	6	54.9
54969	"	6.3	0.7110	4	54.9
54970	"	6.3	0.7103	6	54.7
55037	248	18.0	0.7102	3	54.6
55038	"	18.0	0.7117	3	55.2
55045	"	9.5	0.7113	7	55.8
55046	"	9.5	0.7128	3	55.2
55065	244	5.1	0.7117	10	55.1
55066	"	5.1	0.7125	3	55.1
55067	"	5.1	0.7122	5	54.9
55286	259	5.0	0.7098	6	54.7
55287	"	5.0	0.7114	7	55.0
KOONGARRA					
25	27	2.1	0.7118	12	51.3
99	5	13.8	0.7107	8	55.1
100	"	9.4	0.7105	6	55.0
102	"	22.3	0.7117	9	55.1
104	6	14.7	0.7113	11	55.3
107	9	11.5	0.7125	8	-
108	"	10.1	0.7117	7	55.0
122	16	1.4	0.7100	3	55.1

*Samples from Dr J. Ferguson, Bureau of Mineral Resources. These specimens are near surface hand samples, not drill core.

Table 2. Uranium isotopic abundances in ore samples.

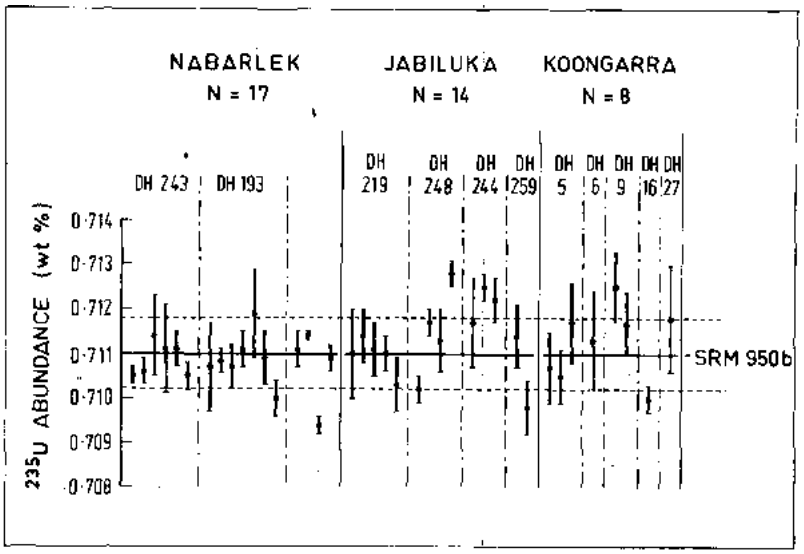


Figure 1. ^{235}U abundance comparison with respect to the standard SRM # 950b. Error bars are 1σ limits. The dashed horizontal line shows 1σ deviations from the standard mean. Drill hole identification is shown for each sample.

The effect has been modelled by Kanno (1971) and Moore *et al.* (1976); it is essentially based on a mass-dependent vaporization rate of molecular species from the sample filament, so that the instantaneous isotopic composition of the ion beam is a function of the fraction of sample remaining on the vaporizing surface. In this work, we have not sought to correct for fractionation, but have accepted the isotopic variation trend as an additive error. For intersample comparison, the error is minimized by ensuring that data are collected in successive sets, commencing at approximately the same point in 'run-time' for each analysis. Typical fractionation changes observed in the study are 0.008% per min for the $^{235}U/^{238}U$ ratio, corresponding to a 0.2% shift over the three sets of data for each sample.

The numerical data of table 2 are condensed pictorially in figure 1, which shows the mean ^{235}U abundance and its associated standard deviation for each sample. The mean value for samples from each ore body is also shown. The data indicate that the means for each ore body are neither distinguishable from each other nor from the value of the standard SRM #950b. The histogram representation of data from all samples is symmetrically distributed about the value for the standard (Fig. 2). Apparent small deviations of ^{235}U abundance of individual samples from the value of the standard are considered to be misleading and caused by isotopic fractionation effects; we conclude from these data that we are unable to find evidence to support the past existence of sustained fission reactors.

Table 2 also lists ^{234}U isotopic abundance data for each sample. This measurement is peripheral to the investigation of reactor evidence but yields information on the state of secular equilibrium in the ^{238}U decay chain. All drill core samples, with the exception of Koongarra #25, are within 2% of the natural abundance value for ^{234}U in secular equilibrium with ^{238}U. Koongarra #25 originates from the weathered zone of the No. 1 orebody (Dickson & Snelling, this volume) and is depleted in ^{234}U. Both depletion and enrichment of ^{234}U is evident in surface samples from Nabarlek.

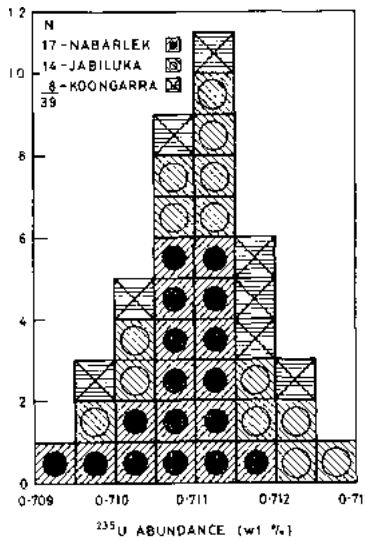


Figure 2. Histogram of all ^{235}U abundance measurements shown with ore body identification.

One preliminary isotopic analysis of neodymium extracted from Nabarlek sample #9097 has been carried out. Only isotopes ^{143}Nd, ^{144}Nd, ^{145}Nd and ^{146}Nd were measured because of possible mass interference by cerium at mass 142 and barium oxide at masses 148 and 150. No samarium was present in the mass spectrum. These results, shown in table 3, are compared with normal abundance data determined on a standard in this laboratory and with analyses from several Oklo samples (Dozol & Neuilly, 1975; Maeck *et al.*, 1975). It is evident that no fission product neodymium is detectable in the sample extract.

The non-fission neodymium data shown in table 4 are compared with standard and rock analyses of De Paolo & Wasserburg (1976), and Richard *et al.* (1976). The data for the standards and 21 rock samples are normalized to assumed ratio values that are not common to all three laboratories, so that interlaboratory comparisons at high precision levels are not justified. However, there is a clear discrepancy between the $^{143}Nd/^{144}Nd$ ratios for the standards and for the Nabarlek sample. The marked enrichment in ^{143}Nd is plausibly explained by the 1.06×10^{11}y. α-decay of ^{147}Sm, thus suggesting that this decay scheme may be of value in dating uraninite.

The tabulated data for $^{146}Nd/^{144}Nd$ and $^{145}Nd/^{144}Nd$ are slightly lower than the corresponding ratios for the standards and grouped rocks analyses. The discrepancy is small. While it may be explicable in terms of uncorrected factionation, an alternative possibility is based on natural neutron activation.

The spontaneous fission neutron emission over the lifetime of the ore body is $\sim 4 \times 10^{24}$ neutrons and the integrated flux is $\sim 10^{16}$ neutrons/cm^2. The thermal capture cross-section for ^{143}Nd is 320 barns and the resonance cross-section ~100 barns. If significant ^{143}Nd has undergone natural (n,γ) activation to ^{144}Nd, then both $^{146}Nd/^{144}Nd$ and $^{145}Nd/^{144}Nd$ ratios will be low in the ore. The concentration of neodymium in this ore sample is not yet known, so that calculations cannot be made to test this possibility.

Sample	U (%)	^{235}U (atom %)	$\frac{^{146}Nd}{^{144}Nd}$	$\frac{^{145}Nd}{^{144}Nd}$	$\frac{^{143}Nd}{^{144}Nd}$
Oklo #1180*	31	0.425	0.4866	0.5483	0.6849
Standard	-	-	0.7219	0.3484	0.5111
Nabarlek #9097	66	0.7110	0.7212	0.3485	0.5147

*Data from Cowan *et al.* (1975) and Dozol and Neuilly (1975)

Table 3. Fission neodymium isotope ratios.

Sample	$\frac{^{146}Nd}{^{144}Nd}$	$\frac{^{145}Nd}{^{144}Nd}$	$\frac{^{143}Nd}{^{144}Nd}$	Source*
Nabarlek #9097	0.72121	0.34848	0.51469	R & K
Koch-Light Standard	0.72282	0.34877	0.51112	R & K
Johnson Matthey Standard	0.72356	0.34887	0.51134	R.S.A.
Rock samples (21)	0.72412	0.34896		DP.W

*R & K, this work; R.S.A., Richard *et al.* (1976); DP.W, De Paolo and Wasserburg (1976)

Table 4. Non-fission neodymium isotope ratios.

CONCLUSIONS

The possibility of the occurrence of natural fission reactor phenomena in uranium ore bodies in the Pine Creek Geosyncline has been assessed. It is probable that mineralization at Koongarra, Jabiluka and Nabarlek has been remobilized at some time(s) subsequent to its emplacement. Uranium isotope analyses of these ore bodies have revealed no depletion of ^{235}U at the 0.1% precision level. An isotopic analysis of neodymium extracted from a high grade zone at Nabarlek shows no isotopic anomalies that would substantiate a sustained fission event. Marked enrichment in ^{143}Nd is observed but considered to be due to α-decay of ^{147}Sm. A small enrichment of ^{144}Nd, marginally decreasing $^{146}Nd/^{144}Nd$ and $^{145}Nd/^{144}Nd$ ratios, may have resulted from natural (n,γ) activation induced by the spontaneous fission flux.

ACKNOWLEDGEMENTS

This project was only made possible by the generous help of several mining companies who supplied samples, data and information on the ore deposits studied. We gradefully acknowledge the aid of Noranda Australia Ltd., Pancontinental Mining Ltd. and Queensland Mines Ltd.

REFERENCES

Cherdynstev, V.V., 1971: *Uranium-234* (Israel Program for Scientific Translations, Jerusalem).

Cowan, G.A., & Adler, H.H., 1976: The variability of the natural abundance of ^{235}U. *Geochim. cosmochim. Acta, 40*, 1487-1490.

Cowan, G.A., Bryant, E.A., Daniels, W.R. & Maeck, W.J., 1975: Some United States studies of the Oklo phenomenon. *in, The Oklo Phenomenon. Proceedings of a Symposium, Libreville.* International Atomic Energy Agency, Vienna, 341-356.

De Paolo, D.J., & Wasserburg, G.J., 1976: Inferences about magma sources and mantle structure from variations of $^{143}Nd/^{144}Nd$. *Geophys. Res. Lett., 3*, 743-746.

Dickson, B.L., & Snelling, A.A., this volume: Movements of uranium and daughter isotopes in the Koongarra uranium deposit. *Proceedings of the International Uranium Symposium on the Pine Creek Geosyncline.*

Dozol, J.F., & Neuilly, M., 1975: Analyse isotopique des terres rares contenues dans le minerai d'Oklo. *in, The Oklo Phenomenon. Proceedings of a Symposium, Libreville.* International Atomic Energy Agency, Vienna, 357-369.

Gulson, B.L. & Mizon, K. J., this volume: Lead isotope studies at Jabiluka. *Proceedings of the International Uranium Symposium on the Pine Creek Geosyncline.*

Hills, J.H., & Richards, J.R., 1976: Pitchblende and galena ages in the Alligator Rivers region, Northern Territory, Australia. *Miner. Deposita, 11*, 133-154.

International Atomic Energy Agency, 1975: *The Oklo Phenomenon. Proceedings of a Symposium, Libreville.* International Atomic Energy Agency, Vienna.

Kanno, H., 1971: Isotopic fractionation in a thermal ion source. *Bull. Chem. Soc. Japan, 44*, 1808-1812.

Maeck, W.J., Spraktes, F.W., Tromp, R.L. & Keller, J.H., 1975: Analytical results, recommended nuclear constants and suggested correlations for the evaluation of Oklo fission-product data. *in, The Oklo Phenomenon. Proceedings of a Symposium, Libreville.* International Atomic Energy Agency, Vienna, 319-339.

Moore, L.J., Heald, E.F., & Filliben, J.J., 1976: An isotopic fractionation model for the multiple filament thermal ion source. *in, Advances in Mass Spectrometry*, Vol. 7, Institute of Petroleum, London, 448-474.

Page, R.W., Compston, W. & Needham, R.S., 1979: Geochronology and evolution of the late Archaean basement and Proterozoic rocks in the Alligator Rivers Uranium Field, Northern Territory, Australia. *Extended Abstracts of the International Uranium Symposium on the Pine Creek Geosyncline*, 151-154.

Richard, P., Shimizu, N., & Allègre, C.J., 1976: $^{143}Nd/^{144}Nd$, a natural tracer: an application to oceanic basalts. *Earth Planet. Sci. Lett., 31*, 269-278.

Ridley, B.H., 1978: Computer control for a thermal ionization mass spectrometer. *in, Australia and New Zealand Society for Mass Spectrometry, Fifth Conference, Program and Abstracts*, 36.

Riley, G.H., Binns, R.A. & Craven, S., this volume: Rb-Sr chronology of micas at Jabiluka. *Proceedings of the International Uranium Symposium on the Pine Creek Geosyncline*.

PETROLOGY AND GEOCHEMISTRY OF ALTERATION ASSOCIATED WITH URANIUM MINERALIZATION AT JABILUKA, NORTHERN TERRITORY, AUSTRALIA

R.A. Binns, D.E. Ayres*, J.R. Wilmshurst and A.R. Ramsden

CSIRO Division of Mineralogy, P.O. Box 136, North Ryde, N.S.W., 2113, Australia
*Present address: Exxon Production Research Company, P.O. Box 2189, Houston Texas 77001, U.S.A

ABSTRACT

An aureole of retrogressive metamorphism in former amphibolite facies schists extends at least 200m from uranium ore zones at Jabiluka. Chloritization of biotite, and replacement of feldspar by sericite-chlorite aggregates, are the most distinctive reactions. Similar but more intense alteration occurs in the immediate vicinity of uraninite-bearing veins and breccia zones.

This retrogressive metamorphism was not isochemical. Compared to their amphibolite facies parents, the altered schists are enriched in Li and Mg, and dramatically depleted in Na, Ca, Sr and Ba. There is little significant geochemical difference between schists in the outer portion of the retrogressed aureole and those closer to ore. However the immediate hosts to ore, within about 1m, are distinctly enriched in uranium associated with chlorite-septechlorite alteration products rather than with disseminated uraninite. Further but mild enrichments in Li and Mg occur, and the immediate hosts are also distinctly depleted in K and Rb.

Compared to the country rocks, Jabiluka uraninite ores are significantly enriched in Ca, Sc, Y, and rare earth elements, and also in radiogenic Pb and certain chalcophile trace metals including Cu, As, Mo, Ag and Sn.

Uranium appears to be its own best pathfinder at Jabiluka for exploration in unweathered rocks. Other geochemical characteristics of the ores and their host rocks may have applications to advanced stages of exploration programs, and they also provide a guide to possible pathfinder elements useful in weathered situations.

INTRODUCTION

Exploration for concealed uranium mineralization in the Pine Creek Geosyncline and for poorly exposed analogues in other provinces is likely to involve increased application of geochemical techniques. Confidence in the method will be enhanced by prior documentation of known deposits and by selection of elements which can be related to mineralogical characteristics of genetic significance. An integrated petrological, geochemical and genetic study has accordingly been made of representative samples from the Jabiluka Two orebody and its vicinity (Rowntree & Mosher, 1975; Hegge, 1977; Hegge & Rowntree, 1978). Various aspects of the project are discussed elsewhere in this volume, and in this paper we concentrate on the geochemistry of rocks and ores, with reference also to petrological and mineralogical features necessary for interpretation.

Drill core samples from three main localities were examined. Drill holes L153V and S180V provided material from mineralized zones and intervening barren intervals between the Upper Graphite Series and the Footwall Series of the Jabiluka Two orebody (see figure 1 of Ryall & Binns, this volume). Drill hole M096V intersected the equivalent unmineralized sequence slightly south of the gap between Jabiluka One and Two, about 200m laterally beyond the limits of ore development in Jabiluka Two. The Cahill Formation schists in these two localities display virtually complete retrogression to greenschist facies assemblages. The third locality lies about 2.5km northwest of Jabiluka, where drill holes DH185 and DH209 (Pancontinental Mining Limited) intersected amphibolite facies schists virtually devoid of retrograde effects. Samples from these two holes were supplemented by graphite schists and marbles from another relatively non-retrogressed amphibolite facies domain about 17km south-southwest of Jabiluka (drill hole R19-S1, Ranger 19 prospect, Geopeko Limited). Because intervening exposure and drill-hole information are scarce or lacking, rocks from the third group cannot be exactly matched stratigraphically to the Jabiluka sequence but they are petrologically representative of the non-retrogressed parents for the latter.

Although the rocks studied do not encompass the entire Jabiluka environment, they

provide initial tests of geochemical differences between high grade schists of the Cahill Formation and their equivalents in the broad retrograde halo surrounding the Jabiluka mineralization, and between altered rocks remote from and close to ore respectively. Typical disseminated and high grade ores from Jabiluka Two were also examined. Elements covered in the analytical programme, and methods used, are shown in figure 1.

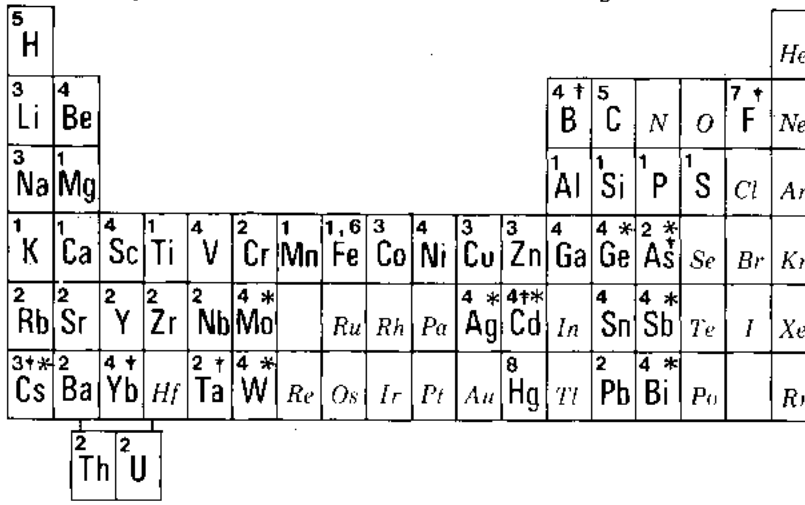


Figure 1. Elements determined (bold symbols) and analytical methods. 1, X-ray fluorescence spectrometry (XRF), fusion method; 2, XRF, pressed method; 3, atomic absorption spectrophotometry; 4, semiquantitative emission spectrography; 5, gravimetric; 6, titrimetric; 7, specific ion electrode; 8, Ryall & Binns, this volume.
* elements generally below detection limit † partial coverage of samples

METAMORPHISM

Intense retrogressive alteration ('chloritization') is a conspicuous feature of the Jabiluka environment and is also referred to in accounts of other East Alligator uranium deposits (Eupene *et al.*, 1975; Foy & Pedersen, 1975). Imperfect exposure does not permit delineation of the shape or size of alteration haloes around mineralization, although they clearly extend for more than 200m at Jabiluka. It is not clear just how widely retrogression occurred throughout the Cahill Formation, nor whether a similar or different style of retrograde alteration is extensive in unmineralized areas. The phenomenon is nevertheless clearly associated with uraninite mineralization, and its salient features will be described below.

Parent Schists

The amphibolite facies schists northwest of Jabiluka are medium to coarse grained and well foliated, with microstructures indicative of polyphase deformation prior to and overlapping high temperature recrystallization. Muscovite and drab to reddish-brown biotite are conspicuous lepidoblastic minerals, and porphyroblasts of almandine garnet are locally abundant. Fine needles and fibrolitic aggregates of sillimanite occur in many pelitic and sedimentary schists. The felsic phases are granoblastic and include quartz, twinned plagioclase (mainly oligoclase) and rarer orthoclase. Zircon, apatite, tourmaline, and opaque oxides are accessory phases. Migmatitic structures indicative of anatexis are lacking in rocks of appropriate composition (although synkinematic quartz veins are common), a feature which, together with the common presence of the critical equilibrium assemblage sillimanite-muscovite-orthoclase-quartz, indicates regional metamorphic conditions close to 600°C, 5kb. Pseudomorphs after sillimanite and almandine are present in retrogressed

Jabiluka schists and the general petrographic similarities, including absence of altered migmatite leucosomes, suggest that similar metamorphic conditions were applicable also to the initial regional metamorphism of rocks that now host the Jabiluka ore deposits. Partly retrogressed schists with some relic sillimanite, biotite, and plagioclase occur in drill hole 24 where it intersects a footwall schist sequence deep below Jabiluka One, and occasional remnants of biotite occur in retrogressed schists from drill hole M096V between Jabiluka One and Two.

Amphibolite facies graphite schists from Ranger 19 resemble those discussed above but contain bands and laminae rich in aligned, fine to medium sized flakes of graphite. Their biotites show minor chloritization, and plagioclase is less abundant and partially sericitized.

Marbles from the locality northwest of Jabiluka are coarse grained and granoblastic, with deformed calc-silicate laminae. Calcite is the dominant phase, accompanied by minor quartz, green clinopyroxene and grossular-andradite garnet. Little-retrogressed marbles from Ranger 19 are granoblastic aggregates of dolomite, with localized quartz, tremolite, or serpentine pseudomorphs after possible olivine. They also contain flakes of a colourless, relatively highly birefringent chlorite which appears a probable product of amphibolite facies metamorphism.

Retrogressed Schists

The two most conspicuous effects of retrogressive metamorphism in schists at and near Jabiluka are chloritization of biotite and alteration of feldspar (Fig. 2). Former biotite is typically replaced epitaxially by single flakes of a colourless or pale green magnesian chlorite. Alternatively the pseudomorph may be a deeper green, almost isotropic chlorite richer in Fe, or a parallel intergrowth of pale brown chlorite and white mica. Sagenitic needles of anatase or brookite, or less commonly rutile, occur in many chloritic pseudomorphs after biotite. Former feldspar grains are replaced by very fine-grained, unoriented intergrowths of white mica ('sericite') and colourless, pale green or pale brown chlorite. X-ray diffraction patterns suggest the presence of 7 Å septechlorite in addition, but no clay minerals have been confirmed. The proportions of these alteration products vary considerably across a thin section, and range from essentially pure sericite to pure chlorite. Complexly zoned pseudomorphs are common, with either phase at the core or margin.

Quartz and muscovite generally remain unaltered. Graphite also persists despite retrogression, and in some schists a possible second generation of very fine graphite occurs in chloritic alteration products of other phases. In some graphite schists, former muscovite flakes are partially replaced by chlorite.

Sillimanite has altered to fine white mica aggregates. In one sample the pseudomorphs are zoned outwards to coarser flakes of Li-rich muscovite. Original garnet porphyroblasts generally form complexly zoned pseudomorphs with varying proportions of chlorite, septechlorite and white mica which, like some feldspar pseudomorphs, suggest fluctuations in potassium activity during retrogression. Similarly composed and zoned pseudomorphs whose shape recalls cordierite also occur in some spotted schists, although this mineral has not been recognised in unaltered equivalents from the amphibolite facies domains.

Accessory zircon and tourmaline remain present, though some needles of the latter are intergrown with sericite or chlorite in a manner indicating a retrogressive origin. Apatite and ilmenite are present but appear less abundant than in the non-retrogressed schists. Some anatase, brookite or Fe-rich rutile needles, or fine-grained sphene, within the schists may represent breakdown of former Fe-Ti oxides.

A remarkable feature of the retrogressed schists at Jabiluka is the preservation of original texture from the parent, as illustrated in figure 2. Formation of late stage alteration products appears to have post-dated even late stage deformational structures such as crenulation. Any alignment rarely seen in the products of alteration is associated with minor

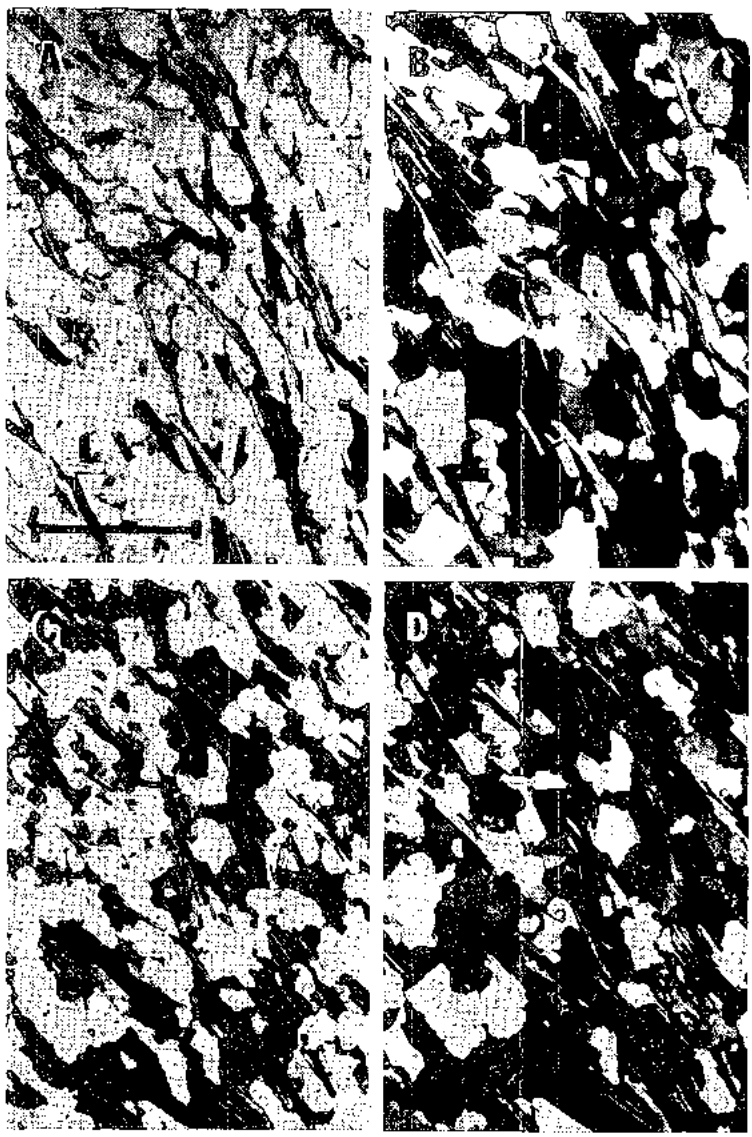


Figure 2. Photomicrographs illustrating retrogressive metamorphism of amphibolite facies schists at Jabiluka. Scale bar represents 1mm for each field.

A, B: Ordinary light and crossed polar views respectively of a non-retrogressed psammitic schist (Group 2A, Table 1) 2.5 km north-west of Jabiluka. Flakes of biotite and muscovite are aligned within granoblastic quartz, oligoclase and minor orthoclase.

C, D: Equivalent views of a retrogressed psammitic schist (Group 2C, Table 1) from a barren zone within Jabiluka Two. Quartz and muscovite remain essentially unaltered. Epitaxial pseudomorphs of pale green chlorite with sagenitic anatase or brookite needles (not visible) have replaced biotite flakes. Feldspar has altered to fine-grained brownish aggregates of chlorite, white mica ('sericite') and possible septechlorite. The former texture of the schist is perfectly preserved.

post-retrogression shearing. The retrogression largely involves hydrolysis reactions. Without assistance by deformation, highly reactive acid fluids, sufficiently reduced to allow preservation of graphite and sulphide and prevent formation of magnetite or hematite, have permeated and altered the former high grade schists for considerable distances (>500m?) from the ore zones at Jabiluka. The only channelways evident are the veins and breccia structures with which uraninite mineralization is itself associated (see below). From the generally greenschist facies assemblage of alteration products, the coexistence of chlorite and septechlorite, and the absence of clays, temperatures for the pervasive retrogressive metamorphism at Jabiluka are estimated to lie in the 300-350°C range.

Marble units within retrogressed schists at Jabiluka range from fine to medium grain size. Although megascopically granoblastic, they show complex fabrics in thin section. Magnesite commonly forms small granules located along or projecting into the margins of dolomite crystals, or the two carbonates may be intergrown, in places almost with graphic texture. Generally, magnesite forms euhedral rhombic crystal outlines against dolomite. Varying proportions of quartz are present, usually with habits suggesting preservation from impurities in amphibolite facies parents. No evidence of 'chert' replacements of marble (compare however Hegge, 1977) has been observed. Some retrogressed marbles contain very coarse veins of rhombic dolomite ± magnesite, or geodes lined by similar crystals.

Pegmatites

The granitic pegmatities at Jabiluka are undeformed except near local shear zones. Their emplacement clearly postdated folding associated with the high grade regional metamorphism, but preceded intense retrograde metamorphism. Large grains or crystals of quartz, muscovite and tourmaline are preserved intact, but the former feldspars are completely altered to massive sericite-chlorite-septechlorite pseudomorphs. In some, relative distribution of chlorite and sericite preserves a palimpsest cleavage structure reminiscent of K-feldspar, and these pseudomorphs appear richer than usual in septechlorite. Former plagioclase grains are replaced by chlorite and quartz with little sericite.

Alteration Close to Mineralization

The retrogressed schists closer to Jabiluka ore veins and breccias (typically 1cm to 1m, less commonly up to 10m in drill core), and schist fragments within breccias, are broadly similar to those described above, except that they tend to contain a noticeably greater abundance of fine-grained chlorite-septechlorite-sericite aggregates. In addition to replacing former feldspar, this material also attacks the margins of former quartz grains, or may occur instead of larger chlorite flakes in pseudomorphs after biotite. Compared to similar material in retrogressed schists more remote from mineralization, it is usually a distinctly brownish colour in thin section (and waxy in reflected light), and the overall proportion of white mica is less. Although much variation occurs, the amount of intergrown white mica ('sericite') falls as mineralized veins or breccia zones are approached. Within about 1cm or so of ore structures, these fine alteration aggregates may contain disseminated uraninite, coffinite or brannerite, and at these same positions graphite and relic muscovite are also replaced by similar chloritic material. Careful microscopic study has failed to reveal any evidence that the chlorite-septechlorite aggregates, which resemble the 'CSQ' gangue described by Binns *et al.* (this volume), have replaced the alteration products more typical of retrogressed schists remote from ore. The relationship appears a perfectly gradational one, dependent on distance from mineralization but with irregularities reflecting the variable abundance of mica-rich or graphitic laminae in the schists. An important point is that a similar gradation exists near the margin of a pegmatite body adjacent to mineralized breccia (see Table 3, column 8D).

LITHOLOGICAL CLASSIFICATION

For the purposes of geochemical comparison, Jabiluka country rocks have been

subdivided into the lithological groups described below. The principal criterion was hand specimen appearance noted during relogging of our diamond drill core collection of retrogressed schists, etc., from Jabiluka, but the classification is supported by microscopic petrography and by inspection of major element chemical analyses. In cases where fine scale interlamination occurred between different schist types in hand specimen, the dominant lithology was used or the major element analysis was relied upon to check the classification. Samples with quartz veins were avoided.

Group 1: Pelitic Schist.

Samples in this group are characterized by relatively abundant and generally coarse-grained muscovite, leading to distinctly lustrous cleavage surfaces.

Group 2: Psammitic Schist.

These are distinctly more felsic in appearance than the pelites, and muscovite is generally finer and less abundant. Comparatively vitreous lustres on core surfaces aid distinction from group 5 (chlorite schist). Groups 1 and 2 tend to form separate populations as might be expected for a sequence of interbedded shales and sands. However some gradational samples exist, and for these the distinction is based on geochemistry, 68% SiO_2 and 16% Al_2O_3 generally serving together to define the boundary.

Group 3: Graphite Schist.

Rocks so classified from their dark and graphitic character in hand specimen generally prove to contain more than 1% elemental carbon on analysis. Most contain less than 9% MgO.

Group 4: Chlorite-rich or Chloritized Graphitic Schist.

This is a heterogenous and probably polygenetic group, many members of which can only be distinguished from group 3 after microscopic examination or chemical analysis. No non-retrogressed equivalents have been studied. Relic pseudomorphs in some samples suggest derivation from garnet-rich graphite schists. However, these are not readily distinguished in hand specimen from other graphitic schists whose abundance of chlorite is a consequence of more intense replacement of quartz, mica and even graphite in the close vicinity of mineralized veins and breccias. To avoid any likelihood of bias in later geochemical comparisons, groups 4 and 3 have been separated on a $\gtrless$10% MgO criterion, which is a distinctive compositional gap between the two populations.

Group 5: Chlorite Schist.

Unlike group 4, the name used for this minor class does not imply exceptional abundance of chlorite. These are dull, medium greenish-grey rocks in hand specimen whose closest affinity lies with group 2. Their distinctiveness arises mainly from scarcity of muscovite, and they appear to be the retrogressed equivalents of comparatively rare muscovite-poor, felsic biotite schists observed in the amphibolite facies domains.

Group 6: 'Greisen'.

This is a distinctive class of considerable genetic importance, found only close to mineralization. It includes rocks which Hegge (1977) termed 'illite' schists, although subsequent X-ray diffraction and chemical analysis has shown the supposed clay to be white mica. The 'greisens' are conspicuously pale golden yellow, yellowish-green, or yellowish brown in drill core, and vary over short distances from coarse-grained lustrous rocks rich in muscovite to duller, fine-grained sericitic types. Their structure ranges from massive to poorly foliated. Many contain large (1-5mm) porphyroblasts of quartz which appear metasomatic in origin. The proportions of white mica and quartz vary considerably. Some chlorite accompanies the sericite. Relatively large grains or aggregates of sphene are a conspicuous accessory, and some samples near uraninite mineralization contain brannerite. In contrast to other schists, the larger muscovites in 'greisens' are commonly bent or kinked, but it is not clear whether this represents imposed deformation prior to sericite formation, or

the effects of growing quartz porphyroblasts. According to M. R. Hegge & G. McArthur (pers. comm., 1979), 'greisens' occur stratigraphically above richer uraninite-bearing zones at Jabiluka. Although not fully applicable to all members, the name for this lithological group has been chosen with some consideration of the genetic implication. Their metasomatic origin is clear in drill core transitions between 'greisen' and schist, where small scale features of the latter, such as quartz veins, chloritic laminae, or in one case a transgressive aplite veinlet, have been replaced by sericite. It is not clear whether the coarser muscovites are cogenetic with the sericites: replacement realtionships in both directions may be observed.

The remaining groups represent comparatively less common lithologies at Jabiluka, or rocks that are not discussed at length below.

Group 7: Marble

Group 8: Pegmatite (see Table 3)

Group 9: Miscellaneous

Cahill Formation lithologies including amphibolite, quartzite, and fine silexite-like rocks that may be deformed quartz veins.

Group 10: Kombolgie Sandstone

Group 11: Metamorphosed regolith below the Kombolgie unconformity (see Riley *et al.*, this volume).

A statistical classification by cluster analysis was performed on geochemical data from drill holes L153V, S180V and M096V, using the MULCLAS and GROUPER programs of Dale *et al.* (1978). These programs form groups of 'most similar' samples by an agglomerative polythetic (multielement) strategy and supply information on the mean composition of each group and the main attributes used in forming them. A total of 46 attributes (chemical components) was taken into account in the analyses.

In general, the statistical classification groups were in good agreement with the prior lithological subdivision. Not surprisingly, distinctive rock types such as marble, amphibolite and the Kombolgie Sandstone were readily separated and rock types such as graphite schist and choloritized graphite schist were also recognized and distinguished from each other. Most overlap between statistical classification groups and lithology was found for rocks described as pelitic schist and chlorite schist and, to a lesser extent, psammitic schist.

OCCURRENCE SUBGROUPS

To allow comparison of specific lithologies from different geological settings, the following suffixes will be used.

A) Non-retrogressed amphibolite facies schists and marbles (N.W. Jabiluka, Ranger 19).

B) Retrogressively altered rocks remote from mineralization (taken as representative of the 'outer alteration halo', drill hole M096V).

C) Barren intervals within the Jabiluka Two orebody, ranging from 2 to 40m vertically from mineralization ('inner alteration halo').

D) Host rocks to uraninite-bearing veins and breccias. This includes unbrecciated samples from which uraninite veins were removed (monitored by radiation detector), or uraninite-free specimens from grab samples within assay intervals (generally 1m) of mineralized drill core. After it was observed that such samples were also U-enriched, and that a distinct gap at 100 ppm U existed in histograms (Fig. 3), any samples with more than 100 ppm U from assay intervals adjacent to definitely mineralized intervals were added to subgroup D. A small number of isolated samples with >100 ppm U, but from generally barren zones more than 2m from ore intersections in the 'mineralized' drill holes, were also included in

subgroup D on the reasonable assumption that they were probably closer laterally to ore.

E) 'Low grade' ores, including uraninite-bearing brecciated schists and samples with minor vein developments. These contain from 0.1% to 3% U, and although a sample bias is possible they appear to form a separate population on this basis from group D.

F) 'High grade' ores (>10% U), including two samples of strongly veined material sawn from drill core, and one heavily mineralized breccia.

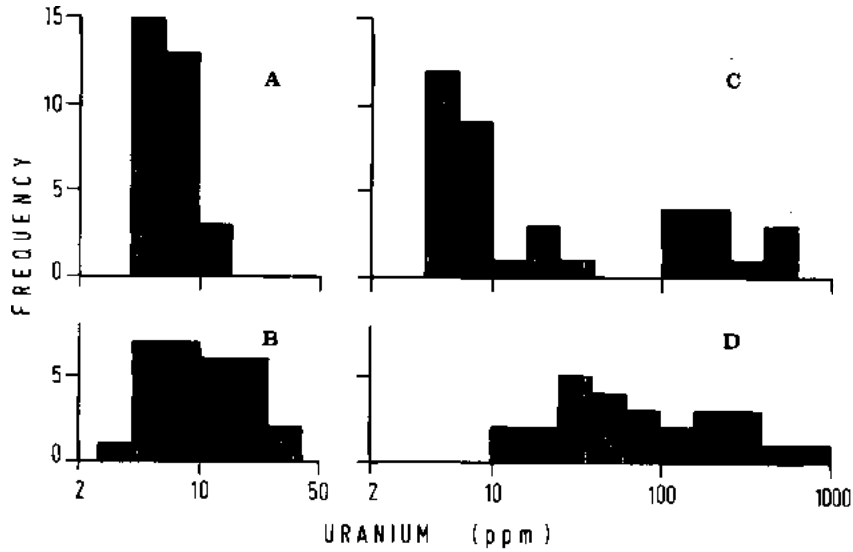


Figure 3. Logarithmic histograms of uranium content in Jabiluka schists. A, B: barren retrogressed schists approximately 200m beyond the Jabiluka Two orebody (drill hole M096V, occurence group B). C, D: similar schists in uraninite-free portions of Jabiluka Two (drill holes L153V and S180V, groups C and D).
Figure 3A and 3C illustrate data for both pelitic and psammitic schists (lithological groups 1 and 2), whereas figures 3B and 3D present the equivalent data for graphite schists (groups 3 and 4). A higher uranium content in graphite schists relative to non-graphitic schists is evident for group B (see Fig. 4). Figure 3C shows two separate uranium populations for pelitic and psammitic schists within Jabiluka Two, which correspond to samples from barren intervals (group C) and immediate hosts to veins (group D) respectively. Graphite schists in the same situations (Fig. 3D) show two overlapping populations with a minimum at *ca* 100 ppm U. The lower population contains significantly more uranium than equivalent graphite schists from the outer retrogressed aureole (Fig. 3B).

GEOCHEMICAL DATA

Average compositions of the more significant Jabiluka country rocks, grouped according to lithology and occurrence as set out above, are presented in tables 1 to 3. Equivalent data for low grade ores (predominantly group 4 hosts) and the uraninite-rich veins and breccia are listed in table 4. Arithmetic means and standard deviations, assuming normal distributions within populations, were calculated for 'major' elements, even though some are in places present only at trace levels. Most trace elements conform to log normal distributions, so 'geometric' means recalculated from logarithms are quoted, together with the standard deviations of the logarithms. The latter typically range from 0.2 to 0.3 for lithophile trace elements, but tend to be higher for the chalcophile traces where distinct bias, for example by occasional chalcopyrite-rich lenticles, is commonly present. These factors must be borne in mind when making comparisons between groups and subgroups. For the low sample numbers in most groups, statistical tests for similarity or difference scarcely

reveal more than direct examination of the values cited. The conclusions reached below should be treated as an initial appraisal of primary geochemistry at Jabiluka, which could now be amplified by further measurements for elements of apparent significance.

The expected differences in major element geochemistry occur between lithological groups. The non-retrogressed pelitic schists (1A), for example, are richer in Fe and Mg relative to their psammitic associates (2A) which contain less biotite. Many trace element differences between these two subgroups reflect relative abundance of micas and feldspars respectively. Subgroup 1A pelites are closely comparable with world average shale (Krauskopf, 1979): although Pb, Th and U are slightly higher, and Sr and Sn lower, the differences are explicable by likely provenance (i.e. the Nanambu Complex, see Needham & Stuart-Smith, this volume).

The graphite schists range from pelitic to psammitic variants, with a bias towards the former indicated by mean values for SiO_2 and Al_2O_3. The relatively high MgO content of subgroup 3A relative to 1A and 2A appears an original feature, for partial chloritization of biotite should reduce K_2O if it were significant. Graphite schists remote from mineralization (subgroups 3A, 3B, 3C) show good correlation between abundance of uranium and elemental carbon (Fig. 4). This may reflect an original sedimentary uranium component in these rocks, falling within the possible range for carbonaceous shales (Bell, 1978). Group 4 schists show a less definite correlation. These correlations become lost as ore is approached in subgroups 3D and 4D. Graphite schists tend to be enriched relative to other schists in chalcophile elements, in conformity with their possession of pyrite-rich sulphide lenticles.

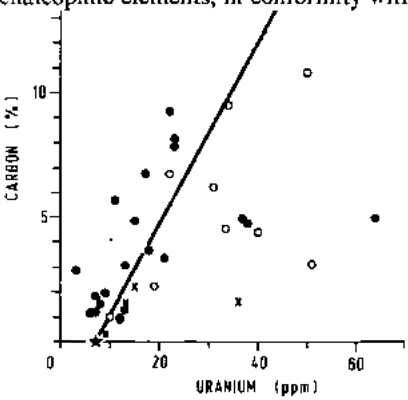


Figure 4. Relationship between uranium and elemental carbon (graphite) contents for non-retrogressed graphite schists (x, subgroup 3A), and equivalents from the outer retrogressed aureole (•, subgroup 3B) and barren intervals within Jabiluka Two (o, subgroup 3C). The two elements are well correlated but uranium contents are slightly higher in subgroup 3C. The star indicates the average composition of comparatively graphite-free pelitic and psammitic schists from groups B and C.

The 'greisens' are distinctly enriched in K and Al, and depleted in Fe and Mg relative to retrogressed schists of other groups. In accordance with their sphene content, Ca and Ti are noticeably higher, as also is Sn. In table 3 this group has been subdivided into variants respectively richer (subgroup 6Ca) and poorer (subgroup 6Cb) in quartz porphyroblasts: column 6E lists a brannerite-bearing greisen of the quartz-poor, sericite-rich type.

Analyses of retrogressed pegmatites are included in table 3 mainly to demonstrate their relatively low contents of trace elements, including uranium. Columns 8B and 8C are not directly comparable, the former representing a large transgressive body ('Mosher Pegmatite', drill hole M135V) and the latter a series of smaller intrusions within Jabiluka Two (drill hole S180V). However column 8D lists the analysis of a heavily chloritized sample near the margin of a 0.3m pegmatite close to breccia ore, the interior of which pegmatite is included within and resembles the average cited in column 8C.

The marbles constitute too variable a group to calculate meaningful averages. A conspicuous decrease in Ca/Mg from non-retrogressed to retrogressed marbles is illustrated in figure 5, where divergence from the calcite-dolomite-magnesite line arises from minor Fe contents in carbonates and the presence of silicate impurities. Although stratigraphic correlation is not established, the trend is consistent with petrological evidence of replacement by magnesite

	PELITIC SCHISTS								PSAMMITIC SCHISTS							
Group	1A		1B		1C		1D		2A		2B		2C		2D	
n	4		11		18		6		4		11		10		6	
Major Elements (wt %, arithmetic means and standard deviations)																
SiO_2	59.4	(5.1)	63.3	(4.1)	63.0	(2.8)	59.7	(8.3)	74.6	(4.9)	70.9	(2.8)	70.6	(1.4)	70.8	(1.1)
TiO_2	0.67	(.04)	0.54	(.14)	0.49	(.08)	0.55	(.13)	0.49	(.04)	0.49	(.18)	0.44	(.22)	0.48	(.17)
Al_2O_3	19.9	(1.4)	17.6	(2.5)	18.0	(1.8)	17.5	(3.3)	13.9	(2.0)	13.8	(.8)	13.7	(1.3)	13.0	(1.0)
Fe_2O_3	1.7	(.4)	1.7	(.4)	1.1	(.8)	0.92	(.47)	0.92	(.65)	1.1	(.2)	0.72	(.29)	0.39	(.25)
FeO	4.5	(.7)	4.5	(.8)	2.2	(.7)	2.0	(1.0)	2.4	(.6)	2.7	(1.1)	1.6	(.6)	1.9	(.8)
MnO	0.11	(.02)	0.07	(.03)	0.04	(.02)	0.04	(.02)	0.07	(.03)	0.06	(.02)	0.04	(.02)	0.05	(.03)
MgO	2.6	(.8)	4.4	(.8)	4.6	(1.9)	8.4	(2.5)	1.1	(.5)	4.0	(1.7)	3.6	(.6)	5.3	(1.7)
CaO	0.50	(.07)	0.10	(.05)	0.10	(.09)	0.15	(.10)	0.59	(.14)	0.06	(.03)	0.06	(.05)	0.11	(.06)
Na_2O	1.2	(.3)	0.10	(.06)	0.12	(.06)	0.08	(.06)	2.1	(.6)	0.05	(.04)	0.02	(.02)	0.05	(.02)
K_2O	4.6	(1.4)	4.3	(1.1)	4.4	(.9)	2.8	(1.0)	1.9	(1.0)	3.5	(.6)	3.2	(.8)	2.3	(.8)
H_2O+	3.7	(.5)	4.2	(1.0)	4.9	(.6)	6.9	(1.5)	1.6	(.5)	3.6	(.9)	4.2	(.4)	4.7	(.5)
H_2O^-	0.5	(.3)	0.4	(.1)	0.8	(.1)	0.8	(.2)	0.4	(.1)	0.4	(.1)	0.9	(.1)	0.7	(.3)
P_2O_5	0.19	(.11)	0.08	(.03)	0.08	(.02)	0.09	(.03)	0.21	(.06)	0.05	(.03)	0.06	(.02)	0.10	(.06)
CO_2	NA		0.05	(.09)	NA		NA		NA		0.07	(.11)	NA		NA	
C	NA		0.12	(.19)	0.15	(.16)	0.23	(.17)	NA		0.12	(.10)	0.12	(.16)	0.17	(.16)
S	0.06	(.04)	NA		NA		0.13	(.18)	0.07	(.09)	NA		NA		0.16	(.02)
TOTAL	99.6		101.5		100.3		100.2		100.4		100.9		99.3		100.6	
Lithophile Trace Elements (ppm, logarithmic means and standard deviations of logarithms)																
Li	30	(.20)	50	(.12)	63	(.23)	182	(.32)	17	(.26)	48	(.23)	84	(.18)	128	(.15)
Be	1.7	(.15)	1.1	(.14)	1.5	(.22)	1.9	(.15)	1.4	(.17)	1.0	(.05)	1.7	(.24)	1.7	(.27)
B	*4	(.76)	NA		NA		NA		<3		NA		NA		NA	
F	1090	(.07)	NA		NA		NA		560	(.11)	NA		NA		NA	
Sc	9	(.08)	12	(.15)	13	(.16)	11	(.30)	4	(.11)	10	(.24)	8	(.18)	7	(.25)
V	63	(.23)	130	(.17)	83	(.11)	153	(.18)	18	(.15)	116	(.14)	54	(.15)	82	(.07)
Cr	114	(.04)	61	(.20)	81	(.15)	72	(.18)	66	(.05)	33	(.48)	32	(.36)	66	(.16)
Ga	22	(.13)	25	(.16)	21	(.07)	16	(.19)	9	(.18)	22	(.16)	20	(.07)	16	(.12)

Ge	<3		<3		<3		<3		<3		<3		<3		<3	
Rb	195	(.13)	130	(.09)	173	(.26)	120	(.38)	69	(.21)	105	(.09)	103	(.33)	63	(.18)
Sr	80	(.16)	11	(.30)	*8	(.23)	14	(.37)	72	(.13)	11	(.31)	*8	(.22)	11	(.34)
Y	36	(.06)	*15	(.34)	20	(.12)	28	(.10)	32	(.04)	19	(.21)	20	(.31)	28	(.17)
Zr	192	(.08)	179	(.15)	158	(.09)	244	(.12)	378	(.15)	218	(.07)	260	(.10)	208	(.07)
Nb	11	(.07)	11	(.09)	13	(.11)	9	(.20)	5	(.12)	12	(.11)	17	(.07)	5	(.05)
Sn	1.6	(.24)	1.5	(.36)	*1.1	(.35)	*1.0	(.29)	<1		4	(.45)	*0.9	(.14)	1.0	(.19)
Cs	NA		3	(.29)	<3		*2	(.19)	NA		3	(.15)	<3		3	(.16)
Ba	900	(.15)	370	(.29)	475	(.25)	267	(.28)	308	(.25)	298	(.28)	103	(.21)	114	(.30)
Yb	2	(.10)	NA		NA		NA		2	(.09)	NA		NA		NA	
Ta	NA		17	(.16)	13	(.23)	NA		NA		12	(.18)	13	(.11)	NA	
W	<50		<50		<50		<50		<50		<50		<50		<50	
Th	22	(.04)	19	(.12)	20	(.08)	19	(.08)	20	(.07)	21	(.05)	22	(.21)	14	(.08)
U	9	(.12)	7	(.12)	8	(.26)	231	(.30)	6	(.05)	7	(.12)	7	(.19)	252	(.20)
Chalcophile Trace Elements (ppm, logarithmic means and standard deviations of logarithms)																
Co	<20		*12	(.17)	*11	(.32)	11	(.15)	<20		<15		*9	(.19)	10	(.11)
Ni	84	(.09)	69	(.19)	65	(.18)	77	(.29)	41	(.12)	60	(.23)	70	(.14)	56	(.25)
Cu	27	(.49)	*8	(.22)	14	(.47)	22	(.57)	*7	(.17)	14	(.45)	29	(.59)	51	(.78)
Zn	76	(.21)	38	(.16)	49	(.24)	42	(.20)	25	(.35)	24	(.18)	24	(.18)	22	(.27)
As	<5		<10		NA		NA		<5		<10		NA		NA	
Mo	<3		<3		<3		*3	(.42)	<3		<3		<3		*3	(.36)
Ag	0.2	(.34)	<.1		*0.1	(.3)	0.1	(.2)	*0.1	(.29)	*0.1		*0.1		0.1	(.00)
Cd	<3		NA		NA		NA		<3		NA		NA		NA	
Sb	<30		NA		NA		<30		<30		NA		NA		<30	
Pb	37	(.15)	12	(.12)	13	(.27)	35	(.49)	21	(.19)	9	(.27)	10	(.26)	40	(.62)
Bi	<1		<1		<1		<1		<1		<1		<1		<1	

* Includes some data below detection limit NA = not analysed or insufficient data

Table 1. Average compositions of pelitic and psammitic schists from Jabiluka and vicinity.

	GRAPHITE SCHISTS								CHLORITE-RICH GRAPHITIC SCHISTS					
Group	3A		3B		3C		3D		4B		4C		4D	
n	4		20		9		9		10		6		2	
Major Elements (wt %, arithmetic means and standard deviations)														
SiO_2	58.9	(8.5)	58.9	(6.0)	54.8	(5.5)	57.5	(5.7)	51.7	(6.3)	47.6	(2.4)	56.2	(4.1)
TiO_2	0.49	(.10)	0.60	(.14)	0.53	(.13)	0.57	(.17)	0.64	(.19)	0.76	(.06)	0.56	(.13)
Al_2O_3	15.1	(2.5)	16.0	(2.5)	15.5	(2.8)	15.9	(2.8)	16.4	(4.6)	20.9	(2.6)	12.6	(4.3)
Fe_2O_3	3.3	(1.8)	3.1	(.9)	3.6	(1.7)	1.7	(2.1)	2.3	(.7)	1.5	(1.4)	2.3	(1.3)
FeO	3.5	(.8)	3.5	(1.5)	2.3	(.6)	2.2	(1.2)	5.1	(1.8)	2.6	(.6)	2.9	(.7)
MnO	0.12	(.04)	0.06	(.02)	0.08	(.06)	0.05	(.04)	0.08	(.03)	0.05	(.02)	0.05	(.02)
MgO	5.0	(.7)	5.3	(2.2)	5.8	(1.5)	5.4	(2.4)	13.5	(3.2)	13.0	(2.8)	12.5	(2.0)
CaO	0.51	(.69)	0.10	(.07)	0.09	(.13)	0.13	(.15)	0.09	(.04)	0.20	(.15)	0.09	(.02)
Na_2O	0.50	(.27)	0.06	(.03)	0.08	(.09)	0.06	(.01)	0.03	(.02)	0.04	(.02)	0.02	(.01)
K_2O	4.7	(1.0)	4.2	(1.3)	3.3	(1.1)	3.2	(1.0)	2.2	(1.9)	1.6	(.7)	0.11	(.15)
H_2O+	3.2	(.6)	4.2	(.9)	4.9	(1.5)	4.7	(1.2)	6.8	(.8)	8.7	(.4)	7.2	(2.0)
H_2O^-	1.1	(.1)	0.5	(.2)	0.7	(.3)	0.6	(.3)	0.6	(.2)	1.1	(.3)	0.8	(.1)
P_2O_5	0.11	(.04)	0.07	(.03)	0.11	(.07)	0.14	(.08)	0.05	(.02)	0.10	(.05)	0.14	(.13)
CO_2	0.9	(1.0)	0.08	(.24)	NA		NA		0.05	(.05)	NA		NA	
C	1.5	(.8)	4.1	(2.6)	5.6	(3.5)	6.7	(3.1)	2.3	(2.4)	2.1	(.8)	3.0	(2.1)
S	1.3	(1.1)	NA		3.3	(2.0)	1.0	(1.0)	NA		0.70	(.39)	NA	
Total	100.2		100.7		100.7		99.9		101.8		101.0		98.9	
Lithophile Trace Elements (ppm, logarithmic means and standard deviations of logarithms)														
Li	74	(.13)	60	(.20)	129	(.17)	113	(.24)	125	(.08)	290	(.09)	220	(.28)
Be	NA		1.0	(.05)	1.9	(.28)	3	(.20)	1.0	(.05)	3	(.18)	3	(.21)
B	10	(.48)	NA		NA		NA		NA		NA		NA	
F	1400	(.12)	NA		NA		NA		NA		NA		NA	
Sc	16	(.17)	16	(.18)	14	(.14)	13	(.28)	13	(.14)	12	(.25)	4	(.07)
V	110	(.37)	218	(.23)	228	(.23)	205	(.11)	137	(.10)	144	(.22)	126	(.28)
Cr	105	(.21)	82	(.33)	79	(.22)	90	(.18)	146	(.27)	205	(.04)	103	(.28)
Ga	8	(.24)	23	(.12)	21	(.11)	18	(.15)	23	(.17)	28	(.07)	24	(.13)

Ge	<3		<3		<3		<3		<3		<3		<3	
Rb	155	(.07)	120	(.14)	87	(.12)	96	(.22)	57	(.44)	46	(.53)	*5	(.2)
Sr	57	(.16)	*11	(.28)	18	(.33)	21	(.42)	*12	(.36)	10	(.23)	*7	(.3)
Y	27	(.06)	14	(.34)	20	(.27)	20	(.29)	*11	(.30)	7	(.15)	*9	(.3)
Zr	175	(.19)	143	(.12)	154	(.08)	144	(.11)	110	(.19)	147	(.06)	131	(.08)
Nb	5	(.17)	13	(.13)	11	(.21)	7	(.20)	11	(.10)	8	(.21)	9	(.34)
Sn	*1	(.37)	4	(.46)	1.7	(.25)	2.1	(.29)	*2	(.66)	1.3	(.21)	*1	(.55)
Cs	NA		3	(.15)	*3	(.22)	*2	(.21)	*2	(.32)	<3		<3	
Ba	560	(.12)	232	(.31)	164	(.26)	157	(.13)	132	(.41)	72	(.33)	28	(.30)
Yb	2	(.09)	NA		NA		NA		NA		NA		NA	
Ta	NA		18	(.17)	19	(.06)	NA		14	(.21)	NA		NA	
W	<50		<50		<50		<50		<50		<50		<50	
Th	15	(.14)	20	(.14)	20	(.10)	21	(.18)	14	(.15)	14	(.15)	12	(.10)
U	16	(.26)	14	(.31)	29	(.23)	255	(.26)	6	(.14)	41	(.33)	131	(.29)
Chalcophile Trace Elements (ppm, logarthmic means and standard deviations of logarithms)														
Co	22	(.09)	*15	(.23)	35	(.24)	18	(.37)	*14	(.18)	25	(.24)	16	(.28)
Ni	120	(.31)	124	(.19)	138	(.20)	89	(.19)	107	(.12)	116	(.32)	126	(.28)
Cu	99	(.23)	73	(1.0)	136	(.50)	140	(.90)	36	(.92)	46	(.43)	104	(1.2)
Zn	73	(.19)	33	(.18)	43	(.13)	47	(.14)	30	(.24)	45	(.13)	50	(.32)
As	NA		<10		NA		NA		<10		NA		NA	
Mo	*15	(.61)	14	(.83)	14	(.78)	11	(.45)	*3	(.52)	*3	(.52)	*4	(.58)
Ag	0.3	(.12)	*0.1	(.1)	0.3	(.3)	0.2	(.2)	<0.1		0.3	(.2)	*0.4	
Cd	NA		NA		NA		<3		NA		NA		<3	
Sb	<30		NA		NA		<30		NA		NA		<30	
Pb	73	(.26)	13	(.17)	79	(.63)	73	(.51)	10	(.16)	101	(.22)	79	(.55)
Bi	<1		*4	(.64)	8	(.33)	3	(.55)	*1	(.61)	2	(.43)	*2	(.71)

* Includes some data below detection limit NA = not detected or insufficient data

Table 2. Average compositions of graphite schists and chlorite-rich graphitic schists from Jabiluka and vicinity.

	'GREISENS'				PEGMATITES				
Group	6C(a)		6C(b)		6E	8B		8C		8D
n	6		5		1	6		5		1
Major Elements (wt %, arithmetic means and standard deviations)										
SiO_2	70.9	(5.3)	53.1	(3.9)	44.9	71.1	(1.1)	66.8	(2.9)	36.6
TiO_2	0.64	(0.15)	0.91	(0.27)	1.07	0.03	(0.01)	0.12	(0.10)	0.86
Al_2O_3	16.2	(3.7)	27.5	(1.3)	32.5	14.7	(0.3)	15.7	(2.3)	20.5
Fe_2O_3	0.51	(0.17)	0.98	(0.17)	0.42	0.50	(0.30)	0.59	(0.09)	0.84
FeO	0.91	(0.24)	0.68	(0.19)	0.35	1.04	(0.41)	1.5	(0.4)	2.85
MnO	0.03	(0.02)	0.03	(0.01)	0.06	0.02	(0.01)	0.04	(0.01)	0.03
MgO	1.3	(0.7)	3.4	(2.7)	1.67	4.0	(1.0)	4.4	(3.1)	23.3
CaO	0.24	(0.13)	0.38	(0.37)	0.16	0.20	(0.05)	0.79	(0.59)	0.58
Na_2O	0.06	(0.03)	0.12	(0.08)	0.09	0.05	(0.02)	0.08	(0.03)	0.03
K_2O	4.8	(1.0)	7.6	(1.3)	8.2	3.1	(0.7)	3.6	(1.4)	0.09
H_2O^+	3.1	(0.7)	5.7	(1.9)	6.2	4.5	(0.6)	4.4	(1.3)	11.4
H_2O^-	0.7	(0.1)	1.0	(0.5)	0.9	0.7	(0.1)	0.7	(0.2)	1.2
P_2O_5	0.15	(0.08)	0.18	(0.12)	0.24	0.07	(0.01)	0.23	(0.13)	0.09
CO_2	NA		NA		NA	0.03	(0.01)	NA		NA
C	0.15	(0.10)	0.20	(0.12)	NA	0.05	(0.02)	0.11	(0.03)	0.18
S	NA		NA		0.26	NA		NA		0.16
Total	99.7		101.8		98.1[#]	100.1		99.1		98.7
Lithophile Trace Elements (ppm, logarithmic means and standard deviations of logarithms)										
Li	29	(.22)	49	(.40)	115	110	(.07)	83	(.45)	330
Be	21	(.26)	4	(.18)	10	4	(.29)	1.6	(.21)	3
B	NA		NA		500	NA		NA		NA
F	NA		NA		1000	NA		NA		NA
Sc	12	(.18)	22	(.23)	150	NA		6	(.26)	7
V	73	(.20)	123	(.20)	80	17	(.28)	78	(.18)	150
Cr	66	(.15)	74	(.35)	160	<10		19	(.41)	138
Ga	21	(.07)	25	(.11)	25	7	(.29)	20	(.10)	30

Ge	<3		<3		<3	< 3		<3		<3
Rb	195	(.16)	340	(.15)	124	<10		175	(.27)	<10
Sr	12	(.22)	16	(.12)	67	<10		36	(.42)	7
Y	30	(.21)	64	(.57)	54	<10		8	(.27)	8
Zr	275	(.17)	345	(.12)	215	20	(.10)	46	(.21)	150
Nb	14	(.15)	32	(.09)	20	13	(.16)	12	(.23)	10
Sn	4	(.51)	10	(.48)	4	1.6	(.31)	22	(.21)	1
Cs	<3		<3		NA	3	(.15)	<3		<3
Be	320	(.29)	470	(.29)	157	43	(.09)	110	(.37)	2
Yb	NA		NA		20	NA		NA		NA
Ta	14	(.30)	14	(.13)	NA	12	(.25)	19	(.20)	NA
W	<50		<50		<50	<50		<50		<50
Th	23	(.27)	35	(.11)	18	<10		<10		<10
U	7	(.11)	9	(.29)	0.87%	11	(.12)	9	(.30)	200
Chalcophile Trace Elements (ppm, logarithmic means and standard deviations of logarithms)										
Co	<10		<10		330	<20		<10		25
Ni	48	(.24)	54	(.66)	150	9	(.43)	65	(.29)	200
Cu	21	(.66)	6	(.31)	470	43	(.70)	30	(1.1)	930
Zn	12	(.21)	22	(.25)	10	17	(.10)	27	(.29)	70
As	NA		NA		3	<10		NA		NA
Mo	<3		<3		60	< 3		<3		3
Ag			<0.1		0.1			<0.1		
Cd	NA		NA		<3	NA		NA		NA
Sb	<30		<30		<30	<30		<30		<30
Pb	13	(.59)	16	(.41)	1070	*10	(.25)	13	(.53)	370
Bi	<1		< 1		5	< 1		< 1		1

NA = Not analysed or insufficient data * Includes some data below detection limit # Includes 1.03% U_3O_8

Table 3. Average compositions of greisens and pegmatites from Jabiluka.

	HIGH GRADE ORES (n = 35)		LOW GRADE ORES (n = 7)	
Major Elements (wt. % see footnote)				
SiO_2	51.9	(2.5)	48.9	(9.7)
TiO_2	0.26	(0.13)	0.51	(0.17)
Al_2O_3	12.4	(2.5)	17.2	(3.7)
Fe_2O_3	-		3.1	(1.5)
FeO**	3.1	(0.4)	2.3	(1.3)
MnO	0.23	(0.02)	0.12	(0.03)
MgO	4.1	(0.1)	12.2	(5.5)
CaO	0.52	(0.16)	0.24	(0.43)
Na_2O	0.04	(0.02)	0.03	(0.02)
K_2O	1.0	(0.7)	1.2	(0.5)
H_2O^+	6.1	(0.1)	8.3	(2.7)
H_2O^-	2.4	(0.2)	1.0	(0.5)
P_2O_5	0.33	(0.04)	0.47	(0.41)
CO_2	0.17	(0.29)	<0.1	
C	0.07	(0.08)	1.6	(1.8)
S	0.30	(0.17)	1.0	(0.7)
U_3O_8	16.5	(2.0)	1.1	(0.9)
Total	99.1		99.3	
Lithophile Trace Elements (ppm, see footnote)				
Li	211	(.08)	255	(.19)
Be	7	(.20)	3	(.17)
B	310	(.28)	127	(.55)
F	746	(.11)	1140	(.24)
Sc	182	(.07)	6	(.30)
V	82	(.08)	107	(.15)
Cr	NA		66	(.22)
Ga	NA		25	(.17)
Ge	NA		≈1	
Rb	55	(.23)	18	(.56)
Sr	11	(.30)	25	(.25)
Y	627	(.06)	113	(.38)
Zr	435	(.08)	155	(.18)
Nb	66	(.09)	6	(.29)
Sn	3.4	(.21)	3.1	(.41)
Ba	29	(.85)	53	(.74)
Yb	1150	(.10)	≈5	(.90)
W	<50		<50	
Th	29	(.23)	21	(.08)
U	13.9%	(.05)	0.60%	(.45)
Chalcophile Trace Elements (ppm, see footnote)				
Co	58	(.02)	41	(.33)
Ni	50	(.02)	99	(.09)
Cu	362	(.47)	840	(.60)
Zn	33	(.07)	58	(.25)
As	77	(.04)	5	(.23)
Mo	37	(.23)	14	(.55)
Ag	0.6	(.07)	0.3	(.32)
Cd	<3		<3	
Sb	<30		<30	
Hg	2.0		0.5	(.30)
Pb	8670	(.08)	680	(.60)
Bi	21	(.44)	6	(.38)

* Includes some data below detection limit (1 ppm)

** Total iron for high grade ores; U interferes with titration

NA Not analysed (U interference)

Arithmetic means and standard deviations are cited for major elements. For trace elements the data are logarithmic means and standard deviations of the logarithms. Mg from Ryall and Binns (this volume).

Table 4. Average compositions of uraninite ores from Jabiluka Two.

during retrogressive alteration. The marbles have low trace element contents: the average Sr content for subgroup 7B is only 21 ppm.

Zirconium (reflecting detrital zircon accessories) is the only trace element of significant abundance in Kombolgie Sandstone; the average U content is only about 1 ppm. However in the basal few metres of sandstone the uranium content increases up to 15 ppm in sympathy with higher Ca and P. This was noted at an unconformable contact in drill hole M096V between Jabiluka One and Two, but was absent from an intersection in T168V through the unconformity above Jabiluka Two mineralization. The increased uranium in the basal Kombolgie Sandstone appears to be due to apatite replacement of sandstone matrix, possibly associated with thin drusy-style quartz veins. Metamorphosed regolith samples below the Kombolgie unconformity are relatively rich in K and Al, reflecting sericite abundance. Trace element contents tend to be intermediate between those of Kombolgie Sandstone and underlying Cahill Formation schists, apart from Sr, which is enriched at approximately 100 ppm.

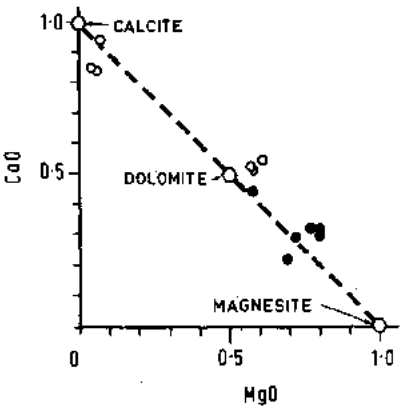


Figure 5. Plot of CaO versus MgO (molecular proportions normalised to CO_2 = 1.00) showing the contrast between amphibolite facies calcite and dolomite marbles (o, subgroup 4A) and their magnesite-rich retrogressed equivalents (●, subgroup 7B).

INTERPRETATION

A rigorous evaluation of geochemical changes associated with mineralization and surrounding alteration at Jabiluka should take into account differences between lithological groups. Statistical tests of the more subtle differences remain to be carried out, preferably when more data are available. The approach in this study has been to examine as wide a range of elements as possible, using samples from a restricted number of representative drill holes. The next step would be to examine, on a wider and more detailed geographic scale, those elements assigned significance below.

Meanwhile, a convenient method of treating the data is to plot various elements against uranium (Fig. 6). Uranium contents display the greatest variation between rocks remote from mineralization, those that are immediate hosts to ore, and the ores themselves. In the following remarks, and in figures 7 to 9, account has been taken of standard deviations listed in tables 1 to 3, and of variations between lithological groups.

Geochemistry of Retrogressive Metamorphism

Geochemical changes associated with retrogressive metamorphism are indicated by a comparison of the analytical data for subgroups A and B and these are summarized in figure 7. It has been assumed that the non-retrogressed schists studied are indeed geochemically representative of parents for their retrogressed petrological equivalents, and the conclusions below are constrained by the validity or otherwise of this assumption.

The most conspicuous geochemical effects of retrogressive alteration are marked depletion in Na and the alkaline earth group Ca, Sr and Ba, and enrichment in Li, Mg and H_2O^+. Lesser depletion in the transition metals Cr, Mn and Fe, in P, and in the chalcophile trace metals Zn and Pb also occur. Mild enrichments in Sc, V, Ga and Nb are also apparent. Some of these changes are not apparent in all lithological groups, or the magnitude of alteration varies between groups. Potassium and Rb contents are generally constant: apparent increases during retrogression of the psammitic schists (2A → 2B) may be in part an artifact reflecting the slightly more siliceous nature of subgroup 2A, and the slight decreases in Rb for groups 1 and 2 appear statistically insignificant.

Most of these differences can be explained in terms of the mineralogy of retrogressive alteration. The increase in Mg and decreases in Cr, Mn and Fe reflect chloritization of biotite. The behaviour of Na and the alkali earths arises from alteration of feldspar to sericite-chlorite-septechlorite aggregates, which also contributes in part to the rise in Mg. A balance evidently existed between release of K from chloritized biotite and its fixation in altered feldspar. The more distinct loss of Ba from groups 1 and 3 compared to group 2 may reflect former proportions of K-feldspar relative to plagioclase. The normally chalcophile elements Zn and Pb may in this instance have displayed a more lithophile character, and their declines probably reflect alteration of the former hosts, biotite and feldspar respectively. The loss of P is consistent with the observed decrease in accessory apatite content, an indication also of the acid nature of retrogressive fluids. The difference in elemental carbon between subgroups 3A and 3B probably represent sample bias.

The immobile character of certain trace elements may also be accounted for mineralogically. For example, accessory zircon is preserved during retrogression, and titanium formerly in biotite is fixed in anatase or brookite needles within sagenitic chlorite replacements.

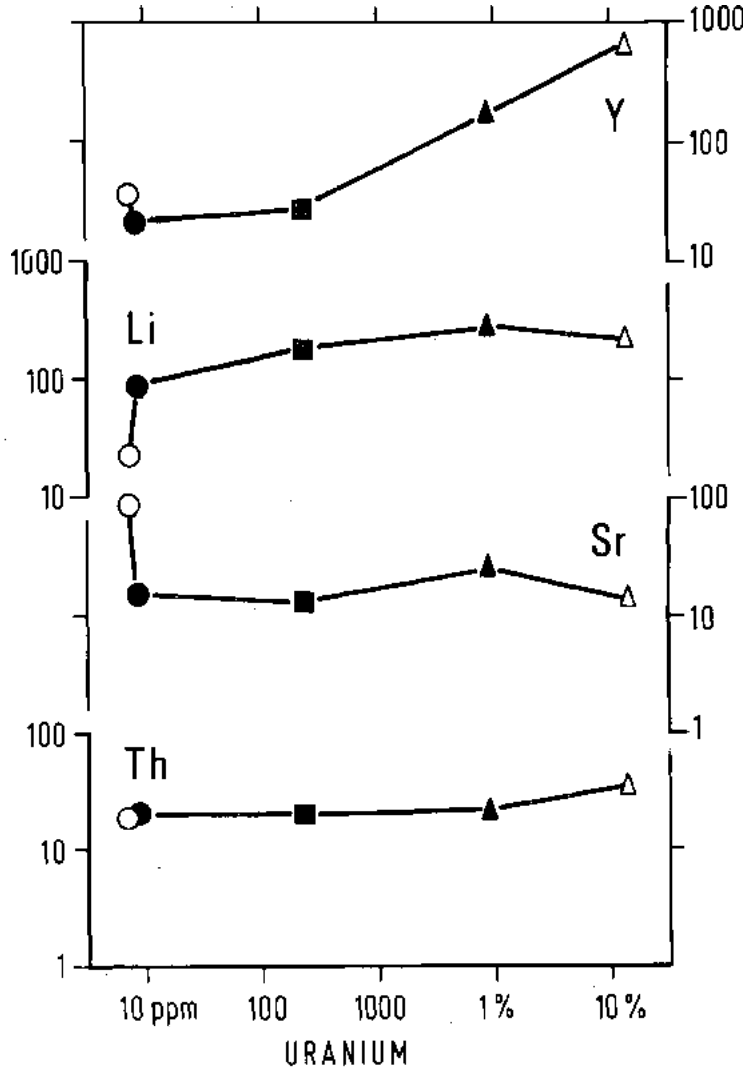


Figure 6. Logarithmic plots illustrating the behaviour of selected average lithophile trace elements in pelitic and psammitic schists from Jabiluka. O, high grade metamorphics > 2 km from Jabiluka (subgroup A); ●, barren retrogressed schists 1-200 m from mineralization (subgroups B and C); ■, immediate host rocks to mineralized veins and breccias (subgroup D); ▲, disseminated ores in brecciated or veined schists (subgroup E); △, high grade ores (subgroup F).
Yttrium illustrates an element conspicuously enriched in ores. Lithium and strontium display enrichment and depletion respectively in the retrogressive halo surrounding mineralization. Thorium is essentially immobile during retrogressive alteration and only slightly enriched in high grade ores.

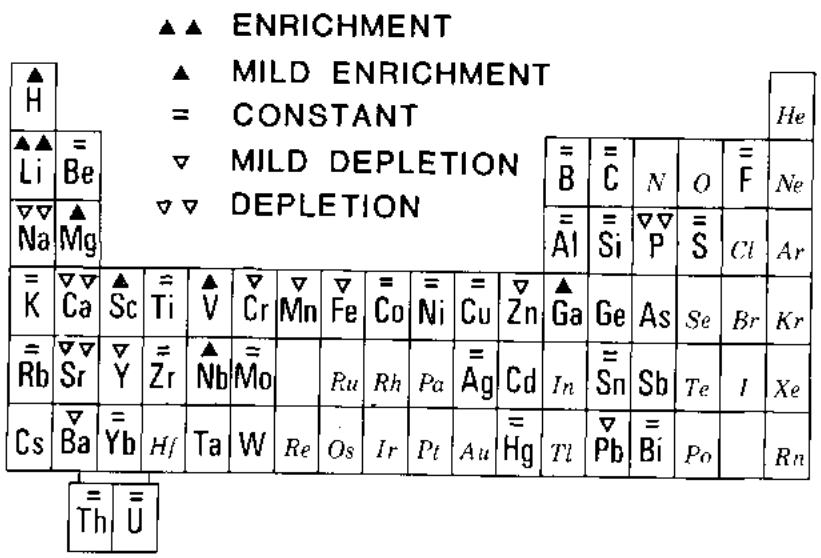


Figure 7. Geochemical changes arising from retrogressive metamorphism of former amphibolite facies schists. These in effect define an outer alteration halo extending >100m from mineralisation. Based on comparisons between subgroup A and subgroups B and C.

Geochemistry of Ores

Differences between Jabiluka ore veins or breccia zones and their immediate host rocks, obtained by comparison of analytical data for subgroup D with those of subgroups E and F, are illustrated in figure 8. When grouped according to the lithology of the veined wall-rock, Jabiluka ores are even further enriched in Mg and are conspicuously depleted in K, Rb and Ba. This reflects abundance of chlorite-septechlorite-quartz intergrowths (CSQ) associated with uraninite, which replace muscovite and other minerals close to veins and breccias. The disseminated ores are slightly enriched in Ca, P and Sr relative to adjacent host rocks, due in part to concentration of apatite in breccia zones. Calcium, and possible Sr, may also be contained in uraninite. Only two of the trace elements examined show enrichments comparable in magnitude to that of uranium itself, namely radiogenic Pb, and Yb (taken as a measure of rare earth element abundances, presumably in uraninite). Scandium and yttrium (Fig. 6) also increase sympathetically with U, but relative to background levels in barren schists the enrichment factors are smaller (about 20x in high grade ores). Copper, correlating with sulphide abundance, is high in ores but erratically distributed. Zirconium, Nb and Th are slightly enriched, as are Be, Sn, Mo and Bi but mostly at levels close to detection limits. Boron and As are relatively high in ores, but few data are available for comparison with host rocks. Ores are also characterized by significantly higher Mn contents and Mn/Fe ratios. Many of these changes in trace elements are also apparent in a comparison of a mineralized greisen (Column 6E, Table 3) with its unmineralized equivalents (subgroup 6Cb). The increases in Sc and Sr are especially notable.

Although all data necessary for comparison are not available, F appears to have the characteristics of an immobile element. Contents in ores (Table 4) are similar to those in non-retrogressed schists (subgroup A, Tables 1 and 2).

Variations Between the Outer and Inner Retrogressed Aureole

Comparisons between subgroup B and subgroup C indicate remarkably little difference

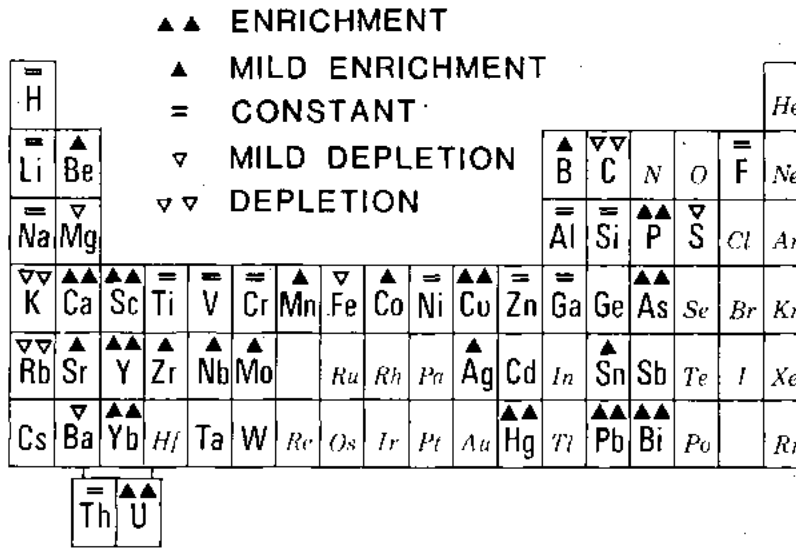


Figure 8. Geochemical characteristics of uraninite mineralization. Based on analyses of breccias and heavily veined samples, compared to subgroup D samples.

in composition of retrogressed country rocks remote from ore and within barren intervals of the Jabiluka Two orebody. There is a consistent and significant decrease in Fe in all lithological groups, which is not explained by changes in sulphide content. Although the complementary increase in Mg is not observable, this nevertheless suggests that a study of chlorite compositions in relation to distance from mineralization might be profitable. In some lithological groups a further increase in Li occurs. Another change between subgroups B and C of possible significance is the slightly higher mean C content of graphitic schists from the latter (Figs. 3 and 4).

Geochemistry of Host Rocks Close to Ore

More distinct changes are apparent upon inspection of data for subgroup D, the immediate host rocks to ore veins and breccias, as summarized in figure 9. Compared to subgroups B and C retrogressed schists, the hosts are enriched by a factor of about 25 in uranium content. Study of thin and polished sections and of long duration autoradiographs shows that this is not due to disseminated uraninite. Rather, it reflects the more intense development of chlorite-septchlorite ± quartz (CSQ) aggregates in the host, replacing quartz especially but in places also muscovite and graphite. Carefully hand-picked CSQ may contain more than 1000 ppm U (see Gulson & Mizon, this volume).

Radiogenic Pb is also high in subgroup D hosts, and it is notable that their U/Pb ratios are lower (about 5) than in ores (about 10-15), which suggests the possibility of detecting a radiogenic aureole surrounding mineralization.

Other characteristics of the host schists relative to their more remote equivalents are increases in Li, Mg and HO^+ further to those arising from retrogression itself (i.e. A → B, C). Mild enrichments in some chalcophile trace elements (Cu, Mo, Hg) are also apparent. Depletion in K and Rb is evident for most lithological groups, reflecting in large part the decrease in the sericite component of CSQ-like replacement products with a contribution from attack on relic muscovite. Insofar as subgroup 4D includes many hosts formed by

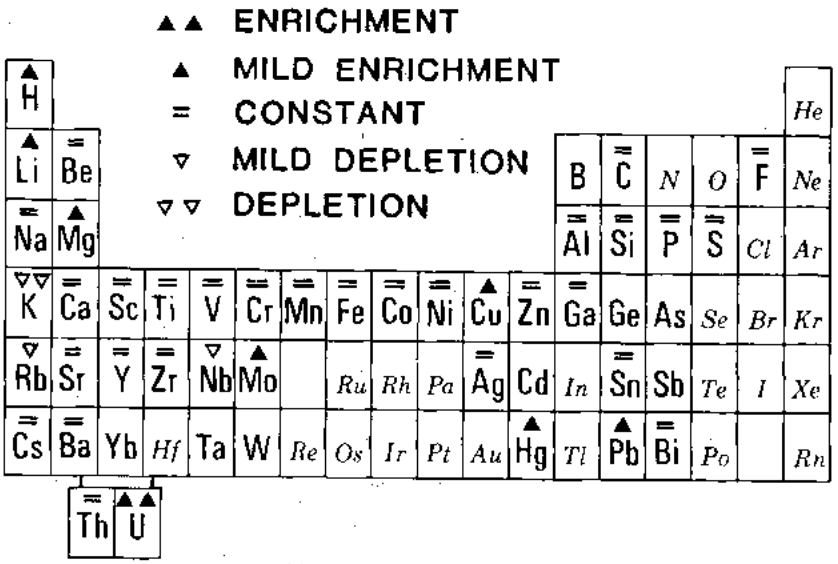


Figure 9. Geochemical characteristics of immediate host rocks to ore, defining an inner alteration halo within metres of uraninite mineralization. Based on comparison of subgroups B and C with subgroup D.

extensive chloritization of graphite schists, these trends are also evident in a comparison of these with subgroup 3C.

EXPLORATION SIGNIFICANCE

When the foregoing results are applied to locating ore in the primary environment, it is immediately apparent that uranium is its own best pathfinder at Jabiluka. Multi-element geochemical techniques will have only a secondary application. The compositional characteristics described above for ores and their immediate host rocks might be applied in advanced evaluation of exploratory diamond drilling for ore extensions or in areas of known mineralization potential. Mercury pathfinder methods and lead isotopic studies (Ryall & Binns, this volume; Gulson & Mizon, this volume) would ideally be undertaken in conjunction with multielement geochemistry. A further application might be in pattern drilling of favourable host rock units (e.g. graphite schists), perhaps recognized by geophysical methods in areas of poor exposure. An important point to be noted is that during advanced stages of exploration it would be beneficial to analyse low level uranium in country rocks that would normally be ignored in early exploration. Figures 3 and 4, and the foregoing discussion, illustrate the potential value of this for graphite schists in particular.

The geochemical changes associated with retrogressive metamorphism form a quite large-scale 'primary geochemical halo' around the Jabiluka orebodies. The alteration patterns described here (A → B) are based on comparatively few drill holes and obviously further studies should be carried out. Even if the parameters indicated, such as enrichment in Li and Mg or depletion in Ca and Sr for example, become substantiated for other localities, geochemical techniques would be unnecessary during early exploratory drilling in the primary environment since retrogressive metamorphism is so obvious from megascopic inspection of core. They may again be applicable in advanced phases of exploration, as for example if it were considered desirable to verify an alteration halo with higher likelihood of

a relationship to mineralization. However geochemical studies of other styles of retrogressive metamorphism would be desirable beforehand.

Geochemical methods have much greater potential application in the secondary environment, where the high mobility of uranium becomes a problem. Although the necessary research remains to be carried out, anomalous enrichments of, for example, Sc, Y, rare earth elements, Pb and Cu in weathered rock or residual soil should reflect underlying Jabiluka-style mineralization. Elements such as Mg, Li, Na, Ca, Sr and Ba would aid delineation in poorly exposed areas of the larger targets created by retrogressive metamorphic haloes, but the differences will be subtle and the deviations large so that statistical multielement approaches including use of element ratios will probably be required. Recent developments in plasma emission spectrometry, providing low cost multielement analyses, greatly increase the commercial feasibility of such approaches.

ACKNOWLEDGEMENTS

We thank the analytical staff of North Ryde Laboratories, CSIRO Institute of Earth Resources for their vital assistance to this project. Most samples were collected with the generous assistance of geological staff from Pancontinental Mining Limited, and Geopeko Limited kindly provided samples from Ranger 19.

REFERENCES

Bell, R.T., 1978: Uranium in black shales - a review. *in* (ed. M.M. Kimberley) *Short Course in Uranium Deposits: Their Mineralogy and Origin, Mineralogical Association of Canada*, 307-329.

Binns, R.A., McAndrew, J. & Sun, S-S., this volume: Origin of uranium mineralization at Jabiluka. *Proceedings of the International Uranium Symposium on the Pine Creek Geosyncline.*

Dale, M., Hain, D., Lance, G., Milne, P. & Williams, W., 1978: *Taxon Users' Manual, CSIRO Division of Computing Research, Canberra.*

Eupene, G.S., Fee, P.F. & Colville, R.G., 1975: Ranger 1 uranium deposits. *in* (ed. C. L. Knight) *Economic Geology of Australia and Papua New Guinea, Australas. Inst. Min. Metall., Monograph Series No. 5, 1. Metals*, 308-317.

Foy, M.F., & Pederson, C.P., 1975: Koongarra uranium deposit. *in* (ed. C.L. Knight) *Economic Geology of Australia and Papua New Guinea*, Australas Inst. Min. Metall., *Monograph Series No. 5, 1. Metals*, 317-321.

Gulson, B.L. & Mizon, K.J., this volume: Lead isotope studies at Jabiluka. *Proceedings of the International Uranium Symposium on the Pine Creek Geosyncline.*

Hegge, M.R., 1977: Geologic setting and relevant exploration features of the Jabiluka uranium deposits. *Proc. Australas. Inst. Min. Metall.*, 264, 19-32.

Hegge, M.R., & Rowntree, J.C., 1978: Geologic setting and concepts on the origin of uranium in the East Alligator River region, N.T., Australia. *Econ. Geol.*, 73, 1420-1429.

Krauskopf, K.B., 1979: *Introduction to Geochemistry*. 2nd edition. McGraw-Hill, New York.

Needham, R.S. & Stuart-Smith, P.G., this volume: Geology of the Alligator Rivers Uranium Field. *Proceedings of the International Uranium Symposium on the Pine Creek Geosyncline.*

Riley, G.H., Binns, R.A. & Craven, S.J., this volume: Rb-Sr chronology of micas at Jabiluka. *Proceedings of the International Uranium Symposium on the Pine Creek Geosyncline.*

Rowntree, J.C., & Mosher, D.V., 1975, Jabiluka uranium deposits. *in* (ed. C.L. Knight) *Economic Geology of Australia and Papua New Guinea, Australas. Inst. Min. Metall., Monograph Series No. 5, 1. Metals*, 321-326.

Ryall, W.R. & Binns, R.A., this volume: Mercury distribution in the Jabiluka Two orebody and its host rocks. *Proceedings of the International Uranium Symposium on the Pine Creek Geosyncline.*

LEAD ISOTOPE STUDIES AT JABILUKA

B.L. Gulson[1] and K.J. Mizon[2]

1. CSIRO Division of Mineralogy, P.O. Box 136, North Ryde, N.S.W., 2113, Australia.
2. CSIRO Fuel Geoscience Unit, P.O. Box 136, North Ryde, N.S.W., 2113, Australia.

ABSTRACT

Analyses of sulphides and whole rocks from Jabiluka demonstrate the potential use of Pb isotopes in exploration for U ore deposits. As mineralization is approached, the $^{206}Pb/^{207}Pb$, $^{206}Pb/^{208}Pb$ and $^{206}Pb/^{204}Pb$ ratios increase dramatically.

The oldest apparent uraninite ages are 1100 - 1300 m.y. from an extensively studied 10cm piece of drill core which contains finely disseminated sulphides associated with chlorite; the sulphides may have stabilized the oxidation of uraninite and thus inhibited loss of radiogenic Pb. Sulphides in this and some other samples contain excess radiogenic Pb derived from uraninite, as does one sample of chlorite. Chalcopyrite from a 'drusy' vein cutting uraninite has an apparent age of ~1380 m.y. and this places a minimum age on the U mineralization.

Analyses of the other carefully selected uraninites (vein and disseminated types) give young apparent ages (~400-900 m.y.) consistent with previous studies in the Alligator Rivers area. These young ages are probably the result of leaching of radiogenic Pb and other daughter products from uraninite during later low temperature alteration processes or Pb loss by diffusion.

Six Jabiluka whole rocks do not define a linear array on any lead isotope plot. One sample with a $^{207}Pb/^{206}Pb$ ratio of ~0.038 exhibits disequilibrium of U and Pb, which may be the result of excess radium. Disequilibrium is also present in a chlorite-septechlorite-quartz vein and may be more widespread, although not as obvious, as in these two samples.

Sulphide lenticles for nine samples located metres from U mineralization define a well-correlated line on a $^{207}Pb/^{206}Pb$ vs $^{204}Pb/^{206}Pb$ plot which has an intercept proportional to an age of 1380 ± 110 m.y. These samples are, however, still within the zone of chloritic alteration. As mineralization is approached, the data become very scattered and little chronological information can be obtained. The apparent age of 1380 ± 110 m.y. does not correlate with any other major isotopic data from the area but is consistent with a later 'event' suggested by U-Pb zircon data (Page *et al.*, this volume), and a single uraninite age. Alternatively, this age may represent the time of uraninite mineralization at Jabiluka.

A mechanism is proposed for transport of U by brines rather than CO_2-rich solutions. This hypothesis is consistent with temperature estimates and can more readily account for corrosion of, and incorporation of U and radiogenic Pb into, pre-existing sulphides. If brines are the transporting mechanism the U can be moved as the U ^{IV} species and no reducing agents at the site of deposition are necessary.

1. EXPLORATION SIGNIFICANCE

Introduction

This investigation was undertaken primarily to ascertain the feasibility of using Pb isotopes in exploration for U deposits by outlining radiogenic halos around deposits. Such a concept has been mooted for more than 20 years (e.g. Cannon *et al.*, 1961; Rossman *et al.*, 1972) but rarely applied, if at all. In U deposits the radioactive decay of ^{238}U to ^{206}Pb and ^{235}U to ^{207}Pb gives radiogenic Pb isotope ratios quite distinct from those occurring in barren rocks or sulphides because of the small amounts of common (initial) Pb in U minerals. The ^{204}Pb gives a measure of the amount of common Pb in a mineral which, at the time of crystallization of uraninites and zircons, is usually very low. The majority of Pb in such minerals is derived by radioactive decay of U and Th (radiogenic Pb) and so we find $^{207}Pb/^{206}Pb$ ratios of 0.2 or less in U ore bodies compared with perhaps 0.9 in base metal sulphide deposits, as well as very high $^{206}Pb/^{204}Pb$ ratios of thousands. On the other hand, many U deposits contain little Th so that very low $^{208}Pb/^{206}Pb$ ratios occur. In a progression from an unmineralized to a mineralized sequence we should therefore observe a decrease in $^{208}Pb/^{206}Pb$ and $^{207}Pb/^{206}Pb$ or increase in $^{206}Pb/^{208}Pb$, $^{206}Pb/^{207}Pb$ and $^{206}Pb/^{204}Pb$ ratios.

For this preliminary investigation, we have analysed pyrite and chalcopyrite from lenticles in graphitic schists from the mineralized zone of the Jabiluka Two orebody, from a zone metres from mineralization and in so-called unmineralized schists between the Jabiluka One and Two orebodies. However, these samples are still from within the chlorite

Sample No.	Pb (ppm)	U (ppm)	$\frac{^{208}Pb}{^{206}Pb}$	$\frac{^{207}Pb}{^{206}Pb}$	$\frac{^{206}Pb}{^{204}Pb}$	$\frac{^{207}Pb}{^{204}Pb}$	$\frac{^{208}Pb}{^{204}Pb}$	$\frac{^{238}U}{^{204}Pb}$	$\frac{^{204}Pb}{^{206}Pb} \times 10^{-4}$	DDH (depth in m)	Sequence Rock type
Near Mineralization											
54943 Cp	22	-	0.0844	0.1333	453	60.40	38.24	-	22.1	S180V (223.6)	MMS Graphite-schist
54954 C Py-A	275	33	0.2499	0.1787	145.0	25.90	36.23	21.6	69.0	S180V	MMS
-B	-	-	0.2497	0.1787	144.6	25.84	36.11	-	69.2	(230.7)	Graphite-schist
54955C Py	107	45	0.3116	0.1853	116	21.53	36.21	63.6	86.1	S180V (231.7)	MMS Graphite-schist
54959B Cp	270	34	0.0355	0.1190	1053	125.4	37.38	135	9.5	S180V (236.3)	MMS Graphite-schist
54959B Py	970	19	0.1230	0.1397	324	45.20	39.78	6.9	30.9	S180V (236.3)	MMS Graphite-schist
55044 Py-1A	3930	-	0.0667	0.0955	596	56.95	39.78	-	16.8	U132V	MMS
-1B	4050	-	0.0667	0.0957	570	54.56	38.03	-	17.5	(156.0)	Graphite-schists
-2	2660	2.34%	0.0584	0.0924	651	60.19	38.04	3290	15.4	U132V (156.0)	MMS Graphite-schist
55046 Py-1	355	-	0.1413	0.1156	272	31.46	38.43	-	36.8	U132V (156.7)	MMS Graphite-schist
-2	364	353	0.1439	0.1168	269	31.39	38.65	285	37.2	"	
55233 Py-1	44	-	0.0990	0.0970	398	38.64	39.43	-	25.1	L153V (292.1)	UGS Graphite-schist
-2	44	408	0.1034	0.0984	383	37.69	39.64	3680	26.1	"	
55266 Py-1	-	-	0.1254	0.1324	308	40.72	38.58	-	32.5	0189V	MMS
-2A	133	126	0.1605	0.1421	232	32.97	37.24	318	43.1	(368.8)	Graphite-schist
B+	-	-	0.1606	0.1422	232	32.99	37.26	-	43.1		
55267 Py-1	157	-	0.0958	0.1192	397	47.24	38.00	-	25.2	0189V (370.0)	MMS Graphite-schist
-2	161	323	0.0918	0.1237	430	53.13	39.42	910	23.3	"	
55288 Py-1	158	-	0.0695	0.1027	528	54.17	36.69	-	18.9	0189V	MMS
-2	158	25	0.0694	0.1033	559	57.75	38.78	91	17.9	(389.0)	Graphite-schist
55289 Py-1	140	-	0.1048	0.1327	357	47.30	37.35	-	28.0	0189V	MMS
-2	139	32	0.1049	0.1317	363	47.87	38.12	90	27.5	(389.2)	Graphite-schist
54964 Cp (drusy vein)	4700	180	0.0264	0.1151	1483	170	39.15	56	6.7	S180V (238.2)	MMS Graphite-schist

Mineralized (metres from ore)											
55235 Py	13.1	6.5	0.9193	0.4401	39.77	17.50	36.56	40	251.4	L153V (294.0)	UGS Graphite-schist
55236 Py	32	7.6	1.3500	0.6094	26.73	16.29	36.09	16.4	374.1	L153V (295.5)	UGS Graphite-schist
55238 Py-1	9.0	10	1.2293	0.5698	28.92	16.48	35.56	80.6	345.8	L153V (298.4)	UGS Graphite-schist
-2++	44	140	0.5967	0.2919	63.9	18.66	38.14	335	157.8		
Unmineralized											
55145 Py	4.7	0.34	1.8050	0.7716	20.44	15.77	36.90	4.7	489.2	M096V (288.9)	MMS Grahite-schist
55172 Py	10.5	4.0	2.0214	0.8750	17.33	15.52	35.85	23.3	564	M096V (388.4)	LMSI Graphite-schist
55174 Py+++	17	7.4	1.6978	0.7384	21.17	15.63	35.94	28.0	472.5	M096V (389.0)	LMSI Graphite-schist
55112 Py	40	40	2.0597	0.8860	17.53	15.53	36.11	59.9	570	M096V (211.0)	UGS Graphite-schist
55126 Py	33	9.3	1.0392	0.4397	40.01	17.59	41.58	24.3	249.9	M096V (228.5)	UGS Graphite-schist
55127 Py	11.6	3.1	0.9510	0.3898	45.85	17.88	43.60	25.1	218.1	M096V (229.8)	UGS Graphite-schist -breccia
65974 Cp	560	1.0	1.0054	0.4131	43.19	17.84	43.42	0.2	231.5	M096V (440.9)	LMS2 Graphite dolomite

+, re-ED; ++, new mineral separation; +++, poor quality data; 1,2, separate dissolution; A,B, reload from same beaker
Blank corrected: 8ng total $^{206}Pb/^{204}Pb = 16.0$ $^{207}Pb/^{204}Pb = 15.3$ $^{208}Pb/^{204}Pb = 35.5$

Table 1. Lead isotope analyses and U and Pb concentrations for sulphides from lenticles in graphitic schists around Jabiluka.

IAEA

alteration zone described by Binns, Ayres, Wilmshurst & Ramsden, (this volume), which is thought to be associated with U mineralization. These sulphides appear to have been recrystallized during the high grade metamorphism and they may have been syngenetic. Pyrite and chalcopyrite were chosen because they are more sensitive indicators of small enrichments in radiogenic Pb than Pb-rich minerals such as galena; moreover galena may not always be present. Details of the geology, mineralogy and geochemistry are given elsewhere in this volume (e.g. Binns, Ayres, Wilmshurst & Ramsden, this volume; Ewers & Ferguson, this volume; Needham & Stuart-Smith, this volume). Sample locations are given in the paper by Ryall & Binns (this volume).

Results

The Pb isotope data and U and Pb concentrations are given in table 1 and plotted in figure 1 on a $^{207}Pb/^{206}Pb$ vs $^{204}Pb/^{206}Pb$ diagram. Advantages of this plot over conventional $^{207}Pb/^{204}Pb$ vs $^{206}Pb/^{204}Pb$ plots are absence of correlated errors in ^{204}Pb, high precision measurement of $^{207}Pb/^{206}Pb$ and small fractionation in $^{207}Pb/^{206}Pb$ (one mass unit separation) compared with $^{207}Pb/^{204}Pb$ (three mass unit separations). Analytical details are given in the Appendix.

In general terms the data support the concept of an increase in the radiogenic nature of the Pb isotope ratios as mineralization is approached. However, there is no direct correlation of radiogenic Pb isotope ratios in the sulphides and U concentration in the whole rocks and/or sulphides. Schematic boundaries of mineralization as a function of isotopic composition are drawn in figure 1. Samples from the mineralized horizons have Pb isotope ratios ranging from 116 to 650 ($^{206}Pb/^{204}Pb$), 0.18 to 0.09 ($^{207}Pb/^{206}Pb$) or 0.31 to 0.06 ($^{208}Pb/^{206}Pb$). Samples within metres of mineralization are less radiogenic whilst four or six samples devoid of mineralization are even less so, i.e. ratios range from 17.5 to 21.1 ($^{206}Pb/^{204}Pb$), 0.73 to 0.88 ($^{207}Pb/^{206}Pb$) or 1.7 to 2.1 ($^{208}Pb/^{206}Pb$). Three samples from the barren drill hole (55126, 55127, 65974 chalcopyrite) have $^{206}Pb/^{204}Pb$ ratios comparable with other samples that are closer to mineralization. However, their $^{208}Pb/^{204}Pb$ ratios are

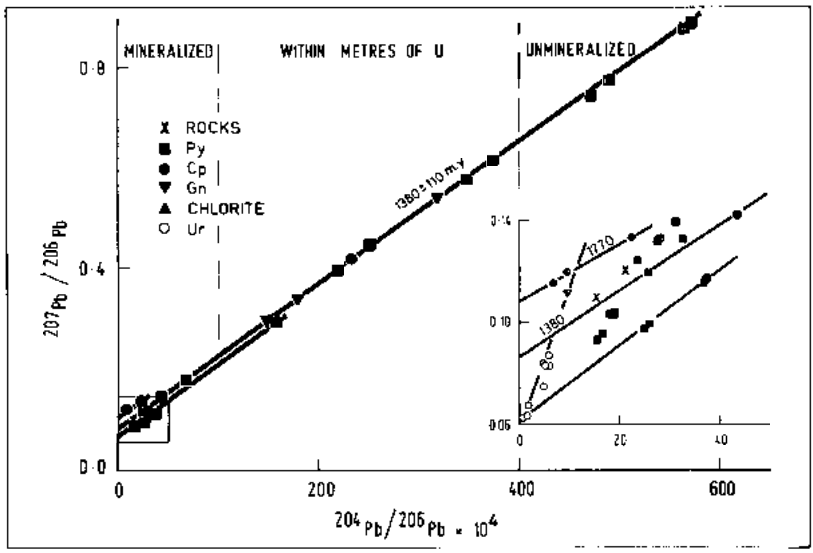


Figure 1. $^{207}Pb/^{206}Pb$ vs $^{204}Pb/^{206}Pb$ x 10^4 plot for sulphides from lenticles. The galena samples are analyses by Hills & Richards (1976). The upper line of apparent age ~1770 m.y. is for three chalcopyrites and a single pyrite and the lower line of apparent age ~900 m.y. is for most samples close to mineralization (see text).

higher (41.6 to 43.6) than those of mineralized samples analysed (35.6 to 39.8) and are consistent ('normal') with the other unmineralized pyrites.

Six whole rock samples were digested in Teflon bombs at 200°C with HF-HNO_3 and their Pb isotope ratios were determined (Table 2). The radiogenic nature of the rocks is in most cases more pronounced than in the sulphides.

Sample No.	Pb (ppm)	U (ppm)	$\frac{^{208}Pb}{^{206}Pb}$	$\frac{^{207}Pb}{^{206}Pb}$	$\frac{^{206}Pb}{^{204}Pb}$	$\frac{^{207}Pb}{^{204}Pb}$	$\frac{^{208}Pb}{^{204}Pb}$	$\frac{^{204}Pb}{^{206}Pb} \times 10^{-4}$	DDH (depth in m)	Sequence Rock type
Whole rocks										
55003 -A	1820	0.88%	0.0605	0.1082	653	70.62	39.49	15.3	S180V	MMS
-B	-	-	0.0605	0.1087	655	71.17	39.61	15.3	(270.2)	Chlorite-schist -breccia
54978	3120	1.22%	0.0794	0.1199	482	57.84	38.30	20.7	S180V (248.3)	MMS Chlorite-schist -breccia
54969	130	560	0.0158	0.0656	3100	203.4	49.0	3.2	S180V (242.7)	MMS Felsic-schist
54970	1.05%	15.7%	0.0082	0.0725	4650	337.1	38.1	2.2	S180V (243.0)	MMS Felsic-schist -breccia
54971 -A	180	211	0.0116	0.0377	3460	130.4	40.1	2.9	S180V	MMS
-B	-	-	0.0123	0.0379	3520	133.5	43.3	2.8	(243.2)	Graphite-schist
54955B-A	840	383	0.0398	0.1069	1016	108.6	40.4	9.8	S180V	MMS
-B	-	-	0.0397	0.1069	998	106.7	39.6	10.0	(231.7)	Graphite-schist
Chlorite-septechlorite-quartz veins+										
54966	60	265	0.033	0.0571	1173	66.98	38.59	8.5	S180V (240.5)	MMS Felsic-schist retrogressed hosts to mineralization
65962++	16	910	0.083	0.089	257	22.9	21.2	38.9	R207V (295.0)	MMS Chloritized graphite schist
65963	85	1270	0.0900	0.0682	5680	387	51.1	1.8	R207V (295.5)	MMS Chloritized graphite schist
65964 -B	440	230	0.0512	0.1136	687	78.0	35.2	14.6	R171V (243.0)	MMS Psammitic schist retrogressed hosts to mineralization

A,B reloads from same beaker

\+ Isotope ratios measured using electron multiplier

++ Very poor quality data

Blank corrected: 8 ng total isotope ratios as in Table 1

Table 2. Lead isotope analyses for whole rocks (HF-HNO_3 bomb digestion) and chlorite-septechlorite-quartz veins from around Jabiluka.

Recommendation and Future Research

Our preliminary data demonstrate the potential of Pb isotopes in U exploration. However, the techniques that we have used involving sophisticated chemistry and mass spectrometer isotopic analyses could not be gainfully employed in an exploration program. The best solution appears to be Pb isotope analysis of whole rocks using a simple HNO_3 leach, thus saving time and cost in mineral separation. Furthermore, the development of instruments capable of measuring Pb isotopes (e.g. Scintrex Corporation, Toronto) even in a very imprecise mode (1-5% standard deviation) would suffice for U exploration as there is no necessity to measure ^{204}Pb; $^{207}Pb/^{206}Pb$ ratios would suffice. In an exploration program, if $^{207}Pb/^{206}Pb$ and $^{208}Pb/^{206}Pb$ ratios less than 0.6 and 1.0 respectively were encountered in a 'barren' intersection, further investigation would be warranted.

2. APPARENT AGES OF SULPHIDES, URANINITES, WHOLE ROCKS AND CHLORITES

Introduction

Our preliminary data (noted in the Symposium Abstracts) for the sulphide lenticles (Table 1, Fig. 1) defined arrays on $^{207}Pb/^{204}Pb$ vs $^{206}Pb/^{204}Pb$ and $^{207}Pb/^{206}Pb$ vs $^{204}Pb/^{206}Pb$ of $\sim$1400 m.y. and 1800 m.y. As these apparent ages were inconsistent with the uraninite data of Hills & Richards (1976) of apparent age $\sim$ 900 m.y., more samples of sulphides associated with mineralization and microscopically selected uraninites and co-existing sulphides were analysed. In our paper, 'uraninite' refers to crystalline UO_2 for which the correct mineralogical name is uraninite. As the oldest U-Pb ages in the Alligator Rivers Uranium Field are from Ranger and based on three whole rock samples (Hills & Richards, 1976), six whole rock samples from Jabiluka were also analysed (Table 2). Chalcopyrites from two 'drusy' veins were also analysed (Tables 1 and 3). These veins consist of quartz-sulphide-carbonate up to 3mm wide which cut uraninite.

Sample No. and type	Pb (2 rad)	U (%)	$\frac{208Pb}{206Pb}$	$\frac{207Pb}{206Pb}$	$\frac{206Pb}{204Pb}$	$\frac{207Pb}{204Pb}$	$\frac{204Pb}{206Pb}$ x10^{-4}	Apparent ages (m.y.) $\frac{206Pb}{238U}$	$\frac{207Pb}{235U}$	$\frac{207Pb}{206Pb}$	Description of sample
54961 A Ur	2.4	34	0.0064	0.0629	7130	448	1.4	470	500	690	Replacement along vein, some reniform. DDH219, 237.3 m common Cp inclusions
54962 B Ur	4.5	59	0.0036	0.0623	13900	867	0.7	515	540	650	Reniform vein along outer portion of sulphide-free chlorite vein DDH219, 237.2 m Rare Cp inclusions
65964 A Ur	3.0	35	0.0168	0.0750	2030	152	4.9	670	720	870	Pb replacement; disseminated in wall rock; No visible Cp DDH203, 243 m
54971 Ur	2.1	23	0.0017	0.0676	5590	378	1.8	600	600	770	Disseminated hard Ja; fine grained crystals with bladed margins. No visible Cp, DDH219, 240.3 m
Sample 54955											
UrV	2.1	14	0.0411	0.0956	770	74.0	12.9	960	1015	1330	Thin reniform band along one margin of vein. Rare Cp inclusions
UrVW	6.0	47	0.0221	0.0861	1550	134	6.4	840	920	1120	Coarser vein replacing wall rock of vein; Rare Cp inclusions
Ur3	(50)	50	0.0216	0.0870	1765	154	5.7	640	720	1170	Along margin of vein - same veins as (1) & (2)
Urp	(0.7)	40	0.0173	0.0821	2150	162	5.1	(47)	(75)	(1080)	Contiguous piece of core. Lower in Cp
Urv	(4.8)	42	0.0239	0.0932	1580	147	6.3	250	900	1400	Richer in Cp
Cp	-	-	0.0360	0.1107	1070	118	9.4	-	-	1580	Coarse Cp segregation in and adjacent to UrP
CS	(9)	0.4	0.0705	0.1242	539	66.9	18.6	18000	221	1595	Sulphide vein between UrV & UrVW. Chlorite (<1% sulphides) Py + cp, cr, sp, Gr
Py	540ppm	0.29	0.0450	0.1100	846	93.1	11.8	1170	1290	1500	Synkinematic pyrite - not sheared
Pyb	102ppm	45ppm	0.3116	0.3857	116	21.53	86.1	-	-	-	Bulk separated pyrite
Cp	160ppm	1.8ppm	0.0852	0.1150	431	49.57	23.2	-	-	-	Quartz-dolomite-Cp uraninite-free drusy vein.
Ir A	840ppm	383ppm	0.0398	0.1089	1016	108.6	9.8	>4600	3420	1490	Wall rock
-B	-	-	0.0397	0.1069	998	106.7	10.0	-	-	1490	

Pb values in parentheses are in error by up to 50% because of underspiking in the analysis. Data are corrected for blank as in Tables 1 and 2. Apparent ages also have a 900 m.y. common Pb correction.

Table 3. Lead isotope and U and Pb concentration data and apparent ages for uraninite (Ur) from Jabiluka. Data for sample 54955 (DDH S180V, 231.7m) are also given. (Data for 54955 pyrite lenticles and whole rocks are given in tables 1 and 2, respectively).

Results and Discussion

Sulphides.

In figure 1 the data mainly lie on three arrays. One array, which has an age* proportional to 1380 ± 110 m.y. (MSWD 1), is defined by the unmineralized samples (65974, 55127,-126,-235,-238,-236,-145,-172,-112). The Jabiluka galenas analysed by Hills & Richards (1976) also lie on this line to within experimental error as they do when the data are plotted on a conventional $^{207}Pb/^{204}Pb$ vs $^{206}Pb/^{204}Pb$ diagram. As illustrated on the inset in figure 1, samples closer to mineralization have a much greater spread in isotope ratios which may be the result of movement of daughter products of U. The high degree of correlation of 12 samples would seem more than fortuitous. However, at this time the significance of the 1380 ± 110 m.y. apparent age is unknown as it can be associated with few geological events except the intrusion of post-Kombolgie Formation phonolite and dolerite dykes (Page *et al.*, this volume). On the other hand, zircons from Granite Hill in the Nanambu Complex (some 3 or 4km south of Jabiluka) have a lower intercept on a Concordia diagram of 1362 ± 6 m.y. (Page, this volume) which probably represents an event that disturbed the zircon U-Pb system. Most of the samples defining the array contain less than 10 ppm U and 40 ppm Pb, values common in graphitic shales associated with base metal mineralization from other areas in Australia (Gulson, 1977; unpubl. data).

There are other samples (55238, 55046, 55044, 55233) which contain higher amounts of U (140 ppm to 1.34%) and Pb (44 to 2660 ppm) and, together with three uraninites and one chlorite, lie on an array of ~900 m.y. Two uraninites studied by Hills & Richards (1976) and four of our uraninites (Table 3), plotted on a coupled $^{206}Pb/^{238}U$ - $^{207}Pb/^{235}U$ diagram, have an upper intersection on Concordia of ~900 m.y. (Fig. 2).

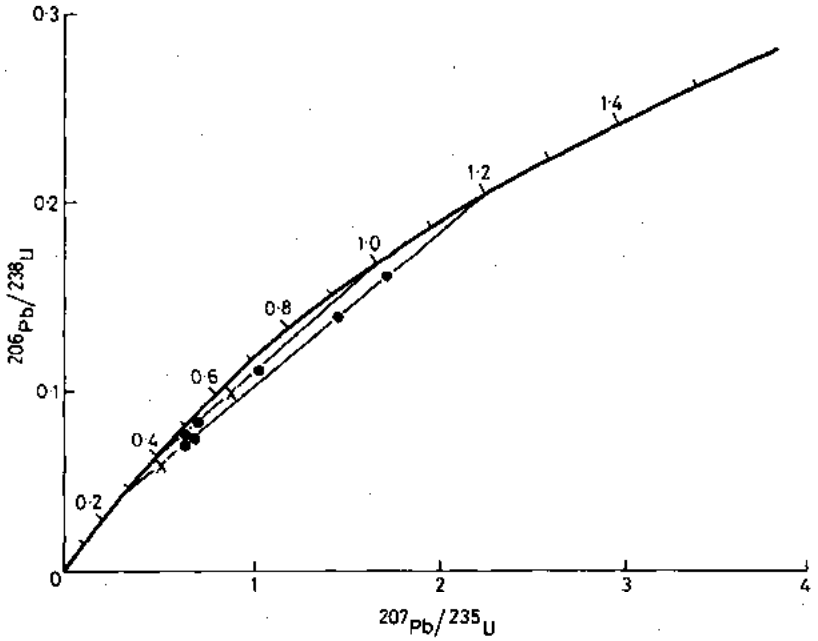


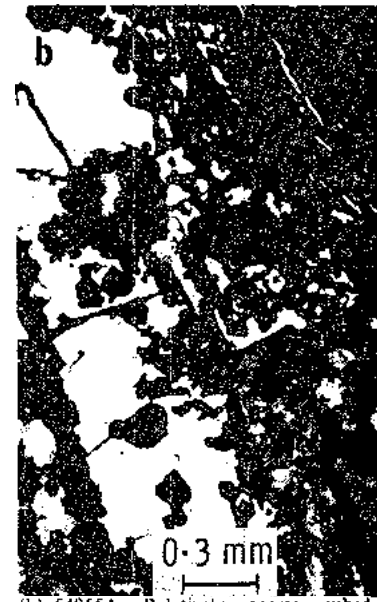
Figure 2. Concordia plot of correctly spiked uraninite data and two uraninites of Hills & Richards (1976) (indicated by crosses).

* All ages quoted in this paper are based on the decay constants of Steiger & Jager (1977).

Figure 3. Photomicrographs of samples analysed, taken pre-excavation.



(a) 54955A Uraninite (light grey) replacing wall of chlorite vein (dark). Chlorite vein contains disseminated sulphides (white).



(b) 54955A Relatively coarse euhedral corroded pyrite (54955 Py, Table 3) in vicinity of chlorite vein. Streaks of chalcopyrite and small amounts of uraninite in chlorite vein.



(c) 54955A Chlorite vein bordered by uraninite with narrower uraninite band containing common galena (54955 Urr, Table 3). The uraninite on the other side of the vein is poor in galena (54955 Urp). Some galena, occasionally coarse-grained (54955 Gn), occurs within the chlorite vein.



(d) 65964A Uraninite (Type Ib) replacing chlorite in chloritized quartz-feldspar-mica schist. Residuals of quartz.



(e) 54971 Disseminated subhedral uraninite (Type 1A) in chloritized host rock. About 3mm from vein.



(f) 54962B Reniform to nodular uraninite with abundant chlorite inclusions in chlorite-rich vein. Sample 54961 is similar to reniform part of 54962B.

The other main array, defined by three chalcopyrites and a co-existing pyrite, has an apparent age of 1770 ± 80 m.y. (MSWD 36), which is consistent with the time of regional metamorphism (Page *et al.*, this volume; Riley *et al.*, this volume). One possible interpretation considered was that the older apparent age (1770 m.y.) of chalcopyrite relative to the 1380 m.y. pyrites resulted from the greater stability of chalcopyrite, which thereby retained its U and Pb. However, chalcopyrite from a drusy vein in 54955 and another disseminated chalcopyrite in 65974, have relatively normal U and Pb concentrations and lie on the 1380 m.y. line. In contrast, 54964 chalcopyrite, which lies on the 1770 m.y. line, is also from a drusy vein cutting uraninite and is thus inconsistent with chalcopyrite from the drusy vein in 54955; this has a possible 'age' of ~1600 m.y. Sample 54964 contains the highest U of any chalcopyrite (180 ppm) and second highest Pb concentration of any sulphide. It is also unusual in that homogenization temperatures of fluid inclusions in co-existing quartz-dolomite are about 300°C, far higher than in any other samples examined by Fuzikawa (pers. comm.).

In view of the above information, we consider the ~1770 m.y. line to be fortuitous and due to inheritance of radiogenic Pb from uraninite (see further discussion below). Furthermore, all the chalcopyrites giving the apparent old 1770 m.y. age are from mineralized samples and as pointed out previously, there is a wide scatter of isotopic data in the mineralized area (see insert, Fig. 1).

Uraninites

No uraninites analysed from Jabiluka give 'ages' as old as the 1770 m.y. chalcopyrite-pyrite data. In fact, the only 'old age' for uraninites in the Pine Creek area is a single sample from a pegmatitic veinlet in the Nimbuwah Complex, reported by Hills & Richards (1976) to have a $^{207}Pb/^{206}Pb$ apparent age of 1855 m.y. Hills & Richards (1976) suggested 1855 m.y.

as an age of economic uranium mineralization but it is in fact the age of crystallization of accessory uraninite, as for example, zircon might give. The only other 'old' ages measured by Hills & Richards (1976) were two whole rocks and a most peculiar low U uraninite (very similar U and Pb concentrations to the whole rocks) from Ranger which gave $^{207}Pb/^{206}Pb$ apparent ages of 1600 - 1680 m.y. Uraninites from Ranger had $^{207}Pb/^{206}Pb$ apparent ages varying from 1150 to 1430 m.y. On a conventional $^{207}Pb/^{204}Pb$ vs $^{206}Pb/^{204}Pb$ diagram five of six points representing uraninite samples from Ranger analysed by Hills & Richards (1976) lie on a line of approximate age 1655 m.y.

The different types of uraninites analysed are illustrated in the photomicrographs in figure 3. No correlation between uraninite type and/or occurrence and apparent ages was obvious from our investigation; similar observations were made by Koeppel (1968). Although carefully selected, our uraninites gave a whole spectrum of apparent ages (which should serve as a warning to those hoping to take a single uncontrolled sample for 'age' determinations).

When plotted on a coupled $^{206}Pb/^{238}U$ - $^{207}Pb/^{235}U$ diagram (Fig. 2) some of our Jabiluka uraninite data (Table 3) are consistent with Hills & Richards (1976) data in that four samples are highly discordant and have $^{207}Pb/^{206}Pb$ ages which range from $\sim$ 630 to 870 m.y. However, two uraninites from sample 54955 gave apparent $^{207}Pb/^{206}Pb$ ages of 1120 m.y. On both the Concordia and $^{207}Pb/^{206}Pb$ vs $^{238}U/^{206}Pb$ plots, the data for the six uraninites lie on an array which intersects Concordia at $\sim$1280 $\pm$ 100 m.y. and the lower intercept is at $\sim$ 450 m.y. (as is the case on the $^{207}Pb/^{206}Pb$ vs $^{204}Pb/^{206}Pb$ plot). Within the error limits, these 'ages' are the same as those for the pyrites from the so-called 'barren' zone (Fig. 1). As these are the oldest uraninites found in the Pine Creek area besides those at Ranger and one Koongarra uraninite (which was extremely discordant and so its upper intersection with Concordia is uncertain), it was necessary to investigate this sample with upper apparent ages (54995) in more detail.

Sample 54955

As well as the two samples of vein uraninite already extracted from the polished section (UrV, UrVW; Table 3), another uraninite sample (Ur3) and a chlorite-sulphide (CS; Fig. 3a) area between uraninites UrV and UrVW were removed. From a contiguous piece of drill core two uraninites, one richer in galena (Urr) and one poorer in galena (Urp) were extracted together with a galena segregation (Gn; $\sim$ 0.1mm^2). The samples are shown in figure 3c. A coarse pyrite (Py) which showed evidence of defomation and occurred millimetres from a uraninite vein (Fig. 3b) was also removed in contrast to a bulk separated pyrite (Pyb) some 5cm from visible uraninite. Chalcopyrite (Cp) was handpicked from a 'drusy' vein and the host rock (TR) lacking visible uraninite veins was also analysed.

The data (Table 3)* for Ur3 uraninite are consistent with the early analyses of UrV and UrVW and the three points lie on a line of approximate apparent $^{207}Pb/^{206}Pb$ age of 1120 - 1170 m.y. (Fig. 4). No microscopic galena inclusions could be seen in any of these uraninites.

The chlorite-sulphide (<15% sulphides) vein (CS) bordered by uraninite Ur3 consists of pyrite with chalcopyrite, chalcocite, galena and sphalerite. It has an apparent $^{207}Pb/^{206}Pb$ age of $\sim$1600 m.y. (Table 3). This sulphide vein contains very high U (0.6% U).

The presence of varying amounts of microscopic galena segregations in uraninites Urp and Urr was verified by their Pb concentrations; both samples contained $\sim$40% U but the sample devoid of galena segregations (Urp) had a Pb concentration approximately an order of magnitude lower. However, the presence or absence of galena segregations may be no verification of the levels of Pb (or apparent ages) as the Pb may still be in solid solution in the uraninite (J. McAndrew, pers. comm.; Koeppel, 1968). The sample poorer in galena segregations (Urp) plots on the same line (Fig. 4) as the other uraninites (UrV, UrVW) with

* The Pb concentrations for Ur3, CS, Urp and Urr are in error because of underspiking in the analysis leading to large error magnifications.

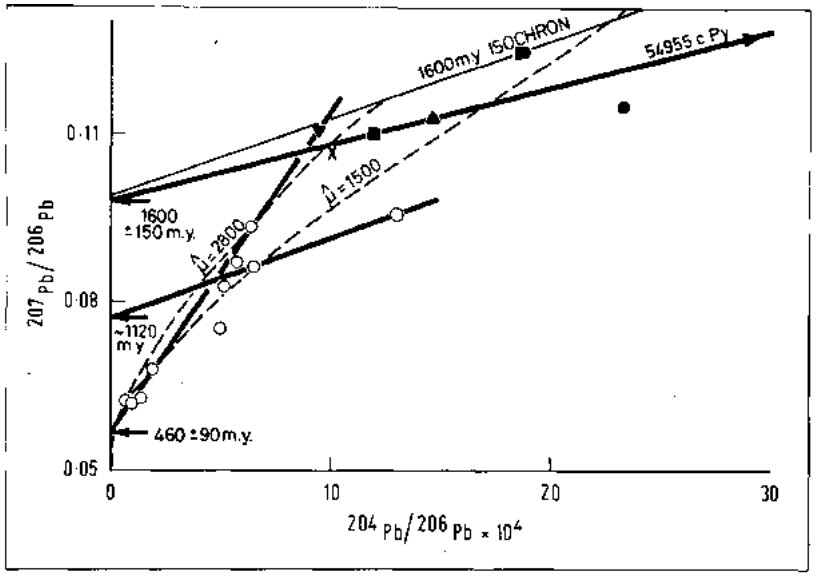


Figure 4. $^{207}Pb/^{206}Pb$ vs $^{204}Pb/^{206}Pb$ x 10^4 plot for data for sample 54955 (uraninites, sulphides, whole rock), other uraninites and one chlorite. Legend as for figure 1. The five uraninite samples below the ~1120 m.y. line are those not intimately associated with fine-grained chlorite-sulphides. One point is from Hills & Richards (1976). Diffusion trajectories for a 1600 m.y. mineralization age and μ values of 1500 and 2800 are shown.

low amounts of visible galena segregations, giving apparent $^{207}Pb/^{206}Pb$ ages of ~1120 - 1170 m.y. Sample Urr, rich in galena segregations, has the oldest apparent $^{207}Pb/^{206}Pb$ age (~1300 m.y.) for any uraninite so far analysed from Jabiluka.

In contrast, the coarse hand-picked galena segregation (Gn) is highly radiogenic suggesting it was derived from uraninite. The galena has an older apparent $^{207}Pb/^{206}Pb$ age than the uraninites but lies on a possible mixing or diffusion line with the uraninites from the same sample, Urr and Urp (Fig. 4). This mixing or diffusion line incorporates most of the other Jabiluka uraninite data including Hills & Richards (1976) analyses (see later discussion). The presence of galena inclusions in uraninite requires a source of sulphur which is post-uraninite. The intersection of the data line for the galena egregation (Gn) and associated uraninites at ~450 m.y. (fig. 4) may perhaps be interpreted as the last period of sulphurization in that particular domain.

The large pyrite (Py) in the host graphitic schist associated with uraninite contains much more U (0.29%) than the bulk separated pyrite lenticle (Pyb) centimetres distant from uraninite veins (45 ppm U). An apparent $Pb/^{206}Pb$ age of ~1600 m.y. can be calculated for Py.

It would appear that the sulphide vein CS, possibly Py pyrite and certainly the galena segregation (Gn) contain unsupported (excess) radiogenic Pb over U and consequently any age interpretations are meaningless. Ludwig (1978) observed that all pyrite separates from the Shirley Basin U ores in Wyoming contained from 130-620 ppm unsupported radiogenic Pb derived from pitchblende. He noted that sulphides near U mineralization incorporated radiogenic Pb with both anomalously young $^{207}Pb/^{206}Pb$ ages due to excess decayed ^{238}U daughters originating from nearby uraninite, and anomalously old ages due to depletion in ^{206}Pb as a result of ^{238}U daughter leakage.

If all the data, except for uraninites, from 54955 are considered as a single unit, a poorly correlated line (MSWD 500) may be drawn which passes through most of the points and intersects the $^{207}Pb/^{206}Pb$ axis with an apparent age of 1600 ± 150 m.y. (Fig. 4). This line is thus defined mainly by sulphides and may be interpreted as representing the time of U mineralization. This apparent age is consistent with the 1600 - 1650 m.y. alteration 'event' reflected by Rb-Sr whole rock data obtained for chloritic and sericitic schists from Nabarlek and Jabiluka by Page *et al.* (this volume) which they suggest may represent the time of uraninite mineralization. Alternatively, in view of the unsupported radiogenic Pb in the galena segregation (Gn) and in the chlorite-sulphide vein (CS), the linearity of the data may be fortuitous.

Gancarz (1978) and Gancarz & Curtis (pers. comm.) interpreted their data from the Oklo U deposit on the basis of Pb-loss by diffusion from uraninite, the Pb being incorporated into sulphide minerals. The uraninite had low apparent $^{207}Pb/^{206}Pb$ ages whereas the sulphides gave older apparent $^{207}Pb/^{206}Pb$ ages (compared with the mineralization). If their systematics are applied to the Jabiluka uraninite and sample 54955 data, a more complex picture emerges than at Oklo. Most uraninite data (Fig. 4) fall on diffusion trajectories, beginning on a 1600 m.y. calculated isochron, which have $\hat{\rho}$ values ranging from 1500 - 2700 ($\hat{\rho}$ is the ^{238}U concentration today divided by the ^{204}Pb concentration at the time of mineralization). In contrast to the Oklo data where lost Pb plots above an isochron representing the age of U mineralization (2050 m.y.), the sulphides from Jabiluka plot either on or below the 1600 m.y. isochron. Ganzarz (1978) and Gancarz & Curtis (pers. comm.) assumed a closed system for the Pb lost and Pb gained. However, the high concentrations of both excess U and radiogenic Pb in some of the sulphides at Jabiluka preclude any simple systematic treatment of our data.

In view of the Rb/Sr alteration ages of 1600 m.y. for both rocks and micas obtained by Page *et al.* (this volume) and Riley *et al.* (this volume), it is tempting to postulate that the 1600 m.y. apparent $^{207}Pb/^{206}Pb$ age for the 54955 samples (excluding uraninite) is the true age of U mineralization. However, the maximum Concordia (Fig. 2) and $^{207}Pb/^{206}Pb$ vs $^{238}U/^{206}Pb$ (not presented) apparent ages of ~1300 m.y. and the well-defined line of 1380 ± 110 m.y. for pyrite lenticles (Fig. 1) within the zone of chloritic alteration are difficult to reconcile as mere coincidences.

The 1600 m.y. isochron (Fig. 4) is a calculated line assuming no Pb loss or gain and although the uraninites lie on diffusion trajectories away from the 1600 m.y. line, the trajectories also intersect isochrons of younger ages such as 1500 or 1400 m.y. The $\hat{\rho}$ is then different, but in view of the variation in $\hat{\rho}$ from at least 1500 to 2700 any differences are minimal.

A McIntyre-York regression analysis of the uraninite data (Model III) gives an intersection on the $^{207}Pb/^{206}Pb$ axis equivalent to an apparent age of 460 ± 90 m.y. (Fig. 4). However, as the data lie on diffusion trajectories which steepen sharply in the region of $^{207}Pb/^{206}Pb$ ~0.055, this apparent age is considered to have no time significance.

It is interesting that 54955, giving the oldest apparent ages for uraninite, is the only sample analysed which contained significant amounts of sulphides in veins associated with the uraninite. Ludwig (1978) observed in the Shirley Basin that the most realistic ages were from massive ore associated with abundant sulphides, which had incorporated radiogenic Pb that might have otherwise diffused out of the system. It may be that the presence of sulphides stabilizes the oxidation of, and inhibits the loss of, daughter products from the uraninite by being more easily oxidized themselves (i.e. chalcopyrite forming chalcocite).

The chalcopyrite (Cp) from the drusy vein plots below the line joining most of the 54955 sulphide-whole rock data points (Fig. 4) and on the 1380 m.y. sulphide line (Fig. 1). As the Pb and U concentrations in this chalcopyrite are not anomalously high, an apparent age of

between 1380 and 1500 m.y. may be assigned to it. Moreover, as this drusy vein cuts uraninite, it places a minimum age of ~1380 m.y. on U mineralization although the incorporation into sulphides of uraninite-leaked radiogenic Pb as outlined above should be kept in mind in assigning ages.

Whole Rocks

Samples free of uraninite veins, except for 54970, were analysed (Table 2). As a control on movement of radiogenic Pb, three whole rocks containing widely differing amounts of U and Pb, were sampled over a distance of less than 0.6m (54969, -970,-971). Sample 54970 contains 15.7% U and 1.05% Pb and has an apparent $^{207}Pb/^{206}Pb$ age of ~1000 m.y. consistent with the low 'ages' of uraninites from this province and some Rb-Sr ages from Nabarlek to which Page *et al.* (this volume) attribute a low-temperature alteration event. Sample 54969 has only 560 ppm U and 130 ppm Pb but it also reflects the lowering of apparent ages to 800-900 m.y.

In contrast, the isotopic data for 54971 (211 ppm U, 180 ppm Pb) indicate long term disequilibrium of the radioactive daughters of U as the $^{207}Pb/^{206}Pb$ ratio (0.038) is anomalously low. Dickson & Snelling (this volume) noted excess radium in the weathered zone of the Koongarra deposit which would decay to give excess ^{206}Pb as we have observed in 54971 and the chlorite-septechlorite-quartz vein, 54966 (see next section). Uraninite from sample 54971 has a young apparent age of ~ 900 m.y. Ludwig (1978) observed a loss of both Pb and radioactive daughters of ^{238}U from pitchblende. Excess radium and ^{206}Pb could have been derived from the adjacent high U sample (54970) which now has a young apparent age if it is assumed that uraninite mineralization took place at ⩾1600 m.y. If the radium is the source of the excess radiogenic Pb, our data are equivocal with regard to the distance of migration of radiogenic Pb. Furthermore, if excess radium is a common feature at Jabiluka, it could explain the large scatter of data in the samples close to mineralization (Fig. 1, insert).

The three other whole rocks give older apparent ages than the above samples; 54978 and 55003 plot on the 1380 m.y. line defined by the pyritic lenticles from the schists away from mineralization whereas 54955D could be as old as ~1600 m.y. (discussed in previous section). The anomalously old apparent $^{206}Pb/^{238}U$ and $^{207}Pb/^{235}U$ ages of 54955D also point to disequilibrium and there appears to be > 700 ppm unsupported radiogenic Pb in this sample.

Chlorite-septechlorite-quartz veins (CSQ)

Small amounts (< 30 mg) of handpicked chlorite from veins were analysed in an attempt to test the model of Binns, McAndrew & Sun (this volume) in which the uranium is introduced with CSQ and later expelled giving uraninite. Because of the small amounts of sample analysed, the isotopic data for the four CSQ's (Table 2) are not of the highest quality but general conclusions can be drawn.

The two U-rich samples (910 and 1270 ppm) are from unmineralized veins whereas those with low U (230 and 265 ppm) are from mineralized veins which lends some support to the Binns, McAndrew & Sun (this volume) model. However, the U-rich samples should have an older age indicative of the time of introduction of the U, say >1600 m.y. In fact, the two U-rich samples have low apparent ages and no correlation between U concentration and apparent ages is obvious. The sample (65964B) with the lowest U has the highest apparent age of ~1600 m.y. and lies on a line joining the 54955 samples (Fig. 4). Although it is tempting to postulate that this approximates the true age of the chlorite and thus U mineralization, as has been suggested previously for the 54955 series samples, the excess of radiogenic Pb over U indicates that either the chlorite has incorporated excess radiogenic Pb from uraninite as have some of the pyrites (see previous section; Ludwig, 1978) or it has lost U but retained its old apparent age. As uraninite from this sample (65964A) contains rare

galena segregations and has lost radiogenic Pb, as indicated by its low apparent age of ~900 m.y., we favour the explanation of a gain of radiogenic Pb for the old apparent age of the chlorite. Furthermore, sample 54966 has anomalously low $^{208}Pb/^{206}Pb$ and $^{207}Pb/^{206}Pb$ ratios which may be due to excess radium as previously suggested for the whole rock samples.

3. SIGNIFICANCE OF Pb ISOTOPE DATA TO GENETIC MODELS

Summary of Pb Isotopic Data

1) Apparent $^{207}Pb/^{206}Pb$ age of 1380 ± 110 m.y. for sulphides metres from, and devoid of, U mineralization. The galena data of Hills & Richards (1976) also plot on this line.
2) Scatter of data near mineralization and excess ^{206}Pb possibly due to excess radium.
3) The apparent $^{207}Pb/^{206}Pb$ ~1770 m.y. line for some chalcopyrites and a pyrite is suggested to be anomalously old due to incorporation of radiogenic Pb that was depleted in ^{206}Pb due to ^{238}U-daughter leakage.
4) Low apparent ages of ~ 450 - 900 m.y. for vein and disseminated uraninites the data for which follow continuous Pb loss diffusion trajectories.
5) Higher apparent $^{207}Pb/^{206}Pb$ ages of ~ 1120 - 1300 m.y. for uraninites associated with chlorite-sulphides.
6) Excess radiogenic Pb in synkinematic sulphides, chlorite-sulphide intergrowths, one sample of CSQ and galena.

Compatability with Other Isotopic Data

1) The ~ 1770 m.y. apparent $^{207}Pb/^{206}Pb$ age is consistent with the regional metamorphism defined by Rb-Sr investigations (Page *et al.*, this volume; Riley *et al.*, this volume) but may be fortuitous.
2) The 1380 ± 110 m.y. apparent $^{207}Pb/^{206}Pb$ age is consistent with the lower intercept on Concordia (Page *et al.*, this volume) for zircon U-Pb data from the Nanambu Complex.
3) Likewise, the 460 ± 90 m.y. intercept of the uraninite data is consistent with their lower Concordia intercept for zircons from the Nimbuwah Complex.
4) The apparent $^{207}Pb/^{206}Pb$ age of 1600 ± 150 m.y. from rocks and sulphides in sample 54955 is consistent with the 1600 - 1650 m.y. low-temperature alteration event measured by Page *et al.* (this volume) which may be the time of U mineralization (however, see following discussion).

Genesis

A number of models have been proposed for the formation of U mineralization in the Alligator Rivers Uranium Field. Binns *et al.* (this volume) propose that U was introduced to Jabiluka within CSQ replacements from which uraninite subsequently 'exsolved'. Ferguson *et al.* (this volume) favour low-temperature CO_2-rich groundwaters carrying U as uranyl carbonate complexes which were adsorbed onto Mg-rich clays (and/or chlorite) and organic material in collapse structures in carbonate-rich sequences. Diagenesis, or heating by Oenpelli dolerite, could then have led to release of U and recrystallization to uraninite. Ypma & Fuzikawa (this volume) suggest that U was carried as carbonate-complexes in CO_2-rich solutions and these were stripped of their U on contact with hypersaline brines.

If the whole rock age for Ranger of 1655 m.y. (Hills & Richards, 1976) is taken as the time of U mineralization in the Alligator Rivers area, any model needs to explain the 1380 m.y. apparent age for sulphides from within the chloritic alteration zone at Jabiluka. The fact that the Jabiluka galenas of Hills & Richards (1976) also plot on this line adds a further complication.

Our estimate of a 1600 m.y. 'age' at Jabiluka is based on the array of five samples of

sulphide and a whole rock for 54955 (Table 3; Fig. 4). However, as at least half these samples contain excess radiogenic Pb and considering the migration of U-daugher products (and U?) near mineralization the 1600 m.y. age may also be fortuitous.

Thus an alternative interpretation for the 1380 m.y. apparent age in the sulphides is that it represents the time of U mineralization at Jabiluka; one uraninite, Urr, also has an apparent $^{207}Pb/^{206}Pb$ age of ~1300 m.y. (Table 3). The other uraninites exhibit varying degrees of Pb loss and follow continuous diffusion trajectories.

If the 'age' of U mineralization is 1380 m.y., why then is it not detected by other isotopic methods? On the basis of fluid inclusion studies at Nabarlek and Jabiluka, Ypma & Fuzikawa (this volume) observe homogenization temperatures of 85°-160°C whilst Donnelly & Ferguson (this volume) suggest temperatures as high as 266°±40°C from their stable isotope investigations. As the estimated threshold retention temperatures ('blocking temperatures') for the K-Ar and Rb-Sr systems in muscovite are >350°C, the alteration event associated with U mineralization may not disturb the mica ages.

If the above explanation for our 1380 ± 110 m.y. data is correct, then the U mineralization post-dates deposition of the Kombolgie Formation at ~1650 m.y. (Page *et al.*, this volume).

Another problem which needs to be explained is the corrosion of synkinematic or syngenetic sulphides (Fig. 3b) within centimetres of ore and the addition of radiogenic Pb (and in some cases, U) to sulphides. Allied to this complex situation are the relatively non-radiogenic galenas from Jabiluka analysed by Hills & Richards (1976) and the chlorite-sulphide veins between uraninite selvedges as in sample 54955 (Fig. 3a).

It is unlikely that dilute CO_2-rich solutions are capable of replacing pyrite and transporting other base metals (A. Giblin, pers. comm.). Furthermore, uranyl carbonate complexes become insignificant above 100°C (A. Giblin, pers. comm.) which is too low a temperature to have any relevance to most of the proposed models of U mineralization.

Alternatively, brines are well known for their capacity to transport metals. From their fluid inclusion studies, Ypma & Fuzikawa (this volume) propose that highly saline solutions were in existence at the time of U mineralization although they did not appeal to them for U transportation. Crick & Muir (this volume) claim to have recognised abundant evaporite pseudomorphs in the Cahill Formation which may not only be the source of the saline fluids but perhaps also the supply of Mg for the Mg-rich chlorites intimately associated with uraninite.

The metals and U (see next section) could have been leached from source rocks and transported to their site of deposition where the low-pH brines reacted with pre-existing pyrite (and chalcopyrite) releasing S which allowed precipitation of the fine-grained pyrite, chalcopyrite, sphalerite and galena associated with chloritic material and uraninite as in 54955. During replacement of the pre-existing sulphides, radiogenic Pb and U could have been deposited, the Pb perhaps as galena utilizing part of the released S. To test this hypthesis, we are currently investigating U distributions in the sulphides using the fission track method.

On the other hand, an external source of Pb may account for the relatively non-radiogenic galenas analysed by Hills & Richards (1976) which they suggested were due to country-rock Pb contamination.

If brines were the leaching and transporting medium then there is no need to postulate transport of U as the U^{VI} species. In all other models, it is proposed that the U is transported as the oxidized U^{VI} species which then requires a reduction mechanism to precipitate the U at the site of deposition. Giblin (1977) has demonstrated that U may be transported by a brine as the U^{IV} species under non-oxidizing conditions if the brine reaches a composition comparable with that in the Salton Sea; Ypma & Fuzikawa's (this volume) fluid inclusion

data would suggest the presence of an even stronger brine. There is therefore no need for the U to have been present in the U^{VI} state and so any requirement for a reducing source, such as sulphides or graphite, is eliminated.

The existence of early coffinite often replacing quartz clasts (Binns, McAndrew & Sun, this volume) may be explained by the transport of U as the reduced species.

The source of the U was possibly primary uraninite such as observed in the Nanambu (McAndrew & Finlay, this volume) and Nimbuwah complexes (Tadpole Prospect, quoted in Hills & Richards, 1976). McAndrew & Finlay (this volume) observed that rocks in the Nanambu Complex with accessory uraninite had very low Th/U ($<<<1$) and that uraninite contributes up to 70% of the total U in the rocks. The extremely low $^{208}Pb/^{206}Pb$ ratios observed in uraninites from the Alligator Rivers area (Hills & Richards, 1976; this paper) indicate that the primary uraninites in granitoid complexes such as Nanambu and Nimbuwah could be the source of economic U mineralization. Zircons also (typically) have low Th/U ratios (although not as low as uraninite) but in view of the resistant nature of zircons and the concordance of U/Pb data in the Nimbuwah (Page *et al.*, this volume), zircons are seen as only a minor source for U in the Alligator Rivers Uranium Field.

Finally, if one appeals to a mechanism of concentration of U by self-heat generation in a high U pluton as suggested by Fehn *et al.* (1978), this occurs over a long period of time beginning with the crystallization of the pluton. Thus any apparent ages may be found in uraninites and these ages need have no relationship to any specific geological event.

ACKNOWLEDGEMENTS

We wish to thank Steve Craven for separating the sulphide lenticles; John McAndrew for handpicking the uraninites and sulphides and pointing out pertinent features of mineragraphy; and Ray Binns for selection of sulphide samples and separation of the chlorites. We would also like to thank Ray Binns, Angela Giblin, John McAndrew and Shen-Su Sun for numerous discussions and Ken Ludwig for an extensive review of our manuscript. Alex Gancarz assisted with the diffusion calculations.

REFERENCES

Binns, R.A., McAndrew, J., & Sun, S-S., this volume: Origin of mineralization at Jabiluka. *Proceedings of the International Uranium Symposium on the Pine Creek Geosyncline.*

Binns, R.A., Ayres, D.E., Wilmshurst, J.R., & Ramsden, A.R., this volume: Petrology and geochemistry of alteration associated with uranium mineralization at Jabiluka, Northern Territory, Australia. *Proceedings of the International Uranium Symposium on the Pine Creek Geosyncline.*

Cannon, R.S., Pierce, A.P., Atweiler, J.C., & Buck, K.L., 1961: The data of lead isotope geology related to problems of ore genesis. *Econ. Geol., 56,* 1-38.

Crick, I.H., & Muir, M.D., this volume: Evaporites and uranium mineralization in the Pine Creek Geosyncline. *Proceedings of the International Uranium Symposium on the Pine Creek Geosyncline.*

Dickson, B.L., & Snelling, A.A., this volume: Movements of uranium and daughter isotopes in the Koongarra uranium deposit. *Proceedings of the International Uranium Symposium on the Pine Creek Geosyncline.*

Donnelly, T.H., & Ferguson, J., this volume: A stable isotope study of three deposits in the Alligator Rivers Uranium Field, N.T. *Proceedings of the International Uranium Symposium on the Pine Creek Geosyncline.*

Ewers, G.R., & Ferguson, J., this volume; Mineralogy of the Jabiluka, Ranger, Koongarra and Nabarlek uranium deposits. *Proceedings of the International Uranium Symposium on the Pine Creek Geosyncline.*

Fehn, U., Cathles, L.M., & Holland, H.D., 1978: Hydrothermal convection and uranium deposits in abnormally radioactive plutons. *Econ. Geol., 73,* 1556-1566.

Ferguson, J., Ewers, G.R. & Donnelly, T.H., this volume: Model for the development of economic uranium mineralization in the Alligator Rivers Uranium Field. *Proceedings of the International Uranium Symposium on the Pine Creek Geosyncline.*

Gancarz, A.J., 1978: U-Pb age (2.05×10^9 years) of the Oklo uranium deposit. *in, Natural Fission Reactors* International Atomic Energy Agency, Vienna, 513-520.

Giblin, A., 1977: A study of uranium mobility in simulated natural surface waters. *M.Sc. Thesis, Macquarie University* (unpubl.), 117p.

Gulson, B.L., 1977: Application of lead isotopes and trace elements to mapping black shales around a base metal sulphide deposit. *J. Geochem. Explor., 8,* 85-103.

Gulson, B.L., & Mizon, K.J., 1979: Preliminary investigation of use of Pb isotopes in uranium exploration with additional U-Pb 'ages' for Jabiluka uraninite. *Extended Abstracts of the International Uranium Symposium on the Pine Creek Geosyncline,* 103-104.

Hills, J.H. & Richards, J.R., 1976: Pitchblende and galena ages in the Alligator Rivers region, Northern Territory, Australia. *Miner. Deposita, 11,* 133-154.

Koeppel, V., 1968: Age and history of the uranium mineralization of the Beaverlodge area, Saskatchewan. *Geol. Surv. Pap. Canada, 67-31*, 111p.
Ludwig, K.R., 1978: Uranium-daughter migration and U/Pb isotope apparent ages of uranium ores, Shirley Basin, Wyoming. *Econ. Geol. 73*, 29-49.
McAndrew, J., & Finlay, C.J., this volume: The nature and significance of the occurrence of uranium in the Nanambu Complex of the Pine Creek Geosyncline. *Proceedings of the International Uranium Symposium on the Pine Creek Geosyncline.*
Needham, R.S., & Stuart-Smith, P.G., this volume: Geology of the Alligator Rivers Uranium Field. *Proceedings of the International Uranium Symposium on the Pine Creek Geosyncline.*
Page, R.W., Compston, W., & Needham, R.S., this volume. Geochronology and evolution of the late Archaean basement and Proterozoic rocks in the Alligator Rivers Uranium Field, Northern Territory, Australia. *Proceedings of the International Uranium Symposium on the Pine Creek Geosyncline.*
Riley, G.H., Binns, R.A., & Craven, S., this volume: Rb-Sr chronology of micas at Jabiluka. *Proceedings of the International Uranium Symposium on the Pine Creek Geosyncline.*
Rossman, G.I., Sychev, I.V., Tarkhanova, G.A. & Chesnokov, L.V., 1972: Use of radiogenic ^{206}Pb halos in prospecting for uranium in acidic volcanic rocks. *Int. Geol. Rev., 14*, 332-337.
Ryall, W.R., & Binns, R.A., this volume: Mercury distribution in the Jabiluka Two orebody and its host rocks. *Proceedings of the International Uranium Symposium on the Pine Creek Geosyncline.*
Steiger, R.H., & Jager, E., 1977: Subcommission on geochronology: Convention on the use of decay constants in geo- and cosmochronology. *Earth Planet. Sci. Lett., 36*, 359-362.
Ypma, P.J.M., & Fuzikawa, K., this volume: Fluid inclusion studies as a guide to the composition of uranium ore forming solutions of the Nabarlek and Jabiluka deposits, N.T., Australia. *Proceedings of the International Symposium on the Pine Creek Geosyncline.*

APPENDIX

Sample Preparation

Sulphides

Pyrite and chalcopyrite were separated from the host schists by crushing to -100 mesh, and heavy liquid and magnetic methods. Concentrates were freed from any remaining schistose material by repeated ultrasonic disintegration treatment. Purity was usually > 95%.

Uraninites

Uraninites were photographed, then removed under a binocular microscope using a tungsten tipped needle. In most cases, pure samples were obtained but occasionally, small amounts of chloritic material were inevitably removed with the uraninite.

Rocks

Rocks were crushed to -200 mesh in a tungsten carbide shatterbox.

Chemical Separation

Sulphides

Sulphides were washed in 6N HCl and rinsed with clean H_2O. Separation of Pb was achieved using HBr anion exchange followed by anodic eletrodeposition. Total processing blank was 4 -8 ng. Uranium was separated in nitric acid medium.

Uraninites

Because of the small amounts involved (1 to 5 mg) no prewashing of the samples was carried out. Samples were dissolved in 7N HNO_3 and treated as for the sulphides.

Rocks

Rocks were dissolved in Krogh hydrothermal vessels and Pb and U separated as for sulphides.

Blanks were of the same order.

Mass Spectrometry

Lead was loaded using silica gel-phosphoric acid and U with tantalum oxide-phosphoric acid.

Isotope ratios were measured with an AVCO series 900A, 35 cm radius, single sector mass spectrometer under computer control for peak search and alignment, ion beam switching, electrometer range selection and data acquisition.

Eight analyses of NBS 981 carried out during this work gave the following averages and standard errors of the means:

$^{208}Pb/^{206}Pb$	$^{207}Pb/^{206}Pb$	$^{206}Pb/^{204}Pb$
2.1605 ± 1	0.9133 ± 1	16.890 ± 3

The data in tables 1-3 have not been normalized to any standard value.

Regression Analyses

Analyses were carried out with a modified McIntyre-York program in which the following errors were assigned:

	$^{207}Pb/^{206}Pb$	$^{204}Pb/^{206}Pb$
Sulphides for 1380 m.y. line (Fig. 1)	0.05%	0.5%
Chalcopyrite-pyrite 1770 m.y. line (Fig. 1)	0.1%	1%
Uraninites (Fig. 4)	0.1%	5%
54955 samples (Fig. 4)	0.1%	1%

Rb-Sr CHRONOLOGY OF MICAS AT JABILUKA

G.H. Riley[1], R.A. Binns[2] and S.J. Craven[2]

1. CSIRO Division of Mineral Physics, P.O. Box 136, North Ryde, N.S.W., 2113, Australia.
2. CSIRO Division of Mineralogy, P.O. Box 136, North Ryde, N.S.W., 2113, Australia.

ABSTRACT

The relative timing of metamorphic and metasomatic events at Jabiluka has been examined by Rb-Sr isotopic measurements on mica concentrates and whole rock samples from specific petrological associations. The deformation associated with high grade regional metamorphism predates emplacement of acid pegmatites whose muscovite component is dated at 1830 ± 5 m.y. Biotites from non-retrogressed, amphibolite facies schists have high enrichments of radiogenic ^{87}Sr and yield concordant model ages of 1805 ± 5 m.y. Associated muscovites have much higher common Sr concentrations than the biotites and radiogenic ^{87}Sr enrichments are therefore much lower. Although their apparent model ages are systematically higher than coexisting biotite, the data cannot be unequivocally related to a single event, but are consistent with an interpretation that peak regional metamorphism was close to the emplacement age of pegmatites. A post-metamorphic cooling rate of 8°C/m.y. is inferred from these data for the Cahill Formation.

Data on 'greisens' strongly suggest that their initial development of coarse-grained muscovite occurred towards the close of the regional metamorphism, possibly due to local potassium metasomatism associated with the transgressive pegmatites.

Retrogressive alteration near the Jabiluka Two ore zone is characterized by extensive development of sericite and chlorite. Age data on relic muscovite in the altered schists are indistinguishable from muscovite ages in non-retrogressed schists. Model ages for retrogressive sericite in pegmatites, greisens and altered schists cover an extended period of time and no conclusive interpretation is possible. Similarly, sericite concentrates from the metamorphosed matrix of Kombolgie Formation sandstone and from the underlying metamorphosed regolith contain relatively high concentrations of common Sr so that model ages are equivocal.

If the retrogressive metamorphism of the Cahill Formation and the prograde metamorphism of the Kombolgie Formation sandstone and its underlying regolith are viewed as an episode in which extensive homogenization of Sr isotopes occurred during crystallization of sericite, an isochron treatment of the data is appropriate and yields an age of 1534 ± 90 m.y. Alternatively, if no such homogenization occurred throughout the Jabiluka wall rocks during retrogression, the lowest model ages measured, namely ca. 1400 m.y., set a maximum limit for the time of alteration.

INTRODUCTION

The timing of mineralization relative to particular stages in the evolution of country rocks is a crucial factor in genetic evaluations of uranium deposits in the Alligator Rivers Uranium Field. A study was accordingly commenced, aimed at a better chronological understanding of the metamorphic and metasomatic development of the Jabiluka environment.

The strategy was to apply Rb-Sr isotopic measurements to various mica concentrates from samples chosen to characterize specific events delineated by petrographic studies described by Binns, Ayres, Wilmshurst & Ramsden (this volume). Anticipating high radiogenic ^{87}Sr enrichments, we expected model ages to discriminate between initial amphibolite facies regional metamorphism of the Cahill Formation and its subsequent retrogressive alteration near the Jabiluka orebodies, and to clarify relationships between the latter and the low grade metamorphism evident in the unconformable Kombolgie Formation sandstone and its underlying regolith. In addition, micas from greisen-like rocks formed by potassium metasomatism apparently closely associated with uraninite mineralization were separated and analysed, together with several mica samples expected to establish the minimum age of pegmatite emplacement and their retrogressive alteration.

The measurements and interpretations given below supersede the preliminary data given in the Extended Abstract volume of this Symposium (Riley *et al.*, 1979).

SAMPLES STUDIED

With the exception of hand-picked muscovite crystals from pegmatites 54920, 55217,

55213 and 54908, mica concentrates were prepared by repetitive combination of heavy liquid and magnetic separation techniques. Fine-grained white micas, of the type called 'sericite' below, proved difficult to separate from intergrown chlorite and, in some samples, from coarser muscovite. Contaminants and purities were estimated from X-ray diffractograms and by optical microscopy.

To define the amphibolite facies regional metamorphism of the Cahill Formation, coexisting muscovite and biotite were separated from three pelitic schists (biotite-muscovite-quartz-oligoclase±sillimanite ±K-feldspar). Samples 65990 and 65994, from 2.5km north-west of Jabiluka, contain very fresh feldspar and display minimal chloritization of biotite. In sample 65957, from a schist sequence below Jabiluka One, the plagioclase is slightly altered and sillimanite has been replaced by fine white mica.

Retrogressed schists from the Jabiluka Two orebody were examined by analysis of two main kinds of mineral separate (see Fig. 2 of Binns, Ayres, Wilmshurst & Ramsden, this volume):

1) Coarse-grained muscovite flakes extracted from altered pelitic schists. This mineral is clearly a relic of the original amphibolite facies metamorphism. Our objective was to establish whether it preserved the regional age or whether its age had been reset during the retrogressive metamorphism.
2) Fine-grained 'sericite' which is a newly crystallized retrogressive alteration product

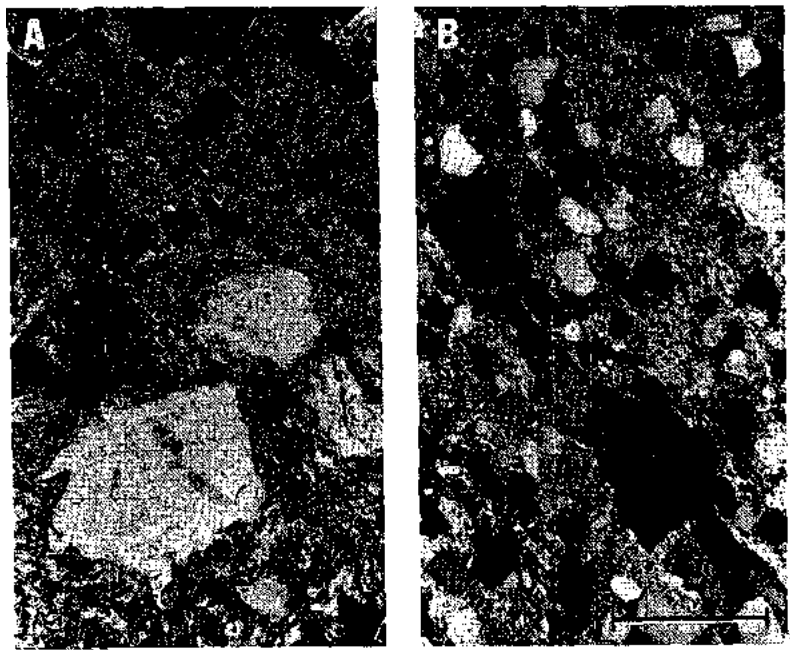


Figure 1. Photomicrographs illustrating metamorphism of Kombolgie Formation Sandstone and underlying regolith.
A: Sandstone 55098. The matrix between detrital quartz clasts is fine-grained, unoriented white mica, which in places has also replaced the clasts.
B: Regolith 55184. Only quartz has survived weathering and subsequent metamorphism. The continuity of a quartz train extending diagonally across the field is a diagnostic feature of regolith samples, and reflects the former foliation of the parental schist. Weathering products have recrystallized to fine white mica and minor chlorite, which also replace quartz along grain boundaries. Crossed polars. Scale bar = 1mm.

of pre-existing feldspar. This component consists of composite microcrystalline particles; it is clearly distinguishable from the relic muscovites of type (1).

In sample 55014 only, chlorite separates (both Mg-rich and Fe-rich), which are alteration products of pre-existing biotite, were also analysed.

Similarly, two kinds of mica sample were studied in the pegmatite bodies. These intrusions appear to have post-dated deformation associated with the high grade regional metamorphism but pre-date retrograde metamorphism. Their large muscovite flakes (2-5mm diameter) represent igneous crystallization products. Former feldspars, however, have been entirely altered to sericitic aggregates during the same retrogressive alteration that affected the schists. Samples 55217 and 55213 are from the large transgressive 'Mosher Pegmatite' intrusion between Jabiluka One and Two. Samples 54920 and 54908 are smaller sills within Jabiluka Two mineralized schists (54920 is actually a muscovite selvedge).

White mica is the dominant constituent of greisen-like rocks formed in large part by potassium metasomatism of pelitic and psammitic schists (Binns, Ayres, Wilmshurst & Ramsden, this volume). The close association of 'greisens' with Jabiluka Two uraninite ore zones, and their local possession of brannerite, imply a genetic relationship to ore occurrence, so the age of potassium metasomatism should also represent that of initial uranium mineralization. The 'greisens' possess large muscovite crystals, usually distinctly kinked, which in thin section resemble relics from the high grade regional metamorphism, and also finer sericite which resembles the products of retrograde metamorphism in schists, although in 'greisens' all earlier minerals, including quartz, may have been replaced. There is no obvious spatial relationship to, nor distinct geochemical affinity with pegmatite, but the potassium introduction responsible for at least the coarser muscovite accumulations was conceivably associated with pegmatite emplacement whereas the sericite enrichments are probably related to retrogressive metamorphism and mineralization. Samples 54931 and 65968 are coarse muscovite-rich 'greisens', whereas 54928 and 65997 contain predominant sericite. All four are from a zone immediately overlying Main Mine Series uraninite ores at Jabiluka Two; 65997 contains minor brannerite intergrown with sericite.

The Kombolgie Formation sandstone unconformably overlying Jabiluka Two is also metamorphosed. Former matrix material has recrystallized to fine sericite-chlorite aggregates which in places replace the margins of detrital quartz grains (Fig. 1A). Immediately below the unconformity there is a 1-2m regolith of partly disintegrated schist. Quartz is the only remnant mineral in the upper portion of the regolith, and the presumed weathering products in which this was set have altered to fine-grained, unoriented white mica (Fig. 1B). The prograde style of alteration resembles burial metamorphism, which obviously must postdate deposition of the Kombolgie Formation sandstone (post 1650 m.y., Page *et al.*, this volume). Close petrographic study of the transition in drill core from sandstone through regolith to underlying schists has provided no clear evidence for superimposition of the Kombolgie metamorphism on retrogressive metamorphic products within the Cahill Formation basement. To test the likelihood that these two events were simultaneous, unweathered sericite concentrates were prepared from sandstone matrices (55094, 55098) and regolith samples (55107, 55184, 55187).

ANALYTICAL TECHNIQUE

Approximately 0.1 g of each sample was dissolved for analysis (in the case of three samples, a smaller quantity of mineral concentrate was used). Digestion by $HClO_4$ and HF was carried out in open Teflon beakers, and the samples were spiked with ^{87}Rb and ^{84}Sr tracers of known concentration after dissolution. After evaporation to dryness, the spiked samples were re-dissolved in 10 M HCl and again evaporated. Standard two-column cation exchange chromatography was used to purify Rb and Sr extracts prior to isotope analysis.

The HCl used in the extractions was made in bulk by dissolving HCl gas in water; its measured Sr concentration is 5×10^{-12} g/g.

The isotope ratios were measured with an AVCO Series 900A, 35-cm radius, single sector, mass spectrometer with computer controlled functions for peak search and alignment, beam switching, electrometer range selection and data acquisition. Samples were run at pressures $<5 \times 10^{-8}$ Torr and 'low temperature' ion beams were generated for analysis. Strontium ratios, when normalized to $^{86}Sr/^{88}Sr = 0.1194$ had an internal precision of ~0.02% for a set of 16 ratios and the means of three blocks of data had a standard error <0.01%. The rubidium level in strontium runs was typically less than 300 ppm.

As all analysed samples were from drill core, only a limited amount of mineral concentrate was obtained for some specimens. In order to verify analytical procedures

Sample	Rb (ppm)	Sr (ppm)	$^{87}Rb/^{86}Sr$	$^{87}Sr/^{86}Sr$	Age (0.705)
Standard K-feldspar (NBS SRM 607)	522.7	65.58	24.196	1.20040	1427.3
	523.5	65.55	24.242	1.20037	1424.5
	522.0	65.89	24.047	1.19893	1431.8
	519.7	65.79	23.979	1.20083	1441.3
	523.4	65.75	24.168	1.20084	1430.2
	517.8	64.99	24.185	1.20048	1428.2
	519.5	65.64	24.026	1.20056	1437.7
	522.0	65.73	24.107	1.20085	1433.8
Mean	521.33	65.62	24.119	1.20041	1431.85
s.e.m.	0.73	0.10	0.33	0.00022	2.00
s.e.m. %	0.14	0.15	0.14	0.018	0.138
NBS values	523.90	65.485	24.213	1.20039	1426.3
Muscovite (65957)	298.2	76.29	11.317	1.00672	1853.0
	297.4	76.30	11.285	1.00737	1862.0
	298.7	76.20	11.347	1.00721	1851.0
	298.7	76.00	11.380	1.00765	1848.4
	298.1	76.06	11.346	1.00766	1854.0
	299.5	76.18	11.384	1.00798	1849.8
Mean	298.4	76.17	11.343	1.00743	1853.0
s.e.m.	0.3	0.05	0.015	0.00018	1.98
s.e.m.%	0.10	0.06	0.14	0.018	0.107

s.e.m. ≡ standard error of mean; s.e.m. % ≡ (s.e.m./mean) 100.

Table 1. Precision test sequence for SRM-607 K-feldspar standard and 65957 Jabiluka muscovite concentrate.

established for this set of samples, the precision of replicate analyses on one of the more abundant micas was compared with the precision of replicates carried out on a standard feldspar (NBS SRM 607). The mica chosen for this comparison test (65957M) had isotopic concentrations of ^{87}Rb and ^{86}Sr and an isotopic ratio $^{87}Sr/^{86}Sr$ of similar magnitude to those in the feldspar standard. Results for these test data are shown in Table 1. An apparent 'age' is calculated for each analysis assuming an initial $^{87}Sr/^{86}Sr$ ratio of 0.705 and a decay constant of 1.42×10^{-11} y^{-1} (Steiger & Jäger, 1977).

The eight replicates for SRM 607 have a mean Rb concentration within 0.5% of the NBS certified value, a mean total Sr concentration within 0.2% of the NBS value and a mean $^{87}Sr/^{86}Sr$ value within 0.002% of the NBS value. Geochronologic information depends only upon the isotope ratios $^{87}Rb/^{86}Sr$ and $^{87}Sr/^{86}Sr$ rather than on elemental concentrations. The standard error of the mean for the set of SRM 607 data is 0.14% for $^{87}Rb/^{86}Sr$, 0.018% for $^{87}Sr/^{86}Sr$ and 0.14% (i.e. 2.0 m.y.) for the apparent age. The apparent age calculated from the mean $^{87}Rb/^{86}Sr$ ratio (24.119 ± 0.033) and the mean $^{87}Sr/^{86}Sr$ ratio (1.20041 ± 0.00022) is equivalent to an age of 1431.8 ± 2.2 m.y. if an initial $^{87}Sr/^{86}Sr$ ratio of 0.705 is assumed. The mean of the ages calculated individually from each replicate is 1431.8 ± 2.0 m.y. The calculated apparent age using NBS data for SRM 607 is 1426.3 m.y., in close agreement with our values.

It is important to extend a measure of the precision statement to the mica samples studied here, rather than base analytical confidence solely on the feldspar standard. In table 1, data for six replicate analyses of muscovite sample 65957M are compared with those for the standard feldspar. The standard error of the mean (as a percentage) for Rb and Sr concentration analyses for six replicates of 65957M is lower, while that for the $^{87}Rb/^{86}Sr$ and $^{87}Sr/^{86}Sr$ ratios is identical. The apparent age based on an initial $^{87}Sr/^{86}Sr$ ratio of 0.705 is 1853 ± 2.0 (s.e.m.) m.y. The technique used in these analyses is thus capable of producing results which have an intrinsic precision at least equal to that attained for analyses of feldspar standard SRM 607.

A comparable precision can be extended to all samples studied here. In table 2, isotopic results are given for 42 samples; 21 of the samples have replicate analyses. The average standard error of the mean for the 21 replicates is less than 0.14% (i.e. 2.5 m.y. at 1800 m.y.). More than half the set of replicate data has a replication standard error of better than 0.10%. Only two replicate pairs have a standard error exceeding 0.4%. The precision of apparent ages is very sensitive to the magnitude of the $^{87}Sr/^{86}Sr$ ratio in the sample measured. In table 2, there are 14 replicated samples with $^{87}Sr/^{86}Sr$ ratios exceeding 1.0. For these relatively radiogenically enriched samples, the average standard error for the replicate mean is less than 0.10%.

RESULTS

Isotopic data and the model age (based on an assumed initial $^{87}Sr/^{86}Sr$ ratio of 0.705) for each sample are listed in table 2. Except for biotites and the pegmatitic muscovite, the micas were found to have lower $^{87}Rb/^{86}Sr$ than anticipated, so that model ages are subject to the inevitable error associated with the choice of the initial $^{87}Sr/^{86}Sr$ ratio.

Cahill Formation

The oldest event recognizable at Jabiluka from the results of this study is the emplacement of the transgressive pegmatites. The enrichment of Rb with respect to common Sr in the coarse pegmatitic muscovites is extremely high and typical of fractionated intrusives. Consequently, enrichment of radiogenic ^{87}Sr is so high that considerations of the initial $^{87}Sr/^{86}Sr$ ratio of the magma at the time of intrusion are irrelevant. The indicated model ages form a conformable set, which fixes a minimum age for the muscovite at 1830 ± 5 m.y. Although relationships are only exposed in drill-core, it is clear that pegmatite

emplacement post-dates deformation responsible for creation of foliation in the regional metamorphic schists.

The high-grade regional metamorphism was examined by analysis of mineral separates from the amphibolite facies pelitic schist samples 65957, 65990 and 65994. Both muscovite

Sample		Rb (μg/g)	Sr (μg/g)	$\frac{^{87}Rb}{^{86}Sr}$	$\frac{^{87}Sr}{^{86}Sr}$	Model age (m.y.)	Sample impurities
Amphibolite Schists							
65957*	M	298.7	78.4	11.35	1.0072	1851	1% C
		299.5	78.4	11.38	1.0080	1850	
65957	B	557	6.63	636.6	17.249	1807	2% C
		561	6.67	637.4	17.247	1804	
54990	M	214.6	33.6	19.40	1.2110	1813	
		214.6	33.5	19.45	1.2125	1814	<1% B
65990	B	398.9	7.73	240.3	6.932	1802	4% C, 2% M
		398.1	7.72	240.0	6.921	1801	
65994	M	278.6	34.6	24.80	1.3542	1820	1% B, tr G
		277.6	34.6	24.72	1.3532	1823	
65994	B	504.7	13.3	152.6	4.6720	1807	4% C, 2% M, tr G
		505.9	13.6	148.4	4.5667	1809	
Pegmatites							
54920	M	1405	19.2	466.1	13.021	1836	<1% C
		1403	19.0	475.0	13.207	1830	
55217	T	121.5	6.78	58.92	2.0917	1638	
	S	119.5	10.04	36.96	1.4424	1391	10% C, 2% Q
	M	767.5	6.66	2361.4	62.850	1829	>99% M
55213	T	125.0	6.49	64.17	2.2429	1668	
	S	177.5	7.77	78.03	2.5344	1632	5% C, 5% Q
	M	490.1	5.77	668.8	18.280	1827	>99% M
54908	T	277.8	42.6	19.86	1.2249	1820	
	S	211.6	138.4	4.48	0.8170	1740	5% C, 1% Q, 1% M
	M	1343.9	15.4	719.7	19.648	1830	>99% M
Retrograde Schists							
55014†	T	105.5	15.1	21.31	1.2363	1735	
	S	139.0	14.0	30.53	1.3208	1407	10% M, 10% C, 2% Q
	M	264.2	27.1	30.42	1.5025	1822	5% S, 3% C
55014	C (Fe)	27.44	4.11	20.25	1.1777	1625	10% M
		27.39	4.15	20.00	1.1737	1631	
55014	C (Mg)	56.52	6.78	25.56	1.3073	1640	15% M, 5% S, 2% R
		56.89	6.87	25.40	1.3132	1666	
55022	T	43.21	8.64	14.97	1.0497	1603	
55022A†	S	90.5	11.92	23.13	1.2296	1570	5% C, 3% Q
55022B†	S	105.8	13.83	23.30	1.2329	1578	5% C, 1% Q
		107.1	13.92	23.44	1.2370	1579	
55140	T	153.5	12.96	37.44	1.6478	1751	
55140	M	305.2	21.84	45.14	1.8859	1819	<1% R
		304.6	21.88	44.95	1.8836	1823	
55170	T	116.9	9.11	40.77	1.7011	1700	
55170	M	329.0	21.92	48.92	1.9927	1830	>99% M
		328.4	21.92	48.85	1.9938	1834	

Table 2. Isotopic data for Jabiluka whole rock samples and mineral concentrates.

Sample		Rb (μg/g)	Sr (μg/g)	$\frac{^{87}Rb}{^{86}Sr}$	$\frac{^{87}Sr}{^{86}Sr}$	Model age (m.y.)	Sample impurities
Greisens							
54928	T	223.0	13.52	54.08	2.0543	1736	
54928	S	342.8	11.14	113.75	3.5362	1731	70% S, 30% M, tr T
		345.2	11.82	106.81	3.3895	1748	
		344.3	11.95	104.91	3.3358	1744	
54931	M	549.2	16.34	129.28	4.0623	1805	90% M, 10% S, 1% Q
		548.4	16.33	129.07	4.0495	1802	
65968	M	511.7	28.01	61.17	2.3053	1819	>99% M
		512.6	28.09	61.10	2.3062	1822	
65997	T	81.76	52.44	4.562	0.8127	1644	
65997	S	133.1	241.1	1.605	0.7452	1742	2% R
		132.2	240.1	1.606	0.7453	1745	
Kombolgie							
55094	S	96.45	59.08	4.781	0.8233	1721	10% C, 5% H, 5% O
		96.88	59.49	4.769	0.8231	1723	
55098	S	86.53	42.84	5.921	0.8338	1515	2% C, 2% Q, 1% H
		81.76	40.95	5.854	0.8332	1525	
55107	T	86.28	99.7	2.519	0.7638	1626	
55107	S	99.15	150.4	1.918	0.7521	1709	20% C
		97.91	150.2	1.896	0.7522	1732	
55184	T	91.77	19.07	14.41	1.0553	1692	
55184	S	137.6	71.80	5.621	0.8369	1634	10% C, 5% R, 2% Q
		137.3	71.52	5.631	0.8369	1630	
55187	T	101.9	52.58	5.685	0.8407	1661	
55187	S	157.4	84.36	5.472	0.8359	1665	5% X, 2% C, 2% Q
		158.8	85.21	5.465	0.8357	1664	

Mineral abbreviations: B, biotite; C, chlorite; G, graphite; H, hematite; M, muscovite; Q, quartz; R, rutile, anatase, brookite or sphene; S, sericite; T, whole rock; X, unidentified high relief phase with prominent line at d = 6.1 Å

* See also Table 1. Data quoted here are for two muscovites analysed in an identical manner to the other samples listed.

† Postscripts A and B refer to different mineral concentrates from the same sample.

Table 2 continued

and biotite separates were studied; the data from the three sample pairs have common characteristics. Biotites contain very low common Sr, high Rb and therefore are very enriched in radiogenic ^{87}Sr. The present day $^{87}Sr/^{86}Sr$ of 65957B is so high that the calculated age is insensitive to reasonable assumptions for the initial $^{87}Sr/^{86}Sr$ ratio and its apparent age is indisputably 1805 ± 5 m.y. The other biotites (65990 and 65994) have lower Rb/Sr ratios, but their excellent model age agreement with 65957 strongly suggests that 1805 m.y. is a meaningful minimum 'age' for the biotite, i.e. at this time, the amphibolite facies schists in this area cooled through approximately 300°C and radiogenic ^{87}Sr was subsequently retained within the mineral (Jäger *et al.*, 1967).

The data on muscovites from these schists are characterized by much higher common Sr, somewhat lower Rb concentrations and relatively low enrichments in the $^{87}Sr/^{86}Sr$ ratio. While all three apparent ages of the muscovites are higher than those of the biotites,

consistent with other studies (e.g. Jäger *et al.*, 1967), these model ages are sensitive to the choice of initial $^{87}Sr/^{86}Sr$ ratio.

Two interpretations are possible. Firstly, we may postulate that each muscovite-biotite pair suffered a short-lived metamorphism and that the age of both minerals is identical and represents the age of that metamorphism. The data for samples 65957, 65990 and 65994 result in ages of 1805 m.y., 1800 m.y. and 1806 m.y., with corresponding initial ratios of 0.713, 0.709 and 0.711. The apparently impressive age agreement is due to the concordance of the single mineral biotite ages and the high enrichment of radiogenic ^{87}Sr in this mineral.

The second interpretation relies on the significance of the data from the pegmatitic muscovites. Although retrogressively altered, the pegmatites show no petrographic indication of recrystallization during a high temperature regional episode. Delicate graphic intergrowths of quartz and former feldspar, for example, are well-preserved. To render the model ages of pegmatite muscovites more compatible with a short-lived regional metamorphic episode it would be necessary to assume high initial $^{87}Sr/^{86}Sr$ ratios that varied grossly within single intrusions. On the other hand, we note that the data for schist muscovite would yield ages concordant with pegmatitic muscovite (i.e. 1830 m.y.) if values slightly different from 0.705 for the initial ratio are chosen. Such values are 0.708 for 65957M, 0.700 for 65990M and 0.702 for 65994M. The very low values calculated for 65990M and 65994M, which originate 2.5km from the retrogressed ore zone, suggest that 1830 m.y. approximates the maximum 'age' for muscovites from these samples.

Our preferred interpretation of the schist data is that the age discrepancy of approximately 25 m.y. between coexisting biotite and muscovite (the latter supported by data from transgressive pegmatites), is due to cooling phenomena and the respective blocking temperatures for strontium in biotite (~300°C) and muscovite (~500°C) (Jager *et al.*, 1967). Studies of the mineral assemblage of the high grade metamorphics indicate a temperature-pressure regime of ~600°C, 5 kb at Jabiluka (Binns, Ayres, Wilmshurst & Ramsden, this volume) or 550-630°C, 6-8 kb at a regional scale corresponding to some 20km of overburden (Ferguson, this volume). Our implicit cooling rate of approximately 8°C/m.y. is compatible with this thickness of cover.

Data on coarse-grained muscovite relics from the retrogressed schists (55014, 55140 and 55170) are very similar to those for muscovites in the high grade schists remote from mineralization. The model ages for the three samples range from 1820 to 1830 m.y., in essential agreement with the indicated age of the pegmatitic muscovites. The slight discrepancies could be due, in part, to sericite and chlorite contaminants. It would appear that the muscovite from the retrogressed schists has retained Rb-Sr isotopic systematics derived from the amphibolite facies regional metamorphism.

Data for two coarse muscovites from 'greisens' are given here. High purity sample 65968M has a model age of 1820 m.y., equatable to the muscovite ages from schists considering the inevitable small error conceivably introduced by an arbitrary choice of 0.705 as the initial $^{87}Sr/^{86}Sr$ ratio. Sample 54931M has a purity of ~90% and the depressed model age of 1804 m.y. is probably due to the residual 'sericite' impurity in the mineral separate.

In attempting to date the retrogressive metamorphism of Cahill Formation schists and pegmatites and the intense sericitization of 'greisen' zones, we have analysed some whole rock samples and chlorite concentrates, as well as sericites. Petrographic studies do not suggest any significant age difference between sericite formation in these three rock groups.

The two sericite samples from the retrogressed schists shown in table 2 have model ages of 1407 and 1579 m.y., both much younger than either the corresponding muscovite ages or the biotite ages of their non-retrogressed equivalents. In figure 2 we show the data for sample 55014, for which whole rock, muscovite, sericite, Mg-rich chlorite and Fe-rich chlorite samples were available for analysis. It is evident that system closure with respect to Rb

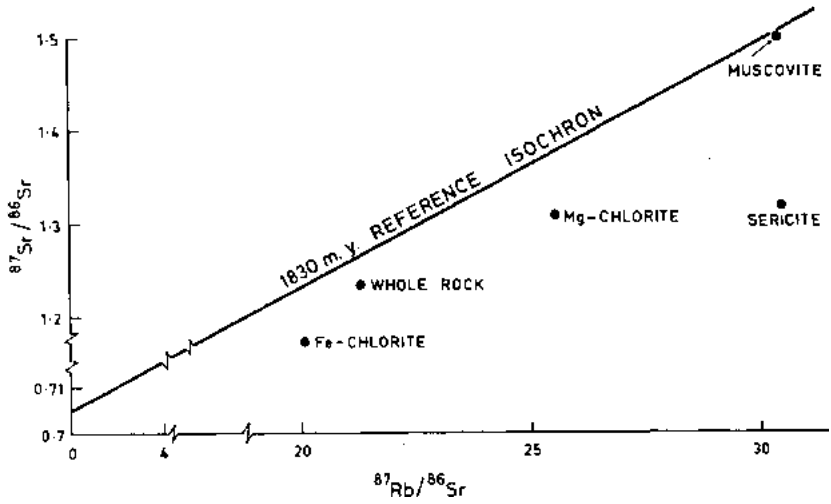


Figure 2. Isotopic data for retrogressed Cahill Formation whole rock and mineral samples plotted relative to an 1830 m.y. reference isochron.

and/or Sr isotopes has not been preserved through any single event subsequent to the retention of radiogenic ^{87}Sr in the muscovite lattice. Since the whole rock data do not plot on the 1830 m.y. (muscovite) reference isochron this sample has evidently either undergone a loss of radiogenic ^{87}Sr and/or an increase in Rb/Sr ratio at a time subsequent to the closure of muscovite (presumably during retrogressive alteration). Similarly, the sericite and the chlorites have even younger apparent ages. The evidence for an open isotopic system with partial response to an alteration event or events, much later than muscovite closure, is clear. While Rb and/or Sr transport is evident in these data, we have analysed no mineral components where *exchange* could have occurred quantitatively, as all data (other than muscovite) indicate only young model ages.

The data for sample 55014 clearly demonstrate the difficulties attached to interpreting 'model' ages of all our Jabiluka sericite samples, and also whole rock samples. Clearly, no single initial ratio is pertinent to all phases of a single sample. Additionally, there is no *a priori* rationale to expect that different samples will derive from a single initial ratio, homogenized during retrogression. This point is emphasized by the highly variable model ages (all calculated assuming an initial ratio of 0.705) for sericites from the greisens and retrogressed pegmatites listed in table 2, which range between 1391 and 1745 m.y.

Kombolgie Formation sandstone

'Sericite' concentrates from the Kombolgie Formation sandstone contain relatively low Rb concentrations, while the regolith samples are distinctly enriched in common Sr when compared with whole rock schist samples. These characteristics presumably reflect the geochemistry of pre-metamorphism weathering. Compared to most Cahill Formation micas, the Kombolgie samples have quite low enrichments of radiogenic ^{87}Sr, so that their calculated model ages have high and indeterminate associated errors. Any attempted interpretation of the data in terms of maximum ages by choice of a minimum feasible initial $^{87}Sr/^{86}Sr$ ratio is unwarranted.

The three regolith samples (55107, 55184 and 55187) have been analysed on a whole

rock and 'sericite' basis. Data on each pair of these samples have an unexpected characteristic. Unlike the retrogressed schist samples, the regolith 'sericites' have lower Rb/Sr ratios than their corresponding whole rocks. The data suffer from the same geochemical deficiency noted previously, namely that the radiogenic enrichment of ^{87}Sr is so low that model age calculations propagate large errors due to arbitrary assumptions of the initial $^{87}Sr/^{86}Sr$ ratio.

DISCUSSION

The minimum age for the deformation associated with the high-grade, amphibolite

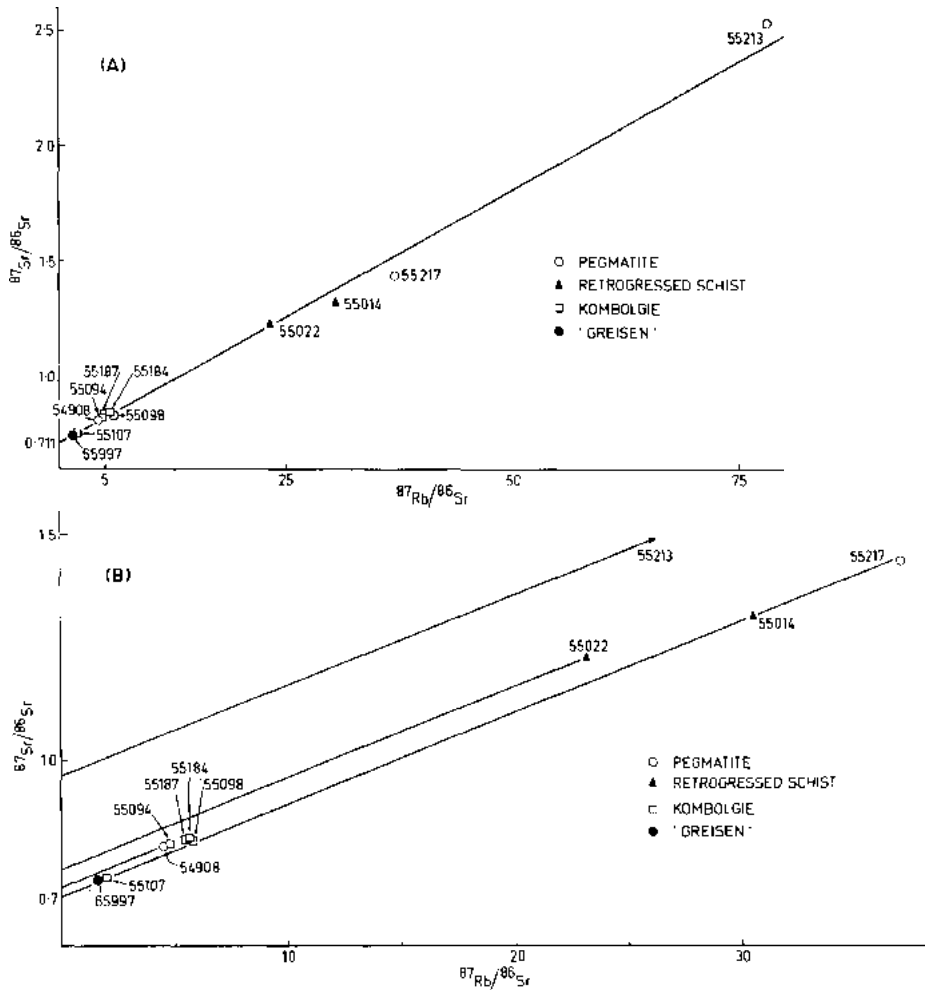


Figure 3A. Sericite 'isochron' assuming crystallization from an isotopically homogenized Sr source. Indicated line and data points correspond to an age of 1534 ± 90 m.y. with an initial $^{87}Sr/^{86}Sr$ ratio of 0.711 ± 0.005.
Figure 3B. Evolution of sericite data assuming crystallization from locally unique $^{87}Sr/^{86}Sr$ sources. Reference lines correspond to 1400 m.y. and this value represents the maximum age of retrogression.

facies regional metamorphism of the Cahill Formation at Jabiluka is 1830 ± 5 m.y. established by muscovite ages of intrusive pegmatites. This age also defines the last time that the Jabiluka host rocks experienced a temperature exceeding 500°C. We interpret younger ages of biotites (1805 ± 5 m.y.) as due to regional cooling to 300°C and thereby calculate a cooling rate of 8°C/m.y.

The retrogressed schists in the vicinity of Jabiluka contain an unaltered muscovite component which retains the older age essentially in agreement with pegmatitic muscovite. Similarly, 'greisen' zones contain muscovite whose age is contemporaneous with muscovite in both schists and pegmatites, suggesting that these zones were developed during the high grade regional metamorphism or as a result of metasomatism associated with pegmatite emplacement.

The regrogression evident in and near the mineralized zone affects schists, pegmatites and 'greisen' zones. A similar style of alteration is evident in the Kombolgie Formation sandstone at Jabiluka and in the regolith immediately underlying it. Our attempts at dating the retrogression in its various manifestations have been frustrated by relatively poor enrichments of radiogenic ^{87}Sr resulting in a range of some 350 m.y. for calculated model ages.

While it is conceded that the present data demonstrate that Rb-Sr techniques are not adequate to resolve fine age detail in the event(s) leading to retrogression in the lithology at Jabiluka, we offer two interpretations of the sericite data that provide information of relevance to the timing of retrogression.

First, if the petrological indications of contemporaneity of the alterations in the Cahill, Kombolgie and 'greisen' zones are accepted, it is reasonable to suggest that extensive fluid involvement during retrogression provided an ambient phase in which strontium isotopes were effectively homogenized during crystallization of sericite. Complete isotopic equilibration between the fluid medium and replaced minerals in the retrogressed schists would permit the formal application of an isochron analysis to data on the sericites. In figure 3A, we show all sericite data (excluding 54928S which has 30% muscovite contamination) on an isochron diagram in which it is quite evident that strontium isotopic equilibration did not occur completely in a single sericitization event over the sampled area. A model 2 age of 1534 ± 90 m.y. is calculated for these data, and represents a reasonable estimate for the age of the alteration episode. The $^{87}Sr/^{86}Sr$ ratio of the fluid responsible for these metamorphic and metasomatic alterations would have been 0.711 ± 0.005.

Alternatively, we may again assume a single alteration event, with the difference that the crystallization of sericite over the sampled region did not involve a homogenized source of strontium isotopes. Rather, each sericite would incorporate a local $^{87}Sr/^{86}Sr$ ratio during its crystallization and the value would be highly dependent on the pre-existing radiogenic component in the altered mineral. In this case each sericite would inherit an independent initial $^{87}Sr/^{86}Sr$ ratio and evolve on an isochron diagram to form an array with a poor linear correlation. The effect is shown in figure 3B in which the sericite data are plotted with individual hypothesized isochrons. In this case, the *minimum* model age calculated assuming a relatively low initial $^{87}Sr/^{86}Sr$ ratio (e.g. 0.705) corresponds to the *maximum* age of the alteration event. Younger ages can be accommodated by assuming initial ratios higher than 0.705. The data from two sericite samples yield model ages approximating 1400 m.y. (based on 0.705) and for these samples the Rb and Sr concentrations fall within the range of possible parent material (e.g. feldspar). On this model, we would conclude that retrogression occurred no earlier than 1400 m.y., long after the regional metamorphism.

Within error limits, both these conclusions are compatible with Pb isotopic data on sulphides in retrogressed graphite schists (Gulson & Mizon, this volume) which suggest an age of 1380 ± 110 m.y. for initial uranium introduction to the Jabiluka environment.

The work reported here has served as a pilot study for detailed Rb-Sr geochronology of a typical mineralized area of the Cahill Formation. Despite rigorous petrological control of sample selection and very careful mineral separation from drill core, it is clear that the Rb-Sr technique has limited application in an area where multiple crystallization events have occurred and whole rock systems have not remained closed with respect to Rb and/or Sr. Further studies of this nature are unlikely to be productive until mining operations allow better access for sampling.

ACKNOWLEDGEMENTS

We thank M. Korsch for assistance with Rb-Sr isotopic measurements, and both B.L. Gulson and R.W. Page for their helpful discussions. This project would not have been possible without the co-operation of Pancontinental Mining Limited; we gratefully acknowledge their contribution in supplying documented drill core.

REFERENCES

Binns, R.A., McAndrew, J. & Sun, S-S, this volume: Origin of mineralization at Jabiluka. *Proceedings of the International Uranium Symposium on the Pine Creek Geosyncline.*

Binns, R.A., Ayres, D.E., Wilmshurst, J.R. & Ramsden, A.R., this volume: Petrology and geochemistry of alteration associated with uranium mineralization at Jabiluka, Northern Territory, Australia. *Proceedings of the International Uranium Symposium on the Pine Creek Geosyncline.*

Ferguson, J., this volume: Metamorphism in the Pine Creek Geosyncline and its bearing on stratigraphic correlations. *Proceedings of the International Uranium Symposium on the Pine Creek Geosyncline.*

Gulson, B.L. & Mizon, K. J., this volume: Lead isotope studies at Jabiluka. *Proceedings of the International Uranium Symposium on the Pine Creek Geosyncline.*

Jäger, E., Niggli, E. & Wenk, E., 1967: Rb-Sr Altersbestimmungen an Glimmern der Centralalpen. *Beitr. Geol. Karte Schweiz, N.F. 134, Liefernung.*

Page, R. W., Compston, W. & Needham, R. S., this volume: Geochronology and evolution of the late Archaean basement and Proterozoic rocks in the Alligator Rivers Uranium Field, Northern Territory, Australia. *Proceedings of the International Uranium Symposium on the Pine Creek Geosyncline.*

Riley, G. H., Binns, R. A. & Craven, S., 1979: Rb-Sr chronology of micas at Jabiluka. *Extended Abstracts of the International Uranium Symposium on the Pine Creek Geosyncline*, 172-173.

Steiger, R. H. & Jäger, E., 1977: Subcommission of geochronology: Convention on the use of decay constants in geo- and cosmochronology. *Earth Planet. Sci. Lett., 36*, 359-362.

MERCURY DISTRIBUTION IN THE JABILUKA TWO OREBODY AND ITS HOST ROCKS

W.R. Ryall and R.A. Binns

CSIRO Division of Mineralogy, P.O. Box 136, North Ryde, N.S.W., 2113, Australia

ABSTRACT

The Jabiluka Two orebody contains a geochemically significant amount of mercury. Uraninite ores from the Upper Graphite Series (UGS) average 360 ppb Hg (range 190 to 470) whereas those from the Main Mine Series (MMS) remote from gold mineralization average 1950 ppb (range 660 to 5920). Higher mercury concentrations are present in the gold-rich, western part of the orebody. Native gold, which occurs principally in breccia zones within the MMS contains up to 450 000 ppb Hg. Uraninite concentrates from auriferous ore contain up to 11 000 ppb Hg, but programmed heating studies indicate about three-quarters of the mercury to be located in gold inclusions. Away from high grade gold mineralization the presence of mercury has been established within both uraninite and associated sulphide minerals.

The immediate host rocks to uraninite veins generally contain more than 100 ppb Hg but only a few metres from ore the levels of both U and Hg fall to background levels of about 7 ppm and 20 ppb, respectively.

Graphite schists adjacent to uraninite veins and breccias in the MMS average 300 ppb and those from unmineralized intervals average 220 ppb. Most Hg in graphite schists is located in pyrite lenticles, which adjacent to ore, average 5000 ppb in the UGS and 9100 ppb Hg in the MMS. Lenticles from a barren drill hole average 1900 ppb in UGS and 2500 ppb Hg in MMS compared with only 200 ppb in graphite schists remote from mineralization.

Greisen-like rocks above mineralized MMS contain anomalously high mercury levels (average 450 ppb). Samples of unweathered Kombolgie Sandstone contain only 10 to 20 ppb Hg.

The mercury content of gold-free uranium ore is strongly correlated with the uranium, arsenic and lead contents. There is no significant correlation of Hg with either total sulphur or other chalcophile elements. This suggests that pyrite and chalcopyrite are genetically unrelated to mercury and supports the contention that Hg was introduced along with uranium and is largely concentrated within uraninite or associated gold.

Except in greisen-like rocks there is no pervasive Hg halo in country rocks surrounding mineralization but the mercury content of pyrite lenticles in graphite schists may indicate proximity to ore. In the secondary environment release of mercury during weathering of uraninite/gold ores may result in soil and soil gas anomalies over deposits lying below flood plain alluvium. Mercury vapour leakage along fault zones may permit exploration on the Kombolgie Sandstone plateau which covers prospective uranium-bearing formations.

INTRODUCTION

Surface or airborne radiometric techniques have so far been largely responsible for discovery of known uranium deposits in the Alligator Rivers Uranium Field. A high potential for additional ore occurrences of similar style lies in concealed situations where alluvium or sedimentary cover rocks hinder the use of radiometric exploration methods. Other techniques capable of reflecting the presence of buried uranium mineralization will play an increasingly important role in future exploration.

One method deserving attention is the mercury pathfinder technique, which has previously been applied with success to locate buried precious and base metal deposits containing from a few to several hundred ppm Hg (Saukov, 1946; McCarthy *et al.*, 1969; Ozerova, 1971; McNerney & Buseck, 1973; Strauss *et al.*, 1977). The mobility of mercury as a vapour is particularly relevant to surface exploration for concealed mineralization.

Few data are available on mercury levels in uranium ores. Trace amounts were reported at the Maureen (Queensland) metasomatic replacement U-F-Mo deposit (O'Rourke, 1975) and from some sandstone Cu-U deposits in Pennsylvania (Lesure *et al.*, 1977). Mercury enrichment at the rims of gold grains in the Mitterberg (Austria) pitchblende deposit were described by Paar (1976). As part of a wider programme designed to evaluate the applicability of the mercury technique in Australian mineral provinces, this paper gives preliminary results for Hg distribution in unweathered samples from the Jabiluka Two orebody, which is overlain by 20 to 70m of Kombolgie Sandstone. The appreciable gold content in parts of this deposit (Rowntree & Mosher, 1975, 1976; Hegge, 1977) was a

promising indication that mercury levels would prove sufficiently high for exploration purposes. Although Rowntree & Mosher (1976) reported the failure of a vehicle-mounted 'mercury sniffer' survey at the nearby Jabiluka One deposit, more sensitive techniques, such as determination of mercury in soil and soil gas, remain untested.

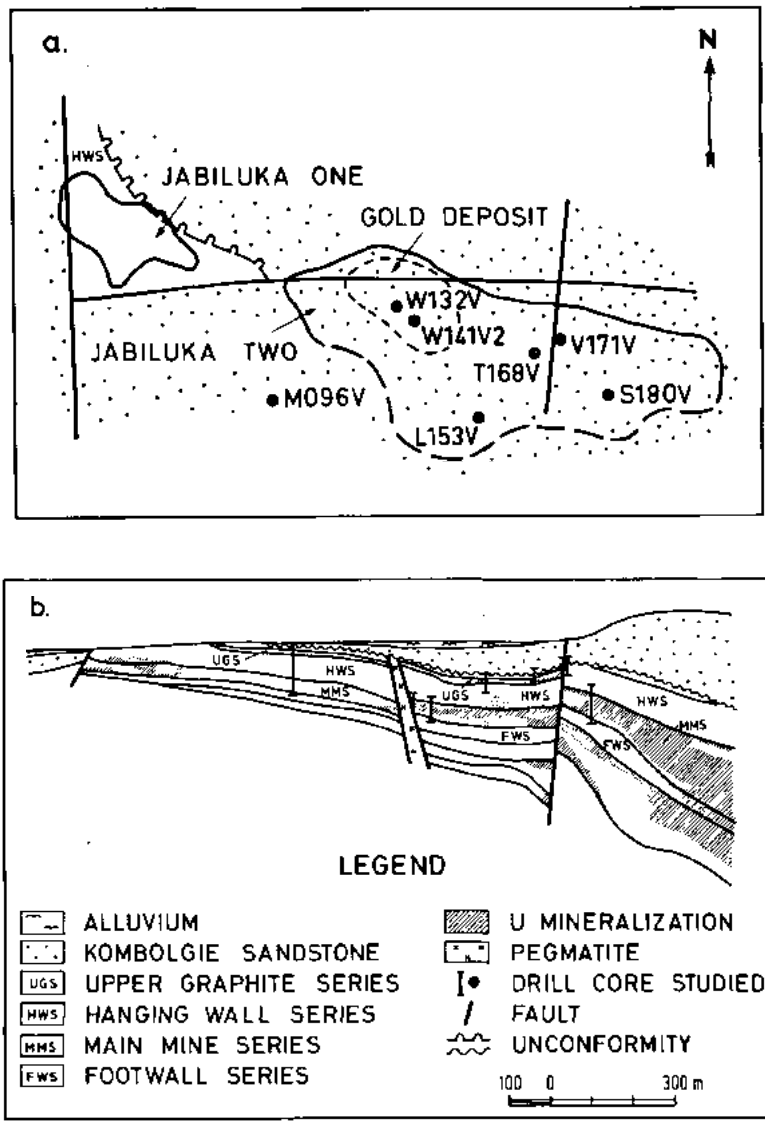


Figure 1. (a) Projection to surface of mineralization at Jabiluka showing diamond drill holes used for mercury analysis.
(b) Longitudinal section showing location of drill core sections. Legend is common to both figures.

SAMPLES STUDIED AND METHODS

Representative samples of fresh diamond drill core from the collection used by Binns, Ayres, Wilmshurst & Ramsden (this volume) were analysed. As indicated on figure 1, drill holes L153V and S180V intersected relatively gold-poor zones of the Jabiluka Two orebody within the Upper Graphite Schist (UGS) and Main Mine Sequence (MMS) respectively, whereas W132V and W141V2 intersected the uranium-gold mineralization. The barren but laterally-equivalent UGS to MMS sequence was examined in M096V, which lies some 200m from mineralization between Jabiluka One and Jabiluka Two, but which is also within the zone of intense greenschist facies retrogressive metamorphism surrounding mineralization.

Comparative data for amphibolite facies pelitic and psammitic schists free from retrogressive effects were obtained from DDH185 and DDH209, located 2.5km northwest of Jabiluka. Biotite-bearing graphite schists showing minimal retrogressive alteration were analysed from DDH R19-S1 at the Ranger 19 prospect 15km south-southeast of Jabiluka. Although these samples cannot be stratigraphically matched with the Jabiluka succession, they provide an indication of mercury contents in potential amphibiolite facies parents for the main component lithologies of the latter.

Samples of Kombolgie Sandstone unconformably overlying Jabiluka were obtained from DDH T168V and M096V, and DDH V171V provided material from a faulted boundary between Cahill Formation and Kombolgie Sandstone directly above mineralization.

Small chips taken along the edges of half drill core were crushed between steel plates and then lightly crushed to minus 150 μm in an agate mortar. This procedure results in negligible mercury loss. Pyrite-rich lenticles in graphite schists were hand-picked from broken core. Samples were analysed soon after preparation to avoid contamination or mercury loss by volatilization.

Mercury contents were determined by the thermal dissociation technique described by Ryall (1979). The sample was heated in an airstream passed through soda asbestos (to absorb CO_2 and SO_2) into a cell positioned in the optical path of an atomic absorption spectrophotometer employing the 253.7 nm Hg emission line. Interferences could be detected by directing the airstream through a gold foil absorber.

To determine total mercury the furnace was held at 900°C and the peak area obtained for the sample was compared with those produced by known volumes of mercury-saturated air. The detection limit of the method is about 10 ppb Hg. Precision ranges from ±35% at 100 ppb to ±20% at 1000 ppb and to ±10% for Hg levels greater than 10 000 ppb.

For certain samples the location and amount of mercury within particular mineral constituents was estimated by using a temperature-programmed furnace and comparing the mercury evolution temperatures with those of pure phases hand-picked from coarse-grained ore samples.

Altogether, 144 samples were analysed. Data for other elements come from the study of Binns, Ayres, Wilmshurst & Ramsden (this volume).

RESULTS

Uraninite ores

The Jabiluka Two deposit is significantly rich in mercury, as indicated in figure 2. Uraninite ores from the UGS DDH L153V average 360 ppb Hg, whereas those from the MMS DDH S180V average 1950 ppb. Programmed heating determinations for hand-picked uraninite (bulk Hg = 5300 ppb) from DDH S180V show that the mercury is liberated in two pulses culminating at 285° and 380°C (Fig. 3a), corresponding to prominent exothemic peaks on differential thermal analysis curves which have been correlated with the two-stage oxidation of uraninite, $UO_2 \rightarrow U_3O_7 \rightarrow U_3O_8$ (Johnson *et al.*, 1957; Kolar *et al.*,

1962). These results suggest either that the mercury substitutes for uranium in the uraninite structure, or that it is present as very fine-grained inclusions of mercuric sulphide, possibly chemisorbed on radiogenic galena inclusions, from which it is released during analysis at the transformation temperatures of the host phase. The absence of a peak near 820°C discounts the possibility that significant mercury is contained within the structure of galena of radiogenic origin which occurs as a common inclusion within Jabiluka uraninite.

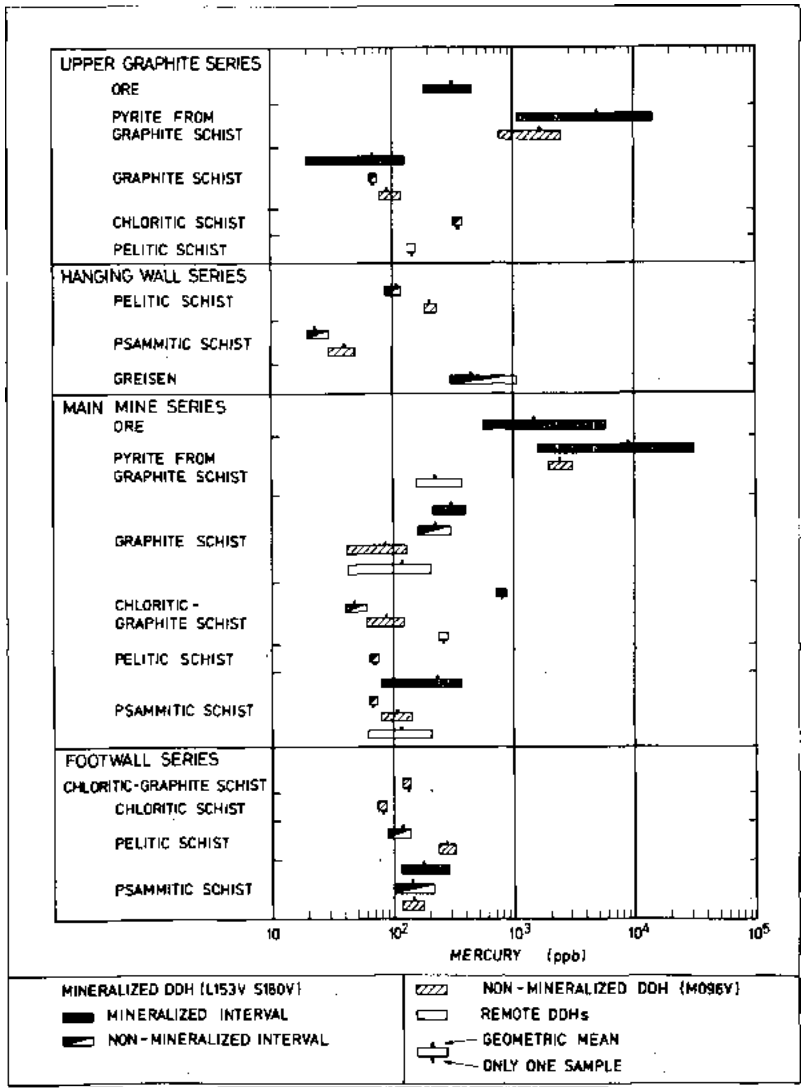


Figure 2. Range of mercury contents and geometric means for Jabiluka Two ores and host rocks.

Much higher mercury contents (average 5200 ppb, range 2000 to 11 000 ppb) were found in the gold-rich, western part of the Jabiluka Two orebody (DDHS W132V, W141V2). Coarse-grained native gold picked from breccia zones with high grade uraninite mineralization contain up to 450 000 ppb Hg. Heating of samples from DDH W132V shows a complex mercury release pattern (Fig. 3b) with peaks at 450°, 510° and 760°C. A small quantity of mercury remained in the gold above 900°C. Uraninite concentrates from auriferous ores contain up to 11 000 ppb Hg but programmed heating determinations indicate that above three-quarters of this is located within fine-grained gold inclusions (Fig. 3c). Some mercury (2500 ppb) is contained within pyrite associated with uraninite mineralization (Fig. 3d), and the presence of a 490°C peak on the auriferous uraninite trace illustrated in figure 3c suggests this also contains Hg-bearing pyrite inclusions.

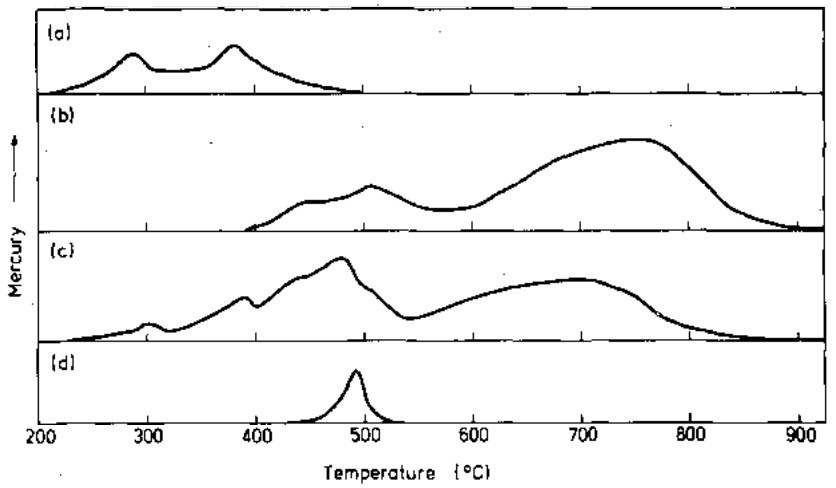


Figure 3. Thermal release curves of mercury from Jabiluka Two samples
(a) Uraninite from graphitic breccia, DDH S180V, 243.8 to 244.1m
(b) Sulphide-free gold grains, DDH W132V, 100.00 to 100.05m
(c) Uraninite containing fine-grained gold and pyrite inclusions, DDH W132V, 155.8m
(d) Pyrite from mineralized graphitic breccia, DDH S180V, 242.8 to 243.1m
Note: no mercury release was detected below 200°C for any samples

Country rocks

The immediate host rocks to the uraninite veins and breccia zones at Jabiluka Two generally contain more than 100 ppb U and are also relatively rich in mercury. However, only a few metres from ore the levels of both U and Hg fall to values comparable with those in similar rocks away from mineralization. No significant differences in Hg have been detected between barren but retrogressively altered country rocks near Jabiluka and their amphibolite facies parents from more remote localities.

Graphite schists adjacent to uraninite veins and breccias in the MMS DDH S180V average 300 ppb Hg and those from unmineralized intervals of MMS in DDH S180V average 220 ppb. Graphite schists from UGS and MMS in the barren DDH M096V average 90 ppb Hg, which is similar to the average in essentially non-retrogressed graphite schists from Ranger 19 (120 ppb Hg). Somewhat discouragingly, the bulk mercury contents are low in UGS graphite schists from DDH L153V, with similar averages of 90 ppb for both mineralized and unmineralized intervals.

Much of the mercury in graphite schists is located in their relatively abundant sulphides, and the contrast between near-ore and remote locations is accentuated by

measurements on pyrite lenticles (typically 1-2cm x 2-3mm) removed from the graphite schists. Those from graphite schists adjacent to ore in the UGS and MMS average 5000 and 9100 ppb Hg, respectively. Equivalent pyrite lenticles from graphite schists in the barren hole M096V are also anomalous with average Hg contents of 1900 ppb in UGS and 2500 ppb in MMS. These levels differ markedly from the 200 ppb Hg average for pyrite lenticles in amphibolite facies graphite schists from Ranger 19.

Pelitic and psammitic schists are depleted in mercury relative to graphite schists, but those from mineralized intervals in DDH S180V contain about twice as much Hg as those from unmineralized intervals of this hole or from the barren hole M096V. The average Hg contents in the latter resemble those in non-retrogressed pelitic and psammitic schists remote from Jabiluka, ranging between 75 and 230 ppb for different stratigraphic intervals.

'Greisens'

The greisen-like rocks rich in muscovite and/or fine-grained white mica, which occur above mineralized MMS (Binns, Ayres, Wilmshurst & Ramsden, this volume), contain an average of 450 ppb Hg. This is an anomalously high value for unmineralized rock and where these greisens (the "illite schists" of Hegge, 1977) surround stronger uranium ores they may host a primary mercury dispersion halo cogenetic with mineralization. A single sample of brannerite-bearing 'greisen' contains 490 ppb Hg.

Kombolgie Sandstone

All samples examined on unweathered Kombolgie Sandstone and the underlying regolith, whether above a barren area (DDH M096V), overlying the Jabiluka Two orebody (DDH T168V), or near a faulted contact (DDH V171V), contained only 10 to 20 ppb Hg. These low levels are not an encouraging indication for application of mercury pathfinder methods in comparably concealed situations elsewhere. Only massive Kombolgie Sandstone was available for analysis, however fractured rock and gouge material from fault zones may contain anomalous mercury levels, that have leaked from underlying mineralization.

GEOCHEMICAL CORRELATIONS

Linear correlation coefficients of mercury with uranium and chalcophile trace elements for 19 samples of ore and immediate host rock are listed in table 1. There is a strong positive correlation of mercury with uranium, arsenic and lead contents. Since most of the lead in these samples is related to uranium by radioactive decay, the Hg-U-Pb correlation also shown indicates mercury to be present in uraninite as shown by the programmed heating analyses.

The correlation of mercury with arsenic may reflect localized presence of arsenide phases in the mineralized veins and breccia zones at Jabiluka Two. A comparable correlation has been reported for base metal deposits (Ryall, 1979), where Hg is commonly contained in part within tetrahedrite. However, at Jabiluka Two a correlation with silver is lacking. Correlation between mercury and antimony is also common in base metal ores, but this cannot be tested at Jabiluka Two where Sb is below the level of detection (Binns, Ayres, Wilmshurst & Ramsden, this volume).

U	0.71[1]
S	-0.28
Ag	-0.14
As	0.46[2]
Bi	0.21
Co	0.19
Cu	0.15
Ni	-0.20
Pb	0.43[2]
Zn	-0.02

[1] Correlation at better than 99.9% significance level
[2] Correlation at better than 90% significance level

Table 1. Values of linear correlation coefficients of Hg with U, S, Ag, As, Bi, Co, Cu, Ni, Pb and Zn in ores and their immediate host rocks (N = 19)

Although some mercury is present in sulphides accompanying Jabiluka Two mineralization (Fig. 3d), table 1 shows no significant correlation of Hg with either total

sulphur or other chalcophile metals, particularly Cu. This suggests that the pyrite and chalcopyrite present in the host rocks are genetically unrelated to mercury and supports the contention that Hg was introduced along with uranium and is largely concentrated within uraninite or, where present, the associated gold.

No gold analyses are available to test their correlation with mercury.

DISCUSSION

The Jabiluka Two deposit contains a geochemically significant concentration of mercury, which is strongly partitioned into uraninite and gold mineralization. Element correlations, and the Hg enrichments in greisen-like rocks associated with ore, suggest a cogenetic relationship (hydrothermal-pneumatolitic?) between mercury and uranium which lends strength to application of the Hg pathfinder technique in exploration.

Except in the immediate vicinity of ore or where greisen-like rocks are present, there appears to be no pervasive primary Hg halo in the country rocks surrounding mineralization, and bulk mercury contents do not discriminate between schists that have undergone or avoided retrogressive metamorphism respectively. The one potential application of mercury methods in the primary zone to be suggested by this study is in analysis of pyrite lenticles within graphite schists (Fig. 4). Even 200m from mineralization these display mercury enrichment of about ten times background (relative to lenticles in non-retrogressed graphite schists) and the contents increase towards ore. These results could aid evaluation of pattern drilling programmes, for example.

It is in the secondary environment that mercury pathfinder techniques may have greater application. Release of mercury during weathering of uraninite and gold ores may result in detectable soil and soil gas anomalies over deposits lying below flood plain alluvium (Fig. 4).

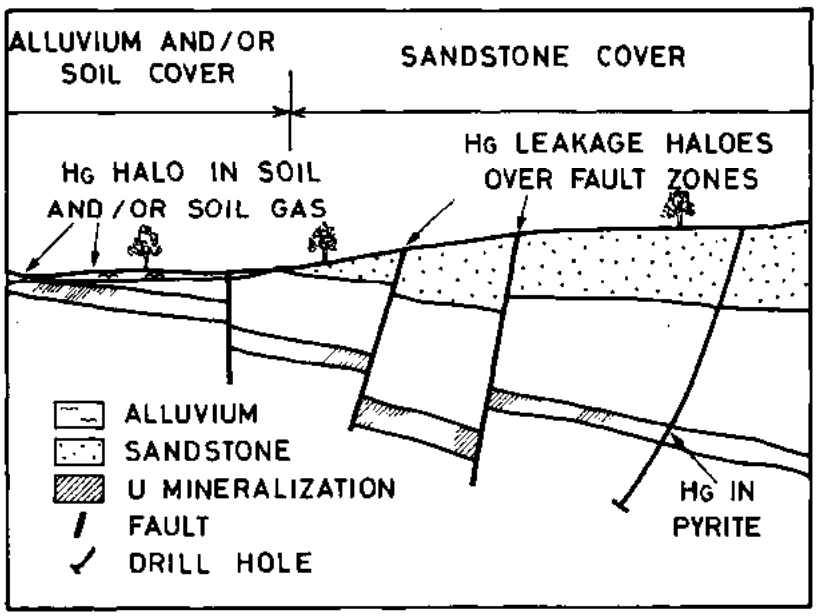


Figure 4. Diagrammatic representation of mercury pathfinder techniques that may have application in the Alligator Rivers Uranium Field.

The presence of sulphide minerals, particularly pyrite, is expected to give rise to enhanced mercury signatures over oxidizing uraninite-gold mineralization since both minerals are unstable at low pH conditions. Although Jabiluka Two is located below the zone of oxidation, modification of the Jabiluka One deposit has occurred to a depth of 15m and in this zone secondary uranium minerals (autunite, sklowdowskite and saleeite) have been identified (Rowntree & Mosher, 1975). Reconnaissance grab samples from the Jabiluka One exploration trench contain 60 ppb (soil) and 30 ppb (weathered schist). Relative to typical barren situations that contain less than 20 ppb Hg, these values are certainly anomalous.

Another mercury exploration technique which may permit exploration over the Kombolgie Sandstone plateau is detection of mercury vapour leakage along fault zones which intersect mineralization at depth. The successful use of this technique relies upon mercury vapour generation occurring by oxidation in permeable fault zones caused by downward migration of oxygenated water (Fig. 4).

ACKNOWLEDGEMENTS

We thank J.R. Wilmshurst for assistance in this study, and also the staff of Pancontinental Mining Limited for their cooperation.

REFERENCES

Binns, R.A., Ayres, D.E., Wilmshurst, J.R. & Ramsden, A.R., this volume: Geochemistry of Jabiluka ores and host rocks. *Proceedings of the International Uranium Symposium on the Pine Creek Geosyncline.*

Hegge, M.R., 1977: Geologic setting and relevant exploration features of the Jabiluka uranium deposits. *Proc. Australas. Inst. Min. Metall. 264,* 19-32.

Johnson, J.R., Fulkerson, S.D. & Taylor, A.J., 1957: Technology of uranium dioxide, a reactor material. *Ceram. Bull., 36,* 112-117.

Kolar, D., Lynch, E.D. & Handwerk, J.H., 1962: Influence of gas flow on DTA curves of UO_2. *J. Am. Ceram. Soc., 45,* 141-142.

Lesure, F.G., Motooka, J.M. & Weis, P.L., 1977: Exploration geochemical studies of some sandstone copper-uranium deposits, Bradford, Columbia and Lycoming Counties, Pennsylvania. *Journal of Research of U.S. geol. Surv., 5,* 609-621.

McCarthy, J.H., Vaughan, W.W., Learned, R.E. & Mueschke, J.L., 1969: Mercury in soil gas and air; a potential tool in exploration. *Circ. U.S. Geol. Surv., 609,* 16 p.

McNerney, J.J. & Buseck, P.R., 1973: Geochemical exploration using mercury vapor. *Econ. Geol., 68,* 1313-1320.

O'Rourke, P.J., 1975: Maureen uranium fluorine molybdenum prospect, Georgetown. *in* (ed. C.L. Knight), *Economic Geology of Australia and Papua New Guinea, Australas. Inst. Min. Metall., Monograph Series No. 5, 1. Metals,* 764-769.

Ozerova, N.A., 1971: Primary dispersion haloes of mercury. *Int. Geol. Rev., 13,* 110 p.

Paar, W., 1976: Telluride der Gold-Nasturan-Paragenese von Mitterberg, Salzburg (Osterreich). *Neues Jb. Miner. Mh., 5,* 193-202.

Rowntree, J.C. & Mosher, D.V., 1975: Jabiluka uranium deposits. *in* (ed. C.L. Knight), *Economic Geology of Australia and Papua New Guinea, Australas. Inst. Min. Metall., Monograph Series No. 5, 1. Metals,* 321-326.

Rowntree, J.C. & Mosher, D.V., 1976: Case history of the discovery of the Jabiluka uranium deposits, East Alligator River region, Northern Territory of Australia. *in, Exploration for Uranium Ore Deposits.* International Atomic Energy Agency, Vienna, 551-573.

Ryall, W.R., 1979: Mercury distribution in the Woodlawn massive sulfide deposit, New South Wales. *Econ. Geol.,* in press.

Saukov, A.A., 1946: Geochemistry of mercury. *Akad. Nauk. SSSR, Inst. Geol. Nauk. No. 78, Series 17,* 129 p.

Strauss, G.K., Madel, J. & Alozo, F. FDEZ, 1977: Exploration practice for strata-bound volcanogenic sulfide deposits in the Spanish-Portugese Pyrite Belt; geology, geophysics and geochemistry. *in* (eds. D.D. Klemm & H.J. Schneider), *Time and Strata-bound Ore Deposits,* Springer-Verlag, Berlin, 55-93.

GROUND WATER GEOCHEMISTRY IN THE VICINITY OF THE JABILUKA DEPOSITS

R.L. Deutscher[1], A.W. Mann[1] and Angela Giblin[2]

1. CSIRO Division of Mineralogy, Private Bag, P.O. Wembley, W.A., 6014, Australia.
2. CSIRO Division of Minerology, P.O. Box 136, North Ryde, NSW, 2113, Australia.

ABSTRACT

Seventeen exploration drill holes in the vicinity of the Jabiluka One and Jabiluka Two deposits were logged for Eh-pH and conductivity at 5 metre intervals to depths of up to 195 metres below ground surface. Forty-seven water samples from exploration drill holes, augered holes on the Magela flood plain and from two billabongs in the vicinity of the deposits were collected and analyzed. Analyses for pH and Fe were conducted in the field, and further analyses for major ions Ca^{2+}, Mg^{2+}, Na^{+}, K^{+}, SO_4^{2-}, Cl^{-}, HCO_3^{-} and Si and minorelements Zn, Cd, Pb, Cu and U were conducted in the laboratory.

The *in situ* Eh-pH and conductivity measurements, and analyses for major and minor elements of ground waters suggest that deep-lying chlorite-graphite schists containing the uranium mineralization are well protected from, or do not react rapidly with, ground water under present-day conditions, i.e. the schists of the Cahill Formation are a stable host for uranium mineralization at depth. In the vicinity of the Magela flood plain where the Cahill Formation and the permanent water table are close to the surface, some samples were found to contain high concentrations of sulphate, zinc, lead and iron. These same samples were characterized by low pH's in the pH range 3.0-4.0. The anomalies suggest weathering of sulphides associated with the mineralized Cahill Formation, where the schists are at shallow depths and in an oxidizing environment. The anomalies are not, however, necessarily indicative of zones of uranium enrichment in this formation.

INTRODUCTION

Hydrogeochemical methods are effective in the search for many different types of mineral deposits, including uranium deposits and those of base metal sulphides. Hydrogeochemical techniques are well suited to the exploration for uranium deposits, since uranium, in the oxidized (VI) valence state, is very soluble either in acid solution as the uranyl, UO_2^{2+}, ion or in neutral and alkaline solutions as the dicarbonate, $UO_2(CO_3)_2^{2-}$ or tricarbonate, $UO_2(CO_3)_3^{4-}$, ions. The potential of hydrogeochemical techniques in the exploration for uranium deposits in the United States was assessed by Fix (1956) and Denson *et al.* (1956). Recent case histories such as those described by Bendix Field Engineering Corporation (1977), Zielinski & Roshold (1978), Culbert & Leighton (1978) and Delany & Fleischer (1978) indicate the widespread suitability of hydrogeochemical techniques for uranium exploration. However, as pointed out by Beus & Grigorian (1975) the size and contrast of an aqueous halo around a particular deposit depends on such factors as:

1) Morphology and composition of the ores, as well as of the primary haloes surrounding them.
2) Physical nature, including permeability of the enclosing and overlying rocks.
3) Hydrogeological and palaeogeochemical environments.
4) Intensity and duration of the erosion process.
5) Landscape geochemical conditions and the migration characteristics of the indicator elements in a given environment.

The Jabiluka deposits are potentially favourable for the formation of a detectable hydrogeochemical anomaly. The market relief on the eastern margin of the Magela flood plain along the Arnhem land escarpment suggests that shallow aquifer groundwater flow at the escarpment should be outwards towards the flood plain, and that the water table along the margin of flood plain should be close to surface.

Hydrogeochemical sampling of the Jabiluka area, and the adjacent parts of the Magela

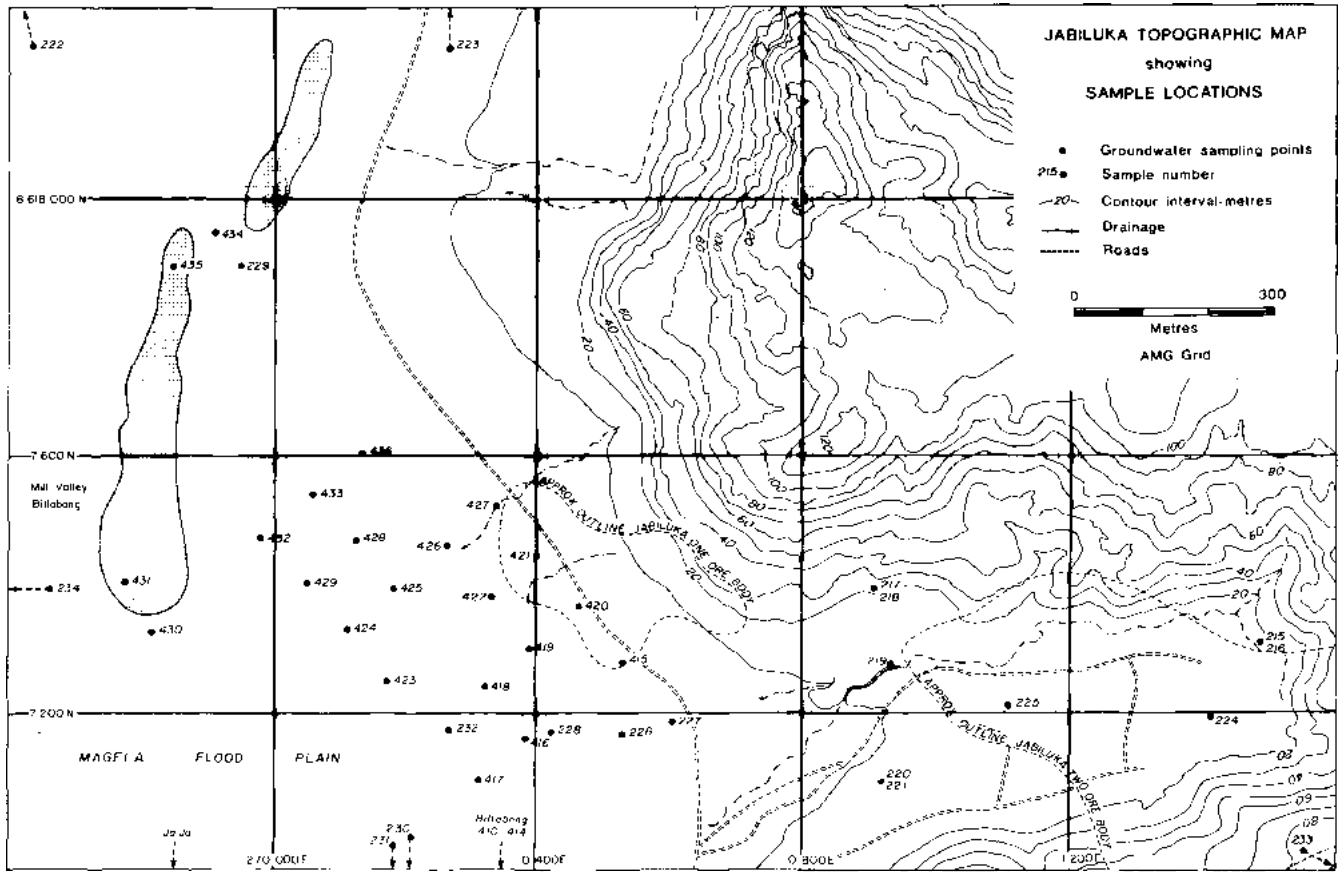


Figure 1. Ground water sampling locations in the vicinity of the Jabiluka deposits.

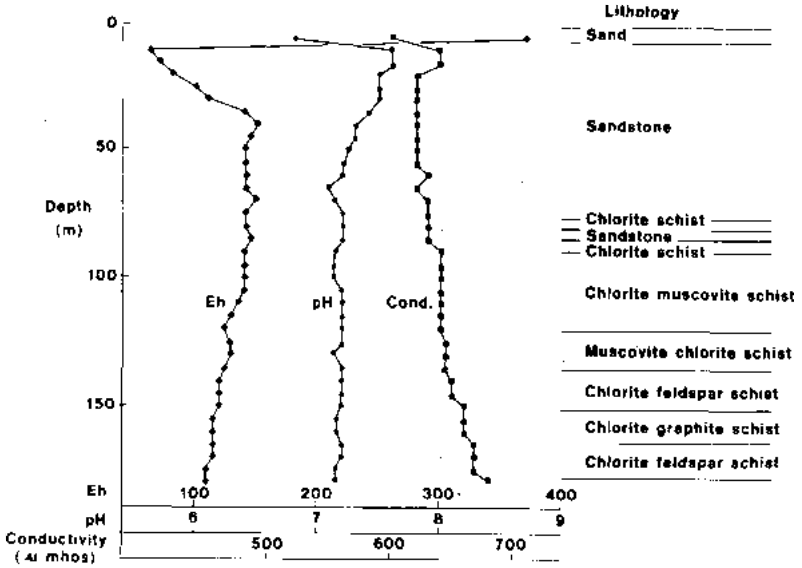


Figure 2. Down-hole Eh-pH and conductivity measurements at sampling location 224.

flood plain, was undertaken at the end of dry season in 1976 and again at the end of the dry season in 1978. Ground water samples were obtained either from drill holes in the immediate vicinity of the Jabiluka One or Jabiluka Two ore bodies (see Fig. 1 and Table 1), from billabongs, or from shallow auger holes in the flood plain. Some drill holes in the area of the ore bodies were logged for Eh, pH and conductivity by a down-hole instrument.

Eh-pH-conductivity measurements

Down-hole measurements of Eh, pH and conductivity were taken in selected drill holes both within and adjacent to the ore bodies. The down-holes probe used was similar to that described by Bolviken *et al.* (1972) and Mann (1974), consisting of a pH electrode with Ag/AgCl reference and two platinum foil electrodes for conductivity and Eh measurements. Eh measurements were made using one of the platinum electrodes and the Ag/AgCl reference. Such probes have been successfully used in the past to locate sulphide zones (Bolviken *et al.*, 1972), oxidation-reduction fronts in uranium containing sandstones and redox fronts related to uranium deposits in calcrete (Mann & Deutscher, 1978).

Measurements were taken at 5m intervals and recorded manually from a Beckman H5 meter, or in the case of conductivity from a portable AC conductivity meter. Ground water in the vicinity of the Jabiluka deposits showed little variation in pH, Eh or conductivity with depth. Reducing ground waters were not detected. Measurements for a typical hole are shown in figure 2.

Apart from an initial change in all parameters in the top 5m of the hole which was collared with iron pipe, little change was observed in any of the parameters down to a depth of 180m. Conductivity was between 620 and 680 μmhos, pH between 7.1 and 7.6, and Eh (apart from the near surface sample) between +60 and +150mV. At this pH, the Eh of the waters is only mildly reducing, being above the redox potential for oxidation of U(IV) to U(VI) and above that for oxidation of Fe(II) to Fe(III). The change in lithology over this same depth range at this location is significant, the major change being from sandstone to schist at 80m. The absence of a major change in water characteristics for this change in lithology indicates two factors:

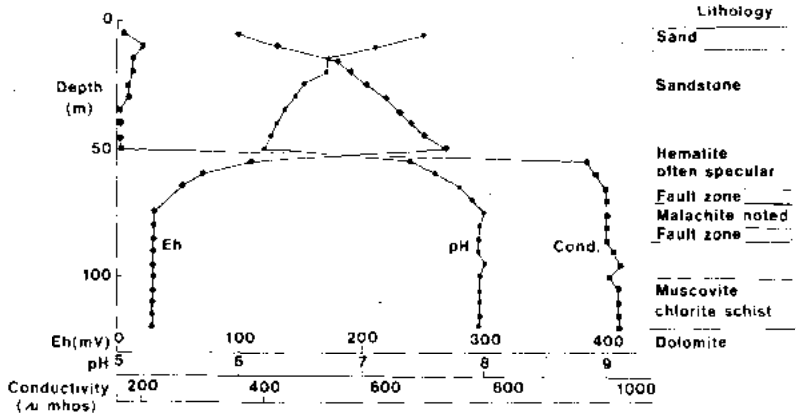


Figure 3. Down-hole Eh-pH and conductivity measurements at sampling location 220.

1) That water in the drill hole is probably from one aquifer probably located near the base of the sandstone.
2) That the schists of the underlying Cahill Formation do not impose a low Eh or low pH on this ground water, i.e. they are unreactive.

In several locations, for example location 220 (see Fig. 3), water of higher conductivity, slightly lower Eh (+030mV), and higher pH (7.60-8.00) was found at depth. In these holes fault zones were recorded in drilling logs, at 65-70m and 80-85m. It appears that ground water associated with these faults has chemical parameters significantly different from that in sandstone above. Again contamination was evident at the top of the hole due to an iron collar. The Eh once again was generally above the redox boundary required for reduction of U(VI) to U(IV) or Fe(III) to Fe(II) (Langmuir, 1978). By comparison, some near-surface acid waters from the Magela flood plain when tested with the same instrument indicated Eh values below the redox potential for reduction of Fe(III) (as $Fe(OH)_3$) to Fe(II).

MAJOR ELEMENT HYDROGEOCHEMISTRY

The major anions, chloride, sulphate and bicarbonate are important indicators of ground water origin and type. Chloride ion, because of its 'inertness' with respect to both chemical precipitation and adsorption is 'conservative' and is useful in determining the amount of evaporation undergone by groundwater, the amount of seawater intrusion, or the degree of contact of ground water with ancient marine deposits or water. The relationships between high sulphate in ground water and sulphide deposits has been widely observed and recorded, for example by Hoag & Webber (1976), Dall'Aglio & Tonani (1972) and Cameron (1978). Sulphate is relatively mobile in groundwater since insoluble sulphates are restricted to cations of trace elements. Reaction between groundwater and carbonate rock is commonly indicated by a high concentration of bicarbonate ion and neutral-alkaline pH. The silica concentration in ground water, similarly, is a useful indicator of reaction between ground water and silicate minerals (Garrels & McKenzie, 1967).

Except for samples 216, 218 and 221 which were taken at depths of 50m, 34m and 60m respectively, all water samples were taken just below the water table. Those from exploration drill holes were obtained with a PVC tube-type sampler, and those from augered drill holes on the flood plain were obtained by suction through a polythene tube into a hand operated PVC pump. Sample locations are shown on figure 1. Samples were placed, unfiltered and unacidified, into 500ml polythene screw top containers. The pH of samples was measured in

the field. Bicarbonate was determined in the laboratory by titration with standardized H_2SO_4 (Brown *et al.*, 1970). Analyses for sodium, potassium, calcium, magnesium and silicon were performed on a Varian Techtron model AA5 Atomic Absorption Spectrophotometer. Sulphate was determined gravimetrically by precipitation of barium sulphate, and chloride was determined by Mohr Titration. Iron, as Fe(II) was measured in the field, by the bipyridine method described by Brown *et al.* (1970). Fluoride was measured with an Orion ion selective electrode. Copper, lead and cadmium were analyzed by anodic stripping voltammetry (Florence, 1972) and zinc was determined by differential pulse anodic stripping voltammetry. Uranium was determined by the delayed neutron activation technique.

All samples from exploration drill holes in the immediate vicinity of the Jabiluka One and Jabiluka Two deposits had extremely low concentrations of chloride, sulphate and silica. Bicarbonate, and major cation concentrations were slightly higher in ground water from several holes, indicating some reaction of ground water with carbonate. Dolomite units, occurring as wedge shaped bodies up to 20m thick in the main mine series between Jabiluka One and Jabiluka Two, were reported by Hegge (1977). The major element hydrogeochemistry in the vicinity of the ore-bodies confirms the suggestion of Eh-pH-conductivity data that there is apparently little reaction between the present-day ground water regime and the schists of the Cahill formation in this area.

In contrast to this, ground water samples from augered holes on the flood plain adjacent to Jabiluka One, near Ja Ja and near the mill valley (sample 223) showed some large variations in major ion concentrations. On the flood plain, soils are generally clay-loam with varying amounts of organic matter (10-30%). Jarosite, $KFe_3(SO_4)_2(OH)_6$ is commonly observed as a powdered yellow white precipitate at the surface. Clay content is high. On the margin of the flood plain and sand/clay ratio varies greatly, and sandy lenses extend into the flood plain through sampling locations 420, 419, 418 and 232.

This section, compiled from information obtained during the augering program, shows the existence of a lens of sand extending some distance into the flood plain. It is probably derived from alluvial material eroded and transported from the adjacent escarpment. Deeper

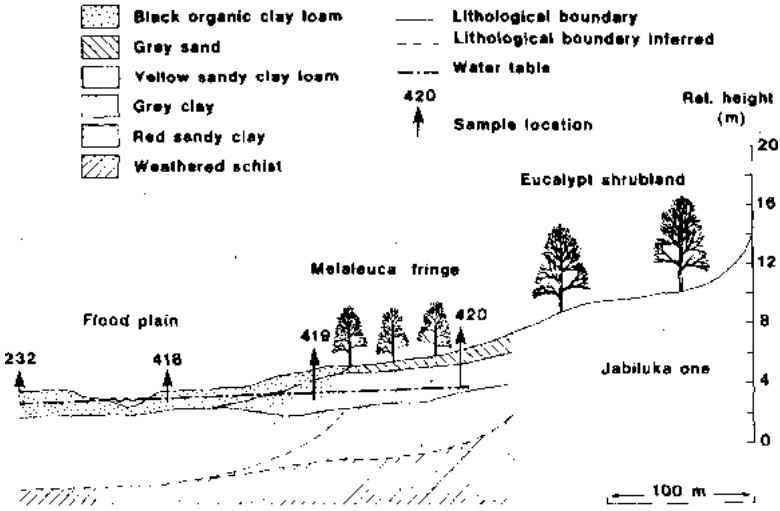


Figure 4. Section of Magela flood plain through sampling locations 420, 419, 418 and 232.

drilling shows that the grey clay of the flood plain is underlain by weathered schist derived from the Cahill Formation. The water table, at the time of sampling (October, 1978) was approximately 1-1.5m below the flood plain surface, with a relatively uniform gradient of 1 in 300 upwards towards the Jabiluka One deposit. Thin films, subsequently verified as iron oxide, were evident on the surfaces of small pools of water formed where ground water seepage occurred.

Ground water samples from the flood plain area showed several interesting features:

1) A large proportion of samples contained high concentrations of sulphate ion (>1000mg l^{-1}).
2) High sulphate concentrations were usually accompanied by low pH and a high concentration of Fe^{2+}.
3) All samples with high sulphate contained higher concentrations of the major cations, Ca^{2+}, Mg^{2+}, Na^{+} and K^{+}.
4) No samples had high cation concentrations without a corresponding high sulphate ion concentration.

Samples with these features, were invariably associated with the grey clay zones of the

Sample No.	pH	Ca^{2+}	Mg^{2+}	Na^{+}	K^{+}	SO_4^{2-}	Si	Cl^{-}	HCO_3^{-}	F^{-}	Fe^{2+}	Zn	Cd	Pb	Cu	U
215	7.80	21	24	60	7	-	8	95	223		-	.034	-	-	-	.003
216	8.20	15	22	12	5	-	8	22	212		-	.028	-	-	-	.003
217	5.60	1	1	2	1	-	5	14	24		1	-	-	-	-	.002
218	5.50	1	1	2	1	-	5	10	18		-	.007	-	-	-	.001
219	8.60	4	8	3	8	-	5	8	212		2	-	-	-	-	.001
220	6.45	1	3	1	1	-	5	6	32		5	.011	-	-	.176	.001
221	7.60	1	5	21	1	-	5	7	59		4	-	-	-	-	.001
222	4.80	3	5	14	4	18	5	27	6		-	.009	-	.006	-	.001
223	3.70	267	890	70	1	6854	66	694	-		3	.164	-	-	.006	.020
224	7.20	1	19	2	1	13	7	9	185		4	.005	-	-	-	.001
225	7.55	1	9	1	1	-	7	6	71		-	.013	-	-	-	.001
226	4.50	1	2	4	3	-	6	10	9		2	.020	-	-	-	.003
227	5.30	1	1	2	1	13	18	6	12		-	.005	-	-	-	.004
228	3.10	18	10	7	7	548	52	31	-		16	.053	-	.006	-	.005
229	4.20	70	180	490	57	1441	34	529	9		-	.027	-	.040	.010	.028
230	3.20	78	114	42	40	1749	43	240	-		55	.256	-	.009	.014	.003
231	6.35	1	3	10	3	-	5	19	12		2	.005	-	-	-	.001
232	6.50	385	464	392	55	1844	25	344	123		3	.040	-	-	.005	.001
233	6.70	1	20	1	1	-	8	7	188		-	.015	-	-	-	.001
234	4.55	39	30	15	3	164	11	143	21		-	.018		-	-	.001
410	5.15	1	1	10	6	-	-	40	7			-	-	-	-	.001
411	5.90	1	1	10	2	14	-	30	13	0.2	-	-	-	-	-	.002
412	5.10	10	13	47	17	310	28	58	6	0.1	48	-	-	-	.016	.002
413	5.00	72	128	196	33	1538	38	65	15	0.2	200	.005	-	.012	-	-
414	5.70	150	196	205	28	1676	43	175	131	0.4	48	.022	-	-	-	.002
415	4.95	3	4	6	1	-	9	24	20	0.2	-	.005	-	-	-	.001
416	3.00	46	19	10	19	1590	73	90	-	3.3	400	.320	.014	.400	.016	.004
417	3.10	152	320	238	1	4132	73	440	-	3.9	720	.480	.008	.162	.009	.007
418	3.65	105	190	360	34	2084	37	615	-	1.1	200	.051	.024	.129	-	.004
420	6.05	3	7	5	2	14	12	20	73	0.2	-	-	-	-	-	.009
421	6.00	1	1	5	2	44	15	22	12	0.2	-	-	-	-	-	.001
422	3.65	7	9	10	5	110	19	34	-	0.1	5	.045	-	.036	-	.007
423	4.60	370	670	610	52	5794	45	910	-	0.5	320	.075	.003	.342	.015	.005
424	5.40	86	141	780	47	1436	16	1895	169	0.1	36	.009	.060	-	.010	.001
425	6.30	221	320	920	59	2324	17	2025	-	0.4	4	-	-	-	.019	.007
426	3.35	50	100	77	37	1614	69	165	-	1.3	560	.132	.010	.660	.008	.004
427	5.55	2	4	5	1	6	8	24	11	0.5	-	.061	-	.009	.018	-
428	6.30	51	106	60	6	912	19	156	-	1.1	40	.052	-	.420	-	.005
429	3.75	192	400	487	41	4356	67	470	-	2.3	-	.036	-	.086	-	-
430	6.75	46	77	1970	83	280	5	2650	-	0.4	-	.005	-	-	-	.005
431	4.25	4	4	47	12	52	-	175	2	-	-	-	-	-	-	.001
437	6.90	48	58	466	33	746	-	415	-	0.2	-	-	-	-	-	.005
433	3.60	142	250	190	19	3464	37	150	-	9.3	720	.076	.021	.144	.109	.012
434	5.35	83	138	190	50	1696	12	240	-	0.3	160	.062	-	.043	.010	.003
435	3.85	3	3	40	11	62	7	138	-	-	-	.013	-	-	-	.005
436	4.00	17	36	75	7	230	20	272	-	0.5	30	.049	-	.088	-	.003
LIMIT OF DETECTION		1	1	1	1	5	5	5	7	0.1	1	.005	.003	.005	.005	.001

- signifies less than limit of detection.
blank signifies no value available.

Table 1. Major and trace element hydrogeochemistry (all values mg/l)

true flood plain, whilst samples along the margin (Melaleuca fringe) and from the sandy alluvial lens(es) were low in major element concentrations and had closer to neutral pH.

Fluoride is often analyzed in ground water as a regional indicator in uranium exploration programs, because of its association with uranium in mineralizing solutions originating from granitic rocks (Doi *et al.*, 1975). Apart from the fact that all samples with concentrations of fluoride >2mg l^{-1} had low pH and high sulphate, there did not appear in the present case to be systematic correlation of fluoride with any other of the measured chemical parameters in the water.

Trace Element Hydrogeochemistry

All water samples were analyzed for U, Cu, Pb, Zn and Cd (see Table 1). Waters from exploration drill holes in the vicinity of the deposit in general contained low concentrations of all of these elements. The highest concentration of uranium observed in waters surrounding the ore-zone was 0.003mg l^{-1}. Samples from the flood plain also had low uranium concentrations, and only in two cases (samples 223 and 229) did the uranium concentration exceed 0.010 mg l^{-1}. Compared to values for other types of uranium deposit, and for activity weathering granite, these ground water concentrations are very low.

Fix (1956), in a study of waters from both mineralized and non-mineralized areas in the U.S., assessed the average background of uranium in water in uraniferous areas as 0.0008mg l^{-1}. Anomalous waters in mineralized areas ordinarily contained from 0.001 to about 0.120mg l^{-1} uranium. Results of systematic sampling in four areas in South Dakota and Wyoming by Denson *et al.* (1956), showed the uranium content in ground water in Oligocene and Miocene units to average between 0.012 and 0.046mg l^{-1}, in Cretaceous, Eocene and Paleocene units to average between 0.004 and 0.006mg l^{-1} and in mineralized areas to average between 0.072 and 0.124mg l^{-1}. Phoenix (1959), in a study of the Colorado plateau sandstone deposits, reported many U concentrations in waters in excess of 0.100mg l^{-1}.

Uranium concentrations in ground water in excess of 0.100mg l^{-1} are a common feature in the vicinity of carnotite deposits in Western Australia (Mann & Deutscher, 1978), (Western Mining Corporation, 1978). 'Upstream' from the ore-zones, actively weathering granite, the probable source of uranium for the carnotite, commonly produces uranium concentrations in ground water of the order of 0.02-0.08mg l^{-1}. Considering the tonnage and grade of the uranium contained in the Jabiluka deposits, the uranium concentrations in ground waters adjacent to the deposits are astonishingly low.

Concentrations of Zn, Cd, Pb and Cu in ground waters are of significance, particularly in samples from the Magela flood plain. One sample (220) from an exploration drill hole between the Jabiluka One and Jabiluka Two deposits, contained 0.175mg l^{-1} of copper. This value is of particular significance, since at the measured pH of the sample, pH-6.45, the solubility of copper in water is low (Mann & Deutscher, 1977). As shown by the lithological record for this hole (Fig. 4), malachite occurs in the fault zone at 75m, and dissolution of this mineral almost certainly causes the high local copper concentration in water.

Higher concentrations of Cu, Pb, Cd and Zn were observed in many of the samples from the Magela flood plain. Five samples (223, 230, 416, 417 and 426) contained greater than 10.100mg l^{-1} zinc, the highest recorded value being 0.480mg l^{-1}. Concentrations in excess of 0.050mg l^{-1} were recorded only once for cadmium and copper in samples 424 and 433 respectively. Three samples (416,423 and 426) and Pb concentrations greater than 0.200mg l^{-1}, the highest being 0.660mg l^{-1}. Only one ground water sample, 433, had a high concentration of copper, lead and zinc. High concentrations of base metals in ground water were invariably associated with low pH and in many, but not all cases, with high Fe(II) concentrations.

DISCUSSION

The unreactivity of the chlorite and graphite schists and the contained mineralization (pyrite and uranium oxides) of the Jabiluka deposits toward the present day ground waters is clearly shown by:

1) Near neutral pH's.
2) High Eh values, with little change from sandstone to schist.
3) Low Cl^-, SO_4^{2-} and Si concentrations.
4) Low concentrations of major cations Ca^{2+}, Mg^{2+}, Na^+ and K^+.
5) Generally low concentrations of U, Cu, Pb, Zn and Cd in ground waters near the ore-zone.

It is not known whether the apparent low rate of chemical reactivity (per unit volume ground water) is due to an inherent chemical stability for the schists, the impermeability of the Cahill formation, or is related to the quantity and/or chemical characteristics of ground water at depth. Pump tests carried out by Kilborn-MWP in the vicinity of the Jabiluka Two deposit showed that transmissibility values and flow of water through the fault systems were low, probably because of chloritic healing in many cases. Tests showed no evidence of significant contribution of ground water from the schist ore body (Kilborn, MWP, 1976). Ground waters from drill holes which were tested during our survey were relatively oxidizing. Both uranium contained in oxides and base metals contained in sulphides must be expected to be mobilized by such solutions if contact between ground water and these minerals occurred. Laboratory tests on crushed drill core samples showed that the pyritic graphite schist was reactive to leaching solutions although bacterial catalysed leaching did not readily occur (Pancontinental Mining Limited, 1977). Ore material when equilibrated with acid mine water maintained a pH high enough (pH 4.0-6.4) to prevent bacterial catalysis conditions occurring. Both the impermeability of host rock, and the buffering effect of reactions involving weathering of country rock appear to contribute to the inhibition of *in situ* oxidation of material in the Jabiluka deposits.

Pyrite, chalcopyrite with rare chalcocite and covellite and galena accompany the primary mineralization at Jabiluka One (Rowntree & Mosher, 1975). These sulphide minerals may occur more extensively in the host rocks than does the uranium mineralization. Pyrite occurs in several members of the Cahill Formation, and the graphite schist may contain up to 5% pyrite. The average grade however, is usually much lower than this (Pancontinental Mining Limited, 1977). In the graphite schists tested from near the ore zone, copper concentrations ranged from 30-1000 ppm, lead from 10-50 ppm and zinc from 30-50 ppm. At Jabiluka, the Upper Graphite Schist Series is from 4-20m thick. The chlorite and muscovite schists contain lower concentrations of sulphur, copper, lead and zinc (Pancontinental Mining Limited, 1977). Some oxidation and weathering of schist material has taken place in the vicinity of the Jabiluka One deposit. Rowntree & Mosher (1975) describe the existence of secondary minerals autunite, sklodowskite and saleeite in the zone of oxidation which extends down to a depth of 15m. Our own, and earlier company drilling, indicates the existence of weathered schist over a wide area on the flood plain, including the area near sampling location 223 in the north, the flood plain adjacent to Jabiluka One, and Ja Ja to the south (see Fig. 1).

Ground water analyses from this flood plain area show:

1) Acid pH's.
2) High Fe(II) concentrations.
3) High SO_4^{2-} concentrations.
4) Moderately high concentrations of cations Ca^{2+}, Mg^{2+}, Na^+, K^+.
5) High concentrations of base metals Cu, Cd, Pb and Zn.

These are features commonly associated with the oxidation of sulphides. As indicated by the

balance overall reaction, the weathering of pyrite produces ferric oxide, H^+ and SO_4^{2-}. These products were all observed on the flood plain.

$$4FeS_2 + 15O_2 + 14H_2O = 4Fe(OH)_3 + 8SO_4^{2-} + 16H^+$$
pyrite

Jarosite ($KFe_3(SO_4)_2(OH)_6$), a noted accessory mineral on the flood plain, is an alternative product of oxidation in the presence of potassium ion. Base metals in solution would be derived from oxidation of the sulphides of copper, lead or zinc, for example galena:

$$PbS + 4H_2O \quad Pb^{2+} + 8H^+ + 8e^-$$
galena

Hoag & Webber (1976) consider that the probability of surface oxidation of sulphides without any microbial activity is slight, and that the soil horizon contains necessary nutrients and plant roots for localized acid conditions favouring growth of bacteria. If sulphide mineralization is sparse, water flow rapid, and silicate and carbonate minerals are available to buffer the pH, then the pH remains near neutral and large scale microbial oxidation does not occur. (It is perhaps more correct to suggest that without the catalytic action of microbial activity, the rate of oxidation is very slow.) These statements perhaps suggest why oxidation of sulphides occurs more rapidly in the schists of the Cahill Formation in the vicinity of the flood plain. Here they are subjected to an annual inundation of water, which below ground surface is slow flowing, rich in nutrients and has availability to organic matter for the production of localized acidic conditions which might favour bacterial activity.

The unreactivity of the schists hosting the mineralization beneath the Kombolgie sandstone at Jabiluka One and Two, is probably a contributing factor to the continued existence of such a large tonnage of high grade reducing ore close to the surface. However it also implies that a widespread secondary geochemical halo from such deposits is unlikely and geochemical methods of exploration are limited to close to the ore zone. In areas where there is seasonal inundation and a slow moving ground water system close to surface, some expression of sulphide weathering could be expected. For this to be a useful exploration technique the relationship between sulphide and uranium distributions in host rock needs to be known. The lack of uranium in ground water samples which contain evidence of sulphide oxidation in the present study, suggests that near the Jabiluka deposits, sulphide is more widespread in the schists of the Cahill Formation than is uranium. Although less likely, it is however possible that uranium has already been preferentially leached from much of the oxidizing zone of these units and flushed out of the Magela system by seasonal discharge.

CONCLUSIONS

The shallow aquifer systems in the vicinity of the Jabiluka deposits have been sampled, and the ground waters analyzed for Eh, pH, conductivity, major elements (Ca^{2+}, Mg^{2+}, Na^+, K^+, SO_4^{2-}, Si, Cl^-, HCO_3^- and Fe^{2+}) and trace elements (F^-, Zn, Cd, Pb, Cu and U). In the immediate vicinity of the Jabiluka One and Jabiluka Two deposits, the Eh-pH-conductivity logs and the ground water analyses indicate that there is very little reaction between present-day ground waters and either the schists of the Cahill Formation containing mineralization, or the mineralization itself. Ground waters in the immediate vicinity of the deposits are of low salinity, and near neutral pH. The unreactivity of the schists, and/or their impermeability to ground water in the vicinity of Jabiluka One and Two deposits, is probably a contributing factor to the continued existence of such a large tonnage of high grade reducing ore close to the surface. A widespread secondary geochemical halo from such deposits in such an environment is unlikely.

On the Magela flood plain, where the schists of the Cahill Formation are close to the

surface, and where there is frequent inundation, ground water samples showed low pH's, and high concentrations of sulphate, iron and base metals. This suggests active weathering of sulphides, probably contained in the schists of the Cahill Formation. It is likely that conditions favourable to microbial activity have contributed to the rate of oxidation of sulphides in this zone.

Concentrations of uranium in ground water, both in the immediate vicinity of the deposits, and on the Magela flood plain, were observed to be low. Uranium in ground water is a poor hydrogeochemical indicator of deposits of the Jabiluka type in this particular environmental setting.

ACKNOWLEDGEMENTS

We acknowledge the help and cooperation of Pancontinental Mining Limited, and Dr. E. Bettenay for his helpful discussion and assistance.

REFERENCES

Bendix Field Engineering Corporation, 1977: Symposium on hydrogeochemical and stream-sediment reconnaissance for uranium in the United States. *U.S. Department of Energy, Grand Junction, Colorado.*, 468p.

Beus, A. A. & Grigorian, S. V., 1977: Geochemical Exploration for Mineral Deposits. *Applied Publishing Ltd., Illionis, U.S.A.*, 286p.

Bolviken, B., Logn, O., Breen, A. & Uddu, O., 1972: Geochemical Exploration 1972. *The Institution of Mining and Metallurgy. London*, 415-419.

Brown, E., Skongstad, M. W. & Fishman, M. J., 1970: Techniques of Water Resources Investigations of the United States Geological Survey. *U.S. Government Printing Office, Washington, D.C.*, 160p.

Cameron, E. M., 1978: Hydrogeochemical methods for base metal exploration in the northern Canadian shield. *J. Geochemical Exploration, 10*, 219-243.

Culbert, R. R. & Leighton, D. G., 1978: Uranium in alkaline waters — Okanagan Area, British Colombia. *Bull. Can. Inst. Min. Metall., 71*, 103-110.

Dall'Aglio, M. & Tonani, F., 1972: Geochemical Exploration, 1972. *The Institution of Mining and Metallurgy. London*, 415-419.

Delany, A. C. & Fleischer, R. L., 1978: Increase in uranium in springs draining Rocky Flats, Colorado. *J. Geochemical Exploration, 19*, 53-62.

Denson, N. M., Zeller, H. D. & Stephens, J. G., 1956: Water Sampling as a guide in the search for uranium deposits and its use in evaluating volcanic units as potential source beds for uranium. *Prof. Pap. U.S. geol. Surv., 300*, 673-680.

Doi, K., Hirino, S. & Sakarnaki, Y., 1975: Uranium mineralization by ground water in sedimentary rocks, Japan. *Econ. Geol., 70*, 628-646.

Fix, P. F., 1956: Hydrogeochemical exploration for uranium. *Prof. Pap. U.S. geol Surv., 300*, 667-671.

Florence, T. M., 1972: Determination of trace metals in marine samples by anodic stripping voltammetry. *J. electroanal. Chem., 35*, 237-245.

Garrels, R. M. & Mackenzie, F. T., 1967: Origin of the chemical compositions of some springs and lakes. *in* (ed. R. F. Gould), *Equilibrium concepts in Natural Water Systems*. American Chemical Society, Washington, D.C., 222-242.

Hegge, M., 1971: Geologic setting and relevant exploration features of the Jabiluka uranium deposits. *Proc. Australas. Inst. Min. Metall., 274*, 19-32.

Hoag, R. B. & Webber, G. R., 1976: Significance for mineral exploration of sulphate concentrations in groundwaters. *Bull. Can. Inst. Min. Metall. 69*, 86-91.

Kilborn-MWP., 1976: Jabiluka uranium project hydrological study and cost estimate. *Private report*, 6-9.

Langmuir, D., 1978: Uranium solution-mineral equilibria at low temperatures which applications to sedimentary ore deposits. *Geochim. cosmochim. Acta, 42*(6), 547-569.

Mann, A. W., 1974: Down-hole Eh-pH probe and water sampler. *CSIRO, Division of Mineralogy, Report No. FP. 5*, 14p.

Mann, A. W. & Deutscher, R. L., 1978: Hydrogeochemistry of a calcrete containing aquifer near Lake Way, Western Australia. *J. Hydrol. 38*, 357-377.

Mann, A. W. & Deutscher, R. L., 1978: Genesis principles for the precipitation of carnotite in calcrete drainages in Western Australia. *Econ. Geol., 73*, 1724-1737.

Pancontinental Mining Limited, 1977: *The Jabiluka project draft environmental impact statement*. 179p.

Phoenix, D. A., 1959: Occurrence and chemical character of groundwater in the Morrison formation. *Prof. Pap. U.S. geol. Surv., 320*, 55-64.

Rowntree, J. C. & Mosher, D. V., 1975: Jabiluka uranium deposits. *in* (ed. C. L. Knight), *Economic Geology of Australia and Papua New Guinea. Australas. Inst. Min. Metall., Monograph Series No. 5., I. Metals*, 321-326.

Western Mining Corporation, 1978: *Draft Environmental Impact Statement, Yeelirrie project, Appendix X.*

Zielinski, R. A. & Rosholt, J. N., 1978: *Uranium in waters and aquifer rocks at the Nevada Test Site, Nye County, Nevada. J. Res. U.S. geol. Surv., 6*, 489-498.

URANINITE AND ITS ALTERATION PRODUCTS, KOONGARRA URANIUM DEPOSIT

A.A. Snelling

Department of Geology and Geophysics, University of Sydney, N.S.W., 2006, Australia.
Present Address: C.R.A. Exploration Pty Ltd., P.O. Box 39598, Winnellie, N.T., 5789, Australia.

ABSTRACT

The secondary uranium minerals so far identified at Koongarra occur in a manner, and are distributed in a pattern, which indicate the mode of their formation. In situ replacement of uraninite veins by the uranium-lead oxides curite, fourmarierite and vandendresscheite, and the uranyl silicates kasolite, uranophane and sklodowskite, occurred immediately above the footwall fault breccia, alteration diminishing towards the high grade ore zone beneath the hanging wall graphitic schist unit. The surviving uraninites and uranyl silicates were, in turn, further altered to the uranyl phosphates renardite, dewindtite, saleeite, sabugalite, metatorbernite, and torbernite, during weathering of the host schists. These processes are attributed to the introduction into the primary ore zones from below of surficial groundwaters and to subsequent changes in their Eh and dissolved phosphate concentrations. Lateral groundwater movement in the weathered zone was also responsible for the formation of a secondary dispersion fan over the No. 1 Orebody.

INTRODUCTION

The secondary uranium minerals have for many years been of particular interest to mineral collectors and professional mineralogists because of the wide variety of them, and their display of many brilliant colours. Being usually of economic, rather than scientific, interest, their presence in many uranium deposits has been merely noted. However, the initial in situ oxidation of uraninite to secondary hydrous uranium oxides, some with lead, surrounded by uranium silicates, and the occurrence of secondary phosphates in a dispersion fan, has previously been described. It is summarised by Frondel (1956), and although clearest in pegmatite deposits, it has been also recognised in the Katangan vein deposits, studied extensively by Schoep (1930), and Thoreau & de Terdonck (1935). Garrels & Christ (1959; 1965 and references therein) also studied in detail the mineralogy of the sandstone-type uranium-vanadium deposits of the Colorado Plateau, U.S.A., paying particular attention to physico-chemical conditions of mineral formation and stability. Langmuir (1978) has updated and summarised all the available thermochemical and mineral-solution equilibria data. In Australia the most detailed mineralogical study of secondary uranium minerals is that of Threadgold (1960), who examined some ores of the South Alligator Uranium Field.

This study seeks to trace the paths of formation from uraninites of the secondary uranium minerals found in the Koongarra uranium deposit. Of particular significance is the pattern of distribution of the uranium minerals. A knowledge of present groundwater circulation aided interpretation of this pattern of distribution, which in turn led to an understanding of the processes which have only recently, relative to the suggested age of the deposit, modified the orebodies. No attempt is made to apply the conclusions to any other deposit in the region, since the precise setting of this deposit, which has ultimately given rise to the modification processes, appears to be unique. Furthermore, published details of secondary uranium mineral distribution and groundwater circulation in other Alligator Rivers Province deposits are generally lacking.

THE KOONGARRA DEPOSIT

The Koongarra deposit has been described by Foy & Pedersen (1975), and Pedersen (1978). The uranium mineralization occurs in two distinct orebodies separated by a barren gap. Both orebodies consist of primary zones of partially coalescing lenses containing

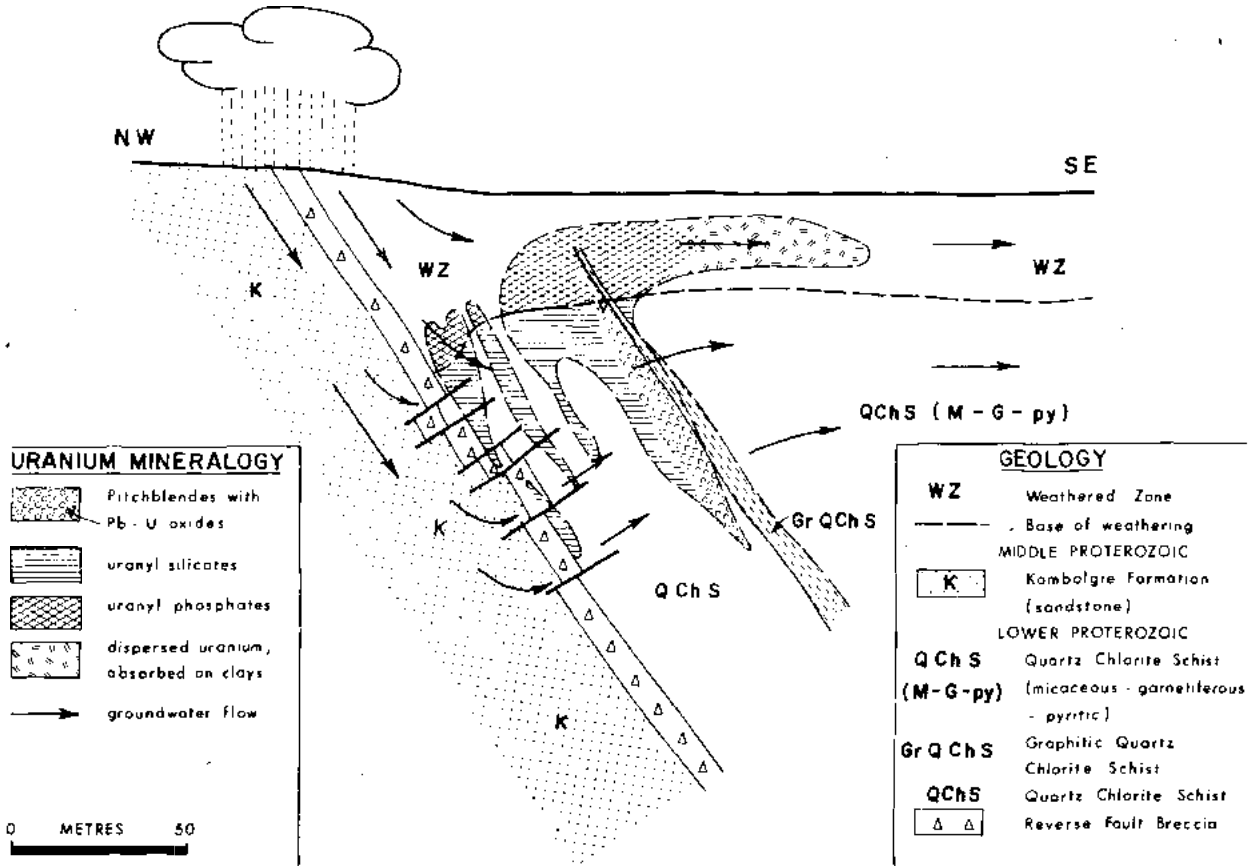


Figure 1. Simplified cross section through the Koongarra No. 1 Orebody. The distribution of the various uranium minerals and the paths of groundwater circulation at the present time are shown schematically.

uraninite veins essentially conformable within steeply dipping quartz-chlorite schists of the lower member, Cahill Formation. The primary deposit therefore is stratabound.

In the No. 1 Orebody, a cross section of which is shown in figure 1, secondary mineralization is present both in weathered schists virtually from the surface to the base of weathering between 25m and 30m down, and in the schists immediately above the footwall fault breccia. The secondary mineralization in the weathered schists forms a tongue-like fan of ore grade material dispersed downslope for about 80m. The primary ore zone averages a true width of 30m at the base of weathering but tapers out at about 100m below surface. The strongest mineralization and highest grades, however, are over a thickness of only several metres stratigraphically just below a thin graphitic quartz-chlorite schist hanging wall unit. Scattered mineralization of varying grades persists down through the schist sequence to the footwall fault breccia, formed by a reverse fault contact with the unconformably overlying Kombolgie Formation sandstone.

In the No. 2 Orebody, 100m to the north-east, the primary ore zone consists of lower grade mineralization over greater widths and persisting to at least 250m below surface. The mineralization also extends stratigraphically above the graphitic schist unit, particularly where this hanging wall unit is less well developed. Since the top of the ore zone is 50m below surface, and thus below the base of weathering, no secondary dispersion fan similar to that above the primary zone of the No. 1 Orebody is present. There is only minor development of secondary mineralization at depth.

THE URANIUM MINERALOGY

1. Primary Mineralization

Uraninites forming the primary ore veins at Koongarra are typical of vein-type and hydrothermal uraninites. Compositionally the uraninites are characterised by their low to negligible contents of thorium and rare earth elements (<0.5%, although McLennan & Taylor, this volume, report that the uraninites are relatively rich in heavy rare earth elements), and by their calcium content, which also divides them into two chemical classes - uraninites with an average CaO content between 1 and 2%, and uraninites whose CaO contents usually reach between 3 and 5%. Lead contents vary considerably both between and within uraninite grains and masses, indicative of partial loss of radiogenic lead resulting in its inhomogeneous distribution within the UO_2 lattice, often as minute galena inclusions. On the other hand, trace to 0.5% amounts of silicon, iron and manganese, like calcium, appear to be homogeneously distributed, suggesting substitution of these elements within the UO_2 lattice.

Hills (1973) showed that the uraninites in each of these two groupings (based on the different uraninite chemistries) have average unit cell dimensions of 5.435Å and 5.404Å, comparable to the median values of 5.437Å and 5.406Å for vein-type and sandstone-type uraninites respectively, as found by Berman (1957). Berman found, however, that values ranged from 5.36Å to 5.50Å for vein-type uraninites, and from 5.35Å to 5.47Å for sandstone-type uraninites.

These two groupings of uraninites are also reflected in uraninite textures. In the first grouping, vein-type uraninites with 1 to 2% CaO occur

1) as thin veinlets, composed of euhedral sub-grains, both parallel to and cross-cutting the schistosity of the host quartz-chlorite schists,
2) as botryoidal masses,
3) as minute spherules (often brecciated) with concentric layering, lacework textures, radial fractures, and infillings of chlorite and chalcedony; and
4) as small disseminated euhedral and sub-euhedral grains.

Uraninites with 3 to 5% CaO content are typically more oxidised supergene uraninites, often with colloform banding, as fracture and cavity infillings, and between quartz gangue

grain boundaries. Their unit cell dimensions and observed textures support the conclusion that they precipitated from low-temperature groundwaters, similar to uraninite precipitation in sandstone-type deposits.

Textural evidence suggests at least two periods of uraninite remobilization (Snelling, 1980). Veins of uraninite euhedra are seen remobilized to varying degrees as massive veinlets. Brecciation of the host quartz-chlorite schists resulted in the schist fragments being cemented together by chlorite and remobilized uraninite veinlets. The remobilized uraninites are compositionally identical to the uraninites from which they were derived. A second period of remobilization corresponds to the precipitation of the supergene uraninites from low temperature groundwaters.

2. Secondary Mineralization

Oxidation and alteration of uraninites has produced a variety of secondary uranium minerals, and those identified to-date are listed, together with their chemical formulae, in table 1. Other species will probably be identified as the deposit is mined.

Oxides	
Curite	$2PbO.\ 5UO_3.\ 4H_2O$[b]
Fourmarierite	$PbO.\ 4UO_3.\ 4H_2O$[d]
Vandendriesscheite	$PbO.\ 7UO_3.\ 12H_2O$[d]
Silicates	
Kasolite	$Pb\ (UO_2)\ SiO_4.\ H_2O$[a]
Sklodowskite-	$(Mg, Ca)\ (UO_2)_2\ Si_2O_7.\ 6H_2O$[b]
Uranophane	$(Ca, Mg)\ (UO_2)_2\ Si_2O_7.\ 6H_2O$[d]
Phosphates	
Saleeite	$Mg\ (UO_2)_2\ (PO_4)_2.\ 8\text{-}10H_2O$[b]
Sabugalite	$HA1\ (UO_2)_4\ (PO_4)_4.\ 16H_2O$[d]
Metatorbernite-	$Cu\ (UO_2)_2\ (PO_4)_2.\ 8H_2O$[b]
Torbernite	$Cu\ (UO_2)_2\ (PO_4)_2.\ 8\text{-}12H_2O$[d]
Renardite-	$Pb\ (UO_2)_4\ (PO_4)_2\ (OH)_4.\ 7H_2O$[b]
Dewindtite	$Pb\ (UO_2)_2\ (PO_4)_2.\ 3H_2O$[d]
Sulphate	
Johannite	$Cu\ (UO_2)_2\ (SO_4)_2.\ 6H_2O$[c]
Vanadate	
Carnotite- Tyuyamunite	$K_2(UO_2)_2\ (VO_4)_2.\ 3H_2O$[a] $Ca\ (UO_2)_2\ (VO_4)_2.\ 5\text{-}8H_2O$[a]

Mineral formulae are after Morton (1978). Identification reported by Tucker (1975)[a], Foy & Pedersen (1975)[b], Gasparrini (1978)[c] and Snelling (1980)[d]

Table 1. Secondary uranium minerals at Koongarra.

Whole uraninite veins, sometimes large veins over 1 cm wide, were altered in situ. Various stages of the process are observed. In one notable case, a large uraninite vein is concentrically sheathed outwards by uranium-lead oxides - vandendriesscheite, fourmarierite and then curite; and finally the uranyl silicate sklodowskite. Other veins are partially or totally replaced by intergrown uranyl silicates - kasolite and sklodowskite (Fig. 2A), kasolite and uranophane (Fig. 2B), or kasolite, sklodowskite and uranophane. In most cases the physical positions and shapes of the replaced uraninite veins, even the euhedra, are preserved (Fig. 2B). Thus the in situ replacement process involved the introduction (to the uraninite) of magnesium, silicon and water, and possibly some calcium, the redistribution within the vein shapes of uranium, lead and calcium, and/or the removal of uranium. Similarly, botryoidal masses of uraninite may also be partially or totally replaced, like the mass shown in figure 2C which is rimmed by sklodowskite.

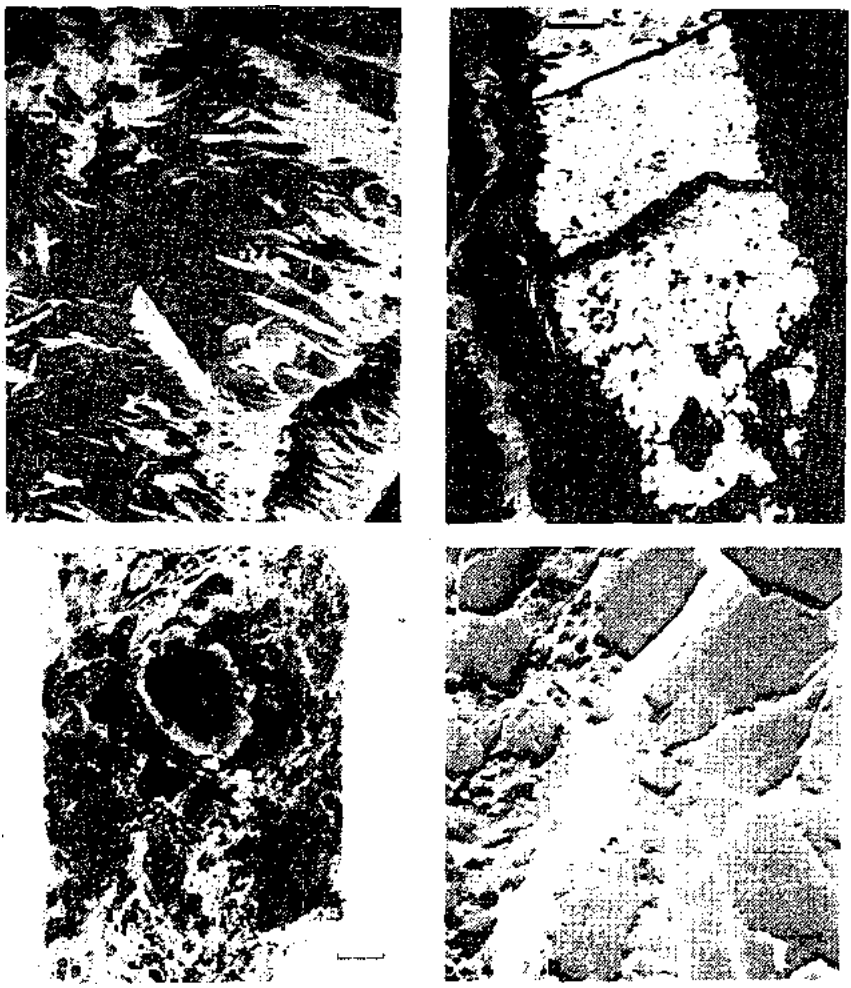


Figure 2. a) A uraninite vein replaced by an intergrowth of kasolite and sklodowskite. Back scattered electron image showing kasolite (white) and sklodowskite (grey). (Scale bar = 50μ).
b) A uraninite vein replaced by kasolite and uranophane. Note that the vein shape, including original euhedra, has been perfectly preserved. (Back scattered electron image; Scale bar = 50μ).
c) Globular botryoidal uraninite mass (just above centre) being altered to sklodowskite (lighter concentric sheath). (Scale bar = 3mm).
d) Uranophane veinlets deposited between quartz grain boundaires. (Back scattered electron image; Scale bar = 50μ)

Uranophane and sklodowskite are also found as veins and stringers within fractures, between grain boundaries and within cleavage planes of chlorites, the major gangue minerals, without either being accompanied by, or replacing, uraninite (Figs. 2D and 3A). Within fractures sklodowskite has crystallised as aggregates of radiating acicular crystals, with chlorite as the infilling matrix (Fig. 3B).

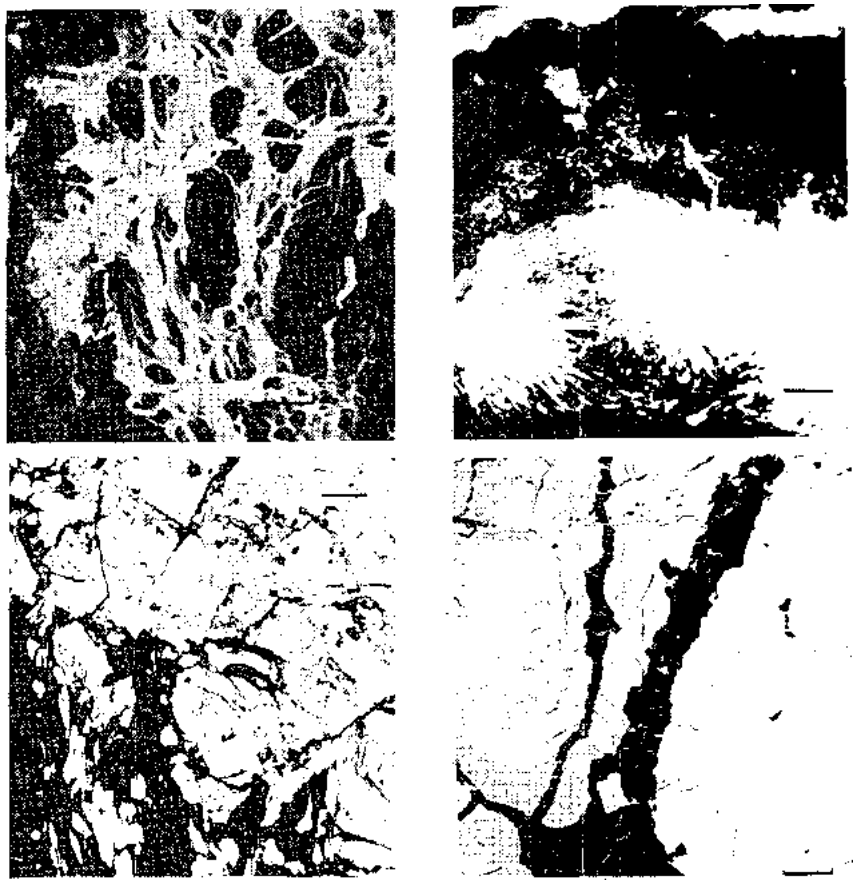


Figure 3. a) Sklodowskite veinlets deposited between chlorite grain boundaries and partly replacing chlorite. (Back scattered electron image; Scale bar = 50μ).
b) A sklodowskite vein composed of radiating aggregates of acicular crystals infilled by a chlorite matrix. (Back scattered electron image; Scale bar = 50μ)
c) Chlorite (black) replacing uraninite (white) along numerous fractures and spots. Fragments of uraninite have also become isolated within massive chlorite away from the uraninite vein. (Reflected light, oil immersion; Scale bar = 100μ).
d) Chemical alteration associated with chlorite veining of uraninite. Back scattered electron image showing chlorite (black) veining uraninite (white) and producing adjacent altered uraninite-sklodowskite (grey). (Scale bar = 50μ).

Gasparrini (1978) reported finding small grains of johannite attached to chalcocite and covellite near uraninite veins, indicating migration of uranyl ions during supergene enrichment of chalcopyrite.

The uranyl phosphates (Table 1) are found exclusively in the tail of the secondary dispersion fan in the weathered schists above the primary ore zone of the No. 1 Orebody (Fig. 1). They occur as veins, stringers, euhedral grains, intergrowths and rosettes amongst the clays-micas-quartz mixtures of the weathered schists. A lone occurrence of uranyl vanadates (carnotite-tyuyamunite) also from the weathered zone is reported by Tucker (1975).

THE FORMATION OF THE SECONDARY URANIUM MINERALS

The onset of in situ oxidation and hydration of uraninites is marked by contemporaneous growth of new chlorites, the last of at least three periods of chlorite growth. This conclusion is based on chlorite textures and compositions, the chlorites forming contemporaneously with the secondary uranium minerals (particularly sklodowskite) being magnesium and silicon-rich talc-chlorites and penninites (Snelling, 1980). This latest growth of new chlorites also coincided with minor uraninite brecciation and remobilization which gives the impression that chlorite is physically attacking and breaking down the uraninites, sometimes replacing them (Fig. 3C). Chlorite is also observed infilling the fractures between the euhedra of uraninite veins.

Oxidation of uraninites along grain and fracture boundaries adjacent to chlorite is noted by a darker reflectance for the altered uraninite. Such alteration is characterised chemically by the addition of magnesium and silicon, as seen in figure 3D which shows sklodowskite in the process of formation between a chlorite vein and uraninite. Elements such as magnesium and silicon were introduced by the same fluids responsible for the growth of new chlorites, chlorites which are themselves magnesium and silicon-rich penninites and talc-chlorites (Snelling, 1980). Circulating low-temperature groundwaters would be capable of producing these results. Continued introduction of such magnesium- and silicon-bearing aqueous fluids would have thus produced both chlorites and uranyl silicate replacement of uraninites.

A combined electron microprobe-scanning electron microscope study of these alteration processes and the secondary uranium minerals produced, reveals that redistribution of magnesium, calcium, silicon, lead and uranium is incomplete. Several series of gradational chemical compositions exist between various species, including some intermediate compositions which may represent distinct, as yet unnamed, species. For instance, in the example already cited where a uraninite vein is sheathed by vandendresscheite, fourmarierite, curite and finally sklodowskite, an analytical traverse from uraninite to sklodowskite shows a steady substitution and redistribution of elements, with species being gradational into one another, particularly the uranium-lead oxides. This suggests that the alteration process is recent, relative to the suggested age of the primary uraninites, and slow, since the uraninites are not all yet completely replaced and/or destroyed, as well as confirming the in situ replacement nature of the alteration process.

Lead was particularly immobile during uraninite alteration, often being retained in kasolite, or partly accommodated in both the uranophane and sklodowskite crystal lattices, substituting for calcium and magnesium respectively.

Gorman & Nuffield (1955) concluded that uranophane and sklodowskite are isostructural, and therefore suggested that the two minerals should be found as end-members of an isomorphous substitution series, the calcium and magnesium cations being structurally interchangeable. Several clear examples of a uranophane-sklodowskite series are found at Koongarra (Snelling, 1980). Iron, with an ionic radius between that of calcium and magnesium, would also be expected to substitute into the uranophane and sklodowskite lattices in place of calcium and magnesium respectively, which it does. However, iron substitution may not go anywhere near to completion, since an iron uranyl silicate end-member has so far not been observed in nature.

In contrast to the uranyl silicates, the uranyl phosphates do not appear to be able to accommodate cationic isomorphous substitution between isostructural end-members, except in the case of the lead uranyl phosphates, where the lead and uranium concentrations change continuously between species, for example, renardite and dewindtite. There is, however, limited substitution between the anions SiO_3^{2-}, AsO_4^{3-} and the PO_4^{3-} in the uranyl phosphates' lattices. A good example is the anionic substitution between sklodowskite and salecite. The presence of the uranyl phosphates only in the weathered zone suggests that they form during

normal surficial weathering of primary ore zone uraninites and associated uranyl silicates. Scattered trace apatites amongst the schists have obviously been weathered at the same time, releasing PO_4^{3-} ions for uranyl phosphate formation.

THE DISTRIBUTION OF THE SECONDARY URANIUM MINERALS

Compilation of the data by plotting on an orebody section the relative positions of all the samples studied, together with their contained secondary uranium minerals, clearly confirms that the uranyl silicates plus the lone uranyl sulphate are found at depth within the primary ore zones of both orebodies, whereas all the uranyl phosphates are found in the tail of the secondary dispersion fan above the No. 1 Orebody (Fig. 1). This medium grade, phosphate-containing tail is now known to be a zone of weathered and leached primary ore (Carson, 1978), and thus formerly an upward extension of the primary ore zone. Away from the tail of the fan, uranium ore grades are progressively lower with uranium dispersed in the weathered schists and adsorbed onto clays towards the leading edge.

This clear division between the observed distribution of uranyl silicates at depth and uranyl phosphates in the weathered zone above, the base of weathering being the dividing line, is clearly significant and points to differing conditions of genesis which require clarification.

Langmuir (1978) compiled and revised thermochemical data for many uranium minerals and uranyl complexes, and studied uranium solution-mineral equilibria at low temperatures. He found that silica forms a relatively weak complex which is more important than uranyl-hydroxy complexes in groundwaters with a pH of around 6 (see Fig. 8 of Langmuir, 1978). It is thus significant that groundwater studies at Koongarra reported by Australian Groundwater Consultants Pty. Ltd. and McMahon *et al.* (1978) showed that the groundwaters at depth within the primary ore zones have a pH between 6 and 6.5, exactly the pH required to maximise the presence and activity of the uranyl silicate complex in groundwaters. Therefore present circulating groundwaters of the measured pH would be capable of producing uranyl silicates from uraninites at depth within both orebodies, the insolubilities of the solid phases relative to ionic and ionic complex concentrations in solution, however, being crucial.

Furthermore Langmuir (1978) also found that because the uranyl silicate complex is relatively weak, the presence of uranyl phosphate complexes, which are stronger complexes, will produce uranyl phosphates rather than uranyl silicates at the same pH (see Fig. 9 of Langmuir, 1978). Thus very high silica and very low total phosphate concentrations in the groundwaters were necessary to precipitate silicates rather than phosphates, although the insolubilities of the solid phases relative to ionic and ionic complex concentrations in solution would again have been crucial. With the weathering of apatite, a common accessory mineral in the host schists, the resulting higher total phosphate concentration in the groundwaters flowing through the weathered schists would therefore favour the precipitation of uranyl phosphates. That the uranyl phosphates were in fact formed from uranium derived from pre-existing uranyl silicates, as well as from uraninites, by the interchange of anions can be inferred from a single sample from the weathered zone in which kasolite is being replaced by renardite. Thus the paths of secondary uranium mineral formation can be summarised as in figure 4.

Since the pH of the groundwaters is the same in both the primary ore zones and the weathered schists above, the other important factor which must have been different between these two horizons, besides the different total phosphate concentrations, was the Eh. Garrels & Christ (1959, 1965) have shown that a slight difference in Eh exists between the conditions for formation of uranyl silicates and uranyl phosphates, the latter favouring the slightly higher oxidation potential of more oxidising conditions. The presence of carnotite-tyuyamunite with

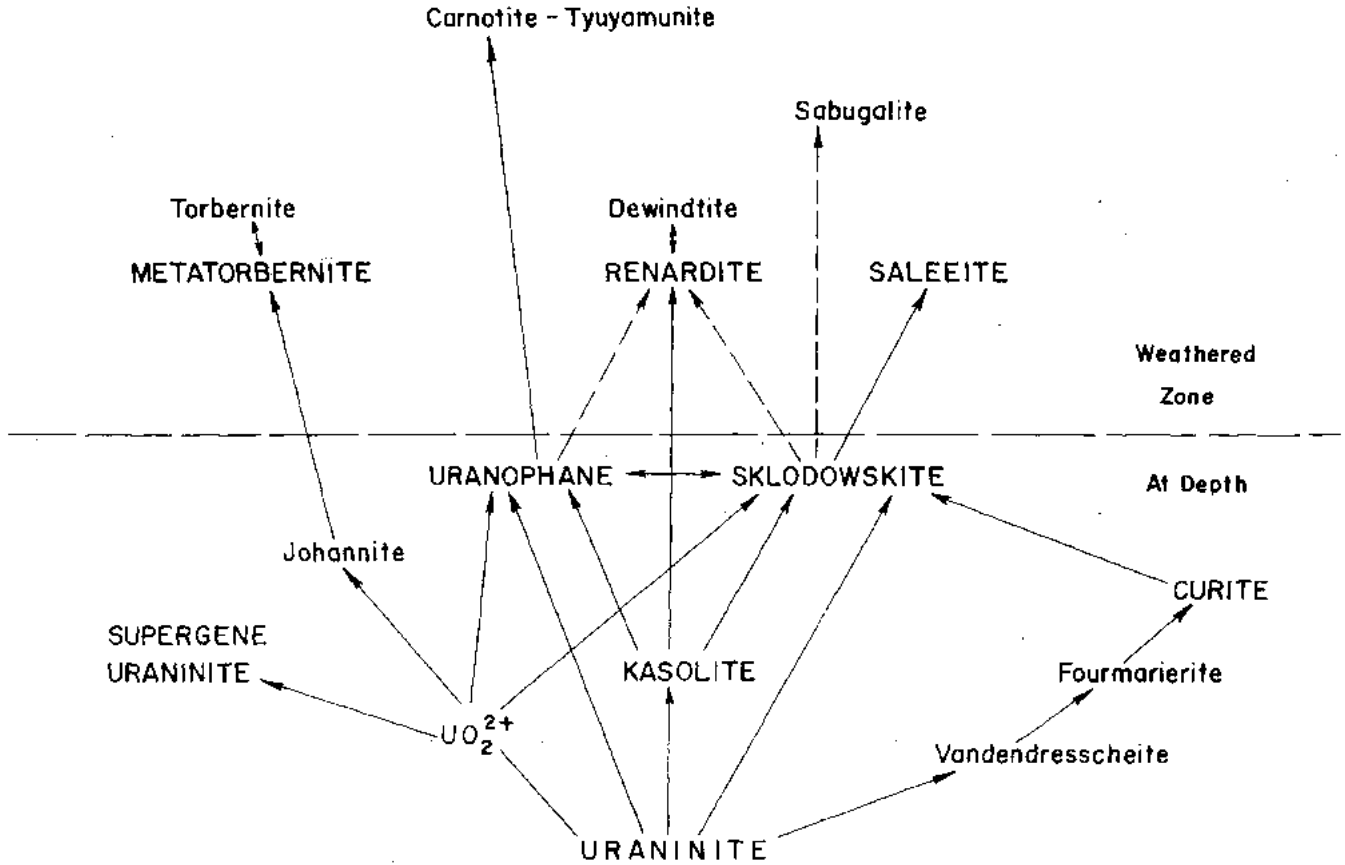


Figure 4. Diagram showing schematically the proposed paths of secondary uranium mineral formation from uraninite.

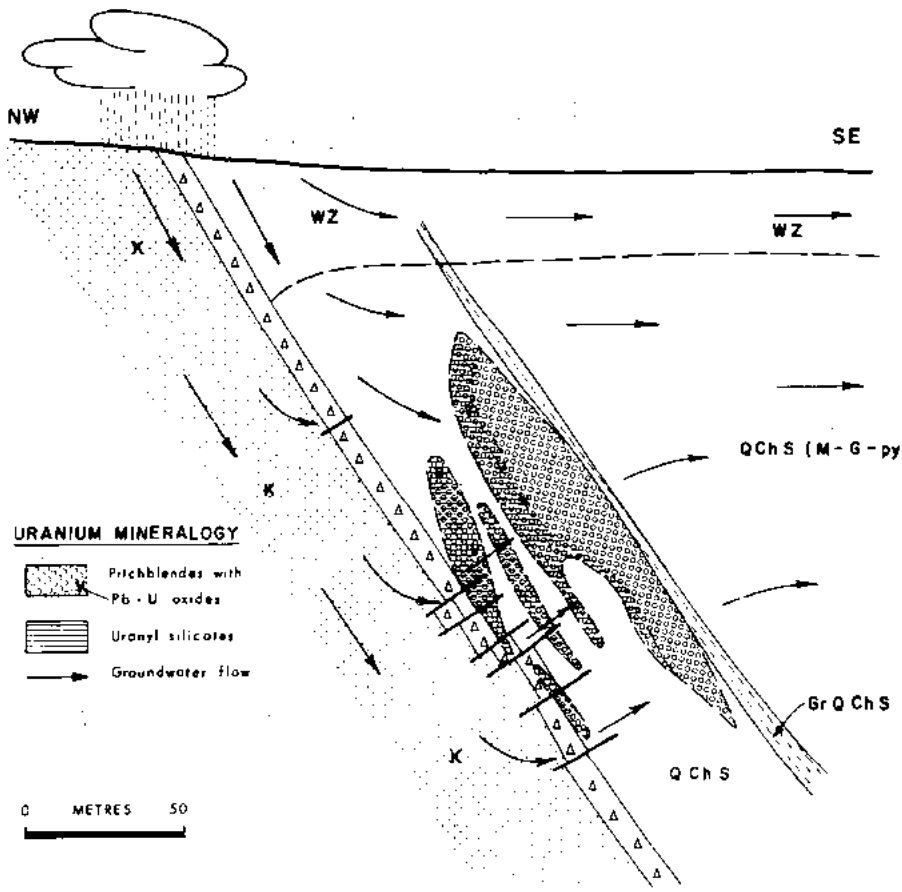


Figure 5. Schematic presentation of distribution and formation of secondary uranium minerals in the No. 1 Orebody, indicating the paths of groundwater circulation responsible after removal of cover rocks sufficient to initiate oxidising groundwater penetration to depth. Note the suggested original tabular shape of the orebody, the top of which is now dispersed as a secondary dispersion fan.

uranyl phosphates in the weathered zone supports the conclusion that the zone is highly oxidised, since carnotite is only stable at high Eh (Langmuir, 1978).

Uraninite on the other hand is still stable in slightly oxidising conditions (Langmuir, 1978), so conditions at depth would not need to be highly reducing for uraninite to still be stable, particularly in view of the fact that much of the uraninite is in the process of being replaced by uranyl silicates. Dickson & Snelling (this volume) have shown, however, that radium is mobile in the groundwaters at depth, and since radium is only transported under reducing and sulphate-free conditions, the Eh below the weathered zone must be on the reducing side of neutral. Thus, as Dickson & Snelling (this volume) also found, the transition zone at the base of weathering is an oxidation-reduction interface between circulating groundwaters of differing chemistry.

The circulation of groundwaters at Koongarra has been studied by Australian Groundwater Consultants Pty Ltd and McMahon, *et al.* (1978). Their conclusions are shown

schematically in figure 1. Recharge of groundwaters to the unweathered Cahill schists occurs via downflow parallel to, and in close proximity to, the reverse fault in both the underlying Kombolgie sandstone and the schists. Although the fault zone breccia was found to be almost impermeable, some water flows from the Kombolgie sandstone into the schists via cross fractures which offset the fault. Once in the schists groundwater flow is towards the south-east, away from the Mount Brockman escarpment. The weathered zone essentially acts as an aquitard or capping which largely prevents percolation downwards of surficial waters. Nevertheless there is a separate flow of surficial groundwaters within the weathered zone, again flowing downslope towards the south-east away from the Mount Brockman escarpment. Their tritium dating of waters from below the weathered zone indicates that flow is very slow.

Dickson & Snelling (this volume) found that this circulation of groundwaters explained observed movements of uranium and daughter isotopes (in particular, radium) within the deposit. The same described pattern of groundwater circulation similarly explains the observed distribution of uranium minerals. Furthermore, as figure 5 attempts to show, the original shape of the No. 1 Orebody can be reconstructed by removing the modifications caused by groundwaters altering the uraninites and transporting uranium.

The No. 2 Orebody, as it is at present, resembles the No. 1 Orebody prior to formation of the secondary dispersion fan. The recharge parallel to, in proximity to, and across the reverse fault has brought oxidising groundwaters into the quartz-chlorite schists below the orebodies, so that uraninites closest to the reverse fault were first to be altered to uranyl silicates (Fig. 5). During passage through the orebodies the Eh of the groundwaters would tend to decrease, being reduced by reaction with the uranium minerals in the rocks. Thus uraninites of the high grade zone just below the graphitic hanging wall which are furtherest from the reverse fault remain unaltered. With time erosion has removed the cover sufficiently to expose the top of the No. 1 Orebody to weathering and surficial groundwaters (Fig. 1), which have destroyed the remaining uraninites and altered the earlier-formed uranyl silicates to uranyl phosphates. Lateral groundwater movement in the weathered zone then dispersed uranium downslope to form the secondary dispersion fan.

Several other features may be accounted for by these groundwater movements. The schists immediately above the reverse fault, and the fault breccia itself, are pervasively hematised, but this alteration is less pronounced higher in the ore zone. Hematitic alteration consequently decreased upwards, but supergene uraninites were increasingly deposited. This latter process, essentially a minor remobilization of uranium, may possibly have been responsible for further upgrading the ore immediately below the graphitic hanging wall schist.

Finally, this model for the previous shape of the No. 1 Orebody implies that the present land surface at Koongarra does not approximate the Middle Proterozoic unconformity surface, since up to 50m or more of schist have been removed to expose the orebody to weathering and surficial groundwater flow.

CONCLUSIONS

The secondary uranium minerals have formed from uraninites during modification of the deposit by circulating groundwaters in the following manner and order:

1) Circulating low temperature groundwaters produced new chlorite growth and brought oxidising and hydrating conditions to the uraninites of the primary ore veins, producing in situ alteration of uraninites to uranium-lead hydrous oxides and uranyl silicates, and the migration and redeposition of uranium as supergene uraninites and uranyl silicates in a low pressure environment, probably after the earliest removal of cover rocks. This represents the present state of the No. 2 Orebody.
2) After further erosion more oxidising surficial weathering intersected the top of the No. 1 Orebody, and with the availability of phosphorus from the weathering of

apatites, produced prolific uranyl phosphates from the weathered and leached former uraninites and uranyl silicates.

3) Simultaneous lateral groundwater movement in the weathered zone began dispersing uranium downslope to eventually form the prominent secondary dispersion fan above the No. 1 Orebody.

ACKNOWLEDGEMENTS

I am grateful to Noranda Australia Limited who made samples available for this study, and in particular, to Company Geologist Chris Pedersen for his help and comments. This work was undertaken while a recipient of a Commonwealth Postgraduate Research Award at the University of Sydney, where help and advice was received from Drs D.A.F. Hendry and K.L. Williams. The University's Electron Microscope Unit made available its electron microprobe and the assistance of Ken Moran with the equipment is acknowledged.

REFERENCES

Australian Groundwater Consultants Pty Ltd. and McMahon, Burgess & Yeates. 1978: Report on investigation of groundwater and the design of water management and tailings retention system for the Koongarra project. *Koongarra Project: Draft Environmental Impact Statement, Noranda Australia Ltd, Melbourne, Appendix XI.*

Berman, R.M., 1957: The role of lead and excess oxygen in uraninite. *Am. Miner.*, 42, 705-731.

Carson, D.J.T., 1978: Contents of deleterious elements in the ore and waste zones of the Koongarra deposit, Australia *Koongarra Project: Draft Environmental Impact Statement, Noranda Australia Ltd, Melbourne, Appendix VI.*

Dickson, B.L., & Snelling, A.A., this volume: Movement of uranium and daughter isotopes in the Koongarra uranium deposit. *Proceedings of the International Uranium Symposium on the Pine Creek Geosyncline.*

Foy, M.F. & Pedersen, C.P., 1975: Koongarra uranium deposit. *in* (ed. C.L. Knight) *Economic Geology of Australia and Papua New Guinea, Australas. Inst. Min. Metall. Monograph Series No. 5, 1. Metals*, 317-321.

Frondel, C., 1956: Mineral composition of gummite. *Am. Miner., 41*, 539-568.

Garrels, R.M., & Christ, C.L., 1959: Behaviour of uranium minerals during oxidation. *in* (eds. R.M. Garrels & E.S. Larsen) *Geochemistry and Mineralogy of the Colorado Plateau Uranium Ores, Prof. Pap. U.S. geol. Surv.*, 320, 81-89.

Garrels, R.M., & Christ, C.L., 1965: *Solutions, Minerals and Equilibria* (Freeman Cooper, San Francisco).

Gasparrini, C., 1978: Mineralogical and chemical study of 35 samples from a uranium deposit in Australia. *Koongarra Project: Draft Environmental Impact Statement, Noranda Australia Ltd, Melbourne, Appendix VII.*

Gorman, D.H., & Nuffield, E.W., 1955. Studies of radioactive compounds; VIII — uranophane and beta-uranophane. *Am. Miner., 40*, 634-645.

Hills, J.H., 1973: Lead isotopes and the regional geochemistry of North Australian uranium deposits. *Ph. D. thesis, Macquarie University* (unpubl.).

Langmuir, D., 1978: Uranium solution-mineral equilibria at low temperatures with applications to sedimentary ore deposits. *Geochim. cosmochim. Acta., 42*, 547-569.

McLennan, S.M., & Taylor, S.R., this volume: Rare earth elements in fine-grained sedimentary rocks and ores from the Pine Creek Geosyncline. *Proceedings of the International Uranium Symposium on the Pine Creek Geosyncline.*

Morton, R.D., 1978: The identification of uraniferous minerals. *in* (ed. M.M. Kimberley) *Short Course in Uranium Deposits: Their Mineralogy and Origin. Mineralogical Association of Canada*, 141-183.

Pedersen, C.P., 1978: The geology of the Koongarra deposits including investigations of contained elements. *Koongarra Project: Draft Environmental Impact Statement, Noranda Australia Ltd, Melbourne, Appendix V.*

Schoep, A., 1930: Les mineraux du gîte uranifère du Katanga. *Annls Mus. r. Congo belge Ser. 8vo, ser. 1., part 2.*

Snelling, A.A., 1980: A geochemical study of the Koongarra uranium deposit, Northern Territory, Australia. *Ph.D. thesis, University of Sydney*, (in prep.).

Threadgold, I.M. 1960: The mineral composition of some uranium ores from the South Alligator River area, Northern Territory. *C.S.I.R.O. Mineragraphic Investigations Technical Paper No. 2.*

Thoreau, J., & de Terdonck, R., 1935: Concentrations uranifères du Katanga. *XIVth Int. geol. Congr., Algers.*

Tucker, D.C. 1975: Wall rock alteration at the Koongarra uranium deposit N.T. *M.Sc. thesis, James Cook University of North Queensland*, (unpubl.).

MOVEMENTS OF URANIUM AND DAUGHTER ISOTOPES IN THE KOONGARRA URANIUM DEPOSIT

B.L. Dickson[1] and A.A. Snelling[2]

1. CSIRO Division of Mineral Physics, P.O. Box 136, North Ryde, NSW, 2113, Australia
2. Department of Geology and Geophysics, University of Sydney, Sydney, NSW, 2006, Australia.

ABSTRACT

Radiometric disequilibrium has been found to occur in the Koongarra uranium deposit among host rocks and in a dispersion fan of weathered ore. High resolution gamma-ray spectroscopy was used to determine which daughter isotopes of uranium have been mobilized by measuring ^{230}Th, ^{227}Th, ^{226}Ra, ^{214}Pb and ^{210}Pb. Uranium was found to have moved slowly in the dispersion fan of uranium in the weathered zone above the main orebody whereas radium was mobilized in the deeper main orebodies. Radium deposition in the transition zone between the two ore zones was also found, indicating upward flow of groundwaters.

INTRODUCTION

The Koongarra uranium deposit contains steeply dipping pitchblende veins covered by a 30m deep layer of weathered ore. In an earlier study of the state of radiometric disequilibrium (which is the degree to which the gamma radiation emitted by the ore is representative of the uranium content) within the Koongarra deposit, a great variety of disequilibrium ratios was found throughout the weathered zone and the host wall rocks (Snelling & Dickson, 1979). The primary ore is however at, or close to, equilibrium.

The decay series of ^{238}U (excluding some short lived isotopes) is

$$^{238}\text{U} \xrightarrow{4.5 \times 10^9 \text{y}} {}^{234}\text{U} \xrightarrow{2.5 \times 10^5 \text{y}} {}^{230}\text{Th} \xrightarrow{8 \times 10^4 \text{y}} {}^{226}\text{Ra} \xrightarrow{1620 \text{y}} {}^{222}\text{Rn} \xrightarrow{3.8 \text{d}} {}^{214}\text{Pb} \xrightarrow{27 \text{m}} {}^{210}\text{Pb} \xrightarrow{20 \text{y}} {}^{206}\text{Pb}\ (\text{stable})$$

When secular equilibrium is reached after some 10^6 years, the activity of each isotope, except ^{206}Pb, in the decay series is equal. Disequilibrium can occur as a result of the different chemical and physical properties of uranium and its long-lived daughter isotopes, ^{230}Th and ^{226}Ra, and as a result of changes in the chemical environment of the sample with time. The types of disequilibrium that can occur and case studies on the use of disequilibrium in uranium exploration have been reviewed by Hambleton-Jones (1978) and Levinson & Coetzee (1978).

With the sealed can method (Scott & Dodd, 1960) used in the previous study, the activity ratio ^{238}U/^{226}Ra is measured approximately, but ratios cannot be determined for the other long-lived isotopes. Recent advances in high-purity germanium detector technology enable the measurement of high resolution gamma-ray spectra in the energy region of 30-300 keV, allowing accurate measurements to be made of many of the isotopes in the uranium decay series which emit gamma-rays in this region. A typical spectrum of a uranium ore in equilibrium is shown in figure 1. A number of investigations have been reported using this technique as it allows disequilibrium to be studied more easily than by traditional radiochemical methods (Ostrinhansky, 1976; Moxham & Tanner, 1977; Szoghy & Kish, 1978). The isotopes and photopeaks of particular interest in this study are listed in table 1. A more extensive tabulation of the various photopeaks emitted by uranium daughter isotopes is given by Szoghy & Kish (1978) and the method is discussed by Moxham & Tanner (1977) and Ostrinhansky (1976).

THE KOONGARRA DEPOSIT

The Koongarra deposit, described by Foy & Pedersen (1976), consists of two separate orebodies, one of which is shown in cross section in figure 2. Both orebodies contain primary

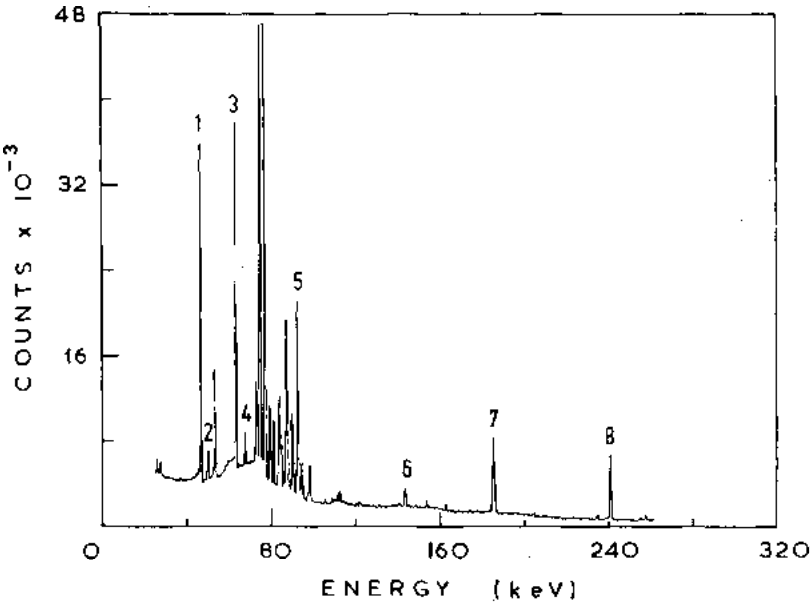


Figure 1. Gamma-ray spectrum of the standard uranium ore NBL-42-4. Numbered peaks are detailed in table 1.

Number in Fig. 1	Isotope	$t_{1/2}$ [a]	Energy[a] (keV)	Relative intensity[b]	Information
1	^{210}Pb	20y	46.5	114	Average of radon retention over 100 years
2	^{227}Th	18d	50.1	13	Occurs in decay ^{235}U after ^{231}Pa
3	^{234}Th	24d	63.3	100	In equilibrium with ^{238}U
4	^{230}Th	8×10^{4}y	67.8	11	Long-lived isotope, relatively immobile
5	^{234}Th	24d	92.3,92.8	105	In equilibrium with ^{238}U
6	^{235}U	7.1×10^{8}y	143.8	7	Measures ^{235}U
7	^{226}Ra	1620y	186.1[c]	21	Can be leached in groundwaters
8	^{214}Pb	27m	241.9	22	Measures ^{222}Rn in sealed sample

[a] Half-life data from Lederer and Shirley (1978)

[b] Relative to ^{234}Th at 63.3 keV for detector system used, corrected for sample absorption effects

[c] Requires subtraction of unresolved contribution from ^{235}U at 185.7 keV

Table 1. Useful photopeaks from isotopes in the uranium decay chain.

zones of pitchblende veins conformable with steeply dipping Lower Proterozoic Cahill Formation quartz-chlorite schists and wedging out with depth at about 100m from the surface. In addition, a 100m long dispersion fan of secondary uranium mineralization occurs in the 30m thick zone of weathered rock above the No 1 Orebody. The strongest mineralization is present in the primary zones stratigraphically just below a graphitic quartz-chlorite schist hanging wall unit. Mineralization of varying grade occurs down the schist sequence to a footwall fault breccia, formed by a reverse fault contact with the unconformably overlying Kombolgie quartz sandstone. The No 2 Orebody, 100m to the north and at greater depth, contains lower grade mineralization, which extends above the graphitic quartz-chlorite schist unit, but is not intersected by the zone of weathering.

Within both primary zones, oxidation and alteration of pitchblendes have taken place *in situ* producing secondary uranium minerals, principally uranyl silicates, as sheaths around, or as total replacement of, pitchblende veins and as thin veins in fractures (Snelling, in prep.). At the base of weathering above the primary ore zone of the No 1 Orebody, there is a strong development of secondary uranium minerals. Dispersion of uranium downslope by moving groundwaters has produced the secondary dispersion fan (Fig. 2). Uranyl phosphates predominate over the uranyl silicates in the higher grade NW tail of the fan, whereas towards the SE leading edge uranium is locked into uranium-rich clays.

In the previous study (Snelling & Dickson, 1979), samples from the No 1 Orebody dispersion fan were found to have a significant trend of increasing disequilibrium ratios in the direction of groundwater flow, indicating movement of uranium in these waters. No conclusive evidence was found for movement of uranium from depth to the dispersion fan so

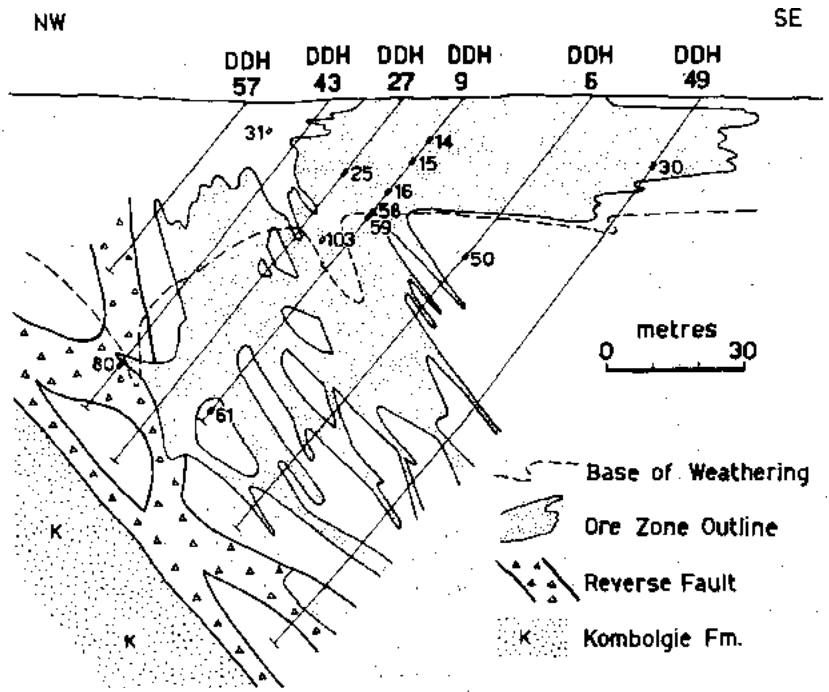


Figure 2. Cross section of Koongarra No 1 Orebody, showing location of samples.

Sample number	U_3O_8 (ppm)	$^{238}U/^{230}Th$	$^{238}U/^{227}Th$	$^{238}U/^{226}Ra$	$^{238}U/^{214}Pb$	$^{238}U/^{210}Pb$	$\frac{U_3O_8}{eU_3O_8}$ [a]	Disequilibrium summary [b]
Estimated error	2%	6%	6%	6%	5%	4%	3%	
No 1 Orebody - weathered zone								
14	1080	0.82 0.92	1.02 1.04	1.01 0.98	0.95 0.93	0.89 0.89	0.91	Th=Ra>U
15	1980	0.90 0.81	0.86 0.88	0.84 0.79	0.98	0.77 0.79	0.82	Th=Ra>U
16	1300	0.78 0.67	0.86 0.80	0.79 0.82	0.98 0.71	0.70 0.67	0.72	Th=Ra>U
25	20800	1.00 1.07	1.04 1.06	0.86 0.89	1.06 1.04	1.07 1.06	1.04	U>Th=Ra
30	930	1.08	0.95	0.93	1.13	1.05	1.11	U>Th=Ra
31	710	0.77	0.87	0.74	0.75	0.69	0.71	Th=Ra>U
No 1 Orebody - transitional zone								
58	210	1.21	1.3	0.38	0.38	0.38	0.27	Ra>U>Th
59	1300	0.60 0.87	0.98 0.96	0.98 0.91	0.88	0.88 0.87	0.92	Th=Ra>U
No.1 Orebody - fractured zones								
80	200	0.86	0.93	1.33	1.35	1.11	1.18	Th>U>Ra
103	6750	0.90	0.90	0.82	0.82	0.76	0.87	Th=Ra>U
No 1 Orebody - host wall rocks								
50	180	0.98	0.96	0.78	0.78	0.72	0.66	Ra>U>Th
61	250	0.88	0.88	0.78	1.03	0.95	0.86	Ra=Th>U
No 2 Orebody								
122	13600	1.04	1.08	0.67	0.75	0.73	0.72	Ra>U>Th

[a] Gamma equivalent uranium by sealed can method

[b] This column summarises the relative equilibrium between ^{238}U, ^{230}Th and ^{226}Ra or its decay daughters, ^{214}Pb and ^{210}Pb. Symbol = represents equilibrium whereas symbol > implies enrichment.

Table 2. Analyses and measured activity ratios for samples from the Koongarra samples.

that the fan is probably a result of weathering processes on a previous upward extension of the primary pitchblende veins. Some redistribution of daughter isotopes was concluded to have occurred at depth as the low grade host wall rocks gave low ratios, though the primary ore was near or at equilibrium.

Samples for this study were chosen from the sample set of the previous study to represent the observed disequilibrium pattern. They were mainly from within the dispersion fan and from the zone between the weathered and primary ore. Since the activity ratios of the low grade host wall rocks are difficult to measure because of low counting rates, only two samples were studied. The samples chosen are listed in table 2 and their locations are shown in figure 2. Sample 122 from the ore zone of the No 2 Orebody is not shown, but was of interest as it is a sample from depth which is very uranium poor (relative to radium).

EQUIPMENT AND TECHNIQUE

Samples were prepared by mixing 50g of ore with 5g of borax powder and pressing into 4.0cm diameter, 2.54cm long nylon cylinders under approximately 5 tonnes pressure. The containers were sealed with nylon discs (3mm thick) using nylon cement and then stored to allow radon regrowth.

The instrument used for this study was a high purity germanium detector with an area of 100mm^2 and a 10mm thickness. Conventional electronics were used in conjunction with a 1024 channel pulse-height analyser to record the spectra and correct for dead-time and pulse pileup effects. The system gain was 4.2 channels per keV and spectra were accumulated for about 6 h per 1% uranium in the sample.

Photopeak areas were calculated by conventional summation of channels and background subtraction assuming a linear continuum under the peak. These intensities were then corrected for the self-absorption within the sample. The absorption coefficients of the

sample at the energies of interest were determined by measuring the transmission through the sample of gamma rays of 43.5 keV (^{238}Pu), 59.6 keV (^{241}Am), 80 keV (^{133}Ba), 122.1 keV (^{52}Co) and 356 keV (^{133}Ba). A number of methods for making the correction for self absorption have been described (see for example, Gunnink & Niday, 1976: Ostrinhansky, 1976; Szoghy & Kish, 1978).

The method used in this study is as follows. The ratio f_a of an absorbing cylindrical source relative to a non-absorbing point source at any energy E_i is given by

$$f_a = \int_{x=0}^{h} \int_{r=0}^{R} \frac{\exp(-\mu_i \times \sec\theta) \cdot E_i(\theta) r\,dr\,dx}{r^2 + (x+a)^2} \qquad (1)$$

where

μ_i = absorption coefficient at E_i
R = radius of sample
h = height of cylinder
a = S + P
S = sample top to detector distance
P = effective penetration depth of radiation E_i into the detector
$\theta = \tan^{-1}(r/x+a)$
$E_i(\theta)$ = relative detector efficiency for energy E_i at angle θ.

The angular efficiency of the detector was measured with the point sources listed above and calibration curves used to obtain the efficiency for the photopeak energies, E_i, of interest. The integration of equation (1) was performed numerically for the sample with a range of values of absorption coefficients, μ. Calibration curves for f_a at each E_i were then obtained as a function of μ, and using the measured μ for each sample, a correction factor was obtained at each E_i.

The activity ratios of each isotope, X (except for ^{226}Ra), relative to ^{238}U were obtained by comparing the sample spectrum with the spectrum of a standard ore. The standard used was US Department of Energy, New Brunswick Laboratory, sample 42-4, which has 0.613% U_3O_8 and is 3% rich in radium. An independent measurement of the ^{234}U/^{238}U ratio of the standard (G.H. Riley, *pers. comm.*) has shown ^{234}U-^{238}U equilibrium (to within ± 1%). ^{230}Th was also assumed to be in equilibrium with ^{238}U. The ^{238}U content of each sample was obtained by assuming the short half life isotope ^{234}Th, the immediate daughter of ^{238}U, to be in equilibrium with ^{238}U. The activity ratio was finally obtained as

$$\text{A.R.}\ \frac{(^{238}\text{U})}{\text{X}} = [(A_u f_u)/(A_x f_x)]_o / [(A_u f_u)/(A_x f_x)]_s$$

where A_u, A_x are the photopeak areas of the 63.3 keV, ^{234}Th peak and of peak X respectively, f_u, f_x are the correction factors of the photopeaks and subscripts o and s denote the ore and standard respectively.

^{226}Ra was estimated from the 186.1 keV photopeak which is unresolvable from a 185.7 keV peak of ^{235}U. Measurements with uranium oxide showed ^{226}Ra contributed 59.1% of this peak. A similar value can be calculated from the data given by Szoghy & Kish (1978). The radium activity ratio was then calculated by first subtracting from the 186 keV peak the correct fraction of the ^{234}Th 63.3 keV peak.

RESULTS AND DISCUSSION

The results obtained from the gamma-ray spectra are detailed in table 2. The first row of the table gives an estimate of the percent error in each of the ratios. These estimates are based on the counting error involved in determining the photopeak area. The errors due to sample packing variations, minor geometry changes and to the sample absorption effects are difficult to estimate. However, by comparing repeat measurements on the same sample the percent variations stated were found to represent the actual differences for samples with uranium contents greater than 1000 ppm. For the few samples around 200 ppm U_3O_8 the increased counting errors lead to actual variations of around double those quoted.

Three of the ratios listed give essentially the same information, namely $^{238}U/^{226}Ra$, $^{238}U/^{214}Pb$ and U_3O_8/eU_3O_8 as the sample container is sealed to allow radon-radium equilibrium. The $^{238}U/^{210}Pb$ ratio should also be similar unless there has been loss or gain of radon or ^{210}Pb to the sample on a 100 year timescale. There is general agreement amongst the four ratios within the estimated errors which is taken to imply that radon and lead movement in the deposit is not large. In a few cases one of the four ratios may have a larger than expected deviation but these are considered to be the result of statistical fluctuations.

The two ratios $^{238}U/^{230}Th$ and $^{238}U/^{227}Th$ enable the loss or gain or uranium on a long time scale to be determined. ^{227}Th occurs after ^{231}Pa in the decay chain of ^{235}U and ^{231}Pa has a half life of 3.2×10^4 years compared to 8.0×10^4 years for ^{230}Th. Precise comparisons of the two may be used to date samples in the 10^5 year time scale (Rosholt, 1967). Here the data of table 2 are used qualitatively to give a description of the disequilibrium as in the last column of table 2.

All the results for the weathered zone samples show approximate equilibrium between ^{230}Th and ^{226}Ra or the short lived isotopes occurring after ^{226}Ra. Equilibrium between ^{230}Th and ^{226}Ra is reached after approximately ten half lives of ^{226}Ra or approximately 16 000

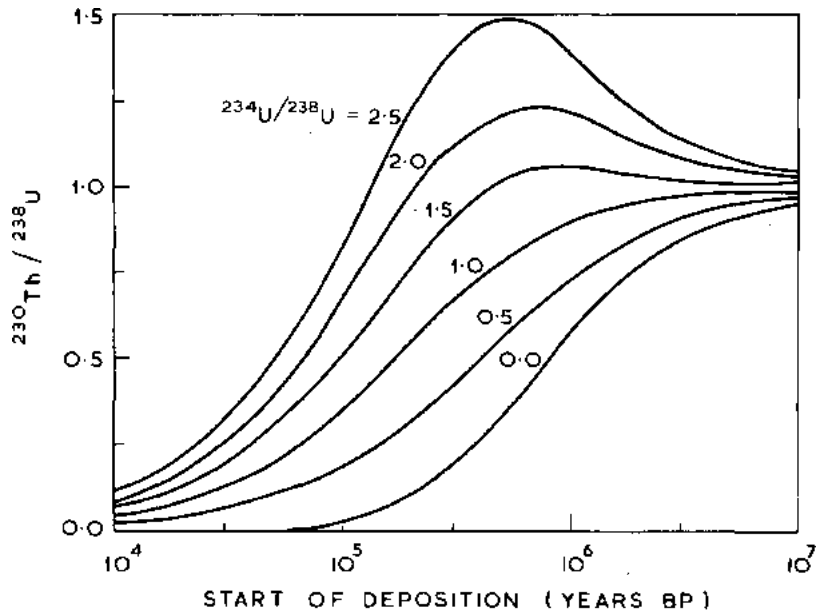


Figure 3. Calculated variation with time in ratio $^{230}Th/^{238}U$ assuming continuous deposition of uranium with different values of the $^{234}U/^{238}U$ ratio.

years. Disequilibrium occurs between ^{230}Th and ^{238}U with the samples at the NW tail of the fan being ^{230}Th rich. Those from the leading edge are ^{230}Th poor. ^{230}Th requires approximately 800 000 years to reach equilibrium with ^{238}U and, as thorium compounds are generally far more insoluble than uranium (Dyck, 1978), the disequilibrium between ^{230}Th and ^{238}U indicates uranium is moving in the weathered zone.

Estimating a time period for movement of uranium from the activity ratios is difficult because the change of ^{230}Th relative to ^{238}U is very dependent on the initial $^{234}U/^{238}U$ ratio. ^{234}U is readily leached in groundwaters as a result of the changes occurring in its formation from ^{238}U (Osmond & Cowart, 1976) so that the uranium being precipitated in the leading edge may be ^{234}U enriched. Figure 3 shows how the $^{230}Th/^{238}U$ ratio varies as a function of the initial $^{234}U/^{238}U$ ratio for an ore body with uranium being continuously deposited at a steady rate. Values of $^{234}U/^{238}U$ can vary considerably, reaching high values in the vicinity of some uranium ore deposits (Osmond & Cowart, 1976). If we assume a value of 1.5, typical for surface waters, for the deposition of uranium at the leading edge of the dispersion fan then uranium deposition in the area of sample 30 would, from figure 3, have been started around 0.35 m.y. BP.

The two samples from the transitional zone at the base of the weathering show that more active movement of isotopes is occurring in this region. Sample 58 is very enriched in ^{226}Ra relative to ^{238}U and also depleted in ^{230}Th. This suggests radium is being deposited and there is a loss of uranium or movement of thorium. The other sample, No 59, has a disequilibrium pattern similar to that for the weathered zone, namely, ^{230}Th-^{226}Ra equilibrium and depletion of ^{238}U which is the pattern for a sample from the NW tail of the fan.

The two fractured zone samples are close to the active weathering zone and also show the effect of recent isotope movements. Sample 103 is from a zone of faulting in the vicinity of massive ore. The disequilibrium pattern is similar to that of sample 59 from the transitional zone, and to that of samples from the weathered zone, with ^{230}Th and ^{226}Ra essentially in equilibrium. Evidently fracturing has allowed the penetration of the weathering process to this depth and allowed removal of uranium. Sample 80 is from the hematite rich Reverse Fault breccia. The fracturing produced by the fault movement has enabled weathering to penetrate down the breccia zone to considerable depth (Fig. 2). The disequilibrium pattern is unusual, the sample being depleted in both ^{238}U and ^{226}Ra relative to ^{230}Th.

The very low uranium content of the host wall rocks makes it difficult to determine the activity ratios as accurately as for the ore samples. With sample 50 the activity ratios indicate equilibrium between ^{238}U and ^{230}Th but ^{226}Ra enrichment relative to ^{238}U. Sample 61 shows both ^{230}Th and ^{226}Ra enrichment relative to ^{238}U. Sample 122 from the top of the No 2 Orebody and located 65m below ground level shows a large gain of radium, with ^{238}U and ^{230}Th being essentially in equilibrium. Sample 122 contains 1.3% U_3O_8 and to explain the 39% increase in radium in this sample requires a specific mechanism of local concentration. This does show however that radium is a very mobile element at depth and that penetrating groundwaters are causing radium, and probably uranium movements, over time periods of up to 5000 years. Such movements may have been taking place for much longer times but the decay of ^{226}Ra precludes confirmation by the technique employed here.

Radium has known mobility in deep groundwaters where reducing conditions prevail (Dyck, 1978) and accumulations of radium are found around mineral springs where Fe and Mn oxides and carbonates precipitate, coprecipitating radium. In comparison, uranium is most mobile in oxidizing near surface groundwaters, as is seen in the Koongarra dispersion fan.

The uranium secondary minerals forming in the Koongarra deposit appear to reflect the two different groundwater chemistries. At depth, where samples enriched in radium indicate that the groundwaters are reducing and mobilizing radium, uranium silicates are found.

However, in the weathered zone where uranium is mobile and the groundwaters oxidizing, uranyl phosphates are the predominant uranium secondary minerals (Snelling, 1979).

As a consequence of this, the transitional zone between the weathered and unweathered ores, which is also a transition from oxidizing to reducing environments, should show the precipitation of either uranium or radium depending on the direction of groundwater flow. Thus an upward flow of reducing groundwaters would precipitate radium on entering the transition zone and mixing with the oxidizing groundwaters. Sample 58, just in the weathered zone, shows ^{226}Ra enrichment indicating upward flow of reducing waters at that location. A similar flow direction is indicated for the locality of sample 122 from the No 2 Orebody. This sample, which has a large radium enrichment, is also notable in that uranium is mainly present as secondary minerals with hematite suggesting that it is in an area of high water flow and that conditions exist for precipitation or adsorption of radium.

The movements of groundwaters implied by these results are in accord with the groundwater studies published by Noranda Australia Ltd. (1978). Recharge of groundwaters to the host schists occurs via downflow parallel to, and in close proximity to, the reverse fault in both the underlying Kombolgie sandstone and the schists. Although the fault zone was found to be almost impermeable, some water flows from the Kombolgie sandstone into the schists via cross fractures which offset the fault. Once in the schists the groundwater flow is towards the south east, away from the Mt Brockman escarpment.

Tritium dating of waters from below the weathered zone (Noranda Australia Ltd, 1978) indicated that flow is very slow. Our results show that there has also been upward flow of groundwater with radium being deposited just below the base of weathering. A summary of these movements with the uranium and radium movements determined in this study is shown schematically in figure 4. These findings also confirm the conclusion from the previous study

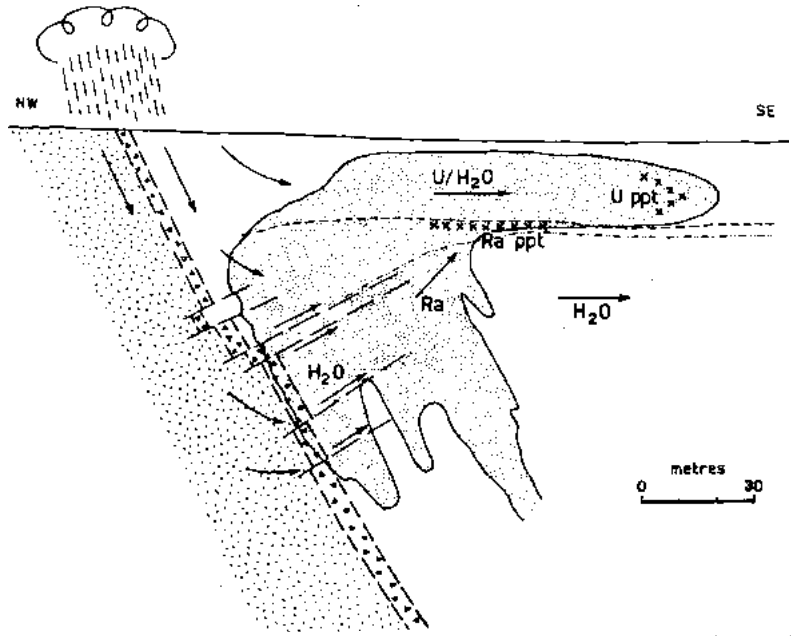


Figure 4. Schematic diagram illustrating proposed movements of groundwater, in the weathered zone and through fractures offsetting the reverse fault breccia, and the resulting displacement and precipitation (ppt) of radium and uranium. Legend as for figure 2.

(Snelling & Dickson, 1979) that the dispersion fan results from weathering of a previous extension upward of the primary ore and not from movement from depth of uranium.

CONCLUSION

This study on the disequilibrium in the Koongarra deposit by the use of high-resolution gamma spectroscopy, shows that there is slow movement of uranium in the weathered zone and more rapid movement of radium at depth in both the No 1 and No 2 Orebodies. One sample in the transitional zone at the base of the weathered zone and one in the top of the No 2 Orebody show considerable radium accumulation. The principal causes of disequilibrium in the deposit are weathering and circulation of groundwaters.

ACKNOWLEDGEMENTS

We wish to thank Noranda Australia Ltd for providing the samples used in this study and Drs P.J. Dallimore and G.R. Newman for discussions on the techniques used.

REFERENCES

Dyck, W., 1978. The mobility and concentration of uranium and its decay products in temperate surficial environments. *in Short Course in Uranium Deposits: their Mineralogy and Origin, Min. Assoc. Canada*, 57-100.

Foy, M.F., & Pedersen, C.P., 1976: Koongarra uranium deposit. *in* (ed. C.L. Knight), *Economic Geology of Australia and Papua New Guinea, Australas. Inst. Min. Metall., Monograph Series No. 5, I. Metals*, 317-321.

Gunnink, R., & Niday, J.B., 1976: A working model for Ge(Li) detector counting efficiencies. *Proceedings ERDA X and Gamma ray Symposium*. (Conf. 760539), 55-58.

Hambleton-Jones, B.B., 1978: Theory and practice of geochemical prospecting for uranium. *Miner. Sci. Eng., 10*, 182-197.

Lederer, C.H., & Shirley, V.S., 1978: *Table of Isotopes*, 7th edition Wiley-Interscience, New York.

Levinson, A.A., & Coetzee, G.L., 1978: Implications of disequilibrium in exploration for uranium ores in the surficial environment using radiometric techniques - a review. *Miner. Sci. Eng., 10*, 19-27.

Moxham, R.M., & Tanner, A.B., 1977: High-resolution gamma-ray spectrometry in uranium exploration. *Journal of research of the U.S. geol. Surv., 5*, 783-795.

Noranda Australia Ltd., 1978: *Koongarra Project Draft Environmental Impact Statement* (Melbourne).

Osmond, J.K., & Cowart, J.B., 1976: The theory and uses of natural uranium isotopic variations in hydrology. *Atomic Energy Review, 14*, 621-679.

Ostrihansky, L., 1976: Radioactive disequilibrium investigations, Elliot Lake area, Ontario. *Geol. Surv. Pap. Can., 75-38*, 21-48.

Rosholt, J.N., 1967: Open system model for uranium-series dating of Pleistocene samples. *Proceedings of Symposium on Radioactive Dating Methods Low Level Counting*. International Atomic Energy Agency, Vienna, 453-466.

Scott, J.H., & Dodd, P.H., 1960: Gamma-only assaying for disequilibrium corrections. *United States Atomic Energy Commission Report, REM-135*.

Snelling, A.A., in prep., A geochemical study of the Koongarra uranium deposit, Northern Territory, Australia. *Ph.D. Thesis, University of Sydney*.

Snelling, A.A., & Dickson, B.L., 1979: Uranium/daughter disequilibrium in the Koongarra uranium deposit, Australia. *Miner. Deposita, 14*, 109-118.

Szoghy, I.M., & Kish, L., 1978: Determination of radioactive disequilibrium in uranium-bearing rocks. *Can. J. Earth Sci., 15*, 33-44.

$^{234}U/^{238}U$ ACTIVITY RATIOS IN CLAY AS A FUNCTION OF DISTANCE FROM PRIMARY ORE

P.J. Shirvington

AAEC Environment and Public Health Unit, Coogee, N.S.W., 2034, Australia.

ABSTRACT

Measurement of $^{234}U/^{238}U$ activity ratios in soil samples is proposed as a useful exploration tool for uranium in the Alligator Rivers Uranium Field. The technique would rapidly distinguish between dispersed uranium and traces of primary mineralization oxidised in place. It relies on the fractionation of ^{234}U and ^{238}U isotopes that occurs in weathered schists associated with uranium mineralization in the area. An enrichment in the ^{234}U isotope occurs by virtue of its lower solubility compared to ^{238}U in oxidising groundwaters. The extent of fractionation is measured α-spectrometrically by comparing $^{234}U/^{238}U$ activity ratios in bulk clay with those in a dilute HNO_3 leachant. An equation is derived to give relative ages of uranium residence in clay and is applied to some of the 60 $^{234}U/^{238}U$ activity ratios obtained from 26 sample sites at the Nabarlek uranium orebody, in order to test the technique. Ages of $\sim 10^3$y were indicated for uranium residence in clay near zones of primary mineralization and up to 30m into the dispersion tail, but ages decreased sharply beyond this point. Selective leaching experiments on weathered schists from Nabarlek and the Austatom uranium prospect indicated a chemical process was involved in the isotope fractionation.

INTRODUCTION

This paper describes isotopic studies that might have application to uranium exploration. The studies were originally undertaken to meet the growing need for data to assist in international assessment of the safety of radioactive waste disposal. Australia's uranium orebodies contain a potential wealth of information that could help in this regard. In this context the mobility of oxidised uranium in groundwater-clay environments is being studied to provide possible upper limits for the migration of the less soluble transuranics, such as plutonium. Data have been obtained from measurements in clays associated with the Nabarlek deposit and the Austatom prospect in the Alligator Rivers Uranium Field (ARUF) in the Northern Territory. A number of results from the study could be relevant to future uranium exploration programs in this Field.

The high grade vein-type uranium deposits found in the ARUF are of world-ranking significance. The deposits may have formed as early as 1800 m.y. ago (Ferguson *et al.*, this volume; Gulson & Mizon, this volume) and were remobilized as recently as 800-900 m.y. ago (Hills & Richards, 1976). All deposits discovered to date lie close to the present erosion surface and have been modified to some extent in recent times by circulating groundwaters and fluctuating water levels. Both of these phenomena can lead to disequilibrium between uranium and its daughter nuclides in the decay series (Fig. 1). Patterns of redistribution of these nuclides may assist in the formulation of a weathering model for the orebodies in the Pleistocene era, which could, in turn, be used to make field predictions of prospective areas for location of primary ore. Several authors have sought to do this in a general way (Syromyatnikov *et al.*, 1967; Morgan, 1972; Levinson & Coetzee, 1976; Hambleton-Jones, 1978) although their models are not clearly applicable to the ARUF. Studies have been made of radioactive disequilibrium and uranium daughter migration in the sandstone, roll-front, uranium deposits in the United States (Rosholt *et al.*, 1965 and references therein; Santos, 1975; Hansink, 1976) and in calcrete deposits in Western Australia (Dickson & Fisher, in press). However, relatively few studies of this nature (Snelling & Dickson, 1979; Dickson & Snelling, this volume) have been made on vein-type uranium deposits.

The Nabarlek Uranium Deposit

Located at 12°18'S, 133°20'E and about 270km due east of Darwin the Nabarlek

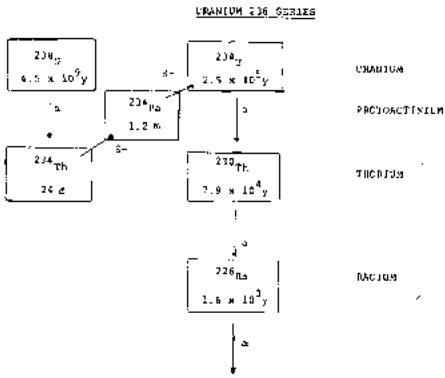


Figure 1. Abbreviated decay series for ^{238}U.

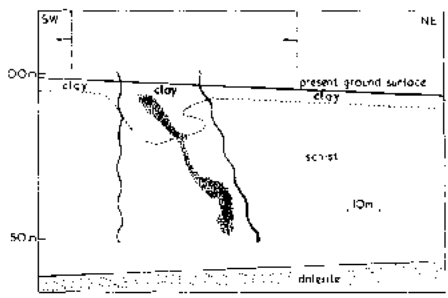


Figure 2. Nabarlek orebody - cross section. uranium ore; high-grade uranium ore, ·····base of weathered zone; – – – postulated earlier positions of sandstone escarpment; boundary of schist crush (deformation) zone.

deposit (Fig. 2) is one of the four large high-grade vein-type deposits discovered in the ARUF. It has estimated reserves (Sept 1971) of 9,530 tonnes of U_3O_8. Anthony (1975) has described the deposit, and detailed accounts of the regional geology are given by Needham & Stuart-Smith (this volume) and by Smart *et al.* (1975).

The Nabarlek orebody is situated within a deformation zone which can be traced on the surface 460m south-east and 120m north-west of the orebody. Traces of primary mineralization occur outside the main orebody in this zone. The rocks enclosing the orebody are contorted and sheared metasomatised schists. The present day gently-sloping erosion surface is believed to approximate closely the unconformity between the mine series schists and the Kombolgie quartz-sandstone formation, which has served as a cover rock for the orebody in the recent past. With erosion, the edge of this thick flat-lying plateau has retreated, exposing the top of the orebody to the zone of weathering of the new erosion surface (Fig. 2).

The uranium mineralization is contained in massive fine-grained chlorite rock, together with sericite and hematite, and is transgressive to the schistosity. Pitchblende is the primary uranium mineral and has unit cell dimensions typical of normal vein-type pitchblende.

The water table in the Mine area is coincident with the surface during the wet season and recedes to a depth of about 15m during the dry season. In the Mine area the metasediments are oxidised to a depth of about 5m but in the orebody the depth of oxidation is about 15m. No significant secondary enrichment has taken place. Some leaching of ore has taken place near the surface resulting in a thin tail of secondary uranium mineralization extending to the north-east of the orebody for a distance of up to 190m. Oxidation has had the effect of considerably widening the low grade envelope near the surface.

The Austatom Prospect

Located at 12°37′S, 132°40′E and about 202km due east of Darwin, in the ARUF, the Austatom Prospect was discovered by AAEC geologists in 1976. A comprehensive report on the prospect has been prepared but is not yet available. Figure 3 is a schematic cross-section of the prospect which consists of secondary uranium mineralization in fully weathered schist, unconformably overlain by Cretaceous sandstone. The schists are underlain by dolomite. Uranium mineralization in the clay is broadly indicated by the dot pattern, the grade being approximately equivalent to the dot density. There is little surface expression of uranium.

Climate

The regional climate is monsoonal with the annual rainfall of 1100-1400mm, nearly all

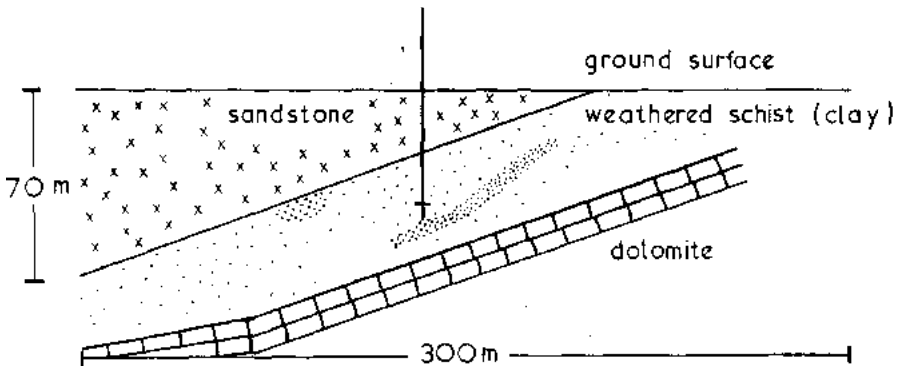


Figure 3. Austatom prospect - cross-section (schematic). U mineralization; low-level U mineralization. $^{234}U/^{238}U$ activity ratios for sample location marked with cross are given in figure 6.

falling in the period November to March. Temperature varies little from a maximum of 35°C in October to 31°C in March.

Uranium Isotope Fractionation

Significant differences would not be expected in the chemistry of two isotopes of the same element, yet the existence of $^{234}U/^{238}U$ disequilibrium has been extensively reported (Cherdyntsev, 1968; Osmond & Cowart, 1976) and attributed to ^{238}U α-decay leaving the ^{234}U atom generated in-situ in a different chemical/physical configuration in the rock to the ^{238}U parent.

In general, groundwaters originating from unweathered rock exhibit considerable enrichment in ^{234}U indicating a greater leachability of the ^{234}U isotope compared to parent ^{238}U, present in the +4 oxidation state. Enrichment in ^{234}U is seldom pronounced in waters emanating from weathered rock and soil horizons where uranium is usually in the +6 state (Osmond & Cowart, 1976), presumably due to insufficient difference in the relative solubilities of the two isotopes. Depletion of ^{234}U in uranium-bearing rocks and soils has been reported (Rosholt *et al.*, 1965; Osmond & Cowart, 1976) where evidence exists for prolonged leaching.

To the authors knowledge it has never been claimed that ^{234}U atoms generated in-situ in the rock are less soluble than ^{238}U in groundwater. Evidence of ^{234}U depletion in groundwater that would substantiate such a claim (Osmond & Cowart, 1976) has been given a different interpretation, viz: that oxidising groundwaters are passing through a zone having a previous history of extensive leaching under reducing conditions. It has been a major finding of the present study that ^{234}U atoms generated in-situ can be less soluble than ^{238}U under some circumstances.

SAMPLING AND ANALYTICAL METHODS

Samples were derived from two sources:

1) Drill cores obtained from the exploration drilling program carried out by Queensland Mines Ltd. at Nabarlek, (diamond-drill holes NA: 32, 55, 71, 110, 145, 195, 220 and 229) and by the AAEC at Austatom (diamond-drill hole ADD-4).
2) A special sampling program along the dispersion tail at Nabarlek taken at depths of 20-40cm. Red clay was normally present at depths greater than 30cm.

The weathered rock/clay samples were pulverished, after first removing quartz pebbles, and air-dried to provide sample stock. One g samples were taken for neutron activation and

delayed neutron counting in the Physics Division. Samples containing 10-100μg U were dissolved in concentrated HF/HNO_3 prior to isotopic analysis ($^{234}U/^{238}U$ activity ratio denoted by 'AR_1'). Coupled to this, separate portions of each sample (usually 1-3g) were leached in a separating funnel with various dilute reagents, accompanied by gentle agitation provided by a mechanical shaker or an air purge. The supernatent was then taken for isotopic analysis ($^{234}U/^{238}U$ activity ratio denoted by 'AR_2').

Uranium was extracted from the pregnant liquors by solvent extraction into tributyl phosphate/kerosene and further separated from other elements by stripping and re-extraction into methyl iso-butyl ketone from an $EDTA/Ca(NO_3)_2$ solution. The methyl iso-butyl ketone was then evaporated and the uranium dissolved in ethanol/dilute HCl and electrodeposited onto a steel planchette at a current density of 50 mA/cm^2. The $^{234}U/^{238}U$ activity ratios were measured by α-spectrometry using an Ortec silicon barrier detector, DC power supply, pre-amplifier, amplifier and multi-channel analyser (260 of 1040 channels). Each determination of $^{234}U/^{238}U$ activity ratio took 0.5 man-days. Counting time varied from a few hours to several days, depending on the uranium concentration in the sample and the time required to accumulate a statistically significant number of counts. A total count of 10,000 per α-peak yields an error of $\sim\pm0.02$ in activity ratio at the 1σ level. Results are quoted to this accuracy unless otherwise stated. Duplicate runs were carried out in some cases as indicated in the text.

Samples of clay from the weathered zone at Nabarlek and Austatom were submitted to the Australian Mineral Development Laboratories for mineralogical examination. The results are summarized in table 1.

Austatom Hole ADD 4, 27.9m		Nabarlek Hole NA 229, 1.2m	
Kaolinite	Dominant	Mica/illite	Dominant
Mica/illite	Sub-dominant	Chlorite	Sub-dominant
Quartz	Accessory	Kaolinite	Sub-dominant
Goethite	Accessory	Gibbsite	Accessory
Montmorillonite	Accessory	Aluminium Geothite	Accessory
		Feldspar	Trace

Key
Dominant: most abundant component
Sub-dominant: next most abundant component, but 20%
Accessory: 5-20%
Trace: < 5%

Table 1. Bulk mineralogy of two samples of uranium-bearing weathered schist from the Alligator Rivers Uranium Field.

RESULTS AND DISCUSSION

In all some 60 $^{234}U/^{238}U$ activity ratios (AR) were obtained from 26 sample sites at Nabarlek and some 10 ARs from one sample site at Austatom.

Nabarlek

Figure 4 shows schematically the variation in AR_1 and AR_2 (defined in previous Section) as a function of distance from the Nabarlek orebody and as a function of depth in the weathered part of the orebody and in the dispersion tail. Uranium concentrations are given in parenthesis and drill hole numbers are given above. A standard leaching time (for AR_2 values) of 48 hours and a standard leachant of 1.6 M HNO_3, were used. Under these conditions, for the samples so indicated, 46±4% of uranium was extracted from the clays. Runs on the same samples only with 1.6 M HNO_3 and 3% hydrogen peroxide, showed no significant difference to results in figure 4 in either activity ratio or fraction of uranium extracted. The effects of peroxide addition likewise had little effect on results for a sample taken from nearer the surface (20cm depth) at the 190m mark, where grey soil colour

indicated a more reducing environment. The remainder of the results obtained at Nabarlek are reported in other forms, later in this Section.

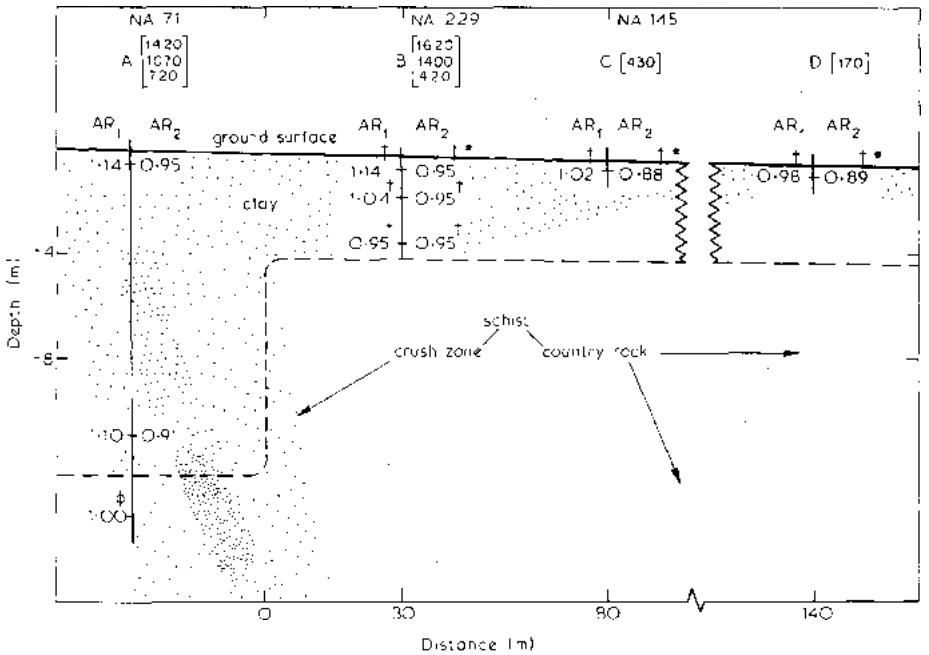


Figure 4. Nabarlek cross section: $^{234}U/^{238}U$ activity ratios (AR) as a function of depth and distance; AR_1 obtained on total U, i.e. clay completely dissolved in conc. HF/HNO_3; AR_2 on accessible U, i.e. that eluted by 1.6 M HNO_3 (* 46 ± 4% of U eluted). U concentrations given in μg g^{-1} in brackets; Company diamond drill hole numbers given above; [ ] U mineralization, intensity of stippling proportional to grade; –– base of weathered zone. 1σ error in AR = 0.02. †mean of duplicates, error within that form counting statistics. ϕ indicative only, based on analysis of unweathered ore at Ranger orebody.

Significant trends in figure 4 are:

1) AR_1: An enrichment in the ^{234}U isotope in the clay in the weathered part of the orebody and at the surface of the dispersion tail near its source. From this latter point ^{234}U enrichment falls away rapidly with depth and with horizontal distance from the orebody.
2) AR_2: Uranium soluble in the dilute HNO_3 leachant exhibits a slight ^{234}U deficiency which is constant with depth in the dispersion tail, but becomes slightly more pronounced with increasing depth in the weathered part of the orebody and with increasing horizontal distance from the orebody.
3) AR_1 - AR_2: The degree of isotope fractionation between bulk uranium and the soluble portion is greatest in the weathered part of the orebody and in the surface clays near the source of the dispersion tail.

Leaching Experiments

This apparent enrichment in ^{234}U in the less soluble uranium fraction in the clay was accentuated artificially in the laboratory by prolonged leaching (Fig. 5). Distilled water, 0.01 M K_2CO_3 and 1.6 M HNO_3 extracted uranium from Nabarlek clay with a constant AR of 0.95 (5% deficiency in ^{234}U) even after prolonged leaching, with the result that (in the case of the latter two), the enrichment of ^{234}U in the clay residue increased from an initial value of 1.07 to 1.16 and 1.28 respectively. Not shown in figure 5, 3 M H_2SO_4 took 7 days to extract

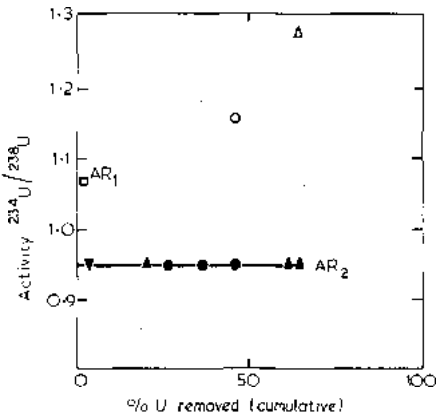


Figure 5. Nabarlek: $^{234}U/^{238}U$ activity ratios as a function of percent uranium removed from clay (clay samples taken from diamond drill hole NA 229, 1.2m, figure 4). ▼ leached with distilled water for 10 days, activity ratio in leachate; ● leached with 0.01 M K_2CO_3 for 2, 6 and 18d, activity ratio in leachate; ▲ leached with 1.6 M HNO_3 for 0.1,5 and 11d, activity ratio in leachate; □ no previous leaching, activity ratio of total uranium, i.e. that completely dissolved in HF/HNO_3; O leached with 0.01 M K_2CO_3 for 18d, activity ratio of residue completely dissolved in HF/HNO_3; Δ leached with 1.6 M HNO_3 for 11d, activity ratio of residue completely dissolved in HF/HNO_3.

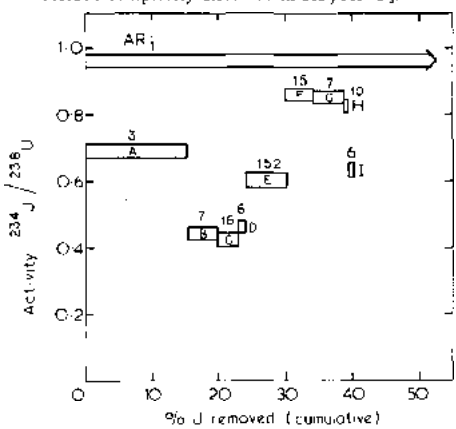


Figure 6. Austatom: $^{234}U/^{238}U$ activity ratios as a function of fraction of uranium removed from clay with various leachants: A, B, C, 1.6 M HNO_3; D 1.6 M HNO_3, 0.3% H_2O_2; E 0.16 M HNO_3, 0.03% H_2O_2; F 1.6 M HCl; G 3% H_2O_2, 0.1 M NaOH; H 0.1 M K_2CO_3; I 1.6 M HNO_3. Leaching time in days, is given above each box. Vertical sides of boxes are counting errors to 1σ level. AR_1, activity ratio of total uranium, i.e. that completely dissolved in HF/HNO_3. Samples taken from diamond drill hole ADD 4, 27.9m (Fig. 3). [U] 730 μg g^{-1}.

83% of the uranium at an AR of 0.98 from a duplicate sample of clay, thereby enriching the residue in ^{234}U by a factor of 1.52 (AR_2 = 1.52).

It is the opinion of most workers in the field (Rosholt *et al.*, 1965; Osmond & Cowart, 1976; and references therein) that ^{234}U enrichment can only be achieved in solids when uranium is deposited from groundwater enriched in the isotope. If this were the case at Nabarlek then the uranium leached from the clay should likewise exhibit an excess of ^{234}U. Since the reverse was found to be true then enrichment in ^{234}U must occur by selective leaching of ^{238}U from the clay. Such a process could only take place if ^{234}U generated in-situ in the clay has entered a chemical/physical configuration that is less soluble then the remainder of the oxidised uranium, including all the ^{238}U.

Since the weathered schists/clays at the Austatom prospect resembled those at Nabarlek in both appearance and mineralogy (Table 1), a drill core sample from the former, taken at 27.9m (Fig. 3), was subjected to a series of leaching experiments. It was considered that the overlying sandstone at Austatom might have insulated the clays from complex processes occurring at the erosion surface, and that the longer resident times possible for uranium in the clay might have enabled a fuller development of the isotope fractionation processes. Figure 6 shows this to be true. Bulk uranium in the sample had an AR of 0.95. Leaching with 1.6 M HNO_3 yielded AR_2 values in the leachate ranging from 0.69 (0-15% fraction) down to 0.42 (20 to 23% fraction). The higher value of the former may be due to contained uranium, near isotopic equilibrium, that has recently been deposited by groundwater and hence is easily extracted by HNO_3. Crystals of secondary uranium minerals in radiometric equilibrium (AR_1 = AR_2 = 1.00) were embedded in clay only 1m from the sample site.

Once the more labile uranium had been removed from Austatom clay the AR of uranium in the leachate could be changed at

will, by selection of appropriate reagents. The addition of H_2O_2 to HNO_3 solutions had a barely significant effect on the AR_2 value. However, reagents which strongly complex uranium (dilute HCl, alkaline peroxide and K_2CO_3 solutions) were less efficient than dilute HNO_3 at separating the ^{234}U and ^{238}U isotopes (AR_2 values of ~ 0.85). This variability suggests a chemical isotope fractionation mechanism and not a physical separation involving implantation of ^{234}U atoms in the clay crystal lattice following α-recoil. Precipitation of the transient ^{234}Th ($t_{1/2}$ 24 d), which is placed between ^{238}U and ^{234}U in the decay series, may be an important component in the chemical fractionation process.

It is possible that our ability to detect the full extent of fractionation present in the clay is limited by the narrow range of leachants tested or by the need to extract uranium at an experimentally convenient rate, which is bound to be rapid in comparison with leaching rates in the field. Therefore the lowest AR obtained (0.42) may not be a lower limit. If uranium has been resident in the clay for periods longer than four or five half-lives of ^{234}U (i.e. $>1 \times 10^6$y) under oxidising conditions and with minimum interference from erosion processes, then the 'theoretical' $^{234}U/^{238}U$ AR of uranium achievable in the leachate may be much lower.

Proposed Model

The $^{234}U/^{238}U$ isotope fractionation process described here appears to have a number of components:

1) Weathering of the schist in order to create the conditions under which this type of fractionation can occur, viz: the presence of clay minerals under oxidising conditions.
2) Entry of uranium in groundwater, if not already present in the pristine schist.
3) A period, commensurate with the half-life of ^{234}U (2.5×10^5y), during which ^{234}U atoms are generated in-situ in the clay and at the same time enter into a chemical configuration which is more resistant to leaching than that of the remainder of the (oxidised) uranium, including all the ^{238}U.
4) Preferential leaching of ^{238}U by oxidising groundwaters resulting in a complex pattern of $^{234}U/^{238}U$ activity ratios, e.g.:
   a) Gradual lowering of the erosion surface in the dispersion tail at Nabarlek may have caused surficial uranium to progressively redissolve in groundwaters and migrate downwards to newly weathered (barren) rock. A $^{238}U/^{230}Th$ isotopic study, to be reported elsewhere, strongly supports such a mechanism. If ^{238}U can be dissolved preferentially compared to ^{234}U during such a process, as indicated by laboratory experiments, then the near-surface clays will have become enriched in ^{234}U in this way and the newly weathered rock (at 3-4m) will have become depleted.
   b) The dispersion tail at Nabarlek may have been produced, in part, by groundwater dissolving uranium and transporting it down-slope via sorption-desorption processes in the clay. If migration times have been commensurate with the half-life of ^{234}U ($\sim 2.5 \times 10^5$y), then the trend towards lower $^{234}U/^{238}U$ activity ratios with increasing distance from the orebody, could have been caused by progressive selective-desorption of ^{238}U from the clay in the dispersion tail. This trend was well developed between 30 and 80m, but vanished at greater distances where sediment, eroded from the top of the orebody and washed downslope, may have been an important contributor of uranium to the groundwater.
   c) If the dispersion tail at Nabarlek has been growing then its leading edge should have recently experienced an influx of new uranium, which would have diluted any residual isotope fractionation of uranium already in the clay. This would

have occurred whether or not new uranium had come from horizontal groundwater transport of from dissolution of relocated solids at the erosion surface immediately above. The result would be a lower measured degree of fractionation between bulk uranium and the soluble portion in the clay. Such a trend is shown quite clearly in figure 4 and in results presented later in the section.

d) Reduction of uranium by organic matter in the soil could give rise to a decrease in the degree of isotope fractionation, through alteration of the relative solubilities of ^{238}U and of ^{234}U generated in-situ. Attempts to achieve the obverse of this in the laboratory, i.e. to oxidise soils rich in organic matter and uranium with a view to changing the degree of isotope fractionation, were unsuccessful. Nevertheless, such processes may still be important in the field.

e) The transport/fractionation processes occurring in the weathered part of the Nabarlek orebody would have been more complex than in the dispersion tail. The effect of downward migration of uranium from the erosion surface would have been superimposed onto fractionation phenomena, already existing in the uranium-rich weathered schist.

The isotope fractionation process can best be described by an equation of the type:

$$AR_1 - AR_2 = \beta(1 - e^{-\lambda t}) \quad (1)$$

where λ is the decay constant for ^{234}U, t is the 'equivalent' age of uranium residence in the clay (assuming uranium concentration to be constant over this time) and β is a coefficient reflecting the efficiency of the fractionation process. The exact value of β is unknown. It may have a number of factors including those mentioned under (1) and (4). It would probably have values between 0 and 1, although the upper limit could be exceeded under some natural leaching conditions. Equation 1 has been derived mathematically in the Appendix.

Application Of The Model

Table 2 gives 'equivalent' ages for uranium residence in clay near the source of the dispersion tail of the Nabarlek ore-body (hole NA 229, 0.5m) calculated from equation 1 using various arbitrary values of β. It is not possible to assign absolute ages due to uncertainty in the value of β.

β	t ($y \times 10^4$)
0.25	52
0.5	17.3
0.75	10.6
1.00	7.6

Table 2. Equivalent ages for uranium residence in clay, in the Nabarlek dispersion tail (hole NA 229, 0.5m), calculated from equation 1 using various values of β.

If sample selection could be standardised in such a way as to keep β constant, then equation 1 or, more simply, the value of $AR_1 - AR_2$, might provide useful information about the relative ages of residence of uranium in clay from various locations. This could enable dispersed uranium to be quickly traced to its source and would allow field-geologists to distinguish between Pleistocene dispersion pheomena and traces of primary ore oxidised in place. Such a standardised procedure might involve, for instance, taking samples from a (constant) depth sufficient to guarantee minimum interference from erosion processes.

All the activity ratio pairs obtained at Nabarlek from a depth of 40-50cm have been converted to an equivalent age, using equation 1 and an arbitrary value of β of 0.5. The results have been used to construct age contours in plan view (Fig. 7). Although the study is incomplete, tentative contours have been drawn for ages of 20, 13 , 8 and 3 x 10^4y. Uranium concentrations in the clay are shown in coded form and the fall-line is indicated by broad arrows. The oldest ages for uranium residence in clay were obtained within the schist crush-zone which contains the orebody; from the weathered part of the orebody (although there

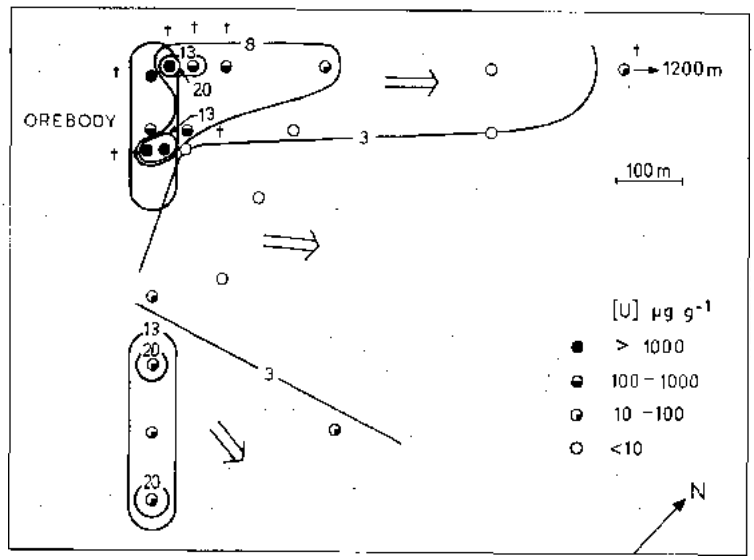


Figure 7: Plan view of Nabarlek orebody and locale, indicating provisional contours for equivalent age of uranium residence in clay in y x 10^4, calculated from equation (1), assuming a β value of 0.5. Sampling points (at 40-50cm depth) are shown. Broad arrows indicate fall-line. Fall is ~2 in 100. For [U] > 100 µg g^{-1} counting error is ± 0.02 in AR at 1σ level. For [U] < 100 µg g^{-1} error is ± 0.03 at 1σ level. † mean of duplicates, error within that from counting statistics.

were some exceptions); and from samples containing 10-100 µg g^{-1} uranium, obtained from south-east of the orebody where some traces of primary mineralization were found during the exploration program. There was no direct correlation between age and uranium concentration except in the dispersion tail where both decreased fairly sharply with distance from the orebody. The pods of uranium-bearing clay immediately over the orebody, having young ages, must have derived their uranium from off-shoots of the primary orebody which have only recently entered the weathering environment. The low-level accumulation of uranium occurring at 1200m exhibits a young age indicating that the uranium is most likely derived from weathering of the main orebody, having arrived there only recently, probably after a long transit time. Although the actual values assigned to the ages depend on the mathematical assumptions, it is possible to draw the general conclusion that the majority of uranium moved from the top of the ore-body over a 10^5y timescale has migrated little further than about 200m.

CONCLUSIONS

Fractionation of ^{234}U and ^{238}U isotopes occurs in weathered schists associated with uranium mineralization in the ARUF. An enrichment in the ^{234}U isotope occurs by virtue of its lower solubility, compared to ^{238}U, in oxidising groundwaters characteristic of the weathering environment. The extent of fractionation may be measured α-spectrometrically by comparing $^{234}U/^{238}U$ activity ratios of bulk clay with those in uranium leached from the clay with dilute HNO_3. Such measurements enable a calculation of the relative ages of uranium residence in clay from various locations. Contours of such ages may assist in tracing dispersed surficial uranium to its source, particularly where ambiguous or conflicting results are obtained from other measurements, e.g. radon daughter activity or uranium

concentration profile. The technique, which would involve taking soil samples at a constant depth of 50cm, would distinguish between uranium dispersed by the weathering process from a zone of primary mineralization and surface traces of primary uranium mineralization oxidised in place. The measurements required for each pair of isotopic ratios involves about 1 man-days work at a cost of about A$100, including overhead for equipment.

ACKNOWLEDGEMENTS

This work would not have been possible without the generous advice and assistance of P. Airey, J. Cook, Y. Meizeitis, N. Conway, D. Roman, A. Camilleri and B. Campbell of the Australian Atomic Energy Commission and P. Anthony of Queensland Mines Ltd.

REFERENCES

Anthony, P.J., 1975: Nabarlek uranium deposit. *in* (ed. C.L. Knight) *Economic Geology of Australia and Papua-New Guinea, Australas. Inst. Min. Metall., Monograph Series No. 5, 1. Metals*, 304-308.

Cherdyntsev, V.V., 1968: Uranium - 234. Israel Program for Scientific Translations, Jerusalem (1971), English Translation of Uran-234 Atomizdat, Moscow.

Dickson, B.L. & Fisher, N.I., 1979: Radiometric disequilibrium analysis of the carnotite-in-calcrete uranium deposit at Yeelirrie, Western Australia. *Bull. Australas. Inst. Min. Metall.*, in press.

Dickson, B.L. & Snelling, A.A., this volume: Uranium daughter isotope movements in the Koongarra uranium deposits. *Proceedings of the International Uranium Symposium on the Pine Creek Geosyncline.*

Ferguson, J., Ewers, G.R. & Donnelly, T.H., this volume: Model for the development of economic uranium mineralization in the Alligator Rivers Uranium Field. *Proceedings of the International Uranium Symposium on the Pine Creek Geosyncline.*

Gulson, G.L. & Mizon, K.J., this volume: Preliminary investigation of the use of Pb isotopes in uranium exploration with additional U-Pb 'ages' for Jabiluka uraninite. *Proceedings of the International Uranium Symposium on the Pine Creek Geosyncline.*

Hambleton-Jones, B.B., 1978: Theory and practice of geochemical prospecting for uranium. *Minerals, Science and Engineering, 10*, 182-196.

Hansink, T.D., 1976: Equilibrium analysis of a sandstone roll-front uranium deposit. *in, Exploration of Uranium Ore Deposits. Proceedings of a Symposium, Vienna.* International Atomic Energy Agency, Vienna, 683-693.

Hills, J.H. & Richards, J.R., 1976: Pitchblende and galena ages in the Alligator Rivers region, Northern Territory, Australia. *Miner. Deposita, 11*, 133-154.

Levinson, A.A. & Coetzee, G.L., 1976: Implications of disequilibrium in exploration for uranium ores in the surficial environment using radiometric techniques — a review. *Minerals, Science and Engineering, 10*, 19-27.

Morgan, J.W., 1972: Radioactive series disequilibrium in uranium economic geology. *Atomic Energy in Australia, 15[2]*, 8-13.

Needham, R.S., & Stuart-Smith, P.G., this volume: Geology of the Alligator Rivers Uranium Field. *Proceedings of the International Uranium Symposium on the Pine Creek Geosyncline.*

Osmond, J.K. & Cowart, J.B., 1976: The theory and uses of natural uranium isotope variations in hydrology. *Atomic Energy Review, 144*, 621-679.

Rosholt, T.N., Tatsumoto, M., Dooley, J.R., 1965: Radioactive disequilibrium studies in sandstone, Powder River Basin, Wyoming, and Slick Rock district, Colorado. *Econ. Geol., 60*, 477-484.

Santos, E.S., 1975: A characteristic pattern of disequilibrium in some uranium ore deposits. *J. Research U.S. geol. Surv., 3*, 363-368.

Smart, P.G., Wilkes, P.G., Needham, R.S. & Watchman, A.L., 1975: Geology and geophysics of the Alligator Rivers region. *in* (ed. C.L. Knight) *Economic Geology of Australia and Papua-New Guinea, Australas. Inst. Min. Metall., Monograph Series No. 5, 1. Metals*, 385-401.

Snelling, A.A. & Dickson, B.L., 1979: Uranium daughter disequilibrium in the Koongarra uranium deposit, Australia. *Miner. Deposita, 14*, 109-118.

Syromyatnikov, N.G., Ibraev, R.A & Mukashev, F.A., 1968: Interpretation of uranometric anomolies in arid regions by means of the $^{234}U/^{238}U$ isotopic ratio. *Geokhimiya, 7*, UK Atomic Energy Authority Translation, AWRE - Trans. 55 (1968).

APPENDIX

Derivation of Equation (1)

At time zero, uranium is first introduced into clay at any point C. ^{238}U has total acitivty $A8_o$ and ^{234}U total acitivity $A4_o$. All uranium absorbed in the clay is accessible to dissolution by groundwater.

After time t (equivalent age of uranium residence in clay), at point C:

for ^{238}U: total activity remains constant and no ^{238}U is inaccessible to groundwater in the clay;

for ^{234}U: that generated in-situ is in a more stable chemical configuration than ^{238}U and is inaccessible to groundwater (and dilute HNO_3). Its activity is given by:

$A4_i$ (inaccessible = $\beta A8_o (1 - e^{-\lambda t})$

where β is a coefficient having values between 0 and 1.
But,
$A4_i$ (inaccessible) $= A4_i$ (total) - $A4_t$ (accessible)
Dividing throughout by $A8_o$:
$A4_i$ (inaccessible)/8_o $= A4_i$ (total)/$A8_o$ - $A4_t$ (accessible)/$A8_o$
$= AR_1 - AR_2$
i.e. $AR_1 - AR_2 = \beta (1 - e^{-\lambda t})$

(The decay of ^{238}U is ignored because of its much greater half-life).

Note that a step function is assumed for uranium deposition into the clay at time zero and, thereafter, total ^{238}U concentration at point C is assumed constant. These are not realistic assumptions. Hence the 'equivalent age' in effect, is a weighted average figure which is approximately correct for most of the uranium in the clay.

THE ROLE OF CLAY ADSORPTION IN GENESIS OF URANIUM ORES

Angela M. Giblin

CSIRO Division of Mineralogy, P.O. Box 136, North Ryde, N.S.W., 2113, Australia

ABSTRACT

Experiments are described in which:

1) The distribution coefficient (K_d) of uranium between a simulated ground water (containing 100 μg/l uranium) and kaolinite, measured over the pH range 3.5 to 10, was found to reach a maximum of 35 000 at pH 6.5.
2) Sequential adsorption-reduction has been demonstrated as one mechanism whereby the enrichment of kaolinite by uranium can exceed 0.01%, the level predicted from K_d measurements when solutions contain $\leqslant 100$ μg U/l.

The relevance of these results to current models for genesis of ores from the Alligator Rivers Uranium Field is to supply a mechanism for generation of economic deposits from waters containing very low levels of uranium. These results also suggest reasons for the antipathy observed between uraninite and base metal sulphide occurrences in the Alligator Rivers Field.

INTRODUCTION

Many models proposed to describe the genesis of uranium ores rely on uranium scavenged by, and carried in, natural surface waters. This concept is popular because it is known that uranium is highly mobile in dilute oxygenated solutions, particularly if complexing species such as carbonate or phosphate are present. However, regardless of the water's potential capacity to carry uranium, the felsic igneous rocks, which are generally seen as the uranium source, contain such low U levels that surface waters draining them usually contain less than 10 μg U/l. Even slowly moving saline ground waters rarely carry more than 100 μg U/l (Fix, 1956) unless they are immediately associated with forming or draining a uraninite deposit. Concentrations in the range 10-100 μg U/l are no doubt adequate, given sufficient time and volume of water, to supply the uranium required for an economic deposit as long as a mechanism is available whereby such low levels of soluble uranium not only become insoluble but also collect in one place, concentrating into economic quantities of crystallized uraninite.

Since oxidized uranium species are generally soluble and therefore mobile whereas reduced uranium species are insoluble unless extremely acid conditions prevail, genesis models generally require some reducing environment to be encountered by the ore-forming solution at the point of deposition. Undoubtedly this sequence of deposition of oxidized mobile uranium as reduced immobile uranium can be demonstrated to have application to many types of uranium ores, in particular, roll front deposits in sandstones. Reduction alone, however, is quite inadequate to explain the deposition of the various types of uraninite present in the Alligator Rivers Uranium Field. For example, Binns, McAndrew & Sun (this volume) describe three related depositional situations for uraninite at Jabiluka, in all of which uraninite has either replaced a chlorite, quartz or other wall rock minerals, or is present as isolated grains within chlorite. It is impossible, therefore, to ignore the frequency of chlorite involvement and to explain uraninite deposition merely in terms of a reduction mechanism.

A further inadequacy of the concept of reduction alone as the ore deposition control in the Alligator Rivers Uranium Field is the reported composition of uraninite minerals. These are apparently not pure UO_2 but contain significant amounts of non-stoichiometric $UO_{(2+x)}$

(Hegge & Rowntree, 1978), which indicates that variations in both pH and redox conditions were involved in their formation.

It should also be noted that the mere formation of chemically insoluble UO_2 within such dilute (≈ 100 μg U/l) solutions does not result automatically in material of particle size sufficiently large for its precipitation from solution. Even in solutions of up to 70 mg U/l, UO_2 formed by reduction in the absence of any nucleating surface is extremely fine grained, possibly colloidal, and as such persists as a mobile species within the aqueous phase (Giblin, 1977). It is thus feasible for very dilute uranium-bearing solutions to traverse reducing fronts without uraninite deposition.

The problem of the generation of economic deposits from very dilute metalliferous waters arises in many ore genesis mechanisms. It is often suggested that low levels of soluble metals are fixed by adsorption on to solids such as clays, hydrous oxides (particularly hydrous ferric oxide) and organic matter. Genetic models proposed by Ferguson, Ewers & Donnelly (this volume) and Ypma & Fuzikawa (this volume) for Alligator Rivers uranium deposits contain suggestions that adsorption of uranium on to clays occurred during the ore forming process. Although there are no reports of uranium-enriched clays in Alligator Rivers uranium ores, there has been persistent reference to an intimate association between the mineralization and a chlorite (Eupene, 1975; Hegge & Rowntree, 1978). The concept of clay adsorption deserves consideration if clays can be demonstrated to be precursors of this present-day chlorite, or if the chlorites can be regarded as clay-like in their surface adsorption characteristics.

The importance of chlorite in the genesis of Alligator Rivers uranium deposits is underlined by three models proposed in contributions in this volume. Although they are all fundamentally different, each refers to a uranium-enriched chlorite or clay. The model proposed by Binns, McAndrew & Sun (this volume) describes a chlorite-septechlorite-quartz intergrowth (CSQ), in which uranium was first introduced at Jabiluka, with uranium levels up to and greater than 1000 μg/g. These authors suggest that discrete concentrations of uraninite formed by exsolution from uraniferous CSQ during events subsequent to the formation of CSQ, but they have no definite evidence as to how uranium is held in CSQ, i.e. whether it is adsorbed or is present as a discrete U-rich phase. They do, however, present evidence which indicates that the fluids from which uraniferous CSQ originally formed were oxidizing, which infers that they were capable of carrying mobile (and therefore sorbable) uranium. In their genesis model Ferguson, Ewers & Donnelly (this volume) suggest the presence of uranium-enriched chlorite which may have been originally a Mg-rich clay that collected uranium by adsorption from low temperature CO_2-rich oxidizing ground waters. These authors also refer to a subsequent crystallization of disseminated uraninite from the uranium originally adsorbed on the chlorite or clay mineral surfaces. Ypma & Fuzikawa (this volume) also suggest that adsorption to clay minerals is an intermediate step between uranium transported in low temperature, CO_2-rich solutions, possibly of meteoric origin, and uraninite deposition initiated by the introduction of concentrated calcium chloride brines.

There is, then a fair consensus that in the Alligator Rivers Uranium Field a chlorite, or possibly a precursor clay was a medium of preconcentration from which economic concentrations of uraninite ultimately formed. Speculations regarding the source of uranium enrichment in the chlorite fall into two categories: syngenetic incorporation during chlorite formation; or surface adsorption onto either already-formed chlorite or a precursor mineral. Lauffenburger *et al.* (1966) have demonstrated experimentally the incorporation of U^{VI} cations into silicates during their formation. Moreover the level of magnesium in solution was shown to control the uranium uptake. This is particularly interesting with regard to the Alligator Rivers uraniferous chlorites because of their high magnesium content. More

generally suggested, however, is the surface adsorption process, presumably because of the restricted conditions required for coeval chlorite formation and uranium collection. Adsorption may also be favoured because the lack of experimental data regarding uranium uptake by chlorites or clays allows its invocation without too much regard for specifics. For example, published values of the uranium distribution coefficient (K_d) for kaolinite, i.e. distribution of uranium between the solution and solid absorbent vary between 10 000 (Muto *et al.*, 1965) and 2 (Langmuir, 1978). Even if the higher figure is the true one, solutions containing 100 μg U/l are unlikely to supply enough uranium by adsorption processes alone to enrich the solids up to the 1000 μg U/l observed in uraniferous chlorites.

In setting up experiments to study the adsorption preconcentration mechanisms, there is a problem of which particular chlorite or clay mineral to use. The layer silicates incorporate a range of minerals, each of which has a characteristic chemical composition and crystal lattice structure. However, adsorption is a surface phenomenon occurring at the interface between a solution and the mineral surface. Thus the total available surface area of a particular clay type mineral is the property of most significance and differences of composition and structure among layer silicates are only significant in an adsorption study to the extent that they affect mineral particle sizes and thus surface areas. O'Connor & Kester (1975) demonstrated this in a series of experiments in which the nature of the solutions containing adsorbable trace metals exerted the main chemical control upon the adsorption capacity of a range of absorbate minerals. They found that adsorption of a specific trace metal was a function of solution pH, Mg^{2+} activity, complex forming ligand activity and ionic strength. The adsorbate mineral concentration was a controlling variable, but its chemical composition was not. O'Connor & Kester suggested an adsorption model in which trace metals are adsorbed in exchange for surface-bound hydrogen ions but since the solid phase composition did not affect adsorption, they assumed that exchangeable hydrogen ions were not those bound to surface OH groups but those attached to surface adsorbed water molecules.

For this study, the mineralogically most simple of the clay minerals, kaolinite, was used, as it has the smallest surface area and thus the least effective sorption properties of all the layer silicates (Grim, 1968). A positive result for kaolinite can therefore be extrapolated to other more adsorptive layer silicates. As a first step an experiment was set up to determine a distribution coefficient for uranium between kaolinite and synthetic natural ground water, which, in the light of O'Connor & Kester's findings, had a fixed solution composition but variable pH.

DETERMINATION OF URANIUM K_d BETWEEN KAOLINITE AND SYNTHETIC NATURAL GROUND WATER

An experimental determination of K_d was undertaken using 10 ml portions of a solution (ionic strength 0.03) containing 128 mg/l NaCl, 1250 mg/l $MgSO_4.7H_20$, 85 mg/l $CaSO_4.2H_20$ and 100 μg/l U mixed with 0.01 g kaolin (Black Mountain, Canberra) in capped centrifuge tubes. Adjustments to pH were made so that solution-kaolinite mixes covered a range of pH 3.8 to 10. The ratio of 0.01 g clay to 10 ml solution (1000 mg/l) was selected on the basis of results of preliminary experiments which considered convenience of reaction mix quantities, analytical detection limits and uranium measurement ranges. O'Connor & Kester's (1975) results, which demonstrate that clay concentration in a solution-clay mix is a controlling factor on the level of trace metal adsorption, also show that above the 1000 mg/l clay-solution ratio there is no further effect on levels of trace metals adsorbed. The capped tubes were suspended for 48 h in a sonic bath in which the temperature was maintained at 25°C ± 0.5°C. The tubes were then centrifuged at 9000

rev/min for 5 min and an aliquot of each clear supernatant solution was analysed for uranium, using a Scintrex UA3 laser fluorescence analyser.

From the solution uranium contents, sorbed uranium was calculated by difference and K_d values determined for each tube. These are plotted against the pH of each mix in figure 1, which shows that uranium adsorption by kaolin was negligible below pH 5, but at higher pH values steadily increased up to pH 6.5 where the K_d reached 35 000. Above pH 6.5 the trend in K_d values was less obviously related to pH, which probably suggests the formation at higher pH levels of neutral and anionic uranium complexes, both hydroxy and possibly carbonate. In contrast to cationic UO_2^{2+} and UO_2OH^+ (stable at lower pH levels), these are not as readily adsorbed by kaolinite flakes on which the principal surface charge is negative (Van Olphen, 1963). This result casts some doubt on assumptions in ore genesis mechanisms that uranium mobilized in CO_2-rich ground waters can be immobilized by clay adsorption processes. It also provides the possible reason for the lower K_d values reported for kaolinite by Muto *et al.* (1965).

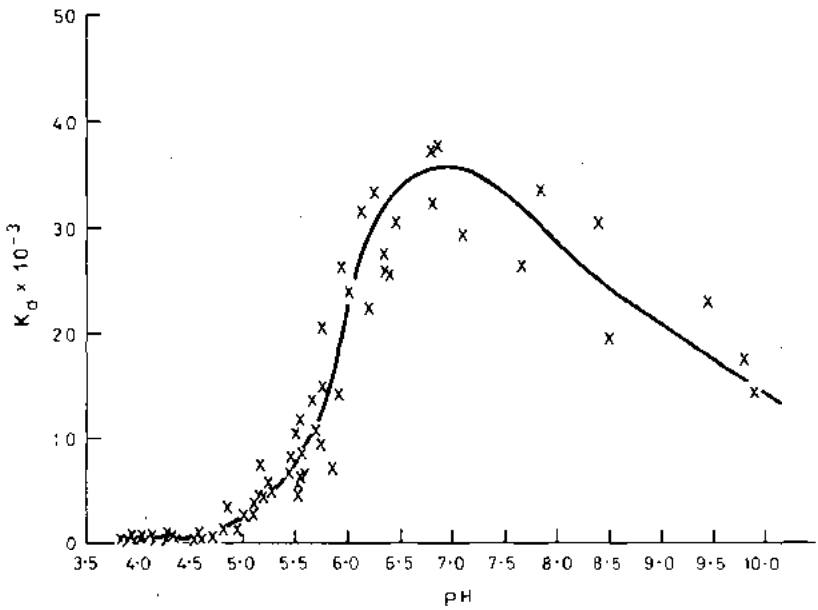


Figure 1. Variation of K_d (measured distribution coefficient of uranium between kaolin and simulated ground water) with pH at 25°C.

The maximum K_d of 35 000 established for the distribution of U between ground waters with maximum concentration of 100 μg U/l and kaolinite is still inadequate to account for enrichment of the chlorite to the 1000 μg U/g level observed at Jabiluka. Calculations from the reaction mixes indicate a uranium enrichment of the kaolinite up to 100 μg/g. Thus there are two factors that could prevent uranium enrichment of a clay up to 1000 μg/g level by adsorption processes alone: the observed natural water uranium concentration and the measured adsorption capacity of the clay, quantified by the distribution coefficient K_d.

In order to explain the distribution of uranium mineralization associated with limonites

and with mudstones containing large amounts of clay minerals, Muto *et al.* (1965) suggested a process which could overcome the above limitations, although their experiments included waters containing levels of uranium much in excess of 100 μg/l. Autoradiographs and chemical investigations demonstrated that uranium, which was previously believed to be present in the adsorbed state, was actually present as fine discrete mineral phases. Muto *et al.* (1965) speculated that discrete uranium minerals developed from uranium initially adsorbed on substrates such as clays or hydrous ferric oxides in response to changes to the chemistry of the systems, leaving the substrates free to adsorb further increments of uranium. They proposed that, over a period of time, accumulations of uranium far in excess of what could be accommodated as adsorbed species developed in intimate association with adsorbate minerals. They demonstrated the feasibility of their theory in experiments which cannot be applied directly to a mechanism which relies on a ground water source for uranium in Alligator Rivers ores, as they used solutions in which the uranium concentrations were too high. However, because their hypothesis could explain how initial adsorption of uranium could ultimately result in the 1000 μg U/g chlorite observed at Jabiluka, an experiment was designed to test its application to uranium solution concentrations which did not exceed 100 μg/l.

The Muto *et al.* (1965) hypothesis requires a sequence of uranium adsorption on to clays, followed by chemical changes which result in formation of discrete uranium minerals. Since reduction is the chemical reaction most often postulated for translating mobile

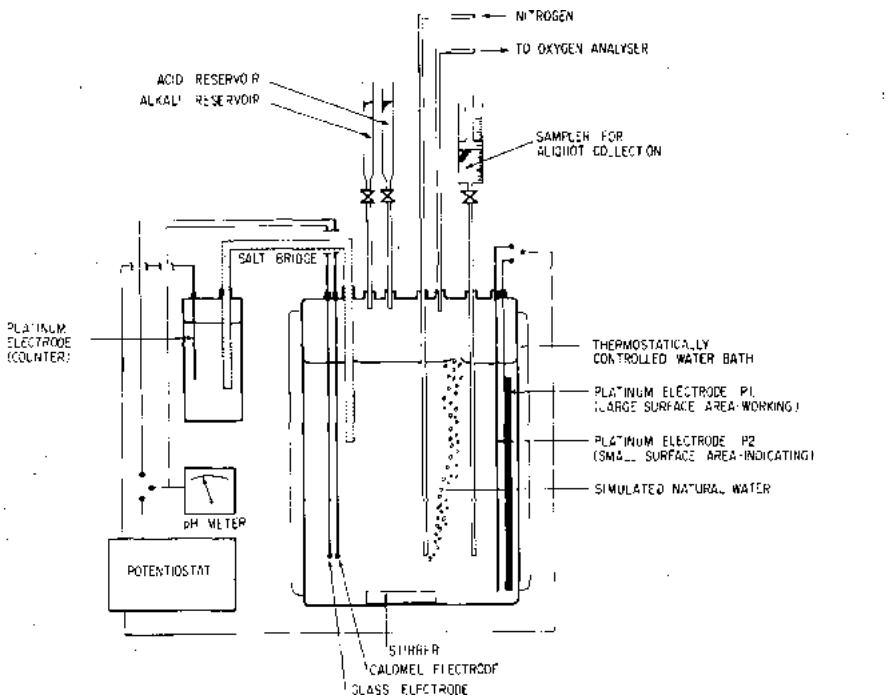


Figure 2. Diagram of apparatus used to study sequential adsorption-reduction of uranium in a kaolinite-simulated ground water system.

uranium into immobile uranium, it was decided to study the effect of lowering Eh between stages during which soluble uranium (at the 100 μg/l level) was adsorbed by kaolinite.

ENRICHMENT OF KAOLIN BY URANIUM FROM 100 μg U/l GROUND WATERS

The solution used in the K_d determinations (500 ml) and 0.5 g of the same kaolinite were contained in a reaction cell in which chemical conditions could be controlled by external pH and redox potential shifts. This solution had a low electrolyte content (ionic strength = 0.03) and simulated a non-specific natural surface water. The reaction apparatus is illustrated diagrammatically in figure 2. Throughout the experiment the temperature was maintained at 25°C ± 0.5°C and nitrogen was continuously bubbled through the cell to exclude oxygen, the presence of which would interfere with external redox control. Initially the pH was held at 6.5 (the optimum range demonstrated by K_d determinations) and the Eh at +300 mV. When analysis indicated maximum loss of uranium from the solution phase, the redox potential of the system was lowered to -100 mV. These Eh values were chosen after consideration of figure 3, which is a plot of predominant uranium species against pH and Eh using thermodynamic data published by Langmuir (1978). Figure 3 defines pH-Eh boundaries where soluble U species have concentrations equal to 24 μg/l at thermodynamic equilibrium. At pH 6.5 and Eh = +300 mV the predominant U species are soluble, whereas at pH 6.5 and Eh = -100 mV the predominant U species is crystalline uraninite. After 12 h at Eh = -100 mV a further increment of dissolved oxidized uranium was added to restore the solution uranium concentration to $\approx$ 100 μg/l and the system Eh was returned to +300 mV. At both high and low redox levels analyses of mobile uranium were made in the solution phase separated from kaolinite by centrifuging a 5 ml aliquot. The analyses were made using laser induced fluorescence measured in a Scintrex UA3 analyser. Each analyser used 1 ml and the remainder of each aliquot was returned to the reaction cell.

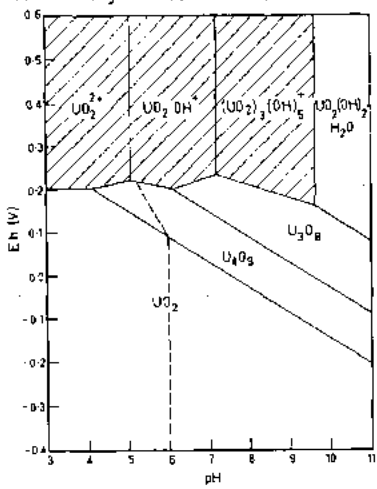


Figure 3. pH-Eh areas of predominance of some uranium species at 25°C in U-H_2O system: Shaded areas indicate regime in which concentration of soluble uranium exceeds 10^{-7} M ($\approx$ 24 μg/l) Data from Langmuir (1978).

The adsorption-reduction uranium addition sequence was repeated until sufficient of the total added uranium had been lost from the solution to enrich the kaolinite to $\approx$ 0.1% U. This occurred after 10 cycles, each one involving a uranium addition of 50 μg. At this stage, on the basis of uranium lost, the kaolinite had been enriched to 0.098% U and the apparent distribution coefficient had risen to 85 000, more than double that achieved when uranium was adsorbed by kaolinite from 100 μg/l solutions without the intermediate reduction steps. Figure 4 illustrates the steady increase in soluble uranium lost from the solution-kaolinite system during the 10 cycles of adsorption-reduction. It also shows that after each cycle the level of uranium in solution did not rise above 20 μg/l, despite additions of soluble uranium totalling 500 μg. It is inferred that the immobilized uranium was associated with the kaolinite but no evidence could be obtained as to the precise nature of this association. A scanning electron microscope (SEM) study with energy dispersive spectrometer (EDS) microanalysis did not locate any discrete concentrations of uranium, but uranium at 0.098% is below the EDS detection limit. It is, however, assumed that uranium is not present as adsorbed solutes because the calculated K_d was so much higher than the measured maximum K_d value of 35 000 (Fig. 1).

This kaolinite thus had a uranium content of the same order as that observed in uraniferous CSQ at Jabiluka (Binns, McAndrew & Sun, this volume). It is also comparable with uraniferous clays observed at the Beverley deposit in South Australia, which contain around 0.24% uranium and in which no positive identification of uranium minerals has been made, although metallurgical tests have indicated uranium present in particles 5-10 μm in size (Haynes, 1975).

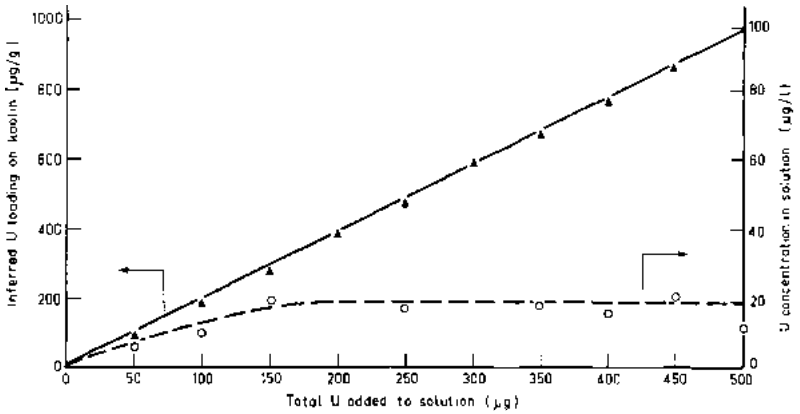


Figure 4. Plot of inferred loading of uranium on kaolinite against cumulative additions of dissolved uranium.

DISCUSSION

Accumulation of discrete uranium minerals from adsorbed uranium solutes involves at least two stages.

1) Chemical alteration of oxidized uranium ions to reduced uranium oxides.
2) Separation of these oxides as discrete phases, however minute their particle size, from the adsorption sites on the clay mineral surface.

The first stage can result from changes in the chemistry of the total system containing the solid adsorbent, such as introduction of new soluble species or changes in the concentration of those already present. In this case the adsorbent is effectively a surface catalyst at which uranium solutes react with new constituents, e.g. migrating H_2S. The chemistry of the total system may also change because physical changes in temperature and pressure alter the equilibrium concentrations of stable phases. For example, thermodynamic calculations on the uranium-water systems demonstrate that the Eh boundary between soluble U^{VI} cations and insoluble U^{IV} oxides moves to more reducing levels when temperatures rise above 25°C. Thus U^{VI} cations adsorbed at 100-150°C and Eh +150 mV would spontaneously alter to U^{IV} oxides during cooling. Alternatively, the chemistry of the bulk system may not be the same as that of the adsorbent mineral surface. For example, the redox state of carbonaceous clays would be much lower than that of oxidized surface waters transporting low levels of uranium. This deposition process is often suggested for uraniferous deposits associated with carbonaceous sediments (Haynes, 1975). Also, Binns, McAndrew & Sun (this volume) suggest graphite schists as reducing agents that could have fixed uranium from hypogene solutions at Jabiluka. These contain chlorite graphite intergrowths on the surfaces of which adsorbed U^{VI} cations could be reduced. Moreover, minute sulphide inclusions in clay particles and substituted reduced iron in clay crystal structures can produce reducing conditions in the micro environment of a clay mineral surface, despite the presence of oxidizing solutions.

Central to the concept of accumulation of discrete uranium phases in uraniferous clays is the separation after formation of reduced uranium oxides from the clay mineral surface as this frees the surface for further collection of mobile uranium. A mechanism is now proposed in which separation is activated by a change in electrostatic surface charge on uranium species when soluble cations are reduced at the clay surface to negatively charged oxide particles. The surface charge on uranium oxide particles is pH dependent; it is negative above the pH of zero surface charge (ZPC) of the oxide and positive below it. Thus if reduction occurs above the oxide ZPC then the negatively charged kaolinite surface repels the oxide, reversing the original adsorption but with the difference that the uranium is now thermodynamically a solid species with the capacity for incorporation into crystalline aggregates.

The pH at which the experimental adsorption-reduction sequences occurred was $\approx$ 6.5 which is above pH 6, the ZPC for UO_2 (Parks, 1965) and so the above mechanism could have applied. Reduction of U^{VI} cations can, however, produce oxides other than UO_2 and the ZPC of a particular uranium oxide is specific to that oxide. Between the Eh domain of the U^{IV} oxide UO_2 and the region where the U^{VI} oxide schoepite, $UO_3.2H_2O$, predominates there is a series of oxides in which the U:O ratio varies from 2 to 3. In the U:O range from 2 to 2.8, the ZPC of the oxide (i.e. pH at which the surface charge reversal occurs) varies from 6 to 3 (Parks, 1965). Thus the release of discrete uranium phases from the clay surface is controlled by the oxidation level of uranium in the oxide, and also by the system pH which determines whether the surface charge of the oxide is positive or negative. Sequential variations in either or both of these parameters will then determine whether uranium oxides accumulate as discrete minerals associated with the clay or whether they remain on the clay surface and block any further collection.

Unfortunately the boundaries for pH-Eh fields of predominance for this range of stoichiometric oxide composition are not precisely known because of the limited free energy data available. Thus a precise pH-Eh boundary cannot be predicted between uranium oxides with positive surfaces and those with negative. However some idea of the boundary location is given by the dashed line on figure 3. Because figure 3 includes U_4O_9 ($UO_{2.45}$) and U_3O_8 ($UO_{2.67}$) (free energy data from Langmuir, 1978) it provides some indication of the general trend of pH-Eh stability fields with oxide stoichiometric compositions.

The position of this boundary indicates that reduction of adsorbed uranium in clay-solution systems of pH >6 will always produce oxides with a negative surface charge, so this pH regime favours the development of uraniferous clays. This is also the regime where uranium oxides have higher oxygen levels than has UO_2. Binns, McAndrew & Sun (this volume) refer to Jabiluka uraninites comprising oxides of variable oxygen content and to the presence of anhydrite in CSQ, whereas Ypma & Fuzikawa (this volume) also infer relatively oxidizing environments in Nabarlek and Jabiluka uranium mineralization from their observations of sulphate and hematite in fluid inclusions from associated quartz and calcite. Thus the pH-Eh conditions inferred for the formation of uraniferous chlorites in the Alligator Rivers Field are compatible with accumulation of uranium minerals by the model proposed here.

This model is also consistent both with the antipathy between uraninite and sulphides observed by Binns, McAndrew & Sun (this volume) at Jabiluka, and the observations of Ferguson, Ewers & Donnelly (this volume) that reduction of U^{VI} complexes by sulphides was not an important process during the main mineralizing event in the Alligator Rivers Uranium Field. If base metal sulphides were the redox lowering control, then their complimentary oxidation would cause release of hydrogen ions to such an extent that the pH of an oxidizing sulphide system would always be below 6. According to the model proposed, reduced uranium oxides formed below pH 6 can have a positive surface charge, which would

inhibit release from the negative clay surface and thus exclude that clay from further adsorption of mobile uranium. However, during continuing infiltration of oxidizing solutions of similar redox-pH character to the original uranium transporting solution the sulphide may be dissolved altogether (possible source of anhydrite), allowing pH to rise above 6 and gradual oxidation of the sorbed oxide to a stoichiometric composition such that it would separate from the clay. Further accumulation of uranium oxides would require application of some other redox lowering mechanism, but such an accumulation would have no apparent sulphide association.

CONCLUSION

A mechanism has been proposed, and in some aspects experimentally tested, to explain the development of uraniferous clays or chlorites such as are described in studies of uranium mineralization in the Alligator Rivers Uranium Field. These minerals contain uranium at higher concentrations than can be accounted for by adsorption processes alone. It is presumed that the uranium is present as discrete phases, although these cannot necessarily be observed by physical techniques such as microscopy or SEM.

The mechanism involves

1) adsorption of soluble oxidized U^{VI} cations by negatively charged clay particles followed by
2) reduction of uranium, while attached to clay surfaces, to reduced uranium oxides which are held to or released from the negative clay surfaces on the basis of their surface charge. This is determined by
3) the oxide uranium-oxygen stoichiometry which is directly controlled by the pH-Eh conditions prevailing in the system at the time they are formed.

REFERENCES

Binns, R.A., McAndrew, J. Sun, S-S., this volume: Origin of uranium mineralization at Jabiluka. *Proceedings of the International Uranium Symposium on the Pine Creek Geosyncline.*

Eupene, G.S., Fee, P.H. & Colville, R.G., 1975: Ranger 1 uranium deposits. *in* (ed. C.L. Knight), *Economic Geology of Australia and Papua New Guinea, Australas. Inst. Min. Metall., Monograph Series No. 5, 1. Metals,* 308-317.

Ferguson, J., Ewers, G.R. & Donnelly, T.H., this volume: Model for the development of economic uranium mineralization in the Alligator Rivers Uranium Field. *Proceedings of the International Uranium Symposium on the Pine Creek Geosyncline.*

Fix, P.G., 1956: Hydrochemical exploration for uranium. *Prof. Pap. U.S. geol. Surv., 300,* 667-671.

Giblin, A.M., 1977: A study of uranium mobility in simulated natural surface waters. *M.Sc. Thesis, Macquarie University* (unpubl.).

Grim, R.E., 1968: *Clay Mineralogy,* 2nd edition (McGraw-Hill, New York) 596 p.

Haynes, R.W., 1975: Beverley sedimentary uranium orebody, Frome Embayment, South Australia. *in* (ed. C.L. Knight), *Economic Geology of Australia and Papua New Guinea, Australas. Inst. Min. Metall.,* Monograph Series No. 5, *1. Metals,* 808-813.

Hegge, M.R. & Rowntree, J.C., 1978: Geologic setting and concepts on the origin of uranium in the East Alligator River region, N.T., Australia. *Econ. Geol., 73,* 1420-1429.

Langmuir, D., 1978: Uranium solution-mineral equilibria at low temperatures with applications to sedimentary ore deposits. *Geochim. cosmochim. Acta, 42(6),* 547-569.

Lauffenberger, I., Siffert, B. & Wey, R., 1966: Incorporation of uranyl cations into silicates during formation. *Bull. Soc. chim. Fr., 5,* 1749-1753.

Muto, T., Hirono, S. & Kurata, H., 1965: Some aspects of fixation of uranium from natural waters. *Min. Geol. Tokyo, 15(74),* 287-298 (in Japanese).

O'Connor, T.P. & Kester, D.R., 1975: Adsorption of Cu and Co from fresh and marine systems. *Geochim. cosmochim. Acta, 39,* 1531-1543.

Parks, G.A., 1965: The isoelectric points of solid oxides, solid hydroxides and aqueous hydrous complex systems. *Chem. Rev., 65,* 177-198.

Van Olphen, H., 1963: *An Introduction to Clay Colloid Chemistry,* Interscience, New York.

Ypma, P.J.M. & Fuzikawa, K., this volume: Fluid inclusion studies as a guide to the composition of uranium ore forming solutions of the Nabarlek and Jabiluka deposits, N.T., Australia. *Proceedings of the International Symposium on the Pine Creek Geosyncline.*

EVAPORITES AND URANIUM MINERALIZATION IN THE PINE CREEK GEOSYNCLINE

I.H. Crick and M.D. Muir

Bureau of Mineral Resources, Box 378, Canberra City, A.C.T. 2601, Australia

ABSTRACT

Gypsum and halite pseudomorphs are found in carbonate rocks of the Coomalie and Celia Dolomites and the Koolpin and Cahill Formations in the three uranium fields of the Pine Creek Geosyncline. Their presence indicates hypersaline intertidal to supratidal depositional environments for these formations. All the evaporites survived metamorphism at ca. 1800 m.y. which reached amphibolite grade in the Cahill Formation. Evaporites were predominantly anhydrite during metamorphism and were rehydrated to gypsum during the Middle Proterozoic (Carpentarian), and later replaced by carbonates, mainly magnesite.

We suggest that the major uranium deposits were formed in a number of stages related to the complex history of these carbonates: (1) primary enrichment of uranium in evaporitic sediments; (2) extrusion of uranium-rich brines during diagenesis; (3) further release of uranium rich brines during metamorphism and (4) possibly still further releases during post-metamorphic phases. Additionally, evaporitic brines released during stages 2 to 4 scavenged uranium and other metals from surrounding sediments and basement before redepositing them along with the evaporite derived uranium. The major phase of uranium concentration in the deposits occurred during stage 4 when the evaporites were replaced by magnesite, which was associated with the formation of high magnesium chlorites

Density contrasts between the evaporites and surrounding sediments may have resulted in pre- and post-metamorphic diapirs. Some of the breccias containing uranium mineralization may have formed as a result of diapirism and/or from partial solution of the evaporites prior to their replacement by carbonates.

Base metal mineralization, commonly associated with uranium deposits in the Rum Jungle Uranium Field may have had a similar genesis. We suggest that this model may also be generally useful elsewhere in explaining the formation of metal deposits associated with replaced evaporites.

INTRODUCTION

Coarse-grained, crystalline magnesite and dolomite rocks crop out widely in the Lower Proterozoic sequence of the Rum Jungle Uranium Field (RJUF) and are also present in the Alligator Rivers Uranium Field (ARUF) N.T. The magnesite reaches refractory grades and is often associated with stromatolites (Prichard, 1976). The carbonate rocks occur in the Celia and Coomalie Dolomites in the RJUF, and in the lower Cahill Formation in the ARUF. Minor amounts are also found in the Koolpin Formation elsewhere in the Pine Creek Geosyncline. The RJUF and ARUF carbonates are closely associated with chloritized breccias and metapelites which are the usual hosts to uranium mineralization in both areas.

All the carbonate units in the four formations are about 300m thick but in the case of the Coomalie Dolomite may be considerably thicker. The Celia and Coomalie Dolomites are almost entirely composed of carbonates whereas the Koolpin and Cahill Formations contain interbedded pelites, which are carbonaceous in places. Stratigraphic relationships and more detailed descriptions of the formations are given by Needham *et al.* (this volume).

Field work on this project has involved study of all the carbonate units in Lower Proterozoic rocks in the Pine Creek Geosyncline and detailed examination of most exposures. We have examined 95 thin sections of carbonates from drill-core and outcrop from all three uranium fields in the Pine Creek Geosyncline, including drill core from the Ranger 1, Koongarra and Jabiluka deposits in the ARUF and from Mt. Fitch, Mt. Burton, Browns and Rum Jungle Creek South deposits in the RJUF. Most of the carbonate outcrop material was collected by us in 1978 and while one of us (IHC) was engaged in regional geological mapping from 1974 to 1978. Drill core thin sections from the ARUF were kindly made available to us by John Ferguson and R.S. Needham and, for the RJUF, from collections made by Kevin Johnson and W.M.B. Roberts.

DESCRIPTION AND INTERPRETATION OF ROCK TYPES

The coarse-grained carbonates have two main forms: in the majority of cases, bladed and discoidal shapes are dominant, with rarer tabular morphologies, many of which can be shown to have three cleavages at right angles (orthorhombic). Some beds however, are almost totally composed of carbonates with cubic shapes. The present rock-forming minerals are magnesite, and, less commonly, dolomite or chert. None of these minerals is cubic or orthorhombic. If the coarsely crystalline carbonates are interpreted as being metamorphic marbles, abundant, frequently disordered twin lamellae should occur in a more or less equant, anhedral grain mosaic (Fig. 1). However, the microscopic textures of the bladed carbonates bear little resemblance to those of metamorphic marble. Bladed (Fig. 2) and discoidal (Fig. 3) crystal forms, and cruciform (Fig. 4) and swallow-tail (Fig. 5) twins occur in many sections. All of the magnesite contains abundant small inclusions (Fig. 6) which, by their optical properties and X-ray micro-analysis have been identified as anhydrite. Elongate, distorted crystals (Fig. 7) are preserved as quartz in a magnesite matrix. This quartz has a form identical to that of lutecite, a variety of silica which pseudomorphs anhydrite, and the form of these crystals from the Coomalie Dolomite is identical with the shape of anhydrite crystals illustrated by Shearman & Fuller (1969, Plate 3) from the Holocene of Abu Dhabi and the Devonian Winnepegosis of Canada. The bladed and discoidal crystal forms (Figs. 2 & 3) and cruciform and swallow-tail twins (Figs. 4 & 5) are all morphologies typical of gypsum crystals which have formed interstitially in pre-existing sediments (Muir, 1979). Teepee and polygon structures indicating resurgence of groundwater have been observed in the Coomalie Dolomite near Batchelor.

The cubic forms (Fig. 8) in the magnesite of the Celia Dolomite in the RJUF contain small cubic inclusions. These contain NaCl and the original cubic mineral was most likely halite.

It seems reasonable, therefore, to interpret all of these coarsely crystalline carbonate rocks as carbonate replacements of evaporites, both sulphates and chlorides. The main carbonate mineral that has replaced the evaporites is magnesite. At White's and Dyson's mines in the RJUF, at least 300m of magnesite has been encountered in drilling in the Coomalie Dolomite, and the magnesite crops out over a strike length of 30km in both the Celia and Coomalie Dolomites (Prichard, 1976). XRD analyses of 6 specimens from an outcrop of carbonate which contains abundant gypsum pseudomorphs, of the Cahill Formation, 8km southwest of Ranger 1, showed magnesite as the major mineral present with minor to trace amounts of dolomite, calcite, quartz and chlorite. Eupene *et al.* (1975) and Rowntree & Mosher (1975) report the presence of magnesite in carbonates associated with the Ranger and Jabiluka deposits, carbonates which also contain abundant gypsum pseudomorphs.

DEPOSITIONAL ENVIRONMENT

Many of the carbonate rocks contain abundant stromatolites with a wide range of morphologies. Stratiform and domal stromatolites occur in the Celia and Coomalie Dolomites and in the Cahill Formation. Conical stromatolites which have an 'organ-pipe' appearance *(Conophyton)* occur in all three formations. The stratiform stromatolites resemble forms of algal mat which in more recent examples are characteristic of intertidal and supratidal environments, whereas the domal stromatolites are more characteristic of intertidal environments. The *Conophyton*-like forms seem generally to be associated with supratidal environments, such as pools or marshes (Walter, 1977). Gypsum casts are also found (although not abundantly) in the small, morphologically distinctive, stromatolites of the Koolpin Formation of the South Alligator Valley (Crick *et al.*, this volume), but near the



Figure 1. Metamorphic magnesite. Koolpin Formation, Burnside Granite area. Scale Bar = 3mm in all micrographs unless otherwise stated. T.S. 7680067.



Figure 2. Typical gypsum rock texture (now magnesite). Long axes of crystals parallel to bedding. Coomalie Dolomite, Mt. Fitch. T.S. 72425126.



Figure 3. Discoidal gypsum crystal (now magnesite). Porphyroblastic sub-crystals of gypsum after anhydrite (Stage V, West, 1964). Coomalie Dolomite, Batchelor. T.S. 73425793.



Figure 4. Cruciform twin. Now magnesite, but after gypsum. Lower Cahill Formation, Ranger I. T.S. 75080226.



Figure 5. Swallow tail twin. Now magnesite, but after gypsum. Koolpin Formation, Burnside Granite. T.S. 76870074.



Figure 6. Bright anhydrite relicts in magnesite. Lower Cahill Formation, Ranger I. T.S. 75080225. Scale bar = 20 m.

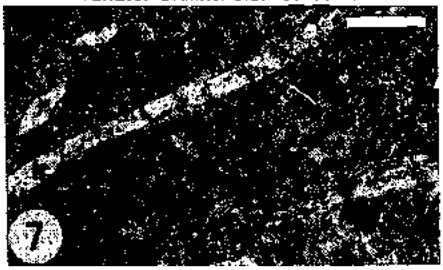


Figure 7. Lutecite crystals after anhydrite. Coomalie Dolomite, Batchelor. T.S. 74425853.



Figure 8. Magnesite casts after halite Celia Dolomite, Batchelor. Scale bar = 20mm. SEM Micrograph CD1.

Burnside Granite, where gypsum casts are common in the Koolpin Formation, no stromatolites have been found.

The palaeontological evidence indicates intertidal to supratidal environments of deposition for the Celia and Coomalie Dolomites, and lower Cahill and Koolpin Formations. This is corroborated by the evidence from associated pale non-evaporitic rocks which occur interbedded with the darker evaporites: stratiform stromatolites occur in these non-evaporitic rocks also and, in addition, cross-bedding, ripple marks, and small scour structures, all of which can be interpreted as intertidal to supratidal. Fine wisps and lenses of early diagenetic chert are preserved in all the sequences as quartz lenses parallel to bedding. It is very difficult to assess the nature of the primary carbonate minerals. By comparison with modern carbonate environments, aragonite and high-magnesium calcite would be the primary minerals.

EARLY DIAGENETIC HISTORY AND ENVIRONMENT

The morphologies of the evaporite crystal casts (Figs. 2, 3 & 7) and the cruciform twins (Fig. 4) are characteristic of gypsum and anhydrite crystals emplaced in part in unlithified sediment formed in a sabkha environment. In a sabkha, the minerals crystallise displacively from pore waters which have become saturated by evaporation from the sabka surface exceeding the replenishment rate of groundwater flow, in a region of very low rainfall. Butler (1969) has described evaporite crystal morphologies from different sabkha zones. The bladed and discoidal crystals (Figs. 2 & 3) grow in the outer flood recharge zone, and the anhydrite morphology (Fig. 7) is characteristic of the supratidal zone. Shearman & Fuller (1969) have illustrated similar crystal forms from calcitised evaporites of the Devonian of Canada, and more recently, Muir (1979) has described and interpreted identical forms from the Middle Proterozoic (Carpentarian) McArthur Group of the Northern Territory, where pseudomorphs are preserved as magnesite and siderite casts.

The halite in the Celia Dolomite appears to be diagenetic (see Neev & Emery, 1967; Muir, 1979) and must have been deposited from brine within the sedimentary pile. Randomly oriented cubic casts are set in a matrix of now slightly more siliceous dolomite or magnesite. The casts are complete six-sided cubes, and bear no resemblance to the partial casts which form after desiccation and re-solution in surface brine pools.

The sabkha environment is one where high evaporation off a submerged water table takes place from an exposed surface. The emergence indicated by this diagenetic environment indicates a regressive phase in the sedimentary column, and a cessation of deposition in the area where the evaporites are forming and this emergence is confirmed by the occurrence of teepee structures (Muir, 1979). In addition, the sub-surface depositional zone forms a mixing area for marine and continental groundwaters, giving rise to a certain flexibility in the chemistry of the evaporites produced. When evaporation reaches the point where halite begins to be deposited, the Mg/Cl ratio reaches 23.1:1 (Morrow, 1978). Peneontemporaneous dolomitisation is one result of this (Shearman, 1966), but in many cases, excess magnesium is trapped in organic matter, only to be released much later on oxidation of the organic matter (Muir, 1979).

EARLY BURIAL HISTORY

Petrological studies show that the amount of evaporite minerals emplaced in the sediment is variable. In some beds, the entire primary carbonate has been replaced and considerable thicknesses of pure gypsum/anhydrite rock must have existed (300m in the Coomalie Dolomite). Where massive gypsum is present, recrystallisation would occur as the first response to burial (Fig. 2). Where scattered crystals occur in fine-grained carbonate rocks, the outline of the initially formed gypsum discoid or anhydrite blade would be

retained even though internal recrystallisation might take place. The silicification of anhydrite to lutecite is believed to take place early in burial diagenesis (West, 1964), and is irreversible. Brines trapped within the sedimentary pile at this stage would be magnesium-rich, because all the calcium would be locked-up as solid sulphate; the brines must also be highly saline, or they would dissolve the soluble evaporite minerals, causing early collapse brecciation in the carbonate beds and overlying clastic sequences. In this latter case, no signs of evaporite pseudomorphs would be found — a situation which does not apply in the Pine Creek Geosyncline.

Initially the evaporites are much denser than the surrounding water-logged sediments, but on compaction and de-watering, the sediments become the more dense. Halite has a density of 2.16 and gypsum 2.32, while the average density of pelitic schists in the Cahill Formation is 2.76 (Tucker *et al.*, this volume). This density contrast could produce diapirism (Kupfer, 1968) of the evaporite beds, producing either salt or gypsum-cored anticlines (Blair, 1975) or piercement structures (Trusheim, 1960). Both types of structures have been described as diapirs (Murray, 1968), and although there is no evidence that large piercement structures ever existed in either the RJUF and ARUF, the lenticular and rounded shapes of many of the evaporitic bodies suggests that at least incipient diapirism may have taken place. The diapiric movement may have been initiated by contemporaneous faulting as has been suggested for the Ekofisk Field in the North Sea (Blair, 1975).

Brecciated and sheared contacts between the surrounding metapelites and the former evaporite bodies occur in the ARUF (Eupene, 1979). This could be interpreted as resulting from movement of the diapirs through compacted sediments to produce a clay-like gouge by shearing of the sediments against the salt (Hanna, 1953). Shales are commonly brecciated outwards for thousands of feet from a diapir, with the breccias grading laterally into undisturbed shale (Kerr & Kopp, 1958). Salt dome breccias have several features distinguishing them from other types of sedimentary breccia (Kerr & Kopp, 1958). Several of Kerr and Kopp's criteria appear to be applicable to the breccias associated with the evaporite bodies in the ARUF.

On continuing burial, gypsum converts to anhydrite (West, 1964) at a depth that is dependent on pressure (Murray, 1964). Anhydrite is denser than compacted sediment; at this stage diapirism would cease, and downwards movement might take place, causing further brecciation.

METAMORPHISM

The rocks in both the RJUF and ARUF were involved in the ca.1800 m.y. metamorphic event (Page *et al.*, this volume) which reached amphibolite grade in the Cahill Formation (Smart *et al.*, 1976). Anhydrite is stable up to temperatures exceeding 1000°C, and survives amphibolite and granulite facies metamorphism (Zimmer, 1947, Scherbanj & Shirokokh, 1970; Leake *et al.*, 1979). The diapiric bodies and associated breccias were sealed in relatively impermeable surrounding sediment, and were protected from invasion by (possibly less saline) metamorphic fluids.

Scapolite has been reported from a number of localities in the amphibolite grade rocks of the Cahill Formation (Ferguson, this volume). Scapolite-bearing metasediments are the products of high-grade metamorphism of evaporites (Ramsay & Davidson, 1970; Serdyuchenko, 1975). It represents a metamorphic concentration of the more volatile elements — Ca, Na, Cl, SO_4, CO_3 and F can all be fixed within scapolite crystals.

POST-METAMORPHIC HISTORY

After the ca. 1800 m.y. metamorphic event, erosion removed considerable thicknesses of metasediment, bringing the evaporite bodies back near to the surface before deposition of

the Kombolgie Formation (at about 1650 Ma., Page *et al.*, this volume). This near-surface region is subject to the influence of meteoric groundwater and during this period, the anhydrite was rehydrated to gypsum. West (1964) illustrates a number of textures associated with rehydration and figure 3 shows porphyroblastic gypsum growing within the crystal boundaries of a primary gypsum discoid (as in West's (1964) Stage V). Numerous anhydrite relicts, in the form of small orthorhombic cleavage flakes, remain in the rehydrated gypsum (Fig. 6). This secondary gypsum is again less dense than the surrounding metasediments and further diapiric movement can take place causing more brecciation and shearing near the contact with the enclosing metasediments. Loading, due to deposition of the Kombolgie Formation, would be sufficient to initiate this second diapiric phase. Eupene (1979) describes a mylonitic gouge at Ranger in the ARUF which may be related to this phase of movement.

The final stage of this history of the evaporites is the replacement of both sulphates and chlorides mainly by magnesite. Large magnesite bodies which replace evaporites are known from several parts of the world, including Siberia (Shcherbakov & Poleatev, 1977) and India (Raha, 1975). The timing of this replacement in the Pine Creek Geosyncline is difficult to assess. The replacement must have been related to changes in groundwater chemistry, and possibly temperatures, and may have begun immediately after the completion of rehydration of the anhydrite, when excess water in the groundwater system would start to leach and replace the gypsum.

The late-stage post-metamorphic chlorites observed in the ore zones of the ARUF (Eupene, 1979) and in sediments overlying the Coomalie Dolomite in the RJUF (Berkman, 1970) are probably related to this final stage. Excess magnesium involved in the conversion of the evaporites to magnesite, derived from surrounding evaporitic sediments, may have also assisted in the conversion of pelitic sediment in the breccias to high magnesium chlorite. Medium to high magnesium chlorites are found in the breccia matrix of the major deposits in the ARUF with iron-rich chlorites, except in the Ranger breccias, where only high magnesium chlorites were found (Ewers & Ferguson, this volume). High magnesium chlorites, formed under burial metamorphic conditions, are reported in the Ringwood evaporites of the Amadeus Basin (Stewart, 1979).

Page *et al.* (this volume) consider that chloritization took place about 1600 m.y. ago under rather low temperature conditions at Jabiluka and Nabarlek. Late-stage growth of secondary sericite and chlorite less than 920 m.y. ago has been reported from Nabarlek (Page *et al.*, this volume). Some replacement of the evaporites mainly by magnesite in the ARUF and possibly the RJUF probably took place about 1600 m.y. ago, probably after the deposition of the Kombolgie Formation at 1650 m.y. (Page *et al.*, this volume).

Magnesium is abundant in evaporitic sequences (Morrow, 1978) and the magnesium required for conversion of much of the Pine Creek Geosyncline evaporites to magnesite and for formation of the high magnesium chlorites, could reasonably have been derived from the evaporitic sediments.

VADOSE AND PHREATIC ENVIRONMENTS

At some time after the replacement of evaporites by secondary carbonates, uplift and erosion affecting the Kombolgie Formation and Buldiva Sandstone and underlying sediments caused the rocks to come into the phreatic and vadose zones. Some of the carbonates in the Coomalie Dolomite exposed near Batchelor exhibit typical solution features in joints, along with coarsely recrystalline magnesite which coats present joint surfaces. These late carbonate solution features are quite distinct from the teepee structures described earlier in that they are not polygonal but follow local joint patterns, and the reprecipitated carbonates have normal carbonate crystal morphologies.

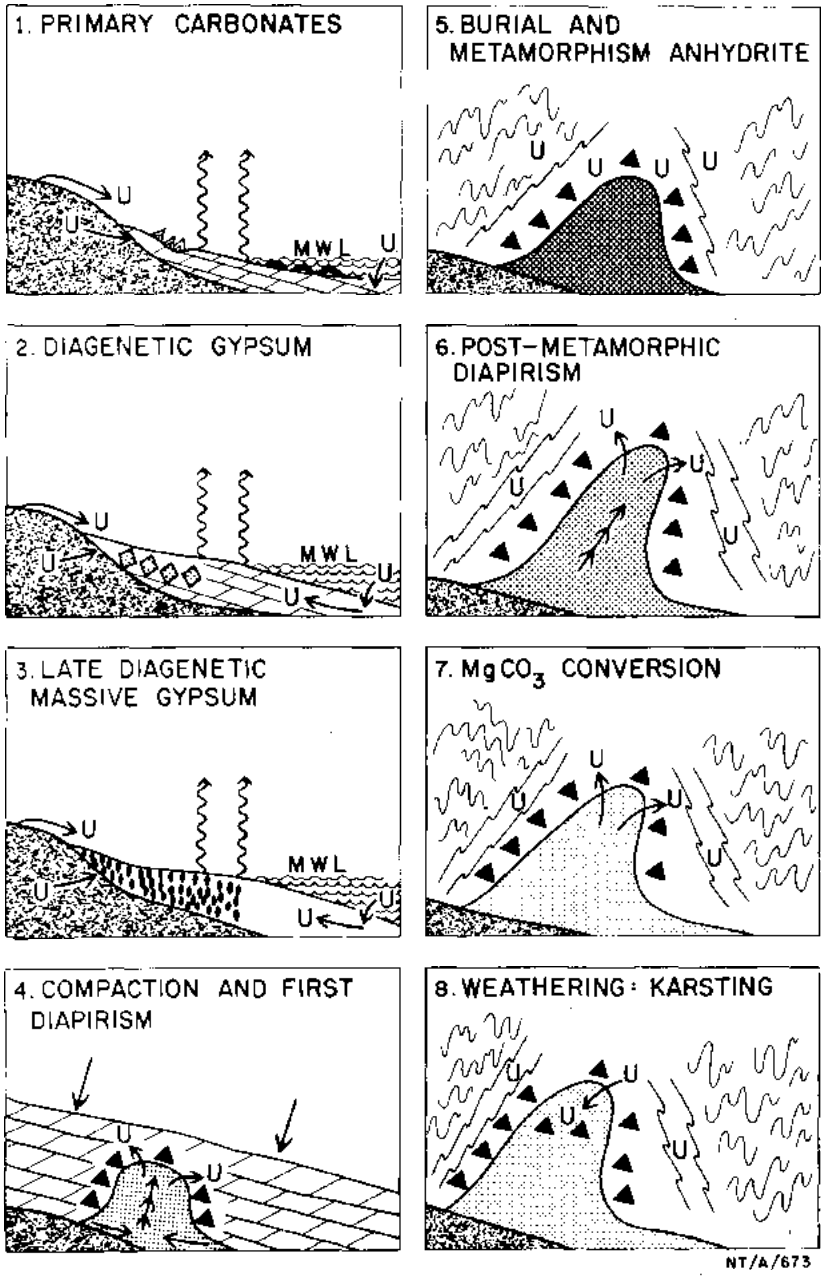


Figure 9. Stages in the development of the uranium deposits in the Alligator Rivers and Rum Jungle Uranium Fields, Pine Creek Geosyncline.

URANIUM ORE GENESIS

The proximity of the former evaporites in the Coomalie Dolomite and Cahill Formation to the uranium deposits of the RJUF and ARUF suggests a genetic relationship. Brines produced from partial solution and replacement of the evaporites, and carbonate rich waters involved in replacing the evaporites would all make potentially very good leaching agents capable of transporting large quantities of uranium. (Dunsmore 1975).

The history of these former evaporites indicates that brines were produced episodically and thus the process of formation of the deposits may have been cumulative. Polyphasic release of brines has been demonstrated for base metals in the Elk Point Basin of Saskatchewan by Thiede & Cameron (1978) and sequential deposition of sulphides in fractures also occurs (Sibson *et al.*, 1975).

Uranium enriched brines produced by evaporation (Dunsmore, 1977) would also have been important, and the production of fractures and breccias through movement of the evaporites may have provided suitable structural traps for at least some of the uranium.

We recognise a number of events, closely associated with the history of the former evaporites in the Pine Creek Geosyncline, which cumulatively could have led towards uranium mineralization and concentration to ore grades (summarised in figure 9).

a) Uranium concentrations

The original source of the uranium in ore deposits in this area is likely to be the Archaean basement which contains about 12 ppm uranium (Ferguson *et al.*, this volume). The uranium was transported, mainly in solution, via surface and groundwater flow to depositional basins. Chemical sediments in the basins incorporated some amount of these metals within crystal lattices, and interstitially. If any of the metals occurred in the basement in a form that could physically survive erosion and surface transport, then detrital, placer deposits might be expected. Biological activity in the form of prolific algal growth, is a potent agent for concentrating and stabilizing by complexing of soluble metals, such as for example, gold, uranium and thorium, and in the RJUF and ARUF there is considerable evidence for biological activity in the form of the abundant stromatolites.

During the evaporitic sabkha phase, there were further influxes of metal-bearing groundwater, of both continental and marine origin. Evaporation during this phase would permit large amounts of metals to be concentrated either within the evaporite crystal lattices, or interstitially. In the high supratidal zones of an arid sabkha, evaporation eventually reaches the point where potassium minerals (sylvite, polyhalite) start to precipitate with anhydrite and halite (Butler, 1979). Dunsmore (1975) has calculated that at this point, the concentration of uranium in solution in evaporitic brine increases some 18 times. If the brines had a normal marine value of 3.2 ppb this would result in a brine containing about 60 ppb uranium (c.f. 12-46 ppb for groundwater emerging from volcanic and tuffaceous sedimentary terranes (Denson *et al.*, 1956)). Uranium concentrated in brines by this process in the RJUF and ARUF would have had values in excess of 60 ppb as probably much higher concentrations of uranium would have initially been in solution through leaching of the anomalously enriched Archaean basement rocks.

During the early stages of burial diagenesis, the influx of metals in continental groundwater continued into the compacting evaporites. Interstitial halite may be dissolved from sulphate rocks (Shearman & Fuller, 1979) providing a secondary porosity for brine trapping concentration of metals. Fluid inclusion studies by Ympa & Fuzikawa (this volume) indicate highly concentrated trapped brines in the carbonates and cherts of the Cahill Formation.

b) Mobilization of uranium

Differences in densities between the evaporites and surrounding sediments during the early stages of diagenesis may have resulted in movement of the evaporites perhaps to the

extent that diapirs were formed. Any physical movement of the evaporites at this stage would result in extrusion of some of the trapped uranium enriched brines into surrounding sediments into fractures and any diapiric breccias formed by this movement, a process similar to that proposed by Dunsmore (1977) for uranium emplacement in the Pictou Group of Nova Scotia and elsewhere.

Conversion of gypsum into anhydrite during a later stage of burial diagenesis released waters of crystallization and more of the trapped uranium enriched brines. Metamorphism and folding of the evaporites at about 1800 m.y. again released connate uranium enriched brines and any residual waters of crystallization.

Alkaline brines were produced by partial solution of the evaporites during burial diagenesis, metamorphism and folding. All these brines were efficient scavengers of uranium and transported uranium to suitable chemical-structural traps where it precipitated. Similar brines were also produced during the rehydration of anhydrite to gypsum after the 1800 m.y. metamorphic event.

Once sufficient volumes of anhydrite had been rehydrated to gypsum, density contrasts between the gypsum beds and surrounding metasediments would again be present and further diapiric movement may have occurred. Any residual, trapped, uranium enriched brines would be released at this stage and partial solution around the edges of the diapirs would produce alkaline brines. Movement of the evaporite beds may have given rise to further fracturing or diapiric breccias and created new structural traps for the emplacement of uranium.

The major stage of brine release took place when the evaporites were finally replaced by carbonates, mostly magnesite. It is probable that the high magnesium chlorites (Ewers & Ferguson, this volume) were also formed at this stage. Magnesium and carbonate-rich fluids responsible for replacement of the evaporites and formation of the high magnesium chlorites, and brines formed from the evaporites as their replacement proceeded, more than likely leached and transported or remobilized existing concentrations of uranium in the surrounding metasediments. The volumes of both types of brines produced at this stage would have been considerable, as the evaporites were virtually totally replaced.

Uranium mineralization is intimately associated with chlorites especially high-magnesium chlorites at Ranger (Ewers & Ferguson, this volume) suggesting that most of the ore-bodies were formed at this stage in the history of the evaporites. Chloritization of breccias and metasediments in the ARUF is a late-stage post-metamorphic event (Eupene, 1979) dated at about 1600 m.y. (Page *et al.*, this volume), a date consistent with some lead isotope ages of sulphides and rocks at Jabiluka (Gulson & Mizon, this volume).

The carbonates which replaced the evaporites would have been subject to solution processes resulting in typical solution features as observed in the Coomalie Dolomite. Further mobilization of uranium may have taken place at this stage, aided by the presence of bicarbonate ions, and still be taking place today. Replacement of the evaporites by carbonates may have been a lengthy process and overlapped with this last stage.

AGE OF URANIUM DEPOSITS IN THE ALLIGATOR RIVERS URANIUM FIELD

Uranium/lead and lead istope ages from mineralization in deposits in the ARUF (Hills & Richards, 1976; Gulson & Mizon, this volume) are widely scattered but are all less than 1800 m.y. A post-metamorphic event or events are therefore largely responsible for the formation of these deposits. It is difficult to derive any satisfactory single age or groups of ages, although Gulson & Mizon (this volume) consider a lead isotope age of 1380 ± 110 m.y. for sulphide lenticles at Jabiluka as possibly indicating the time of uraninite mineralization. In our model we suggest that copious brines were produced when the evaporites were replaced by magnesite and were largely responsible for the formation of the ores, an event we

link with the formation of high magnesium chlorites formed at about 1600 m.y. The discrepancy in ages between the formation of chlorites and sulphide lenticles at Jabiluka may indicate separate events or alternatively, the process of replacement of the evaporites may have taken a considerable time and perhaps proceeded only in stages. Essentially, the replacement of the evaporites by carbonates stands out as one of the major brine-producing events in the history of the former evaporites, although brines were produced at different times, probably in smaller amounts, before, during and after the 1800 m.y. metamorphic event. We suggest that the present deposits are the product of a series of events which cumulatively led to their formation, with a major stage in their formation being related to the time when the evaporites were replaced by carbonates.

FURTHER IMPLICATIONS

The model we have proposed for most of the uranium mineralization in the Pine Creek Geosyncline with the exception of the South Alligator Valley Uranium Field (see Crick *et al.*, this volume), may also explain the presence of other metals associated with these deposits, particularly in the RJUF. Copper mineralization is associated with uranium at Mount Burton and White's deposits and the latter also contains cobalt, nickel and lead. The Intermediate deposit near White's was mined for copper only and several prospects in this area contain lead, lead-copper or lead-zinc mineralization (Fraser, this volume). Mineralization in the Woodcutters lead-zinc prospect is present in near-vertical fissures in the axial part of an anticline containing a carbonate core of Coomalie Dolomite (Roberts, 1973), a structure which, using our model, may have formed by incipient diapirism.

Copper, as well as uranium, can be concentrated in evaporites (Rose, 1976; Dunsmore, 1977), and evaporite brines are efficient leaching agents of a wide range of metals. In the RJUF it seems probable that brines, generated from the former evaporites in the Celia and Coomalie Dolomites played a role in this mineralization at a number of times, but particularly during their replacement by magnesite.

Our model may also prove generally useful in explaining mineralization in rocks associated with replaced evaporites. The wholesale replacement by carbonate (mainly by magnesite) of large amounts of evaporites in the Pine Creek Geosyncline is not a unique phenomenon. Recognition of massive replacement of evaporites in rocks elsewhere (e.g. in the McArthur Basin; Muir, 1979), indicates that similar replaced evaporites may be found elsewhere in the world. In particular, carbonates associated with the Rabbit Lake uranium deposits in the Athabasca Basin in Canada, which Sibbald (1977, 1978) interprets as having an evaporitic origin because of their high sodium content, appear from his descriptions to be similar to the carbonates containing evaporite pseudomorphs of the Pine Creek Geosyncline.

ACKNOWLEDGEMENTS

The authors publish with the permission of the Director, Bureau of Mineral Resources, Geology and Geophysics, Canberra. One of the authors (IHC) gratefully acknowledges the assistance given to him in the field by Mr. M.J. Roarty (N.T. Geological Survey), and we both thank Mr. M.J. Jackson for field assistance and helpful discussion.

REFERENCES

Berkman, D., 1970: Geology of the Rum Jungle uranium deposits. *Atom. Energy, Sydney, 13*, 12-22.

Blair, D.G., 1975: Structural styles in North Sea Oil & Gas Fields *in* (ed. A.W. Woodland) *Petroleum and the Continental Shelf of North-West Europe. Volume I. Geology*. 327-334. Institute of Petroleum, B.B., Applied Science Publishers, Ltd., Barking, England.

Butler, G.P., 1969: Modern evaporite deposition and geochemistry of coexisting brines, the Sabkha, Trucial Coast, Arabian Gulf. *J. sedim. Petrol., 39*, 70-89.

Crick, I.H., Muir, M.D., Needham, R.S. & Roarty, M. J. this volume: The geology and mineralization of the South Alligator Valley Uranium Field. *Proceedings of the International Uranium Symposium on the Pine Creek Geosyncline.*

Denson, N.M., Zeller, H.D. & Stephens, J.G., 1956: Water sampling as a guide in the search for uranium deposits and its use in evaluating widespread volcanic units as potential source beds for uranium. *Prof. Pap. U.S. geol. Surv., 300*, 673-680.

Dunsmore, H.E., 1975: Origin of lead-zinc ores in carbonate rocks: a sedimentary-diagenetic model. *Ph.D. Thesis, Imperial College, University of London* (unpubl.)

Dunsmore, H.E., 1977: A new genetic model for uranium-copper mineralization, Permo-Carboniferous basin, Northern Nova Scotia. Report of Activities, Part B. *Geol. Surv. Pap. Can., 77-1B*, 247-253

Eupene, G.S., 1979: Stratigraphic, Structural and Temporal Control of Mineralization in the Alligator Rivers Uranium Province, Northern Territory, Australia. *in* (ed. J.D. Ridge) *Proceedings of the Fifth International Symposium on the Genesis of Ore Deposits, Snowbird, Utah, August, 1978* (in press).

Eupene, G.S., Fee, P.H. & Colville, R.G., 1975: Ranger 1 uranium deposits. *in* (ed. C.L. Knight) *Economic Geology of Australia and Papua New Guinea, Australas. Inst. Min. Metall., Monograph Series No. 5, 1, Metals*, 308-317.

Ewers, G.R., & Ferguson, John, this volume: Mineralogy of the Jabiluka, Ranger, Koongarra and Nabarlek uranium deposits. *Proceedings of the International Uranium Symposium on the Pine Creek Geosyncline.*

Ferguson, J., this volume: Metamorphism on the Pine Creek Geosyncline and its bearing on Stratigraphic relationships. *Proceedings of the International Uranium Symposium on the Pine Creek Geosyncline.*

Fraser, W.J., this volume: Geology and exploration in the Rum Jungle Uranium Field. *Proceedings of the International Uranium Symposium on the Pine Creek Geosyncline.*

Fyfe, W.S., Price, N.J. & Thompson, A.B., 1978: Fluids in the earth's crust. *Developments in Geochemistry, 1*, 1-383. Elsevier Scientific Publishing Company, Amsterdam.

Gulson, B.L. & Mizon, K.J., this volume: Lead isotope studies at Jabiluka. *Proceedings of the International Uranium Symposium on the Pine Creek Geosyncline.*

Hanna, M.A., 1953: Fracture Porosity in Gulf Coast. *Bull. Am. Ass. Petrol. Geol., 37*, 266-281.

Hills, J.H. & Richards, J.R., 1976: Pitchblende and Galena Ages in the Alligator Rivers Region, Northern Territory, Australia. *Miner. Deposita, 11*, 133-154.

Kerr, P.F., & Kopp, O.C., 1958: Salt Dome Breccia. *Bull. Am. Ass. Petrol. Geol., 42*, 548-560.

Kupfer, D.H., 1968: Relationship of internal to external structure of salt domes. *Mem. Am. Petrol. Geol., 8*, 79-89

Leake, B.E., Farrow, C.M. & Townend, R., 1979: A pre-2000 m.y. old granulite facies metamorphosed evaporite from Caraiba, Brazil. *Nature, Lond., 277*, 49-50.

Morrow, D.W., 1978: The influence of the Mg/Ca ratio and salinity on dolomitisation in evaporite basins. *Bull. Can. Petrol. Geol., 26*, 389-392.

Muir, M.D., 1979: A sabkha model for deposition of part of the Proterozoic McArthur Group of the Northern Territory, and implications for mineralization. *BMR J. Aust. Geol. Geophys., 4*, 149-162.

Murray, G.E., 1968: Salt structures of Gulf of Mexico Basin — a Review. *in* (eds. J. Braunstein & G.D. O'Brien), Diapirism and Diapirs, Mem. Am. Ass. Petrol. Geol., 8, 99-121.

Murray, R.C., 1964: Origin and diagenesis of gypsum and anhydrite. *J. Sedim. Petrol., 34*, 512-23.

Needham, R.S., Crick, I.H. & Stuart-Smith, P.G.; this volume: Regional Geology of the Pine Creek Geosyncline. *Proceedings of the International Uranium Symposium on the Pine Creek Geosyncline*

Neev, D. & Emery, K.O., 1967: The Dead Sea. *Bull. geol. Surv. Israel, 41*, 1-144.

Page, R.W., Compston, W., & Needham, R.S., this volume: Geochronology and evolution of the late Archaean basement and Proterozoic rocks in the Alligator Rivers Uranium Fields, Northern Territory, Australia. *Proceedings of the International Uranium Symposium on the Pine Creek Geosyncline.*

Prichard, C.E., 1976: Magnesite — Northern Territory. *in* (ed. C.L. Knight) *Economic Geology of Australia and Papua New Guinea, Australas. Inst. Min. Metall., Monograph Series No. 5, 4. Industrial Minerals and rocks*, 222-223.

Raha, P.K., 1975: Crystalline magnesite deposit in Jammu Limestone, near Katra, Jammu — its nature and origin. *Indian Miner., 29*, 18-24.

Ramsay, C.R. & Davison, L.R., 1970: The origin of scapolite in the regionally metamorphosed rocks of Mary Kathleen, Queensland, Australia. *Contrib. Mineral. Petrol., 25*, 41-51.

Roberts, W.M.B., 1973: Dolomitization and the genesis of the Woodcutters Lead-Zinc Prospect, N.T., Australia. *Miner. Deposita, 8*, 35-56.

Rose, A.W., 1976: The effects of cuprous chloride complexes in the origin of red-bed copper and related deposits *Econ. Geol., 71*, 1036-1048.

Rowntree, J.C. & Mosher, D.V., 1975: Jabiluka Uranium Deposits. *in* (ed. C.L. Knight). *Economic Geology of Australia and Papua New Guinea, Australas. Inst. Min. Metall., Monograph Series No. 5, 1, Metals*, 321-326.

Scherbanj, I.P. & Shirokikh, I.N., 1970: Thermodynamical and experimental data on the stability of gypsum, semihydrate and anhydrite under hydrothermal conditions. *Geolog. i. Geophis., 9*, 102-105, Norosibirsk.

Serdyuchenko, D.P., 1975: Some Precambrian scapolite-bearing rocks evolved from evaporites. *Lithos, 8*, 1-7.

Shcherbakov, A.F. & Poletaev, I.A., 1977: Magnesite ore of the Sarina Deposit. *Litologia i Poleznye Iskopaemye, 6*, 140-143.

Shearman, D.J., 1966: Origin of marine evaporites by diagenesis. *Trans. Instn Min. Metall. (Applied Earth Sciences), B75*, 208-215.

Shearman, D.J. & Fuller, J.C., 1979: Anhydrite diagenesis, calcitization, and organic laminites, Winnepegosis Formation, Middle Devonian, Saskatchewan. *Bull. Can. Petrol. Geol., 17*, 469-525.

Sibbald, T.I.I., 1977: Uranium Metallogenic Studies: I Rabbit Lake, Geology. *in* (eds. J.E. Christopher & R. MacDonald) *Summary of Investigations 1977. Sask. Geo. Surv. Misc. Rep.*, 111-123.

Sibbald, T.I.I., 1978: Uranium metallogenic studies: Rabbit Lake, Geology. *in* (eds. J.F. Christopher & R. MacDonald) *Summary of Investigations 1978, Sask. Geo. Surv. Misc. Rep.*, 56-60.

Sibson, R.H., Moore, J.McM. & Rankin, A.H., 1975: Seismic pumping — a hydrothermal fluid transport mechanism. *J. geol. Soc. Lond., 131*, 653-659.

Smart, P.G., Wilkes, P.G., Needham, R.S. & Watchman, A.L., 1976: Geology and Geophysics of the Alligator Rivers Region. *in* (ed. C.L. Knight) *Economic Geology of Australia and Papua New Guinea, Australas. Inst. Min. Metall., Monograph Series No. 5, 1. Metals*, 285-301.

Stewart, A.J., 1979: A barred-basin marine evaporite in the Upper Proterozoic of the Amadeus Basin, central Australia. *Sedimentology, 26*, 33-62.

Trusheim, F., 1960: Mechanism of salt migration in northern Germany. *Bull. Am. Ass. Petrol. Geol., 44*, 1519-1540.

Thiede, D.S. & Cameron, E.N., 1978: Concentration of heavy metals in the Elk Point Evaporite Sequence, Saskatchewan. *Econ Geol., 73*, 405-415.

Tucker, D.H., Hone, I.G. & Sampath, N., this volume: The characteristics and interpretation of regional gravity, magnetic and radiometric surveys in the Pine Creek Geosyncline. *Proceedings of the International Uranium Symposium on the Pine Creek Geosyncline*, 206-208.

Walter, M.R., 1977: Interpreting stromatolites. *Am Scient., 65*, 563-571.

West, I.M., 1964: Evaporite diagenesis in the Lower Purbeck Beds of Dorset. *Proc. Yorks. geol. Soc., 34*, 315-330.

Ypma, P.J.M. & Fuzikawa, K., this volume. Fluid inclusion studies as a guide to the composition of uranium ore forming solutions of the Nabarlek and Jabiluka deposits N.T., Australia. *Proceedings of the International Uranium Symposium of the Pine Creek Geosyncline*.

Zimmer, P.W., 1947: Anhydrite and gypsum in the Lion Mountain magnetite deposit of the north-eastern Adirondacks. *Am. Miner., 32*, 647-653.

ORIGIN OF URANIUM MINERALIZATION AT JABILUKA

R.A. Binns, J. McAndrew and S-S. Sun

CSIRO Division of Mineralogy, P.O. Box 136, North Ryde, NSW, 2113, Australia.

ABSTRACT

Petrological, mineragraphic, and isotopic investigations of drill core samples from the Jabiluka Two uranium deposit indicate a prominent role for hydrothermal fluids, with comparatively high initial temperatures (300°-350°C), in the main mineralization episode. The Cahill Formation host sequence of former amphibolite facies metasedimentary schists shows pronounced retrogressive alteration for distances exceeding 200m from ore. Mineralization is associated with vein and breccia structures characterized by abundance of fine-grained uraniferous chlorite-septechlorite-quartz (CSQ) intergrowths as the dominant gangue and as replacements of rock fragments and immediately adjacent wall rocks. Uraninite, the principal ore mineral, formed relatively late in the mineralization sequence, by replacement of CSQ in particular. Coffinite and brannerite also occur, as replacements in breccia clasts and wall rock. Thucholite is a rare phase.

The chlorite-dominated alteration halo surrounding mineralization also extends into the unconformable Kombolgie Formation sandstone cover sequence. During hydrothermal fluid activity, potassium was transported upwards from Jabiluka ore zones to form overlying bodies of sericite-rich rocks resembling greisen.

Replacement processes or deposition during brecciation and opening of veins dominate the ore structures, which lack clear evidence of open space filling. The latter is more pronounced in a suite of barren, post-uraninite drusy veins containing crystalline quartz, carbonates, and sulphides. Hydraulic fracturing associated with introduction of mineralizing fluids is the suggested mechanism for creation of the uraninite-bearing veins and breccias. Declining temperatures, and reduction of fluids by reaction with graphite schists governed deposition of uraniferous CSQ and probably also of uraninite. Stable isotope data indicate a deep-seated source for the initial mineralizing fluids, which were possibly modified by mixture with surface water towards the closing stages of the ore-forming episode.

Remobilization from country rocks during their polymetamorphic alteration does not explain the uranium content of the ores. Supergene sources are not compatible with ore characteristics including their structures and the indicated depositional temperatures for uraniferous CSQ. A hypogene souce is favoured, preference being assigned to granitic gneisses, which carry partly altered primary uraninite, within the reactivated Archaean Nanambu Complex underlying Jabiluka. It is postulated that the deposit is located in the upwelling discharge zone of a large fluid convection cell penetrating these source rocks and probably initiated by radiogenic heat within them. Fracturing due to epeirogenic movements associated with deposition of the Kombolgie Formation sandstone, or with its subsequent faulting, is suggested as a reason why the mineralization episode was deferred until the 1550-1400 m.y. age period indicated by available geochronological data.

INTRODUCTION

Effective exploration for uranium deposits in the Pine Creek Geosyncline, or in similar environments elsewhere, requires sound genetic models for known ore occurrences. In the Alligator Rivers Uranium Field (ARUF) a major constraint to understanding the origin of mineralization is imposed by the scarcity of surface exposure and the present lack of mine workings. Between the broad regional setting and features observable in drill core there are few crucial data such as, for example, are necessary to assess possible structural controls of ore location. Great reliance must therefore be placed on microscopic, geochemical, and isotopic characteristics of ores and their host rocks.

The following remarks derive from a study of drill hole intersections of the Jabiluka Two deposit and its environment, chosen to illustrate general features described by Rowntree & Mosher (1975), Hegge (1977) and Hegge & Rowntree (1978). Drill holes L153V, S180V and M096V were the main source of material, covering the deposit to a depth of about 300m below the Kombolgie unconformity (see figure 1 of Ryall & Binns, this volume). In addition, core samples to illustrate specific features were provided from other parts of the deposit by geologists of Pancontinental Mining Limited.

GEOLOGICAL SETTING OF MINERALIZATION

The Jabiluka uranium deposits occur within the deformed and metamorphosed Lower Proterozoic Cahill Formation, in close proximity to an upper, sharply defined unconformity

overlain by flat-dipping Middle Proterozoic Kombolgie Formation sandstone, and above an older, modified unconformity underlain by the remobilized Archaean Nanambu Complex. Their geological characteristics are described in the references cited above, and mineralization throughout the ARUF has been reviewed by Ryan (1979), Eupene (in press), and Hegge *et al.* (this volume). Further details of the regional setting and geochronology are given by Needham & Stuart-Smith (this volume) and Page *et al.* (this volume) respectively. Salient features of the Jabiluka host rocks are summarized below from Binns *et al.* (this volume).

The mineralized sequence is dominated by psammitic, pelitic and graphitic schists, with lesser marble and rare quartzite and amphibolite. These rocks underwent sillimanite-grade, amphibolite facies metamorphism (*ca* 600°C, 5kb) towards the close of an intense episode of polyphase deformation. Complexly transposed microstructures suggest that detailed stratigraphy may not be resolvable. Synkinematic or synmetamorphic quartz veins occur in the schists, but there are no migmatites. Relatively undeformed pegmatites and occasional aplites intrude the sequence.

A pervasive retrogressive metamorphism* to greenschist facies assemblages is characteristic of the mineralized environment. Chloritization of biotite and garnet, replacement of sillimanite by white mica, and alteration of feldspars to very fine grained chlorite-septechlorite-white mica aggregates have generally proceeded to completion in schists within at least 200m of ore. The pegmatites were similarly altered. Replacement of dolomite by magnesite is the equivalent alteration in marbles. This retrogression occurred under essentially static conditions: without assistance by deformation, highly reactive acid fluids - sufficiently reduced to allow preservation of graphite and sulphide - have soaked and altered the former high grade schists for considerable distances without significantly disturbing their earlier metamorphic fabric. Temperatures in the vicinity of 300°-350°C are suggested by mineral assemblages, particularly the coexistence of chlorite and septechlorite (Nelson & Roy, 1958). Fluctuations in K and Mg activity are indicated by complexly zoned chlorite-septechlorite-white mica pseudomorphs. The retrogressive metamorphism was distinctly allochemical, in particular involving introduction of Mg and removal of Na, Ca and P.

Within about 1 metre of ore zones at Jabiluka Two, the immediate host schists show even more thorough replacement by chlorite-septechlorite aggregates. Former quartz and muscovite have been attacked as well as other phases. These rocks are relatively enriched in uranium (>100 ppm), which resides mainly in chlorite-septechlorite intergrowths, and are depleted in potassium due to diminished sericite contents and the chloritization of relic muscovite.

'Greisen'-like rocks rich in muscovite and/or sericite, and with variable development of metasomatic quartz porphyroblasts, are prominent above uraninite ores at Jabiluka Two. Their coarser muscovites may be relics from the high grade regional metamorphism (Riley *et al.*, this volume), but their fine sericite represents potassic replacement of other minerals including quartz. They were derived from a variety of pelitic and psammitic schists. Boundary relationships at the metasomatic front indicate that sericites in both 'greisens' and 'normal' retrogressed schists were coeval.

The Kombolgie Formation sandstone overlying Jabiluka Two, and the 1-2 metre regolith in formerly weathered schists immediately below the unconformity, have also been metamorphosed. Decussate chlorite-sericite aggregates replace sandstone matrices or weathering products respectively, and in drill hole intersections through the unconformity

* This might be considered to constitute a large wall-rock alteration halo about mineralization. However, the term 'retrogressive metamorphism' is preferred, to avoid prejudging such a genetic relationship, to emphasize its unusual extent, and to distinguish it from more intensive alteration closer to ore.

zone these appear contiguous with retrogressive metamorphic assemblages in the underlying schists. Locally, chloritic alteration is more intense in the Kombolgie Formation sandstone and detrital quartz grains have been replaced. We have not examined any sandstones containing or directly above uraninite mineralization.

CHARACTERISTICS OF MINERALIZATION

Uranium concentrations at Jabiluka occur in and near veins and breccia zones, concentrated in but not restricted to graphitic units of the sequence. Primary ore minerals include predominant uraninite, lesser coffinite and brannerite, and rare thucholite. Coatings of chlorite and coffinite on uraninite aggregates commonly produce a sooty appearance in hand specimens.



Figure 1. Transmitted light photomicrograph showing uraninite concentration (black) at a typical vein selvedge. The interior of the vein (right) consists of fine grained CSQ gangue (see text), which has fractured during preparation of the section. This vein is concordant to foliation of the enclosing schist (left), of which a quartz rich lamina forms the immediate wall. The schist is extensively replaced by patches of CSQ resembling that in the vein interior. Disseminated uraninite occurs especially within a formerly micaceous lamina of the schist (far left). Scale bar, 1mm.

Uraninite occurs in three main situations.

1) As selvedges along veins, and less commonly as internal layers or disseminations within them (Fig. 1). These veins are both transgressive and conformable to schistosity, and occur mainly in graphitic and chlorite-muscovite schists. The vein gangue may be subhedral quartz (Fig. 2), but more generally it is a distinctive microcrystalline intergrowth of chlorite-septechlorite-quartz (CSQ) which in places has replaced former gangue quartz (Figs. 1, 3). The CSQ usually appears brownish in thin section and conspicuously waxy in polished section. As will be illustrated below, uraninite has itself replaced the CSQ or quartz gangue, and also the retrograde phases in immediately adjacent wall rock.
2) Surrounding angular rock fragments and as disseminated grains within narrow microbreccia zones or thicker breccia intervals (up to 10-20cm). The matrix of these breccias and microbreccias includes fine rock and mineral fragments, especially quartz, extensively replaced by a brownish CSQ similar to that in the aforementioned veins. Localised growths of coarser, subhedral quartz also occur. Where this quartz and/or CSQ become particularly abundant, the breccia zones are essentially indistinguishable from those veins that carry isolated rock fragments (Fig. 2). Uraninite occurs in the breccias as selvedges to rock fragments and also as isolated grains within matrix CSQ, generally near quartz fragments. However the margins of the quartz clasts are replaced locally by botryoidal coffinite which in turn is replaced either by CSQ or by uraninite.
3) Within narrow, irregular replacement zones of CSQ extending outwards (1-2cm) from either veins or breccias into adjacent schistose wall rock (Figs. 1, 4). As well as showing replacement of quartz relics by coffinite, these zones also contain brannerite associated with anatase or brookite. Uraninite once more appears a late-

stage replacement within CSQ, its abundance decreasing markedly with distance from the 'source' vein or breccia.



Figure 2. Subhedral quartz gangue in a bifurcating vein. The schist fragment above left from centre represents incipient development of breccia, while other dark areas are the vein walls. Uraninite (black) has extensively replaced the schist, especially along contacts of walls and the fragments. Some CSQ gangue occurs at the left side of the vein. Scale bar 1mm. Transmitted light.



Figure 3. Uraninite at the edge of a vein which shows replacement of gangue quartz by fine CSQ (transmitted light, cross polars). A narrow selvedge of chlorite occrus between uraninite and quartz. The thin black line parallel to and left of the uraninite is a crack formed during section preparation. Scale bar, 1mm

Transitions occur between these typical forms of uraninite occurrence. Some specimens show veins developing into breccia zones, or well-defined CSQ-rich veins emanating outwards into country rock from the matrix portions of breccias. Also, irregular CSQ replacement zones extending out from thicker veins may develop into narrow, transgressive, satellitic veins. These clearly replaced the schist since occasional partly corroded relic muscovite flakes extend from one wall to the other. Thus all three kinds of uraninite occurrence listed above appear cogenetic.

While megascopic relationships in typical uraninite-bearing veins and breccias indicate overall dilation, we have observed no microscopic evidence within them of the open-space filling suggested by Hegge (1977) and Hegge & Rowntree (1978). Quartz appears to have been the first new mineral deposited, but the lack of drusy or cockade structures and the presence in veins of what would otherwise have been unsupported schist fragments suggest either a replacement origin for this quartz, or a gradual separation of the vein walls simultaneously with, or even consequent upon, its crystallization. A replacement origin is more clearly established for some of the subsequent CSQ in veins, breccia matrices, and wall

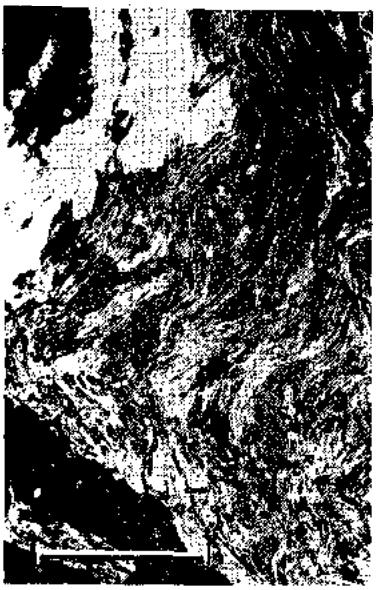


Figure 4. Contact between a uraninite vein (lower left corner) and a crenulated graphite schist. The white zone is a recrystallized syn-metamorphic quartz vein parallel to foliation of the schist. Opaque graphite is abundant in the upper part of the field of view, but towards the vein this has become oxidized and replaced by CSQ. Disseminated uraninite and coffinite occur within the CSQ-rich 'bleached' zone of ozidized schist adjacent to the vein wall. Some original muscovite of the schist persists up to the vein wall, but it is also progressively replaced by CSQ. Scale bar, 1mm. Transmitted light.

rocks (see, e.g., Figs. 1, 3), but in veins free of coarse quartz the CSQ gangue may also have been deposited during vein widening.

In narrow microbreccia zones or where veins grade into breccias, the contained rock fragments are similar in lithology to the adjacent country rock. The fragments in wider breccia zones commonly consist entirely of, or are dominated by rock types occurring in adjacent unbrecciated drill core. Some breccias contain a mixture of fragment lithologies, but even then the centimetre scale of lamination typical of Jabiluka schists does not rule out an essentially local derivation. One breccia sample studied contains a number of fragments of graphite schist with portions of a narrow, boudinaged vein of synmetamorphic quartz parallel to their foliations, and these were almost certainly derived from a comparable vein in the adjacent graphite schist wall. Although the foliations of rock fragments in breccia zones, and of their less common equivalents in veins, have become totally disoriented relative to schistosity in the country rocks, there is generally no sign of comparable deformation in the adjacent walls other than spalling at the immediate margin. These features, together with the angularity of the fragments despite their commonly soft character, appear to rule out a tectonic origin for the mineralized veins and breccias other than that implied by the necessity for incipient fractures and possibly by their concentration near the axial zones of broad flexures or cross folds in the schistose country rocks (Hegge, 1977).

Several kinds of later veins also occur at Jabiluka Two, the most abundant being drusy-structured quartz-dolomite-magnesite veins commonly carrying appreciable pyrite and chalcopyrite. These veins appear dilational—many showing obvious open-space filling structures — and they cut across the uraninite-bearing veins and breccias. Although this cannot be established in drill core, they may be related to the occasional geodes observed in dolomite-magnesite marbles between Jabiluka One and Jabiluka Two. More than one generation of drusy vein could be present. Similar quartz veins occur in the basal Kombolgie Sandstone. An even later, but much rarer form of earthy dolomitic vein within graphitic schist may carry minor uraninite.

Mineragraphy

Typical features of uraninite mineralization at Jabiluka are illustrated in figures 5 to 8. In the *veins* a large proportion of the uranium occurs as reniform to micro-nodular uraninite (Fig. 5), frequently with angular to sub-rectangular inclusions of microcrystalline chlorite-septechlorite, concentrated into zones and bands parallel to the vein margin. Reniform uraninite locally passes into reticulate uraninite replacing chlorite-septechlorite over an area continuous with adjoining reniform uraninite. Some reniform uraninite shows fracturing and micro-brecciation, but genuine shrinkage cracks are absent. Disseminated euhedral to



Figure 5. Uraninite (white) in a CSQ vein (black, centre). The band of reticulate uraninite on the right replaces CSQ near the vein margin (further along the vein this grades into a band of reniform uraninite). A fragment of brecciated reniform uraninite with CSQ or chlorite inclusions occurs at the upper left. Reflected light. Scale bar, 0.1mm.



Figure 6. Uraninite (light grey) along the edge of a birfucating CSQ vein, replacing the wall rock to the vein and partly grown into the vein. Sulphides (white) also occur within the CSQ gangue of the vein. Reflected light. Scale bar, 0.1mm.

subhedral uraninite cubes, and aggregates of these, are less common. The textures reveal growth of uraninite subsequent to vein development or, at the earliest, contemporaneously with CSQ which replaced earlier vein quartz or was deposited during vein widening. Thin selvedges of coffinite may border uraninite, with a narrow intervening band of darker chlorite. Preferential fracture along these selvedges exposes a dull black surface concealing the underlying dark grey submetallic uraninite.

In many specimens, there is more replacement by uraninite in the immediate *wall rock* to veins than within the vein (Fig. 6). Irregular anastomosing replacements may pass into disseminated subhedral uraninite within CSQ-rich patches in the wall rock (Fig. 7). The amount of uraninite decreases away from the vein walls. Relic quartz within uraninite-bearing areas of retrogressed schist has a thin selvedge of chlorite free of uraninite. In contrast, coffinite has formed along the margins of relic quartz corroded by CSQ (cf. Fig. 8). Commonly less than 25 μm in diameter or width, this coffinite is developed in botryoidal fashion into quartz, with its concentric banding truncated by the CSQ. Some coffinite bodies are altered to uraninite, or have a core of uraninite. The coffinite appears to have developed by reaction between relic quartz from the country rock schist and the fluids associated with CSQ deposition. Brannerite occurs associated with anatase or brookite in or near chloritized biotite, evidently having formed wherever titanium was available for reaction with uraniferous fluids.

Mineragraphic relationships in mineralized *breccias* are essentially similar to those described above for country rock adjacent to veins. The matrix of such breccias is extensively



Figure 7. Coalescing uraninite cubes and subhedral crystals (white) in a CSQ rich patch within retrogressed schist next to a vein (lower right). Reflected light. Scale bar, 0.02mm.



Figure 8. Botryoidal coffinite (light grey) and uraninite (white) in the matrix of a breccia. The coffinite is located at the interface between quartz clasts and replacive CSQ, and appears itself replaced by uraninite. Reflected light. Scale bar, 0.02mm.

replaced by CSQ, and uranium minerals again tend to concentrate at the interface between relic mineral grains or rock fragments and the CSQ mesostasis. This leads to a more disseminated appearance of mineralization within breccia zones compared to veins, but in reality the two environments are mineragraphically analagous.

Despite a variable but close association of sulphides with uraninite in veins, breccias, and adjacent wall rocks, with rare exceptions galena is the only sulphide to occur within or directly in contact with the uranium minerals. Some uraninite lacks microscopically visible galena, but most contains euhedral to cuspate galena inclusions, variable in amount. Lenticular galena occupies crossfractures in reniform uraninite, while larger galena segregations up to a few millimetres across are associated with later carbonate-quartz veins, which may contain unreplaced residuals of uraninite or local thucholite with uraninite inclusions where they cut CSQ veins or mineralized breccias. The mobilization and sulphurization of radiogenic lead from uraninite thus appears to have occurred repeatedly as well as to varying extents. The variation in lead isotope ratios observed in Jabiluka uraninites and rocks (Gulson & Mizon, this volume) may arise from this phenomenon as well as, or rather than, from repeated deposition of uraninite.

Sulphides of iron and copper range in age from possible regional metamorphic relics in retrogressed schist to those in the late stage drusy veins. Pyrite and chalcopyrite of the former type become corroded close to uraninite-bearing veins and breccia zones, and chalcopyrite may here be replaced by chalcocite. Post-kinematic growth of some large pyrite

crystals in lenticles within graphite schists is revealed by unreplaced poikiloblastic graphite inclusions in bands continuous with adjoining foliation. Disseminated sulphides are locally abundant in the interior of CSQ-uraninite veins, as monomineralic or composite grains generally not exceeding 20 μm. Less commonly, these occur also in chloritized wall rock. Chalcopyrite and pyrite predominate and are commonly associated, while galena may occur separately. Chalcopyrite may be partly altered to chalcocite and covellite. Sphalerite is distinctive in being observed only within veins, commonly as cores to galena plus chalcopyrite. There is a marked antipathy between sulphides (other than galena) and uraninite, which never occur in direct contact.

The late-stage drusy veins contain varying amounts of much coarser-grained pyrite and chalcopyrite, and occasional sphalerite, generally located interstitially to euhedral quartz or dolomite crystals. These veins clearly cut across uranium-mineralized veins and breccias, causing no conspicuous alteration.

The nature of 'CSQ'

Fine-grained intergrowths of chlorite-septechlorite ± quartz (CSQ) occur as the gangue component in veins, as matrix to breccias, as extensive replacements of immediately adjacent country rock, and also (in association with sericite) as an alteration product of feldspar in retrogressed schists more remote from mineralization. The nature and origin of CSQ are obviously key factors in elucidating ore genesis at Jabiluka.

Scanning electron microscope images show the CSQ to be composed of 1-20 μm interlocking platelets of phyllosilicate. Tiny rosettes of anhydrite crystals about 5-10 μm in diameter are scattered throughout. Preliminary high resolution transmission electron microscope studies (I.D.R. Mackinnon, pers. comm., 1979), and convergent beam and reflection electron diffraction patterns (A.W.S. Johnson, pers. comm., 1979) reveal most phyllosilicate crystallites to be single homogeneous phases with either 7Å (septechlorite) or 14Å (chlorite) basal spacings. Some lattice images show intergrown domains of these two phases, and also rare crystallites with other basal spacings yet to be interpreted. No electron diffraction patterns indicative of random mixed-layer phyllosilicates have been obtained. Varying proportions of chlorite and septechlorite in different samples are suggested by relative peak intensities on X-ray powder diffraction traces, and the peaks near 7Å for the two main phases may occasionally be resolved. There is no evidence for detectable aluminosilicate clay mineral in CSQ.

Long-duration autoradiographs of polished sections indicate the CSQ in veins, breccias, and immediately adjacent host rocks to be distinctly uraniferous. Gulson & Mizon (this volume) measured up to 1270 ppm uranium in carefully hand-picked CSQ samples free from opaque phases at x50 magnification. Fluorescent X-ray images with the scanning electron microscope show some phyllosilicate cleavage surfaces or crystal faces to be enriched in uranium, but it is not clear whether this is adsorbed or present as a separate phase. The uraniferous CSQ possibly explains the lower grade population (averaging 0.14% U_3O_8) of the bimodal assay distribution reported at Jabiluka by Hegge (1977). Further study of CSQ is in progress.

MINERALIZING PROCESSES

At present it is not possible to establish conclusively whether the uranium content of CSQ predates uraninite. Although lead isotopic measurements (Gulson & Mizon, this volume) do not indicate an older age for uranium in CSQ relative to that in uraninite, the uranium contents of CSQ remote from uraninite are distinctly higher than those from the interior of uraninite-lined veins. Together with the mineragraphic data presented above, particularly on distribution of coffinite and brannerite, this leads us to the provisional

conclusion that uranium enrichments within and in the immediate vicinity of Jabiluka ore structures were first introduced via the fluids responsible for abundant generation of CSQ. Less confidently, we suggest that subsequent uraninite developed in part by redistribution of this uranium. However on a local scale the uranium geochemical budget rules this out as the sole mechanism for forming uraninite.

The occurrence of anhydrite rosettes within CSQ, and the conspicuous oxidation and removal of graphite in the vicinity of mineralized veins and breccias (Fig. 4), indicate that the fluids from which CSQ originally formed were relatively oxidized and thus capable of transporting hexavalent uranium. The corrosion of pyrite in adjacent country rocks and the replacement of chalcopyrite appear relevant to the geochemistry of these fluids, but their significance is not yet clear. Further studies are required to delineate the factors responsible for deposition of uranium within CSQ, and more importantly for the crystallization of the main ore mineral, uraninite, which clearly formed at a comparatively late stage replacing CSQ and coffinite in particular. At least locally, the influence imposed on mineralizing fluids by the oxidation of graphite (Fig. 4) offers strong suggestions of a redox control. At Jabiluka, this would be consistent with the localization of orebodies in more graphitic schist sequences, particularly when account is taken of the likelihood that many exceptionally chloritic host rocks may be altered graphite schists (Binns *et al.*, this volume). Declining temperatures are also likely to be important in governing the behaviour of uranium within the mineralizing fluids.

In understanding the broader controls of ore formation at Jabiluka, the relationship between CSQ-depositing fluids and those responsible for the extensive retrogressive aureole around mineralization is a crucial issue. As a brannerite-forming reaction occurred between CSQ fluids and titanium released during chloritization of biotite, the time sequence must be that retrogression was simultaneous or earlier. There are definite similarities both mineralogically (e.g. septechlorite) and texturally between CSQ replacements in and near veins or breccias, and retrogressive alteration products of feldspar in more remote schists. CSQ patches grade into normal retrogressive assemblages without evidence of superimposition. Consequently we interpret retrogressive metamorphism and creation of uraniferous CSQ as cogenetic and essentially contemporaneous, the more oxidized and possibly lower temperature fluids associated with the latter being introduced slightly later.

A further indication of the close relationship between retrogressive metamorphism and at least the initial mineralization is provided by the 'greisen'-like rocks developed above uraninite-rich zones at Jabiluka Two. These represent accumulations of sericite similar to that which replaces former feldspar in retrogressed schists. At least in part, they appear the sink for potassium removed in solution from CSQ-rich areas of the underlying mineralized zone. Locally they contain brannerite intergrown with sphene and the associated silicates, particularly sericite. Their large quartz porphyroblasts could represent the ultimate fate of silica removed from the heavily chloritized ore zones. If these interpretations are borne out when mine exposures become available, they provide an important indication of the direction of fluid transport, namely upwards.

One implication of this evident relationship between retrogressive metamorphism and uranium introduction at Jabiluka is the relatively high temperature (300°-350°C) suggested for initial mineralizing fluids by the CSQ paragenesis (Nelson & Roy, 1958). Another is that improved knowledge of the geometry of the retrogressive aureole would greatly clarify fundamental questions about mineralization controls and ore genesis. It is clear from drilling that both retrogression and mineralization extend at least 300m vertically below the Kombolgie unconformity. Together with the indicated temperatures, the relatively reduced nature of the retrogressive metamorphism (as shown by the persistence of sulphides and virtual absence of hematite or hydrated ferric oxides), and the fact that similar metamorphic

Sample No.	Mineral	$\delta^{34}S_{CDT}$ (‰)	Notes
1. Sulphide Lenticles from Retrogressed Graphite Schists			
54955C	pyrite	+4.0	From Main Mine Series (MMS) near mineralization
55235	pyrite	+3.7	From Upper Graphite Series (UGS) near mineralization
55145	pyrite	+4.6	From MMS, unmineralized
55112	pyrite	+5.5)	From UGS, unmineralized
55126	pyrite	+3.5)	
54959B	pyrite	+6.1	From separate bands in MMS near mineralization
	chalcopyrite	+5.0	
65974	chalcopyrite	+2.3	From graphitic dolomite in barren LMS2
54943	chalcopyrite	+2.3	From MMS near mineralization
2. Sulphides from Drusy Veins			
54955D	chalcopyrite	+3.5)	From quartz-dolomite-chalcopyrite vein
55254	chalcopyrite	+5.5)	
54932	chalcopyrite	+3.6	From quartz-dolomite-chalcopyrite vein cutting greisen
54964	chalcopyrite	+3.5	From quartz-chalcopyrite vein cutting uraninite vein
65971	chalcopyrite	+6.2	From quartz-chalcopyrite-marcasite vein. Marcasite growth on top of chalcopyrite
	marcasite	+14.5	

Table 1. $\delta^{34}S_{CDT}$ data for sulphide samples from Jabiluka Two.

alteration extends upwards through the former regolith into the overlying Kombolgie Formation sandstone, this appears to rule out a pre-Kombolgie palaeosurface control of the initial mineralization.

Future mine exposures would also clarify the nature and origin of the veins and breccia zones with which ore deposition was obviously associated. These were clearly the channelways for CSQ-forming fluids and possibly, though not necessarily, for the fluids responsible for more extensive retrograde metamorphism of Cahill Formation schists. As discussed above, observations on drill core do not support a fundamentally tectonic character for these structures. Nor does their distribution, the progression from breccia zones into veins, and the lack of open-space filling structures appear consistent with the collapse origin suggested by Hegge (1977). While acknowledging that careful mapping of mine-scale

exposures is needed to demonstrate the point conclusively, we believe that the characteristics of breccias and their contained fragments (particularly the replacement phenomena) are more compatible with a hydraulic fracturing mechanism (Phillips, 1973; Fyfe *et al.*, 1978). This is highly likely in an environment where fluids played such a clearly important role. An excess fluid pressure relative to lithostatic pressure could explain the otherwise puzzling pervasiveness of the retrogressive metamorphism in country rocks subjected to no significant contemporaneous deformation.

ISOTOPIC EVIDENCE

Oxygen, carbon and sulphur isotopes

Stable isotope studies have concentrated on examining the relationship between sulphides in the schists and those in post-uraninite drusy veins, between carbonates in marbles and these same drusy veins, and on estimating the characteristics of retogressive and mineralizing fluids from oxygen isotope ratios in various minerals.

Sulphur isotope data are listed in table 1. Pyrites from lenticles in graphite schists have $\delta^{34}S$ values from +3.5 to +6.1‰, and those of chalcopyrites from similar occurrences range from +2.3 to +5.0. Our pyrite data differ from those reported by Donnelly & Ferguson (this volume) but the chalcopyrite data are similar. The pyrite and chalcopyrite samples from 54959B occur in adjacent laminae, and if they have equilibrated the fractionation factor of 1.1‰ corresponds to a temperature of 360°C. This is consistent with the temperature estimate given previously for retrogressive metamorphism and CSQ emplacement (the sample is from a mineralized section of core). Chalcopyrites from post-uraninite drusy veins have $\delta^{34}S$ values between +3.5 and +6.2‰. A simple explanation of their isotopic similarity to wall-rock sulphides is that sulphides in the drusy veins were derived by leaching of those occurring in nearby retrogressed schists with little opportunity for fractionation. A rare sample of tiny marcasite crystals projecting from chalcopyrite into a drusy cavity has a high $\delta^{34}S$ value of +14.5‰, which suggests limited introduction of isotopically heavy solutions with decreased SO_4^{2-}/HS^- ratios at a very late stage in evolution of the Jabiluka enviroment.

Carbon and oxygen isotope data for carbonates are listed in table 2. Dolomites from magnesite-rich retrogressed marbles were carefully separated by heavy liquid techniques. Both the carbon and oxygen isotope ratios of carbonate minerals from marble units fall within the range for early Proterozoic marine carbonates (Veizer & Hoefs, 1976) but dolomites from the retrogressed, magnesite-bearing marbles have $\delta^{18}O$ values about 5‰ lower than their non-retrogressed amphibolite facies parental equivalents. Dolomites from drusy veins have more variable $\delta^{13}C$ values than those in either group of marbles, but the ranges overlap. We interpret this to mean the latter were the source of carbonates in the former. The oxygen isotopic compositions of drusy dolomites are similar to those in retrogressed, magnesite-bearing marbles, but this has little meaning since it could arise either through equilibration with the same hydrothermal fluids, or from various fortuitous combinations of isotopically-different fluids at different temperatures (Fig. 9). Samples from two thin, late-stage carbonate veins in graphite schist have anomalous carbon isotope ratios, which could suggest a minor contribution of ^{13}C-depleted carbon from graphite or of supergene organic origin towards the close of fluid activity. These, and also dolomites from a layered geode (55254) have higher $\delta^{18}O$ values than other drusy vein samples, indicative of their lower temperature formation. No statistical correlation between carbon and oxygen isotopic compositions is evident, contrary to the suggestion by Donnelly & Ferguson (this volume).

Oxygen isotope data for quartz and white mica from different parageneses are listed in table 3. Coexisting quartz and muscovite from a non-retrogressed,

Sample No.	Mineral	$\delta^{13}C_{PDB}$ (‰)	$\delta^{18}O_{SMOW}$ (‰)	Notes
1. Non-retrogressed Marbles				
67560	calcite	-0.7	+14.6	
65980	dolomite	+0.2	+21.0	
67557	dolomite	+1.6	+19.3	
2. Magnesite Marbles				
55132B	dolomite	-0.3	+14.8	Assuming dolomite-water equilibration at 300°C, $\delta^{18}O$ of the metamorphic fluid is estimated to be ∿ +7‰
55149	dolomite	-0.3	+15.4	
55150	dolomite	-0.3	+15.2	
3. Drusy Veins				
54995	dolomite	+0.3	+14.9	From MMS, coarse rhombic carbonate vein in chlorite schist breccia
54955	dolomite	-3.1	+15.6	From MMS, quartz-dolomite-chalcopyrite vein in graphite schist
55000	dolomite	-3.0	+15.2	From MMS, dolomite vein in chlorite schist breccia
65975	dolomite	+0.3	+14.2	From MMS, massive coarse crystalline dolomite with vughs; fluid inclusion filling temperature ∿ 120°C. $\delta^{18}O$ of equilibrating hydrothermal water is estimated to be -3‰
4. Layered Geode				
55254A	dolomite	+4.5	+22.4)	In chlorite breccia from UGS. A is on top of B which in turn lies on top of quartz with fluid inclusion temperature ∿120°C
55254B	dolomite	+4.1	+24.6)	
5. Late Thin Veins				
55004	dolomite	-8.6	+23.2	From MMS, thin transgressive earthy vein with probable late stage remobilized uraninite
55240	dolomite	-21.8	+19.9	

Table 2. $\delta^{13}C_{PDB}$ and $\delta^{18}O_{SMOW}$ data for carbonates from Jabiluka Two.

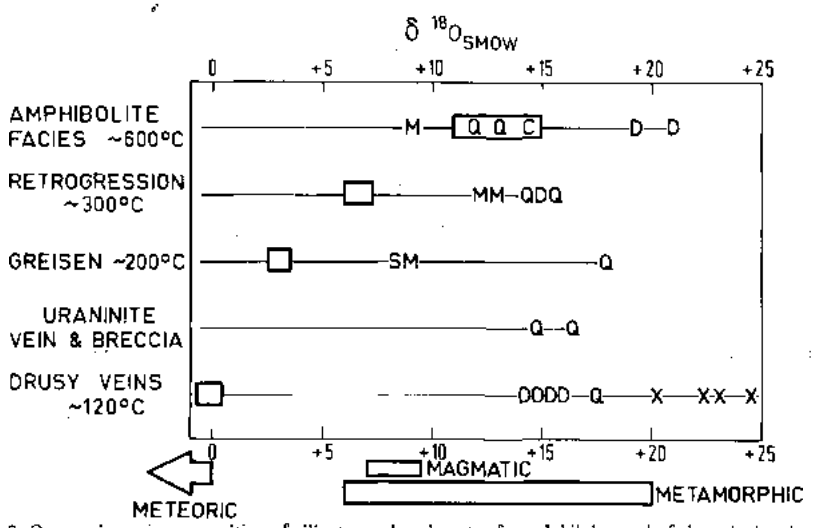


Figure 9. Oxygen isotopic composition of silicates and carbonates from Jabiluka, and of the calculated aqueous fluids (boxes) that would have been in equilibrium with those at the estimated temperatures (based either on metamorphic parageneses or fluid inclusions). The fields for typical magmatic, metamorphic, and low-latitude meteoric fluids are also shown. M, muscovite; S, sericite; Q, quartz; D, dolomite; X, late-stage dolomite from complex geode and minor veins.

amphibolite facies pelitic schist have a fractionation factor of 2.8‰, corresponding to an equilibration temperature of 650°C (from Blattner, 1975) which agrees well with that estimated from the mineral assemblage. Quartz-muscovite pairs from retrogressed schists appear not to be isotopically equilibrated. The pair from a coarse-grained 'greisen' gives a fractionation factor of +6.9‰ which corresponds to a temperature of approximately 200°C (after Friedman & O'Neil, 1977) if equilibration occurred. Quartz gangue samples from uraninite-CSQ veins have $\delta^{18}O$ values lying between those of quartz in retrogressed schist and in later drusy veins respectively.

Using fractionation relationships between water and dolomite, quartz and muscovite respectively (Friedman & O'Neil, 1977), the oxygen isotopic constitution of fluids equilibrated with carbonate and silicate phases has been estimated for the various parageneses. No corrections for solutes in fluid have been applied (cf. Ypma & Fuzikawa, this volume), and extrapolation was necessary at low temperatures. Details of the temperature estimates used in calculation are given in tables 1 to 3. The results are shown diagrammatically in figure 9.

A picture of declining fluid $\delta^{18}O$ values with falling temperature emerges. The estimated fluid composition for non-retrogressed amphibolite facies schists and marbles ($\delta^{18}O$ = +11 to +15‰) is typical of high grade regional metamorphic metasedimentary terranes (Hoefs, 1973). The composition of fluids responsible for retrogressive metamorphism ($\delta^{18}O \sim +6$‰) resembles magmatic waters. Those associated with the drusy veins have $\delta^{18}O$ values close to zero, which is significantly higher, by about 5‰ (Veizer, pers. comm., 1979; Perry *et al.*, 1978), than mid-Proterozoic seawater or low latitude meteoric water.

If 'greisens' and the CSQ-uraninite veins equilibrated at temperatures similar to those of the retrogressive metamorphism, their fluid compositions would also have been close to +6‰. However if they formed at lower temperatures, say 200°C, fluids with $\delta^{18}O$ values about +1 to +3 are indicated (Fig. 9).

Sample No.	Mineral	$\delta^{18}O_{SMOW}$ (‰)	Notes
1. Amphibolite Facies Schists			
65990	quartz	+11.8	Quartz-muscovite fractionation factor α = 2.8‰, corresponding to ~650°C. $\delta^{18}O$ of metamorphic fluid equilibrating with quartz is ~+11‰
	muscovite	+ 9.0	
65993	vein quartz	+13.3	
2. Retrogressed Schists			
55170	quartz	+15.3	Quartz-muscovite α = 2.7 and 2.2‰ respectively, indicating incomplete isotopic adjustment during retrogressive metamorphism. Assuming quartz and metamorphic fluid equilibrated at 300°C, $\delta^{18}O$ value for fluid is estimated to be +6‰
	muscovite	+12.6	
55176	quartz	+14.4	
	muscovite	+12.2	
3. Greisens			
65968	quartz	+15.9	Quartz-muscovite α = 6.9‰, corresponding to ~200°C equilibration temperature
	muscovite	+ 9.0	
54928	sericite	+ 8.4	
65997	vein quartz	+18.2	
4. CSQ-uraninite Veins			
54955A	quartz	+14.6	
54996	quartz	+16.5	
5. Drusy Veins			
55240	quartz	+17.5	
55254	quartz	+17.5	On the basis of drusy dolomites (Table 3) the fluid inclusion filling temperature of this quartz sample is ~120°C. The corresponding $\delta^{18}O$ of the hydrothermal fluid is ~0‰

Table 3. $\delta^{18}O_{SMOW}$ data for quartz and muscovite samples from Jabiluka Two.

Several interpretations of the data are possible.

1) A progressive mixing has occurred between deep-seated waters and surface water during evolution of the Jabiluka environment. This could have occurred in a large-scale circulatory system in the Cahill Formation, with surface waters descending well away from the mineralized centre, or when upwelling fluids encountered an aquifer near the Kombolgie unconformity. Any effects of such mixing are only clearly established for the post-uraninite drusy veins. A surface water component could be the source for additional new material required by S and C isotope data on

late-stage marcasite and the thin dolomite veins, though these are by no means significantly abundant at Jabiluka.

2) The fluids had only one, deep-seated, source and have evolved to lower $\delta^{18}O$ values with decreasing temperature by progressive reaction with country rocks.

Further oxygen isotope studies of minerals from amphibolite facies and retrogressed Cahill Formation schists, and particularly from the mineralized veins and breccias, may help to better evaluate these alternatives.

Geochronology

Isotopic studies to clarify age relationships in Jabiluka mineralization and its environment are reported separately by Gulson & Mizon (this volume: U-Pb and Pb-Pb) and Riley *et al.* (this volume: Rb-Sr).

Following detailed investigation of different uraninite and sulphide parageneses in a single specimen, Gulson and Mizon express strong reservations about the geological significance of apparent Pb 'ages' obtained from ore-bearing samples. However a 1380 ± 110 m.y. event is well established for pyrites and chalcopyrites from retrogressed graphite schists outside the ore zones, and for their uranium-enriched equivalents close to mineralization. Equilibration of sulphides with the retrogressive and mineralizing fluids respectively appears the most acceptable explanation for the isotopic systematics of these samples, in which case the result appears the best available estimate for the age of ore development at Jabiluka and (within error limits) the apparently contemporaneous alteration aureole surrounding mineralization. Chalcopyrite from a late drusy vein cutting a uraninite zone conforms to this isochron, setting 1380 ± 110 m.y. as a minimum age for uranium introduction and, on mineragraphic grounds, for uraninite crystallization also.

The Rb-Sr data on Jabiluka micas provide good age estimates for pegmatite emplacement (1830 ± 5 m.y.), which evidently occurred near the peak of the amphibolite facies regional metamorphism after which cooling to about 300°C had occurred by 1805 ± 5 m.y. (Riley *et al.*, this volume; see also Page *et al.*, this volume). Attempts to use sericite concentrates to date retrogressive metamorphism of Cahill Formation host rocks at Jabiluka, and to compare this with apparently simultaneous prograde metamorphism of the Kombolgie Formation sandstone and its underlying regolith, were less conclusive, due mainly to low enrichments in radiogenic strontium. A moderately-fitted isochron suggests some validity for an assumption that all these sericites crystallized in isotopic equilibrium with a single fluid phase, in which case 1534 ± 90 m.y. is suggested as the age of the alteration episode. Alternatively, it might be assumed that the lowest Rb-Sr model ages obtained for sericites, close to 1400 m.y., established a maximum age limit for alteration. Within error limits both results are compatible with the 1380 ± 110 m.y. lead isotope age indicated for sulphides in retrogressed graphite schists from Jabiluka.

SOURCE OF URANIUM

Although the limitations of observations based solely on drill core must be recognized, the foregoing discussion indicates characteristics of mineralization and mineralized structures at Jabiluka, and conditions relating to the mineralizing and retrogressive fluids, which are not easily reconciled with a supergene origin for the contained uranium.

It has been suggested previously (e.g. Hegge & Rowntree, 1978) that Alligator Rivers uraninites were remobilized from syngenetic protore, for example from uranium first concentrated in carbonaceous metasediments after supergene aqueous transport from uraniferous granitoids exposed and weathered in basement source areas. If retrogressive metamorphism (whatever its cause) were to be the remobilizing factor in such a scenario, then a pronounced depletion of uranium should be apparent in the extensive aureole of altered schists surrounding the Jabiluka orebodies. Average uranium contents reproduced in

	Graphite Schist	Psammitic Schist	Pelitic Schist
1. Unaltered amphibolite facies schists distant from Jabiluka	16	6	9
2. Retrogressed schists remote from mineralization	14	7	7
3. Retrogressed schists close to mineralization	29	7	8
4. Immediate hosts to veins (with veins removed)	255	250	230

Table 4. Average uranium contents (ppm, log normal means) for Jabiluka schists (from Binns *et al.*, this volume)

table 4 contradict this requirement. No disseminated uranium minerals were observed in the rocks used to obtain these data: the pronounced rise in U content near ore reflects presence of CSQ-rich patches and veinlets. Both these, and any contained uraninite adjacent to ore veins or breccias, are clearly replacements emanating from the main mineralized structures.

Remobilization from sediments during the original high grade regional metamorphism does not accord with the observed intimate association of mineralization with retrogression and formation of CSQ. It would require these latter features to be fortuitously superimposed. Eupene (in press) also presents analytical and abundance data arguing against remobilization of uranium from host rocks.

An extraneous and hypogene source for Jabiluka uranium is strongly indicated. The granitic pegmatites intruding the area are unsuitable source rocks on two grounds. First, they are comparatively low in uranium and other trace elements, and secondly they themselves suffered extensive retrogressive metamorphism and have become enriched in uranium where intensely replaced by CSQ at their margins (Binns *et al.*, this volume).

A subjacent heat source appears essential to create the unique and voluminous retrogressive metamorphic aureole surrounding Jabiluka mineralization. One possibility is a concealed granitic pluton, which could also provide the retrogressive fluids and the uranium, as well as a suitable explanation for hydraulic fracturing in its roof rocks. Jabiluka ores are enriched in elements such as Be, Sc, Y, Nb, Sn, Mo, Bi, possibly B (Binns *et al.*, this volume; Ferguson & Winer, this volume), and in Hg (Ryall & Binns, this volume). They are conspicuously low in thorium. Lithium is enhanced in both ores and the retrogressed aureole. These geochemical relationships recall pneumatolytic-hydrothermal situations associated with acid magmas. However a direct magmatic-hydrothermal origin of this type appears to be ruled out by geochronological data discussed above for the age of mineralization and retrogressive alteration, for there is no evidence of granitic activity in the province much younger than 1780 m.y. (Riley, this volume; Page *et al.*, this volume) despite the abundance of uranium occurrences similar to Jabiluka.

Uraninite-bearing granitic gneisses of the Nanambu Complex, as described by McAndrew & Finlay (this volume) from 'Granite Hill', 5km south of Jabiluka, and

elsewhere, represent an alternative source rock for uranium in the mineralizing solutions. Their primary accessory uraninite shows evidence of oxidation and dissolution well below the level of weathering. Convective fluid circulation, possibly driven by the heat generated from abnormal contents of radioactive trace elements (Fehn *et al.*, 1978), could transfer uranium into the overlying Cahill Formation and also cause the retrogressive alteration. The chronological problems associated with this potential source are discussed further below.

Other alternative subjacent uranium sources might be considered such as the migmatized Cahill-Nanambu contact (cf. Ryan, 1979) but like the above suggestions they cannot be adequately tested at present or they fail to meet heat source or chronological requirements.

GENETIC MODEL AND EXPLORATION SIGNIFICANCE

Many genetic aspects of Jabiluka ores remain to be settled by further research and when mine exposures become available. On the basis of present evidence, we propose an essentially conventional, epigenetic hydrothermal model. According to this, uranium mineralization has been introduced by aqueous fluids along vein and breccia structures created by hydraulic fracturing of schists subjected, essentially simultaneously, to pervasive retrogressive alteration. These processes account for abundant replacement structures in the ores, their immediate country rocks, and the broader retrogressive aureole. Uranium deposition was controlled, at least in part, by redox reactions between fluids and country rocks (particularly graphite schists), and by the declining temperature of these mineralizing fluids. The detailed geochemistry of the fluids, and especially the factors controlling crystallization of uraniferous chlorite-septechlorite-quartz (CSQ) intergrowths and uraninite respectively, remain to be determined.

The uranium in Jabiluka ores was not remobilized from their polymetamorphic country rocks. Since the extensive chlorite-rich wallrock alteration expressed as retrogressive metamorphism of the Cahill Formation schists extends also into the overlying Kombolgie Formation sandstone as an apparently prograde metamorphism, we discount a supergene uranium source related to the pre-Kombolgie weathering surface, evidence of which is limited to a 1-2m thick metamorphosed regolith below the unconformity. A post-Kombolgie supergene origin is inconsistent with the characteristics and distribution of vein and breccia structures observable in drill core, with the relatively high temperatures indicated for retrogressive metamorphism and CSQ replacements early in the mineralizing cycle, and with the removal of potassium from ore zones into *overlying* 'greisen' bodies.

Several alternative hypogene sources for the uranium may be postulated. Fluids expelled during crystallization of a subjacent granitic pluton are geochemically and mechanistically attractive, but their existence at the right time is not supported by available geochronological data.

Our preferred alternative is that mineralization centres such as Jabiluka represent the upwelling zone of broad circulatory fluid systems induced by radiogenic heat built up in subjacent granitic bodies over a period of time. Such sources could include the relatively uranium-rich post-kinematic granitoids (1780 m.y.) of the Pine Creek Geosyncline (Ferguson *et al.*, this volume), or the gneisses carrying primary uraninite accessories within the reactivated Archaean Nanambu Complex underlying the ARUF (McAndrew & Finlay, this volume). The latter are favoured by their ability to release uranium to the convecting fluid cell through alteration of uraninite. Uranium in the post-kinematic granitoids is contained mainly within more refractory phases such as zircon, monazite, and sphene (C. J. Finlay, pers. comm., 1979).

The feasibility of such processes, in particular their potential for producing fluids with sufficiently high temperatures to conform with the characteristics of Jabiluka

mineralization, is supported by the mathematical modelling carried out by Fehn *et al.* (1978). They calculated that steady state temperatures some 140°C higher than the normal geothermal gradient would develop at the centre of the base of a modest-sized, shallowly buried, abnormally radioactive granitic sheet by generation of internal radiogenic heat. Extrapolating from this to larger, more deeply buried plutons or gneissic bodies within or remobilized from the Nanambu Complex, temperatures exceeding those required for initial mineralizing fluids at Jabiluka are readily imagined. Once rendered permeable by fracturing, the model of Fehn *et al.* demonstrates comparatively rapid development of fluid convection cells in and above the radioactive rock body. Since consolidation of potential Nanambu Complex source rocks appears unlikely to be younger than 1800 m.y. (Page *et al.*, this volume), it is necessary that they remained relatively impermeable for an appreciable time span if the convective cells were not to operate significantly before the time indicated by isotopic age estimates for Jabiluka mineralization, namely around 1530 to 1400 million years ago. Epeirogenic movements associated with the deposition of the Kombolgie Formation sandstone, or its subsequent fracturing, possibly initiated the fluid convection.

A major difficulty with the hypogene source model, for which we have no adequate explanation, is the Mg-rich character of the CSQ-uraninite veins and of the retrogressed schists surrounding the Jabiluka Two deposit, arising from the intense replacement by chlorite and septechlorite. Magnesium is not an expected major component in hydrothermal fluids expelled from or reacting with granitic rocks. The existence of a Mg-depleted zone in schists or gneisses beneath mineralization cannot be evaluated and seems unlikely. Interaction between ascending fluids and either the dolomite-magnesium marbles (cf. Eupene, in press) or the Oenpelli Dolerite is one possibility. However abundance relationships appear unsuitable and, in the marbles, magnesite replaces dolomite as a result of retrogressive alteration so Mg has been added rather than removed. We have not studied the Oenpelli Dolerite, but references to its marginal chloritization (Page *et al.*, this volume; Ypma & Fuzikawa, this volume) suggest a similar contradiction. Supergene sources for Mg suffer from the same problems as apply to uranium, and the distinct depletion in Na, Ca and Sr exhibited by retrogressed schists may also be noted in this respect.

In a simplistic epigenetic hydrothermal model for uranium mineralization at Jabiluka, no genetic significance appears attached to the Kombolgie unconformity. This would be of extreme importance to exploration strategy, for it implies an equivalent ore potential in the more deeply eroded portions of the Cahill Formation, most of which are poorly exposed. Indeed the model does not rule out a mineralization potential for the Kombolgie Formation sandstone itself. Uraniferious solutions could continue migrating upwards into this overlying Formation and become fixed by a variety of redox processes. However to draw this conclusion with certainty would be premature at present. Although interpreting their fluid inclusion data in terms of a supergene uranium source, Ypma & Fuzikawa (this volume) assign importance to mixing between saline fluids and contrasted groundwaters moving along or close to the Kombolgie unconformity. It is conceivable that a similar effect might be responsible for the deposition of uraninite rather than, or as well as, uraniferious CSQ when hypogene mineralizing fluids encounter the influence of the Kombolgie aquifer. This is possible at Jabiluka according to one interpretation of the stable isotope data. While difficult to reconcile with the known existence of mineralization more than 300m below the unconformity at Jabiluka, and at even greater depths (1000m) in other occurrences (Eupene, in press), any such mechanism would place an important additional constraint on exploration models. The issue is clearly one deserving greater attention.

Our present genetic model provides exploration criteria relating mainly to occurrences of initial CSQ-associated mineralization. The existence of uraniferous granitoids in metamorphic regions which display localized centres of retrogressive alteration and possess

reduced lithologies such as graphite schist or sulphide-rich units, would appear highly favourable indications for the source, transport and depositional requirements. In this context, proximity to remobilized Nanambu basement is important more in terms of increased likelihood of granitic sources for uraniferous hydrothermal fluids than as a potential uranium supply dating back to the sedimentary stage. Graphite schists would be significant not so much as protores from which syngenetic uranium might become redistributed, but instead as reducing agents that will fix uranium from hypogene solutions. Pronounced retrogressive metamorphism in prospective areas would indicate upwards discharge zones of the necessary hydrothermal activity. It also provides opportunity for creation of geochemical haloes potentially useful in exploration, as discussed by Binns *et al.* (this volume).

ACKNOWLEDGEMENTS

We thank our colleagues at the CSIRO Division of Mineralogy for fruitful discussion, and the staff of Pancontinental Mining Ltd. for their cooperation. Dr. P. Blattner (DSIR, New Zealand) and Mr. K. Fuzikawa (University of Adelaide) kindly assisted with some isotopic measurements and with fluid inclusion studies respectively.

REFERENCES

Binns, R.A., Ayres, D.E., Wilmshurst, J.R. & Ramsden, A.R., this volume: Petrology and geochemistry of alteration associated with uranium mineralization at Jabiluka, Northern Territory, Australia. *Proceedings of the International Uranium Symposium on the Pine Creek Geosyncline.*

Blattner, P., 1975: Oxygen isotopic composition of fissure-grown quartz, adularia, and calcite from Broadlands geothermal field, New Zealand. *Am. J. Sci., 275,* 785-800.

Donnelly, T.H. & Ferguson, J., this volume: A stable isotope study of three deposits in the Alligator Rivers Uranium Field, N.T. *Proceedings of the International Uranium Symposium on the Pine Creek Geosyncline.*

Eupene, G.S., in press: Stratigraphic, structural and temporal control of mineralization in the Alligator Rivers Uranium Province, Northern Territory, Australia. *Proc. 5th International Symposium on the Genesis of Ore Deposits, Snowball, Utah (IAGOD).*

Fehn, U., Cathles, L.M. & Holland, H.D., 1978: Hydothermal convection and uranium deposits in abnormally radioactive plutons. *Econ. Geol., 73,* 1556-1566.

Ferguson, J., Chappell, B.W. & Goleby, A.B., this volume: Granitoids in the Pine Creek Geosyncline *Proceedings of the International Uranium Symposium on the Pine Creek Geosyncline.*

Ferguson, J. & Winer, P., this volume: Pine Creek Geosyncline: statistical treatment of whole rock chemical data. *Proceedings of the International Uranium Symposium on the Pine Creek Geosyncline.*

Friedman, I. & O'Neill, J.R., 1977: Compilation of stable isotope fractionation factors of geochemical interest. *in, Data of Geochemistry, 6th edition, Chapter KK., Prof. Pap. U.S. geol. Surv., 440-KK.*

Fyfe, W.S., Price, N.J. & Thompson, A.B., 1978: *Fluids in the Earth's Crust.* Elsevier, Amsterdam, 383p.

Gulson, B.L. & Mizon, K.J., this volume: Lead isotope studies at Jabiluka. *Proceedings of the International Uranium Symposium on the Pine Creek Geosyncline.*

Hegge, M.R., 1977: Geological setting and relevant exploration features of the Jabiluka uranium deposits. *Proc. Australas. Inst. Min. Metall., 264,* 19-32.

Hegge, M.R., Mosher, D.V., Eupene G.S. & Anthony, P.J., this volume: Geologic setting and comparative review of the East Alligator uranium deposits and prospects. *Proceedings of the International Uranium Symposium on the Pine Creek Geosyncline.*

Hegge, M.R. & Rowntree, J.C., 1978: Geological setting and concepts on the origin of uranium in the East Alligator River region, N.T., Australia. *Econ. Geol., 73,* 1420-1429.

Hoefs, J., 1973: *Stable isotope geochemistry.* Springer-Verlag, New York, 140p.

McAndrew, J. & Finlay, C.J., this volume: The nature and significance of the occurrence of uranium in the Nanambu Complex of the Pine Creek Geosyncline. *Proceedings of the International Uranium Symposium on the Pine Creek Geosyncline.*

Needham, R.S. & Stuart-Smith, P.G., volume: Geology of the Alligator Rivers Uranium Field. *Proceedings of the International Uranium Symposium of the Pine Creek Geosyncline.*

Nelson, B.W. & Roy, R., 1958: Synthesis of the chlorites and their structural and chemical constitution. *Am. Miner., 43,* 707-725.

Page, R.W., Compston, W. & Needham, R.S., this volume: Geochronology and evolution of the late-Archaean basement and Proterozoic rocks in the Alligator Rivers Uranium Field, Northern Territory, Australia. *Proceedings of the International Uranium Symposium on the Pine Creek Geosyncline.*

Perry, E.C., Ahmad, S.N. & Swulius, T.M., 1978: The oxygen isotope composition of 3800 m.y. old metamorphosed chert and iron formation from Isukasia, West Greenland. *J. Geol., 86,* 223-239.

Phillips, W.J., 1972: Hydraulic fracturing and mineralization. *Quart. J. Geol. Soc., 128,* 337-355.

Riley, G.H., this volume: Granite ages in the Pine Creek Geosyncline. *Proceedings of the International Uranium Symposium on the Pine Creek Geosyncline.*

Riley, G.H., Binns, R.A. & Craven, S.J., this volume. Rb-Sr Chronology of micas at Jabiluka. *Proceedings of the International Uranium Symposium on the Pine Creek Geosyncline.*

Rowntree, J.C. & Mosher, D.V., 1975: Jabiluka uranium deposits. *in* (ed. C.L. Knight) *Economic Geology of Australia and Papua New Guinea, Australas. Inst. Min. Monograph Series No. 5, I. Metals,* 321-326

Ryall, W.R. & Binns, R.A., this volume: Mercury distribution in the Jabiluka Two orebody and its host rocks. *Proceedings of the International Uranium Symposium on the Pine Creek Geosyncline.*

Ryan, G.R., 1979: The genesis of Proterozoic uranium deposits in Australia. *Phil. Trans. R. Soc. Lond., A291,* 339-354.

Veizer, J. & Hoefs, J., 1976: The nature of O^{18}/O^{16} and C^{13}/C^{12} secular trends in sedimentary carbonate rocks. *Geochim. Cosmochim. Acta, 40,* 1387-1395.

Ypma, P.J.M. & Fuzikawa, K., this volume: Fluid inclusion studies as a guide to the composition of uranium ore-forming solutions of the Nabarlek and Jabiluka deposits, N.T., Australia. *Proceedings of the International Uranium Symposium on the Pine Creek Geosyncline.*

MODEL FOR THE DEVELOPMENT OF ECONOMIC URANIUM MINERALIZATION IN THE ALLIGATOR RIVERS URANIUM FIELD

John Ferguson[1], G.R. Ewers[1] and T.H. Donnelly[2]

1. Bureau of Mineral Resources, P.O. Box 378, Canberra City, A.C.T., 2601, Australia.
2. CSIRO Baas Becking Laboratory, P.O. Box 378, Canberra City, A.C.T., 2601, Australia.

ABSTRACT

Major uranium deposits occur in the Alligator Rivers Uranium Field within the Lower Proterozoic Cahill Formation. This uranium mineralization post-dates an ~1800 m.y. metamorphic event; isotopic dating of uraninite and galena indicates two periods of mineralization or mobilization dated at ~1600 and ~900 m.y. The orebodies have a number of features in common; all occur in the same stratigraphic unit (strata-bound); location within breccia zones; contained in rocks that underwent low-temperature retrogressive metamorphism; proximity to granitoids, and occurrence below the Middle Proterozoic unconformity. An additional feature at three of the deposits is the extreme thinning or disappearance of massive bedded carbonate sequences within the ore-zones and reappearance external to these zones.

The Lower Proterozoic meta-sediments are enriched in uranium, having been derived from an Archaean provenance containing 2 to 6 times normal uranium abundance for granitoids. Black shale units and carbonaceous-rich carbonates within the Lower Proterozoic sediments concentrated uranium but no syngenetic deposits are known to have developed. During the ~1800 m.y. metamorphic event, uranium does not appear to have been mobilized on any extensive scale. Peneplanation of the terrane followed on the ~ 1800 m.y. regional metamorphic event, and during this period solution cavity and accompanying karst topography is thought to have developed. The insolubles, mostly meta-psammitic and meta-pelitic material, collapsed into these solution cavities (dolines). Additional insolubles like clay and carbonaceous matter were probably washed into these structures. The breccia zones provided a plumbing system and sites for ore-formation. It is postulated that oxidising and mildly alkaline to neutral meteoric water percolated along bedding planes and fracture systems and scavenged uranium from the Lower Proterozoic metamorphic rocks. Black shales and insoluble carbonaceous matter are thought to have supplied most of the uranium as the elements concentrated in these carbonaceous-rich meta-pelites are also those found concentrated in the ore-zones (e.g. U, W, As, Nb, Mo, Pb, Li, Sc, Co, Cu, B and REE). En route to the ore zones, the uranium-bearing solutions may have evolved a slightly acid condition as a result of oxidization of the sulphides within the black shales. The very high U/Th ratios (> 500) encountered within the uranium ore-zones suggest that the uranium was transported as a uranyl species. Enrichment within the ore-zones of REE and in particular HREE suggests uranyl carbonate complexing. Because some experimental evidence suggests that carbonate complexing becomes less effective with increasing temperature, it is postulated that the original uranium concentration was at low temperature. Within dolines and fracture systems, the solutions would enter an environment where adsorption could take place. Experimental work demonstrates that clays, ferric hydroxides and carbonaceous matter are excellent adsorbers of uranium under slightly acid conditions. Cyclic stripping of adsorbed uranium by reduction would precipitate uraninite and allow further adsorption and concentration to take place. Reduction of the uranyl complexes could be brought about by a number of mechanisms including oxidation of the Fe^{2+} in clays/chlorites and consumption of graphite to produce methane.

At ~1700 m.y. the breccia columns are thought to have been largely sealed by infill and alluvium. High heat-flow conditions were probably encountered in the area due to igneous activity associated with the pre-Kombolgie, Oenpelli Dolerite at 1688 m.y. and intercalated lava flows in the Kombolgie Formation at 1648 m.y. It is thought that the heat associated with the latter event remobilized the uranium deposits in situ resulting in the ~270°C temperatures estimated from stable isotope data. The euhedral disseminated uraninite at Ranger, dated at ~1600 m.y., is thought to have been produced at this time. Reworking of the uranium deposit took place at low temperature at ~900 m.y., during a period of marked epeirogenesis in the area. The colloform and massive vein uraninite at Jabiluka, Nabarlek, and Koongarra is thought to have been produced in situ during this event.

The apparent absence of massive carbonate sequences at Nabarlek makes this deposit atypical of the area. The ore occurs in a crush zone with abundant hematite, clay/chlorite and minor graphite. It is suggested that the brecciated plumbing system allowed uranium-enriched meteoric water to penetrate with fixation of uranium on ferric hydroxides in the breccia zones. Cyclic variations in pH and/or Eh and/or temperature may have precipitated the uranium, clearing the adsorption sites for further concentration of uranium. During dehydration, the ferric hydroxides were converted to hematite.

INTRODUCTION

Major uranium deposits occur in the Alligator Rivers Uranium Field (ARUF) within the Lower Proterozoic Cahill Formation, these are: Nabarlek (Anthony, 1975), Jabiluka (Hegge, 1977), Ranger (Eupene *et al.*, 1975) and Koongarra (Foy & Pedersen, 1975). These deposits and many prospects occur within zones of major disruption and extensive

retrogressive metamorphism. Uraninite and galena ages from this uranium field indicate two periods of possible mineralization or mobilization at ~1600 and ~900 m.y. (Hills & Richards, 1976; J.H. Hills, R.W. Page, B.L. Gulson & G.H. Riley, pers. comm.).

A number of models which have been advanced to explain the origin of these uranium deposits share the concept of an epigenetic origin, but opinion is divided as to whether the mineralization is formed by hypogene or supergene processes. A hypogene model is supported by Hills (1973), who considered that some preconcentration of uranium took place during orogenesis concentrating in the metamorphic rocks and intrusive granites. Hills proposed that the hydrothermal emplacement of the ores was followed by later remobilization. Ryan (1977) proposed hydrothermal emplacement of the uranium from unknown sources, which were likely to have been associated with granitization and anatexis, accompanied by expulsion of metal-bearing connate waters. Binns *et al.* (1979) favour "hydrothermal extraction or emanation from suitable subjacent granitoids" to account for uranium mineralization at Jabiluka. Needham & Stuart-Smith (1976) advocate a hydrothermal origin for Nabarlek. Eupene (1979) suggested that mineralizing waters were liberated from the Lower Proterozoic portions of the Nanambu Complex and mingled with water reservoirs in the carbonate units of the lower Cahill Formation to form the U-deposits. Similarly, Dodson *et al.* (1974) suggest that mineralizing connate solutions were mobilized during igneous and contemporaneous tectonic phases. Modifications of the epigenetic model have been put forward by a number of workers. The models mostly involve initial syngenetic concentration of uranium in the Lower Proterozoic sediments followed by ore-forming event(s) which occurred:

1) during or following Lower Proterozoic metamorphism, with reconstitution during later orogenic events (Hegge 1977; Hegge & Rowntree, 1977);
2) "a number of times" corresponding to the periods of isotopic dating of mineralization (Needham & Stuart-Smith, 1976);
3) due to low-temperature meteoric solutions transporting colloidal urano-compounds with fixation by a strong electrolyte (Ypma & Fuzikawa, this volume);
4) when brines were released, at different periods, from evaporates in the Lower Proterozoic sequence that were "possibly enriched in uranium" (Crick & Muir, this volume).

A number of recent field, mineralogical and chemical results were investigated and evaluated and from this a model has been derived for mineralization in the ARUF.

REGIONAL SETTING

The regional geological setting and a comparative review of the major uranium deposits in the ARUF has been presented elsewhere Needham *et al.* (1977), Needham & Stuart-Smith (this volume) and Hegge *et al.*, (this volume).

The oldest rocks in the area, Archaean to Lower Proterozoic, comprise the mantled gneiss dome of the Nanambu Complex. This Complex contains Archaean granitoids with a primary age of about 2500 m.y. (Page *et al.*, this volume) and Lower Proterozoic feldspathic and quartzitic gneisses and schists which were accreted during an ~1800 m.y. regional metamorphic event. The base of the Lower Proterozoic succession is represented by sheared gneisses and the rudite-rich assemblage of the Kakadu Group. The Cahill Formation overlies the Kakadu Group with apparent conformity and in places is contiguous with the Nanambu Complex. The Cahill Formation is overlain, in places unconformably, by a dominantly clastic assemblage of rocks which belong to the Nourlangie Schist. Extensive intrusion of continental tholeiite sills followed; orogenesis occurred at about 1800 m.y. and was accompanied by granitoid development which continued into the early Middle Proterozoic. Rocks in the ARUF have undergone medium to high-grade metamorphism

(Ferguson & Needham, 1978; Ferguson, this volume) and four periods of deformation resulting in multiple isoclinal folding and extensive thrusting (Needham & Stuart-Smith, 1976; this volume). Intrusion of post-orogenic mafic lopoliths at 1688 m.y. (Page *et al.*, this volume) post-date late orogenic granitoid development. Peneplanation and deposition of the Middle Proterozoic Kombolgie Formation followed. This Formation is dominantly massive rudite and contains minor intercalated volcanics, dated at about 1650 m.y. (Page *et al.*, this volume).

Needham & Stuart-Smith (1976) have divided the Cahill Formation into two members: a lower member, which is host to the uranium mineralization and is characterized by the presence of carbonaceous and carbonate units, and also contains an interlayered sequence of mica schist, chloritized feldspathic quartzite, quartz schist, para-amphibolite and calc-silicate rock; the upper more psammatic member contains quartz schist, feldspathic schist, felspathic quartzite and conglomerate. Both members contain orthoamphibolite and have been regionally metamorphosed to medium-grade (Ferguson & Needham, 1978).

GEOLOGY OF URANIUM DEPOSITS

A number of authors (Needham & Stuart-Smith, 1976; this volume; Eupene, 1979) have noted the spatial association of the known uranium ore-zones with the following geological features:

1) the regional unconformity surface which separates Lower and Middle Proterozoic, and proximity to the Kombolgie escarpment;
2) the lower member of the Cahill Formation;
3) contact of metasediments with granitoid complexes;
4) zones of retrograde metamorphism;
5) absence of massive bedded carbonates within the ore-zones, and their reappearance outside the ore-zones, except at Nabarlek where carbonate rocks do not appear to be involved (Eupene *et al.*, 1975; Foy & Pedersen, 1975).

Recently discovered uranium prospects, namely Ranger 68 and Austatom, are farther from the escarpment than previous discoveries (16 and 42km respectively), but they lie close to the Lower-Middle Proterozoic unconformity which corresponds very closely to the present land surface. All uranium deposits in the ARUF are stratabound within the lower member of the Cahill Formation, and occur in the lowermost 300-600m, a unit dominated by carbonaceous schist and bedded carbonates. All these ore-zones are close to granitoid/metasedimentary contacts. Koongarra is the fartherest removed from this contact, occurring 6.5km from the Nanambu Complex.

Rocks of the ARUF have been regionally metamorphosed to medium and high-grade with anatexis and the development of granulites. The most recent P-T estimates for metamorphic conditions in the Cahill Formation are in the range 5-8kb and 550-630°C (Ferguson, this volume). Within areas of uranium mineralization, very low-temperature retrograde metamorphism is found.

One of the most striking features of the ore deposits is the tendency for mineralization to be intimately associated with zones of brecciation and chloritization (Binns *et al.*, this volume; Ewers & Ferguson, this volume). The breccia fragments are typically chlorite and/or sericite-bearing meta-arenites, strongly chloritized material, and chert which is commonly a replacement of carbonate. (Ewers & Ferguson, this volume). The fragments are generally angular and rotated, and are cemented by chlorite/clay ± hematite ± chert ± quartz ± graphite ± sulphides ± uraninite. Vugs can be present, generally infilled with euhedral quartz and chlorite and sometimes hematite. The primary uranium mineralization is uraninite, although Binns *et al.* (this volume) report the lesser presence of coffinite and brannerite at Jabiluka. Eupene (1979) mentions "minor incursions" of uranium mineralization in the top

of the Nanambu Complex. Within the brecciated ore-zones there are tabular intrusions of granitoid pegmatites, amphibolite and chloritized dolerite. At Jabiluka, uranium zones thicken on the upperside of pegmatites (M.R. Hegge, pers. comm). Jabiluka One is underlain by the large mafic Zamu Dolerite intrusive that pre-dates uranium mineralization.

Uraninite and galena ages from the ARUF indicate two different periods of possible mineralization or mobilization, namely ~1600 m.y. and ~900 m.y. (Hills & Richards, 1976; J.H. Hills, R.W. Page, B.L. Gulson & G.H. Riley, pers. comm.). Rb-Sr ages on rocks from the alteration zones associated with uranium mineralization at Nabarlek and Jabiluka give an average model age of about 1600 m.y., additionally a younger event <920 m.y., is recorded at Nabarlek (Page *et al.*, this volume). K-Ar muscovite ages from altered and unaltered Cahill Formation rocks at Jabiluka are consistent at about 1800 m.y. - an indication that the alteration associated with this ore-zone took place below the threshold retention temperature at about 350°C (Page *et al.*, this volume).

With the exception of Nabarlek, the uranium deposits are associated with massive bedded dolomite and/or magnesite. A feature of this association is the disappearance, or marked thinning of, the carbonate sequences within the ore-zones (Eupene *et al.*, 1975; Foy & Pedersen, 1975). Chert replacement of the carbonates is also a common feature (Ewers & Ferguson, this volume). Eupene *et al.* (1975) suggested for Ranger 1 No. 1 ore-body that disrupted zones in "the Upper Mine Schists, the Footwall Shear Zone, and other features indicating disturbance as at least partly generated by collapse of the Lower Mine Sequence within the mineralized zones". J. Ferguson (BMR Workshop, May 1977) suggested that, with the exception of Nabarlek, the zones of disruption found in the ore-zones could result from solution cavity development of the massive bedded carbonate sequences, accompanied by collapse. Eupene (1979) attributes the disruption in the ore-zones to silicification of carbonate which resulted in volume reduction and collapse. At Nabarlek the ore-zone is located in a discordant crush-zone removed from massive carbonate sequences (Anthony, 1975). Binns *et al.* (1979) are of the oninion that the brecciated ore zones at Jabiluka were produced by "hydraulic fracturing arising from excessive pressure of either the retrogressive or the earliest mineralizing fluids . . .". This concept is favoured by these authors on the grounds that "there would appear to have been nothing available to dissolve and collapse" (p.22) despite the contrary evidence for massive carbonate units occurring juxtaposed to the ore-zones at Ranger 1 (Eupene *et al.*, 1975), Koongarra (Foy & Pedersen, 1975), and Jabiluka (Hegge, 1977).

CONSTRAINTS OF ORE-FORMING SOLUTIONS

The composition of the ore-forming solutions can, in part, be inferred from the mineralogy of the ore-zones and wall-rock alteration, and additionally from: (1) whole-rock chemistry; (2) mineral chemistry; (3) stable isotopes; (4) fluid inclusions.

Correlation matrices of whole-rock chemistry of the Cahill Formation (Ferguson & Winer, this volume) show uranium correlates with W, As, Nb, Mo, Pb, Li, Sc & Co at the 99 percent confidence limit. The larger number of rocks analysed in the Cahill Formation (143), made it possible to examine elemental correlations at the 99 percent confidence level for 4 subsets of rocks based on U content:

1) U in excess of 500 ppm - U correlates with As, Nb, La, Ce, Mo, Pb & Co.
2) U in excess of 40 ppm - U correlates with As, Nb, Mo, Pb, Sc & Co.
3) U less than 40 ppm - U correlates with P.
4) U less than 30 ppm - U shows no correlation.

Analyses of samples from Jabiluka One and Two indicate the following elemental correlations (99% level) for two data subsets:

1) U in excess of 40 ppm - U correlates with Cu, W, As, Nb, Mo, Pb, Sc & Co.

2) U less than 30 ppm - U shows no correlation.

G.A. Cowan (unpublished data) established that uraninite from Jabiluka concentrates Li, B, HREE, Bi, Sb, Ga, Co and Ti. Concentration of REE with enrichment in HREE in ore-zones is confirmed by McLennan & Taylor (this volume). Limited available gold analyses in whole-rocks suggest that there is no correlation with uranium (Ferguson & Winer, this volume). However, high gold contents (greater than 4 ppm) are restricted to rocks with a high uranium content (greater than 1000 ppm).

Metapelitic and psammitic schists in the broad retrograde halo surrounding mineralization show the following changes compared to their unaltered equivalents: enrichment in Mg and Li; depletion in Ca, Na, Sr, Ba, and, to a lesser extent, Rb and possibly P, Fe, Mn and Cr (Binns *et al.*, 1979). Within the retrogressively metamorphosed ore-grade rocks, there is further enrichment in Mg and depletion in K. The disseminated ores are slightly enriched in Ca, P and Sr. Yb and radiogenic Pb show enrichment comparable to that of uranium in the ore-zones.

Minerals consistently associated with uranium mineralization throughout the ARUF are a variety of chlorites, clay-structured chlorites, and clays (Ewers & Ferguson, this volume). There is a tendency for these chlorite-clays that are associated with the uraninite to be magnesium-rich and to have low Fe^{2+}/Fe^{3+} ratios (Ewers & Ferguson, this volume).

Stable isotope data (Donnelly & Ferguson, this volume) from minerals in the ore-zones and in the medium-grade metamorphic assembledges of the Cahill Formation suggest:

1) Bedded sulphides, adjacent to the ore-zones, formed from H_2S of juvenile origin. These sulphides formed in a marine environment in which, at this time, sulphate, if present, also had an isotopic composition indicating a juvenile origin.
2) That the sulphides within ore-zones are isotopically different to bedded sulphides and indicate that at the time of their formation isotopically heavy seawater sulphate was present. That is, biological sulphate reduction was an established process. Two explanations can account for the sulphur isotope values found in the ore-zones:
   a) a single step, low temperature, process in which the sulphides formed by bacterial sulphate reduction under conditions of a restricted sulphate supply, or
   b) a multiple step, higher temperature, process in which some sulphides formed from hydrothermal solutions under changing redox conditions (increasing Eh and the presence of sulphate); some bedded sulphides may have been moved to the ore-zones; and high temperature sulphate reduction.
3) Sulphur isotope, geothermometry indicates high temperatures, around 270°C, for both bedded and ore sulphides at Jabiluka. The most probable explanation is that these temperatures indicate a heat event after the formation of the deposit which caused re-equilibration of the isotopic compositions of coexisting sulphides, without changing overall isotopic ranges.
4) Carbon isotopic compositions of carbonates away from the ore-zones are typically of Lower Proterozoic marine carbonates.
5) That the carbonates from ore-zones have carbon isotopic values which indicate formation in an organic-rich environment, in the presence of organically-derived CO_2.
6) Correlations between $\delta^{13}C$ and $\delta^{18}O$ for ore-zone carbonates at Jabiluka One and Two and Ranger 1 are explained, most simply, as the result of low temperature oxidising groundwater circulation into organic-rich zones.

Two types of fluid inclusions have been observed in quartz and calcite associated with zones of uranium mineralization in the Nabarlek and Jabiluka deposits (Ypma & Fuzikawa, this volume). Type I fluid inclusions, in their pure form, are characterized by extreme

salinities, predominance of $CaCl_2$, and occurrence of Mg chlorides and sulphates and NaCl, KCl and Fe chlorides. Type II inclusions, in their pure form, are characterized by lower salinities and CO_2 in the vapour phase. For Type I inclusions, homogenization temperatures differ but are mainly between 100° and 160°C; Type II inclusions give various homogenization temperatures but are commonly as low as 85°C.

A downward percolation is suggested for the direction of flow of the mineralizing solutions; evidence for this includes ponding effects with uranium enrichment on the upper side of steeply dipping, impermeable barriers in the ore-zones and bottoming out of the ore-zone against an impermeable mafic intrusive at Jabiluka One.

Photosynthesis has probably taken place from at least 2500 m.y. b.p. (Cloud, 1976), and so it is likely that any younger meteoric waters were to varying degrees oxidising and uranium would then have been transported as the U^{6+} complex. As Th is diadochic with U^{4+} (Naumov, 1959) the U/Th ratio is a critical parameter in deciding the ionic species being transported. That the uranium was probably transported in the hexavalent state is supported by the marked increase in U/Th ratios within the ore bodies (>500), as compared to the granitoids (< 1.1), granitic pegmatites (~12.5), and black shales (~2.3). (Ferguson & Winer, this volume). At typical concentrations in groundwater, the most important uranyl complexes are found with carbonate, P, F and sulphate (Langmuir, 1978). Fluoride and sulphate complexing may be significant in acid conditions up to ~pH4. The presence of carbonates and micas in the metasediments would buffer ground water pH to neutral or slightly alkaline. Under these conditions phosphate, carbonate, and hydroxy uranyl complexes would be the most important (Langmuir, 1978). With increasing temperature, they are minor species at all pH's at temperatures of 100°C and $P_{CO_2} \leq 10^{-2}$ atm (Langmuir, 1978). Since P is not an important element in any of the rocks associated with the ore-zones, whereas the REE show enrichment in the ore-zones and are known to be transported by carbonate complexes (Kosterin, 1959), the latter is the preferred uranyl complex. That CO_2 was present in the ore-zones is supported by the presence of chert after carbonate - a condition resulting from increased P_{CO_2} (von Engelhardt, 1977).

SOURCE OF URANIUM

The Archaean granitoids within the Pine Creek Geosyncline are thought to be representative of the provenance area for the Lower Proterozoic sediments. The granitoids are enriched in uranium by 2 to 6 times world average abundances for granitoids (Ferguson *et al.*, 1979). The uranium in the granitoids is present in the accessory minerals uraninite, monazite, zircon, uranothorite, xenotime and apatite (McAndrew & Finlay, this volume). This uranium anomaly in the provenance area led to an enrichment in the derived sediments, those closer to source probably being more enriched. Most metasedimentary rock types within the geosynclinal pile are enriched in uranium relative to world aboundances for equivalent rock types. As discussed earlier, the ore-solutions were meteoric, oxidising and probably mildly alkaline, a condition well suited to uraninite solubility in the provenance granitoids and to transport of the uranium as a U^{6+} complex. Fixation of uranium in the sediments could have been brought about either by adsorption onto clays, organic matter, ferric-, titanium- and manganese-hydroxides, or by chemical reduction under anaerobic conditions. The greatest concentrations of uranium in the Pine Creek Geosyncline away from the ore-zones are in pyritic, carbonaceous black shales of the Koolpin, Masson and Cahill Formations (Ferguson & Winer, this volume). This association suggests that the uranium concentrated by adsorption either onto living and/or decaying organisms, or alternatively was directly precipitated in an anaerobic environment by H_2S generated during bacterial sulphate reduction. However, the syngenetic uranium concentrating mechanism was inadequate to produce ore deposits, as all of the major uranium deposition in the ARUF

postdate the ~1800 m.y. regional metamorphic event (Ewers & Ferguson, this volume). During the medium-grade metamorphism of the Cahill Formation, the carbonaceous matter was converted to graphite. There is no evidence of concentration of uranium during this metamorphic event (Ferguson & Winer, this volume).

The proposed model for uranium mineralization which we develop here applies specifically to the Jabiluka, Ranger, and Koongarra deposits, which show marked similarities and probably have parallel origins. Where possible reference has also been made to Nabarlek; however, Nabarlek shows some significant differences from the other deposits, and has not been studied in the same detail.

THE MODEL

Development of the brecciated ore-zones took place in the carbonate-rich sequences at Jabiluka, Ranger and Koongarra after peneplanation of the Lower Proterozoic sediments and before depositon of the Kombolgie Formation. Solution of these carbonate rocks appears to have produced a karst topography with collapse structures, or large caverns, containing insoluble fragments and other insoluble residues such as micas, chlorite, clays, and graphite. These dolines may have either been open or overlain by only a thin cover of rock with a well-developed fracture system. Textures and lithology clearly indicate that the breccias developed after the regional metamorphism (Ewers & Ferguson, this volume) and that there was a high percentage of voids between the fragments, at times reaching 50 percent by volume.

The main mineralizing event was probably low-temperature, and took place after the development of the collapse dolines. During this period, Mg-rich clays (and/or chlorite) and possibly decaying organic matter, now represented by thucholite, were washed into the structures. The apparent activity of sulphate respirers and biogenic carbonates within the breccia zones further supports the presence of organic matter. The introduced material was probably already enriched in uranium, and may well have been capable of further enrichment through adsorption. Experimental studies indicate that organic material and clays readily adsorb large quantities of uranium in the pH range 5 to 8.5 (Rozhkova *et al.*, 1959; Muto *et al.*, 1965; Dio *et al.*, 1975). Muto *et al.* (1965) found that uranium, presumed to be in a metastable state when adsorbed on clays, was released and formed in time a stable uranium mineral and that, in the process, the clays recovered their sorptive capacity. Muto *et al.* (1965) quote an enrichment factor of 10,000. The experimental work of Giblin (this volume) shows that the adsorption capacity of kaolin, known to have the least effective sorption properties of all clay minerals, reached a maximum Kd at 25°C of 35,000 at pH 6.5. In order for desorption to take place the surface charge of the adsorbed uranium ion must be made incompatible with the negative sorbent surface of the clay or clay-sized chlorite. This incompatibility can be brought about by increasing the CO_2 content at constant pH, raising the pH (Langmuir, 1978), or varying the temperature (Giblin, this volume). The accumulation of organic material within the collapse structures would create an anaerobic environment in which CH_4 and CO_2 might be present at a pH between 5 and 7. It is postulated, that while the clays and organic material were accumulating within the dolines, the plumbing system of these structures was such that low-temperature CO_2-rich groundwater, carrying uranium as uranyl carbonate complexes, passed through them. As the trace elements concentrated in the black shales are those also found in the ore-zones (for example U, W, As, Nb, Mo, Pb, Li, Sc, Co, Cu, B and REE) it seems likely that the meteoric solutions scavenged most of these components from the black shales (Table 1). Additionally the ore-zones could have partly inherited this geochemistry from carbonaceous-rich residue produced during doline formation.

The meteoric solutions are thought to have been originally neutral to slightly alkaline,

and oxidising, a condition that would allow ready dissolution of uraninite (Hostetler & Garrels, 1962; Langmuir, 1978), the main uranium mineral found in the provenance Archaean granitoids. The Eh and pH of the solutions could have evolved significantly before they reached the sites of deposition in the dolines. On entering the now carbonate poor collapse structures, reduction in pH would enhance the adsorption of uranium onto particulate matter. The reduction of uranyl complexes may have been facilitated by the oxidation of Fe^{2+} in clay, chlorite or other Fe-bearing minerals (Ewers & Ferguson, this volume).

It is suggested that around 1700 m.y. the deposits were effectively sealed by infill and alluvium, and that all subsequent events recorded within the deposits, including the high temperature features, represent reworking in situ. High heat-flow conditions were probably present in the area due to igneous activity associated with the pre-Kombolgie Oenpelli Dolerite at 1688 m.y. and intercalated lava flows in the Koombolgie Formation at 1648 m.y. (Page *et al.*, this volume). It is probable that the heat associated with the latter igneous event resulted in the ~270°C temperature recorded in the ore-zone from stable isotope data; additionally amorphous uranium oxides could have crystallized in a disseminated euhedral form about 1600 m.y. ago. It appears to be significant that this disseminated euhedral form of uraninite is particularly well developed at Ranger and that Ranger also records this ~1600 m.y. event very clearly. Russian studies of hydrothermal uranium deposits (Tugarinov & Naumov, 1969) indicate that the formation of uraninite occurs above 250°C whereas pitchblende, the massive microcrystalline and commonly colloform variety of uraninite, forms at temperatures not exceeding 220°C and probably less than 200°C. It is not clear whether clay, or chlorite, or both accumulated in the dolines. However, if Mg-rich clays were originally present, diagenesis (Rowsell & De Swart, 1976) or heating by an igneous event would have been sufficient to convert them to chlorite. The ~1600 m.y. dates recorded within the ore-zones would belong to this period. It is suggested that, whereas the Type II fluid inclusions of Ypma & Fuzikawa (this volume) may represent the original mineralizing groundwater, the very saline brine of the Type I inclusions were produced at the time of igneous intrusion by derivation from evaporites in the Cahill Formation (Crick & Muir, this volume).

Petrographic work shows that solution of the disseminated uraninite and its redeposition as stringers and colloform uraninite has occurred in these deposits (Ewers & Ferguson, this volume; Binns *et al.*, this volume) and it would seem that the conditions required for this to take place may be very mild. The ~900 m.y. event can be correlated with epeirogenesis and development of Adelaidean (Upper Proterozoic) sedimentation to the south of the Pine Creek Geosyncline. Hydrostatic imbalance at high levels in the crust would be well-developed during periods of thermal activity associated with epeirogenesis.

COMMENTS ON THE MODEL

Although our model favours adsorption, with reduction, as the process responsible for the early syngenetic concentration of uranium and the main mineralizing event, other depositional mechanisms cannot be precluded. If uranium is transported as uranyl carbonate complexes, experimental work would indicate that redox reactions, pH changes, and the loss of CO_2 may individually or collectively assist the deposition of uraninite.

The presence of graphite and sulphides in the ore-zones is enigmatic. Graphite has clearly developed in the carbonaceous-rich units during the regional metamorphic event. Its presence in the ore-zones may represent an insoluble residue in the solution-collapse structures, and/or a second generation of carbonaceous matter introduced at the time of the main mineralizing event. Thucholite has been reported from the Ranger I No. 3 orebody (G.H. Taylor *in* Eupene, 1979) and Jabiluka (Binns *et al.*, this volume), which may indicate

Element	Av. PCG	Av. "normal" Shale	Black Shales Median	Black Shales Metal rich	Black Sea Muds
	(a)	(b)	(c)	(d)	(e)
Ba	235	580	300	700	
Rb	110	140			
Sr	45	300			
Pb	39	20	20	70	
Th	15	12			
U	34	3.7		>20	12
Zr	137	160	70	150	107
Nb	9	18			
Y	24	41			
La	34	40			
Ce	71	95			
Li	27	66			
Cs	5	5.5			
Sc	16	13			
V	242	130	150	700	177
Co	22	19	10	20	30
Ni	45	68	50	200	92
Cu	70	45	70	150	106
Zn	50	95	<300	1000	
Ga	19	19			
Be	3	3			
As	9	10			
Mo	12	2.6	10		77
Sn	3	6			
Hf	5	2.8			
W	4	1.8			
F	1064	740			
Cl	45	180			

(a) Ferguson & Winer, this volume. Pine Creek Geosyncline - black shale average of PCG 26, 31, 32, 33, 36, 37, 40, 42, 43, 84, & 85.
(b) Wedepohl (1970) (c) & (d) Vine & Tourtelot (1970)
(e) Volkov (1973)

Table 1. Average Chemical analyses of Black Shales.

a second generation of organic material. However, there appears to be no correlation between the occurrence of carbon and the concentration of uranium, and if such a correlation did exist, its absence can only be argued in terms of the removal of carbon as CH_4 and CO_2. Experimental work (French, 1966) demonstrates that at temperatures around 200°C, interaction of diagenetic solutions with graphite generates methane and carbon dioxide by the reaction:

$$2C + 2H_2O = CH_4 + CO_2$$

The temperatures subsequently generated within the orebodies (i.e. ~ 270°C) by the event associated with igneous activity would have been sufficient for the removal of graphite in the presence of water by the above reaction. However the fact that biogenic carbonates are present only in the ore-zones (Donnelly & Ferguson, this volume) argues against this reaction. The presence of organic materials at the time of the main mineralization event, may have facilitated the localization of gold in the orebodies through adsorption (Lakin *et al.*, 1974). The absence of a broad correlation between sulphur and uranium (Ferguson & Winer, this volume) suggests that the reduction of uranyl complexes by sulphide ions was not an important process during the main mineralizing event. However, subsequent remobilization of the deposits in situ in the presence of sulphides may have caused local redeposition of uraninite. The positive correlation of U with Cu at Jabiluka (Ferguson & Winer, this volume) may be an indication of this.

Although the Nabarlek deposit is broadly similar to the Jabiluka, Ranger, and Koongarra deposits, it shows a significant difference, which affects the application of the above model, that is, there are no massive bedded carbonates in the vicinity of Nabarlek. The mineralization occurs within a well-developed crush zone, and hematite becomes a major constituent of the host rock (together with chlorite) towards the centre of the orebody (Anthony, 1975). Minor graphite has also been recognised recently (R. Tammekand & S. Lees, pers. comm.). It could be argued that this crush-zone may have acted as a structural trap for washed-in clays and/or chlorite and hydrated iron oxides, which have subsequently been dehydrated to hematite. The remarkable sorptive power of ferric oxyhydroxides for uranyl complexes is well documented (Van der Weijden *et al.*, 1976; Langmuir, 1978) and may account for the high ore grades found at Nabarlek.

Most of the uranium deposits and prospects in the Rum Jungle and South Alligator Valley Uranium Fields have features in common with those occurring in the ARUF. They all occur within zones of disruption usually involving carbonaceous and chlorite-rich shales, slates, and schists that overlie or are in faulted contact with massive carbonate units (Berkman, 1968; Fraser, 1975; Foy, 1975; Ayres & Eadington, 1975). However, dissimiliarities are that they occur within terranes of low-grade regional metamorphism; some contain major associated base-metal mineralization; the South Alligator Valley deposits occur at a higher stratigraphic level compared to the other two Fields; a few deposits in the South Alligator Valley are associated with salic volcanics rocks.

ACKNOWLEDGEMENTS

We are indebted to Geopeko Ltd., Noranda Australia Ltd., Pancontinental Mining Ltd. and Queensland Mines Ltd. for supply and access to rock samples. M.R. Hegge, J.T. Nash, and G.H. Taylor offered valuable criticism of an earlier draft of this manuscript.

Published with permission of the Director, Bureau of Mineral Resources, Geology & Geophysics, Canberra, Australia.

REFERENCES

Anthony, P.J., 1975: Nabarlek uranium deposit. *in* (ed. C.L. Knight) *Economic Geology of Australia and Papua New Guinea, Australias. Inst. Min. Metall., Monograph Series No. 5, 1. Metals*, 304-308.

Ayres, D.E., & Eadington, P.J., 1975: Uranium mineralisation in the South Alligator River Valley. *Miner. Deposita, 10*, 27-42.

Berkman, D.A., 1968: The geology of the Rum Jungle uranium deposits. *Australas. Inst. Min. Metall. Symposium, Uranium in Australia*, 12-31.

Binns, R.A., McAndrew, John & Sun, S-S., 1979: Origin of uranium mineralisation at Jabiluka. *Extended Abstracts of the International Uranium Symposium on the Pine Creek Geosyncline*, 20-25.

Binns, R.A., McAndrew, John & Sun, S-S., this volume: Origin of uranium mineralization at Jabiluka. *Proceedings of the International Uranium Symposium on the Pine Creek Geosyncline.*

Cloud, Preston, 1976: Major features of crustal evolution. *Du Toit Memorial Lecture 14, Geol. Soc. Sth. Africa, Annexure to Volume 79.*

Crick, I.H. & Muir, M.D., this volume: Evaporites and uranium mineralisation in the Pine Creek Geosyncline. *Proceedings of the International Uranium Symposium on the Pine Creek Geosyncline.*

Dodson, R.G., Needham, R.S., Wilkes, P.G., Page, R.W., Smart, P.G. & Watchman, A.L., 1974: Uranium mineralisation in the Rum Jungle — Alligator Rivers province, N.T., Australia. *Rec. Bur. Miner. Resour. Geol. Geophys. Aust., 1974/37*, (unpubl.).

Doi, K., Kirono, S. & Sakamari, Y., 1975: Uranium mineralisation by groundwater in sedimentary rocks, Japan. *Econ. Geol., 70*, 628-646.

Donnelly, T.H. & Ferguson, John, this volume: A stable isotope study of three deposits in the Alligator Rivers Uranium Field, N.T. *Proceedings of the International Uranium Symposium on the Pine Creek Geosyncline.*

Eupene, G.S., 1979: Stratigraphic, structural and temporal control of mineralisation in the Alligator Rivers Uranium province, N.T., Australia. *in* (ed. J.D. Ridge) *Proceedings of the fifth International Symposium on the Genesis of ore deposits Snowbird, Utah, August 1978* (in press).

Eupene, G.S., Fee, P.H. & Colville, R.G., 1975: The Ranger One uranium deposits. *in* (ed. C.L. Knight) *Economic Geology of Australia and Papua New Guinea, Australas. Inst. Min. Metall., Monograph Series No. 5, 1. Metals*, 308-317.

Ewers, G.R. & Ferguson, John, this volume: Mineralogy of the Jabiluka, Ranger, Koongara and Nabarlek uranium deposits. *Proceedings of the International Uranium Symposium on the Pine Creek Geosyncline.*

Ferguson, John, this volume: Metamorphism in the Pine Creek Geosyncline and its bearing on stratigraphic correlations. *Proceedings of the International Uranium Symposium on the Pine Creek Geosyncline.*

Ferguson, John, Chappell, B.W. & Goleby, A.B., this volume: Granitoids in the Pine Creek Geosyncline. *Proceedings of the International Uranium Symposium on the Pine Creek Geosyncline.*

Ferguson, John & Needham, R.S., 1978: The Zamu Dolerite : A lower Proterozoic preorogenic continental tholeiitic suite from the Northern Territory, Australia. *J. geol. Soc. Aust., 25*, 309-322.

Ferguson, John & Winer, Paul, this volume: Pine Creek Geosyncline : Statistical treatment of whole rock chemical data. *Proceedings of the International Uranium Symposium on the Pine Creek Geosyncline.*

Foy, M.F., 1975: South Alligator Valley uranium deposit. *in* (ed. C.L. Knight), *Economic Geology of Australia and Papua New Guinea, Australas. Inst. Min. Metall., Monograph Series No. 5, 1 Metals*, 301-304.

Foy, M.F. & Pedersen, C.P., 1975: The Koongarra uranium deposit. *in* (ed. C.L. Knight), *Economic Geology of Australia and Papua New Guinea, Australas. Inst. Min. Metall., Monograph Series No. 5, 1. Metals, 317-321.*

Fraser, W.J., 1975: The Embayment line of mineralisation, Rum Jungle. *in* (ed. C.L. Knight), *Economic Geology of Australia and Papua New Guinea, Australas. Inst. Min. Metall., Monograph Series No. 5, 1. Metals*, 271-277.

French, B.M., 1966: Some geological implications of equilibrium between graphite and a C-H-O gas phase at high temperatures and pressures. *Rev. geophys., 4*, 223-253.

Giblin, A.M., this volume: Experiments on the role of day adsorption in genesis of uranium ores. *Proceedings of the International Uranium Symposium on the Pine Creek Geosyncline.*

Hegge, M.P., 1977: Geologic setting and relevant exploration features of the Jabiluka uranium deposits. *Proc. Australas. Inst. Min. Metall., 264*, 19-32.

Hegge, M.R. & Rowntree, J.C., 1978: Geologic setting and concepts on the origin of uranium deposits in the East Alligator Rivers Region, N.T., Australia. *Econ. Geol., 73*, 1420-1429.

Hegge, M.R., Mosher, D.V., Eupene, G.S. & Anthony, P.J., this volume: Geologic setting of the East Alligator uranium deposits and prospects. *Proceedings of the International Uranium Symposium on the Pine Creek Geosyncline.*

Hills, J.H., 1973: Lead isotopes and the regional geochemistry of North Australian uranium deposits. *Ph.D. thesis, Macquarie University, Sydney* (unpubl.).

Hills, J.H. & Richards, J.R., 1976: Pitchblende and galena ages in the Alligator Rivers Region, Northern Territory, Australia. *Miner. Deposits, 11*, 133-154.

Hostetler, P.B. & Garrels, R.M., 1962: Transportation and precipitation of U and V at low temperatures with special reference to sandstone-type U-deposits. *Econ. Geol., 57*, 137-167.

Kosterin, A.V., 1959: The possible modes of transport of the rare earths by hydrothermal solutions. *Geochemistry, 4*, 381-387.

Lakin, H.W., Curtin, G.C. & Hubert, A.E., 1974: Geochemistry of gold in the weathering cycle. *Bull. U.S. geol. Surv., 1330*, 80p.

Langmuir, Donald, 1971: Particle size effect on the reaction geothite = hematite + water. *Am. J. Sci., 271*, 147-156 and *Am. J. Sci., 272*, 972 (1972).

Langmuir, Donald, 1978: Uranium solution — mineral equilibria at low temperatures with applications to sedimentary ore deposits. *Geochim. cosmochim. Acta, 42*, 547-569.

McAndrew, John & Finlay, C.J., this volume: The nature and significance of the occurrence of uranium in the Nanambu Complex of the Pine Creek Geosyncline. *Proceedings of the International Uranium Symposium on the Pine Creek Geosyncline.*

McLennan, S.M. & Taylor, S.R., this volume: Rare earth elements in sedimentary rocks, granites and uranium deposits of the Pine Creek Geosyncline. *Proceedings of the International Uranium Symposium on the Pine Creek Geosyncline.*

Muto, T., Hirono, S. & Kurata, H., 1965: Some aspects of fixation of uranium from natural waters. *Mining Geol. (Tokyo), 15(74),* 287-298.

Naumov, G.B., 1959: Transportation of Uranium in hydrothermal solution as a carbonate. *Geochemistry, 1,* 5-20.

Needham, R.S., Crick, I.H. & Stuart-Smith, P.G., this volume: Regional Geology of the Pine Creek Geosyncline. *Proceedings of the International Uranium Symposium on the Pine Creek Geosyncline.*

Needham, R.S. & Stuart-Smith, P.G., 1976: The Cahill Formation — host to uranium deposits in the Alligator Rivers Uranium Field, Australia. *BMR J. Aust. Geol. Geophys., 1,* 321-334.

Needham, R.S. & Stuart-Smith, P.G., this volume: Geology of the Alligator Rivers Uranium Field. *Proceedings of the International Uranium Symposium on the Pine Creek Geosyncline.*

Page, R.W., Compston, William & Needham, R.S., this volue: Geochronology and evolution of the late Archaean basement and Proterozoic rocks in the Alligator Rivers Uranium Field, Northern Territory, Australia. *Proceedings of the International Uranium Symposium on the Pine Creek Geosyncline.*

Rozhkova, E.V., Rasumnaya, E.G., Serebryakova, M.B. & Shcherbak, O.V., 1958: The role of sorption in the process of uranium concentration in sedimentary rocks.*Proceedings of the International Conference on Peaceful Uses of Atomic Energy, U.N., Geneva, 1958,* 420-431.

Ryan, G.R., 1977: Uranium in Australia. *in* (ed. M.J. Jones) *Geology, mining and extractive processing of uranium. Inst. Min. Metall. London,* 24-42.

Tugarinov, A.I. & Naumov, V.B., 1969: Thermobaric conditions of formation of hydrothermal uranium deposits. *Geochem. Int., 6,* 89-102.

Van Der Weijden, C.H., Arthur, R.C. & Langmuir, Donald, 1976: Sorption of uranyl by hematite: Theoretical and geochemical implications. *Geol. Soc. Am. Abstracts with Program, 1976 Annual Meeting, Denver, Colorado.*

Vine, J.D. & Tourtelot, E.B., 1970: Geochemistry of black shale deposits — a summary report. *Econ. Geol., 65,* 253-272.

Volkov, I.I., 1973: The main patterns characterising the distribution of chemical elements through the deep sea sediments of the Black Sea. *Litologiya i Poleznye Iskapaemye.*

Von Engelhardt, W., 1977: The Origin of Sediments and Sedimentary Rocks. *Sedimentary Petrology, 3,* 359p. John Wiley & Sons, Halsted Press.

Wedepohl, K.H., 1970: Environmental Influence on the Chemical Composition of Shales and Clays. *in* (eds. L.H. Ahrens, F. Press, S.I. Runcorn & H.C. Urey). *Phys. Chem. Earth, 8,* 305-333. Pergamon Press.

Ypma, P.J.M. & Fuzikawa, Kazuo, this volume: Fluid inclusion studies as a guide to the composition of uranium ore forming solutions of the Nabarlek and Jabiluka deposits, N.T., Australia. *Proceedings of the International Uranium Symposium on the Pine Creek Geosyncline.*

ATHABASCA BASIN UNCONFORMITY-TYPE URANIUM DEPOSITS: A SPECIAL CLASS OF SANDSTONE-TYPE DEPOSITS?

J. Hoeve[1], T.I.I. Sibbald[2], P. Ramaekers[3] and J.F. Lewry[4]

1. Saskatchewan Research Council, 30 Campus Drive, Saskatoon, Canada, S7N OX1.
2. Saskatchewan Geological Survey, 1914 Hamilton Street, Regina, Canada, S4P 4V4.
3. Saskatchewan Geological Survey, Subsurface Laboratory, 201 Dewdney Avenue, Regina, Canada, S4N 4G3.
4. Department of Geological Sciences, University of Regina, Regina, Canada, S4S OH2.

ABSTRACT

Two major episodes of uranium metallogenesis are recognized in Northern Saskatchewan. The first is of late-Hudsonian age and gave rise to metamorphic-hydrothermal pitchblende deposits of simple mineralogy at Beaverlodge (primary mineralization: 1780 ± 20 m.y.). The second and more important episode of approximately Grenvillian age rendered unconformity-type deposits in the Athabasca Basin (primary mineralization: 1000-1300 m.y.). The late-Hudsonian deposits at Beaverlodge were overprinted by this second event and new deposits of complex mineralogy were formed in that area. The metallogenetic importance of a third and much later episode which gave rise to mineralization within the Athabasca Formation is uncertain at the moment.

With regards to metallogenesis of the unconformity-type deposits, presently available evidence favours a diagenetic-hydrothermal rather than a near-surface supergene or a magmatic/metamorphic hydrothermal model. The diagenetic-hydrothermal model relates uranium mineralization to 'red bed-type' diagenetic processes in the Athabasca Formation involving post-depositional oxidation and leaching, which continued for several hundred million years after deposition. Ore deposits were formed by interaction, under conditions of deep burial at elevated temperatures and pressures, of a uraniferous oxidizing Athabasca aquifer with reducing, graphite-bearing, metamorphic rocks of the basin floor. The large-scale convection required for such interaction may have been induced by mafic magmatic activity coeval with the episode of mineralization.

The diagenetic-hydrothermal model displays close similarities with metallogenetic models developed for certain sandstone-type deposits.

INTRODUCTION

Northern Saskatchewan has been known as a uranium producing area since the early 1950's, with active mines at Beaverlodge, the region around Uranium City (Fig. 1). During the exploration boom of the 1950's, hundreds of showings and occurrences were discovered and several mines went into production, most of which have since been closed. The more important deposits and occurrences are described by Beck (1969), who distinguishes between syngenetic and epigenetic deposits. None of the syngenetic deposits, represented by uranium-bearing pegmatites, are economically viable at present.

The epigenetic deposits contain pitchblende veins of variably complex parageneses and have been cited as examples of classical hydrothermal Ag-Ni-Co-Bi-U-type deposits (Maucher, 1962). Beck (1969) and Tremblay (1972) advocated a metamorphic hydrothermal origin and more recently supergene concepts have been proposed (Langford, 1974, 1977; Robertson & Lattanzi, 1974; Barbier, 1974).

During the past decade, the Athabasca Basin located south of Lake Athabasca has emerged as one of the most important uranium districts of the world. Presently known deposits are those of Rabbit Lake, Cluff Lake, Raven and Horseshoe, Key Lake, Collins Bay, West Bear Lake, Maurice Bay and Midwest Lake. With the possible exception of Raven and Horseshoe, and of Maurice Bay all of these belong to the so-called unconformity-type of deposits (Derry, 1970; Beck, 1976), being spatially associated with and presumably genetically related to the major regional unconformity between a metamorphosed Archaean and Aphebian (Lower Proterozoic) crystalline basement and overlying unmetamorphosed rocks of the Helikian (Middle Proterozoic) Athabasca Formation.

Less important uranium occurrences in the Athabasca Basin are known from Fond-du-Lac, from Isle-Brochet, Stewart Island and Johnson Island in Lake Athabasca, and from

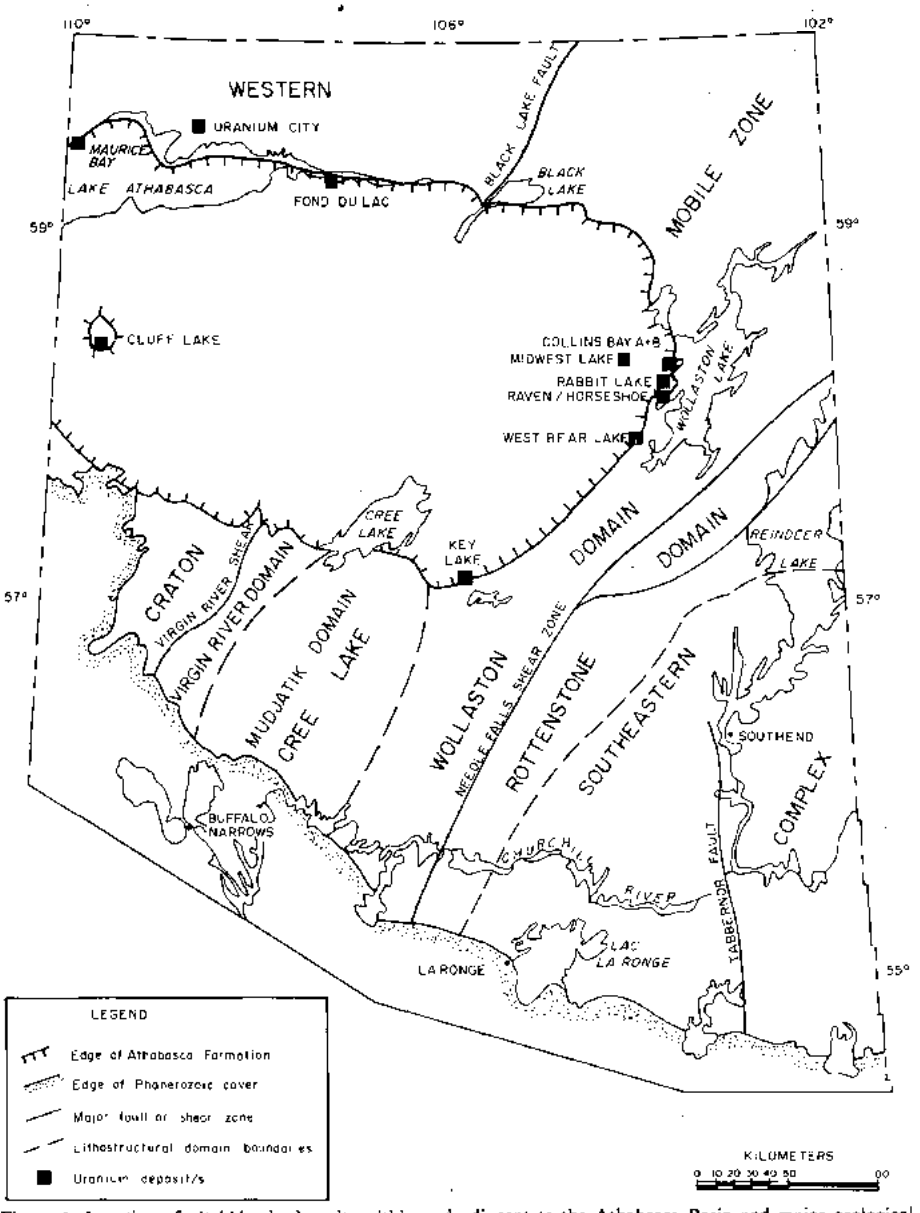


Figure 1. Location of pitchblende deposits within and adjacent to the Athabasca Basin and major geological subdivisions of the Saskatchewan Shield (after Sibbald *et al.*, 1976).

various locations within the interior of the Basin. These are located above the unconformity, entirely within the Athabasca Formation and differ from the aforementioned unconformity-type deposits with respect to mineralogy and host rock alteration. Furthermore, judging from preliminary age dating studies, they may be much younger. Since little published information is available, they will not be further considered herein.

The Athabasca Basin unconformity-type deposits have much in common with those of the Pine Creek Geosyncline in the Northern Territory of Australia. Deposits in the two districts share characteristics related to geological setting and age, host rock alteration, mineralogy, geochemistry and, most important of all, a general spatial association with graphite and carbonaceous rocks (Dodson *et al.*, 1974; Needham & Stuart-Smith, 1976, this volume; Needham *et al.*, this volume; Ryan, 1977; Stuart-Smith *et al.*, this volume; Kalliokoski *et al.*, 1978). This is particularly the case for the deposits located in the South Alligator Valley Uranium Field (Ayres & Eadington, 1975; Foy, 1975; Crick *et al.*, this volume).

Although the origin of unconformity-type deposits is still disputed, in view of the many existing similarities it seems clear that whatever metallogenetic model will eventually be agreed upon, it should be applicable in both districts. With regards to the Athabasca Basin, three main metallogenetic concepts have been advanced, advocating, respectively,

1) a near surface supergene origin;
2) a magmatic/metamorphic-hydrothermal origin;
3) a diagenetic-hydrothermal origin.

The present contribution is focused on the Athabasca Basin unconformity-type deposits. Their geological setting, general characteristics, relationships with Beaverlodge vein-type deposits and metallogenesis are discussed.

GENERAL GEOLOGY OF NORTHERN SASKATCHEWAN

The crystalline basement of northern Saskatchewan is part of the Churchill structural province of the Canadian Shield. It comprises an Archaean substratum overlain by an Aphebian (Lower Proterozoic) supracrustal cover, both of which were variably affected by Hudsonian (ca. 1750 m.y.) deformation, metamorphism and anatectic mobilization.

In the Uranium City area, this metamorphic basement is unconformably overlain by unmetamorphosed red beds of the Palaeohelikian (Lower-Middle Proterozoic) Martin Formation (Fig. 1). Intercalated lava flows have been dated by the K/Ar method at 1630 ± 180 m.y. (Wanless *et al.*, 1965). Further south, the basement is overlain by sandstones and conglomerates of the more extensive Helikian (Middle Proterozoic) Athabasca Formation, dated by the Rb/Sr-isochron method at 1428 ± 30 m.y. (Armstrong & Ramaekers, in press). The Athabasca Formation has red bed characteristics, which are less pronounced than in the Martin Formation. It is underlain by a partially preserved palaeo-weathering profile of lateritic character, developed in rocks of the metamorphic basement.

The metamorphic basement, as well as the Martin and Athabasca Formations, are intruded by diabase dykes of approximately Grenvillian age, which generally follow NW-SE directions.

The Crystalline Basement

On the basis of lithologic, structural and metamorphic criteria, several lithostructural domains have been recognized in the metamorphic basement of northern Saskatchewan (Sibbald *et al.*, 1976; Lewry & Sibbald, 1977), which can be grouped within major crustal units (Lewry *et al.*, 1978) namely Western Craton, Cree Lake Mobile Zone, Rottenstone Domain, and the Southeastern Complex (Fig. 1). The following review largely derives from Lewry & Sibbald (1979).

The Western Craton, incorporating the Firebag, Clearwater and Western Granulite

domains and the region north of Lake Athabasca (Figs. 1 & 2) represents a relatively stable cratonic foreland to the west of the main Hudsonian mobile belt. It comprises catazonal Archaean continental crust on which undisputed Aphebian (Lower Proterozoic) platform desposits are only locally preserved (Thluicho Lake Group). Hudsonian reworking is generally slight and marked by development of narrow zones of intense brittle to plastic deformation and by pervasive greenschist to amphibolite facies retrogressive metamorphism. Less reworked portions of the craton show only mild regression of Archaean upper amphibolite and granulite facies metamorphic assemblages.

The Cree Lake Zone, bounded by the Virgin River-Black Lake Shear Zone and by the Needle Falls Shear Zone, encompasses the Virgin River, Mudjatik and Wollaston domains. It comprises a continuous Archaean substratum originally overlain by Aphebian (Lower Proterozoic) shelf to miogeosynclinal sediments. In contrast to the Western Craton, the zone represents a belt of intensive Hudsonian orogenesis marked by high-grade metamorphism and anatexis, which resulted in ductile interaction of the Archaean substratum with the overlying Aphebian (Lower Proterozoic) supracrustals. The structural evolution is complicated and several deformation events are recognized. The Mudjatik domain, representing the most mobile core of the Cree Lake Zone, consists of flat-lying migmatite lobes, separated by intervening screens of infolded Aphebian (Lower Proterozoic) metasediments. The cooler and less mobile margins represented by the Wollaston and Virgin

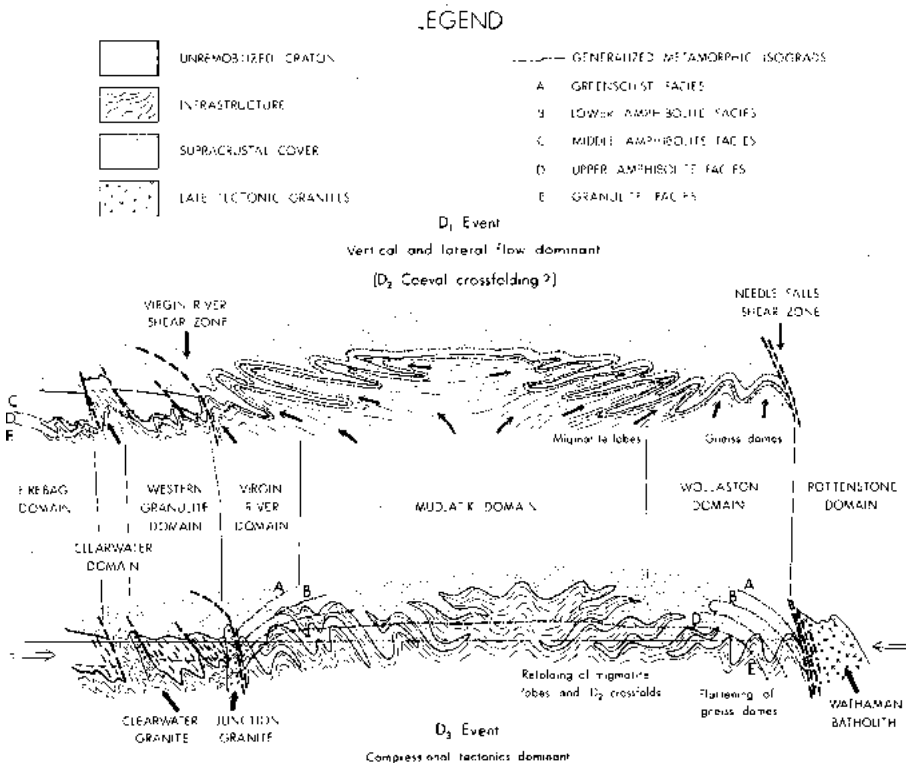


Figure 2. Hudsonian structural and metamorphic evolution of the crystalline basement in Northern Saskatchewan (after Lewry & Sibbald, 1979).

River domains, are characterized by mantled gneiss domes, consisting of Archaean granitoid cores wrapped in Aphebian (Lower Proterozoic) supracrustals. Coincident with this decrease in mobility, metamorphic grade declines from granulite facies in the core to lower amphibolite facies at the margins of the Zone (Fig. 2).

The Rottenstone Domain, located to the east of the Needle Falls Shear Zone, is considered as a Hudsonian Batholithic regime. It comprises early- to late-syntectonic Hudsonian tonalitic to granitic intrusives and associated injection migmatites. The late-tectonic Wathaman Batholith, which forms a dominant element of the domain, has been dated 1865 ± 10 m.y. (Wanless & Ray, 1979; in press).

The Southeastern Complex comprises probably eugeosynclinal Aphebian (Lower Proterozoic) to early Hudsonian volcanic arcs, related subjacent plutonics and primitive sub-arc crust, proximal to distal clastic fringe and basinal sediments and later flysch deposits.

In most of the above crustal units, the stratigraphic record of the Aphebian supracrustals originally overlying the Archaean substratum is either poorly preserved (Western Craton, Rottenstone Domain) or is poorly understood (Southeastern Complex). It is only within the Cree Lake Zone that a coherent stratigraphy is apparent. Nonetheless, a major transition, located in close proximity to the Needle Falls Shear Zone or within the adjacent Rottenstone Domain, is recognized in Aphebian (Lower Proterozoic) crustal character and depositional environment. Supracratonic shelf sedimentation in the west contrasts transitional and oceanic conditions and eugeosynclinal sedimentation in the east.

In the Cree Lake Zone, the thickness of the Aphebian (Lower Proterozoic) supracrustal sequence, denoted as 'Wollaston Group' (Ray, 1977), is at least 3-4km (Hoeve & Sibbald, 1978). Four main stratigraphic units are distinguished (Lewry & Sibbald, 1979):

1) A basal clastic unit of variable thickness, which is developed principally along the eastern margin of the Cree Lake Zone. It comprises mature quartzitic to arkosic psammites with locally developed basal conglomerate and semi-pelitic to pelitic mica schists. It may locally be underlain by a sequence of highly immature meta-arkoses, metaconglomerates and interbedded mafic volcanics. To the west it is generally not identified or is seen only as a thin basal quartzite.
2) A predominantly pelitic unit which is typically graphitic and contains interbedded quartzitic psammite, calc-silicate rocks and occasionally marble. The unit rests directly on the Archaean substratum throughout most of the Wollaston and Mudjatik domains. To the west in the Mudjatik and Virgin River domains it appears to be associated with mafic to ultramafic volcanics and intrusives and also with oxide-silicate facies banded iron formation.
3) A thick unit of calcareous and non-calcareous meta-arkose which is interlayered with subordinate calc-silicate rocks and thin pelite horizons.
4) An upper amphibolite-quartzite unit characterized by these two rock types and containing interlayered calcareous sediments and graphitic pelites. This unit may be equated with the Hidden Bay Assemblage (Wallis, 1971) and is only definitely known to outcrop in the Wollaston Lake area.

Martin Formation

The Martin Formation, unconformably overlying the metamorphic basement near Uranium City, comprises a sequence of red beds composed of continental arkoses, sandstones, siltstones and conglomerates, intercalated with andesitic and basaltic lava flows (Tremblay, 1972). These sediments were locally derived and deposited in a number of small 10 x 30km, 4-6km deep depressions controlled by major faults (e.g. Black Bay Fault). This sequence was gently folded more or less contemporaneously with deposition, but was not affected by Hudsonian metamorphism.

Palaeo-current data (Tremblay, 1972; Scott, 1978) suggest that the Martin basins were

fault-bounded on both sides forming troughs with talus slopes and alluvial fans entering from the sides and with drainage to the southwest. A palaeo-latitude of 16°N (Evans & Bingham, 1973) suggests a warm, possibly arid climate, during deposition of the Martin strata.

The Formation is marked by extensive hematitization, which preceded the folding, as indicated by palaeomagnetic studies (Evans & Bingham, 1973), and hence must have taken place almost immediately after deposition. The hematite has not been remobilized since. Feldspar, up to 60% of the rock, is well preserved despite some sericitization and partial replacement by calcite or hematite. The clastic grains are embedded in a carbonate cement; secondary quartz is absent or rare. Thus, palaeomagnetic and petrographic evidence corroborates structural evidence for rapid deep burial, folding and compaction of the Martin Formation, suggesting that the sediments were effectively sealed at an early stage and subsequently were little affected by later groundwater movements. Hence, uranium mineralization present in fractures within intercalated lava flows, was probably introduced along younger or reactivated fault and fracture zones.

Athabasca Formation

The Athabasca Formation unconformably overlies the metamorphic basement to the south of Lake Athabasca, covering an area of approximately 100,000km^2. The formation is about 1400m thick and consists of flat-lying, predominantly fluviatile, poorly to well-sorted often clay-rich quartz sandstones with minor conglomerate, siltstone and mudstone (Ramaekers, 1979). Conglomerate is concentrated towards the bottom of the sequence.

Colours range from buff, grey cream, white to pink, brick-red, maroon and purple to black, depending on the absence or presence and abundance of hematite pigment along grain boundaries. The hematite content ranges between 0-30%, but is typically in the order of 1-2%. Detrital grains of quartz are commonly and variably overgrown by up to three generations of authigenic quartz, (Ramackers & Dunn, 1976), the degree of induration ranging from complete to absent. An early-diagenetic carbonate cement, replaced by secondary quartz, is locally observed. In sandy units, a clay matrix, essentially authigenic kaolinite and illite, is typically present, but also variably developed, ranging between 2-40%. Heavy minerals are rare and marked by an extremely stable suite comprising tourmaline with minor proportions of rutile, zircon, monazite and hematite. Centimetre-sized clastic pebbles of hematite are locally present near the base of the formation. Several colour varieties of detrital tourmaline have been recognized, all of which may show overgrowths of colourless, presumably Mg-rich tourmaline, dravite (Gravenor, 1959). Authigenic overgrowths of colourless tourmaline are also reported by Fahrig (1961). As noted below, dravite overgrowths also occur in host rock alteration haloes of the ore deposits at Rabbit Lake, Cluff Lake, Key Lake and Midwest Lake.

There is evidence that the present red bed aspects of the formation largely result from diagenetic processes involving oxidation and intensive post-depositional leaching. Relics of the original detrital mineral assemblage are preserved only within rocks that underwent early reduction of permeability such as certain clay beds and zones with a chert, carbonate or apatite cement. In such rocks feldspars are found, as are detrital grains of biotite and clay-hematite pseudomorphs after amphibole and pyroxene. In more permeable zones, feldspars were completely altered to kaolinite and illite, as evidenced by pseudomorphs after clastic grains; mafic and heavy minerals (except for the mentioned ultrastable suite) were oxidized, leached and transformed to clay. Dickite is fairly common as fracture fillings and one occurrence of nacrite was found. This assemblage suggests intensive leaching of the formation, as does the occurrence in conglomeratic zones, of relics of granite pebbles, whose feldspars are apparently leached to a clay residue.

Although clastic pebbles of hematite are locally observed in conglomeratic zones, much

of the hematite pigment of the formation is of diagenetic origin (Ramaekers, 1976; 1977; 1978; Ramaekers & Dunn, 1976). It is concluded from petrographic evidence that specular hematite crystallized prior to, concomittantly with and after diagenetic silicification. This interpretation is supported by Pagel's (1975a) observation of euhedral hematite platelets enclosed in fluid inclusions of quartz overgrowths. Furthermore, hematite forms induration zones and colour banding commonly oblique to sedimentary layering. Recent iron mobility is indicated by limonitic stains cross-cutting hematitic layers.

A number of diabase dykes intrusive into the Athabasca Formation show the effects of diagenetic alteration. The Moore Lake dyke (dated 1080 m.y.; Armstrong & Ramaekers, *in* press) and others are locally fractured, impregnated with hematite, veined by quartz and completely altered to kaolinite and illite. Post-depositional alteration of the Athabasca Formation must, therefore, have continued for hundreds of millions of years after deposition. This is consistent with evidence obtained from fluid inclusion studies. Pagel (1975a; 1975b) recognized an episode of basin-wide, late, diagenetic silicification marked by an increase in salinity and temperature as a function of depth of burial. Conditions at the unconformity ($T = 200°C$; $P = 1500b$; salinity = 39% equ. NaCl), indicate a total sediment cover of 4800m, implying that diagenesis continued during deep burial.

Late chemical reduction of basin-wide magnitude is indicated by widespread bleaching phenomena in permeable zones and haloes around fractures (Plate IV *in* Fahrig, 1961) which may be filled with siderite. Rare hematite clasts occurring near the base of the Formation, may be replaced by siderite. These reduction phenomena may be equated with bleaching effects in the sub-Athabasca palaeo-weathering profile and with reducing host rock alterations associated with uranium mineralization.

Although details of the diagenesis are not well known, it appears from the above features that the diagenetic history of the Athabasca Formation has been very complex. Present evidence suggests that the formation has been subjected to processes of intrastratal oxidation and leaching similar to those invoked in the formation of more recent red beds (Chukhov, 1973; Hubert & Reed, 1978; Jawad Ali & Braithwaite, 1977; Turner, 1977; Walker, 1967; 1976; Walker *et al.*, 1978). Such processes may possibly have started shortly after deposition, but certainly continued during deep burial, several hundreds of millions of years after deposition of the formation, as attested by the diagenetically altered diabase dykes.

Mafic Dykes

A series of mafic dykes of basaltic composition intrudes the Athabasca Formation following north-westerly trends. Age limits suggested by K/Ar dating methods are 938 m.y. (Tremblay, 1978) and 1230 m.y. (Burwash *et al.*, 1962); however, Rb/Sr dates suggest a narrower interval of 1080-1116 m.y. (Armstrong & Ramaekers, in press).

The pattern of dyke intrusion and faulting suggests that late movements along some of the northeast-trending major shear zones (e.g. Black Lake-Virgin River Shear Zone) were left-lateral in nature (Ramaekers & Hartling, 1979). Dyke outcrops are uncommon and typically distributed along prominent linear magnetic anomalies. Individual bodies display a great variation in strike and dip; some may be sill-like complexes.

The dykes comprise labradorite, augite and locally olivine. They show evidence of rapid cooling and of baking the adjacent sandstone, which for a distance of up to 30m, may be fractured, silicified and leached of hematite.

Dyke rocks have been mineralized by pitchblende, which occurs along fractures and is accompanied by chloritic host-rock alteration. Thermally altered sandstone near the dykes may also be mineralized.

PRE-ATHABASCA WEATHERING

The Athabasca Formation is underlain by a palaeo-weathering profile developed in

rocks of the metamorphic basement. Present thicknesses are in the order of 50m. Mineralogical and chemical characteristics of the palaeo-weathering profile are similar to those of the lower levels of present-day laterites, indicating that the profile has only been partially preserved (Hoeve, 1977; Hoeve & Sibbald, 1978). The upper levels of the original profile must have been eroded prior to deposition of the conglomeratic basal Athabasca Formation. A mineralogical zoning is generally recognized, marked by kaolinite in the upper zones and by illite accompanied by some chlorite in the lower. Red staining due to hematite impregnation is pervasive, except at the base of the profile.

Throughout the Athabasca Basin, the palaeo-weathering profile is variably affected by superimposed alteration, correlated with late reducing phenomena in the Athabasca Formation and with reducing host rock alterations accompanying uranium mineralization in unconformity-type deposits.

In the kaolinite portions of the profile this alteration manifests itself by hematite removal, whereas in other zones it is marked by chloritization and development of siderite. In the common case of weak superimposed alteration, only the top few centimetres of the profile are affected, however, where it is severe, as in the vicinity of uranium mineralization, weathered as well as unweathered rocks are intensively chloritized and a thin, bleached, chalky-white kaolinitic zone immediately below the unconformity is the only remaining evidence of previous weathering.

GENERAL DISTRIBUTION OF URANIUM MINERALIZATION

Uranium occurrences in northern Saskatchewan may be grouped into types with syngenetic and epigenetic mineralization. The latter are represented by the economically important late Hudsonian vein-type deposits of Beaverlodge and the approximately Grenvillian age unconformity-type deposits of the Athabasca Basin, whereas the former comprise various types of Aphebian (Lower Proterozoic) and/or Hudsonian pegmatoid and stratabound deposits. None of the syngenetic deposits are economically viable at present.

The majority of the syngenetic and all of the epigenetic deposits are located to the west of the Needle Falls Shear Zone. To the east of the Shear Zone, uranium mineralization is unimportant and confined within granites and pegmatites of presumed Hudsonian age, whereas to the west a diversity of deposit types and ages is apparent.

In the Western Craton uranium mineralization, both syngenetic and epigenetic, appears closely associated with the restricted, linear belts of Hudsonian reworking and related retrograde metamorphism. Syngenetic mineralization manifests itself as disseminations of radioactive minerals in granite pegmatites and less commonly in country rocks. Uraninite, the typical ore mineral, is associated with monazite and thorite. Rare earth minerals are locally present and rarely important. Epigenetic mineralization is represented by the fracture-controlled, late-Hudsonian Beaverlodge-type pitchblende deposits. Brittle-plastic deformation, characterizing the linear belts of Hudsonian reworking, seems to have been important in providing structural traps favourable for this type of mineralization (Sibbald *et al.*, 1976; Lewry & Sibbald, 1979).

A much different situation prevailed in the Cree Lake Zone which in contrast to the Western Craton was subjected to ductile Hudsonian deformation and recrystallization under high-grade metamorphic conditions. It is believed that the absence of brittle structural traps and the high-grade metamorphic evolution precluded the formation of Beaverlodge vein-type pitchblende deposits in this zone. The most easterly occurrence of this type of mineralization is found in some showings on the west side of Black Lake, located in mylonites of the Black Lake Shear Zone at the junction of the Western Craton and the Cree Lake Zone.

The Cree Lake Zone is characterized by syngenetic pegmatoid and/or stratabound

uranium occurrences. Some uranium mineralization is present in granitic and pegmatitic anatectic fractions of early Hudsonian or possibly late Kenoran age within the remobilized Archaean substratum (Sibbald, 1975; Sibbald *et al.*, 1976; Lewry & Sibbald, 1979). However, most uranium mineralization is found in the Aphebian (Lower Proterozoic) supracrustals and exhibits a lithologic and stratigraphic, rather than a structural control. On the basis of dominant host rock, Sibbald *et al.* (1976) and Lewry & Sibbald (1979) distinguish arkosic, pelite-pegmatite and calc-silicate types of deposits. Occurrences of the first two types are for the most part located near the base of the Aphebian (Lower Proterozoic) succession, whereas those in calc-silicate rocks are encountered at several stratigraphic levels.

The arkosic type is represented by an occurrence at Duddridge Lake, located near the southern end of the Wollaston domain. It comprises disseminations of pitchblende, copper, sulphides, galena, sphalerite, molybdenite and skutterudite within graphitic, pelitic lenses in arkosic rocks, belonging to the basal unit of the Wollaston Group. Mineralization is locally concentrated along fractures; however, the overall control seems to be stratigraphic. Geochemically, mineralization is represented by an element suite comprising U, Ni, Co, As, Sc, Pb, Ag, Au, Mo, and V. Although the deposit has been suggested to represent a metamorphosed sandstone-type deposit (Bretzlaff, 1976), its origin is still uncertain.

The pelite-pegmatite type is typified by pegmatoid bodies containing disseminated uraninite in often graphitic pelitic gneisses. Uraninite is associated with molybdenite and values in lead, copper and zinc have been reported. Field relations suggest that uranium may have segregated with the pegmatoid material during high-grade metamorphism and anatexis. In this event it ultimately derives from concentrations existing in the host pelites and the occurrences can be interpreted as Aphebian (Lower Proterozoic) black shale concentrations redistributed during Hudsonian metamorphism.

The calc-silicate type comprises uraninite concentrations in calc-silicate host rocks. In some occurrences uraninite is confined within certain layers of host rock, in others it is concentrated in coarse-grained zones and pods. Mineralization is characterized by the association of uraninite-molybdenite, locally accompanied by fluorite and less commonly by uraninite-molybdenite-apatite. The occurrences of the calc-silicate type may be interpreted, analogously to those of the pelite-pegmatite type, as Aphebian (Lower Proterozoic) syngenetic sedimentary concentrations recrystallized and mobilized during Hudsonian metamorphism.

The important unconformity-type deposits are confined to the Athabasca Basin which covers portions of both the Cree Lake Mobile Zone and the Western Craton (Fig. 1). The Cluff Lake deposits are located within the Western Craton, the others within the Cree Lake Zone. The deposits are spatially related to the unconformity at the base of the Athabasca Formation and are generally associated with graphitic metamorphic rocks of the basin floor. Mineralization seems to have been controlled by the presence of the sub-Athabasca unconformity rather than by factors related to Aphebian (Lower Proterozoic) sedimentation or Hudsonian structural and metamorphic evolution, because outside the Athabasca Basin no such mineralization is encountered.

BEAVERLODGE VEIN-TYPE PITCHBLENDE DEPOSITS

Pitchblende deposits at Beaverlodge are located in fractured basement rocks and in overlying red beds of the Martin Formation. Pitchblende is the chief ore mineral and thorium and rare earths are absent.

The deposits can be divided into two groups, one showing simple mineralogy, the other complex mineralogy (Robinson, 1955; Beck, 1969). The larger group with simple mineralogy is characterized by pitchblende and coffinite in association with brannerite and

locally nolanite, and small amounts of pyrite, chalcopyrite and galena, whereas in deposits with complex mineralogy, pitchblende and coffinite are found with sulphides, arsenides and selenides of nickel, cobalt, copper, lead, zinc and native gold and silver, specular hematite, locally thucholite. Paragenetic relationships in both types of deposits are complicated by the fact that several of the constituent minerals are present in multiple generations and modes of occurrence, e.g. submicroscopic, colloform, massive and botryoidal pitchblende. Gangue minerals include calcite, quartz and chlorite.

The mineralization exhibits a strong structural control, occurring as veins and as disseminations in the fractured wall rocks of faults which often may be of large vertical and horizontal extent. Mineralization of this type appears to be most common in rocks of the Fay Complex near the base of the exposed stratigraphic succession and, hence, a possible stratigraphic control has also been advocated (Tremblay, 1972). Although mineralization is found in a wide range of rock types, mafic rocks appear to be the most favourable host (Robinson, 1955).

Red hematitic alteration of wall rocks accompanied by albitization and development of chlorite and calcite (Robinson, 1955; Dawson, 1951) is typical adjacent to pitchblende veins, though variable in intensity.

Fluid inclusion and stable isotope studies conducted on gangue carbonates from the Fay mine and Bolger open pit indicate mineralization temperatures evolving from 500°C to 80°C (Sassano *et al.*, 1971).

Uranium-lead dating suggests a complicated evolution for uranium deposits in the Beaverlodge area. Koeppel (1968) on the basis of a systematic study of different generations of pitchblende and galena and clausthalite concluded that the epigenetic pitchblende deposits were formed 1780±20 m.y. ago and suffered episodic lead losses at 1110±50 m.y., 270±20 m.y. and 100±0 m.y.

The age of pitchblende mineralization in relation to the Martin Formation, dated 1630 ±180 m.y. by the K-Ar method (Wanless *et al.*, 1966) is the subject of varied opinion. Beck (1969) and Tremblay (1972) subscribe to the view that initial pitchblende deposition predates the Martin Formation, however, as some veins cross cut the Martin Formation, Koeppel (1968) argues that all veins must post-date it.

Koeppel's U-Pb data from samples of pitchblende mineralization in the Martin Formation are ambiguous and do not plot on a chord defining the age of primary mineralization (Koeppel, 1968; Fig. 2), or themselves define a unique chord. Some samples in fact plot on or close to the chord defining the 1110±50 m.y. episode of lead loss, suggesting the possibility that all Martin-hosted mineralization, may have been emplaced during this event. Significantly, the samples of Martin-hosted mineralization as well as others from basement hosted deposits plotting on the 1110±50 m.y. chord, are characterized by complex mineralogy. On the basis of an inferred correlation between mineralogy (simple or complex) and age, Hoeve (1978) and Hoeve & Sibbald (1978b) have suggested two main episodes of epigenetic mineralization in Saskatchewan, the first at 1780±20 m.y. giving rise to deposits of simple mineralogy and the second at 1110±50 m.y. resulting in the Beaverlodge area in reworking of the existing deposits and in formation of new ones of complex mineralogy. During the later event, the unconformity-type deposits of the Athabasca Basin marked by complex mineralogy (discussed below) originated.

The Beaverlodge pitchblende deposits have in the past been regarded as prime examples of classical hydrothermal uranium deposits (Maucher, 1962). Beck (1969), Sassano *et al.* (1971) and Tremblay (1972) have argued for a metamorphic hydrothermal origin. Others (Barbier, 1974; Langford, 1974; 1977; Robertson & Lattanzi, 1974) have suggested a surficial origin for the Beaverlodge deposits, mainly on the basis of a spatial relationship with the sub-Martin unconformity. However, Lewry & Sibbald (1979) have interpreted this

relationship in terms of a depth zoning of uranium mineralization. They argued that in the Western Craton within the linear belts of Hudsonian reworking syngenetic and epigenetic uranium mineralization may reflect different levels of Hudsonian orogenesis and that pitchblende veins developed at higher structural levels and lower metamorphic grade than the uraninite-bearing pegmatites. Since the Martin Formation occurs as down-faulted erosional relics it might be anticipated that the underlying basement rocks occupy a higher structural level than those of the surrounding area from which the Martin cover has been removed.

The authors subscribe to the metamorphic-hydrothermal model for initial (1780±20 m.y.) pitchblende mineralization in the Beaverlodge area, recognizing that new ore constituents have been introduced during reworking of existing deposits and formation of new ore in a later (1110±50 m.y.) diagenetic-hydrothermal event (Hoeve & Sibbald, 1978).

ATHABASCA BASIN UNCONFORMITY-TYPE DEPOSITS

Of the presently known unconformity-type deposits in the Athabasca Basin, only Rabbit Lake (Hoeve & Sibbald, 1978; Rimsaite, 1978) and to a lesser degree Key Lake (Dahlkamp, 1978; Kirchner *et al;* this volume) have been studied in any detail. Published data on the other deposits are limited, however, they appear to share the characteristic features of these two deposits.

The deposits occur in close and undeniable spatial association with the sub-Athabasca unconformity. They are located in altered basement rocks just below the unconformity (Rabbit Lake; N-zone, Claude and Dominique at Cluff Lake), at the unconformity in bleached and altered, palaeo-weathered rocks (Collins Bay B, Midwest Lake, Key Lake) and above the unconformity in bleached and altered Athabasca Formation (D-zone at Cluff Lake; Collins Bay B; Midwest Lake; Key Lake). In those deposits where the protective cover of the Athabasca Formation is still present, ore bodies are seen to be rooted in basement rocks and to extend above the unconformity into the overlying sandstone (Key Lake, Midwest Lake, Collins Bay B). Mineralization is known to extend along faults 200m below the unconformity (Rabbit Lake, Key Lake) and at least 200m above it into the Athabasca Formation (Midwest Lake).

Mineralization is structurally controlled, occurring as veins, breccia fillings and associated impregnations. Deposits are located in fracture and breccia zones, which in many cases are related to reverse faults which offset the unconformity and strike approximately parallel to basement lithology. The ore body at the Rabbit Lake deposit is located in a probably pre-Athabasca, steeply dipping NNE-SSW-trending fault zone, which was cut off and reactivated by the ENE-WSW-trending post-Athabasca low-angle reverse Rabbit Lake fault. At Collins Bay B (Jones, in press) mineralization is contained within a NNW-SSE-trending zone of intense intricate thrust faulting which offsets the unconformity. At Key Lake the Deilmann and Gaertner ore bodies are located within or near a NE-SW striking fault zone (Dahlkamp, 1978).

In most deposits there is evidence of repeated fault movement in part contemporaneous with and after the main stage of mineralization. At Collins Bay B, late fault movements have displaced part of the ore body (Jones, in press). At Rabbit Lake several episodes of mineralization and host rock alteration, tied to intermittent brecciation have been recognized (Hoeve, 1977; Hoeve & Sibbald, 1976; 1978). Although brecciation was tectonically induced, dissolution and redistribution of dolomitic marbles probably also played a role. For the Key Lake ore bodies, Dahlkamp (1978) reports brecciation and cementation of ore.

Mineralization is also lithologically controlled, since the deposits display a general association with graphitic basement rocks. Basal Aphebian (Lower Proterozoic) metapelites

appear as a most favourable host (Collins Bay A and B; Key Lake; Midwest Lake), although other graphite-bearing rocks are also associated with mineralization (Rabbit Lake; Cluff Lake). In detail, however, the relationship is less direct, because ore grade and graphite concentration do not seem to correlate, even though at Collins Bay B the ore grade drops significantly where the graphitic metapelite gives way for pegmatoid masses (Jones, in press). The bulk of the ore is often located in adjacent non-graphitic basement rocks (Key Lake) or even at and above the unconformity in the Athabasca Formation (Collins Bay A and B; D-zone at Cluff Lake; Midwest Lake).

The geometric relationships are illustrated by deposits such as Deilman at Key Lake and Collins Bay B. These deposits can be schematically depicted as to comprise a long, half cylindrical ore zone, located at and above the unconformity, aligned parallel to and rooted in graphitic metapelite (Fig. 3). The portion of the ore body lying above the unconformity is laterally displaced with respect to its roots in the graphitic basement rocks.

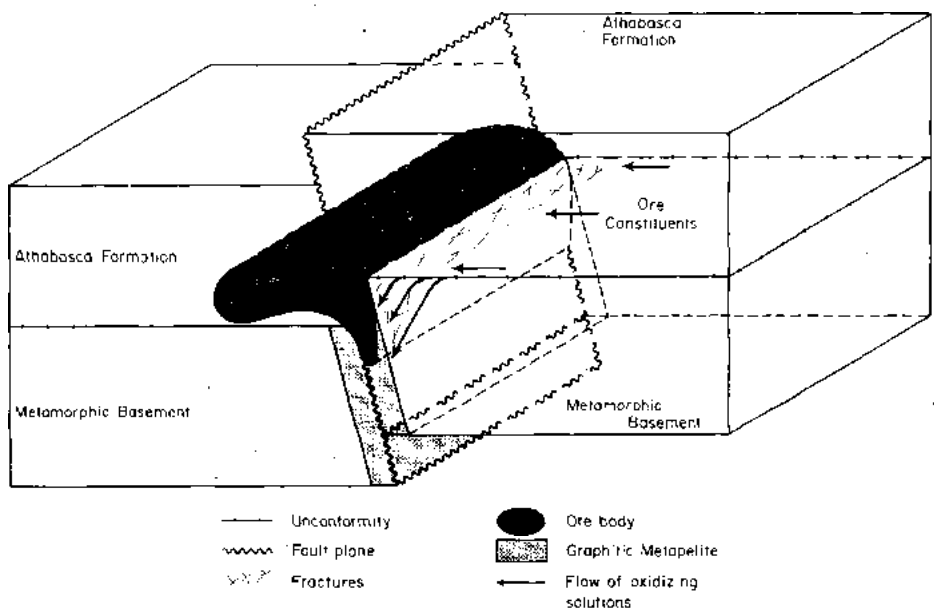


Figure 3. Schematic representation of Athabasca Basin unconformity-type uranium deposit.

Mineralization is contained within an envelope of host rock alteration, which extends a few hundred metres from the ore body and is chemically and mineralogically distinct from the effects of palaeo-weathering (Hoeve, 1977; Hoeve & Sibbald, 1978). Alteration is superimposed upon the sub-Athabasca lateritic weathering profile and also effects the overlying Athabasca Formation. It is marked by chloritization, sericitization and tourmalinization. At Rabbit Lake, chloritization and tourmalinization are accompanied by large-scale introduction of magnesium (probably derived from dissolved dolomitic marbles) and boron. Tourmalinization is also recognized at Cluff Lake, Midwest Lake and Key Lake. At Rabbit Lake, chloritization is associated with destruction of graphite (Hoeve, 1978; Sibbald, 1978) and at the Collins Bay B deposit altered and mineralized graphite pelites contain less graphite than their less-altered counterparts (Jones, in press).

Several types of chloritization can be recognized. At Rabbit Lake, dark green

(presumably iron-bearing) chlorite characterizes the rock hosting primary mineralization, whereas red hematitic and pale green chlorite (magnesium rich, almost iron-free) marks alterations connected with dispersion and remobilization of the deposit. In the Dominique showing at Cluff Lake, primary mineralization is in dark green chloritized basement rock, whereas at the D-zone it is in dark green chloritzed Athabasca sandstone and siltstone. However, in the Claude and the N-zone mineralization is located in weathered basement rocks affected by superimposed pale green chloritization, sericitization, and bleaching.

At Midwest Lake, mineralization is associated with pale green chloritization of basement rock and with bleaching and sericitization in the overlying Athabasca Formation. At Collins Bay host rock alteration in the Athabasca Formation is marked by extensive development of sericite (Jones, in press).

At Key Lake, Dahlkamp (1978) reports various types of alteration including kaolinitization, sericitization and chloritization, but fails to identify the effects of palaeo-weathering as distinct from those related to mineralization. Judging from his descriptions, it seems possible that at Key Lake kaolinitization, as elsewhere at the sub-Athabasca Formation unconformity, ultimately derives from paleo-weathering.

The unconformity-type deposits are often of high grade and marked by an extremely diverse mineralogy and geochemistry. Intersections of several percent or even tens of percent are common. Pitchblende and coffinite, the primary uranium minerals, are accompanied by pararammelsbergite, rammelsbergite, niccolite, gersdorffite, millerite, carrollite, skutterudite, safflorite, maucherite, linneite-polydymite, bravoite, pyrite, arsenopyrite, molybdenite, various copper sulphides, clausthalite, galena, sphalerite, hematite, goethite, psilomelane, native copper, gold and selenium, and others. Gangue minerals comprise quartz, calcite, dolomite, ankerite, siderite, chlorite, sericite and adularia.

At Key Lake, Dahlkamp (1978) noted a crude mineral zoning and mineralogical contrasts between 'Athabasca ore' and 'basement ore' i.e. lustrous colloform primary pitchblende versus sooty pitchblende and coffinite. Although mineralogical zoning is also known from other deposits, no difference in pitchblende morphology has been observed below and above the unconformity. At Collins Bay B, lustrous, colloform primary pitchblende occurs below *and* above the unconformity (Jones, in press).

In addition to uranium, a broad suite of elements is present, including Ni, Co, Mo, Cu, Pb, Zn, Mn, Fe V, Ag, Au, Pt-group elements, S, Se, As. In deposits such as Rabbit Lake these constituents occur in trace quantities, whereas in others they may occur in mineable quantities. The D-zone at Cluff Lake contains, besides uranium, considerable concentrations of selenium and gold. Key Lake is characterized by uranium, nickel and arsenic, Midwest Lake by uranium, nickel, cobalt, molybdenum and arsenic. At Collins Bay uranium is accompanied by significant values in nickel, cobalt, silver, gold and arsenic (Jones, in press).

Solid, glossy, amorphous hydrocarbons are present in most, if not all, deposits. They occur in mineralized rock, intimately associated with ore, as well as in unmineralized rocks of the alteration envelope. In some deposits, like Collins Bay B and the D-zone at Cluff Lake, they are present in appreciable amounts. At Rabbit Lake they are most abundant in high-grade ore, but also occur as vein fillings on top of euhedral quartz in the chloritization envelope. Although they are found in all of the Cluff Lake ore bodies, they are particularly abundant in the D-zone. Here the solid hydrocarbons are intermixed with ore minerals. They also occur as clusters of mm-sized beads of lustrous, pitchlike material, which form haloes around fractures in chloritized Athabasca host rock.

The association of hydrocarbon compounds with mineralized and altered rocks is also suggested by the fact that in most deposits, gases with a strong hydrocarbon odour are released during drilling operations and splitting of core. Qualitative analysis of gas samples collected from Rabbit Lake and Collins Bay B core identified carbon dioxide and methane.

Pagel (1975b; 1977) reports the presence of carbon dioxide, methane and ethane in fluid inclusions in euhedral quartz from Rabbit Lake.

Fluid inclusion studies by Pagel (1975b; 1977) suggest that conditions of mineralization were similar to those prevailing at the base of the Athabasca Formation during diagenetic silicification. For inclusions in gangue quartz from Rabbit Lake, Pagel reports trapping conditions: T= 160±10°C; P=700-800b; salinity=28% equ. NaCl. He also notes close compositional similarities between mineralizing and diagenetic solutions.

Redox reactions have probably played a major role in primary mineralization as well as in later reworking of the deposits. At Rabbit Lake repeated oscillations between oxidizing and reducing conditions, intimately tied to intermittent brecciation and paralleled by remobilization and redeposition of mineralization are recognized (Hoeve, 1977; Hoeve & Sibbald, 1976; 1978). Jones (in press) reports oscillations between oxidizing and reducing conditions at Collins Bay B.

Published radiometric ages for primary mineralization are similar for various deposits; 1281 m.y. at Rabbit Lake (Cumming & Rimsaite, 1979), 1200 m.y. at Key Lake (Wendt *et al.*, 1978); 1330 m.y. and 1050 m.y. at the Cluff Lake D-zone (Gancarz, this volume). These ages define a time interval which is younger than the Athabasca Formation dated at 1428± 30 m.y. (Armstrong & Ramaekers, in press), but approximately coeval with the episode of Grenville age mafic magmatism in the Athabasca Basin. K/Ar ages of diabase dykes intrusive into the Athabasca Formation range between 938±33 m.y. (Tremblay, 1978) and 1230 m.y. (Burwash *et al.*, 1962).

It is noted that primary mineralization for unconformity-type deposits in the Athabasca Basin is coeval with the first reworking episode at Beaverlodge, dated by Koeppel (1968) at 1110±50 m.y., which gave rise to the pitchblende vein-type deposits of complex mineralogy in that region.

METALLOGENESIS

Current concepts on the metallogenesis of unconformity-type uranium deposits in the Athabasca Basin fall into three groups, advocating

1) a near-surface supergene origin;
2) a magmatic or metamorphic hydrothermal origin;
3) a diagenetic-hydrothermal origin.

Near-surface supergene concepts, as proposed by several authors (Knipping, 1974; Langford, 1974; 1977; Robertson & Lattanzi, 1974; Ruzicka, 1975), involve leaching of uranium and other ore constituents from basement rocks during development of the sub-Athabasca weathering profile, transportation by ground and surface waters and reprecipitation wherever a suitable reducing environment is encountered. Basement rocks (Knipping, 1974; Langford, 1974; 1977) and 'organic-rich shales' of the basal Athabasca Formation (D-Zone at Cluff Lake; Robertson & Lattanzi, 1974; Ruzicka, 1974; Pagel *et al.*, this volume) have been suggested to provide such chemical traps.

These concepts, though attractive, do not fit the characteristics of the deposits as listed in the previous section. For example, it is doubtful whether under near-surface conditions graphitic metapelites which typically contain some sulphide, would have created a stronger reducing environment than other sulphide-bearing, non-graphitic basement rocks. The 'organic-rich shales' at the Cluff Lake D-Zone are considered by supergenetists as primary sediments deposited in shallow ponds that developed upon the ancient land surface prior to deposition of the Athabasca Formation sandstones and conglomerates (Anonymous, 1974; Robertson & Lattanzi, 1974; Ruzicka, 1975; Pagel *et al.*, this volume). As there is no evidence elsewhere in the Athabasca Basin for the existence of primary organic-rich sediments, others (Hoeve & Sibbald, 1978) have argued that the 'organic-rich shales'

represent previously hematitic Athabasca Formation which was chemically reduced and chloritized and into which the carbonaceous matter was introduced as part of the ore forming process, rather than acted as a precipitant for uranium. Near-surface supergene concepts attribute host rock alteration to palaeo-weathering, however, it has been shown (Hoeve, 1977; Hoeve & Sibbald, 1978) that host rock alteration, superimposed upon the palaeo-weathering profile and also affecting the overlying Athabasca Formation, is mineralogically and chemically distinct. The results of the age-dating studies, referred to in the previous section, indicate that primary mineralization took place up to several hundred million years after deposition of the Athabasca Formation, dated at 1428±30 m.y. (Armstrong & Ramaekers, in press). Homogenization studies of fluid inclusions in quartz and dolomite from Rabbit Lake (Pagel, 1975; 1977; Pagel *et al.*, this volume) indicate that during mineralization, conditions were similar to those of diagenetic silicification at the base of the Athabasca Formation. Pagel (1977) also noted compositional similarities between mineralizing and diagenetic solutions. Langford (1978) and also Dahlkamp (1978) suggested that initial precipitation occurred under surficial conditions and that the age dating and fluid inclusion data reflect a later diagenetic event which took place at elevated temperatures and under a thick sedimentary cover, obliterating all evidence of the early near-surface supergene history. Such a possibility can, of course, not be ruled out entirely. The hypothesis requires no supportive evidence and has obvious attractions to theorists lacking data.

A variation of the near-surface supergene model has been recently advanced by Robertson *et al.* (1978) and Tilsley (this volume), who proposed that an electrochemical process might have played a role in the formation of unconformity-type uranium deposits. They pointed out that a significant electrical potential difference may develop within a weathering profile between the upper zones that are being oxidized and the lower reduced zones where hydrolysis of silicates takes place. If a conductive rock such as a graphitic metapelite connects the two zones, an electrochemical cell may arise. In such a situation, uranium leached from the weathering profile and transported by ground and surface waters is thought to be drawn towards the graphite electrode and precipitated. Although the model could explain the association between mineralization and graphitic rocks, the other arguments against the near-surface supergene model remain and additional objections can be raised. The electrically negative character of the electrode requires that uranium, in order to be precipitated at the graphitic conductor, be transported as positively charged ions such as UO_2^{2+} or as uranyl-hydroxyl complexes such as UO_2OH^+. However, under near-surface conditions and in a solution in contact with atmospheric carbon dioxide, most of the dissolved uranium is present as uranyl-carbonate or uranyl-phosphate complexes (Langmuir, 1978), which are negatively charged or neutral and, hence, would not collect at the negative electrode of the cell. Neither would ore constituents such as S and As, which in the near-surface environment are also transported as anions. The foregoing implies that the role of electrochemical cells in the formation of unconformity-type uranium deposits must have been very limited.

A magmatic- or metamorphic-hydrothermal origin of the deposits was proposed by Little (1974) and Morton (1977) who envisage mineralization by ascending solutions from a deep-seated source. Arguments in favour of such a concept derive from the post-Athabasca age of initial mineralization and from the fluid inclusion data, indicating elevated temperatures, pressures and salinities for the mineralizing solutions. The fact that primary mineralization is approximately coeval with mafic magmatic activity in the Athabasca Basin could be taken as further supportive evidence. However, the magmatic/metamorphic-hydrothermal model cannot satisfactorily explain the spatial association of deposits with the sub-Athabasca unconformity and with graphitic basement rocks. The notion that uranium

precipitation took place in response to CO_2-ebullition with the emergence of ascending solutions at the unconformity is not supported by Pagel's (1975; 1977) fluid inclusion studies. Mafic magmatism alone is incompatible with the characteristic, broad geochemical spectrum of the ore deposits. Even if Ni, Co, As, Au had been derived from a mafic magma, some additional process would have to be called upon in order to account for U and B. Furthermore, there is no evidence to suggest that the intrusion of diabase dykes in the Athabasca Formation was accompanied by significant hydrothermal activity. A metamorphic-hydrothermal as opposed to a magmatic-hydrothermal origin is unlikely in the absence of significant metamorphism coeval with mineralization.

The diagenetic-hydrothermal model, presented by the authors (Hoeve & Sibbald, 1976) and expanded on (Hoeve & Sibbald, 1978), relates uranium mineralization to the action in the Athabasca Formation of diagenetic processes similar to those invoked in the development of red beds. The spatial association with the sub-Athabasca unconformity is attributed to interaction, under conditions of deep burial, of an oxidizing uraniferous Athabasca aquifer with reducing rocks of the underlying basement. Because the basin floor consists of metamorphic rocks with low permeability, all such interaction must have been restricted to the immediate vicinity of the unconformity and the sub-Athabasca palaeo-weathering profile, except in the vicinity of fault and breccia zones of increased secondary permeability.

The model proposes that saline, oxidizing, uraniferous, diagenetic solutions of the Athabasca Formation, at elevated temperatures of around 200°C and at a depth of 4-5km (Pagel, 1975), penetrated the metamorphic basement along fault and breccia zones and reacted with graphite rocks to yield reducing solutions containing carbon dioxide and methane (French, 1966). Provided these newly generated solutions formed part of a percolating system, they will have flowed upwards along other portions of the same fault or breccia zone, eventually reaching the unconformity. Mineralization resulted from interaction of flows of the reducing methane-bearing solutions and of the oxidizing diagenetic solutions carrying ore constituents and, hence, was subject to hydrological control. The geometry of ore bodies such as Collins Bay B and the Deilman (Key Lake) suggests that a flow of reducing solution, discharging into the Athabasca aquifer, was laterally deflected by a flow of diagenetic oxidizing solution directed along the unconformity (Fig. 3). Exceptionally high grades as encountered in many unconformity-type deposits may have developed in a situation of prolonged stationary hydrodynamic equilibrium, as the system is marked by continuous replenishment of ore constituents and methane reductant. Repeated oscillations between oxidizing and reducing conditions as documented at Rabbit Lake (Hoeve, 1977; Hoeve & Sibbald, 1976; 1978) may have arisen from changes in the hydrological regime in response to modification of the plumbing system by intermittent brecciation.

The question of the ultimate source of the ore constituents is difficult to answer. However, they cannot have been derived directly from the palaeo-weathering profile, in view of the post-Athabasca age of mineralization. Pre-existing, late Hudsonian, Beaverlodge-type pitchblende deposits, contrary to Dahlkamp's (1978) and Rimsaite's (1978) suggestions, are not considered a likely source. Despite considerable exploration efforts no such deposits have been discovered east of the Virgin River-Black Lake Shear Zone and in view of the contrasting Hudsonian orogenic evolution east and west of this zone, their existence is unlikely (Sibbald *et al.*, 1976; Hoeve & Sibbald, 1978; Sibbald & Lewry, 1979). Gancarz' (this volume) uranium-lead and lead isotope studies at Cluff Lake suggest that the ore constituents were not derived from precursor ores, but were leached from ordinary rocks not enriched in lead or uranium. If confirmed, his data rule out Hudsonian syngenetic-metamorphic concentrations or late Hudsonian Beaverlodge-type pitchblende deposits as

sources of ore matter, and also surficial concentrations related to pre-Athabasca weathering.

The authors consider the Athabasca Formation as the most likely direct source, rather than rocks of the metamorphic basement, in view of the evidence that the formation has been subjected to extensive post-depositional oxidation and leaching. Destruction of feldspars, mafic and heavy minerals by intrastratal weathering must have liberated a broad suite of trace elements including U, Ni, Co, As, Cu and Zn and other ore constituents in addition to iron, magnesium, calcium and alkalis. Alternatively, ore constituents may also have been introduced into the Athabasca Basin adsorbed to iron hydroxides and to detrital clay minerals to be released during diagenetic recrystallization to the present authigenic assemblage. The coincidence in the Athabasca Basin of the episode of primary mineralization with mafic magmatism ($\simeq$900-1250 m.y.) is considered significant. Steepening of the geothermal gradient accompanying the initiation of mafic magmatism may have induced within the Athabasca Formation the large-scale convection of diagenetic pore solutions required for extraction of ore constituents to take place in the vicinity of the unconformity. Coincident tectonism, giving rise to thrust faulting, provided structural preparation of the ground and induced the increased secondary permeability, which allowed the oxidizing diagenetic solutions access to reducing basement rocks.

The diagenetic-hydrothermal model shows close similarities with metallogenetic models developed for certain epigenetic sandstone-type deposits, which involve either movement of oxidizing groundwaters into reduced sediments, or migration of mobile reductants such as H_2S and hydrocarbons into red beds containing uraniferous pore solutions (Adler, 1974). Examples of the latter are found in southern Texas (Goldhaber *et al.*, 1978; Eargle & Weeks, 1973), and in northwestern Colorado (Adler, 1974). Typical roll-front deposits as in the Wyoming basins, develop in direct response to post-depositional oxidation of initially reduced sediments. Slowly advancing tongues of oxidized sandstone extend inwards from the basin margin, roll-front deposits forming at the redox interface between altered and unaltered rock. With time and favourable hydrological conditions, the whole basin might eventually become oxidized. In such a situation the fate of uranium would depend on hydrological factors. Robertson *et al.* (1978), discussing the time-bound character of uranium deposits, attributed the virtual absence of sandstone-type deposits in pre-Permian host rocks to flushing with oxidizing groundwaters through time leading to destruction of any such ore deposits that once might have been present.

Although the initial oxidation state of the Athabasca Formation is unknown, considering the nature of the extensive diagenetic alteration of the formation, it can be speculated that roll-front or related redox controlled deposits might once have been present and that a situation as observed in the Wyoming basins might represent a transient stage in a process of intrastratal oxidation that has gone to completion in the Athabasca Basin. Mafic magmatism may have added this process by inducing convection within the aquifer, thus allowing interaction of large volumes of oxidizing uraniferous pore solutions with the basin floor. In contrast to Phanerozoic sediments, post-depositional oxidation of the Proterozoic Athabasca Formation may have been facilitated by the absence of organic trash.

Further similarities between Athabasca Basin unconformity-type deposits and those of sandstone-type are in host rock alteration and geochemistry. For the Powder River Basin in Wyoming, Langen & Kidwell (1971) report destruction of mafic minerals such as pyroxene, amphibole and biotite, accompanying the oxidation of host sediments. They also note feldspar alteration to montmorillonite and nontronite. For the Grants Belt, New Mexico, Granger (1962) and Lee (1976) observed chlorite enrichment in the ore zones proportional to the uranium, organic carbon and magnesium contents, and Riese *et al.* (1978) indicate clay mineral zoning with montmorillonite in front of ore, chlorite in the ore zone and kaolinite behind the ore.

Langford (1977) noted that many sandstone-type deposits in the U.S.A. are characterized by element suites strikingly similar to those of Athabasca Basin unconformity-type deposits i.e. U, V, Cu, Pb, Zn, Ni, Co, Mo, Cr, Ag, S, As, Se (Shoemaker *et al.*, 1959; Finch, 1967; Fischer, 1970; Hartman, 1974) and Riese *et al.* (1978) report enrichment in the ore zone, in addition to uranium, of Ni, Co, Cr, Mo, Ti, As, Sb, organic C, Mg and other elements.

Working group IV of the IAEA Symposium on the Formation of Uranium Ore Deposits, Vienna, 1974, observed similarities between sandstone and vein-type uranium deposits, suggestive of the possibility of a common ancestry. They recommended that study of U.S.A. sandstone-type deposits might be beneficial in reaching an understanding of Proterozoic vein-type deposits. In the above discussion the authors pointed to common factors of geochemistry and host rock alteration between Athabasca Basin unconformity-type and sandstone-type uranium deposits. In addition, both types of deposits are associated with continental red beds confined to relatively close basins. Although general conditions in the Athabasca Basin have been somewhat different, reflecting deep burial rather than a more surficial environment, processes and mechanisms involved in the formation of Athabasca Basin unconformity-type deposits, as outlined by the diagenetic-hydrothermal metallogenetic model, appear closely related to those involved in the formation of sandstone-type deposits.

REFERENCES

Anonymous, 1974: The Carswell circular structure and the Cluff Lake Uranium ore bodies. *in* (ed. G. R. Parslow) *Fuels: a Geological appraisal. Spec. Publs geol. Soc. Sask., 2,* 47-61.

Ayres, D.E. & Eadington, P.J., 1975: Uranium Mineralization in the South Alligator River Valley. *Miner. Deposita, 10,* 27-41.

Barbier, J., 1974: Continental weathering as a possible origin of vein-type uranium deposits. *Miner. Deposita, 9,* 271-288.

Beck, L.S., 1969: Uranium Deposits of the Athabasca region, Saskatchewan. *Rep. Sask. Dep. Miner. Resour., 126,* 140p.

Beck, L.S., 1976: History of uranium exploration in Saskatchewan with special references to changing ideas on metallogenesis. *in* (ed. C.E. Dunn) *Uranium in Saskatchewan. Spec. Publs geol. Soc. Sask., 3,* 1-10.

Bretzlaff, R.E., 1976: Genesis of uranium mineralization of Duddridge Lake, Saskatchewan. *M.Sc. Thesis, Carlton University* (unpubl.).

Burwash, R., Badsgaard, H. & Morton, R.D., 1962: Precambrian K-Ar dates from the Western Canada sedimentary basin. *J. geophys. Res., 67,* 1617-1625.

Chukhov, F.W., 1973: On mineralogical and geochemical criteria in the genesis of Red-Beds. *Chem. Geol.,* 12, 67-75.

Crick, I.H., Muir, M.D., Needham, R.S. & Roarty, M.J., this volume: The Geology and Mineralization of the South Alligator Valley Uranium Field. *Proceedings of the International Uranium Symposium on the Pine Creek Geosyncline.*

Cumming, G.L. & Rimsaite, J., 1979: Isotopic studies of lead-depleted pitchblende, secondary radioactive minerals, and sulphides from the Rabbit Lake uranium deposit, Saskatchewan. *Can. J. Earth Sci., 16,* 1702-1715.

Dahlkamp, F.J., 1978: Geological appraisal of the Key Lake U-Ni deposits, northern Saskatchewan. *Econ. Geol., 73,* 1430-1449.

Dawson, K.R., 1951: A petrographic description of wall-rocks and alteration products associated with pitchblende-bearing veins in the Goldfields region, Saskatchewan. *Geol. Surv. Pap. Can., 51-24.*

Derry, D.R., 1970: Geochemistry — The link between ore genesis and exploration. *Bull. Can. Inst. Min. Metall., 63,* 655-658.

Dodson, R.G., Needham, R.S., Wilkes, P.G., Page, R.W., Smart, P.G. & Watchman, A.L., 1974: Uranium mineralization of the Rum Jungle — Alligator Rivers province, Northern Territory, Australia. *in Formation of Uranium Ore Deposits. Proceedings of a Symposium, Athens.* International Atomic Energy Agency, Vienna, 551-566.

Eargle, D.H., & Weeks, A.M.D., 1973: Geologic relations among uranium deposits, South Texas, Coastal Plain region, U.S.A. *in* (eds. G.C. Amstutz & A.J. Bernard) *Ores in Sediments.* Springer-Verlag Berlin, Heidelberg, New York, 101-114.

Fahrig, W.F., 1961: A Geology of the Athabasca Formation. *Bull. Geol. Surv. Can., 68,* 41p.

Finch, W.I., 1967: Geology of epigenetic uranium deposits in sandstone in the United States. *Prof. Pap. U.S. geol. Surv., 538,* 121p.

Fischer, R.P., 1970: Similarities, differences and some genetic problems of the Wyoming and Colorado Plateau types of uranium deposits in sandstone. *Econ. Geol., 65,* 778-784.

French, B.M., 1966: Some Geological Implications of Equilibrium between Graphite and a C-H-O Gas Phase at High Temperatures and Pressures. *Rev. Geophys., 4(2)*, 223-253.
Foy, M.F., 1975: South Alligator Valley Uranium Deposits. *in* (ed. C.L. Knight) *Economic Geology of Australia and Papua New Guinea, Australas. Inst. Min. Metall., Monograph Series No. 5, 1. Metals*, 301-303.
Goldhaber, M.B., Reynolds, R.L. and Rye, R.O., 1978: Origin of a South Texas Roll-type Uranium Deposit. *Econ. Geol., 73*, 1690-1705.
Granger, H.C., 1962: Clays in the Morrison Formation and their spatial relation to the uranium deposits at Ambrosia Lake, New Mexico. *in, Geological Survey Research, 1962. Prof. Pap. U.S. geol. Surv., 450-D*, D15-D20.
Gravenor, C.P., 1959: Heavy minerals of the Athabasca Sandstone. *J. Alberta Soc. Petrol. Geol., 7(1)*, 1-6.
Harshman, E.N., 1974: Distribution of elements in some roll-type uranium deposits. *in, Formation of Uranium Ore Deposits. Proceedings of a Symposium, Athens.* International Atomic Energy Agency, Vienna, 169-181.
Hoeve, J., 1977: Uranium Metallogenetic Studies, 11 Rabbit Lake: Mineralogy and Geochemistry. *in* (eds. J.E. Christopher & R. MacDonald) *Summary of Investigations 1977. Sask. Geol. Surv. Misc. Rep.*, 124-135.
Hoeve, J., 1978: Uranium Metallogenetic Studies: Rabbit Lake: Mineralogy and Geochemistry. *in* (eds. J.E. Christopher & R. MacDonald) *Summary of Investigations 1978. Sask. geol. Surv. Misc. Rep.*, 61-65.
Hoeve, J. & Sibbald, T.I.I., 1976: Rabbit Lake Uranium Deposit. *in* (ed. C.E. Dunn) *Uranium in Saskatchewan. Spec. Publs. geol. Soc. Sask., 3*, 331-354.
Hoeve, J. & Sibbald, T.I.I., 1978a: Uranium concentration related to the sub-Athabasca unconformity, northern Saskatchewan, Canada. *in* (ed. M.M. Kimberley) *Short Course in Uranium Deposits: Their Mineralogy and Origin. Mineralogical Association of Canada*, 475-484.
Hoeve, J. & Sibbald, T.I.I., 1978b: On the origin of Rabbit Lake and other unconformity-type uranium deposits in northern Saskatchewan, Canada. *Econ. Geol., 73*, 1450-1473.
Hubert, J.F., & Reed, A.A., 1978: Red-bed diagenesis, in the East Berlin Formation, Newark Group, Connecticut Valley. *J. sedim. Petrol., 48(1)*, 175-184.
Jawad Ali, A. & Braithwaite, C.J.R., 1977: Penecontemporaneous Weathering of the Old Red Sandstone of the Midland Valley of Scotland. *Scott. J. Geol, 13(4)*, 305-312.
Jones, B., in press: Geology of the Collins Bay uranium deposits, Saskatchewan. *Bull. Can. Inst. Min. Metall.*
Kalliokoski, J., Langford, F.F. & Ojakangas, R.W., 1978: Criteria for Uranium occurrences in Saskatchewan and Australia as guides to favorability for similar deposits in the United States. *Technological University, Department of Geology Geological Engineering*, 480p.
Kirchner, G., Lehnert-Thiel, K., Rich, J. & Strnad, J.G., this volume: Key Lake and Jabiluka: Models for Lower Proterozoic Uranium Deposition. *Proceedings of the International Uranium Symposium on the Pine Creek Geosyncline.*
Koeppel, V., 1968: Age and history of the uranium mineralization of the Beaverlodge area, Saskatchewan. *Geol. Surv. Pap. Can., 68-31*, 11p.
Langen, R.E. & Kidwell, A.L., 1974: Geology and geochemistry of the Highland uranium deposit, Converse County, Wyoming. American Institute of Mining, Metallurgical and Petroleum Engineers Paper 71-1-37, 17p.
Langmuir, D., 1978: Uranium solution-mineral equilibria at low temperatures with applications to sedimentary ore deposits. *Geochim. cosmochim. Acta, 42(6)*, 547-569.
Lee, M.J., 1976: Geochemistry of the sedimentary uranium deposits of the Grants Mineral Belt, Southern San Juan Basin, New Mexico. *PhD. Thesis, University of New Mexico*, (unpubl.), 241p.
Lewry, J.F. & Sibbald, T.I.I., 1977: Variation in lithology and tectonometamorphic relationships in the Precambrian basement of Northern Saskatchewan: *Can. J. Earth Sci., 14(6)*, 1453-1467.
Lewry, J.F. & Sibbald, T.I.I., 1979: A review of pre-Athabasca basement geology in Northern Saskatchewan. *in* (ed. G.R. Parslow) *Spec. Publs. geol. Soc. Sask., 4*, in press.
Lewry, J.F., Sibbald, T.I.I. & Rees, C.J., 1978: Metamorphic patterns and their relation to tectonism and plutonism in the Churchill Province in northern Saskatchewan. *in, Metamorphism in the Canadian Shield. Geol. Surv. Pap. Can., 78-10*, 139-154.
Little, H.W., 1974, Uranium in Canada. Report of Activities, Part A. *Geol. Surv. Pap. Can., 74-1.*, 137-139.
Morton, R.D., 1977: The western and northern Australian uranium deposits — exploration guides or exploration deterrants for Saskatchewan? *in* (ed. C.E. Dunn) *Uranium in Saskatchewan, Spec. Publs Geol. Soc. Sask., 3*, 211-255.
Maucher, A., 1962: *Die Lagerstätten des Urans, Vieweg and Sohn.* Braunschweig.
Needham, R.S., Crick, I.H. & Stuart-Smith, P.G., this volume: Regional Geology of the Pine Creek Geosyncline. *Proceedings of the International Uranium Symposium on the Pine Creek Geosyncline.*
Needham, R.S. & Stuart-Smith, P.G., 1976: The Cahill Formation, host to uranium deposits in the Alligator Rivers Uranium Field, Australia. *BMR J. Aust. Geol. Geophys., 1*, 321-333.
Needham, R.S. & Stuart-Smith, P.G., this volume: Geology of the Alligator Rivers Uranium Field. *Proceedings of the International Uranium Symposium on the Pine Creek Geosyncline.*
Pagel, M., 1975a: Cadre Géologique de Gisements d'uranium dans la structure Carswell (Saskatchewan-Canada). "Etude des phases fluides". *Thèse de de Docteur de Spécialite (3e cycle), L'Université de Nancy 1.*
Pagel, M., 1975b: La diagénèse des grés et les gisements d'uranium du bassin Athabasca (Canada). *in, Rapport d'activité 1975. Equipe de Récherches sur les Equilibres entre fluides et minéreaux, Nancy.*
Pagel, M., 1975c: Déterminations des conditions physio-chimiques de la silicifications diagénétique des grés Athabasca (Canada) au moyen des inclusions fluides. *C.R. Acad. Sci. Paris, T. 280, Ser. D.*, 2301-2304.
Pagel, M., 1977: Microthermometry and chemical analysis of fluid inclusions from the Rabbit Lake uranium deposit, Saskatchewan, Canada (Abstract). *Trans. Instn Min. Metall., 86*, B157.

Ramaekers, P., 1976: Athabasca Formation, Northeast Edge (64L, 74I, 74P); Part I Reconnaissance geology. *in* (eds. J.E. Christopher & R. MacDonald) *Summary of Investigations 1976. Sask. Geol. Misc. Rep.*, 73-77.
Ramaekers, P., 1977: Athabasca Formation, South-Central Edge (74G Area): Part I Reconnaissance geology, *in* J.E. Christopher & R. MacDonald) *Summary of Investigations 1977. Sask. geol. Surv. Misc. Rep.*, 157-163.
Ramaekers, P., 1978: Athabasca Formation, Southwestern Edge: Part I Reconnaissance Geology (NTS Areas 74F, 74K), *in* (eds. J.E., Christopher & R. MacDonald) *Summary of Investigations 1978. Sask. geol. Surv. Misc. Rep. 78-10*, 124-128.
Ramaekers, P., 1979: Stratigraphy of the Athabasca Basin. *in* (eds. J.E. Christopher & R. MacDonald) *Summary of Investigations 1979. Sask. geol. Surv. Misc. Rep., 79-10* (in press).
Ramaekers, P. & Dunn, C.E., 1976: Geology and Geochemistry of the Eastern Margin of the Athabasca Basin. *in* (ed. C. E. Dunn) *Uranium in Saskatchewan. Spec. Publs geol. Soc. Sask, 3*, 297-322.
Ramaekers, P. & Hartling, A., 1979: Structural geology and intrusive events of the Athabasca Basins, and their bearing on uranium mineralization. *in* (ed. G. R. Parslow) *Uranium Exploration techniques. Spec. Publs geol. Soc. Sask., 4*, in press.
Ray, G.E., 1977: The geology of Highrock Lake — Key Lake vicinity. *Rep. Sask. geol. Surv., 197*, 29p.
Riese, W.C., Brookins, D.B., Lee, M.J. & Della Valle, R., 1978: Application of trace element geochemistry to prospecting for sandstone-type uranium deposits. *7th Int. Geoch. Expl. Symposium, Denver, 1978. Program and Abstracts*, 64-65.
Rimsaite, J., 1978: Application of mineralogy to the study of multi-stage uranium mineralization in remobilized uranium deposits, Saskatchewan. *in* (ed M. M. Kimberley) *Short Course in Uranium Deposits: Their Mineralogy and Origin. Mineralogical Association of Canada*, 475-484.
Robinson, S.C., 1955: Mineralogy of Uranium Deposits, Goldfields, Saskatchewan. *Bull. geol. Surv. Can., 31*, 128p.
Robertson, D.A. & Lattanzi, C.R., 1974: Uranium deposits of Canada. *Geoscience Canada, 1*, 8-19.
Robertson, D.S., Tilsley, J.E. & Hogg, G.M., 1978: The time-bound character of uranium deposits. *Econ. Geol., 73*, 1409-1419.
Ruzicka, V., 1975: Some metallogenic Features of the "D" Uranium Deposit at Cluff Lake, Saskatchewan. Report of Activities. *Geol. Surv. Pap. Can., 75-1C*, 279-283.
Ryan, G. R., 1977: Uranium in Australia. *in* (ed. M. J. Jones) *Geology, Mining and Extractive processing of Uranium. Inst. Min. Metall., London*, 24-42.
Sassano, G.P., Fritz, R. & Morton, R.D., 1972: Paragenesis and isotopic composition of some gangue minerals from the uranium deposits of Eldorado, Saskatchewan. *Can. J. Earth Sci., 9*, 141-157.
Scott, B.P., 1978: The geology of an area east of Thluichio Lake, Saskatchewan. *Rep. Sask. geol. Surv., 167*, 52p.
Sibbald, T.I.I., 1975: Investigation of certain radiometric anomalies in Crown Reserve 621. *in* (eds. J. E. Christopher & R. MacDonald). *Summary of Investigations 1976. Sask. geol. Surv. Misc. Rep.*, 123-129.
Sibbald, T.I.I., Munday, R. J. C. & Lewry, J. F., 1976: The geological setting of uranium mineralization in northern Saskatchewan. *in* (ed C. E. Dunn) *Uranium in Saskatchewan. Spec. Publs geol. Soc. Sask., 3*, 51-98.
Stuart-Smith, P. G., Wills, K., Crick, I. H. & Needham, R. S., this volume: Evolution of the Pine Creek Geosyncline. *Proceedings of the International Uranium Symposium on the Pine Creek Geosyncline.*
Tremblay, L. P., 1972: Geology of the Beaverlodge Mining Area, Saskatchewan. *Mem. geol. Surv. Can., 367.*
Tremblay, L. P., 1978: Geologic setting of Beaverlodge-type uranium deposits and its comparison to that of unconformity-type. *in* (ed M. M. Kimberley) *Short Course in Uranium Deposits: Their Mineralogy and Origin. Mineralogical Association of Canada*, 431-456.
Turner, P., 1974: Origin of Red-beds in the Ringerlike Group (Silurian) of Norway. *Sediment. geol., 12*, 215-235.
Walker, R. T., 1967: Formation of Red-beds in modern and ancient deserts. *Bull. geol. Soc. Am., 78*, 353-368.
Walker, T. R., 1976: Diagenetic origin of Red-beds. *in, The Continental Permian in Central, West and South Europe*. Reidel Publ Co., Dordrecht, Holland.
Walker, R. T., Waugh, B. & Crone, A. J. 1978: Diagenesis in first-cycle desert alluvium of Cenozoic age, southwestern United States and northwestern Mexico. *Bull. geol. Soc. Am., 89, 19-32.*
Wallis, R. H., 1971: The Geology of the Hidden Bay Area, Saskatchewan. *Rep. Sask. geol. Surv., 137.*
Wendt, I., Hohndorf, A., Lenz, H. & Voultsidis, V., 1978: Radiometric age determinations on samples of the Key Lake Uranium deposits. *in* (ed R. E. Zartmann) *Short Papers of the Fourt International Conference, Geochronology, Cosmochronology, Isotope Geology, 1978., USGS Open File Report, 78-701*, 448-449.
Wanless, R. K., Stevens, R. D., Lachange, G. R. & Rimsaite, J. Y. H., 1966: Age determinations and geological studies, K-Ar isotope ages, Report 6. *Geol. Surv. Pap. Can.*, 65-17.

URANIUM GEOLOGY IN THE AMER — DUBAWNT — YATHKYED — BAKER LAKES REGION, KEEWATIN DISTRICT, N.W.T. CANADA

Laurence Curtis[1] and A.R. Miller[2]

1. Research School of Earth Sciences, Australian National University, P.O. Box 4, Canberra, A.C.T., 2601, Australia.
2. Geological Survey of Canada, 601 Booth Street, Ottawa, Ontario. K1A OE8, Canada

ABSTRACT

Numerous showings of uranium occur in the Keewatin District of Central Canada. The uranium mineralization is found predominantly within Proterozoic supracrustals which unconformably overlie a basement complex consisting of granites, metasediments and metavolcanics. The Proterozoic rocks consist of an older shelf facies sequence of Lower Proterozoic (Aphebian) age which are unconformably overlain by the Middle Proterozoic continental Dubawnt Group. The Dubawnt Group comprises basal conglomerates and sandstones, which in the Baker Lake basin are overlain by subaerial alkaline volcanics and intercalated fluviatile sediments related to a period of rift tectonics. These are in turn overlain by calc-alkaline volcanics. A subsequent period of crustal stability is indicated by the development of a thick section of mature continental sandstones, possibly correlative with the Athabasca sandstone. Uranium occurs within granitoid basement rocks of probable Archaean age, as stratabound concentrations within Lower Proterozoic metasediments and as vein and disseminated mineralization in the vicinity of Lower-Middle Proterozoic unconformities. Fracture controlled and disseminated uranium is found in a diverse number of geological settings within the Dubawnt Group. Several of the uranium occurrences have economic potential further highlighting the comparison between the Keewatin and Pine Creek uranium provinces.

INTRODUCTION

An area in excess of 100,000km² of Proterozoic supracrustals overlying Archaean basement occurs in the Districts of Keewatin and Mackenzie, Northwest Territories Canada (Fig. 1). Uranium mineralization hosted by this Proterozoic sequence has been the focus of exploration activity for the past decade. There are no producing mines in the area at present, but at least one potentially economic ore deposit has been located and several other significant discoveries are presently being evaluated.

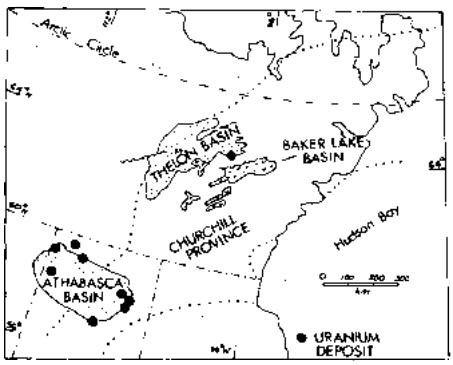


Figure 1. Location of the Thelon and Baker Lake Basins, Keewatin and Mackenzie Districts, Northwest Territories, Canada . . . Probable extent of Lower Proterozoic Geosyncline (McGlynn, 1976).

In this paper we describe the geological history and stratigraphy of the region and examine the distribution of the various mineralization types with respect to time. The greater number of known uranium showings are found within an area defined geographically by the Amer, Dubawnt, Yathkyed and Baker Lakes. This area contains the Baker Lake, Yathkyed and subsidiary basins in addition to the northeast portion of the Thelon basin (Fig. 2). Potential uranium-bearing areas also occur in the lesser known portions of the Thelon basin in the Mackenzie District.

The detailed mineralogical descriptions were carried out by the second author on samples collected during mapping programmes conducted by the Geological Survey of Canada and on samples provided by several companies.

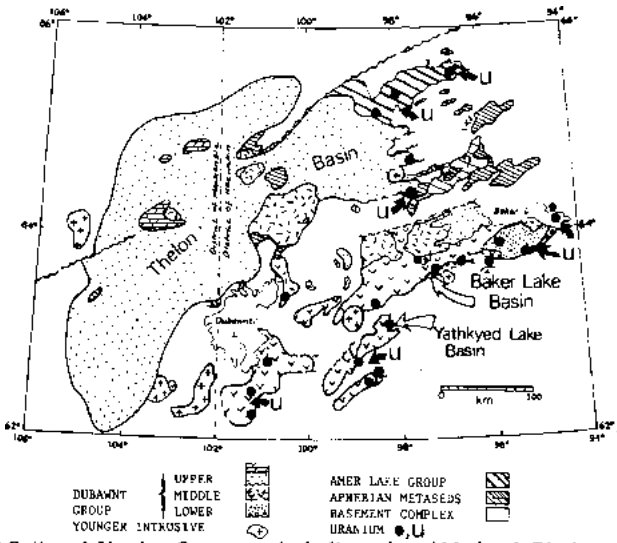


Figure 2. Regional Geology & Uranium Occurrences in the Keewatin and Mackenzie Districts, after Wright (1967), Donaldson (1965; 1969), LeCheminant & Miller (1978) and this paper.

GEOLOGICAL HISTORY OF THE URANIUM PROVINCE

The region of interest lies within the Churchill Structural Province (Stockwell, 1961). The northern portion of the province has been subdivided into blocks defined by major east-west and northeast trending fault systems. These blocks are characterised by different metamorphic grades and structural styles, which are believed to reflect differing levels of crustal exposure (Heywood & Schau, 1978).

The Archaean basement rocks consist of granite gneisses and lesser infolded greenstone belts and have been reworked and metamorphosed. Metamorphic grades range from amphibolite to granulite facies. In the southern portion of the Churchill province the Archaean rocks have undergone deformation during the Kenoran orogeny, dated at approximately 2550Ma (Wanless & Eade, 1975). Diabase dykes intrude the basement complex and have been dated in the southern portion of the Churchill Province at ~2550Ma (Wanless *et al.*, 1973).

Intermittent periods of relative tectonic stability are suggested by the presence of Lower Proterozoic (Aphebian) shelf facies sediments deposited in local basins in the northern, central and southern portions of the province. These rocks were in turn strongly folded and deformed during the Hudsonian orogeny, an event which in the area of interest appears to have preceded deposition of the late Lower(?) to early Middle Proterozoic (Palaeohelikian) cover rocks. This deformational overprinting has complicated interpretations of the structural history of the basement complex. The extent and age limits of the Hudsonian orogeny in this region are at present a matter of debate, although the culmination of the event appears to have been between 1735-1800Ma.

The Lower Dubawnt Group was deposited in response to a period of active faulting which was followed by alkaline volcanism within a complex graben structure. An ensueing period of calc-alkaline volcanism was closely followed by intrusion of numerous anorogenic granites. After a considerable period of tectonic stability a blanket of mature sandstones was deposited particularly within the structure now defined as the Thelon Basin.

A later phase of fracturing and faulting in a predominantly north-westerly direction was superimposed on the region. The Mackenzie diabase dykes emplaced around 1200Ma (Patchett *et al.*, 1978) parallel these trends.

STRATIGRAPHY

A simplified stratigraphy, modified after Wright (1967) is presented in table 1, an expanded version of which is shown in table 2. Simplified stratigraphic columns from locations within the Thelon and Baker Lake basins are given in table 3. The age relationships between various units, particularly those which constitute the basement complex are uncertain. There are also some difficulties in correlating Lower Proterozoic (Aphebian) metasediments of the Hurwitz Group which occur in the Kaminak-Henik Lakes area with similar lithologies found north and west of Baker Lake. These units have yet to be given group status

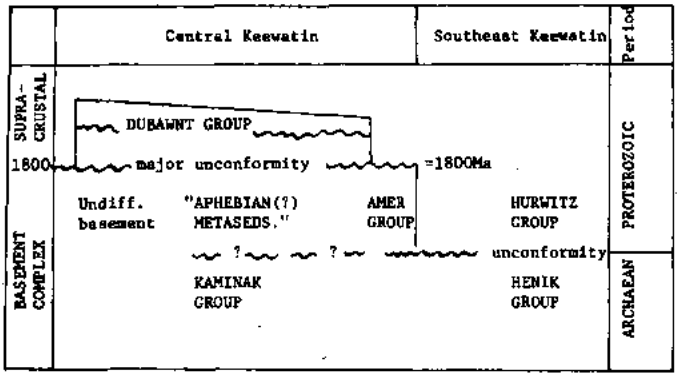
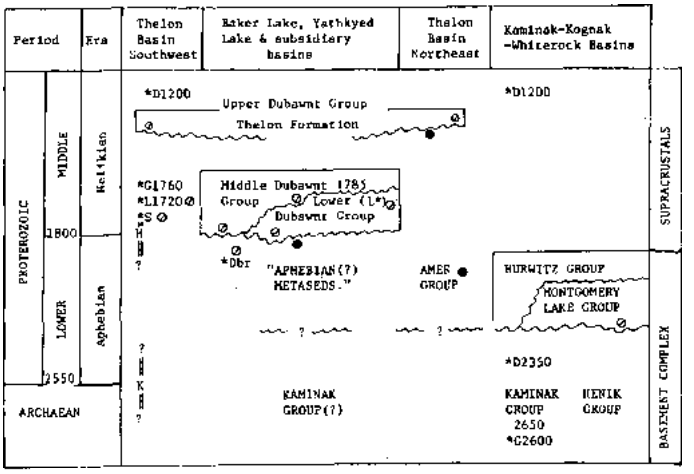


Table 1. Simplified Regional Stratigraphy.



K, H = Kenoran & Hudsonian orogenies

*G,S,D,L,Dbr - Granite, syenite, diabase, lamprophyre and diatreme breccia; ages in Ma

Stratigraphic position of mineralisation

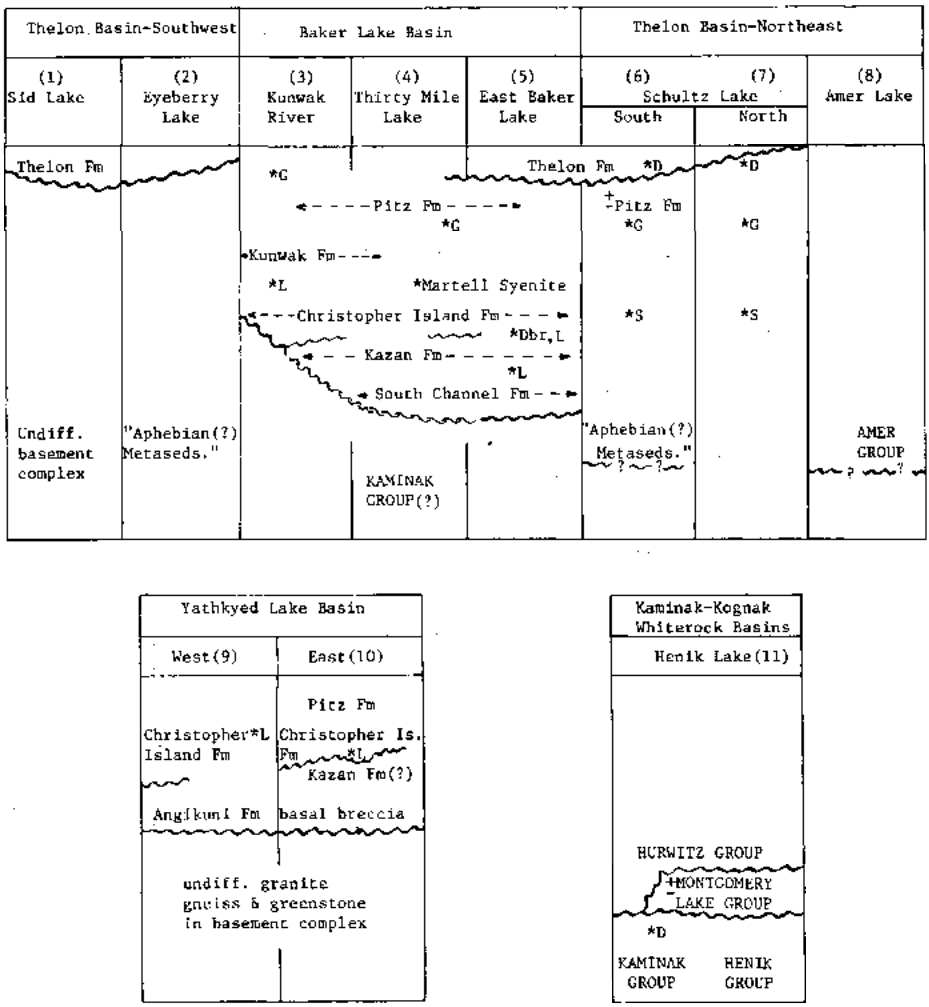
Table 2. Regional Stratigraphy and Uranium Occurrences.

and we will refer to them as 'Aphebian(?) metasediments'. The name Amer Group has been applied by Tippett & Heywood (1978) to define a similar belt of metasediments occurring north of Baker Lake. Reference is made to the Kaminak-Whiterock-Kognak basins for comparative purposes only.

Archaean and Lower Proterozoic(?) Basement Complex

Granitoid gneiss complexes

Granitoid gneiss complexes of Archaean and probably Lower Proterozoic age predominate in the basement assemblage. The complexes consist of ortho- and paragneisses, gneissic granodiorites, granites and migmatites. These felsic gneisses are commonly infolded



* G,D,S,Dbr,L= Granite, Diabase, Syenite, Diatreme breccia, Lamprophyre

unconformity fault ( ) Section on Figure 3

Table 3. Simplified Stratigraphic Sections, Keewatin and Mackenzie Districts, N.W.T.

with linear belts of metavolcanics and metasediments. The granite gneisses have been quite strongly deformed, with two phases of deformation commonly observed and up to three phases recognized locally (LeCheminant *et al.*, 1977, 1979b). Zones of migmatisation and the presence of pegmatites attest to moderate to high thermal regimes. Amphibolite facies assemblages are present in the basement complex, however, extensive retrogression to greenschist facies occurred during the Hudsonian event. Granulite facies rocks are present northeast of Baker Lake (Schau & Hulbert, 1977) and probable retrograde granulite facies rocks have been recognized west of Thirty Mile Lake (LeCheminant *et al.*, 1977).

Archaean metavolcanic and metasedimentary belts

Archaean metavolcanic and metasedimentary belts occur south of the Baker Lake basin and in the vicinity of the Yathkyed Lake basin (Eade & Blake, 1977; Reinhardt & Chandler, 1973; LeCheminant *et al.*, 1976, 1977). In some areas west of Baker Lake it is difficult to distinguish overlying Lower Proterozoic(?) units from the presumed Archaean greenstones.

Intrusives

Intrusives of probable Archaean age are found within the region although only a few have compatible age dates. There is also a possibility that some of the mafic intrusives originally mapped by Wright (1955, 1967), which consist of diorites, gabbros, ultramafics and anorthosites could be of late Archaean age.

A large number of gabbro dykes intrude the basement complex in the region and although not dated, are considered to be Lower Proterozoic (early Aphebian) age. K/Ar dates obtained from similar dykes in the Kaminak Lake area (southeast of the region under consideration) average about 2370Ma (Wanless *et al.*, 1973).

Lower Proterozoic Hurwitz Group, Amer Group and 'Aphebian(?) Metasediments'

Within the basement complex in the Keewatin District a number of metasedimentary belts considered to be of Lower Proterozoic (Aphebian) age were assigned to the Hurwitz Group by Wright (1955). Further mapping in the type area southeast of the uranium province has resulted in a more detailed stratigraphy in the Kaminak-Kognak-Whiterock basins, (Eade, 1964, 1974; Bell, 1968; Ridler, 1974; Davidson, 1970) which is summarised in table 2.

It has since become evident that although the metasediments which comprise the Hurwitz Group in areas southeast of the Baker Lake basin (viz. the Whiterock-Kaminak-Kognak basins) are demonstrably correlative (Bell, 1968), a correlation with similar lithologies north and west of Baker Lake as originally proposed by Wright (1955) cannot be as readily justified. For these reasons the 'Hurwitz-like' sediments west and north of Baker Lake are referred to as 'Aphebian(?) metasediments'.

These sediments were probably deposited intermittently over an extended period of Lower Proterozoic time within a northeast trending basin or geosyncline of unknown extent (Fig. 1). A more detailed description of the Hurwitz Group, Amer Group and Hurwitz-like Aphebian(?) metasediments follows.

Hurwitz Group

As previously noted the stratigraphy of the Hurwitz Group is defined and best studied in areas south and southeast of the uranium-bearing region under consideration. Nonetheless as some of the host rocks to the uranium mineralization are considered to be correlative with the Hurwitz Group the following descriptions after Eade (1974) are useful as a reference stratigraphy. The most complete section examined by Eade has a combined thickness of about 2450m, however, thickness of individual units is extremely variable:

1) Padlei Formation: Basal conglomerate.
2) Kinga Formation: Orthoquartzite marker unit.
3) Ameto Formation: Slate, shale and siltstone. Minor dolomite. Splitic shallow marine tholeiites (up to 900m) of the Happotiyik Member are developed locally (Ridler, 1974).

4) Watterson Formation: Dolomite, argillite, siltstone and greywacke. Minor iron formation.
5) Ducker Formation: Greywacke and some siltstone.
6) Tavani Formation: Impure quartzite, arkose and quartz-sericite schist.
7) Gabbro: Sills, probably coeval with the Happotiyik Member.

The Hurwitz rocks in this region have been folded and contain assemblages typical of low to medium grade greenschist facies metamorphism. Dynamic metamorphism has affected the Hurwitz Group locally and this is due mainly to syn- and, post-tectonic intrusives associated with the Hudsonian event. Wanless & Eade (1975) obtained a K-Ar age of 1815±116 Ma on an amphibole from a Hurwitz gabbro still within the Hurwitz Group, and a Rb/Sr whole rock isochron on a quartz latite intercalated with Hurwitz Group sediments returned a similar age of 1801±35Ma*. These data imply a late Lower Proterozoic (late Aphebian) age for the Hurwitz Group, a conclusion which has been challenged by Young (1975) and Church (1977) who infer that the Hurwitz Group could be of early Lower Proterozoic (early Aphebian) age.

Amer Group

The Amer Group occupies a discrete fold belt which occurs approximately 125km northwest of the hamlet of Baker Lake. The belt strikes in a ENE-WSW direction and forms a canoe shaped synclinorium which is overlain unconformably to the west by the Thelon sandstone of Middle Proterozoic (Palaeohelikian) age. The Amer Group as defined by Tippett & Heywood (1978) has a minimum thickness of 3500m and consists of seven units, representing two major clastic sequences (units 2 and 7) which are separated by a series of thin transitional units (units 3-6). The sequence in ascending order is as follows:

1) Feldspathic sandstone and muscovite schist (0-30m)
2) Orthoquartzite (400-1000m)
3) Impure clastic unit (5-20m)
4) Cross-bedded feldspathic quartzite (10-30m)
5) Dolomite limestone (30-50m)
6) Slate (50-300m)
7) Feldspathic sandstone-siltstone-slate(3000m+), a heterogeneous assemblage in which feldspathic sandstone, siltstone and slate predominate; calcareous feldspathic sandstones are also a significant constituent.

The upper clastic unit of the Amer Group hosts the majority of the stratiform uranium showings described below. The belt is tightly folded and complexly faulted. The grade(s) of metamorphism have not yet been adequately determined as P-T estimates based on existing mineral assemblages are conflicting (Tippett & Heywood, 1978). The Amer Group is generally believed to be of Lower Proterozoic (Aphebian) age by virtue of the Hurwitz Group correlation.

Undifferentiated Aphebian(?) Metasediments

As noted previously this terminology is used to refer to Lower Proterozoic(?) belts assigned to the Hurwitz Group by Wright (1955, 1967), but which have not yet been studied in sufficient detail to warrant such a correlation. The stratigraphic position of these belts relative to the Amer Group is not known, however, they are distinguished from the Amer belt by absence of the distinctive dolomite units and by presence of metavolcanics and cherty magnetite-bearing units. As yet insufficient work has been done to determine if the belts are facies equivalents of the Amer Group, or if they are at all correlative. These are important considerations particularly since the Amer Group hosts stratiform uranium mineralization

*All Rb/Sr data quoted are recalculated using $\lambda^{87}Rb = 1.47 \times 10^{-11} a^{-1}$

and the Aphebian(?) metasediments west of Baker Lake host the Sissons Lake uranium prospect.

The relationships between the Aphebian(?) metasediments and the basement complex are not well defined. For our purposes we will consider the Aphebian(?) metasediments north and west of Baker Lake to be Hurwitz equivalents, however, it is possible that at least some of these units could be of late Archaean age.

Lower(?)-Middle Proterozoic Dubawnt Group

Occupying some 90,000km² of the Keewatin and Mackenzie Districts, the Dubawnt Group forms an extensive blanket of continental volcanic and clastic sedimentary rocks resting unconformably upon the basement complex previously described (Fig. 2). The Dubawnt Group consists of six named units defined by Donaldson (1965), plus two additional units of restricted occurrence, recently defined by Blake (in press) and LeCheminant *et al.* (1979b). These have been divided into a lower clastic sedimentary (redbed) cycle, a middle volcanic-volcaniclastic-intrusive cycle and an upper mature sedimentary cycle (Table 4).

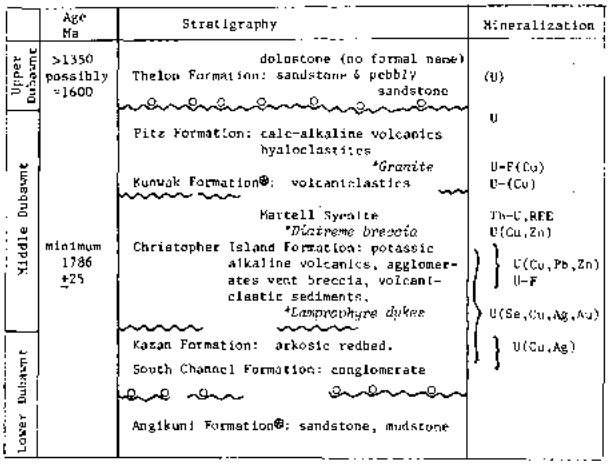


Table 4. Stratigraphy of the Dubawnt Group and Uranium Occurrences.

A major unconformity at the base of the Group is marked locally by a hematite and clay-rich regolith. Local unconformities and disconformities occur within the succession, a feature not unexpected in regions where volcanic and fluvial activity is commonly of local extent and short duration. The Dubawnt Group is host to numerous occurrences of uranium mineralization (Blake *et al.*, 1977) and for this reason the stratigraphy is presented below in some detail.

Description of the main units (in ascending order)

1) Angikuni Formation: Defined by Blake (in press), this Formation is of local extent and comprises a lower sequence of feldspathic sandstone (1400+m) and a conformable upper sequence consisting of interbedded siltstone, mudstone and fine grained sandstone (1500+m).
2) South Channel Formation: This basal polymict conglomerate unit occurs discontinuously along the eastern and southern rim of the Baker Lake basin where it commonly attains thicknesses up to 1800m (LeCheminant *et al.*, 1977, 1979a,b).
3) Kazan Formation: This unit conformably overlies the South Channel conglomerates

and consists predominantly of a maroon feldspathic sandstone (arkose). Lesser quantities of siltstone and mudstone are intercalated and increase up sequence. Thicknesses of up to 1000m are recorded south of Baker Lake. Rocks possibly correlative with the Kazan Formation have also been recognized in the Yathkyed basin (Eade, 1976).

4) Christopher Island Formation: Extensive subaerial lavas, pyroclastics, agglomerates, vent breccias and volcaniclastic sediments comprise this unit which occurs in the Baker Lake and subsidiary basins, but has yet to be identified in the Thelon basin. The basal contact is diachronous; the unit may be conformable or unconformable with underlying units. The volcanics consist predominantly of potassic trachybasalts, trachyandesites, trachytes and minor rhyolites and have shoshonitic affinities (Blake, in press). Blake notes that in comparison to most other volcanics they have high P and Ba, high but variable Sr and U and lower Ti and Fe contents. Thicknesses are extremely variable ranging from 60m to 7300m (Donaldson, 1965; Eade & Blake, 1977; LeCheminant *et al.*, 1978). A Rb/Sr whole rock isochron determined on the volcanics by Wanless & Loveridge (1972) gave an age of 1786Ma.
5) Kunwak Formation: Defined by LeCheminant *et al.* (1979b) the Kunwak Formation is of restricted occurrence and consists of volcaniclastic sediments which unconformably overlie the Christopher Island Formation.
6) Martell Syenite: Laccoliths, dykes and sills of syenite, monzonite and rarely alkali granite constitute this unit (Donaldson, 1965; LeCheminant *et al.*, 1977) which is considered to be comagmatic with the Christopher Island volcanics (Blake, in press).
7) Pitz Formation: In the type locality west of Pitz Lake, this unit consists predominantly of red porphyritic flows and lesser volcaniclastic sediments (Donaldson, 1965). LeCheminant *et al.* (1977) also distinguished some hyaloclastites. The Pitz volcanics have calc-alkaline affinities (Analysis V, Table 5), are widely distributed and average about 100m in thickness.
8) Thelon Formation: This is by far the most extensive unit of the Dubawnt Group, and is composed predominantly of fluvial quartzose sandstones, lesser amounts of pebbly sandstone and locally contains lenses of conglomerate and siltstone (Donaldson, 1965). The basal contact is a disconformity which is often marked by a hematitic regolith. Although only about 100m thick in the eastern Baker Lake basin, the sandstones probably thicken in the central Thelon basin. The Thelon sediments in the Thelon basin are generally more mature and less indurated than the Kazan redbeds and were deposited under highly stable tectonic conditions (Donaldson, 1968; Cecile, 1973). The age of the Formation is bracketed by the underlying Dubawnt volcanics with a currently accepted age of about 1800Ma and cross-cutting diabase dykes dated at 1200Ma (Patchett *et al.*, 1978). Another guide to the age of the Thelon Formation is the inferred correlation with the Athabasca Formation (Donaldson, 1967; Fraser *et al.*, 1970; Fahrig *et al.*, 1978) which has been dated at 1428±30Ma (Ramaekers, 1979).

Dolostones and basalts which overlie the Thelon Formation have been included by Donaldson (1967, 1969) in the Dubawnt Group, but have not been formally named.

Intrusive Rocks related(?) to the Dubawnt Group

Porphyritic granite and quartz-feldspar porphyry dykes which intrude Dubawnt Group volcanics are considered by LeCheminant *et al.* (1978) to be comagmatic with the Pitz volcanics. Wright (1967) describes a number of syenite, gabbro and lamprophyre intrusions occurring north of Baker Lake which he believes could be intrusive equivalents to the Dubawnt Group volcanics. One such mafic syenite north of Amer Lake gave a K/Ar age of

%	I	II	III	IV	V	VI	VII	VIII*
SiO_2	62.0	58.9	75.8	71.1	73.0	60.8	67.4	54.4
TiO_2	0.97	0.55	0.23	0.19	0.40	0.91	0.61	
Al_2O_3	15.2	15.3	9.44	14.4	13.5	16.6	15.0	12.8
ΣFeO	6.30	6.11	1.20	1.30	2.12	5.80	3.76	9.24
MnO	0.08	0.06	0.07	0.01	0.04	0.05	0.05	0.57
MgO	1.39	2.92	0.62	0.40	0.33	0.76	0.93	4.89
CaO	2.33	3.59	4.35	1.44	0.62	1.30	0.46	5.71
Na_2O	3.00	1.99	1.57	3.51	3.26	6.03	4.26	0.44
K_2O	5.22	4.39	3.71	5.46	5.39	4.80	5.71	6.70
P_2O_5	0.28	0.11	0.08	0.06	0.07	0.00	0.08	0.62
H_2O	1.54	5.09	3.27	1.65	1.16	0.77	0.82	2.39
	99.1	99.7	100.4	99.7	100.1	98.5	99.6	99.1
ppm								
U	3	860	3500	5	4	210	43	1650
Th	19	15	8	38	42	520	320	14
Pb	50	85	1020	10	20	170	170	410

I Basement gneiss, Nowleye Lake.
II Metasiltstones, Amer group Sandhills Showing.
III Metasiltstone, "Aphebian(?) meta-sediment" outlier.
IV Non-foliated granite, south of Schultz Lake.
V Pitz Formation, east of Kunwak River.
VI Fine grained bostonitic syenite; 25km northwest of Nutarawit Lake.
VII Porphyritic microsyenite, 25km northwest of Nutarawit Lake.
VIII Fractured & chloritised microsyenite, same outcrop as VII.

* All analyses by X-ray Assay Laboratories, Toronto major elements XRF: U, Th neutron activation; Pb by AA.

Table 5. Selected Chemical Analyses.

1833±32Ma (Tella & Heywood, 1978), which is the presumed age of emplacement. Numerous 'lamprophyre' dykes intrude the Dubawnt volcanics and also occur away from the main Baker Lake basin; one of these gave a minimum K/Ar age of 1720Ma (Wright, 1967). On the eastern rim of the Baker Lake basin a number of alkalic mafic intrusives and diatreme breccias occur which may be cogenetic with the Dubawnt volcanic episode. The relationship between the informally named Nueltin Lake granites (Wright, 1967) and the Dubawnt volcanic suite is, however, less certain. These granites are typically non-foliated, and porphyritic and commonly occupy areas of 500+km² within the southern Keewatin and southeast Mackenzie Districts. The Neultin Lake granites are commonly fluorite-bearing, and are generally enriched in Th and to a lesser extent U. A Rb/Sr age determination of 1760ma* was obtained forNueltin Lake granite in the type area (Wanless & Eade, 1975) and Wanless & Loveridge (1972) dated satellite plutons of the Nueltin granite at 1775Ma*. On present knowledge these dates do not preclude the possibility that some of the Nueltin Lake granites could be correlative with the calcalkaline Pitz Formation of the Dubawnt Group, as suggested by LeCheminant *et al.* (1978).

* Recalculated using $\lambda^{87}Rb = 1.47 \times 10^{-11} a^{-1}$

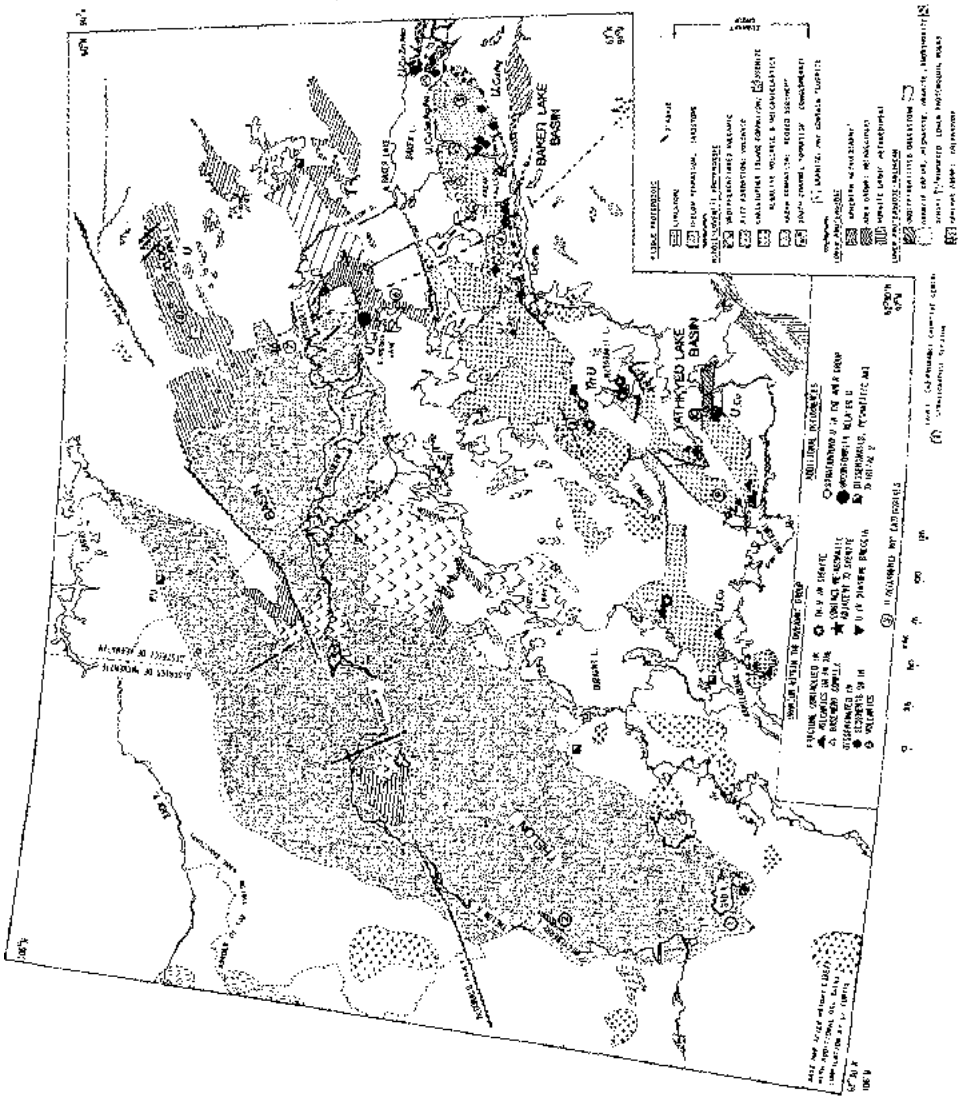


Figure 3. Detailed geology and Uranium Occurrences in the Keewatin Uranium Province.

MINERALIZATION

Uranium mineralization in the Keewatin District occurs in a wide variety of geological situations and is hosted by rocks ranging in age from Archaean(?) to Middle Proterozoic. At present only a limited amount of data are available and in many instances the absence of detailed studies or their confidentiality precludes informed genetic interpretations. For this reason the various uranium occurrences have been classified on a descriptive basis placing emphasis upon their mode of occurrence (e.g. pegmatitic, detrital, stratiform, vein) and the age of their host rocks rather than upon genetic processes. The location of the more important prospects is shown on figure 3, and their relative stratigraphic positions are indicated on figure 5a and b.

Disseminated or Pegmatitic Uranium Mineralization in Basement Rocks

Radioactive basement granites, ortho- and paragneisses and pegmatites of Archaean(?) to Lower Proterozoic age are a common occurrence in the Keewatin District (Fig. 3). Uranium occurs within primary disseminated minerals such as monazite, within heavy mineral concentrates such as apatite and as U-Th concentrations (including uranothorite) in pegmatites. In several of the occurrences there is an association between high radioactivity and zones of hematisation. U and Th contents are not of economic significance, although locally high values (in excess of 500ppm) of both elements have been recorded.

Detrital Uranium Mineralization in Lower Proterozoic Pyritic Quartz-Pebble Conglomerates

This type of mineralization has been described from an occurrence near *Kinga Lake*, approximately 280km south of the hamlet of Baker Lake. The Lower Proterozoic Montgomery Lake Group (Table 1) which hosts the mineralization consists of feldspathic quartzite, grit, siltstone and quartz-pebble conglomerate. The lower unit is a polymict boulder conglomerate which rests unconformably upon volcanics of the Archaean Kaminak Group (Bell, 1970; Heywood & Roscoe, 1967). More recent data suggest that this lower unit represents a basal till deposit (Lord *et al.*, 1979). A drilling programme carried out by Denison Mines Limited in 1970 indicated that the mineralization is confined to pyritic quartz-pebble conglomerate within the sequence. Several low grade intersections were obtained from both lower and upper portions of the sequence, the best of which assayed 0.017% over 3.7m.

The radioactive minerals consist of fine grained disseminated uranothorite, a titanium-bearing phase (brannerite?) and zircon (Lord *et al.*, 1979), and are considered to be of *detrital* origin, derived locally from the Kaminak Group.

Stratabound Uranium Mineralization in Lower Proterozoic Metasediments

The majority of uranium showings of this type are associated with pelitic, quartzitic and feldspathic metasediments of the upper clastic unit of the Amer Group, the stratigraphy of which is described above. Stratiform mineralization of a similar nature is known to occur in outlying Aphebian(?) metasedimentary belts (Fig. 5a).

Mineralization within the Amer Group

The *Amer Lake* showings consist of low grade laterally continuous and stratabound mineralization which is locally remobilized along fracture zones. The predominant host rocks are folded quartzitic and pelitic metasediments within which proven mineralized lenses extend for 600-1525m with typical intersections of 0.05-0.12% U_3O_8 over 1-2m (Laporte, 1974). Thin and laterally discontinuous feldspathic sandstone lenses within the metasiltstone sequence are sometimes strongly mineralized. An examination of one such sample indicates that high lead pitchblende occurs as a cement between quartz grains and mantles or replaces feldspar grains. Fine grained disseminated pyrite, chalcopyrite and traces of molybdenite accompany uranium mineralization.

As the pitchblende is interstitial to what are interpreted to be diagenetic phases, the

uranium mineralization is considered to be *syn-* or *post-diagenetic;* similar observations have been made by Ruzicka (1979).

Another group of showings *southwest of Amer Lake* occur within rocks probably equivalent to the upper clastic unit of the Amer Group (Knox, 1979). Uraniferous metasiltstones are the predominant hosts, and these are locally siliceous and interbedded within arenaceous and calcareous metasediments. The showings are scattered over a distance of some 40km between Amer Lake and the basal Thelon Formation unconformity (Fig. 2). Mineralized magnetite-bearing feldspathic quartzite, siliceous biotite marble and magnetite-bearing calcareous meta-arkose from these showings were examined by qualitative microprobe methods. The predominant uranium-bearing phase is a high lead pitchblende which occurs as colloform bands or as cubic grains and which is sometimes associated with traces of a lower lead, silicon-uranium phase (coffinite?). Iron oxides, principally magnetite and/or pyrite and in rare instances chalcopyrite, pyrite, cubanite, pyrrhotite, galena and cobaltite occur with very fine grained (1-5μ) pitchblende.

Uranium mineralization within the Amer Group at the *Sandhills* showing has been studied by Taylor (1978). A sequence of interbedded argillaceous and arenaceous and sometimes calcareous metasediments, host the mineralization (Analysis II, Table 5). The sandstones are commonly oxidised containing hematite whereas the siltstones represent a reduced facies and are commonly pyritic. Carbonate occurs as a matrix cement or as veins within the arenaceous rocks. Uranium mineralization occurs as disseminations within siltstones particularly at siltstone-sandstone contacts. The uranium mineralization consists mainly of fine grained pitchblende disseminations and layers, and sometimes is associated with pyrite and chlorite-bearing spheroids and magnetite grains. Hematite alteration, particularly of feldspars is characteristic of the mineralized zones. Qualitative microprobe scans of one of the siltstones indicate that uranium also occurs as a uranium-silicon phase (coffinite?) and traces of uranium were also noted in iron-rich chlorite. Taylor (op. cit) considers the mineralization to have been formed during a *low temperature hydrothermal replacement* event accompanying low grade regional metamorphism. On the basis of the available evidence, however, it is reasonable to postulate that the uranium could have been formed syngenetically, was concentrated during diagenesis and in some instances remobilized and reconcentrated during metamorphism.

Mineralization within Aphebian(?) Metasediments

Uranium mineralization has been identified in some Lower Proterozoic(?) outliers of the basement complex, south of the Amer Lake belt. Host rocks at one such occurrence consists of feldspathic quartzite and calcareous feldspathic quartzite (Analysis III, Table 5). Qualitative microprobe scans of one sample indicate that the mineralization consists of disseminated pitchblende which occasionally concentrates into layers. The pitchblende contains a very high lead content and is associated with minor amounts of chlorite, hematite/limonite, biotite and sphene (in which pitchblende is also found as inclusions). Chalcopyrite, arsenopyrite and iron sulphide (pyrrhotite?) occur in trace quantities. In contrast to stratabound mineralization within the Amer Group, which occurs relatively high in the stratigraphic succession, stratabound mineralization in these Aphebian(?) metasediments occurs preferentially near the base of the succession.

Uranium Mineralization Related to Unconformities Within the Lower(?)-Middle Proterozoic Dubawnt Group

Several significant uranium occurrences are found in the vicinity of these unconformities and they can be classified on the basis of their host rocks into (a) mineralization within basement granitoid gneisses or greenstones (b) mineralization within basement Aphebian(?) metasediments, and (c) mineralization within rocks of the Dubawnt Group. These divisions form the basis for the following discussion:

Unconformity Related Uranium Mineralization Within Basement Granitoid Gneisses and Greenstones

Fracture controlled uranium and base metal mineralization occurs near *Kazan Falls*, approximately 60km south of the hamlet of Baker Lake (Fig. 5b). Epigenetic mineralization is found in three main zones associated with a major northwest-trending fracture zone within cataclastic and brecciated migmatite and felsic augen gneiss of the basement complex (LeCheminant & Miller, 1978; Laporte, *et al.*, 1978, Lord *et al.*, 1979). In the Kazan Falls area, Dubawnt rocks north of the unconformity consist of Kazan arkose overlain by trachyte flows and volcaniclastic sediments of the Christopher Island Formation, and are presumed to be faulted against the gneiss complex. Pitchblende-base metal mineralization has been recognized up to 2.5km south of the present erosional trace of the Dubawnt unconformity. The pitchblende is colloform, sooty or rarely subhedral and is associated paragenetically with pyrite, chalcopyrite, bornite and galena. Minor molybdenite is sometimes present. Extensive hematisation, chloritisation, silicification and carbonatisation (predominantly calcite) characterises the mineralized fracture zones. Pan Ocean Oil Limited drilled the prospect in 1970 and outlined one mineralized zone to a depth of 100m, a width of 5m and a strike length of 200m; best intersections obtained averaged 0.46% U_3O_8 over 2m. (Laporte *et al.*, 1978).

Several other minor showings of pitchblende within fractured, chloritised and hematised granitoid gneisses in the vicinity of the basal Dubawnt Group unconformity occur elsewhere along the southern rim of the Baker Lake basin (Miller, 1979).

Fracture related vein type mineralization in a similar geological environment is found in the Yathkyed-Angikuni Lakes area (Fig. 3) southwest of the Baker Lake basin (Ruzicka, 1978; Laporte *et al.*, 1978; Lord *et al.*, 1979). At the east end of the Yathkyed basin mineralization occurs as pitchblende veinlets within fractured Archaean greenstones, and is generally accompanied by trace amounts of pyrite, chalcopyrite and less commonly galena. Silver is also reported in assays from these occurrences. Outcrops of basal Dubawnt Group sediments and hematised regolith occur in close proximity to the prospects. On the west end of the basin similar fracture controlled mineralization occurs within hematised basement gneisses in contact with volcanics of the Christopher Island Formation. The pitchblende is accompanied by chalcopyrite, pyrite and calcite. Northeast of Dubawnt Lake (Fig. 3), samples from mineralized fractures within basement gneisses, Outlet Bay granite and unconformably overlying Dubawnt volcanics contain up to 1.17% U_3O_8 (Lord *et al.*, 1979).

The nature of this type of mineralization and the associated alteration and gangue assemblages is reminiscent of mineralization within the Beaverlodge District in Saskatchewan, Canada (Tremblay, 1972).

Unconformity Related Mineralization Within Basement Aphebian(?) Metasediments

At present the most economically significant occurrence of this type is the *Sissons Lake* prospect which occurs approximately 75km west of the hamlet of Baker Lake (Fig. 3). The prospect occurs within an area underlain by shallowly dipping 'Hurwitz Group' impure quartzites and conformably overlying orthoquartzites which are intruded by fluorite-bearing granite, syenite, lamprophyre and diabase (Lord *et al.*, 1979). We have designated the 'Hurwitz-Group' rocks in this area as Aphebian(?) metasediments, for reasons discussed above. In the vicinity of the prospect Donaldson (1967) has mapped extensive areas of regolith (Fig. 4), a significant observation since it suggests that much of the basement exposure in this area has been only recently stripped of the unconformably overlying Middle Proterozoic sandstone cover rocks (Thelon Formation). The regolith zone is characterised by kaolinised feldspars and is commonly cemented by opaline silica. The mineralization occurs within the underlying metasediments, approximately 3km from the present erosional trace of the unconformity. Pitchblende is the dominant uranium-bearing phase associated with kaolin, limonite, hematite and chlorite. One of several mineralized intersections obtained from

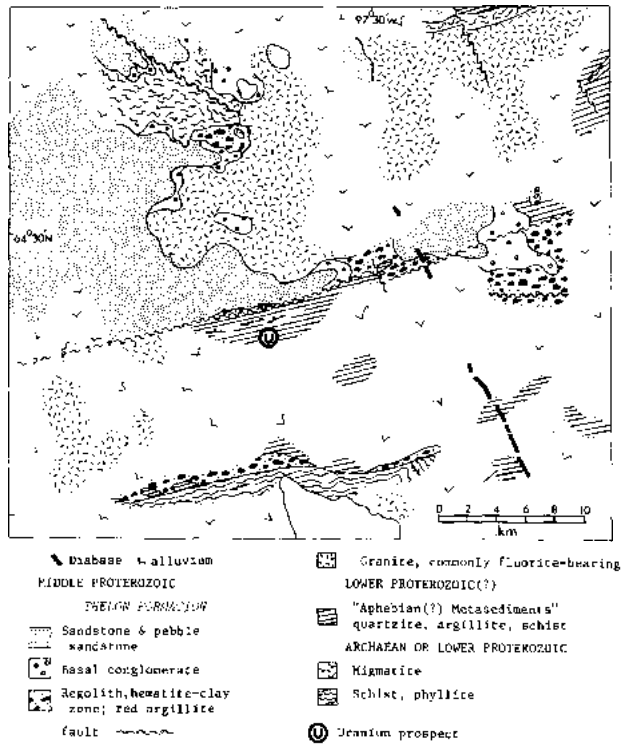


Figure 4. Geology in the vicinity of the Sissons Lake prospect, Keewatin District (Modified after Donaldson, 1965).

drilling the prospect average approximately 1% U_3O_8 over 33m (Northern Miner, 1978).

This type of occurrence is similar in some respects to the *unconformity-vein type* deposits within the Alligator Rivers Uranium Field (ARUF) in northern Australia.

Unconformity Related Mineralization Within the Dubawnt Group

Miller (1979) has described epigenetic copper-uranium mineralization on the southern rim of the Baker Lake basin. One such occurrence is at the contact between Christopher Island Formation trachytes and unconformably overlying fanglomerates of the Kunwak Formation. Weak mineralization is associated with post-depositional alteration of the overlying clastic red-beds which are cemented by calcite and hematite. Secondary minerals such as malachite and metatyuyamunite are present. Disseminated uranium-copper mineralization also occurs at the contact between South Channel Formation conglomerates and underlying basement gneisses. The mineralization consists of pitchblende, pyrite and chalcopyrite disseminated within the chlorite- and calcite-bearing arkosic matrix of the basal conglomerate. The underlying felsic gneiss is comparatively unaltered and devoid of uranium mineralization.

Weak uranium mineralization with basal Dubawnt Group clastic sediments is also reported from the Yathkyed Lake basin (Lord *et al.*, 1979; Ruzicka, 1978) and is known to occur at the contact between Dubawnt Group volcanics and volcaniclastics and underlying basement rocks in the Nowleye-Kamilukuak Lakes area (Fig. 3).

Mineralization Within the Dubawnt Group

A total of six mineralization types are recognised within the Dubawnt Group or within intrusives considered to be comagmatic with Dubawnt Group volcanics. (Table 4). Within the Baker Lake & Yathkyed Lake basins the showings are concentrated in the Lower and Middle Dubawnt Group, whereas only traces of mineralization occur in the Upper sequence (Figure 3).

Fracture Controlled Mineralization

Showings related to fractures and zones of brecciation or cataclastics within the Lower-Middle Dubawnt Group are widespread, and occur particularly at the eastern terminus and along the southern margin of the Baker Lake basin (Fig. 3). Several of the showings coincide with zones of faulting and fracturing which transect or parallel the unconformity. Two metal associations have been recognized by Miller:

1) pitchblende + copper, silver and lead selenides and electrums of Au-Ag and Ag-Au.
2) pitchblende + lead, iron, copper - iron and zinc sulphides.

An example of the first type is the mineralization on *Christopher Island*, which occurs within fractures and breccia zones in Kazan Formation arkose and in tuffaceous arkose and intrusive biotite trachyte of the Christopher Island Formation (LeCheminant & Miller, 1978; Pringle & Miller, 1977; Miller, in press) Iron-rich chlorite, calcite, ubiquitous hematite and minor quartz accompany the mineralization.

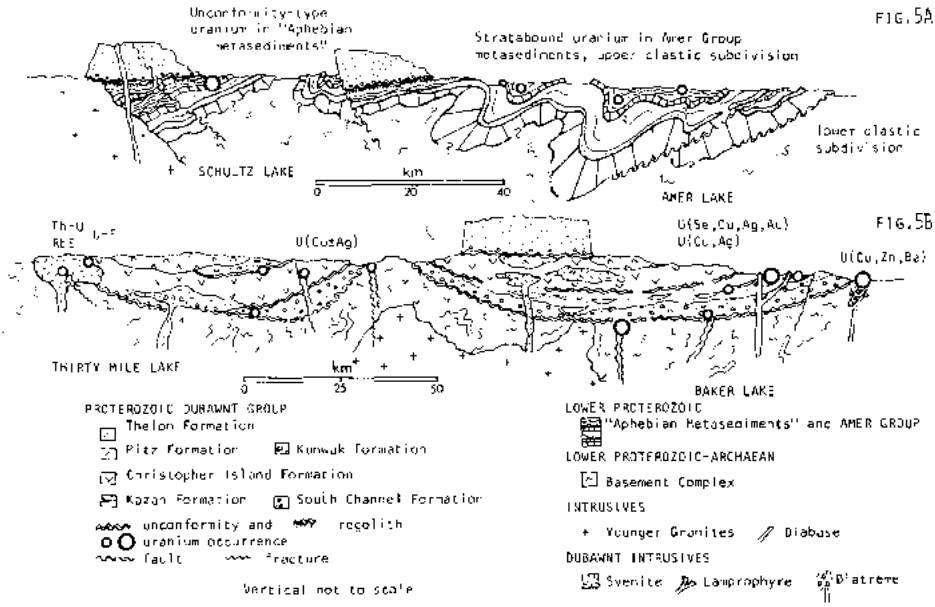
Propylitised porphyritic trachytes host the second metal assemblage in the *Thirty Mile Lake* area. The mineralization is localised within fractures related to a major east-northeast structural dislocation on the southern boundary of the Baker Lake basin (LeCheminant & Miller, 1978). The uranium-base metal association is similar to that observed in the basement occurrences described above, but no molybdenum mineralization has been identified. Pervasive chloritisation and hematisation is a feature of the mineralized zones and chlorite, sphene, calcite, anatase, barite, calcite and quartz accompany the mineralization.

Additional fracture related pitchblende showings within the Dubawnt Group volcanics and sediments have been reported in the Yathkyed Lake basin (Laporte *et al.*, 1978; Lord *et al.*, 1979) and southeast of Dubawnt Lake (J. Douglas, *pers. comm.*).

Mineralization Within Lower Dubawnt Group Red-Beds Adjacent to Dubawnt Intrusives

The best documented showings of this type occur in the eastern portion of the Baker Lake basin (LeCheminant & Miller, 1978; Laporte *et al.*, 1978; Lord *et al.*, 1979; Miller, in press). The mineralization occurs within South Channel Formation conglomerate and lower portions of Kazan Formation arkose where they are intruded by lamprophyre dykes. The epigenetic silver-copper-uranium mineralization is concentrated within symmetrical alteration envelopes which surround the dyke(s). The dykes are extensively chloritised and carbonated. The surrounding redbeds are albitised and the hematite and calcite cements have been redistributed coincident with the development of Fe-Mg chlorite (clinochlore) and minor anatase. The uranium mineralization, principally pitchblende and minor Ti-U compounds, occurs as interstitial impregnations in the alteration halo in association with chlorite and hematite, and is accompanied by copper-iron and iron sulphides and native copper and silver. Pb/U ratios are extremely variable suggesting post-depositional remobilization. Drilling of one showing (74-1W) by the Cominco-Pan Ocean consortium resulted in one intersection in mineralized arkose of 0.088% U_3O_8 over 176m, including 17.5m of 0.284% U_3O_8 (Laporte, 1979), however, subsequent drilling indicated that the mineralization was of only local extent. Extension of the original hole resulted in mineralized intersections to a depth of 350m (Northern Miner, 1979).

LeCheminant & Miller (1978) and Miller (in press) have suggested a two stage genetic process of ore formation, consisting of (1) precipitation of iron and copper-iron sulphides and



native silver within the thermal aureole formed during emplacement of the lamprophyres and (2) later reduction of uranium-bearing groundwaters by the sulphide zones.

Mineralization Associated with Diatreme Breccias

A number of diatreme breccias rim the eastern margin of the Baker Lake basin and two showings associated with these structures occur on the northeast side of Baker Lake (LeCheminant & Miller, 1978; Laporte *et al.*, 1978; Lord *et al.*, 1979). The intrusives represent satellitic stocks and dykes of the Christopher Island suite which have been forcefully emplaced within Archaean granulitic gneiss approximately 2km north of the faulted Dubawnt Group-basement unconformity. Mineralization is confined to the matrix of loosely packed granulitic breccia which surrounds an ellipsoidal syenite stock. The paragenetic sequence involved deposition of botryoidal pitchblende, chalcopyrite and resinous sphalerite, accompanied by quartz, hematite, chlorite, calcite-dolomite and barite (Miller, in press).

The genetic process for uranium-base metal concentration clearly involved channelling of hydrothermal fluids through zones of high permeability within the diatreme structure. Such a process may have accompanied or closely followed volatile degassing during formation of the breccia pipe such as envisaged by Tilsley (1978). Another alternative would be post intrusive introduction of uranium-bearing fluids related to the nearby faulted unconformity.

Contact Aureole Mineralization

In the central portion of the Baker Lake basin uranium mineralization occurs within metasomatised Christopher Island Formation volcanics and breccias which have been intruded by miarolitic fluorite-bearing granite (Miller, 1979; LeCheminant *et al.*, 1979b). Minor pyrite and chalcopyrite accompany the pitchblende mineralization and fracture coatings of uranophane and masuyite in addition to a uranium-bearing Ca-Ti-Si phase have been observed.

Disseminated Syngenetic Mineralization in Dubawnt Group Intrusives and Volcanics

Syenite stocks and dykes intrude Dubawnt Group volcanics and gneiss complex west and

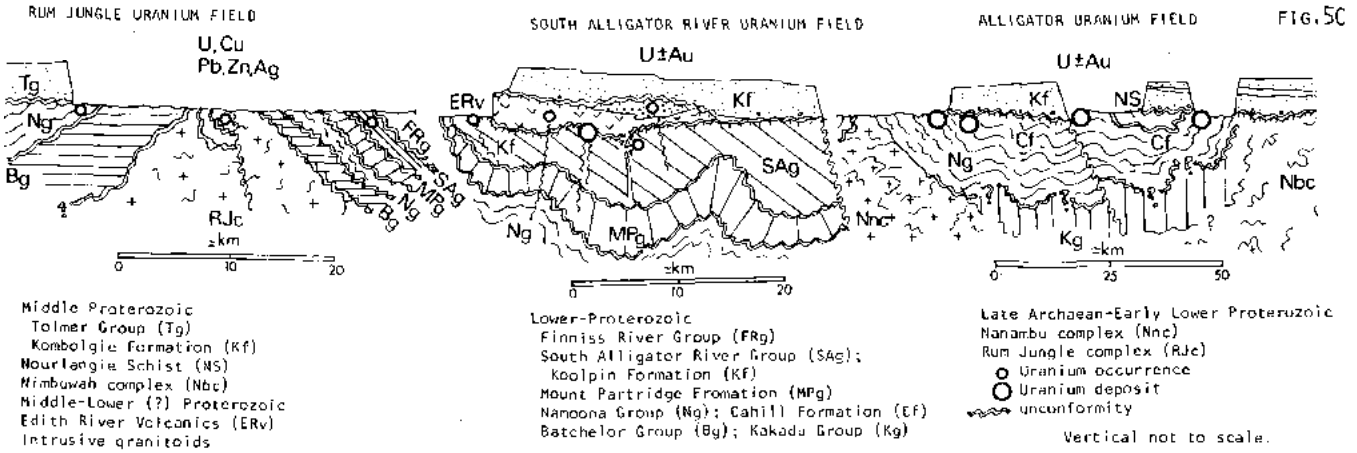


Figure 5. (a) Schematic cross section, Schultz and Amer Lakes, Northeast Thelon Basin.
(b) Schematic cross section, Thirty Mile and Baker Lakes, Baker Lake Basin.
(c) Schematic cross section, Pine Creek Uranium Province.

northwest of Yathkyed Lake and contain anomalously high quantities of U and Th (Miller, 1979; Lord *et al.*, 1979), particularly in the finer grained bostonitic variants. High total alkalis, high Fe^{3+}/Fe^{2+} ratios and low Mg contents characterise the host rocks. Disseminated metamict phases possibly monazite and thorite and uranium-bearing zircon, variety cyrtolite are responsible for the anomalous radioactivity of the rocks. Although probably not economic in this form, the high U-Th intrusives may have economic potential in situations where they are sufficiently disrupted and fractured to enable late stage metasomatic fluids to scavenge and reconcentrate the contained uranium. Alternatively the fractured syenites may provide a repository for late stage uranium-bearing hydrothermal fluids. Relative to high U-Th syenites, fractured syenites from the same outcrop are enriched in U, Fe, Ca and Mg and depleted in Si and Na (Analyses VII & VIII, Table 5).

Diseminated uranium mineralization occurs in hematised Christopher Island volcanics east of Dubawnt Lake (Fig. 3). Minor Pb and Cu are associated with the U, which typically assays 250-500ppm U (J. Douglas, pers. comm.). No structural control has to date been identified at these prospects, and no Th is present.

Mineralization Within the Thelon Formation

A few scattered uranium occurrences in the Thelon Formation have been documented (Lord *et al.*, 1979); these include concentrations of radioactive heavy minerals in the southwest portion of the Thelon basin, pockets of uraniferous apatite in the northeast portion of the Thelon basin and anomalous radioactivity within mottled sandstones and intraformational conglomerates in the central portion of the Thelon basin. The Thelon sandstones are thoroughly oxidised and contain only a small proportion of intercalated siltstones and from this point of view are poor targets for sandstone-type uranium mineralization.

DISCUSSION

The preceding descriptions illustrate the diversity of mineralization types that have been distinguished in the Keewatin uranium province. Concentration of the uranium appears to have been part of an ongoing process initiated in Archaean-Lower Proterozoic time. The presence of stratabound mineralization within the Lower Proterozoic sediments indicates that substantial amounts of uranium were concentrated within some of the depositional basins prior to the advent of Dubawnt Group sedimentation and volcanism in late Lower(?) to early Middle Proterozoic times. The primary source for this uranium was the Archaean to Lower Proterozoic basement terrane, consisting predominantly of granitoid gneisses, some of which have been metamorphosed to granulite facies. Mobilization of U and various incompatible elements during such high grade metamorphism is not uncommon (Heier & Thoresen, 1971). Transported uranium derived from weathering of the basement could then have been fixed within the pelitic sediments occupying the shallow cratonic(?) basins. It is quite probable that during and following diagenesis uranium was concentrated or mobilized. Subsequent metamorphism during the Hudsonian orogeny may have remobilized or reconcentrated this mineralization in some instances. The resultant mineralization is still broadly conformable and characterized by a simple mineralogy and metal association.

The Dubawnt sedimentary-volcanic episode marked a period of rift tectonics which culminated in the extrusion of alkaline lavas enriched in uranium (Blake, in press). Intrusives considered to be comagmatic with the lavas are enriched in both uranium and thorium. Not surprisingly the uranium mineralization associated with the Dubawnt suite is characterized by a more complex metal association; for example the U-Cu-Se±Ag-Au assemblage on Christopher Island or the U-Cu-Zn assemblage in the diatreme breccias. The association of trace amounts of Cu, Pb and Ag in many of the fracture controlled showings within, or in close

KEEWATIN URANIUM PROVINCE	PINE CREEK URANIUM PROVINCE*
Mackenzie dolerite dykes ≈1200Ma *Thelon Formation:* fluvial sandstone Upper >1200 <1785Ma, poss.1600Ma major hiatus DUBAWNT GROUP Middle calc-alkaline & alkaline volcanics, syenite, lamprophyre, diatreme minimum age ≈1785Ma Lower fluvial sediments U(trace Cu,Ag,Au,Pb,Se,Mo Zn) within sediments, volcanics & in basement rocks in close proximity to the Dubawant Group; Baker Lake & Yathkyed Lake Basins. Th+U in syenites. Late orogenic granite, granodiorite & syenite ≈1830-1735Ma Regional metamorphism ≈1800Ma greenschist/amphibolite	minor dolerite ≈1200Ma *Kombolgie Formation:* fluvial sandstone >1370 <1690Ma major hiatus DENPELLI DOLERITE ≈1688 Ma EDITH RIVER VOLCANICS: locally developed and volcanics, minor syenite and basalt: sandstone & conglomerate minimum age ≈1760Ma U±Au (trace Cu,Ag,Ni,Pb) minor occurrences within the volcanics & sediments in SARUF** Late orogenic granite, granodiorite & adamellite ≈1780-1735Ma Regional metamorphism ≈1800Ma greenschist/amphibolite/minor granulite
Lower Proterozoic dolerite dykes ≈2350Ma; gabbros coeval with Hurwitz Group tholeiitic volcanics	ZAMU DOLERITE, sills & dykes <2500 >1800Ma
	FINNISS RIVER GROUP: flysch sediments
AMER GROUP, "Aphebian Metasediments" & HURWITZ GROUP: shallow marine platform pelitic, psammitic & carbonate sediments; minor iron formation & carbonaceous sediments; shallow marine tholeiitic basalt. <2500 >1800Ma U stratabound in AMER GROUP in "Aphebian Metasediments" in proximity to the *Thelon Formation* unconformity. MONTGOMERY LAKE GROUP	SOUTH ALLIGATOR GROUP and NAMOONA GROUP: shallow marine sediments, chemical, detrital & volcanic. MOUNT PARTRIDGE GROUP: fluviatile sediments <2400 >1870Ma U±Au fracture/fault controlled within *Koolpin Formation* in SARUF** U±Au stratabound in *Cahill Formation* in proximity to *Kombolgie Formation* unconformity ARUF** U,U-Cu stratabound in *Masson Formation* in RJUF**
Archaean or early Lower Proterozoic undifferentiated granite-gneiss, schist, amphibolite & granulite; metasediments & metavolcanics of the HENIK & KAMINAK GROUPS; granite, quartz monzonite.	KAKADU & BATCHELOR GROUPS: Lower Proterozoic fluviatile sediments Archaean & early Lower Proterozoic NANAMBU (2470Ma) & RUM JUNGLE COMPLEXES; granite gneiss, granite, schist, migmatite & metasediment.

* Crick *et al.*, Page *et al.*, Needham *et al.*, Stuart-Smith *et al.*, this volume

** Alligator River, South Alligator River & Rum Jungle Uranium Fields.

Table 6. Comparison between Keewatin and Pine Creek Uranium Provinces.

proximity to Dubawnt Group rocks appears to be a genetic signature indicative of a primary volcanic/magmatic origin for these metals.

The ensueing erosional period, perhaps of the order of 200 + Ma, provided ample time for leaching of the uraniferous volcanics and for the operation of supergene processes. Subsequent deposition of the Thelon sandstone effectively protected the sequence from further chemical weathering. The Thelon blanket may not have played a static role in terms of ore genesis, as the presence of abrupt colour changes and mottling of the sandstones sometimes in association with weak radioactivity suggests that this formation may have provided a leach source for uranium during diagenesis or weathering. The present state of knowledge suggests, however, that this was not a prime source of uranium for the showings described.

Analogies with the Pine Creek Uranium Province

Several comparisons between the Keewatin and the Pine Creek uranium provinces are possible both on a regional and detailed scale. The more obvious regional similarities are summarized in figure 5 and table 6. In both provinces there exists (1) a complex basement assemblage which includes Lower Proterozoic pelitic rocks containing stratabound uranium mineralization, (2) unconformably overlying volcanics and sediments of late Lower Proterozoic (?) - early Middle Proterozoic age which host or are in close promixity to uranium ± base metal ± Au and/or Ag mineralization, (3) evidence for a major orogeny around 1800 Ma, followed closely by late orogenic plutonism, and (4) unconformably overlying Middle Proterozoic fluviatile sandstones formed on a stable platform.

The localization of uranium within particular stratigraphic units is a feature common to both provinces. In the Alligator Rivers Uranium Field (ARUF) the major uranium deposits are stratabound within the Cahill Formation (Needham & Stuart-Smith, 1976); this Formation represents a shallow marine sequence deposited within an intracratonic basin (Stuart-Smith *et al.*, this volume). In the Keewatin province, the Amer Group and possible correlatives in the Aphebian(?) metasediments are the uranium-bearing equivalents of the Cahill Formation. It is significant that to date the most promising prospect (Sissons Lake) within the Keewatin uranium province occurs within the Aphebian(?) metasediments in close proximity to a Middle Proterozoic unconformity, a situation directly analogous to the unconformity-type deposits in the ARUF in the Pine Creek province. Uranium mineralization associated with and directly below the Edith River volcanics in the South Alligator River Uranium Field in the Pine Creek province is similar in some respects to the mineralization within or below the Dubawnt Group volcanics in the Keewatin province.

In summary, the geological and metallogenic associations in both the Alligator Rivers and the Keewatin uranium provinces show marked similarities. Although only a few uranium showings of economic potential have been found so far in the Keewatin District, analogies with the Pine Creek Geosyncline suggest that major uranium deposits remain to be discovered in this region.

ACKNOWLEDGEMENTS

For provision of samples and the permission to publish data collected on these samples we are grateful to Dr G. Bundrock of Urangesellschaft Canada Limited, Dr R. McMillan & Mr E. Nutter of Western Mines Limited and Mr R. Foster of Pan Ocean Oil Limited. J. Douglas of Shell Canada Resources Limited provided additional data. Dr A. LeCheminant, Dr A. Davidson and Dr D.H. Blake helpfully commented on the manuscript. We are particularly indebted to Dr A.G. Plant for supervising the microprobe analysis. Dr D.H. Blake, Dr A. LeCheminant and Mark Taylor kindly provided access to unpublished material. P. Laporte provided Mineral Industry reports used in the compilation. Comments by S. Needham and P. Stuart-Smith were useful for the Pine Creek Geosyncline comparisons. The manuscript was written whilst the first author was on leave at the Research School of Earth Sciences at the Australian National University, the facilities of which are gratefully acknowledged.

REFERENCES

Bell, R.T., 1968: Preliminary notes on the Proterozoic Hurwitz Group, Tavani (55K) and Kaminak Lake (55I) areas, District of Keewatin. *Geol. Surv. Pap. Can., 68-36.*

Bell, R.T., 1970: The Hurwitz Group, a prototype for deposition on metastable cratons. *in* (ed. A.J. Baer), Symposium on basins and geosynclines of the Canadian Shield. *Geol. Surv. Pap. Can., 70-40,* 159-169.

Blake, D.H., in press: Volcanic rocks of the Palaeohelikian Dubawnt Group in the Baker Lake-Angikuni Lake areas, District of Keewatin, N.W.T. *Bull. geol. Surv. Can., 309.*
Blake, D., Miller, A., & Schau, Mikkel, 1977: Potassic volcanic rocks of the Palaeohelikian Dubawnt Group and associated Cu, U, and Sc mineralization, Christopher Island Region, District of Keewatin, N.W.T. *Geological Association of Canada, Program with Abstracts, 2,* 8.
Cecile, M.P., 1973: Lithofacies analysis of the Proterozoic Thelon Formation, Northwest Territories. *M.Sc. thesis, Carlton University, Ottawa* (unpubl.).
Church, W.R., 1977: Early Aphebian basaltic volcanism in the southern District of Keewatin, Northwest Territories: Discussion. *Can. J. Earth. Sci., 14,* 2425-2426.
Crick, I.H., Muir, M.D., Needham, R.S., & Roarty, M.J., this volume: The geology and mineralization of the South Alligator Uranium Fleld. *Proceedings of the International Uranium Symposium on the Pine Creek Geosyncline.*
Davidson, A., 1970: Precambrian geology, Kaminak Lake map-area, District of Keewatin. *Geol. Surv. Pap. Can., 69-51.*
Donaldson, J.A., 1965: The Dubawnt Group, Districts of Keewatin and Mackenzie. *Geol. Surv. Pap. Can., 64-20.*
Donaldson, J.A., 1966: Geology, Schultz Lake, District of Keewatin. *Geol. Surv. Can., Map 7-1966.*
Donaldson, J.A., 1967: Two Proterozoic clastic sequences: a sedimentological comparison. *Proc. geol. Ass. Can., 18,* 33-54.
Donaldson, J.A., 1969: Descriptive notes (with particular reference to the late Proterozoic Dubawnt Group) to accompany a geological map of central Thelon Plain, Districts of Keewatin and Mackenzie (65M, NW½, 66B, C, D, 75 P E½, 76A E½). *Geol. Surv. Pap. Can., 68-49.*
Eade, K.E., 1964: Preliminary report, Kognak River map-area (east-half) District of Keewatin. *Geol. Surv. Pap. Can., 64-27.*
Eade, K.E., 1974: Geology of the Kognak River map-area, District of Keewatin. *Mem. geol. Surv. Can., 377.*
Eade, K.E., 1976: Geology of the Tulemalu Lake map-area (65J), District of Keewatin. Report of Activities, Part A. *Geol. Surv. Pap. Can., 76-1A,* 379-381.
Eade, K.E., & Blake, D.H., 1977: Geology of the Tulemalu Lake map-area, District of Keewatin. Report of Activities, Part A. *Geol. Surv. Pap. Can., 77-1A,* 409-410.
Fahrig, W.F., Christie, K.W., & Freda, G., 1978: The paleolatitude and paleomagnetic age of the Athabasca Formation, northern Saskatchewan. Current Research, Part C. *Geol. Surv. Pap. Can., 78-1C,* 1-6.
Fraser, J.A., Tremblay, L.P., Donaldson, J.A., & Fahrig, W.F., 1970: Helikian basins and geosynclines of the northwestern Canadian Shield. *in* (ed. A.J. Baer), Symposium on basins and geosynclines of the Canadian Shield, *Geol. Surv. Pap. Can., 70-40,* 213-231.
Heywood, W.W., & Roscoe, S.M., 1967: Pyritic quartz pebble conglomerate in the Hurwitz Group, District of Keewatin. Report of Activities, Part A. *Geol. Surv. Pap. Can., 67-1,* 21-22.
Heywood, W.W., & Schau, Mikkel, 1978: A subdivision of the northern Churchill Structural Province. Current Research Part A. *Geol. Surv. Pap. Can., 78-1A,* 139-143.
Heier, K.S., & Thoresen, K., 1971: Geochemistry of high grade metamorphic rocks, Lofoten-Vesteralen, North Norway. *Geochim. cosmochim. Acta, 35,* 89-99.
Knox, A., in prep: Relationship of uranium minerals to stratigraphy in the Amer Group. *M.Sc. thesis, University of Calgary, Alberta,* (unpubl.).
Laporte, P.J., 1974: Mineral Industry Report 1969 and 1970 vol. 2 of 3, Northwest Territories, east of 104°; Indian and Northern Affairs *EGS 1974-1.*
Laporte, P.J., Gibbins, W.A., Hurdle, E.J., Lord, C., Padgham, W.A. & Seaton, J.B., 1978: Keewatin Region. *in* Mineral Industry Report 1975, Northwest Territories. Indian & Northern Affairs. *EGS 1978-5,* 7-22.
Lord, C., Laporte, P.J., Gibbins, W.A., Hurdle, E.J., Seaton, J.B. & Padgham, W.A., 1979: Keewatin Region. *in* Mineral Industry Report 1975, Northwest Territories. Indian & Northern Affairs. *EGS 1978-11,* 28-52.
LeCheminant, A.N., Hews, P.C., Lane, L.S., & Wolff, J.M., 1975: MacQuoid Lake (55M west half) and Thirty Mile Lake (65P east half) map-areas. District of Keewatin. Report of Activities, Part A. *Geol. Surv. Pap. Can., 76-1A.* 383-386.
LeCheminant, A.N., Blake, D.H., Leatherbarrow, R.W., & Debie, L., 1977: Geological Studies: Thirty Mile Lake and MacQuoid Lake map-areas, District of Keewatin. Report of Activities, Part A. *Geol. Surv. Pap. Can., 77-1A,* 205-220.
LeCheminant, A.N., & Miller, A.R., 1978: Five types of Uranium Occurrence Studied in Baker Lake Basin. *Nth. Miner. November 30, 1978,* D1,22.
LeCheminant, A.N., Lambert, M.B., Miller, A.R., & Booth, G.W., 1979a: Geological studies: Tebesjuak Lake map area, District of Keewatin. Current Research. Part A. *Geol. Surv. Pap. Can., 79-1A,* 179-186.
LeCheminant, A.N., Leatherbarrow, R.W., & Miller, A.R., 1979b: Thirty Mile Lake (65P W½) map-area, District of Keewatin. Current Research, Part B, *Geol. Surv. Pap. Can., 79-1B,* 319-329.
Miller, A.R., 1979: Uranium Geology in the Central Baker Lake Basin. Current Research, Part A. *Geol. Surv. Pap. Can., 79-1A,* 57-59.
Miller, A.R., in press. Uranium geology of Eastern Baker Lake Basin, District of Keewatin, N.W.T. *Geol. Surv. Pap. Can.*
McGlynn, J.C., 1976: Geology of the Canadian Shield. *in* (ed. R.J. Douglas) *Geology and Economic Minerals of Canada, Part A, Geol. Surv. Can. Economic Geology Report No. 1,* 86.
Needham, R.S., Crick, I.H., & Stuart-Smith, P.G., this volume: Regional geology of the Pine Creek Geosyncline. *Proceedings of the International Uranium Symposium on the Pine Creek Geosyncline.*
Needham, R.S., & Stuart-Smith, P.G., 1976: The Cahill Formation - host to uranium deposits in the Alligator Rivers uranium field, Australia. *BMR J. Aust. Geol. Geophys, 1,* 321-333.

Northern Miner, 1978: Urangesellschaft "U" Find in Baker Lake Area, N.W.T., *Nth. Miner, September 21, 1978*, 1.

Northern Miner, 1979: Deepened hole at Baker Lake adds 'U' values, *Nth. Miner, October 4, 1979*, 1.

Page, R.W., Compston, W., & Needham, R.S., this volume: Geochronology and evolution of the late Archaean basement and Proterozoic rocks in the Alligator Rivers uranium field, Northern Territory, Australia. *Proceedings of the International Uranium Symposium on the Pine Creek Geosyncline.*

Patchett, P.J., Bylund, G., & Upton, B.G.J., 1978: Palaeomagnetism and the Grenville Orogeny: New Rb-Sr ages from Dolerites in Canada and Greenland. *Earth Planet. Sci. Lett., 40*, 349-364.

Pringle, G.J., & Miller, A.R., 1977: A study of Cu-S-Se minerals; electron microprobe analyses and X-ray powder. Report of Activities, Part B. *Geol. Surv. Pap. Can., 77-1B*, 113-116.

Ramaekers, P., 1979: Stratigraphy, sedimentology and structural geology of the Middle Proterozoic basins in the Athabasca area, Saskatchewan, Canada, and their bearing on uranium mineralization. *Extended Abstracts of the International Uranium Symposium on the Pine Creek Geosyncline.* 163-165.

Reinhardt, E.W., & Chandler, F.W., 1973: Gibson-MacQuoid Lakes map-area, District of Keewatin. Report of Activities, Part A. *Geol. Surv. Pap. Can., 73-1A*, 162-165.

Ridler, R.H., 1974: Shallow Marine Plateau Basalts of the Aphebian Hurtwitz Group at Last Lake, District of Keewatin. *Geol. Surv. Pap. Can., 74-1, Part B*, 195-199.

Ruzicka, V., 1978: Evaluation of selected uranium-bearing areas in Canada. Current Research, Part A. *Geol. Surv. Pap. Can., 78-1A*, 269-274.

Ruzicka, V., 1979: Uranium and thorium in Canada, 1978: Current Research, Part A. *Geol. Surv. Pap. Can., 79-1A*, 139-155.

Schau, Mikkel & Hulbert, L., 1977: Granulites, anorthosites and cover rocks northeast of Baker Lake, District of Keewatin. Report of Activities, Part A. *Geol. Surv. Pap. Can., 77-1A*, 399-407.

Stockwell, C.H., 1961: Structural provinces, orogenies and time classification of rocks of the Canadian Pre-cambrian Shield. Age determination by the Geological Survey of Canada, Report 2, isotopic ages. *Geol. Surv. Pap. Can., 61-17*, 108-118.

Stuart-Smith, P.G., Wills, K., Crick, I.H., & Needham, R.S., this volume: Evolution of the Pine Creek Geosyncline. *Proceedings of the International Uranium Symposium on the Pine Creek Geosyncline.*

Taylor, M.A., 1978: An investigation of the Uranium Mineralization at the Sandhills showing, District of Keewatin, Northwest Territories. *B.Sc. thesis, Queen's University, Kingston, Ontario* (unpubl.).

Tella, S., & Heywood, W.W., 1978: The structural history of the Amer Mylonite Zone, Churchill Structural Province, District of Keewatin. Current Research, Part C. *Geol. Surv. Pap. Can., 78-1C*, 79-88.

Tilsley, J., 1978: Uranium mineralization in shallow intrusive environments. *in* (ed. M.M. Kimberley), *Short Course on Uranium Deposits: Their Mineralogy and origin. Mineralogical Association of Canada.* 281-289.

Tippett, Clinton R., & Heywood, W.W., 1978: Stratigraphy and structure of the northern Amer group (Aphebian), Churchill Structural Province. District of Keewatin. Current Research, Part B. *Geol. Surv. Pap. Can., 78-1B*, 7-11.

Tremblay, L.P., 1972: Geology of the Beaverlodge Mining Area, Saskatchewan. *Mem. geol. Surv. Can., 367*, 265p.

Wanless, R.K., & Loveridge, W.D., 1972: Rubidium-strontium isochron age studies, Report 1. *Geol. Surv. Pap. Can., 72-23.*

Wanless, R.K., Stevens, R.D., Lachance, G.R., & Delabio, R.N., 1973: Age determination and geological studies, K-Ar isotopic age Report 11. *Geol. Surv. Pap. Can., 73-2.*

Wanless, R.K., & Eade, 1975: Geochronology of Archaean and Proterozoic rocks in the Southern District of Keewatin. *Can. J. Earth Sci., 12*, 95-114.

Wright, G.M., 1955: Geological notes on central District of Keewatin, Northwest Territories. *Geol. Surv. Pap. Can., 55-17.*

Wright, G.M., 1967: Geology of the southeastern barren grounds, Northwest Territories. *Mem. geol. Surv. Can.*, 350.

Young, G.M., 1973: Tillites & aluminous quartzites as possible time markers for Middle Precambrian (Aphebian) rocks of North America. *in* (ed. G.M. Young), Huronian Stratigraphy and Sedimentation, *Spec. Pap. geol Ass. Can., 12*

THE KEY LAKE U-Ni DEPOSITS: A MODEL FOR LOWER PROTEROZOIC URANIUM DEPOSITION

G. Kirchner, K. Lehnert-Thiel, J. Rich and J.G. Strnad

Uranerz Exploration and Mining Limited,#204, 229 - 4th Avenue South, Saskatoon, Saskatchewan, S7K 1N1, Canada.

ABSTRACT

The Key Lake deposits comprise one of the largest concentrations of uranium and nickel in the Athabasca basin of Saskatchewan. The principal hosts to mineralization are pelitic metasediments of the Lower Proterozoic (Aphebian) Wollaston domain, and the overlying Middle Proterozoic (Helikian) Athabasca sandstone. Ore controls include a major post-Athabasca strike fault within graphitic metasediments and the Lower-Middle Proterozoic (Aphebian-Helikian) unconformity.

Principal uranium minerals include crystalline pitchblende (tetragonal U_3O_7), sooty pitchblende (U_3O_8 + X) and coffinite. Mineralization is most intense at and up to 20 metres below the sandstone interface, within kaolinite and chlorite gouge formed through intense tectonic destruction and *post* sandstone hydrothermal alteration. Age dates of 960 to 1228 Ma are indicated for primary ore deposition.

Younger dates of 89-370 Ma attest to numerous episodes of post depositional remobilization. Significantly, sandstone ore contains only sooty secondary pitchblende dating 107-250 Ma. This is considered strong evidence for a hypogene origin.

Lower Proterozoic (Aphebian) pelites were syngenetically enriched in uranium. Progressive upgrading during the Lower Proterozoic (Hudsonian) Orogeny and pre-Athabasca weathering, culminated in a major hydrothermal remobilization into structurally and geochemically favourable traps at and below the Middle Proterozoic Helikian unconformity.

Using Jabiluka as an example, the applicability of this model to deposits of the Alligator Rivers Uranium Field of Australia is discussed.

INTRODUCTION

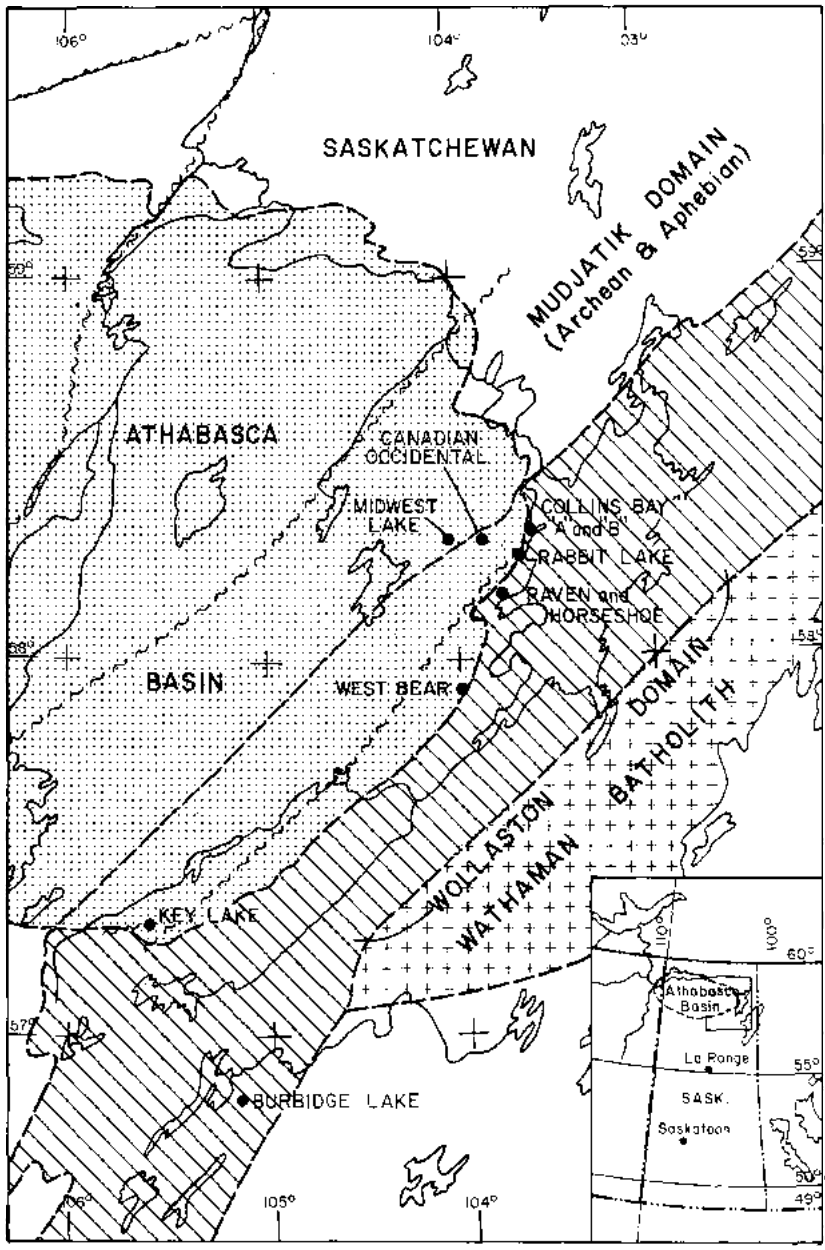
The Key Lake deposits comprise one of the largest concentrations of uranium and nickel in the Athabasca sandstone basin. The Jabiluka deposits in the Alligator Rivers Uranium Field of Australia contain even greater metal reserves, which probably exceed 188×10^6 kilograms U_3O_8 and 8.09×10^6 grams of gold, (Hegge, 1977). Both Key Lake and Jabiluka are considered representative of Lower Proterozoic uranium deposition. This paper discusses the Key Lake deposits with emphasis on their geologic setting and genetically significant features. A depositional model based on Key Lake is presented, and using Jabiluka as an example, its applicability to Australian deposits is discussed.

Key Lake is located in Northern Saskatchewan on the south rim of the Athabasca sandstone basin. The area is completely mantled by unconsolidated Pleistocene glacial deposits of boulder till and outwash sand up to 80 metres thick, which completely mask the underlying geology. The closest outcrops occur 5 kilometres to the southwest. A considerable part of the known mineralization occurs beneath a chain of three postglacial lakes. The continental climate, which varies from -50°C in winter to +30°C in summer, facilitates year-round drill exploration from both land and lake ice. All geologic data to date, are based on drill core information only.

REGIONAL GEOLOGY

The southeast rim of the Athabasca sandstone basin is underlain by the north-easterly trending Wollaston linear domain. In addition to Key Lake, this structural belt also hosts a number of other uranium deposits including Rabbit Lake and possibly Midwest Lake (Fig. 1).

In early Lower Proterozoic (early Aphebian) time, the Wollaston domain supracrustals were deposited in a tectonically stable marine-terrestrial environment, probably under shallow water to sub-aerial conditions (Sibbald *et al.*, 1976). During the Lower Proterozoic



EASTERN ATHABASCA BASIN

Figure 1. Uranium Deposits of the Eastern Athabasca Basin.

(Hudsonian) Orogeny, thermal deformation produced doming of the underlying Archaean basement. The domes moved upwards without penetrating or seriously disrupting the cover rocks, so that their stratigraphic relationships remained essentially preserved (Ray, 1977). Later periods of compressive strain resulted in flattening of these mantled domes into doubly plunging northeasterly elongated antiforms (Sibbald *et al.*, 1976). Their Archaean cores

OROGENY OR THERMAL EVENT	AGE		DEPOSIT THICKNESS	LITHOLOGY
	PLEISTOCENE	10,000 years	GLACIAL DEPOSITS 0-80m	SANDY BOULDER TILL KAME MORAINE ESKERS OUTWASH SAND
GRENVILLE		955 Ma		
	M. PROTEROZOIC (HELIKIAN)	935-1260 Ma	DIABASE DYKES	DIABASE, GABBRO
		1350 Ma	ATHABASCA FORMATION 0-1450m.	SANDSTONE WITH MINOR SHALE. CONGLOMERATE
HUDSONIAN		1735 Ma		
	L. PROTEROZOIC (APHEBIAN)	2480 to 1735 Ma	WOLLASTON DOMAIN est 3500m.	ORTHOQUARTZITE META-ARKOSE PELITIC AND SEMI-PELITIC SCHISTS AND GNEISSES, BIOTITE >10% PLUS LOCAL CORDIERITE, SILLIMANITE, GARNET AND GRAPHITE.
KENORAN		2480 Ma		
	ARCHAEAN	AGE UNCERTAIN MAYBE EARLY L. PROT. (EARLY APHEBIAN)		AMPHIBOLITE GRANITE GNEISS

Table 1. Stratigraphy of the Key Lake Area.

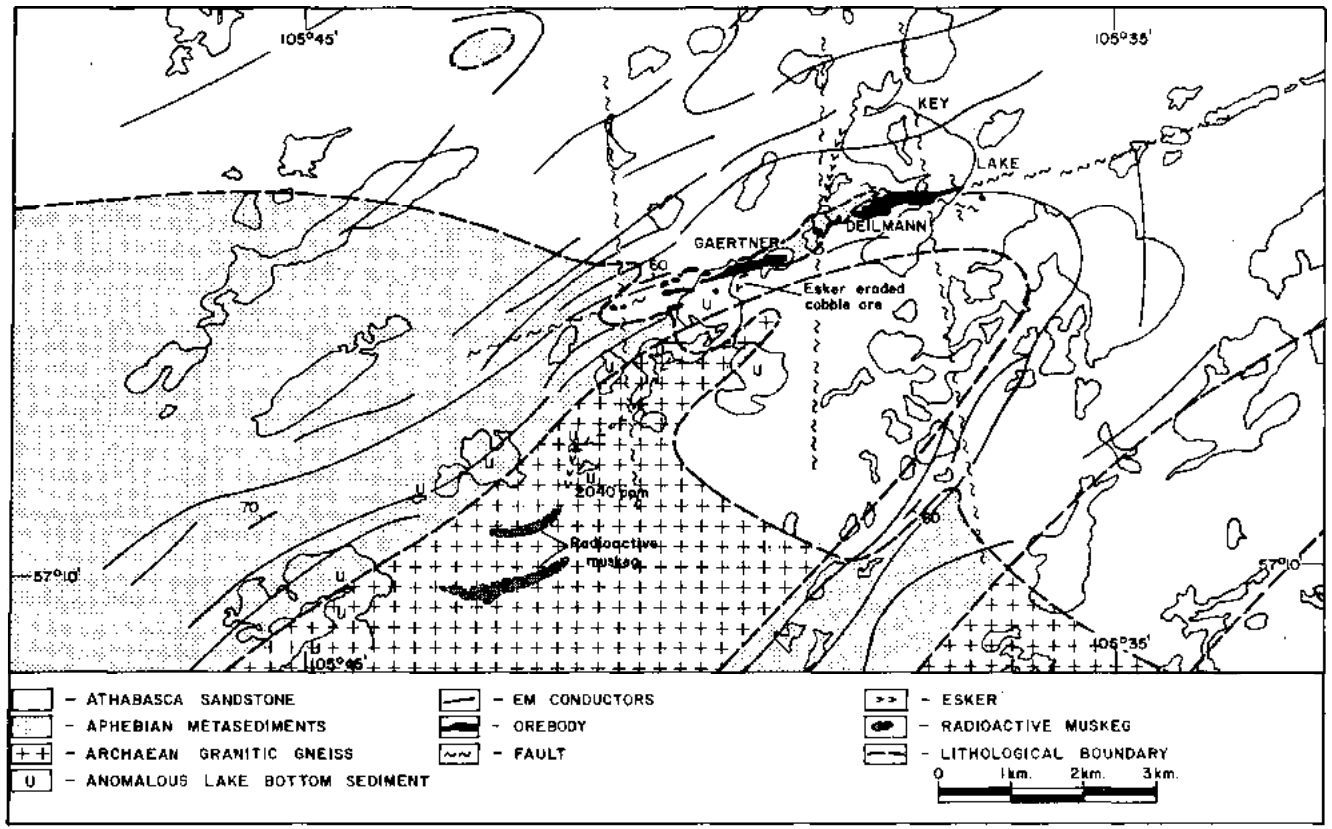


Figure 2. Geological Plan of the Key Lake Area.

were subsequently exposed during an extensive period of post Lower Proterozoic (post Hudsonian) peneplanation preceeding deposition of the Athabasca sandstone. This flat lying sequence of sandstones and conglomerates has remained virtually undisturbed for 1350 Ma (Table 1).

In the Key Lake area, the Wollaston domain metasediments have been metamorphosed to the upper amphibolite facies, locally reaching granulite facies within the adjacent Archaean basement.

Although basal the Wollaston domain rocks are estimated to vary up to 3500 metres in thickness, the graphitic zones appear limited to the lower-most 200 metres (Ray, 1977). Tight folding of these rocks has resulted in numerous steeply dipping repetitions of the graphitic horizons. These result in pronounced linear geophysical conductors. Where an exposed domal antiform plunges under basal Wollaston rocks, the graphitic horizons produce arcuate conductors which wrap around the nose of the Archaean core. The Key Lake deposits occur where faulted graphitic metasediments flank one such inlier of complexly folded Archaean granitoid gneiss (Fig. 2).

EXPLORATION HISTORY

Two distinct deposits, occur over a strike length of 4000 metres. Both are covered by Athabasca sandstone and overburden. Glacial scouring between the two deposits eroded the original sandstone cover, resulting in a window of Lower Proterozoic (Aphebian) metasediments. During the last ice advance, erosion of the exposed ore resulted in a train of uranium and nickel mineralized cobbles in glacial till, which comes to surface beneath Seahorse Lake (Fig. 5). During glacial retreat, an esker which now cuts diagonally across Karl Ernst Lake, eroded a portion of this cobble ore, and transported it 6 kilometres to the southwest where much of it was dispersed in an esker delta (Fig. 2). A chain of post glacial lakes and kettle holes associated with the esker, were found to carry sediment anomalies of over 700 ppm U_3O_8 (Tan, 1976). The discovery, in 1971, of uranium and nickel mineralized boulders in and around radioactive muskegs associated with the esker delta, (Watkinson *et al.*, 1975), led to a 5 year program of lake geochemistry, boulder prospecting and drilling of graphite related EM conductors resulting in discovery of the 'Gaertner' ore body in 1975, followed by the 'Deilmann' in 1976. There were no surficial radiometric anomalies over either ore body. A distinct surficial anomaly was present, however, over the esker delta. Initial work on the geology and mineralogy of the Key Lake deposits was described by Dahlkamp & Tan (1977), Dahlkamp (1977 & 1978) and Gatzweiler *et al.*, (1979).

KEY LAKE

Mineralization is controlled by a simple to complex ENE trending reverse fault which has caused a down-throw of the southern block of up to 30 metres. The attitude of the fault system coincides with the strike and dip of the surrounding graphitic Lower Proterozoic (Aphebian) metasediments.

In the structurally simpler Gaertner, graphite schist occupies the up-thrown hanging wall. Sheared kaolinite and chlorite gouge resulting from intense tectonic destruction and post sandstone hydrothermal alteration occupy the fault zone and form the principal hosts of mineralization. Alteration is most intense at, and up to 20 metres below, the sandstone interface. There is a gradation, at depth, from altered to fresh biotite-plagioclase-cordierite gneiss. Substantial mineralization is also present in the over-lying sheared sandstone. In the structurally complex Deilmann, multiple graphite horizons and faulting have produced massive mineralized 'roots' extending more than 100 metres down dip. The Deilmann achieves a maximum width of 160 metres where younger cross faulting has augmented the tectonic dilation. Typical cross sectional configurations are illustrated in figure 3. In the

Deilmann, satellite bodies in the sandstone (Fig. 3A), represent younger periods of post depositional remobilization. Disjointed satellite bodies along the Middle Proterozoic (Helikian) unconformity (Fig. 3B), appear to be localized by younger cross faults. Subsidiary faulting parallel to and probably contemporaneous with the main fault has produced similar satellite ore zones in the Gaertner (Fig. 3F).

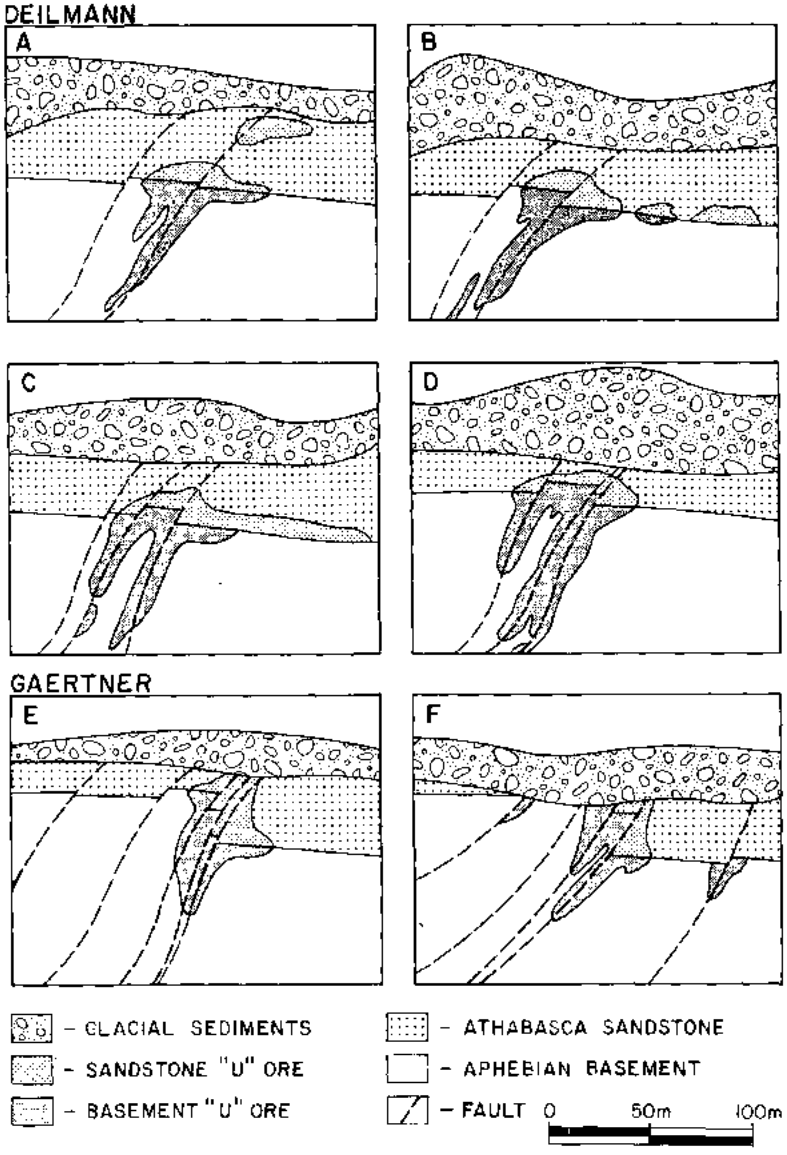


Figure 3. Geometry of Key Lake Orebodies and schematic cross-sections.

Ore grades over 2.0 metres of 40% U_3O_8 and 20% nickel have been reported. A sympathetic relationship between uranium and nickel mineralization has been observed in both ore bodies, and in exploration testing of the basal Wollaston domain pelites around Key Lake.

ORE MINERALOGY

Uranium and nickel ore minerals in decreasing abundance are: pitchblende I (crystalline pitchblende, tetragonal $U_3O_7=UO_{2.33}$), pitchblende II ('sooty' pitchblende U_3O_8+X), coffinite ($USiO_4$), gersdorffite (NiAsS), millerite (NiS), niccolite (NiAs), rammelsbergite ($NiAs_2$), bravoite ($FeNiS_2$), and safflorite ($CoAs_2$).

Repeated cycles of pre and post tectonic uranium and nickel mineralization occurred contemporaneously with the formation of kaolinite and chlorite gouge. Pitchblende II and coffinite, can constitute the matrix for gersdorffite, millerite and niccolite or vice versa (Gatzweiler *et al.*, 1979). Colloform intergrowths of niccolite with chlorite and pitchblende I with chlorite, have been reported by Dahlkamp (1977). A broad vertical zonation of uranium and nickel mineralization exists with generally greater nickel concentration at depth (Fig. 5).

Basement ore

Pitchblende II + Coffinite > Pitchblende I

Niccolite + Gersdorffite > Millerite

Sandstone ore

Pitchblende II + Coffinite ONLY

Millerite > Niccolite + Gersdorffite

Pitchblende I is considered to represent the first generation of uranium ore deposition. Pitchblende II and coffinite are younger replacement products of pitchblende I.

DEPOSITIONAL MODEL

Data from Key Lake suggests a polygenetic history. The following sequence of events is envisioned:

Syngenetic Precipitation 2200 Ma

Basal Wollaston domain pelites were deposited in shallow, sappropelic, marine basins. These sediments were immediately underlain by, and derived from, U-rich Archaean rocks. A sufficiently oxidizing atmosphere permitted the transport of uranium and other metallic ions. Uranium dissolved in sea water may have been adsorbed by clays, or by organic material, and precipitated as colloidal pitchblende. Within the sediments, uranium entering the basin in ground water could have been reduced under the influence of gases such as H_2S or CH_4. Average uranium values would probably be less than 10 ppm. Thorium values would also be low, since even in simple oxide form, thorium is much less soluble than oxidized uranium (Gabelman, 1977).

Exploration drill testing of the basal Wollaston pelites shows an increase in uranium ranging from 1 to 50 ppm U_3O_8 close to graphitic horizons over background values of 1 to 2 ppm U_3O_8. The presence of such syngenetic preconcentrations in graphitic shales and their potential as source rocks is well documented in the literature (i.e. Pretorius, 1968; Bell, 1978). It is also reasonable to expect that the original Lower Proterozoic (Aphebian) sedimentary basins contained areal variations in uranium content, which implies that the stage may have been set for Key Lake two billion years ago.

Conversely, many of the graphitic pelites in the Athabasca basin presently considered to be priority exploration targets may in fact be of reduced potential due to low depositional preconcentrations.

KEY LAKE DEPOSIT

SCHEMATIC INTEGRAL GEOLOGICAL CROSS-SECTION

FIGURE 4

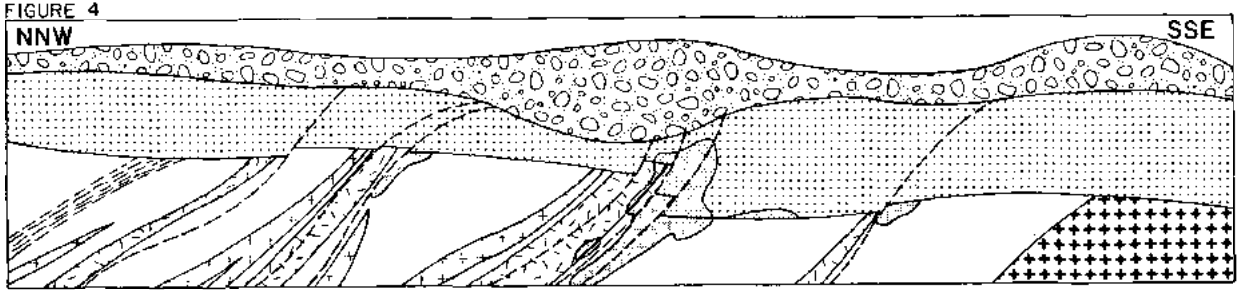


Figure 4. Schematic integral geological cross-section of the Key Lake Deposit.

VERTICAL ZONALITY OF U,Ni,As - SCHEMATIC LONGITUDINAL SECTION

FIGURE 5

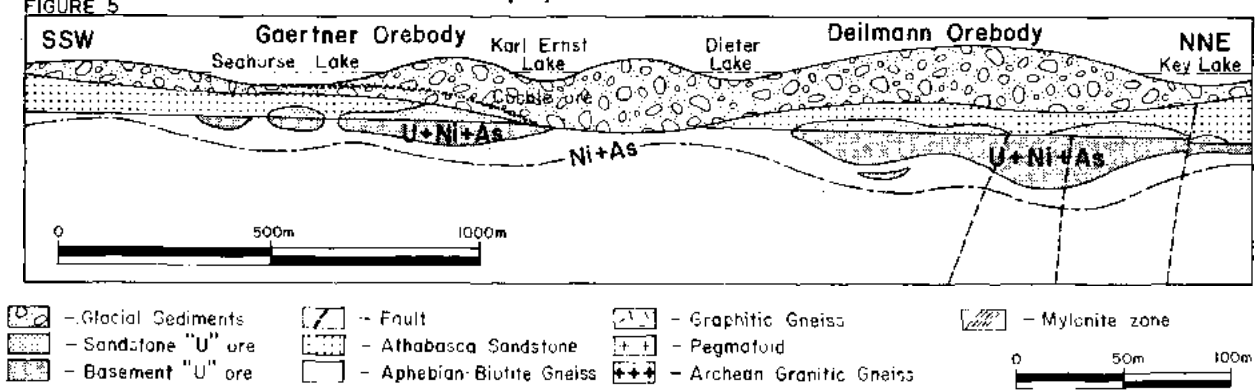


Figure 5. Schematic longitudinal section of the Key Lake Deposit.

Diagenetic Enrichment 2200-1800 Ma

Dewatering of the sedimentary pile through progressive compaction and lithification resulted in redistribution and further concentration of uranium in the pelitic horizons.

Lower Proterozoic (Hudsonian) Orogenesis 1800-1700 Ma

Prograde metamorphism accompanied thermal doming of the Archaean basement. In these granitic rocks, uranium and thorium may have been mobilized and expelled during partial melting, along with H_2O, CO_2, F, Cl and other volatiles. The passage of these gases and fluids through the *adjacent* pelites would augment, remobilize and further concentrate, the uranium. These *protore* concentrations have been intersected in numerous exploration drill holes within a 40 kilometre radius of Key Lake, where concentrations of 50 to 300 ppm U_3O_8 and 50 to 600 ppm Ni occur in unfaulted biotite gneisses immediately adjacent to graphitic gneisses. At Key Lake, anatectic pegmatoids are ubiquitous throughout the ore bodies (Fig. 4). They appear to have formed in situ and may be spatially related to the Archaean domes. Similar rocks are commonly found in exploration drill holes and often show association with protore concentrations. These pegmatoids may reflect the partial melting and expulsion of uranium and thorium from the Archaean. This mechanism would also explain the thorium enrichment in the Key Lake ores. The presence of Archaean rocks in close proximity to these types of deposits may be genetically significant.

Pre-Athabasca Peneplanation 1700-1350 Ma

In the Key Lake area, the Wollaston sedimentary pile was at least 2500 to 3500 metres thick (Ray, 1977). The cores of the Archaean domal antiforms were subsequently exposed during an extensive period of post-Lower Proterozoic (post-Hudsonian) peneplanation. Isostatic readjustment along faults would maintain them as principal passage ways for migrating solutions, and result in further metal redistribution and concentration during retrograde metamorphism.

Weathering 1350 Ma

A long period of slow weathering occurred close to the present position of the Middle Proterozoic (Helikian) unconformity. The existence of a widespread fossil weathering zone up to 50 metres thick, has been confirmed in exploration drilling. Along fault zones, this weathering would have been deeper. In immediate pre-Athabasca times, the Key Lake fault trace was, therefore, a topographic low, locallizing both ground water and surface drainage. Various authors have suggested that initial supergene deposition occurred at this time since surface drainage would carry metals leached during weathering. Langford (1974), postulated that the same supergene processes which formed the calcrete deposits of Western Australia could also be invoked to explain unconformity vein deposits. Although such mechanisms may have been operative, their effects would have been largely removed by fluvial scouring, which accompanied initial Athabasca conglomerate deposition. Athabasca sedimentation was probably complete by 1300 Ma.

Hydrothermal Deposition of Uranium Ore 1350-900 Ma

Following Athabasca sedimentation, the Key Lake fault was reactivated due to isostatic readjustment. A widespread thermal event possibly associated with the Upper Proterozoic (Grenville) Orogeny (955 Ma), triggered the upward movement of fluids within the fault, and redistribution of protore upward to the Middle Proterozoic (Helikian) unconformity. P-T conditions below 1500 bars and 300°C are indicated by open space fillings and pentlandite-pyrrhotite exsolution. Lower temperatures are indicated for primary uranium deposition since tetragonal U_3O_7 only forms below 137°C. Although the exact mechanisms of ore emplacement are not known, the following should be considered: alteration in the ore zones at Key Lake is post-sandstone hydrothermal and not pre-sandstone weathering; conditions in the Athabasca sandstone were oscillating between oxidizing and reducing; sandstone diagenesis would promote water flow in basement faults; fluids rising in the Key Lake fault

HEADINGS	KEY LAKE	JABILUKA
HOST ROCK	Lower Proterozoic (Aphebian), graphitic quartz-biotite-plagioclase-cordierite gneiss altered to chlorite and kalolinite in ore zone.	Lower Proterozoic, graphitic dolomitic quartz-chlorite-feldspar schist.
HOST ROCK Preconcentration	Background 2-10 ppm near graphitic zones, locally reaching 300+ ppm U_3O_8.	Unaltered pelitic schists distant from Jabiluka 9 ppm, graphite schists remote from Jabiluka 13 ppm[1]
STRATIGRAPHIC Distance Above Archaean Granite	Approximately 400 metres	Estimated 200-300 metres
ARCHAEAN	Rejuvenation 1800 Ma. Anatectic pegmatoid in Wollaston pelites.	Rejuvenation 1800 Ma. Transitional migmatitic contact with Cahill Fm.[2]
U_3O_8 in Archaean	2 ppm to 15 ppm.	Nanambu Complex average 10 ppm U[3]
METAMORPHISM	Prograde 1800 Ma to upper amphibolite facies. Possible retrograde metamorphism? (may be confused with hydrothermal alteration in ore zone)	Prograde 1800 Ma to amphibolite facies. Retrograde to green schist facies. ~1600-1700 Ma[4] [5]
STRUCTURAL CONTROL	Faulting, pre and post sandstone.	Collapse breccias[6] [7]
ORE Emplacement	Tetragonal $U_3O_8 = UO_{2.33}$ (pitchblende I) remobilized and redeposited as sooty pitchblende (pitchblende II) and coffinite accompanied by tectonism and formation of chlorite.	Uraninite, remobilized and redeposited as pitchblende accompanied by formation of chlorite.
THERMAL Event Accompanying Main Redistribution (ore forming event)	955 Ma (Grenville Orogeny) Diabase Dykes 935-1230 Ma.	> 900 Ma[8] ~ 900Ma[7] Epeirogenic (?) activity
TEMPERATURE Ore Formation	<137°C dep. pitchblende I.	<85°-260°C - stable isotopes[9] 75°-160°C fluid inclusions[10]
REPORTED AGE Dates	1228-960 Ma ore in Athabasca Sandstone returns only young dates 370-89 Ma.	800-900 Ma[11]
RELATIONSHIP To Helikian Unconformity	Completely covered at time of ore forming event. Athabasca Fm. 1350 Ma	Completely covered at time of ore forming event. Kombolgie Fm. 1650 Ma[4]

(1) Binns *et al.* (this volume)
(2) Needham & Stuart-Smith (this volume)
(3) Ferguson, Chappell & Goleby (this volume)
(4) Page *et al.* (this volume)
(5) Riley *et al.* (this volume)
(6) Hegge (1977)
(7) Ferguson, Ewers & Donnelly (this volume)
(8) B.L. Gulson, J.H. Hills, R.W. Page & G.H. Riley (pers. comm. 1979)
(9) Donnelly & Ferguson (this volume)
(10) Ypma & Fuzikawa (this volume)
(11) Hills & Richards (1976)

Table 2. Comparative geology of Key Lake and Jabiluka.

may have found the basal sandstone relatively less permeable than the fault; water flow may have been in the form of convection cells fueled by heat associated with the intrusion of diabase dykes which occur throughout the Athabasca basin and date 935-1230 Ma; P-T changes or the accumulation of reductants at the unconformity could have triggered uranium precipitation. Sibbald (1978) and Hoeve (1978) report strong evidence from Rabbit Lake, suggesting that graphite consumption and production of CH_4 and CO_2 occurred during ore deposition.

AGE DATING

U/Pb age determinations indicate primary ore deposition at 1228, 1155 and 960 Ma. Post depositional redistribution occurred at 370, 250, 107 and 89 Ma. Supergene theories for similar deposits such as Rabbit Lake (Hoeve, 1978), advocate the migration of uranium mineralizing solutions within the Athabasca sandstone from unspecified distant sources. Haloes of CH_4 generated from graphite would trigger uranium precipitation at the unconformity. The supergene approach fails to explain the lack of uranium in the Athabasca sandstone, and ignores the ubiquitous uranium protore present in graphitic pelites throughout the Wollaston domain. At Key Lake, the presence of only 'sooty' secondary pitchblende in the sandstone, dating 250-107 Ma, is strong evidence for a hypogene origin.

JABILUKA

Lower Proterozoic uranium deposits in the Athabasca Basin and Pine Creek Geosyncline, exhibit many striking similaries in geologic setting, host rocks, alteration, mineralogy and structural controls. Key Lake and Jabiluka may be considered representative of Lower Proterozoic uranium deposition in these two uranium provinces. Hegge (1977), proposed that Lower Proterozoic pelitic and chemical sediments with higher than normal background uranium were the source rocks for the Jabiluka U-Au deposits. Collapse breccias formed through dolomite silicification at Jabiluka had a similar effect as strike faulting at Key Lake, providing channel ways and depositional traps for metal bearing fluids. As in the model proposed for Key Lake, uranium and other metals might also have entered the Cahill Formation in varying amounts during anatectic reactivation of the Archaean Nanambu Complex or during retrograde metamorphism from circulating brines.

The similarities between these two deposits can be seen in table 2, which is a comparison of their genetically significant features.

CONCLUSIONS

In light of work to date, we consider the essential requirements for Lower Proterozoic, unconformity vein type deposits to be:

1) Fertile host rocks
2) Structural dilation
3) Middle Proterozoic (Helikian) cover rocks

The most important single criteria, is their intimate association with Middle Proterozoic (Helikian) unconformities which implies that the ultimate ore forming events occurred following Middle Proterozoic (Helikian) sedimentation. This also implies that deposits will only be found beneath, or close to, the erosional edge of Middle Proterozoic (Helikian) basins. In Saskatchewan, this is reflected by the fact that all areas of the Athabasca basin are presently held, and being actively explored, despite known sandstone thicknesses of up to 1450 metres. Added impetus in this search for deeply buried deposits has come from the discovery in early 1978 of the high grade deposit at Midwest Lake covered by 160 metres of sandstone and the realization that the Cluff Lake deposits were formed beneath over 1200 metres of sandstone. The meteor impact which formed the Carswell circular structure in

Ordovician time served only to remove the sandstone cover. Similar deeply buried deposits should occur under the Kombolgie Formation sandstones at their interface with graphitic Cahill Formation sediments.

ACKNOWLEDGEMENTS

The authors wish to thank the management of Key Lake Mining Corporation and Uranerz Exploration and Mining Limited of Saskatoon, Canada, and Uranerzbergbau, Bonn, West Germany, for giving permission to publish this paper.

REFERENCES

Bell, R.T., 1978: Uranium in Black Shales — A Review, *in* (ed. M.M. Kimberley) *Short Course on Uranium Deposits: Their Mineralogy and Origin. Mineralogical Association Canada,* 307-329.

Binns, R.A., McAndrew, J. & Sun, S-S., this volume: Origin of Uranium Mineralisation at Jabiluka. *Proceedings of the International Uranium Symposium on the Pine Creek Geosyncline.*

Dahlkamp, F.J., 1977: Geologic Appraisal of the Key Lake U-Ni Deposits, Northern Saskatchewan. *Annual Meeting Soc. Econ. Geol. and G.S.A., November 7-9, Seattle, Washington.*

Dahlkamp, F.J. & Tan, B., 1977: Geology and Mineralogy of the Key Lake U-Ni Deposits, Northern Saskatchewan, Canada. *in* (ed. M.J. Jones) *Geology, Mining and Extractive Processings of Uranium. Symposium, London,* 145-157.

Dahlkamp, F.J., 1978: Geologic appraisal of the Key Lake U-Ni Deposits, Northern Saskatchewan. *Econ. Geol., 73,* 1430-1449.

Donnelly, T.H. & Ferguson, J., this volume. A stable isotope study of three deposits in the Alligator Rivers Uranium Field, NT. *Proceedings of the International Uranium Symposium on the Pine Creek Geosyncline.*

Ferguson, J., Chappell, B.W. & Goleby, A.B., this volume: Granitoids in the Pine Creek Geosyncline. *Proceedings of the International Uranium Symposium on the Pine Creek Geosyncline.*

Ferguson, J., Ewers, G.R. & Donnelly, T.H., this volume: Model for the development of economic uranium mineralisation in the Alligator Rivers Uranium Field. *Proceedings of the International Uranium Symposium on the Pine Creek Geosyncline.*

Gabelman, J.W. 1977: Migration of Uranium and Thorium — Exploration Significance. *Am. Ass. Petrol. Geol., Studies in Geology, 3.*

Gatzweiler, R., Lehnert-Thiel, K., Classen, D., Voultsidis, V., Strnad, J.G. & Rich, J., 1979: The Key Lake Uranium-Nickel Deposits. *Bull. Can. Inst. Min. Metall., 70, 807,* 73-97.

Hegge, M.R. 1977: Geologic setting and Relevant Exploration Features of the Jabiluka Uranium Deposits. *Bull. Can. Inst. Min. Metall., 70, 788,* 50-61.

Hegge, M.R. & Rowntree, J.C., 1977: Geologic setting and concepts on Origin of Uranium Deposits in the East Alligator River Area, N.T., Australia. *Annual Meeting Soc. Econ. Geol. and G.S.A., November 7-9, Seattle, Washington.*

Hegge, M.R. & Rowntree, J.C., 1978: Geologic setting and concepts on the Origin of Uranium Deposits in the East Alligator River Region, N.T. Australia. *Econ. Geol., 73,* 1420-1429.

Hills, J.H. & Richards, J.R., 1976: Pitchblende and galena ages in the Alligator Rivers Region, Northern Territory, Australia. *Miner. Deposita, 11,* 133-154.

Hoeve, J., 1978: Uranium Metallogenetic Studies: Rabbit Lake, Mineralogy and Geochemistry. *in* (eds. J.E. Christopher & R. MacDonald) *Summary of Investigations 1978, Saskatchewan Geological Survey Miscellaneous Report, 78-10,* 61-65.

Hoeve, J. & Sibbald, T.I.I., 1978: On the genesis of Rabbit Lake and other unconformity-type Uranium Deposits in Northern Saskatchewan, Canada. *Econ. Geol., 73,* 1450-1473.

Langford, F.F., 1974: A supergene origin for vein-type uranium ores in light of the Western Australian calcrete-carnotite deposits. *Econ. Geol., 69,* 516-526.

Needham, R.S. & Stuart-Smith, P.G., 1976: The Cahill Formation — host to Uranium deposits in the Alligator Rivers Uranium Field, Ausralia. *BMR J. Aust. Geol. Geophys., 1,* 321-333.

Needham, R.S. & Stuart-Smith, this volume: Geology of the Alligator Rivers Uranium Field. *Proceedings of the International Uranium Symposium on the Pine Creek Geosyncline.*

Page, R.W., Compston, W. & Needham, R.S., this volume: Geochronology and evolution of the late Archaean basement and Proterozoic rocks in the Alligator Rivers Uranium Field, Northern Territory, Australia. *Proceedings of the International Uranium Syumposium on the Pine Creek Geosyncline.*

Pretorius, D.A., 1968: Mineral Exploration in Southern Africa: Problems and Prognosis for the Next Twenty Years. *University of Witwatersrand, Economic Research Unit, Information Circular, 50.*

Ray, G.E., 1977: The Geology of the Highrock Lake — Key Lake Vicinity. *Rep. Sask. geol. Surv., 197.*

Riley, G.H., Binns, R.A. & Craven, S., this volume: Rb-Sr chronology of micas at Jabiluka. *Proceedings of the International Uranium Symposium on the Pine Creek Geosyncline.*

Sibbald, T.I.I. Munday, R.J.C. & Lewry, J.F., 1976: The geological setting of Uranium Mineralisation in Northern Saskatchewan. *Spec. Publs geol. Soc. Sask., 3,* 51-98.

Sibbald, T.I.I., 1978: Uranium Metallogenic Studies: Rabbit Lake Geology. *in* (eds. J.E. Christopher & R. MacDonald). *Summary of Investigations 1978, Saskatchewan Geological Survey Miscellaneous Report, 78-10,* 56-60.

Strnad, J.G., 1979: Genetic Models and their impact on Uranium Exploration in the Athabasca Sandstone Basin, Saskatchewan, Canada. *Extended Abstracts of the International Uranium Symposium on the Pine Creek Geosyncline*, 192-195.

Tan, B., 1977: Geochemical case history in the Key Lake Area. *in* (eds. J.E. Christopher & R. MacDonald). *Summary of Investigations 1978, Saskatchewan Geological Survey Miscellaneous Report, 78-10*, 323-330.

Watkinson, D.H., Heslop, J.B. & Ewert, W.D., 1975: Nickel Sulphide — Arsenide Assemblages Associated with Uranium Mineralisation Zimmer Lake Area, Northern Saskatchewan. *Can. Mineralogist, 13*, 198-204.

Ypma, P.J.M. & Fuzikawa, K.,, this volume: Fluid inclusion as a guide to the composition of uranium ore forming solutions to the Nabarlek and Jabiluka deposits, NT, Australia. *Proceedings of the International Uranium Symposium on the Pine Creek Geosyncline*

GENETIC MODELS AND THEIR IMPACT ON URANIUM EXPLORATION IN THE ATHABASCA SANDSTONE BASIN, SASKATCHEWAN, CANADA

Jiří G. Strnad

Uranerz Exploration and Mining Ltd., 204-229 4th Avenue South, Saskatoon, Saskatchewan, S7K 4K3, Canada.

ABSTRACT

While the Beaverlodge area of Northern Saskatchewan became an important uranium-producing district during the 1950s, the Athabasca sandstone basin, located in the immediate vicinity, was considered to be non-prospective in Canada's regional assessment. Twenty years later, with the introduction of the supergene model into the basin's exploration strategy, the favourability of the host-rock for uranium deposits was shown. However, in some instances the search for local targets was enriched by implementing non-supergene models.

Most geologists originally favoured the Middle Proterozoic (sub-Helikian) unconformity as a unique ore-controlling feature. Later, the concept of Lower Proterozoic (Aphebian) syngenetic protore, as represented by graphite-bearing strata in Archaean proximity, was added. In the author's view the combination of these factors is productive only within specialized segments of Archaean-Lower Proterozoic (Archaean-Aphebian) contact zones.

ASSESSMENT OF REGIONAL POTENTIAL

The Athabasca sandstone basin was a virgin territory where the complexity of geological thought and its involvement in the discovery of uranium potential can be demonstrated with relative ease.

In July 1935, the first pitchblende was found in the Beaverlodge district during prospecting for base and precious metals. By the mid 1960s virtually all of today's vein type uranium deposits in the immediate vicinity of the basin were known. The basin's monotonous plain of flat-layered sandstone remained almost untouched despite the presence of hundreds of prospectors and a dozen uranium shafts in its northern vicinity. In 1951 autunite at Middle Lake was discovered within the regolith at the base of the Athabasca sandstone on the basin's north rim. The decline of exploration in this vicinity brought out the first evaluation of the basin's potential in a remarkably perceptive account. "The Athabasca sandstone is an unfavourable rock in which to seek vein deposits. The grade (of Middle Lake occurrence) is unfavourable, but the possibility of finding worthwhile deposits in the Athabasca series should not be ignored" (Blake, 1956). The existence of vein deposits within the basement rocks in the Beaverlodge district led Gussow (1959) to predict that "possibly the basal sandstones and conglomerates of the Athabasca Formation are the host for Blind River-type mineralization" and to recommend that "the possibility of uranium mineralization should be investigated".

The step-wise retreat from these early positive views is suggested in the same period by Lang (1961) when he writes that "on the whole, the region is not considered as being favourable for prospecting . . . occurrences may nonetheless be found". Lang *et al.*, (1962) completely excluded the Athabasca basin from the regional prospective scenario. Thus the results of two of the most important nation-wide regional works of those years, a preliminary study of metallogenic provinces and a uranium deposits review, under the competitive image of a favoured conglomeratic type, depressed the potential of the Athabasca basin to zero. As evidenced by the passage of time, the simple local assessment of the basin by Blake (1956) was more visionary in comparison to the regionally-balanced assessment.

THE PREDISCOVERY DEVELOPMENT OF GENERAL STRATEGY

While the cold winds of a negative regional assessment blew across the barrenness of the Athabasca plain, several companies based their remote general strategy on the *supergene*

model, which had been developed as being viable in the *Proterozoic* of Western Africa. The selection of the Athabasca basin was reduced to the principle of analogy of the favourable host rock for supergene uranium concentrations and the proximity to known uranium deposits in older formations regardless of their different genetic type. Years of patient work culminated in the discovery of the Rabbit Lake deposit by Gulf Mineral Ltd. in 1968, the Cluff Lake deposits by Amok (Canada) Ltd. in 1969 and the Key Lake ore bodies by Uranerz Exploration and Mining Limited in 1975-76.

The substantial discoveries are still mainly the result of aggressive field activity guided by flexible geological thinking. This was confirmed by discoveries in the Athabasca basin and exhaustively illustrated by the case history of the Jabiluka deposit. It's hard to imagine how computer programs such as Monte Carlo and Play Prospect being desirably a "tool . . . in any uranium exploration project" (Ruzicka, 1976) would handle the data available before the East Alligator River region had been selected as a regional target. Sometimes it happens that in terrane where the geological maps are considered as being of "limited reliability" (Rowntree & Mosher, 1976), there is usually not so much to be computerized. In other cases, with an excess of data, "the computer discovered the districts already known" (Gabelman, 1976) as reported from the United States sandstone provinces.

A SHORT REVIEW OF GENETIC MODELS AND EXPLORATION TACTICS AS USED IN THE DISCOVERIES

After the general strategical framework has been firmly erected, the difficulties start, as usual, in the second phase, i.e. in the search for targets. The problem is, that the 'correct host rock' and the general ' 'genetic model' are still only very generalized guidelines. *The specifics of the terrane* become decisive and need to be studied in adequate detail. The case histories from the Athabasca basin show the lengthy laborious process of discovery.

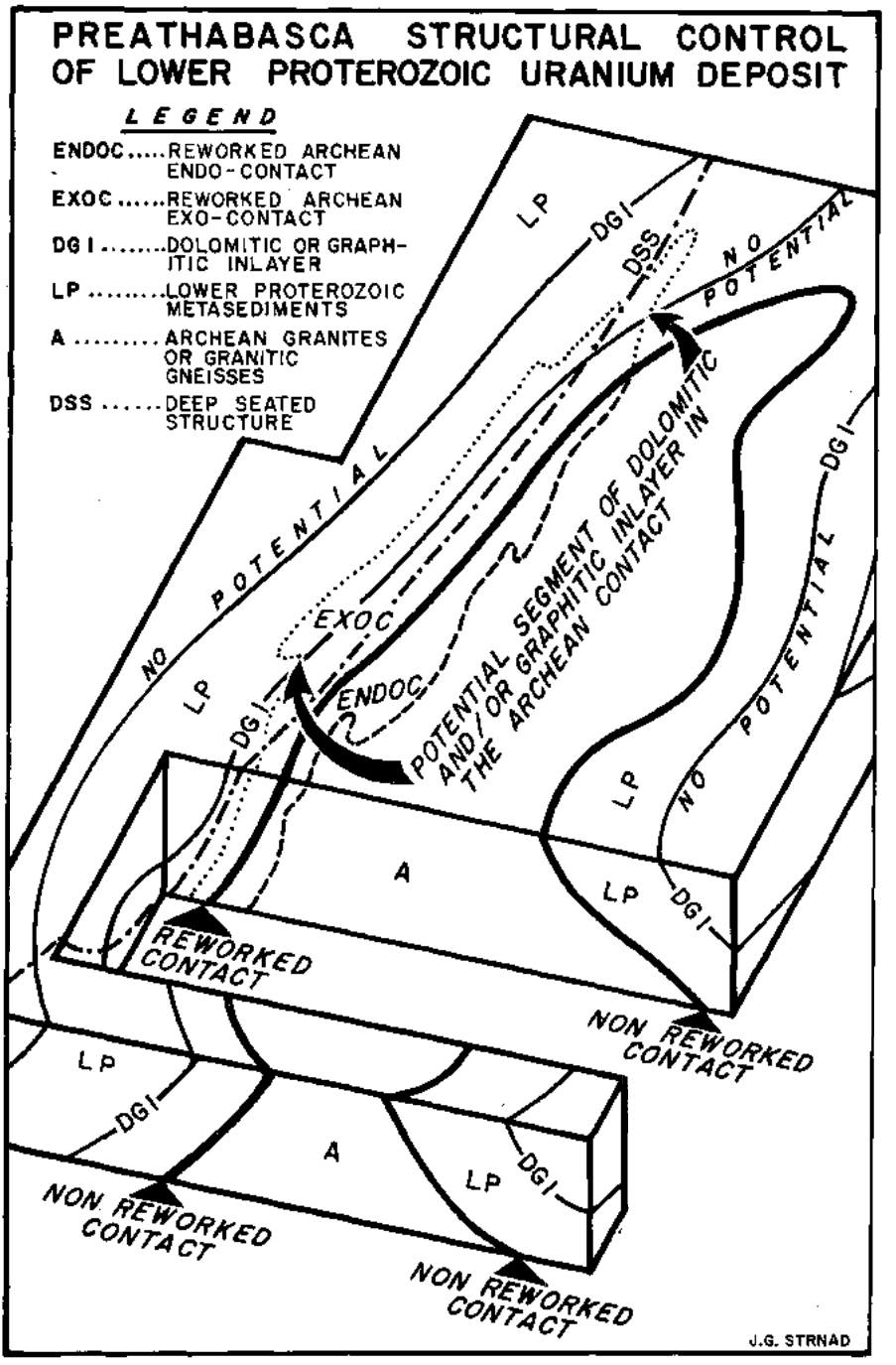
Two examples will show the complexity encountered. In one locality, the mineralized clasts were predominantly sandstone cobbles. This fact understandably matched the supergene theory and the thinking had been easily channeled into an apparently correct conclusion that the orebody lay within the sandstone. Thus the geometry of the sought-after orebody, in accordance with the known sandstone types, was surely not expected to be expressively linear. Then, the initial drilling intersected a graphitic zone with nickel mineralization and traces of uranium within the basement. It took a certain period to implement a linear model to test the target against the prevailing classical intraformational sandstone-type image. Consequently, the corresponding exploration methods and an adequate drilling pattern has been fully enforced, which finally led to a discovery of the ore body. In another locality geologists tried to locate a sandstone source by tracing mineralized sandstone cobbles. Years of disappointing results from searching for the intraformational target (within the sandstone), afterwards changed into a discovery when the approach switched to taking a closer look at the basement.

These examples show that while we recognize the role of the supergene school in its ultimately abstracted essence, by showing the *regional host-rock target*, the supergene school may not be fully operational during the search for *specific targets*.

The main workload during the exploration phase is centered on the selection of exploration methods according to the specifics of the terrane. An excellent example of the use of a combination of different techniques has been demonstrated by the exploration case history of Key Lake (Tan, 1976; Kirchner & Tan, 1977).

THE RECENT STAGE OF GENETIC MODELS AND THEIR INTERACTIONS

The diversity of existing genetic models have been analyzed by Beck (1976), Hoeve (1978) and Treblay (1978). To repeat the words of Charles Lyell we do not know which of the


PREATHABASCA STRUCTURAL CONTROL
OF LOWER PROTEROZOIC URANIUM DEPOSIT
LEGEND
ENDOC.....REWORKED ARCHEAN ENDO-CONTACT
EXOC.....REWORKED ARCHEAN EXO-CONTACT
DGI.....DOLOMITIC OR GRAPHITIC INLAYER
LP.....LOWER PROTEROZOIC METASEDIMENTS
A.....ARCHEAN GRANITES OR GRANITIC GNEISSES
DSS.....DEEP SEATED STRUCTURE
LP
DGI
DSS
NO POTENTIAL
NO POTENTIAL
EXOC
ENDOC
POTENTIAL SEGMENT OF DOLOMITIC AND/OR GRAPHITIC INLAYER IN THE ARCHEAN CONTACT
NO POTENTIAL
A
REWORKED CONTACT
NON REWORKED CONTACT
NON REWORKED CONTACT
NON REWORKED CONTACT
J.G. STRNAD

models will be "adopted by universal consent". Regardless of their variety, they all have enough in common which can be used during the exploration. The generally-accepted optimum feature in the Athabasca basin is the unconformity separating the folded Lower Proterozoic (Aphebian) and Archaean units from the overlying Athabasca sandstone formation. Some workers assume that this unconformity has a unique advantage in the formation of uranium mineralization. The problem centres on recognizing the function of the unconformity. In the case of the Athabasca basin it is still questionable if the unconformity is an *'ore-forming' structure* (and if so, to what extent?) or only an *'ore-bearing' feature* having the important function of a plane of physico-chemical discontinuity.

For simplification, we may reduce the importance of the unconformity to the plane where the ore bodies are localized. If only a horizontal plane would be considered as unqiuely important we would expect a multitude of flat-lying ore accumulations within or above the unconformity, but recent discoveries show the expressive linearity of orebodies. This means that there exists another important factor required for large concentrations of uranium. In general these complementary features are marked mainly by the strike faults coinciding with certain strata within the Lower Proterozoic (Aphebian). Thus, the final geometry of a uranium ore body within the Athabasca basin is related to the intersection line between the subhorizontal unconformity and a subvertical unconformity-crossing (or unconformity-reaching) fault. Both are needed to build the potential conditions for a sizeable ore body. Small and/or low grade deposits in different positions and of different geometry might exist within each of the two formations while related to one of the above-mentioned structural planes. One subtype, important from the exploration point of view, is represented by *intraformational bodies* within the sandstone strata. Such bodies in a stratigraphically-higher position are probably the main source of mineralized surficial boulder trains. Despite their generally low grade and smaller size these could be important indicators for the main deposits at depth in the commonly-known unconformity/fault arrangement.

THE APPROXIMATE FEATURES OF AN OPTIMAL MODEL

The diversity of geological units within, and specifically beneath, the Athabasca basin creates the general condition for the existence of uranium deposits with a variety of size, uranium concentration, geometry, position and mineral association. Despite intensive exploration activity, today's mosaic of diversity is surely not yet final. However, we may assume that the recently recognized main type of unconformity/fault arrangement is relatively known by its typical development in the Key Lake deposit and that such a model completed by knowledge from other places might be viable for further exploration.

The role of the unconformity in the author's view occupies just one part of the whole model. As in any other important and complex deposit, one controlling feature alone is not sufficient for ore deposition. The most important events centre on the pre-Athabasca development of specific zones within the basement.

Several authors have emphasized the controlling factor of graphitic layers developed within the basal portion of the Lower Proterozoic (Aphebian) sequence close to Archaean inlayers. In their view the Archaean represents the *ultimate source* of uranium through the passive pre-lower Proterozoic (pre-Aphebian) weathering processes. The role of Lower Proterozoic (Aphebian) graphitic inlayers has been restricted to those developed in a paleogeographically favourable position i.e. close to the Archaean source. Such enriched inlayers were the postulated uranium protore. This scheme, however, follows the probable sequence of events rather than presenting the regional-wide evidence for such a process. We still do not possess the type of data which convincingly shows how the uranium background of Archaean rocks differs from Lower Proterozoic (Aphebian) one, based on fresh rock samples. Neither do we know how much the uranium content in the graphitic layers compares with the pelitic

metamorphics, nor finally, if and by how much the protore uranium content of the basal graphitic members exceeds that of the graphites of stratigraphically higher positions. Similarly, weathering processes acting during the time of Archaean-Lower Proterozoic (Archaean-Aphebian) and Lower Proterozoic-Middle Proterozoic (Aphebian-Helikian) unconformities have hardly been touched by any regionally-based clay-mineralogical or clay-geochemical studies.

In the author's view, such a simple combination of Archaean and Lower Proterozoic (Aphebian) features as mentioned above leads to a large number of possibilities. Reality, nevertheless shows that the favouable combination of controlling factors is less common and spatially restricted to the more *specifically developed segments* of the basement. Within such segments the Archaean-Lower Proterozoic (Archaean-Aphebian) boundaries are not of simple transgressive character, but rather that the contact is intensively reactivated. Lower Proterozoic (Hudsonian) events cover a wide range of metamorphic, intrusive, metasomatic and tectonic processes within such zones. Xenoliths of amphibole-gneisses floating within remobilized Archaean granitic gneisses, the assimilation of Lower Proterozoic (Aphebian) rocks within the granitic gneisses, intrusive pegmatites, syenitic dykes, migmatization and the still poorly deciphered metasomatites (albitization) are all phenomena demonstrating the complex *metamorpho-intrusive* development of certain segments along the Archaean-Lower Proterozoic (Archaean-Aphebian) contact. This multitude of Hudsonian events has been complemented by a sequence of post-Lower Proterozoic (post-Hudsonian) and pre-Athabasca tectonics represented by mylonite zones and younger shearing. Considering the average Lower Proterozoic (Aphebian) rock block, the major physico-mechanical anisotropy is located around the thick graphitic member and close to the Archaean block. Other graphitic members probably had few chances to be involved in major tectonic movements.

Ideal conditions for the multistage concentration of uranium are provided by those tectonic zones which along their strike coincide with the reactivated Archaean-Lower Proterozoic (Archaean-Aphebian) contact. In addition, hydrothermal processes along shear zones and subsequent weathering complete the multiphase picture of pre-Athabasca event. The syn- and early post-Athabasca event played the role of further developing the physico-chemical discontinuity of the unconformity, which was important for the culmination of uranium concentration processes.

Most uranium accumulations or redistribution phases sensitively reflect *tectonic perturbations*. The reactivation of consolidated blocks is a commonly-known phenomenon and the lack of orogenic evidence within the sediments after their deposition within the Athabasca basin does not prove their overall tectonic inactivity. Tectonic studies in the regional vicinity of the Athabasca basin also indicate that numerous events contradict the simplified atectonic view of the supergene school.

Haites (1960) distinguishes within Western Canada's Phanerozoic the following movements: early Palaeozoic Taconic, late Palaeozoic Appalachian, post-Upper Cretaceous, Tertiary Laramide and even late Pleistocene movements. Byers (1962) relates the fault perturbations within the Western part of the Canadian Shield to late Precambrian, post-Devonian and post-Cretaceous periods. Probably, the range of the uranium geochemical cycle, within the basin deposits, including redistribution, includes *several younger tectonic events* occurring after the Upper Proterozoic (Grenvillian) which has been promoted by Morton (1977). The author suggests that the *mosaic of a multitude of faults* within the basin is of primary importance from a different point of view.

An association of uranium accumulation with diabase has frequently been reported. On a regional scale, the Proterozoic Oenpelli dolerite are described from the East Alligator River province (Smart *et al.*, 1975). Gangloff (1970) reported the close association of Proterozoic uranium-phosphatic Bakouma layers with dykes and sills of dolerite. The diabase intrusions

are considered to be substantially more efficient heat generators than granitic bodies of similar size (Winkler, 1965 p. 220). Their internal development might cover a large time range which might be necessary for differentiation into syenites, sodic syenites, gabbro and albite pegmatoids (Granger, 1955; Smart *et al.*, 1975). Few authors even relate the uranium mineralization directly to "emanations from . . . igneous masses of mafic composition" (Page, 1960) or to "late-stage hydrothermal fluids derived from diabasic magma" (Nuffield, 1978). During the processes of formation of endogenic halos related to the stage of pre-ore development, mafic rocks with their higher Fe and Ti yield a higher coefficient of uranium concentration in comparison with siliceous environment (Yelisieyeva & Omelyayenko, 1976). In some cases, the pre-ore halos are characterized by Na-metasomatites with albite-aegirine and/or riebeckite or with an albite-carbonate and/or chlorite assemblage. Rocks possibly having such an affinity have been reported from the deposits within the Athabasca basin and from its periphery. The syenite from Gunnar Mine (Beck, 1969), porous calcitic granites from Dubyna Lake (Trueman & Fortuna, 1976), plagioclasite from Rabbit Lake (Hoeve & Sibbald, 1978), and newly-found syenites from the Key Lake deposit are examples. The role of diabases and granites as the immediate uranium sources has been negated by Tremblay (1970). On the other hand, the numerous world-wide examples of uranium remobilization related to the heating effects of cratonic mafic intrusions might also be a viable guideline for the Athabasca basin.

THE GENERAL ROLE OF CLASSIFICATION OF URANIUM DEPOSITS IN THE EXPLORATION STRATEGY

Genetical aspects have been used in many classification schemes resulting in generalized guidelines for the *known* types of deposits. However, the excursions of the classifications into the *unknown* realm are less bright. Substantial enhancements of classification schemes are recorded mostly after the more or less unpredicted discoveries of new types of deposits are made.

The problems observed probably lie in the *selection of correct criteria possessing an operational value.* In this connection, reference should be made to a sphere which is not commonly analyzed.

By reading 83 pages dedicated to uranium deposits of the USSR (Smirnov, 1977) one finds some striking features which merit much closer look. First there is an evident emphasis on the *metamorphogenic* and *endogenic* deposits while the exogenic deposits are accorded only one quarter of the attention. As a result there is noticeably a great variety within the metamorpho- and endogenic deposits. The relatively small review of exogenic deposits might be partially a reflection of a certain uneasiness about making the imported models fully operational. On the other hand we have to suspect that the wider spectrum of metamorpho- and endogenic deposits probably indicates not only a greater geological availability, but also a *broader knowledge* of *metasomatic processes* (traditionally in the theoretical field of these processes and in the practical field by the intense use of *litho-geochemistry* (i.e. whole rock geochemistry s.s.). Secondly, the development of USSR uranium resources has been, at least during the 1950s and 60s, potentially enriched by the physical contact of Russian geologist with uranium districts in the Erzgebirge. Besides the emphasis placed on the endogenic types, the geotectonic concept is another leading approach used within the USSR for the classification of ore deposits in general (Danchev & Strelyanov, 1976; Smirnov, 1977). We may expect that this approach is a reflection of unified training established within a large territory.

In conclusion, it is still difficult to say how close this or other systems are to the idealized criteria under which classifications will be apparently operational for exploration. Nevertheless, the intention was to indicate that the scope and the processing of observed

geological phenomena might be strongly influenced by different schools of thought. To establish the correctness of abstractive processes covering our realm, probably also requires a deeper understanding of similar intentions carried out within a large region with a different autonomous path of geological thought.

CONCLUSION

The large scale regional concepts (regional assessments, uranium-deposits classifications etc.) are still influenced by a more or less subjective path of particular geological school of thought and by the waves of preference given for specific type of deposits. The operationality of such concepts is mostly limited to their highly abstracted essence — to the simple selection of *favourable host-rock and preferentially in the vicinity of known uranium* cumulations.

Within the particular case of the Athabasca basin, the optimum features for recently recognized main type of unconformity/fault arrangement focus on the *location of an intersection line* of both important planes. Thus the *general* controlling features are acceptable by most of the differing genetic models. Further specification of both important geometric elements, however, depends on the genetical assumptions. In the author's view, the *specific development of the lower structural level* is essential for the initiation and development of uranium cumulative processes, while the unconformity, syn- and early post-Athabasca events complete the process of concentration. Most of the post-Athabasca events probably play the regressive role within the uranium cycle.

ACKNOWLEDGEMENTS

The author expresses his thanks to the Management of Uranerzbergbau GmbH, Bonn, German Federal Republic and Uranerz Exploration and Mining Ltd., Saskatoon, Canada, for their permission and support in preparing this paper. Numerous discussions with colleagues from both companies substantially enriched the author's ideas. Special thanks are directed to Mr Roland Loewer for anglicizing the text and general help in obtaining the necessary literature.

REFERENCES

Baasgaard, H., *et al.*, 1964: *Limitations of Radiometric Dating. Geochronology in Canada.* University of Toronto Press.

Beck, L.S., 1969: Uranium Deposits of the Athabasca Region, Saskatchewan. *Rep. DMR Prov. Sask., 126,* 193.

Beck, L.S., 1976: History of Uranium Exploration in Saskatchewan with special reference to the changing ideas on Metallogenesis. *Uranium in Saskatchewan, Spec. Publs geol. Soc. Sask., 3,* 1-10.

Blake, D.A.W., 1956: Geological Notes on the Region South of Lake Athabasca and Black Lake, Saskatchewan and Alberta. *Geol. Surv. Pap. Can., 55-33,* 12.

Byers, A.R., 1962: *Major Faults in Western Part of Canadian Shield with Special Reference to Saskatchewan. Tectonics of the Canadian Shield.* Toronto University Press, 40-59.

Danchev, V.I. & Strelyanov, N.P., 1976: Stages in Ore Deposition and Classification of Exogenic Uranium Deposits. *Geologiya Rudn. Mestorozh., 3,* 11-24.

Gableman, J., 1976: *Exploration for Uranium Ore Deposits, Proceedings of a Symposium, Vienna.* International Atomic Energy Agency, Vienna, 682.

Gangloff, A., 1970: Notes sommaires sur la geologie des principaux districts uraniferes etudies par la CEA. *Uranium Exploration Geology. Proceedings of a Panel, Vienna.* International Atomic Energy Agency, Vienna, 77-104.

Granger, H.C., 1955: Dripping Spring Quartzite. *US Geol. Survey, Trace Elements Investigation Report, TE 1-590,* 187-191.

Gussow, W.C., 1959: Athabasca Formation of Western Canada. *Bull. geol. Soc. Am., 70,* 1-18.

Haites, T.B., 1960: Trancurrent Faults in Western Canada. *Journal of the Alberta Society of Petroleum Geologists, 8(2),* 33-79.

Hoeve, J., 1978: Classification of Uranium Deposits in Northern Saskatchewan. *in* (ed.M.M. Kimberley) *Short Course in Uranium Deposits: Their Mineralogy and Origin. Mineralogical Association of Canada,* 397-402.

Hoeve, J. & Sibbald, T.I.I., 1978: On the Genesis of Rabbit Lake and Other Unconformity-Type Uranium Deposits in Northern Saskatchewan, Canada. *in* (ed. M.M. Kimberley) *Short Course in Uranium Deposits: Their Mineralogy and Origin. Mineralogical Association of Canada.* 457-474.

Kirchner, G. & Tan, B.H., 1977: Prospektion, Exploration and Entwicklung der Uranlagerstätte Key Lake, Kanada. *Erzmetall, Bd. 30, H.12,* 584-589.

Lang, A.H., 1961: A Preliminary Study of Canadian Metallogenic Provinces. *Geol. Surv. Pap. Can., 60-33,* 54.

Lang, A.H., Griffith, J.W. & Steacy, H.R., 1962: Canadian Deposits of Uranium and Thorium. *Geol. Survey of Canada. Economic Geology Series,* 16.

Morton, R.D., 1977: The Western and Northern Australian Uranium Deposits — Exploration Guides or Exploration Deterrents for Saskatchewan? *Uranium Spec. Publs geol. Soc. Sask., 3,* 211-255.

Nuffield, E.W., 1950 and 1955 *in* Robertson, J.A., 1978: Uranium Deposits in Ontario. *in* (ed. M.M. Kimberley) *Short Course in Uranium Deposits: Their Mineralogy and Origin. Mineralogical Association of Canada,* 229-280.

Page, L., 1960: The Source of Uranium in Ore Deposits. *21st Int. geol. Congr. Norden, Report Part 15,* 149-164.

Rowntree, J.C. & Mosher, D.V., 1976: Case History of the Discovery of the Jabiluka Uranium Deposits, East Alligator River Region, Northern Territory of Australia. *Exploration for Uranium Ore Deposits. Proceedings of a Symposium, Vienna.* International Atomic Energy Agency, Vienna, 551-570.

Ruzicka, V., 1976: Uranium Resources Evaluation Model as an Exploration Tool. *Exploration for Uranium Ore Deposits. Proceedings of a Symposium, Vienna.* International Atomic Energy Agency, Vienna, 673-681.

Smart, P.G., Wilkes, P.G., Needham, R.S. & Watchman, A.L., 1975: Geology and geophysics of the Alligator Rivers Region. *in* (ed. C.L. Knight) *Economic Geology of Australia and Papua New Guinea, Australas. Inst Min. Metall. Monograph Series No. 5, 1. Metals,* 285-301.

Smirnov, V.I., 1977: Ore Deposits of the USSR. Volume 2. Pitman, London, San Francisco, Melbourne. Translated by D. A. Brown.

Tan, B.H., 1976: Geochemical Case History in the Key Lake Area, Uranium in Saskatchewan. *Spec. Publs geol. Soc. Sask, 3,* 27-50.

Tremblay, L.P., 1970: The Significance of Uranium in Quartzite in the Beaverlodge Area, Saskatchewan. *Can. J. Earth Sci., 7(2),* 280-305.

Tremblay, L.P., 1978: Geologic Setting of the Beaverlodge-Type of Vein-Uranium Deposit and its Comparison to that of the Unconformity-Type. *in* (ed. M.M. Kimberley) *Short Course in Uranium Deposits: Their Mineralogy and Origin. Mineralogical Association of Canada,* 431-455.

Trueman, T. & Fortuna, P.A., 1976: Dubyna Lake Uranium Deposit (31 zone) Eldorado, Saskatchewan. *Spec. Publs geol. Soc. Can., 3,* 355-382.

Winkler, H.G.F., 1965: *Petrogenesis of Metamorphic Rocks.* Springer-Verlag, Berlin-Heidelberg-New York, 220.

Yeliseyeva, O.P. & Omelyayenko, B.O., 1976: The Local Distribution of Uranium in Rocks and Minerals as Indicator for the Petrogenetic Processes. *Soviet Geologia, I,* 76-91 (in Russian).

CONTRIBUTION TO SOME SASKATCHEWAN URANIUM DEPOSITS MAINLY FROM FLUID INCLUSION AND ISOTOPIC DATA

Maurice Pagel[1-2], Bernard Poty[1] and Simon M.F. Sheppard[2]

1. Centre de Recherches sur la géologie de l'Uranium, B.P. 23, 545000 — Vandoeuvre (France).
2. Centre de Recherches Pétrographiques et Géochimiques, C.O. No. 1, 54500 — Vandoeuvre (France).

ABSTRACT

Mineralogical, fluid inclusion homogenisation temperature and composition studies, and D/H, $^{13}C/^{12}C$ and $^{18}O/^{16}O$ isotope studies have been performed on the Cluff Lake and Rabbit Lake uranium deposits and their host rocks. The following aspects are emphasized:

1) Metamorphism of the basement in presence of an essentially carbonic fluid (granulite facies);
2) Evaporitic type of sedimentation with high Mg-Li-B- and organic matter at the beginning of the Athabasca basin sedimentation;
3) Presence of highly concentrated brines (~30% eq. weight NaCl) during diagenesis of the sandstone;
4) Hydrothermal alteration (around 200°C), at the boundary between basement and cover.

Solutions during at least one stage of uranium mobilization and deposition were very similar to these diagenetic brines from the point of view of temperature, pressure, salinity, Cl/Br and stable isotopes (D/H and $^{18}O/^{16}O$). $^{13}C/^{12}C$ ratios on CO_2 are consistant with a derivation from organic matter by thermal degradation. However chloritization cannot be related to this stage and is not yet understood.

Diagenesis of the Athabasca sandstone was an important step in the formation of economic uranium concentrations.

INTRODUCTION

The origin of Saskatchewan uranium deposits has been debated since their discovery particularly as several deposits are related, at least spatially, to the unconformity between the basement rocks and the overlying Athabasca sandstones. The principal aim of this work is to provide some additional data from fluid inclusion and isotopic studies to help in understanding the genesis of these deposits. These data are restricted to the Cluff Lake and Rabbit Lake deposits and their host rocks.

GENERAL GEOLOGY

The uranium deposits studied are located geographically near the boundary between the pre-Lower Proterozoic (Prehelikian) basement and the Athabasca sandstone basin (Fig. 1) and geologically near the unconformity between these two formations. Sibbald *et al.* (1977) have shown that within the pre-Lower Proterozoic (Prehelikian) basement a distinction is made between the Archaean craton, only mildly reworked by Lower Proterozoic (Hudsonian) events, and the Lower Proterozoic (Hudsonian) mobile zones comprising extensively remobilized Archaean rocks and Lower Proterozoic (Aphebian) supracrustals. The Athabasca formation rests unconformably on this basement and its age is still in debate since Ramaekers & Dunn (1977) have found an age of 1350 + 50 m.y. by Rb/Sr isochron methods on clay pebbles and Fahrig *et al.* (1977) an age of 1550 m.y. by paleomagnetic data. The Athabasca sandstones have been studied regionally by Fahrig (1961) and by Ramaekers & Dunn (1978). They consist of conglomerates at the base overlain by relatively pure quartzites with minor amounts of shale layers. In the Carswell area (Fig. 1), the Athabasca formation passes gradually from fine grained sediments, the Douglas Formation, to the Carswell Formation, which consists of dolomitic layers preserved by a meteoritic impact event (Innes, 1964; Pagel, 1975a). The uranium deposits studied in this paper (Rabbit Lake, Cluff Lake) and the other deposits found in this province (Key Lake, Maurice Bay, Midwest Lake) are located near the unconformity between the Athabasca formation and the basement. Geochronological data related to the genesis of the

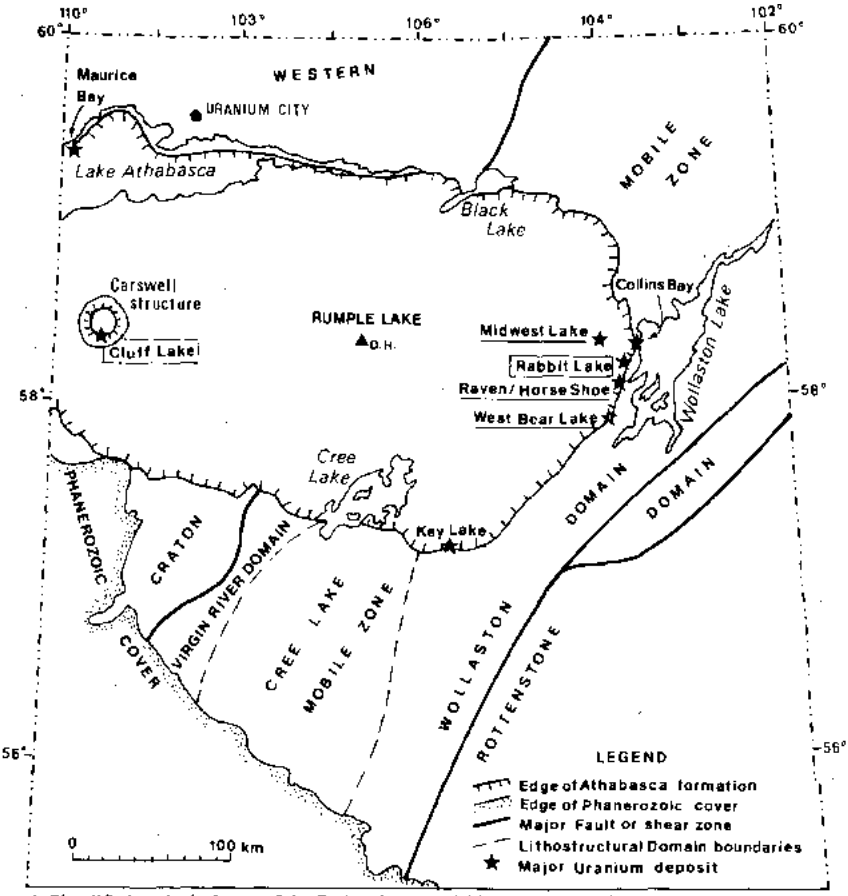


Figure 1. Simplified geological map of the Saskatchewan shield with location of the major uranium deposits, after Sibbald *et al.* (1979).

deposits, although abundant, are not always easy to interpret. A summary of the published data is presented in figure 10.

REGIONAL METAMORPHISM IN BASEMENT ROCKS

In the Carswell structure (Pagel, 1975a; Herring, 1976) and Rabbit Lake area (Sibbald *et al.*, 1977) metamorphism reached the granulite facies. Sibbald *et al.* (1977) and Hoeve & Sibbald (1978) have described uranium concentrations in anatectic zones which they interpret as a result of high grade metamorphism of a uraniferous black shale. Some U and Th concentrations in pegmatoids are also cited by Harper (1978) for the Carswell area. The composition of the fluid phase during the metamorphism is thus of great importance. In the Carswell structure, Pagel (1975a) has shown that a carbonic fluid is contemporaneous with the granulite facies metamorphism. The homogenization temperatures of carbonic inclusions (in the liquid phase) are between - 18°C and + 31°C, with most values in the range + 15°C to + 15°C. The melting temperatures which are close to -56.6°C, the triple point of

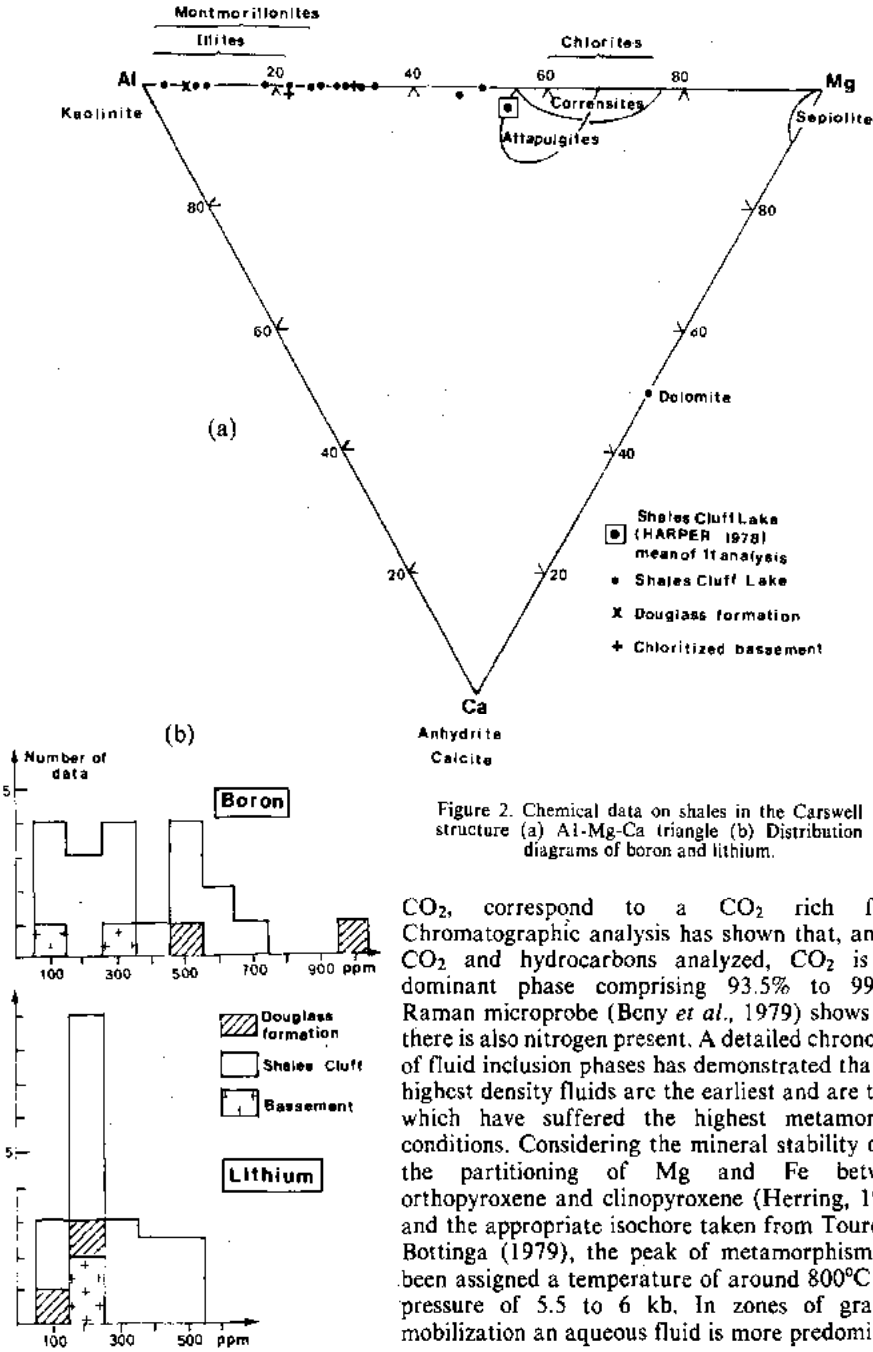


Figure 2. Chemical data on shales in the Carswell structure (a) Al-Mg-Ca triangle (b) Distribution diagrams of boron and lithium.

CO_2, correspond to a CO_2 rich fluid. Chromatographic analysis has shown that, among CO_2 and hydrocarbons analyzed, CO_2 is the dominant phase comprising 93.5% to 99.2%. Raman microprobe (Beny *et al.*, 1979) shows that there is also nitrogen present. A detailed chronology of fluid inclusion phases has demonstrated that the highest density fluids are the earliest and are those which have suffered the highest metamorphic conditions. Considering the mineral stability data, the partitioning of Mg and Fe between orthopyroxene and clinopyroxene (Herring, 1976) and the appropriate isochore taken from Touret & Bottinga (1979), the peak of metamorphism has been assigned a temperature of around 800°C at a pressure of 5.5 to 6 kb. In zones of granitic mobilization an aqueous fluid is more predominant

although inclusions containing carbonic fluids do occur. These aqueous inclusions have salinities of the order of 5 to 8 weight percent equivalent NaCl and a mean homogenization temperature of +210°C. The proportions of $P(CO_2)$ and $P(H_2O)$ in the fluid phase are probably very important in the genesis of the different types of metamorphism since high $P(CO_2)$ has been shown to be characteristic of granulite facies metamorphism (Touret, 1971). Variations in the composition of the fluid are critical for explaining the U-concentrations in remobilized metasediments and depletions in granulite facies rocks (Collerson & Fryer, 1978).

SHALES

Shales are not abundant in the Athabasca basin but they have been observed at some localities especially in the Carswell structure at the base of the Athabasca Formation. These shales are abundant in the D zone ore body (Cluff Lake deposit) and show several characteristics:

1) MgO is high, up to 15% and this Mg cannot be accommodated in montmorillonites or illites; boron is high, 100 to 1000 ppm and lithium varies from 60 to 550 ppm (Fig. 2). This is indicative of marine evaporitic or close to evaporitic sedimentation (Trauth, 1977; Jarousse *et al.*, 1978).
2) their organic matter content is high: this organic matter, which may come from algal mats, has been studied by Rouzaud (1979). Its H/C and O/C atomic ratios do not plot in a Van Krevelen diagram in the normal kerogen evolution path for algae but in the path of continental plants. This contradiction shows that not only has the organic matter released most of its hydrogen during burial — which was expected — but also that it has been oxidized.

DIAGENESIS OF ATHABASCA SANDSTONES

The diagenetic evolution of sandstones is marked by quartz overgrowths, pressure solution of detritic quartz grains, specular hematite, authigenic kaolinite and illite/chlorite assemblages (Ramaekers & Dunn, 1977). Fluid inclusions, associated with the siliceous diagenesis, have been studied by Pagel (1975a). The inclusions around the detritic quartz grains are always formed by two fluid phases, commonly a cube of halite and sometimes platelets of hematite; argillaceous solids are also present in some cases. If the cube of halite is a daughter mineral, platelets of hematite and argillaceous solids result from heterogeneous trapping. They show that the silicification of Athabasca sandstones was produced by brines. This has been observed both in the Carswell area and in a deep drill hole in the Rumple Lake area, near the centre of the Athabasca basin (Fig. 1). Variations of both the chemical composition of the fluid inclusions and the homogenization temperatures have been determined.

These fluid inclusion studies have shown that relatively high temperatures have been attained in the Athabasca basin (220°C at the base of sandstones in the Carswell area).

Assuming that the estimated diagenetic silicification temperatures are real, the pressure can be estimated using the H_2O - 30% NaCl system. But in this system, the isochores are known only when the cube of halite dissolves in the presence of liquid and vapor. Furthermore the first melting temperature which is much lower than the eutectic point of the H_2O-NaCl system shows that divalent ions (Ca and Mg) are in significant concentration.

Despite the complex fluid composition, it should be noted that these heated brines are of regional occurrence and that the geothermal gradient, 35°C/km, is plausible.

HYDROTHERMAL ALTERATION AT THE BASEMENT - SANDSTONE INTERFACE

A special hydrothermal alteration, restricted to the rocks along the unconformity, has

been noted by Pagel (1975a) and by Tremblay (1978) in the Carswell structure. In the basement rocks, it involves the crystallization of chlorite and white mica and is posterior to a red alteration which has been attributed to pedogenetic processes. Fluid inclusion studies have shown that the alteration took place at around 200°C. In the sandstones, hydrothermal alteration is also marked by a strong dissolution of detrital quartz grains and subsequent authigenic silicification. Herring (1976) has dated the alteration products of a cordierite and places the time of alteration at 988 m.y.

In this altered basement there are rare quartz veins with fine dravite. Ramaekers & Dunn (1977) have clearly demonstrated, for the east margin of the Athabasca sandstones, the superposition of different alteration patterns. This hydrothermal alteration is probably a regional process, superimposed on the regolith but only developed locally, implying different physicochemical conditions and probably tectonic events.

GANGUE MINERALS AND FLUID INCLUSIONS IN THE RABBIT LAKE DEPOSIT

Euhedral quartz, dolomite, calcite, a pale green fine grained chlorite after feldspar and a coarser grained pale chlorite were sampled in the open pit in July 1975.

The position of these minerals in the paragenetic sequence established by Hoeve & Sibbald (1978a & 1978c) is uncertain. The quartz and carbonates should be related, probably, to their second stage of mineralization. The pale green fine grained chlorite, is spatially related to a euhedral quartz vein. Close observation of the sample shows that the quartz vein is younger than the chloritic alteration and not contemporaneous as outcrop observation would have suggested.

Isotopic results on minerals

The principles of H-, C- and O- isotope geochemistry and their application to the study of hydrothermal systems have been reviewed by Rye & Ohmoto (1974), Taylor (1974) and Sheppard (1977). The H-, C- and O- isotope fractionation factors, or their extrapolations, used in calculations are those summarised in Taylor (1974), Ohmoto (1972) and Sheppard & Schwarcz (1970).

Standard analytical procedures were used for all isotopic analyses. Absorbed water was removed under high vacuum from all mineral and fluid inclusion samples before commencing the hydrogen isotopic analysis. All isotopic data are reported as δ-values in per mil. The standard for both hydrogen and oxygen isotope data is SMOW and for carbon isotope data PDB. Analytical precision for minerals is 0.1 per mil for oxygen and carbon and 1 per mil for hydrogen.

1) Deuterium

The D/H ratio of five chlorites were determined: the two pale green fine grained chlorites (95-1 and 95-2) after feldspar are isotopically identical $\delta D = -60$ and -57‰. The three coarser grained pale chlorites (RL-C, 97, 95-1) have values of -59, -66 and -60 respectively. Assuming equilibrium between chlorite and water, the calculated H-isotope composition of the water is estimated to about -10‰ for temperatures in the range 100°-200°C. Because H-isotope fractionation factors between chlorite and water are probably not very temperature sensitive below 300°C (Taylor, 1974) the H-isotope composition of the waters in equilibrium with the fine grained and coarser chlorites are indistinguishable even if there was an important difference in their temperature of formation.

Small differences ($\sim$10-15‰) among the waters are possible if variations in the chemical composition of the Mg-rich chlorites (Rimsaite, 1978) and temperature of formation are considered. Because the H-isotope fractionation factors between chlorite-H_2O are not well known below $\sim$350°C the waters in equilibrium with the chlorites are currently considered indistinguishable.

2) Oxygen

Four dolomites have similar O-isotope compositions in the range 14.4 to 15.4‰ (SMOW). A later calcite is slightly enriched in ^{18}O with $\delta = +16.7‰$.

Assuming isotopic equilibrium between dolomite and water the calculated O-isotope composition of the water using the fluid inclusions homogenization temperature of 130°C is $\delta\,^{18}O \sim -1.3$ to $-2.3‰$. For the calcite the calculated composition of water at a temperature of 120°C is $\delta\,^{18}O \sim +1.5‰$.

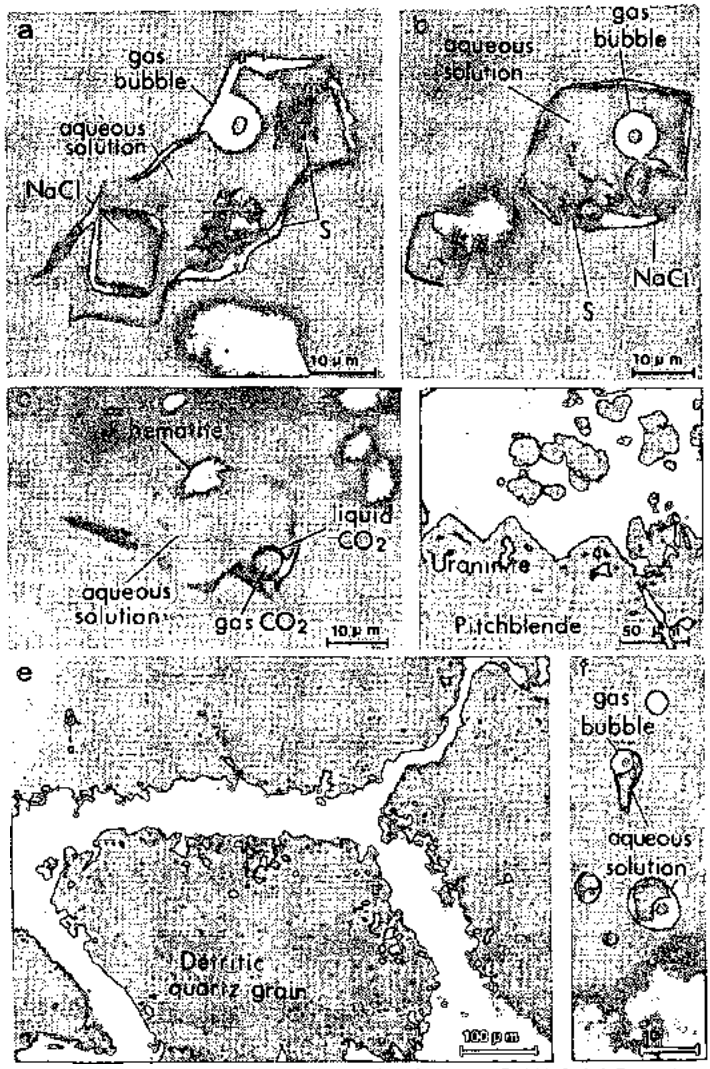


Figure 3. Photomicrographs: (a) and (b) Multiphase inclusions in quartz (Rabbit Lake) S = unknown solid phase; (c) Multiphase inclusion with liquid and gaseous CO_2, plus hematite in dolomite (Rabbit Lake); (d) Pitchblende and uraninite in an argillaceous matrix; (e) Sandstone in D deposit (Cluff Lake) - Numerous late fluid inclusions (see text); (f) Detail of inclusions in (e).

3) Carbon

The C-isotope composition of the four dolomites are uniform with $\delta^{13}C$ = -6.2 to -6.5‰ (PDB). The later calcite is slightly more depleted in ^{13}C with δ= -7.6‰. The C-isotope composition of the fluid can be calculated if we know the dominant carbon bearing species in solution. In these samples the fluid inclusion studies demonstrate that the gas is essentially carbon dioxide with no methane. The calculated C-isotope composition of the fluid is thus $\delta^{13}C$ = -10.2‰ for dolomite and -10.5‰ for the calcite.

We see that the C- and O- isotope composition of the fluids which precipitated dolomite and later calcite are rather similar.

Fluid inclusions

Fluid inclusions have been studied by microthermometry, Raman spectroscopy and for their D/H ratio.

Fluid inclusions in quartz from euhedral quartz veins

The fluid inclusions observed in euhedral quartz crystals can be classified in several groups.

1) Multiphase inclusions containing a gas bubble, a liquid and several solid phases including a cube of halite and acicular birefringent solids (Fig. 3). The volume of the gas bubble is always small. Temperature measurements show two groups of data related with different quartz veins (Fig. 4):

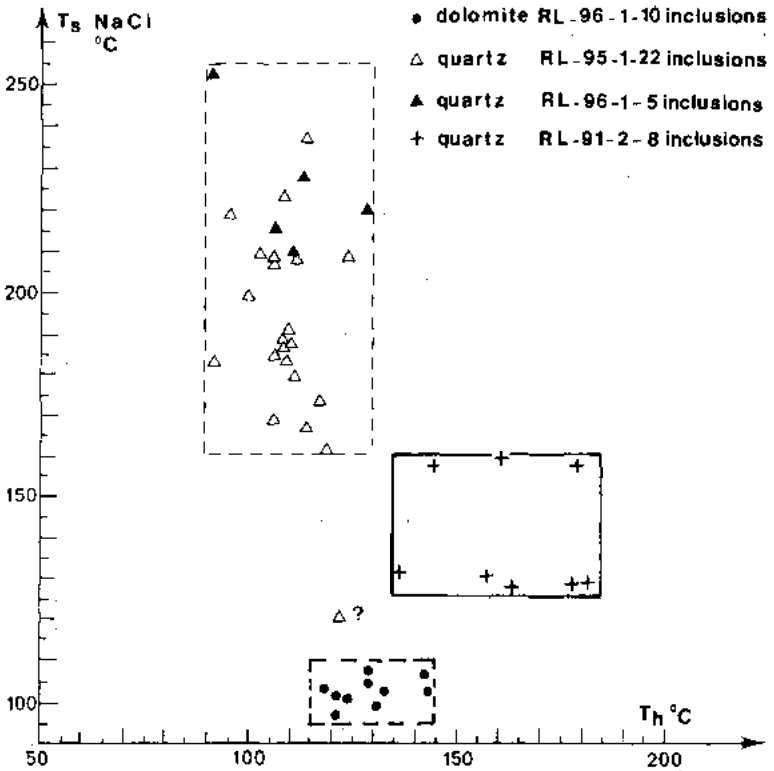


Figure 4. Temperature of disappearance of the gas bubble (Th) versus temperature of disappearance of the halite cube T_s NaCl for fluid inclusions in quartz and dolomite veins from Rabbit Lake.

a) a high and variable salinity with a rather constant homogenization temperature which is lower than the temperature of dissolution of the cube of halite (sample 95-1). Such data are usually interpreted (Touray, 1970) as the trapping of a saturated aqueous solution with cubes of salts. Using the minimum temperature of dissolution of the cube of halite one may infer from the isochore the pressure of trapping. In this case the pressure would be close to 700 bars for a temperature of 160°C±10°C.

b) Multiphase inclusions with a lower salinity and a higher homogenization temperature up to 191°C. These brines were close to saturation with NaCl but not always saturated at a minimum temperature of 160 ± 20°C.

The Ca/Na atomic ratios of these brines range between 0.16 to 0.34 (Pagel & Jaffrezic, 1977). This indicates that NaCl is the dominant species in solution. Cl/Br ratio of these brines has been determined by neutron activation (Pagel & Jaffrezic, 1977). It is very constant at a value of 55 (by weight). This value is much lower than sea water (~300) and different from meteoric waters having dissolved halite (n x 1000). Cl/Br decreases when a brine is precipitating halite (Braitsch, 1971) and also when organic matter releases Br during its evolution (Wickman & Khattab, 1972). Thus this value of 55 suggests either a marine evaporitic environment or thermal degradation of marine organic matter, or both.

2) Scarce fluid inclusions contain H_2 and O_2 (Beny *et al.*, 1979).

The δ D value for fluid inclusions from a euhedral quartz vein is -78±3‰. This vein sample is immediately adjacent to the fine grained and near the coarse grained chlorite (95-1) which probably equilibrated with a water having δ D ~ -10‰. Such a difference of 60-70‰ in the H-isotope composition of the fluids associated with chloritization and the quartz vein is orders of magnitude larger than estimated uncertainties in the chlorite-water fractionation factors. Thus the processes of chloritization and quartz vein formation must have been achieved by different fluids and could not have been contemporaneous.

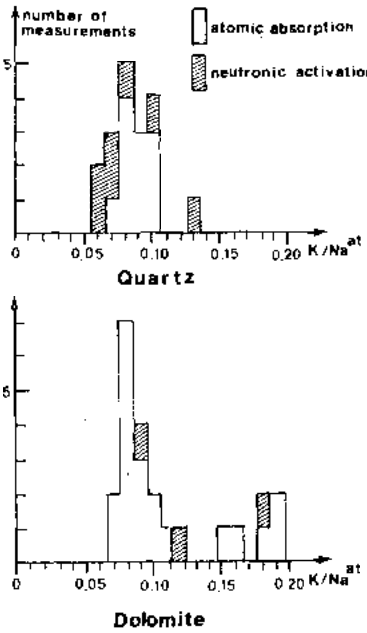


Figure 5. Distribution diagrams of the K/Na ratio for brine inclusions in quartz and dolomite of Rabbit Lake.

Fluid inclusions in dolomite

In dolomite two or three fluid phase inclusions are observed with solid phases, a cube of halite and an hexagonal flake of hematite. The volume of the CO_2 rich-phase is highly variable in these inclusions. The melting temperatures of solid CO_2 are -56.6 ± 0.2°C. This indicates that the carbonic fluid is nearly pure CO_2, a determination which is confirmed by Raman spectroscopy (Beny *et al.*, 1979). The melting of hydrates is between -6.3°C and +7.1°C. Homogenization temperatures of the two CO_2 rich phases lie between +13.8°C and +30.7°C. When there is no cube of halite inclusion, the melting temperatures of ice are between -25.8°C and -26.9°C. When there is a cube of halite the average dissolution temperature is +105°C, which corresponds to a 30% concentration in NaCl after the data of Keevil (1942). A birefringent hexagonal solid forms during cooling and dissolves at temperatures lying between 40.4°C and 46°C.

These data show that the solution is complex. Complementary data have shown that the K/Na ratio (Fig. 5) of brine is very constant near 0.8 and neutron activation analysis of leachates (Pagel & Jaffrezic, 1977) have determined a Cl/Br weight ratio of 65 + 4 in dolomite.

The H_2O - CO_2 inclusions decrepitate at temperatures above +130°C, before total homogenization. The homogenization temperatures when the CO_2 content is very low, vary from +119.5°C to +144.7°C. δD values of fluid inclusions in dolomites have been determined for sample 96-1, 2 and 3 (Fig. 6). They are -76, -94 and -79‰. Duplicate analyses agree within ±2‰ except for 96-1 where 5 analyses range from -63 to -87‰. Although it is known that the fluid inclusions are not homogeneous on the scale of our sampling (crushing up to 9 gm) it is not known why the data are so much more variable for 96-1 relative to the other fluid inclusion samples analysed.

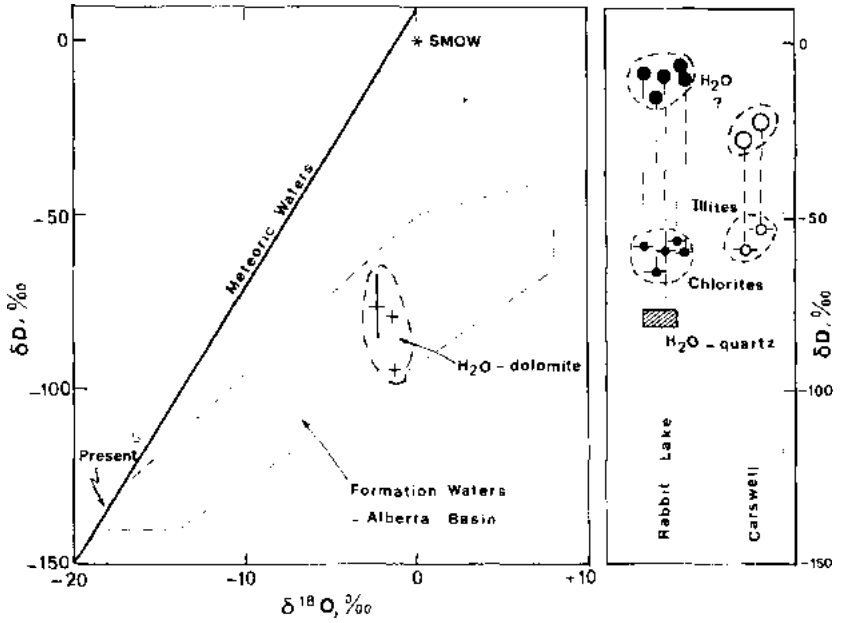


Figure 6. Plot of δD versus $\delta^{18}O$ in fluids (measured and calculated) and minerals at Rabbit Lake and Carswell.

The D/H ratio of the fluid inclusions in the dolomite samples falls within the range observed for the quartz sample. Although the O-isotope composition of the fluid associated with the quartz is not yet known a common fluid could be present in quartz and dolomite samples. The fluid inclusion studies are consistent with this interpretation.

Fluid inclusions in calcite

Two fluid phase inclusions are observed in calcite. They consist of a low salinity (1% w eq. NaCl) aqueous solution with an homogenization temperature varying from +150°C to +127°C.

FLUID INCLUSIONS IN THE CLUFF LAKE D DEPOSIT

In the Carswell structure, two types of mineralization have been distinguished (Harper, 1978). One type with a relatively simple mineral assemblage and a second type, represented

by the D orebody occurring in carbonaceous shales at the base of the Athabasca Formation above the inverted unconformity. The complex mineralogy includes the coexistence of uraninite and pitchblende, and the existence of clausthalite, gold tellurides, Co-Ni sulfo-arsenides and uraniferous bitumens. Reconnaissance fluid inclusion studies have been made on some important minerals.

Quartz veins

In sandstones, there are quartz veins containing two-phase fluid inclusions cross-cutting a green alteration (chloritization). Melting temperatures range from -22.5°C to -28°C, hydrate melting are between -12°C and +5.6°C for variable homogenization temperatures between 250°C and 150°C. These quartz veins are very similar to those of Rabbit Lake. They are also characterized by the existence of a brine at temperatures similar to the diagenetic silicification although they are posterior.

Fractured sandstones

At the contact of sandstones with the high grade zones, a series of small planes of two fluid phase inclusions, generally having a highly variable bubble to total volume ratio, are observed around the borders of detritic grains or in the authigenic quartz overgrowths where such occur (Fig. 3). Melting temperatures of these inclusions vary from 0.1°C to -14°C which correspond to salinites of 0.5 to 18% eq. weight NaCl with a mean salinity between 8 and 14%. The homogenization temperatures are very variable (Fig. 7) with maximum temperatures of 380°C, in the case of a homogeneous plane of inclusions. Most of the inclusions decrepitated between +300 and +350°C (Fig. 7).

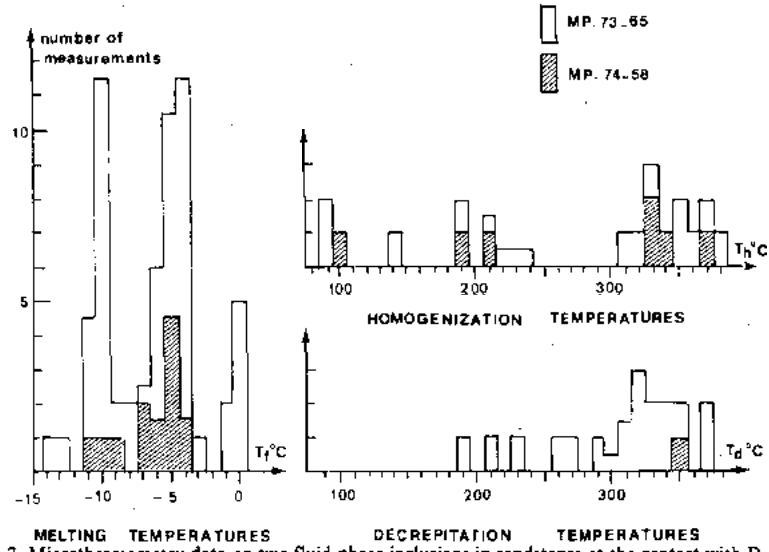


Figure 7. Microthermometry data on two fluid phase inclusions in sandstones at the contact with D deposit (Cluff Lake).

Chloritized basement

At the contact between the Athabasca sandstones and the basement, which is complex in detail, chlorite-rich basement preserves its original gneissic texture as shown by the quartz grains. Around these quartz grains, there are quartz rims with numerous platelets of hexagonal hematite and fluid inclusions. The melting temperatures of these aqueous one or two phase inclusions vary from -11.7°C to -47.4°C for homogenization temperatures up to +172°C.

Calcite veinlets

Some calcite veinlets have been observed, cutting the U mineralization, with two phase fluid inclusions. Melting temperatures are between -1.4°C and -1.9°C for a mean homogenization temperature of 120°C (Fig. 8). These characteristics are very similar to those of the Rabbit Lake calcite.

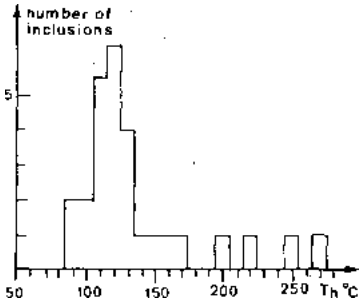


Figure 8. Homogenization temperatures of two fluid phase inclusions in late calcite veinlets in the D deposit (Cluff Lake).

DISCUSSION

The new data place additional contraints on the evolution of the Athabasca Basin and the formation of uranium ore deposits.

1) What is the significance of pelites at the base of the Athabasca sandstones?

The chemical composition of the shales in indicative of a marine evaporitic or close to evaporitic type sedimentation (Fig. 2). Although a simple increase in Mg might be interpreted as a later Mg metasomatism, this would not be consistent with the high B which is a characteristics of Cluff Lake and Rabbit Lake deposits, and high Li as we have seen at Cluff Lake. Furthermore this interpretation is consistent with the high salinity of the brines which are found on a regional scale.

2) Organic matter which is closely associated with these pelites has a very special character: it suffered a strong catagenesis with a sharp decrease of the H/C ratio. Thus this organic matter must have released during its burial quantities of CO_2, H_2O, oil and gas, all components which are reactive with uranium bearing minerals. Furthermore this organic matter is abnormally oxidized and this is evidence for circulation of oxidized waters at the base of the Athabasca formation during its diagenesis.

3) Fluid inclusions found at the beginning of silicification of Athabasca sandstone at Cluff Lake (Pagel, 1975a) as well as in the centre of the basin (Pagel, 1975b) were the first source of evidence of a deep burial of the Athabasca basin. Fluid inclusion studies in quartz and dolomite crystals show that the brines associated with these minerals — and apparently with the economic uranium concentration — are of the same nature as the formation waters of the sandstone. In addition the Cl/Br ratio of the brines shows that they do not come from the leaching of evaporite beds by meteoric waters, but that they are formation waters, either enriched originally in bromide during the deposition of halite or, more probably, by the catagenesis of organic matter.

The waters that were equilibrated with quartz and dolomite are isotopically directly comparable to saline formation waters as found to-day in sedimentary basins (Fig. 6). The field for the formation waters in the Alberta, Canada sedimentary basin, which are associated with oil and gas fields are shown for comparison ($T \leq 118$°C, salinity ≤ 30%, Hitchon & Friedman (1969)). The formation waters are not of direct connate water origin in the sense of dominantly being of sea water origin. They contain a major meteoric water component modified by mixing with diagenetically modified sea water and isotopic (and chemical) exhange with the sediments.

4) Most chlorites have been considered up to now as part of the uranium mineralization process. But the chlorites that we analysed cannot be part of the quartz and dolomite formation studied here. This is suggested by the D/H values of waters equilibrated with chlorites. Some of the chlorites may have formed at the time of this peculiar sedimentation or soon after, but before silicification of the Athabasca sandstones because at that time

formation waters have acquired a different character. New field and petrologic studies should be undertaken taking this point into account.

5) *Origin of the Carbon*

There are three principal reservoirs for carbon in the crust with the following isotopic compositions (Degens, 1969) (Fig. 9).

a) marine carbonate -3 to +3‰
b) organic carbon -30 to -15‰
c) mantle carbonate and CO_2 -8.5 to -3‰

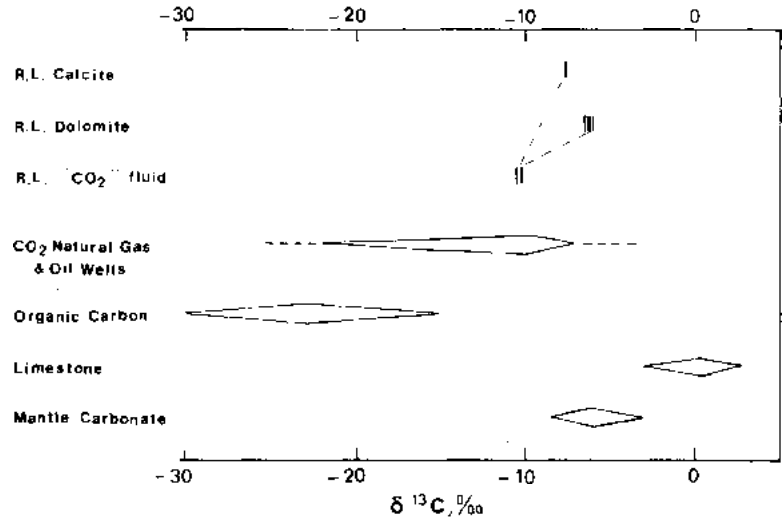


Figure 9. Comparison of measured $\delta^{13}C$ values of dolomites and calcite at Rabbit Lake and calculated $\delta^{13}C$ values of CO_2 fluid with major reservoirs for carbon (see text for discussion).

By comparison with the oxidised carbon reservoirs, direct derivation of the fluid CO_2 with δ = -10‰ from both a limestone source, by either dissolution or thermal decomposition during metamorphism, and mantle carbonate -CO_2 source can be excluded.

Carbon dioxide can be derived from organic matter in a number of ways, many of which are complex and incompletely understood in detail. C-isotope fractionation factors associated with some of these processes are also not known. During early diagenesis by bacterial fermentation processes, CO_2 and CH_4 are generated. This CO_2 is often enriched in ^{13}C by 10 to 20 ‰ relative to the organic source (Oana & Deevey, 1960; Degens, 1969). The small quantities of CO_2 associated with many relatively shallow gas fields often have δ-values around -10‰ and can be explained by such bacterial fermentation processes. Carbon dioxide generated during the thermal degradation of organic matter often has $\delta^{13}C$ values which are similar to the organic starting material (e.g. Sackett & Chung, 1979), but fractionations associated with some of these processes ar not well known.

Excluding the bacterial fermentation reactions it is thus, at present, difficult to predict the istopic composition of CO_2 generated from organic matter. We note, however that although a large range of values have been observed for $\delta^{13}C$ on a relatively small number of samples from natural gas and oil fields, the prevailing value, including those from deep oil fields, is about -10% (Zartman *et al.*, 1961; Wasserburg *et al.*, 1963) (Fig. 9).

Taking into account all the available information on the field, derivation of the CO_2 carbon from a sedimentary source, by thermal degradation of organic matter, is considered

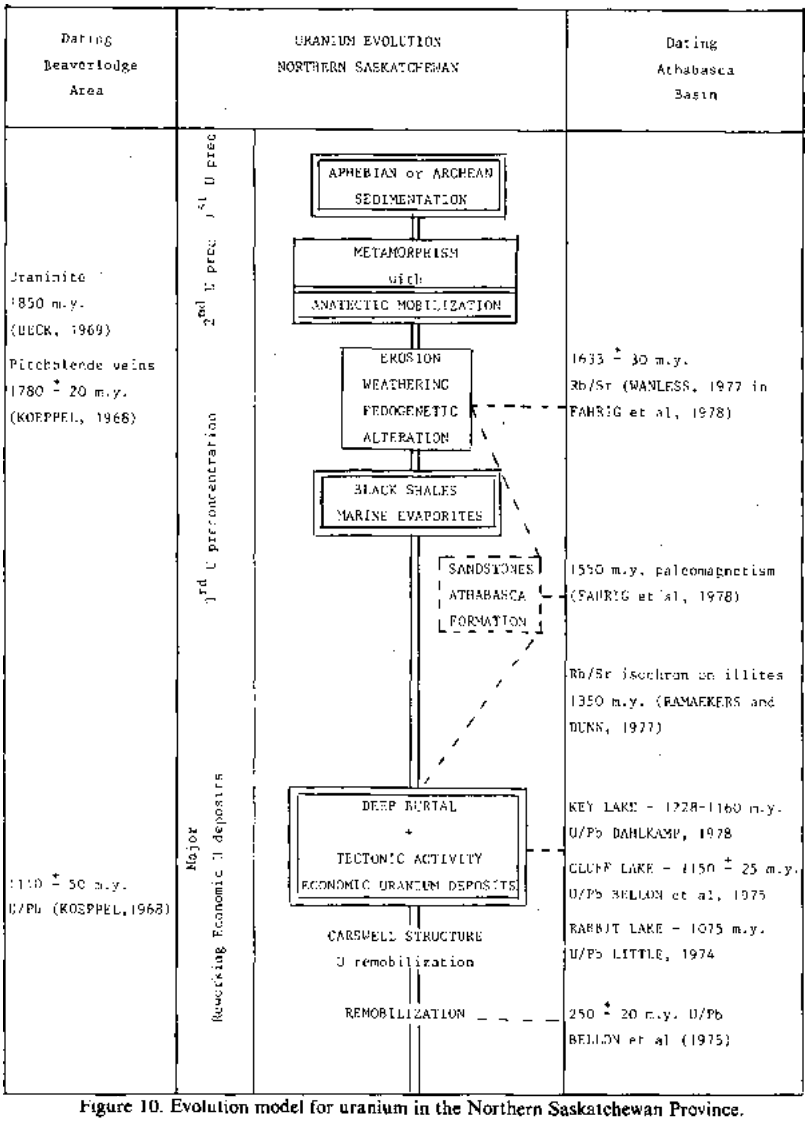


Figure 10. Evolution model for uranium in the Northern Saskatchewan Province.

most probable. Mixing and/or exchange of such CO_2 with limestone carbon is possible. A contribution from a 'profound' source, such as mantle CO_2 or CO_2 released from graphite bearing metamorphic rocks cannot be completely excluded by the isotopic data.

6) In the Carswell structure, a high temperature event, probably related to the formation of the structure itself, induced mineralogical modifications in the deposit. Rimsaite (1978) considers that temperatures higher than 300°C were attained in the N deposit. An age of 478 m.y. has been obtained on melted rocks in the Carswell structure by K/Ar methods. Such an age has not yet been found using U/Pb methods.

The high temperatures recorded by fluid inclusions in the Carswell structure are also recorded by the crystallization of uraninite, such as has been suggested for the Oklo deposit where temperatures over 450°C were determined (Openshaw *et al.*, 1978). There are at least three possibilities for producing these high temperatures (a) natural nuclear reaction (b) radioactive decay (c) formation of the Carswell structure. The third hypothesis is considered to be the most probable explanation because fluid inclusions studied in the impact breccias, melted rocks and in planar fractures have the same characteristics as those occurring in the fractured sandstones (Pagel, 1975; see also Pagel & Poty, 1975, for comparison with the Charlevoix structure).

GENETIC MODEL FOR THE SASKATCHEWAN UNCONFORMITY RELATED URANIUM DEPOSITS

Many genetic models have been proposed for the Saskatchewan unconformity related uranium deposits. These models range from a per descensum origin (Knipping, 1974; Langford, 1978) to a deep origin (Little, 1974) through a diagenetic process origin (Pagel & Jaffrezic, 1977; Hoeve & Sibbald, 1978a & b). Our data support the last model but a multistage evolution must be considered in addition (Fig. 10).

1) Uranium preconcentration has been demonstrated in metamorphic rocks (Dahlkamp, 1978) and thus U was already present in Lower Proterozoic (Aphebian) or Archaean sediments, some of which are interpreted as black shales (Sibbald *et al.*, 1977; Hoeve & Sibbald, 1978). A further concentration step for uranium may have been the anatectic mobilization of these rocks.
2) Pedogenetic alteration at the Lower Proterozoic (Hudsonian) unconformity must have released uranium. Part of this uranium was trapped in algal mats which are characteristic of the intertidal zone of lagoons where a Mg, B and Li rich sedimentation, of an evaporitic type, was occurring. Formation of the economic deposits at this time is negated by both fluid inclusion and isotopic data.
3) Deposition of the Athabasca sandstones and later sediments.
4) During burial the formation waters acquired their chemical and isotopic character (density, Cl/Br ratio, δD, $\delta^{18}O$, $\delta^{13}C$ etc . . .).
5) Probably as a consequence of tectonic activity during the Grenville orogeny, there was major migration of the formation waters and redistribution of uranium. The economic uranium deposits date from this period. The source of uranium must be located in these argillaceous and organic rich sediments (fossil lagoons?) and not in the sandstones which are very mature, rather clean and apparently quite different from those of typical sandstone type uranium deposits.

ACKNOWLEDGEMENTS

Part of this work was supported by a grant from Compagnie de Mokta. We thank the geologists of Amok and Gulf Minerals for their help in sampling the Cluff Lake and Rabbit Lake deposits and for fruitful discussions, particularly J. Dardel. Chemical analyses were performed in the laboratories of K. Govindaraju and M. Vernet, and P. Coget assisted with the isotopic analyses.

REFERENCES

Beck, L.S., 1969: Uranium deposits of the Athabasca region, Saskatchewan. *Department of Mineral Resources, Province of Saskatchewan, Report 126*, 140p.

Bellon, H., Devillers, C., Hagemann, R. & Touray, J.C., 1976: Dater les mineralisations. *Mém. h. sér. Soc. géol. France, 7*, 265-268.

Beny, J.M., Pagel, M. & Poty, B., 1979: in prep.

Braitsch, O., 1971: *Salt deposits: their origin and composition*. Springer, Berlin.

Collerson, K.D. & Fryer, B.J., 1978: The role of fluids in the formation and subsequent development of early continental crust. *Contrib. Mineral. Petrol., 67*, 151-167.

Dahlkamp, F.J., 1978: Geological appraisal of the Key Lake U-Ni deposits, northern Saskatchewan. *Econ Geol., 73*, 1430-1449.

Degens, E.T., 1969: Biogeochemistry of stable carbon isotopes. *in* (eds. G. Eglinton & M.T.J. Murphy) *Organic Geochemistry*. Springer, Berlin.
Fahrig, W.F., 1961: The geology of the Athabasca formation. *Bull. geol. Surv. Can., 68.*
Fahrig, W.F., Christie, K.W. & Freda, G., 1978: The paleolatitude and paleomagnetic age of the Athabasca formation, Northern Saskatchewan. Current Research, Part. C. *Geol. Surv. Pap. Can., 78-1C*, 1-6.
Harper, C.T., 1978: The geology of the Cluff Lake uranium deposits. *Can. Min. metall. Bull.*, 1-11.
Herring, B.F., 1976: The metamorphism and alteration of the basement rocks in the Carswell circular structure, Saskatchewan. *MSc. Thesis, Univ. of B.C.*, (unpubl.), 134p.
Hitchon, B. & Friedman, I., 1969: Geochemistry and origin of formation waters in the Western Canada sedimentary basin — I Stable isotopes of hydrogen and oxygen. *Geochim. cosmochim. Acta, 33*, 1321-1349.
Hoeve, J. & Sibbald, T.I.I., 1978a: Mineralogy and geological setting of unconformity type uranium deposits in northern Saskatchewan. *in* (ed. M.M. Kimberley) *Short Course in Uranium Deposits: Their Mineralogy and Origin, Mineralogical Association of Canada*, 457-474.
Hoeve, J. & Sibbald, T.I.I., 1978b: Uranium concentration related to the sub-Athabasca unconformity, northern Saskatchewan, Canada. *in* (ed. M.M. Kimberley) *Short Course in Uranium Deposits: Their Mineralogy and Origin. Mineralogical Association of Canada*, 475-484.
Hoeve, J. & Sibbald, T.I.I., 1978c: On the genesis of Rabbit Lake and other unconformity type uranium deposits in northern Saskatchewan, Canada. *Econ. Geol., 73*, 1450-1473.
Innes, M.J.S., 1974: Recent advances in meteorite crater research at the Dominion observatory, Ottawa, Canada. *Meteoritics, 2*, 219-249.
Jarousse, J., Moine, B. & Sauvan, P., 1978: Etude chimique de séries évaporitiques en vue de leur identification dans les ensembles métamorphiques. *C.R. Acad. Sci. Paris, Série D, 286*, 1057-1060.
Keevil, N.B., 1942: Vapor pressures of aqueous solutions at high temperatures. *An. Chem. Soc. J., 6A*, 841-850.
Knipping, H.D., 1974: The concepts of supergene versus hypogene emplacement of uranium at Rabbit Lake, Saskatchewan, Canada. *in, Formation of Uranium Ore Deposits. Proceedings of a Symposium, Athens.* International Atomic Energy Agency, Vienna, 531-549.
Koeppel, V., 1968: Age and history of the uranium mineralization of the Beaverlodge area, Saskatchewan. *Geol. Surv. Pap. Can., 67-31.*
Langford, F.F., 1978: Origin of unconformity type pitchblende deposits in the Athabasca basin of Saskatchewan. *in* (ed. M.M. Kimberley) *Short Course in Uranium Deposits: Their Minerology and Origin. Mineralogical Association of Canada*, 485-499.
Little, H.W., 1974: Uranium in Canada. Report of activities, Part A. *Geol. Surv. Pap. Can., 74-1*, 137-139.
Oana, S. & Deevey, E.S., 1960: Carbon-13 in lake waters and its possible bearing on paleolimnology. *Am. J. Sci., 258A*, 253-272.
Ohmoto, H., 1972: Systematics of sulfur and carbon isotopes in hydrothermal ore deposits. *Econ. Geol., 67*, 551-578.
Openshaw, R., Pagel, M. & Poty, B., 1978: Phases fluides contemporaines de la diagenèse des grès, des mouvements tectoniques et du fonctionnement des réacteurs nucléaires d'Oklo (Gabon). *in, Les réacteurs de fission naturels. Proceedings of a Technical Committee Meeting, Paris.* International Atomic Energy Agency, Vienna, 267-296.
Pagel, M., 1975a: Cadre géologique des gisements d'uranium dans la structure Carswell (Saskatchewan - Canada) - Etude des phases fluides. *Thèse de spécialité, Université Nancy I*, 157p.
Pagel, M., 1975b: Détermination des conditions physico-chimiques de la silicification diagénétique des gres Athabasca (Canada) au moyen des inclusions fluides. *C.R. Acad. Sci. Paris, Série D, 280*, 2301-2304.
Pagel, M. & Poty, B., 1975: Fluid inclusion studies in rocks of the Charlevoix structure (Quebec, Canada). *Fortschr. Miner., 52, Special Issue, IMA - Papers 9th Meeting Berlin Regensburg 1974*, 479-489.
Pagel, M. & Jaffrezic, H., 1977: Analyses chimiques des saumures des inclusions de quartz et de la dolomite du gisement d'uranium de Rabbit Lake (Canada). Aspect méthodologique et importance génétique. *C.R. Acad. Sci. Paris, Serie D, 284*, 113-116.
Ramackers, B. & Dunn, C.E., 1977: Geology and geochemistry of the eastern margin of the Athabasca basin. *Spec. Publs geol. Soc. Sask., 3*, 297-322.
Rimsaite, J., 1978: Application of mineralogy to the study of multi-stage uranium mineralization in remobilized uranium deposits, Saskatchewan. *in* (ed. M.M. Kimberley) *Short Course in Uranium Deposits: Their Mineralogy and Origin. Mineralogical Association of Canada*, 403-430.
Rimsaite, J., 1978: Layer silicates and clays in the Rabbit Lake uranium deposit, Saskatchewan. Current Research, Part. A. *Geol. Surv. Pap. Can., 78-1A*, 303-315.
Rouzaud, J.N., 1979: Etude structurale de matières carbonées associées à des minéralisations uranifères. *Thèse de Spécialité, Université d'Orléans*, 108p.
Rye, R.O. & Ohmoto, H., 1974: Sulfur and carbon isotopes and ore genesis, a review. *Econ. Geol. 69*, 826-842.
Sackett, W.M. & Chung, H.M., 1979: Experimental confirmation of the lack of carbon isotope exchange between methane and carbon oxides at high temperatures. *Geochim. cosmochim. Acta, 43*, 273-276.
Sharma, T. & Clayton, R.N., 1965: Measurement of O^{18}/O^{16} ratios of total oxygen of carbonates. *Geochim. cosmochim. Acta, 29*, 1347-1354.
Sheppard, S.M.F., 1977: IDentification of the origin of ore-forming solutions by the use of stable isotopes *in, Volcanic Processes in Ore Genesis. Inst. Min. Metall. and Geol. Soc., London*, 25-41.
Sheppard, S.M.F. & Schwarcz, H.P., 1970: Fractionation of carbon and oxygen isotopes and magnesium between metamorphic calcite and dolomite. *Contrib. Mineral. Petrol., 26*, 161-198.
Sibbald, T.I.I., Munday, R.J.C. & Lewry, J.F., 1977: Setting of uranium mineralization in northern Saskatchewan. *Spec. Publs geol. Soc. Sask., 3*, 51-98.

Taylor, H.P., Jr., 1974: The application of oxygen and hydrogen isotope studies to problems of hydrothermal alteration and ore deposition. *Econ. Geol., 69*, 843-883.

Touray, J.C., 1970: Analyse thermo-optique des familles d'inclusions à dépôts salins (principalement halite). *Schweiz. Min. Petr. Mitt., 1*, 67-79.

Touret, J., 1971: Le faciès granulite en Norvège méridionale - II - Les inclusions fluides. *Lithos, 4*, 423-426.

Touret, J. & Bottinga, Y., 1979: Equation d'état pour le CO_2; application aux inclusions carboniques. *Bulletin de Mineralgoie, 5-6*, in press.

Trauth, N., 1977: Argiles evaporitiques dans la sédimentation carbonatée continentale et épicontinentals tertiaire. Bassins de Paris, de Mormoiron et des Salinelles (France), Ibel Ghassoul (Maroc). *Sciences Géologiques, Strasbourg, Mem. 49*, 195p.

Tremblay, L.P., 1978: Uranium subprovinces and types of uranium deposits in the precambrian rocks of Saskatchewan. Current Research, Part A. *Geol. Surv. Pap. Can. 78-1A*, 427-435.

Wasserburg, G.J., Mazor, E. & Zartman, R.H., 1963: Isotopic and chemical composition of some terrestrial natural gases: *in* (eds. T. Geiss & E.D. Goldberg) *Earth Science and Meteoritics*, North-Holland Publ. Co. Amsterdam, 219-240.

Wickman, F.E. & Khattab, K.M., 1972: Non destructive activation of fluid inclusions in fluorite. *Econ. Geol., 67*, 236-239.

Zartman, R.E., Wasserburg, C.J. & Reynolds, J.J., 1961: Helium, argon and carbon in some natural gases: *J. geophys. Res., 66*, 277-306.

PRESENT EXPLORATION STATUS OF THE LIANSHANGUAN URANIUM DEPOSIT, NORTHEAST CHINA

Qin Fei[1] and Hu Shaokang[2]

1. Liaoning Exploration Team of Uranium Geology, The People's Republic of China.
2. Beijing Research Institute of Uranium Geology, The People's Republic of China.

INTRODUCTION

During recent years surface radiometry has revealed a series of anomalies and uranium occurrences in the Lianshanguan region of Northeast China which are present in Proterozoic Formations. Several significant uranium occurrences were tested by trenching and core drilling which resulted in the discovery of the Lianshanguan uranium deposit in 1978. The ore bodies of economic significance are located at a depth of 38-250m. Potential reserves are 1000 tons of U_3O_8.

The geological setting of the Lower Proterozoic Lianshanguan uranium deposit has a certain similarity to the Alligator Rivers Region, Northern Territory, Australia. However, the Lianshanguan deposit occurs in detrital formations (in the lower part of the Lower Proterozoic sequence), adjacent to a migmatitic zone; it is overlain by carbonate argillitic rocks.

The discovery of the Lianshanguan deposit indicates a potential for further uranium discoveries in northeast China, where Proterozoic sequences are well developed.

The Lianshanguan uranium deposit is located approximately 100km south of Shenyang at 40°59'N and 123°30'E (Fig. 1).

The area is one of low mountains. The maximum elevation above sea level is 700m and the relative elevation of the area is 300m. There are shallow surficial deposits on the slopes of the mountains.

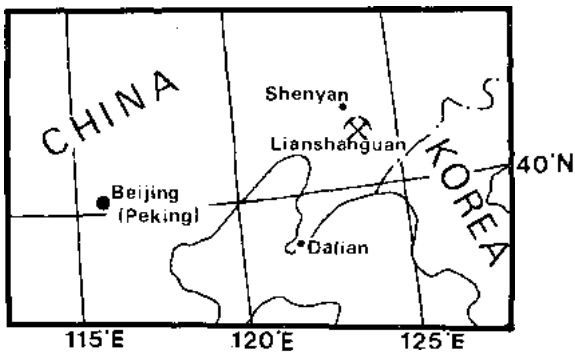


Figure 1. Location Map of the Lianshanguan Uranium Deposit

Climatically the area belongs to the humid northern temperate zone. The average annual rainfall is 920mm which is mostly recorded during July-September. Annual evaporation is 1036mm. Temperature ranges from 36.1°C to -36.6°C. The drainage system is well developed and characterized by ephemeral short streams and multiple sources. The discharge of streams is controlled by the seasonal rainfall.

REGIONAL GEOLOGY

The Lianshanguan area is located on the northeast end of the Northern China Platform in the Lianshanguan anticline, which is composed of the Lower Proterozoic Liaohe Group. The core of the anticline is formed by migmatitic granite with a west-east strike in which inliers of Archaean metamorphic rocks and ferruginous quartzite occur. The migmatitic granite massif surrounded by metamorphic rocks of the Lower Proterozoic Liaohe Group

measures approximately 40 by 10km. Archaean and Lower Proterozoic metamorphic sequences are unconformably overlain by an Upper Proterozoic Group which consists of shallow sea detrital-carbonate sequences of platform type. This essentially unmetamorphosed unit has limited distribution in the area occurring in the northwest part of the region (Fig. 2 and Table 1).

Upper Proterozoic (600-1700 m.y.)	Sinian (Z)	Shale, limestone, marl, quartz-sandstone, quartzite intercalated with slate
Lower Proterozoic (1700-2400 m.y.)	Liaohe Group (Ptl)	Schist, marble, quartzite intercalated with metamorphic tuff and granulite
Archaean (>2400 m.y.)	Anshan Group (Ara)	Schist, gneiss, granulite, magnetic quartzite and amphibolite

Table 1. Simplified Stratigraphy of the Lianshanguan area

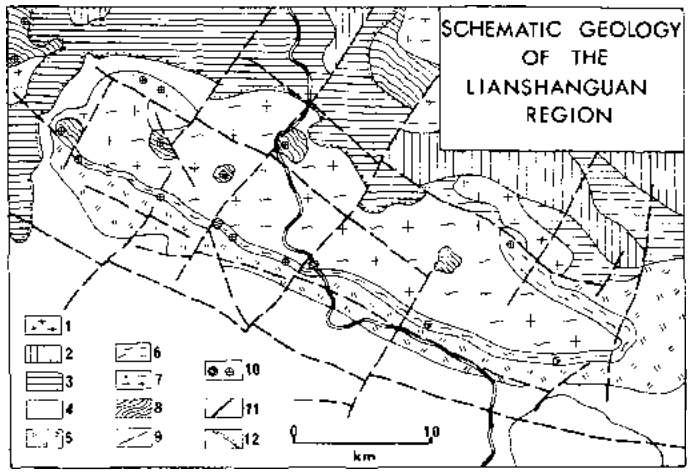


Figure 2. Schematic Geological Map of the Lianshanguan Region
MESOZOIC: 1. Granite; CAMBRIAN: 2. Limestone, shale; UPPER PROTEROZOIC: 3. Quartz-sandstone, phyllite; LOWER PROTEROZIC: 4. Marble; 5. Schist, quartzite; 6. Migmatitic metasediments; ARCHAEAN: 7. Red migmatitic granite; 8. Anshan Group; 9. Fault; 10. Uranium deposit and prospect; 11. Geological boundary; 12. Unconformity.

1. Metamorphic sequences

Archaean Anshan Group

The Archaean Anshan Group is composed of gneiss, amphibolite, granulite, schist and magnetic quartzite; it is basement to the region and has a total thickness of more than 10km. The rocks of this group are exposed in several small ($< 8km^2$) inliers bounded by migmatitic granite in the axial part of Lianshanguan anticline. The Anshan Group has been metamorphosed to amphibolite facies; the age of the main metamorphism and

migmatization is 2400 ± 50 m.y. The original rocks were mafic and intermediate-felsic volcanics and pelitic sediments accompanied by subvolcanic intrusions.

Lower Proterozoic Liaohe Group

The Lower Proterozoic Liaohe Group is made up of eugeosyncline shallow-sea clayey sand-clayey carbonate-sandy clay sediments up to 4-10km thick which are intercalated in the middle part with mafic intermediate-felsic volcanic rocks. The ages of major metamorphic events are 1900 and 1700 m.y. The amphibolite facies has been retrogressed to greenschist facies. Regionally, the contact beween Anshan and Liaohe Groups is unconformable; but in the Lianshanguan area itself exposure of the Liaohe Group represents only the lower subgroup, composed of carbonate clayey-detrital formations up to 500m thick. The contact between these two groups is partly one of migmatitic metasomatism, and partly migmatite-metasomatic intrusion.

2. Migmatite

Both Archaean and Lower Proterozoic rocks underwent strong migmatization. Migmatite is well developed along the axis of the brachyaxial anticline, and occupies the greater part of the anticline. The intensity of migmatization is variable. In general, intensity decreases outwards from Archaean to Lower Proterozoic rocks and from the axial part to the margin of the anticline. This gradation is reflected by a regional zonation from an inner red migmatitic granite zone to an outer white migmatitic metasediment zone, the original rocks of which were the Liaohe Group.

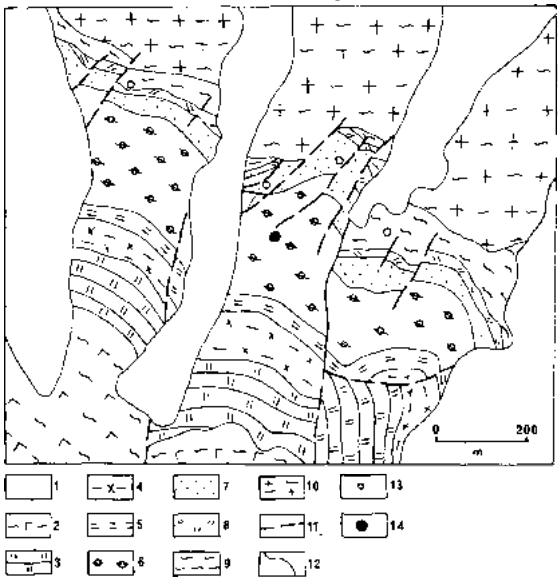


Figure 3. Geological Sketch map of the Lianshanguan Uranium Deposit.

QUARTERNARY: 1. Alluvial and slope wash; LOWER PROTEROZOIC: 2. Meta-rhyolitic-tuff; 3. Tremolite-calcite-marble; 4. Garnet-biotite-quartz schist; 5. Garnet-mica-quartz schist, garnet-biotite-feldspar-quartz schist; 6. Graphite-garnet-biotite-feldspar-quartz schist; 7. Staurolite-garnet-mica-quartz schist, garnet-amphibole schist; 8. Quartzite intercalated with mica-quartz schist; 9. Migmatitic metasediments; ARCHAEAN: 10. Red migmatitic granite; 11. Fault, 12. Geological boundary; 13. Uranium prospect; 14. Uranium deposit.

The inner zone contains homogeneous red migmatitic granite rich in potash feldspars which appears to have been derived by anatexis of the Archaean Anshan Group. The age of the main migmatization is 2400 m.y. This migmatite was reworked by a second stage of migmatization at 1900 m.y.

The white marginal migmatitic netasediment zone extends along the margin of the red migmatitic granite massif along the southern flank of the anticline. The lithology of the migmatitic sediments is rather complex (see description of stratigraphy under Lianshanguan Uranium Deposit). Taxitic textures are well developed. The content of plagioclase is relatively high ($Na_2O > K_2O$). Isotopic dating gives an age of the order of 1900 m.y. for the main stage of migmatization, which was affected by regional metamorphism at 1700 m.y.

3. The distribution of uranium mineralization in the Lianshanguan area.

Uranium mineralization has been discovered on both flanks of the

anticline in belts along the contact between quartzite and white migmatitic metasediment zone. Quartzite occurs at the base of the lower Proterozoic metasediments, and contains lenses of marble. Apart from this, uranium mineralization has also been found in the inliers of Anshan Group rocks bounded by red migmatitic granite in the axial part of the anticline.

The limited isotopic age data suggest uranium mineralization formed at 1800 ± 50 m.y., i.e. slightly later than the second stage of migmatization.

THE LIANSHANGUAN URANIUM DEPOSIT

The Lianshanguan uranium deposit is localized in quartzite and the white migmatitic metasediment zone at the base of carbonate-clayey detrital sub-sequence on the Liaohe Group on the southwestern flank of the Lianshanguan Anticline (Fig. 3).

1. Stratigraphy

Overburden is composed of recent alluvium, slope and residual accumulations from 0.5-10m thick.

The Lower Proterozoic strata form a monocline structure, and dip at 25°-50° to the south. They can be divided into four lithological zones as shown in table 2, which are described below (from upper to lower).

1) Metamorphosed volcanic zone — submarine volcanic eruptives, mainly metamorphosed rhyolite-tuff and local metamorphosed tuff-breccia;
2) Tremolite-marble zone — mainly tremolite-marble intercalated with graphite-mica-schist beds;
3) Schist zone — mainly garnet-mica-quartz-schist, with garnet-hornblende-schist at the base. In the middle and lower parts interstratified silica lenses probably related to migmatization are developed. Perhaps the garnet-hornblende-schist was derived from terrestrial volcanic-sedimentary sequences. Schist is persistently distributed throughout the mineralized area, and serves as an index horizon to define the uranium-bearing quartzite;
4) Quartzite zone — the host of the uranium ore, which consists of quartzite interbedded with leucogranulite, mica-quartz-schist and metamorphic quartz-conglomerate. The quartzite is characterised by presence of muscovite (sericite), quartz, and argillaceous bands, and is rich in impurities, such as clay, iron, boron and sulphur.

Interstratified brecciation, compressional schistosity and silicification are widely developed. Uranium content of quartzite, one of the hosts of the Lianshanguan deposit, reaches 17 ppm.

The base of the quartzite zone is converted into migmatitic metamorphosed rock which follows the contact between the ore-bearing quartzite and the Archaean red migmatitic granite. Relict fabrics preserved in the original metasediments bounded by white migmatite, and spatial location of the latter, suggest the white migmatite may be equivalent to the ore-bearing quartzite.

Migmatization involves both Na and K metasomatism. Na metasomatism is represented by the replacement of quartz by albite. With further migmatization the Na metasomatism gives way to K metasomatism. The migmatite zone can be divided into four subzones: migmatitic metasediments, taxitic migmatite, homogeneous migmatite, and transitional white migmatitic granite.

The average U content of the migmatitic metasediment zone, the main host rocks to the mineralisation, reaches 35 ppm.

2. Mode of Occurrence

Mineralization of economic significance has developed locally in the Quartzite zone and

Cenozoic	Alluvium, slope and residual accumulations		0-10m. Sand, gravel and clay
Lower Proterozoic	Carbonate-clayey Detrital Sub-sequence	Metamorphosed volcanic zone >25m	Metamorphosed rhyolite-tuff.
		Tremolite-marble zone 95m	Tremolite-calcite marble; Graphite-sericite-schist, Graphite-muscovite-quartz-schist; Tremolite marble.
		Schist zone 180-290m.	Garnet-biotite-quartz-schist; Garnet-mica-quartz-schist; Garnet-muscovite-feldspar-quartz-schist; Graphite-garnet-feldspar-quartz-schist; Staurolite-garnet-muscovite-biotite-quartz-schist; Garnet-hornblende-schist.
		*Quartzite zone 0-80m.	Quartzite intercalated with mica-quartz-schist containing metamorphosed quartz-conglomerate lenses.
		*Migmatitic meta-sediment zone	Migmatitic schist, quartzite subzone; Taxitic migmatitic subzone; Homogeneous migmatite subzone; Transitional white migmatite granite subzone.
Archaean	Red migmatitic granite, muscovitic gneissose and migmatitic granite		

* Ore-bearing horizons.

Table 2. Summary of Stratigraphy in the area of the Lianshanguan deposit.

IAEA

the Migmatitic schist and quartzite and Taxitic migmatite subzones (Table 2). To date, known mineralization extends down dip to a depth of about 300m.

Lenticular ore bodies occur at depth in three modes (Fig. 4).

A. Veins occur in interstratified breccia zones in the migmatitic metasediments zone and Taxitic migmatite subzone. The ore is mainly composed of pitchblende, metallic sulphides and detritus and breccia cemented by clay minerals. The size and location of the ore bodies depends upon the structure and form the contact between the Lower Proterozoic and Archaean rocks. In the convex part of the migmatite-metasomatic contact, tectonic fracturing is accompanied by more extensive mineralization. The main ore body occurs as lenses up to 5.6m in average thickness, 90m in length and 40m down dip. The grade is variable, with an average uranium content of 0.5%. The tonnage of uranium in the main ore body accounts for 75% of the total reserve of the Lianshanguan deposit.

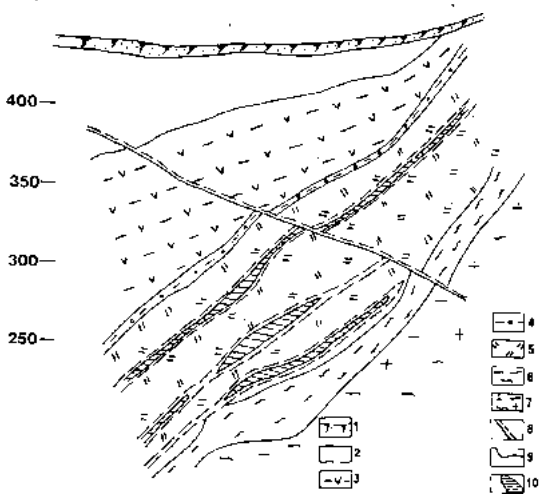


Figure 4. Schematic Cross Section No. VII
1. Slope wash; 2. Graphite-garnet-mica-feldspar-quartz schist; 3. Staurolite-garnet-muscovite-quartz schist; 4. Garnet-hornblende schist; 5. Quartzite intercalated with mica-quartz schist; 6. Migmatitic metasediments; 7. Red migmatitic granite; 8. Tectonoblastic zone; 9. Geological boundary; 10. Orebody.

B. Layered lenses are localized in mica-quartz-schist interbedded with uranium-bearing quartzite of the Quartzite zone and also in the Migmatitic metamorphic subzone. The lenses form the upper ore zone of the deposit. Uranium mineralization is distributed along the schistosity and gneissose foliation. The ore bodies measure approximately 200 by 15-40m, in plan they have discontinuous form, with thickness from 0.6 to 8.5m. The ore grade is lower than that of the veins and lenses-type mineralization, but is relatively uniform.

C. Irregular uranium-bearing veinlets are distributed in the homogeneous migmatite subzone; they are composed of pitchblende filling the shear-compressional fracture systems. Individual veinlets vary from ten centimetres to more than ten metres in length, and from millimetres to several centimetres in width. The intensity of mineralization depends upon the size and density of the fracture system. Veinlets of this type have no economic significance.

3. Mineralogy

The composition of the ore is similar to the composition of the host rocks; these rocks can be divided into 4 lithological varieties.

1) Cataclastic taxitic migmatite and breccia;
2) Microgneissic biotite migmatite;
3) Quartzite;
4) Mica-quartz-schist

Secondary uranium minerals are poorly developed and include gummite, uranophane, β-lambertite, kasolite, billietite, autunite and torbernite.

The main economic mineral is pitchblende, which occurs in both disseminated and massive forms. The disseminated pitchblende is distributed along the schistosity and

gneissosity, and also between other mineral grains. The massive pitchblende has colloform structure and is represented in vein, veinlet and cemented breccia forms. Microprobe analysis shows the pitchblende contains U 71.9%, Pb 3.0%, Si 1.8% and Ca 0.5%.

The primary ore contains minor amounts of metallic sulphides, such as pyrite, pyrrhotite, chalcopyrite, galena, sphalerite and molybdenite. The most common ore is pyrite. Native gold exists in small amounts. Maximum content of gold in samples reaches 0.3 g/t.

No elements other than uranium are economic. Analysis of associated elements indicates that U is positively correlated with Mo and Pb.

Wall rock alteration: With the exception of the alkalic metasomatism of the main stage of migmatization (1900 m.y.) in the middle and late stages of mineralization the alterations were fairly weak. Among these chloritization, sericitization and carbonization are spatially related with uranium mineralization. Chlorite veinlets cut or extend along the massive pitchblende. Sericite is closely associated with pitchblende. Fine-grained cryptocrystalline carbonates are concentrated in the rich ore shoots.

METALLOGENESIS

The characteristics of the Lianshanguan uranium deposit can be identified as follows:

1) The uranium mineralization is mainly situated in a metamorphosed detrital sequence at the base of the Lower Proterozic Liaohe Group and its migmatitic lower part. The main host rock is grey and black-grey quartzite, generally rich in clay, iron, carbon, sulphur and other impurities. In this region, the uranium content of ore-bearing horizons averages 25 ppm, with the maximum content up to 35 ppm. In the uranium-bearing quartzite, microcrystalline pitchblende is in the metamorphic minerals (garnet, tourmaline, biotite, chlorite and so on) or/and associated with them.
2) Uranium ore bodies occur in the transitional zone between metamorphic and migmatitic sequences and are tectonically controlled in fracture zones. Pitchblende in the form of veins and veinlets is localized in the interstratified breccia zones, and forms rich ore-shoots where the migmatite is in irregular contact with metamorphic rocks.
3) Wall-rock alteration is rather weak and mainly reflected by chloritization and sericitization.
4) The composition of the ore is simple; the primary uranium mineral is pitchblende. The age of mineralization is about 1800 m.y.

Genesis of the deposit was probably complex. It is possible that the original shallow-sea detrital sediments contained low-grade uranium mineralization. During regional metamorphism uranium in quartzite was mobilized and concentrated initially. Migmatization associated with regional metamorphism probably caused the remobilization of uranium and yielded the ore-bearing hydrothermal solution from which uranium was deposited in the favourable fracture zones to form the rich orebodies.

The deposit has not yet been studied in detail. The suggested genesis is preliminary and further investigations are required.

LE GISEMENT D'OKLO ET SES REACTEURS DE FISSION NATURELS

F. Gauthier-Lafaye,[1] F. Weber,[1] R. Naudet,[2] J.P. Pfiffelmann,[3] R. Chauvet,[4] B. Michel,[4] et J.C. Reboul[4]

1. Centre de Sédimentologie et Géochimie de la Surface (C.N.R.S.), Strasbourg, France.
2. Commissariat à l'Energie Atomique — France.
3. Mokta, Paris, France.
4. Compagnie des Mines d'Uranium de Franceville, Mounana, Gabon.

ABSTRACT

In the uranium deposit of Oklo (Republic of Gabon), seven zones have been discovered since 1972, in which natural fission reactions took place.

Since 1974, a thorough geological study of these zones has been undertaken. It includes field studies, observations of drilled samples and laboratory studies. These studies permit the authors to define the geological environment of the reactors (from sedimentological, tectonic, petrographic and mineralogical view points) and to point out the influence of nuclear reactions on the surrounding formations. All this work was completed by a geological and metallogenic study of the deposit of Oklo and of the uraniferous basin of Franceville.

The deposit of Oklo is situated in a detrital, sandstone-like and pelitic series belonging to the Francevillian. The Francevillian and the mineralization are dated as Middle Precambrian (1800-2000 M.A.).

The ore of Oklo is the result of two concentration stages. In the first, uranium seems to have been fixed by hydrocarbons that were concentrated in oil traps. After a tectonic event, circulations of oxidizing solutions generated reconcentrations that are associated with hematite and have contents of UO_2 between 1 and 20%.

The fission reactions developed in the high-graded ores which had formed during the last phase of UO_2 concentration. A thorough tectonic analysis of the ore deposit shows that high-graded ores and fission reactors are controlled by fractures.

The working of nuclear reactors results in a local increase of temperature which gave a rise to circulation of warm water. The results of this hydrothermal circulation and of the neutron bombardment are seen in a succession of facies surrounding the reactors. At the centre of the reactor all sedimentary structures have been destroyed within the reaction zone the following clays mineral zones are founded: (1) 1 Md illite and ferrous chlorite corresponding to the common Francevillian sediment; (2) 2 Md illite, (3) magnesium chlorite and (4) 1 Md illite and chlorite-vermiculite in the very rich uraninite ore. These dydrothermal circulations also caused removal of silica toward the outer zones which reacted affecting the geometry of the reactors by fracturing.

INTRODUCTION

En 1972, une anomalie dans la composition isotopique d'un minerai d'uranium en provenance du Gabon été découverte par les laboratoires de C.E.A. Très vite, il a été démontré que ce minerai provenait du gisement d'Oklo et que cette anomalie de composition isotopique était due à la présence, dans ce gisement, de zones ayant été le siège de réactions de fission naturelles (Bodu *et al.*, 1972; Neuilly *et al.*, 1972).

En 1974 et dans le cadre du 'Projet Franceville', une étude géologique détaillée des réacteurs de fission a été entreprise. Cette étude, encore en cours, comprend des relevés géologiques qui s'effectuent durant l'exploitation des zones de réaction, des études sur carottes de sondage et d'importants travaux en laboratoire qui font intervenir de nombreux centres de recherche.

PRESENTATION DE FRANCEVILLIEN ET DU GISEMENT D'URANIUM D'OKLO

Le Francevillien

Le Francevillien est une série détritique et volanco-sédimentaire, non métamorphique du Précambrien moyen qui affleure dans le quart SE de la République du Gabon (Fig. 1).

Les mesures radiochronologiques effectuées sur la fraction argileuse des sédiments du Francevillien par les méthodes K-Ar et Rb-Sr et les études sur les réacteurs d'Oklo amènent à proposer un âge de sédimentation du Francevillien antérieur à 2000 M.A. L'âge de 2600

M.A. mesuré sur le substratum métamorphique du Francevillien donne une limite extrême pour l'âge da la sédimentation de cette série (IAEA, 1975; IAEA, 1978).

D'un point de vue stratigraphique, la série du Francevillien est subdivisée en 5 formations (Weber, 1968) qui sont, de la base vers le sommet (Fig. 2): le FA, essentiellement gréso-conglomératique, d'origine fluviatile et fluvio-deltaïque, le FB à dominante pélitique et ampélitique à la base (FB_1), puis plus gréseux au sommet (FB_2), et les formations, FC, FD et FE volcano-sédimentaires avec, dans la formation FC, un épisode plus chimique (jaspes, dolomies).

La minéralization se localise toujours dans le FA.

Le degré de diagenese subi par les grès FA du Bassin de Franceville a été estimé par des

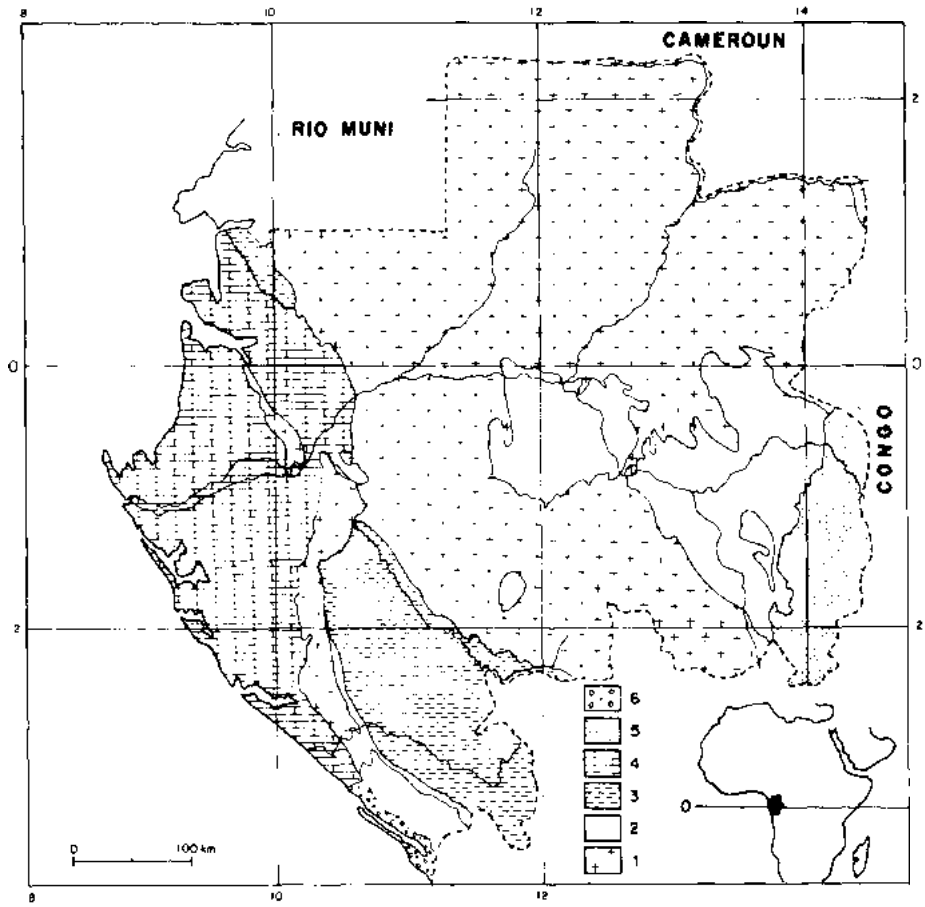


Figure 1a. Esquisse Géologique du Gabon. *Geological sketch of Gabon.*

1. Précambrien Inférieur
1. Lower Precambrian
2. Précambrien moyen
2. Middle Precambrian
3. Précambrien Supérieur
3. Upper Precambrian
4. Secondaire et Tertiaire
4. Mesozoic and Cainozoic
5. Tertiaire des plateaux Batéké
5. Tertiary of the Bateke plateaux
6. Quaternaire
6. Quaternary

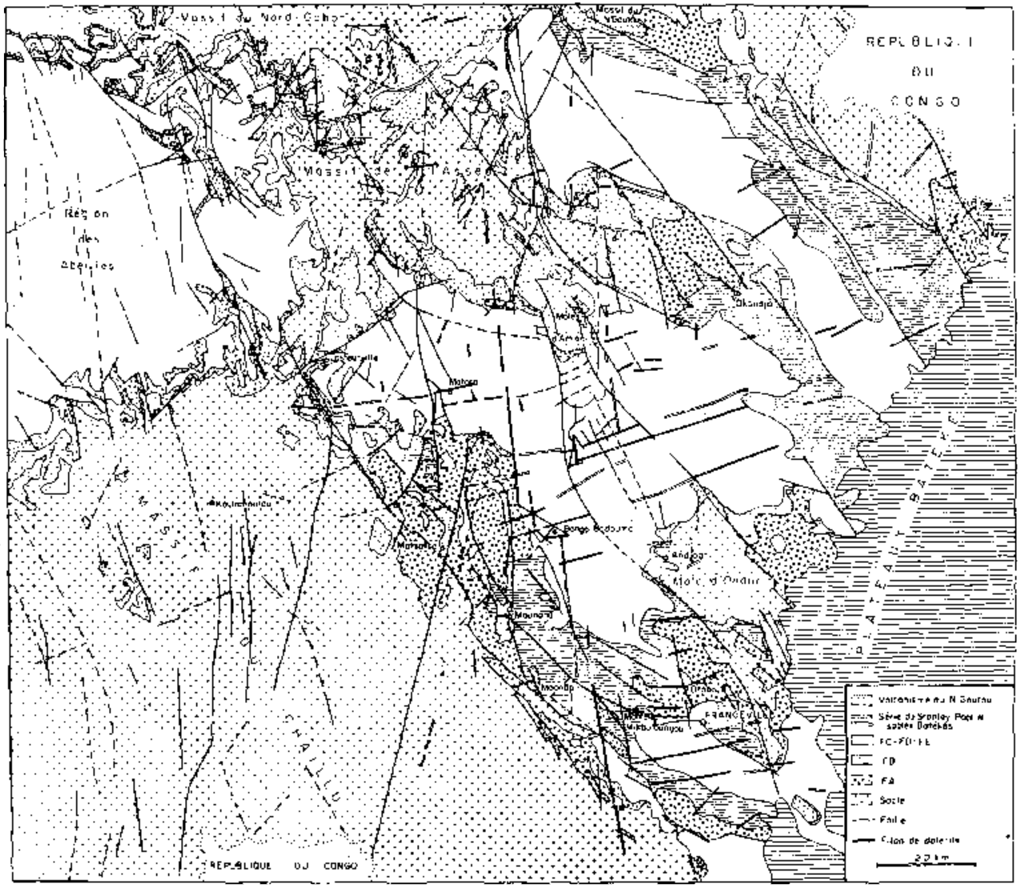


Figure 1b. Carte géologique simplifee du Bassin du Francevillien. (D'après la carte au 1/500 000 de Franceville O et E 1968, BRGM).
Simplified geologic map of the Francevillien Basin.

IAEA

études pétrographiques, l'étude au R.X. de la fraction argileuse des grès (IAEA, 1978) (Indice de cristallinité et types polymorphes de l'Illite) des études sur les matières organiques (IAEA, 1978) et sur les inclusions fluides contenues dans les auréoles de silices secondaires entourant les quartz détritiques (IAEA, 1978). On estime qu'une température voisine de 200°C (238 ± 17° selon (Openshaw *et al.*, 1978) par l'étude des inclusions fluides) peut être retenue comme température maximum subie par les sédiments au cours de la diagenèse sous un enfouissement de 3000 à 5000m.

Les gisements d'uranium du Francevillien se localisent tous dans le bassin de Franceville où ils constituent un groupe de 4 gisements qui bordent une remontée de socle (Fig. 3). Ce sont les gisements de Boyindzi, Mounana, Oklo et Okelobondo. Ce dernier gisement constitue la prolongation méridionale du gisement d'Oklo. Tous ces gisements sont impliqués dans des structures tectoniques en décrochement.

Le Gisement d'Oklo

Le gisement d'Oklo s'étend plus ou moins uniformément sur 900m dans le sens N-S et 600m dans le E-W. Il se prolonge sur 1km vers le Sud pour former le gisement d'Okelobondo (Fig. 4).

Sédimentologie du gisement d'Oklo

L'essentiel de la minéralization uranifère se situe dans les derniers niveaux de grès du FA supérieur, dans un épisode sédimentaire de 7 à 8m de puissance appelé 'couche C1' surmonté des pélites FB.

A Oklo, la 'couche C1' est composée de 6 séquences pélitiques à conglomératiques bien définies (Fig. 5). Elles appartiennent à une grande structure sédimentaire orientée N-S qui longe la boutonnière de socle de Mounana. Vers le Sud, au niveau du gisement d'Okelobondo, cette structure est un chenal plus ou moins divaguant où la 'couche C1' est épaissie et à dominante de grès grossiers et conglomératiques. Vers le Nord, ce 'chenal' s'étale en une vaste zone d'épandage où la 'couche C1' est plus mince, présente une granulométrie plus fine et surtrout des séquences à plus grande extension latérale. C'est dans cette zone d'épandage que se situe la gisement d'Oklo.

Tectonique du gisement d'Oklo

L'analyse tectonique du gisement d'Oklo a fait apparaître deux types de structures majeures (IAEA, 1975; IAEA, 1978). Le premier type est la large flexure subméridienne qui borde l'Est de la boutonniere de Mounana. Elle est responsable du pendage moyen des couches de 30° à 40° vers l'Est. Cette flexure donne au gisement d'Oklo l'allure d'un piège structural comparable aux pièges du type pétrolier.

Le deuxième type de structure est un système de décrochements orienté N 140 qui découpe la flexure subméridienne suivant une maille décamétrique. Les mouvements de coulissage plus ou moins importants le long de ces décrochements se compensent par la formation de plis métriques à hectométriques aux axes orientés N 50° à N 60° et pentés de 40° vers le NE.

La Minéralization Uranifère à Oklo: hypothèses sur la genèse du gisement

Les études pétrographiques effectuées sur le minerai d'Oklo ont montré que l'essentiel de la minéralization se présente sous forme de pechblende et que les minéraux à U^{6+} sont rares et toujours rattachés à des remaiements secondaries (IAEA, 1975).

A Oklo, la pechblende est, soit en inclusion dans des matières organiques (IAEA, 1975), soit associée à des fronts d'oxydo-réduction. Ces deux cas nous permettent de distinguer deux types de minerai qui se sont formés suivant des processus différents (Gauthier-Lafaye, 1977).

Dans le premier cas, le minerai (minerai I) correspond à un grès noir, silicifié riche en pyrite et matière organique dont la teneur en UO_2 est de quelques ‰ à quelques %. Les études entreprises sur les matières organiques (IAEA, 1978), ont montré que celles-ci

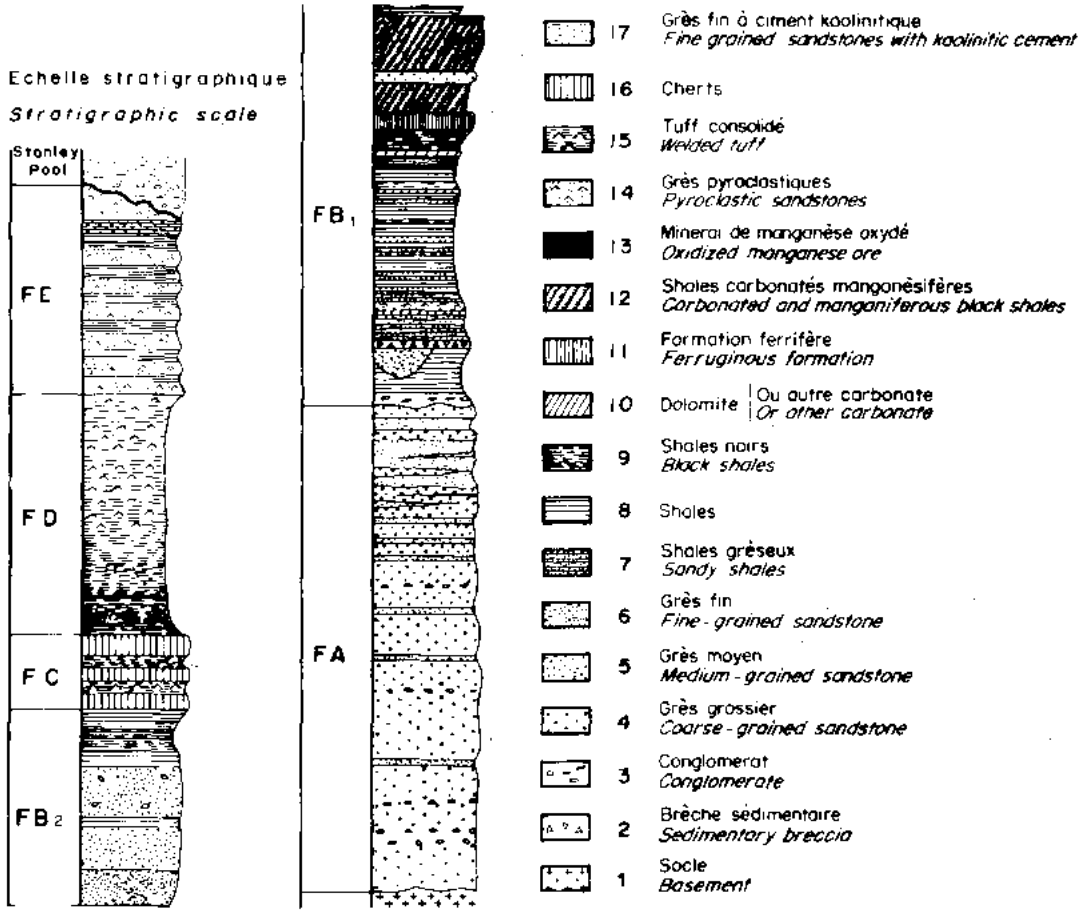


Figure 2. Coupe stratigraphique du Francevillien dans le Bassin de Franceville. *Stratigraphic section of the Francevillian series in the Franceville Basin.*

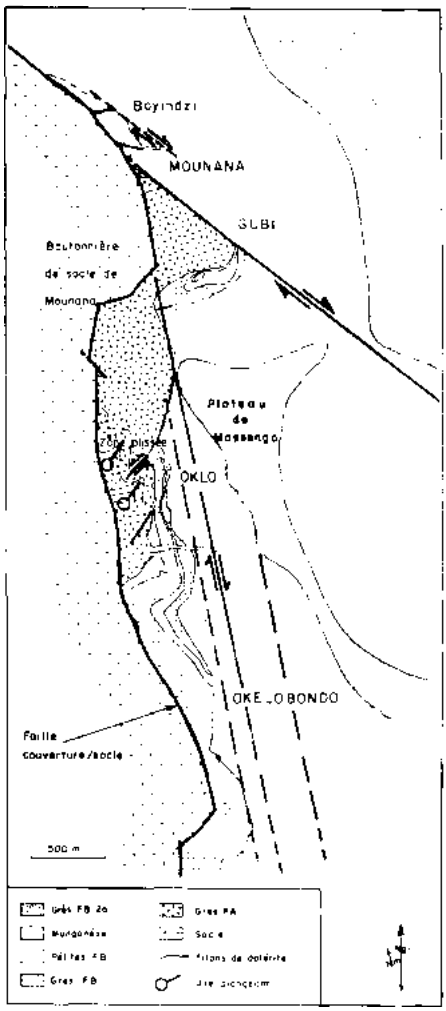


Figure 3. Carte du secteur E boutonnière de Mounana. *Map of eastern sector of Mounana Inlier.*

étaient essentiellement des bitumes correspondant à d'anciens hydrocarbures migrés ayant subi une diagenèse à gaz.

Dans le deuxième cas, le minerai est constitué d'un grès peu à pas silicifié, noir à 'taches' hématiteuses, dont la teneur UO_2 varies de 5 à 20% (minerai II). La minéralization se répartit autour de taches hématiteuses dont elle est séparée par une frange décolorée centimétrique. La frontière entre taches hématiteuses et grès minéralisés apparaît ainsi comme un petit front d'oxydo-réduction d'échelle décimétrique.

Ce type de minerai est généralement associé à des zones fortement tectonisées. L'uranium tapisse des plans de micro-fractures qui affectent les quartz et la matrice argileuse des grès.

Le modèle métallogénique proposé ici considère trois étapes importantes dans la mise en place des concentrations uranifères à Oklo. Les deux premières étapes sont à l'origine du minerai I. Elles aboutissent à l'élaboration d'un gisement à hydrocarbure et à l'introduction d'uranium au sein de ce gîte. L'Uranium est amené, soit par des solutions oxydantes qui sont connues dans les zones périphériques du gisement, soit directement par les hydrocarbures.

La troisième étape est une étape de surconcentration qui aboutit à la formation du minerai II. Elle implique la circulation de solutions oxydantes dans des zones tectonisées qui remobilisent l'uranium contenu dans le minerai I et le concentrent plus en 'aval' lorsqu'elles ont perdu leur pouvoir oxydant.

LES REACTEURS DE FISSION NATURELS D'OKLO

Les gisements d'Oklo et Okelobondo renferment 3 groupes de 'réacteurs' qui s'alignent suivant une direction N 140° en s'approfondissant vers le SE (Fig. 4).

Le premier groupe se situe à l'extrémité Nord du gisement d'Oklo, sur le pourtour d'un pli d'axe orienté N 50°. Il s'étend sur une longueur de 140m et comprend 4 zones de réaction numérotées dans l'ordre de leur découverte. Ce sont, du N vers le S les zones 1, 2, 5-6 et 3-4. Leur exploitation est maintenant achevée.

Le deuxième groupe de réacteurs, découvert récemment, se situe à 200m au Sud de premier. Il comporte, du Nord vers le Sud, les zones 7, 9 et 8 qui s'étendent sur une trentaine de mètres. Son exploitation est actuellement en cours. Enfin, le troisième groupe se situe dans le gisement d'Okelobondo. Ces réacteurs, accessibles que par sondage et sous 400m de

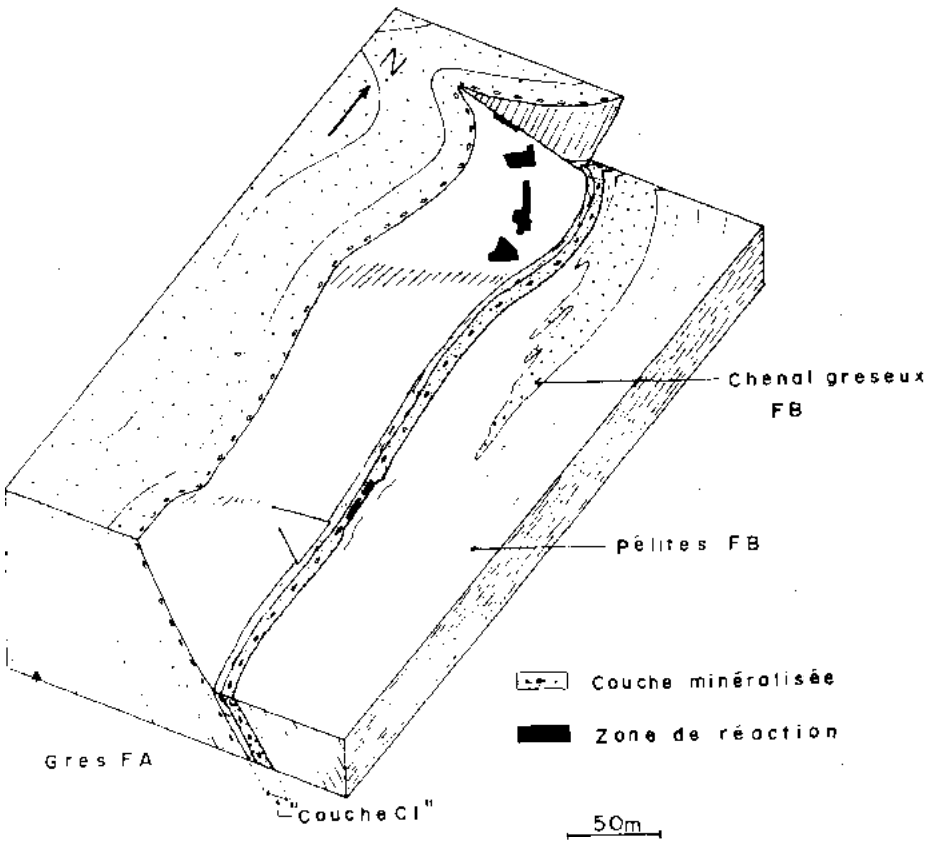


Figure 4. Bloc diagramme schématique de la structure d'Oklo.
Schematic block diagram of the structure at Oklo.

couverture pélitique, sont encore très mal connus. Leur extension n'a pas encore pu être précisée.

Description géologique des réacteurs

Sur le terrain, les réacteurs se caractérisent par la présence d'un minerai particulièrement riche (U 25 a 50%) entouré d'une gangue argileuse totalement depourvue de quartz et formant les épontes (Fig. 6). C'est ce minerai riche ou 'faciès pile' qui est entré en réaction. Les argiles sont vertes ou noires et dépourvues de toute structure sédimentaire à l'approche du faciès pile. Elles constituent un faciès bien particulier qui n'est connu nulle part ailleurs dans le Francevillien et dans l'environnement d'Oklo.

L'étude des sondages et des coupes géologiques traversant les zones de réaction montre que la présence d'un réacteur s'accompagne toujours d'une diminution de puissance de la 'couche C1' (Fig. 6). Cette diminution de puissance est due à la disparition de certaines séquences gréseuses de la couche et leur 'remplacement' par les argiles et le faciès pile. Dans certaines zones, cette 'argilisation' peut affecter l'ensemble de la 'couche C1' qui est alors constituée de 3 a 4m d'argile depuis le conglomérat du mur jusqu'aux pélites du FB. Des

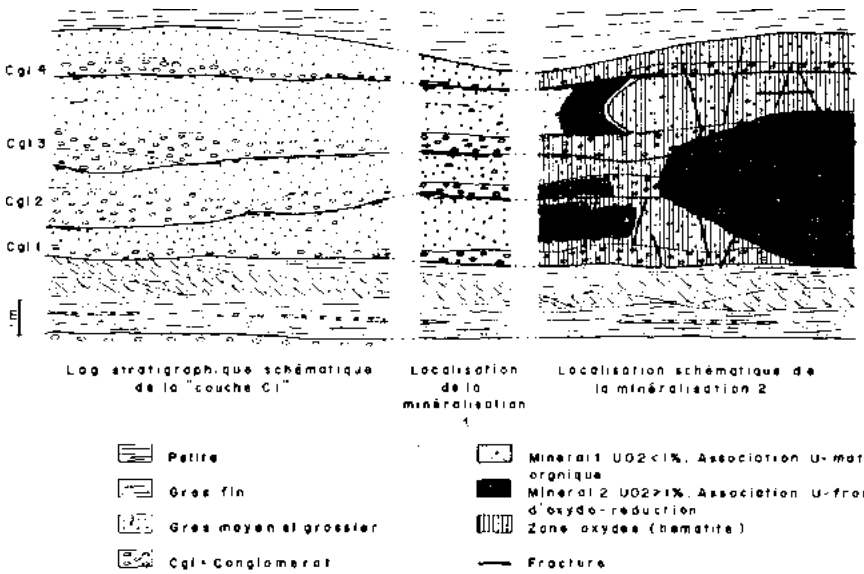


Figure 5. Stratigraphie de la 'couche C1' minéralisée d'Oklo. Localization des différents types de minéralization.
Stratigraphy of the 'couche C1' mineralization at Oklo, and locality of the different types of mineralization.

images particulières comme l'effondrement du toit de 'C1' compensent fréquemment cette diminution de puissance de la couche.

Dans l'espace, l'épaisseur totale de la gangue argileuse et du 'minerai pile' varie entre 0,2 à 3m sur des longueurs pouvant atteindre 15 à 20m suivant les zones. Cet ensemble, plus ou moins concordant aux plans de stratification a une géométrie qui est guidée par des systèmes de fractures bien définis: fractures associées au dôme et décrochements N 140 et N 0 pour l'essentiel.

Description pétrographique et minéralogique

Les descriptions qui vont suivre ne concernent que les réacteurs situés à l'extrémité Nord du gisement d'Oklo. Les études sur les réacteurs situés plus au Sud sont actuellement en cours. Les premières observations faites sur ces zones de réaction nous permettent cependant de dire que si les différents faciès associés aux réacteurs présentent le même aspect macroscopique — ils ont cependant la particularité d'être très riches en matière organique. Cette dernière, presque totalement absente dans les zones de réaction Nord, est ici souvent présente dans le coeur des réacteurs ou en tapissage dans les plans de fracture.

Les études pétrographiques et minéralogiques ont mis en évidence, autour des zones de réaction Nord plusieurs auréoles qui peuvent se caractériser par la nature de leurs minéraux phylliteux. Depuis la périphérie des 'réacteurs' vers le coeur, la succession des auréoles est la suivante (Fig. 7):

— auréole à illite 1 Md et à chlorite ferrifère: ces minéraux appartiennent au sédiments communs du Francevillien;
— auréole à illite 2 M: elle apparaît à une distance de 1 à 2 mètres du 'faciès pile';
— auréole à chlorite magnésienne;
— auréole à illite 1 M et à chlorite-vermiculite: hématite et leucoxènes sont abondants.

A partir de l'auréole à illite 2 M, jusque dans l'auréole à chlorite magnésienne, on observe une dissolution des quartz détritiques et un effacement progressif de toutes les

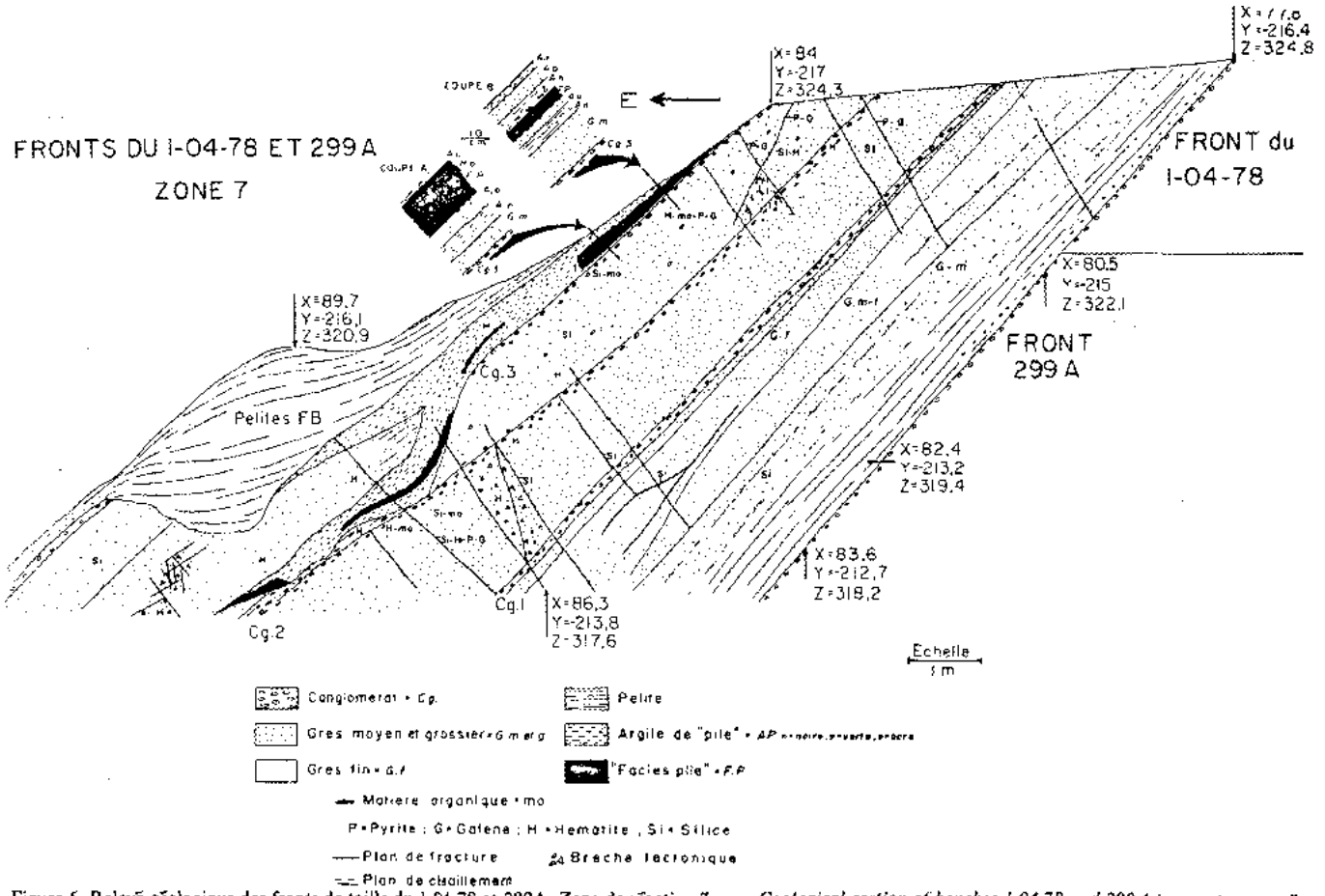


Figure 6. Relevé géologique des fronts de taille du 1.04.78 et 299A. Zone de réaction 7. *Geological section of benches 1.04.78 and 299A in reaction zone 7.*

IAEA

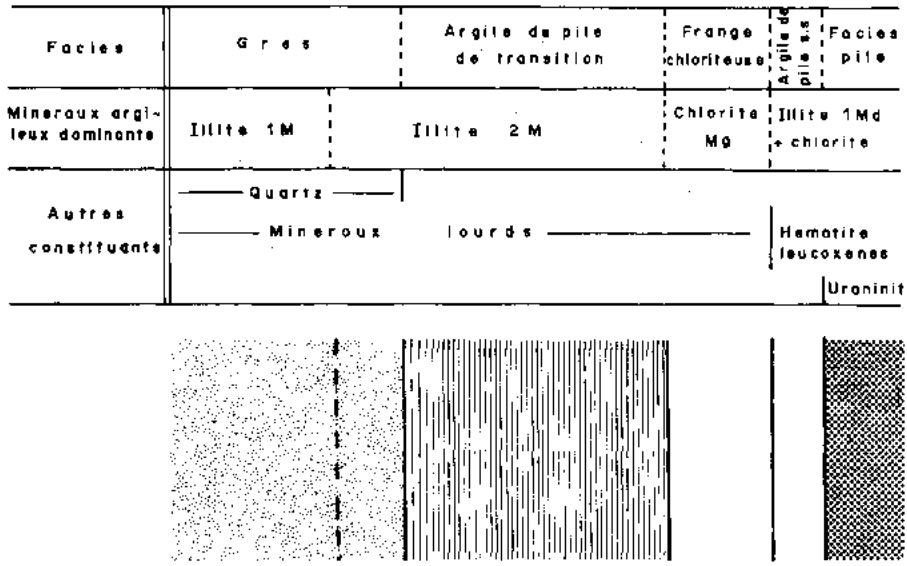


Figure 7. Répartition schématique des minéraux au voisinage des zones de réaction.
Schematic distribution of the minerals in the vicinity of the reaction zones.

structures sédimentaires d'échelles macroscopiques à microscopiques. Dans les zones externes (zones à illite 2 M ou à chlorite magnésienne suivant les cas), une épigénie des quartz par de la séricite est observable: dans ce cas les structures sédimentaires sont encore conservées. Dans la zone à illite 1 M, le disparition des quartz est toujours totale et les argiles ont ici une structure cryptocristalline. Selon (Vidale, 1977), certaines chlorites de l'environnement des réacteurs dériveraient de biotites néoformées pendant les réactions puis rétrogradées.

Dans le coeur du 'réacteur', l'UO_2 est cristallisé sous forme d'uraninite, ce qui le distingue du minerai 'normal' (à teneur isotopique normale) d'Oklo ou seule la pechblende est présente (Geffroy & Lissilour, 1974). L'uraninite est associée à l'illite 1 M et à la chlorite-vermiculite. L'illite 2 M peut parfois persister mais toujours en quantité mineure. L'hématite et les leucoxènes sont abondants.

Interprétation

La gangue argileuse des zones de réaction résulte d'une désilicification des grès de la 'couche C1'. Cette désilicification s'accompagne de transformations chimiques et minéralogiques des argiles intitiales qui sont liées au fonctionnement des réactions nucléaires.

L'effet thermique le plus net associé au fonctionnement des réacteurs est la transformation des illites 1 M en illite 2 M, qui ne se manifeste que dans l'auréole la plus externe et non dans le coeur. Les argiles du coeur ont en effet été destructurées par le bombardement neutronique et n'ont recristallisé qu'après l'arrêt des réactions, durant le refroidissement. Au contraire, dans les épontes, à une distance trop grande pour subir l'effet des neutrons, les minéraux phylliteux ont enregistré l'effet thermique des réactions. Cet effet thermique ne se manifeste toutefois qu'à une distance relativement faible du coeur: 1,5 à 2m, ce qui est très peu, compte tenu de la quantité de chaleur dégagée au cours des réactions. Ceci montre que l'évacuation de chaleur devait se faire plus par circulation d'eau dans les fractures que par conduction à travers les terrains encaissants. On peut penser que les

réactions nucléaires ont déclenché un véritable siphon thermique drainant, à travers les fractures, les eaux de la nappe des grès. Ces eaux étaient minéralisées et contenaient en particulier du magnésium qui s'est fixé dans la gangue du minerai et ses épontes, induisant la cristallization de chlorites magnésiennes. Ces circulations d'eau ont également participé à l'élimination massive de la silice entraînant ainsi une concentration en UO_2 et la formation du 'faciès pile'. Cette désilicification autour des réacteurs a également favorisé la propagation des réactions de fission.

CONCLUSION

La présence de réacteurs de fission dans le gisement d'Oklo est attribuée à la convergence de plusieurs circonstances favorables dont les principales sont:

1) l'âge ancien du gisement 2000 M.A.
2) une métallogénie particulière qui aboutit à l 'élaboration d'un minerai à forte teneur en UO_2 (10 à 20.%)
3) une fracturation importante des minerais riches en UO_2. Cette fracturation favorise les circulations d'eau qui sont favourables au déclenchement des réactions nucléaires et à leur propagation.
4) une géochimie favorable et en particulier l'absence de 'poison' comme B ou V par exemple.

D'un point de vue géologique, le déclenchement de réaction de fission se marque principalement par la mise en place d'un phénomène hydrothermal auquel est associé des transformations géochimiques et minéralogiques bien particulières et des perturbations géométriques décamétriques à microscopiques des roches encaissantes.

REFERENCES

Bodu, R., Bouzigues A., Morin N. & Pfiffelmann, J.P., 1972: Sur l'existence d'anomalies isotopiques rencontrées dans l'uranium du Gabon. *C.R. Acad. Sci. Paris, sér. D 275,* 1731.

Dunoyer de Segonzac, G., 1969: Les minéraux argileux dans la diagenèse. Passage au métamorphisme. *Mém. Serv. Carte Géol. Als-Lorr., 29.*

Gauthier-Lafaye, F. 1977: Oklo et les gisements d'uranium du Francevillien aspects tectonique et métallogénique. *Ph.D. Thesis, University of Strasbourg,* 81p (unpubl.).

Geffroy, J. & Lissilour, J., 1974: Étude microscopique des minerais uranifères d'Oklo. *Bull. Inf. Sci. Tech. (Paris), 193,* 51-58.

IAEA, 1975: *The Oklo Phenomenon. Proceedings of a Symposium, Libreville.* International Atomic Energy Agency, Vienna.

IAEA, 1978: *Natural Fission Reactors — Les Reacteurs de Fission Naturels. Proceedings of Technical Committee Meeting, Paris.* International Atomic Energy Agency, Vienna.

Neuilly, M., Bussac, J., Frejacques, C., Nief, G., Vendryes, G. & Yvon, J., 1972: Sur l'existence dans un passé recule d'une réaction en chaîne naturelle de fission, dans le gisement d'uranium d'Oklo (Gabon). *C.R. Acad. Sci. Paris, 275,* 1847-1849.

Openshaw, R., Pagel, M. & Poty, B., 1978: Phases fluides contemporaines de la diagenèse des grès, des mouvements tectoniques et du fonctionnement des réacteurs nucléaires d'Oklo (Gabon). *in, Natural Fission Reactors — Les Reacteurs de Fission Naturels. Proceedings of Technical Committee Meeting, Paris.* International Atomic Energy Agency, Vienna, 267.

Vidale, R.J., 1977: The highest temperatures recorded by the Oklo mineral phase assemblages and rock textures. *in, Natural Fission Reactors — Les Reacteurs de Fission Naturels. Proceedings of Technical Committee Meeting, Paris.* International Atomic Energy Agency, Vienna, 235-240.

Weber, F., 1968: Une série précambrienne du Gabon: le Francevillien; sédimentologie, géochimie. Relation avec les gîtes minéraux associés. *Mém. Serv. Carte Géol. Als-Lorr., 28,* 328p.

URANIFEROUS PHOSPHORITE AND APATITE-BEARING GNEISSES IN THE PROTEROZOIC OF FINLAND

Olli Äikäs

Geological Survey of Finland, P.O. Box 237, SF-70101 Kuopio 10, Finland

ABSTRACT

Uranium is known to occur in the Proterozoic of Finland (1) within the Lower Proterozoic/Archaean boundary zone, (2) as strata-bound mineralizations in the Lower Proterozoic (Karelian) quartzites, (3) in albitite and albite diabase dykes cutting across these quartzites, (4) as uraninite-carbonate veins in a Lower Proterozoic (Karelian) greenstone-phyllite formation in northern Finland, (5) in migmatized Lower Proterozoic (Svecofennian) schists in southern Finland, and (6) in metamorphic phosphatic rocks of the Lower Proterozoic (both Karelian and Svecofennian) schist belts. However, the uranium occurrences found so far are too small or of too low grade to be of economic importance for the present. Here, the uranium- and phosphorous-bearing (U-P-type) occurrences at Nuottijarvi, Lampinsaari, and Temo are briefly described, and the characteristics of this type of uranium mineralization are summarized. The U-P occurrences are usually bedded, and the host rocks include fine-grained apatite-quartz-feldspar rock, and apatite-bearing or phosphorite-banded dolomite and skarn rock. Uranium occurs as uraninite crystallites within the apatite grains; it may also be contained in the apatite as a substitute for calcium. The grade of the occurences is usually 0.03-0.04% U and 3-5% P_2O_5, and their Th content less than 10 ppm. Radiometric U-Pb dates indicate that the U-P occurrences were most probably deposited 1900-2080 Ma ago and were subjected to regional metamorphism about 1880 Ma ago. The metamorphic grade varies from intermediate greenschist to high amphibolite facies. The U-P occurrences are interpreted to be syngenetic and of marine sedimentary or mixed sedimentary and volcanic origin. It is also suggested that the uraniferous phosphatic rocks and other Proterozoic phosphorite occurrences in Finland and Sweden may belong to a possible Lower Proterozoic phosphogenic province of the Baltic shield.

INTRODUCTION

As early as the 1950s, uranium exploration in Finland was based on geological analogies with uraniferous formations elsewhere in the world. As a result, several small uranium occurrences were discovered, most of them in the Proterozoic rocks. On the basis of the recent findings of major uranium deposits in the Proterozoic of Australia and Canada, it may be said that geological analogies are now even more important than before in guiding uranium exploration in Finland.

Excepting a small area of Palaeozoic rocks, the bedrock of Finland belongs to the Precambrian ranging from Archaean to Middle Proterozoic. The Archaean basement

Age, Ma	Episode	Rocks
1250-1300	Postjotnian instrusion	diabase
1300-1400	Jotnian sedimentation	sandstone, siltstone
1540-1700	Postorogenic intrusion	rapakivi granites
	SVECOKARELIAN OROGENY:	
1860-1900	Synorogenic intrusion	mainly granitic intrusive and plutonic rocks
2100-	Sedimentation and volcanism: SVECOFENNIAN KARELIAN — Kalevian; Marine Jatulian; Jatulian	schists and gneisses
2425-2450	Prejatulian intrusion	mafic intrusive rocks

Table 1. Geochronology of the Proterozoic of Finland, after Kouvo (1976) and Vaasjoki (1977).

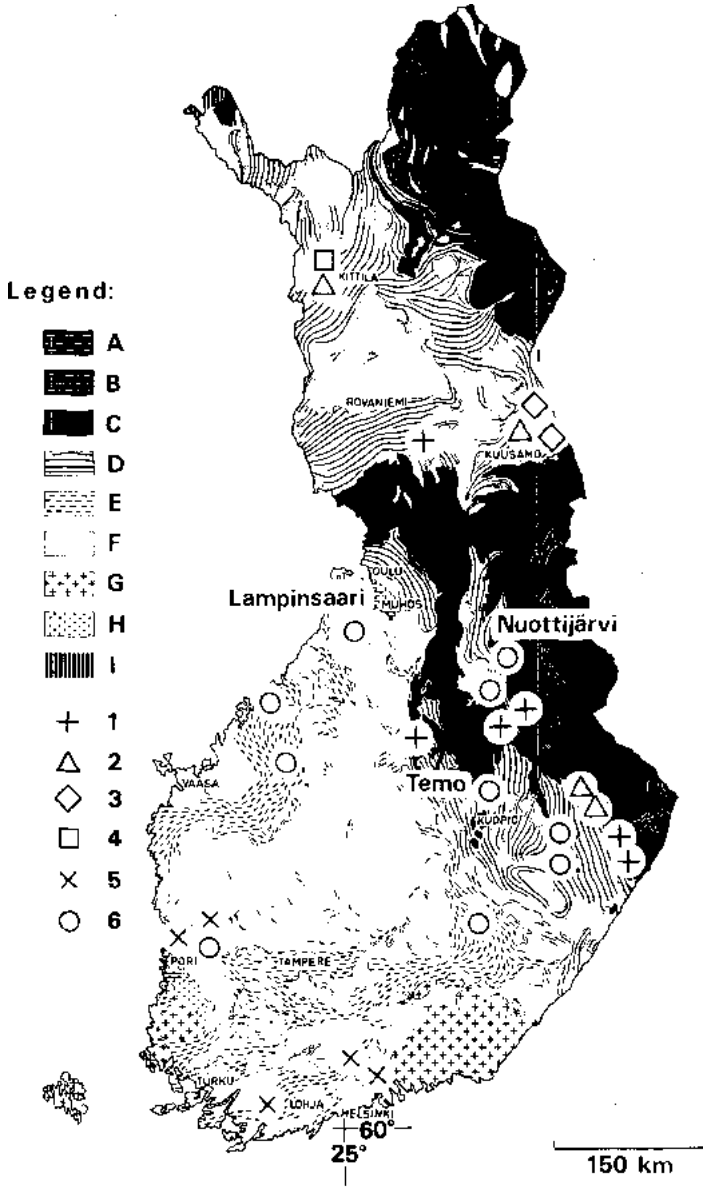


Figure 1. Main lithologic units and Proterozoic uranium occurrences of Finland, compiled after geological and ore deposit maps (Simonen, 1971; Kahma *et al.*, 1976) as well as unpublished reports of Outokumpu Oy and the Geological Survey of Finland. Lithology: — Archaean: (A) schist and paragneiss; (B) granulite; (C) orthogneiss; — Proterozoic: (D) Karelian schists; (E) Svecofennian schists; (F) Svecokarelian intrusive and plutonic rocks; (G) rapakivi granites; (H) Jotnian sedimentary rocks; — Phanerozoic: (I) Caledonian schists. Symbols 1-6 denote the uranium occurrences of (1) Proterozoic/Archaean boundary zone; (2) quartzite areas; (3) albitite zone; (4) veined-type (Pahtavuoma deposit); (5) migmatite zone; (6) U-P zone.

complex in eastern and northern Finland (Fig. 1) is composed of granitic and granodioritic ortho- and paragneisses, with zones of metasediments and metavolcanics about 2800 Ma old. The Proterozoic began with the emplacement of mafic and ultramafic intrusions in northern Finland (Table 1). The deposition of the Lower Proterozoic Svecokarelian sedimentary and volcanogenic rocks started with the transgressive mature Jatulian sediments on the marginal areas of the Archaean craton, the minimum age for the Jatulian quartzites being 2100 Ma. The upper part of the Karelian metasediments (Kalevian) and the Svecofennian supracrustal rocks were deposited about 1900-2000 Ma ago, representing the main phase of the Svecokarelian sedimentation. According to radiometric dating of the synorogenic intrusive rocks, the culmination of the Svecokarelian orogeny took place about 1860-1900Ma ago, causing the regional metamorphism of the Svecokarelian supracrustal rocks, now known as the Karelian and Svecofennian schist belts.

In western and southern Finland, postorogenic rapakivi granite and Jotnian (Upper Proterozoic) sedimentary rocks cover small areas.

URANIUM IN THE PROTEROZOIC OF FINLAND

The uranium occurrences in the Proterozoic of Finland can be divided into six groups, according to their relation to the Svecokarelian lithostratigraphy (Fig. 1). The potential uranium-bearing zones delineated on the basis of this classification (Fig. 2) indicate middle and northern Finland as the most critical areas for uranium exploration. The following supplements the division worked out by Sarikkola (1974):

1) Within the Archaean basement complex, near the contact between Lower Proterozoic and Archaean, a few occurrences exist with a mineral association of uraninite, molybdenite, and in some cases coarse-grained fluorapatite in closely spaced lenses or veins of biotite-rich pegmatoids. Thorium is also present.
2) Strata-bound uranium mineralizations occur in the Jatulian quartzites from eastern to northern Finland. The mineralizations are comparable to the tecto-lithologic sandstone type of uranium deposits (Dahlkamp, 1978); they have also been called the U-V-type occurrences (Piirainen, 1978). The most important of these occurrences are the deposits at Paukkajanvaara, Eno (Piirainen, 1968) and Kesänki, Kolari (Ketola *et al.*, 1975). The grade of these deposits is 0.12 and 0.06% U, respectively. At Paukkajanvaara, uranophane is the main ore mineral with subordinate pitchblende, gummite, and meta-autunite (Piirainen, 1968).
3) In northern Finland, uraninite disseminations and uraninite-carbonate veins have been found in albitite and albite diabase dykes cutting across the Jatulian quartzites (Sarikkola, 1974; Piirainen, 1978). In addition to the uraninite, there occur davidite and chalcopyrite as well as, in places, selenide and telluride minerals.
4) Uraninite-carbonate veins intersect the Pahtavuoma copper deposit in a Karelian (Lower Proterozoic) greenstone-phyllite formation in northern Finland (Ketola, *et al.*, 1975). This veined-type of uranium mineralization appears to be a favourable target for future exploration.
5) In the intensively migmatized Svecofennian (Lower Proterozoic) schists in southern Finland, a few uranium- and thorium-bearing occurrences are known, mostly connected with granitic and pegmatitic parts of the migmatites. Uranium-bearing minerals in these occurrences are uraninite, zircon, monazite, and allanite.
6) Uraniferous phosphatic rocks, commonly associated with calcareous metasediments, have been found in both the Karelian and Svecofennian (Lower Proterozoic) schist belts. In the following, these occurrences are called the U-P deposits.

URANIFEROUS PHOSPHATIC OCCURRENCES

Since 1959, a dozen occurrences of uraniferous phosphatic rocks have been discovered in Finland, most of them by the exploration department of the Outokumpu Oy mining company. In 1975, when research on this type of mineralization was started, ten occurrences were known. Here, the deposits at Nuottijärvi, Lampinsaari, and Temo (Fig. 1), are briefly described, and the characteristics of the occurrences of the U-P-type are presented.

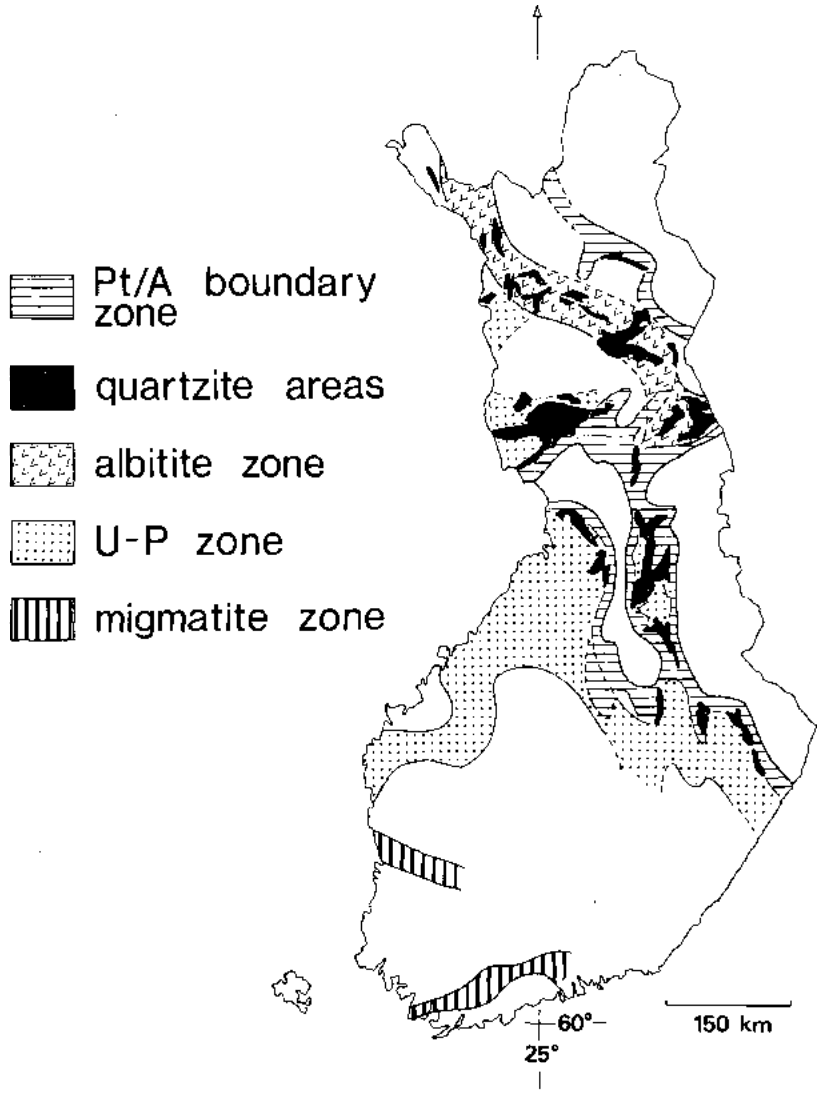


Figure 2. Zones of different types of uranium occurrences in the Proterozoic of Finland, based on the unpublished map prepared by R. Sarikkola, Outokumpu Oy. — Pt/A: Proterozoic/Archaean; U-P zone: zone of uraniferous phosphatic occurrences.

In a series of steeply dipping Karelian metasediments, the Nuottijärvi deposit (Fig. 3) underlies a graphite schist horizon in the upper contact of the Jatulian quartzite. An intraformational breccia characterizes the deposit: quartzite and skarn fragments or balls up to 2m in diameter are cemented by compact breccia consisting of quartzite, tremolite skarn, carbonate rock, and uraniferous, fine-grained apatite-quartz-feldspar rock. The deposit is a wedge-shape body about 400m long and up to 90m broad, which narrows downwards. According to the investigations made by the Outokumpu company (unpubl. reports; Sarikkola, 1974), it is estimated to average 0.04% U and 4.0% P_2O_5, and to contain about 1000 tons of uranium.

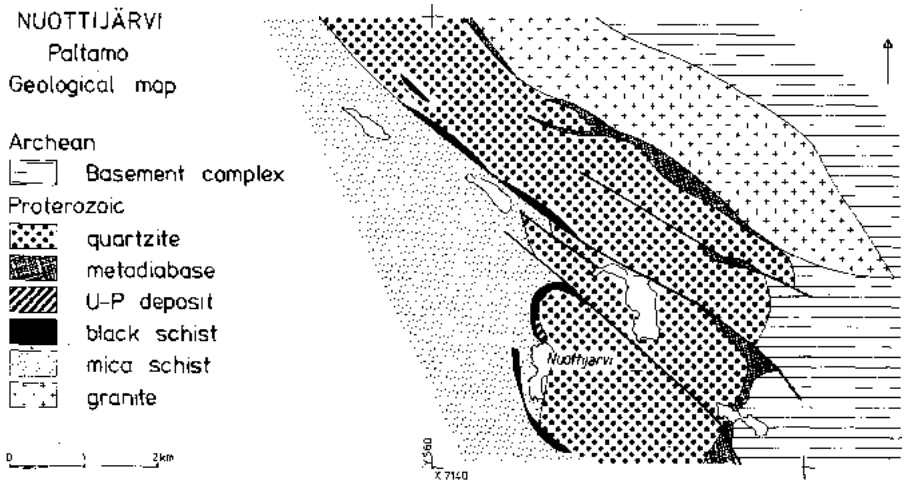


Figure 3. Geological map of the Nuottijärvi area, Paltamo, eastern Finland, showing the location of the uranium- and apatite-bearing deposit (U-P deposit) on the northern shore of Nuottijärvi. Mapped by the exploration department of Outokumpu Oy.

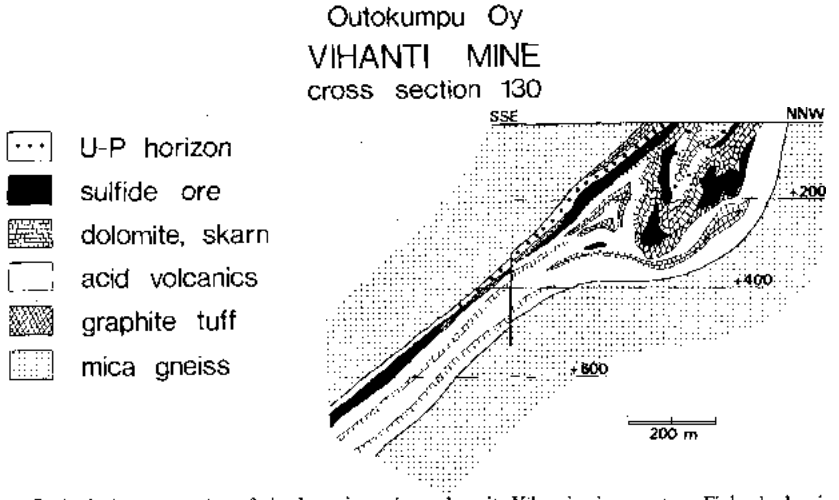


Figure 4. Geological cross section of the Lampinsaari ore deposit, Vihanti mine, western Finland, showing the uranium- and apatite-bearing zone (U-P horizon) (Rauhamaki *et al.*, 1978).

The uranium- and apatite-bearing rocks at Lampinsaari, Vihanti are closely connected with the sulphide orebodies of the Lampinsaari ore complex (Fig. 4), forming a zone up to 50m thick near the hanging wall of the complex. The U-P horizon shows two main types of uraniferous rocks, phosphorite-banded dolomite and fine-grained apatite-quartz-plagioclase gneiss, which is interpreted to be a metamorphic derivative of phosphatic tuff (Rehtijärvi *et al.*, 1979). The grade of the mineralization is 0.03% U and 3-5% P_2O_5.

The U-P deposit at Temo, Nilsiä forms a 3.5km long and up to 90m wide zone overlaying the Jatulian quartzite of the Nilsiä schist belt. The stratigraphic position is similar to that at Nuottijärvi. However, the structure is bedded, and the host rocks for uranium are apatite-quartz-feldspar gneiss, apatite-bearing dolomite and skarn rocks, and phosphorite-banded dolomite. Barren beds of dolomite, skarn rocks, amphibolite, and cherty quartzite alternate with the mineralized beds. This association is overlain by graphite gneiss and migmatized mica gneiss. Numerous veins varying from granite to gabbro in composition cut the deposit. Because of the barren interbeds and veins, the grade of the deposit is as low as 0.01-0.15% U and 1-2% P_2O_5.

The metamorphic grade of the U-P occurrences in Finland varies from intermediate greenschist to high amphibolite facies. The uranium-bearing rocks include dolomitic and calcitic marbles, skarn rocks, and quartz-feldspar gneisses; they are mostly fine grained and bedded, the thickness of the beds varying from less than 0.1m to 1.5m. Apatite occurs in these rocks as dissemination, streaks, bands, and as thin phosphorite intercalations and lenses. Apatite-biotite (phlogopite) rocks have also been found.

The apatite is fluorapatite, and usually very fine grained. Uranium occurs as uraninite crystallites within the apatite grains (Rehtijärvi *et al.*, 1979). Another mode of occurrence of uranium may be as a substitute for calcium in the apatite structure. Other uranium-bearing minerals found are sphene and thucholite. The REE contents of the apatites from the U-P occurrences reveal a uniform distribution pattern slightly depleted in Ce and resembling those found in Phanerozoic marine phosphorites (P. Rehtijärvi, pers. comm.).

Geochemically, the occurrences show two prominent features: the P_2O_5/U-ratio varies between 100 and 300, and the thorium content of the rocks is low, usually less than 10 ppm. The average uranium and phosphorus contents of the investigated occurrences do not exceed 0.04% U and 5% P_2O_5. However, samples from the phosphorite interbeds may contain 0.1-0.2% U and 10-25% P_2O_5 (Rehtijärvi *et al.*, 1979).

In most of the occurrences, there is a close relationship between uraniferous and sulphide-bearing rocks, such as cherty quartzites, skarn rocks, and graphite schists. In the surrounding areas of the Lampinsaari deposit, where U-P-type mineralizations have been found to follow a zone of felsic volcanics + dolomite + skarn rocks + graphite tuff among the areally dominant mica gneisses (Rauhamäki *et al.*, 1978), this connection has been used in prospecting sulphide ores by means of radiometric survey.

Isotopic U-Pb analyses of whole rock samples from deposits at Lampinsaari and Temo yield an age of about 1880 Ma reflecting the time of the Svecokarelian regional metamorphism. An analysis of a uranium thucholite from the Nuottijärvi deposit gives an age of 1897 ± 7 Ma (Vaasjoki *et al.*, 1979). This suggests that the deposition of the U-P occurrences took place not later than 1900 Ma ago, and, judging from the study of Sakko and Laajoki (1975) in the area west of Nuottijärvi, not earlier than 2080 Ma ago.

The lithologic characteristics, the close geochemical correlation of uranium and phosphorus, the low thorium content, and the results of the REE analyses of the apatites indicate that the uraniferous phosphatic occurrences in Finland are syngenetic, and of marine sedimentary or mixed sedimentary and volcanic origin. U-P occurrences have been discovered in both the Karelian and Svecofennian schist belts (Fig. 1); in the Karelian belt they are closely associated with the calcareous and graphitic Marine Jatulian

metasediments. The occurrences in the Svecofennian belt have a similar affinity to calcareous and graphitic host rocks, but their detailed stratigraphic relations remain unclear. The presence of metavolcanics in the association produces the basic differences as compared with the occurrences of the Karelian belt.

CONCLUSIONS

At present, a dozen uranium-bearing phosphatic occurrences are known in the Proterozoic of Finland. The deposition of the occurrences took place most probably between 1900 and 2080 Ma, and they were metamorphosed about 1880 Ma ago. The investigated occurrences are of a low grade, and, as yet, are not economically exploitable. A group of such deposits, in addition to other Proterozoic phosphorite occurrences in Finland (Laajoki & Saikkonen, 1977) and in northern Sweden (Frietsch, 1974) indicate however, that there exists a Lower Proterozoic phosphogenic province within the Baltic shield, comparable to the younger provinces listed by Cook (1976) in his classifications of the world's sedimentary phosphate deposits. Recent studies elsewhere suggest that analogous occurrences may exist in, for instance, the Canadian shield (Cannon & Klasner, 1976; Grauch, 1978) and the Aldan shield (Tugarinov *et al.*, 1977).

REFERENCES

Cannon, W.R. & Klasner, J.S., 1976: Phosphorite and other apatite-bearing sedimentary rocks in the Precambrian of northern Michigan. *Circ. U.S. geol. Surv., 746*, 6 p.

Cook, P.J., 1976: Sedimentary phosphate deposits. *in* (ed. K.H. Wolf) *Handbook of strata-bound and stratiform ore deposits. Vol. 7*, 505-535. Elsevier, Amsterdam.

Dahlkamp, F.J. 1978: Classification of uranium ore deposits. *Miner. Deposita, 13*, 83-104.

Frietsch, R., 1974: The occurrence and composition of apatite with special reference to iron ores and rocks in northern Sweden. *Sver. geol. Unders., ser. C, 694*, 49p.

Grauch, R.L., 1978: Precambrian uranium and massive sulfide deposits in metamorphosed volcanogenic rocks: southeastern New York. *Econ. Geol., 73*, 1407 (abstract).

Kahma, A., Saltikoff, B. & Lindberg, E., 1976: Ore deposits in Finland. 1:1 000 000 map, *Geological Survey of Finland*.

Ketola, M., Piiroinen, E. & Sarikkola, R., 1975: On feasibility of airborne radiometric surveys for uranium in Finland. *Geol. Surv. Finl. Rep. Invest., 7*, 43p.

Kouvo, O., 1976, Chronostratigraphy of the Finnish bedrock. *in, Stratigrafia-symposio 08.09.1976, Geologiliitto, Koulutusmoniste 2*, 1-13 (in Finnish).

Laajoki, K. & Saikkonen, R., 1977: On the geology and geochemistry of the Precambrian iron formations in Väyrylänkylä, South Puolanka area, Finland. *Geol. Surv. Finl. Bull., 292*, 137p.

Piirainen, T., 1968: Die Petrologie and die Uranlagerstätten des Koli-Kaltimogebiets im finnischen Nordkarelien. *Bull. Commn. géol. Finl., 237*, 99p.

Piirainen, T., 1978: General geology and metallogenetic features of Finland. *in, Metallogeny of the Baltic Shield Helsinki Symposium 1978, IGCP Project 74/1/91 "Metallogeny of the Precambrian", Excursion Guide, the Academy of Finland*, 1-19.

Rauhamäki, E., Isomäki, O-P. & Mäkelä, T., 1978: Geology of the Vihanti mine. *in, Metallogeny of the Baltic Shield Helsinki Symposium 1978, IGCP Project 74/1/91 "Metallogeny of the Precambrian", Excursion Guide, the Academy of Finland*, 35-56.

Rehtijärvi, P., Äikäs, O. & Mäkelä, M., 1979: A middle Precambrian uranium- and apatite-bearing horizon associated with the Vihanti zinc ore deposit, western Finland. *Econ. Geol., 74*, 1102-1117.

Sakko, M. & Laajoki, K., 1975: Whole rock Pb-Pb isochron age for the Pääkkö iron formation in Väyrylänkylä, South Puolanka area. *Geol. Soc. Finl. Bull., 47*, 113-116.

Sarikkola, R., 1974: Uranium deposits in Finland. *Geologi, 26*, 61-64 (in Finnish).

Simonen, A., 1971: Das finnische Grundgebirge. *Geol. Rdsch, 60*, 1406-1421.

Tugarinov, A.I. Bibikova, E.V., Gracheva, T.V., Lyalikov, A.V. & Smirnov, F.L., 1977: On the age of apatite mineralization of the Aldan shield. *Geokhimiya, 6*, 847-853.

Vaasjoki, M., 1977: Rapakivi granites and other postorogenic rocks in Finland: their age and the lead isotopic composition of certain associated galena mineralizations. *Geol. Surv. Finl. Bull., 294*, 64p.

Vaasjoki, M., Äikäs, O., & Rehtijärvi, P., 1980: The age of Mid-Proterozoic phosphatic metasediments in Finland as indicated by radiometric U-Pb dates. *Lithos* (in press).

GEOLOGY OF URANIUM VEIN DEPOSITS (INCLUDING SCHARTZWALDER MINE) IN PROTEROZOIC METAMORPHIC ROCKS, FRONT RANGE, COLORADO

Richard H. De Voto[1] and Jim A. Paschis[2]

1. Colorado School of Mines, Geology Department, Golden, Colorado, 80401, U.S.A.
2. Rocky Mountain Energy Co., RT 2 Box 658A, Golden, Colorado, 80401, U.S.A. (formerly with Cotter Corporation).

ABSTRACT

The Schartzwalder uranium deposit is one of many uranium vein occurrences in the Lower Proterozoic metamorphic rocks of the Front Range, Colorado. The principal veins of significant uranium content occur marginal to the Colorado Mineral Belt; are localized by structural dilation zones, vein junctions, fault deflections or branching; and occur dominantly within or at the contact of certain preferred metamorphic-stratigraphic units, particularly the siliceous, garnetiferous gneisses, where these rock units are broken by faults and fractures associated with the north-northwest-trending throughgoing faults.

Uranium at the Schwartzwalder mine occurs primarily as open-space brecciated vein filling along the steeply west-dipping Illinois vein and numerous east-dipping subsidiary veins where they cut preferred metamorphic host rocks that are tightly folded. Uraninite occurs with molybdenite, adularia, jordisite, ankerite, pyrite, base-metal sulphides, and calcite in vein-filling paragenetic sequence. Minor wall-rock alteration is mainly hematite alteration and bleaching. Vertical relief on the developed ore deposit is 900 metres and still open-ended at depth. No vertical zonation of alteration, vein mineralogy, density of the subsidiary veins, or ore grade has been detected. The Schwartzwalder uranium deposit is of substantial tonnage (greater than 10,000 metric tons of U_3O_8) and grade (averaging 0.57% U_3O_8).

Structural mapping shows that the Illinois vein-fault is a Proterozoic structure. Discordant Proterozoic (suggested) and Laramide dates have been obtained from Schwartzwalder ore. The data suggest, therefore, a Proterozoic ancestry of this heretofore presumed Laramide (Late Cretaceous-Early Tertiary) hydrothermal uranium deposit.

The authors suggest a polygenetic model for the origin of the Schwartzwalder uranium deposit. Such a genetic hypothesis would include:

1) initial syngenetic enrichment of uranium in the Lower Proterozoic (1800-2000 million years) marine shales and/or sandstones,
2) regional metamorphism (1690-1750 million years), heating, and dewatering along pressure-dilation zones with the movement of great quantities of uranium and other metals in solution in the metamorphic-hydrothermal fluids, culminating with the Boulder Creek intrusive event (1710 million years),
3) precipitation of uraninite and accompanying minerals along Proterozoic structures (veins) with the pressure decrease, attendant CO_2 loss, and resulting pH increase nearer the surface during the regional metamorphic event, and
4) local uranium remobilization and redistribution during later thermal events, possibly the Silver Plume intrusive phase (1400-1460 million years), the Pikes Peak event (950-1040 million years), and/or the Laramide (50-70 million years) intrusive event.

Thus, the regional metamorphic event may have been the single most important event in the formation of the Schwartzwalder uranium deposit.

INTRODUCTION

Numerous small uranium vein occurrences in the Proterozoic metamorphic terrane of the Front Range, Colorado, have been discovered and prospected since the 1940's. Mining activities at the Schwartzwalder mine, 13km northwest of Golden, Colorado, during the past decade have revealed that such occurrences can be of substantial tonnage and grade and have disclosed geologic aspects which suggest a Proterozoic ancestry of this heretofore presumed Laramide (Late Cretaceous-Early Tertiary) hydrothermal uranium deposit.

GEOLOGY OF THE FRONT RANGE

Precambrian

The Precambrian terrane of the central Front Range is dominated by Proterozoic metasedimentary and metavolcanic rocks (probably 1800-2000 million years of age) that

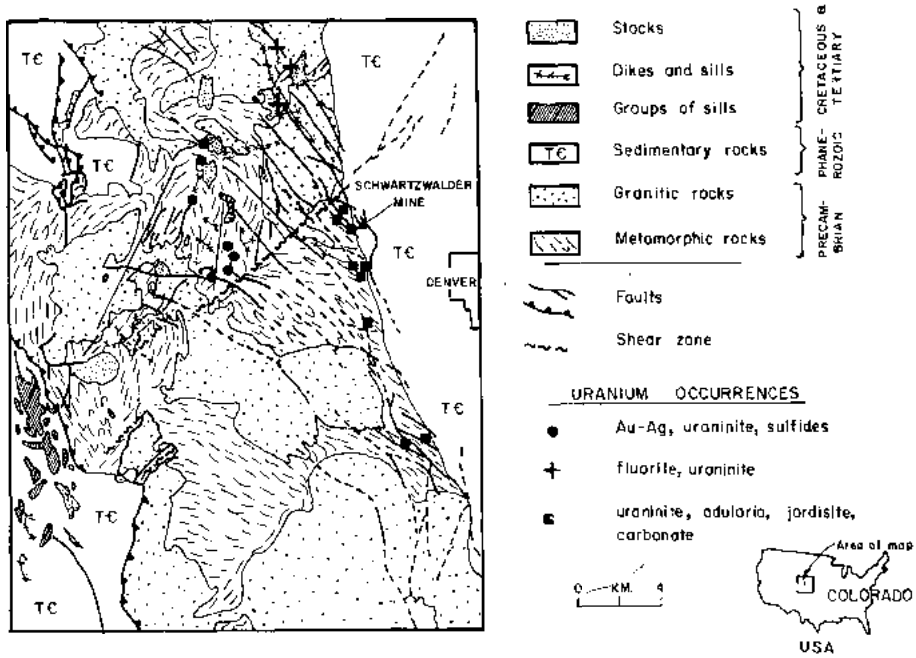


Figure 1. Geologic map of the Central Front Range, Colorado (after Tweto & Sims, 1963; Sims & Sheridan, 1964).

have been intruded by numerous granodiorite to granite stocks and batholiths of three major Proterozoic intrusive events (Fig. 1) (Sims & Sheridan, 1964). The Proterozoic shales and sandstones and rhyolite, dacite and andesite volcanic rocks underwent regional metamorphism to the amphibolite facies during the 1690-1750 million year metamorphic event. Intensive isoclinal folding along east-west and northeast-trending structures developed during the plastic deformation associated with the regional metamorphism. Later Proterozoic brittle deformation created northeast-trending shear zones with intensive cataclasis and mylonitization. The Boulder Creek granodiorite and quartz monzonite (1710 million years) formed syntectonically with regional metamorphism. There is little evidence of much fluid phase fractionation associated with the catazonal Boulder Creek plutons.

The granite to quartz monzonite batholiths and stocks of the Silver Plume thermal event intruded the metamorphic terrane with abundant fluid phase activity in the form of pegmatites and hydrothermal mineralization from 1400-1460 million years ago. The Silver Plume granites in places contain as much as 15-30 ppm uranium (Carpenter *et al.*, 1979). The Pikes Peak granite to granodiorite batholith and related stocks intruded the southern Front Range with late-stage fluid-phase differentiation from 950-1040 million years ago (Hutchinson, 1976).

Palaeozoic and Mesozoic

Lower and Middle Palaeozoic marine carbonate rocks and possibly some sandstones were deposited on the Proterozoic metamorphic and igneous rocks exposed beneath the pre-Palaeozoic unconformity. In the area of the central Front Range, Late Palaeozoic block-faulting created a mountainous uplift of thousands of metres of relief, so that the Lower and Middle Palaeozoic strata were removed and the Proterozoic rocks were deeply dissected and eroded. Upper Carboniferous (Pennsylvanian) alluvial fan and braided-river deposits of the

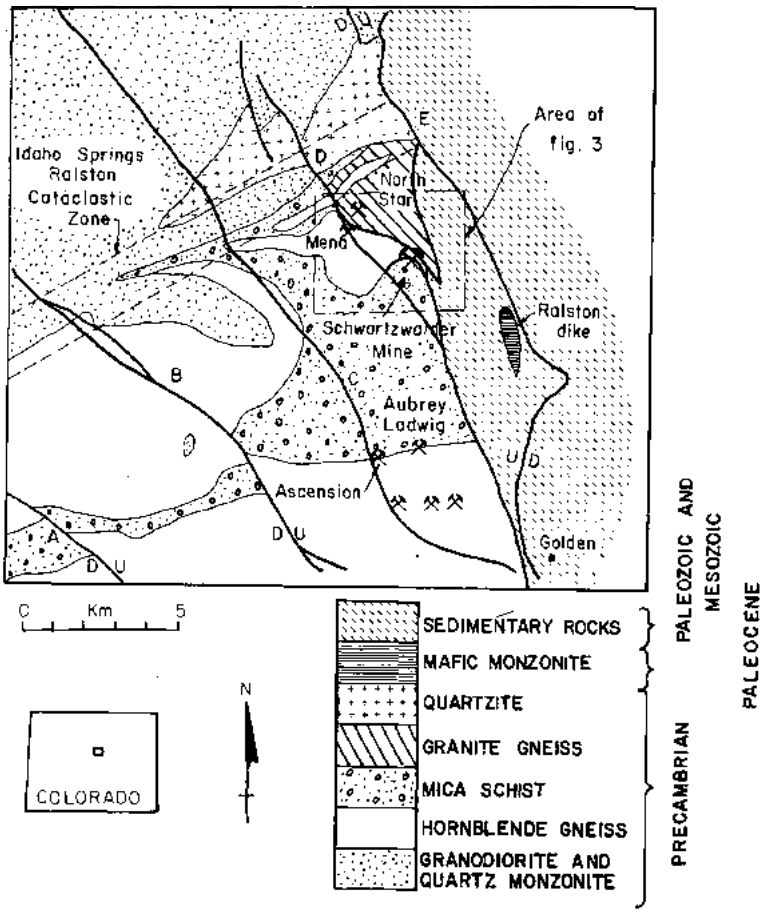


Figure 2. Geologic map and uranium occurrences of Front Range northwest of Golden, Colorado (Young, 1977). Faults identified: A, Black Hawk; B, Junction Ranch; C, Hurricane Hill; D, Rogers, east and west branches; E, Livingstone-Golden. Idaho Springs-Ralston cataclastic zone outlined by dashed lines.

red, arkosic sandstones, conglomerates, and few siltstones of the Fountain Formation were shed eastward off the flank of the mountain range. Upper Carboniferous (Pennsylvanian) red beds now rest unconformably on the Proterozoic rocks of the core of the Front Range, as shown on figures 1, 3 and 5. No soil or weathered bedrock of any appreciable thickness occur beneath the unconformity in the central Front Range area. Subsequent relative tectonic quiescence, erosion, and marine transgression permitted the Cretaceous sea to advance from the northeast and southeast across central Colorado so that from 3000 to 4000 metres of marine and coastal-plain sediments were deposited over the entire Front Range and surrounding areas.

Cenozoic

Late Cretaceous and Tertiary block faulting, principally along north-and northwest-trending faults (Fig. 1), once again created a Front Range uplift from which nonmarine sediments have been shed eastward intermittently since the Late Cretaceous. Porphyritic

intrusions of intermediate composition were emplaced along the northeast-trending Colorado Mineral Belt during the Laramide (50-70 million years ago) and extensive vulcanism of intermediate rocks occurred in the mid-Tertiary (25-40 million years ago) within Colorado. Gold-siver-base metal veins in the Front Range are related to the Laramide intrusive activity and stockwork molybdenum deposits in porphyries are related to the mid-Tertiary vulcanism (Lovering & Goddard, 1950).

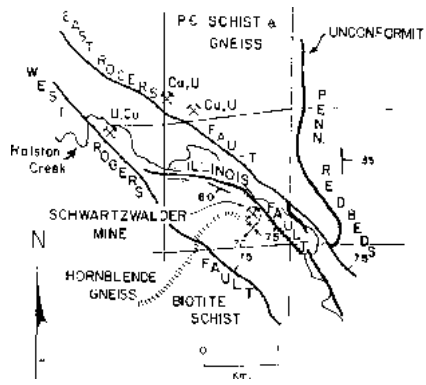


Figure 3. Geologic map of Schwartzwalder Mine area (courtesy of Cotter Corporation). Lithologies within hachured zone are shown on table 1.

URANIUM OCCURRENCES

Regional

The uranium vein deposits are generally concentrated in the east-central Front Range (Fig. 1). The deposits generally occur as discontinuous mineralization along open dilation zones in fractures and faults. There appears to be a rough zonation of uranium vein mineralogy spatially with respect to the Colorado Mineral Belt, the presumed site of a deep-seated heat source during the Laramide (Fig. 5). Within the Colorado Mineral Belt in the Central City area, anomalous uranium concentrations occur in quartz monzonite and syenite intrusions (10-40 ppm), quartz bostonite dykes (30-170 ppm) and the Au-Ag-quartz-uraninite-sulphide veins, all of Early Tertiary-Late Cretaceous age (50-70 million years) (Sims & Sheridan, 1964; Phair & Jenkins, 1975). Fluorite-uraninite veins occur as well on the north edge of the Mineral Belt in the Jamestown area.

Several uraninite-molybdenite-adularia-jordisite-sulphide-carbonate veins systems, including the Schwartzwalder mine, occur to the south of the Colorado Mineral Belt, particularly along the eastern edge of the Front Range near the unconformity with the overlying Phanerozoic rocks. The principal veins of significant uranium content occur marginal to the Colorado Mineral Belt; are localized by structural dilation zones, vein junctions, fault deflections or branching; and occur dominantly within or at the contact of certain preferred metamorphic stratigraphic units, particularly the siliceous, garnetiferous gneisses, where these rock units are broken by faults and fractures associated with the north-northwest-trending throughgoing faults (Fig. 2).

Schwartzwalder Uranium Deposit

In the area of the Schwartzwalder mine, the Proterozoic metasediments have been folded isoclinally into an overturned east-west antiform (Fig. 2) and subjected to regional amphibolite-grade metamorphism. The strike of the foliation is locally northwest and the dips 65°W to vertical. A secondary synform which plunges steeply to the southwest has been developed on the overturned north limb of the gently west-plunging antiform by approximately 800 metres of left-lateral movement along the Illinois fault system (Fig. 3). The Schwartzwalder orebody occurs in particular host rocks where this synform is cut by the Illinois vein-fault and the host rocks are tightly folded and fractured. These structures and the Schwartzwalder uranium deposit occur between the major, throughgoing, northwest-trending, east-dipping West and East Rogers faults (Figs. 3 & 4). These faults are highly brecciated and have been shown to be unmineralized by deep drilling from the surface.

Uranium at the Schwartzwalder mine occurs primarily along the steeply west-dipping Illinois vein-fault and numerous east-dipping veins which branch from the Illinois on its west

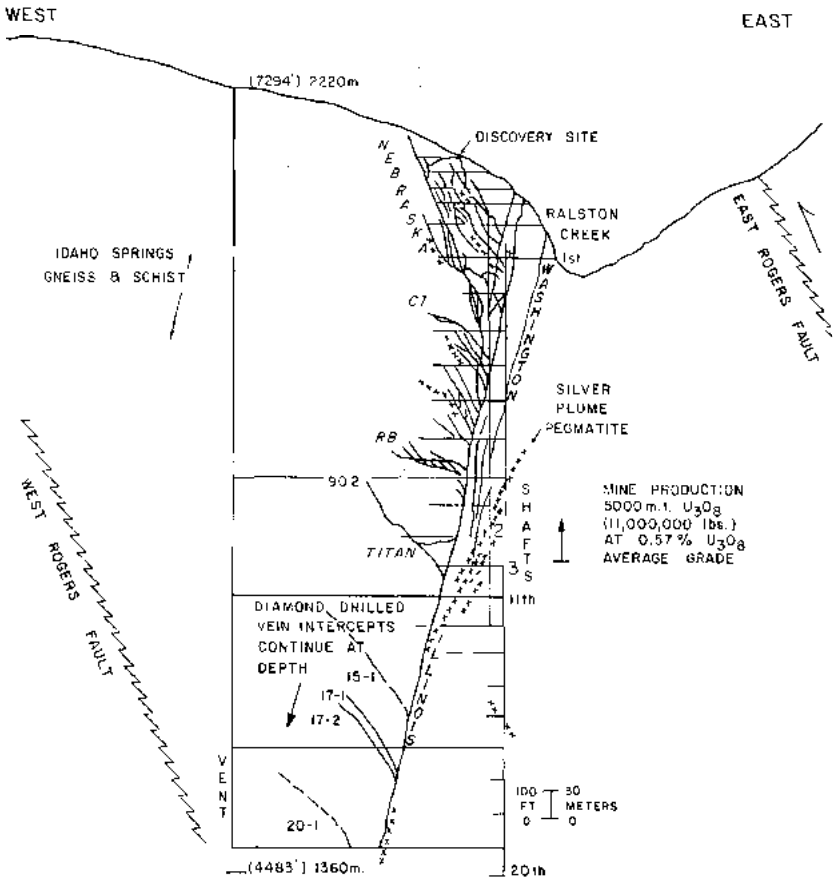


Figure 4. Schwartzwalder Mine cross section showing major developed uraninite veins.

(hanging wall) side (Fig. 4). These 'horsetail' veins dip 10°-60°E and steepen as they approach the Illinois vein. This structure appears to be a cymoid fault within the Rogers fault zone and is manifested variously as a wide shear, an open fault zone, and a uranium-mineralized breccia. The Schwartzwalder orebody occurs principally where the siliceous garnetiferous gneiss has been tightly folded into the synform and broken by the Illinois vein-fault and its associated horsetail veins. Recent underground mapping has shown that pegmatites of Silver Plume age occur in orientations parallel to both the Illinois and its east-dipping horsetail veins. Thus, the structural data suggest that the Illinois vein-fault is a Proterozoic structure which was possibly active during regional metamorphism 1690-1750 million years ago but, in any case, prior to the intrusion of the Silver Plume pegmatites 1400-1460 million years ago.

Metasediments of the Idaho Springs Formation, principally garnet-biotite gneiss, quartz-biotite schist, and quartzite, are the principal host rocks to uraninite veins. In general, the schists and gneisses can be stratigraphically interpreted as resulting initially from sedimentation of a marine to shoreline regressive sequence. Offshore shales now are

represented by biotite schists capped by pyritic-almandine-biotite gneiss. Shoreline and distributary facies are now represented by quartz-biotite schists and quartzites. The local stratigraphic sequence is capped by a thick hornblende gneiss of uncertain origin, possibly carbonate muds or basalt. Pegmatites of Silver Plume age are to a minor extent host to ore. Recent analyses of the background uranium content of some of the metamorphic host rocks show the following (Table 1).

Table 1
(In order of stratigraphic succession)

	U (ppm)
Silver Plume pegmatite dykes	2
lime silicate-hornblende gneiss	< 2
quartzite	< 2
quartz-biotite schist	8
garnet-biotite gneiss	3
biotite schist	2

Limited analytical data worldwide suggest that rocks undergo systematic depletion in their uranium content with increasing grades of metamorphism. Therefore, the pre-metamorphism uranium contents may have been somewhat (up to two to three times) higher than now.

Uraninite ore at the Schwartzwalder mine occurs as open-space, brecciated vein filling within the synformally folded, more siliceous host rocks. The wall rocks are not replaced by uraninite, nor are they extensively altered. Alteration is propyllitic in nature, with locally common bleaching, hematization, or chloritization, although a complete absence of alteration also occurs adjacent to some uraninite veins. The uranium at the Schwartzwalder mine is associated with 25 vein minerals. Events generally in order of their genetic sequence are: (a) brecciation and hematite alteration of breccia fragments and, to a limited extent, in the wall rock, (b) precipitation of adularia, uraninite, and jordisite coating the breccia fragments and vein wall, (c) precipitation of ankerite, pyrite/marcasite, and base-metal (Cu, Pb, Zn) sulphides, and (d) calcite precipitation (Rich & Barabas, 1976). The breccia fragments are extensively altered to fine-grained aggregates of hematite, ankerite, quartz, and adularia. Anomalous amounts of Cu, Pb, Zn, and Zr, as well as anomalous trace amounts of Co, Ni, Ag, and Be occur in the uranium ore. Fluid inclusion data (Rich & Barabas, 1976) and the increased zirconium and beryllium content with the uraninite mineralization (Young, 1977) suggest a high temperature (>380°C), initial vein filling, followed by a lower temperature (120-130°C), post-uraninite, calcite vein filling.

Vertical relief on the developed ore deposit is 900 metres and uranium ore has been encountered at the bottom of the deepest drillhole at the Schwartzwalder mine. No vertical zonation of alteration, vein mineralogy, density of horsetail veins, or ore grade has been detected in the drilling and mining activities to date. The overall geometry of the Schwartzwalder uranium vein system is greater than 900 metres in depth (along the dip of the Illinois vein), approximately 130 to 180 metres in strike length (along the Illinois vein), and approximately 50 to 100 metres in width (perpendicular to and on the west side of the Illinois vein). Five thousand metric tons of U_3O_8 in rock of average grade of 0.57% U_3O_8 have been produced to date from the Schwartzwalder mine. Reserve estimates show that an additional 5000 metric tons of U_3O_8 have been indicated to date and the ore deposit is still open-ended at depth.

Uranium ore from the upper third of the Schwartzwalder deposit has yielded wide ranges in ages using Pb-U and Pb-Pb methods. Discordant Proterozoic and Laramide dates are known from the ores (Heyse, 1971). Laramide dates in the 52-76 million year (Late Cretaceous to Early Tertiary) range have also been obtained from a number of other vein occurrences in the Front Range (Sheridan *et al.*, 1967; Phair, 1979). These data, along with the Proterozoic origin of the Illinois vein and its horsetail structures, which are the sites of the uranium mineralization, suggest a possible Proterozoic ancestry of the uranium mineralization at the Schwartzwalder mine with a later Late Cretaceous to Early Tertiary thermal overprint.

GENESIS OF SCHWARTZWALDER URANIUM DEPOSIT

The Schwartzwalder uranium deposit had, until recently, been widely accepted as being of Laramide (56-70 million years) magmatic-hydrothermal origin related to uraniferous hot waters emanating from the monzonite and related intrusions associated with a presumed deep-seated batholith beneath the Colorado Mineral Belt (Fig. 5) (Sims & Sheridan, 1963; Sheridan *et al.*, 1967; Bird, 1979). Recent workers, however, have proposed that the uranium may have been derived from above the unconformity between the Phanerozoic and Proterozoic rocks, which can be reconstructed to have existed approximately 800 metres above the ground surface at the Schwartzwalder mine (Fig. 6) (Rich & Barabas, 1976; Maslyn, 1978). This hypothesis would invoke Laramide leaching of uranium from Precambrian granites exposed to the west in the core of the Front Range anticline, its migration in oxidizing ground waters beneath greater than 3000 metres of sedimentary cover within the red Upper Carboniferous (Pennsylvanian) sandstones that rest on the unconformity, and its movement at least 1700 metres beneath the unconformity along the Illinois vein and back up along the eastward-dipping, dead-end horsetail veins where uraninite precipitation occurred due to the reducing environment provided by the favorable pyritic host rocks.

The authors, however, suggest that a third alternative may more reasonably fit the data. The data which are particularly important to integrate into a single genetic hypothesis include:

1) the fundamental structural control of the mineralization, yet its limitation to certain favourable stratigraphic horizons,
2) the essential vertical aspect of the deposit without diminution to a depth of at least 900 metres,
3) the apparent variable temperature, initially high temperature (>380°C) followed by low temperature (120-130°C) vein filling, and the limited wall-rock alteration,
4) the polymetallic aspect of the ore,
5) the Proterozoic origin of the vein structures,
6) the absence of any uranium vein deposits in pre-Laramide Phanerozoic rocks overlying the unconformity,
7) the suggested Proterozoic dates obtained from some of the uranium ore, and
8) the multiple thermal events which have apparently affected the uranium deposit, as evidenced by the multiple intrusive activity and suggested by the multiple Pb-U and Pb-Pb dates.

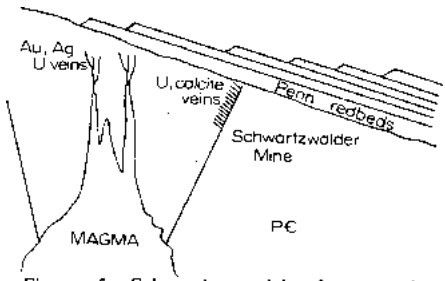


Figure 5. Schematic model of magmatic-hydrothermal genesis of Schwartzwalder Uranium Deposit.

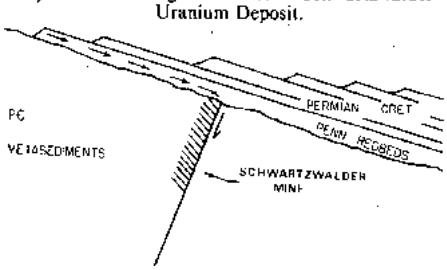


Figure 6. Schematic model of unconformity-related (supergene) genesis of Schwartzwalder Uranium Deposit.

The genetic hypothesis herein proposed includes an initial syngenetic enrichment of uranium in the Lower Proterozoic (1800-2000 million years) marine shales and/or sandstones. The syngenetic uranium concentrations may have been as much as 10-30 ppm uranium in some of the unmetamorphosed sediments. Upon regional metamorphism,

heating, and dewatering along pressure-dilation zones, great quantities of uranium and other metals would have been mobilized and moved in solution in the metamorphic-hydrothermal fluids (Fig. 7). Upon pressure decrease nearer the surface, CO_2 loss would cause an increase in the pH of water, which could cause the precipitation of uraninite and associated minerals. Thus, the regional metamorphic event (1690-1750 million years) could have been a major uranium-concentrating event at the Schwartzwalder area. Later nonmetamorphic thermal events, particularly the Silver Plume intrusive phase (1400-1460 million years), the Pikes Peak event (950-1040 million years), and the Laramide (50-70 million years) intrusive event, could have significantly affected the uranium concentration and distribution within the Proterozoic structures. The two principal facts which demonstrate the importance of post-metamorphic thermal events in the development of the Schwartzwalder uranium deposit are the uraninite vein mineralization which cross cuts Silver Plume pegmatite dykes in the mine and the common Laramide (50-70 million years) dates of uranium vein mineralization of the Front Range. It is not clear as to the relative importance of these post-metamorphic thermal events on the ultimate development of the Schwartzwalder uranium deposit (Fig. 5). It is likely, however, that massive movement of water through the whole rock mass, porosity and permeability, and availability of readily mobilized uranium were greater during the regional metamorphic event than at any later time, and, therefore, that the regional metamorphic event may have been the single most important event in the formation of the Schwartzwalder uranium deposit.

COMPARISON OF SCHWARTZWALDER URANIUM DEPOSIT WITH THE ALLIGATOR RIVERS URANIUM FIELD

Striking similarities exist between the Schwartzwalder uranium deposit of the Front Range, Colorado, and the uranium deposits of the Alligator Rivers Uranium Field (ARUF), Northern Territory, Australia. Geologic similarities include the following factors:

1) The uranium deposits are hosted by marine to shoreline Lower Proterozoic metasediments of anomalous uranium content.
2) The host rocks were regionally metamorphosed to amphibolite facies during an 1800 million-year event.

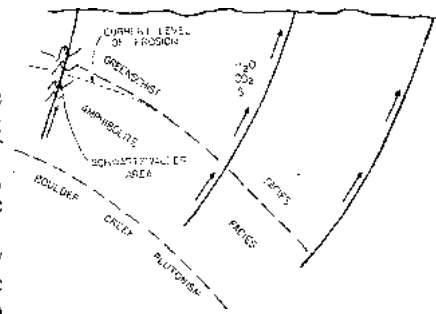


Figure 7. Schematic model of metamorphic-hydrothermal genesis of Schwartzwalder protore in highly folded and associated highly fractured zone at 1690-1750 million years.

3) The uranium deposits occupy open spaces in favorable host strata.
4) The principal uranium mineral is uraninite.
5) The mineralization is polymetallic.
6) Hematite alteration is commonly associated with the uranium deposits.
7) The uranium deposits have undergone remobilization during several thermal events, initially at the regional metamorphic event (Hegge & Rowntree, 1978; Morton, 1977).

The major dissimilarities include the fact that retrograde metamorphism and massive chloritization is evident at all the uranium deposits in the ARUF and is not apparent at the Schwartzwalder or other Front Range uranium deposits. The deposits of the ARUF occur close below a Proterozoic unconformity, whereas the only unconformity near the Schwartzwalder uranium deposit is the Late Palaeozoic surface of erosion. The many striking similarities in the nature of the uranium deposits, the alteration, the host rock

stratigraphy, and metamorphic and recurrent thermal history, all suggest that the Schwartzwalder uranium deposits may have had a similar genesis to those of the ARUF.

SUMMARY

The Schwartzwalder uranium deposit is one of many uranium vein occurrences in the Lower Proterozoic metamorphic rocks of the Front Range, Colorado. The principal veins of significant uranium content occur marginal to the Colorado Mineral Belt; are localized by structural dilation zones, vein junctions, fault deflections or branching; and occur dominantly within or at the contact of certain preferred metamorphic-stratigraphic units, particularly the siliceous, garnetiferous gneisses, where these rock units are broken by faults and fractures associated with the north-northwest-trending throughgoing faults.

Uranium at the Schwartzwalder mine occurs primarily as open-space brecciated vein filling along the steeply west-dipping Illinois vein and numerous east-dipping subsidiary veins where they cut preferred metamorphic host rocks that are tightly folded. Uraninite occurs with molybdenite, adularia, jordisite, ankerite, pyrite, base-metal sulphides, and calcite in vein-filling paragenetic sequence. Minor wall-rock alteration is mainly hematite alteration and bleaching. Vertical relief on the developed ore deposits is 900 metres and still open-ended at depth. No vertical zonation of alteration, vein mineralogy, density of the subsidiary veins, or ore grade has been detected. The Schwartzwalder uranium deposit is of substantial tonnage (greater than 10,000 metric tons of U_3O_8) and grade (averaging 0.57% U_3O_8).

Structural mapping shows that the Illinois vein-fault is a Proterozoic structure. Discordant Proterozoic (suggested) and Laramide dates have been obtained from Schwartzwalder ore. The data suggest, therefore, a Proterozoic ancestry of this heretofore presumed Laramide (Late Cretaceous-Early Tertiary) hydrothermal uranium deposit.

The authors suggest a polygenetic model for the origin of the Schwartzwalder uranium deposit. Such a genetic hypothesis would include:

1) initial syngenetic enrichment of uranium in the Lower Proterozoic (1800-2000 million years) marine shales and/or sandstones.
2) regional metamorphism (1690-1750 million years), heating, and dewatering along pressure-dilation zones with movement of great quantities of uranium and other metals in solution in the metamorphic-hydrothermal fluids.
3) precipitation of uraninite and accompanying minerals along Proterozoic structures (veins) with the pressure decrease, attendant CO_2 loss, and resulting pH increase nearer the surface during the regional metamorphic event, and
4) local uranium remobilization and redistribution during later thermal events, possibly the Silver Plume intrusive phase (1400-1460 million years), the Pikes Peak event (950-1040 million years), and/or the Laramide (50-70 million years) intrusive event.

Thus, the regional metamorphic event may have been the single most important event in the formation of the Schwartzwalder uranium deposit.

BIBLIOGRAPHY

Bird, A.G., 1979: An epigenetic model for the formation of the Schwartzwalder uranium deposit — a discussion. *Econ. Geol., 74(4)*, 947-948.

Carpenter, R.H., Gallagher, J.R. & Huber, G.C., 1979: Modes of uranium occurrences in Colorado Front Range. *U.S. Dept. of Energy GJBX-15 (79)*, 293p.

De Voto, R.H., 1978: Uranium Geology and Exploration. *Lecture notes, Colorado School of Mines*, 396p.

Downs, G.R. & Bird, A.G., 1965: The Schwartzwalder uranium mine, Jefferson County, Colorado. *The Mountain Geologist, 2(4)*, 183-191.

Fisher, J.C., 1976: Remote sensing applied to exploration for vein-type uranium deposits, Front Range Colorado. *Remote Sensing Report 76-2, Colorado School of Mines.*

Hegge, M.R. & Rowntree, J.C., 1978: Geologic setting and concepts on the origin of uranium deposits in the East Alligator River Region, N.T., Australia. *Econ. Geol., 73(8)*, 1420-1429.

Heyse, J.V., 1971: Mineralogy and paragenesis of the Schwartzwalder Mine uranium ore, Jefferson County, Colorado. *Lucius Pitkin, Inc., U.S. AEC GJO-912-1, 44p.*

Hutchinson, R.M., 1976: Precambrian geochronology of western and central Colorado and southern Wyoming. *Colorado School of Mines, Professional Contributions, 8,* 73-77.

Johnson, S.M., 1977: The geology and geochemistry of uranium and thorium in the Late Cretaceous intrusives and the enclosing Idaho Springs Formation, Black Hawk Quadrangle, Gilpin County, Colorado. *M.Sc. Thesis, Colorado School of Mines,* 238p, (unpubl.).

Lovering, T.S. & Goddard, E.N., 1950: Geology and ore deposits of the Front Range, Colorado. *Prof. Pap. U.S. geol. Surv., 223,* 319p.

Lovering, T.S. & Tweto, O., 1953: Geology and ore deposits of the Boulder County Tungsten District, Colorado. *Prof. Pap. U.S. geol. Surv., 245,* 199p.

Maslyn, R.M., 1978: An epigenetic model for the formation of the Schwartzwalder uranium deposit. *Econ. Geol., 73(4),* 552-557.

Morton, R.D., 1977: The western and northern Australian uranium deposits-exploration guides or exploration deterrents for Saskatchewan? *in* (ed. C.E. Dunn) *Uranium in Saskatchewan. Spec. Publs. geol. Soc. Sask., 3,* 211-254.

Paschis, J.A., 1979: Mining and geologic developments at Cotter Corporation's Schwartzwalder uranium mine, Jefferson County, Colorado. *1979 Mining Yearbook, Colorado Mining Association,* 123-129.

Phair, G., 1979: Interpretation of lead-uranium ages of pitchblende deposits in the central Front Range, Colorado. *Bull. geol. Soc. Am., 90(9), Part 1,* 858-870.

Phair, G. & Gottfried, D., 1964: *The Colorado Front Range, Colorado, as a uranium and thorium province, in The Natural Radiation Environment.* Chicago Press, 7-38.

Phair, G. & Jenkins, L.G., 1975: Tabulation of uranium and thorium data on the Mesozoic-Cenozoic intrusive rocks of known chemical composition in Colorado. *U.S. geol. Surv. Open-File Report 75-501.*

Rich, R.A. & Barabas, A., 1976: Mineralogy, paragenesis, fluid inclusions, and origin of the Schwartzwalder uranium deposit, Jefferson County, Colorado, (abstract). *Abstracts with Programs, Geol. Soc. Am., 6,* 1068.

Rich, R.A., Holland, H.D. & Petersen, U., 1977: Hydrothermal Uranium Deposits. *Developments in Economic Geology, 6.* Elsevier, Amsterdam, 264p.

Sheridan, D.M., Maxwell, C.H. & Albee, A.L., 1967: Geology and uranium deposits of the Ralston Buttes District, Jefferson County, Colorado. *Prof. Pap. U.S. geol. Surv., 520,* 121p.

Sims, P.K., 1956: Paragenesis and structure of pitchblende-bearing veins, Central City District, Gilpin County, Colorado. *Econ. Geol., 51(8),* 739-756.

Sims, P.K., Drake, A.A. & Tooker, E.W., 1963: Economic geology of the Central City District, Gilpin County, Colorado. *Prof. Pap. U.S. geol. Surv., 359,* 231p.

Sims, P.K. & Sheridan, D.M., 1963: Geology of uranium and associated ore deposits of the central part of the Front Range Mineral Belt, Colorado. *Prof. Pap. U.S. geol. Surv., 371,* 119p.

Sims, P.K. & Sheridan, D.M., 1964: Geology of uranium deposits of the Front Range, Colorado. *Bull. U.S. geol. Surv., 1159,* 116p.

Tweto, O. & Sims, P.K., 1963: Precambrian ancestry of the Colorado Mineral Belt. *Bull. geol. Soc. A. 74,* 991-1014.

Wells, J.D., 1960: Petrography of radioactive Tertiary igneous rocks, Front Range Mineral Belt, Colorado. *Bull. U.S. geol. Surv., 1032-E,* 233-272.

Young, E.J., 1977: Radiometric and mineralization maps and underground workings of the Schwartzwalder uranium mine area, Jefferson County, Colorado. *U.S. geol. Surv. Open-File Report 77-725,* 38p.

THE ASSOCIATION OF URANIUM AND SKARN DEVELOPMENT IN THE MARY KATHLEEN AREA, QUEENSLAND

B.I. Cruikshank, John Ferguson and G.M. Derrick

Bureau of Mineral Resources, P.O. Box 378, Canberra City, A.C.T. 2601, Australia.

ABSTRACT

Several uranium anomalies in the Mary Kathleen Syncline, the most important being the Mary Kathleen orebody, are contained in units of garnet-rich skarn.

The Corella Formation, which is host to the uranium deposits, is intruded by the Burstall Granite and a swarm of rhyolite dykes in the eastern part of the syncline, and by the Wonga Granite to the west. Regional metamorphism centred around the Wonga Granite has produced amphibolite facies rocks in the syncline. Conditions during the regional metamorphism are considered to have been:
T = 500°C to 600°C; P = 3-4 kb; X_{CO_2} — 0.2 (probably much less).

Subsequent metasomatic alteration, during intrusion of the Burstall Granite and emplacement of the associated rhyolite dykes, formed large areas of garnet-rich skarn. These skarns have formed from such diverse rock types as marble and calc-silicate granofels (The Elaine Dorothy and Rita prospects) and conglomerate (the Mary Kathleen orebody).

By petographic examination and recalculation of averaged whole rock analyses, the regionally metamorphosed marble was found to comprise calcite (40-50%), clinopyroxene (15-20%), garnet (ca. 10%), wollastonite (ca. 10%) and K-feldspar (ca. 10%) with minor scapolite, albite and vesuvianite. Petrographic examination of the most altered skarns showed these to comprise garnet (60-70%) and clinopyroxene (20-25%) with minor scapolite, albite and in some cases calcite, wollastonite, amphibole and epidote.

The Mary Kathleen orebody is contained within a unit of garnet-rich skarn apparently formed by alteration of an open-textured breccia-conglomerate and other units. This skarn is chemically and mineralogically identical to skarn formed from marble.

The genesis of both the Mary Kathleen orebody and the garnet-rich skarns appears to be related to the release of the residual, hydrous phase of the crystallising Burstall Granite and associated rhyolite dykes. The fluid introduced many elements, including uranium, into the metasomatic system and possibly remobilised others.

Decomposition of carbonate during alteration of marble gave rise to fluids rich in CO_2; it appears likely that these fluids transported uranium and the rare-earth elements to suitable sites of deposition. Deposition of uraninite and retrograde reaction of garnet to allanite, the host mineral for much of the mineralisation, probably occurred during a period of decreasing CO_2 content of the metasomatic-mineralising fluid.

INTRODUCTION

The Mary Kathleen uranium deposit is some 60km east of Mount Isa in northwest Queensland (Fig. 1). It has been previously described by Matheson & Searl (1956), Whittle (1960), Hughes & Munro (1965), Hawkins (1975), and Derrick (1977). Uranium is present as finely dispersed uraninite in massive allanite, which forms along irregular fracture zones in a massive garnet-rich replacement skarn. The main orebody and two smaller prospects (Elaine Dorothy and Rita) are located within the Proterozoic Corella Formation of the Mary Kathleen Group (Derrick *et al.*, 1977), which is between 1780 and 1670 m.y. old (Page, 1978).

Figure 1 shows the general geology of the Mary Kathleen region. The oldest rocks are gneissic felsic metavolcanics (Argylla Formation) overlain, possibly disconformably, by a thin quartzite (Ballara Quartzite) and at least 2000m of laminated calc-silicate and quartzofeldspathic granofels of the Corella Formation, which also contains lenses and bands of conglomerate, schist, marble, and quartzite. The sequence is tightly folded to form the Mary Kathleen Syncline.

To the west, the Wonga Granite intrudes the Argylla Formation but is thought also to post-date the Corella Formation; to the east, the Burstall Granite intrudes the Corella Formation with slight discordance. Wollastonite, diopside, garnet, vesuvianite, and sillimanite in the syncline indicate relatively low-pressure amphibolite facies metamorphism; this medium-grade metamorphic belt forms a regional envelope around

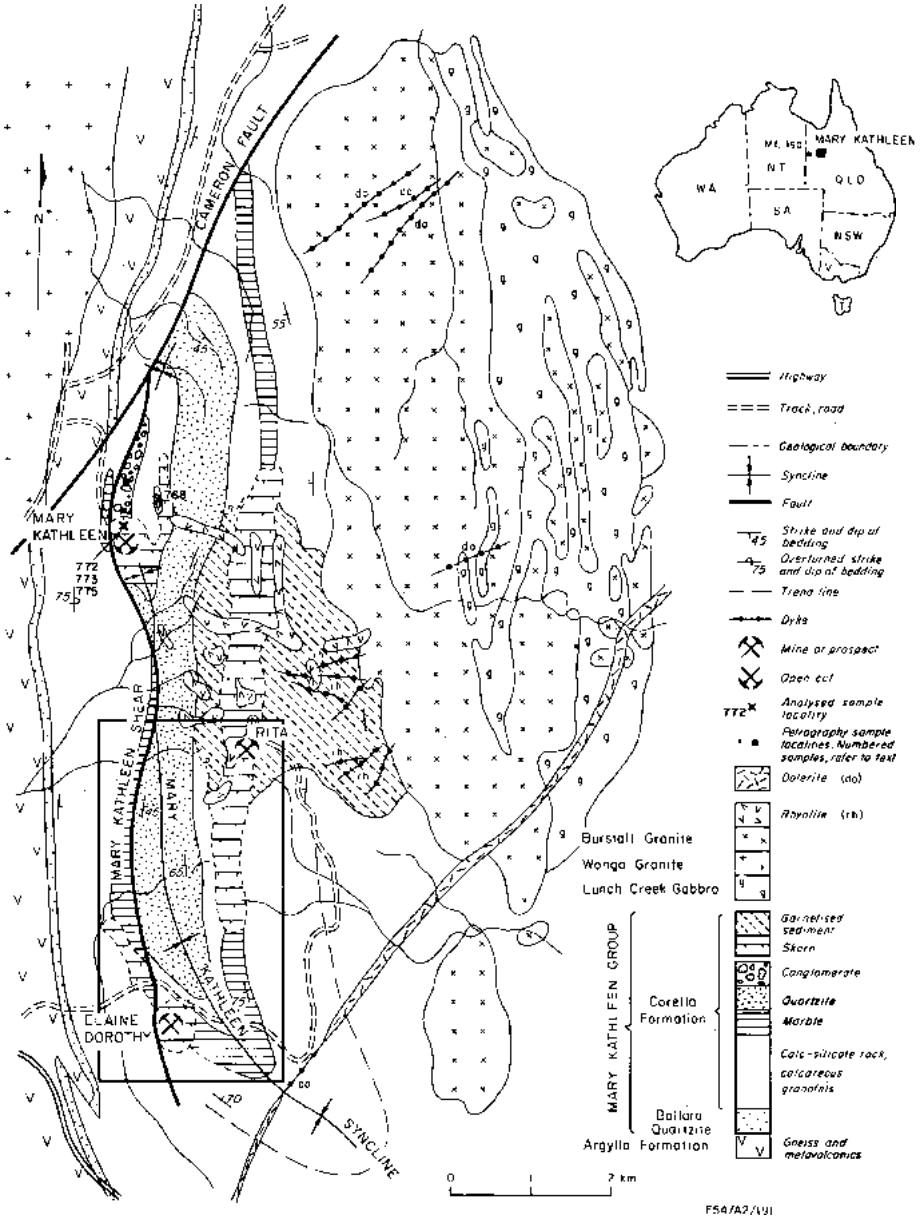


Figure 1. Geological map, Mary Kathleen area. The rectangle outlines the area covered in figure 2 (after Derrick, 1977).

areas of Wonga Granite. Hydrothermal effects of the Burstall Granite overprint the regional metamorphic rocks and the Burstall Granite must therefore post-date the main regional metamorphism (Derrick, 1978).

Metasomatism and Skarn Formation

Two metasomatic events (Derrick, 1977) are evident in the syncline, both of which have caused major alteration of the regional metamorphic rocks. The first, involving fluids rich in Na, K, and Cl, resulted in the formation of diopside, scapolite, and K-feldspar-rich metasomatic bands grossly parallel to original bedding in the calc-silicate granofels; a second metasomatic event resulted in the formation of massive garnet-allanite skarn from parental rocks as diverse as granofels, marble and conglomerate. Skarn development is controlled by proximity to the Burstall Granite-rhyolite dyke system and associated fractures, by rock composition, and by permeability. Some of the skarn is associated with uranium mineralisation.

Previous workers (Matheson & Searl, 1956; Whittle, 1960; Hughes & Munro, 1965; Derrick, 1977) have proposed that fluids enriched in uranium, associated with the intrusion of Burstall Granite and dykes, were the main source of uranium mineralisation at Mary Kathleen. Hawkins (1975) suggested the uranium was derived by concentration from source beds within the syncline.

In this study, we supplement the work of Derrick (1977) by presenting new petrochemical data on the transformation of marble and conglomerate to skarn, and its

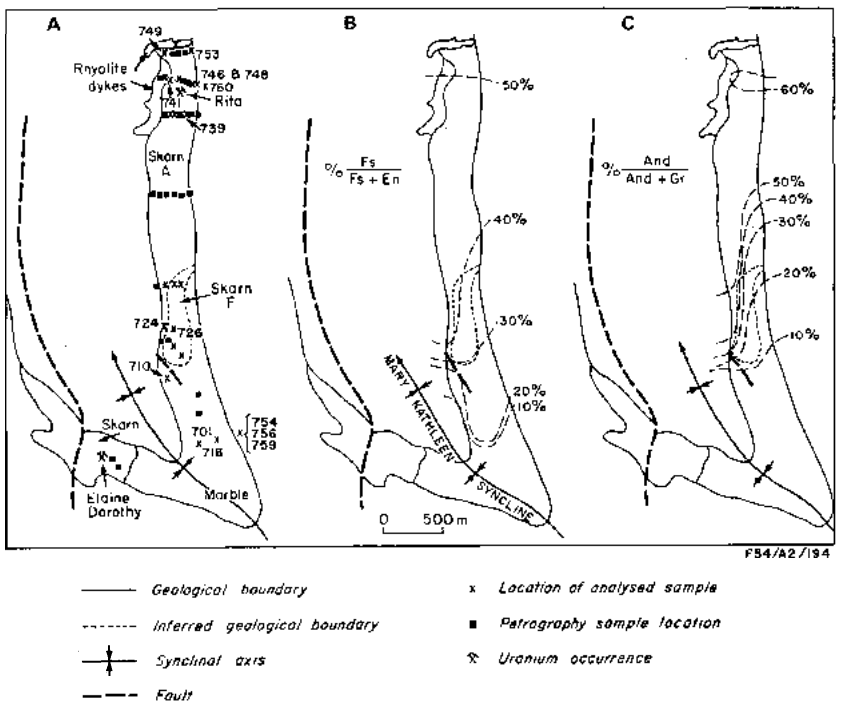


Figure 2. (a) Sample localities in marble, skarn F, and skarn A.
(b) Proportion of iron-bearing end-member in clinopyroxene.
(c) Proportion of iron-bearing end-member in garnet.

	1. Marble	2. Skarn F	3. Skarn A	4. Rhyolite Dykes	5. Barren Skarn (772)	6. Mineralised Skarn (775)
Weight %						
SiO_2	30.73	44.05	41.54	75.96	40.15	31.00
TiO_2	0.18	0.15	0.39	0.11	0.47	0.10
Al_2O_3	3.94	3.44	8.91	11.77	6.72	11.52
Fe_2O_3	0.23	1.67	12.14	0.72	13.16	4.28
FeO	1.11	5.57	3.56	0.29	3.56	7.72
MnO	0.14	0.57	0.47	0.15	0.49	0.16
MgO	3.43	5.06	1.93	0.02	2.92	2.34
CaO	38.96	31.19	29.02	0.61	28.75	20.73
Na_2O	0.14	0.07	0.41	1.94	0.60	0.06
K_2O	1.95	0.07	0.23	7.86	0.30	---
P_2O_5	0.12	0.13	0.14	---	0.22	1.36
H_2O^+	0.11	0.35	0.57	0.27	0.66	1.75
H_2O^-	0.09	0.18	0.14	0.09	0.08	0.11
CO_2	19.18	7.36	0.45	0.10	0.95	4.45
S	0.03	0.01	0.01	0.13	---	0.03
F	0.10	0.13	0.12	0.02	0.16	0.13
Cl	0.03	0.02	0.09	0.03	0.04	0.01
Total	100.47	100.02	100.12	100.07	99.15	**
$-O_2$	0.06	0.06	0.08	0.08	0.08	
Total	100.41	99.96	100.04	99.99	99.07	
ppm						
Ba	189	<5	42	2960*	117	<5
Ce	63	118	199	77	872	44 900
Cr	17	24	31	<3	16	8
La	12	61	106	29	625	30 200
Rb	84	<2	9	253	18	3
Sn	<2	5	33	3	65	53
Sr	41	20	14	19	22	51
Th	6	5	14	75	14	566
U	2.5	3.0	4.5	21	12	1680
V	13	11	76	<5	112	60
Y	10	9	49	55	49	22
Zr	60	65	87	194	62	20
No. of samples	5	5	12	3	1	1

* one sample 7800 ppm ** 94.5% including Ce_2O_3, La_2O_3 & U_3O_8

Table 1. Averaged analyses for marble, skarn F, skarn A and rhyolite dyke units, plus barren (772) and mineralised (775) orebody skarn.

bearing on the nature of the uranium ore-forming fluids. (Detailed petrographic notes are available, on request, from the authors).

Sampling and Analysis

Samples were collected from skarn containing the Rita and Elaine Dorothy prospects, from the skarn-marble unit, and from calc-silicate units in the east limb of the syncline (Figs. 1 & 2A). A separate suite of altered conglomerate and skarn was collected from within the Mary Kathleen orebody and over a distance of some 400m northward from the pit edge (Fig. 1).

Following petrographic examination, a suite of 35 samples was selected for whole-rock analysis. No attempt was made at whole-rock analysis of the conglomerate suite owing to the extreme inhomogeneity of the samples. However, reference will be made to analyses by Derrick (1977; Tables 3 & 4) of primary sedimentary matrix and altered (garnetised) matrix material in the conglomerate.

An A-CO_2-F (Fig. 3) diagram shows that samples originally designated as skarn are of two distinct types, one richer in the F-component elements (Mg, Fe^{2+}, and Mn), representative of clinopyroxene-rich mineralogy, the other richer in the A-component elements (Al and Fe^{3+}), indicating garnet-rich mineralogy. These skarn groupings will be referred to as 'skarn F' and 'skarn A' respectively, with skarn F forming an intermediate zone between marble and garnet-rich skarn A (Fig. 2A). Separation of the rock groupings is accentuated by substituting CO_2 for Ca in the ACF diagram emphasising the calcite content of the rocks.

Averaged analyses for the marble, skarn F, and skarn A units, and the rhyolite dykes are listed in table 1. Also included are examples of barren (772) and mineralised (775) skarn material from within the orebody.

Cation proportions (per 100 oxygen atoms) were calculated for each analysed sample. The mean and standard deviation for each element were estimated, and are listed in table 2(a), for the marble, skarn F, and skarn A units. The significance of element variation between rock units were tested using Student's *t* test at 95% confidence limits, and significant variations are listed in table 3.

Normative mineral compositions, based on an idealised suite of seven common materials, were calculated from mean cation proportions

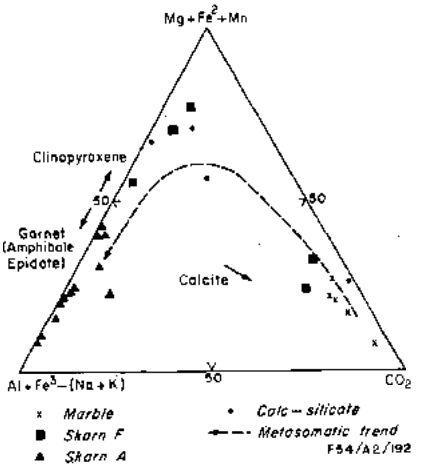


Figure 3. Composition variations during metasomatism on A-CO_2-F diagram.

	Marble		Skarn F		Skarn A	
	Mean	Std.Dev.	Mean	Std.Dev.	Mean	Std.Dev.
Si	18.02	5.41	26.99	7.31	26.87	1.40
Ti	0.08	0.03	0.07	0.08	0.19	0.03
Al_{III}	2.72	1.04	2.48	1.33	6.80	1.65
Fe_{II}	0.10	0.11	0.76	0.84	5.93	1.35
Fe^{3}	0.55	0.26	2.85	0.50	1.92	1.10
Mn	0.07	0.01	0.30	0.11	0.26	0.02
Mg	2.98	1.28	4.62	1.19	1.86	0.82
Ca	24.53	3.01	20.34	3.48	20.26	1.48
Na	0.16	0.12	0.09	0.04	0.52	0.51
K	1.47	1.13	0.05	0.11	0.15	0.22
P_2	0.06	0.01	0.07	0.03	0.08	0.04
H^+	0.43	0.11	1.42	1.07	2.44	0.98
C	15.21	4.97	5.97	7.36	0.19	0.60
Ba	49.0	44.9	2.0	4.56	12.0	11.7
Ce	15.6	2.65	31.1	27.6	54.3	94.7
Cr	11.6	5.03	15.7	18.5	22.8	6.33
La	3.0	1.01	16.2	23.4	29.8	64.3
Rb	34.6	25.6	1.0	2.33	4.0	5.69
Sc	0.2	0.40	1.4	1.42	10.9	2.27
Sr	36.6	4.01	8.3	1.56	6.1	4.61
Th	0.91	0.48	0.77	0.86	2.34	3.19
U	0.40	0.26	0.49	0.26	0.71	0.38
V	9.2	8.78	8.0	11.4	58.3	25.9
Y	5.8	1.14	3.5	1.04	21.5	6.80
Zr	23.0	9.18	26.2	12.7	97.0	15.4
total	66.21	0.47	65.02	1.36	67.62	1.22
No. of Samples	5		5		12	

Table 2a. Cation proportions (major elements and total per 100 'O'atoms — trace elements per 1 000 000 'O' atoms) for marble, skarn F and skarn A units as means and standard deviations.

	Marble	Skarn F	Skarn A
Calcite	45	15	1
Clinopyroxene	20 (0.7)*	50 (0.4)	25 (0.5)
Garnet	10 (0.1)	20 (0.5)	65 (0.4)
Wollastonite	10	5	--
K-feldspar	10	≤1	≤1
Albite **	≤1	≤1	5
Quartz	≤1	5	≤1

* proportion of Fe end member - e.g. ferrosilite/ferrosilite + enstatite for clinopyroxene and andradite/andradite + grossular for garnet.

** includes scapolite.

Table 2b. Idealised normative mineral compositions for marble, skarn F and skarn A units.

for the marble, skarn F, and skarn A units and are listed in table 2(b).

Minerals in a number of samples were analysed by electron microprobe (Reed & Ware, 1975), (Fig. 4).

Petrogenesis

1) Marble

Minerals in the pre-metasomatic pelitic, calc-silicate and marble units in the syncline allow estimation of pressure (P), temperature (T), and CO_2 mole fraction (X_{CO_2}) conditions prevailing during regional metamorphism.

The apparent equilibrium between mineral phases in the samples studied suggests the absence of steep P, T, and X_{CO_2} gradients in the metamorphic system. The presence of cordierite, and of andalusite and sillimanite in pelitic units west of the marble (Derrick, 1977), places an upper limit on P of 4-5 kb and a lower limit on T of 500°C during metamorphism (Winkler, 1976).

Dolomite, although widespread elsewhere in the region, was not found in the samples studied, all carbonate analysed was pure calcite. The only magnesium-bearing mineral present is diopside which can be formed by reaction involving dolomite, calcite, tremolite, talc and quartz (equations 1, 2, and 3). Tremolite is widespread in the lower grade metamorphic areas to the east of the Mary Kathleen region.

$$3CaMg(CO_3)_2 + 4SiO_2 + H_2O \rightleftharpoons Mg_3Si_4O_{10}(OH)_2 + 3CaCO_3 + 3CO_2 \quad (1)$$

dolomite quartz talc calcite

$$5Mg_3Si_4O_{10}(OH)_2 + 6CaCO_3 + 4SiO_2 \rightleftharpoons 3Ca_2Mg_5Si_8O_{22}(OH)_2 + 6CO_2 + 2H_2O \quad (2)$$

tremolite

$$Ca_2Mg_5Si_8O_{22}(OH)_2 + 3CaCO_3 + 3SiO_2 \rightleftharpoons 5CaMgSi_2O_6 + 3CO_2 + H_2O \quad (3)$$

diopside

The formation of diopside, as represented by equation 3, goes to completion at temperatures between 500°C and 550°C for P_{fluid} (P_f) = 1 kb, and between 590°C and 650°C for P_f = 5 kb for X_{CO_2} values in the range 0.1 to 0.9 (Winkler, 1976; Metz & Trommsdorff, 1968). By extrapolation, for P_f = 3 kb, a temperature range of 550°C to 650°C could be expected for this range of X_{CO_2} values.

Wollastonite forms (equation 4) at temperatures ranging from 400°C for $X_{CO_2} \sim 0$ (actually 1 atmosphere) to 780°C for X_{CO_2} = 0.9, for P_f = 3 kb. This reaction is obviously favoured by low X_{CO_2} values (Greenwood, 1967).

$$CaCO_3 + SiO_2 \rightleftharpoons CaSiO_3 + CO_2 \quad (4)$$

wollastonite

Grossular plus quartz is restricted to $X_{CO_2} \leqslant 0.2$ and to a temperature range of 500°C to 600°C for P_f = 2 kb (equation 5; Gordon & Greenwood, 1971).

$$CaAl_2Si_2O_8 + 2CaCO_3 + SiO_2 \rightleftharpoons Ca_3Al_2Si_3O_{12} + 2CO_2 \quad (5)$$

anorthite grossular

The absence of calcic plagioclase may place an upper limit of 600°C (at least at 2 kb - equation 6) on the temperature, although its absence can also be explained by the higher proportion of meionite found in scapolite in the marble unit (equation 7).

$$Ca_3Al_2Si_3O_{12} + SiO_2 \rightleftharpoons CaAl_2Si_2O_8 + 2CaSiO_3 \quad (6)$$

$$3CaAl_2Si_2O_8 + CaCO_3 \rightleftharpoons Ca_4[Al_6Si_6O_{24}]CO_3 \quad (7)$$

meionite

Conditions prevailing during regional metamorphism of the marble and adjacent units can be summarised as:—

$T = 550°C$ to $600°C$
X_{CO_2} — ≤ 0.2
$P = 3$ to 4 kb

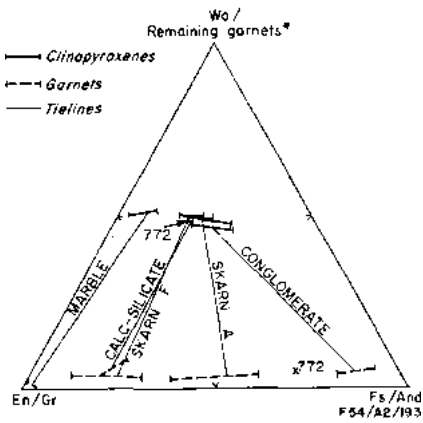


Figure 4. Composition variations of clinopyroxene (Wo = Wollastonite; En = enstatite; Fs = ferrosilite) and garnets (Gr = grossular; And = Andradite; Remaining garnets = almandine, pyrope and spessartine).

2) Burstall Granite and Rhyolite Dykes

The Burstall Granite is exposed to the east of the Mary Kathleen Syncline and has been described (Derrick, 1978) as having formed by fractional crystallisation of an undersaturated melt of tonalitic composition at pressures between 3 and 4kb. Residual fluids of the crystallising magma accumulated at the apex of the domed western margin of the pluton and subsequently escaped into fractures in the overlying roof zone of Corella Formation rocks, accompanied by the emplacement of mainly east-west-trending rhyolite dykes (Whittle, 1960; Derrick, 1977 & 1978). The hydrous phase remaining after crystallisation of the dykes, percolated outward through favourable zones in the Corella Formation and along fractures, to form skarn. This phase, probably admixed with connate water, facilitated the massive transfer of elements necessary for skarn formation.

Derrick (1977) concluded that remobilisation of uranium from the sediments as a source of the mineralisation was unlikely, given the uniformity of distribution of uranium in individual sedimentary units and their approximation, in uranium content, to world averages for similar rock types. An alternative source is the residual, hydrous phase of the Burstall Granite and related dykes which are enriched in uranium relative to the world average for granites (average 7 ppm and 12 ppm respectively compared with 4.8 ppm world average; Taylor, 1964; Turekian & Wedepohl, 1961). Uranium enrichment in the dykes increases to the west, with one rhyolite sample (768) from near the Mary Kathleen orebody containing 29 ppm uranium, more than twice the average for the dykes.

The granite is also enriched in Ce, La and, presumably, other rare-earth elements (Derrick, 1978), whereas the rhyolites are not. The granite, however, contains accessory amounts of rare-earth-bearing allanite, a mineral not observed in the rhyolites. Both granite and rhyolite contain abundant accessory fluorite, and the rhyolites especially show evidence of extensive K-Na metasomatism (Derrick, 1978).

Since uranium and the rare-earth elements are known to concentrate in the residual hydrous phases of crystallising magmas, U-enriched rocks should have evolved correspondingly enriched fluids. Such fluids might also contain volatile compounds of the halogens, P, and S, as well as Si, Al, Na, and K which usually remain in excess after crystallisation of even the most siliceous rocks (Krauskopf, 1967).

3) Skarn from Marble

Large areas of the marble unit in the syncline (Figs. 1 & 2A) have been altered to garnet-rich skarn. In the east limb the area of most intense alteration centres on the swarm of east-west-trending dykes, just south of which is the Rita uranium prospect. In the west limb, skarn containing the Elaine Dorothy prospect has formed from marble and calc-

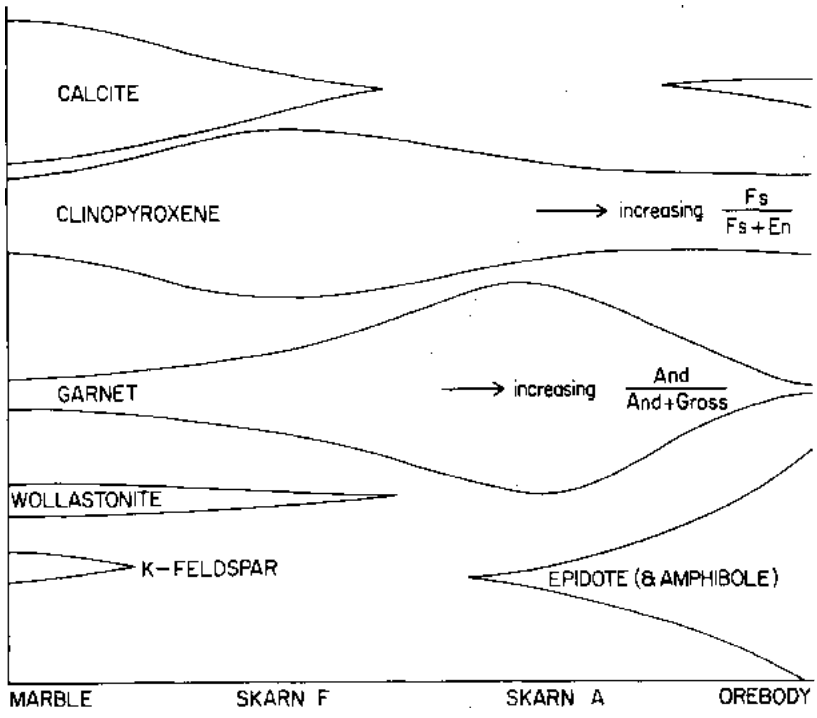


Figure 5. Paragenetic sequence of minerals within skarns (after Morgan, 1975).

silicate granofels, along extensions of the Mary Kathleen Shear. Although no rhyolite dykes are exposed in the vicinity of this skarn body, it has been postulated (Derrick, 1977) that fluids from the eastern dykes and the Burstall Granite may have migrated to the Elaine Dorothy prospect. Surface exposure and geophysical evidence indicates that the Burstall Granite is inclined at about 60°C to the west and probably underlies much of the syncline at moderate depths.

Rock-unit transformations	Significant additions	Significant losses
Marble to Skarn F	Fe^{2+}, Mn	K, C, Ba, Rb
Marble to Skarn A	Si, Ti, Al, Fe^{3+}	Mg, Ca, K, C
	Fe^{2+}, Mn, H*, Cr	Ba, Rb, Sr
	Sn, V, Y	
Skarn F to Skarn A	Ti, Al, Fe^{3+},	Mg, C
	Sn, V, Y	

Note: The significance of some additions (e.g. Si, Fe^{3+}, and Mg for marble → skarn F and Na for marble → skarn A) are masked by large variations (i.e. standard deviations) in the populations.

Table 3. Significant additions and losses at 95% confidence limits.

The clinopyroxene-rich transitional unit, skarn F, exists between unmetasomatised marble and the dominant garnet-rich skarn, skarn A (Fig. 2A). The paragenetic sequence shown in figure 5 (modified from Morgan, 1975) depicts mineralogical changes from marble, through skarn F, to skarn A and finally, with some omissions, to orebody material. These changes can be related to the statistically significant metasomatic gains and losses listed in table 3.

Initial loss of C (as CO_2) and of K, Ba, and Rb can be related to decomposition of calcite (equations 8, 9, and 12) and K-feldspar (equation 8) respectively.

$$3CaCO_3 + 2KAlSi_3O_8 \rightarrow Ca_3Al_2Si_3O_{12} + 3CO_2 + 3SiO_2 + [K_2O]^* \quad (8)$$
K-feldspar

A large hand specimen of layered skarn from the Elaine Dorothy prospect comprised semi-parallel, discontinuous lenses of clinopyroxene in a K-feldspar-rich groundmass. Where the rock is faulted, a garnet-rich vein, containing scapolite, has been introduced. Garnet has also developed in the adjacent host rock, replacing K-feldspar between the clinopyroxene-rich lenses.

The initial gain of Fe^{2+} and Mn relate to the increase of clinopyroxene, contained in the iron-bearing end member hedenbergite (equations 9 and 10), although a discernible but statistically insignificent increase in Mg occurs (Tables 2a & 3). Analysis of individual mineral grains by electron probe showed that the relative abundance of the iron-bearing end members of the clinopyroxenes (Fig. 2B) and the garnets (Fig. 2C) increases towards the rhyolite dyke swarm. The ranges of composition of these minerals are depicted in figure 4.

$$CaCO_3 + 2SiO_2 + [FeO] \rightarrow CaFeSi_2O_6 + CO_2 \quad (9)$$
hedenbergite

$$CaSiO_3 + SiO_2 + [FeO] \rightarrow CaFeSi_2O_6 \quad (10)$$

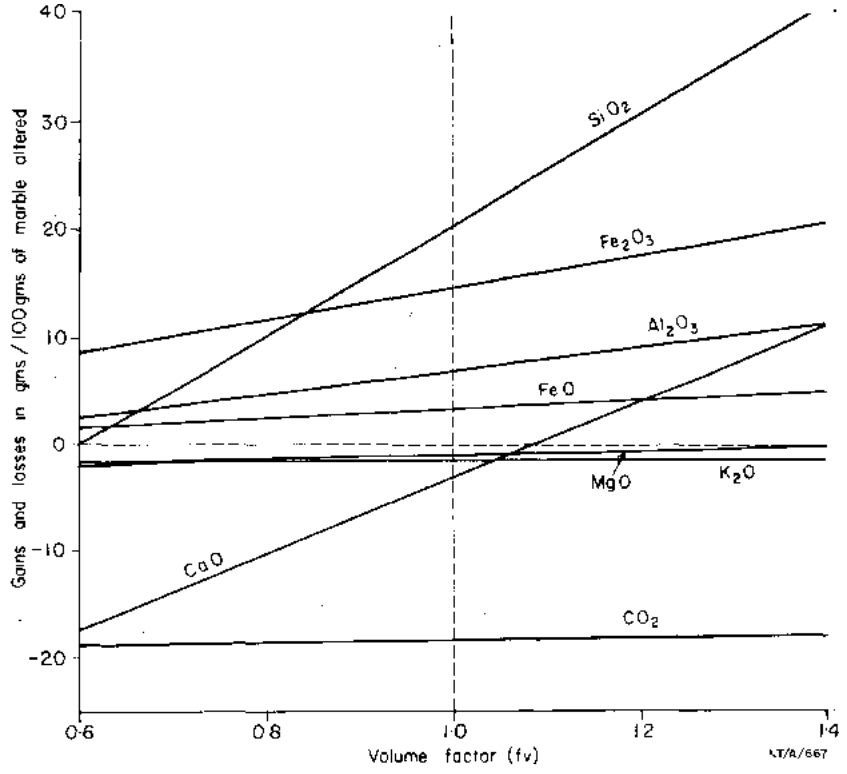


Figure 6. Metasomatic gains and losses as a function of volume factor, from 40% loss, to 40% gain of volume.

*(In this and following equations, [ ] indicates a component introduced or removed by the metasomatic fluid).

Subsequent loss of Mg and C relates to the decline of clinopyroxene (equation 11), compounded by further increase in the proportion of the iron-bearing end member and by continued decomposition of calcite respectively, whereas gains in Ti, Al, Fe^{3+}, Cr, Sn, V, and Y reflect the formation of garnet (quations 11 and 12).

$$Ca(Mg, Fe^{2+})Si_2O_6 + [Al_2O_3 + O_2] \xrightarrow[\text{balanced}]{\text{not}} Ca_3(Al,Fe^{3+})_2Si_3O_{12} + [MgO] \quad (11)$$

$$3CaCO_3 + [(Al,Fe^{3+})_2O_3] + 3SiO_2 \rightarrow \underset{\text{grossular-andradite}}{Ca_3(Al,Fe^{3+})_2Si_3O_{12}} + 3CO_2 \quad (12)$$

To compute actual gains and losses that have occurred during matasomatism it is necessary to know the chemical compositions and specific gravities of unaltered and altered rocks, and the accompanying volume change. The average chemical compositions of marble and skarn A are listed in table 1; average specific gravities were determined as 2.86 g/cm³ and 3.52 g/cm³ respectively. Little is known of the volume changes that accompanied alteration of the marble to skarn; however, using the method of Gresens (1967), gains and losses were computed for the range of volume changes from 40 percent loss to 40 percent gain of volume. The results are shown in figure 6 although five components (TiO_2, MnO, Na_2O, P_2O_5, and H_2O^+), which had gains between 0 and 1 g/100 g of marble, are not included.

Making the simple assumption that 1 volume of marble is altered to 1 volume of skarn [volume factor (fv)= 1.0] gains and losses/100g and /1m³ of marble are listed in table 4.

	g/100 g marble	x 10^5 g/1 m³ marble
Gains		
SiO_2	20.4	5.85
TiO_2	0.30	0.09
Al_2O_3	7.03	2.01
Fe_2O_3	14.7	4.21
FeO	3.27	0.94
MnO	0.44	0.13
Na_2O	0.36	0.10
P_2O_5	0.05	0.01
H_2O^+	0.59	0.17
Total	47.1 g	13.5 x 10^5 g
Losses		
MgO	1.05	0.30
CaO	3.24	0.93
K_2O	1.67	0.48
CO_2	19.6	5.62
Total	24.6 g	7.03 x 10^5 g
Net gain	22.5 g/10 g marble	6.5 x 10^5 g /1 m³ marble

Table 4. Metasomatic gains and losses for marble to skarn A (assuming equal volume).

The evolution of 5.3 x 10^5 g (1.2 x 10^4 moles) of CO_2/m^3 of marble metasomatised should have a profound effect on the composition of the fluid. However, the persistence of, and subsequent formation of, grossular during metasomatism indicates that X_{CO_2} remained below the upper stability limit of 0.2 (Gordon & Greenwood, 1971) and probably was much lower. Taylor & O'Neil (1977) estimated from stable isotope studies that X_{CO_2} during crystallisation of garnet, pyroxene, and wollastonite in a massive Ca-Fe-Al-Si in the Osgood Mountains, Nevada, was ≤ 0.035.

Assuming a similar value for X_{CO_2}, some 6.5 x 10^6 g of water must have passed through each m³ of metasomatised marble to form an H_2O/CO_2 fluid of the desired composition. Since water at 600°C and 3 kb has a density of 0.7 g/cm³ (Fisher, 1976), the volume of water is approximately 10m³. This is, however, consistent with the total weight of solute estimated to have been introduced (1.3 x 10^6g) during skarn genesis.

The metasomatic gains and losses characterise, respectively, the compositions of the fluid on arrival at and departure from the site of metasomatic activity, but not necessarily its original composition. In equilibrium with the rhyolitic magma the fluid would typically be rich in Si, Al, K, and Na (Krauskopf, 1967) which, after crystallisation of quartz and feldspars in the rhyolite, could explain the introduction of Si, Al, and Na. Less

clear is the origin of the introduced iron, since the granite from which the fluid was derived is slighly low in iron compared with the world average. The iron may have been remobilised from within the sedimentary pile (Derrick, 1977), or it may well be that the amount of iron introduced is insignificant in terms of the total amount of iron in the granite, rhyolite, and hydrous phase.

The zone of contact between unmetasomatised marble and the fluid is preserved in the area designated as skarn F (Fig. 2A). Since iron-bearing clinopyroxene is the most abundant mineral in the area, iron may have been introduced as Fe^{2+}. Hedenbergite has an extensive f_{O2} - P_f - T stability range, with maximum f_{O_2} lying slightly above NNO buffer (Gustafson, 1968). At higher f_{O_2}, hedenbergite is replaced by andradite (equation 13), a plausible source of oxygen being the mixing of large amounts of CO_2 with hydrous magmatic fluids such as exist during contact metasomatism (Nokleberg, 1973).

$$9CaFeSi_2O_6 + 2O_2 \rightarrow \underset{\text{andradite}}{3Ca_3Fe_2Si_3O_{12}} + \underset{\text{magnetite}}{Fe_3O_4} + 9SiO_2 \qquad (13)$$

Both garnet and clinopyroxene have undergone retrogressive reactions, probably in pockets of CO_2-rich fluid, to form amphibole, epidote group minerals (including allanite), calcite, and some mica (equations 14 and 15).

$$5Ca(Mg,Fe)Si_2O_6 + 3CO_2 + H_2O \rightarrow 3CaCO_3 + SiO_2 + \underset{\text{amphibole}}{Ca_2(Mg,Fe)_5Si_8O_{22}(OH)_2} \qquad (14)$$

$$3Ca_3(Al,Fe)_2Si_3O_{12} + 5CO_2 + H_2O \rightarrow 5CaCO_3 + 3SiO_2 + \underset{\text{epidote}}{2Ca_2(Al,Fe)_3Si_3O_{12}OH} \qquad (15)$$

The Al/Fe ratio in the epidote group minerals is invariably higher than in the garnet from which the epidotes are presumed to have formed, such that the epidotes have compositions between clinozoisite and epidote. The amphibole is typically ferrohastingsite with considerable Al, Na, and K substitution.

Such retrograde reactions in skarns relate, with some degree of uncertainty, to variations in T and X_{CO_2} (Morgan, 1975). Iron-rich clinopyroxene would, with decrease in T and increase in the CO_2 content with respect to water, regress to amphibole + calcite + quartz. Alternatively, stable clinopyroxene and retrograde alteration of garnet to epidote + calcite + quartz would be favoured by low molar contents of CO_2 during dooling.

4) Skarn from Congolomerate

The Mary Kathleen orebody is contained within a unit of garnet-rich skarn formed in part by metasomatic alteration of a breccia-conglomerate unit (Matheson & Searl, 1956). Breccia-congolomerate outside the ore-zone comprises quartzitic and feldspathic pebbles in a quartz-clinopyroxene-K-feldspar-rich matrix, and its relatively open texture no doubt facilitated migration of the metasomatic fluid and intense intergranular metasomatic reaction (Whittle, 1960). As the degree of metasomatism increases, quartzitic pebbles are essentially replaced by green clinopyroxene (equation 16) and feldspathic pebbles by garnet (equation 17).

The skarn (sample 772) comprises about 65 percent garnet, 20 percent clinopyroxene, and 5 percent albite, with accessory calcite, sphene, scapolite, K-feldspar, fluorite, apatite, and allanite. Surprisingly, in view of the contrasted nature of the parent rocks, it is chemically (Table 1) and mineralogically (Table 2b) comparable to skarn formed from marble, as in the east limb of the syncline. Analysis of garnetised and primary matrix materials (Derrick, 1977) suggests metasomatic gain of Fe, Mn, Mg, Ca, P, and possibly Na, and loss of Si and K. These gains and losses correspond to the change from quartzo-feldspathic mineralogy of the primary conglomerate to the garnet-clinopyroxene-rich mineralogy of the skarn (equations 16 and 17).

$$2SiO_2 + [CaO + (Mg,Fe^{2+})O] \rightarrow Ca(Mg,Fe)Si_2O_6 \qquad (16)$$

$$2KAlSi_3O_8 + [3CaO] \rightarrow Ca_3Al_2Si_3O_{12} + [K_2O + 3SiO_2] \qquad (17)$$

The proportions of the iron-bearing end members of garnets and clinopyroxenes in

the conglomerate suite initially increase with increasing degree of metasomatic alteration, but peak towards the middle of the suite collected. Thereafter, increasing degree of metasomatic alteration resulted in decreasing proportions of the iron-bearing end members, a trend which is evident in the skarn (see sample 772, Fig. 4).

Uraninite in ore-grade material is contained largely in allanite, an epidote-group mineral unusual for its ability to accommodate rare-earth elements, e.g. $(Ca,RE)_2(Fe^{2+},Fe^{3+})Al_2Si_3O_{12}OH$. Invariably a silica sheath separates the uraninite and allanite (Whittle, 1960). Allanite has formed by retrograde reaction of garnet (equation 15), apparently under conditions of low, or even decreasing, CO_2 content (Morgan, 1975). Uraninite is also included to a lesser extent, in apatite.

5) Transport and Deposition

Available evidence indicates that residual fluids from the crystallising Burstall Granite, probably admixed with connate water, were the source of uranium, rare-earth elements, fluorine, phosphorus, silica, aluminium, and sodium; and possibly iron, which were introduced into and distributed within the metasediments of the Corella Formation during metasomatic alteration. It remains to discuss element transport and deposition in the metasomatic process, with emphasis on the formation of economic uranium mineralisation.

Residual fluid leaving a crystallising granite magma would contain volatile components such as HCl, HF, oxides of sulphur, in the largely hydrous phase and would therefore be acidic. Since magnetite is the most abundant iron oxide in granites oxygen fugacities somewhere in its field of stability are suggested. As the residual fluid percolated through country rock rich in carbonates, acids in the fluid would be neutralised (equation 18) and CO_2 would evolve.

$$2H^+ + CaCO_3 \rightarrow Ca^{2+} + H_2O + CO_2 \qquad (18)$$

While excess carbonate remains, the system is buffered by solution of additional carbonate as a bicarbonate species solution of additional carbonate as a bicarbonate species (equation 19), resulting not only in reduced acidity but also marked increases in the concentrations of HCO_3^- and $CO^2{}_3$.

$$CaCO_3 + H_2O + CO_2 \rightleftharpoons Ca^{2+} + 2HCO_3^- \qquad (19)$$

Almost all experimental and theoretical studies of uranium complexes in natural systems relate to surface or near-surface environments, i.e. to temperature ranges of 25-100°C, pressure of 1 atmosphere, and CO_2 partial pressures of up to 0.01 atmospheres. Since these are not wholly applicable to systems at the elevated temperatures (> 500°C) and pressures (up to 4 kb) and hight CO_2 contents (possibly up to $X_{CO_2} \sim 1$) obtaining during contact metasomatism, the species which actually exist in such systems can only be inferred.

Under the relatively oxidising conditions represented by the upper end of the magnetite stability range, the uranyl ion, UO_2^{2+}, is the stable uranium species. That uranium was transported in the hexavalent state is supported by the marked decrease in the Th/U ratio of the orebody (0.4/1) relative to the granite (11/1) and dyke (5/1) source. Thorium has chemical similarities with U^{4+} but not UO_2^{2+} (Naumov, 1959). The uranyl ion is known to form stable complexes with fluoride ions (under acid conditions), phosphate ions (weakly acid to neutral), an carbonate ions (weakly acid to alkaline) (Langmuir, 1978), all of which would have been present in the metasomatic fluid. However, the level of acidity in the buffered fluid and its relatively high CO_2 content suggests that a carbonate complex most likely predominated. Unpublished experimental work by B. Poty (pers. comm.) indicates the effectiveness of uranyl carbonate complexing at temperatures as high as 700°C. The two possibilities are the uranyl dicarbonate complex (UDC), $[UO_2(CO_3)_2(H_2O)_2]^{2-}$ or $[UO_2(CO_3)_2]^{2-}$, and the uranyl tricarbonate complex (UTC), $[UO_2(CO_3)_3]^{4+}$. Because of the inferred acidity, the former is more likely (equation 20).

$$UO_2^{2+} + 2HCO_3^- \rightleftharpoons [UO_2(CO_3)_2]^{2-} + 2H^+ \qquad (20)$$

Transport in carbon dioxide-bicarbonate-carbonate-rich fluid applies not only to uranium and calcium, but also to the rare-earth elements as $[RE(CO_3)_3]^{3-}$ (Kosterin, 1959), and to Mg^{2+} and Fe^{2+} (equations 21 and 22) as bicarbonate species,

$$FeCO_3 + H_2O + CO_2 \rightleftharpoons Fe^{2+} + 2HCO_3^- \quad (21)$$

$$Fe_2SiO_4 + 4CO_2 + 4H_2O \rightleftharpoons 2Fe^{2+} 4HCO_3 + H_4SiO_4 \quad (22)$$

whereas such conditions would not inhibit transport of Na, K, Si, and Al.

Providing the fluid contains enough carbon dioxide, the uranyl carbonate complex can "coexist with such concentrations of reducing agents, for example Fe^{2+} or S^{2-} as would reduce it (the uranyl ion) in the absence of CO_2, that is both hexavalent uranium and the reducing agent may be transported in the same hydrothermal solution" (Naumov, 1959). This follows a decrease in the oxidation-reduction potential of the U^{IV}/U^{VI} couple with increase in dissovled CO_2. The deposition of uranium would be preceded by the destabilisation of the carbonate complex owing to a decrease in the bicarbonate-carbonate concentration brought about by either an increase in the acidity of the fluid or, more likely, by release of CO_2 (equations 23, 24). Indeed, in the Erzgebirge deposit, fluid inclusions in minerals deposited just before the deposition of uraninite contained high concentrations of CO_2, whereas those deposited immediately after uraninite contained considerably lower concentrations (Naumov, 1973; Tugarinov & Naumov, 1974), indicating that uraninite precipitated from highly carbonated fluid because of a sharp decrease in the CO_2 content.

$$Ca^{2+} + 2HCO_3 \rightarrow CaCO_3\downarrow + H_2O + CO_2\uparrow \quad (23)$$

$$[UO_2(CO_3)_2]^{2-} + H_2O \rightarrow UO_2\downarrow + 2HCO_3^- + \tfrac{1}{2}O_2 \quad (24)$$

Conditions of low or decreasing CO_2 content also favour the retrograde formation of allanite (the host mineral of uraninite in the orebody) from garnet. It is allanite which, significantly, also contains most of the rare-earth elements found in the orebody. The presence of Fe^{2+} in allanite indicates that even though iron in the parent garnet occurs predominantly as Fe^{2+}, either significant concentrations of Fe^{2+} still remained in the fluid, or another reducing agent, possibly the sulphide ion, was active. Indeed, the highest concentrations of rear-earth elements, and therefore of Fe^{2+}, in allanite occur in the richest ore. The orebody also contains much sulphide veining which postdates deposition of the uraninite (Whittle, 1960).

The open texture of the breccia-conglomerate unit, after facilitating ingress of the powerful metasomatic and mineralising fluid, could have ultimately provided for the escape of CO_2 leaving the fluid. The full extent of the original mineralisation is not apparent because the orebody is truncated in the west by the roughly north-south Mary Kathleen Shear. The west block was upthrown by about 1500m, and the absence of garnet and allanite west of the shear indicates that the Mary Kathleen Shear almost certainly post-dates the garnet, and probably also the mineralisation (Mary Kathleen Uranium, 1976).

CONCLUSIONS

The genesis of both the Mary Kathleen orebody and the garnet-rich skarns appears to be related to the release of the residual, hydrous phase of the crystallising Burstall Granite and associated rhyolite dykes. The fluid introduced many elements, including uranium, into the metasomatic system and possibly remobilised others.

Decomposition of carbonate during alteration of marble gave rise to fluids rich in CO_2; it appears likely that these fluids transported uranium and the rare-earth elements to a suitable site of deposition, in this case an open-textured conglomerate. Deposition of uraninite and retrograde reaction of garnet to rare-earth-bearing allanite probably occurred during a period of decreasing CO_2 content of the metasomatic-mineralising fluid.

The Cahill Formation in the Pine Creek Geosyncline lacks the high temperature skarn-type uranium enrichment found in the Mary Kathleen area, despite the similarity in metamorphic grade and the development of juxtaposed uranium-enriched granitoids. The main difference in lithology in the uranium host formation in the two areas is the predominance of and calcsilicate rocks in the Mary Kathleen area. The calcareous units in the Cahill Formation are volumetrically small compared with those in the Corella Formation at Mary Kathleen. Other differences between the two areas possibly relate to the compositions of the initial fluids associated with the granitoids and to their interaction with host rocks, as well as the involvement of connate hydrous solutions.

ACKNOWLEDGEMENTS

The authors which to thank R. A. Binns, A. G. L. Paine and A. K. Scott for criticism of this paper: J. G. Pyke, T. I. Slezak, the late J. C. W. Weekes, and K. H. Ellingsen who performed the chemical analyses: and N. G. Ware for his instruction in the use of the electron microprobe.

Published with the permission of the Director, Bureau of Mineral Resources, Geology and Geophysics, Canberra, A.C.T.

REFERENCES

Derrick, G. M., 1977: Metasomatic history and origin of uranium mineralisation at Mary Kathleen, northwest Queensland. *BMR J. Aust. Geol. Geophys., 2,* 123-130.

Derrick, G. M., 1978: Proterozoic igneous and sedimentary rocks and associated metamorphism and metasomatism at Mary Kathleen, northwest Queensland. *Ph.D Thesis, University of Queensland* (unpubl.).

Derrick, G. M., Wilson, I. H. & Hill, R. M., 1977: Revision of stratigraphic nomenclature in the Precambrian of northwestern Queensland. VI Mary Kathleen Group. *Qld. Govt. Min. J., 78,* 15-23.

Fisher, J. R., 1976: The volumetric properties of H_2O — A graphical portrayal. *J. Research U.S. geol. Surv., 4,* 189-193.

Gordon, T. M. & Greenwood, H. J., 1971: The stability of grossularite in H_2O-CO_2 mixtures. *Am. Miner., 56,* 1674-1688.

Greenwood, H. J., 1967: Wollastonite, stability in H_2O-CO_2 mixtures and occurrence in a contact metamorphic aureole near Salmo, British Columbia, Canada. *Am. Miner., 52,* 1669-1680.

Gresens, R. L., 1967: Composition-volume relationships of metasomatism. *Chem. Geol., 2,* 47-65.

Gustafson, W. I., 1968: Stabilities of andradite and hedenbergite and their relation to skarn equilibria. *Spec. Pap. geol. Soc. Am., 121,* 122-123.

Hawkins, B. W., 1975: Mary Kathleen uranium deposit. *in* (ed. C. L. Knight), *Economic geology of Australia and Papua New Guinea, Australas. Inst. Min. Metall., Monograph Series No. 5, 1. Metals,* 398-402.

Hughes, F. E. & Munro, D. L., 1965: Uranium ore deposit at Mary Kathleen. *in* (ed. J. McAndrew) *Geology of Australian ore deposits (2nd edition), 8th Commonwealth Mining and Metallurgical Congress, 1,* 256-263.

Kosterin, A. V., 1959: The possible modes of transport of the rare earths by hydrothermal solutions. *Geochemistry, 4,* 381-387.

Krauskopf, K. B., 1967: *Introduction to Geochemistry.* McGraw-Hill Book Company, New York.

Langmuir, D., 1978: Uranium solution-mineral equilibria at low temperatures with applications to sedimentary ore deposits. *Geochim. cosmochim. Acta, 42,* 547-569.

Mary Kathleen Uranium Limited, 1976: *Description of Operations* (prepared by the company's staff, June, 1976), 8-9.

Matheson, R. S. & Searl, R. A., 1956: Mary Kathleen uranium deposit, Mount Isa-Cloncurry district, Queensland, Australia. *Econ. Geol., 51,* 528-540.

Metz, P. & Trommsdorff, V., 1968: On phase equilibria in metamorphosed siliceous dolomites. *Contrib. Mineral. Petrol., 18,* 305-309.

Morgan, B. A., 1975: Mineralogy and origin of skarns in the Mount Morrison Pendant, Sierra Nevada, California. *Am. J. Sci., 275,* 119-142.

Naumov, G. B., 1959: Transportation of uranium in hydrothermal solution as a carbonate. *Geochemistry, 1,* 5-20.

Naumov, G. B., 1961: Some physiochemical characteristics of the behaviour of uranium in hydrothermal solutions. *Geochemistry, 2,* 127-147.

Naumov, G. B., 1973: The behaviour of the radioactive components in hydrothermal process. *in* Radioactive elements in rocks, *IZD-VO NAUKA SO AN SSR, NOVOSIBIRSK.*

Nokleberg, W. J., 1973: CO_2 as a source of oxygen in the metasomatism of carbonates. *Am. J. Sci., 273,* 498-514.

Page, R. W., 1978: Response of U-Pb zircon and Rb-Sr total rock systems to low grade regional metamorphism in Proterozoic igneous rocks, Mount Isa, Australia. *J. geol. Soc. Aust., 25,* 141-164.

Reed, S. J. B. & Ware, N. G., 1975: Quantitative electron microprobe analysis of silicates using energy-dispersive x-ray spectrometry. *J. Petrology, 16,* 499-519.

Taylor, S. R., 1964: Abundance of chemical elements in the continental crust. *Geochim. cosmochim. Acta, 28,* 1280-1281.

Taylor, B. E. & O'Neil, J. R., 1977: Stable isotope studies of metasomatic Ca-Fe-Al-Si skarns and associated metamorphic and igneous rocks, Osgood Mountains, Nevada. *Contrib. Mineral. Petrol., 63,* 1-49.

Tugarinov, A. I. & Naumov, G. B., 1974: Die migrations — und absatsverhältnisse des urans bei der endogenen erzbildung. *Z. angew. Geol., 20,* 410-413.

Turekian, K. K. & Wedepohl, K. H., 1961: Distribution of elements in some major units of the earth's crust. *Bull. geol. Soc. Am., 72,* 186.

Whittle, A. W. G., 1960: Contact mineralisation phenomena at the Mary Kathleen uranium deposit. *Neues Jb. Miner. Abh., 94,* 798-830.

Winkler, H. G. F., 1976: *Petrogenesis of metamorphic rocks.* 4th Edition. Springer-Verlag, New York, 334p.

THE DISTRIBUTION OF U,Th and K THROUGH A SECTION OF THE GRANITIC CRUST OF THE VREDEFORT BASEMENT

(EXTENDED ABSTRACT)

Roger J. Hart,[1] Louis O. Nicolaysen[2] and Noel H. Gale[3]

1. Nuclear Physics Research Unit, University of the Witwatersrand, Johannesburg, South Africa
2. Bernard Price Institute of Geophysical Research, University of Witwatersrand, Johannesburg, South Africa
3. Department of Geology and Mineralogy, University of Oxford, England.

The Vredefort basement granite in South Africa forms the core of an updomed and overturned sequence of Precambrian strata. The granitic core which is about 50km in diameter, outcrops near the centre of the Witwatersrand Basin. The southern and eastern portions of the structure are covered with flat-lying Palaeozoic Karroo strata. On the northern and western sides of the dome overturned Precambrian strata of the Lower Witwatersrand Group form a rim around the central hub of Archaean granite, and dip steeply inwards towards the granite core. Slawson (1976) proposed that the granite core has also been overturned, exposing to view a thick section through the Archaean crust, increasing in depth towards the centre of the dome. Recent geophysical, geochemical and geological studies (Hart, 1978) strongly support this proposal. Profiles across the Vredefort basement provide an opportunity for studying the distribution of the major and trace elements, particularly U, Th, and K with depth in the upper and middle crust.

GENERAL GEOCHEMISTRY

Two distinct annular zones within the basement core and which were identified by their geologic and petrographic character have distinct major element attributes. The deepest crustal levels, exposed in the central parts of the dome, are represented by the Inlandsee leucogranofels (ILG) which is characterised by the absence of ferro-magnesium minerals, and a strongly marked tectonic fabric. Inclusions of metasedimentary supracrustals and pyroxene granulites occur interlayered with the Inlandsee leucogranofels. This inner zone occurs in high grade granulite facies metamorphism. The outer granite gneiss (OGG) which forms a 10km wide peripheral zone to the inner core occurs in a lower grade amphibolite facies metamorphism. The gneisses vary in composition, and in general show a progressive increase in cafemic character from the margins inwards.

RADIOELEMENT GEOCHEMISTRY

Detailed radioelement concentration profiles across the granitic basement showed that:

1) the central part of the basement core is depleted in U and Th relative to the perimeter, and the concentration of U and Th falls off regularly from the basement margin inwards (Fig. 1). The average concentrations of U and Th in the central regions of the core are 0.31 ppm and 6.95 ppm respectively and increase to a maximum of 28 ppm U and 67 ppm Th near the outer margins of the granite basement.
2) the average distribution of the radioelements, and the distribution of heat production with depth over the outer 8km, is consistent with an exponential depth function. The main zone of exponential decline in the concentration of U and Th occurs within the OGG annulus. Thus, although there is a broad spatial correlation between the decline in radioelement concentrations and the approach towards

granulite facies metamorphism, the bulk of the fall off occurs within a zone that exhibits a lower grade of metamorphism.

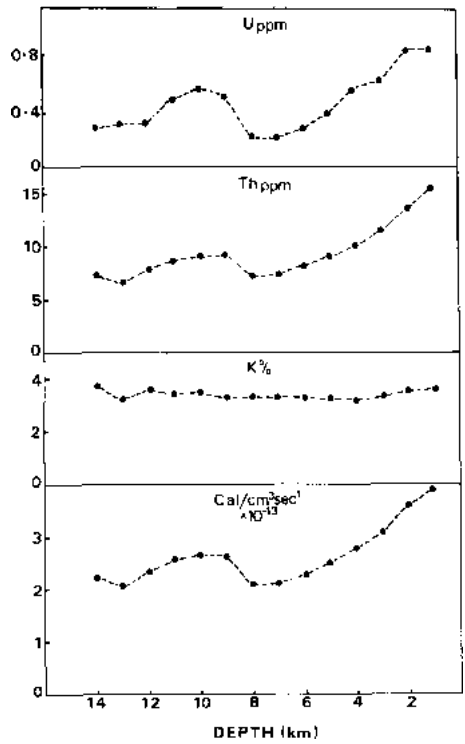


Figure 1. Averaged radioelement and heat production profiles for the Vredefort basement.

3) the felsic granulites in the central regions of the Vredefort basement are characterised by extremely high K/U (12.8×10^4) and Th/U (22.5) ratios, compared to a crustal average of 1×10^4 (Wasserburg *et al.*, 1964) and 3 to 4 (Rogers & Adams, 1969) for K/U and Th/U respectively. Both these ratios increase from the margins inwards. Mafic granulites which occur in the central regions of the granitic core have "normal" K/U, K/Th and Th/U ratios.

CONCLUSIONS

It is argued that a high grade metamorphic environment resulted in the depletion of both U and Th relative to K in the greater proportion of the felsic rocks from the central regions of the Vredefort basement. Depletion of U was far greater than that of Th. The normal Th/U, K/U and K/Th ratios in mafic rocks, in close proximity to the felsic rocks, suggest that mineral assemblages have a strong control on the behaviour of the radioelements during regional metamorphism in the Vredefort basement. Isotopic evidence (Hart, in preparation) suggests that the geochemical regime at Vredefort was established at least ~2700 m.y. ago.

REFERENCES

Hart, R.J., 1978: A study of the isotopic and geochemical gradients in the old granite of the Vredefort structure, with implications to continental heat flow. *Ph.D thesis, University of the Witwatersrand,* (unpubl.).

Hart, R.J., in prep., Geochronology of the deep profile through the Archaean Basement of Vredefort, with implications for early crustal evolution.

Rogers, J.J.W. and Adams, J.A.S., 1969: Uranium. *in* (ed. K.H. Wedepohl) *Handbook of Geochemistry, Vol. II/1 Ch. 92,* Springer-Verlag

Slawson, W.F., 1976, Vredefort core: a cross section of the upper crust? *Geochim. cosmochim. Acta, 40,* 117-121

Wasserburg, G.H., MacDonald, G.J.F., Houle, F. and Fowler, W.A., 1964: *Science, 143,* 565-567

SYNGENETIC MODEL FOR SOME EARLY PROTEROZOIC URANIUM DEPOSITS: EVIDENCE FROM OKLO

Douglas G. Brookins

Department of Geology University of New Mexico, Albuquerque, New Mexico 87131 U.S.A.

ABSTRACT

Massive, vein-like accumulations of uranium in Early Proterozoic metamorphic rocks have conventionally been explained by hydrothermal processes (± tectonic control), metamorphism of original syngenetic or early epigenetic sedimentary deposits, mechanical accumulations, supergene processes, or some combination of these processes. Many of these deposits are located at unconformities and may be controlled by basement fault systems, but the unconformities are not necessarily the primary control for ore formation. Exploration of Proterozoic sedimentary basins is, for economic factors, usually restricted to the basin edges where distance to the unconformities is minimal. The interiors of the basins thus have not received as intensive exploration.

The 2.0 ± 0.1 billion year old Oklo uranium deposit, Republic of Gabon, is unique in that very high grade ore has apparently been derived from low grade ore in unmetamorphosed sedimentary rocks. The low grade ore is similar to Phanerozoic syngenetic or early epigenetic sandstone type deposits; the assemblage pitchblende-illite (1Md polytype)-chlorite-organic carbon-dolomite is common. Uranium was mobilized from the low grade ore zones and concentrated as high grade ore in fractures. Pitchblende (± some uraninite and coffinite)-illite (2M_1 polytype)-chlorite-hematite-pyrite in the virtual absence of quartz and carbon is common in the high grade ore. Crystallization temperatures near 200°C at P = 0.5-2 kb(?) and Eh conditions favouring formation of either pyrite or hematite, in the pH range of 6-8 were likely. The reductant for the mobilized uranium was apparently carbon which was oxidized as fractures opened, thus also accounting for the absence of quartz. The high grade ore, concentrated in shale-rich material down-filled into broken sandstone layers, was then severely folded and fractured. In cross sections, then, much of the Oklo ore resembles cross sections of high grade uranium ore in metamorphic rocks. It is proposed that Oklo may either be a hybrid type of deposit or a precursor to typical deposits in metamorphic rocks noted in Canada and elsewhere. It is considered significant that the Oklo deposit is located within the sedimentary sequence and not at the unconformity between this sequence and the basement granitic massif.

INTRODUCTION

The possibility of syngenetic or very early epigenetic uranium deposits in the interiors of Proterozoic sedimentary basins has received relatively little attention from explorationists or academics. Most Proterozoic uranium accumulations of economic importance discovered to date are located at unconformities between Precambrian units of a wide range of geologic ages. Commonly these deposits are controlled by faults or folds in the rocks below the unconformity, but this need not be the primary control for mineralization. The literature describing these types of deposits is voluminous and the reader is referred to Rich *et al.* (1978), Kimberley (1978), Bowie *et al.* (1972), Knipping (1974), Dodson *et al.* (1974), Smith (1974), for descriptions of specific Proterozoic deposits.

Some general features of these Proterozoic deposits are

1) localization of the ore at or near an unconformity;
2) vein or vein-like geometries of the ore bodies;
3) pitchblende (here used to mean botryoidal to reinform material of approximate composition, $UO_{2.6}$, as opposed to well crystallized uraninite, UO_2) as the dominant ore mineral;
4) chlorite — quartz gangue, commonly with variable amounts of carbon, carbonates, and sulphides.

Hypotheses on the origin of these deposits are covered in the references cited above. A commonly accepted hypothesis is that the deposits are hydrothermal in origin, although fluid inclusion and other data argue for a wide range in temperature of fluids such that the deposits can be interpreted as being anywhere from essentially ground water hydrothermal to metamorphic hydrothermal. The proximity of some deposits to igneous masses suggests a near-hypogene origin. Alternatively, the igneous processes are interpreted as essential for

elemental migration. At times, even supergene processes are assumed important for original accumulation of the uranium at favourable structural sites (Langford, 1978). None of these hypotheses satisfies all Proterozoic deposits but at the same time each has some merit for specific deposits.

Lacking in the discussion of the origin of most Proterozoic deposits, however, is the significance of the sedimentary (including metasedimentary) rocks which unconformably overlie the older rocks. Although these may be inferred to provide local sources for some uranium, the general assumption is that they provided sufficient lithostatic load to promote tectonic control. Even where geochemical prospecting techniques are employed the assumption is common that any anomaly may be indicative of ore at the unconformity. While I dispute neither the tremendous amount of uranium located at unconformities in Proterozoic rocks nor the exploration methods in use, I do feel it necessary to examine the possibility of preserved uranium deposits in sedimentary/metasedimentary rocks above the conventional and convenient unconformities.

The hypothesis to be explored in the remainder of this paper, then, is the possibility of the accumulation of significant amounts of uranium in Proterozoic basin filling sedimentary rocks prior to tectonism and/or metamorphism. Such deposits would be analogous to those of the central and western United States of America where argillaceous sandstones account for well over 95 percent of the Nation's reserves. The origin of these sandstone deposits has been thoroughly covered by Finch (1967), Brookins (1976) and others. Ore is usually interpreted as early epigenetic as opposed to syngenetic (Finch, 1967) although true syngenetic deposition of uranium cannot be unequivocally ruled out in some deposits. Criteria commonly thought to be useful in prospecting for uranium in these deposits include:

1) argillaceous sandstone of low to moderate permeability overlain and underlain by mudstones,
2) local increases in argillaceous matter to serve as traps for solutions and/or colloidal matter, or organic trash,
3) presence of organic matter which may act as a reductant for U(VI)-bearing solutions.

It is generally accepted that a characteristic suite of oxyions, U-V-Se-Mo, is segregated from many other elements and transported together until a chemically reducing environment is encountered. At that time these elements are reduced to a lower valence and precipitated from solution, although each element may be concentrated in a different mineral (i.e. U in pitchblende or coffinite, V in clay minerals or in oxides, Se in seleniferous pyrite or as native Se, Mo in jordisite). The place where precipitation occurs is commonly at the redox interface between up-dip, hematitic, oxidized rocks and down-dip, pyritiferous, reduced rocks. If additional oxygenated waters infiltrate the rocks, the redox front is moved down-dip, destroying much of the early formed ore while transporting the U-V-Se-Mo suite, again as oxyions, toward a new, chemically reducing environment. Prospecting for deposits in the immediate vicinity of the redox front is thus common in the deposits of Wyoming and Texas (both Eocene and younger(?)). In the Grants Mineral Belt, New Mexico, prospecting along the present redox front is most useful only for that ore which has been formed by sulphide-sulphate dependent reactions. Deeper in reduced rocks massive accumulations of ore are found which apparently were dependent on the presence of organic carbon to reduce U(VI) to U(IV). Commonly this ore (usually referred to as trend ore of presumed Late Jurassic age) occurs at point bars or other traps in the original, buried stream regime. Ore occurrences can, at times, be used to reconstruct palaeochannel systems.

In order to address the possibility of Colorado-type (here used to imply Grants Mineral Belt ore including both trend and redistributed ore; cf. Brookins, 1976) ore as being important in the Proterozoic, the larger part of the remainder of this paper will deal with

some well known characteristics of deposits in Gabon and the reader is again referred to Gauthier-Lafaye *et al.* (1978) and Weber (1978) for the key background articles.

AN OVERVIEW OF THE URANIUM DEPOSITS OF GABON

The geology of Gabon has been described in detail by Weber (1969) and others (see Gauthier-Lafaye *et al.*, (1978) and Weber (1978)). In brief, the majority of the land consists of pre-2 billion year old massifs on which several Middle Precambrian basins are preserved. The largest are the Booue, Lastourville, Franceville, and Okondja basins. Only the Franceville basin has been extensively explored; and, it is noteworthy that most of the uranium in Gabon is from deposits in this basin. The uranium deposits of the Franceville basin are located usually, but not always, at the break in sedimentation between basal (F1A) sandstones and overlying (F1B) arenaceous shales-argillaceous sandstones. Several repetitions in the sedimentary history are indicated. Common to the less conglomeratic parts of the Francevillian rocks is the presence of organic matter in which are found preserved fossil algae (Weber, 1969) plus 1Md illite, chlorite, quartz, carbonates, and both volcanogenic and plutonic detritus.

Uranium deposits are commonly described as due to control by lineaments within the basin at the F1A:F1B unconformity, but, strictly speaking, this is true only for the high (to 70% U at Oklo) grade ore. Commonly overlooked is the fact that much of the ore is located in relatively undisturbed, organic-rich argillaceous sandstones from which the high grade ore has been derived. The major deposits at Mounana, Boyindzi, Oklo and Okelobondo all show marked enrichment of uranium along fault and joint planes and uranium in at least part of Oklo has been locally derived (Gauthier-Lafayne, 1978).

Combinations of tectonic and stratigraphic controls are proposed for all the deposits mentioned above; at Boynidzi and Mounana, tectonic control is most important; at Oklo, although the highest grade ore does occur as in-fillings in a fractured system, the bulk of the ore occurs in the sandy-to-conglomeratic part of the unit known as Couche 1 and averages 0.4% U_3O_8. The ore at Okelobondo is less precisely known (Naudet, 1978) but may be similar to that at Oklo since they are only one kilometre apart and have similar mineralogies and other characteristics (Gauthier-Lafaye, 1978).

The ore at Oklo has received worldwide attention because the highest grade ore sustained a critical fission reaction for 0.5 to 2.0 million years at about 2 billion years ago (Bonhomme & Weber, 1975; Bonhomme *et al.*, 1978). This has led to a detailed study of the Oklo deposit over the last few years and a brief account of important parameters is given below.

The age of low grade ore formation at the Oklo deposit is about 2.0 ± 0.5 billion years (Gancarz, 1978), and this age is within the experimental limits of error for that assigned to the high grade ore; i.e. 1.9-2.0 billion years based on U-Ru, U-Nd, some U-Pb, and indirect methods based on interpretation of various rare earth element isotopic patterns as a function of uranium fission yield and fluence (Bonhomme *et al.*, 1978). A younger date of 1.85 ± 0.15 billion years has been reported for the Franceville Series by Bonhomme and co-workers (Weber & Bonhomme, 1975; Bonhomme, *et al.*, 1978), but this date is assumed to be a minimum as it is now interpreted as a diagenetic-silicification, post-ore age (Naudet, 1978). Of importance, however, is that Bonhomme and co-workers determined this date plus K-Ar dates on materials from the low grade zones and from barren host rocks, thus placing a minimum age on the Oklo deposit. Of special importance is the presence of 1Md illite in the Francevillian Series near the sites of the high grade ore. The mere fact that dates as old as approximately 1.8 billion years are obtained from such material indicates a relatively shallow burial; burial to depths in excess of 0.5 to 0.8 kilometers would have not only driven off radiogenic ^{40}Ar from the 1Md illites but probably would have caused more ordered illites

(1M, $2M_1$) to form. This point is stressed because the host rock of the high grade ore which sustained the nuclear reactions must have reached much higher temperatures of the order of 400°C or so (*note:* a controlling factor here is the critical point of water, which must have been present to sustain the nuclear reactions; temperatures greater than the critical temperature at any depth would drive off water and thus shut down the nuclear reactions for lack of medium for neutron transfer). Various depth estimates from 300 metres (P=80 bars; Holliger *et al.*, 1978) to 3500 metres (P=1 kilobar; Openshaw *et al.*, 1978) have been proposed for the high grade reactor ore. Although the writer does not dispute very high temperatures (possibly in excess of 500°C very locally; Vidale, 1978), much lower temperatures, certainly not in excess of 200°C, are more likely for the overall deposit with the higher temperatures reached in the reactor zones. It is also significant that in the reactor zones high temperature polytypes of chlorite and illite ($2M_1$) are present as opposed to low temperature polytypes 1Md in the low grade ore and in barren rocks. Further, fossil algae are preserved in the Franceville Series which also attests to low temperatures. Finally, although phyllitic material which is presumed in part to be a product of hydrothermal reactions at slightly elevated temperatures is noted in the reactor zones, no such authigenic material is noted away from the reactor zones.

Another estimate of temperature and an estimate of the range in oxidation potential and pH can be determined from study of the minerals present in the high grade reactor zones and from Eh-pH diagrams. Space does not permit the showing of Eh-pH diagrams. The reader is referred to Langmuir (1978), Garrels & Christ (1965) and Brookins (1979a) for the pertinent diagrams and discussion. The reactor ores are thought to have been subjected to local, oxidizing conditions during the operational lifetime of the reactors because both pyrite (and other sulphides) and hematite are noted, and native copper is found in close association with hematite but not in contact with pitchblende nor coffinite. Since the uranium minerals are commonly veined or rimmed by sulphides, the separation of native copper from them is explained as due to Eh-pH conditions slightly above the sulphide-sulphate boundary. At 25°C, 1 bar pressure, the field of native copper is well above the sulphide-sulphate boundary. At 200°C, 80 bars, however, the field of native copper overlaps the hematite field just above the sulphide-sulphate boundary (Brookins, 1979a). At temperatures closer to 400°C (P=80 bars to 300 bars) the field of native copper overlaps the sulphide-sulphate boundary such that a possible native copper-sulphide U-mineral assemblage should be common, but this is not the case. This information, then, argues for temperatures for the low grade ore of somewhere in the near vicinity of 200°C at a pressure of probably less than 300 bars (Brookings, 1979a). This lower temperature for the overall deposit is certainly more in line with the preservation of fossil algae, and the existence of low temperature polytypes of chlorite and illite.

The geometry of high grade ore has been worked out in fine detail by Gauthier-Lafaye *et al.* (1978). An extremely complex, vein-like geometry is common for much of the high grade ore, although it grades into blanket like ore at the edge of the deposit (Gauthier-Lafaye, 1978) who further shows that in places, due to faulting and other factors, there is no gradation of uranium from high grade to low grade ore, but that within a few meters, chemical gradations from low grade to high grade ore are observable. A gradational change in mineralogy and chemistry from low-grade to high-grade ore is noted in some places; where faulting and folding has been severe, no such gradation is noted.

The abundance of carbonates, many of which are probably penecontemporaneous with ore formation (Bonhomme *et al.*, 1978) argues for pH conditions greater than 7. This in turn suggests that UDC (uranyl dicarbonate ion; $(UO_2(CO_3)_2.2H_2O)^{2-}$) may have been responsible for transport of uranium from low-grade ore into the fracture filling, high-grade zones. This would allow for transport of U(VI) while not allowing for remobilization of V-Se-Mo as the Eh conditions were such that (a) sulphides were stable (hence no Se or Mo

migration), and (b) V was probably retained in host minerals in the low-grade ore even if oxidized (*note:* the ionic radi of V(III), V(IV), V(V) are within 5 percent of each other). Further, oxidation of U(IV) in the low-grade ore to soluble U(VI) would not affect the rare earth elements, hence they would remain in the low-grade ore. This must have happened as both the V and REE would, if transported with U(VI), have acted as sufficient poisons to prevent the nuclear reactions which occurred at Oklo. Because the waters for transport were slightly oxygenated, then oxidation of organic carbon in the fracture fillings could well have been the reducing mechanism for U(VI) to U(IV). This would also explain the lack of carbon in the high-grade ore zones.. The absence of quartz is not readily explainable, although it may be a simple matter of quartz paucity in the shale forced into the fractures.

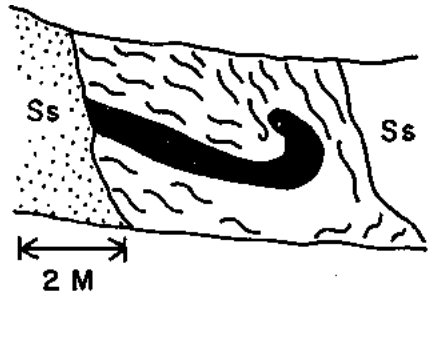
Regardless of all the uncertainties surrounding the genesis of the high grade ore at Oklo, what is clear is that sedimentation was either accompanied by syngenetic uranium accumulation or that the uranium in the low grade ore was early epigenetic. Further, the tilting and fracturing which followed the deposition of the F1B Series was, in terms of geologic time, close to the age of formation of the low grade ore as attested to by the fact that the radiometric age dating cannot unequivocally distinguish between the ages of low grade ore and high grade ore although the geologic control clearly shows the latter to have formed from the low grade ore. Further, even the end of diagenetic reactions may have occurred within 100 m.y. after low grade ore formation.

During all these steps ore of very different geometries was formed. The low grade ore tends to be concentrated into preferential layers (Couche 1 for example) whereas the high grade ore fills fractures and is usually vein-like in such sites while, less commonly, it grades both into high grade blanket-like accumulations or into the low grade ore. Weber (1975, p.606) has compared the Oklo deposit to the roll-type deposits of the Colorado Plateau, presumably like the Wyoming or Texas types (*note:* roll-type ore in the Grants Mineral Belt, New Mexico is explained by various hypotheses and is not as simple as the other occurrences). No block diagrams to verify a roll geometry for the Oklo deposit have been presented, although Chauvet (1975) has presented diagrams suggesting down-dip migration of ore after tilting of the Franceville Series just prior to fracturing. His interpretation can only be verified by detailed block diagrams which as yet have not been published. In short, and especially when one remembers that the signs for an oxidation front (i.e. hematite, etc.) are found only in the fracture systems where oxidizing waters are postulated to have moved, then a roll-type geometry for the low grade ore is speculative at best. Due to the abundance of U(IV) minerals with organic carbon, low temperature chlorite and illite, carbonates, and sulphides in the low grade ore with quartz and both volcanic and plutonic detritus as part of the gangue; the low grade Oklo ore is not dissimilar from ore formed in reduced rocks (i.e. below the sulphate-sulphide boundary) in the Grants Mineral Belt, New Mexico (Brookins, 1976). If true, then original mineralization was controlled by the reduction of U(VI) to U(IV) due to the presence of the organic matter and not by sulphate-sulphide equilibria. Two billion years ago oxidizing conditions were less common than during the Mesozoic. In addition, fossil algae were the source of organic carbon at Oklo, whereas lignin-derived organic carbon was common during the formation of the Grants Mineral Belt ore. Further, coffinite is much less abundant than pitchblende in Proterozoic deposits whereas the opposite is commonly true for Mesozoic deposits. This last fact, however, is due to the greater instability of coffinite to even slightly oxidizing conditions relative to pitchblende, thus Proterozoic deposits may, when first formed, have contained more coffinite than is now noted. At Oklo, a low silica activity in the fracture fillings would also favour pitchblende formation relative to coffinite. Geffroy (1975) has described secondary coffinite at Oklo altering from pitchblende where secondary quartz has formed.

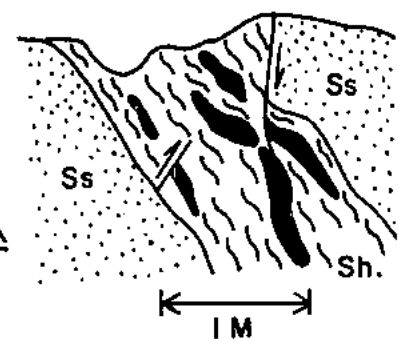
Yet despite these differences, there are several similarities between the low grade Oklo ore and many Mesozoic deposits:

1) uranium occurs in organic-rich, argillaceous sandstones;
2) organic carbon served as a reductant for U(VI) to U(IV);
3) uranium is associated with V, Mo, Se; this implies transport as oxyions of these elements prior to reduction;
4) some stack ore (i.e. ore remobilized during orogeny and reprecipitated in fault systems) in the Grants mineral belt resembles the fracture filling ore at Oklo and, although of much lower grade than Oklo, it contains less organic carbon than the primary, trend ore;
5) both the low grade Oklo and Grants trend ore can be interpreted as early epigenetic or syngenetic.

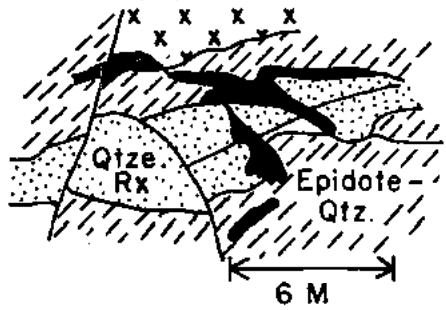
It is of interest to speculate on how the uranium deposits of the Grants Mineral Belt might be changed had they been formed approximately 1.5 billion years (or more) age. The deposits occur in Late Jurassic rocks of the Morrison Formation, which consists of a thick sequence of non-marine sandstones and mudstones. Local unconformities are noted between some of the Members of the Morrison although most boundaries are conformable. The Morrison rocks were tilted prior to uplift, peneplanation, and subsequent subsidence and deposition of Cretaceous marginal marine to marine sandstones and shales. Some of the Morrison ore is truncated at the angular unconformity with the Cretaceous rocks. The angularity is quite low, 0.5 to 3 degrees apparent dips are common. If these rocks, which



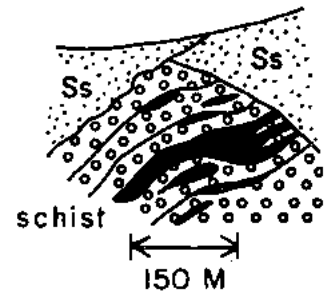
A. Oklo, (modified from Gauthier-Lafaye, 1978, p.95).



B. Oklo, Gabon. (Modified from Gauthier-Lefaye, 1978, p.113).



C. Rayrock Mine, Northwest Territories, Canada. (Modified from Rich *et al.*, 1978, p.113).



D. Jabiluka, Australia. (Modified from Kimberley, 1978, p. 212).

Figure 1. Sketches of ore deposits from Oklo, Canada and Australia to illustrate similarites.

represent about 50 million years of first-to-remobilized ore formation, were truely formed about 1.5 billion years ago and subjected to burial to some 500 metres to 1,500 metres, and to the same degree of tilting, folding and other processes effective in the Franceville Basin, then it would be logical to expect the Grants Mineral Belt ores to be effected in an equivalent fashion as those at Oklo. The uranium in the uppermost Morrison would certainly be mobilized and, if Cretaceous mudstones were downfilled into fractures in the sandstones, uranium would also likely be enriched in these newly formed traps. Two billion years ago U(IV) would also preferentially be oxidized to soluble U(VI) relative to V, Mo, Se and thus be concentrated alone as at Oklo. Further, the sequence of rocks would consist of non-marine to marine sandstones and mudstones with both subtle and well defined unconformities present. At Oklo, Bonhomme's work (1975, 1978) suggests a period of earth history covering perhaps 200 m.y., hence the hypothetical sequence of events for the Grants Mineral Belt uranium deposits is not at all unreasonable.

DISCUSSION

The many geometries for vein or vein-like massive accumulations of uranium have been extensively covered in the literature (see references cited earlier in this paper) and need no extensive review here. Figure 1 (Brookins, 1979b) illustrates some similarities between parts of the Oklo ore and ore from both Canada and Australia, although the scales are admittedly quite different. What is important to note, however, is that a deposit such as that at Oklo could, if subjected to low to moderate prograde metamorphism, yield ore geometries similar to those described from Saskatchewan or from Australia. To illustrate this point consider figure 2 which is a simplified version of the model proposed for the Key Lake deposit, Saskatchewan, Dahlkamp (1978). In figure 2a, deposition of lagoonal or shelf sediments is accompanied by uranium mineralization; the source of the uranium being syngenetic processes at the surface and by lateral secretion from basement rocks below the surface. It can be argued that processes operative at Oklo represent this stage (Chauvet, 1975). Figure 2b depicts the scenario after the Lower Proterozoic (Hudsonian Orogeny) (1.8-1.9 billion years ago) where low grade, more-or-less uniform ore is now concentrated due to remobilization into favourable sites parallel or subparallel to original bedding planes. Figure 2c shows early deposited Martin sediments (M) somewhat irregularly distributed relative to the much thicker overlying Athabasca Formation (about 1.3 billion years ago ?), and some faulting and diabase dyke intrusion as indicated. Note that some of the ore has again been mobilized and fixed away from original bedding planes in the folded rocks. Figure 2d is assumed to represent the commonly accepted scenario at Kay Lake from about 200 million years ago to the present. Destruction of the Athabascan sediments by erosion and destruction-redistribution of some surface or near-surface uranium at the unconformity of the Athabascan with the post-Archaean-Kenoran rocks may now occur thus further confusing an exact reconstruction of events. A similar mechanism may account for some Australian deposits (Fig. 1d).

Now consider an hypothetical multistage model for the Gabonese deposits as depicted in figure 3. In figure 3a, a highly idealized and simplified view of the Francevillian Series (F) is shown in a tilted syncline surrounded by granitic massifs; the high grade ore is shown as inclined to the Francevillian bedding planes and low grade ore as podlike for convenience. The basic difference between figure 2a and figure 3a is that the uranium in the Francevillian rocks may be syngenetic with little (if any?) lateral secretion. Otherwise the diagrams are similar in that shelf to lagoonal sediments are proposed. The Francevillian Series was never buried to any appreciable depths as were the pre-Martin, post-Archaean-Kenoran host rocks at Key Lake; hence figures 3b and 3c are intended as situations which might have arisen had the section shown in figure 3a been buried to depths sufficient to promote metamorphism. In

figure 3b burial to a depth to modify and in part obliterate the high grade fracture system is proposed, accompanied by mobilization of the low grade, disseminated ore into more concentrated masses. Evidence for the original low temperature origin of these rocks may be destroyed but may be inferred from elemental distributions within the rocks and possibly by fluid inclusion work. In figure 3c is shown a hypothetical sequence somewhat analogous to figure 2c. If sufficient depth for situations at either 3b or 3c was achieved, then graphitic schists would form from the carbonaceous parts of the Francevillian sediments. As depicted in figure 3c, where subsequent uplift, peneplanation, subsidence and sedimentation has been proposed, the margins of exposed ore will be destroyed or locally redistributed and, due to lead loss, very young U-Pb ages would be obtained from such remobilized ore.

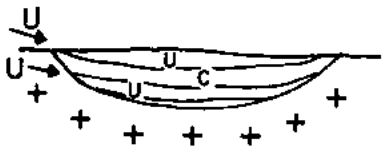


Figure 2a. Deposition of post Archaean-Kenoran: pre-Martin carbonaceous (C) and uraniferous (U) sediments; U derived syngenetically and by lateral secretion.

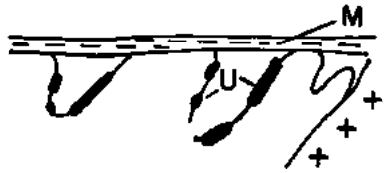


Figure 2b. Metamorphism of sediments (2a) with deposition of Martin Sediments (M) following erosional cycle. U fixed as indicated.

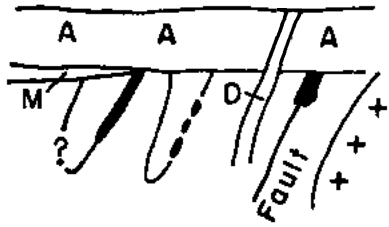
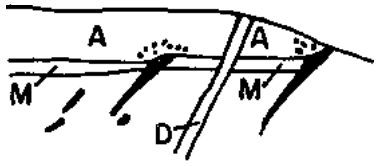


Figure 2c. Long post-Martin period followed by deposition of Athabasca Formation (A) with later intrusion of diabase dykes (D). Some U remobilized, truncated, etc.



(Modified from Dahlkamp, 1978)

Figure 2d. Present (from 200 m.y. ago (?)) view of Key Lake U deposits with young U remobilization.

Whereas the foregoing discussion is admittedly speculative, the point is that every step hypothesized for the Gabonese deposits, had they been formed in more tectonically active parts of Africa, are reasonable in view of what is proposed as the logical sequence events for such deposits as Key Lake (and the writer reminds the reader once again that Key Lake is only one of any number of deposits where such a scenario might be envisaged).

An important facet of the hypotheses (Figs. 3a-3c) is that some remobilization and concentration occurred under low temperature conditions. While the nuclear reactions at Oklo have made local temperature measurements unreasonably high relative to the surrounding low grade ore, the deposits at Boyindzi and Mounana should be more easy to study by conventional fluid inclusion and mineral paragenetic interpretation of temperatures of formation. The deposit at Okelobondo will be more difficult to assess as some ^{235}U depleted ore has been discovered there (Naudet, 1978) which, due to nuclear reactions, will thus result in high temperatures in some ore zones.

CONCLUDING STATEMENTS

Whereas numerous conclusions are not warranted from the foregoing discussion, some statements are in order. (1) Conditions accompanying sedimentation at about 2.1-1.6 billion years ago were sufficiently reducing such that U(IV) could be syngenetically fixed in shelf or lagoonal sediments. (2) Assuming relatively large amounts of uranium; the amounts of other elements transported as oxyions and fixed with U(IV) during reduction in Proterozoic deposits would be extremely variable as local versus widespread transport of uranium may have been the rule. (3) Simple basin filling during subsidence accompanied

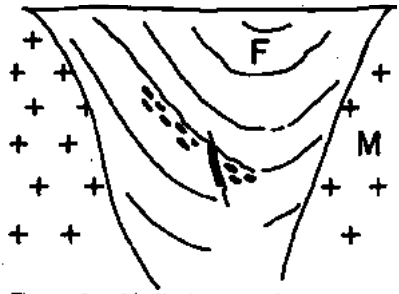


Figure 3a. Idealized view of tilted and synclinally folded Francevillian Series with both disseminated-blanket ore (pods) and local high grade ore in fracture fillings.

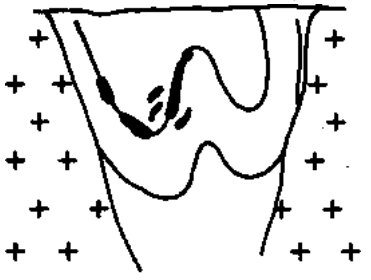


Figure 3b. Hypothetical Oklo scenario post-2 Gyr with U remobilization as indicated.

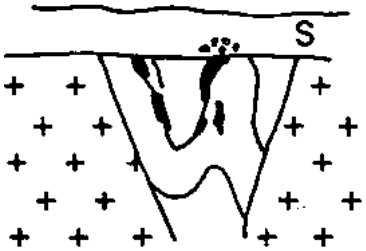


Figure 3c. Deposition of post-Francevillian sediments (S) accompanied by U redistribution as indicated; events may occur any time after 3b.

by innerbasin faulting and fracturing, followed by infiltration of slightly oxidizing waters could mobilize uranium as U(VI) while not necessarily mobilizing other elements. This is proposed for Oklo although the exact mechanism(s) responsible for carbon-depletion in the high grade ore zones is not known. (4) Burial with accompanying folding and faulting of rocks equivalent to the Gabonese deposits could easily result in the varied vein and vein-like geometries noted in many Proterozoic uranium deposits in metamorphic rocks where deposits are parallel to original bedding planes, controlled by faults, or at angles to original bedding planes. The fact that the deposits at Mounana, Boyindzi, Oklo and Okelobondo are all different in some aspects yet are all of the same age and preserved at approximately the same temperature, pressure conditions emphasises just how easily complex ore geometries can evolve from syngenetic and early epigenetic sedimentary deposits. (5) Exploration targets in Proterozoic basins are unusually focused on unconformities; either around the basin edges or looking for some surface or near-surface evidence of dispersed ore from a truncated ore body as depicted in figure 2c or figure 2d. Spot mineralization in the basin interiors, especially along lineaments, is commonly interpreted as due to favourable remobilization of deep seated uranium upward toward the surface. In fact, as evidenced by the Gabonese deposits, downward leaching of ore may also result. (6) There are a large number of Proterozoic basins with, infilling sediments favourable in age 1.5-2.1 billion years old), carbonaceous matter (or evidence for former accumulations), close to favourable uranium source areas (either granites, volcanics, arkosic sediments or metasediments), and trace element distributions that warrant exploration for sandstone-type accumulations in the interiors of the basins, as well as at the basin edges. Basins in tectonically stable areas are of course favourable targets as are smaller basins in tectonically active areas where remobilization and reconcentration are plausible. (7) These host rocks are also not unique in terms of favourability for uranium accumulation. Syngenetic or early epigenetic models, possibly with a greater favourability for high uranium accumulations in smaller total areas in the Proterozoic relative to Phanerozoic basins due to the more reducing conditions in the Proterozoic, are certainly as viable as more complex models for uranium mineralization in such rocks. One attractive feature of such an hypothesis is, of course, that very complex models and hence tedious and perhaps unjustified exploration programs for originally syngenetic deposits in metamorphic rocks interpreted as hydrothermal, etc. deposits can possibly be distinguished.

REFERENCES

Bonhomme, M., Leclerc, J. & Weber, F., 1978: Etude radiochronologique complementaire de la serie du Francevillien et de son environment *in, Natural Fission Reactors — Les Reacteurs de Fission Naturels. Proceedings of Technical Committee Meeting, Paris.* International Atomic Energy Agency, Vienna, 19-24.

Bowie, S.H.U., Davis, M. & Ostle, D., 1972: Proceedings of a NATO-sponsored Advanced Study Institute on Methods of Prospecting for Uranium Minerals London. *London Inst. Min. Metall.*, 346p.

Brookins, D.G., 1976: Uranium deposits of the Grants, New Mexico mineral belt. *U.S. Energy Res. Dev. Agency, Rpt GJO-1636-1*, 120p.

Brookins, D.G., 1979a: Thermodynamic considerations underlying the migration of radionuclides in geomedia: Oklo and other examples. *in* (ed G. McCarthy) *Scientific Basis for Nuclear Waste Management, 1*, 355-366.

Brookins, D.G., 1979b: Syngenetic model for some early Proterozoic uranium deposits: evidence from Oklo. *Extended Abstracts of the International Uranium Symposium on the Pine Creek Geosyncline*, 26-29.

Chauvet, R.J., 1975: Description de gisement d'uranium d'Oklo. *in, The Oklo Phenomenon. Proceedings of a Symposium, Libreville.* International Atomic Energy Agency, Vienna, 53-66.

Dahlkamp, F.J., 1978: Geologic appraisal of the Key Lake U-Ni deposits, northern Saskatchewan. *Econ. Geol., 73*, 1430-1449.

Dodson, R.G., Needham, R.S., Wilkes, P.G., Page, R.W., Smart, P.G. & Watchman, A.L., 1974: Uranium mineralization in the Rum Jungle-Alligator Rivers Province, Northern Territory, Australia. *in, Formation of Uranium Ore Deposits. Proceedings of a Symposium, Athens.* International Atomic Energy Agency, Vienna, 551-568.

Finch, W.I., 1967: Geology of epigenetic uranium deposits in sandstone in the United States. *Prof. Pap. U.S. geol. Surv.*, 538, 121p.

Gancarz, A., 1978: U-Pb age (2.05 x 10^9 years) of the Oklo uranium deposit. *in, Natural Fission Reactors — Les Reacteurs de Fission Naturels. Proceedings of Technical Committee Meeting, Paris.* International Atomic Energy Agency, Vienna, 513-520.

Gauthier-Lafaye, F., 1977: Oklo et les gisements d'uranium du Francevillien aspects tectonique et metallogenique. *Ph.D. Thesis, University of Strasbourg*, 81p, (unpubl.).

Gauthier-Lafaye, F., 1978: Suivi geologique de l'exploitation des reacteurs naturels d'Oklo. *in, Natural Fission Reactors — Les Reacteurs de Fission Naturels. Proceedings of Technical Committee Meeting, Paris.* International Atomic Energy Agency, Vienna, 75-130.

Gauthier-Lafaye, F., Besnus, Y. & Weber, F., 1978: Donnees nouvelles sur l'environnement geologique des reacteurs naturels, *in, Natural Fission Reactors — Les Reacteurs de Fission Naturels. Proceedings of Technical Committee Meeting, Paris.* International Atomic Energy Agency, Vienna, 35-71.

Geffroy, J., 1975: Etude microscopique des minerais uraniferes d'Oklo. *in, The Oklo Pheomenon. Proceedings of a Symposium, Libreville.* International Atomic Energy Agency, Vienna, 133-152.

Holliger, P., Devillers, C. & Retali, G., 1978: Evaluation des temperatures neutroniques dans les zones de reaction d'Oklo par l'etude des rapports isotopiques. *in, Natural Fission Reactors — Les Reacteurs de Fission Naturels. Proceedings of Technical Committee Meeting, Paris.* International Atomic Energy Agency, Vienna, 553-568.

Hostetler, P.B. & Garrels, R.M., 1962: Transportation and precipitation of uranium and vanadium at low temperatures, with special reference to sandstone-type uranium deposits. *Econ. Geol., 57*, 137-168.

Kimberley, M.M., 1978: *Short Course in Uranium Deposits: Their Mineralogy and Origin. Mineralogical Association of Canada*, 521p.

Knipping, H.D., 1974: The concepts of supergene versus hypogene emplacement of uranium at Rabbit Lake, Saskatchewan, Canada. *in, Formation of Uranium Ore Deposits. Proceedings of a Symposium, Athens.* International Atomic Energy Agency, Vienna, 531-550.

Langford, F.F., 1978: Uranium deposits in Australia. *in* (ed. M.M. Kimberley) *Short Course in Uranium Deposits: Their Mineralogy and Origin. Mineralogical Association of Canada*, 205-216.

Langmuir, D., 1978: Uranium solution-mineral equilibria at low temperatures with applications to sedimentary ore deposits. *Geochim. cosmochim. Acta, 42*, 547-570.

Naudet, R., 1978: Problemes poses pal le deroulement de phenomene d'Oklo: tentative d'interpretation globale. *in, Natural Fission Reactors — Les Reacteurs de Fission Naturels. Proceedings of Technical Committee Meeting, Paris.* International Atomic Energy Agency, Vienna, 715-734.

Openshaw, R., Pagel, M. & Poty, B., 1978: Phases fluides contemporaines de la diagenese des gres, des mouvements tectoniques et du fonctionnement des reacteurs nucleaires d'Oklo. *in, Natural Fission Reactors — Les Reacteurs de Fission Naturels. Proceedings of Technical Committee Meeting, Paris.* International Atomic Energy Agency, Vienna, 267-296.

Rich, R.A., Holland, H.D. & Peterson, U., 1977: *Hydrothermal Uranium Deposits.* Elsevier, Amsterdam, 264p.

Siever, R. & Kastner, M., 1972: Shale petrology by electron microprobe: pyrite-chlorite relations. *J. sedim. Petrol., 42*, 350-355.

Smith, E.E.N., 1974: Review of current concepts regarding vein deposits of uranium. *in, Formation of Uranium Ore Deposits. Proceedings of a Symposium, Athens.* International Atomic Energy Agency, Vienna, 515-530.

Vidale, R.J., 1978: The highest temperatures recorded by the Oklo mineral phase assemblages and rock textures, *in, Natural Fission Reactors — Les Reacteurs de Fission Naturels. Proceedings of Technical Committee Meeting, Paris.* International Atomic Energy Agency, Vienna, 235-242.

Weber, F., 1969: Une serei Precambrienne du Gabon: la Francevillien sedimentologie, geochimie, relations avec les gites mineraux associes. *Ph.D. Thesis, University of Strasbourg*, 328p. (unpubl.).

Weber, F., 1978: Etat des etudes geologiques entreprises en France sur le gite d'Oklo depuis le Colloque de Libreville. *in, Natural Fission Reactors — Les Reacteurs de Fission Naturels. Proceedings of Technical Committee Meeting. Paris.* International Atomic Energy Agency, Vienna, 181-198.

Weber, F. & Bonhomme, M., 1975: Donnees radiochronologiques nourvelles sur le Francevillien et son environnement *in, The Oklo Phenomenon. Proceedings of a Symposium, Librebille.* International Atomic Energy Agency, Vienna, 17-36.

CONTINENTAL WEATHERING AND DEVELOPMENT OF PALAEOSURFACE-RELATED URANIUM DEPOSITS: SOME GENETIC CONSIDERATIONS

J. E. Tilsley

David S. Robertson & Associates Limited, Suite 2000, 62 Queen St. West, Toronto, Canada.

ABSTRACT

The uranium deposits of the Alligator Rivers Uranium Field, Northern Territory, Australia, and the Athabasca basin area, Saskatchewan, Canada, are of major importance in terms of the world's future energy supply. Their genesis has been interpreted variously in terms of metamorphic events, hydrothermal activity and syngenetic processes.

It is believed that the most highly enriched of these deposits are the result of epigenetic concentration related to the weathering process. Subsequent modification by what appear to be hydrothermal events may, in part, be related to thermal anomalies developed due to the heat of radioactive decay of the uranium in the ore during burial by younger sedimentary rocks. Thermal anomalies can also be expected to be associated with graphitic zones that are commonly spatially related to this sort of deposit.

A genetic model for paleosurface-related vein-type deposits is proposed. It involves preconcentration of uranium in Lower Proterozoic (Aphebian) carbonaceous pelitic and argillaceous sediments that were later altered to graphitic schists during regional metamorphism. Subsequent continental weathering released the uranium to surface and groundwater from which it was concentrated in suitable physical-chemical traps. It is proposed that naturally occurring, direct current electrical fields played a dominant role in deposition and preservation of the mineralization.

This model supplies criteria useful to the exploration process as follows:

1) Lower Proterozoic (Aphebian) sediments are preferred source and host rocks.
2) High grade mineral concentration appears to be related to electrically conductive zones in the basement. These zones can be located and traced geophysically through significant thicknesses of cover rock.
3) Post-depositional remobilization of UO_2 for several hundred metres up into cover rocks may result from hydrothermal circulation due to heat of radiogenic decay of the ores. Such mineralization may be a useful guide to ore at depth.
4) Thermal anomalies are not to be expected at surface but detection of temperature rise near ore zones beneath cover rocks may be of some exploration value.

INTRODUCTION

Uranium deposits that appear to be spatially related to Proterozoic weathering surfaces have been located in the Northern Territory, Australia, and in northern Saskatchewan, Canada. Among deposits of this type are ore bodies that contain large reserves of uranium in material of exceptionally high grade. Such ore bodies are of great importance in assuring future energy supplies.

The genesis of these vein-type deposits is variously interpreted in the literature as related to metamorphic events (Ryan, 1977) or hydrothermal activity (Morton & Beck, 1978) or supergene processes (Knipping, 1974). Other genetic models that require a combination of these processes have been suggested (Hoeve & Sibbald, 1978).

It is not the purpose of this paper to discuss these concepts which are thoroughly described in the papers referenced above and in recent reviews (McMillan, 1976 and 1977; Nash, 1978; Langford, 1978). Instead a genetic model is proposed that considers the source of the metals involved, the history of concentration, post-depositional behaviour of the mineralization, environmental constraints on each phase of the genetic cycle and the energy requirements of each stage.

While the major uranium deposits of the Alligator Rivers Uranium Field, for example, Ranger and Jabiluka, may have only an accidental relationship to the pre-Kombolgie weathering surface, the high-grade deposits of the Athabasca region (e.g. Key Lake, Midwest Lake) lie at the unconformity at the base of the Athabasca sandstone. Mineralization is hosted by either basement or cover rocks, or both. The proposed processes of concentration and modification apply to the high-grade Athabasca-type deposits,

however, the geological environment in the Alligator Rivers Uranium Field appears to be particularly favourable for development of similar ore bodies.

GENETIC MODEL: PALAEOSURFACE-RELATED URANIUM DEPOSITS MODELLING CRITERIA

Development of a mineral concentration is dependent on fulfillment of several basic requirements: There must be a source of readily available metal(s) within the environment under consideration. An effective collection and transportation system must be operating while the metal(s) are readily available. The collection and transportation media must carry the metal(s) into an environment where energy conditions permit their deposition and concentration. Subsequent to deposition, mineral assemblages may be modified by a variety of geologic processes. Such modification may be tolerated up to the point beyond which the element(s) of interest are made unrecoverable or are dispersed.

If these requirements are satisfied and if the nature of the mineralization, its degree of concentration, and other factors, permit economic recovery of one or more of its constituents, an ore body exists. If any of the requirements cannot be fulfilled, there can be no ore body. The inter-relationship of these factors is illustrated in figure 1.

PROPOSED GENETIC MODEL

The proposed genetic model is illustrated in figure 2.

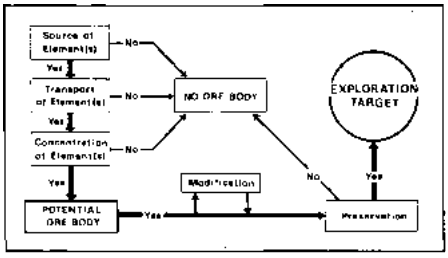


Figure 1. Conceptual Model: Formation of Ore Deposits.

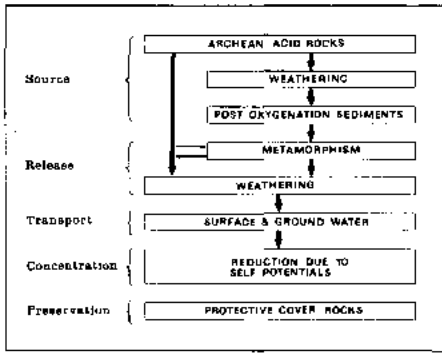


Figure 2. Genetic Model: Palaeosurface-related Uranium Deposits.

General Environmental Constraints

During Archaean and Early Proterozoic time, uranium was, in general, probably chemically mobile only in certain magmatic and metamorphic environments.

In the surface environment, however, available uranium would not have been chemically active. Its minerals would have been insoluble and reported as detrital materials in alluvial deposits such as at Elliot Lake, Canada, and in the Dominion Reef and Witwatersrand Systems in South Africa (Robertson, 1974; Theis, 1978).

With significant increase in the oxygen content of the atmosphere in early Proterozoic time (about 2200 Ma; Roscoe, 1973; Cloud, 1976; Walker, 1977) uranium minerals in the surface environment became as notably soluble as they are today. Uranium was released by weathering of all rocks reported in surface and groundwaters. With this mobility of uranium in the surface environment, low-temperature chemical concentration of the metal became possible. Ore deposits that require uranium to be mobile in low-temperature near-surface environments cannot be older than this change. It is proposed herein that palaeosurface-related vein-type uranium deposits are the result of low-temperature chemical-electrochemical activity and

are intimately related to weathering processes. This relationship is further considered following the sequence of modelling criteria outlined earlier.

Source of Metal(s)

Certain Archaean felsic igneous rocks and their metamorphic equivalents are known to be modestly to moderately enriched in uranium (Robertson, 1978). It has been proposed that weathering of these rocks during Lower Proterozoic and late Archaean time provided the uraninite of the Elliot Lake and Witwatersrand ores (Robertson, 1974; Roscoe, 1973; Theis, 1978; Robertson, 1978).

Post-oxygenation weathering of similar rocks, which can contain two to ten parts per million uranium or more, may have provided, directly, the uranium for concentration in palaeosurface-related deposits being considered. It appears more likely, however, that there was an intermediate stage of uranium concentration. Carbonaceous pelitic sediments are well known to be enriched in a variety of metals, including uranium. Sometimes these enrichments approach economically recoverable levels as in the Cambrian Alum shales of Sweden (OECD-IAEA, 1977).

Uranium deposits of the Athabasca basin are found in, and immediately overlying, post-oxygenation Lower Proterozoic (Aphebian), commonly graphitic, metasedimentary rocks. The Cahill formation which hosts the major Australian deposits of the Alligator Rivers Uranium Field is of similar age. The spatial relationship of the Australian ores with graphitic, fine-grained metasediments suggests an originally syngenetic collection of metal.

Carbonaceous pelitic sediments are usually pyritic to some extent and often contain more than 5% iron sulphide (Bayley & James, 1973). Uranium values in such sequences tend to be highest in the more graphitic and iron sulphide-bearing sections (Gandhi, 1978). This is presumably reflective of the more strongly reducing conditions within these parts of the sedimentary sequence during deposition. The contained uranium is considered to have been introduced syngenetically prior to diagenesis of the sediment, since permeability of argillaceous and pelitic sediments is notably low even at the time of sedimentation and decreases further during lithification. Subsequent remobilization of metal is often observed to be due apparently to metamorphism of the sediments. But there is little evidence to indicate widespread post-depositional accumulation of uranium.

Although igneous and metamorphic terranes may be relatively enriched in uranium contained in minerals that will release the metal to surface and groundwater during weathering, it would appear, on the basis of exploration evidence, that early post-oxygenation pelitic sediments are preferred source rocks.

Release of Metal(s)

Uranium may be present in rocks in a variety of minerals. Only those minerals that are destroyed by weathering will release metal to surface or groundwater. It is this available or 'labile' uranium that is of importance in the low-temperature geochemical cycle.

Uranium in carbonaceous shales is often bound into organic complexes (Å. Anderson, pers. comm. 1979). These complexes must be partially destroyed before the metal becomes readily available (Stapleton, 1978; Bell, 1978). Metamorphism of an uranium-enriched sedimentary sequence to a level in excess of greenschist facies or complete oxidation during weathering is necessary to decompose the organic component adequately to free contained metals. Metamorphism of carbonaceous materials to graphite expells all elements from the crystal lattice excepting boron.

Metamorphism up to, but not including, anatexis would therefore appear to be beneficial in preparation of a sedimentary sequence for most efficient release of metal during the weathering process.

It appears that the pH of the weathering environment is a critical factor in the genetic equation. Unless a relatively low pH is maintained (pH = 5 or less), uranium in waters that

contain CO_2 will likely be transported as uncharged $UO_2CO_3^0$ or as a $UO_2(CO_3)_2^{2-}$ complex (Langmuir, 1978). Such complexes are not likely to be concentrated readily by the sort of electro-chemical influences interpreted to be responsible for development of high-grade paleosurface-related uranium deposits.

Rate of Erosion

The palaeosurfaces with which the Australian and Canadian deposits are related are described as gently to moderately undulating peneplanes. Some areas show evidence of deep weathering, while in other cases younger sediments of the Athabasca and Kombolgie Formations lie upon a clean-swept surface (Hoeve & Sibbald, 1978; Climie, pers. comm. 1978; Curtis, pers. comm. 1978 and pers. comm. 1979).

The rate of weathering for this sort of topography in what appears to have been an alternatively wet-dry seasonal environment (McMillan, pers. comm. 1979) is likely to range between 30 and 3,000 Bubnoff units (Kukal, 1971). The Bubnoff unit is defined as 1 micron/year = 1mm/thousand year = 1m/million years (Fischer, 1969).

Calculations based on dissolved load in rivers flowing in mature topography and rate of sedimentation of reservoirs (Gottschalk, 1964) indicate an erosion rate of 100 Bubnoff units (1m per 10,000 years) as a likely denudation rate, slightly more than the average for all continents of 80B calculated by Kukal (1971, p.29) from data given by Schumm (1963).

Assuming a relatively small catchment of 10km wide and 20km long being eroded at the rate of 100B, mass balance calculations for available uranium contents in bedrock of 5, 10, 20 and 50 ppm give the results shown in table 1. An annual basin discharge of 50 x $10^6 m^3$ H_2O, equivalent to 0.25 metres total runoff is assumed.

	Uranium Released		
Available U ppm	Tonnes/Vertical Meter	Tonnes/Year	Average U Concentration in Catchment Discharge
5	1,500	0.25	5.0 ppb
10	5,000	0.50	10.0
20	10,000	1.00	20.0
50	25,000	2.50	50.0

Table 1. Release of uranium during weathering.

Transportation

In this model it is assumed that the uranium released by weathering is transported from the catchment in the total runoff which is made up from surface and groundwater. This water, flowing through surface drainage systems, could carry the volume of uranium common to this type of deposit into the area of influence of a concentration cell of the sort proposed herein, in a relatively short time (Table 1).

The efficiency of such a transportation system is obviously many times greater than that of groundwater moving in even the most permeable aquifers.

Concentration

Behaviour of Charged Species in Solution

Ions and charged complexes in natural and man-made solutions respond to applied electrical potential gradients by migrating at a rate which is a function of the voltage gradient and a constant peculiar to the ion or complex. Ions that carry a positive charge move counter to electron flow, i.e., from relatively positive toward relatively more negative voltages. Negatively charged ions and complexes migrate toward relatively more positive voltages.

At a potential gradient of 100 mV per metre, the hydrogen ion would migrate 1.14 metres per year in a static aqueous solution at 20°C. Metal ions move at a slower rate, about 0.15 to 0.25 metres per year under the influence of the same potential gradient (Moore, 1972).

Spontaneous Polarization or Self-Potentials

Self-potentials are developed in the earth when volumes of differing Eh are connected electrically. Such contrasting conditions in nature exist between relatively positive Eh (oxidizing conditions) in the weathering environment and relatively negative Eh (reducing conditions) at depth.

Bolviken & Logn (in press) proposed the Primary Redox Field model (Fig. 3), which assumes uniformly decreasing Eh and increasing pH with depth. The effect of a conductive body in the primary Redox Field is illustrated in figure 4.

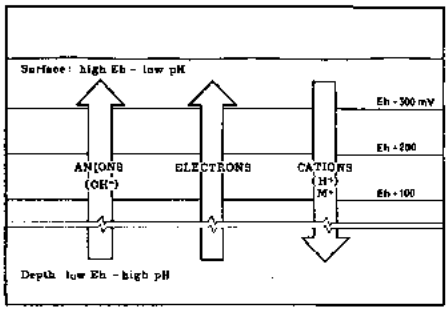


Figure 3. Bolviken's (Bolviken & Logn, in press) Primary Redox Field.

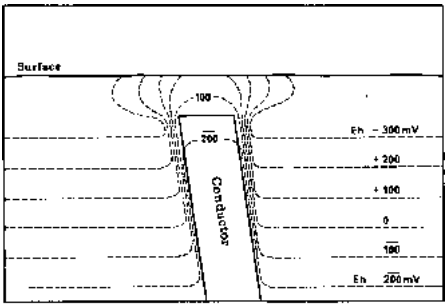


Figure 4. Effect of conductor on Primary Redox Field.

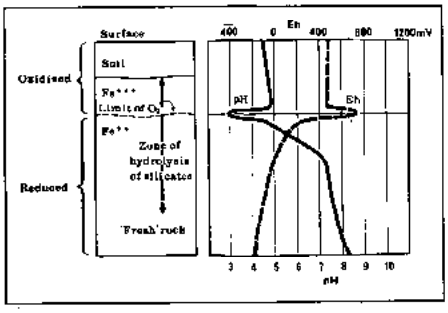


Figure 5. Primary Redox Field - Deep Weathering.

We find that Eh changes, at least in areas of deep weathering, are less regular. Significant Eh contrast is observed across what appears to be the limit of free oxygen in groundwater (Fig. 5). The Bolviken model (Figs. 3 & 4) however, serves to illustrate the origin of self-potentials in an uncomplicated system. In areas of active chemical weathering, it seems that electrical activity on a conductive structure would tend to be most concentrated at the limit of free oxygen.

Voltage differences across the axis of a conductive body such as massive sulphides or graphitic schists are frequently in the order of 500 to 700mV and, in some cases (Kelly, 1957; Chisholm, 1957) are in excess of 1,000mV. Near the axis of conductive structures, voltage gradients of 50 to 100mV or more per metre are possible.

Electro-precipitation of Uranium Minerals

Uranium in solution as a positively charged complex, UO_2^{2+} or $UO_2(OH)^+$ for example, would tend to migrate toward the low voltage superimposed on the surface environment by a conductive body extending from the zone of weathering to reducing conditions at depth.

These uranium-bearing complexes will be precipitated as UO_2 if the voltage applied by the self-potential cell is lower than the upper stability limit of the solid phase. This limit is about Eh +50mV at pH5 (Hostetler & Garrels, 1962). More recent data (Langmuir, 1978) suggest that this upper stability limit may be somewhat higher, at about Eh 200mV at the same pH. In any

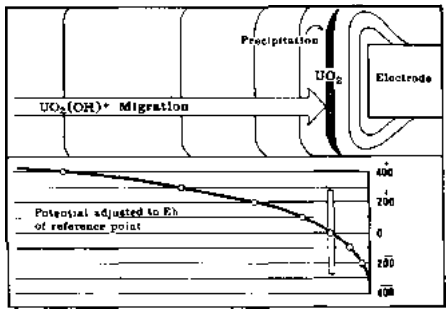


Figure 6. Electroprecipitation of UO_2 from $UO_2(OH)^+$

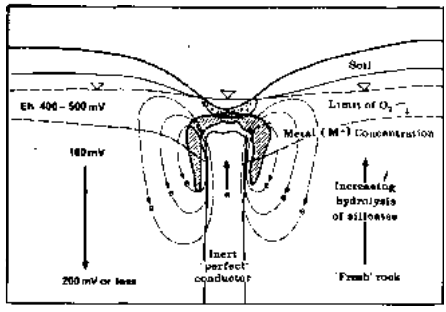


Figure 7. Uranium Concentration at 'Good' conductor.

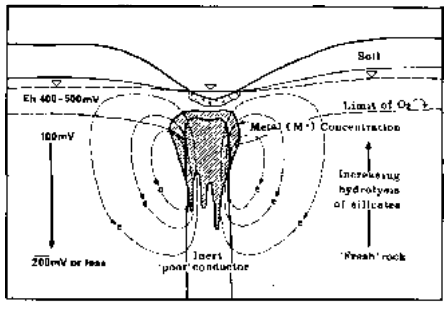


Figure 8. Uranium Concentration at 'Poor' conductor.

event, if the applied voltage is less than the upper stability limit, or if the complex migrates into a chemical environment having a lower Eh, UO_2 will precipitate.

If voltages are not more negative than this limit, there will be no precipitation of UO_2, although migration toward the electron source (upper terminus of the conductor) will still continue.

In natural systems, electrode geometry is ill-defined since most wet geologic materials are somewhat conductive and become extensions of the electrode.

A 'perfect' conductor will not draw uranium into itself since, in a perfect conductor, the potential gradient approaches zero and ion migration is therefore not appreciable. UO_2 precipitation would take place in the surrounding rock or soil where voltage (Eh) becomes more negative than the upper stability limit of the solid phase (Fig. 8).

A 'poor' conductor, by definition, will have an internal potential gradient. Positively charged ions and complexes will migrate into the conductive structure and be precipitated at a point where voltage conditions are favourable.

The concentrating efficiency of such an electrochemical cell would vary depending upon the voltage gradients developed, the velocity of runoff through the area of influence of the cell, and the concentration of metal in the fluid. The probable efficiency of the proposed mechanism cannot be estimated accurately for any given case due to the number of independent variables. It seems likely, however, that low velocity discharge, steep potential gradients and relatively elevated uranium content in the transporting fluids are all desirable factors.

Consideration of the hypothetical catchment and the uranium contents listed in table 1 indicate that an electrochemical cell, operating at 1% efficiency, could collect 25,000 tonnes U in ten million years if the labile uranium content were 5 ppm.

A higher grade source, such as a Proterozoic equivalent of the Swedish Alum shales or even the Chattanooga shales, having an average labile uranium content of 50 ppm, would yield 25,000 tonnes U in one million years. The land surface would be lowered 1,000 metres in the first case and 100 metres in the second. The probability of deposit formation and preservation through the palaeo-erosion cycle obviously increases with the grade of source area.

A variation of this model that may be applicable to development of significant ore

bodies of a somewhat different but related genesis, is as follows: Metal that is released during weathering of steeply inclined uraniferous graphitic schists is likely to migrate downward for the electrochemical reasons given and reprecipitate ahead of the vertically descending limit of free oxygen. 'Secondary enrichments' of this nature may not achieve the high grades of other palaeosurface-related deposits of the Key Lake or Midwest lake type, but ore bodies that may be of economic interest appear possible.

Preservation

During lowering of the weathering surface the potential gradients, which contribute to collection of uranium (and other metals) from surface or groundwaters, also preserve existing metal concentrations by causing migration to depth of positively charged complexes of any mineral destroyed by contact with descending oxidization conditions.

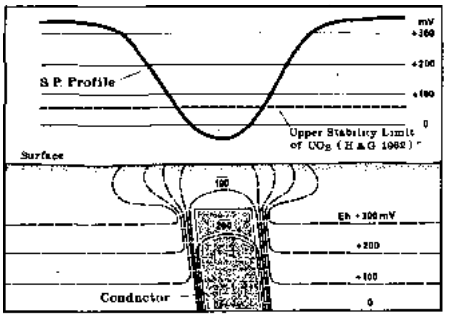


Figure 9. Effect of conductor on preservation of UO_2.

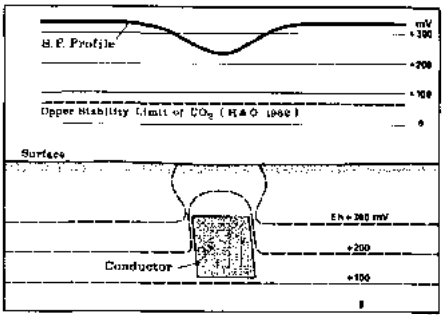


Figure 10. Effect of shallow conductor in Primary Redox Field.

In the event that weathering and erosion reduces the depth of a conductive structure to the extent that it no longer traverses an adequate range of Eh conditions, associated voltage gradients will be reduced so that ion migration slows and the superimposed voltage rises above the stability limit of UO_2. The metal concentration will then tend to be destroyed (Fig. 10).

Assuming that the metal concentration is not lost to weathering by the latter process, preservation through time must be due to burial by younger rocks. In both the Northern Territory, Australia, and the Athabasca basin, Saskatchewan, cover rocks are continental sandstone (quartzite) sequences. Deposition of cover rocks protects the deposit from chemical weathering and mechanical dispersal. As depth of cover increases, the Eh of the environment surrounding the mineralization is usually maintained at a level below the upper stability limit of UO_2 at low temperatures.

During burial, there may be some remobilization as discussed in a later section, but it appears that this sort of uranium concentration would not be dispersed by metamorphism at any grade below anatexis, excepting under rather special conditions of fluid movement.

Redistribution

Uranium may be redistributed from high grade concentrations during burial by younger sedimentary rocks. Such redistribution appears to have taken place, for example, at the Midwest Lake desposit in Saskatchewan. Uranium oxides are found in the Athabasca sandstones up to two hundred metres above the unconformity. This has been interpreted as evidence of a hydrothermal origin of the deposit. It is proposed, however, that convection cells that post-date the ores are responsible for redistribution of uranium. The thermal energy involved is provided by radioactive decay of the uranium in high grade ores. Remobilization of uranium minerals in this fashion may also be responsible for the variety of radiometric ages determined in these deposits (Fig. 12).

Radiogenic Heat in Uranium Ores

Radiogenic decay of natural uranium at the present time produces approximately three joules per gram U per year ($\sim 9.5 \times 10^{-8}$ watts). The temperature increase that may be generated by radioactive decay of a body of natural uranium is a function of thermal energy produced and heat flow from the body. Heat flow from the surface of a source depends upon the thermal conductivity of the enclosing rock, temperature gradient and the thickness of cover.

This subject lends itself to treatment by computer modelling and the thermal anomalies related to a high-grade uranium deposit would appear to be described easily by existing programmes (Cathles, pers. comm. 1979).

Figure 11 is illustrative of the proposed thermal model constrained as follows:

1) An uncomplicated geological environment with homogenous basement and cover rock;
2) An ore body of rectangular cross-section and a semi-infinite length;
3) Initially no influence from fluid convection;
4) Heat flow patterns which are essentially vertical;
5) Calculation for equilibrium conditions.

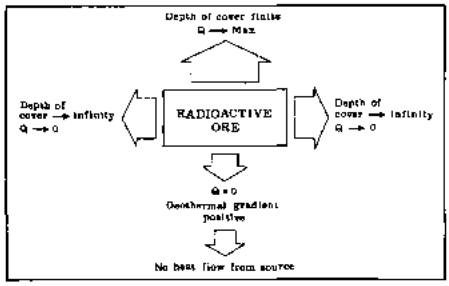


Figure 11. Simplified Thermal Model.

Accepting these points, it can be shown that there is little heat flow horizontally from the ore body since the temperature gradient in this direction is much lower than that from the upper termination of the ore body to surface. There can be no heat flow to depth against the geothermal gradient. The geothermal temperature pattern is distorted to produce a thermal 'spike' extending from some distance above the ore body to the depth at which the temperature is equal to the ambient temperature at the ore body level plus temperature rise due to radioactive decay. In a dry environment where convection of pore water does not take place, the temperature increase within a body containing 10% U may exceed 50°C at a depth of burial at 1,000 metres.

The temperature that may develop in an ore zone is dependent upon its geometry as well as the grade of the mineralized body.

Assuming that heat flow is essentially through the upper surface of the ore zone with little loss through the sides and no heat flow from the bottom surface, the temperatures given in table 2 are calculated for a prism one metre square and ten metres deep located at the centre line of the ore body. Heat losses due to heatflow through the sides of the prism are

Ore Grade %U	Energy Flow Upper Surface of Prism W/(m.K)	T1 Maximum Temperature Rise in Ore Due to Radiogenic Heat °C	Temperature Due to Depth of Burial °C	T2 Temperature in Ore due to T1 + T2 °C
2	3.84×10^{-4}	14.5	40	54.5
5	1.24×10^{-5}	49.5	40	89.5
10	2.49×10^{-3}	99.1	40	139.1
20	4.98×10^{-3}	198.2	40	238.2

Table 2. Temperature due to radioactive decay of uranium ore.

taken to be minimal and temperature reduction expectable along the upper edges of the larger prism is assumed to have negligible influence on the calculated temperature of this internal ore block.

This, in effect, assumes a semi-infinite width for the ore zone which, it is recognized, may tend to overstate temperatures attainable, particularly as thickness of mineralization becomes narrower than about ten times the central prism width.

It has been assumed also that the section to which these calculations apply is located near the mid-point of an ore body of semi-infinite length so that no consideration need be given to end effects.

The calculation uses the heat flow equation given by Clark (1966) simplified to

$$Q = K \frac{T}{X} A$$

Q = heat flow
K = thermal conductivity
T/X = thermal gradient, °C per unit thickness
A = surface area

Heat energy produced by radioactive decay of the uranium ore is calculated on the basis of the thermal constant for the present rather than the higher constants given to exist in earlier geologic time. (Lee, 1969 and *in* Yoder 1976). This value is added to the heat flow calculated at the ore body position using a representative thermal conductivity for quartzites of K = 2.5 watts per metre Kelvin, and a temperature gradient of 20°C/km.

A new thermal gradient is calculated for a depth of cover of 1,000 metres and a range of uranium grades. A surface temperature of 20°C is assumed. These data are used to determine the temperature in the ore zone and, by inspection, the temperature difference between the ore and the surrounding rocks. A temperature anomaly of this sort will result in development of a thermal spike in heat flow pattern as has been mentioned earlier. The thermal anomaly is likely to extend into the cover rock above the mineralization only some modest distance. The most extensive influence will be observed below the ore body. As an example, in a geothermal gradient of 20°C/km a temperature rise of 20°C in an ore body will cause the isotherm that lies 1,000 metres below to be drawn up and pass through the mineralized zone.

High grade uranium ore bodies are relatively small volumes that must be considered to be, at best, linear energy sources. Temperatures can be expected to fall rapidly above the upper surface of the mineralization approximately in inverse proportion to distance. The thermal anomaly below the ore body, however, would appear to contribute to circulation of groundwater through the ore zone and into the overlying cover rocks. Convection of groundwater will depend upon permeability of the rock adjacent to and within the limits of the thermal anomaly. In a rock of high permeability, cooling may proceed to the minimum temperature required to maintain activity of the circulation cell. Water circulation will tend to reduce the width of the temperature anomaly and increase its height. Maximum fluid movement would appear to be above the mid-point of the upper surface of an ore body.

The response of pore fluids to thermal anomalies has been investigated and reported in the literature. Combarnous & Bories (1975) discussed hydrothermal convection in saturated porous media and other models have been presented by Donaldson (1968), Elder (1967) and Katto & Masuoka (1967). The influence of geothermal convection cells on metal distribution in the earth has been discussed by, among others, Fehn *et al.*, (1978) and Norton & Cathles (in press).

Such detailed studies are beyond the scope of the present discussion. However, preliminary consideration of the matter, as outlined above, leads us to believe that

hydrothermal convection cells of significant proportions can develop due to heat of radioactive decay of uranium in a high grade ore body.

The temperature rise reasonably expected is in the range of 10° to 100°C. Reference to Lemoine's (1975) data shows that solution of UO_2 would take place within the ore body and that re-precipitation higher in the cell during cooling of the rising fluids could easily account for the distribution of uranium minerals observed in overlying sediments. (Fig. 12).

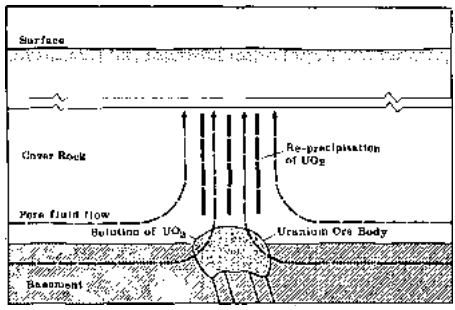


Figure 12. Fluid movement and redistribution of UO_2 driven by radiogenic heat of ore.

It should be stressed that temperature rise in an uranium ore body requires significant depth of cover and that there will be no detectable increase in temperature at surface due to the thermal anomaly at depth (Mogro-Campero & Fleischer, 1976).

Thermal Anomalies and Graphitic Bodies

It would appear possible that thermal anomalies as suggested above might be detectable in drill holes passing near high grade uranium bodies. If this is so, temperature measurement could prove useful in detection of this sort of ore at distances greater than possible with gamma ray measuring devices. During consideration of this possibility, potential sources of thermal 'noise' were studied.

Thermal conductivity of common rocks varies less than 0.9W/(m.K) to more than 8W/(m.K). The more indurated rocks, such as quartzite, have higher thermal conductivities than porous rocks such as sandstones. Gneisses and schists often display greater thermal conductivity parallel to foliation than at 90° to it (Clark 1966; Lee & Clark 1966).

Determinations of thermal conductivity of graphitic schists are not available to us. However, judging from data given by Clark (1966) a small quantity of oriented graphite in schists tends to raise the thermal conductivity several times to several orders of magnitude above that of most rocks.

Thermal anomalies therefore can be expected in association with thermally conductive bodies that extend to depth in basement below cover rocks.

Calculations indicate that the thermal gradients in graphitic schists are likely to be in the order of 2°C/km or less. This contrasts with 'normal' geothermal gradients of 15° to 30°C/km. (Lubimova & Polyak, 1969; Clark, 1966) and results in a temperature at the upper termination of the graphitic body only a few degrees lower than the ambient temperature at its deepest point. Temperature anomalies of 10° to 25°C may be associated with graphitic zones that extend 1,000 metres into the basement below cover rocks.

These temperature anomalies are likely to interfere with thermal prospecting for high grade ores. It is interesting, however, to speculate on the effect of these anomalies on circulation of pore water in the basement and porous cover rocks, and on the sort of alteration and mineralization that consequently might result.

CONCLUSIONS

Palaeosurface-related uranium bodies appear to form at an erosion surface as a result of weathering-related processes. Preferred source rocks are pyritic post-oxygenation pelitic sediments. Weathering of these sediments or their metamorphic equivalents tends to produce a relatively low pH and high Eh in the near surface environment. Under these conditions, uranium in solution migrates as a positively charged UO_2^{2+} complex that will respond to natural potential gradients. Graphitic zones in the pelites are ideal self-potential

axes along which electrochemical concentration of uranium can take place. Preservation of metal concentrations during the palaeo-weathering cycle is assisted by electrical potential gradients which tend to continually draw metal released during lowering of the weathering surface into reducing conditions at depth.

During subsequent burial, thermal anomalies, due to heat of radiogenic decay of uranium in the ore body, may result in development of low-temperature hydrothermal convection cells with consequent remobilization of ore minerals and alteration of host rock.

Similar thermal anomalies of somewhat lesser amplitude may be expected in proximity to steeply inclined graphitic zones that extend to depth in basement beneath cover rocks. But thermal anomalies of either type are unlikely to be detectable at surface.

The initiation of such a hydrothermal cell is dependent upon thickness of cover rock above the ore body. Until the required cover is developed, there will be insufficient temperature rise to drive the 'thermal pump'. Removal of cover rock will ultimately result in cessation of cell activity.

The range of radiometric ages obtained for high grade uranium deposits may be related, in part, to remobilization of uranium minerals due to phenomena such as these described. The evidence suggestive of hydrothermal activity may be due to influence of the ore body itself rather than indicating a mode of original genesis.

These factors can be of significance in exploration for palaeosurface-related uranium deposits.

The preferred basement rocks below the unconformity are post-oxygenation Proterozoic pelitic sediments or their metamorphic equivalents.

Conductive structures that could be loci of mineral concentration can be located and traced electromagnetically through several hundred metres of cover rocks.

Prospecting for high grade uranium concentrations at a buried unconformity may be made somewhat easier if there is redistribution of UO_2 into cover rocks, as at Midwest Lake, Saskatchewan, possibly by hydrothermal convection cells driven by radiogenic heat from the ore itself.

Thermal detection of high grade ore bodies at surface is not possible but temperature measurement in bore holes may be useful. Thermal prospecting at depth may be complicated by temperature anomalies related to steeply dipping, thermally conductive structures in the basement rocks but these latter anomalies are not likely to be as pronounced as those related to large high grade deposits.

REFERENCES

Bayley, R.W. & James, H.L., 1973: Precambrian iron formations of the United States. *Econ. Geol., 68,* 934-959.

Bell, R.T., 1978: Uranium in Black Shales, A Review. *in* (ed. M.M. Kimberley), *Short Course in Uranium Deposits: Their Mineralogy and Origin. Mineralogical Association of Canada,* 307-329.

Bolviken, B. & Logn, O., in press: The redox potential field of the earth. *Internat. Assoc. Geochem. Cosmochem. and UNESCO: Second symposium on the origin and distribution of the elements, Paris,* 1977.

Chisholm, E.O., 1957: Geophysical exploration of a lead-zinc deposit in Yukon Territory. *in, Methods and Case Histories in Mining Geophysics, 6th Commonwealth Mining and Metallurgy Congress,* 269-277.

Clark, S.P., Jr., 1966: Thermal Conductivity. *Mem. geol. Soc. Am., 97,* 459-482.

Cloud, P., 1976: Major features of Crustal evolution. *Du Toit Memorial Lecture 14, Geol. Soc. Sth. Africa, Annexure to Volume 79.*

Combarnous, M.A. & Bories, S.A. 1975: Hydrothermal convection in saturated porous media. *in* (ed. Ven Te Chow) *Advances in Hydroscience, 10,* 231-207. New York Academic Press.

Donaldson, I.G., 1968: A possible model for hydrothermal systems and method of studying such a model. *Aust. Conf. Hydral. Fluid Mech.*

Elder, J.W., 1967: Steady free convection in a porous medium heated from below. *J. Fluid Mech., 27,* 29-48.

Fehn, U., Cathles, L.M. & Holland, H.D., 1978: Hydrothermal convection and Uranium deposits in abnormally radioactive plutons. *Econ. Geol, 73,* 1556-1566.

Fischer, A.G., 1969: Geological Time-Distance Rates: The Budnoff Unit. *Bull. geol. Soc. Am., 80,* 549-552.

Gandhi, S.S., 1978: Geological setting and genetic aspects of uranium occurrences in the Kaipokok Bay - Bay River Area, Labrador. *Econ. Geol., 73,* 1492-1522.

Gottschhalk, L.C., 1964: Sedimentation. Part I. Reservoir sedimentation. *in* (ed. Ven Te Chow) *Handbook of Applied Hydrology, Section 17,* 1-34.
Hoeve, J. & Sibbald, T.I.I., 1978: On the genesis of Rabbit Lake and other unconformity type uranium deposits in northern Saskatchewan, Canada. *Econ. Geol., 73,* 1450-1473.
Hostetler, P.B. & Garrels, R.M., 1962: Transportation and precipitation of uranium and vanadium at low temperatures, with special reference to sandstone type uranium deposits. *Econ. Geol., 57,* 137-167.
Katto, Y. & Masuoka, T., 1967: Criteria for onset of convective flow in a fluid in a porous medium. *Int. J. Heat Mass Transfer, 10,* 297-309.
Kelly, S.F., 1957: Spontaneous polarization, or self-potential methods. *in, Methods and Case Histories in Mining Geophysics, 6th Commonwealth Mining and Metallurgy Congress,* 55-58.
Knipping, H.D., 1974: The concepts of supergene vs hypogene emplacement of uranium at Rabbit Lake, Saskatchewan, Canada. *in, Formation of Uranium Ore Deposits. Proceedings of a Symposium, Athens. International Atomic Energy Agency, Vienna,* 531-549.
Kukal, Z., 1971: The rate of denudation of continents. In Geology of Recent Sediments. *Cont. Geol. Surv. Prague.* Academic Press, London, 25-40.
Langford, F.F., 1978: Origin of unconformity-type pitchblende deposits in the Athabasca Basin of Saskatchewan. *in* (ed. M.M. Kimberley) *Short Course in Uranium Deposits: Their Mineralogy and Origin. Mineralogical Association of Canada,* 485-499.
Langmuir, D., 1978: Uranium solution-mineral equilibria at low temperatures with application to sedimentary ore deposits. *Geochim. cosmochim. Acta, 42,* 547-569.
Lee, W.H.K. & Clark, S.P., Jr., 1966: Heat flow and volcanic temperatures. *Mem. geol. Soc. Am., 97,* 483-512.
Lemoine, A., 1975: Contribution de l'etude du comportment de UO_2 en milieu aqueux a haute temperature et haute pression: Ph.D. thesis, Nancy (unpubl.) *in,* Rich, R.A., Holland, H.P., & Petersen, U., 1977: *Hydrothermal Uranium Ore Deposits. Developments in Economic Geology, 6.* Elsievier, Amsterdam.
Lubimova, E.A. & Polyak, B.G., 1969: Heat Flow Map of Eurasia. *in* (ed. P.V. Hart) *Amer. Geophys. Union. Mono. 13,* 83-88.
Moore, W.J., 1972: *Physical Chemistry.* 4th edition. Prentice-Hall. 435p.
Morton, R.D. & Beck, L.S., 1978: The origin of the uranium deposits of the Athabasca Region, Saskatchewan, Canada. (Abstract) *Econ. Geol., 73,* 1408.
Mogro-Campero, A. & Fleischer, R.L., 1976: Are measurements of radiogenic heat useful for uranium exploration? *Geophys. Res. Lett., 3,* 459-462.
McMillan, R.H., 1976: Metallogenesis of Canadian Uranium Deposits: A Review. *in,* (ed. M.J. Jones) *Geology, Mining and extractive processes of uranium. Inst. Min. Metall. and E.E.C.,* 43-55.
McMillan, R.H., 1977: Uranium in Canada, *Bull. Can. Petrol. Geol. 26,* 1222-1249.
Nash, J.T., 1978: Preface - Uranium Geology in resource evaluation and exploration. *Econ. Geol., 73,* 1401-1408.
Norton, D.L., & Cathels, L.M., in press: Thermal aspects of ore deposition *in,* (ed. H.L. Barnes). *Geochemistry of hydrothermal ore deposits.* 2nd edition New York, Wiley-Interscience.
OECD-IAEA, 1977: *Uranium resources, production and demand.* Organisation for Economic Co-operation and Development, O.E.C.D. Publications, France, 136p.
Robertson, D.S., 1974: Proterozoic units as fossil time markers and their use in uranium prospecting. *in, Formation of Uranium Ore Deposits. Proceedings of a Symposium, Athens. International Atomic Energy Agency, Vienna,* 495-512.
Robertson, J.A., 1978: Uranium deposits in Ontario. *in,* (ed. M.M. Kimberley) *Short Course in Uranium Deposits: Their Mineralogy and Origin. Mineralogical Association of Canada,* 229-512.
Roscoe, S.M., 1973: The Huronian supergroup, a paleo-Aphebian succession showing evidence of atmospheric evolution. *Spec. Pap. geol. Ass. Can., 12,* 31-47.
Ryan, B.R., 1977: Uranium in Australia. *in,* (ed. M.J. Jones) *Geology Mining and extractive processing of uranium. Inst. Min. Metall., 86,* 24-42.
Schumm, S.A., 1963: The disparity between present rates of denudation and orogeny. *Prof. Pap. U.S. geol. Surv., 454-A,* 1-13.
Stapleton, R.P., 1978: Organic metamorphism and uranium occurrences in the Beaufort Group of South Africa. *Econ. Geol., 73,* 283-285.
Theis, N.J., 1978: Mineralogy and setting of Elliot Lake deposits. *in,* (ed. M.M. Kimberley) *Short Course in Uranium Deposits: Their Mineralogy and Origin. Mineralogical Association of Canada,* 331-338.
Walker, J.C.C., 1977: *Evolution of the Atmosphere.* McMillan, 264-278.
Wetherill, G.W., 1966: Radioactive decay constants and energies. *Mem. geol. Soc. Am., 97,* 513-519.
Yoder, H.S., 1976: *Generation of Basaltic Magma.* National Academy of Science, Washington, D.C.

A COMPARISON OF EXPLORATION TECHNIQUES IN SASKATCHEWAN AND THE NORTHERN TERRITORY

C. W. Armstrong and N. E. Brewster

A.C.A. Howe International Limited, 159 Bay Street, Toronto, Canada M5J 1J7

INTRODUCTION

The unique physical properties of uranium, such as its radioactive decay series and its distinctive geochemical cycle involving marked mobility in the hexavalent state and fixation in reducing environments, have led to the development of a sophisticated range of direct exploration techniques. In addition more orthodox methods can be used both at an early state to outline a geological environment suitable for uranium mineralization and also in a later phase to trace host lithologies or structures which are outside the range of the more specific methods.

With the recognition of the Alligator Rivers and Northern Saskatchewan areas as two of the world's major uranium districts with broadly similar regional geology and mineral deposits, it would seem a useful exercise to study how this wide range has been utilised in each area. It is beyond the scope of this paper to provide a detailed study of the application of every possible technique of whatever significance, or detailed case histories of the major discoveries. The object will be to trace the effect of developments in technology, instrumentation and geological understanding on each area and to determine the lessons to be learnt for future exploration, within these two regions.

The available options and the stages at which their use may be considered during the development of an exploration programme are listed in table 1.

TECHNIQUE	APPLICATION
Geological Evaluation	Regional
Airborne Radiometrics	Regional to sub-regional
Ground Radiometrics	Sub-regional to detailed
Lake and Stream Sediment Geochemisry	Sub-regional
Soil Geochmeistry	Detailed
Hydrogeochemistry (U and Rn)	Sub-regional
Radon Emanometry	Detailed
Geobotany and Biogeochemistry	Sub-regional to detailed
Geological Mapping	Sub-regional to detailed
Non-radiometric geophysics	Sub-regional to detailed
Non-radiometric geochemistry	Sub-regional to detailed
Exploration Drilling	Sub-regional to detailed

Table 1. Uranium Exploration Methods
(Based on IAEA Panel 1972)

CLIMATE AND PHYSIOGRAPHY

Although other extraneous factors, most noteably the attitudes of respective governments to the uranium industry, have affected the timing and extent of developments in each area it is the markedly dissimilar climates and natural features which have probably had most influence on the varying exploration approaches used. It is therefore important to recognise the extent of these differences before studying the history of exploration in each area.

The relevant features of the tropical climate of the Alligator Rivers area as opposed to the subarctic climate of northern Saskatchewan are summarized in table 2.

These extremes of climate with an extended period of flooding in Australia and snow

	Northern Territory (Oenpelli)	Saskatchewan (Uranium City)
Mean summer temperatures		
max	36°C	15°C
min	24°C	4°C
Mean winter tempertatures		
max	33°C	-15°C
min	19°C	-31°C
Normal precipitation	140cm	35cm
Summer precipitation	130cm	20cm
Winter precipitation	10cm	15cm

Table 2. Climatic Data

cover in Canada have had a twofold effect on mineral exploration. Firstly they have had the obvious direct effects on access, on the length of the efficient field season, the applicability of certain exploration techniques and the development of vegetation. Secondly, and possibly even more important, the broadly chemical weathering system caused by the Northern Territories' tropical climate and the largely physical weathering in Saskatchewan, compounded by an even more extreme arctic paleaoclimate, have produced very different physiographies and subsurface conditions. Thus in the Northern Territory there has been extensive lateritisation of the exposed Lower Proterozoic and the development of a prominent scarp along the Lower-Middle Proterozoic contact due to the resistive nature of the Kombolgie sandstone. In Canada the arctic palaeoclimate has left a glacial peneplain covered by till and glaciofluviatile deposits which the slightly less extreme present climate has done little to modify.

EARLY EXPLORATION

Uranium was first reported in Saskatchewan in 1935 when two pitchblende-bearing veins with associated sulphides were discovered on the north shore of Lake Athabasca.

The impetus for vigorous exploration activities however did not occur until 1944 when uranium was categorized as a strategic material. Regional evaluation efforts undertaken by Eldorado Nuclear, private mining companies and prospectors in the Beaverlodge area resulted in the discovery of the Ace-Fay-Verna and Gunnar deposits along with many smaller deposits more than a dozen of which reached production. Exploration techniques employed during this period included Geiger prospecting, overburden stripping, rock trenching, channel sampling and diamond drilling.

In 1952, Eldorado Nuclear located radioactive pegmatities in the Foster Lakes area and in 1953 pitchblende was discovered in calc-silicate rocks in the Burbidge Lake area. Associated exploration activities elsewhere resulted in the discovery of uranium in the Athabasca Sandstone near Uranium City in 1955, of uranium bearing pegmatites in the Black Lake-Charlebois Lake area during the 1946-1958 period, uranium in fault contact with Athabasca sandstone at Black Lake and an occurrence of secondary uranium in regolith underlying the Athabasca sandstone at Middle Lake.

The discovery of the Rum Jungle Uranium Field in 1949, similarly instigated by government incentives, was made by local prospectors using simple Geiger-Muller counters facilitated by the development of distinctive secondary uranium minerals in that environment. Subsequent work in this area relied on standard follow-up techniques of trenching and drilling with emphasis placed on locally recognised geological controls.

An extension of the search area using very basic airborne radiometry and ground prospecting led to the discovery of the South Alligator Valley Uranium Field in 1953.

These early phases of exploration in both areas not only resulted in the discovery of a number of small, though important, deposits using relatively unsophisticated instrumentation, but also allowed a later generation of geologists to capitalise on a sounder understanding of the uranium geology and geochemistry. Once these areas had been

established, their evaluation from a basic geological and geophysical viewpoint was greatly facilitated by a wealth of regional data made available by the respective governments institutions. These agencies have continued their contribution in both countries by providing a correlation service and overview which has been of considerable use to operating companies. It is interesting to speculate here on why these early phases of exploration did not themselves result in the discovery of the major deposits in each area, several of which were marked by significant radioactive anomalies. Certainly the later rapid development in airborne radiometric systems is a mitigating circumstance, as it greatly increased the area of search relatively economically, but it may also be argued that had more attention been paid at this stage to the geological controls of known mineralization the area of search would have expanded anyway and the larger deposits could have been found some years earlier. This should emphasise to current operators the need to relate data generated from all forms of exploration approach to a sound geological framework rather than to rely solely on a 'black box' in isolation from the geological context.

AIRBORNE RADIOMETRICS

The major exploration effort which commenced in both areas in the late 1960's was assisted by rapid developments during this period in the field of aeroradiometry. After the somewhat disappointing results of earlier surveys with simple Geiger instrumentation or small crystal total count scintillometers, the use of systems with large crystal volumes linked to multi-channel spectrometers proved to be rapid, relatively inexpensive and successful. This technique resulted in the direct discovery of the Ranger, Koongarra, Nabarlek, Cluff Lake and Rabbit Lake deposits, which may be considered surprising given the widely different problems occurring in each area. The Northern Territory has a zone of heavy lateritic weathering and a very high water table during the summer months which persists for much of the effective field season and flying is best conducted in September or October. One major advantage here is the clearly marked escarpment along the Lower-Middle Proterozoic unconformity which enabled overflying of the Kombolgie Sandstone to be kept to a minimum and also directed rim flying to a prime target area with negligible surficial overburden. Whether the former advantage is still seen as such after recent discoveries in Canada is open to debate and may cause a change in exploration policy at some stage in the future. The major subcropping orebodies discovered in this phase had surface expressions ranging from a zone of up to 12 times background 6.5 kilometres long and 1 kilometre wide at Ranger to the more localised high intensity anomaly at Nabarlek which was recorded on only two flight lines with a spacing of 400 feet (Tipper & Lawrence, 1972). In Canada a potentially more serious problem for aeroradiometry was the effect of up to 100 feet of till together with large areas permanently under water. However, a combination of glacial plucking and frost-heaving has generally produced a surface expression of the subcropping orebodies. The other marked disadvantage in Canada was the imprecise delineation of the contact between the Lower Proterozoic (Aphebian) metasediments and the overlying Middle Proterozoic Athabasca Sandstone due to the till cover. Some companies flew entire properties on the same spacing regardless, whilst others conducted boulder population density studies or drilled to bedrock to determine the contact more precisely, prior to flying the sandstone areas on a wide spacing. Similar techniques were utilised to locate windows through to the basement Lower Proterozoic metasediments. Either approach involved a substantial increase in effective costs compared with Australia.

The success of aeroradiometric surveys at the start of the present uranium exploration boom in two areas of widely different climate and physiography, and despite problems ranging from excessive leaching to snow, water and till cover, demonstrates that the widely publicised view that radiometric surveys are serverely limited by such problems is obviously more apparent than real.

Although the carborne radiometric surveying technique has proved to be a useful and popular prospecting technique in such relatively treeless environments as the southwestern United States and parts of southern Africa and some western European countries with a dense road network it is clearly impractical in Saskatchewan and has had limited crude use in the Northern Territory.

PRIMARY GROUND FOLLOW-UP

It is in the ground follow-up phase where differences either necessitated by environment or chosen by the local industry due to varying genetic concepts become most noticeable. It is probably relevant at this state to comment on the effect which climate, physiography and vegetation have had on access and the effective field season in each area.

Summer exploration in Canada is hampered by thick bush, extensive permanent water cover and very few roads or tracks. Camps must therefore be set up and serviced using air transport and crews are often moved to their work place by helicopter. Line-cutting is essential for location and access in the bush and is both time-consuming and costly. In winter the ice and snow cover precludes certain techniques and necessitates better camp conditions for crews, but ground access is simplified and diamond drilling and geochemical sampling through lake ice is possible. Limited programmes are therefore generally conducted all winter and it is only at freeze-up and ice break-up that programmes are shut down.

Light bush cover and generally dry conditions make the Northern Territory an ideal place for winter fieldwork. Vehicle access is possible to most areas during this period, camps are easily maintained and line-cutting, where necessary, is simple and inexpensive. Summer access during the wet season however is limited by surface flooding. Companies which have operated at this time have been forced to use all-terrain vehicles such as the Canadian Bombadier for mounting or movement of drilling rigs and general property access.

In Canada, primary ground follow-up by direct approaches was conducted along two avenues. Firstly, the technique of lake water and lake sediment geochemistry which had been largely developed by the Geological Survey of Canada was, and still is, widely employed on a sub-regional to detailed basis to allow coverage both for orebodies masked by lakes and a further check for subcropping deposits where the effects of frost-heaving or glacial plucking may have been obscured. Rapid transportation by a float-equipped helicopter between sites and sample collection by means of weighted 'bombs' enabled operators to work at half the cost of a stream sediment survey in a similar environment. The second widely applied primary follow-up technique was ground radiometric surveying both along cut lines and on a random prospecting basis. Both approaches were expensive due to the cost of line-cutting in northern Canadian forests and to the fact that no geological guidelines were evident for prospectors. However, economies could be made in staff grades as untrained personnel could cope with this job quite adequately. The instruments used at this stage were generally total-count scintillometers as these had proved to be more rugged for rough traversing work with less down time than the more sensitive spectrometers which were only used for assessment of any anomaly discovered. As the prime target was individual boulders or small trains not detected by airborne surveys, the choice of instrument varied accordingly, partly on purely individual preference for those who felt that the Geometrics GR101 for instance was small, lightweight, reasonably sensitive and left the hands free for boulder mapping or those who insisted that the somewhat cumbersome though highly sensitive Srat SPP2N was essential for this type of work.

Further 'ground' surveys are now possible with the development by George Goldak, Scintrex and the U.K. Institute of Geological Sciences of lake bottom loggers both to test for orebodies subcropping beneath the extensive lake cover in northern Saskatchewan, and as a geochemical mapping tool. Some companies have further advanced this approach by using

divers to obtain some idea of the lake bottom sediment conditions or percentage of outcrop so that results can better be evaluated.

In Australia ground follow-up of the less pronounced airborne radiometric anomalies and supplementary checking for any orebodies with little or no surface expression was initially far more restricted by the environment. Lake water and sediment and stream sediment geochemistry were inapplicable in this area and there was no other readily available subregional exploration method. Operators therefore had to rely extensively on ground radiometric surveys in an area of heavy surface leaching. However, the precise location of the Lower-Middle Proterozoic unconformity along the scarp of the Kombolgie sandstone enabled a concentration of effort in the target area of minimal overburden. Contemporaneous geological mapping also allowed a better understanding of the radiometric results. Another major advantage was the relative ease of access compared with northern Saskatchewan; lines, where necessary, could be established very readily and vehicle and pedestrian access was possible to most prospective areas. This approach to ground follow-up in Australia led to the discovery of several areas of mineralization, most notably the Jabiluka One anomaly which had registered no response to airborne surveys.

Evaluation of anomalies delineated on the ground has also followed a different course. As it could reliably be assumed that there had been limited transportation of anomalies in Australia, detailed grid surveying could be carried out immediately to give some idea of the configuration of sub-surface mineralization. Due to the relatively thin overburden this could be followed by trenching or shallow auger drilling into weathered bedrock. Trenching at this stage was found to be invaluable as it enabled lithological and structural interpretation to be made at an early point prior to diamond drilling into unweathered rock at depth. Once again the Canadians were somewhat less fortunate due partly to the fact that anomalies have been transported up to 9 kilometres and bedrock is obscured by 30-80 metres of glacial overburden. These factors have led to the development of a variety of sophisticated Pleistocene mapping techniques involving surface studies of boulder population densities, percussion drilling and reverse circulation drilling to sample both till and bedrock.

SOIL GEOCHEMISTRY

In neither of the areas under consideration are soils widely or deeply developed. In Australia much of the surface is either obscured by alluvium or consists of leached laterite. Soil sampling has therefore not been effective under these conditons.

Because of the heavy glacial overburden in Saskatchewan and the need to trace mineralized boulders to their source, deep sampling techniques became necessary. Mobile low cost durable equipment was necessary to retrieve samples from the till profile suitable for trace element and lithological analysis. Atlas Copco percussion drills and Akar reverse circulation rotary drills are currently being employed for this work. The latter device is capable of collecting continuous samples at predetermined intervals down the hole whereas with the Atlas Copco system samples are typically taken at the till-bedrock interface. Reverse circulation drill holes can also be radiometrically logged.

HYDROGEOCHEMISTRY

Hydrochemical methods include sampling both for uranium and its daughter products — radium, radon and helium, and is a widely accepted technique for regional to subregional evaluation. The Northern Territory however, with extensive summer flooding and rapid disappearance of minor stream network during the winter, is poorly suited to this approach. Northern Saskatchewan, on the other hand, has an ideal environment with large areas permanently under cover of slow-moving water.

Dyck (1975) has shown the usefulness of the method in the Canadian environment.

Uranium in water samples at a density of one every twelve square miles still indicated the potential of the Beaverlodge area, whereas radon indications started to disappear at sample densities of greater than one per square mile. Even in this environment, however, it may be noted that the Midwest Lake deposit did not register as a noticeable anomaly even at a sampling density of one to one square mile despite weak airborne and ground radiometric anomalies.

RADON EMANOMETRY

Early trials into the measurement of radon in soil air in Canada were successful in outlining zones of uranium mineralization beneath several metres of soil cover, but all too often could not be widely used due to the paucity of soil cover and the abundance of lakes in the known districts of Elliot Lake, Beverlodge and Bancroft.

However, both the uranium provinces under consideration should, at first glance, be ideally suited to this type of approach; Saskatchewan with its extensive till cover and the Northern Territory with its cover of leached alluvium and laterite. In both cases it was felt that only the largest deposits would have been detected by direct radiometric measurement and radonometry would be a useful additional tool.

The earliest form of emanometers, where soil gas was pumped through an ionization chamber and recorded have now been developed from the rather bulky impractical prototypes to lightweight models more appropriate to field use. Their first application in Australia was in 1971 when a Scintrex instrument was used in the Northern Territory. Initial surveys were not encouraging as the dust filter and dessicants were inadequate for the conditions and despite field modifications reproducible results were unobtainable. Improved design has now largely eliminated these problems and emanometers have now successfully outlined mineralized areas beneath several metres of overburden cover. In Saskatchewan field work conducted by Dyck and several mining companies indicate comparability of results between emanometer, Alpha-Cup, Track Etch, and gamma ray methods over ore zones covered by 1-7 metres of coarse sand and gravel-bearing overburden.

Despite modest successes and the benefits of immediate recordings it was realized that emanometer results were not wholly reliable due to marked variations in radon readings caused by changes in temperature, humidity and barometric pressure. The integrated method that was required was provided by the Alpha Nuclear, Track Etch and Westinghouse systems in which the detector can remain in the ground as long as necessary to overcome local climatic variations. These systems require more than one visit to the sample site and the Track Etch method involves a further delay while the results are computed by the manufacturer.

Trach Etch has been quite widely applied in both areas. In the East Alligator area it was used to delineate a known orebody at a depth of 75 metres with an anomaly of 40 times background (Gingrich & Fisher, 1976). It is not known which orebody this is. The method has also been used to outline mineralization near Koongarra which was not detected by airborne spectrometry and only gave a weak ground radiometric response. Tests over known orebodies beneath relatively thin cover of Kombolgie sandstone have been negative, though anomalies as yet untested have been located through major fractures. Anomalies in Australia are rather more subtle due to excessive leaching resulting in a background of one third of the worldwide average. In Saskatchewan the Cluff Lake deposit was also outlined by Track Etch subsequent to drilling, but so were a number of barren anomalies. Many Track Etch anomalies in this area appear to reflect secondary radium concentrations which have migrated some distance from the uranium source.

Very little information is available on the use of alphametry in either area and although it has a number of practical advantages to the field operator many have undoubtedly been

dissuaded by the high initial capital outlay, although long term costs to committed uranium exploration are probably cheaper than Track Etch. However, it does not seem as if this method has had an important bearing on any of the discoveries in either area to date.

The attractions of all forms of radon measurement, with claims of detection of orebodies at depths of several hundred feet will doubtless encourage steady use in both areas though this use must be in conjunction with other techniques and where possible geological input due to the number of spurious anomalies that have been recorded. The operators must remember that radon can probably only move 20 feet by true diffusion. Possibly the most interesting development in this field, if it is ever allowed, will be the drilling of anomalies located above fractures and major joints in the Kombolgie sandstone.

Helium gas surveys have also ben propounded in recent years, based on the same decay principles as radon emanometry, but with the advantage of a more stable nature as opposed to the 3.8 day half life of radon, and more fugitive tendencies due to its markedly lower specific gravity. However, helium surveys are in their infancy in both areas despite these seeming advantages, as operators are suspicious of the very low anomalies projected and the cost of helium analyses.

INDIRECT METHODS

At this stage the approach in both areas has been to rely on direct evidence of uranium concentrations and apart from its use in recognition of the regional potential, geological interpretation was not a prime consideration, probably because extensive surface mapping was not possible in either area. However, as geological information gradually began to emerge from drilling of the known deposits, a change of emphasis emerged in the recongnition of significant lithological geochemical and alteration features.

The view that deposits were predominantly restricted to the plane of Lower-Middle Proterozoic unconformity was gradually modified to allow other key features to be fitted into the developing model. Most notably these included the apparent relationship of mineralization to graphitic and chloritic metasediments flanking granite gneiss domes and the possible effect of major fracturing on these. The genetic interpretation of these relationships has varied in each country but the main effect on exploration has been in the presumed area of prospective mineralization which is more limited in Canada by the emphasis placed on proximity to the plane of the Lower-Middle Proterozoic unconformity. The Canadians tend to put more emphasis on direct proximity to graphite horizons which restricts the target within the stratigraphic succession more than in Australia.

Although full advantage of this knowledge could not be taken in Australia due to sociopolitical problems, what exploration has taken place in recent years has relied largely on locating and tracing favourable lithologies and structures. Both magnetic and gravity surveys have been used to delineate the granite gneiss complex boundaries and favourable horizons flanking these have been traced by auger and diamond drilling and resistivity surveys. The results of this approach are difficult to compare directly with Canada as by necessity they have largely been restricted to areas of subcropping Lower Proterozoic, but a number of areas of economic potential have been outlined.

In Canada, exploration by indirect techniques based on a sounder geological understanding has been possible on both subcropping and Athabasca sandstone covered areas and has provided a new dimension to exploration of the area by markedly increasing the depth of detection from the more limited direct techniques. The most widely used approach has been to conduct airborne magnetic and electromagnetic surveys over a property to locate conductive metasediments on the flanks of magnetic granite gneiss domes. Airborne anomalies are then located more precisely by ground surveying and are subsequently drilled. Resistivity and induced polarization techniques have been used to a

lesser extent. Considerable success has been achieved by this method in the discovery of West Bear, the Collins Bay deposits, and the Asamera and Occidental discoveries. However, it is apparent that such an approach is not a panacea as some deposits have only a minor graphite or sulphide content and others are not intimately associated with graphitic schists. Many barren graphitic conductors have already been drilled in Canada, and it seems that more emphasis should be placed on geology and supplementary exploration techniques to allow better discrimination of this type of target. The emphasis placed on electromagnetometry in Canada cannot be applied in Australia at the present time as those areas available for exploration, or likely to be in the foreeeable future, are complicated by the presence of conductive overburden. Trial electromagnetometer surveys over Jabiluka One in 1971 for instance gave very inconclusive results but recent surveys using more sophisticated instrumentation appear to offer better possibilities.

Various sulphide minerals are commonly associated with Northern Saskatchewan deposits and have led to geochemical analysis of till samples for Cu, Ni, Mo and As as pathfinder elements. This approach has also proved suitable for waters and sediments and is carried out on a routine basis by many of the exploration companies operating in the area. Lakes in the immediate vicinity of the Key Lake area were marked by anomalous base metals and their presence is thought to provide additional evidence of uranium mineralization.

FUTURE TRENDS

The authors feel that in both these regions there are large areas, as yet untested, where standard techniques will still apply. However, there are also areas where difficulty of access, overburden or thick sandstone cover might warrant some variation in technique or emphasis. Variations will also doubtless occur due to the development of geological knowledge and genetic theories. For instance the widespread presence of uranium mineralization in sandstone in Saskatchewan may lead to grid drilling techniques as applied on the Colorado Plateau.

GEOBOTANY/BIOGEOCHEMISTRY

Both these techniques are usually widely decried due to the expense, necessity for skilled samplers and the fact that other techniques are more effective. However, it may be seen from this general survey of the techniques applied that none is foolproof and that the explorationist must keep an open mind on all available methods.

In Australia, especially as electromagnetic methods cannot be used for tracing favourable lithologies, subregional geobotany from satellite imagery interpretation combined with limited field traverses might be invaluable in geological interpretation of subcrop regions where the Kombolgie sandstone has been eroded.

Trial biogeochmeical surveys in 1971 by Howe Australia also gave indications that this may be a useful method, though the work was limited and has not been duplicated. Plant ash samples from the Colorado Plateau and from New Zealand have shown that samples containing more than 1 ppm U_3O_8 are anomalous. In the Alligator Rivers Uranium Field most genera tested were significantly higher than this, and in particular the eucalypts ranged up to 182 ppm. Insufficient sampling was possible at the time from control areas. The Bureau of Mineral Resources Geology and Geophysics has recently carried out a detailed geobotanical survey over Ranger 1 Number 3 ore body; results of this survey will be known shortly. The technique might be particularly suited to areas such as swamp, ravine and talus slopes where alternative subsurface techniques cannot be used or are likely to prove expensive.

Recent test surveys of pine needle sampling in Canada offer some evidence that the technique may be effective even over areas of Athabasca Sandstone cover.

STRUCTURE

There are indications from both areas that deposits may be located along major linear or arcuate structural features. These are as yet largely unspecified but may be major faults or possibly channels at the base of the Middle Proterozoic sandstones. Certainly, companies in Canada are basing costly programmes on locating the intersections of these features with favourble lithologies, and it seems possible that a similar approach - which was first proposed in Australia in 1972 - may be attempted there when exploration resumes in earnest.

Satellite imagery and seismic surveys could possibly both be used in projecting such features beneath sandstone cover to considerable depths, and could markedly increase the effectiveness of 'blind' drilling of airborne electromagnetic anomalies. In addition faults in the sandstone cover rocks may represent reactivated Lower Proterozoic structures which could be discriminated by radon and helium surveys.

CONLUSIONS

Table 3 shows in summary the differences in exploration approach in these two areas, mainly influenced by the climate and physiography but also by varying genetic concepts and external sociopolitical problems. Some methods have been particularly successful, others marginally so, thereby reinforcing the view that those techniques best suited to the area in question must be found, developed and integrated into a balanced programme with a sound background of geological interpretation which is not restructed by a genetic straitjacket.

	AUSTRALIA	CANADA
Regional Geological Evaluations	Essential	Essential
Geological mapping	Essential	Essential
Airborne Radiometrics	Extensive successful use	Extensive successful use
Carborne Radiometrics	Limited use	Not possible
Ground Radiometrics	Extensive - more cost effective in Australia	Extensive
Lake & Stream Sediments Geochemistry	Not used	Widespread use
'Soil' Geochemistry	Uncommon	Extensive till sampling
Hydrogeochemisty and Emantometry	Not used	Widespread
Radonometry	Limited trial survey	Limited trial survey
Geobotany & Biogeochemistry	Limited use	Not used
Non-Radiometric Geophysics	Magnetometry and resisitivity	Magnetometry, electro-magnetometer and seismic
Non-Radiometric Geochemistry	Not used	Common for Ni, Co, Cu, Au, As, Mo
Exploration Drilling	Auger and diamond	Percussion, Reverse circulation and diamond

Table 3. Comparison Summary

ACKNOWLEDGEMENTS

The authors wish to extend their appreciation to their colleagues A. C. A. Howe and J. B. Felderhof for helpful discussion and to Dr. R. H. McMillan of Western Mines Limited, Toronto, for critically reviewing the manuscript.

BIBLIOGRAPHY

A.C.A. Howe Australia Pty. Limited, 1971: Proprietary Report, No. 48, Sydney.

A.C.A. Howe Australia Pty. Limited, 1972: Proprietary Report, No. 53, Sydney.

Beck, L.S., 1970: Genesis of Uranium in the Athabasca Region and its significance in Exploration. *Trans. Can. Inst. Min. Metall., 73,* 59-69.

Cole, M.M., 1971: The Importance of Environment in Biogeographical/Geobotanical and Biogeochemical Investigations. *Can. Inst. Min. Metall., Special Volume 11,* 1-12.

Darnley, A.G., 1972: Airborne Gamma-Ray Survey Techniques. *Uranium Prospecting Handbook, Inst. Min. Metall.*, 174-211.
Dyck, W., 1975: Geochemistry Applied to Uranium Exploration. *Geol. Surv. Pap. Can., 75-26*, 33-48.
Dyck, W., 1976: The Use of Helium in Mineral Exploration. *Journal of Geochemical Exploration, 5*, 3-20.
Gingrich, J.E. & Fisher, J.C., 1976: Exploration for Uranium Utilizing the Track Etch Technique. *25th Int. geol. Congr., Sydney, Abstracts, 2*, 390.
Hegge, M.R., 1977: Geologic Setting and Relevant Exploration Features of the Jabiluka Uranium Deposit. *Bull. Can. Inst. Min. Metall., 70*.
Kirwan, L.D., 1978: History of the Midwest Lake Uranium Discovery. *Saskatchewan Geological Society Symposium on Uranium Exploration Techniques* (in press).
Linfott, K.G., Pyke, M.W. & Netolitzky, R.K., 1976: Uranium Exploration in Saskatchewan. *Can. Min. J., 97*, 60-69.
McMillan, R.H., 1977: Uranium in Canada. *Bull. Can. Petrol. Geol., 25*, 1222-1249.
McMillan, R.H., Heenan, P.R. & McKnight, B.K., 1978: Uranium Exploration: Canada. *Proceedings of the Topical Symposium Uranium Resources: An Internation Veiwpoint.* Las Vegas, Nevada, Sept. 10-13, 1978. American Nuclear Society; U.S. Dept. of Energy.
Morton, R.D., 1976: Western and Northern Australia Uranium Deposits — Exploration Guides and Exploration Deterrents to Saskatchewan. *Spec. Publs geol. Soc. Sask., 3*, 211-254.
Munday, R.J., 1979: Uranium Mineralization in Northern Saskatchewan. *Bull. Can. Inst. Min. Metall., 72*, 102-111.
Pedersen, C.P., Dunbier, J. & Gingrich, J.E., this volume: Experience with the Track Etch Method for Uranium Exploration in Northern Australia. *Proceedings of the International Uranium Symposium on the Pine Creek Geosyncline.*
Porritt, J.W.M., 1979: Radon in Soil Measurements in Uranium Exploration using the RE 279 Radon Counter. *Research Division, Bondar Clegg & Company Limited.*
Rowntree, J.C. & Mosher, D.V., 1976: Case History of the Jabiluka Uranium Deposits, East Alligator River region, Northern Territory of Australia. Exploration for Uranium Ore Deposits. *Proceedings of a Symposium, Vienna. International Atomic Energy Agency, Vienna*, 551-571.
Ryan, G.R., 1972: Ranger 1: A Case History. *Uranium Prospecting Handbook, Inst. Min. Metall.*, 296-300.
Tipper, D.B. & Lawrence, G., 1972: The Nabarlek Area, Arnhemland, Australia: A Case History. *Uranium Prospecting Handbook, Inst. Min. Metall.*, 301-305.

URANIUM DEPOSITS OF THE FUTURE

Derek M. Taylor[1] and James Cameron[2]

1. OECD Nuclear Energy Agency, Paris
2. International Atomic Energy Agency, Vienna

ABSTRACT

A report was published by the OECD in December 1978 entitled 'World Uranium Potential: An International Evaluation'. This report, which was based on the first phase of the International Uranium Resources Evaluation Project (IUREP), contained an estimate of the world's 'Speculative Resources'. Using the data developed during the evaluation the authors have estimated that between 2 million and 4.5 million tonnes of the world's Speculative Resources could occur in deposits of the Proterozoic unconformity-related type and have indicated the areas of the world in which these deposits could be located. The areas which are already known to contain deposits of the unconformity-related type, notably Australia and Canada, have the greatest potential for further deposits of this type but significant new resources could also be discovered in other areas of the world, in particular in the Francevillian sediments in central Africa and the sub-Roraima metamorphic rocks in the northeast of South America.

In view of the projected uranium demand, and the possible constraints on the discovery and availability of many of the world's Speculative Resources, the authors emphasize the urgent need for exploration for these resources and in particular for those contained in deposits of the unconformity-related type.

INTRODUCTION

A report (OECD, 1978) was published by the OECD in December 1978 entitled 'World Uranium Potential: An International Evaluation'. That report was based on a study which constituted Phase I of the International Uranium Resources Evaluation Project. During the study, members of the Steering Group on Uranium Resources of the OECD Nuclear Energy Agency and the International Atomic Energy Agency, together with consultants engaged by the two agencies, compiled a large volume of data on 185 countries of the world.

The greater part of the information collected concerned the geology of the countries with particular reference to areas containing known uranium occurrences and those thought favourable for the location of uranium deposits. Information was also collected on known resources, past production, past and present uranium exploration activities and general geographical features that may influence such activity in the future. Using this data the Group identified areas which they believed to be favourable for the discovery of uranium resources in addition to those Reasonably Assured Resources (RAR) and Estimated Additional Resources (EAR) reported in 'Uranium Resources, Production and Demand, December 1977' (OECD, 1977). For each country an estimate was made of the order of magnitude of this additional potential which, for the purpose of making a summation, was assigned a range of tonnages. These tonnage ranges were called 'Speculative Resources' and the summation, by continent, is shown in table 1.

For the purpose of the IUREP evaluation, the major uranium resources of the world were assigned, on the basis of their geological setting, to the following six categories of ore types:

1) Quartz-pebble conglomerate deposits
2) Proterozoic unconformity-related deposits
3) Disseminated magmatic, pegmatitic and contact deposits in igneous and metamorphic rocks
4) Vein deposits
5) Sandstone deposits
6) Other types of deposits (includes deposits in calcretes, limestones, etc.).

We are here concerned with deposits of the Proterozoic unconformity-related type and these are described in the OECD report as deposits which "occur spatially close to major erosional unconformities developed during a generally world-wide orogenic period about

CONTINENT	NUMBER OF COUNTRIES	SPECULATIVE RESOURCES (MILLION TONNES U)
Africa	51	1.3-4.0
Asia and Far East*	41	0.2-1.0
Australia and Oceania	18	2.0-3.0
North America	3	2.1-3.6
South and Central America	41	0.7-1.9
Western Europe	22	0.3-1.3
TOTAL	176	6.6-14.8
China, Eastern Europe and USSR	9	3.3-7.3**

* Excluding Peoples Republic of China and eastern part of USSR.

** The potential shown here is 'Estimated Total Potential' and includes an element for 'Reasonably Assured Resources' and 'Estimated Additional Resources' although those data were not available to the Steering Group.

Table 1. Speculative Resources listed by continent.

1800-1600 m.y. They are represented by the ore bodies of Cluff Lake, Key Lake and Rabbit Lake in northern Saskatchewan, Canada, and those in the Alligator Rivers areas in northern Australia". In this paper we have used the name 'Proterozoic unconformity-related' and this description as a guide, but we have not completely excluded the possibility that deposists similar to those mentioned could occur in rocks of ages other than Lower Proterozoic or in rock units not clearly related to major unconformities.

Using the data developed during Phase I of IUREP the authors have estimated how much of the world's Speculative Resources could occur in Proterozoic unconformity-related deposits and where these undiscovered deposits could occur. The ranges shown in table 2 were calculated in two stages. First an estimate was made as to what percentage of each country's Speculative Resources, as initially estimated by the Steering Group, could be expected to occur in unconformity-related deposits. Then the high values and the low values of the ranges for all the countries within each continent were added to give the ranges in the table. As in the IUREP study, this technique was felt to be appropriate in view of the subjective nature of the

CONTINENT	SPECULATIVE RESOURCES (1,000 TONNE U)
Africa	171-635
Asia and Far East*	15-75
Australia and Oceania	1500-2250
North America	600-1200
South and Central America	222-475
Western Europe	2-10
TOTAL	2510-4645
China, Eastern Europe and USSR	1255-2290**

* Excluding Peoples Republic of China and the eastern part of USSR.

** A portion of these resources may already have been discovered.

Table 2. Speculative Resources in Proterozoic unconformity-related deposits.

exercise and the uncertainty associated with the tonnage ranges originally applied to each country.

In table 2 the estimate shown for Eastern Europe, China and the USSR was made simply by assuming that the uranium in the area covered by these countries would be distributed in the same proportions as in the rest of the world.

FAVOURABLE AREAS OF THE WORLD

It can be seen from table 2 that the potential for Proterozoic unconformity-related deposits is not equally distributed between the continents but ranges from a low potential in Western Europe to a very high potential in Australia. This distribution of potential is, of course, to be expected, being influenced primarily by the amount of Precambrian rocks underlying the continents and also by the presence of known resources of the unconformity-related type (Fig. 1). This should be kept in mind when using the numbers in the table and during the following brief continent by continent review of the favourable areas.

Africa

A large part of the Speculative Resources shown for Africa in table 2 is expected to occur in the Francevillian sediments or their equivalents of Gabon and Zaire. Several geologists refer to known deposits in the Francevillian as examples of standstone type uranium deposits. We believe that they also have many features in common with the deposits of the Wollaston Lake Fold Belt and of the Pine Creek Geosyncline. It is interesting to note that in the past these sediments have frequently been referred to as Middle Proterozoic but recent work on the Oklo deposit, Gancarz (1978), has indicated that the host sediments and the original mineralization may be older than 1800 m.y. and possibly older than 2000 m.y.

The case for including, in the Speculative Resource figures in table 2, an element for the potential of the Katanga System is not as convincing as for the Francevillian, especially as the rocks are not Lower Proterozoic in age. However, there are similarities between the known mineralizations in the basal Katanga rocks (Roan Formation) and deposits of the unconformity-related type. Deposits of this type could occur in these rocks under the correct tectonic conditions in Zaire and Zambia.

A large area of Rwanda and Burundi is underlain by a series of Precambrian, mainly Proterozoic, granites and metasediments. The radiometric anomalies detected by an airborne

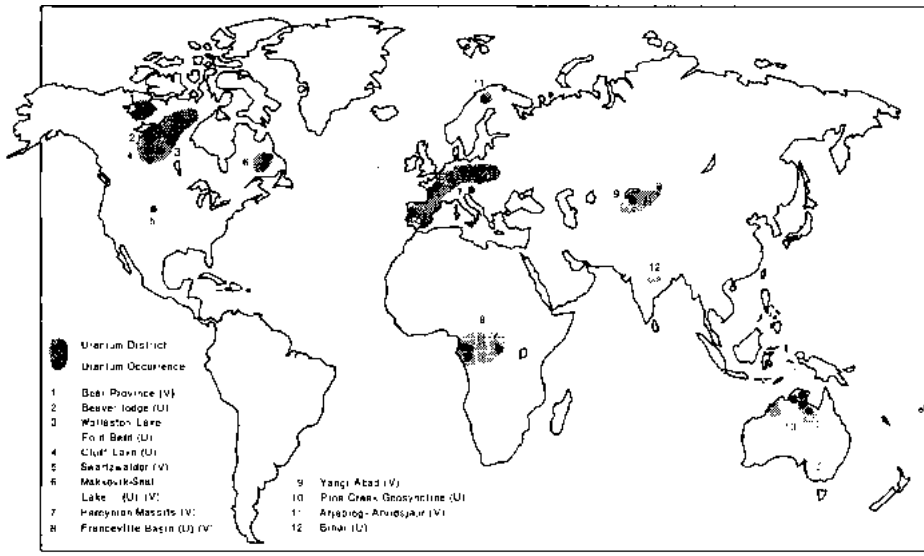


Figure 1. Areas of Proterozoic unconformity-related (U) and vein (V) deposits (From: World Uranium Potential: An International Evaluation, 1978).

survey over the countries and the pitchblende boulders collected in Rwanda are an indication that these countries have potential for uranium deposits, possibly of the unconformity-related type.

Other areas which could contain significant deposits include those underlain by the Middle Proterozoic Oendolongo System in Angola, the Dahomeyan/Atacorian unconformity of Togo and Dahomey, the unconformity between the Buganda-Toro System and the Karagwe-Ankolean System of Uganda, and the pre-Moyombe unconformity of Congo.

Several other African countries have a lesser potential for these types of deposits. These include Botswana, Cameroon, Central African Empire, Ethiopia, Ghana, Mozambique and Nigeria.

Asia

With the exception of one recently described deposit in China, there are no known Proterozoic unconformity-related deposits in Asia. If we exclude China and the eastern part of the USSR the only areas of the continent where such deposits could be found are those underlain by the rocks of the Indian Shield. Here thick assemblages of sediments, including rocks of the Lower Proterozoic Dharwar System and Aravalli Supergroup, overlie a highly metamorphosed Archaean basement. These sediments were deformed and metamorphosed during the Early Karelian Orogeny, dated at 2000 m.y, and again by the Late Karelian Orogeny which started around 1600 m.y. The three uranium provinces, Singhbhum, Rajasthan and Madhya Pradesh, which contain deposits as disseminations in metamorphic rock may be the most attractive targets especially the metasediments of the Aravalli Supergroup in Rajasthan province.

Studies of the Arabian Shield have failed to detect any rocks older than 1100 m.y. Though rocks older than this could be present, it appears unlikely that significant areas of Archaean or Early Proterozoic rocks will be found.

Australia and Oceania

Only one country in the grouping, Australia, has potential for additional uranium in

unconformity-related deposits. The North Australian Orogenic Province contains the Pine Creek Geosyncline, the Tennant Creek Block, the Granites-Tanami Block, the Nicholson Block and the Halls Creek Belt. In the Pine Creek Geosyncline the Cahill Formation extends over an area of about 6,000km² but less than 1% outcrops. The limited exploration completed to date has resulted in the discovery of large reserves and it is considered that there is a potential of the order of five to ten times the known reserves yet to be found. This formation could then host nearly half of the resources contained in the world's* unconformity-related deposits. In other words, this relatively small area in which approximately one-sixth of the world's* reserves occur, could also contain one-sixth of Speculative Resources. In addition, there is some potential for further discoveries in all the blocks of this orogenic province and in other Precambrian metamorphic complexes, in particular the Georgetown Block and the Gawler Block.

Europe

The potential for unconformity-related deposits in Western Europe is severely limited with the only areas which could be favourable for deposits of this type being within the Fennoscandian Shield. The numbers shown in table 2 should, in this instance, be viewed as uranium potential relative to that of other continents rather than an indication that these tonnages of uranium are expected to exist.

Uranium mineralization is known in Precambrian (Lower Proterozoic?) sediments which occur in eastern Finland. These metasediments were deposited marginally to a pre-Karelian basement gneissic complex and have been intruded by orogenic plutons at around 1800 m.y. Parts of Norway and Sweden could also be studied further.

North America

The most recently discovered deposits in Canada are of the unconformity-related type and we believe that the majority of the undiscovered resources in Canada are also of this type. Geological environments similar to those containing the known deposits occur elsewhere in the Wollaston Lake and Tazin-Nonacho Fold Belts and in the East Arm and other fold belts of the Churchill Structural Province (including the Baker Lake and Amer Lake Areas). Similar environments also occur in portions of the Bear and Slave Provinces and parts of the Nain and Superior Structural Provinces, the former including the Makkovik Fold Belt and the Labrador Fold Belt.

It is worth stressing that in Canada, as in Australia, we have a relatively small area, the Wollaston Lake Fold Belt, that contains an appreciable percentage of the world's reserves and is expected to contain a similar percentage of the world's Speculative Resources.

There is little possibility of finding major uranium deposits of the unconformity-related type outside of Canada, in North America though there are geologists who believe that some of the vein deposits in the Precambrian Idaho Spring Formation of the Front Range of Colorado belong to this type. The Precambrian rocks of the Southern Canadian Shield outcrop in Minnesota, Wisconsin and Michigan and minor uranium occurrences are known. These formations could be studied further.

South and Central America

The most favourable area for the location of Proterozoic unconformity-related deposits in South America is that underlain by the Guyana Massif and overlain by the Roraima Formation. Here, in parts of Venezuela, Brazil, Guyana, French Guiana and Surinam, the geological conditions of the sub-Roraima unconformity closely resemble those of the sub-Kombolgie and sub-Athabasca unconformities of the Wollaston Fold Belt and the Pine Creek Geosyncline. Many of the rocks that underlie the Roraima are moderately folded and faulted Lower Proterozoic metasediments, many of which are pyritic and some are carbonaceous. These rocks commonly overlie a gneissic basement. The Middle Proterozoic Roraima

* Excluding USSR, China and Eastern Europe

Formation, which covers an area of over 10,000km², is continental, consisting of fluviatile sandstones with minor conglomerates near the base.

There is the possibility that sandstones present on the Guapore Massif in Bolivia, and on the Guyana Shield and in the mesas of the Llanos Basin in Colombia, are Precambrian units correlative with the Roraima Formation. The rocks below these units could be prospective.

There are several areas of Brazil, in addition to those already mentioned, where Proterozoic sediments and metasediments occur which could be favourable for unconformity-related deposits. The unconformity between the Minas Series and the overlying Itacolomi Series in the Quadrilatero Ferrifero may be interesting, even though the latter is predominantly marine, and the unconformity between the Caico Group and the later Serido Group in the Serido Geosyncline could be a good exploration target.

China, Eastern Europe and the USSR

The knowledge outside of China, Eastern Europe and the USSR of their uranium deposits is very limited, and the published geological information is commonly generalized. The following observations may be made in support of the resource figures shown in table 2.

In China miogeosynclinal and eugeosynclinal deposits of Early Proterozoic age were laid down around the Archaean North China-Korean and South China nuclei. Many of these sediments were later deformed by the Luliangian orogeny around 1800 m.y. and some have been incorporated in the nuclei. These metasediments could now be favourable targets for exploration for unconformity-related deposits especially in areas where overlying Middle Proterozoic sediments, such as those of the Changcheng System, have been removed by erosion.

Outside of the USSR there is little possibility of finding Proterozoic unconformity-related deposits in Eastern Europe. Within the USSR, however, there must be tremendous potential for such deposits. Lower Proterozoic rocks are well developed in the Russian Platform especially in the Kola Peninsula and to the south of the White Sea. On the Siberian Platform the Lower Proterozoic is developed as a thin cover along the northern slope of the Eastern Sayan Massif but in other regions as a thick (10-12km) sequence of highly folded metamorphic schists, phyllites, quartzites, crystalline limestones and dolomites. Proterozoic rocks also outcrop in the Palaeozoic Uralian and Angora geosynclines, in the Mesozoic and Cainozoic Mediterranean and Pacific Ocean geosynclines, and in the geologically complex area of Central Asia. Archaean rocks also occur in all these areas. There is no indication in the available literature that unconformity-related deposits have been found in the USSR but with the large areas which could contain favourable environment for such deposits it is expected that large resources would exist.

URANIUM DEMAND

At present we have sufficient uranium reserves to meet demand. This is fortunate as most of the Speculative Resources discussed in this paper will take many years to be moved into the reserve category, if they do so at all. What we are interested in here is uranium demand in the longer term and a recent forecast of demand is illustrated here by figure 2. This figure shows the predicted cumulative uranium committments, using the fuel requirements for a 30-year reactor lifetime, to the year 2025, with the unbroken curves showing the two extreme cases of possible committments using Light Water Reactors (LWR) without recycle and the broken curves showing the predicted uranium committments, for the same energy output, if Fast Breeder Reactors (FBR) using oxide fuel are gradually introduced. The horizontal lines represent quantities for Reserves, Resources and the lower and upper limits of the range of Speculative Resources.

From figure 2 we can see that the Reserves would all be committed around 1990 and that the additional resources, if they can be transformed into Reserves, which is of course not

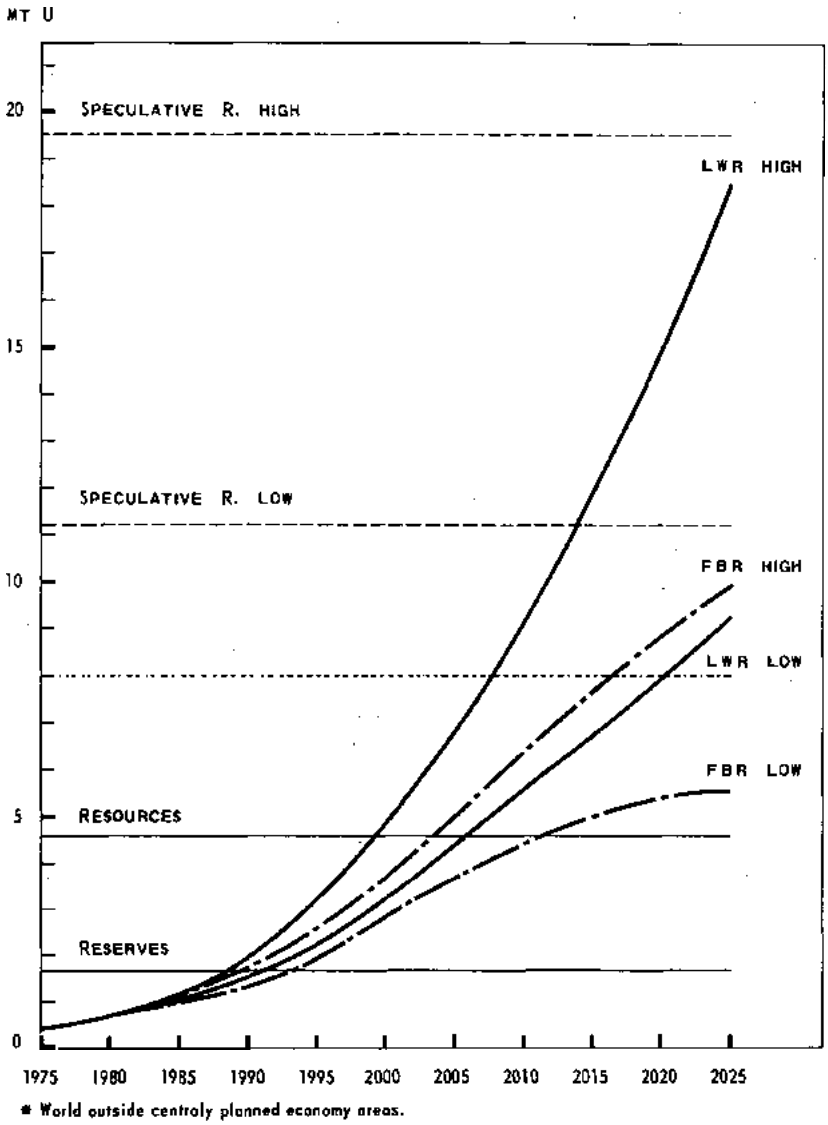


Figure 2. Uranium Commitments (WOCA)*. After Häussermann, 1979).

certain, would be committed between 2000 and 2005 for the high LWR and low LWR cases respectively. After these dates new reactors would need to be fuelled by what is, at this time, 'speculative uranium'. By the year 2025, if only LWRs are installed, cumulative uranium committments would be between 9 and 19 million tonnes.

URANIUM SUPPLY

The situation appears at the present time to be a comfortable one with adequate uranium

reserves to meet demand in the short term and enough Speculative Resources to meet 'speculative demand' in the longer term, especially if breeder reactors are introduced. We use the word 'appears' as there are, unfortunately, many uncertainties in the basic assumptions.

We are as confident as geologists can be that the reserves of 1.7 million tonnes of uranium exist. What we do not know is if they will all be produced and made available. Many of you will know of uranium reserves that are not being exploited and may not be exploited in the foreseeable future. Nearly 80% of the remaining resources fall into the 'Estimated Additional Resources' category and there is appreciably less confidence in these estimates than in those for Reserves. Therefore we are not confident that all these resources exist and less confident that they will be produced. It may also be important that over a quarter of the 4.7 million tonnes of resources are in a high cost ($80-130/kg U) category.

There is, of course, even less confidence in the Speculative Resources estimates. In the Foreword to 'World Uranium Potential' it is emphasized that "even if these Speculative Resources exist, there is no guarantee that the resources will be discovered or, if discovered, that they can be made available. In other words, these estimates imply nothing about *discoverability or availability*. Serious constraints may well arise on many fronts, such as the restriction of access to the favourable areas for the purpose of exploration, inadequacies in uranium exploration techniques, the rate of discovery once exploration has commenced, conflicts in land use where discoveries are made, difficulties of capital formation and allocation, and availability of trained manpower . . . because of these constraints, and in view of the long lead times for exploration, mine development and production, it is likely that a major part of these Speculative Resources may not be discovered and brought into production during the first quarter of the 21st century".

It is then going to require substantial exploration efforts to move the Speculative Resources and, in many instances, the Estimated Additional Resources into the Reasonably Assured Resources category. After these efforts there will remain, as we are sure you know only too well, the major step of converting resources in the ground to reactor fuel.

Exploring for uranium is very expensive and becoming increasingly so. Many of the resources still to be discovered will occur in blind orebodies and the percentage of exploration budgets spent on drilling will rapidly increase. The most attractive exploration targets will be large orebodies, preferably of course high grade ones. Preference will also be given to areas where the geology is well known, where expertise in exploration and, if possible, in production, is available and where the laws governing uranium exploration are clearly defined.

CONCLUSIONS

Approximately one third of the world's Speculative Resources are expected to occur in Proterozoic unconformity-related deposits and three quarters of these resources, outside of the communist countries, could occur in Australia and North America. They are, unfortunately, still Speculative Resources. Many of them could become the deposits of the future, and we must hope that, with an increased exploration effort, the future will not be too far away.

REFERENCES

Gancarz, A.J., 1978: U-Pb age (2.05 x 10^9 years) of the Oklo Uranium Deposit *in* Natural Fission Reactors. *Proc. Tech. Comm., Paris, 1977.* International Atomic Energy Agency, Vienna.

Häussermann, W., 1979: Adequacy of World Uranium Resources. *Atomic Industrial Forum Fuel Cycle Conference 79, Atlanta.*

OECD Nuclear Energy Agency and International Atomic Energy Agency, Uranium Resources, Production and Demand, December 1977: *Joint OECD(NEA)/IAEA Report, OECD, Paris.*

OECD Nuclear Energy Agency and International Atomic Energy Agency, World Uranium Potential; An International Evaluation, 1978: *Joint OECD(NEA)/IAEA Report, OECD, Paris.*

THE SYMPOSIUM — RETROSPECT AND DISCUSSION

G.H. Taylor[1] and J.C. Rowntree[2]

1. CSIRO Fuel Geoscience Unit, P.O. Box 136. North Ryde, N.S.W. 2113, Australia.
2. Pancontinental Mining Ltd., 50 Bridge Street, Sydney, N.S.W., 2001, Australia.

INTRODUCTION

In this chapter an attempt is made to review briefly and discuss some of the material presented during this Symposium. Inevitably, we must be highly selective in this task; the reader is encouraged to refer to the individual papers in this volume*.

Much of the Symposium centred around two main questions:

1) What are the characteristic features of the known uranium mineralization in the Pine Creek Geosyncline?
2) How did the known uranium mineralization in the Pine Creek Geosyncline form?

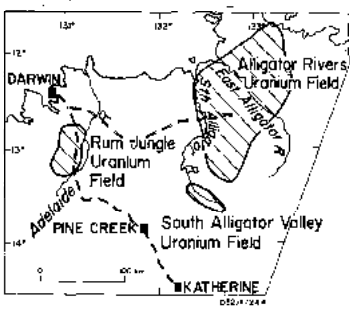


Figure 1. Locality of the three Uranium Fields in the Pine Creek Geosyncline.

It is convenient to begin by reviewing briefly the models which were proposed during the Symposium. The present authors have had to base this review and discussion paper on the papers presented at the Symposium. They do not in any way seek to pass judgement on these papers, but attempt to make constructive comments and draw attention to some problems. While the Symposium is a landmark in our progress towards gaining a full understanding of uranium mineralization in the Proterozoic rocks of northern Australia, we forward to further work which will confirm or modify some of the concepts put forward.

For the most part we will not refer to mineralization other than of uranium. Indeed, most of this paper will be concerned with the very rich uranium mineralization which occurs in the Alligator River Uranium Field (ARUF) (Fig. 1).

The major features of the ARUF deposits may be summarized as follows (not necessarily in order of importance). Some of these features were also listed by Mosher *et al.* (1979):

1) There is intense and pervasive chloritization, magnesium metasomatism, and lesser sericite alteration of the mineralized and surrounding lithologies including the Kombolgie Formation.
2) Although most deposits are bounded by lithological units, a major localizing feature appears to have been the presence of open spaces, especially in and near zones of brecciation.
3) Pitchblende is the main ore mineral; gold is the only associated metal which is concentrated in economic quantities. Disseminated sulphides occur.
4) There appears to be a spatial relationship of the deposits to the Lower/Middle Proterozoic unconformity. There may be other prominent discontinuities, faults or aquifers close to ore concentrations.
5) The proximity to the older granitic migmatite complexes and their pegmatitic apophyses to mineralization appears likely to be significant.

*All references without dates are to papers in this volume.

6) There is a regional association of mineralization with carbonate strata but commonly an antipathetic relationship with carbonate within the ore zones.
7) The content of thorium in the ore is very low.
8) Ore commonly occurs in or near graphitic rocks (graphitic here being used for rocks containing graphite or other carbonaceous matter). Such rocks are now known to be present at Narbarlek as well as near other deposits.
9) There is virtually no mineralization in the Kombolgie sandstone despite some chlorite veining.
10) The ARUF deposits include numerous small occurrences as well as several very large ore bodies.
11) There is a wide spread of apparent ages of mineralization. Perhaps the only certainty is that the mineralization in its present form is younger than the ~1800 Ma metamorphic event.

MODELS PROPOSED

The various models proposed at the Symposium are grouped rather arbitrarily into those relevant to the ARUF deposits, those relevant to other uranium mineralization in the Pine Creek Geosyncline, and those relevant to deposits in other countries. The brief notes given here do not constitute summaries approved by the various authors, and the reader is encouraged to consult the various papers presented in this volume.

Deposits in the Alligator Rivers Uranium Field (ARUF)

Crick & Muir postulate the formation of primary carbonate in a sabkha environment and the deposition of uranium from the surrounding terrane. Diagenetic gypsum was formed in the evaporitic deposits, and this later changed to anhydrite. With post-metamorphic diapirism, uranium was transported into the rocks around the upper parts of the diapirs.

Ypma & Fuzikawa conclude that uranium was transported in low temperature waters of meteoric origin along or close to the Upper/Middle Proterozoic unconformity. These waters encountered $CaCl_2$-rich brines perhaps generated as proposed by Crick & Muir. Methane may have been involved in the chemical reduction which accompanied precipitation of the uranium.

Gulson & Mizon, while not postulating a model, believe that the uranium was transported in the uranous state, presumably as chloro-complexes in highly saline waters.

Binns, McAnderew & Sun propose hydrothermal fluids from a concealed granite as the agent of mineralization. These fluids moved to favourable sites (graphitic rocks) where the uranium was initially incorporated in a chlorite-septechlorite-quartz (CSQ) rock. The uraninite was formed from the CSQ rock during a later event.

Ferguson, Ewers & Donnelly postulate the derivation of uranium from weathering of rocks exposed in the post-orogenic terrane. This uranium became incorporated in carbonate complexes in surface and near-surface waters. These waters then carried uranium into collapse breccias which were part of a karst-type topography. The reduction to uraninite occurred in situ.

Needham & Stuart-Smith also favour the movement of uranium in surface and ground waters to a site where carbonaceous matter was present. The uranium was perhaps concentrated on clays and deposited in open structures. These authors also regard mineralization from brines as a possibility.

Giblin did not advance a model but reported work which was invoked by a number of other authors. She showed that soluble uranyl species may be immoblized by adsorption on clay. Subsequent lowering of the Eh leads to crystallization of the uranium as uraninite with reactivation of the clay surface. Repeated cycling of Eh values makes possible a high degree of uranium enrichment.

Deposits in Other Areas of Australia

Pine Creek Geosyncline

Berkman & Fraser suggest that the Mount Fitch copper-uranium deposits in the Rum Jungle Uranium Field (Fig. 1) began as disseminated mineralization which was concentrated by weathering and movement into a breccia zone.

Crick, Muir, Needham & Roarty propose that the uranium in deposits of the South Alligator Valley Uranium Field (SAVUF) (Fig. 1) deposits was derived through the leaching of the Edith River Volcanics by groundwater. The solutions moved into the Koolpin Formation where the uranium was deposited in the vicinity of carbonaceous and ferruginous rocks.

Mary Kathleen area

Cruikshank, Ferguson & Derrick conclude that the uranium in the Mary Kathleen garnet-rich skarn deposit originated from residual fluids associated with the crystallization of granitic magma. The uranium was transported in carbonate complexes which were later destabilized to precipitate uraninite. Such destablization could have occurred when acidic solutions were neutralized by reaction with carbonates.

Deposits in Other Countries

There is not space to review the papers presented at the Symposium on deposits in countries other than Australia. These included the account by Qin & Hu of the Lianshanguan deposit in northeast China, and that by De Voto & Paschis of deposits in the Front Range, Colorado, U.S.A. Several papers on the Athabasca deposits were of special interest because of their possible relevance to the ARUF deposits:

1) Hoeve, Sibbald & Ramaekers;
2) Kirchner, Lehnert-Thiel, Rich & Strnad;
3) Pagel, Poty & Sheppard;
4) Ramaekers; and
5) Tilsley.

It is clear that workers on the Canadian deposits put much more emphasis on the Athabasca Formation sandstone than Australian workers do on the Kombolgie Formation. There is, of course, some reason for this, since only minor mineralization is known at present to occur in rocks of the Kombolgie Formation whereas major uranium mineralization is present in the Athabasca Formation. We should ask ourselves whether this is a real or apparent difference and, if real, what this implies for genetic modelling in the two areas.

GENESIS

The genesis of the uranium mineralization will be considered under the headings of age, source of uranium, transport, and controls of deposition.

Age

It is clear, from papers to this Symposium, that the dating of rocks and events in the Pine Creek Geosyncline presents a great problem and is a task for specialists. There was general satisfaction that the specialists at the Symposium were able to contribute a joint account of the present state of knowledge. (B.L. Gulson, J.H. Hills, R.W. Page and G.H. Riley, pers. comm.)

On the basis of field relationships, the following sequence of events seems to be beyond challenge:

- Intrusion of Archaean granitoids
- Deposition of sedimentary rocks prior to ~1800 Ma[1]
- ~1800 Ma metamorphism[1][2]
- Intrusion of Oenpelli Dolerite at 1688 Ma[1]
- Deposition of Kombolgie Formation [1] ~1650 Ma

- Intrusion of phonolites (1316 Ma[1]) and mafic dykes (1200 Ma [1])

[1]Page, Compston & Needham; [2]Riley, Binns & Craven.

It also seems to be generally accepted, on the basis of field and laboratory work, that uranium mineralization in the Pine Creek Geosyncline is later than the ~1800 m.y. metamorphic event.

There is no doubt that uranium in these deposits has been remobilized, probably repeatedly. As Gulson & Mizon emphasized, the ages which were presented during the Symposium are apparent ages and should be treated as such. Some late ages must represent remobilization. The whole matter of time relationships is of such importance to the elucidation of the uranium mineralization that it is an appropriate field for collaboration by those able to provide data.

On the basis of metamorphic grade Ferguson raised the question as to whether the metasediments to the east of the South Alligator Hinge Zone (SAHZ) are of comparable age to those in the west, as has been widely assumed. It would be desirable to have any doubt removed since a marked difference of age on the two-sides of the SAHZ could have profound implications for ore genesis and exploration, depending on the favoured process of mineralization.

Source of Uranium

Most would agree that the Pine Creek Geosyncline is a uranium-rich province, although Rossiter & Ferguson imply that it may not be unique in Australia in this respect. Other areas within the large Archaean continental margin may yet be shown to contain more uranium mineralization than has yet been found.

McAndrew & Finlay showed how uranium occurs in the granitic rocks which are important as sources for subsequent mineralization, and suggested tests to show whether the rock could have contained uraninite capable of being moved to a site of concentration elsewhere. Rossiter and Ferguson considered the possibility of mantle plumes, rich in uranium and other refractory elements, rising from the lower mantle as a logical consequence of hypothetic inhomogeneous planetary accretion. Alternatively or additionally, mechanisms of high heat flow can be invoked to produce anatexis with resulting production of U-enriched potassic granitoids.

Needham & Roarty accept the basement as the source of uranium, except perhaps in the South Alligator Valley where the uranium may have come from the Edith River Volcanics. Needham and Roarty consider that, elsewhere, concentration could have occurred in shallow marine or tidal conditions during the Lower Proterozoic. These initial concentrations acted as a secondary source, in their view, during subsequent ferromagnesian metasomatism.

Binns, McAndrew & Sun derive their uranium from a granitoid — presumably one of the post-orogenic granitoids which are commonly enriched in uranium (slightly more so than the Archaean granitoids, according to Ferguson, Chappell & Goleby). Binns, McAndrew & Sun prefer a granitic source because of their assessment that the mineralization was derived from ascending hydrothermal solutions. The high uranium content of the post-orogenic granitoids may be relevant to their case for mineralization via solution from such a granitoid.

Ferguson and his co-workers and most other authors derive their uranium from the supergene alteration, in the post-orogenic phase (i.e. <1800 Ma), of rocks containing significant amounts of uranium. These rocks would have included the granitoids and the Lower Proterozoic carbonaceous and pelitic shales. Although the degree of enrichment of such sediments seems to be debatable, they are invoked by several authors as the main source of uranium for the ARUF deposits, whether the movement of uranium is directly from the peneplaned surfaces (as Ferguson, Ewers & Donnelly suggest) or along the Kombolgie contact (as proposed by Ypma & Fuzikawa). This contrasts with the suggestion by

Ramaekers (1979) that the uranium in Saskatchewan has come from the Athabasca Formation. Such suggestions should remind us that we know very little about the provenance of the Kombolgie Formation. Did it come from a uranium-rich terrane and does it now have less uranium than its provenance rocks, as is claimed for the Canadian case? If it could be established that some rocks of the Kombolgie Formation have been significantly depleted in uranium, this may be a feasible source for the ARUF deposits. Moreover, there could then be some hope of significant mineralization within favourable zones of the Kombolgie Formation itself.

Transport of Uranium

It seems clear from the mineral associations and general geology that the uranium, now in the ARUF deposits, was transported in aqueous solution, even though there are diverse views as to the origin and composition of the water.

Ypma & Fuzikawa found two sets of fluid inclusions in quartz and calcite, in the vicinity of the Jabiluka and Nabarlek deposits. They suggest that the uranium was carried as uranyl carbonate complexes in CO_2-rich solutions of low temperature (probably meteoric) origin. The uranium was stripped when these waters came in contact with hypersaline brines. (Can we be confident that these brines have, in fact, been involved in the uranium mineralization? May they have been associated, for instance, with the movement of gold at another time?)

Several possible mechanisms for the precipitation of uranium were suggested at the Symposium, including the possibility that methane may have been the reductant in the change from a uranyl compound to uraninite. Since, in some models at least, the methane was brought in with the CO_2-rich solution which transported the uranium, it is hard to see why reduction did not occur earlier if, indeed, it was going to occur at all. We are not aware of evidence that methane is an effective reductant under the conditions suggested and consider it much more likely that carbonaceous matter was the reductant. It is true that, above about 200°C, methane may be an equilibrium product (not, incidentally, higher hydrocarbons as have been suggested) but it seems unlikely to be of great significance in the present context.

The model proposed by Ypma & Fuzikawa calls for transport along or close to the Kombolgie contact with Lower Proterozoic rocks. (One wonders why the chlorite veins which transgress the contact and pass into the Kombolgie are not significantly mineralized.) Ypma & Fuzikawa invoke the adsorption of uranium on to phyllosilicates in line with Giblin's work (although the CO_2-rich nature of the fluid may lead to unfavourable conditions for maximum adsorption). The question also arises as to why the solutions would traverse so much rock containing abundant clays and chlorite before adsorption actually occurred.

Crick & Muir also invoke brines, associated with evaporites, for transport of the uranium. Without dwelling here on the diapirism with which these continental brines were associated, Crick and Muir consider that these fluids were released before and during the ~1800 m.y. metamorphism. They visualize these brines, possibly enriched in uranium and thought to have been rich in magnesium, as having provided the raw materials for later carbonate-rich groundwaters to convert clay to chlorite and to deposit uranium. This model would seem to suggest that not only uranium but also thorium and base metals in chloro-complex form would have been expected in the brine. However these elements may have dropped out of solution as the brine became less concentrated. One recalls the thorium and uranium/thorium deposits mentioned by various authors.

Binns, McAndrew & Sun move their uranium in via a retrogressive fluid from a concealed intrusion. This fluid carried, together with uranium, elements such as Be, Sc, Y and others but must have been of extremely low Th content. These authors propose that the

uranium was transported in uranyl form and that subsequent reduction occurred with the consumption of graphite. Binns, McAndrew & Sun note the presence of occasional sulphides in veins which elsewhere carry uraninite. Despite recent works by Langmuir (1978) one could envisage a possible problem in transporting uranyl compounds and depositing sulphides from the same solution. Perhaps the answer is that we do not have to assume that the fluids necessarily remained of constant character throughout. Indeed, we have evidence for the replacement of chlorite by uraninite and of uraninite by chlorite at different stages, suggesting that there were significant changes in the nature of the mineralizing fluids.

Ferguson, Ewers & Donnelly also move their uranium in the uranyl form, although in their model the leaching is of surface-exposed granitoids or Lower Proterozoic sediments. The uranium was fixed by adsorption on clays or hydrated iron oxides or by chemical reduction under anaerobic conditions – for example on pyritic carbonaceous black shales. In the second stage of transport, CO_2-rich groundwater extracted and moved the uranium along as uranyl carbonate complexes which entered collapse structures where the uranyl complex was adsorbed and later reduced to uraninite.

Crick & Muir favour ground water for transport of uranium to the SAVUF deposits, following Ayres & Eadington (1975). They suggested that the ground water leached uranium from the Edith River Volcanics and that water movement through the Coronation Sandstone, especially at faults and other discontinuities, brought the solutions to positions in the Koolpin Formation where reduction could occur. The events which produced mineralization may have been related to weather cycles. Crick & Muir mentioned pre- and post-glacial pluvials to fit in with inferred ages. We comment that the problem may not be so much to get extra water but rather to get oxygen into the system to render the uranium mobile. Crick & Muir mentioned red beds and these conditions of deep weathering may have been quite significant.

The association of sulphides, gold and tourmaline with uranium mineralization was mentioned at the Symposium in discussion of the SAVUF deposits and there may be something of the same kind to explain in the ARUF deposits. It is possible that hydrothermal solutions may have used the same pathways, but not necessarily at the same time, as the solutions which brought in uranium. It seems interesting that, as Ferguson & Winer reported, there is no positive correlation between gold and uranium at Jabiluka. The stable isotope work of Donnelly & Ferguson also suggests a magmatic source for the sulphur in the bedded sulphides in areas removed from mineralization.

It is difficult not to conclude that the water bringing in the uranium was sufficiently oxidizing for uranyl species to be transported. As Giblin has pointed out, recent work by Langmuir (1978) has shown that the switch from oxidizing to reducing conditions is not as dramatic a change as had been thought. Nevertheless, there seems to be no doubt that once sufficiently reducing conditions are established uranium is virtually immobile, except in brines or very acid solutions, so that the presence of a major deposit may not be detected from analysis of nearby ground water.

We see no real evidence for transport of uranium by brines to the present site since the thorium content is very low; there are also comparatively low amounts of other elements which would have been expected had highly saline conditions made possible the transport of metals as chloro-complexes. Moreover, in places where sulphides do seem to have been transported in brines, whether formed by dewatering of the Gerowie Tuff as suggested by Goulevitch or from sea-floor brine pools as proposed by Nicholson, there is a notable absence of uranium.

We would make one final comment on the transport of uranium. Most authors of papers to the Symposium have proposed solutions moving up or down. It may be worth giving more

consideration to the circulation of water, a subject which has received much consideration in relation to porphyry copper deposits.

Controls of Deposition

Why are the deposits where they are? Much was made at the Symposium of the presence of breccias. Although there is considerable controversy as to how the breccia formed, when it formed and perhaps why it formed, there is not doubt that it and other open structures constitute favoured sites for mobility of fluids and deposition of new mineral phases.

Ypma & Fuzikawa see the uranium depositing as a result of the mixing of two fluids of contrasting composition. One of these fluids were of comparatively low salinity and carried the uranium; the other was of high salinity and may have had a carbonate-evaporite origin. Deposition would presumably have been of a uranyl salt which was later reduced to uraninite. If the Crick & Muir model is accepted this may provide an explanation of the localization of the ARUF deposits in the Cahill Formation.

Ferguson, Ewers & Dennelly envisage a karst-type topography — collapsed dolines — into which low temperature, CO_2-rich groundwater carrying uranium as uranyl carbonate complexes could enter. They postulate Mg-rich clays (and/or chlorite) and possibly decaying organic matter to have been washed into the structures. The uranium was fixed and on subsequent heating by igneous activity the previously adsorbed uranium crystallized at about 1600 Ma.

Binns, McAndrew & Sun doubt the collapse origin of the breccias, and, despite comparatively high inferred pressures, prefer to read them as the result of hydraulic fracturing from introduced fluids. Into the channelways formed by the fluids associated with retrogressive metamorphism was introduced the uraniferous CSQ (chlorite-septechlorite-quartz rock). Some later episode, for example, superjacent fluid movement, would have released the uranininte as a separate phase from the CSQ.

On the basis of her recent experimental work, Giblin showed that clays can adosrb uranium from dilute uranyl solution and, with cycling ten times from oxidizing to reducing, ore grade cencentrations can form. Moreover, chlorite was stated to adsorb even more strongly than clay. This leads to the question as to why particular phyllosillicates have been the locus for deposition of uranium. Certainly, the fluctuation of Eh as in Giblin's experiments implies a reductant in the actual mineralization process. If we envisage pulses of a relatively oxidizing solution into rocks at depth, reducing conditions would be restored between pulses by reaction with carbonaceous matter, chlorite, sulphide or some other reductant. It may be highly significant that Ewers & Ferguson found the Fe^{2+}/Fe^{3+} ratio in chlorites decreased with increasing whole rock uranium. Ferguson & Winer also showed a correlation of uranium and copper at Jabiluka. The apparent activity of sulphate reducers and the presence of biogenic carbonates within the breccia (Donnelly & Ferguson) are consistent with the presence of organisms (and of the thucholite reported by several authors). All these relationships seem to be good evidence that redox controls were indeed important. However, we suspect that the greater part of the reductant role is likely to have been played by the graphite/carbonaceous matter. Certainly it was stated many times at the Symposium that the sites of mineralization were close to, or within, graphitic metasediments and instances were shown by Binns, McAndrew & Sun, and others, where oxidation of graphite had occurred. Donnelly & Ferguson have also shown that carbon isotopes from carbonate in ore suggest a contribution of carbon from the oxidation of graphite. Despite this, there appears to be a broad, rather than immediate, association between graphite and ore. The explanation may be this: the oxidation of graphite occurs at modest temperatures but is very slow. Graphite undergoes reaction at measurable rates even with water at temperatures of 200°C and more. After a pulse of oxidizing fluid, equilibrium would have

been restored and intermediate reductants like chlorite would again have been rendered active at the ultimate expense of graphite which was progressively consumed to form, eventually, CO_2. Perhaps the 'carbon button' shown by Ypma & Fuzikawa was a carbonaceous fragment from the country rock not yet completely consumed in solution.

It seems to us, then, that the sort of mechanism suggested by Giblin for those models where the uranium was introduced as the uranyl ion could have been most important. However, there remains the question as to why the particular phyllosilicates have been the site of deposition. Since graphitic rocks are very commonly involved it does seem probable that we can at least extend the control to phyllosilicates in the vicinity of a graphitic metasediment or other carbonaceous matter. Since some permeability of the rocks is essential, the presence of breccias or fractures must have been very important to give a plumbing system.

We suspect that the contribution of permeability near the unconformity was the main role of the carbonates, and while deposition was not always in breccia, mineralization does usually appear to be filling previous open space which can hardly have occurred at any great depth.

The characteristic association of ore with graphite has different significance for authors. In the model proposed by Binns, McAndrew & Sun, the fluids which brought in the uranium also caused the retrogressive metamorphism, i.e. chloritization. These authors recognize a problem with the Mg-rich character of the CSQ-uraninite veins. In view of the richness of the possibly evaporitic carbonates in Mg, this seems to be a possible source of magnesium. Ferguson, Ewers & Donnelly conceived the magnesium as having arrived in low temperature solutions of meteoric origin.

The role of the Kombolgie is a tanalising question. If subsequent work confirms that mineralization does not extend into the Middle Proterozoic rocks above the unconformity, even though chlorite veins do cross this boundary, the reason is likely to lie in the more oxidizing conditions which existed in the Kombolgie rocks during mineralization or have existed since. There seem to be many good reasons for paying a good deal of attention to the Kombolgie Formation in the future in order to establish whether its role was that of: 1) a source of uranium; 2) an aquifer with U-solution transport close to the lower contact, and/or 3) an impervious cap-rock which has acted to preserve the U-deposits from subsequent weathering and transport.

REFERENCES

Ayres, D.E. & Eadington, P.J., 1975: Uranium mineralization in the South Alligator River Valley. *Miner. Deposita, 10(1)*, 27-42.

Langmuir, D., 1978: Uranium solution - mineral equilibria at low temperatures with application to sedimentary ore deposits. *Geochim. cosmochim. Acta, 42*, 547-569.

Mosher, D.V., Hegge, M.R., Anthony, P.J., Eupene, G.S. & Pedersen, C.P., 1979: Geologic Setting and Comparative Review of the East Alligator Uranium Deposits and Prospects. *Extended Abstracts of the International Uranium Symposium on the Pine Creek Geosyncline*, 128-129.

Ramackers, P., 1979: Stratigraphy, sedimentology and structural geology of the Middle Proterozoic Basins on the Athabasca area, Saskatchewan, Canada and their bearing on uranium mineralization. *Extended Abstracts of the International Uranium Symposium on the Pine Creek Geosyncline*, 163-165.

SOLID GEOLOGY OF THE PINE CREEK GEOSYNCLINE

NORTHERN TERRITORY

1979

Scale 1:500 000

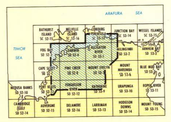
10 0 10 20 30 40 50 KILOMETRES

Transverse Mercator Projection

LOCALITY MAP



INDEX TO 1:250 000 MAP SHEETS



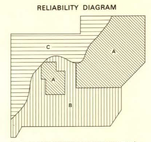
Geology by BMR 1951–59, 1962, 1965–78
Geology revised 1971–78 by I. Needham, P. G. Smart, P. D. Tucker (BMR); I. H. Crick, A. L. Watchman, D. A. Wallace, D. H. Tucker (BMR); K. Wills (CRAE); M. Roarty (NTGS); D. A. Berkman (IAGS)

Map compiled 1978 by R. S. Needham
Legend compiled by R. S. Needham, I. H. Crick, P. G. Stuart-Smith, P. D. Hohnen
Edited by J. Mitchell, P. D. Hohnen, A. S. Mikkelsen
Design and drafting by Cartography Section, BMR
Drawn by P. Moffat
Printed by Mercury-Walch, Hobart, Australia

Published by the Bureau of Mineral Resources, Geology and Geophysics, Department of National Development, issued under the authority of the Minister for National Development
Topographic base compiled by the Bureau of Mineral Resources, Geology and Geophysics, Canberra, ACT, from National Chart, ICAO 1:1 000 000 series produced by the Division of National Mapping, Department of National Development
© Commonwealth of Australia 1979

Copies of this map may be obtained from the Bureau of Mineral Resources, Geology and Geophysics, Canberra, ACT, or Darwin, NT

RELIABILITY DIAGRAM



A –Good; recently mapped, little cover or scattered drilling information in covered areas

B –Fair; detailed but dated mapping, modified by extrapolation from recently mapped areas

C –Poor; extensive cover with little drilling information, geology by gravity and magnetic interpretation and conceptual extrapolation

MAIN DATA SOURCES

(Predominant source shown for each area)



A –BMR and BMR–NT Geological Survey 1:100 000 scale mapping, 1971–77

B –BMR 1:63 360 scale mapping, 1954–59

C –BMR 1:250 000 scale mapping, 1969–70

D –BMR 1:250 000 scale mapping, 1972–73

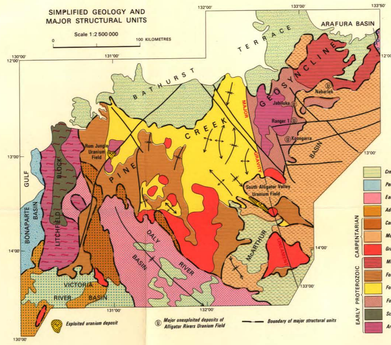
E –BMR 1:250 000 scale mapping, 1962

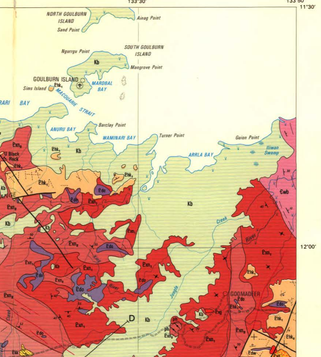
F –BMR 1:250 000 scale mapping, 1951–59

SIMPLIFIED GEOLOGY AND MAJOR STRUCTURAL UNITS

Scale 1:2 500 000

0 100 KILOMETRES

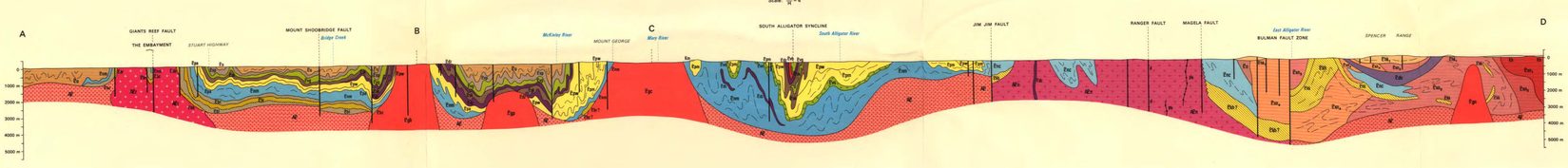


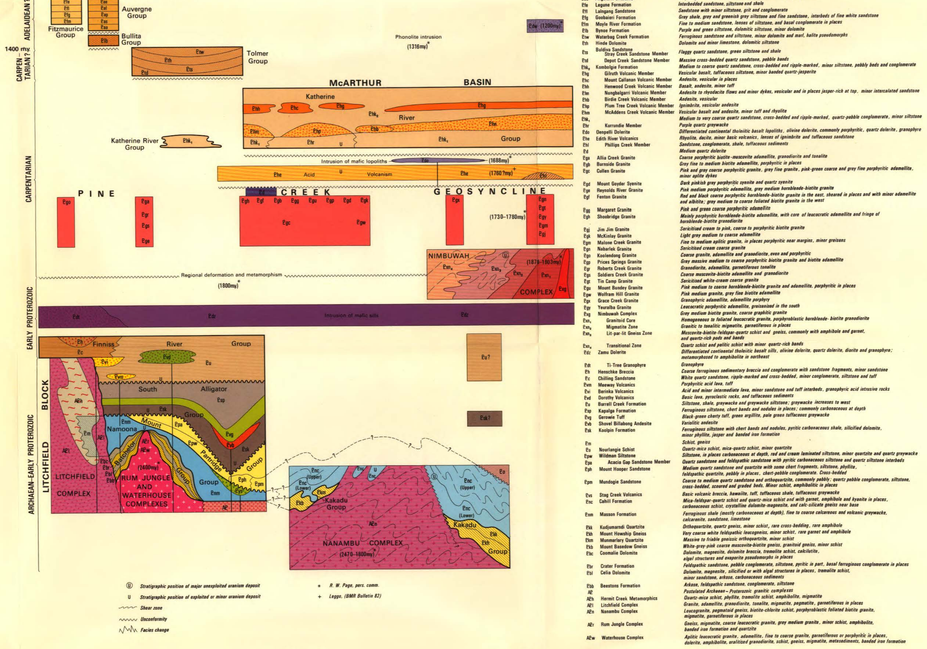


SCHEMATIC SECTIONS

Basement configuration calculated from gravity data: 5 mGals to 1 km depth

Scale: $\frac{V}{H} = 4$





Tb	Bathurst Island Formation	Fine to medium sandstone, siltstone: mainly marine
Km	Petrel Formation	Medium to coarse sandstone, siltstone, conglomerate; mainly terrestrial
P		Siltstone, silty sandstone, minor limestone, basal conglomerate, diamictite
Do	Dolloo Limestone	Flaggy pink-grey limestone, common oolicrinal
Cl		Stromatolitic limestone, minor siltstone, sandstone
Cl[b]	Jinduckin Formation	Fine sandstone, siltstone and siltstone, minor marl, dolomite and chert; baritic pseudomorphs common
Cm	Mandorah Limestone Member	Limestone; commonly partly silicified
Cm	Tindall Limestone	Crystalline limestone with minor calcilutite, chert nodules
Cmb	Buckingham Bay Sandstone	Coarse white sandstone, clayey sandstone; massive to blocky
Cm	Antrim Plateau Volcanics	Massive and vesicular basalt, minor agglomerate
Cj	Jarang Conglomerate	Boulder and pebble conglomerate
Cw	Wilch Wai Conglomerate	Ferruginous sandy boulder and pebble conglomerate
Dw	Warrego Dolerite	Medium ophitic dolerite
Dm	Spencer Sandstone	Quartz sandstone, minor silty and dolomitic sandstone
Dl	Lloyd Creek Formation	Algal and oolitic dolomite, minor sandy and silty dolomite and grey-green siltstone
Dp	Pinkerton Sandstone	White massive quartz sandstone, minor siltstone and shale
Dm	Saddle Creek Formation	Basal blocky cross-bedded sandstone, upper flaggy quartz sandstone and siltstone
Dm	Angalarri Siltstone	Grey-green siltstone, minor fine sandstone, minor silty sandstone
Dg	Legune Formation	Interbedded siltstone, sandstone and dolomite
Dm	Mount Goodwin Member	Siltstone, minor sandstone, grit and conglomerate
Dm	Sinbaum Formation	Grey shale, grey and grey-green siltstone and fine sandstone, interbeds of fine white sandstone
Dm	Moyle River Formation	Fine to medium sandstone, lenses of siltstone, and basal conglomerate in places
Dm	Reeys Formation	Purple and green siltstone, dolomitic siltstone, minor dolomite
Dw	Waterbag Creek Formation	Ferruginous sandstone and siltstone, minor dolomite and marl, baritic pseudomorphs
Dh	Hinkler Dolomite	Dolomite and minor limestone, dolomitic siltstone
Ds	Sullivan Sandstone	Flaggy quartz sandstone, green siltstone and shale
Dsd	Stray Creek Sandstone Member	Massive cross-bedded quartz sandstone, pebbly beds
Dsd	Depot Creek Sandstone Member	Medium to coarse quartz sandstone, cross-bedded and ripple-marked, minor siltstone, pebbly beds and conglomerate
Dm	Mount Partridge Rhyolite	Rhyolite, dacite, minor basalt volcanics, lenses of sandstone and tuffaceous sandstone
Dm	Silverb Volcanic Member	Vesicular basalt, tuffaceous siltstone, minor banded quartz-jasperite
Dmc	Mount Callanan Volcanic Member	Andesite, vesicular in places
Dmh	Horsewood Creek Volcanic Member	Basalt, andesite, minor tuff
Dmn	Nunghalgarri Volcanic Member	Andesite to rhyodacite flows and minor dykes, vesicular and in places jasper-rich at top, minor intercalated sandstone
Dmb	Bridle Creek Volcanic Member	Andesite, vesicular
Dmp	Plum Tree Creek Volcanic Member	Ignimbrite, vesicular andesite
Dmm	McAdams Creek Volcanic Member	Vesicular basalt and andesite, minor tuff and rhyolite
Dm,		Medium to very coarse grantz sandstone, cross-bedded and ripple-marked, quartz-pebble conglomerate, minor siltstone
Dp		Purple quartz greywacke
Dd	Dengalli Dolerite	Differentiated continental tholeiitic basalt lopolith, olivine dolerite, commonly porphyritic; quartz dolerite, granophyre
Dm	Edith River Volcanics	Rhyolite, dacite, minor basalt volcanics, lenses of sandstone and tuffaceous sandstone
Dsl	Phillips Creek Member	Sandstone, conglomerate, shale, tuffaceous sediments
Dsl		Quartz sandstone, minor conglomerate
Dp	Allia Creek Granite	Coarse porphyritic biotite-muscovite adamellite, granodiorite and tonalite
Dgb	Burnside Granite	Grey fine to medium biotite adamellite, porphyritic in places
Dgc	Callen Granite	Pink and grey coarse porphyritic granite, grey fine granite, pink-green coarse and grey fine porphyritic adamellite, minor aplite dykes
Dgd	Mount Goodger Syenite	Dark pinkish-grey porphyritic syenite and quartz syenite
Dgr	Reynolds River Granite	Pink medium porphyritic adamellite, grey medium hornblende-biotite granite
Dgd	Tenton Granite	Red and bluish coarse porphyritic hornblende-biotite granite in the east, sheared in places and with minor adamellite and aplitite; grey medium to coarse foliated biotite granite in the west
Dgg	Margaret Granite	Pink and green coarse porphyritic adamellite
Dgh	Shoobridge Granite	Mainly porphyritic hornblende-biotite adamellite, with core of leucocratic adamellite and fringe of hornblende-biotite granodiorite
Dgj	Jim Jim Granite	Sericitized cream to pink, coarse to porphyritic biotite granite
Dgk	McKinlay Granite	Light grey medium biotite granite, minor gneiss
Dgm	Malone Creek Granite	Fine, cream-weathering aplitic granite, in places porphyritic near margins, minor gneisses
Dgn	Nimbuwah Granite	Sericitized cream coarse granite
Dgp	Kooleenbong Granite	Coarse granite, adamellite and granodiorite, even and porphyritic
Dgp	Prices Springs Granite	Grey massive medium to coarse porphyritic biotite granite and biotite adamellite
Dgr	Roberts Creek Granite	Granodiorite, adamellite, gneissose in places
Dgs	Soldiers Creek Granite	Coarse muscovite-biotite adamellite and granodiorite
Dgt	Tin Camp Granite	Sericitized white-cream coarse granite
Dgm	Mount Boorabby Granite	Pink medium to coarse hornblende-biotite granite and adamellite, porphyritic in places
Dgw	Wolfram Hill Granite	Pink medium granite, grey fine adamellite
Dgg	Grace Creek Granite	Granophyric adamellite, adamellite porphyry
Dgy	Yeuralba Granite	Leucocratic porphyritic adamellite, gneissose in the south
Dng	Nimbuwah Complex	Grey medium biotite granite, coarse graphitic granite
Dm,	Granitoid Core	Homogeneous to foliated porphyritic granite, porphyroblastic hornblende- biotite granodiorite
Dm,	Migmatite Zone	Granodiorite, adamellite, granitoid gneiss
Dm,	Lit-par-lit Gneiss Zone	Metamorphic biotite-feldspar-quartz schist and gneiss, commonly with amphibole and garnet, and quartz-rich pods and bands
Dm,	Transitional Zone	Quartz schist and pelitic schist with minor quartz-rich bands
Dd	Zamu Dolerite	Differentiated continental tholeiitic basalt sills, olivine dolerite, quartz dolerite, dacite and granophyre; metamorphosed to amphibolite in northeast
Dt	Ti-Tree Granophyre	Granophyre
Dh	Henschke Breccia	Coarse ferruginous sedimentary breccia and conglomerate with sandstone fragments, minor sandstone
Dc	Chilling Sandstone	White quartz sandstone, ripple-marked and cross-bedded, minor conglomerate, siltstone and tuff
Dvm	Mawney Volcanics	Porphyritic acid lava, tuff
Dv	Berinka Volcanics	Acid and minor intermediate lava, minor sandstone and tuff interbeds, granophyric acid intrusive rocks
Dd	Dorothy Volcanics	Basic lava, pyroclastic rocks, and tuffaceous sediments
Dr	Barrell Creek Formation	Siltstone, silty sandstone, minor greywacke siltstone, greywacke increases to west
Dp	Kapalga Formation	Ferruginous siltstone, shale, marl and sandstone in places; cosmonoh carbonaceous at depth
Dg	Gerowie Tuff	Rhyolitic welded tuff, grey-green argillite, pale green tuffaceous greywacke
Dsh	Shovel Billabong Andesite	Dacitic andesite
Dk	Kadjera Formation	Ferruginous siltstone with chert bands and nodules, pyritic carbonaceous shale, silicified dolomite, minor phyllite, jasper and banded iron formation
Ps		Schist, gneiss
Pz	Nourlangie Schist	Quartz-mica schist, mica-quartz schist, minor quartzite
Pzw	Wildman Siltstone	Siltstone, in places carbonaceous at depth, red and cream laminated siltstone, minor quartzite and quartz greywacke
Pzw	Acacia Gap Sandstone Member	Quartz sandstone and feldspathic sandstone with pyritic carbonaceous siltstone and quartz siltstone interbeds
Pzph	Mount Hooper Sandstone	Medium quartz sandstone and quartzite with some chert fragments, siltstone, phyllite, feldspathic quartzite, pebbly in places; chert pebble conglomerate at base in places
Pzph	Munduyle Sandstone	Coarse to medium quartz sandstone and siltstone/shale, commonly pebbly; quartz pebble conglomerate, siltstone, minor beds of chert breccia, ferruginous sandstone, amphibolite in places
Pzc	Stag Creek Volcanics	Rhyolitic welded breccia, ignimbrite, tuff, tuffaceous shale, tuffaceous greywacke
Pzc	Cahill Formation	Mica-feldspar-quartz schist and quartz-mica schist and with garnet, amphibole and kyanite in places, carbonaceous schist, crystalline dolomite-magnesite, and calc-silicate gneiss near base
Pzw	Masson Formation	Ferruginous shale (mostly carbonaceous at depth), fine to coarse calcareous and volcanic greywacke, calcarenite, sandstone, limestone
Pzk	Kadjamarrdik Quartzite	Orthoquartzite, quartz gneiss, minor schist, rare cross-bedding, rare amphibolite
Pzh	Mount Howship Gneiss	Very coarse white feldspathic leucogneiss, minor schist, rare garnet and amphibole
Pzm	Mumeralarry Quartzite	Massive to friable gneissic orthoquartzite, minor schist
Pzb	Mount Bonnefoy Gneiss	White-grey-pink coarse muscovite-biotite gneiss, granitoid gneiss, minor schist
Pzc	Coomalie Dolomite	Dolomite, magnesite, dolomite breccia, tremolite schist, cacholarite, algal structures and magnetite pseudomorphs in places
Pzr	Crater Formation	Feldspathic sandstone, pebble conglomerate, siltstone, pyritic in part, basal ferruginous conglomerate in places
Pzc	Celia Dolomite	Dolomite, minor limestone, dolomite breccia, tremolite in places, tremolite schist, minor sandstone, schists, carbonaceous sediments
Pzb	Beestons Formation	Arkose, feldspathic sandstone, conglomerate, siltstone
AE		Foliated Archaean–Proterozoic granitic complexes
AEh	Hermit Creek Metamorphics	Quartz-mica schist, phyllite, tremolite schist, amphibolite, migmatite
AEl	Litchfield Complex	Granite, adamellite, granodiorite, tonalite, migmatite, pegmatite, gamet/leucos in places
AEn	Nanambu Complex	Leucogranite, pegmatoid gneiss, biotite-chlorite schist, porphyroblastic foliated biotite granite, migmatite, gamet/leucos in places
AEr	Rum Jungle Complex	Gneiss, migmatite, coarse leucocratic granite, grey medium granite, minor schist, amphibolite, banded iron formation and quartzite
AEw	Waterhouse Complex	Aplitic leucocratic granite, adamellite, fine to coarse granite, gamet/leucos or porphyritic in places, dolerite, amphibolite, scattered granodiorite, schist, gneiss, migmatite, metavolcanics, banded iron formation

PINE CREEK GEOSYNCLINE
1:500 000

RADIOMETRIC CONTOURS — TOTAL COUNT OF THE PINE CREEK GEOSYNCLINE

NORTHERN TERRITORY

1979

Scale 1:500 000

10 0 10 20 30 40 50 KILOMETRES

Transverse Mercator Projection

Design and drafting by Cartography Section, BMR
Printed by Mercury-Walch, Hobart, Australia

Published by the Bureau of Mineral Resources, Geology and Geophysics, Department of National Development. Issued under the authority of the Minister for National Development

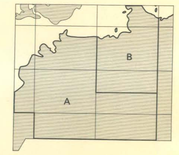
© Commonwealth of Australia 1979

Copies of this map may be obtained from the Bureau of Mineral Resources, Geology and Geophysics, Canberra, ACT, or Darwin, NT

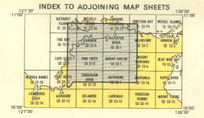
This map serves as an overlay to the Pine Creek Geosyncline geological map.

SURVEY PARAMETERS

	Area A	Area B
Source	BMR	BMR
Date of survey	1974–76	1971–72
Line spacing	1500m	1500m
Altitude	150m above G.L.	150m above G.L.
Total Count Window	0.84–3.00 met	0.84–3.00 met
Detector volume	3700cm³ NaI	3700 cm³ NaI
Recording system	digital	analogue
Background correction	applied	applied
Height correction	applied	nil
Filtering	applied	nil
Contouring	1500×600 grid	contour cuts
Exposure rate Conversion	1 μ R/h approx. 7.5cps	1 μ R/h approx. 7.5cps



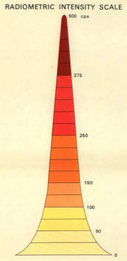
INDEX TO ADJOINING MAP SHEETS

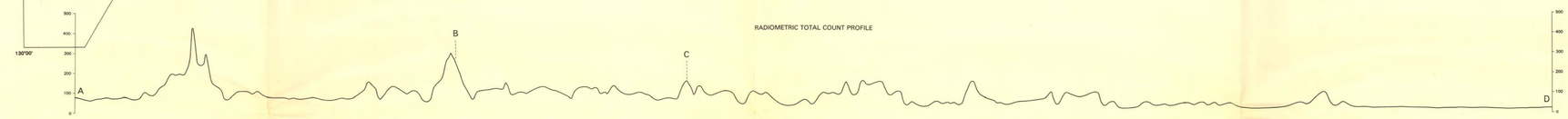


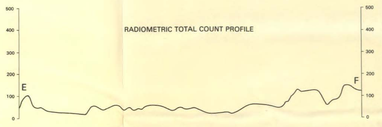
LOCALITY MAP



RADIOMETRIC INTENSITY SCALE







PINE CREEK GEOSYNCLINE
1:500 000

TOTAL MAGNETIC INTENSITY CONTOURS OF THE PINE CREEK GEOSYNCLINE NORTHERN TERRITORY 1979

Scale 1:500 000

10 0 10 20 30 40 50 KILOMETRES

Transverse Mercator Projection

Design and drafting by Cartography Section, BMR

Printed by Mercury-Walch, Hobart, Australia

Published by the Bureau of Mineral Resources, Geology and Geophysics, Department of National Development, issued under the authority of the Minister for National Development

© Commonwealth of Australia 1979

Copies of this map may be obtained from the Bureau of Mineral Resources, Geology and Geophysics, Canberra, ACT, or Darwin, NT

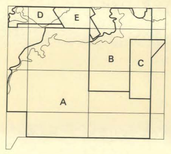
This map serves as an overlay to the Pine Creek Geosyncline geological map

SURVEY PARAMETERS

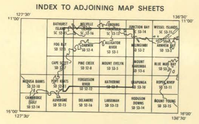
	Area A	Area B	Area C	Area D	Area E
Source	BMR	BMR	Queensland Mines Limited	Alliance Oil Development Australia N.L.	Flinders Petroleum N.L. (BMR Subsidy)
Date of survey	1974–76	1971–72	1970	1963	1969
Line spacing	1500m	1500m	800m	Groups of 3 lines 1600m apar 17000m between centres of groups	Groups of 3 lines 1600m apart 000m between centres of groups
Line direction	EW	EW	NS	NE and EW	NW
Altitude	150m above G.L.	150m above G.L.	120m above G.L.	600m above G.L.	600m above G.L.
Recording system	digital	analogue	analogue	analogue	digital
Corrections	IGR Field removed	IGR Field removed	IGR Field removed	IGR Field removed	IGR Field removed
Contouring	1500÷600m grid	Contour cuts	contour cuts	contour cuts	contour cuts
Contour interval	10nT	10nT	10nT	10nT	10nT

Magnetic Low

SURVEY PARAMETERS

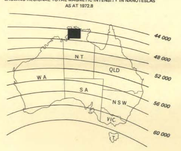


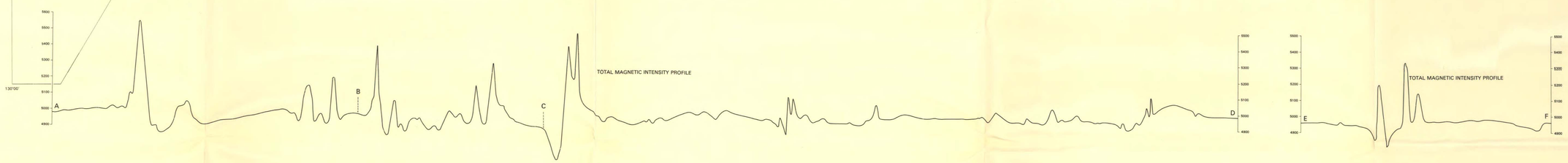
INDEX TO ADJOINING MAP SHEETS



LOCALITY MAP

SHOWING REGIONAL TOTAL MAGNETIC INTENSITY IN NANOTESLAS AS AT 1972.0





PINE CREEK GEOSYNCLINE
1:500 000

BOUGUER ANOMALY CONTOURS OF THE PINE CREEK GEOSYNCLINE

NORTHERN TERRITORY

1979

Scale 1:500 000

10 0 10 20 30 40 50 KILOMETRES

Transverse Mercator Projection

Contour interval 1Gum.s^{-2} (1μm.s^{-2} ≡ 1μNKg^{-1} ≡ 0.1 mGal)

For the calculation of Bouguer anomalies 2.67 t.m^{-3} has been adopted as an average rock density

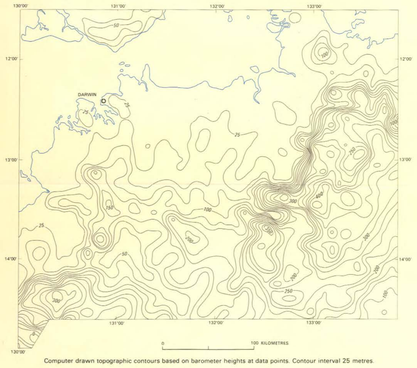
Compiled by A. S. Murray
Design and drafting by Cartography Section, BMR
Drawn by A. J. Maxwell
Printed by Mercury - Walch, Hobart, Australia

Published by the Bureau of Mineral Resources, Geology and Geophysics, Department of National Development. Issued under the authority of the Minister for National Development
Topographic base compiled by the Bureau of Mineral Resources, Geology and Geophysics from the Australian Aeronautical Chart, ICAO 1:500 000 series produced by the Division of National Mapping, Department of National Development

© Commonwealth of Australia 1979

Copies of this map may be obtained from the Bureau of Mineral Resources, Geology and Geophysics, Canberra, ACT, or Darwin, NT.

This map serves as an overlay to the Pine Creek Geosyncline geological map.



Computer drawn topographic contours based on barometer heights at data points. Contour interval 25 metres.

Sources of data

The sources of data, for about 85 percent of the contoured area, are the contract surveys carried out for the Bureau of Mineral Resources (BMR), to provide a regional coverage of Australia and the surrounding marine areas. Surveys used helicopters for transport and barometers to determine heights. The stations were spaced on a regular 11 km grid. The remaining data were obtained by BMR, using a spacing which ranged from 0.5-5km. The locations of all data points are shown on the face of the map.

Reduction of anomalies

The values of observed gravity throughout the map are controlled by the Australian National Gravity Network. The positions of the helicopter stations were determined using aerial photographs to tie to the Australian Geodetic Datum, and heights where determined by barometer ties to third-order levelling traverses, which in turn are tied to the Australian Height Datum. The observed gravity values have been reduced to the simple Bouguer anomaly (BA)

$$BA = g_o + g_n + 0.3086h - 0.0419\rho h$$

where h is the altitude in metres and ρ is taken as 2.67 t.m^{-3}. No terrain corrections have been applied.

Accuracy of anomalies

The usual precision within each helicopter land gravity survey is better than 3μm.s^{-2} for observed gravity differences, less than 5m for altitude, and about 0.1 minutes of arc for latitudes and longitudes, resulting in Bouguer anomalies with a relative precision of about 10μm.s^{-2}. The precision of ties between surveys is less than 5μm.s^{-2} and 10m, or about 20μm.s^{-2} in Bouguer anomaly. Gravity values of the national network are estimated to have a standard error of 1μm.s^{-2} relative to other stations on the same east-west line, and a standard error of 2μm.s^{-2} relative to the network as a whole.

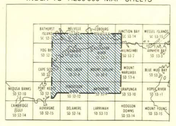
Smoothing and contouring gravity anomalies

The data were interpolated onto a 2-minute square grid over the whole map area. The contour lines are based on the computed grid values - not directly on the anomaly values - and are precise to only about half a grid spacing, or about 1 minute of arc.
The graticule and gravity contours were scribed on BMR's Calcomp 745 flatbed plotter.

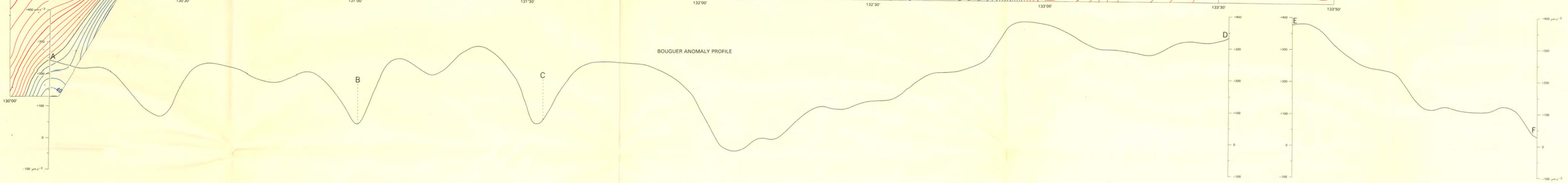
LOCALITY MAP



INDEX TO 1:250 000 MAP SHEETS



BOUGUER ANOMALY PROFILE



PINE CREEK GEOSYNCLINE
1:500 000

AUTHOR INDEX

The Arabic numerals refer to the first page of a paper by the author concerned.

Äikäs, Olli: 675
Anthony, P.J.: 259
Armstrong, C.W.: 733
Ayres, D.E.: 417
Berkman, D.A.: 299, 343
Binns, R.A.: 417, 457, 469, 543
Brewster, N.W.: 733
Brookins, D.G.: 709
Cameron, J.: 743
Chappell, B.W.: 73
Chauvet, R.: 663
Compston, W.: 39
Craven, S.J.: 457
Crick, I.H.: 1, 23, 273, 531
Cruikshank, B.I.: 693
Curtis, L.: 595
Derrick, G.M.: 693
Deutscher, R.L.: 477
De Voto, R.H.: 683
Dickson, B.L.: 499
Donnelly, T.H.: 397, 563
Dunbier, J.: 351
Eupene, G.S.: 259
Ewers, G.R.: 363, 563
Fei, Qin: 655
Ferguson, John: 73, 91, 191, 209, 363, 397, 563, 693
Finlay, C.J.: 357
Fraser, W.J.: 287, 343
Fuzikawa, Kazuo: 375
Gale, N.H.: 707
Gauthier-Lafaye, F.: 663
Giblin, A.M.: 477, 521
Gingrich, J.E.: 351
Goleby, A.B.: 73
Goulevitch, J.: 307
Green, A.A.: 141
Gulson, B.L.: 439
Hart, R.J.: 707
Hegge, M.R.: 259
Hochman, M.B.: 335
Hoeve, J.: 575
Hone, I.G.: 101
Huntington, J.F.: 141
Kirchner, G.: 617
Korsch, M.J.: 407
Lehnert-Thiel, K.: 617
Leishman, J.: 141
Lewry, J.F.: 575
Mann, A.W.: 477
McAndrew, J.: 357, 543
McLennan, S.M.: 175
Michel, B.: 663
Miller, A.R.: 595
Mizon, K.J.: 439
Mosher, D.V.: 259
Muir, M.D.: 273, 531
Naudet, R.: 663
Needham, R.S.: 1, 23, 39, 157, 233, 273
Nicholson, P.M.: 319
Nicolaysen, L.O.: 707
Page, R.W.: 39
Pagel, M.: 639
Paschis, J.A.: 683
Pedersen, C.P.: 351

Pfiffelmann, J.P.: 663
Poty, B.: 639
Ramaekers, P.: 575
Ramsden, A.R.: 417
Reboul, J.C.: 663
Rich, J.: 617
Riley, G.H.: 69, 407, 457
Roarty, M.J.: 157, 273
Rossiter, A.G.: 209
Rowntree, J.C.: 751
Ryall, W.R.: 469
Sampath, N.: 101
Shaokang, Hu: 655
Sheppard, S.M.F.: 639
Shirvington, P.J.: 509
Sibbald, T.I.I.: 575
Simpson, C.J.: 141
Snelling, A.A.: 487, 499
Strnad, J.G.: 617, 631
Stuart, D.C.: 101
Stuart-Smith, P.G.: 1, 23, 233
Sun, S-S.: 543
Taylor, D.M.: 743
Taylor, G.H.: 751
Taylor, S.R.: 175
Tilsley, J.E.: 721
Tucker, D.H.: 101
Weber, F.: 663
Wills, K.: 23
Wilmshurst, J.R.: 417
Winer, P.: 191
Ypma, P.J.M.: 375

HOW TO ORDER IAEA PUBLICATIONS

An exclusive sales agent for IAEA publications, to whom all orders and inquiries should be addressed, has been appointed in the following country:

UNITED STATES OF AMERICA UNIPUB, 345 Park Avenue South, New York, NY 10010

In the following countries IAEA publications may be purchased from the sales agents or booksellers listed or through your major local booksellers. Payment can be made in local currency or with UNESCO coupons.

ARGENTINA	Comisión Nacional de Energía Atomica, Avenida del Libertador 8250, RA-1429 Buenos Aires
AUSTRALIA	Hunter Publications, 58 A Gipps Street, Collingwood, Victoria 3066
BELGIUM	Service Courrier UNESCO, 202, Avenue du Roi, B-1060 Brussels
CZECHOSLOVAKIA	S.N.T.L., Spálená 51, CS-113 02 Prague 1 Alfa, Publishers, Hurbanovo námestie 6, CS-893 31 Bratislava
FRANCE	Office International de Documentation et Librairie, 48, rue Gay-Lussac, F-75240 Paris Cedex 05
HUNGARY	Kultura, Hungarian Foreign Trading Company P.O. Box 149, H-1389 Budapest 62
INDIA	Oxford Book and Stationery Co., 17, Park Street, Calcutta-700 016 Oxford Book and Stationery Co., Scindia House, New Delhi-110 001
ISRAEL	Heiliger and Co., Ltd., Scientific and Medical Books, 3, Nathan Strauss Street, Jerusalem 94227
ITALY	Libreria Scientifica, Dott. Lucio de Biasio "aeiou", Via Meravigli 16, I-20123 Milan
JAPAN	Maruzen Company, Ltd., P.O. Box 5050, 100-31 Tokyo International
NETHERLANDS	Martinus Nijhoff B.V., Booksellers, Lange Voorhout 9-11, P.O. Box 269, NL-2501 The Hague
PAKISTAN	Mirza Book Agency, 65, Shahrah Quaid-e-Azam, P.O. Box 729, Lahore 3
POLAND	Ars Polona-Ruch, Centrala Handlu Zagranicznego, Krakowskie Przedmiescie 7, PL-00-068 Warsaw
ROMANIA	Ilexim, P.O. Box 136-137, Bucarest
SOUTH AFRICA	Van Schaik's Bookstore (Pty) Ltd., Libri Building, Church Street, P.O. Box 724, Pretoria 0001
SPAIN	Diaz de Santos, Lagasca 95, Madrid-6 Diaz de Santos, Balmes 417, Barcelona-6
SWEDEN	AB C.E. Fritzes Kungl. Hovbokhandel, Fredsgatan 2, P.O. Box 16356, S-103 27 Stockholm
UNITED KINGDOM	Her Majesty's Stationery Office, Agency Section PDIB, P.O.Box 569, London SE1 9NH
U.S.S.R.	Mezhdunarodnaya Kniga, Smolenskaya-Sennaya 32-34, Moscow G-200
YUGOSLAVIA	Jugoslovenska Knjiga, Terazije 27, P.O. Box 36, YU-11001 Belgrade

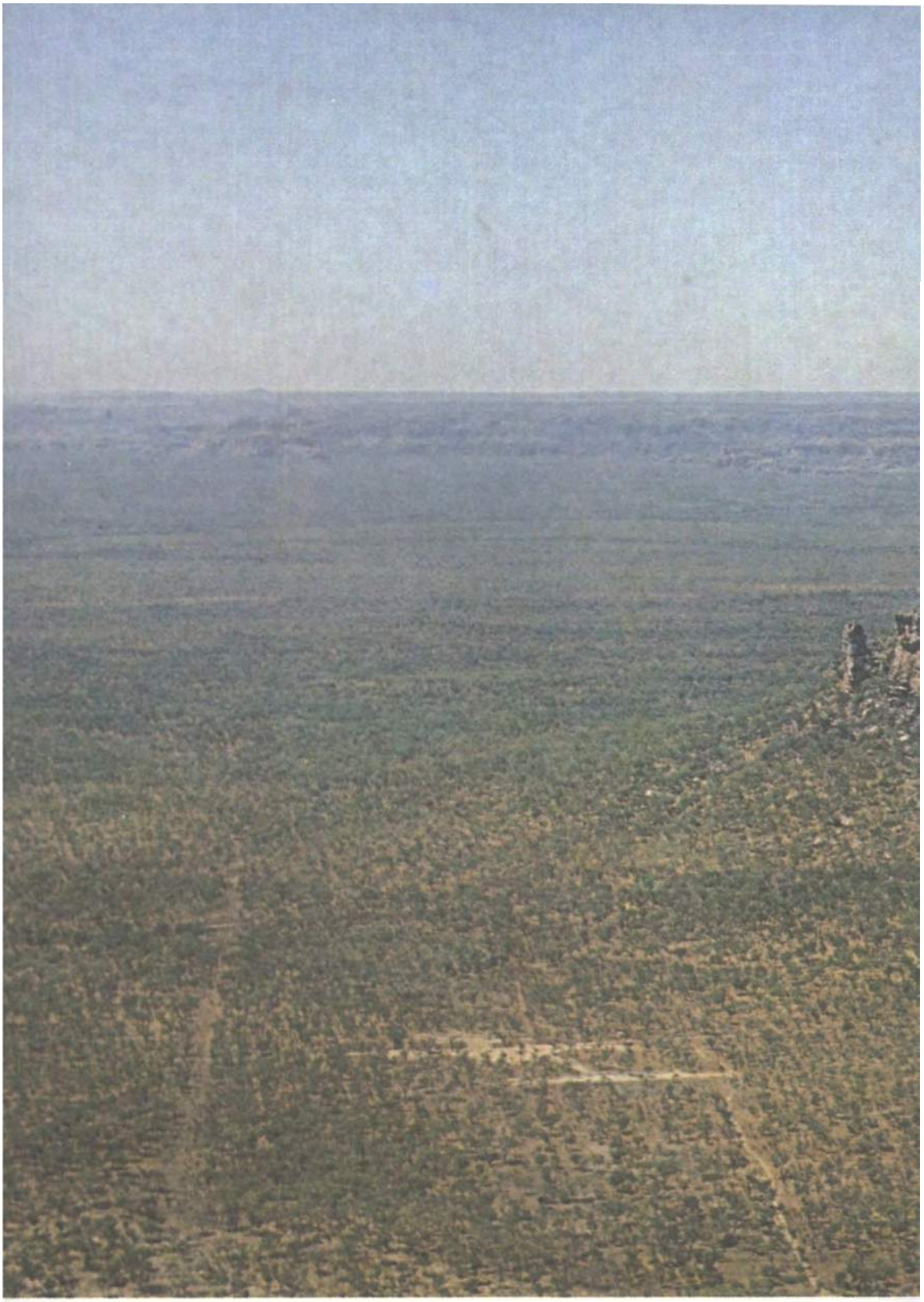
---

Orders from countries where sales agents have not yet been appointed and requests for information should be addressed directly to:



Division of Publications
International Atomic Energy Agency
Wagramerstrasse 5, P.O. Box 100, A-1400 Vienna, Austria

80. 00936



INTERNATIONAL
ATOMIC ENERGY AGENCY
VIENNA, 1980

SUBJECT GROUP: IV
Chemistry, Geology and Raw Materials/Geology
PRICE: Austrian Schillings 1080.–